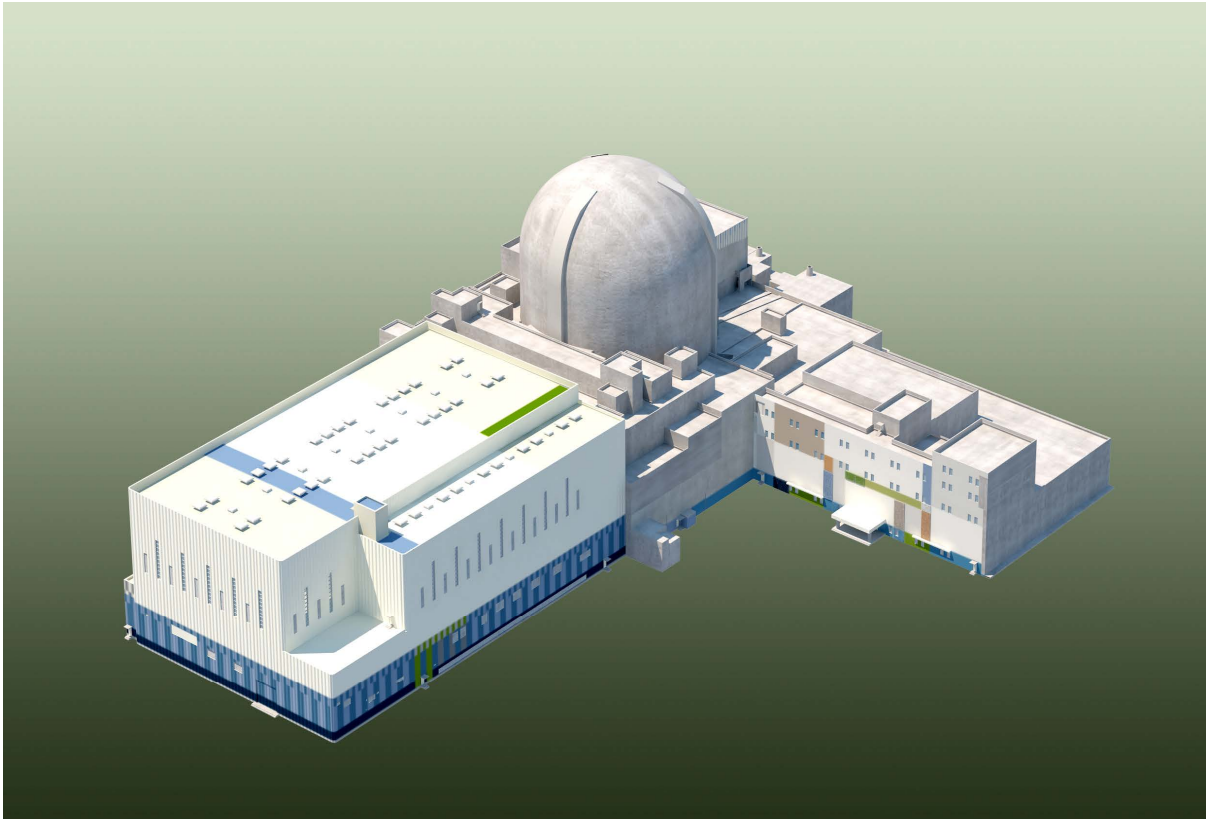


PLUS7 Fuel Design for the APR1400

APR1400-F-M-TR-13001-NP-A

August 2018



KOREA ELECTRIC POWER CORPORATION



KOREA HYDRO & NUCLEAR POWER CO., LTD

CONTENTS

| SECTION | DESCRIPTION |
|---------|-------------|
|---------|-------------|

- | | |
|---|--|
| A | Letter from William Ward(NRC) to Han-Gon KIM (KHNP), ADVANCED POWER REACTOR 1400 FINAL SAFETY EVALUATION FOR TOPICAL REPORT APR1400-F-M-TR-13001-P,REVISION 1, “PLUS7 FUEL DESIGN FOR THE APR1400,” dated on May 25, 2018. |
| B | PLUS7 FUEL DESIGN FOR THE APR1400 Topical Report, APR1400-F-M-TR- 13001-NP-A |
| C | KHNP Response to ‘Request for Additional Information 4-7542, dated May 27, 2014,’ dated on June 26, 2014 |
| D | Response to ‘Request for Additional Information 5-7954, dated June 18, 2015,’ dated on July 21, 2015 Response to ‘Request for Additional Information 5-7954, dated June 18, 2015,’ dated on July 29, 2016 Revised Response to ‘Request for Additional Information 5-7954, dated June 18, 2015,’ dated on August 11, 2017 Revised Response to ‘Request for Additional Information 5-7954 Rev. 2, dated June 18, 2015,’ dated on October 16, 2017 Revised Response to ‘Request for Additional Information 5-7954 Rev.3, dated June 18, 2015,’ dated on December 1, 2017 |
| E | Revised Response to ‘Request for Additional Information 6-8322, dated October 27, 2015,’ dated on January 27, 2016 Revised Response to ‘Request for Additional Information 6-8322, dated October 27, 2015,’ dated on July 31, 2017 |

This document was prepared for the design certification application to the U.S. Nuclear Regulatory Commission and contains technological information that constitutes intellectual property of Korea Hydro & Nuclear Power Co., Ltd. Copying, using, or distributing the information in this document in whole or in part is permitted only to the U.S. Nuclear Regulatory Commission and its contractors for the purpose of reviewing design certification application materials. Other uses are strictly prohibited without the written permission of Korea Electric Power Corporation and Korea Hydro & Nuclear Power Co., Ltd.

Non-Proprietary

SECTION A

Non-Proprietary

Page intentionally left blank

OFFICIAL USE ONLY – PROPRIETARY INFORMATION



UNITED STATES
NUCLEAR REGULATORY COMMISSION
WASHINGTON, D.C. 20555-0001

May 25, 2018

Dr. Han-Gon Kim, Project Manager
APR1400 Design Certification
Advanced Reactors Development Laboratory
Korea Hydro and Nuclear Power Co., Ltd.
70-1312-gil, Yuseong-daero
Yuseong-Gu, Daejeon
34101 Korea (Republic of)

SUBJECT: ADVANCED POWER REACTOR 1400 FINAL SAFETY EVALUATION
FOR TOPICAL REPORT APR1400-F-M-TR-13001-P, REVISION 1,
"PLUS7 FUEL DESIGN FOR THE APR1400"

Dear Dr. Kim:

The U.S. Nuclear Regulatory Commission (NRC) staff has prepared a final Topical Report Safety Evaluation (TRSE) for Topical Report APR1400-Z-M-TR12003-P, Revision 1, "Plus7 Fuel Design for the APR1400." This TRSE is also valid for the non-proprietary version of the topical report (TR). This action is supported by the letter dated March 26, 2018 (Agencywide Documents Access and Management System Accession No. ML18074A379), whereby the Advisory Committee on Reactor Safeguards agrees with the NRC staff's conclusions, within the limits and conditions that are specified in the TRSE. This evaluation is in support of the review of the APR1400 design certification application submitted by Korea Hydro and Nuclear Power (KHNP) and Korea Electric Power Corporation on December 23, 2014.

The staff requests that KHNP publish the accepted enclosed proprietary and non-proprietary versions of this TR within one month of receipt of this letter. The accepted versions shall incorporate this letter and the enclosed final TRSE after the title page. Also, they must contain historical review information, including NRC requests for additional information and your responses. The accepted versions of the TR shall include an "-A" (designated accepted) following the report identification number.

If the NRC's criteria or regulations change such that its conclusion that the accepted TR is invalidated, KHNP and/or the applicant referencing the TR will be expected either to revise and resubmit its respective documentation or to submit justification for continued applicability of the TR without revision of the respective documentation.

Document transmitted herewith contains sensitive unclassified information. When separated from the enclosure, this document is "DECONTROLLED."

OFFICIAL USE ONLY – PROPRIETARY INFORMATION

OFFICIAL USE ONLY – PROPRIETARY INFORMATION

Dr. Kim

- 2 -

If you have any questions or comments concerning this matter, please contact me at (301) 415-7038, or via e-mail at William.Ward@nrc.gov, or George Wunder at (301) 415-5207, or via e-mail at George.Wunder@nrc.gov.

Sincerely,

A handwritten signature in blue ink, appearing to read "William Ward", is positioned above the typed name.

William Ward, Senior Project Manager
Licensing Branch 2
Division of New Reactor Licensing
Office of New Reactors

Docket No. 52-046

Enclosure:
As stated

cc w/ encl.: See next page

OFFICIAL USE ONLY – PROPRIETARY INFORMATION

Email

| | |
|--|--------------------|
| <u>kimhg1108@khnp.co.kr</u> | [Han-Gon Kim] |
| <u>hansang.kim@khnp.co.kr</u> | [Hansang Kim] |
| <u>dohwan.lee@khnp.co.kr</u> | [Do-Hwan Lee] |
| <u>junghokim@khnp.co.kr</u> | [Jung-Ho Kim] |
| <u>yunho.kim@khnp.co.kr</u> | [Yun Ho Kim] |
| <u>jiyong.oh@khnp.co.kr</u> | [Jiyong Andy Oh] |
| <u>ahn.daegeun@khnp.co.kr</u> | [Daegeun Tony Ahn] |
| <u>iksuh@khnp.co.kr</u> | [Jeong Kwan Suh] |
| <u>hachewung@khnp.co.kr</u> | [Che Wung Ha] |
| <u>kang.deogji@khnp.co.kr</u> | [Deog Ji Kang] |
| <u>sunguk.kwon@khnp.co.kr</u> | [Sun Guk Kwon] |
| <u>ptmaster300@kepco.co.kr</u> | [Hyun Chul Park] |
| <u>sisk1rb@westinghouse.com</u> | [Rob Sisk] |
| <u>david.wagner@aecom.com</u> | [David Wagner] |
| <u>robert.sweeney@consultant.aecom.com</u> | [Robert Sweeney] |

KHNP Mailing List

9/22/2015

Daegeun Tony Ahn
Director
KHNP Washington DC Center
8100 Boone Blvd, Suite 620
Vienna, VA 22182

SAFETY EVALUATION BY THE OFFICE OF NEW REACTORS

TOPICAL REPORT (TR) APR1400-F-M-TR-13001, REVISION 1.

“PLUS7 FUEL DESIGN FOR THE APR1400,” KOREA HYDRO & NUCLEAR POWER CO. LTD

PROJECT NO. PROJ0782

1.0 INTRODUCTION AND BACKGROUND

By letter dated September 17, 2013 (Reference 1), as supplemented by letters dated June 26, 2014 (Reference 2), July 21, 2015 (Reference 3), and July 31, 2017 (Reference 4), Korea Hydro & Nuclear Power Co. LTD (the applicant) requested review and approval of Topical Report (TR) APR1400-F-M-TR-13001, “PLUS7 Fuel Design for the APR1400.” By letter dated August 11, 2017 (Reference 5), the applicant submitted a revision to the TR which included updates to address the U.S. Nuclear Regulatory Commission (NRC) staff’s requests for additional information (RAIs). This TR describes the PLUS7 assembly mechanical design for the applicant’s APR1400 nuclear steam supply system (NSSS).

2.0 REGULATORY EVALUATION

Regulatory guidance for the review of fuel system designs and adherence to applicable General Design Criteria (GDC) of Title 10 of the *Code of Federal Regulations* (10 CFR) Part 50, “Domestic Licensing of Production and Utilization Facilities,” Appendix A, “General Design Criteria for Nuclear Power Plants,” is provided in NUREG-0800, “Standard Review Plan for the Review of Safety Analysis Reports for Nuclear Power Plants” (SRP), Section 4.2, “Fuel System Design” (Reference 6). These regulations include:

1. 10 CFR 50.46, “Acceptance Criteria for Emergency Core Cooling Systems for Light-water Nuclear Power Reactors,” 10 CFR 50.34, “Contents of applications; technical information,” and 10 CFR 50.67, “Accident source term” as they relate to the cooling performance analysis of the emergency core cooling system (ECCS) using an acceptable evaluation model and establishing acceptance criteria for light-water nuclear power reactor ECCSs.
2. General Design Criterion (GDC) 10, “Reactor Design,” as it relates to assuring that specified acceptable fuel design limits (SAFDLs) are not exceeded during any condition of normal operation, including the effects of AOOs.
3. GDC 27, “Combined Reactivity Control Systems Capability,” as it relates to control rod insertability under postulated accident conditions.
4. GDC 35, “Emergency Core Cooling,” as it relates to the reactor fuel system being designed such that the performance of the Emergency Core Cooling System will not be compromised following a postulated accident.
5. 10 CFR 52.47(b)(1), which requires that a DC application contain the proposed inspections, tests, analyses, and acceptance criteria (ITAAC) that are necessary and sufficient to provide reasonable assurance that, if the ITAACs are performed and the acceptance criteria are met, a plant that incorporates the design certification is built and

will operate in accordance with the design certification, the provisions of the Atomic Energy Act, and the NRC's regulations.

In accordance with SRP Section 4.2, the objectives of the fuel system safety review are to provide assurance that:

1. The fuel system is not damaged as a result of normal operation and anticipated operational occurrences (AOOs),
2. Fuel system damage is never so severe as to prevent control rod insertion when it is required,
3. The number of fuel rod failures is not underestimated for postulated accidents, and
4. Coolability is always maintained.

An approved mechanical design methodology is utilized to demonstrate compliance with the NRC regulations identified in SRP 4.2 Section II. The staff's objectives for the review of TR APR1400-F-M-TR-13001 are to ensure that the fuel mechanical design methodology adequately addresses SRP Section 4.2 criteria. In addition, based upon Lead Test Assemblies (LTAs) and Commercial Surveillance Assemblies (CSAs), post-irradiation examinations (PIEs), mechanical testing, past operating experience of similar designs and materials, and fuel performance code predictions, the staff reviewed expected performance of the PLUS7 assembly to ensure it satisfied these objectives. The staff's review is similar in scope to past reviews, e.g. CE (Combustion Engineering) 16x16 NGF fuel assembly design (Reference 7).

3.0 SUMMARY OF TECHNICAL INFORMATION

The applicant jointly developed the PLUS7 fuel assembly design with Westinghouse to improve upon the Guardian fuel performance. This TR describes the design evaluation of the PLUS7 fuel assembly based on in-reactor performance data and calculations based on previously approved fuel analysis codes and methods.

The general approach of the TR is based on the guidance provided in SRP Section 4.2. In Sections 2, "Fuel Assembly and Components Design," and 3, "Fuel Rod Design," of the TR, the applicant presented design bases, criteria, and evaluations for potential failure mechanisms. The staff summarized these in Section 4.0, "Technical Evaluation," of this safety evaluation report (SER) as part of the staff's review. While the applicant analyzed and presented the majority of the failure mechanisms identified in SRP Section 4.2 in this TR, there are a few that are not. The applicant addressed failure mechanisms such as fuel seismic response and core coolability related failure mechanisms (e.g. fuel rod ballooning, cladding embrittlement, bursting, etc.) in other topical and technical reports. For these items, the applicant presented the basis and criteria for these failure mechanisms in this TR but refers the reader to other reports for the evaluation.

Section 3.3 of the TR discusses the codes and methods used to perform the analyses. The applicant presented the applicability of each code to the PLUS7 and APR1400 designs as well as the compliance with the applicable SERs.

Revision 1 to this TR includes discussions and analyses regarding the impacts of burnup dependent Thermal Conductivity Degradation (TCD) in Sections 3.4 and 3.5. This information supplements some of the information presented in other sections. For example, Section 3.2.2

discusses the design basis, criteria, and evaluation for cladding strain, but Section 3.4.2 later presents additional information regarding the impact of TCD on strain. Therefore, in order for the reader to understand the applicant's analysis of strain for the PLUS7 fuel assembly as a whole, both Section 3.2.2 and Section 3.4.2 must be reviewed.

The applicant presented a summary of the PLUS7 fuel operational experience in Section 4, "PLUS7 Fuel Experience," to support the analyses in Sections 2 and 3.

4.0 TECHNICAL EVALUATION

The staff's review of TR APR1400-F-M-TR-13001, Revision 1, is summarized below:

- Verify that the fuel assembly component and fuel rod design criteria are consistent with acceptance criteria identified in SRP Section 4.2 or are otherwise justified.
- Verify that the fuel mechanical design methodology is capable of accurately or conservatively evaluating each component with respect to established design criteria.
- Verify that the operating experience data database (in-reactor residence, post-irradiation examinations, and out-of-pile testing) supports the operating limits being requested and provides reasonable assurance that no anomalous behavior will occur during batch implementation.

The layout of this SER closely follows that of TR APR1400-F-M-TR-13001.

4.1 Fuel Assembly and Components Design

Section 2 of TR APR1400-F-M-TR-13001 provides a description of the PLUS7 fuel assembly with comparisons to Guardian and RFA fuel. Throughout this section, the applicant made comparisons between calculated physical phenomena and data obtained from LTAs and CSAs.

4.1.1 Fuel Assembly

4.1.1.1 Fuel Assembly Structural Integrity

The staff reviewed the fuel assembly structural integrity design basis, criteria, and evaluation as presented in Section 2.2.2.1 of APR1400-F-M-TR-13001, Revision 1. The staff's review is summarized below.

Basis

In Section 2.2.2.1 of APR1400-F-M-TR-13001, Revision 1, the applicant stated that, "[t]he objectives of the fuel assembly safety are to provide assurance that (a) the fuel system is not damaged as a result of normal operation and anticipated operational occurrences (AOOs), (b) fuel system damage is never so severe as to prevent control rod insertion when it is required, (c) the number of fuel rod failures is not underestimated for postulated accidents, and (d) coolability is always maintained."

This design basis is consistent with SRP Section 4.2. Therefore, the staff finds this basis to be acceptable.

Criteria

In Section 2.2.2.1 of APR1400-F-M-TR-13001, Revision 1, the applicant stated that the criteria used to evaluate the PLUS7 fuel assembly structural integrity are those taken from Section III of the American Society of Mechanical Engineers (ASME) Boiler and Pressure Vessel (B&PV) Code; specifically,

For normal conditions:

$$P_m \leq S_m$$

$$P_m + P_b \leq 1.5 S_m$$

For accident conditions:

$$P_m \leq S_m'$$

$$P_m + P_b \leq 1.5 S_m'$$

Where:

P_m = primary membrane stress

P_b = primary bending stress

S_m = allowable design stress

S_m' = allowable design strength for the accident conditions

Additionally, the methodology described by the applicant used normal operation and AOO stress limit criteria even under postulated accident conditions in order to preclude plastic deformation for components important to control element assembly (CEA) insertion.

These criteria are consistent with SRP Section 4.2, Appendix A. Therefore, the staff finds these criteria to be acceptable.

Evaluation

The structural integrity of the assembly components are verified in the following sections describing the individual assembly components. The fuel assembly evaluation for seismic and loss of coolant accident (LOCA) loads is performed in accordance with the NRC licensed CE methodology, CENPD-178-P, Revision 1 (Reference 12). The staff issued RAI 7954, Question 22 (ML15169A118), requesting the applicant to provide clarification regarding the evaluation for seismic and LOCA loads since the TR stated that the analysis was performed in Section 4.2 of the APR1400 design control document (DCD), but Section 4.2 of the DCD stated that the analysis was performed in the TR. In its response to RAI 7954, Question 22 (ML15202A676), the applicant stated that the evaluation is presented in Technical Report APR1400-Z-M-NR-14010-P, "Structural Analysis of Fuel Assemblies for Seismic and LOCA Loading." The staff confirmed that this information was presented in the referenced technical report and that the staff's SER for DCD Section 4.2 would address the staff's evaluation of the fuel assembly structural analysis of external loads. Therefore, the staff's evaluation will not be presented in this SER.

4.1.1.2 Rod to Top Nozzle Axial Clearance

The staff has reviewed the fuel assembly structural integrity design basis, criteria, and evaluation as presented in Section 2.2.2.2 of the APR1400-F-M-TR-13001, Revision 1. The staff's review is summarized below.

Basis

In Section 2.2.2.2 of the TR, the applicant stated that, "[i]f a fuel rod were to be fully constrained axially by contact with top and bottom nozzles, large axial load could be generated. This load could result in fuel rod bowing, overstressing of guide thimbles, or overstressing of guide thimble joints to nozzles." This is consistent with SRP Section 4.2 (1)(A)(v). Therefore, the staff finds this basis to be acceptable.

Criteria

Section 2.2.2.2 of the TR states that "[t]he axial clearance between the fuel rod and top nozzle shall be maintained during the fuel life time."

This criterion will preclude interference between the fuel rods and the nozzles and is acceptable.

Evaluation

The applicant performed a simple calculation of axial gap between the fuel rod and top nozzle that includes the fuel rod and assembly irradiation growth to ensure that axial clearance is maintained during the fuel lifetime. Additionally, pool side examination data is provided to confirm that there is sufficient gap after three cycles of irradiation.

The staff reviewed the analysis and finds that this evaluation, supported by pool side examination data, demonstrates compliance with the stated criteria in that there will be rod to top nozzle axial clearance throughout the requested fuel assembly lifetime.

4.1.1.3 Hydraulic Stability

The staff has reviewed the fuel assembly structural integrity design basis, criteria, and evaluation as presented in Section 2.2.2.3 of the APR1400-F-M-TR-13001, Revision 1. The staff's review is summarized below.

Basis

In Section 2.2.2.3 of APR1400-F-M-TR-13001, Revision 1, the applicant stated that, "[s]ince the fuel assembly lift-off may cause the fuel assembly and in-core structure failure, the fuel assembly shall not be lifted off during the normal operation. The fuel assembly and fuel rod vibration causing the fuel failure shall not occur over the full range of flow rates of the plant." This is consistent with SRP Section 4.2(1)(A)(iii) and (1)(A)(vii). Therefore, the staff finds this basis to be acceptable.

Criteria

The applicant provided the following criteria regarding hydraulic stability:

- The fuel assembly shall not be lifted off during normal operation.
- Fuel rod vibration causing the fuel failure shall not occur over the full range of flow rates.
- The fuel rod vibration caused by the cross-flow between the fuel assemblies shall not result in fretting wear-induced cladding failure.

These criteria are consistent with the guidance provided in SRP Section 4.2 (1)(A)(iii) and (1)(A)(vii). Therefore, the staff finds these criteria to be acceptable.

Evaluation

The applicant stated that the assembly lift off and fuel rod vibration failure criteria are met as demonstrated through prototype testing and operating experience. The staff reviewed the information provided and confirmed that it covered the full range of flow rates and demonstrated that a fuel assembly will not lift off due to the hydraulic loads nor generate abnormal fluid-induced vibration which could lead to fuel rod failure.

The applicant also provided documentation regarding 500 hours of endurance tests performed in the VIPER high temperature loop on PLUS7 and Guardian fuel to confirm that cross flow-induced vibration did not produce grid to rod fretting failure. Additional pool side examinations confirmed that there has been no fuel rod fretting failure of PLUS7 fuel since its introduction in 2002. The staff reviewed the provided testing and pool side examination information and concludes that the applicant has adequately demonstrated that PLUS7 fuel cladding will not experience fretting wear-induced failures due to fuel rod vibration caused by cross-flow.

Based on the above staff evaluations, the staff finds that the applicant adequately demonstrated that PLUS7 fuel meets the hydraulic stability criteria and is, therefore, acceptable.

4.1.1.4 Shipping and Handling Loads

The staff has reviewed the fuel assembly structural integrity design basis, criteria, and evaluation as presented in Section 2.2.2.4 of APR1400-F-M-TR-13001, Revision 1. The staff's review is summarized below:

Basis

In Section 2.2.2.4 of APR1400-F-M-TR-13001, Revision 1, the applicant stated, "[t]he fuel assembly shall withstand loads encountered during normal shipping and handling conditions."

There are no rules or regulations regarding shipping loads as covered by the guidance provided in SRP Section 4.2. However, this basis is consistent with SRP Section 4.2 regarding fuel failure. Therefore, the staff finds this basis to be acceptable.

Criteria

In Section 2.2.2.4 of APR1400-F-M-TR-13001, Revision 1, the applicant defined the applicable criteria as: (1) the fuel assembly shall meet the stress criteria of normal operation with an axial

load of 4g acceleration and a lateral load of 6g acceleration that may occur during shipping and (2) the fuel assembly shall meet the stress criteria of normal operation with the maximum load of 4g acceleration that may occur during handling.

SRP Section 4.2 does not specify that stress criteria must be met at a specific acceleration, only that the stress criteria must be met. Therefore, the staff does not make a finding regarding the 4g and 6g acceleration criteria, but does find the underlying stress criteria to be consistent with SRP Section 4.2 and is, therefore, acceptable.

Evaluation

The applicant provided the results of an evaluation which credits the grid springs to provide initial pre-loads greater than 4g axially and 6g laterally. Additionally, the applicant performed prototype testing to confirm that the grids would not deform under 6g lateral loading. The staff's evaluation of the grid testing is captured in the SER for APR1400 DCD, Section 4.2.

The staff reviewed the prototype testing presented in the TR and finds that the results and analysis demonstrate that the PLUS7 fuel assembly will not be damaged by 4g axial and 6g lateral loads. This analysis and evaluation does not cover the cask nor its ability to limit the loads on the fuel assembly, but instead covers the ability of the PLUS7 fuel assembly to withstand 4g axial and 6g lateral loads. The staff finds that the applicant adequately demonstrated that PLUS7 fuel assemblies can withstand these loads and therefore meets the stress criteria.

4.1.1.5 Mechanical Compatibility

The staff has reviewed the mechanical compatibility design basis, criteria, and evaluation as presented in Section 2.2.2.5 of APR1400-F-M-TR-13001, Revision 1. The applicant's basis for this criterion is that the PLUS7 fuel assembly can be loaded with no interference with reactor internals and maintain mechanical compatibility with core components.

The staff notes that this criterion does not directly correlate to any NRC rules or regulations; however, there would be secondary relationships with other criteria for which the NRC does have clear requirements (e.g. control rod insertability, clad stress, etc.). Therefore, the staff makes no finding specifically regarding this criterion other than to state that the implementation of this criterion by the applicant supports, but does not individually address, the other related criteria. The criteria that do correlate to NRC rules or regulations are evaluated in the appropriate sections of this SER.

4.1.2 Fuel Assembly Components

4.1.2.1 Bottom Nozzle

The staff finds that the bottom nozzle design has been adequately described in the TR such that an evaluation of the proposed methods may be performed. The following sections detail the staff's review of the applicant's basis, criteria, and evaluation used to analyze the bottom nozzle in terms of: (1) providing structural support of the fuel assembly, (2) preventing fuel rod ejection, (3) maintaining compatibility with the lower support structure, and (4) maintaining compatibility with the instrument.

4.1.2.1.1 Structural Support of the Fuel Assembly

Basis

In Section 2.3.1.2 of APR1400-F-M-TR-13001, Revision 1, the applicant stated that, “[t]he bottom nozzle integrity is maintained for lateral and vertical loads from normal, AOOs, postulated accidents, and shipping & handling conditions.”

There are no regulatory requirements regarding shipping loads as covered by the guidance provided in SRP Section 4.2. However, this basis is consistent with the SRP Section 4.2 (1)(A)(i) basis regarding fuel failure. Therefore, the staff finds this basis to be acceptable.

Criteria

In Section 2.3.1.2 of APR1400-F-M-TR-13001, Revision 1, the applicant defined the applicable criterion as, “[t]he bottom nozzle shall withstand lateral and vertical loads without exceeding the stress limits described for the assembly structural integrity discussed in Section 2.2.2.1.”

The staff finds that by complying with the stated criterion, the PLUS7 fuel assembly bottom nozzle would maintain its structural integrity.

Evaluation

The applicant performed a finite element analysis to verify the mechanical integrity of the bottom nozzle for the loads from fuel assembly shipping and handling, normal operation, AOOs, and postulated accidents. This analysis showed that for a conservative estimate of loading there is significant margin to the allowable stress limit.

The staff reviewed the analysis presented in APR1400-F-M-TR-13001, Revision 1, and found that it demonstrates that the PLUS7 bottom nozzle complies with the stated criteria and is, therefore, acceptable.

4.1.2.1.2 Prevention of Fuel Rod Ejection

Basis

In Section 2.3.1.2 of APR1400-F-M-TR-13001, Revision 1, the applicant stated, “[t]he fuel rod shall not be ejected out of fuel assembly [sic].”

Although the SRP does not provide direct guidance regarding fuel rod ejection, the basis presented by the applicant followed the overall guidance provided in SRP Section 4.2 (1)(C) regarding coolability and is, therefore, acceptable.

Criteria

In Section 2.3.1.2 of APR1400-F-M-TR-13001, Revision 1, the applicant defined the applicable criterion as, “[t]he bottom nozzle will be designed so fuel rods are not ejected through the nozzle.”

The staff notes that SRP Section 4.2 does not provide specific guidance regarding the ejection of a fuel rod (as opposed to the guidance provided regarding Rod Control Cluster Assembly (RCCA) ejection), but the proposed criterion does relate to SRP Section 4.2 (1)(C) regarding coolability. Therefore, the staff finds this criterion to be acceptable.

Evaluation

The PLUS7 bottom nozzle is designed to provide an offset in the centerline of the fuel rod array and the nozzle's primary flow hole array to prevent fuel rod ejection.

The staff reviewed the drawings and confirmed that there is no direct path for a fuel pin to fall through. Therefore, the staff finds that this design feature is acceptable to prevent fuel rod ejection.

4.1.2.1.3 Compatibility with the Lower Support Structure

Basis

In Section 2.3.1.2 of APR1400-F-M-TR-13001, Revision 1, the applicant stated, "[t]he bottom nozzle can mate with the lower support structure without interference."

This basis is consistent with the SRP Section 4.2 basis regarding fuel failure. Therefore, the staff finds this basis to be acceptable.

Criteria

In Section 2.3.1.2 of APR1400-F-M-TR-13001, Revision 1, the applicant defined the applicable criterion as, "[t]he bottom nozzle shall be acceptable with the lower internal by mating between the bottom nozzle and the lower support structure."

The staff notes that SRP Section 4.2 does not present specific guidance regarding bottom nozzle mating with the lower support structure, but the proposed criterion is consistent with SRP Section 4.2(1)(A)(v) regarding prevention of dimensional changes which could cause fuel failures. Therefore, the staff finds this criterion to be acceptable.

Evaluation

The applicant evaluated the geometric compatibility using worst case dimensional tolerances and it was demonstrated that there will be no interference.

The staff has reviewed the applicant's evaluation and finds that it demonstrates the PLUS7 fuel assembly complies with this criterion.

4.1.2.1.4 Compatibility with the Instrument

Basis

In Section 2.3.1.2 of APR1400-F-M-TR-13001, Revision 1, the applicant stated, "[p]roper alignment with the in-core instrument will assure reliable function of core monitoring and protection."

This basis is consistent with the SRP Section 4.2 basis regarding fuel failure. Therefore, the staff finds this basis to be acceptable.

Criteria

In Section 2.3.1.2 of APR1400-F-M-TR-13001, Revision 1, the applicant defined the applicable criterion as, “[t]he bottom nozzle shall be dimensionally compatible with the in-core instrument while providing adequate cooling.”

The staff notes that SRP Section 4.2 does not present specific guidance regarding bottom nozzle maintaining alignment with the in-core instrument, but the proposed criterion is consistent with SRP Section 4.2(1)(A)(v) regarding prevention of dimensional changes which could cause fuel failures. Therefore, the staff finds this criterion to be acceptable.

Evaluation

In Section 2.3.1.2 of APR1400-F-M-TR-13001, Revision 1, the applicant described the design of the bottom nozzle that directs the in-core instrument through the bottom nozzle plenum region.

The staff reviewed the design description and the diagram, and the staff finds that the design shows that the bottom nozzle is dimensionally compatible with the in-core instrument while providing adequate cooling and complies with this criterion. Therefore, the staff finds this criterion to be acceptable.

4.1.2.2 Top Nozzle

The applicant provided a description of the top nozzle and associated figures in Section 2.3.2 of APR1400-F-M-TR-13001, Revision 1. The staff finds that the top nozzle design has been adequately defined in the TR such that an analysis of the proposed methods may be performed.

The applicant identified five areas where analysis should be performed to ensure that the top nozzle meets its design requirements. The staff’s review of these areas is presented below.

4.1.2.2.1 Structural Support of the Fuel Assembly

Basis

In Section 2.3.2.2 of APR1400-F-M-TR-13001, Revision 1, the applicant stated, “[t]he top nozzle integrity is maintained for lateral and vertical loads from normal, AOOs, postulated accidents, and shipping & handling conditions.”

There are no regulatory requirements regarding shipping loads as covered by the guidance provided in SRP Section 4.2. However, this basis is consistent with the SRP Section 4.2 basis regarding fuel failure. Therefore, the staff finds this basis to be acceptable.

Criteria

In Section 2.3.2.2 of APR1400-F-M-TR-13001, Revision 1, the applicant defined the applicable criterion as, “[t]he top nozzle shall withstand lateral and vertical loads without exceeding the stress limits of Section 2.2.2.1”.

The staff notes that SRP Section 4.2 does not present specific guidance regarding top nozzle structural integrity, but the proposed criterion is consistent with SRP Section 4.2(1)(A)(i) regarding stress, strain, and load limits for fuel assembly components in order to prevent fuel failures. Therefore, the staff finds this criterion to be acceptable.

Evaluation

The applicant performed a finite element analysis to verify the mechanical integrity of the bottom nozzle for the loads from fuel assembly shipping and handling, normal operation, AOOs, and postulated accidents. This analysis showed that for a conservative estimate of loading there is greater than 60 percent margin to the allowable stress limit.

There are no regulatory requirements regarding shipping loads as covered by the guidance provided in SRP Section 4.2. However, the staff reviewed the evaluation presented in the TR and finds that the basis, criterion, and analysis provided demonstrate that the bottom nozzle design complies with stress limits regarding the fuel failure criterion for normal operation, AOOs, and postulated accidents.

4.1.2.2.2 Prevention of Fuel Rod Ejection

Basis

In Section 2.3.2.2 of APR1400-F-M-TR-13001, Revision 1, the applicant stated, “[t]he fuel rod shall not be ejected out of the fuel assembly.”

Although the SRP does not provide direct guidance regarding fuel rod ejection, the basis presented by the applicant followed the overall guidance provided in SRP Section 4.2 (1)(C) regarding coolability and is, therefore, acceptable.

Criteria

In Section 2.3.2.2 of APR1400-F-M-TR-13001, Revision 1, the applicant defined the applicable criterion as, “[t]he top nozzle shall be designed fuel rods not to be ejected through the nozzle [sic].”

The staff notes that SRP Section 4.2 does not provide specific guidance regarding the ejection of a fuel rod (as opposed to the guidance provided by RCCA ejection), but the proposed criterion does relate to SRP Section 4.2 (1)(C) regarding coolability. Therefore, the staff finds this criterion to be acceptable.

Evaluation

The applicant stated that the top nozzle is designed to provide ligaments that are oriented above the fuel rod centerlines to prevent fuel rod ejection and flow holes that are offset laterally from the fuel rod horizontal position.

The staff reviewed the drawings and confirmed that there is no direct path for a fuel pin to fall through. Therefore, the staff finds that this design feature is acceptable to prevent fuel rod ejection.

4.1.2.2.3 Compatibility with the Upper Guide Structure

Basis

In Section 2.3.2.2 of APR1400-F-M-TR-13001, Revision 1, the applicant stated that, “[t]he top nozzle can mate with the upper guide structure without interference.”

This basis is consistent with the SRP Section 4.2 basis regarding fuel failure. Therefore, the staff finds this basis to be acceptable.

Criteria

In Section 2.3.2.2 of APR1400-F-M-TR-13001, Revision 1, the applicant defined the applicable criterion as, “[t]he top nozzle shall be acceptable with the upper internal by mating between the top nozzle and the upper guide structure.”

The staff notes that SRP Section 4.2 does not present specific guidance regarding top nozzle mating with the upper guide structure, but the proposed criterion is consistent with SRP Section 4.2(1)(A)(v), regarding prevention of dimensional changes which could cause fuel failures. Therefore, the staff finds this criterion to be acceptable.

Evaluation

The applicant evaluated the geometric compatibility using worst case dimensional tolerances and concluded that there is no interference.

The staff has reviewed the applicant’s evaluation and finds that it demonstrates the PLUS7 fuel assembly complies with this criterion because the evaluation confirms that the top nozzle and guide structure would mate without causing interference. Therefore, the staff finds this to be acceptable.

4.1.2.2.4 Remote Reconstitutability

In Section 2.3.2.2 of APR1400-F-M-TR-13001, Revision 1, the applicant provided a criterion regarding remote reconstitutability of the fuel assembly. There is no guidance in SRP Section 4.2 regarding remote reconstitutability and it does not directly tie to any regulations listed in SRP Section 4.2. Therefore, the staff makes no findings regarding this criterion and did not perform an evaluation other than to note that it does not directly conflict with any NRC regulations.

4.1.2.2.5 Compatibility with Handling Equipment

There is no guidance in SRP Section 4.2 regarding compatibility with handling equipment and it does not directly tie to any regulations listed in SRP Section 4.2. Therefore, the staff makes no findings regarding this criterion and did not perform an evaluation other than to note that it does not directly conflict with any NRC regulations.

4.1.2.3 Holddown Spring

In Section 2.3.3 and Figure 2-13 of APR1400-F-M-TR-13001, Revision 1, the applicant presented a description of the holddown spring. The staff finds that the holddown spring design has been adequately defined in the TR such that an analysis of the proposed methods may be performed.

The applicant identified three areas where analysis should be performed to ensure that the holddown spring meets its design requirements. The staff’s review of these areas is presented below.

4.1.2.3.1 Holddown Force in Normal Operation

Basis

In Section 2.3.3.2 of APR1400-F-M-TR-13001, Revision 1, the applicant stated that, “[f]uel assembly lift-off during normal operating conditions can result in fuel assembly or core support structural damage. If lift-off occurs during normal operation, large amplitude fuel assembly oscillations could ensue. These oscillations can cause impact forces on the core structures and fuel assembly.”

This basis is consistent with the SRP Section 4.2 basis regarding fuel failure. Therefore, the staff finds this basis to be acceptable.

Criteria

In Section 2.3.3.2 of APR1400-F-M-TR-13001, Revision 1, the applicant defined the applicable criterion as, “[t]he fuel assembly shall not lift-off the core support structure during the normal operation.”

The staff notes that this criterion is the same criterion used in Section 2.2.2.3 of APR1400-F-M-TR-13001, Revision 1. The criterion is also consistent with the guidance in SRP Section 4.2 (1)(A)(vii). Therefore, the staff finds this criterion to be acceptable.

Evaluation

The applicant presented results from prototype testing and operating experience in order to evaluate the PLUS7 fuel assembly against this criterion. The testing results presented in Section A.2.9 of APR1400-F-M-TR-13001, Revision 1, demonstrate that the lift force for the PLUS7 assembly in the APR1400 reactor design would not result in assembly liftoff. The staff reviewed the information provided and finds that the applicant adequately demonstrated that the PLUS7 fuel assembly will not become unseated during normal operation, and therefore complies with this criterion. Therefore, the staff finds this to be acceptable.

4.1.2.3.2 Maximum Deflection Range and Solid Condition

Basis

In Section 2.3.3.2 of APR1400-F-M-TR-13001, Revision 1, the applicant stated that, “[l]oad of solid spring may cause improper load distribution through the top nozzle, and may have an adverse effect on the spring itself. The load of solid spring on the fuel assembly can cause extensive structural damage and subsequent fuel failure.”

The staff finds that this basis is consistent with the guidance provided in SRP Section 4.2 regarding fuel failure. Therefore, the staff finds this basis to be acceptable.

Criteria

In Section 2.3.2.2 of APR1400-F-M-TR-13001, Revision 1, the applicant defined the applicable criterion as, “[t]he clearance between the holddown working height and spring solid height shall be maintained under normal operation.”

This criterion follows the guidelines in SRP Section 4.2 (1)(A)(v). Therefore, the staff finds this criterion to be acceptable.

Evaluation

The applicant stated that the holddown working height was calculated based on the maximum fuel assembly growth. This working height was compared to the solid spring height to ensure margin between these values.

The staff reviewed the method used to calculate the holddown working height and solid spring height and finds that the applicant demonstrated that the PLUS7 top nozzle spring does not go solid under normal operation. Therefore, the staff finds this to be acceptable.

4.1.2.3.3 Holddown Spring Shear Stress

Basis

In Section 2.3.3.2 of APR1400-F-M-TR-13001, Revision 1, the applicant stated that, “[t]he spring shear stress shall meet the ASME Boiler and Pressure Vessel Code.”

The staff finds that this basis is consistent with the guidance provided in SRP Section 4.2 regarding fuel failure. Therefore, the staff finds this basis to be acceptable.

Criteria

In Section 2.3.3.2 of APR1400-F-M-TR-13001, Revision 1, the applicant defined the applicable criterion as, “[t]he spring shear stress for normal operation except lift-off shall be less than 0.8 S_m .”

This criterion for spring shear stress is consistent with ASME B&PV Code Section III, NB-3227.2, specifically the second part which specifies that the maximum primary shear stress at the periphery of a solid circular section in torsion shall be limited to 0.8 S_m .

Additionally, the criterion includes the words “normal operation except lift-off.” Assembly lift-off is precluded by the design of the spring as discussed in Section 4.1.1.3 of this SER.

The staff finds that this criterion is consistent with the guidance provided in SRP Section 4.2 (1)(A)(i). Therefore, the staff finds this criterion to be acceptable.

Evaluation

The applicant provided the results of a design calculation that demonstrate margin to the shear stress limit. The staff reviewed the results and finds that the applicant demonstrated that the PLUS7 fuel assembly complies with this criterion. Therefore, the staff finds this to be acceptable.

4.1.2.4 Guide Thimble and Instrument Tube

In Section 2.3.4, Figure 2-1, and Figure 2-17 of APR1400-F-M-TR-13001, Revision 1, the applicant presented a description of the guide thimbles and instrument tube. The staff finds that the guide thimble and instrument tube spring design has been adequately defined in the TR such that an analysis of the proposed methods may be performed.

The applicant identified two areas where analysis should be performed to ensure that the guide thimbles and instrument tube meet their design requirements. The staff concurs that these two

areas are appropriate to analyze the guide thimbles and instrument tubes, and the staff's review of these areas is presented below.

4.1.2.4.1 Structural Support of the Fuel Assembly

Basis

In Section 2.3.4.2 of APR1400-F-M-TR-13001, Revision 1, the applicant stated that, "[t]he guide thimble maintains its structural integrity for lateral and vertical loads from normal, AOOs, and shipping and handling conditions."

The staff's review, based on the guidance provided in SRP Section 4.2, does not cover shipping and handling loads. However, the staff finds that the basis is consistent with the guidance in SRP Section 4.2 regarding fuel failure. Therefore, the staff finds this basis to be acceptable for supporting the fuel failure requirements.

Criteria

In Section 2.3.4.2 of APR1400-F-M-TR-13001, Revision 1, the applicant stated that the criterion is the same as the structural design criteria of the fuel assembly described in Section 2.2.2.1 of APR1400-F-M-TR-13001, Revision 1 for the fuel assembly. These criteria follow the guidance of Section III of the B&PV Code of ASME. For ease of use, these criteria are repeated below.

For normal conditions:

$$P_m \leq S_m$$

$$P_m + P_b \leq 1.5 S_m$$

For accident conditions:

$$P_m \leq S_m'$$

$$P_m + P_b \leq 1.5 S_m'$$

Additionally, the methodology described by the applicant used normal operation and AOO stress limit criteria even under postulated accident conditions in order to preclude plastic deformation for components important to CEA insertion.

These criterion are consistent with SRP Section 4.2, Appendix A. Therefore, the staff finds these criterion to be acceptable.

Evaluation

The applicant provided the results of a design calculation of the guide thimble tube during shipping and handling. The applicant concluded that the shipping and handling loads are greater than the loads during normal operation and AOO. Additionally, the applicant stated that the circumferential stress acting on the guide thimble tube from the pressure difference between inner and outer guide thimble tube around the dashpot region was evaluated to satisfy the stress design limit and that, conservatively assuming that the CEA drop occurs once a day, the guide thimble tube stress was calculated to be so small that the fatigue-induced guide thimble tube failure does not occur.

The staff reviewed the analyses and results presented by the applicant and, for the reasons stated above, finds that the applicant demonstrated that the PLUS7 fuel assembly complies with the stated criteria. As stated in the Basis section, there are no regulatory requirements regarding shipping loads as covered by the guidance provided in SRP Section 4.2. However, the basis, criterion, and analysis provided do demonstrate compliance with stress limits regarding the fuel failure criterion. Therefore, the staff finds this to be acceptable.

4.1.2.4.2 CEA Drop Time

Basis

In Section 2.3.4.2 of APR1400-F-M-TR-13001, Revision 1, the applicant stated that, “[p]lant reactivity control systems must be capable of reducing power within a maximum specified time to preclude fuel damage.”

The staff finds that the basis is consistent with the guidance in SRP Section 4.2 regarding fuel failure. Therefore, the staff finds this basis to be acceptable.

Criteria

In Section 2.3.4.2 of APR1400-F-M-TR-13001, Revision 1, the applicant defined the applicable criterion as, “[t]he geometrical shape of the guide thimble tube shall meet the control rod drop time limit.”

The staff has reviewed the information provided and notes that this criterion is consistent with the guidance provided in SRP Section 4.2 (1)(A)(vii) regarding control rod insertability. Therefore, the staff finds this criterion to be acceptable. The staff notes that this criterion is specific to the design of the guide tubes and not the actual drop time analysis itself which is covered in Chapter 4 of the staff’s SER for the APR1400 DCD.

Evaluation

As stated in the Basis section above, the staff notes that CEA drop times are analyzed as part of the APR1400 DCD, Chapter 4 review. Therefore, the staff makes no specific finding here.

4.1.2.5 Grid

In Section 2.3.5.1 of APR1400-F-M-13001-P, Revision 1, Figures 2-3, 2-4, 2-5, 2-6, 2-19, 2-20, and 2-21, the applicant presented a description of the PLUS7 grids (top grids, bottom grids, protective grids, and mixing vane mid grids). The staff finds that the grid designs have been adequately defined in the TR such that an analysis of the proposed methods may be performed.

The applicant identified six areas where analysis should be performed to ensure that the grids meet their design requirements. The staff finds that these six areas cover the failure mechanisms identified in SRP Section 4.2 regarding fuel system damage. The staff’s review of these areas is presented below.

4.1.2.5.1 Fuel Rod Support

Basis

In Section 2.3.5.2 of APR1400-F-M-TR-13001, Revision 1, the applicant stated that, “[t]he grid shall support the fuel rod axially and laterally.”

The staff finds that the basis is consistent with the guidance in SRP Section 4.2 regarding fuel failure. Therefore, the staff finds this basis to be acceptable.

Criteria

In Section 2.3.5.2 of APR1400-F-M-TR-13001, Revision 1, the applicant defined the applicable criterion as, “[t]he positive spring force of the bottom grid shall be maintained up to EOL.” The applicant provided an additional design criterion regarding the minimum spring force for the PLUS7 bottom grid.

The staff has reviewed the information provided and notes that this criterion is consistent with the guidance provided in SRP Section 4.2 (1)(A)(1) regarding loading limits. Therefore, the staff finds this criterion to be acceptable.

Evaluation

In Section 2.3.5.2 of APR1400-F-M-TR-13001, Revision 1, the applicant described an evaluation of the bottom grid spring forces of the PLUS7 fuel and shows that the spring force is larger than the minimum spring force criterion at EOL.

The staff has reviewed this information and finds that this evaluation demonstrates that the PLUS7 bottom grid design meets this criterion. Therefore, the staff finds this to be acceptable.

4.1.2.5.2 Shipping and Handling

Basis

In Section 2.3.5.2 of APR1400-F-M-TR-13001, Revision 1, the applicant stated that, “[t]he fuel should be designed to withstand shipping and handling loads without damage.”

There are no specific regulatory requirements regarding shipping loads in Title 10 of the *Code of Federal Regulations* (10 CFR), Part 52, “Licenses, Certifications, and Approvals for Nuclear Power Plants,” for the fuel system design, as found in the guidance provided by SRP Section 4.2. However, the inclusion of this criteria does not interfere with regulatory requirements. Therefore, the staff finds this basis to be acceptable, but not necessary in order to support the fuel system design regulatory requirements.

Criteria

In Section 2.3.5.2 of APR1400-F-M-TR-13001, Revision 1, the applicant stated that, “[t]he grid shall withstand 4g axial and 6g lateral accelerations without allowing the fuel rods to shift or the grid to permanently deform during the shipping and handling.”

As already noted, there are no regulatory requirements regarding shipping and handling loads within the guidance provided in SRP Section 4.2. However, the use of 4g axial and 6g lateral acceleration limits does not conflict with staff guidance regarding loading limits provided in SRP Section 4.2 (1)(A)(i). Therefore, the staff finds this criterion to be acceptable.

Evaluation

The applicant performed an evaluation to ensure that the friction loads associated with the spring force on the grids is greater than an axial load of 4g and the grid spring force is greater than a lateral load of 6g.

Additionally, the applicant performed grid buckling tests to demonstrate that the buckling strength of the grids is greater than a lateral load of 6g.

As already noted, the staff has no regulations or guidance regarding shipping loads within 10 CFR Part 52 or SRP Section 4.2 in terms of the fuel system design. Therefore, the staff makes no specific regulatory finding regarding this criterion.

4.1.2.5.3 Fuel Rod Fretting Wear

Basis

In Section 2.3.5.2 of APR1400-F-M-TR-13001, Revision 1, the applicant stated, “[t]he fuel rods should not fail due to the grid-to-rod fretting wear caused by the fuel assembly-induced or the fuel rod-induced vibration during normal operation.”

The staff has reviewed the information provided and notes that this criterion is consistent with the guidance provided in SRP Section 4.2 regarding loading limits and fuel failure. Therefore, the staff finds this basis to be acceptable.

Criteria

In Section 2.3.5.2 of APR1400-F-M-TR-13001, Revision 1, the applicant stated, “[t]he fuel rod should not fail due to fretting wear during fuel lifetime.”

The staff has reviewed the information provided and notes that this criterion is consistent with the guidance provided in SRP Section 4.2 (1)(A)(iii) regarding fuel rod fretting. Therefore, the staff finds this criterion to be acceptable.

Evaluation

The applicant used prototype testing and operating experience to evaluate the PLUS7 fuel assembly against this criterion. The applicant stated that fluid-induced assembly vibration tests have been performed to confirm that the symmetric arrangement of the PLUS7 grid mixing vanes will cause very little fluid-induced vibration. Furthermore, 500-hour wear resistance tests show that the PLUS7 fuel will not generate fretting wear-induced fuel failure for the fuel lifetime. Finally, operating experience demonstrates that the PLUS7 fuel assembly has not shown any fretting wear failure for the fuel lifetime.

The staff has reviewed the test descriptions and results presented in Section 2.3.5.2 and Appendices A.2.2 and D of APR1400-F-M-TR-13001 Revision 1. The staff finds that Figure 2-10 demonstrates that for the range of flow rates for APR1400, the maximum vibrational amplitude remains small and would not lead to hydraulic instabilities. Additionally, the long-term fretting wear test results from Appendix A.2.2 demonstrate that no measurable fretting wear occurs on oxidized rods and that the fretting wear on non-oxidized rods meets KHNP’s internal criterion. Appendix D shows through extrapolation and use of a conservative failure criterion, a non-oxidized rod would not experience failure for the PLUS7 fuel assembly in an APR1400 plant design. Based on these tests results and analyses, the staff finds that the applicant demonstrated that the PLUS7 fuel assembly will not experience fuel rod fretting wear failure over the lifetime of the fuel. Therefore, the staff finds this to be acceptable.

4.1.2.5.4 Fuel Rod Bow

Basis

In Section 2.3.5.2 of APR1400-F-M-TR-13001, Revision 1, the applicant stated that, "...the grids shall accommodate the fuel rod length change caused by the thermal expansion and neutron irradiation growth without inducing unacceptable fuel rod bow."

The staff has reviewed the information provided and notes that this criterion is consistent with the guidance provided in SRP Section 4.2 regarding rod bowing and fuel failure. Therefore, the staff finds this basis to be acceptable.

Criteria

In Section 2.3.5.2 of APR1400-F-M-TR-13001, Revision 1, the applicant stated, "[t]he grid shall not permit or cause rod bowing that exceeds the allowable limits for channel closure for the fuel assembly lifetime."

The staff has reviewed the information provided and notes that this criterion is consistent with the guidance provided in SRP Section 4.2(1)(A)(v) regarding fuel rod bowing. Therefore, the staff finds this criterion to be acceptable.

Evaluation

The applicant performed an evaluation to determine if a departure from nucleate boiling ratio (DNBR) penalty is needed for the PLUS7 fuel design based on the expected reduction in fuel channel spacing due to rod bow. The applicant provided results of in-reactor tests to conclude that the PLUS7 rod bow is less than the limit, therefore no penalty is needed to ensure that the rod bow criterion is met.

The staff reviewed the test results used by the applicant to evaluate rod bow and finds that the applicant demonstrated that the PLUS7 fuel assembly design complies with this criterion.

4.1.2.5.5 Mid Grid Buckling Strength

Basis

In Section 2.3.5.2 of APR1400-F-M-TR-13001, Revision 1, the applicant stated that, "[c]ore coolability and safe shutdown of the reactor should be maintained under the most limiting load on the mid grid assembly."

The staff has reviewed the information provided and notes that this criterion is consistent with the guidance provided in SRP Section 4.2, Appendix A, regarding fuel assembly structural response to externally applied forces. Therefore, the staff finds this basis to be acceptable.

Criteria

In Section 2.3.5.2 of APR1400-F-M-TR-13001, Revision 1, the applicant stated, "[t]he grids must provide a coolable geometry and allow the control rod insertion for the postulated accidents, such as seismic and LOCA."

The staff has reviewed the information provided and notes that this criteria is consistent with the guidance provided in SRP Section 4.2, Appendix A, regarding determination of strength for grids. Therefore, the staff finds this criteria to be acceptable.

Evaluation

The applicant used an NRC-approved CE methodology to perform grid strength evaluation. Grid buckling strength was determined from dynamic impact testing for comparison with predicted grid impact force. The details of this analysis are contained in Technical Report APR1400-Z-M-NR-14010-P, Revision 2, and the staff's review is contained in the SER for APR1400 DCD Section 4.2.

4.1.2.5.6 Grid Width

Basis

In Section 2.3.5.2 of APR1400-F-M-TR-13001, Revision 1, the applicant stated that, "[t]he grid width will grow due to neutron irradiation as the fuel burnup increases. This grid irradiation growth should not affect the fuel loading and unloading operation in the reactor core."

The staff has reviewed the information provided and notes that this criterion is consistent with the guidance provided in SRP Section 4.2 regarding rod bowing and fuel failure. Therefore, the staff finds this basis to be acceptable.

Criteria

In Section 2.3.5.2 of APR1400-F-M-TR-13001, Revision 1, the applicant stated, "[a]n adequate space between the fuel assemblies should be maintained to load and unload the fuel assembly safely for the fuel lifetime."

The staff notes that SRP Section 4.2 does not provide specific guidance regarding irradiation induced grid width growth, but this criterion generally supports the guidance provided in SRP Section 4.2 (1)(A)(v) regarding dimensional changes. Therefore, the staff finds this criterion to be acceptable.

Evaluation

The applicant's evaluation referred to poolside examination of PLUS7 fuel to confirm that there is adequate space between the fuel assemblies after the three cycle irradiation. The applicant also credited the designs of the grid guide tab, grid guide vane, and grid corner shape of PLUS7 fuel as being based on the previous designs used successfully in commercial nuclear power plants.

The staff has reviewed the applicant's evaluation and finds that fuel assemblies at EOL conditions will not experience growth to an extent which would allow neighboring fuel assemblies to interfere with each other. The staff finds that the PLUS7 fuel assembly design meets this criterion. Therefore, the staff finds this to be acceptable.

4.1.2.6 Joint and Connection

Five joint and connections are identified for the PLUS7 fuel assembly. These include; top nozzle/guide thimble, top grid/guide thimble/instrument tube, mid grid/guide thimble/instrument

tube, bottom grid/guide thimble/instrument tube, and bottom muzzle/protective grid/guide thimble. These joints and connections have been adequately defined in the TR such that an analysis of the proposed methods may be performed.

In Section 2.3.6.1 of APR1400-F-M-TR-13001, Revision 1, and Figures 2-22, 2-23, and 2-25, the applicant presented a description of the PLUS7 fuel assembly joints and connections. The staff finds that the joints and connections have been adequately defined in the TR such that an analysis of the proposed methods and analysis can be performed.

The applicant identified five areas where analysis should be performed to ensure that the joints and connections meet their design requirements. The staff agrees that these five analysis areas are sufficient to demonstrate compliance. The staff's review of these areas is presented below.

4.1.2.6.1 Top Nozzle/Guide Thimble

Basis

In Section 2.3.6.2 of APR1400-F-M-TR-13001, Revision 1, the applicant stated, "[t]he top nozzle/guide thimble joint and connections shall not be damaged under the loads of normal operation and AOOs."

The staff has reviewed the information provided and notes that this criterion is consistent with the guidance provided in SRP Section 4.2 regarding stress, strain, and loading limits which can lead to fuel failure. Therefore, the staff finds this basis to be acceptable.

Criteria

In Section 2.3.6.2 of APR1400-F-M-TR-13001, Revision 1, the applicant stated:

Under the loads of normal operation and AOOs, the top nozzle/guide thimble joint and connections shall not be damaged and must meet the following design criteria:

$$P_m \leq \text{a smaller value of } 0.9 S_y \text{ and } 2/3 S_u$$

$$\tau \leq 0.6 S_y$$

Where,

P_m = calculated primary membrane stress

τ = calculated primary shear stress

S_u = minimum ultimate tensile strength at unirradiated condition

S_y = minimum yield tensile strength at unirradiated condition

The staff has reviewed the information provided and notes that this criterion is consistent with ASME Section III, Division 1, Subsection NG-3232.1 for threaded structural fasteners. Therefore, the staff finds this criterion to be acceptable.

Evaluation

The applicant provided results from a design calculation which demonstrate that the stress limits will not be exceeded. The staff has reviewed the applicant's evaluation and finds that the PLUS7 fuel assembly meets this criterion. Therefore, the staff finds this to be acceptable.

4.1.2.6.2 Grid/Guide Thimble/Instrument Tube

Basis

In Section 2.3.6.2 of APR1400-F-M-TR-13001, Revision 1, the applicant stated that, "[d]imensional stability of the fuel assembly must be maintained under operating, shipping, and handling conditions. The joint must remain intact under operating, shipping, and handling conditions. Since the spot-welds are not expected to yield significantly before failure, the design limits are based on failure loads."

There are no regulatory requirements regarding shipping loads as covered by the guidance provided in SRP Section 4.2. However, this basis is consistent with the SRP Section 4.2 basis regarding stress, strain, and loading limits which can lead to fuel failure. Therefore, the staff finds this basis to be acceptable.

Criteria

In Section 2.3.6.2 of APR1400-F-M-TR-13001, Revision 1, the applicant stated, "[u]nder the loads of normal operations and AOOs, the grid/guide thimble/instrument tube joint and connections shall not be damaged."

The staff has reviewed the information provided and notes that this criterion is consistent with the guidance provided in SRP Section 4.2 (1)(A)(1) regarding loading limits. Therefore, the staff finds this criterion to be acceptable.

Evaluation

The applicant stated that the largest load acting on the grid/guide thimble welding point is a slip load at the fuel rod/grid interface caused by the difference in their thermal expansion. The applicant stated that it calculated this stress and that it was evaluated to be far less than the weld strength of the grid/guide thimble connection measured by test.

The staff reviewed this evaluation and found that it is acceptable in identifying the largest load and in calculating the stress due to this load and demonstrates that the PLUS7 fuel assembly complies with this criterion. The staff finds this to be acceptable.

4.1.3.2.3 Bottom Nozzle/Guide Thimble

Basis

In Section 2.3.6.2 of APR1400-F-M-TR-13001, Revision 1, the applicant stated that, "[f]uel assembly dimensional stability must be maintained under shipping, handling, operating, and accident conditions. The lifting force requirement ensures that the joint can withstand the maximum possible force exerted on the fuel assembly by the fuel handling equipment during removal from the core."

The staff has reviewed the information provided and notes that this criterion is consistent with the guidance provided in SRP Section 4.2 regarding stress, strain, and loading limits which can lead to fuel failure. Therefore, the staff finds this basis to be acceptable.

Criteria

In Section 2.3.6.2 of APR1400-F-M-TR-13001, Revision 1, the applicant stated:

Under the loads of normal operation and AOOs, the top nozzle/guide thimble joint and connections shall not be damaged and must meet the following design criteria:

$$P_m \leq \text{a smaller value of } 0.9 S_y \text{ and } 2/3 S_u$$

$$\tau \leq 0.6 S_y$$

Where,

P_m = calculated primary membrane stress

τ = calculated primary shear stress

S_u = minimum ultimate tensile strength at unirradiated condition

S_y = minimum yield tensile strength at unirradiated condition

There are no regulatory requirements regarding shipping loads as covered by the guidance provided in SRP Section 4.2. However, this basis is consistent with the SRP Section 4.2 basis regarding fuel failure for normal operation and AOOs. The staff has reviewed the information provided and notes that this criterion is consistent with ASME Section III, Division 1, Subsection NG-3232.1 for threaded structural fasteners. Therefore, the staff finds this criterion to be acceptable.

Evaluation

The applicant provided results from a design calculation which demonstrate that the stress limits will not be exceeded. The staff reviewed the applicant's evaluation and finds that the PLUS7 fuel assembly meets this criterion. Therefore, the staff finds this to be acceptable.

4.2 Fuel Rod Design

In Section 3 of APR1400-F-M-TR-13001, Revision 1, the applicant described the 16 identified design bases that have been identified for the thermal-mechanical performance of PLUS7 fuel. For each of these design bases, the applicant described the criteria and evaluation used to show that the PLUS7 fuel would meet these bases. The following sections describe the staff's review of the acceptability of each of these design bases, criteria, and evaluations for thermal-mechanical performance of PLUS7 fuel.

4.2.1 Fuel Design Bases, Criteria, and Evaluation

The staff has reviewed the information provided by the applicant in the TR and finds that the fuel rod design has been adequately defined such that an analysis of the proposed methods can be performed.

Typically, an applicant requests that a methodology for showing compliance with the fuel rod design bases on a cycle-specific basis be reviewed and approved. In Revision 1 of APR1400-F-M-TR-13001, the applicant did not present a specific methodology to perform these analyses on a cycle-specific basis, but rather showed that within a given operating envelope, the design bases will be met. The operating window that has been requested by the applicant is as follows:

- Linear Heat rate specified acceptable fuel design limit (SAFDL) of [] for normal operation and AOO.
- Radial fall-off shown in Figure 1 for UO_2 and $\text{Gd}_2\text{O}_3\text{-UO}_2$ fuel rods where powers are normalized to [].
- Maximum radial peaking factor of [].
- Maximum fuel rod average burnup of 60 GWD/MTU (Gigawatt-days per metric ton of uranium).

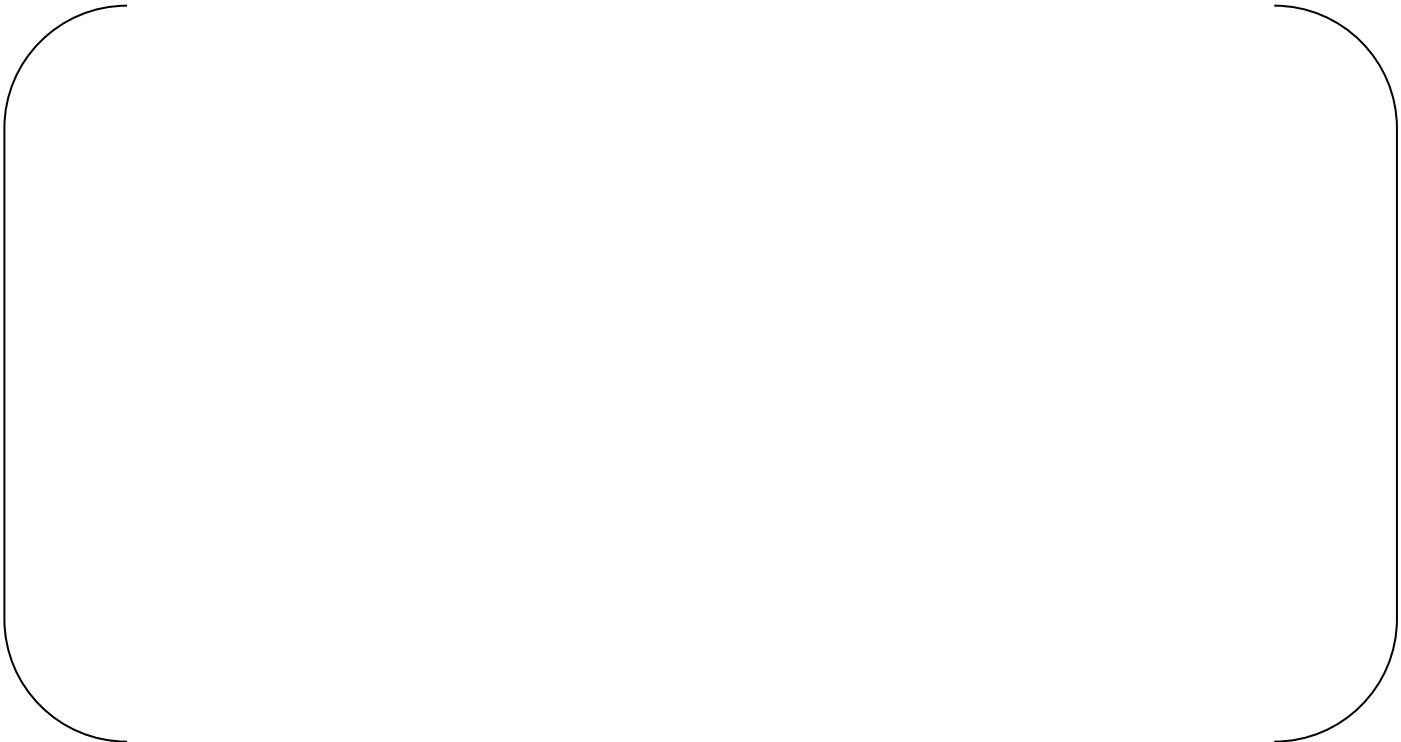


Figure 1: Rod Power History Used for PLUS7 Fuel Rod Performance Analysis (powers normalized to [])

The primary code that the applicant used to calculate fuel performance parameters is FATES3B. This code was developed in the 1970s and 1980s and does not include the effect of burnup on fuel thermal conductivity and therefore will under predict fuel rod temperatures with increasing burnup. The applicant has determined that some fuel rod criteria will not be impacted by the lack of burnup dependent fuel TCD such as cladding corrosion and hydrogen pickup, cladding collapse, and fuel rod growth. In these cases, FATES3B and the associated methods may be used to demonstrate compliance with the design bases. However, other

criteria such as cladding stress, cladding strain, cladding fatigue, rod internal pressure, and overheating of fuel pellets are affected by TCD. In these cases, an alternative code and/or method will be used to demonstrate compliance within the requested operational window. The applicant presented the results of the burnup dependent TCD analysis in Section 3.4 of APR1400-F-M-TR-13001, Revision 1, with results that sometimes supersede analyses without TCD earlier in the TR. For clarity, the staff's safety evaluation will include the analysis of the effects of TCD directly in the evaluations of cladding stress, cladding strain, cladding fatigue, rod internal pressure, and overheating of the fuel pellets, instead of handling TCD separately.

4.2.1.1 Cladding Stress

Basis

In Section 3.2.1 of APR1400-F-M-TR-13001, Revision 1, the applicant stated that, "[a] fuel system will not be damaged due to excessive stress under normal operation including AOOs."

The staff has reviewed the information provided and notes that this criterion is consistent with the guidance provided in SRP Section 4.2 regarding stress, strain, and loading limits which can lead to fuel failure. Therefore, the staff finds this basis to be acceptable.

Criteria

In Section 3.2.1 of APR1400-F-M-TR-13001, Revision 1, the applicant provided two criteria by which to evaluate cladding stress:

During normal operation and AOOs, primary tensile stress in the clad and the end cap welds must not exceed [] at the applicable temperature.

During Normal operation and AOOs, primary compressive stress in the clad and end cap welds must not exceed [] at the applicable temperature.

The applicant further specified that, "...the unirradiated cladding yield strength is conservatively used as the cladding stress design criterion."

The staff has reviewed the information provided and notes that this criterion is consistent with ASME Section III of the B&PV Code. The staff finds that by following the ASME Section III stress limits, these criteria are consistent with the guidance provided in SRP Section 4.2 (1)(A)(i), and are, therefore, acceptable. Additionally, the staff agrees that the use of unirradiated cladding yield stress is conservative for this analysis. Therefore, the staff finds this criterion to be acceptable.

Evaluation

In Section 3.2.1 of APR1400-F-M-TR-13001, Revision 1, the applicant summarized analyses used to evaluate the PLUS7 fuel design against the clad stress criteria. Design calculations were provided that demonstrate that the primary tensile and compressive stresses in the cladding and end cap welds are within the allowable limits.

Additionally, in Section 3.4.1 of APR1400-F-M-TR-13001, Revision 1, the applicant discussed the impact of burnup dependent TCD on cladding stress. The applicant stated that the cladding

stress analysis is unaffected by TCD since rod internal pressure is also not affected by TCD (per Section 3.4.4 of the TR).

The staff reviewed the statements regarding TCD and agrees that cladding stress would only be affected by TCD if rod internal pressure is affected since it is the primary cause of cladding stress. As detailed in Section 4.2.1.5 of this SER, the staff finds that rod internal pressure is not affected by FATES3B's lack of a burnup dependent TCD model, and therefore, the staff agrees that the analysis methods used by the applicant to evaluate cladding stress remain valid.

The staff reviewed the results of the applicant's cladding stress analysis and finds that the PLUS7 fuel design complies with the clad stress criteria, because the primary tensile and compressive stresses in the cladding and end cap welds are within the allowable limits. The analysis and the staff's finding are based on the operating window as discussed in Section 4.2.1 of this SER.

4.2.1.2 Cladding Strain

Basis

In Section 3.2.2 of APR1400-F-M-TR-13001, Revision 1, the applicant stated that the, "[f]uel system will not be damaged due to excessive strain under normal operation including AOOs."

The staff has reviewed the information provided and notes that this criterion is consistent with the guidance provided in SRP Section 4.2 regarding cladding strain limits which can lead to fuel rod failure. Therefore, the staff finds this basis to be acceptable.

Criteria

In Section 3.2.2 of APR1400-F-M-TR-13001, Revision 1, the applicant provided three criteria by which to evaluate cladding strain: (1) the permanent (plastic) hoop strain will remain below [] relative to beginning of life dimensions, (2) the total change in hoop strain (elastic plus plastic) from a single AOO will remain below [] relative to the pre-transient dimensions, and (3) the applicant stated that they expect ZIRLO to have greater than [] ductility at burnups greater than 60 GWd/MTU.

The staff has reviewed the information provided and notes that this criterion is consistent with the guidance provided in SRP Section 4.2 (1)(B)(vi). Therefore, the staff finds this criterion to be acceptable.

Evaluation

In Section 3.2.1 of APR1400-F-M-TR-13001, Revision 1, the applicant performed an evaluation of hoop strain for normal operation and AOOs using the methodology from the previously approved TR CENPD-404-P-A, "Implementation of ZIRLO Cladding Material in CE Nuclear Power Fuel Assembly Design," (Reference 10).

The staff noted and independently confirmed that TCD (which is not included in FATES3B) has a significant impact on the prediction of total hoop strain and strain increment. The staff issued RAI 7954, Question 18 (ML15169A118), requesting the applicant to provide a sample calculation showing the total strain increment resulting from a typical AOO at 0, 20, 40, and 60 GWd/MTU. The staff performed confirmatory calculations using FRAPCON to compare with KHNP's response (ML17223B382) and are shown in Figure 2. In its response to RAI 7954,

Question 18 (ML17223B382), the applicant showed that the FATES-3B calculation of transient hoop strain is always greater than those calculated using FRAPCON.

As detailed in Section 3.4.2 of the TR, the applicant re-performed these strain calculations to account for burnup dependence using FATES3B with the modified NFI fuel thermal conductivity model from FRAPCON. The staff notes that since FATES3B is not tuned to this model, this should result in an overestimate of cladding strain. The resulting cladding plastic strain was [] and the total (elastic+plastic) strain was [] which still showed margin to the limit of [] strain.

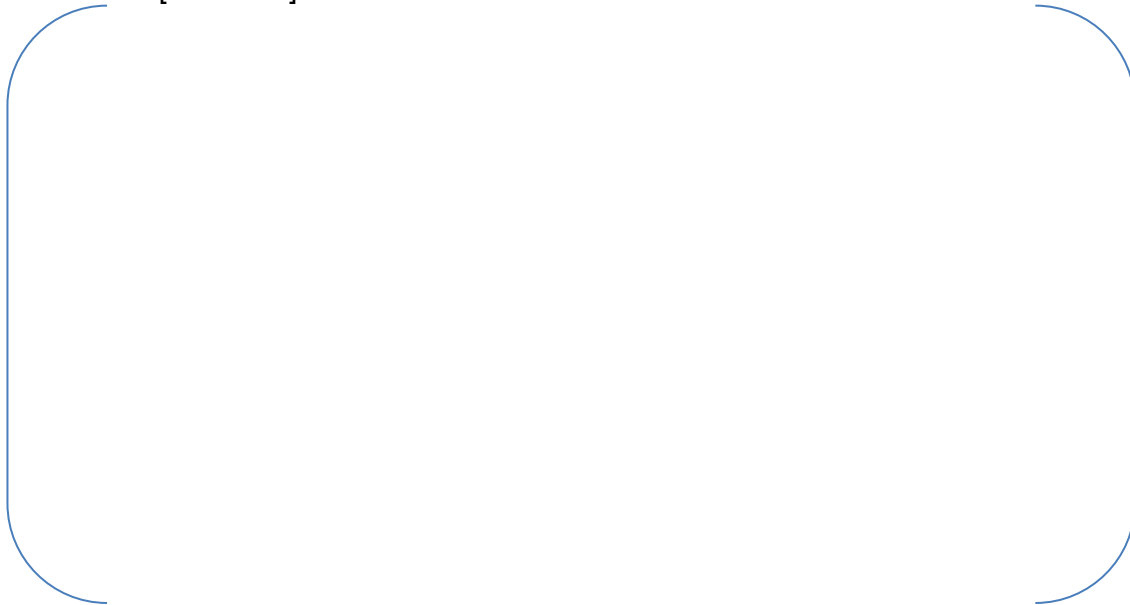


Figure 2: Comparison of the applicant and FRAPCON calculated cladding total hoop strain.

Based on the applicant's revised analysis which accounts for burnup dependent TCD, the staff finds that the PLUS7 fuel assembly meets the strain criteria.

4.2.1.3 Cladding Fatigue

Basis

In Section 3.2.3 of APR1400-F-M-TR-13001, Revision 1, the applicant stated that the, "[f]uel system will not be damaged due to excessive fatigue under normal operation."

The staff has reviewed the information provided and notes that this criterion is consistent with the guidance provided in SRP Section 4.2 regarding loading limits and fuel failure. Therefore, the staff finds this basis to be acceptable.

Criteria

In Section 3.2.3 of APR1400-F-M-TR-13001, Revision 1, the applicant stated, "[f]or the number and type of transients which occur during normal operation, end-of-life (EOL) cumulative fatigue damage in the cladding must be less than []." Additionally, the applicant provided further description of the cladding fatigue criteria by stipulating that the analysis is performed with the Langer-O'Donnell fatigue design curve and a safety factor of 2 on the stress or a safety factor of 20 on the number of cycles is imposed on the curve.

The staff notes that this criterion is conservative as fatigue failure is typically predicted at a fatigue damage fraction of 1.0 and the Langer-O'Donnell fatigue design curve already includes a safety factor of 2 on the stress or a safety factor of 20 on the number of cycles as recommended by SRP Section 4.2 (1)(A)(ii). Therefore, the staff finds this criterion to be acceptable.

Evaluation

In Section 3.2.3 of APR1400-F-M-TR-13001, Revision 1, the applicant presented the results of a fatigue analysis for the PLUS7 fuel assembly.

The staff noted that TCD (which is not included in FATES3B) has a significant impact on the prediction of cumulative fatigue damage fraction. The staff issued RAI 7954, Question 16, requesting the applicant to describe how the fatigue analysis would be performed on a cycle-specific basis given the demonstration that FATES3B without TCD is inadequate to assess the fatigue damage fraction. In its response to RAI 7954, Question 16 (ML17223B382), the applicant clarified that this methodology will not be used on a cycle-specific basis, but rather will demonstrate that the PLUS7 fuel design can meet fatigue limits within the requested operational window.

In Section 3.4.3 of APR1400-F-M-TR-13001, Revision 1, the applicant addressed burnup TCD by performing the fatigue analysis with the same modified version of FATES3B used in the cladding strain analysis (which replaced the Lyons thermal conductivity model with the modified NFI thermal conductivity model). The revised analysis also included a more limiting radial peaking factor. The resulting total cumulative fatigue damage factor remained below the limit. Based on the staff's review of the revised cladding fatigue analysis, the staff finds that the PLUS7 fuel assembly complies with the cladding fatigue criterion for the requested operating limits. Therefore, the staff finds this to be acceptable.

4.2.1.4 Cladding Oxidation and Hydriding

Basis

In Section 3.2.4 of APR1400-F-M-TR-13001, Revision 1, the applicant stated that the, "[f]uel system will not be damaged due to excessive oxidation under normal operation including AOOs."

The staff has reviewed the information provided and notes that this criterion is consistent with the guidance provided in SRP Section 4.2 regarding fuel system damage and fuel rod failure. Therefore, the staff finds this basis to be acceptable.

Criteria

In Section 3.2.4 of APR1400-F-M-TR-13001, Revision 1, the applicant stated, "[t]he best estimate cladding oxide thickness shall be less than []." It is further stated that, "[t]he clad hydrogen pickup is limited to [] at EOL to preclude loss of ductility due to hydrogen embrittlement by formation of zirconium hydride pellets."

The staff notes that these criteria have been widely used by the industry and is consistent with the guidance provided in SRP Section 4.2 (1)(A)(iv) and (1)(B)(i). Therefore, the staff finds these criteria to be acceptable.

Evaluation

In Section 3.2.3 of APR1400-F-M-TR-13001, Revision 1, the applicant presented an end of life oxidation and hydrogen content evaluation of PLUS7 fuel using the PAD4 code.

The staff issued RAI 7954, Question 17 (ML15169A118), requesting the applicant to justify the use of a [] hydrogen pickup fraction for ZIRLO. In its response to RAI 7954, Question 17 (ML15202A676), the applicant responded by comparing data and changing the pickup fraction to [] based on qualitative comparisons to data. The staff reviewed the applicant's response and performed a confirmatory analysis which supported the proposed [] pickup fraction.

In Section 3.3.4 of APR1400-F-M-TR-P, Revision 1, the applicant discussed the use of the PAD code for the PLUS fuel design and concludes that a corrosion multiplier on the Zircaloy-4 model of [] should be used to determine a best estimate oxide thickness for ZIRLO cladding. PAD4 typically uses a corrosion multiplier of []. Based on KNF operational experience, a corrosion multiplier of [] was selected for the analysis of PLUS7 fuel. The staff performed comparisons of the model and data and found that this is acceptable.

The applicant's analyses using the PAD4 code with the pickup fraction of [] and the corrosion multiplier of [] resulted in oxidation and hydrogen content below the stated limits. Based on the staff's review of the methods and analysis, the staff finds that the PLUS7 fuel design complies with the cladding oxidation criteria within the proposed operating limits. Therefore, the staff finds this to be acceptable.

4.2.1.5 Fuel Rod Internal Pressure

Basis

In Section 3.2.5 of APR1400-F-M-TR-13001, Revision 1, the applicant stated that the, "[f]uel system will not be damaged due to excessive rod internal pressure under normal operation."

This design basis is very similar to that given in SRP Section 4.2 (1)(A)(vi). Therefore, the staff finds this basis to be acceptable.

Criteria

In Section 3.2.5 of APR1400-F-M-TR-13001, Revision 1, the applicant provided three criteria for fuel rod internal pressure: (1) that cladding creep rate does not exceed fuel swelling rate (no cladding liftoff), (2) that reorientation of hydrides in the radial direction in the cladding shall not occur, and (3) that the radiological dose consequences of departure from nucleate boiling (DNB) failures are within the specified limits.

These criteria are consistent with the guidance provided in SRP Section 4.2 (1)(A)(vi). Therefore, the staff finds these criteria to be acceptable.

Evaluation

The applicant provided a rod internal pressure evaluation in Section 3.2.5 of the TR based on the use of the FATES3B code to calculate the critical pressure where cladding creep rate exceeds the fuel swelling rate. The staff issued RAI 7954, Question 15, requesting the applicant to provide the rod internal pressure limit used for the PLUS7 fuel and the basis for the

limit. In its response to RAI 7954, Question 15 (ML15202A673), (Reference 3), the applicant stated that FATES3B calculates the critical pressure limit when the rod internal pressure exceeds the systems pressure. The applicant also stated that this critical pressure is around []. The critical pressure is based on the cladding creep rate and the fuel swelling rate. The applicant confirmed that FATES3B will use the PAD4 ZIRLO creep model which the staff has previously found to be acceptable (ML003735452) (Reference 13). The staff notes that the fuel swelling mode in FATES3B is known to overpredict swelling in comparison to results from the staff's confirmatory code, FRAPCON[

].

This will lead to overpredicting (non-conservative) the lift-off pressure. However, in this case, the applicant demonstrated that the maximum rod internal pressure for the PLUS7 fuel within the operating envelope requested will not exceed the system pressure. Therefore, the staff finds that although FATES3B may overpredict the critical lift-off pressure, for this application and the requested operating envelope, the rod internal pressure will not exceed system pressure. This is consistent with guidance provided in SRP Section 4.2 (1)(A)(vi).

The staff requested, in RAI 7954, Question 18 (ML15169A118), for the applicant to provide a sample calculation showing rod internal pressure for a bounding power history up to a rod-average burnup of 62 GWd/MTU. In its response to RAI 7954, Question 18 (ML15202A675), as supplemented by letter dated August 11, 2017 (ML17223B382), the applicant provided the information requested. The staff performed confirmatory calculations using FRAPCON, which are shown in Figure 3. It can be seen that the FATES3B calculation of rod internal pressure predicts the same or greater rod internal pressure as those calculated using FRAPCON.

In Section 3.4.4 of APR1400-F-M-TR-13001, Revision 1, the applicant stated that TCD is inherently accounted for in FATES3B, since the model was calibrated to measure data for a full range of fuel rod burnup and operating conditions. There was insufficient information supporting this claim for the staff to review. In its response to RAI 7954, Question 18, the applicant additionally discussed conservatisms that are included in the original FATES3B calibration process, and in the design methodology, which the applicant described would offset any potential increase of rod internal pressure due to reduction of void volume caused by TCD-induced fuel thermal expansion. The staff's confirmatory analysis based on the applicant's response to RAI 7954, Question 18, confirms that the applicant's results are conservative in comparison to FRAPCON.



Figure 3: Comparison of the applicant and FRAPCON calculated rod internal pressure for sample calculation.

The applicant evaluated DNB propagation using the NRC approved methodology based on the INTEG code. This analysis was based on limiting DNB transients and internal pressure. The results from the applicant's analysis demonstrated that the calculated strains would not induce DNB propagation. The staff has reviewed the information provided and finds that the PLUS7 fuel assembly design would not exhibit DNB propagation within the requested operating parameters.

The applicant evaluated the PLUS7 fuel assembly in terms of hydrogen reorientation by noting that the calculated rod internal pressure is well below the pressure at which hydrogen reorientation occurs.

Based on the applicant's analysis, as supported by the staff's confirmatory analysis, the staff finds that the PLUS7 fuel assembly meets the fuel rod internal pressure criteria for the requested operating parameters. The staff notes that since the calculated maximum rod internal pressures for the requested operating parameters are below system pressure, the DNB propagation and hydrogen reorientation criteria are not necessary per the guidance provided in SRP Section 4.2; they do, however, provide additional defense in depth.

4.2.1.6 Internal Hydriding

Basis

In Section 3.2.6 of APR1400-F-M-TR-13001, Revision 1, the applicant stated that the, "[f]uel system will not be damaged due to excessive hydriding."

The staff has reviewed the information provided and notes that this criterion is consistent with the guidance provided in SRP Section 4.2 regarding hydriding and fuel rod failure. Therefore, the staff finds this basis to be acceptable.

Criteria

In Section 3.2.6 of APR1400-F-M-TR-13001, Revision 1, the applicant stated that to avoid internal hydriding the moisture content in the pellet will remain below 2.0 ppm.

The staff has reviewed the information provided and notes that this criterion is more conservative than the guidance provided in SRP Section 4.2 (1)(B)(i). Therefore, the staff finds this criterion to be acceptable.

Evaluation

The applicant provided a qualitative analysis which discusses the manufacturing process controls as the method by which the internal hydriding analysis is met.

The staff reviewed the applicant's evaluation and finds that the PLUS7 fuel assembly internal hydrogen levels are kept lower than the limits provided by the guidance in SRP Section 4.2(1)(B)(i). Therefore, the staff finds that the PLUS7 fuel assembly complies with the guidance provided in SRP 4.2(1)(B)(i) regarding internal hydriding.

4.2.1.7 Cladding Collapse

Basis

In Section 3.2.7 of APR1400-F-M-TR-13001, Revision 1, the applicant stated that, "[f]uel rod failure will not occur due to cladding collapse."

The staff has reviewed the information provided and notes that this criterion is consistent with the guidance provided in SRP Section 4.2 regarding cladding collapse and fuel rod failure. Therefore, the staff finds this basis to be acceptable.

Criteria

In Section 3.2.7 of APR1400-F-M-TR-13001, Revision 1, the applicant stated that radial buckling of the clad will not occur if axial gaps longer than [] will not occur between fuel pellets and that the plenum spring radial support capacity is sufficient to prevent clad collapse. Therefore, the staff finds this criterion to be acceptable.

Evaluation

In Section 3.2.7 of APR1400-F-M-TR-13001, Revision 1, the applicant presented a clad collapse analysis based on a previously approved methodology, CENPD-187-P-A (Reference 11), which uses the CEPNAFL and FATES3B codes. The applicant also stated that the PAD4 ZIRLO creep model is used as part of this evaluation.

The applicant provided results from its cladding collapse evaluation which conclude that cladding collapse will not occur within the operating range proposed over the entire life of the rods for both UO₂ and Gd₂O₃-UO₂ rods. The results also confirmed that the plenum spring provides sufficient radial support to the cladding to preclude cladding collapse.

The applicant additionally stated that operational experience indicates that collapse does not occur for fuel rods with initial pellet density of 95 percent theoretical density and having initial helium pressurization of [].

The staff finds that by using approved codes and methods, the applicant has demonstrated that the clad collapse criterion is met and the fuel cladding in the PLUS7 fuel assembly will not experience buckling.

4.2.1.8 Overheating of Cladding

Basis

In Section 3.2.8 of APR1400-F-M-TR-13001, Revision 1, the applicant stated that, “[f]uel rod failure will not occur due to the overheating of cladding under normal operation including AOOs.”

The staff has reviewed the information provided and notes that this criterion is consistent with the guidance provided in SRP Section 4.2, regarding thermal margin and fuel rod failure. Therefore, the staff finds this basis to be acceptable.

Criteria

In Section 3.2.8 of APR1400-F-M-TR-13001, Revision 1, the applicant stated that, “[t]here should be a 95% probability at the 95% confidence level that a hot fuel rod in the reactor core will not experience a DNB during normal operation or AOOs. For postulated accidents, the rods that experience DNB are assumed to fail for radiological dose calculation purposes.”

SRP Section 4.2 (1)(B)(iii) states that ensuring a thermal margin such as DNBR for PWRs is acceptable to demonstrate cladding will not overheat and that for postulated accidents, the rods that experience DNB should be assumed to fail for radiological dose calculation purposes. SRP Section 4.4 states that there should be at least a 95-percent probability at the 95-percent confidence level that the hot fuel rod in the core does not experience a DNB or transition condition during normal operation or AOOs. The staff finds that this criterion is consistent with the guidance provided in SRP Sections 4.2 and 4.4. Therefore, the staff finds this criterion to be acceptable.

Evaluation

The evaluation for overheating cladding is addressed in the plant specific transient and accident analysis (Chapter 15 of DCD). Therefore, the applicant did not request review and approval for the evaluation itself as part of this TR.

4.2.1.9 Overheating of Fuel Pellets

Basis

In Section 3.2.9 of APR1400-F-M-TR-13001, Revision 1, the applicant stated that, “[f]uel rod failure will not occur due to the overheating of fuel pellets under normal operation including AOOs. For postulated accidents, the total number of rods that experience centerline melting should be considered for radiological dose calculation.”

The staff has reviewed the information provided and notes that this criterion is consistent with the guidance provided in SRP Section 4.2 regarding thermal margin and fuel rod failure. Therefore, the staff finds this basis to be acceptable.

Criteria

In Section 3.2.9 of APR1400-F-M-TR-13001, Revision 1, the applicant stated that during normal operation and AOOs the fuel melting temperature will not be exceeded. The melting temperature of unirradiated UO_2 is 5080 °F and decreases by [] per 10 GWd/MTU and [] for each weight percent of Gd_2O_3 . During a postulated accident if the fuel melts, the fuel rod is considered to be failed and will be considered in the radiological consequence calculation.

The staff notes that the applicant's criteria is consistent with the high level guidance provided in SRP Section 4.2 (1)(B)(iv). However, in order to independently confirm the applicant's specific criteria, the staff compared the applicant's correlation for fuel melting temperature versus the corresponding correlation in FRAPCON and found it to be very conservative. Figure 4 shows the results of this comparison. Based on the discussion provided by the applicant, and with supporting staff confirmatory analysis, the staff finds this criteria to be acceptable.



Figure 4: Comparison of the applicant and FRAPCON fuel melting limits for UO_2 and Gd_2O_3 - UO_2 with 10 wt. percent Gd_2O_3 .

Evaluation

In Section 3.2.9 of APR1400-F-M-TR-13001, Revision 1, the applicant used FATES3B and the previously approved C-E Fuel Evaluation Model methodology to calculate the maximum fuel centerline temperature. FATES3B is used to calculate a power-to-melt curve as a function of burnup and the anticipated maximum powers are compared to this curve.

The staff notes that FATES3B will underpredict fuel centerline temperature as a function of burnup because TCD is not considered in FATES3B. The staff issued RAI 7954, Question 12

(ML15169A118), requesting the applicant to discuss how an analysis will be performed for UO_2 and $\text{Gd}_2\text{O}_3\text{-UO}_2$ fuel each cycle to ensure that the fuel will not melt since FATES3B is non-conservative in its prediction of fuel centerline temperature. In its supplemental response to RAI 7954, Question 12, dated August 11, 2017 (ML17223B382), the final methodology was eventually changed to use FATES3B and a temperature penalty on fuel centerline temperature as presented in Section 3.4.5 of APR1400-F-M-TR-13001, Revision 1.

Using FATES3B and temperature penalty, the applicant produced a power-to-melt curve for UO_2 and $\text{Gd}_2\text{O}_3\text{-UO}_2$ fuel. These power-to-melt curves are compared to the radial fall-off curves from Figure 3-1 of APR1400-F-M-TR-13001, Revision 1, and are confirmed to be greater than the maximum requested power for the entire burnup range. These comparisons are shown in Figure 3-3 of the TR.

The staff performed confirmatory calculations to confirm that the power to melt curves produced using FATES3B with the temperature penalty were acceptable. Figure 5 shows these comparisons with FRAPCON in blue and FATES3B with the temperature penalty in red. It can be seen in this figure that FATES3B with the temperature penalty predicts a lower power to melt than FRAPCON for all burnup ranges and both fuel types. This demonstrates that FATES3B with the temperature penalty is conservative relative to FRAPCON.



Figure 5: Comparison of the applicant and FRAPCON calculated power to melt for sample calculations with UO_2 and $\text{Gd}_2\text{O}_3\text{-UO}_2$ rods.

Based on the applicant's analysis, as independently confirmed by the staff with FRAPCON, the staff finds that the PLUS7 fuel design will meet the overheating of the fuel pellets criteria within the operating limits proposed. Therefore, the staff finds this to be acceptable.

4.2.1.10 Excessive Fuel Enthalpy

Section 3.2.10 of APR1400-F-M-TR-13001, Revision 1, states that the fuel rod failure is not underestimated for postulated accidents. Additionally, Section 3.2.10 of the TR provides failure criteria for determining the number of failed fuel rods. The staff evaluated these criteria and finds that these criteria match the criteria for determining the number of fuel failures provided in Appendix B to SRP 4.2 (Reference 6) and are therefore, acceptable. The TR, however, states that the evaluation of excessive fuel enthalpy is addressed in the plant specific transient and accident analysis. Accordingly, no finding regarding the evaluation of this criterion is made in this SER.

4.2.1.11 Pellet-to-Cladding Interaction

Section 3.2.11 of APR1400-F-M-TR-13001, Revision 1, states that fuel rod failure will not occur due to pellet cladding interaction (PCI) under normal operation including anticipated operational occurrences. The TR provided criteria on cladding strain and fuel melting. The staff finds this criteria to be consistent with the acceptance criteria provided in SRP Section 4.2, Item II.1.B.vi (Reference 6). The staff's evaluation of the cladding strain and fuel melt analyses are provided in Section 4.2.1.2 and Section 4.2.1.9 of this SER, respectively.

4.2.1.12 Bursting

Section 3.2.12 of APR1400-F-M-TR-13001, Revision 1, states that fuel rod failures are permitted during postulated accidents but that they will be accounted for in the dose analysis. The staff determined that the criteria provided in the TR matches the acceptance criteria provided in SRP Section 4.2, Item II.1.B.vii (Reference 6). Therefore, the staff finds this to be acceptable. The TR, however, states that the evaluation of this criterion is addressed in the plant specific transient and accident analysis. Accordingly, no finding regarding the evaluation of this criterion is made in this SER.

4.2.1.13 Cladding Embrittlement

Section 3.2.13 of APR1400-F-M-TR-13001, Revision 1, states that coolability is always maintained under postulated accidents. The staff evaluated the criteria provided in the TR and find them to match the requirements of 10 CFR 50.46(b)(1), "Peak cladding temperature," and 10 CFR 50.46(b)(2), "Maximum cladding oxidation." Therefore, the staff finds this to be acceptable. The TR, however, states that the evaluation of this criterion is addressed in the plant specific transient and accident analysis. Accordingly, no finding regarding the evaluation of this criterion is made in this SER.

4.2.1.14 Violent Expulsion of Fuel

Section 3.2.14 of APR1400-F-M-TR-13001, Revision 1, states that coolability is always maintained under postulated accidents. The staff evaluated the criteria provided by the applicant and finds them to match the core coolability criteria provided in Appendix B to SRP 4.2 (Reference 6). Therefore, the staff finds this to be acceptable. Additionally, the staff compared these criteria to the criteria provided in Draft Regulatory Guide DG-1327 (Reference 8) and finds the criteria specified in Section 3.2.14 of the TR to be more restrictive than the criteria provided in DG-1327. The TR, however, states that the evaluation of this criterion is addressed in the plant specific transient and accident analysis. Accordingly, no finding regarding the evaluation of this criterion is made in this SER.

4.2.1.15 Generalized Cladding Melting

Section 3.2.16 of APR1400-F-M-TR-13001, Revision 1, states that cladding embrittlement is more stringent than the melting criteria provided in Section 3.2.13 of the TR. The staff compared the 1204 °C (2200 °F) embrittlement criteria to the solidus temperature for Zircaloy provided in MATPRO (Reference 9) and determined that the embrittlement temperature is much lower than the temperature at which zirconium based alloys begin to melt. Accordingly, the staff finds that the cladding embrittlement criterion is more stringent than the generalized cladding melting criterion for ZIRLO.

4.2.1.16 Fuel Rod Ballooning

Section 3.2.16 of the TR states that coolability is always maintained under postulated accidents and that fuel rod ballooning must be accounted for in the analysis of the core flow distribution. The staff finds that this basis is consistent with the acceptance criterion provided in SRP Section 4.2, Item II.1.C.iv (Reference 6). The TR, however, states that the evaluation of this criterion is taken into account in the plant specific LOCA analyses. Accordingly, no finding regarding the evaluation of this criterion is made in this SER.

5.0 LIMITATIONS AND CONDITIONS

This TR does not address the evaluation of the fuel assembly for seismic and LOCA loads. As mentioned in Section 2.2.2.1 of the TR, the evaluation of fuel assembly for seismic and LOCA loads will be addressed in APR1400 DCD, Tier 2, Section 4.2.

The staff's approval is limited to a maximum peak rod average burnup of 60 GWD/MTU.

The fuel centerline temperature penalty presented in Section 3.4 of the TR is based on the operating parameters (e.g. peak linear heat generation rate) covered by the TR. The temperature penalty would need to be reevaluated for any core designs not bounded by these operating parameters.

The staff's approval is limited to baseload operations. Any applicant or licensee referencing this topical report who wishes to use non-baseload operations must justify the fission gas release model for the intended operation and demonstrate that any impacted safety analyses do not exceed the limits.

6.0 CONCLUSION

The staff concludes that the PLUS7 fuel assembly has been designed so that: (1) the fuel system will not be damaged as a result of normal operation and anticipated operational occurrences, and (2) fuel damage during postulated accidents will not be severe enough to prevent control rod insertion when it is required, thereby meeting the related requirements of GDC 10, "Reactor design," GDC 27, "Combined reactivity control systems capability," and GDC 35, "Emergency core cooling," in Appendix A to 10 CFR Part 50 and 10 CFR 50.34. This conclusion is based on the following:

1. The applicant provided sufficient evidence that these design objectives will be met based on operating experience, prototype testing, and analytical predictions.
2. The applicant provided for testing and inspection of new fuel to ensure that it is within design tolerances at the time of core loading. The applicant made a commitment to

perform online fuel failure monitoring and postirradiation surveillance to detect anomalies or confirm that the fuel has performed as expected.

Core coolability is addressed within the TR in part, but since the analyses supporting coolability such as large break LOCA are contained in separate topical and/or technical reports, no final finding is made by the staff in this SER regarding coolability. The staff's review of core coolability following a LOCA will be documented in the SER associated with the topical report APR1400-F-A-TR-12004-P, "Realistic Evaluation Methodology for Large-Break LOCA of the APR1400."

The staff concludes that the applicant described methods of adequately predicting fuel rod failures during postulated accidents so that radioactivity releases are not underestimated and thereby meets the related requirements of 10 CFR 50.34 (for new reactors).

7.0 REFERENCES

1. "Transmittal of Topical Report APR1400-F-M-TR-13001-P/NP, Revision 0, 'PLUS 7 Fuel Design for the APR1400' for Safety Evaluation," MKD/NW-13-0028L, dated September 17, 2013 (ML13298A413).
2. "The applicant Response to RAI 4-7542," MKD/NW-0020L, dated June 26, 2014 (ML14177A219).
3. "Response to RAI 5-7954 on Topical Report 'PLUS7 Fuel Design for the APR1400,' APR1400-F-M-TR-13001, Rev. 0)," MKD/NW-15-0055L, dated July 21, 2015 (ML15202A673).
4. "Revised Response to RAI TOP 6-8322," MKD/NW-17-0130L, dated July 31, 2017 (ML17212B078).
5. "Transmittal of Topical Report APR1400-F-M-TR-13001-P Revision 1, "PLUS7 Fuel Design for the APR1400," MKD/NW-17-0205-L, dated August 11, 2017 (ML17223B416).
6. NUREG-0800, Standard Review Plan, Section 4.2, "Fuel System Design," Revision 3, dated March 2007.
7. WCAP-16500-P-A, "CE 16x16 Next Generation Fuel Core Reference Report," (ML072500331).
8. DG-1327, "Pressurized Water Reactor Control Rod Ejection and Boiling Water Reactor Control Rod Drop Accidents," dated November 2016 (ML16124A200).
9. NUREG/CR-6150, Volume 4, Revision 2, "SCDAP/RELAP5/MOD 3.3 Code Manual: MATPRO – A Library of Materials Properties for Light-Water-Reactor Accident Analysis," dated January 2001 (ML010330400).
10. CENPD-404-P-A, "Implementation of ZIRLO™ Cladding Material in CE Nuclear Power Fuel Assembly Designs," dated November 2001 (ML031080082).
11. CENPD-187-P-A, Supplement 1-P-A, "CEPAN Method of Analyzing Creep Collapse of Oval Cladding" dated April 1985.

12. CENPD-178-P, Rev. 1-P, "Structural Analysis of Fuel Assemblies for Seismic and Loss of Coolant Accident Loading," August 1981.
13. WCAP-15063-P-A, Revision 1, "Westinghouse Improved Performance Analysis and Design Model (PAD 4.0)," dated April 2000 (ML003735452).

Non-Proprietary

SECTION B

Non-Proprietary

Page intentionally left blank

Non-Proprietary

PLUS7 Fuel Design for the APR1400

APR1400-F-M-TR-13001-NP-A

PLUS7 Fuel Design for the APR1400

(Approved Version)

Non-Proprietary

August 2017

Copyright © 2017

**Korea Electric Power Corporation &
Korea Hydro & Nuclear Power Co., Ltd
All Rights Reserved**

REVISION HISTORY

| Revision | Date | Page | Description |
|----------|-------------|-----------|---|
| 0 | August 2013 | All | Original issue |
| 1 | July 2017 | 1-1 | Revised the percentage of buckling strength increase based on the through-grid long-pulse test results |
| | | 2-3 | Added the description on the stress limit of fuel assembly components for CEA insertability |
| | | 3-3 | Updated strain results |
| | | 3-5 | Updated oxide thickness and hydrogen content results |
| | | 3-6 | Added content for critical pressure limit |
| | | 3-8 | Modified trip setpoint value |
| | | 3-16~3-19 | Updated the impact of thermal conductivity degradation (TCD) on fuel rod design criteria |
| | | 3-22 | Modified peak LOCA limit LHR |
| | | 3-23 | Modified parameter local power for APR1400 |
| | | 3-28 | Added two figures for power to melt and comparison of predicted & measured fuel centerline temperatures |
| | | 4-7 | Updated hydrogen pickup fraction |
| | | 4-47 | Updated Figure 4-44 |
| | | A-2~A-5 | Revised title of tables and figures (Mid grid crush test → Through-grid long-pulse test) |
| | | A-14~A-17 | Revised Appendix A.2.3 for the through-grid long-pulse test |
| | | A-6, A-38 | Added the comparison table between test condition and APR1400 operating condition |
| | | D-4 | Corrected the Appendix number (Appendix A.2.3 → Appendix A.2.2) |

This document was prepared for the design certification application to the U.S. Nuclear Regulatory Commission and contains technological information that constitutes intellectual property of Korea Hydro & Nuclear Power Co., Ltd. Copying, using, or distributing the information in this document in whole or in part is permitted only to the U.S. Nuclear Regulatory Commission and its contractors for the purpose of reviewing design certification application materials. Other uses are strictly prohibited without the written permission of Korea Electric Power Corporation and Korea Hydro & Nuclear Power Co., Ltd.

ABSTRACT

Eight Westinghouse type PWRs, eleven Combustion Engineering type OPR1000s, and four CANDU type PHWRs are currently operating in the Republic of Korea. Additionally, one OPR1000 will start operation sequentially by 2013 and four APR1400s are under construction and four more APR1400s will be constructed.

KEPCO NF had jointly developed PLUS7 fuel from 1999 to 2002 with Westinghouse to improve the fuel performance relative to Guardian fuel. Four lead test assemblies (LTAs) were loaded in an OPR1000 nuclear power plant (Ulchin unit 3) and irradiated for three cycles from 2002 to 2007. The LTAs were confirmed to have been irradiated within the design limits through the pool-side examinations and hot-cell examinations at each end of cycle operation. Additionally, four commercial surveillance assemblies (CSAs) were examined in Yonggwang unit 5 for three cycles from 2006 to 2010. The in-pile performance of PLUS7 fuel was confirmed through the LTAs and CSAs. Based on the successful in-reactor performance of the LTAs and CSAs, more than 2,300 PLUS7 fuel assemblies have been supplied to OPR1000 nuclear power plants from 2006 to 2012.

This topical report describes the design evaluation of PLUS7 fuel and the results of its in-reactor performance. The designs of PLUS7 fuel assembly and its components are evaluated in order to verify the mechanical integrity of the PLUS7 fuel during the in-reactor operations. The results of the design evaluations confirmed that all the out-of-pile and in-reactor mechanical integrity-related design criteria on the PLUS7 fuel are satisfied.

LIST OF ACRONYMS

| | |
|---------|---|
| AOO | Anticipated Operational Occurrences |
| APR1400 | Advanced Power Reactor 1400 |
| ASME | American Society of Mechanical Engineers |
| BOC | Beginning of Cycle |
| CEA | Control Element Assembly |
| CEDM | Control Element Drive Mechanism |
| CHF | Critical Heat Flux |
| CSA | Commercial Surveillance Assembly |
| DCD | Design Control Document |
| DFBN | Debris Filter Bottom Nozzle |
| DNB | Departure from Nucleate Boiling |
| DNBR | Departure from Nucleate Boiling Ratio |
| ECT | Eddy Current Test |
| FACTS | Fuel Assembly Compatibility Test System |
| FDF | Fatigue Damage Factor |
| KSNP | Korean Standard Nuclear Power Plants |
| LOCA | Loss Of Coolant Accident |
| LTA | Lead Test Assembly |
| LVDT | Linear Variable Differential Transducer |
| OPR1000 | Optimized Power Reactor 1000 |
| PSE | Poolside Examination |
| RCS | Reactor Coolant System |
| SSE | Safe Shutdown Earthquake |
| VIPER | Vibration Investigation and Pressure drop Experimental Research |

TABLE OF CONTENTS

| | |
|--|-------------|
| LIST OF TABLES | vii |
| LIST OF FIGURES..... | viii |
| | |
| 1. INTRODUCTION | 1-1 |
| 2. FUEL ASSEMBLY AND COMPONENTS DESIGN..... | 2-1 |
| 2.1 OVERVIEW | 2-1 |
| 2.2 Fuel Assembly | 2-1 |
| 2.2.1 Design Features | 2-1 |
| 2.2.2 Design Basis, Criteria and Evaluation | 2-2 |
| 2.2.2.1 Structural Integrity..... | 2-2 |
| 2.2.2.2 Rod-to-Top Nozzle Axial Clearance | 2-3 |
| 2.2.2.3 Hydraulic Stability | 2-3 |
| 2.2.2.4 Shipping and Handling Loads..... | 2-4 |
| 2.2.2.5 Mechanical Compatibility | 2-5 |
| 2.3 FUEL ASSEMBLY COMPONENTS | 2-5 |
| 2.3.1 Bottom Nozzle | 2-5 |
| 2.3.2 Top Nozzle | 2-7 |
| 2.3.3 Holddown Spring | 2-9 |
| 2.3.4 Guide Thimble/Instrument Tube | 2-11 |
| 2.3.5 Grid | 2-12 |
| 2.3.6 Joint and Connection | 2-16 |
| 3. FUEL ROD DESIGN | 3-1 |
| 3.1 OVERVIEW | 3-1 |
| 3.2 DESIGN BASIS, CRITERIA AND EVALUATION | 3-1 |
| 3.2.1 Cladding Stress | 3-2 |
| 3.2.2 Cladding Strain | 3-3 |
| 3.2.3 Cladding Fatigue..... | 3-4 |
| 3.2.4 Cladding Oxidation and Hydriding | 3-5 |
| 3.2.5 Fuel Rod Internal Pressure..... | 3-5 |
| 3.2.6 Internal Hydriding..... | 3-6 |
| 3.2.7 Cladding Collapse..... | 3-7 |

| | | |
|-----------|--|------------|
| 3.2.8 | Overheating of Cladding | 3-7 |
| 3.2.9 | Overheating of Fuel Pellets | 3-8 |
| 3.2.10 | Excessive Fuel Enthalpy | 3-9 |
| 3.2.11 | Pellet-to-Cladding Interaction | 3-9 |
| 3.2.12 | Bursting..... | 3-10 |
| 3.2.13 | Cladding Embrittlement | 3-10 |
| 3.2.14 | Violent Expulsion of Fuel | 3-10 |
| 3.2.15 | Generalized Cladding Melting | 3-11 |
| 3.2.16 | Fuel Rod Ballooning | 3-11 |
| 3.3 | APPLICABILITY OF FUEL PERFORMANCE CODES AND METHODOLOGIES FOR DESIGN EVALUATION | 3-11 |
| 3.3.1 | Safety Evaluation Report Compliance..... | 3-11 |
| 3.3.2 | Applicability of FATES3B Code to PLUS7 Fuel Rod Design | 3-13 |
| 3.3.3 | Applicability of CEPANFL Code to PLUS7 Fuel Rod Design | 3-14 |
| 3.3.4 | Applicability of PAD Code to PLUS7 Fuel Rod Design | 3-15 |
| 3.4 | IMPACT OF THERMAL CONDUCTIVITY DEGRADATION (TCD) ON FUEL ROD DESIGN CRITERIA | 3-16 |
| 3.4.1 | Cladding Stress | 3-16 |
| 3.4.2 | Cladding Strain | 3-17 |
| 3.4.3 | Cladding Fatigue..... | 3-17 |
| 3.4.4 | Fuel Rod Internal Pressure..... | 3-17 |
| 3.4.5 | Overheating of Fuel Pellets | 3-17 |
| 3.5 | IMPACT OF TCD ON SAFETY ANALYSIS | 3-18 |
| 3.5.1 | Determination of TCD penalty | 3-18 |
| 3.5.2 | Fuel Rod Interface Data for Safety Analyses | 3-19 |
| 3.6 | IMPACT OF FUEL ENTHALPY | 3-19 |
| 3.7 | CONCLUSION | 3-19 |
| 4. | PLUS7 FUEL EXPERIENCE | 4-1 |
| 4.1 | OVERVIEW | 4-1 |
| 4.2 | POOL-SIDE EXAMINATIONS..... | 4-1 |
| 4.2.1 | Fuel Assembly Irradiation Growth | 4-2 |
| 4.2.2 | Fuel Assembly Bow and Twist..... | 4-2 |
| 4.2.3 | Rod-to-Top Nozzle Axial Clearance (Shoulder Gap) | 4-3 |
| 4.2.4 | Fuel Rod Bow | 4-3 |
| 4.2.5 | Grid Width..... | 4-3 |

| | | |
|-------------------|--|------------|
| 4.2.6 | Cladding Oxide Thickness | 4-4 |
| 4.2.7 | Fuel Rod Outer Diameter | 4-4 |
| 4.3 | HOT-CELL EXAMINATIONS | 4-5 |
| 4.3.1 | Fuel Rod Fretting Wear | 4-5 |
| 4.3.2 | Cladding Oxide Thickness | 4-5 |
| 4.3.3 | CRUD Thickness | 4-6 |
| 4.3.4 | Fuel Rod Outer Diameter | 4-6 |
| 4.3.5 | Cladding Hydrogen Contents and Hydride Orientation | 4-6 |
| 4.3.6 | Fission Gas Release | 4-7 |
| 4.4 | TESTING, INSPECTION AND SURVEILLANCE PLANS | 4-7 |
| 5. | CONCLUSION..... | 5-1 |
| 6. | REFERENCES | 6-1 |
| | | |
| Appendix A | Summary of PLUS7 Fuel Assembly Tests | A-1 |
| Appendix B | Commercial Operating Experience of KEPCO NF PWR Fuel | B-1 |
| Appendix C | PLUS7 Scram Data Verification | C-1 |
| Appendix D | PLUS7 Wear Performance Analysis | D-1 |

LIST OF TABLES

| | | |
|------------|---|------|
| Table 2-1 | Comparison of Design Features of PLUS7, Guardian, and RFA Fuel | 2-19 |
| Table 3-1 | Comparison of PLUS7 Fuel Rod with Guardian Fuel Rod | 3-20 |
| Table 3-2 | Codes Used for Analyses of Fuel Rod Design | 3-21 |
| Table 3-3 | Cladding Stress Evaluation Results | 3-21 |
| Table 3-4 | Main Design Parameters Used for PLUS7 Fuel Rod Performance Analysis | 3-22 |
| Table 3-5 | Description of Data Base Used for FATES3B Verification | 3-23 |
| Table 3-6 | Design Parameters for Rods in the Verification Data Base | 3-24 |
| Table 3-7 | Thermal-Hydraulic Parameters for Rods in the Fission Gas Release Verification Data Base | 3-24 |
| Table 3-8 | Comparison of Measured Oxide Thickness and Predicted Oxide Thickness Using modified Corrosion Model Multiplier | 3-25 |
| Table 3-9 | Mean Value and Standard Deviation of M/P for H615 and H605 Assemblies | 3-26 |
| Table 3-10 | Operating Conditions of APR1400, OPR1000, and Westinghouse Type Plants | 3-26 |
| Table 4-1 | Commercial Loading of PLUS7 up to 2012 | 4-8 |
| Table 4-2 | Burnup Data of PLUS7 LTAs and CSAs | 4-9 |
| Table 4-3 | Irradiation Growths of the PLUS7 LTAs and CSAs | 4-9 |
| Table 4-4 | Shoulder Gaps of the PLUS7 LTAs and CSAs | 4-10 |
| Table 4-5 | Rod-to-Rod Gaps of the PLUS7 LTAs and CSAs | 4-10 |
| Table 4-6 | Grid Widths of the PLUS7 LTAs and CSAs | 4-11 |
| Table 4-7 | Summary of Fuel Rod for Hot Cell Examination | 4-12 |
| Table 4-8 | Fuel Rod Internal Gas Pressure and Fission Gas Release | 4-12 |

LIST OF FIGURES

| | | |
|-------------|--|------|
| Figure 2-1 | PLUS7 Fuel Assembly Configuration | 2-20 |
| Figure 2-2 | Comparison of Fuel Rod Designs | 2-21 |
| Figure 2-3 | Mid Grid Designs | 2-22 |
| Figure 2-4 | Spring and Dimple Configurations of PLUS7 Mid Grid | 2-23 |
| Figure 2-5 | Comparison of Top and Bottom Grids | 2-24 |
| Figure 2-6 | Debris Filtering Design of PLUS7 | 2-25 |
| Figure 2-7 | Reconstitutable Design of PLUS7 Top Nozzle | 2-26 |
| Figure 2-8 | Comparison of Bottom Nozzles | 2-27 |
| Figure 2-9 | Comparison of Guide Thimbles | 2-28 |
| Figure 2-10 | Vibration Test Results of PLUS7 Fuel Assembly | 2-29 |
| Figure 2-11 | PLUS7 Bottom Nozzle | 2-30 |
| Figure 2-12 | 1/8 Bottom Nozzle Finite Element Model | 2-30 |
| Figure 2-13 | PLUS7 Top Nozzle | 2-31 |
| Figure 2-14 | PLUS7 Top Nozzle/Guide Thimble Joint & Connection | 2-32 |
| Figure 2-15 | 1/8 Top Nozzle Adapter Plate Finite Element Model | 2-33 |
| Figure 2-16 | 1/8 Top Nozzle Holddown Plate Finite Element Model | 2-33 |
| Figure 2-17 | PLUS7 Guide Thimble and Instrument Tube | 2-34 |
| Figure 2-18 | CEA Drop Time | 2-35 |
| Figure 2-19 | PLUS7 Top and Bottom Grid | 2-36 |
| Figure 2-20 | PLUS7 Protective Grid | 2-36 |
| Figure 2-21 | PLUS7 Mid Grid | 2-37 |
| Figure 2-22 | PLUS7 Grid/Guide Thimble and Instrument Tube Joint & Connection | 2-38 |
| Figure 2-23 | PLUS7 Bottom Grid/Guide Thimble and Instrument Tube Joint & Connection | 2-39 |
| Figure 2-24 | PLUS7 Bottom Nozzle and P-Grid/Guide Thimble Joint & Connection | 2-40 |
| Figure 3-1 | Rod Power History Used for PLUS7 Fuel Rod Performance Analysis | 3-27 |
| Figure 3-2 | Comparison of Measured Oxide Layer Thickness and Predicted Oxide Layer Thickness for H615 and H605 Assemblies | 3-27 |
| Figure 3-3 | Power to Melt and Maximum Attainable Power for UO ₂ and Gd ₂ O ₃ -UO ₂ Rods | 3-28 |
| Figure 3-4 | Comparison of Predicted and Measured Fuel Centerline Temperatures as a Function of Burnup vs. Determined TCD Penalty (red line) | 3-28 |

| | | |
|-------------|---|------|
| Figure 4-1 | Development & Commercial Supply Status of PLUS7 | 4-13 |
| Figure 4-2 | Configuration of Fuel Rods in PLUS7 LTAs and CSAs | 4-14 |
| Figure 4-3 | Core Loading Pattern with PLUS7 LTAs | 4-15 |
| Figure 4-4 | Core Loading Pattern with PLUS7 CSAs | 4-18 |
| Figure 4-5 | Measured Irradiation Growths of PLUS7 LTAs and CSAs | 4-21 |
| Figure 4-6 | Measured Rod-to-Top Nozzle Clearances of PLUS7 LTAs and CSAs | 4-21 |
| Figure 4-7 | Measured Rod-to-Rod Gaps of PLUS7 LTAs and CSAs | 4-22 |
| Figure 4-8 | Measured Grid Widths of PLUS7 LTAs and CSAs | 4-22 |
| Figure 4-9 | Measured Cladding Oxide Layer Thickness of PLUS7 LTA and CSAs | 4-23 |
| Figure 4-10 | Comparison of Measured Cladding Oxide Layer Thickness and Predicted Cladding Oxide Layer Thickness of PLUS7 LTA and CSAs | 4-23 |
| Figure 4-11 | Diameter of HA03-A03 Fuel Rod | 4-24 |
| Figure 4-12 | Diameter of HA03-A14 Fuel Rod | 4-25 |
| Figure 4-13 | Diameter of HA03-B03 Fuel Rod | 4-26 |
| Figure 4-14 | Diameter of HA03-B14 Fuel Rod | 4-27 |
| Figure 4-15 | Diameter of HA03-C03 Fuel Rod | 4-28 |
| Figure 4-16 | Diameter of HA03-K07 Fuel Rod | 4-28 |
| Figure 4-17 | Diameter of HA03-C16 Fuel Rod | 4-29 |
| Figure 4-18 | Diameter of HA03-D15 Fuel Rod | 4-30 |
| Figure 4-19 | Diameter of HA03-D16 Fuel Rod | 4-31 |
| Figure 4-20 | Diameter of H615-E01 Fuel Rod | 4-32 |
| Figure 4-21 | Diameter of H615-N01 Fuel Rod | 4-32 |
| Figure 4-22 | Diameter of H615-D01 Fuel Rod | 4-33 |
| Figure 4-23 | Diameter of H615-N03 Fuel Rod | 4-33 |
| Figure 4-24 | Diameter of H615-H04 Fuel Rod | 4-34 |
| Figure 4-25 | Diameter of H615-S16 Fuel Rod | 4-34 |
| Figure 4-26 | Diameter of H615-N02 Fuel Rod | 4-35 |
| Figure 4-27 | Diameter of H615-L11 Fuel Rod | 4-35 |
| Figure 4-28 | Visual Inspection Results of Fuel Rods at Grid Positions | 4-36 |
| Figure 4-29 | Visual Inspection Results of B14 Fuel Rod at Grid Positions | 4-38 |
| Figure 4-30 | Cross-Section Inspection Results of B14 Fuel Rod (10 th Grid, Spring 0°) | 4-39 |
| Figure 4-31 | Oxide Thickness of HA03-A14 Fuel Rod | 4-40 |
| Figure 4-32 | Oxide Thickness of HA03-B14 Fuel Rod | 4-40 |
| Figure 4-33 | Oxide Thickness of HA03-C03 Fuel Rod | 4-41 |
| Figure 4-34 | Oxide Thickness of HA03-D15 Fuel Rod | 4-41 |
| Figure 4-35 | Oxide Thickness of HA03-D16 Fuel Rod | 4-42 |

| | | |
|-------------|--|------|
| Figure 4-36 | Oxide Thickness of HA03-K07 Fuel Rod | 4-42 |
| Figure 4-37 | CRUD and Bonding Layer of HA03-C03 Fuel Rod (3094 mm) | 4-43 |
| Figure 4-38 | Diameter of HA03-A14 Fuel Rod | 4-44 |
| Figure 4-39 | Diameter of HA03-B14 Fuel Rod | 4-44 |
| Figure 4-40 | Diameter of HA03-C03 Fuel Rod | 4-45 |
| Figure 4-41 | Diameter of HA03-D15 Fuel Rod | 4-45 |
| Figure 4-42 | Diameter of HA03-D16 Fuel Rod | 4-46 |
| Figure 4-43 | Diameter of HA03-K07 Fuel Rod | 4-46 |
| Figure 4-44 | Hydrogen Content of ZIRLO Cladding | 4-47 |
| Figure 4-45 | Calculated Hydrogen Content of PLUS7 LTA | 4-47 |
| Figure 4-46 | Hydride Microphotograph of HA03-C03 Fuel Rod (3255 mm) | 4-48 |

1. INTRODUCTION

PLUS7 fuel was jointly developed from 1999 through 2002 with Westinghouse to enhance the fuel performance relative to Guardian fuel. In the process of the design, various out-of-pile mechanical, thermal, hydraulic, and vibration characteristic tests were performed.

For the in-pile tests, four lead test assemblies (LTAs) were loaded in an OPR1000 nuclear power plant in the Republic of Korea and irradiated from 2002 through 2007. Additionally, four commercial surveillance assemblies (CSAs) were examined in Yonggwang unit 5 for three cycles from 2006 to 2010. The in-pile performance of PLUS7 fuel was confirmed through poolside examinations (PSEs) of the LTAs and CSAs, and hot-cell examinations of the LTA. Based on the successful in-reactor performance of the LTAs and CSAs, more than 2,300 PLUS7 fuel assemblies have been supplied to OPR1000 nuclear power plants from 2006 to 2012. PLUS7 fuel will also be supplied to APR1400 nuclear power plants from the initial cores.

PLUS7 fuel has the following advanced design features with respect to Guardian fuel:

- High burnup performance
Batch average burnup increase from 45,000 to 55,000 MWD/MTU
- High thermal performance
Overpower margin increase by more than 10%
- High mechanical strength
Mid grid dynamic buckling strength increase by 35%
- Improved economy
Enhanced uranium utilization (optimized H/U ratio) and neutron economy
- Improved fretting wear resistance
Increased grid-to-rod fretting wear resistance with the conformal grid springs and dimples
- Multi-devices for debris filtering
Improved debris filtering efficiency with a small-hole bottom nozzle and the protective grid
- Enhanced fuel production
Standardized design and manufacturing processes

This report describes the design features, evaluation results, and in-reactor performance results of PLUS7 fuel.

In Chapter 2, the mechanical design features, design criteria and evaluation results of PLUS7 fuel assembly and components are described.

Chapter 3 covers the design and the evaluation results of the PLUS7 fuel rods with ZIRLO™ cladding up to 60,000 MWD/MTU.

In Chapter 4, the fuel experiences of PLUS7 are described based on the operating experiences, including results of the pool-side examinations and hot-cell examinations of PLUS7 LTAs and CSAs.

In the appendices, the summary of out-of-pile test results, the commercial operating experiences, the scram data verification, and the wear performance analysis for PLUS7 fuel are described.

2. FUEL ASSEMBLY AND COMPONENTS DESIGN

2.1 Overview

In this chapter, the design features and evaluation results of the PLUS7 fuel assembly are described. The evaluation results show that the PLUS7 fuel assembly maintains high burnup performance, thermal performance, mechanical performance, and the structural integrity needed for the in-reactor operations.

2.2 Fuel Assembly

2.2.1 Design Features

The PLUS7 fuel assembly is composed of a reconstitutable top nozzle, a debris filtering bottom nozzle with small holes, a debris filtering protective grid, nine mid grids with mixing vanes, a vaneless top grid, a vaneless bottom grid, four guide thimbles, an instrument tube, and 236 fuel rods inserted into the cells of each grid, as shown in Figure 2-1.

The PLUS7 fuel assembly incorporates the same basic structural features and geometries as those of Guardian fuel assembly to have mechanical compatibility with the Guardian fuel as well as CE type reactor internals. The critical geometric dimensions of the both fuel assemblies are same, such as overall length, diameters of guide thimbles and instrument tube, axial elevations of top and mid grids, fuel rod pitch, and top and bottom nozzle interface with reactor internals.

In addition, the PLUS7 fuel assembly incorporates proven features and materials of Westinghouse type fuel assembly to improve fuel assembly performance. The incorporated features are ZIRLO cladding, ZIRLO guide thimbles and instrument tube, ZIRLO mid grids with mixing vanes, Inconel top grid, Inconel protective grid, debris filter bottom nozzle, fuel rod diameters, axial blanket, variable pitch plenum spring and straight type of grid straps. Table 2-1 shows the comparison of design features of PLUS7 fuel, Guardian fuel and RFA fuel.

Figure 2-2 shows that the PLUS7 fuel rod adopts ZIRLO cladding and a variable pitch plenum spring to secure high burnup performance. The PLUS7 fuel rod diameter is reduced by $\left(\frac{D_{PLUS7}}{D_{Guardian}} \right)^{TS}$ relative to the Guardian fuel rod, which reduces the rod-induced pressure drop and improves the uranium utilization. The axial blankets at the top and the bottom of the fuel stack region reduce the axial leakage of neutrons.

As shown in Figure 2-3, the PLUS7 mid-grids adopt mixing vanes to increase the overpower margin by more than 10% compared with Guardian fuel. The grid straps are in a straight shape to enhance the buckling strength. PLUS7 uses the conformal spring and dimple to reduce the grid-to-rod fretting wear. The conformal spring and dimple make grid-to-rod area contacts instead of the point contact in Guardian fuel. The springs and dimples are designed to minimize the grid-induced pressure drop, as shown in Figure 2-4.

As shown in Figure 2-5, the PLUS7 top and bottom grids have straight-shaped straps to enhance the buckling strength. The pressure drop of the top and the bottom grids is reduced by designing the dimple in the horizontal direction. These grids adopt Inconel material to maintain a sufficient rod supporting force during the fuel life-time since Inconel has the property of low irradiation growth and relaxation.

Figure 2-6 shows that the protective grid connected to the top of the bottom nozzle divide the round flow hole into four and the slotted flow holes into two. This feature reduces the size of debris passing through the bottom nozzle. Moreover, the debris passing through the bottom nozzle flow holes and the inner straps of the protective grid will be captured by the dimples of the protective grid. The protective grid contains four dimples in each grid cell that provide a co-planar contact with long end plug of the fuel rod.

Figure 2-7 shows the reconstitutable top nozzle of PLUS7 fuel. The PLUS7 top nozzle components are not dismantled when the inner extension tube is disconnected from the guide thimble flange during the fuel assembly reconstitution process (integral design concept). In comparison, the Guardian top nozzle requires the installation of a temporary post to prevent dismantling of the top nozzle components. This PLUS7 top nozzle design makes the fuel reconstitution work easier and less time-consuming.

As shown in Figure 2-8, the flow hole of the PLUS7 bottom nozzle is about half size of the Guardian's flow hole in order to enhance the debris-filtering efficiency. To minimize the pressure drop, the bottom nozzle is designed with round holes and slotted holes.

The configurations of the guide thimbles in the Guardian fuel and PLUS7 fuel are shown in Figure 2-9. To improve the manufacturability, the PLUS7 guide thimbles have two steps of tube diameters rather than three steps in the Guardian guide thimbles. However, there are no difference in the CEA insertability between PLUS7 fuel and Guardian fuel since inner and outer diameters and flow hole dimensions of the guide thimbles are identical.

All the dimensions of the PLUS7 instrument tube are the same as those of the Guardian.

2.2.2 Design Basis, Criteria and Evaluation

2.2.2.1 Structural Integrity

(1) Basis

The objectives of the fuel assembly safety are to provide assurance that (a) the fuel system is not damaged as a result of normal operation and anticipated operational occurrences (AOOs), (b) fuel system damage is never so severe as to prevent control rod insertion when it is required, (c) the number of fuel rod failures is not underestimated for postulated accidents, and (d) coolability is always maintained.

(2) Criteria

The fuel assembly shall maintain the structural integrity under any load occurring at all operating conditions during the entire lifetime.

For the normal operation and AOO conditions, the stress limits for the fuel assembly and its components are given below:

$$\begin{aligned}P_m &\leq S_m \\P_m + P_b &\leq 1.5 \cdot S_m\end{aligned}$$

Worst case abnormal loads during the postulated accidents are represented by seismic and LOCA loads. For these conditions, the stress limits for the fuel assembly and its components are given below:

$$P_m \leq S_m'$$

$$P_m + P_b \leq 1.5 \cdot S_m'$$

Where,

P_m = calculated primary membrane stress

P_b = calculated primary bending stress

S_m = allowable design stress intensity defined in the ASME Section III

S_u = minimum ultimate tensile strength at unirradiated condition

S_m' = allowable design strength for the accident conditions (a smaller value of $2.4 S_m$ and $0.7 S_u$)

Additionally the stresses of the fuel assembly components for the CEA insertion are evaluated using the normal operation and AOO stress limits to assure that the components do not deformed severely enough to interfere with CEA insertion even under the faulted conditions. The fuel assembly components for CEA insertion are guide thimble, outer guide post, adapter plate and holddown plate. The stress limits of fuel assembly components for CEA insertion are same as the normal operation and AOO stress limits.

(3) Evaluation

The structural integrity of the PLUS7 components is verified in Section 2.3 for all conditions.

The fuel assembly evaluation for seismic and LOCA loads is performed in accordance with the NRC licensed CE methodology (Reference 2-1). The fuel assembly model and characteristics were determined as analysis of fuel assembly mechanical test and used to the core analysis predicted fuel assembly deflected shapes and grid impact forces. Grid buckling strength was determined from dynamic impact testing for PLUS7 grids, and compared with predicted grid impact forces. The stresses for remaining components during seismic and LOCA are calculated through deflection shapes and axial loads, and then evaluated against each stress criteria. The evaluation of fuel assembly for seismic and LOCA loads will be addressed in DCD tier 2, Section 4.2.

2.2.2.2 Rod-to-Top Nozzle Axial Clearance

(1) Basis

If a fuel rod were to be fully constrained axially by contact with top and bottom nozzles, large axial load could be generated. This load could result in fuel rod bowing, overstressing of guide thimbles, or overstressing of guide thimble joints to nozzles.

(2) Criteria

The axial clearance between the fuel rod and top nozzle shall be maintained during the fuel life time.

(3) Evaluation

Based on the calculation of the axial gap between the fuel rod and top nozzle considering their irradiation growths, the axial clearance is maintained during the fuel lifetime. The PLUS7 PSE results confirmed the sufficient gap after three cycles of irradiation as shown in the Section 4.2.3.

2.2.2.3 Hydraulic Stability

(1) Basis

Since the fuel assembly lift-off may cause the fuel assembly and in-core structure failure, the fuel assembly shall not be lifted off during the normal operation. The fuel assembly and fuel rod vibration causing the fuel failure shall not occur over the full range of flow rates of the plant.

(2) Criteria

- The fuel assembly shall not be lifted off during normal operation.
- Fuel rod vibration causing the fuel failure shall not occur over the full range of flow rates.
- The fuel rod vibration caused by the cross-flow between the fuel assemblies shall not result in fretting wear-induced cladding failure.

(3) Evaluation

The fuel assembly was confirmed not to be lifted off over the full range of flow rates, based on the fuel assembly lift-off tests at the FACTS loop test facility, as described in Appendix A.2.9.

The PLUS7 fuel assembly vibration tests were performed at the FACTS loop test facility to evaluate its vibration characteristics (see Appendix A.2.1). The test results showed that PLUS7 fuel maintained dynamic stability and did not generate abnormal fluid-induced vibration in the reactor operating flow range, as shown in Figure 2-10.

Five hundred hours of endurance tests were performed in the VIPER high temperature loop having two kinds of fuel assemblies, PLUS7 fuel and Guardian fuel. This test is to evaluate the grid-to-rod fretting wear-induced failure that may be caused by the cross-flow between the two fuel assemblies. Based on these test results, it was confirmed that the cross flow-induced vibration did not produce the grid-to-rod fretting wear-induced failure (see Appendix A.2.2).

Hydraulic stability of PLUS7 fuel assembly was also confirmed by successful operating experience (see Section 4). There was no fuel rod fretting failure for the LTA and commercially supplied PLUS7 fuel assemblies since 2002.

2.2.2.4 Shipping and Handling Loads**(1) Basis**

The fuel assembly shall withstand loads encountered during normal shipping and handling conditions.

(2) Criteria

- The fuel assembly shall meet the stress criteria of the normal operation with an axial load of 4g acceleration and a lateral load of 6g acceleration that may occur during the shipping.
- The fuel assembly shall meet the stress criteria of the normal operation with the maximum load of 4g acceleration that may occur during the handling.

(3) Evaluation

The shift of fuel rods and the deformation of the grid springs do not occur during fuel assembly shipping because the grid springs have initial pre-loads greater than an axial load of 4g acceleration and a lateral load of 6g acceleration.

Grids are not deformed during fuel assembly shipping because the grid impact strength measured from the tests is found to be larger than the lateral load on the grid surface generated by 6g acceleration (see Appendix A.2.3).

It was evaluated that the stress acting on the fuel assembly was less than the stress allowable for the normal operation even when the load of 4g acceleration of fuel assembly mass was applied to the bottom nozzle, top nozzle, and guide thimble, as shown Section 2.3.

2.2.2.5 Mechanical Compatibility

(1) Basis

Fuel Assembly should properly interface with core components and the internal structure.

(2) Criteria

The fuel assembly shall be loaded without any interference with the reactor internals and the adjacent fuel assemblies. It also shall maintain mechanical compatibility with core components (control element assembly and neutron source rods).

(3) Evaluation

There is no impact on the mechanical compatibility because the PLUS7 designs are same as the Guardian at the interface with reactor internals and core components. Compatibility has been proved through the extensive operating experiences since 2002.

2.3 Fuel Assembly Components

2.3.1 Bottom Nozzle

2.3.1.1 Description

As shown in Figure 2-11, the bottom nozzle is composed of an adapter plate, four legs including skirt plates, and a cylindrical instrument guide. The bottom nozzle is attached to the four guide thimbles by thimble screws that penetrate through the adapter plate and mate with threaded end plugs of the guide thimbles. The thimble screws are locked in place by crimping on the underside of the adapter plate to prevent loosening.

The adapter plate of the bottom nozzle together with the protective grid can protect the fuel rods from debris entering the fuel assembly. The adapter plate consists of 188 round flow holes and 372 slotted flow holes, preventing the inflow of debris and minimizing the pressure drop of the bottom nozzle. The skirt plates and legs are welded to the adapter plate.

The instrument guide to guide instrument into the reactor core is fixed on the underside of the adapter plate at its center by a spot weld.

2.3.1.2 Design Basis, Criteria and Evaluation

(1) Structural support of the fuel assembly

1) Basis

The bottom nozzle integrity is maintained for lateral and vertical loads from normal, AOOs, postulated accidents, and shipping & handling conditions.

2) Criteria

The bottom nozzle shall withstand lateral and vertical loads without exceeding the stress limits of Section 2.2.2.1.

3) Evaluation

The finite element analysis was performed to verify the mechanical integrity of the bottom nozzle for the loads arising from the fuel assembly shipping and handling as well as normal operation, AOOs and postulated accidents.

Figure 2-12 shows the finite element analysis model of the bottom nozzle. The maximum load applied to the bottom nozzle during a postulated accidents is conservatively assumed to be []^{TS}. The stress analysis result of bottom nozzle show that the stress intensity is []^{TS} for the []^{TS}. The allowable stress is []^{TS} for the postulated accident condition. Therefore, bottom nozzle integrity is maintained for the postulated accident condition including shipping & handling, normal operation, AOOs since the resultant stress for postulated accident condition is higher than other conditions.

(2) Prevention of fuel rod ejection

1) Basis

The fuel rod shall not be ejected out of fuel assembly.

2) Criteria

The bottom nozzle shall be designed fuel rods not to be ejected through the nozzle.

3) Evaluation

The bottom nozzle design provides optimal offset in the centerline of the fuel rod array and the nozzle's primary flow hole array. This offset prevents fuel rod ejection.

(3) Compatibility with the lower support structure

1) Basis

The bottom nozzle can mate with the lower support structure without interference.

2) Criteria

The bottom nozzle shall be acceptable with the lower internal by mating between the bottom nozzle and the lower support structure.

3) Evaluation

The geometrical compatibility between the bottom nozzle and the reactor lower internals was evaluated considering the worst dimension tolerances of the bottom nozzle and the reactor lower support structure. It was evaluated that the bottom nozzle maintained compatibility with the reactor lower internals.

(4) Compatibility with the instrument

1) Basis

Proper alignment with the in-core instrument will assure reliable function of core monitoring and protection.

2) Criteria

The bottom nozzle shall be dimensionally compatible with the in-core instrument while providing adequate cooling.

3) Evaluation

The bottom nozzle design employs a cylindrical, thick-walled instrument guide that directs the in-core instrument through the bottom nozzle plenum region, as shown in Figure 2-11. The inside diameter of the guide matches the outside diameter of the instrument. Chamfering is provided on the inner diameter at the guide's lower end for the lead-in of the instrument.

2.3.2 Top Nozzle

2.3.2.1 Description

As shown in Figure 2-13 and Figure 2-14, the top nozzle is composed of an adapter plate, four outer guide posts, a holddown plate, four helical holddown springs, and an instrument housing.

The outer guide posts are threaded externally at their lower ends for connection to the adapter plate and welded to the underside of the adapter plate against unlocking. The outer guide post provides a groove on its outside for crimping against unlocking.

The inner extension is inserted through the outer guide post, threaded into the guide thimble flange and crimped with outer guide post.

The holddown plate accommodates the fuel handling tool to the fuel assembly. The holddown plate is a key component of the top nozzle that prevent the fuel assembly lift-off by the holddown spring force occurring when the insert tube of the upper structure holds it down (Figures 2-7 and 2-13).

The instrument housing is attached at the center of the adapter plate by a threaded joint, and it accommodates and protects the in-core instrument.

2.3.2.2 Design Basis, Criteria and Evaluation

(1) Structural support of the fuel assembly

1) Basis

The top nozzle integrity is maintained for lateral and vertical loads from normal, AOOs, postulated accidents, and shipping & handling conditions.

2) Criteria

The top nozzle shall withstand lateral and vertical loads without exceeding the stress limits of Section 2.2.2.1.

3) Evaluation

Finite element analysis was performed to verify the mechanical integrity of the top nozzle for the loads from the fuel assembly shipping and handling as well as normal operation, AOOs and postulated accidents.

Figures 2-15 and 2-16 show the finite element analysis model of the top nozzle components. The maximum load applied to the top nozzle during a postulated accidents is conservatively assumed to be { }^{TS}. The stress analysis results of holddown plate show that the stress intensity is { }^{TS} and adapter plate is { }^{TS} for the { }^{TS}. The allowable stress is { }^{TS} for the postulated accident condition. Therefore, top nozzle integrity is maintained for the postulated accident condition including shipping & handling, normal operation, AOOs since the resultant stress for postulated accident condition is higher than the other conditions.

(2) Prevention of fuel rod ejection

1) Basis

The fuel rod shall not be ejected out of fuel assembly.

2) Criteria

The top nozzle shall be designed fuel rods not to be ejected through the nozzle.

3) Evaluation

The top nozzle design provides that ligaments are oriented above fuel rod centerlines preventing from fuel rod ejection and that the flow holes are offset laterally from the fuel rod horizontal position.

(3) Compatibility with the upper guide structure

1) Basis

The top nozzle can mate with the upper guide structure without interference.

2) Criteria

The top nozzle shall be acceptable with the upper internal by mating between the top nozzle and the upper guide structure.

3) Evaluation

The geometrical compatibility between the top nozzle and the reactor upper internals was evaluated, considering the worst dimensional tolerances of the top nozzle and the reactor upper guide structure. It was evaluated that the top nozzle maintained compatibility with the reactor upper internals.

(4) Remote reconstitutability

1) Basis

The fuel assembly design requires all necessary features to allow remote reconstitution at the plant site by removal of the top nozzle.

2) Criteria

The components of the top nozzle and fuel assembly must interface with each other such that smooth remote removal and replacement of the top nozzle can be performed. All parts removed during the reconstitution must be captured to preclude the loss of parts in the reactor. Adequate clearance must be provided after removal of the top nozzle to allow the removal of the fuel rods.

3) Evaluation

The top nozzle is disengaged from the fuel assembly by removing the four inner extensions and lifting the top nozzle off the guide thimble flanges. A sliding fit between the inner diameter of the outer guide post and the outer diameter of the inner extension is provided for smooth removal or replacement process.

(5) Compatibility with handling equipment

1) Basis

The top nozzle design must assure that proper handling and storage of new and irradiated fuel assemblies can be performed.

2) Criteria

The top nozzle design must ensure that the fuel assembly can be installed in fuel storage racks, fuel transfer equipment, fuel elevators, and in the core. All components of the top nozzle must be designed for proper fit-up with plant handling equipment.

3) Evaluation

All available information on the handling tools and procedures has been reviewed. The containment handling tool grapple was found to provide the most limiting fit with the top nozzle holddown plate. These interface dimensions of the top nozzle related the handling tools are identical to those of Guardian fuel.

2.3.3 Holddown Spring

2.3.3.1 Description

The holddown spring is designed to provide a sufficient holddown force for the fuel assembly in order not to lift-off during normal operation. As shown in Figure 2-13, the holddown coil spring of Inconel-718 surrounds the outer guide post and generates the holddown force.

2.3.3.2 Design Basis, Criteria and Evaluation

(1) Holddown force in normal operation

1) Basis

Fuel assembly lift-off during normal operating conditions can result in fuel assembly or core support structural damage. If lift-off occurs during normal operation, large amplitude fuel assembly oscillations could ensue. These oscillations can cause impact forces on the core structures and fuel assembly.

2) Criteria

The fuel assembly shall not lift-off the core support structure during the normal operation.

3) Evaluation

As explained in Section 2.2.2.3 and shown by the fuel assembly lift-off tests in the FACTS loop, the fuel assembly did not lift-off at normal operation (see Appendix A.2.9).

(2) Maximum deflection range and solid condition

1) Basis

Load of solid spring may cause improper load distribution through the top nozzle, and may have an adverse effect on the spring itself. The load of solid spring on the fuel assembly can cause extensive structural damage and subsequent fuel failure.

2) Criteria

The clearance between the holddown working height and spring solid height shall be maintained under normal operation.

3) Evaluation

The holddown working height was calculated based on the maximum fuel assembly growth. It was evaluated that the holddown working height is greater than the solid spring height.

(3) Holddown spring shear stress

1) Basis

The spring shear stress shall meet the ASME Boiler and Pressure Vessel Code.

2) Criteria

The spring shear stress for normal operation except lift-off shall be less than $0.8 S_m$.

3) Evaluation

A functional analysis of the fuel assembly holddown spring was performed to optimize the geometric configuration of the spring based on both holddown spring static stress and fatigue considerations. As a result of calculating the shear stresses, the maximum shear stress of the holddown spring was respectively calculated to be $\{\quad\}^{TS}$ at cold, $\{\quad\}^{TS}$ at hot. The results are less than the allowable design criteria which are $\{\quad\}^{TS}$ at cold, $\{\quad\}^{TS}$ at hot.

2.3.4 Guide Thimble and Instrument Tube

2.3.4.1 Description

As the structural components of the fuel assembly skeleton, four guide thimbles are located toward the corners of the square envelope and an instrument tube located at the center of the fuel assembly. The guide thimbles and the instrument tube guide the control element assembly, the neutron source rods, and the in-core instrument into the fuel assembly (See Figure 2-1).

As shown in Figure 2-17, the lower section of the guide thimble tube has a smaller diameter than the upper section. This design feature provides for hydraulic deceleration of CEAs during SCRAM to reduce impact forces on the upper guide structure. Two flow holes of guide thimbles accommodate cooling of the CEAs and the neutron source rods.

The upper portion of the guide thimble tube is welded to the internally threaded flange, which is attached to the top nozzle by an externally threaded inner extension inserted into the outer guide post. The internally threaded end plug is welded to the lower portion of the guide thimbles and the guide thimble screw is inserted into the end plug from the underside of the bottom nozzle, connecting the guide thimble tube to the bottom nozzle.

Two pairs of inward dimples, offset in a radial direction by 90° are formed on the instrument tube at each mid-span elevation. The 40 dimples formed axially along the instrument tube support the in-core instrument laterally when inserted into the instrument tube. The coolant flows through one flow hole of the instrument tube, cooling the in-core instrument.

2.3.4.2 Design Basis, Criteria and Evaluation

(1) Structural support of the fuel assembly

1) Basis

The guide thimble maintains its structural integrity for lateral and vertical loads from normal, AOOs, and shipping and handling conditions.

2) Criteria

The design criteria of guide thimble and instrument tube are same as the structural integrity design criteria of the fuel assembly described in Section 2.2.2.1.

3) Evaluation

The stress analysis result of guide thimble tube is $\{\quad\}^{TS}$ at shipping and handling condition and allowable stress is $\{\quad\}^{TS}$. Therefore, the guide thimble stress intensity is maintained for the

shipping and handling condition. Since the shipping and handling load is higher than that for the normal operation and AOOs, the resultant stress intensities are well within allowable limits.

The circumferential stress acting on the guide thimble tube from the pressure difference between inner and outer guide thimble tube around the dashpot region was evaluated to satisfy the stress design limit.

Assuming that the CEA drop occurs once a day conservatively, the guide thimble tube stress was calculated to be so small that the fatigue-induced guide thimble tube failure does not occur.

(2) CEA drop time

1) Basis

Plant reactivity control systems must be capable of reducing power within a maximum specified time to preclude fuel damage.

2) Criteria

The geometrical shape of the guide thimble tube shall meet the control rod drop time limit.

3) Evaluation

The CEA drop time depends on the geometrical configurations (the inner diameter of the guide thimble tube, the number of flow holes and their diameters, the control rod diameter), the CEA weight, and the fuel assembly pressure drop. The results of CEA scram analysis show that the CEA design meets the drop time and displacement limits, as shown in Figure 2-18. In addition, it is verified that scram analysis provides reasonable CEA drop time data, as described in Appendix C.

2.3.5 Grid

2.3.5.1 Description

The PLUS7 grids are composed of a top grid minimizing fuel rod bow due to fuel rod irradiation growth, a bottom grid preventing fuel rod failure due to fretting wear at high burnup, a protective grid enhancing the debris filtering efficiency, and nine mid grids with mixing vanes to improve thermal performance as a result of better coolant mixing. The design feature of each grid is described as follows.

(1) Top and bottom grids

Top and bottom grids are brazed among the inner straps, outer straps and sleeves, and have horizontal dimples in each grid cell to minimize pressure drops. Top and bottom grid have an anti-sag design to minimize adverse assembly interactions during core loading and unloading.

The spring force of the top grid is designed small enough to minimize the rod bow due to fuel rod irradiation growth. The spring force of the bottom grid is designed large enough to support the fuel rods sufficiently up to the target design burnup. The PLUS7 top and bottom Inconel grids are shown in Figures 2-5 and 2-19.

(2) Protective grid

The PLUS7 protective grid is located directly above the small-hole bottom nozzle for additional debris filtering. The protective grid also reduces the flow induced fuel rod fretting wear by supporting the end region of the fuel rod with the bottom grid.

The protective grid contains four dimples in each grid cell that provide a co-planar contact with the fuel rod bottom end plug. These dimples are combined with the long solid end plug and the small-hole bottom nozzle to provide multi-debris filtering capability (see Figures 2-6 and 2-20). As shown in Figure 2-6, the protective grid straps divide the round holes of the bottom nozzle into four equal parts and the slotted holes of the bottom nozzle into two equal parts. The debris captured by the protective grid cannot cause a fuel rod failure since the debris is to contact the long solid end plug instead of the cladding of the fuel rod.

Four washers are welded to the underside of the protective grid cells containing the guide thimbles. Then, the protective grid is attached to the bottom nozzle by the guide thimble screws through the washers.

(3) Mixing Vane Mid Grid

The PLUS7 mid grid has mixing vanes to increase the overpower margin by more than 10% (see Figures 2-3 and 2-4). The fluid-induced fuel assembly vibration may occur when hydraulic force balance in the fuel assembly is not achieved due to the asymmetrical mixing vane pattern of the mid grid. The mixing vane pattern of the PLUS7 mid grid is optimized to have hydraulic force balance.

The mid grid, like the top and the bottom grids, is designed to decrease the possibility of grid hang-up during the loading and unloading of fuel assembly.

As shown in Figures 2-4 and 2-21, the mid grid has conformal grid springs and dimples creating area contacts with the fuel rods, which can help prevent grid-to-rod fretting wear-induced fuel failure. The conformal shapes increase the fretting wear-induced fuel rod perforation time significantly since the area contact will result in less wear depth than the point or line contact even when the same wear volume is made.

Also, the seismic-resistance of the fuel assembly is largely improved due to a large increase in the buckling strength of the mid-grids due to the straight-shaped grid strap.

2.3.5.2 Design Basis, Criteria and Evaluation

(1) Fuel Rod Support

1) Basis

The grid shall support the fuel rod axially and laterally.

2) Criteria

The positive spring force of the bottom grid shall be maintained up to EOL.

3) Evaluation

The internal design criteria for the spring force of the PLUS7 bottom grid at EOL is conservatively set to $\left[\quad \right]^{TS}$. The evaluation results of the bottom grid spring forces of the PLUS7 fuel show that the spring force is larger than $\left[\quad \right]^{TS}$ at EOL.

(2) Shipping and Handling

1) Basis

The fuel should be designed to withstand shipping and handling loads without damage.

2) Criteria

The grid shall withstand 4g axial and 6g lateral accelerations without allowing the fuel rods to shift or the grid to permanently deform during the shipping and handling.

3) Evaluation

The grid should withstand 4g axial and 6g lateral accelerations without allowing the fuel rods to shift or the grid to permanently deform under the loads resulting from the design level of axial and lateral accelerations during the fuel assembly shipping and fuel assembly handling.

The frictional load associated with the spring force of the PLUS7 grids on fuel rod is greater than the axial load of 4g acceleration so that the fuel rods should not be shifted from the grids. The grid spring force is larger than the fuel rod lateral load by 6g acceleration. Therefore, the fuel rod lateral movement was evaluated to have been restrained.

The grid buckling test results (see Appendix A.2.3) indicated that the buckling strength was greater than the lateral load of 6g acceleration generated by the fuel rods' weight of the grid-to-grid span length. Therefore, the permanent deformation of the grid assembly was evaluated not to occur.

(3) Fuel Rod Fretting Wear

1) Basis

The fuel rods should not fail due to the grid-to-rod fretting wear caused by the fuel assembly-induced or the fuel rod-induced vibration during normal operation.

2) Criteria

The fuel rod should not fail due to fretting wear during fuel lifetime.

3) Evaluation

The fuel rods must not fail due to the grid-to-rod fretting wear caused by the fuel assembly-induced or the fuel rod-induced vibration during normal operation. The grid-to-rod fretting wear resistance performance can be verified by the following three kinds of verification tests:

- Fluid-induced fuel assembly vibration test
- 500-hour long-term wear-resistance test

The mixing vanes of the PLUS7 grids were arranged symmetrically to have the hydraulic balance for preventing the fluid-induced fuel assembly vibration. As shown in Figure 2-10, the PLUS7 fuel assembly vibration is very small over the range of flow rates of the plants.

The 500-hour long-term wear-resistance test results showed that the PLUS7 fuel did not generate the fretting wear-induced fuel failure for the fuel lifetime (see Appendices A.2.2 and D). Fuel rod fretting wear performance of PLUS7 fuel assembly was verified by successful operating experience without any fuel rod fretting wear failure for the fuel lifetime (see Section 4.3.1).

(4) Fuel Rod Bow

1) Basis

An excessive grid spring force may restrain the fuel rods from slipping, which may generate the fuel rod bow, making the fuel rod channel spacing smaller and subsequently overheating the fuel rods. Therefore, the grids shall accommodate the fuel rod length change caused by the thermal expansion and neutron irradiation growth without inducing unacceptable fuel rod bow.

2) Criteria

The grid shall not permit or cause rod bowing that exceeds the allowable limits for channel closure for the fuel assembly lifetime.

3) Evaluation

The fuel rod bow is used to determine if the Departure from Nucleate Boiling Ratio (DNBR) penalty is to be imposed or not. The DNBR penalty is not imposed if the reduction of the fuel rod channel spacing due to the fuel rod bow is less than $\left[\quad \right]^{TS}$ of the initial fuel rod channel spacing. As seen in the in-reactor irradiation test results in Section 4.2.4, the minimum fuel rod channel spacing measured after the three cycles operation is less than $\left[\quad \right]^{TS}$ of the initial fuel rod channel spacing. Therefore, PLUS7 fuel was evaluated to meet the fuel rod bow-related design criteria for the fuel lifetime.

(5) Mid Grid Buckling Strength

1) Basis

Core coolability and safe shutdown of the reactor should be maintained under the most limiting load on the mid grid assembly.

2) Criteria

The grids must provide a coolable geometry and allow the control rod insertion for the postulated accidents, such as seismic and LOCA.

3) Evaluation

Grid impact strength evaluation is performed in accordance with the NRC licensed CE methodology (Reference 2-1). Grid impact force associated with the seismic/LOCA is generated for the mid grid by analysis. Grid buckling strength was determined from dynamic impact testing for comparison with predicted grid impact force. Due to differences in the seismic/LOCA input to the analysis, the

implementation in specific plant will include a plant-specific analysis to confirm compliance with this criterion.

(6) Grid Width

1) Basis

The grid width will grow due to the neutron irradiation as the fuel burnup increases. This grid irradiation growth should not affect the fuel loading and unloading operation in the reactor core.

2) Criteria

An adequate space between the fuel assemblies should be maintained to load and unload the fuel assembly safely for the fuel lifetime.

3) Evaluation

With taking account of the increase in the grid width due to the neutron irradiation in the reactor core, an adequate space between the fuel assemblies should be maintained to load and unload the fuel assembly safely after irradiation. Also a proper guide chamfer should be provided on the outer grid strap to prevent the fuel failure caused by interferences between adjacent fuel assemblies during fuel handling.

The poolside examination (PSE) results of PLUS7 fuels confirmed that an adequate space between the fuel assemblies could be maintained after the three cycle irradiation (see Section 4.2.5). Furthermore, the designs of the grid guide tab, grid guide vane, and grid corner shape of PLUS7 fuel were based on the previous designs used successfully in commercial nuclear power plants. Therefore, there should be no fuel assembly interference-induced fuel failure (see Appendix A.2.6).

2.3.6 Joint and Connection

2.3.6.1 Description

(1) Top nozzle/guide thimble

As shown in Figure 2-14, the top nozzle/guide thimble are assembled such that the inner extension tube is inserted into the outer guide post and then threaded into the guide thimble flange, and the upper head of the inner extension tube is crimped on the upper part of the outer guide post to prevent un-torqueing due to vibration.

(2) Top grid/guide thimble/instrument tube

As shown in Figure 2-22, the top grid/guide thimble/instrument tube are assembled so that the sleeves of zirconium alloy located at the upper and the lower sides of the Inconel top grid are spot welded to the guide thimble tube and the instrument tube at four points positioned at intervals of 90° to fix the position of the Inconel top grid.

(3) Mid grid/guide thimble/instrument tube

As shown in Figure 2-22, the mid grid/guide thimble/instrument tube are assembled so that the sleeves of zirconium alloy laser-welded at the lower sides of the mid grid are spot welded to the

guide thimble tube and the instrument tube at four points positioned at intervals of 90° to fix the position of the mid grid.

(4) Bottom grid/guide thimble/instrument tube

As shown in Figure 2-23, the bottom grid/guide thimble/instrument tube are assembled so that the sleeves of zirconium alloy located at the upper and the lower sides of the bottom grid are spot welded to the guide thimble and the instrument tube at four points positioned at intervals of 90° to fix the position of the Inconel bottom grid.

(5) Bottom nozzle/protective grid/guide thimble

As shown in Figure 2-25, the bottom nozzle/protective grid/guide thimble are assembled so that the protective grid having welded washers are inserted between the bottom nozzle and the guide thimble end plugs, and then the guide thimble screws inserted from the lower side of the bottom nozzle are threaded into the guide thimble end plugs.

2.3.6.2 Design Basis, Criteria and Evaluation

(1) Top nozzle/guide thimble

1) Basis

The top nozzle/guide thimble joint and connections shall not be damaged under the loads of normal operation and AOOs.

2) Criteria

Under the loads of normal operation and AOOs, the top nozzle/guide thimble joint and connections shall not be damaged and must meet the following design criteria:

$$P_m \leq \text{a smaller value of } 0.9 S_y \text{ and } 2/3 S_u$$

$$\tau \leq 0.6 S_y$$

Where,

P_m = calculated primary membrane stress

τ = calculated primary shear stress

S_u = minimum ultimate tensile strength at unirradiated condition

S_y = minimum yield strength at unirradiated condition

3) Evaluation

The largest load acting on the top nozzle/guide thimble joint and connections is a preload caused by a torque occurring during the screw connection process. The maximum predicted stress intensity due to preload is calculated to be $\left\{ \right\}^{TS}$ which satisfies the allowable limit of $\left\{ \right\}^{TS}$.

(2) Grid/guide thimble/instrument tube

1) Basis

Dimensional stability of the fuel assembly must be maintained under operating, shipping, and handling conditions. The joint must remain intact under operating, shipping, and handling conditions. Since the spot-welds are not expected to yield significantly before failure, the design limits are based on failure loads.

2) Criteria

Under the loads of normal operation and AOOs, the grid/guide thimble/instrument tube joint and connections shall not be damaged.

3) Evaluation

The largest load acting on the grid/guide thimble welding point is a slip load at the fuel rod/grid interface caused by the difference in their thermal expansion. As a result of calculating the stress, it was evaluated to be far less than the weld strength of the grid/guide thimble connection measured by the test.

(3) Bottom nozzle/guide thimble

1) Basis

Fuel assembly dimensional stability must be maintained under shipping, handling, operating, and accident conditions. The lifting force requirement ensures that the joint can withstand the maximum possible force exerted on the fuel assembly by the fuel handling equipment during removal from the core.

2) Criteria

Under the loads of normal operation and AOOs, the bottom nozzle/guide thimble joint and connections shall not be damaged and must meet the following design criteria:

$$P_m \leq \text{a smaller value of } 0.9 S_y \text{ and } 2/3 S_u$$

$$\tau \leq 0.6 S_y$$

Where,

P_m = calculated primary membrane stress

τ = calculated primary shear stress

S_u = minimum ultimate tensile strength at unirradiated condition

S_y = minimum yield strength at unirradiated condition

3) Evaluation

The largest load acting on the bottom nozzle/guide thimble joint and connections is a preload caused by a torque occurring during the screw connection process. The maximum predicted stress intensity due to preload is calculated to be $\left(\frac{P}{A} \right)^{TS}$ which satisfies the allowable limit of $\left(\frac{P}{A} \right)^{TS}$.

Table 2-1 Comparison of Design Features of PLUS7, Guardian, and RFA Fuel

| Fuel Components | Guardian | PLUS7 | RFA |
|---------------------------------|----------|-------|-----|
| Fuel Assembly | | | |
| Overall assembly height, inches | | | |
| Fuel assembly weight, lbs | | | |
| Number of grids | | | |
| Fuel Rod | | | |
| Pellet diameter, inches | | | |
| Cladding I.D., inches | | | |
| Cladding O.D., inches | | | |
| Cladding Material | | | |
| Plenum Spring | | | |
| Fuel rod length, inches | | | |
| Axial Blanket | | | |
| Mid Grid | | | |
| Mixing Vane | | | |
| Strap Shape | | | |
| Spring/Dimple Shape | | | |
| Number / Material | | | |
| Top/Bottom Grid | | | |
| Mixing Vane | | | |
| Strap Shape | | | |
| Spring/Dimple Shape | | | |
| Material | | | |
| Top Nozzle | | | |
| Reconstitution | | | |
| Holddown Spring Material | | | |
| Bottom Nozzle | | | |
| Flow Hole shape | | | |
| Reconstitution | | | |
| Protective Grid | | | |
| Material | | | |
| IFM Grid | | | |
| Number/Material | | | |
| Guide Thimble | | | |
| Number of Diameter Steps | | | |
| Material | | | |
| Instrument Tube | | | |
| Material | | | |

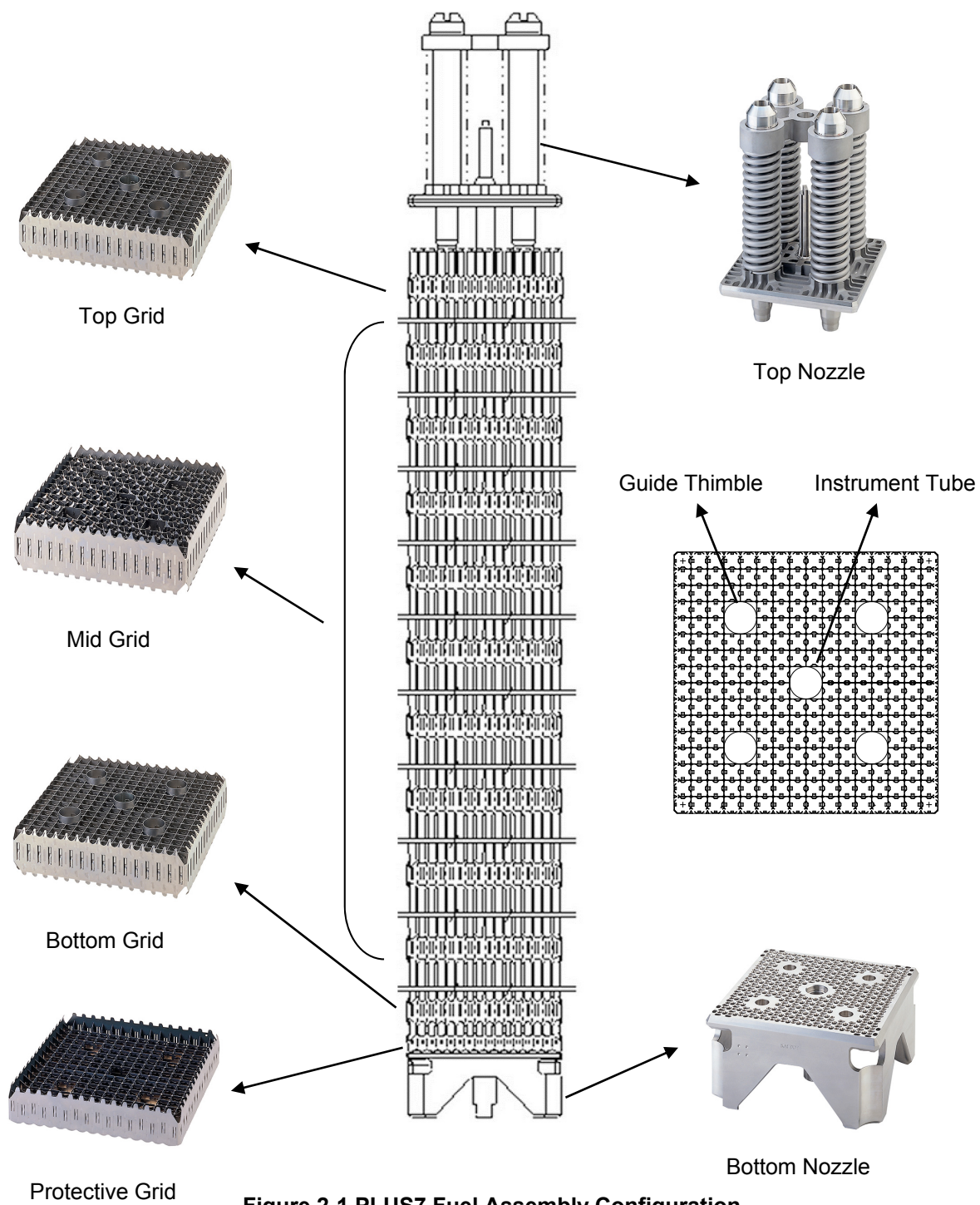


Figure 2-1 PLUS7 Fuel Assembly Configuration

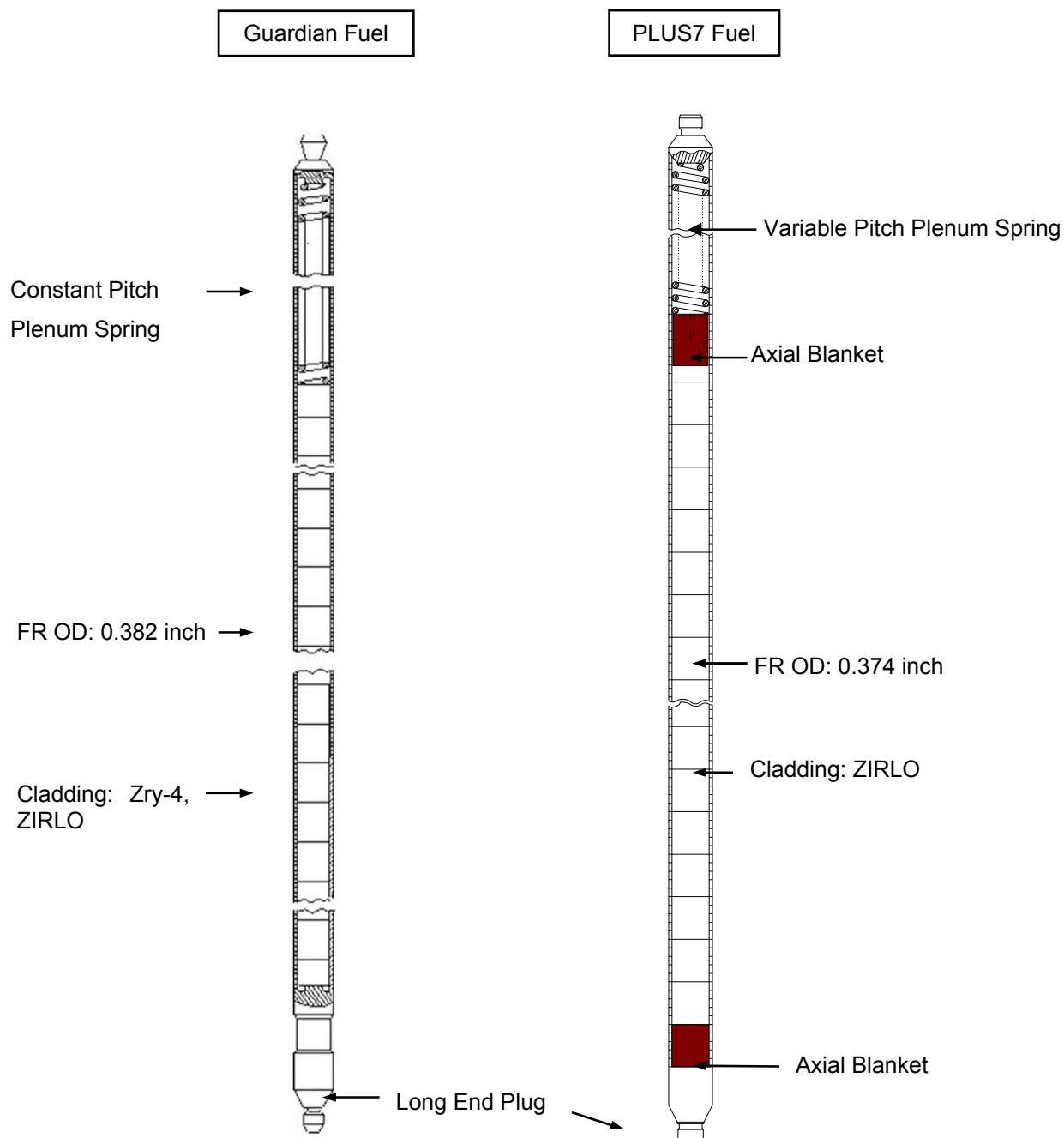


Figure 2-2 Comparison of Fuel Rod Designs

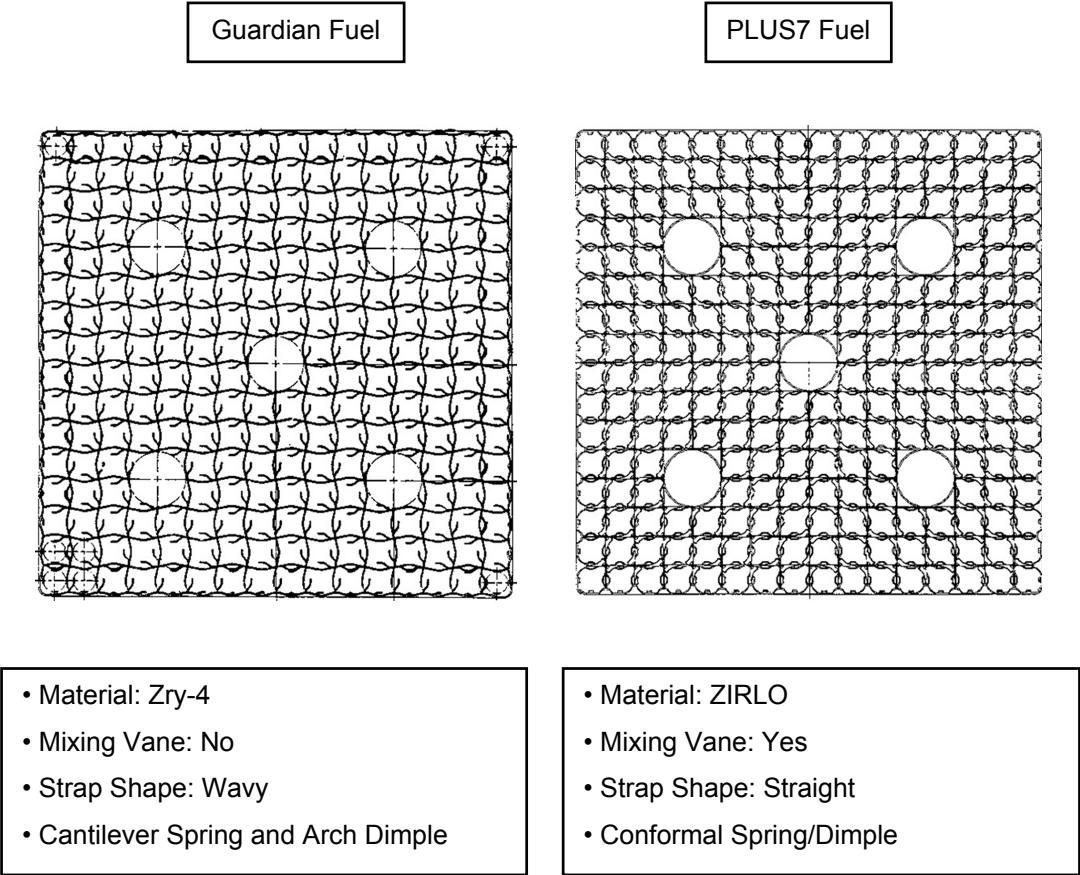


Figure 2-3 Mid Grid Designs

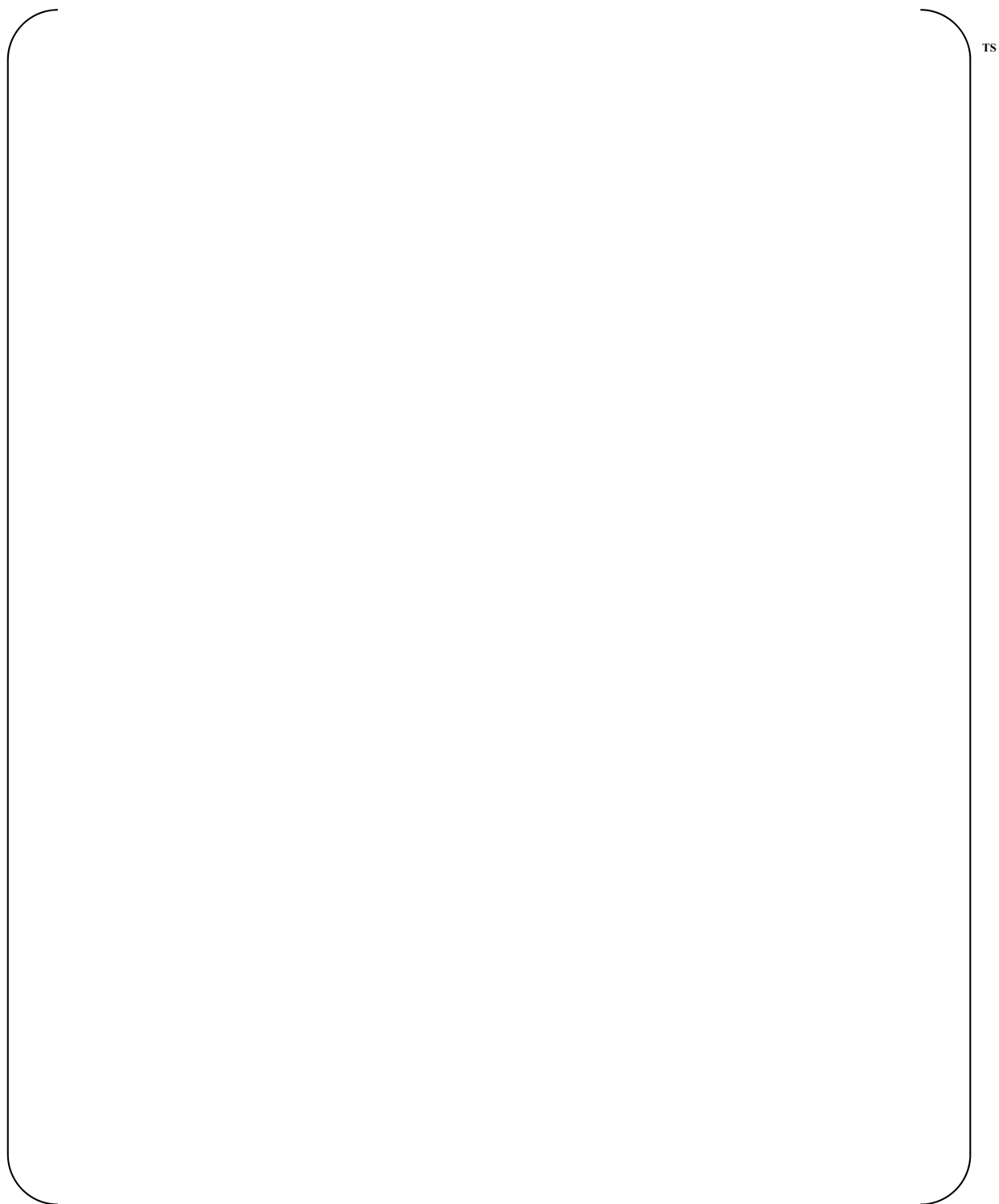
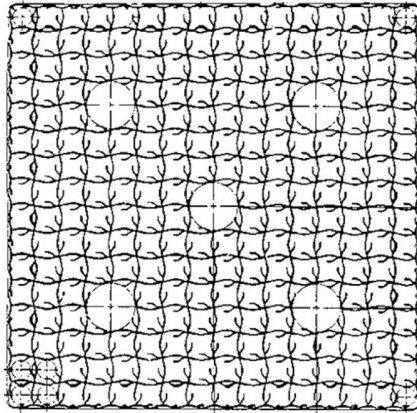
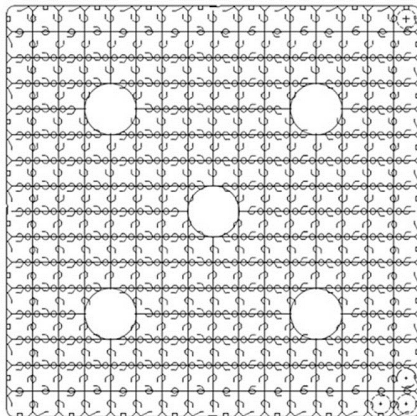


Figure 2-4 Spring and Dimple Configurations of PLUS7 Mid Grid

Guardian Fuel



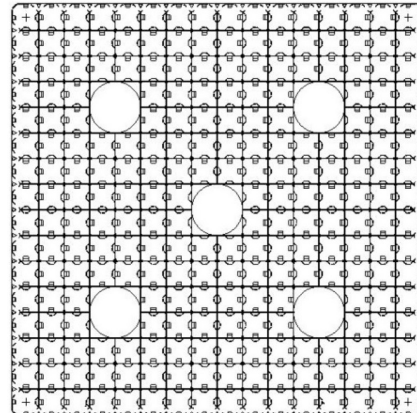
< Top Grid >



< Bottom Grid >

- Material
 - Top: Zry-4
 - Bottom: Inconel-625
- Mixing Vane: No
- Strap Shape:
 - Top: Wavy
 - Bottom: Straight
- Cantilever Spring and Arch Dimple

PLUS7 Fuel



< Top/Bottom Grid >

- Material
 - Top: Inconel-718
 - Bottom: Inconel-718
- Mixing Vane: No
- Strap Shape: Straight
- Vertical Spring and Horizontal Dimple

Figure 2-5 Comparison of Top and Bottom Grids

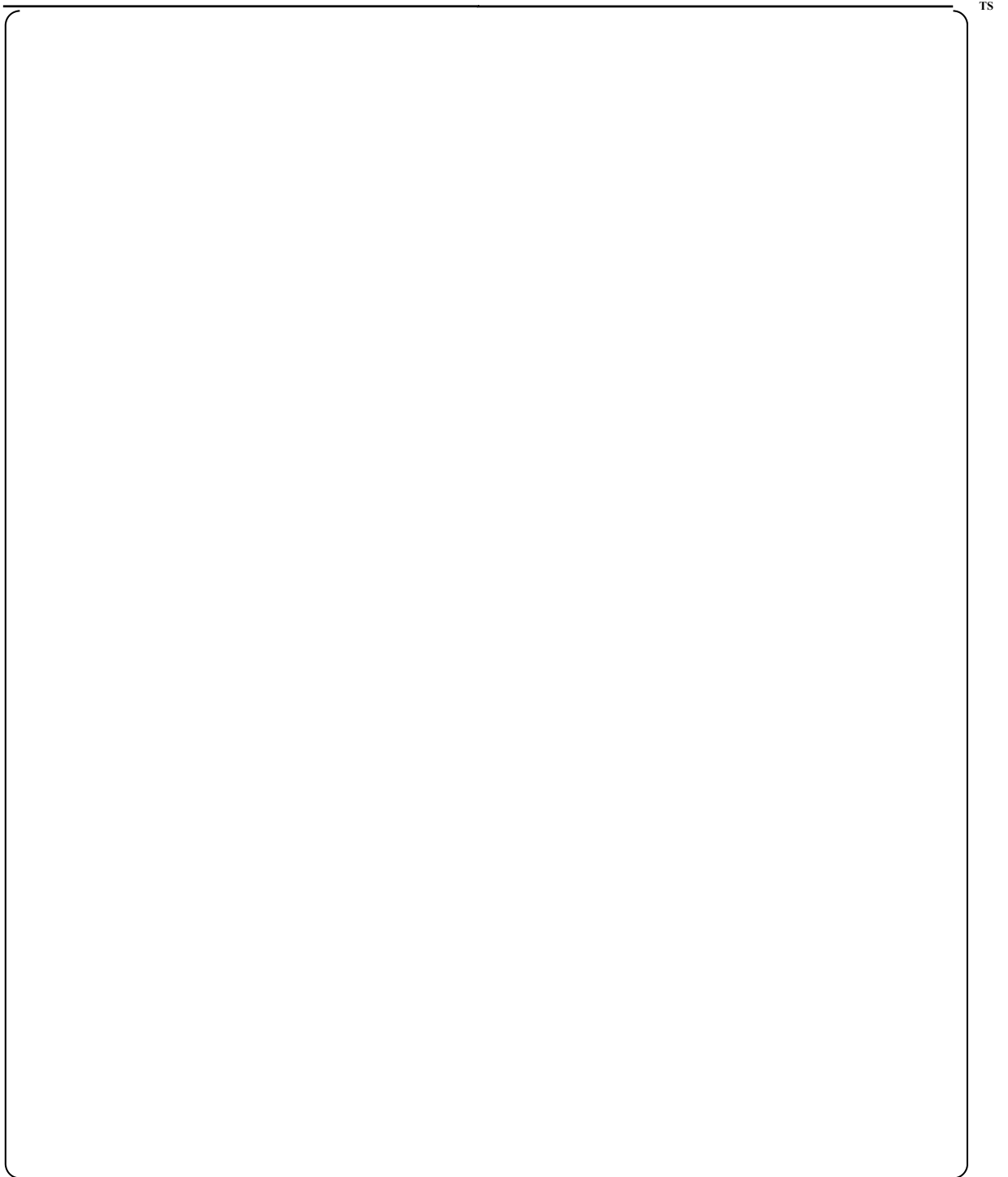


Figure 2-6 Debris Filtering Design of PLUS7

<Before Constituting Inner Extension>



TS

Figure 2-7 Reconstitutable Design of PLUS7 Top Nozzle

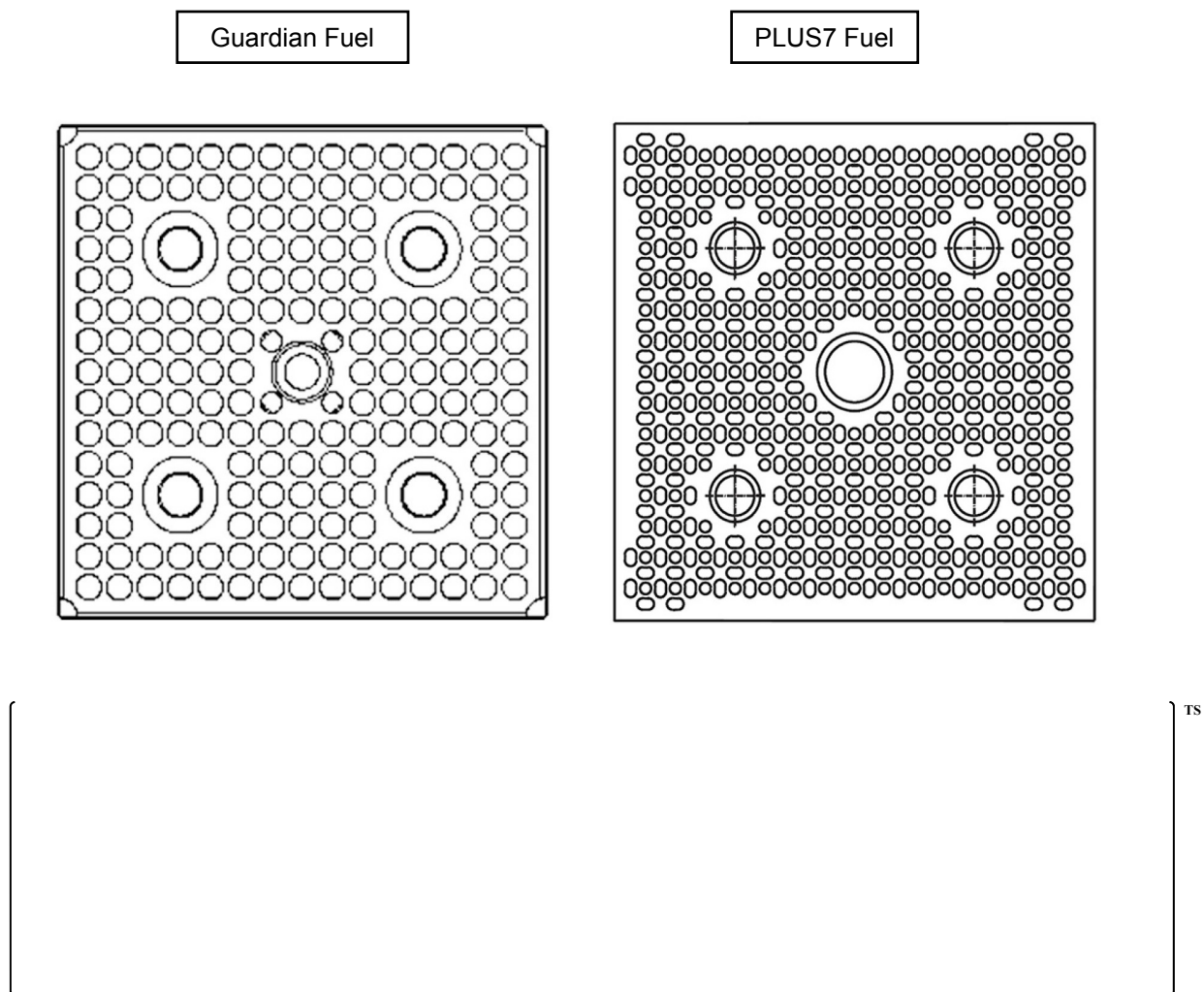


Figure 2-8 Comparison of Bottom Nozzles

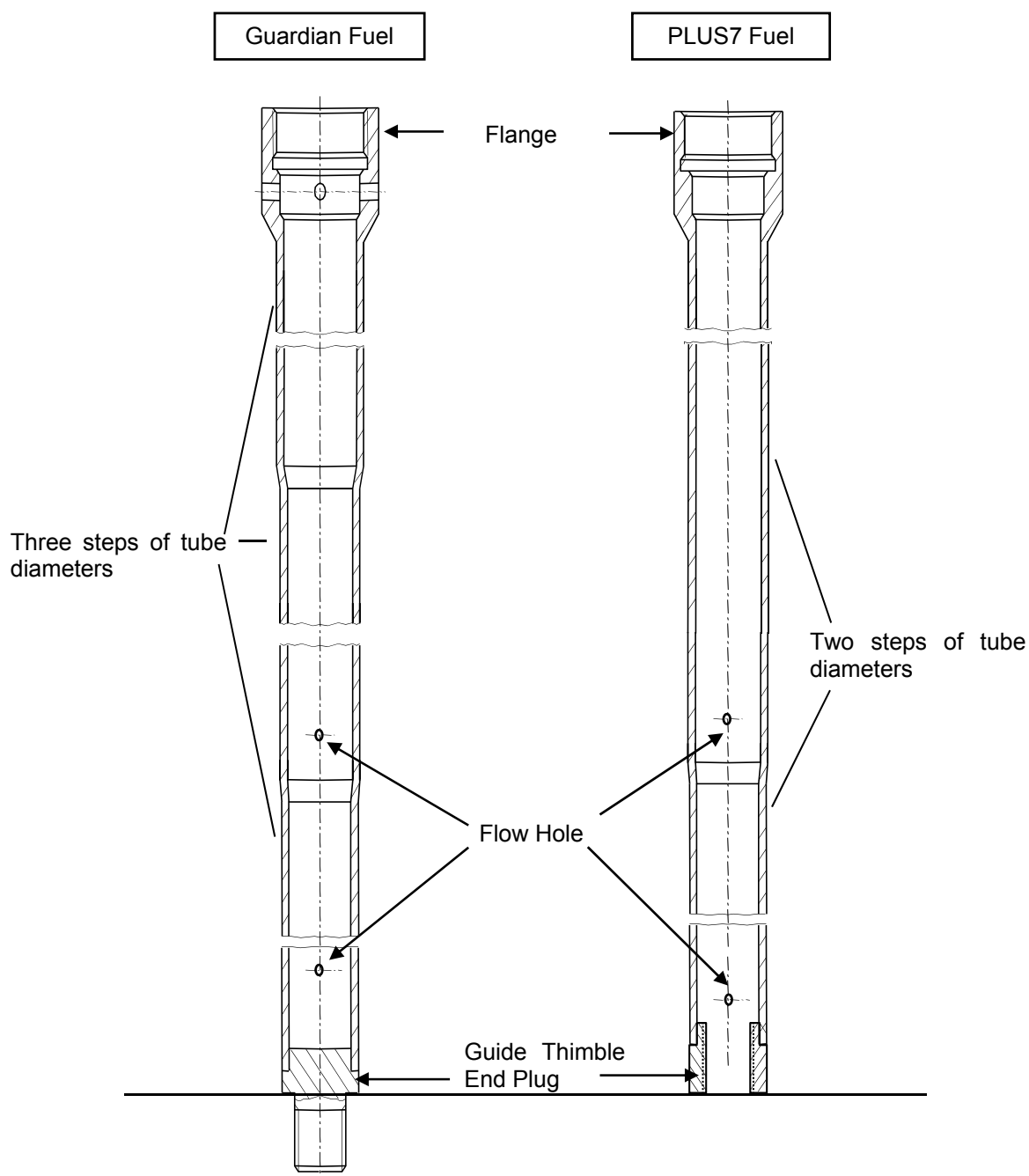


Figure 2-9 Comparison of Guide Thimbles



Figure 2-10 Vibration Test Results of PLUS7 Fuel Assembly

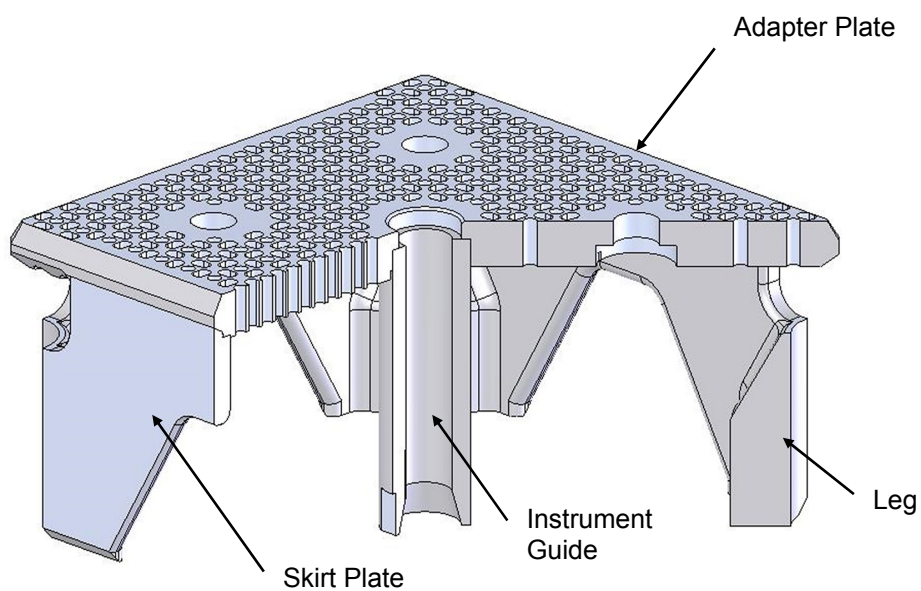


Figure 2-11 PLUS7 Bottom Nozzle

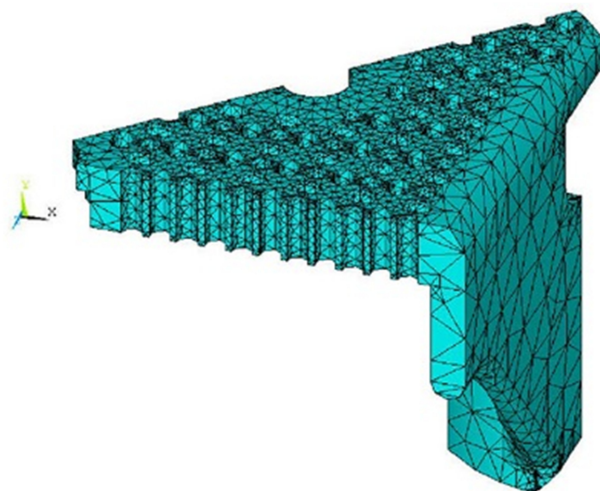
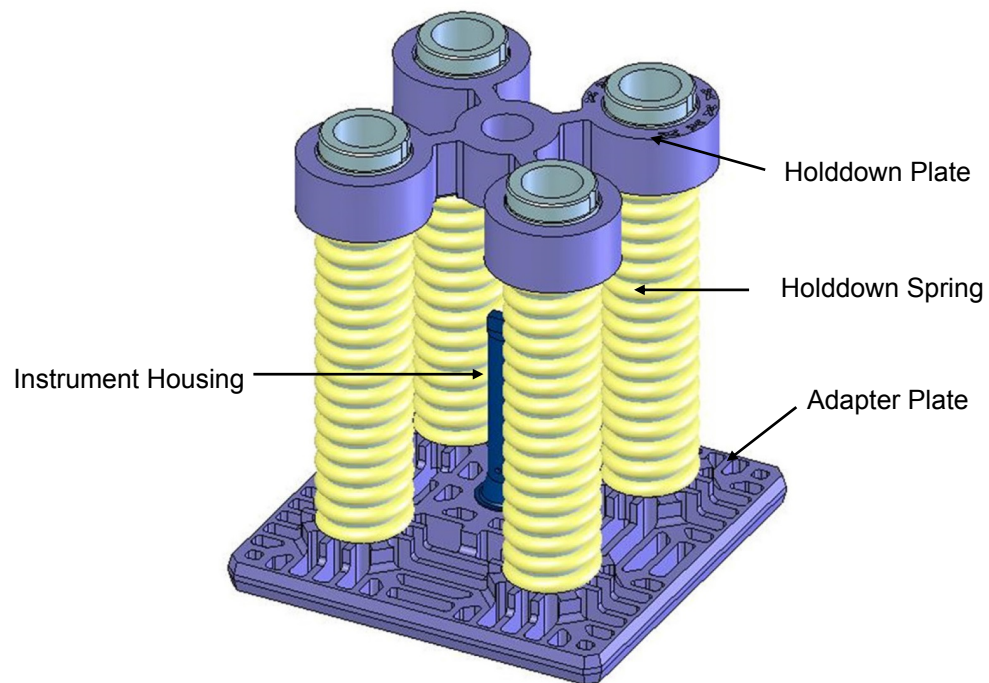
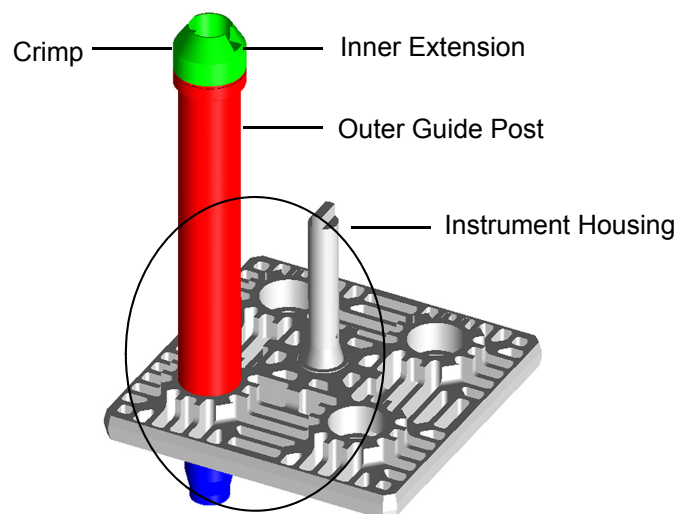


Figure 2-12 1/8 Bottom Nozzle Finite Element Model



TS

Figure 2-13 PLUS7 Top Nozzle



TS

Figure 2-14 PLUS7 Top Nozzle/Guide Thimble Joint & Connection

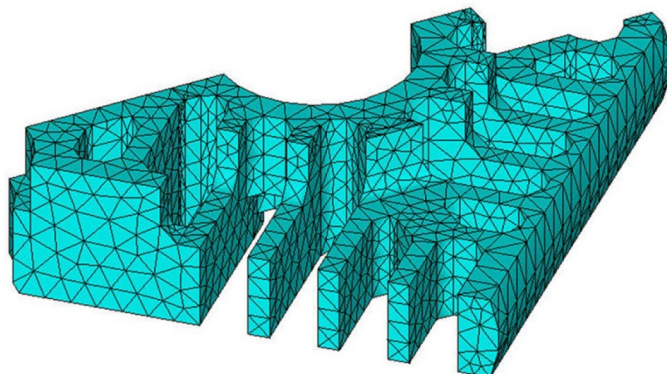


Figure 2-15 1/8 Top Nozzle Adapter Plate Finite Element Model

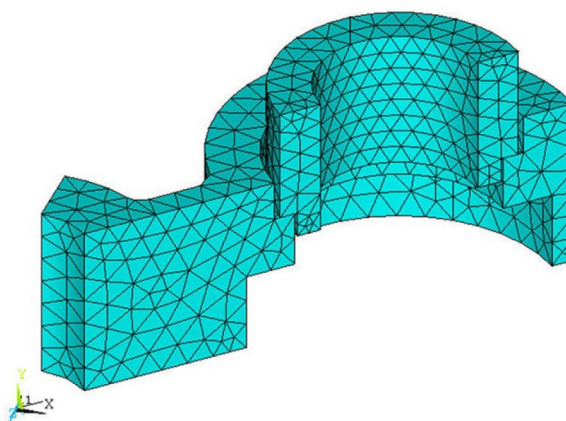


Figure 2-16 1/8 Top Nozzle Holddown Plate Finite Element Model

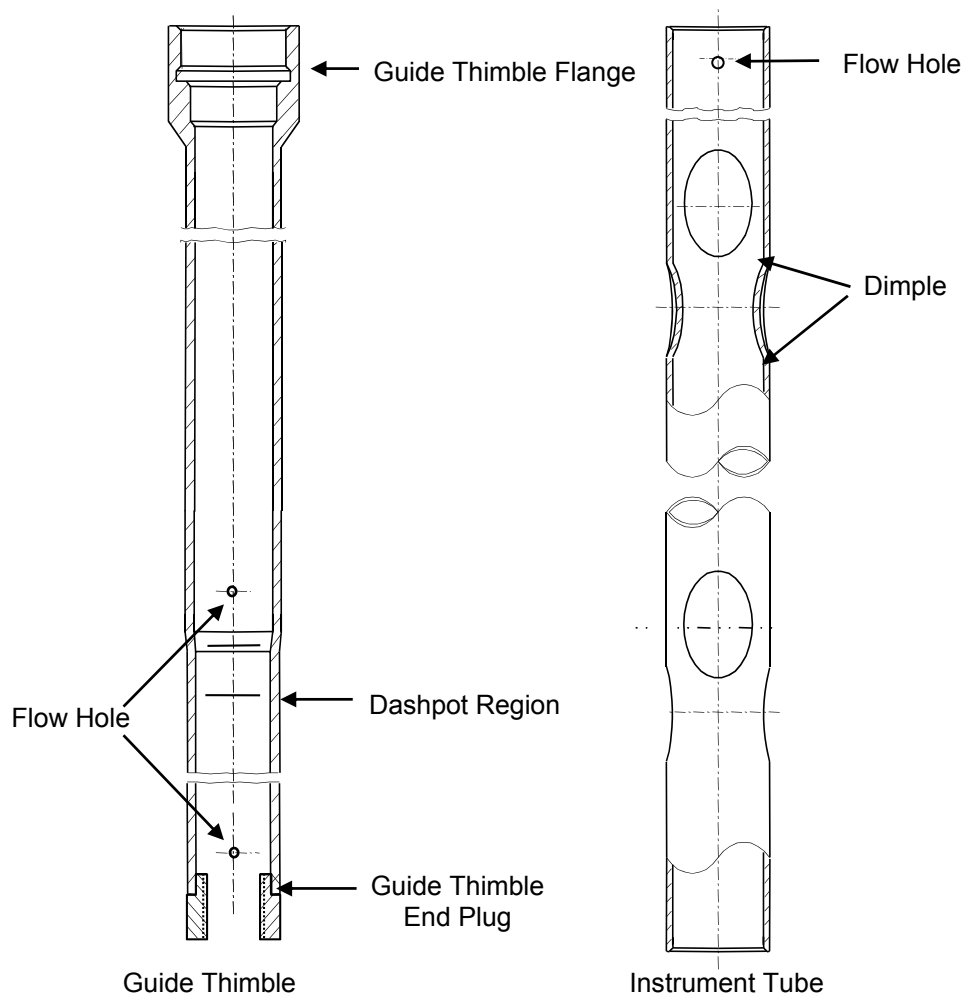


Figure 2-17 PLUS7 Guide Thimble and Instrument Tube



Figure 2-18 CEA Drop Time

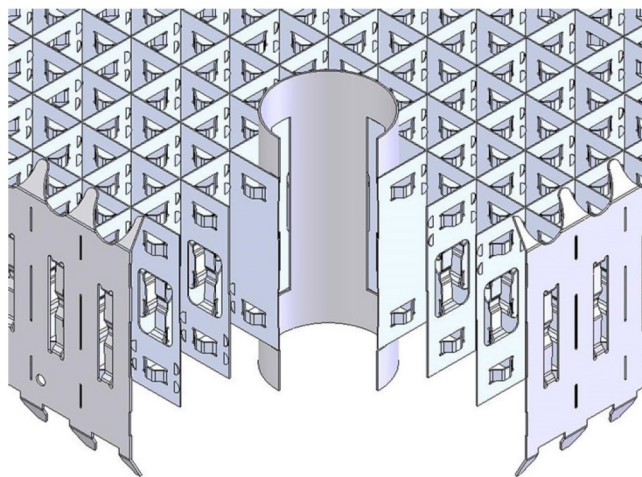


Figure 2-19 PLUS7 Top and Bottom Grid

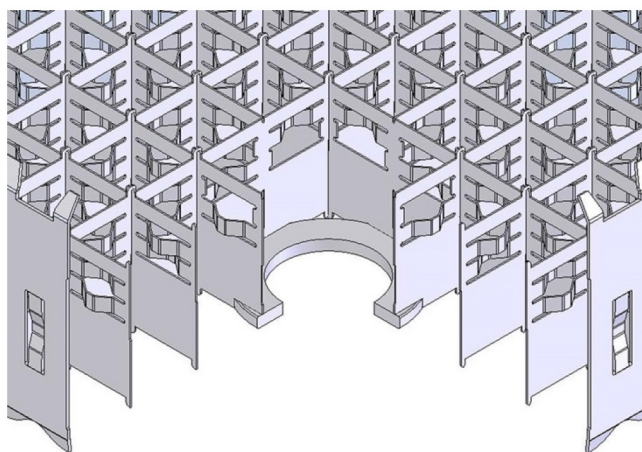


Figure 2-20 PLUS7 Protective Grid

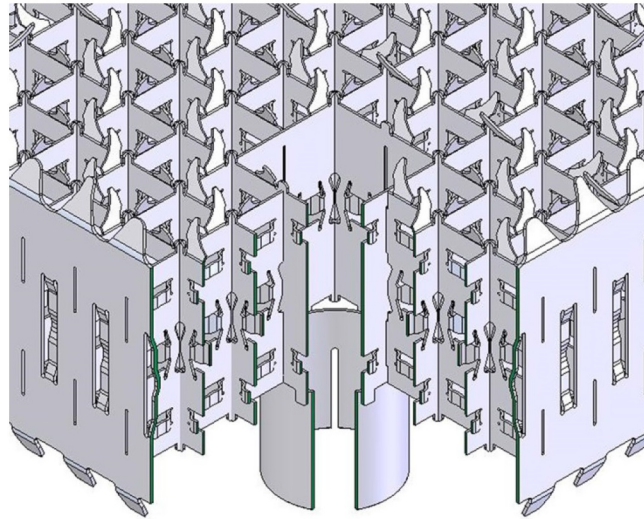


Figure 2-21 PLUS7 Mid Grid

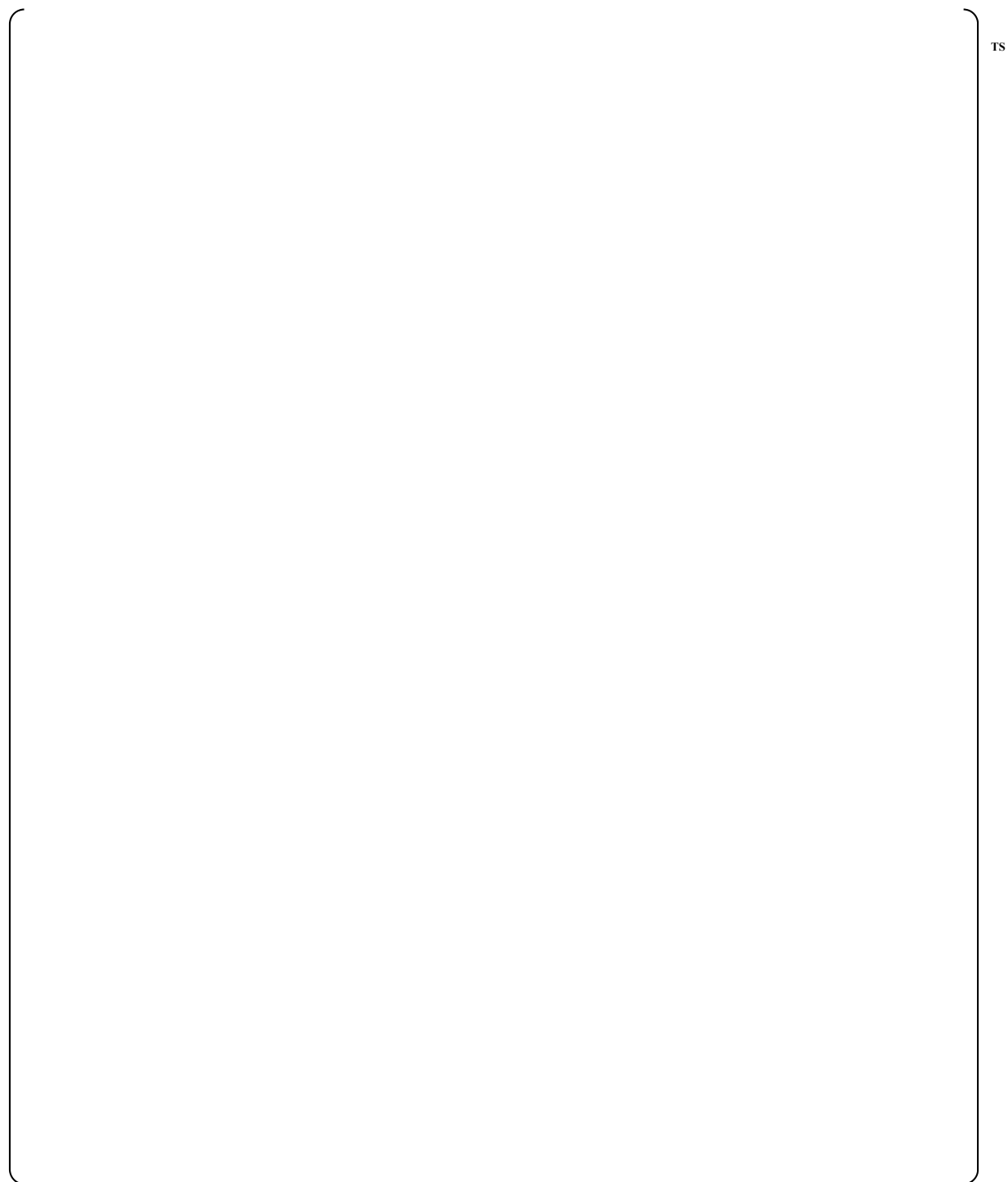


Figure 2-22 PLUS7 Grid/Guide Thimble and Instrument Tube Joint & Connection

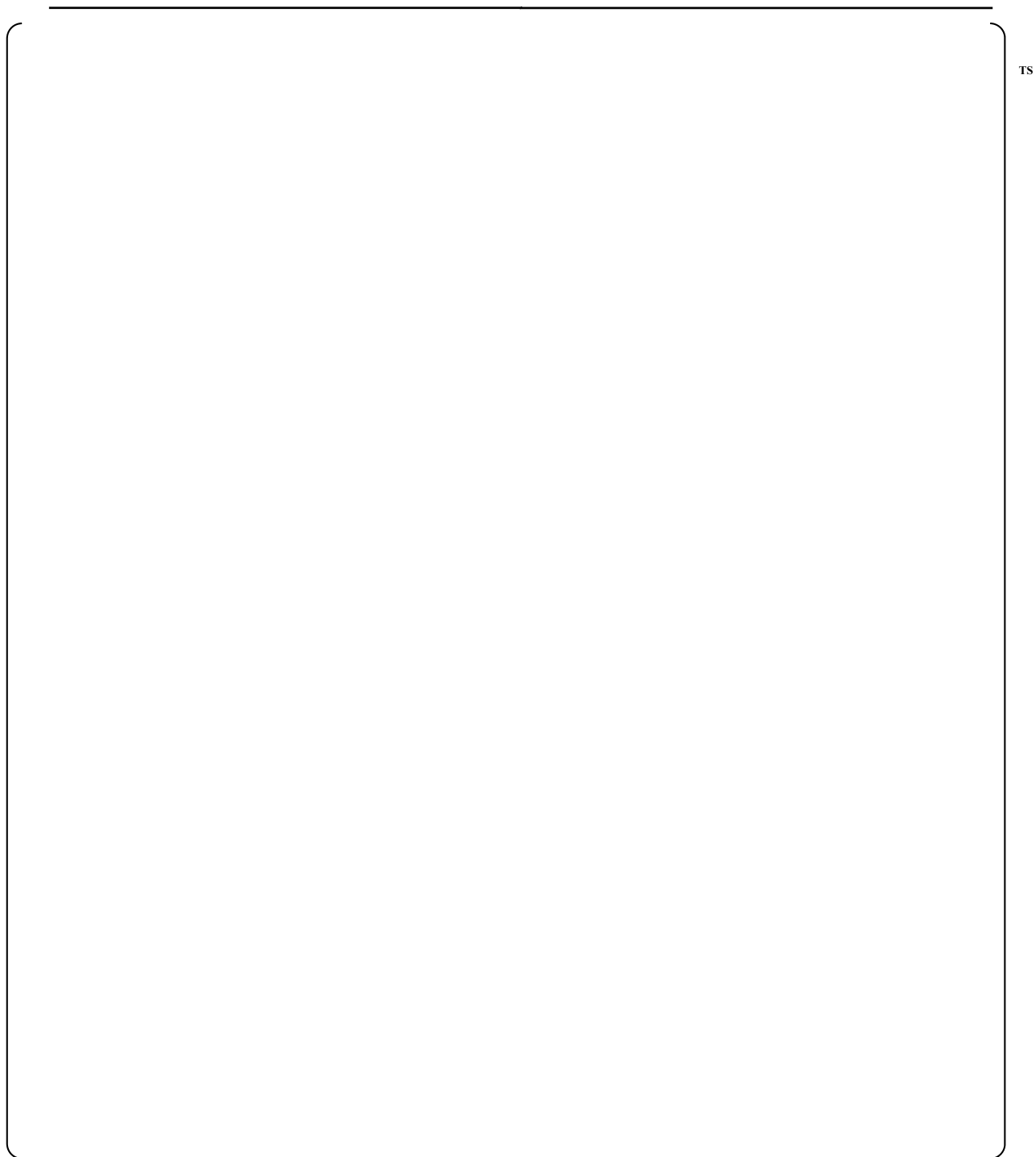


Figure 2-23 PLUS7 Bottom Grid/Guide Thimble and Instrument Tube Joint & Connection

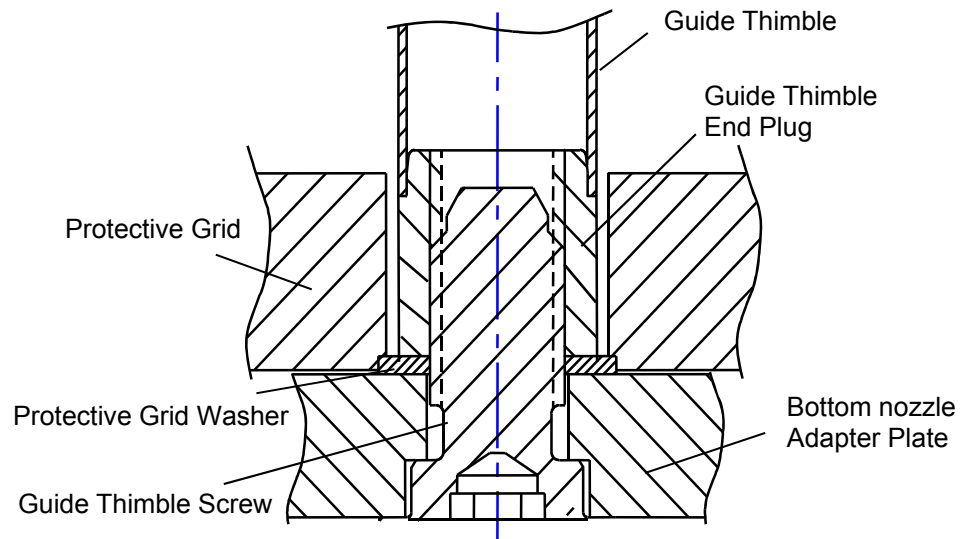


Figure 2-24 PLUS7 Bottom Nozzle and P-Grid/Guide Thimble Joint & Connection

3. FUEL ROD DESIGN

3.1 Overview

The PLUS7 fuel had been developed to improve the fuel performance against the Guardian fuel. Table 3-1 shows the design differences between the PLUS7 fuel rod and the Guardian fuel rod. The key design features of the PLUS7 fuel rod are summarized as follows:

- Fuel rod diameter of ()^{TS} to reduce the fuel rod-induced pressure drop and to enhance neutron economy
- Axial blankets (low enriched UO₂) at the top and bottom of the fuel stack region of the UO₂ fuel rod to reduce neutron leakage
- Gadolinia (Gd₂O₃-UO₂) fuel rod as a burnable absorber
- Optimized initial helium gas pressure of ()^{TS}
- Lower volume variable pitch plenum spring to increase void volume
- ZIRLO cladding to improve corrosion-resistance

The fuel rods consist of slightly enriched UO₂ cylindrical ceramic pellets and a round wire helical type 302 stainless steel compression spring, both encapsulated within a cladding and seal welded with Zircaloy-4 end caps. The fuel rods are internally pre-pressurized with helium during assembly. The pellets are dished at both ends in order to better accommodate thermal expansion and fuel swelling. The nominal density of the UO₂ pellets is ()^{TS} which corresponds to ()^{TS} of 10.96 g/cm³, the theoretical density of UO₂.

The cladding tube is Westinghouse's 1% niobium-tin-iron zirconium based alloy, ZIRLO, having a microstructure comprising second phase precipitates homogeneously distributed throughout the zirconium matrix. The upper end cap has external features to allow remote underwater fuel rod handling during repair and reconstitution work. The lower end cap has an external tip which is seized by the gripper during fuel rod loading. It is round to minimize chances of damage to the grid dimples, springs, or straps during installation or removal of the rod. Compression spring located at the top of the fuel pellet column maintains the column in its proper position during handling and shipping.

3.2 Design Basis, Criteria and Evaluation

Fuel system damage applies to normal operation and Anticipated Operational Occurrences (AOOs). To meet the requirements of General Design Criterion 10 as it relates to Specified Acceptable Fuel Design Limits for normal operation including AOOs, fuel system damage criteria should be given for all known damage mechanisms. Such damage criteria involve cladding stress, cladding strain, stress and loading limit for other than cladding, cladding fatigue, fretting wear, cladding oxidation/hydriding, dimensional change, fuel rod internal pressure and assembly lift-off.

Fuel rod failure applies to normal operation, AOOs, and postulated accidents. To meet the requirements of (a) General Design Criterion 10 as it relates to Specified Acceptable Fuel Design Limits for normal operation, including AOOs, and (b) 10 CFR Part 100 as it relates to fission product release for postulated accidents, fuel rod failure criteria should be given for all known fuel rod failure mechanisms. Such failure criteria involve fuel rod internal hydriding, cladding collapse, overheating of cladding, overheating of fuel pellets, excessive fuel enthalpy, pellet-to-cladding interaction, bursting and fuel rod mechanical fracturing.

Fuel coolability applies to postulated accidents. To meet the requirements of GDC 27 and 35 as they relate to control rod insertability and core coolability for postulated accidents, fuel coolability should be provided for all severe damage mechanisms. Fuel coolability criteria involves cladding embrittlement, violent expulsion of fuel, generalized cladding melting, fuel rod ballooning and structural deformation.

In this section, evaluations have been done to verify that the fuel rod design bases and criteria can be met for the PLUS7 fuel design. The fuel rod design criteria for cladding stress, cladding strain, cladding fatigue, cladding corrosion/hydriding, rod internal pressure, cladding collapse, overheating of fuel pellets, pellet-to-cladding interaction have been evaluated using the NRC approved Westinghouse fuel rod performance codes and methodologies (References 3-1 through 3-9, 3-12, 3-13). The codes applied for evaluating each fuel rod design criterion are summarized in Table 3-2.

The design bases and limits for PLUS7 fuel rod are the same as NRC approved design bases and limits for Westinghouse CE PWR fuel designs (Reference 3-10).

The stress and loading limit for other than cladding, fretting wear, dimensional change, assembly lift-off, rod mechanical fracturing and structural deformation are described in Chapter 2. The criteria and evaluations related to safety analyses will be described in DCD Chapter 15 in detail.

3.2.1 Cladding Stress

(1) Basis

A fuel system will not be damaged due to excessive stress under normal operation including AOOs.

(2) Criteria

During normal operation and AOOs, primary tensile stress in the clad and the end cap welds must not exceed $\left[\frac{S_y}{F} \right]^{TS}$ at the applicable temperature.

During normal operation and AOOs, primary compressive stress in the clad and the end cap welds must not exceed $\left[\frac{S_y}{F} \right]^{TS}$ at the applicable temperature.

Even though the cladding yield strength increases due to the fast neutron flux during irradiation, the unirradiated cladding yield strength is conservatively used as the cladding stress design criterion.

(3) Evaluation

The evaluation methodology for the fuel rod stress is discussed in Reference 3-5, which was reviewed and approved by the NRC for Westinghouse CE PWR fuel designs.

The rod internal pressures used to perform the stress analyses of the fuel rod designs accounts for power dependent and time dependent changes (e.g., fuel rod void volume, fission gas release and gas temperature, differential cladding pressure, cladding creep and thermal expansion) that can affect stresses in the fuel rod cladding. The rod external pressures are consistent with the event being analyzed and are biased in the conservative direction (maximum for compressive stresses, minimum for tensile stresses). The maximum tensile and compressive stresses were calculated for

normal operation involving fuel handling and storage, reactor servicing, power operation and reactor trip, heatup and cooldown, and minor fuel handling accident using the standard formulas.

The stress analyses for AOOs such as “Inadvertent Opening of an Atmospheric Dump Valve”, “Uncontrolled CEA Withdrawal at Power”, “Total Loss of Reactor Coolant Flow and “Loss of Condenser Vacuum” events were performed using the FATES3B code [3-1 through 3-4].

The results of the evaluation indicate that the primary tensile and compressive stresses in the cladding and end cap welds are within the allowable limits as shown in Table 3-3.

3.2.2 Cladding Strain

(1) Basis

Fuel system will not be damaged due to excessive strain under normal operation including AOOs.

(2) Criteria

At any time during the fuel rod lifetime, the net unrecoverable circumferential tensile cladding strain shall not exceed $\left[\right]^{TS}$ based on the beginning-of-life (BOL) cladding dimensions. This criterion is applicable to normal operating conditions and following a single AOO.

The total (elastic plus plastic) circumferential cladding strain increment produced as a result of a single AOO shall not exceed $\left[\right]^{TS}$ relative to the pre-transient condition.

Ductility is a function of irradiation and hydride formation in the cladding wall. Because the waterside corrosion for ZIRLO is significantly lower and should result in less hydrogen uptake and less hydride formation, total strain capability of ZIRLO is projected to be in excess of $\left[\right]^{TS}$ at burnups of 60,000 MWD/MTU. Thus, a $\left[\right]^{TS}$ strain limit will continue to be applied as a strain criterion.

(3) Evaluation

The evaluation methodology for the fuel rod cladding strain is discussed in Reference 3-5, which was reviewed and approved by NRC for Westinghouse CE PWR fuel designs.

The first part of the strain limit concerns that the total plastic strain incurred as a result of cladding creep and cladding yielding during long term normal operation and the following short transient conditions. Cladding creep strain and plastic strain due to cladding yielding are driven by the stress in the cladding that results from differential pressure and interface with the fuel pellets. The method used to evaluate the strain accounts for power dependent and time dependent changes (e.g., fuel rod void volume, fission gas release and gas temperature, differential cladding, cladding creep and thermal expansion) that can produce strain in the fuel cladding. In addition, the strain analysis accounts for both long term, normal operating condition, and short term, transient condition.

For the present application, the predicted plastic strain using FATES3B code is $\left[\right]^{TS}$ and the total (elastic plus plastic) circumferential cladding strain increment produced as a result of a single AOO is $\left[\right]^{TS}$. As the calculated strains are less than $\left[\right]^{TS}$ the design criteria are satisfied.

3.2.3 Cladding Fatigue**(1) Basis**

Fuel system will not be damaged due to excessive fatigue under normal operation.

(2) Criteria

For the number and type of transients which occur during normal operation, end-of-life (EOL) cumulative fatigue damage in the cladding must be less than $\left(\frac{1}{2} \right)^{TS}$.

A fatigue analysis for the ZIRLO cladding is performed using the Langer-O'Donnell fatigue design curve. A safety factor of 2 on the stress or a safety factor of 20 on the number of cycles is imposed on this curve conservatively. The fatigue damage is defined as the ratio of the number of calculated cycles in a given strain range to the permitted number of cycles determined by fatigue curve at strain range.

(3) Evaluation

The method used for fatigue analysis of fuel rod accounts for power dependent and time dependent changes (e.g., rod void volume, fission gas release and gas temperature, cladding creep and thermal expansion, and pellet swelling and thermal expansion) that can produce cyclic straining of the fuel cladding. With respect to determining changes in cladding and pellet diameters, the methodology used to evaluate the fatigue damage from power cycling is the same for the strain evaluation during normal operation, except that some of the parameters are biased in the opposite direction to provide results that are conservative for fatigue analysis.

The number of load cycles assumed in the fatigue evaluation is defined below for startup/shutdown, power variations and reactor trip during normal operation. The stress amplitudes for the cyclic loads are calculated using the FATES3B code.

a) Startup/shutdown

A startup/shutdown cycle is defined as the change from the 0% cold stand-by-state to the 0% hot stand-by state. $\left(\frac{1}{2} \right)^{TS}$ startups/shutdowns between 0% power and room temperature conditions are considered for fatigue evaluation.

b) Power variation during normal operation

Load follow operation is the most limiting condition of normal operation for fatigue evaluation. The power variation for load following is conservatively assumed to vary between 10% and 100% on a daily basis, and for each day.

c) Reactor Trip

The limiting condition for power change due to the AOOs is the reactor trip from 100 power to hot condition, conservatively. $\left(\frac{1}{2} \right)^{TS}$ reactor trips are considered for fatigue evaluation.

The total cumulative fatigue damage factor from power cycling, reactor trips and startups/shutdowns is $\left(\frac{1}{2} \right)^{TS}$, which is below the limit of $\left(\frac{1}{2} \right)^{TS}$. It was demonstrated that the fuel rod fatigue criterion was satisfied.

3.2.4 Cladding Oxidation and Hydriding**(1) Basis**

Fuel system will not be damaged due to excessive oxidation under normal operation including AOOs.

(2) Criteria

The best estimate cladding oxide thickness shall be less than $\{ \quad \}^{TS}$

The clad hydrogen pickup is limited to $\{ \quad \}^{TS}$ at EOL to preclude loss of ductility due to hydrogen embrittlement by formation of zirconium hydride platelets.

(3) Evaluation

The cladding oxide thickness and hydrogen content of the PLUS7 fuel rod are evaluated by the same methodology and model as are used for Westinghouse PWR fuel rod designs. The best estimate oxide thickness and hydrogen content at the end of irradiation are calculated with NRC approved PAD code [3-11] during normal operation. Since cladding oxide thickness and hydrogen content do not increase during AOOs due to short time, it is not necessary to consider the AOOs for oxide thickness and hydrogen content.

The following parameters were used for evaluation.

- a) Nominal design inlet temperature, system pressure, and core mass velocity based on Thermal Design Flow Rate
- b) A crud thickness of $\{ \quad \}^{TS}$
- c) A ZrO_2 thermal conductivity of $\{ \quad \}^{TS}$

The maximum cladding thickness and hydrogen content up to rod average burnup of 60,000 MWD/MTU for APR1400 are 69.4 μm and 554.3 ppm, respectively. The criteria of cladding oxide thickness and hydrogen content are satisfied.

3.2.5 Fuel Rod Internal Pressure**(1) Basis**

Fuel system will not be damaged due to excessive rod internal pressure under normal operation.

(2) Criteria

The fuel rod internal hot gas pressure shall not exceed the critical maximum pressure determined to cause an outward clad creep rate that is in excess of the fuel radial growth rate anywhere locally along the entire active fuel length of the fuel rod.

Reorientation of the hydrides in the radial direction in the cladding shall not occur.

The radiological dose consequences of DNB failures shall remain within the specified limits.

(3) Evaluation

FATES3B was used to calculate the rod internal pressure and corresponding critical limit according to the NRC approved methodology described in Reference 3-6. Where appropriate, the approved gadolinia methodology of References 3-7 and 3-8 has been applied. The critical limit is the internal hot gas pressure at which the outward tensile creep rate of the cladding exceeds the fuel pellet radial growth rate due to fuel swelling, thus creating any potentially damaging effects on the fuel rod due to detrimental thermal feedback effects within the fuel rod during normal operation.

Maximum rod internal pressure is calculated using conservative biasing of nominal fuel rod data including cladding outer diameter, cladding inner diameter, pellet outer diameter, active fuel length, fill gas pressure and will usually include additional conservatisms in the power levels representing each successive cycle of projected residency in the reactor core. The input power history to the code is important for rod internal pressure calculation. The methodology and conservatism for determining the rod power history are described in Reference 3-9. The main parameters and rod power histories considered in representative fuel rod internal pressure calculation are summarized in Table 3-4 and Figure 3-1, respectively.

The evaluation shows that the maximum rod internal pressures are $\{ \quad \}^{TS}$ and $\{ \quad \}^{TS}$ for the UO_2 fuel rod and $Gd_2O_3-UO_2$ burnable absorber fuel rod, respectively. Therefore, no clad lift-off (NCLO) criterion is satisfied since the calculated gas pressures are less than the system pressure. FATES3B code calculates the critical pressure limit to prevent clad lift-off only when the rod internal pressure exceeds the system pressure.

DNB propagation evaluations for transients and DNB accidents are performed using the NRC approved methodology with INTEG code, which is a standalone computer code to predict fuel rod deformation and burst behavior under conditions of DNB (Reference 3-6).

The time-dependent DNB transient local properties are obtained from the appropriate transient analysis methodology for any given plant. These inputs include time, heat flux, quality, mass flow, system pressure, rod internal pressure, and fuel rod initial geometry. To evaluate the potential for DNB propagation, the limiting DNB transients and internal pressure of $\{ \quad \}^{TS}$ are applied.

The results indicate that the clad strains induced by high temperature creep for limiting transients are less than $\{ \quad \}^{TS}$. This amount of strain does not induce DNB propagation to adjacent fuel rods.

Finally, hydride reorientation does not occur at internal pressure of $\{ \quad \}^{TS}$, which is well above the predicted rod internal pressure of $\{ \quad \}^{TS}$ on PLUS7 fuel (Reference 3-6).

3.2.6 Internal Hydriding**(1) Basis**

Fuel system will not be damaged due to excessive hydriding.

(2) Criteria

Primary hydriding is prevented by maintaining the level of moisture very low during the pellet manufacturing. The moisture content shall remain below the limit of 2.0 ppm (hydrogen from all sources for fuel pellets).

(3) Evaluation

The hydrogen levels in the fuel pellet are maintained at very lower than the design criterion through manufacturing process controls. Current PLUS7 fuel pellets have a total hydrogen content of less than { }^{TS} at 95% confidence. As a result of these controls, the failures due to internal hydriding have not experienced for PLUS7 fuel.

3.2.7 Cladding Collapse**(1) Basis**

Fuel rod failure will not occur due to cladding collapse.

(2) Criteria

The time required for the radial buckling of the clad in any fuel rod must exceed the reactor operating time necessary for the appropriate fuel batch to accumulate its design average burnup. This criterion must be satisfied for continuous reactor operation at any reasonable power level and during normal operating condition and AOOs. It will be considered satisfied if it can be demonstrated that axial gaps longer than { }^{TS} will not occur between fuel pellets and that the plenum spring radial support capacity is sufficient to prevent clad collapse under all design conditions.

(3) Evaluation

The evaluation of the cladding collapse accounts for power dependent and time dependent changes (e.g., differential cladding pressures, cladding temperature, cladding flux, and cladding thinning due to oxidation) that can affect the ovalization of the cladding during operation. The methodology for the cladding creep analysis is described in References 3-12 and 3-13, which was approved by the NRC. The methodology involves the use of the CEPANFL code which calculates cladding ovality as a function of time until the rate of ovality increases becomes excessive. To predict the minimum collapse time, the BOL cladding properties of midwall radius, wall thickness, and ovality are defined based on worst case drawing dimensions. In addition, oxide thickness as a function of time is defined. The time dependent operating conditions include the differential pressure across the cladding (based on a conservative minimum rod internal pressure history from the FATES3B code), cladding temperature, and fast neutron flux.

The evaluation results of the cladding collapse using CEPANFL in the active region indicate that the cladding collapse does not occur for both UO₂ fuel rod and Gd₂O₃-UO₂ burnable absorber fuel rod during entire fuel lifetime of { }^{TS}. The evaluation of cladding collapse in the plenum region demonstrated that PLUS7 plenum spring design provides sufficient radial support to the cladding to preclude collapse.

On the basis of the operating experience of PLUS7 fuel, cladding collapse does not occur for fuel rods with initial fuel pellet density of 95 percent theoretical density(T.D) or greater and having initial fuel rod pressurization with helium. Maintaining current pellet fabrication process controls with initial pellet density of 95 percent T.D or greater and with current initial helium pressurization levels is therefore sufficient to prevent cladding collapse.

3.2.8 Overheating of Cladding

(1) Basis

Fuel rod failure will not occur due to the overheating of cladding under normal operation including AOOs.

(2) Criteria

There should be a 95% probability at the 95% confidence level that a hot fuel rod in the reactor core will not experience a DNB during normal operation or AOOs. For postulated accidents, the rods that experience DNB are assumed to fail for radiological dose calculation purposes.

(3) Evaluation

The evaluation for overheating cladding is addressed in plant specific transient and accident analysis (Chapter 15 of DCD).

3.2.9 Overheating of Fuel Pellets**1) Basis**

Fuel rod failure will not occur due to the overheating of fuel pellets under normal operation including AOOs. For postulated accidents, the total number of rods that experience centerline melting should be considered for radiological dose calculation.

(2) Criteria

During normal operating and AOOs, the fuel centerline temperature shall not exceed the melting temperature accounting for degradation due to burnup and addition of burnable absorbers.

The fuel rod is considered to be failed []^{TS} during postulated accidents. In the event of fuel failure, the radiological consequences of fuel failure must be accounted in the dose calculations.

The melting temperature of UO₂ is taken to be 5,080 °F (unirradiated) and to decrease []^{TS} per 10,000 MWD/MTU fuel burnup. For Gd₂O₃-UO₂ burnable absorber fuel rod, the melting temperature decreases additionally []^{TS} per weight percent of Gd₂O₃.

(3) Evaluation

The fuel centerline temperatures as a function of burnup are calculated using the NRC approved FATES3B code and methodology described in References 3-1 through 3-5 for UO₂ rod and References 3-7 and 3-8 for Gd₂O₃-UO₂ burnable absorber fuel rod.

The powers to fuel melting are calculated as a function of rod burnup. To preclude fuel melting, the peak local power experienced in normal operation and AOOs should be less than the power to fuel melting at all burnups.

The minimum design margin occurs at the end of cycle 1 because of the reduced power capability with burnup, which is caused by the depletion of the fissile material in the fuel and the buildup of fission products. The calculated power to fuel melting at the end of cycle 1 is []^{TS} which is bounded by the local power density for trip setpoint of []^{TS}.

The linear heat rate corresponding to centerline melt of Gd_2O_3 - UO_2 burnable absorber fuel rod is always less than that of UO_2 fuel rod. Therefore, the lower power of Gd_2O_3 - UO_2 burnable absorber fuel rod compared to UO_2 fuel rod ensures that UO_2 fuel rod remains limiting for centerline melt.

3.2.10 Excessive Fuel Enthalpy

(1) Basis

The number of fuel rod failures is not underestimated for postulated accidents.

(2) Criteria

The total number of fuel rods that must be considered in the radiological assessment is equal to the sum of all of the fuel rods failing each of the criteria below.

- The high cladding temperature failure criteria for zero power conditions is a peak radial average fuel enthalpy greater than 170 cal/g for fuel rods with an internal rod pressure at or below system pressure and 150 cal/g for fuel rods with an internal rod pressure exceeding system pressure. For intermediate (greater than 5% rated thermal power) and full power conditions, fuel cladding failure is presumed if local heat flux exceeds thermal design limits (DNBR).

The PCMI failure criteria is a change in radial average fuel enthalpy greater than the corrosion-dependent limit depicted in Figure B-1 in the NRC standard review plan, Revision 3.

(3) Evaluation

The evaluation for excessive fuel enthalpy is addressed in plant specific transient and accident analysis (Chapter 15 of DCD).

3.2.11 Pellet-to-Cladding Interaction (PCI)

(1) Basis

Fuel rod failure will not occur due to pellet cladding interaction (PCI) under normal operation including AOOs.

(2) Criteria

While there is no current criterion for fuel failure resulting from PCI, two related design criteria are applied.

- Cladding strain during AOOs must remain below 1%
- Fuel centerline melting does not occur

(3) Evaluation

Evaluations on the cladding strain and fuel centerline melting are described in Sections 3.2.2 and 3.2.9, respectively. Based on such evaluation results, it can be concluded that the criteria regarding the pellet-to-cladding interaction are satisfied.

3.2.12 Bursting**(1) Basis**

Fuel rod failures are permitted during postulated accidents, but they will be accounted for in the dose analysis.

(2) Criteria

To meet the requirements of 10 CFR 50.46, as it relates to ECCS performance evaluation, the ECCS evaluation model should include a calculation of the swelling and rupture of the cladding. Regulatory Guide (RG) 1.157 provides guidelines for performing a realistic model to calculate the degree of cladding swelling and rupture.

(3) Evaluation

The evaluation of this criterion is addressed in plant specific transient and accident analysis (Chapter 15 of DCD).

3.2.13 Cladding Embrittlement**(1) Basis**

Core geometry shall be such that the core remains amenable to cooling under postulated accidents.

(2) Criteria

The ECCS performance analysis must satisfy the fuel design criteria specified within 10 CFR 50.46(b). These criteria ensure a coolable core geometry by preserving adequate post-quench ductility in the fuel rod cladding. The current criteria require that (1) the peak cladding temperature remains below 2200 °F and (2) the peak cladding oxidation remains below 17% ECR.

(3) Evaluation

The evaluation of this criterion is addressed in plant specific transient and accident analysis (Chapter 15 of DCD).

3.2.14 Violent Expulsion of Fuel**(1) Basis**

Coolability is always maintained under postulated accidents.

(2) Criteria

- Peak radial average fuel enthalpy must remain below 230 cal/g.
- Peak fuel temperature must remain below incipient fuel melting conditions.

-
- Mechanical energy generated as a result of (1) non-molten fuel-to-coolant interaction and (2) fuel rod burst must be addressed with respect to reactor pressure boundary, reactor internals, and fuel assembly structural integrity.
 - No loss of coolable geometry due to (1) fuel pellet and cladding fragmentation and dispersal and (2) fuel rod ballooning.

(3) Evaluation

The evaluation of this criterion is addressed in plant specific transient and accident analysis (Chapter 15 of DCD).

3.2.15 Generalized Cladding Melting

Generalized (i.e., nonlocal) melting of the cladding could result in the loss of rod-bundle fuel geometry. Criteria for cladding embrittlement in Section 3.2.13 above are more stringent than melting criteria. Therefore, additional specific criteria are not used.

3.2.16 Fuel Rod Ballooning

(1) Basis

Coolability is always maintained under postulated accidents.

(2) Criteria

To meet the requirements of 10 CFR 50.46 as it relates to ECCS performance during postulated accidents, the analysis of the core flow distribution must account for burst strain and flow blockage caused by ballooning (swelling) of the cladding. Those non-LOCA accidents that result in clad ballooning should examine the possibility of DNB propagation.

(3) Evaluation

The burst strain and flow blockage caused by ballooning (swelling) of the cladding are taken into account in the plant-specific LOCA analyses (Chapter 15 of DCD). The possibility of ballooning and DNB propagation is examined in the plant-specific non-LOCA analyses (Chapter 15 of DCD).

3.3 Applicability of Fuel Performance Codes and Methodologies for Design Evaluation

3.3.1 Safety Evaluation Report Compliance

The fuel rod performance analysis for PLUS7 fuel was performed using the codes and methodologies which have been licensed by NRC through the several topical reports. As a result of review for topical reports, a number of limitations, restrictions and conditions on the use of codes and methodology are issued and described in SERs (Safety Evaluation Reports).

The topical reports regarding to fuel performance codes, methodology for core designs containing gadolinia-urania burnable absorbers, application of 1-pin burnup limit of 60 MWD/kgU for C-E 16x16 PWR fuel, methodology for fuel rod maximum gas pressure, and application of ZIRLO cladding material in CE nuclear power fuel assembly designs were submitted to NRC and

Non-Proprietary

PLUS7 FUEL DESIGN for the APR1400

APR1400-F-M-TR-13001-NP-A

approved. The following is a summary of limitations, restrictions and conditions specified in SERs for these topical reports and compliance for the PLUS7 fuel rod performance analysis.

| Item No. | Limitations, Restrictions and Condition (LRCs) | Compliance |
|---|---|--|
| CENPD-275-P Revision 1-P-A “C-E Methodology for Core Designs Containing Gadolinia-Urania Burnable Absorbers” | | |
| 1 | Based on review, we conclude that the gadolinia fuel properties are acceptable for licensing applications up to 8 weight percent gadolinia concentration | APR1400 uses gadolinia fuel of up to 8 weight percent. |
| CEN-386-P-A “ Verification of the Acceptability of a 1-Pin Burnup Limit of 60 MWD/kgU for Combustion Engineering 16x16 PWR Fuel” | | |
| 1 | It was noted that factors affecting cladding corrosion performance at extended burnup cannot differ substantially from that in the existing database without conducting additional corrosion evaluations. The specific factors identified in CEN-386-P are : <ul style="list-style-type: none"> - Average linear heat rate - Reactor coolant temperature - Reactor coolant lithium level | The cladding oxidation is evaluated using the analysis computer code on a reactor-specific basis. |
| 2 | CEN-386-P states that the impact of cladding changes to improve in-reactor corrosion resistance compared to the cladding used in the current database should be included in these additional evaluations. | The impact of ZIRLO cladding on fuel rod design has been evaluated in Reference CENPD-404-P-A “Implementation of ZIRLO™ Cladding Material in CE Nuclear Power Fuel Assembly Designs” |
| 3 | It was observed that the stress analyses at extended burnup should include the effects of cladding thinning due to cladding oxidation. | The effects of cladding thinning due to cladding oxidation are accounted for PLUS7 fuel rod stress analyses. |
| 4 | It was further observed that since cladding oxidation is dependent upon reactor specific conditions (e.g., reactor coolant temperature, and water chemistry), it is necessary to examine cladding oxidation on a reactor-specific basis. | The cladding oxidation is evaluated on a reactor-specific basis using the analysis computer code. |
| CEN-161(B)-P Supplement 1-P-A “Improvements to Fuel Evaluation Model” | | |
| 1 | The approval of the fission gas release and fuel thermal expansion model is based on ; 1) verification of FATES3B predictions against in the ranges of the code's intended applications, 2) verification that the code and input are adequately conservative for its intended applications. | Operating ranges of verification data cover the operating conditions of APR1400. The fuel fabrication and power history input described in Reference 3-9 are used. |

| CEN-372-P-A Fuel Rod Maximum Allowable Gas Pressure” | | |
|---|---|--|
| 1 | Those licensees referencing this high pressure topical report are required to 1) provide plant-specific LOCA analyses to determine the impact of maximum calculated rod pressures on cladding rupture timing and peak cladding temperatures and 2) provide analyses for DNB propagation in postulated accidents if the bounding 14x14 steam line break is not applicable for calculating maximum cladding rupture strain and percent flow blockage for the licensees applications, as described in Section 2.4.2. | The plant specific LOCA and DNB propagation analyses are performed for limiting postulated accidents of APR1400. |
| CENPD-404-P-A “Implementation of ZIRLO™ Cladding Material in CE Nuclear Power Fuel Assembly Designs” | | |
| 1 | The corrosion limit, as predicted by the best-estimate model will remain below 100 microns for all locations of the fuel. | The corrosion limit based on best estimate for APR1400 is 100 microns. |
| 2 | All the conditions listed in the SEs for all the CENPD methodologies used for ZIRLO fuel analysis will continue to be met, except that the use of ZIRLO cladding in addition to Zircaloy-4 cladding is now approved. | This table shows that all the conditions listed in the SEs for other CENPD are met. |
| 3 | Until data is available demonstrating the performance of ZIRLO cladding in CENP designed plants, the fuel duty will be limited for each CENP designed plant with some provision for adequate margin to account for variations in core design (e.g., cycle length, plant operating conditions, etc.). Details of this condition will be addressed in a plant specific basis during the approval to use ZIRLO in a specific plant. | The cladding oxidation is evaluated using the analysis computer code on a reactor-specific basis. Therefore, the fuel duty would not be limited for APR1400 plant. |
| 4 | The burnup limit for this approval is 60 MWD/kgU. | The fuel rod burnup limit of APR1400 is 60 MWD/kgU. |

3.3.2 Applicability of FATES3B Code to PLUS7 Fuel Rod Design

A total of 92 fuel rods and 14 fuel rods were used for verifying the predictive capability of FATES3B for fission gas release and fuel temperature, respectively.

Table 3-5 gives the number of rods and their use as well as the peak local power and rod average burnup ranges for each data set. Important design and operating variables for each data set including the high burnup data set (Zorita, BR-3, Super-Ramp, DOE High Burnup Ramp, and DOE Background Ramp data) are summarized in Table 3-6 and 3-7. The data base for FATES3B fission gas release and fuel temperature verification are as following.

- 12 Calvert Cliffs-1, 25 Over-Ramp, 10 Petten and 2 IFA-418 rods for fission gas release verification.
- 4 four-cycle Calvert Cliffs-1 rods for fission gas release verification
- 5 unpressurized BWR RISO rods for gas release verification

-
- 7 Zorita test rods for fission gas release verification
 - 13 fuel rods ramp tested at the R2 reactor in Studsvik, Sweden for fission gas release verification including four large grain fuel rods as well as nine additional 3 and 4 cycle rods.
 - 5 test rods irradiated in the BR-3 reactor at Mol, Belgium for fission gas release verification
 - 9 higher burnup fuel rods from Petten ramp tests for fission gas release verification
 - 2 IFA 418, 6 IFA428 and 6 IFA 11+21 rods for fuel temperature verification

The data base for model development and for overall verification has been broad in the range of fuel designs and irradiation histories covered [Reference 3-4]. The broad nature of the data base is typical of the high burnup fission gas release data used to develop and verify the fission gas release model in FATES3B. The verification data base of Table 3-6 includes fuel designs ranging in diameter from smaller than the C-E 16x16 designs to larger than the C-E 14x14 designs. This includes fuel fabricated by other U.S. fuel vendors (e.g., Westinghouse) as well as foreign fuel vendors (e.g., KWU) and also includes fuel rods irradiated in both commercial cores and special test reactors.

The FATES3B input was designed such that it can be used to describe fuel design features that may differ (such as diameters, fill gas pressure, etc.) and to describe specific fuel fabrication characteristics and/or microstructure that will influence behavior during irradiation (such as fuel grain size, porosity, surface roughness, densification, etc.).

Comparison of the operating conditions indicates that the peak local power and rod average burnup ranges of FATES3B verification data base bound or nearly the same as those of APR1400 plant.

Table 3-7 shows that the coolant pressure and inlet temperature of FATES3B verification data base bound those of APR1400. The coolant pressure and inlet temperature of APR1400 are 2250 psia and 555 °F, respectively.

It is, therefore, concluded that the FATES3B is generally applicable for PLUS7 fuel rod designs in APR1400.

3.3.3 Applicability of CEPANFL Code to PLUS7 Fuel Rod Design

CEPANFL is a theoretical model for the analysis of the creep deformation of fuel cladding containing initial ovality. Solution of the governing equations is accomplished with a finite difference method based on the engineering principles of shell theory. This means that the applicability of CEPANFL code can be extended to all kinds of commercially used fuel rod designs including PLUS7 fuel.

The time-to-collapse predictions are primarily dependent upon the creep correlations employed for the cladding deformation. The creep correlation of CEPANFL is an empirical equation developed by fitting a selected form to in-reactor creep data. It is the same as that of FATES3B verified in Reference 3-5.

3.3.4 Applicability of PAD Code to PLUS7 Fuel Rod Design

- ZIRLO Corrosion Data Base

ZIRLO in-reactor corrosion data have been obtained from the BR-3 and North Anna fuel program. The BR-3 test fuel residence times extend to 47,500 hours, and the North Anna fuel has achieved a 10,150 EFPH residence time after one cycle of irradiation. Comparison of the corrosion data from the BR-3 ZIRLO rods with sibling Zr-4 rods show ZIRLO peak corrosion ranging from 66% to 83% of Zr-4 peak corrosion. Peak corrosion data from the one cycle North Anna rods range from 0.3 to 0.6 mil for the ZIRLO rods, and from 0.5 to 0.9 mil for the Zr-4 rods.

Based on these data, a corrosion multiplier of 0.75 relative to the Zr-4 corrosion model has been determined for use in ZIRLO fuel rod performance evaluations.

- Increase of Corrosion Model Multiplier

However, it was found that the model multiplier of 0.75 is less conservative for ZIRLO claddings irradiated in Yonggwang unit 2, Yonggwang unit 4 and Ulchin unit 3 through the Post Irradiation Examination Program.

Using the measured oxide layer thickness data of Yonggwang unit 2, Yonggwang unit 4 and Ulchin unit 3, the new corrosion model multiplier was determined to evaluate the best estimate predictions of oxide thickness. A total of 25 oxide thickness data with high burnup exceeding 50 MWD/kgU was used to determine best estimate corrosion model multiplier for Yonggwang unit 2, Yonggwang unit 4 and Ulchin unit 3. Those oxide thickness data consist of 6 fuel rods of V5H fuel irradiated in Yonggwang unit 2, 6 fuel rods of GUARDIAN fuel irradiated in Yonggwang unit 4 and 13 fuel rods of PLUS7 fuel irradiated in Ulchin unit 3 were used.

Through the process of statistical analyses and evaluations, the corrosion model multiplier of 0.92 was determined for best estimate oxide thickness prediction for ZIRLO cladding. Table 3-8 shows the comparison of measured oxide thickness and predicted oxide thickness using corrosion model multiplier of 0.92. The results of statistical analyses are as follows.

| | |
|-----------------------------|------|
| Number of Data : | 25 |
| Mean Value of M/P : | 0.89 |
| Standard Deviation of M/P : | 0.19 |

- Verification of Corrosion Model Multiplier

In order to verify the accuracy of corrosion model multiplier determined based on measured oxide thickness data from Yonggwang unit 2, Yonggwang unit 4 and Ulchin unit 3, the verification of modified corrosion model multiplier was performed using the measured oxide thickness data of PLUS7 fuel rods irradiated in Yonggwang unit 5. The 72 thrice burnt fuel rods with fuel rod average burnups of up to 58,000 MWD/MTU were selected for verification of corrosion model multiplier.

Figure 3-2 shows the comparison of measured oxide thickness and predicted oxide thickness. The predicted oxide thicknesses were generated using the corrosion model multiplier of 0.92.

As shown in Figure 3-2, the predicted values are much higher than those of measured values for both H614 and H605 PLUS7 fuel assemblies. In addition, the means values and standard deviations of M/P are summarized in Table 3-9 for H615 and H605 assemblies.

- Comparison of operating conditions of OPR1000, Westinghouse Type Plants and APR1400

As explained in previous section, oxide thickness data to use the development of corrosion model multiplier and verification were measured at Ulchin unit 3, Yongggwang unit 2, Yongggwang unit 4 and Yongggwang unit 5. However, there are no available APR1400 plant specific corrosion data because the APR1400 plant was not started its first commercial operation yet.

It is, therefore, necessary to compare the operating conditions of Ulchin unit 3, Yongggwang unit 4 and Yongggwang unit 4 with those of APR1400 because the corrosion buildup on cladding material is mainly dependent on operating conditions in terms of coolant temperatures, mass flow rate, lithium concentration and core average power.

Table 3-10 shows the operating conditions of APR1400 and OPR1000 (Yongggwang unit 4 and Ulchin unit 3) as well as Westinghouse type plant of Yongggwang unit 2. As shown in Table 3-10, the coolant inlet temperature and outlet temperature of APR1400 plant are less than those of OPR1000 and Yongggwang unit 2 as well as the core average coolant mass flow rate of APR1400 plant is well within the range of OPR1000 and Yongggwang unit 2. In addition, the allowable maximum lithium concentration of APR1400 plant is the same as those of OPR1000 and Yongggwang unit 2. On the other hand, the core average linear heat rate of APR1400 plant is about four percent higher than that of OPR1000. However, it is expected that four percent increase of core average power does not give a significant effect on oxide buildup of cladding tube. Therefore, the applicability of PAD code with increased corrosion multiplier to PLUS7 fuel in APR1400 for corrosion evaluation was confirmed.

3.4 Impact of Thermal Conductivity Degradation (TCD) on Fuel Rod Design Criteria

The FATES3B fuel performance code is used for fuel rod design and generation of fuel rod interface data for safety analyses. The FATES3B, however, does not explicitly model TCD with burnup. The FATES3B uses the burnup-independent thermal conductivity of the Lyons correlation. Compared with measured data, the Lyons model produces a relatively less conservative temperature distribution within fuel pellet.

Nonetheless, some cladding-related criteria, such as cladding corrosion and hydrogen pickup, cladding collapse, and fuel rod growth are not affected by TCD. Cladding temperature is not affected since the heat flux is not changed by TCD, so cladding corrosion and hydrogen criteria are unaffected. Fuel densification is not also affected by TCD, so cladding collapse criterion is not impacted by TCD. Fast neutron fluence does not change due to TCD, so fuel rod growth criterion is also not impacted by TCD. However, the other criteria such as stress, strain, fatigue, rod internal pressure, and overheating of fuel pellets are affected by TCD. Thus, the evaluations for the fuel rod design criteria that are affected by TCD are described as follow.

3.4.1 Cladding Stress

As described in Section 3.2.1, cladding stress criterion is established to prevent fuel damage from the excessive primary stress which results from the pressure difference between rod internal pressure and system pressure. In Section 3.4.4, it was evaluated that the rod internal pressure predicted by FATES3B includes the effect of TCD.

Therefore, considering the conservatism of FATES3B with regarding the rod internal pressure and design margin for cladding stress, it is judged that the cladding stress design criterion is still met with consideration of TCD.

3.4.2 Cladding Strain

The cladding strain considering the effect of TCD was calculated using the convenient codes of FATES3B which fuel thermal conductivity model, Lyons correlation, is replaced with the modified NFI thermal conductivity model. According to the evaluation results considering the TCD effect, the cladding plastic strain during normal operation and following a single AOO is $\{ \quad \}^{TS}$ and, total (elastic plus plastic) circumferential strain increment produced as a result of a single AOO is $\{ \quad \}^{TS}$. Because the calculated strains are less than $\{ \quad \}^{TS}$, the strain design criteria are still satisfied with the consideration of TCD.

3.4.3 Cladding Fatigue

The fatigue damage factor for the daily load following operation was calculated using the same convenient code of FATES3B as used for cladding strain evaluation. In this calculation, more conservative radial peaking factor (RPF) than the cycle specific RPF curve was used. On the other hand, the fatigue damage factors for reactor trips and startups/shutdowns are determined by hand calculation using a simple formula. The total cumulative fatigue damage factor from daily load following operation, reactor trips and startups/shutdowns was $\{ \quad \}^{TS}$ which is below the limit of $\{ \quad \}^{TS}$. Therefore, it was confirmed that the cladding fatigue criterion is still satisfied with the consideration of TCD.

And then, to confirm the applicability for a given subsequent cycle, the conservative RPF used in the calculation will be validated on a cycle-by-cycle basis.

3.4.4 Fuel Rod Internal Pressure

The fuel rod internal gas pressure is determined by the combination of fission gas release and fuel rod void volume. The effect of increased fuel temperature due to TCD on fission gas release is inherently accounted for in the current performance code, FATES3B (References 3-1 through 3-4), because the model was calibrated to measured data for a full range of fuel rod burnup and operating conditions. Additionally, conservatism is considered in the original FATES3B calibration process and in design methodology. In contrast, the rod internal pressure may be increased due to the TCD-induced fuel thermal expansion, which reduces the total fuel rod void volume. However, the potential increase of rod internal pressure due to reduction of void volume can be sufficiently offset with the inherent conservatism of FATES3B and available design margin to the design limit. It is also noted that the rod internal pressure is conservatively calculated assuming the RPF curve and biased input to generate higher rod internal gas pressure. Therefore, it can be concluded that rod internal pressure criteria are still satisfied considering the effects of TCD.

3.4.5 Overheating of Fuel Pellets

The power to melt (PTM) decreases as fuel rod burnup increases because the fuel melting temperature is decreased. The local linear powers that preclude fuel centerline melting are calculated for UO_2 and Gd_2O_3 - UO_2 rods as a function of burnup using FATES3B code considering the TCD effect. In this calculation, as explained in section 3.5.1, TCD effects was considered by adding a penalty on fuel centerline temperature that linearly increases from $\{ \quad \}^{TS}$ over

the burnup range from zero to $\{ \quad \}^{TS}$ and remains constant for higher range of burnup. The calculated power to fuel melting considering the TCD penalty is presented in Figure 3-3. As shown in Figure 3-3, the PTM limit with TCD penalty for UO_2 rod is decreased below a SAFDL of $\{ \quad \}^{TS}$ above $\{ \quad \}^{TS}$ but the fuel will not melt because the decreasing rate of the maximum attainable rod power will be much higher than that of the PTM due to the reduced power capability caused by the depletion of the fissile material in the fuel and the buildup of fission products. In Figure 3-3, each maximum attainable power of UO_2 and Gd_2O_3 - UO_2 rods can be obtained from radial fall-off values, namely from the normalized radial power in Figure 3-1. Since the maximum attainable power for both UO_2 and Gd_2O_3 - UO_2 rods is limited up to $\{ \quad \}^{TS}$ which is a SAFDL value for APR1400, it can be defined that the maximum attainable power of $\{ \quad \}^{TS}$ is only available with a normalized UO_2 rod radial power of $\{ \quad \}^{TS}$. In addition, the maximum attainable power after about $\{ \quad \}^{TS}$ in Figure 3-3 is derived from the proportional decrease of normalized radial power fall-off curve in Figure 3-1. Based on the same reasoning, the maximum attainable powers of Gd_2O_3 - UO_2 rods are obtained by considering the normalized radial power ratio of UO_2 and Gd_2O_3 - UO_2 rods over all burnup ranges shown in Figure 3-1.

As shown in Figure 3-3, the PTM values are well above the attainable powers for UO_2 and Gd_2O_3 - UO_2 rods along whole range of burnup. Therefore, it can be concluded that there will be no melting for UO_2 and Gd_2O_3 - UO_2 rods. In addition, fuel melting of Gd_2O_3 - UO_2 rods will not be occurred even when the rod power for UO_2 rod reaches the SAFDL value of $\{ \quad \}^{TS}$. Therefore, the lower power of Gd_2O_3 - UO_2 rod compared to UO_2 rod ensures that UO_2 rod remains limiting for centerline melt. This melting analysis will be performed on a cycle specific basis with FATES3B code considering the TCD penalty. This will ensure that the linear heat rate SAFDL of $\{ \quad \}^{TS}$ is valid.

In summary, the fuel rod design criteria have been reviewed with respect to the potential impacts of TCD, and it is concluded that TCD can be accommodated to the fuel rod design criteria that satisfied for current APR1400 fuel rod designs.

3.5 Impact of TCD on Safety Analyses

As previously described, the FATES3B code uses the fuel pellet thermal conductivity model which does not consider the TCD effects. Therefore, it is necessary to evaluate the non-conservatism of the FATES3B code on the generation of fuel rod interface data for safety analyses. In this section, the degree of non-conservatism in the FATES3B temperature prediction (TCD penalty values) is determined based on the comparison results with the measured temperature data from Halden test reactor.

3.5.1 Determination of TCD Penalty

The verification of the TCD penalty of FATES3B code for fuel centerline temperature was completed using the measured Halden test reactor data. Halden data with the power range of $\{ \quad \}^{TS}$ and burnup range of $\{ \quad \}^{TS}$ are applied to the comparison and include the comparable conditions of APR1400.

- Hot Rod Fuel Temperature Penalty

The deviation of M-P (measured minus predicted) at an upper bound basis which is indicated as red line in Figure 3-4 is linearly increased from $\{ \quad \}^{TS}$ at $\{ \quad \}^{TS}$ to $\{ \quad \}^{TS}$ to $\{ \quad \}^{TS}$ and remains constant for above $\{ \quad \}^{TS}$. The upper bound deviation line in Figure 3-4 bounds over $\{ \quad \}^{TS}$ of all M-P comparison data. Therefore, the deviation line in red of Figure 3-4 represents as reasonable centerline temperature penalty due to TCD for

FATES3B prediction. The fuel volume-averaged temperature is assumed as $\left(\frac{T_{CL} + T_{FA}}{2} \right)^{TS}$ of the fuel centerline temperature with TCD penalty.

- Average Rod Fuel Centerline Temperature Penalty

The centerline temperature penalty is linearly increased from $\left(\frac{T_{CL} + T_{FA}}{2} \right)^{TS}$ at $\left(\frac{T_{CL} + T_{FA}}{2} \right)^{TS}$ to $\left(\frac{T_{CL} + T_{FA}}{2} \right)^{TS}$ to $\left(\frac{T_{CL} + T_{FA}}{2} \right)^{TS}$ and remains constant for above $\left(\frac{T_{CL} + T_{FA}}{2} \right)^{TS}$. This best-estimated penalty was determined based on the comparison of FATES3B and Halden test data which are similar to the APR1400 core average power.

For the mass and energy calculations used in the containment pressure analysis, 95 % upper bounded penalty was determined as the linear increasing of centerline temperature from $\left(\frac{T_{CL} + T_{FA}}{2} \right)^{TS}$ at $\left(\frac{T_{CL} + T_{FA}}{2} \right)^{TS}$ to $\left(\frac{T_{CL} + T_{FA}}{2} \right)^{TS}$ and remaining constant for above $\left(\frac{T_{CL} + T_{FA}}{2} \right)^{TS}$.

3.5.2 Fuel Rod Interface Data for Safety Analyses

To generate the fuel rod interface data with TCD effect for safety analyses, the TCD penalty determined as a function of burnup is added to the temperatures calculated by FATES3B code and those TCD penalty-added centerline temperatures of hot and average rod should be provided to safety analyses team.

3.6 Impact of Fuel Enthalpy

The impacts of TCD result in increasing the fuel enthalpy and the fuel centerline temperature. The impact on the fuel enthalpy due to TCD would be negligible for fresh fuel even though the maximum power peaking factors exist in the low burnup fuel in the APR1400 reload core designs. For the high burnup fuel which is affected by TCD, the fuel enthalpy and the fuel centerline temperature increase due to TCD are not significant because of the peaking factor burndown effect at higher burnups. The event specific evaluation considering the TCD penalty described in the Section 3.5 was performed and described in DCD Tier 2 Chapter 15.4.8.

3.7 Conclusion

The PLUS7 fuel rod design criteria considering TCD effect is evaluated using NRC approved FATES3B code and verified acceptable up to rod average burnup of 60,000 MWd/MTU. In addition, the potential impact of TCD on the fuel rod design criteria was evaluated, and it is concluded that TCD can be accommodated. Fuel rod interface data accounting for TCD penalty are generated and transmitted to safety analyses team.

Table 3-1 Comparison of PLUS7 Fuel Rod with Guardian Fuel Rod

| Parameter | Guardian | PLUS7 |
|---|----------|-------|
| UO₂ Pellet | | |
| Diameter, inches | | |
| Length, inches | | |
| Density (%TD) | | |
| Enrichment(w/o U-235) | | |
| Dish Configuration | | |
| Chamfer | | |
| Roughness, inches | | |
| Gd₂O₃-UO₂ Pellet | | |
| Diameter, inches | | |
| Length, inches | | |
| Density (%TD) | | |
| Enrichment(w/o U-235) | | |
| Gd ₂ O ₃ Weight% | | |
| Dish Configuration | | |
| Chamfer | | |
| Axial Blanket | | |
| Configuration | | |
| Enrichment (w/o U-235) | | |
| Diameter, inches | | |
| Pellet Length, inches | | |
| Total Length, inches | | |
| Axial Cutback | | |
| Configuration | | |
| Enrichment (w/o U-235) | | |
| Diameter, inches | | |
| Pellet Length, inches | | |
| Total Length, inches | | |
| Cladding | | |
| Material | | |
| Outer Diameter, inches | | |
| Inner Diameter, inches | | |
| Thickness, inches | | |
| Roughness, inches | | |
| UO₂ and Gd₂O₃-UO₂ Fuel Rod | | |
| Stack Length, inches | | |
| Pellet-to-Cladding Gap, inches | | |
| Initial Helium Pressure, psig | | |
| Plenum Length, inches | | |
| Plenum Spring | | |
| Plenum Spring Volume, in ³ | | |
| Plenum Volume, in ³ | | |
| Upper End Cap Length, inches | | |
| Lower End Cap Length, inches | | |
| Fuel Rod Length, inches | | |
| Fuel Rod Pitch, inches | | |
| Rod Internal Void Volume, in ³ | | |

TS

Table 3-2 Codes Used for Analyses of Fuel Rod Design

| Design Criteria | Code |
|------------------------------|------|
| Cladding Stress | |
| Cladding Strain | |
| Cladding Fatigue | |
| Cladding Oxidation/Hydriding | |
| Rod Internal Pressure | |
| DNB Propagation | |
| Cladding Collapse | |
| Fuel Pellet Temperature | |

TS

Table 3-3 Cladding Stress Evaluation Results

| Component | Stress | Condition | Allowable Stress (psi) | Calculated Stress (psi) |
|--------------|-------------|------------------|------------------------|-------------------------|
| Cladding | Tensile | Normal operation | | |
| | | AOOs | | |
| | Compressive | Normal operation | | |
| | | AOOs | | |
| End Cap Weld | Tensile | Normal operation | | |
| | | AOOs | | |
| | Compressive | Normal operation | | |
| | | AOOs | | |

TS

Table 3-4 Main Design Parameters Used for PLUS7 Fuel Rod Performance Analysis

| Type of Parameter | Design Parameter | |
|------------------------------|--|--|
| Physics Parameter | Core Thermal Power, MW_{th} | |
| | Core Average Power (at 100% Power), kW/ft | |
| | Maximum Radial Peaking Factor | |
| | Peak LOCA Limit LHR, kW/ft | |
| | Peak Fuel Rod Average Burnup, MWD/MTU | |
| | Core Average Fast Flux, $(n/cm^2\text{-sec}, E > 1.0 \text{ MeV})$ | |
| Thermal Hydraulics Parameter | Core Coolant Inlet Temperature, °F | |
| | Coolant Pressure, psia | |
| | Coolant Flow Rate, lbm/hr-ft ² | |
| | Equivalent Hydraulic Diameter, ft | |

TS

Table 3-5 Description of Data Base Used for FATES3B Verification

| Parameter | Number of Rods | Used For (*) | Parameter Local Power(kw/ft) | Rod Average Burnup(MWD/kgU) |
|------------------|----------------|--------------|------------------------------|-----------------------------|
| Calvert Cliffs-1 | 16 | F | | |
| Over-Ramp | 25 | F | | |
| Petten | 10 | F | | |
| IFA-418 | 2 | F, T | | |
| IFA-428 | 6 | T | | |
| IFA-11+21 | 6 | T | | |
| RISO | 5 | F | | |
| Zorita | 7 | F | | |
| BR-3 | 5 | F | | |
| Super-Ramp | 13 | F | | |
| DOE Ramp | 9 | F | | |
| APR1400 (**) | - | - | | |

(*) F – Fission gas release T – Fuel temperature

(**) Design values

Table 3-6 Design Parameters for Rods in the Verification Data Base

| Parameter | Calvert Cliffs-1 | Over Ramp | Petten | IFA418 | Zorita | BR-3 | Super Ramp | DOE Ramp | APR1400 (PLUS7) |
|---|------------------|-----------|--------|--------|--------|------|------------|----------|-----------------|
| Clad OD, in | | | | | | | | | |
| Clad ID, in | | | | | | | | | |
| Initial Pellet-Clad Diametral Gap, mils | | | | | | | | | |
| Initial Grain Size, μm | | | | | | | | | |
| Initial Fuel Density, %TD | | | | | | | | | |
| Fill Gas Pressure at 70 °F, psia | | | | | | | | | |
| Enrichment, %U235 | | | | | | | | | |

TS

Table 3-7 Thermal-Hydraulic Parameters for Rods in the Fission Gas Release Verification Data Base

| Parameter | Coolant Pressure(psia) | Coolant Inlet Temperature(°F) |
|------------------|------------------------|-------------------------------|
| Calvert Cliffs-1 | | |
| Over-Ramp(*) | | |
| Petten(*) | | |
| IFA-418 | | |
| IFA-428 | | |
| IFA-11+21 | | |
| Zorita | | |
| BR-3 | | |
| Super-Ramp(**) | | |
| DOE Ramp(*) | | |
| APR1400 | | |

TS

(*) The coolant pressure and inlet temperature during power ramping are 2100 psia and 642 °F

(**)The coolant pressure and inlet temperature during power ramping are 2100 psia and 507-597 °F

Table 3-8 Comparison of Measured Oxide Thickness and Predicted Oxide Thickness Using Modified Corrosion Model Multiplier

| Rod ID | Rod Average Burnup (MWD/MTU) | Measured Maximum Oxide Thickness (μm) | Predicted Oxide Thickness (μm) | M/P |
|--------|------------------------------|---------------------------------------|--------------------------------|-----|
| | | | | |

TS

Table 3-9 Mean Value and Standard Deviation of M/P for H615 and H605 Assemblies

| Statistics | H615 Assembly | H605 Assembly | Total |
|---------------------------|---------------|---------------|-------|
| Number of Samples | | | |
| Mean Value of M/P | | | |
| Standard Variation of M/P | | | |

TS

Table 3-10 Operating Conditions of APR1400, OPR1000, and Westinghouse Type Plants

| Rod ID | Core Inlet Temperature (°F) | Core Outlet Temperature (°F) | Maximum Lithium Concentration (ppm) | Core Average Mass Flow (lbm/hr-ft ²) | Core Average Linear Heat Rate(kw/ft) |
|------------------|-----------------------------|------------------------------|-------------------------------------|--|--------------------------------------|
| Yonggwang unit 2 | | | | | |
| Yonggwang unit 4 | | | | | |
| Ulchin unit 3 | | | | | |
| Yonggwang unit 5 | | | | | |
| APR1400 | | | | | |

TS



Figure 3-1 Rod Power History Used for PLUS7 Fuel Rod Performance Analysis



Figure 3-2 Comparison of Measured Oxide Layer Thickness and Predicted Oxide Layer Thickness for H615 and H605 Assemblies



Figure 3-3 Power to Melt and Maximum Attainable Powers for UO₂ and Gd₂O₃-UO₂ Rods



Figure 3-4 Comparison of Predicted and Measured Fuel Centerline Temperatures as a Function of Burnup vs. Determined TCD Penalty (red line)

4. PLUS7 FUEL EXPERIENCE

4.1 Overview

KNF has developed advanced PWR fuel for the OPR1000s, PLUS7, because Guardian fuel for the OPR1000s was not enough to meet Korean customers' requirements, such as sufficient overpower margin to employ full low leakage loading patterns as well as safe implementation of power uprating, elimination of fuel failure attributable to grid-to-rod fretting wear and debris, better fuel economics, fuel integrity maintenance even at high burnup beyond the current licensed burnup of 60,000 MWD/MTU. For these purposes, PLUS7 fuel development activities, such as fuel assembly and its components design, their manufacturing technology, out-of-pile mechanical /thermal/hydraulic/vibration characteristic tests, were performed from 1999 to 2001 as shown in Figure 4-1.

Four PLUS7 lead test assemblies (LTAs) were loaded into the fifth cycle of Ulchin unit 3 (UCN-3) in December of 2002. The first commercial operation of PLUS7 fuel started in Ulchin unit 4 (UCN-4) cycle 6 in 2006 (see Appendix B.1.0). More than 2,300 PLUS7 fuel assemblies had been loaded in all OPR1000 NPPs in Korea (Yonggwang-3, 4, 5 & 6, Ulchin-3, 4, 5 & 6, Shin-Kori 1) by 2012 (see Table 4-1). Except Shin-Kori unit 1, all OPR1000s in operation have equilibrium cores with PLUS7 fuel at the present. Shin-Kori unit 2 and Shin-Wolsung units 1&2 are scheduled to load PLUS7 fuel from their second cycles. PLUS7 fuel will be loaded into APR1400s from the initial cores in near future.

An overview of the poolside examinations (PSEs) of the PLUS7 LTAs and commercial surveillance assemblies (CSAs) are described in Section 4.2. Moreover, Section 4.3 discusses about the experience gained from hot-cell examination programs for the LTAs.

4.2 Pool-Side Examinations

Four PLUS7 LTAs were loaded into the fifth cycle of UCN-3 to verify the in-reactor performance of PLUS7 fuel. Figure 4-2 shows the fuel rods configuration of the PLUS7 LTAs and Figure 4-3 shows the fuel loading patterns from the fifth to the seventh cycles of UCN-3 where the four PLUS7 LTAs were loaded.

The inlet temperature of the UCN-3 reactor core is []^{TS} at 100% power and the average power of the reactor core is []^{TS}. The effective full power days, the fuel assembly average burnup, and peak fuel rod average burnup of the LTAs are as shown in Table 4-2.

At the end of cycles 5, 6, and 7 of UCN-3, PSEs of the LTAs were conducted. Among the four LTAs, the LTA of U3HA06 was only selected for the full-scope PSE since the four LTAs were manufactured with the same specifications and were loaded at the symmetrical position of the reactor core. In addition, the U3HA03 LTA was examined for some additional information.

Since PSE results of the four PLUS7 LTAs confirmed that the PLUS7 fuel assembly and the fuel rod satisfied all the design criteria, PLUS7 fuel started its commercial supply to all OPR1000 reactors in Korea, starting from UCN-4 cycle 6. Additionally, two assemblies scheduled to be burned twice and two assemblies scheduled to be burned thrice in Yonggwang unit 5 (YGN-5) cycle 5 were selected to be CSAs. At the end of cycles 5, 6, and 7 of YGN-5, PSEs of the CSAs were conducted. PSE results of the CSAs re-verified that the PLUS7 fuel assembly and the fuel rod satisfied all the design criteria. Figure 4-2 shows the fuel rods configuration of the PLUS7 CSAs

and Figure 4-4 shows the fuel loading patterns from the fifth to the seventh cycles of YGN-5 where the four PLUS7 CSAs were loaded.

Fuel assembly irradiation growth, fuel assembly bow and twist, rod-to-top nozzle axial clearance (shoulder gap), fuel rod bow, spacer grid width, cladding oxide thickness, and fuel rod outer diameter were measured during the PSE. The PSE measurement methods, results and evaluations for the LTAs and CSAs are described in below sections. Tables 4-3 through 4-6 present maximum or minimum measured values and allowable limits for each examination. Measured data are plotted in Figures 4-5 through 4-8, and upper or lower 95% prediction bound is plotted on the graph to show that the PLUS7 in-reactor performance for each measurement items are well within its allowable limits.

4.2.1 Fuel Assembly Irradiation Growth

(1) Measurement Method

A visual image recording technique with an underwater camera was used to measure the length change of irradiation-induced fuel assembly. Each length from the bottom nozzle to each grid and to the top nozzle was measured at the end of cycles.

(2) Measurement Results and Evaluation

The irradiation-induced fuel assembly growth is used for evaluating the compatibility with the reactor internals and the interference between the top nozzle and the fuel rods. Fuel assembly growth is calculated by the differences between the initial fuel assembly length and the lengths after the first, second, and third cycle burnup. Table 4-3 and Figure 4-5 show the measurement value of the irradiation-induced fuel assembly length changes and an allowable design limit for maintaining the compatibility with the reactor internals. The maximum irradiation-induced growths of LTAs measured after the first, second, and third cycle burnup are $\{ \quad \}^{TS}$, respectively. For the CSAs, the maximum irradiation-induced growths measured after the first, second, and third cycle burnup are $\{ \quad \}^{TS}$, respectively. This shows that there is no effect of the PLUS7 fuel assembly irradiation growth on the reactor internals integrity since a sufficient margin exists for the PLUS7 assembly growth against the allowable design limit of $\{ \quad \}^{TS}$ for the compatibility maintenance. The effect of the assembly growth on the interference between the top nozzle and the fuel rod is described in Section 4.2.3.

4.2.2 Fuel Assembly Bow and Twist

(1) Measurement Method

The assembly bow is measured from two adjacent faces of the assemblies. At first the line is installed on the right-hand side of the assembly. Then, the assembly bow is obtained for one face, measuring distance from the line to the adjacent assembly face. After rotating the assembly 90°, the assembly bow is obtained for the other face using the same method.

The assembly twist can be obtained by measuring the twist angle of the top nozzle with reference to the bottom nozzle or by measuring the twist angle of the bottom nozzle with reference to the top nozzle. In detail, two lines are installed on the right-hand side of the assembly at the front and back rows, respectively, and then the assembly twist angle is obtained by measuring an angle between the plane made by two lines and the adjacent face of the top and bottom nozzles.

(2) Measurement Results and Evaluation

For the LTAs, U3HA03 and U3HA06, after three cycles of irradiation, the maximum assembly bows are { }^{TS} respectively, and the maximum twist angles are { }^{TS} respectively. For the CSAs, KY5H605 and KY5H615, after three cycles of irradiation, the maximum assembly bows are { }^{TS} respectively, and the maximum twist angles are { }^{TS} and { }^{TS} respectively. Since a sufficient margin exists against the allowable design limit of { }^{TS} mm for the fuel assembly bow and { }^{TS} for the twist, the PSE result assures that the PLUS7 has no impact on the CEA insertion and withdrawal, and the compatibility with the reactor internals, or on the fuel assembly unloading and loading.

4.2.3 Rod-to-Top Nozzle Axial Clearance (Shoulder Gap)**(1) Measurement Method**

The shoulder gap, which is defined as the distance between the lower surface of the top nozzle and the upper end of the fuel rod top end plug, is determined by the difference in the irradiation growth between the fuel rod and the fuel assembly.

(2) Measurement Results and Evaluation

The measured shoulder gap is used to check whether the interference between the fuel rod and the top/bottom nozzles occurs or not, and if it maintains a positive (+) value for the entire fuel lifetime. Table 4-4 and Figure 4-6 show the measured shoulder gaps and allowable limit for the LTAs and CSAs at the end of each cycle. After the burnup of three cycles, the measured minimum shoulder gaps are { }^{TS} for U3HA03 and U3HA06, and { }^{TS} for KY5H605 and KY5H615, respectively. Therefore, as shown in this table and figure, the positive (+) value of the criteria for the shoulder gap is sufficiently satisfied.

4.2.4 Fuel Rod Bow**(1) Measurement Method**

To evaluate the PLUS7 fuel rod bow, peripheral rods of the LTAs and CSAs were selected and the rod-to-rod distances were measured at the middle of the adjacent grids.

(2) Measurement Results and Evaluation

The fuel rod bow is used to check whether the DNBR penalty is to be imposed or not. The DNBR penalty is not imposed if the reduction of the fuel rod channel spacing due to the fuel rod bow is less than { }^{TS} of the initial fuel rod channel spacing. Table 4-5 and Figure 4-7 shows the initial rod-to-rod spacing and the measured rod-to-rod spacing for the LTAs and CSAs. The LTAs' least fuel rod channel spacing measured at the end of their first, second, and third cycles' burnup are { }^{TS} respectively, and for the CSAs' at the end of their second and third cycles' burnup are { }^{TS} respectively. These results sufficiently satisfy the criteria of { }^{TS} of the initial fuel rod channel spacing.

4.2.5 Grid Width**(1) Measurement Method**

The grid widths were measured using the Linear Variable Differential Transformer (LVDT).

(2) Measurement Results and Evaluation

The excessive growth of grid width caused by the neutron irradiation may have an impact on the fuel assembly unloading and loading. Hence, the neutron irradiation-dependent grid width is limited to less than the fuel assembly pitch to facilitate the assembly unloading and loading. The maximum grid widths were measured at the ninth grids. Table 4-6 and Figure 4-8 show the grid widths measured at the end of each cycle.

After the first, second, and third cycles of burnup, the maximum measured grid widths of LTAs were { }^{TS}, respectively. Grid widths of the CSAs were measured after the second and third cycles of burnup, and the maximum values were { }^{TS}, respectively. The PLUS7 fuel assembly has a sufficient margin compared to the fuel assembly pitch ({ }^{TS}), so it was evaluated that the PLUS7 LTAs had no impact on the fuel assembly unloading and loading due to the irradiation growth of the grid.

4.2.6 Cladding Oxide Thickness

(1) Measurement Method

The oxide thicknesses of 36 fuel rods were measured for LTAs using ECT (Eddy Current Test) apparatus manufactured by Framatome at the end of cycles 5, 6 and 7. The maximum burnup of the fuel rods is 57,535 MWD/MTU.

For CSAs, the oxide layer thicknesses were measured for 72 fuel rods of H615 and H605 assemblies at the end of cycle 7. The maximum burnup of fuel rods is 58,353 MWD/MTU.

(2) Measurement Results and Evaluation

The measured oxide layer thickness of fuel rods with ZIRLO cladding as a function of rod average burnup is shown in Figure 4-9. The maximum measured oxide thickness are { }^{TS} for the LTAs and { }^{TS} for the CSAs, which are less than the oxide thickness design limit of { }^{TS}. Therefore, the cladding corrosion performance of the PLUS7 fuel rod was confirmed.

The comparison of measured values and predicted values for LTAs and CSAs is shown in Figure 4-10.

4.2.7 Fuel Rod Outer Diameter

(1) Measurement Method

The outer diameters for fuel rods for LTAs and CSAs were measured using the Linear Variable Differential Transducer (LVDT) at the end of cycle 7. The measurements were performed for two faces, 0° face and 90° face.

(2) Measurement Results and Evaluation

Figures 4-11 through 4-19 and Figures 4-20 through 4-27 present the fuel rod outer diameters of LTAs and CSAs. The results show that the outer diameters range { }^{TS} for both

LTAs and CSAs. Therefore, it was confirmed that fuel rod diameter increases resulting from the cladding creep and swelling are within the strain limit of $\left[\quad \right]^{TS}$ based on initial diameter of 9.5 mm.

4.3 Hot-Cell Examinations

The hot cell examinations for 6 fuel rods of HA03 fuel assembly which was irradiated in UCN-3 from cycle 5 to cycle 7 were performed. The major objective of hot cell examination was to confirm the integrity of PLUS7 fuel rods and obtain data relevant to fuel rod performance and data useful for evaluating fuel rod performance models.

The details of selected fuel rods and examinations are shown in Table 4-7.

The examinations of fretting wear, cladding oxide thickness, CRUD thickness, fuel outer diameter, cladding hydrogen pickup, and fission gas release were performed.

4.3.1 Fuel Rod Fretting Wear

(1) Measurement Method

The fuel rods were visually examined and the fuel rod that shows large spring/dimple wear mark was sectioned to measure the fretting wear depth on the fuel rod wear area.

(2) Measurement Results and Evaluation

The visual examination results of the fuel rods show that the wear mark is increased from bottom to top grid typically as shown in Figure 4-28. Also the visual examination results show that the B14 fuel rod in inner cell has bigger wear mark than other rods in outer cell and near guide thimble cell. Figure 4-29 shows the wear mark at the 3rd, 7th and 10th grid position of the fuel rod B14 that shows bigger wear mark than the others. Figure 4-30 shows the cross section inspection results for the spring wear mark at 10th grid location that show the largest wear mark on the fuel rod B14. The wear mark area was sliced in 8 pieces with 1 mm thickness to measure the wear depth. As shown in Figure 4-30, not any wear depth was shown in the cross section of the wear mark. Therefore, it was confirmed that not any measureable fretting wear has occurred in the PLUS7 fuel rods.

4.3.2 Cladding Oxide Thickness

(1) Measurement Method

The oxide thicknesses on cladding were measured for A14, B14, C03, D15, D16 and K07 fuel rods using Eddy Current Test (ECT). The oxide thickness measurements were carried out for each fuel rod at 0, 90, 180 and 270 degree directions.

(2) Measurement Results and Evaluation

The results of cladding oxide thickness for A14, B14, C03, D15, D16 and K07 fuel rods are shown in Figures 4-31 through 4-36. Even though the maximum local oxide thickness of A14 fuel rod is greater than $\left[\quad \right]^{TS}$, the circumferential averaged oxide thickness is less than $\left[\quad \right]^{TS}$ as for other measured fuel rods.

In addition, the predicted oxide thickness are also shown in Figures 4-31 through 4-36. Figures 4-31 through 4-36 indicate that the predicted values well bound the measured circumferential averaged oxide thicknesses for 6 fuel rods.

4.3.3 CRUD Thickness

(1) Measurement Method

The CRUD thickness and bonding layer between pellet and cladding were measured at 3094 mm height from bottom of fuel rod for C03 fuel rod using electron microscope.

(2) Measurement Results and Evaluation

Figure 4-37 shows the bonding layer between pellet and cladding inner surface as well as CRUD layer on cladding outer surface for C03 fuel rod.

As shown in Figure 4-37, no gap exists between the inner surface of the cladding and the periphery of the fuel pellet. This means that the pellet and cladding is in complete contact around the full circumference of the transverse specimens. The observed bonding layer is about { }^{TS}

CRUD thickness was observed on outer surface of cladding. From Figure 4-37, it was evaluated that CRUD thickness is { }^{TS}. The thickness of { }^{TS} is similar to the assumed CRUD thickness for evaluating clad oxide thickness using fuel rod performance code.

4.3.4 Fuel Rod Outer Diameter

(1) Measurement Method

Continuous profilometry measurements were made on 6 fuel rods to characterize local fuel rod diameter using the LVDT.

(2) Measurement Results and Evaluation

The diameters as a function of axial position are shown in Figures 4-38 through 4-43 for A14, B14, C03, D15, D16 and K7 fuel rods. The measured diameters range { }^{TS}. These results are consistent with the results of PSE for PLUS7 LTAs.

Therefore, it was confirmed that fuel rod diameter increases resulting from the cladding creep and swelling are within the strain limit of { }^{TS} relative to initial diameter.

4.3.5 Cladding Hydrogen Content and Hydride Orientation

(1) Measurement Method

The cladding hydrogen content measurement was performed for C03 fuel rod of PLUS7 LTA. Three samples were taken at 1550 mm, 2781 mm, and 3280 mm heights from bottom of fuel rod. The measurements were carried out at 3 positions of circumferential direction for each sample. The average hydrogen contents along circumferential positions are calculated from hydrogen contents of circumferential positions. In addition, the hydride orientations were also examined for C03 fuel rod of PLUS7 LTA.

(2) Measurement Results and Evaluation

Figure 4-44 shows the measured hydrogen contents in cladding as a function of oxide thickness. Figure 4-44 includes C03 fuel rod data and ZIRLO data irradiated in commercial reactors of Yonggwang unit 4, V.C. Summer, []^{TS}. The hydrogen contents of LTA fuel are within the ZIRLO cladding database.

The hydrogen content absorbed in cladding depends on the hydrogen pickup fraction and oxide layer thickness. The hydrogen pickup fraction is one of the material properties, which is []^{TS} for ZIRLO based on best estimate. This value is not dependent on the fuel types as well as the plant operating conditions. Therefore, the hydrogen content absorbed in ZIRLO cladding is based on oxide layer thickness generated by oxidation reaction.

Using the oxide thicknesses in Figure 4-9, the hydrogen contents averaged over the entire wall thickness is calculated using a hydrogen evolution model. The results are shown in Figure 4-45. For discharge burnup up to 60,000 MWD/MTU, the circumferential average hydrogen concentrations are less than []^{TS} for PLUS7 fuel in APR1400.

A photomicrograph of the etched C03 fuel rod cladding is shown in Figure 4-46. Figure 4-46 shows that the concentration of hydrides increases with increasing distance from the cladding inner surface due to the radial thermal gradient in the cladding. The cladding hydrogen contents exist mostly in the form of circumferential hydrides distributed in the outer region of the clad wall as shown in Figure 4-46.

4.3.6 Fission Gas Release

(1) Measurement Method

During the hot cell examination, A14 and C03 fuel rods of PLUS7 LTA irradiated in UCN-3 cycle 5 through cycle 7 were punctured and gases from these rods were collected and analyzed to determine the fractional fission gas release.

(2) Measurement Results and Evaluation

Table 4-8 shows the predicted values and measured data obtained in hot cell examination. As shown in Table 4-8, the fission gas released are []^{TS} for A14 and C03 fuel rods, respectively. In addition, the rod internal pressures were measured for A14 and C03 fuel rods. The measured rod internal pressures of []^{TS} are well within the database of PWR fuel rod internal pressure at the condition of room temperature.

4.4 Testing, Inspection, and Surveillance Plans

Testing and inspection of new fuel and post-irradiation surveillance are described in DCD tier 2, Section 4.2.

Table 4-1 Commercial Loading of PLUS7 up to 2012

| Plant | Cycle loaded PLUS7 | No. of Fuels | No. of Rods | Max. Assembly Burnup (MWD/MTU) | Max. Rod Burnup (MWD/MTU) |
|------------------|--|--------------|-------------|--------------------------------|---------------------------|
| Yonggwang unit 3 | Cycle 11, Cycle 12, Cycle 13, Cycle 14 | | | | TS |
| Yonggwang unit 4 | Cycle 10, Cycle 11, Cycle 12, Cycle 13, Cycle 14 | | | | |
| Yonggwang unit 5 | Cycle 5, Cycle 6, Cycle 7, Cycle 8, Cycle 9 | | | | |
| Yonggwang unit 6 | Cycle 5, Cycle 6, Cycle 7, Cycle 8 | | | | |
| Ulchin unit 3 | Cycle 8, Cycle 9, Cycle 10, Cycle 11, Cycle 12 | | | | |
| Ulchin unit 4 | Cycle 7, Cycle 8, Cycle 9, Cycle 10 | | | | |
| Ulchin unit 5 | Cycle 4, Cycle 5, Cycle 6, Cycle 7 | | | | |
| Ulchin unit 6 | Cycle 3, Cycle 4, Cycle 5, Cycle 6, Cycle 7 | | | | |
| Shin-Kori unit 1 | Cycle 2 | | | | |
| Total | 2006 ~ 2012 | | | | |

Table 4-2 Burnup Data of PLUS7 LTAs and CSAs

| | | 1 st Cycle | 2 nd Cycle | 3 rd Cycle |
|-----|--|---|-----------------------|-----------------------|
| LTA | Effective full power days (EFPDs) | <div style="border: 1px solid black; width: 100%; height: 100%; border-radius: 10px; position: relative;"> TS </div> | | |
| | Fuel assembly average burnup (MWD/MTU) | | | |
| | Peak fuel rod average burnup (MWD/MTU) | | | |
| CSA | Effective full power days (EFPDs) | | | |
| | Maximum fuel assembly average burnup (KY5H615) (MWD/MTU) | | | |
| | Peak fuel rod average burnup (KY5H615) (MWD/MTU) | | | |

* Values in () are cumulated values
P14, C03: See Figure 4-2

Table 4-3 Irradiation Growths of the PLUS7 LTAs and CSAs

(Unit: mm)

| | Fuel Assembly No. | 1 st Cycle | 2 nd Cycle | 3 rd Cycle | Allowable Limit |
|-----|---|-----------------------|-----------------------|-----------------------|-----------------|
| LTA | <div style="border: 1px solid black; width: 100%; height: 100%; border-radius: 10px; position: relative;"> TS </div> | | | | |
| | | | | | |
| CSA | | | | | |
| | | | | | |

NM : Not measured (or not to be measured)

Table 4-4 Shoulder Gaps of the PLUS7 LTAs and CSAs

(Unit: mm)

| | Fuel Assembly No. | Initial | 1 st Cycle | 2 nd Cycle | 3 rd Cycle | Allowable Limit | |
|-----|-------------------|--|-----------------------|-----------------------|-----------------------|-----------------|----|
| LTA | | <div><div></div><div></div><div></div><div></div><div></div><div></div><div></div><div></div><div></div><div></div><div></div></div> | | | | | TS |
| | | | | | | | |
| CSA | | | | | | | |
| | | | | | | | |
| | | | | | | | |
| | | | | | | | |
| | | | | | | | |
| | | | | | | | |
| | | | | | | | |
| | | | | | | | |
| | | | | | | | |

NM : Not measured (or not to be measured)

Table 4-5 Rod-to-Rod Gaps of the PLUS7 LTAs and CSAs

(Unit: mm)

| | Fuel Assembly No. | Initial | 1 st Cycle | 2 nd Cycle | 3 rd Cycle | Allowable Limit (No Penalty on DNB) |
|-----|-------------------|--|-----------------------|-----------------------|-----------------------|--|
| LTA | | <div><div></div><div></div><div></div><div></div><div></div><div></div><div></div><div></div><div></div><div></div><div></div></div> <div>TS</div> | | | | |
| | | | | | | |
| CSA | | | | | | |
| | | | | | | |
| | | | | | | |
| | | | | | | |
| | | | | | | |

NM : Not measured (or not to be measured)

Values in () indicate channel closure

Table 4-6 Grid Widths of the PLUS7 LTAs and CSAs

(Unit: mm)

| | Fuel Assembly No. | Initial | 1 st Cycle | 2 nd Cycle | 3 rd Cycle | Allowable Limit |
|-----|-------------------|---------|-----------------------|-----------------------|-----------------------|-----------------|
| LTA | | | | | | |
| | | | | | | |
| | | | | | | |
| CSA | | | | | | |
| | | | | | | |
| | | | | | | |

NM : Not measured (or not to be measured)

Table 4-7 Summary of Fuel Rod for Hot Cell Examination

| Assembly | Rod ID | Burnup (MWD/MTU) | Cell Position | Examinations |
|---|--------|---------------------|------------------|--------------|
| <div style="border: 1px solid black; height: 300px; position: relative;"> <div style="position: absolute; top: 0; right: 0; font-size: 10px;">TS</div> </div> | | | | |
| | | | | |
| | | | | |
| | | | | |
| | | | | |
| | | | | |

Table 4-8 Fuel Rod Internal Gas Pressure and Fission Gas Release

| Rod ID | Burnup (GWD/MTU) | Internal Pressure (MPa) | | Void Vol. (cc) | | Fission Gas Gen.(cc) | | Fission Gas Rel.(cc) | | Fraction of FGR | |
|-------------|------------------|-------------------------|---|----------------|---|----------------------|---|----------------------|---|-----------------|---|
| | P | M | P | M | P | M | P | M | P | M | P |
| <div></div> | | | | | | | | | | | |

P : Predicted M : Measured

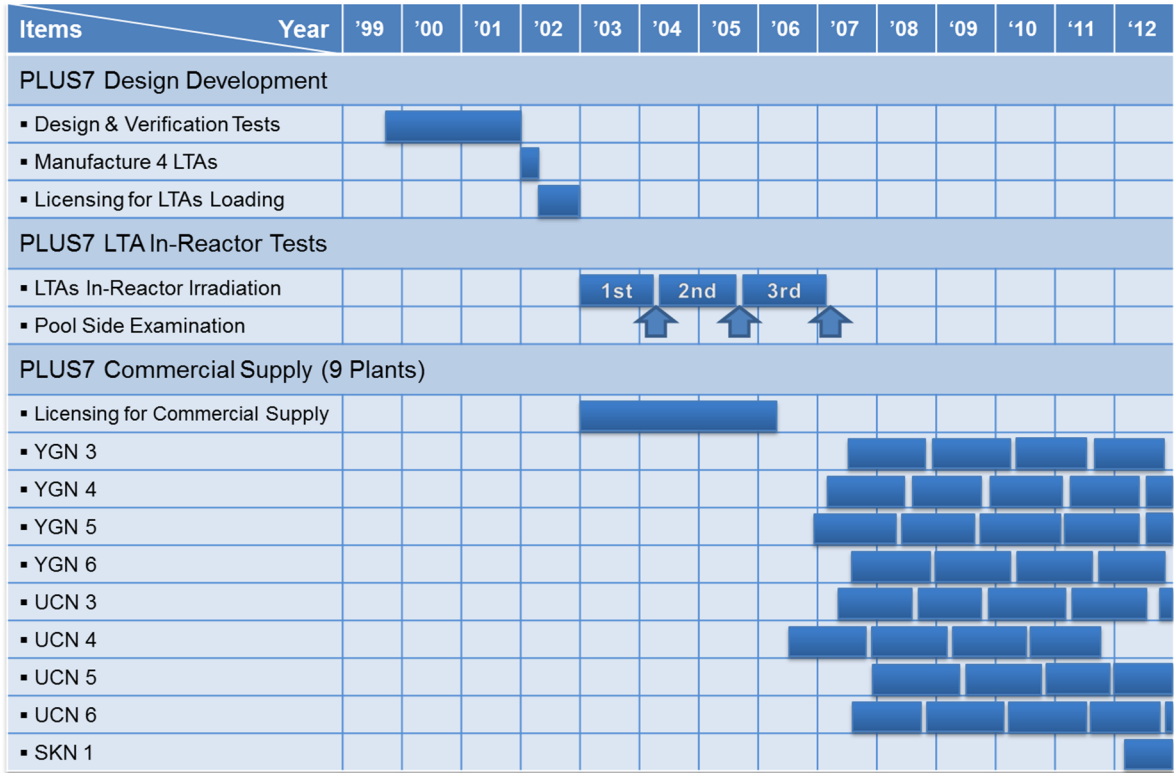
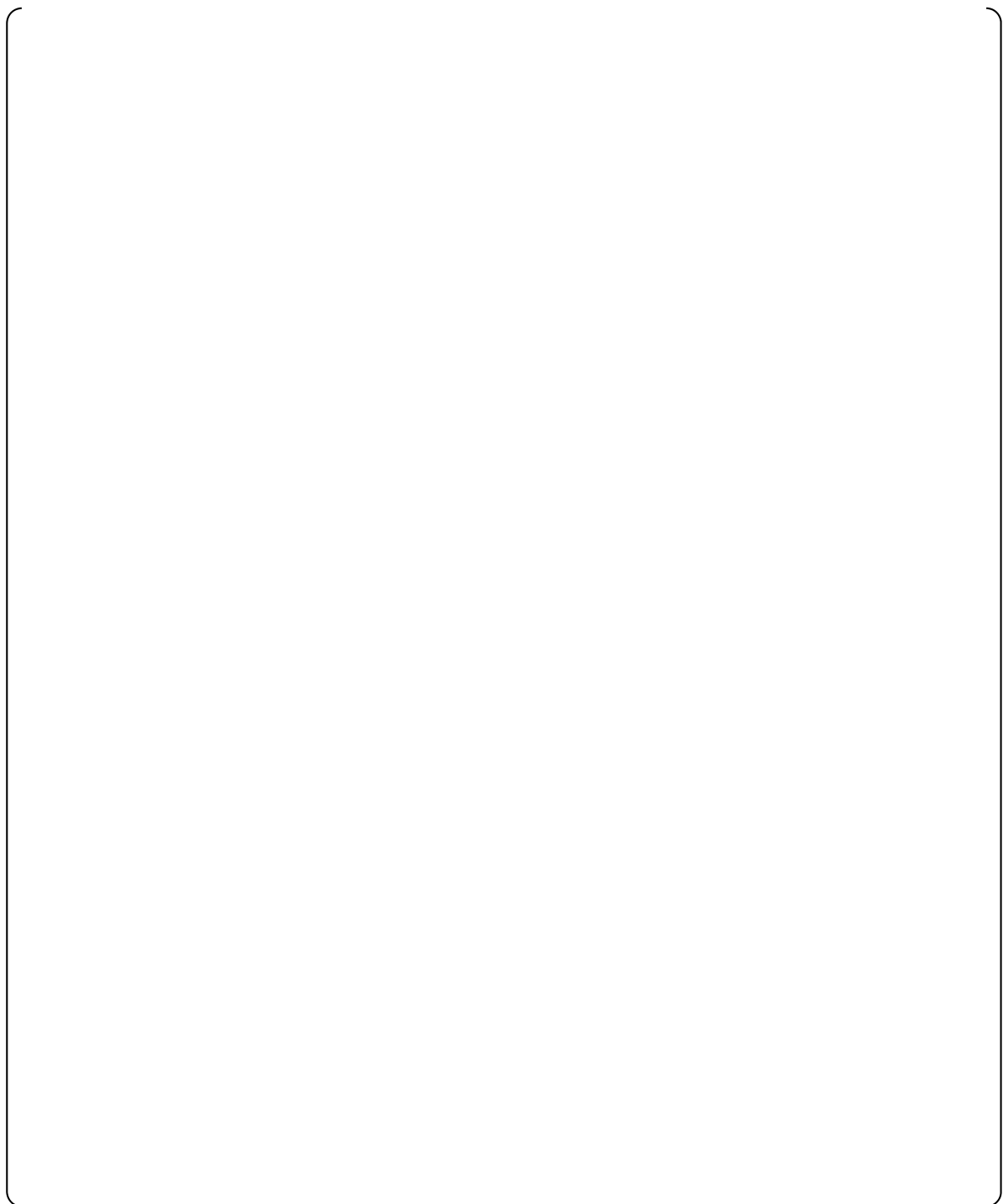
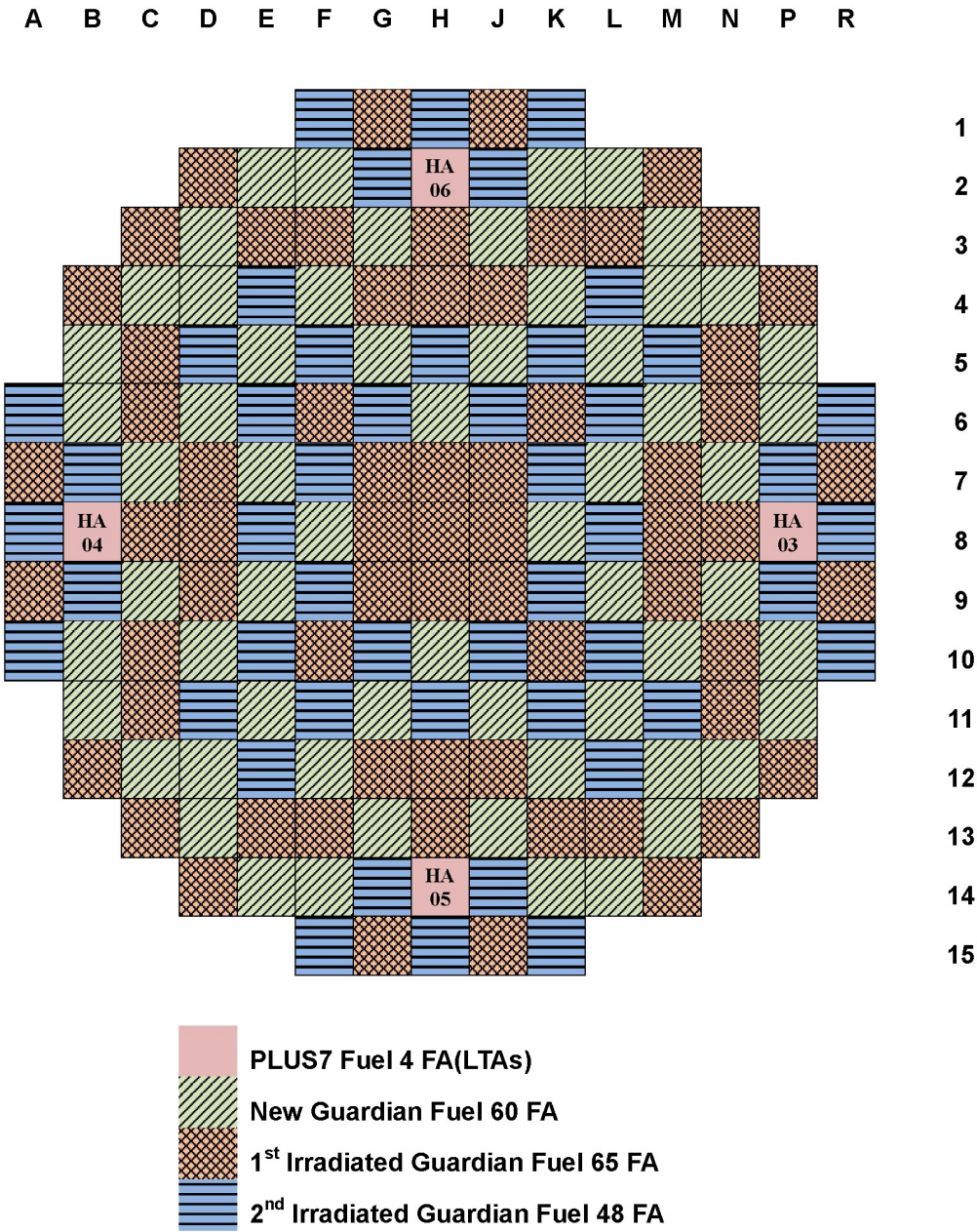


Figure 4-1 Development & Commercial Supply Status of PLUS7



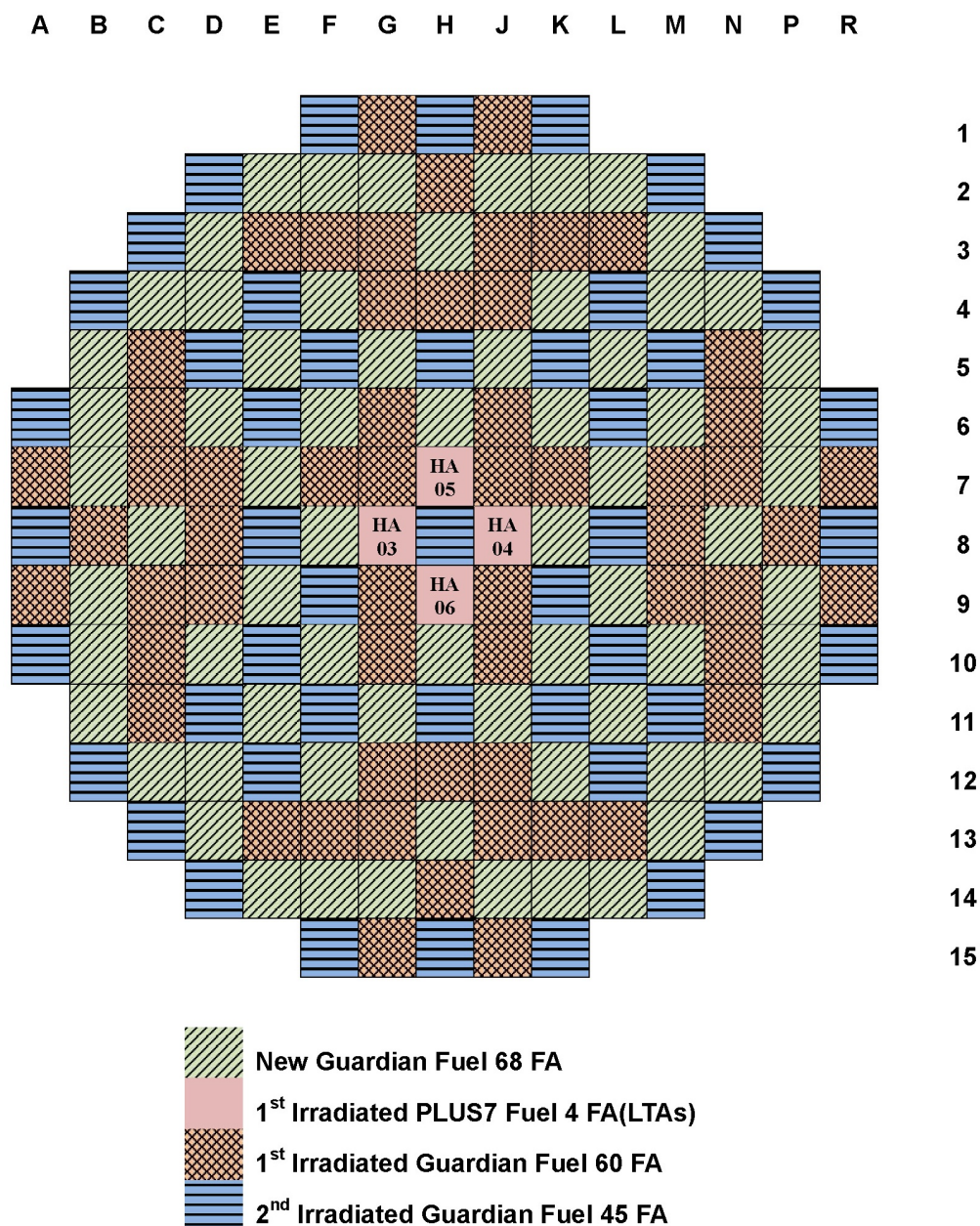
TS

Figure 4-2 Configuration of Fuel Rods in PLUS7 LTAs and CSAs



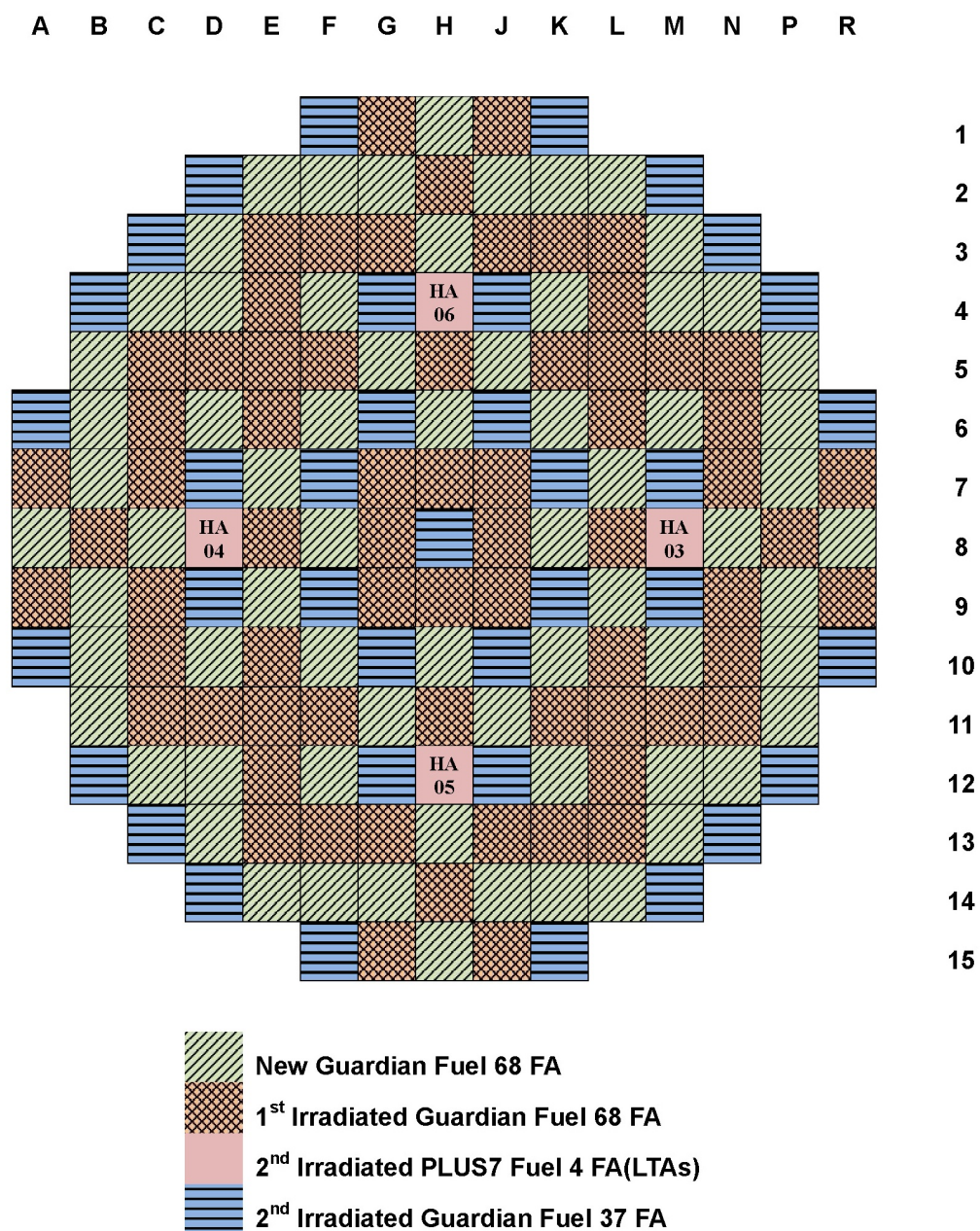
(a) The core of loading pattern of the UCN-3 5th cycle

Figure 4-3 Core Loading Pattern with PLUS7 LTAs



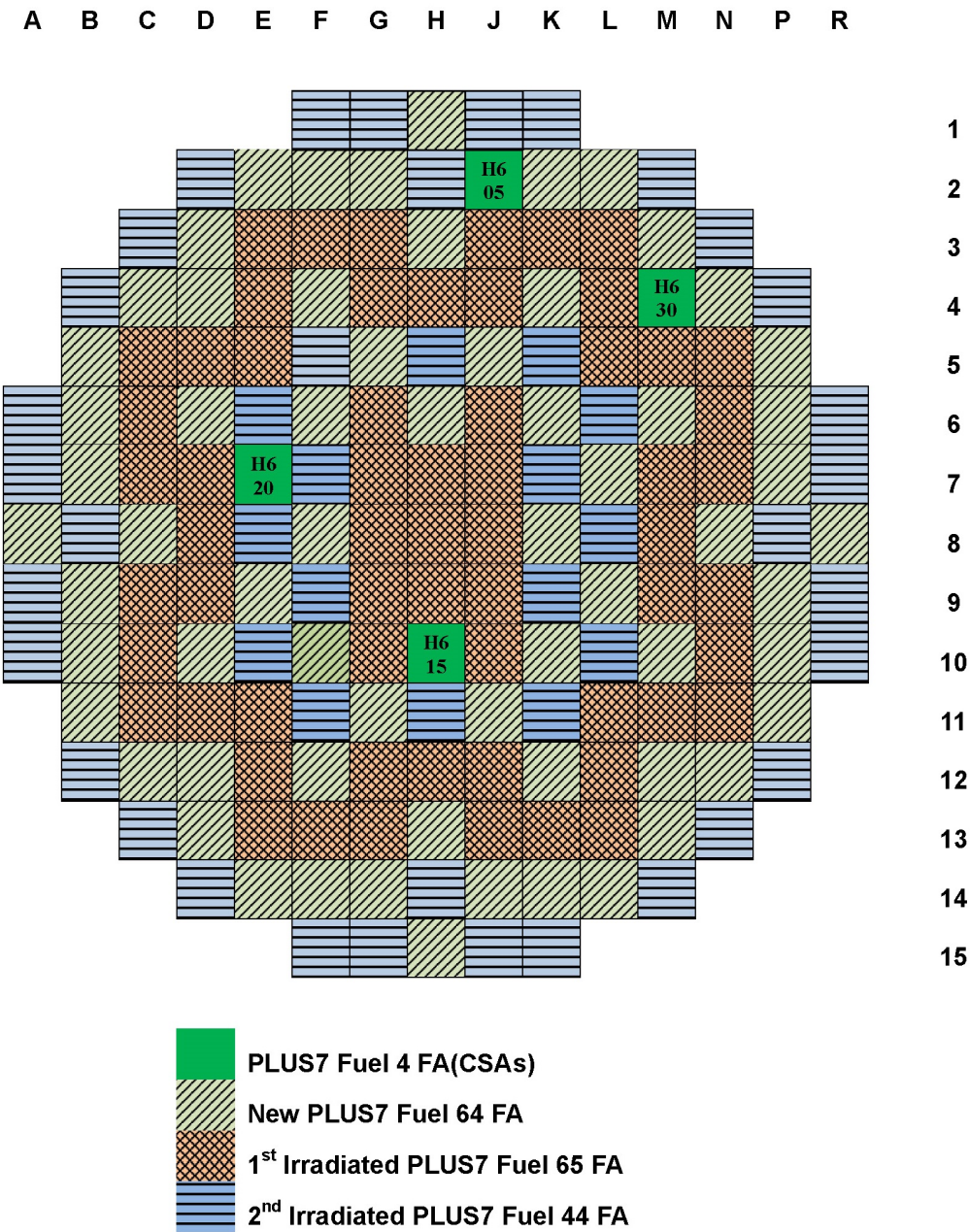
(b) The core of loading pattern of the UCN-3 6th cycle

Figure 4-3 Core Loading Pattern with PLUS7 LTAs (Continued)

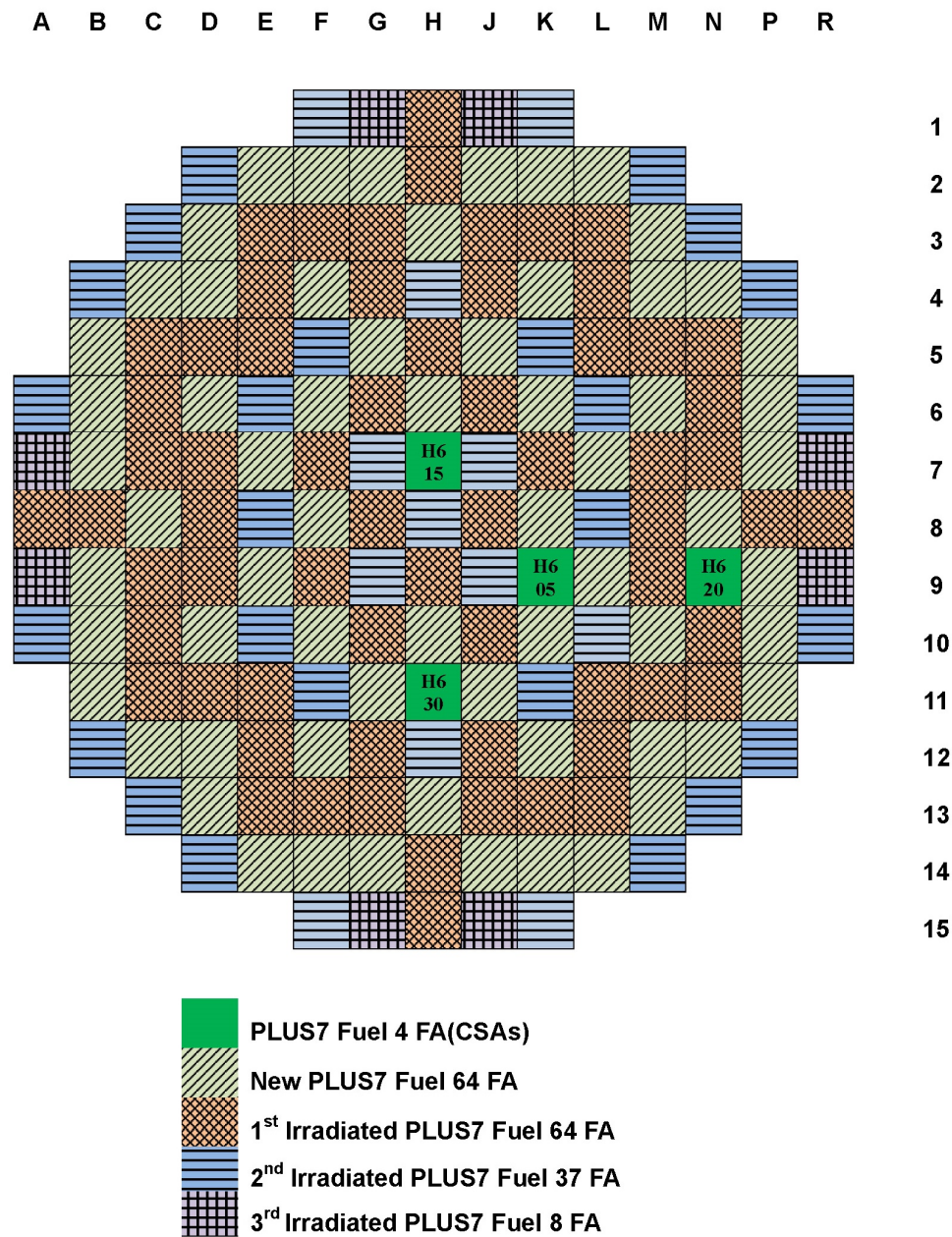


(c) The core of loading pattern of the UCN-3 7th cycle

Figure 4-3 Core Loading Pattern with PLUS7 LTAs (Continued)

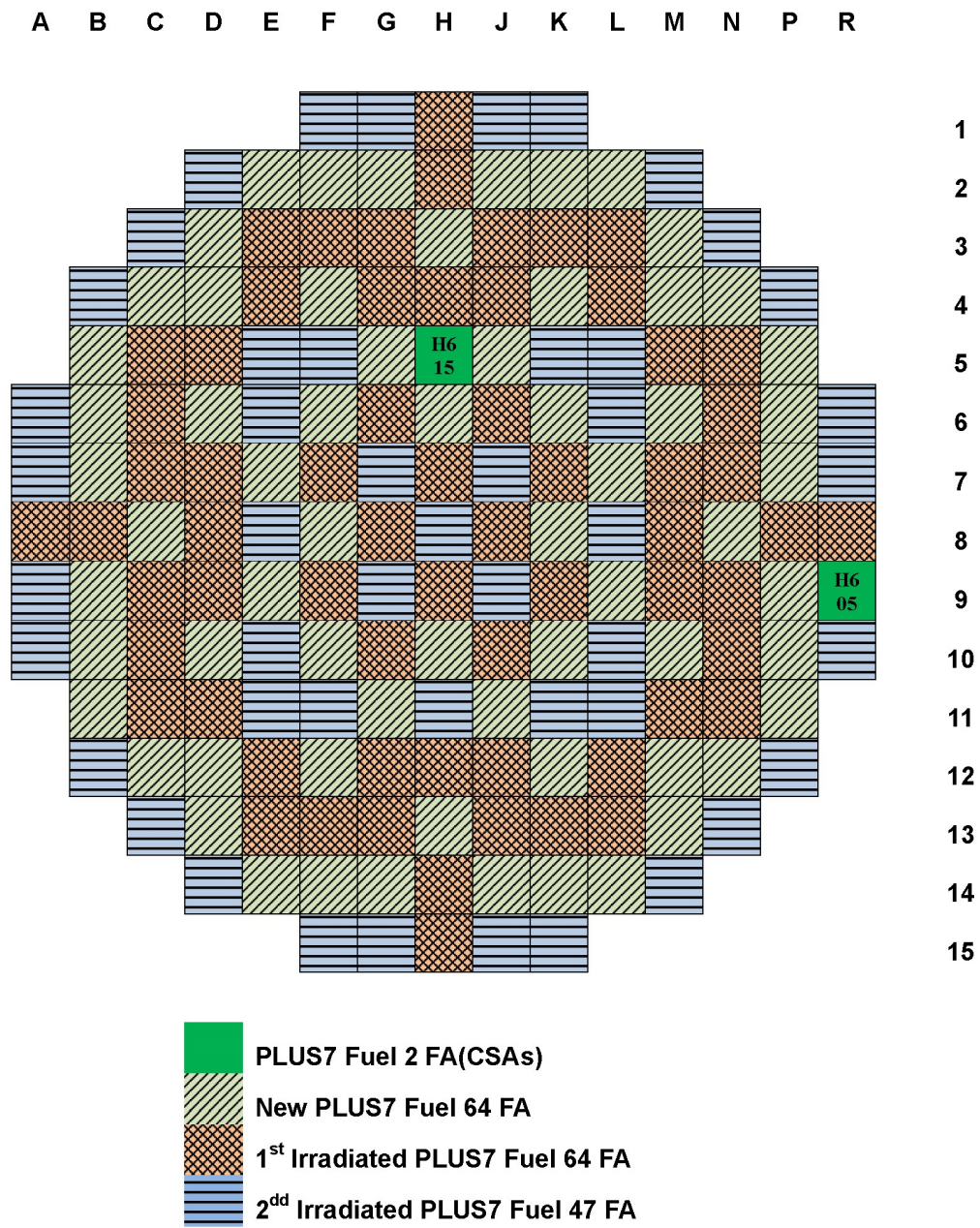


(a) The core of loading pattern of the YGN-5 5th cycle
Figure 4-4 Core Loading Pattern with PLUS7 CSAs



(b) The core of loading pattern of the YGN-5 6th cycle

Figure 4-4 Core Loading Pattern with PLUS7 CSAs (Continued)



(c) The core of loading pattern of the YGN-5 7th cycle
Figure 4-4 Core Loading Pattern with PLUS7 CSAs (Continued)



Figure 4-5 Measured Irradiation Growths of PLUS7 LTAs and CSAs



Figure 4-6 Measured Rod-to-Top Nozzle Clearances of PLUS7 LTAs and CSAs



Figure 4-7 Measured Rod-to-Rod Gaps of PLUS7 LTAs and CSAs



Figure 4-8 Measured Grid Widths of PLUS7 LTAs and CSAs

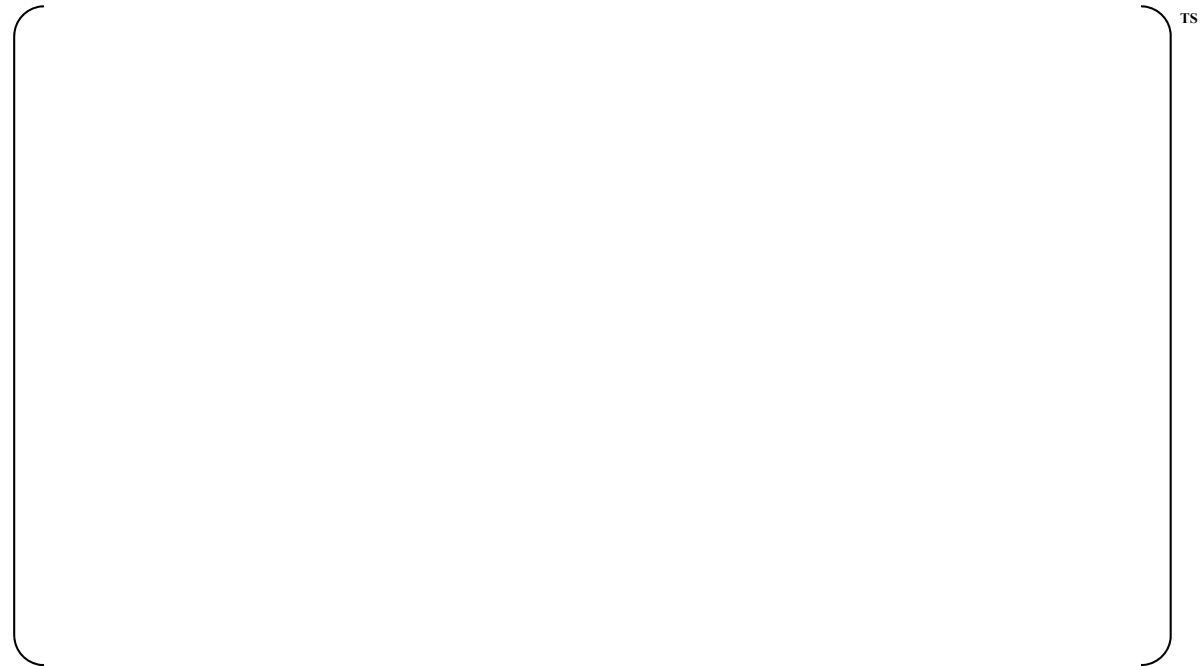


Figure 4-9 Measured Cladding Oxide Layer Thickness of PLUS7 LTA and CSAs



Figure 4-10 Comparison of Measured Cladding Oxide Layer Thickness and Predicted Cladding Oxide Layer Thickness of PLUS7 LTA and CSAs

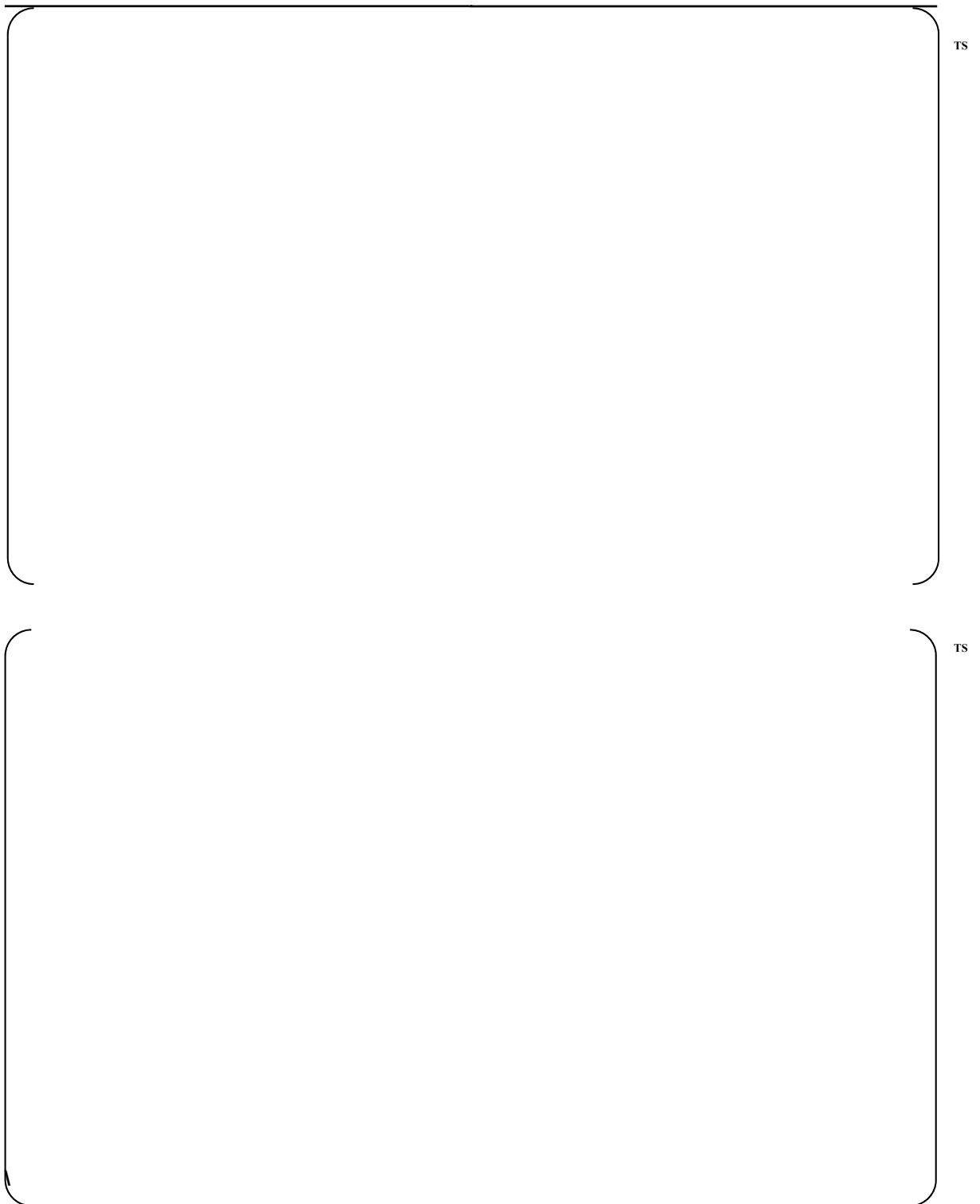


Figure 4-11 Diameter of HA03-A03 Fuel Rod

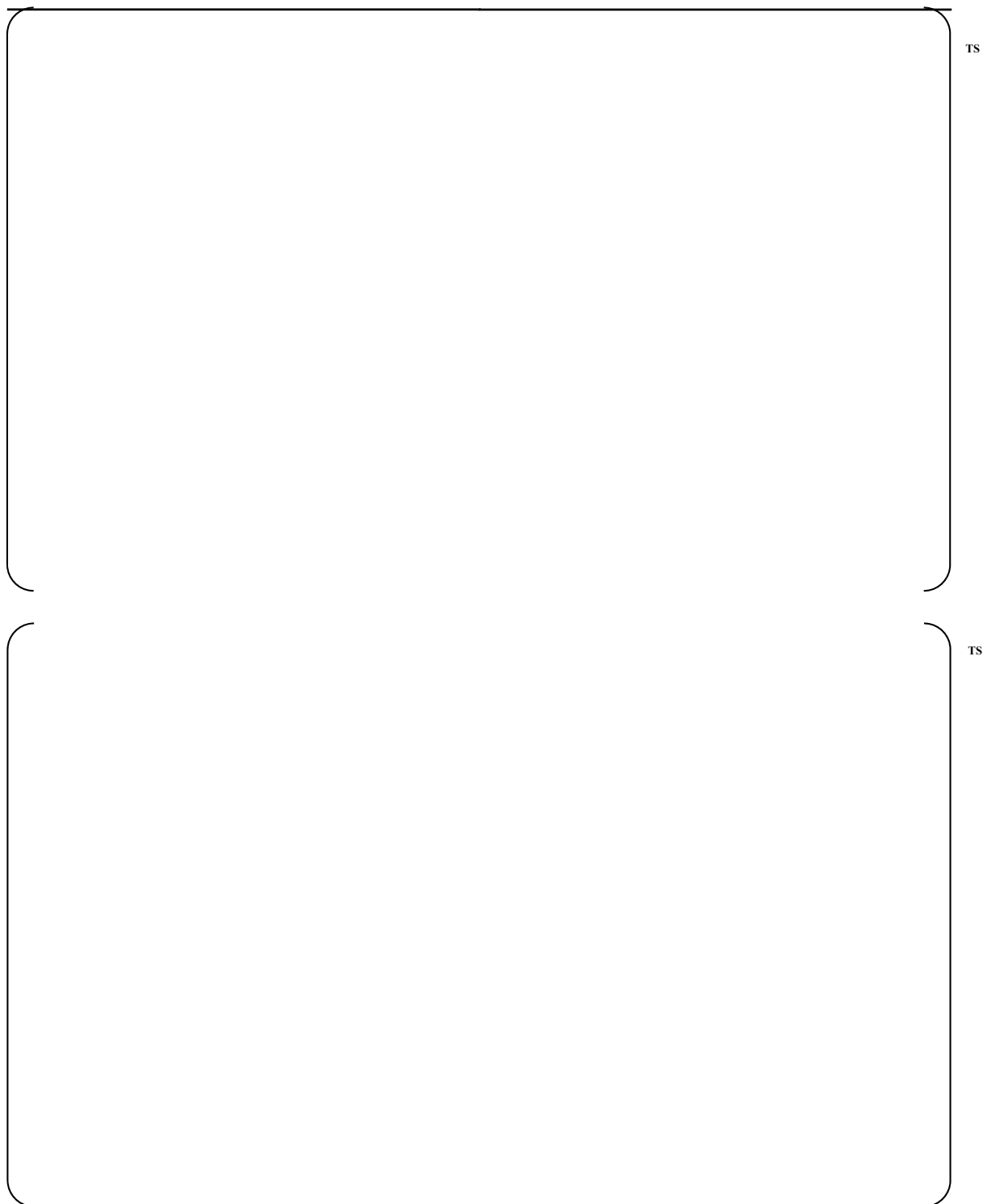


Figure 4-12 Diameter of HA03-A14 Fuel Rod

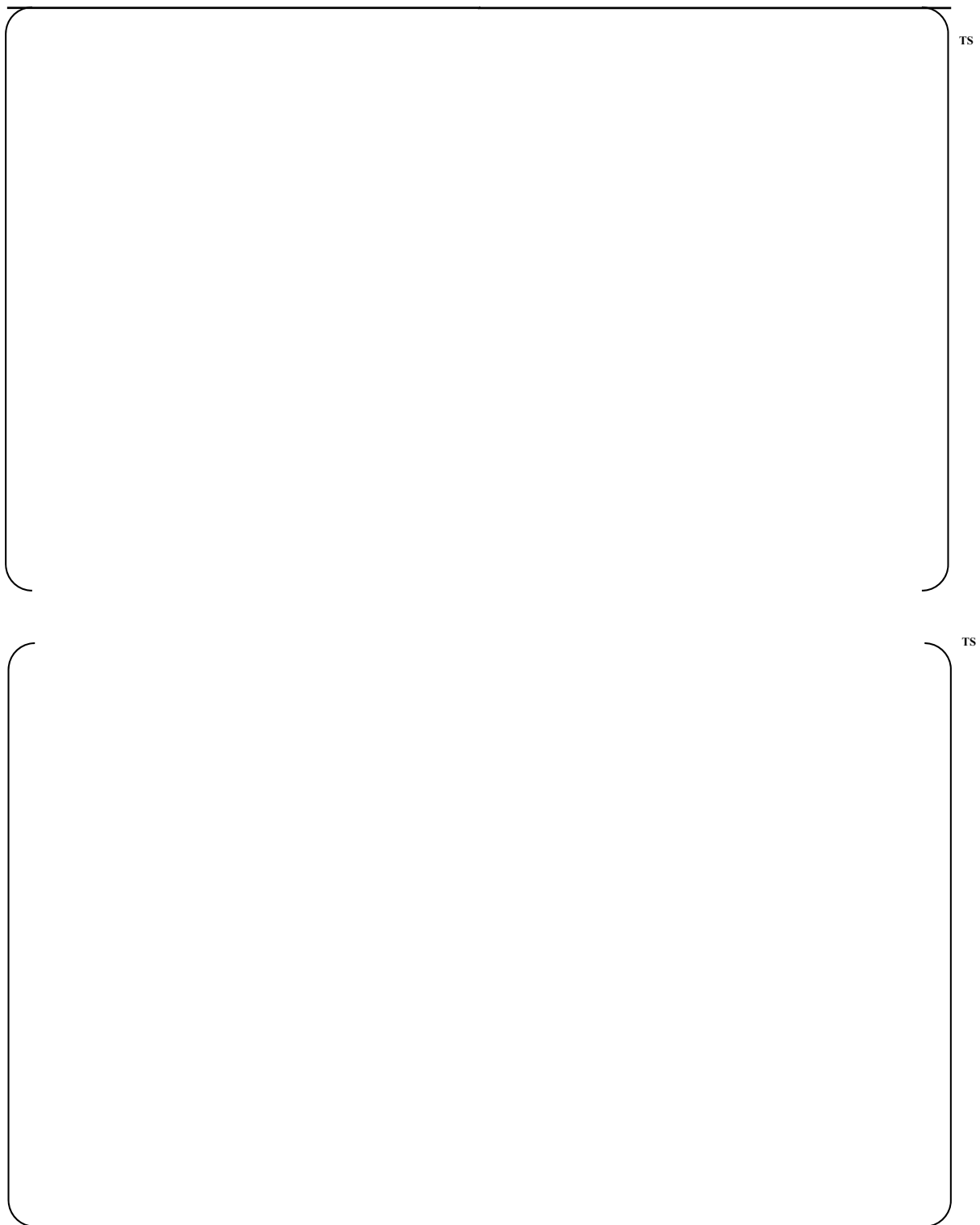


Figure 4-13 Diameter of HA03-B03 Fuel Rod

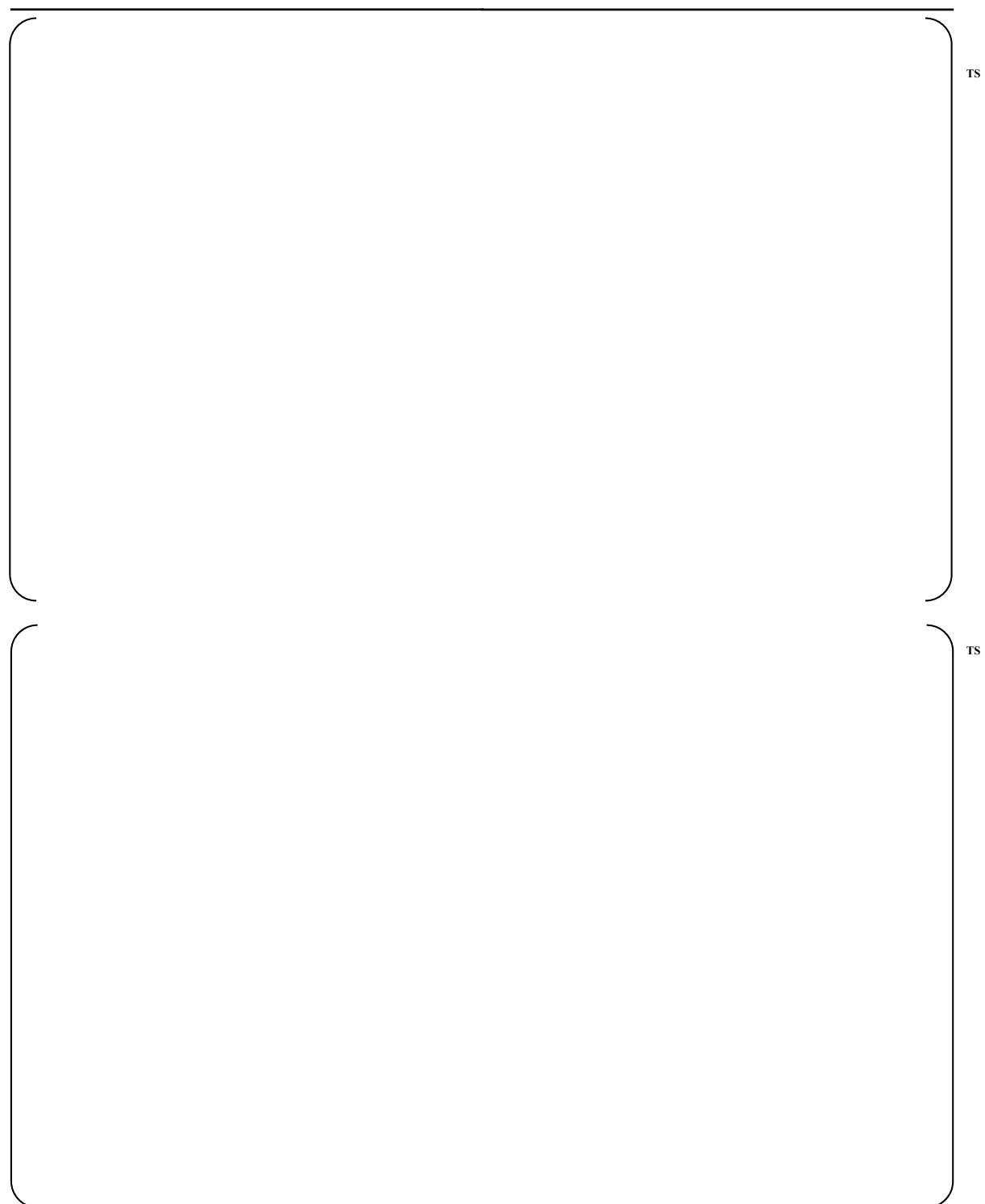


Figure 4-14 Diameter of HA03-B14 Fuel Rod

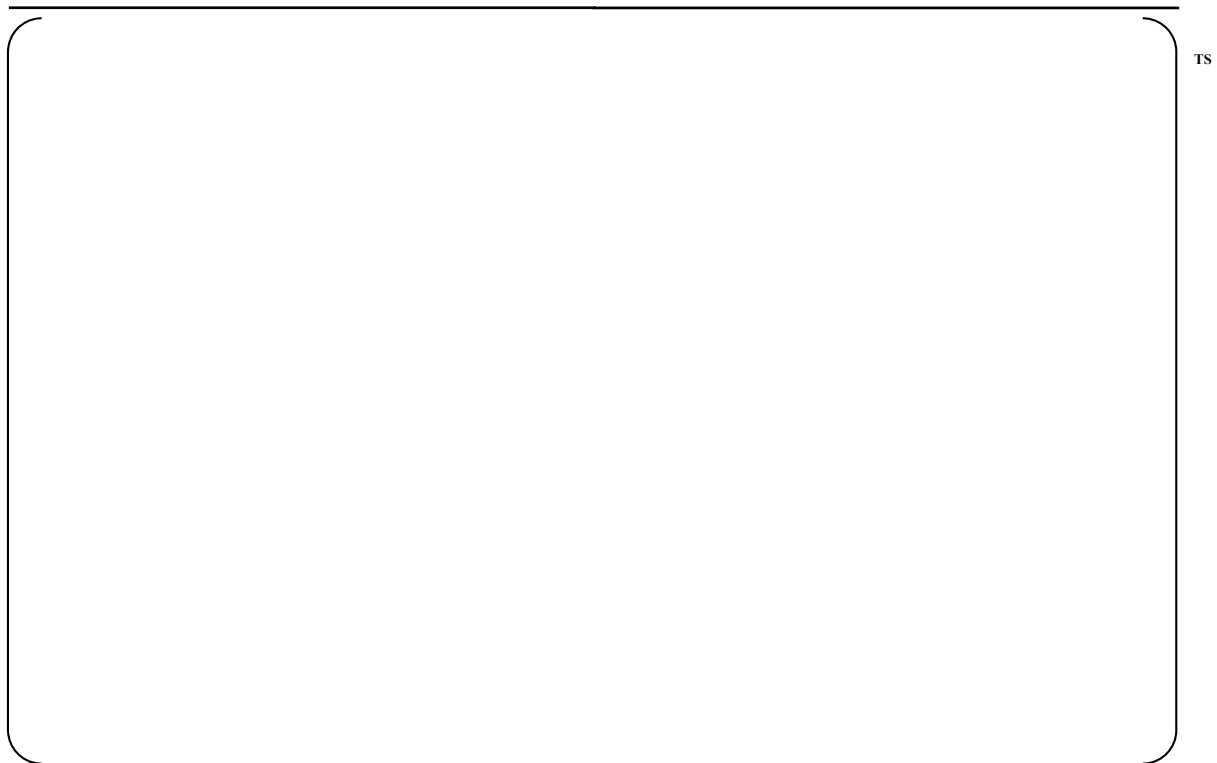


Figure 4-15 Diameter of HA03-C03 Fuel Rod (0°)

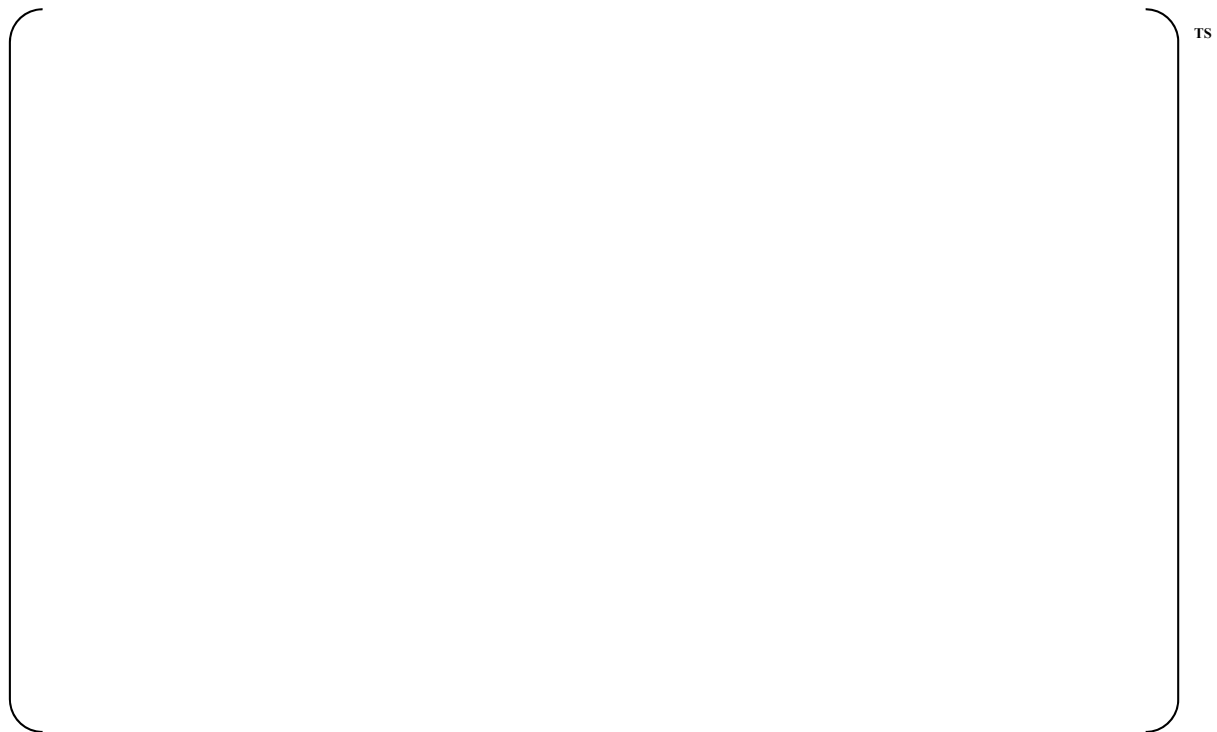


Figure 4-16 Diameter of HA03-K07 Fuel Rod (0°)

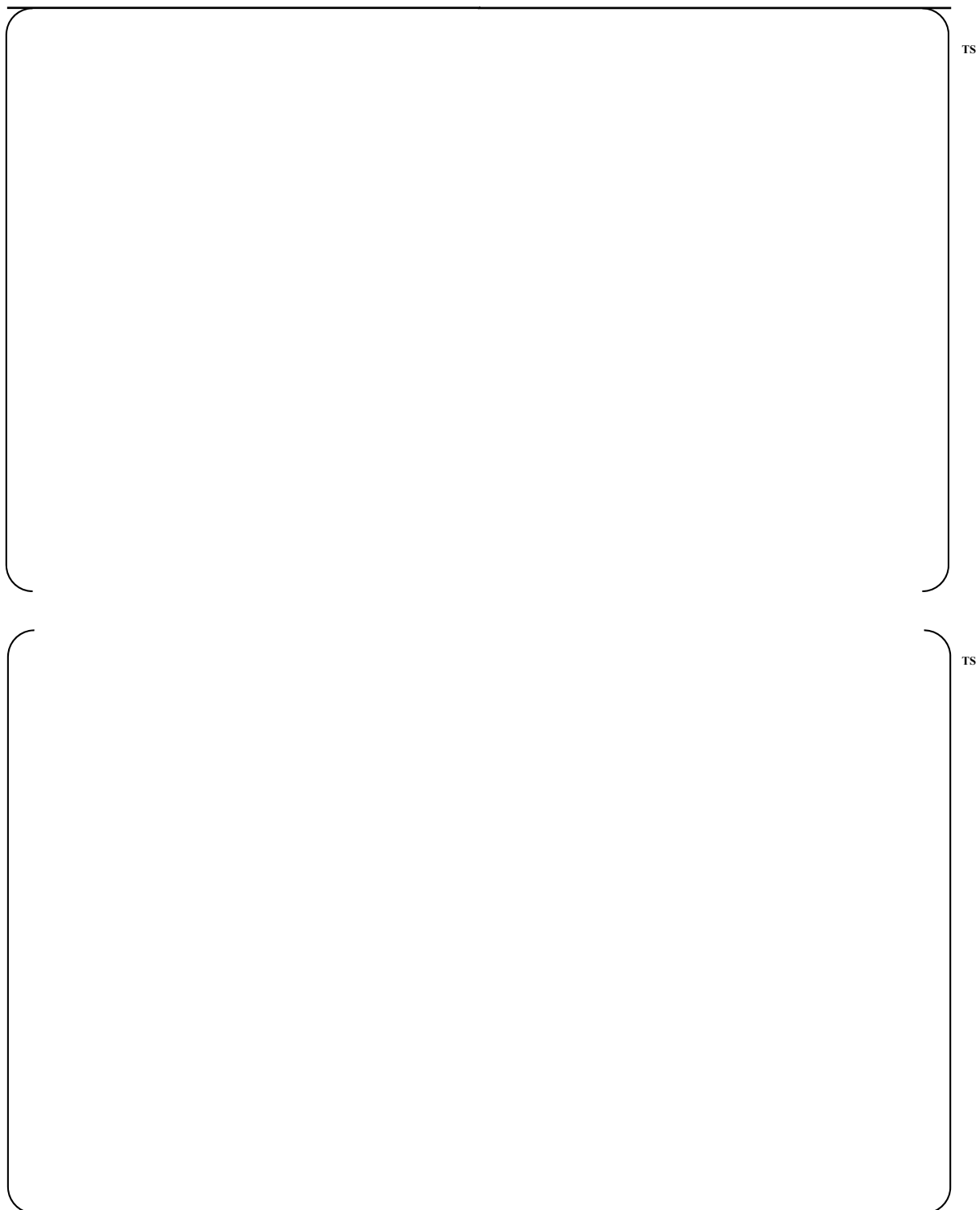


Figure 4-17 Diameter of HA03-C16 Fuel Rod

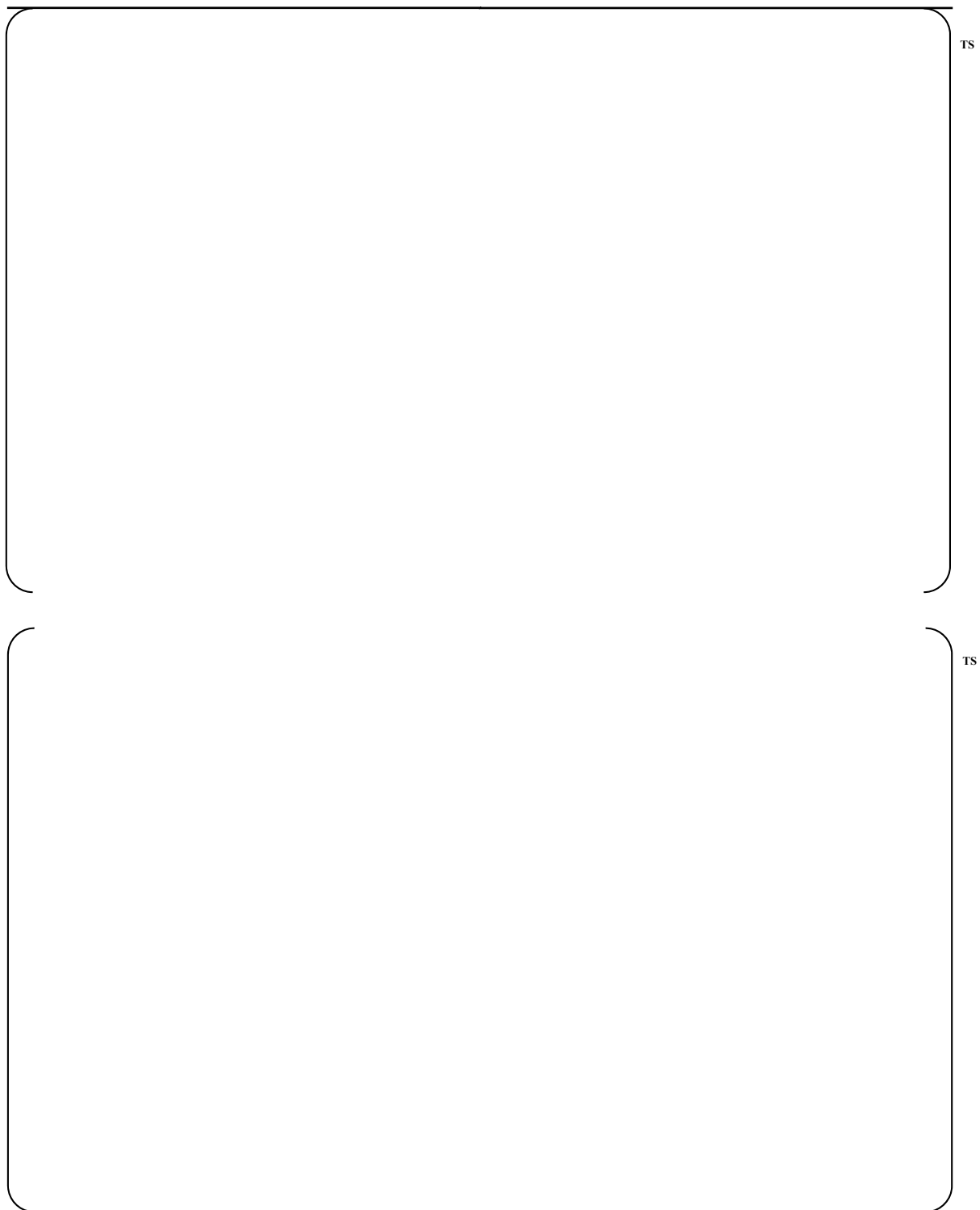


Figure 4-18 Diameter of HA03-D15 Fuel Rod

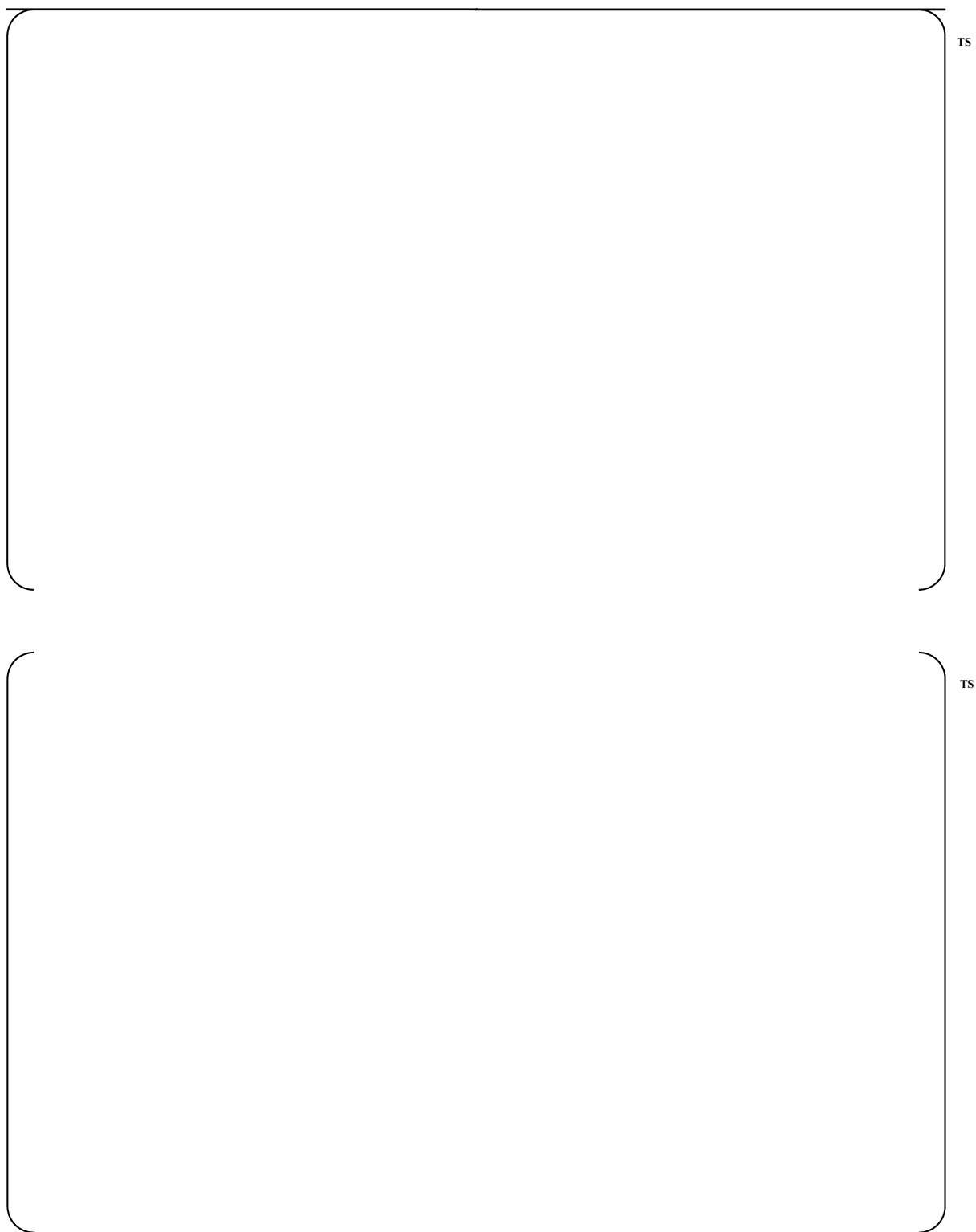


Figure 4-19 Diameter of HA03-D16 Fuel Rod



Figure 4-20 Diameter of H615-E01 Fuel Rod



Figure 4-21 Diameter of H615-N01 Fuel Rod Conclusion



Figure 4-22 Diameter of H615-D01 Fuel Rod



Figure 4-23 Diameter of H615-N03 Fuel Rod



Figure 4-24 Diameter of H615-H04 Fuel Rod



Figure 4-25 Diameter of H615-S16 Fuel Rod



Figure 4-26 Diameter of H615-N02 Fuel Rod



Figure 4-27 Diameter of H615-L11 Fuel Rod

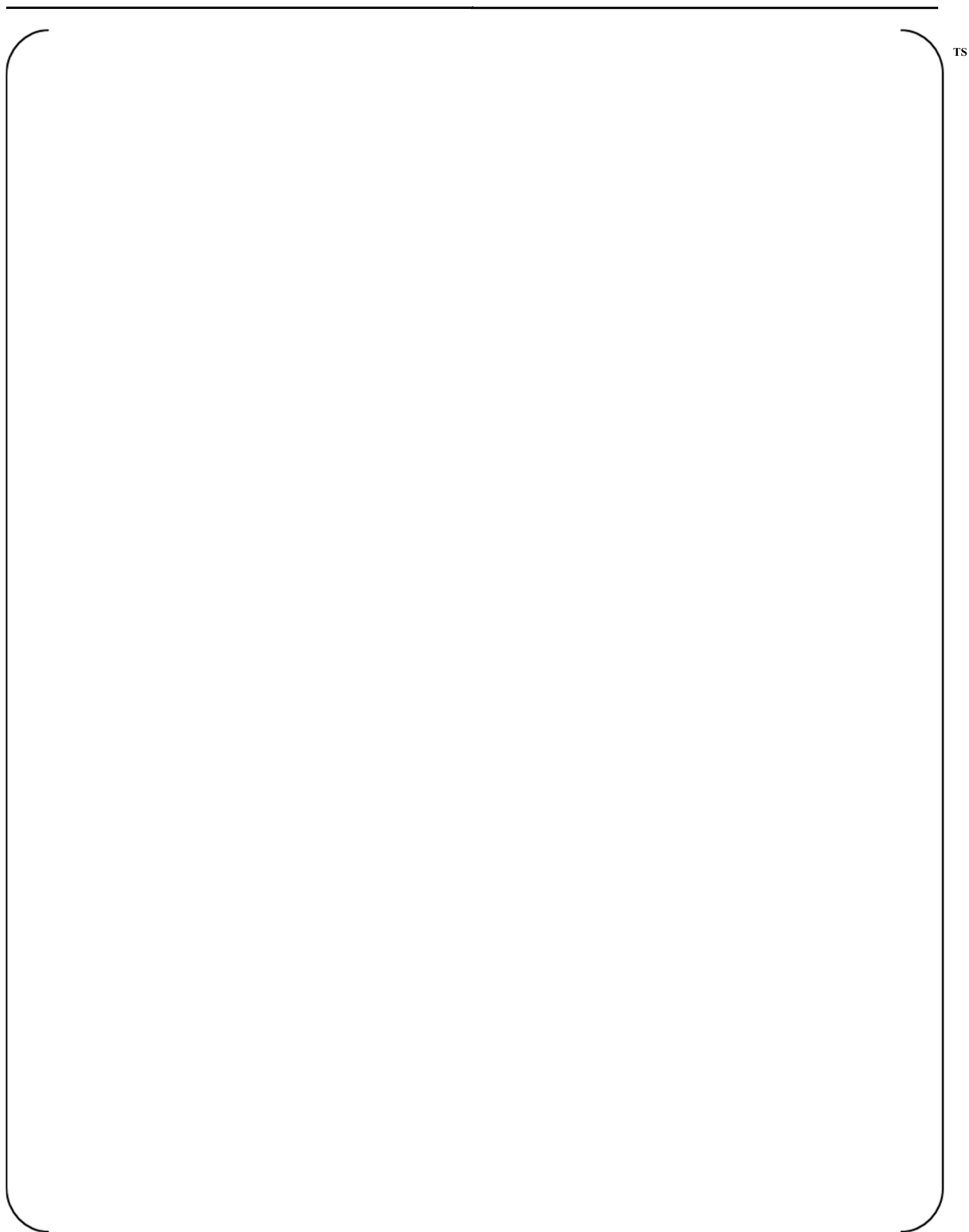


Figure 4-28 Visual Inspection Results of Fuel Rods at Grid Positions

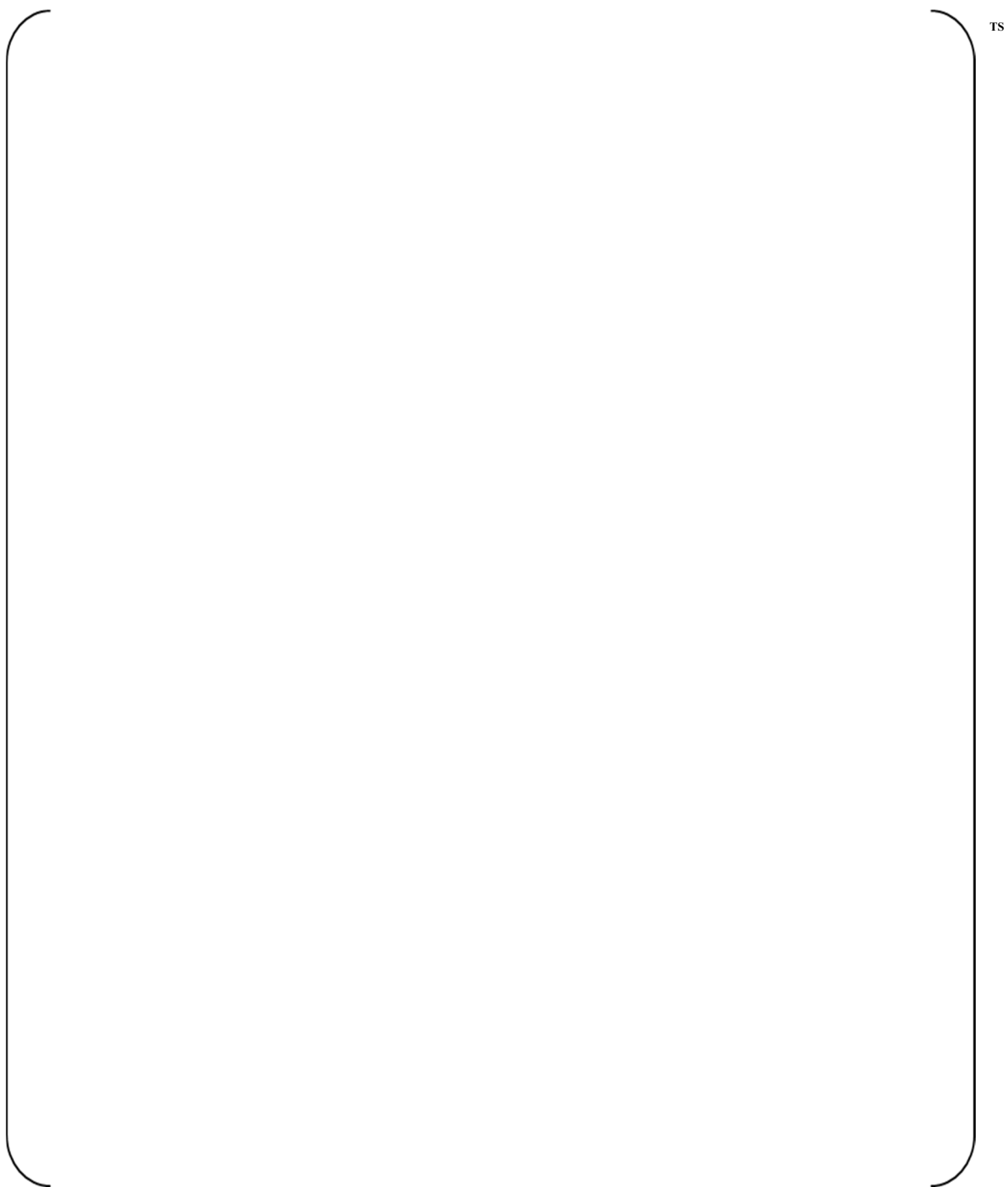


Figure 4-28 Visual Inspection Results of Fuel Rods at Grid Positions (Continued)



Figure 4-29 Visual Inspection Result of B14 Fuel Rod at Grid Positions

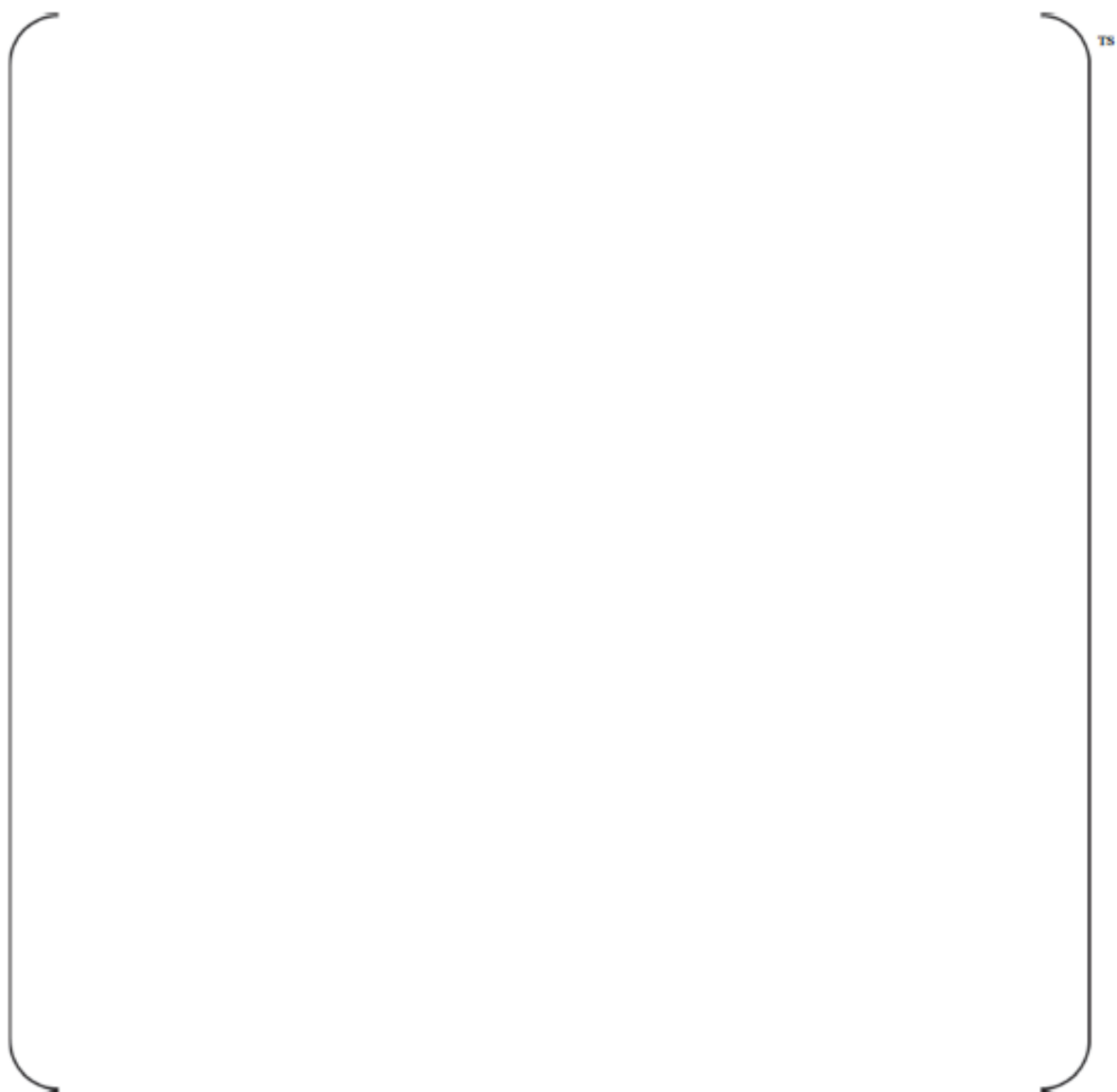


Figure 4-30 Cross-Section Inspection Results of B14 Fuel Rod (10th Grid, Spring 0°)



Figure 4-31 Oxide Thickness of HA03-A14 Fuel Rod



Figure 4-32 Oxide Thickness of HA03-B14 Fuel Rod



Figure 4-33 Oxide Thickness of HA03-C03 Fuel Rod

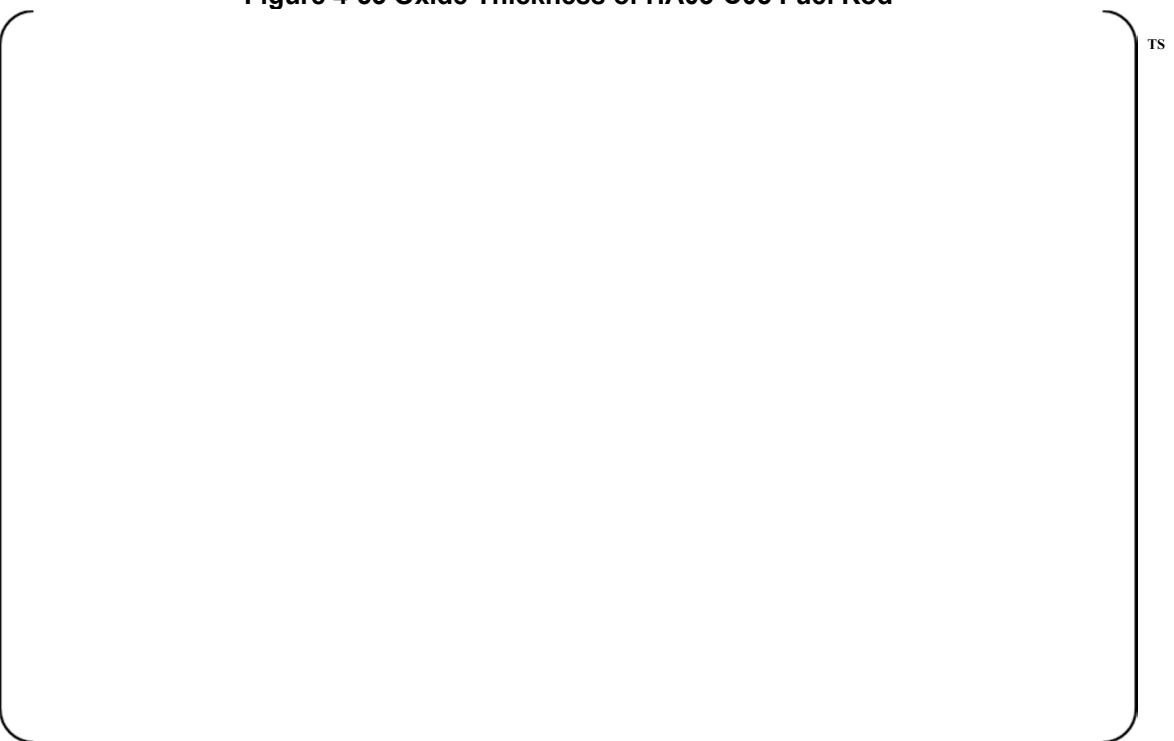


Figure 4-34 Oxide Thickness of HA03-D15 Fuel Rod



Figure 4-35 Oxide Thickness of HA03-D16 Fuel Rod

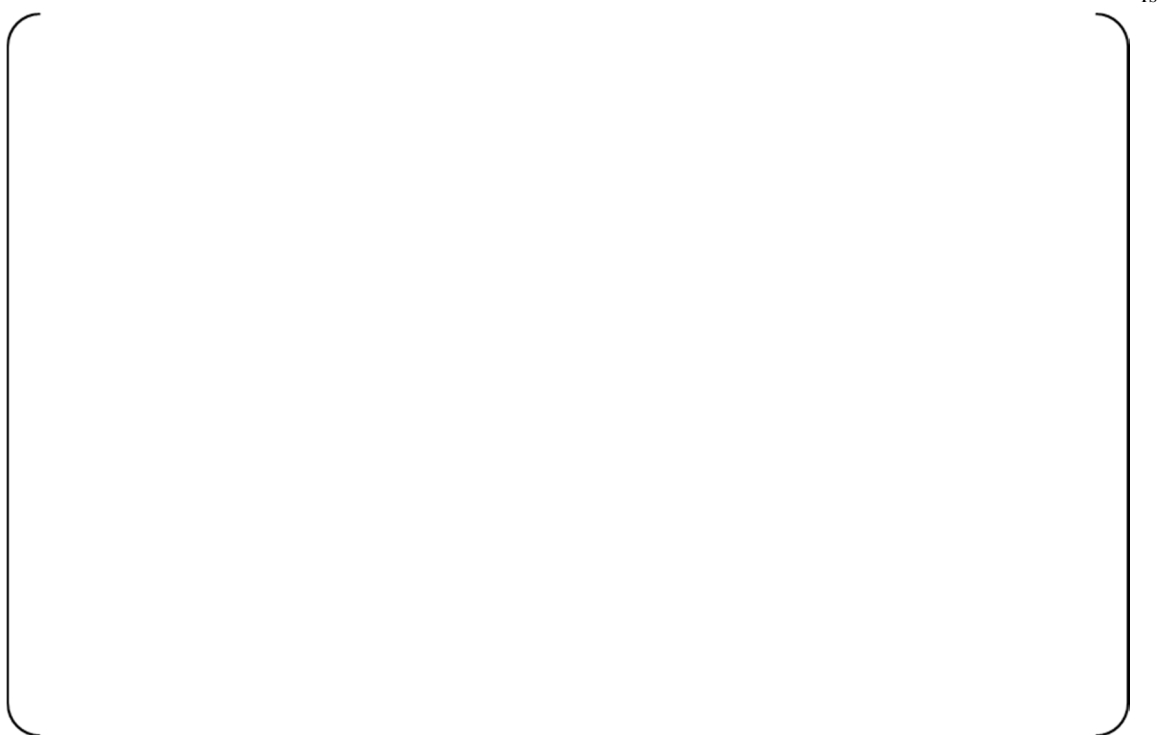


Figure 4-36 Oxide Thickness of HA03-K07 Fuel Rod



Figure 4-37 CRUD and Bonding Layer of HA03-C03 Fuel Rod (3094 mm)



Figure 4-38 Diameter of HA03-A14 Fuel Rod



Figure 4-39 Diameter of HA03-B14 Fuel Rod



Figure 4-40 Diameter of HA03-C03 Fuel Rod



Figure 4-41 Diameter of HA03-D15 Fuel Rod



Figure 4-42 Diameter of HA03-D16 Fuel Rod

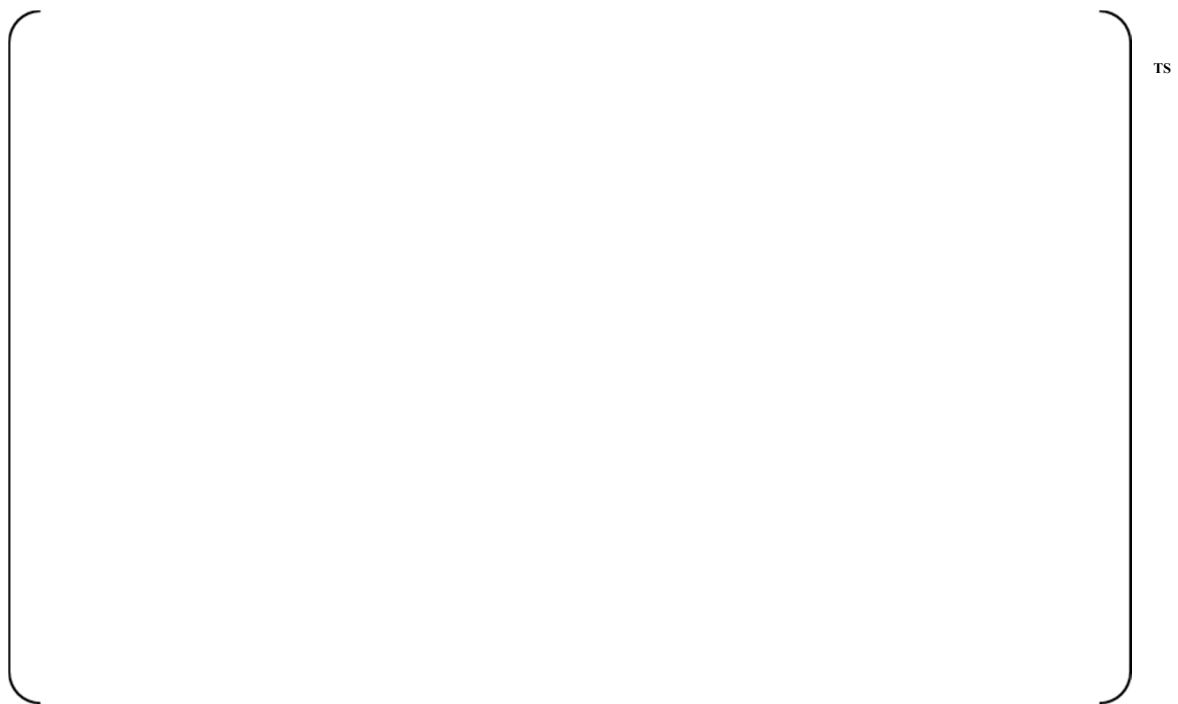


Figure 4-43 Diameter of HA03-K07 Fuel Rod



Figure 4-44 Hydrogen Content of ZIRLO Cladding

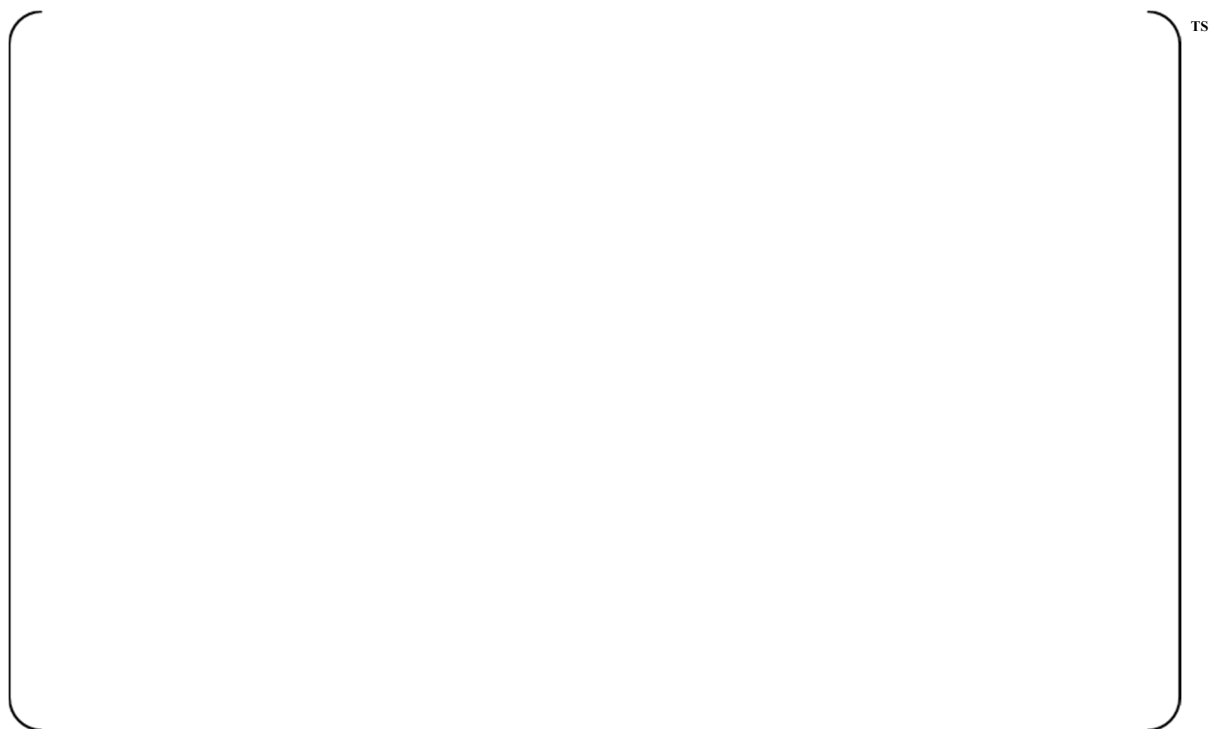


Figure 4-45 Calculated Hydrogen Content of PLUS7 LTA



Figure 4-46 Hydride Microphotograph of HA03-C03 Fuel Rod (3255 mm)

5. CONCLUSION

PLUS7 fuel has been developed to improve fuel performance relative to Guardian fuel. The integrity and safety evaluation results for fuel assembly and fuel rods are summarized as follows.

- Fuel assembly and its components design

The performance of the PLUS7 fuel assembly and its components was evaluated. The evaluation results showed that the PLUS7 fuel assembly met all the design criteria related to the in-reactor mechanical integrity. It was confirmed that the PLUS7 fuel assembly and its components were irradiated within the design limit based on the in-reactor performance data measured for the PLUS7 fuels.

- Fuel rod design

The thermal performance and mechanical integrity of the PLUS7 fuel rods adopting ZIRLO cladding were evaluated up to the maximum fuel rod average burnup of 60,000 MWD/MTU. The results confirmed that the PLUS7 fuel rod satisfied all the design criteria related to the rod thermal performance and mechanical integrity. It was confirmed that the PLUS7 fuel rods have been irradiated within the design limit based on the in-reactor performance data measured for the fuel rods in PLUS7 fuels.

6. REFERENCES

- 2-1 CENPD-178-P, Revision 1-P, "Structural Analysis of Fuel Assemblies for Seismic and Loss of Coolant Accident Loading," Combustion Engineering Inc., August 1981.
- 3-1 CENPD-139-P-A, "C-E Fuel Evaluation Model Topical Report," Combustion Engineering Inc., July 1974.
- 3-2 CENPD-139, Supplement 1, Revision 01, "C-E Fuel Evaluation Model Topical Report," Combustion Engineering Inc., July 1974.
- 3-3 CEN-161(B)-P-A, "Improvements to Fuel Evaluation Model," August 1989.
- 3-4 CEN-161(B)-P Supplement 1-P-A, "Improvements to Fuel Evaluation Model," January 1992.
- 3-5 CENPD-404-P-A, "Implementation of ZIRLO™ Cladding Material in CE Nuclear Power Fuel Assembly Designs," November 2001.
- 3-6 CEN-372-P-A, "Fuel Rod Maximum Allowable Gas Pressure," May 1990.
- 3-7 CENPD-275-P, Revision 1-P-A, "C-E Methodology for Core Designs Containing Gadolinia-Urania Absorbers," May 1998.
- 3-8 CENPD-275-P, Revision 1-P, Supplement, 1-P-A, "C-E Methodology for Core Designs Containing Gadolinia-Urania Absorbers," April 1999.
- 3-9 CEN-193(B), Supplement 2-P, Partial Response to NRC Questions on CEN-161(B)-P, "Improvements to Fuel Evaluation Model," March 21, 1982.
- 3-10 WCAP-16500-P-A, Rev.0 "CE 16x16 Next Generation Fuel Core Reference Report," August 2007.
- 3-11 WCAP-15063-P-A, Rev.1, with Errata, "Westinghouse Improved Performance Analysis and Design Model (PAD4.0)," July 2000.
- 3-12 CENPD-187-P-A, CEPAN Method of Analyzing Creep Collapse of Oval Cladding, Combustion Engineering, Inc., April 1976 ; Supplement 1-P-A, June 1977.
- 3-13 EPRI NP-3966-CCM, "CEPAN Method of Analyzing Creep Collapse of Oval Cladding-Volume 5: Evaluation of Interpellet Gap Formation and Cladding Collapse in Modern PWR Fuel Rods," Combustion Engineering, Inc., April 1985.

Appendix A

Summary of PLUS7 Fuel Assembly Tests

JULY 2017

**Copyright © 2017
All Rights Reserved**

TABLE OF CONTENTS

| | |
|---|-------------|
| LIST OF TABLES | A-3 |
| LIST OF FIGURES..... | A-4 |
| | |
| A.1.0 INTRODUCTION | A-5 |
| A.2.0 SUMMARY OF TESTS | A-6 |
| A.2.1 FUEL ASSEMBLY VIBRATION TEST (FACTS)..... | A-6 |
| A.2.2 VIPER PLUS7 Fuel Assembly Long-Term Wear Test | A-9 |
| A.2.3 Through-Grid Long Pulse Test..... | A-14 |
| A.2.4 Top Nozzle Mechanical Test..... | A-17 |
| A.2.5 DFBN Mechanical Test | A-23 |
| A.2.6 Grid Hang-up Test..... | A-27 |
| A.2.7 FACTS Hydraulic Test for PLUS7 Fuel Assembly | A-30 |
| A.2.8 Grid Spring Test | A-32 |
| A.2.9 FACTS Lift-off Test for the PLUS7 Fuel Assembly | A-37 |
| A.3.0 CONCLUSION | A-42 |

LIST OF TABLES

| | | |
|---------------|--|------|
| Table A.2.1-1 | Comparison of the Assembly Vibration Test Condition Ranges to the APR1400 Operating Condition Ranges | A-6 |
| Table A.2.2-1 | Test Loop Conditions | A-9 |
| Table A.2.2-2 | PLUS7 Assembly Measurable Wear Scar | A-10 |
| Table A.2.3-1 | Through-Grid Long Pulse Test Result | A-14 |
| Table A.2.7-1 | Pressure Loss Coefficients | A-31 |
| Table A.2.8-1 | Summary of Grid Spring Load Deflection Test Results | A-33 |
| Table A.2.9-1 | Comparison of the Liftoff Test Condition Ranges to the APR1400 Operating Condition Ranges | A-37 |
| Table A.2.9-2 | Fuel Assembly and Specifications | A-38 |
| Table A.2.9-3 | Results of the Lift-off Tests Based on the Accelerometer Indications | A-39 |

LIST OF FIGURES

| | | |
|----------------|--|------|
| Figure A.2.1-1 | Placement of Inductive Displacement Transducers and Flow Housing Accelerometer | A-8 |
| Figure A.2.1-2 | Results of Vibration Test on PLUS7 Fuel Assembly | A-8 |
| Figure A.2.2-1 | Fretting Wear Scar Locations | A-11 |
| Figure A.2.2-2 | Fretting Wear Scar Elevations | A-12 |
| Figure A.2.2-3 | PLUS7 Assembly Wear Scar Distribution Along Grid Elevations | A-13 |
| Figure A.2.3-1 | Through-Grid Long Pulse Test Arrangement | A-15 |
| Figure A.2.3-2 | Impact Force & Deformation versus Run Number | A-16 |
| Figure A.2.4-1 | Shipping Test Setup | A-19 |
| Figure A.2.4-2 | Handling Test Setup | A-20 |
| Figure A.2.4-3 | Holddown Load Test Setup | A-21 |
| Figure A.2.4-4 | Holddown Spring Load Deflection Curve | A-22 |
| Figure A.2.5-1 | Shipping and Handling Load Test Setup | A-25 |
| Figure A.2.5-2 | LOCA Load Test Setup | A-26 |
| Figure A.2.6-1 | Grid Hang-up Test Setup | A-28 |
| Figure A.2.6-2 | Fuel Assembly Grid Hang-up Test Series | A-29 |
| Figure A.2.8-1 | Spring Test Apparatus Setup | A-34 |
| Figure A.2.8-2 | Load Deflection Tool | A-34 |
| Figure A.2.8-3 | ZIRLO Mid Grid Test Locations (Bottom View) | A-35 |
| Figure A.2.8-4 | Inconel Top Grid Test Locations (Bottom View) | A-35 |
| Figure A.2.8-5 | Inconel Bottom Grid Test Locations (Top View) | A-35 |
| Figure A.2.8-6 | Protective Grid Test Locations (Bottom View) | A-35 |
| Figure A.2.8-7 | ZIRLO Mid and Inconel Top/Bottom/Protective Grid Inner Cell Load Deflection | A-36 |
| Figure A.2.9-1 | FACTS Flow Diagram | A-40 |
| Figure A.2.9-2 | K11 (inlet) from the Lift-off Test | A-41 |
| Figure A.2.9-3 | K8 (outlet) from the Lift-off Test | A-41 |

A.1.0 INTRODUCTION

The following tests were conducted to verify the hydraulic and mechanical characteristics of the PLUS7 fuel assembly:

| Test Item | Test Objectives | Facility |
|---------------------------------------|--|--------------------|
| 1. Fuel Assembly Vibration Test | To determine the flow induced fuel assembly vibration characteristics | FACTS |
| 2. Fuel Rod Fretting Wear Test | To evaluate the fuel rod fretting wear | VIPER |
| 3. Through-Grid Long Pulse Test | To obtain the through-grid buckling strength | Grid Impact Tester |
| 4. Top Nozzle Mechanical Test | To obtain strain levels and displacements of the adapter plate and holddown plate at selected locations as a function of axial loading | FA Test Facility |
| 5. DFBN Mechanical Test | To obtain fuel assembly mechanical characteristics | FA Test Facility |
| 6. Grid Hang-up Test | To confirm FA to FA grid hang-up performance | FA to FA test |
| 7. FACTS Hydraulic Pressure Drop Test | To measure the fuel assembly and component pressure drop | FACTS |
| 8. Grid Spring Test | To determine the inner and outer cell spring load deflection characteristics of grid assemblies. | Grid Spring Tester |
| 9. Fuel Assembly Lift-off Test | To determine the flow rates at which the fuel assembly lifts off | FACTS |

A.2.0 SUMMARY OF TESTS

A.2.1 Fuel Assembly Vibration Test (FACTS)

1.0 Introduction and Objectives

The objective of this test is to confirm that the PLUS7 design is not susceptible to high resonance flow-induced assembly vibration over a range of plant operating flow rates. This is assessed by reviewing the vibration spectra from displacement transducers (see Figure A.2.1-1) and the instrumented fuel rod accelerometers for the presence of abnormal, flow-dependent, resonant vibration peaks. The absence of such peaks will be sufficient to determine the acceptability of the fuel assembly design.

2.0 Test Conditions

The test flow conditions were systematically varied in an effort to excite the vibration modes of the fuel assembly. Such a variation consisted of setting the loop at the required temperature of { }^{TS} and sweeping the loop flow rate from { }^{TS} to the maximum achievable flow rate. The flow rate was then returned to { }^{TS} at a same rate. The maximum achievable flow rate for this test was { }^{TS}. The PLUS7 fuel assembly will be placed at { }^{TS}. The equivalent mechanical design flow in the FACTS test is { }^{TS}. Although the FACTS loop could not reach the elevated test flow rate { }^{TS} the maximum achievable flow rate does bound all possible operating flow rates, representing over 117% of the best estimate flow { }^{TS}, which is the flow rate at which PLUS7 fuel assembly will be placed. The maximum achievable flow rate is more than adequate to confirm that the PLUS7 design does not exhibit flow-induced resonant fuel assembly vibration. The test conditions and APR1400 operating conditions are compared in Table A.2.1-1.

Table A.2.1-1 Comparison of the assembly vibration test condition ranges to the APR1400 operating condition ranges

| Assembly Vibration Test Condition in FACTS Loop | | APR1400 Operating Condition | |
|---|-------------------|---|-------------------|
| Temperature (°F) | { } ^{TS} | Average Temperature (°F) | { } ^{TS} |
| Corresponding Mechanical Design Flow in FACTS (gpm) | | Mechanical Design Flow (gpm) per Assembly | |
| Test Flow Range (gpm) | | | |

3.0 Test Results

The flow sweep test was performed at { }^{TS}. In this test, the loop flow rate was increased in a constant manner from { }^{TS} to the maximum achievable loop flow rate of { }^{TS} in six minutes. Because the instrumented rod accelerometers were mounted at mid-grid elevations with as-built cell conditions, the accelerometer outputs represent the fuel assembly vibration.

Figure A.2.1-2 shows that the assembly did not experience the high resonance flow-induced fuel assembly vibration. There was no indication of abnormal flow-induced vibration response throughout the test flow range.

4.0 Summary and Conclusion

A FACTS loop test was conducted to verify that the PLUS7 design did not exhibit high resonance flow-induced fuel assembly vibration. Displacement transducers and instrumented fuel rods at grid locations measured the fuel assembly vibration. There was no indication of abnormal flow-induced vibration response throughout the test flow range.

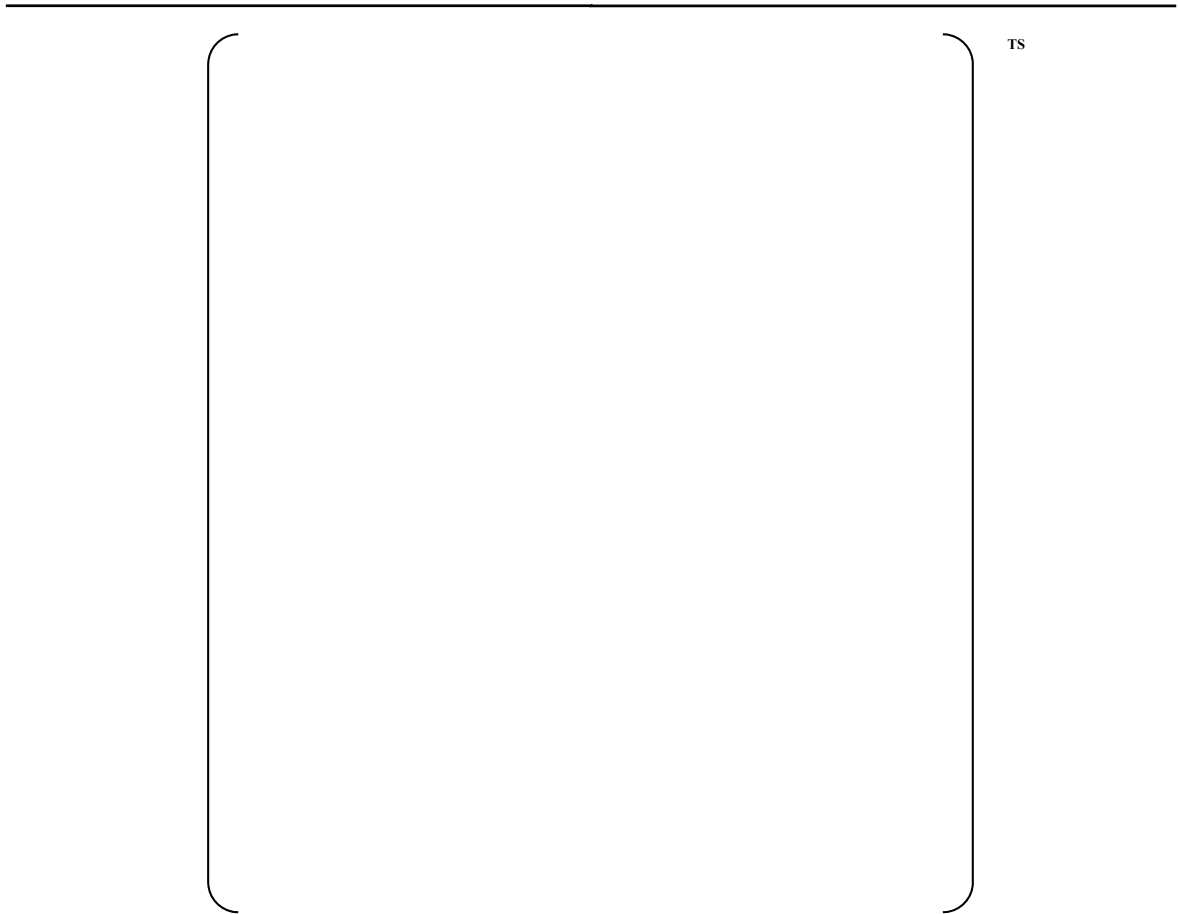


Figure A.2.1-1 Placement of Inductive Displacement Transducers and Flow Housing Accelerometer

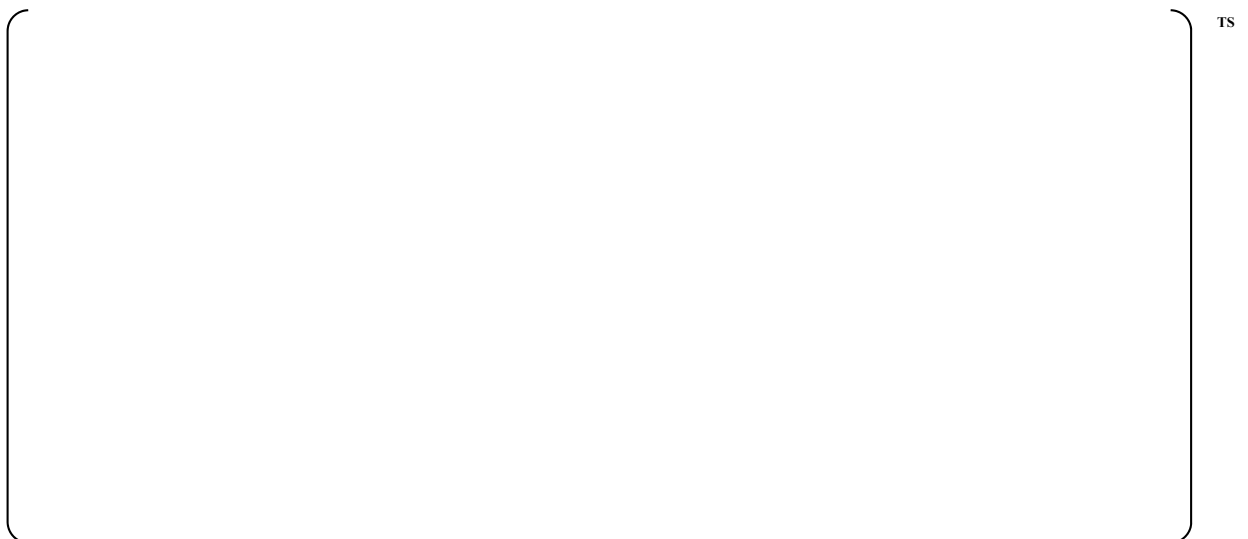


Figure A.2.1-2 Results of Vibration Test on PLUS7 Fuel Assembly

A.2.2 VIPER PLUS7 Fuel Assembly Long-Term Wear Test**1.0 Introduction and Objectives**

In this test, a PLUS7 fuel assembly with mixing vanes and a Guardian fuel assembly without mixing vanes were placed in the loop side by side. The PLUS7 fuel assembly consists of a reconstitutable top nozzle, a debris filter bottom nozzle, 4 ZIRLO guide thimbles and an instrument tube with a 0.98 inch diameter, 236 ZIRLO fuel rods with a 0.374 inch diameter, Inconel top and bottom grids, 9 ZIRLO mid grids, and an Inconel protective grid. The Guardian fuel assembly consists of a reconstitutable top nozzle, a standard bottom nozzle, 4 Zry-4 guide thimbles and an instrument tube with a 0.98 inch diameter, 236 Zry-4 fuel rods of 0.382 inch diameter, 10 Zry-4 grids, and an Inconel bottom grid. These two assemblies have nearly the same grid spacing. The PLUS7 ZIRLO mid grids have conformal spring and dimple features, while the Guardian Zry-4 mid grids and the top grid have wavy spring and dimple features.

Test objectives:

- To obtain grid-rod fretting wear data for the PLUS7 in a transition core environment and severe flow conditions

The test acceptance criteria for PLUS7 test assembly are as follows:

- Oxidized rods located in realistic gap cells [],^{TS} when projected to the expected operating life of the assembly, will not result in wear through the cladding

2.0 Test Conditions

The duration of the long-term wear test was 500 hours. The axial flow was intended to remain at [].^{TS} The average test conditions are listed below.

Table A.2.2-1 Test Loop Conditions

| T_{inlet} | P_{inlet} | P_{outlet} | Q_{total} | Q_{axial} | Viscosity | Density |
|--------------------------|--------------------------|---------------------------|--------------------------|--------------------------|------------------------|------------------------|
| (deg. F) | (psia) | (psia) | (gpm) | (gpm) | (ft ² /sec) | (lbm/ft ³) |
| [] ^{TS} | | | | | | |

3.0 Test Results

The PLUS7 assembly had a combination of pre-oxidized rods and non-oxidized rods in a checkerboard pattern. Figure A.2.2-1 shows the locations of rods with wear in the assembly. The value in a cell is the maximum depth of the worst dimple or spring wear scar on each rod. Figure A.2.2-2 shows the wear scar grid elevations corresponding to Figure A.2.2-1 and the order of the grid number in each cell corresponds to the wear severity up to three grids. A bar chart, Figure A.2.2-3, shows the wear scar distribution along the grid elevation.

Some observations and conclusions are obtained from the PLUS7 assembly wear results.

1. Under the axial flow test conditions and using the normal size flow housing with non-perforated side walls, the PLUS7 assembly wear pattern showed a basic random distribution radially. Since Guardian assembly and PLUS7 assembly had different pressure drops at local mid grid and mid-span, some local cross flow was generated between two assemblies. Even though the wear at the side facing Guardian assembly was slightly higher, deep wear also occurred in the other side. The effect of local cross flow was not significant.

2. The rods in { }^{TS} gap cells showed less wear than those in { }^{TS} gap cells. Eight rods showed wear scars in the { }^{TS} gap cells. Three rods in { }^{TS} gap cells had over { }^{TS} deep wear (all three scars were single dimple wears). The maximum wear depth in a { }^{TS} gap cell was { }^{TS} from a spring wear scar (See Figure A.2.2-1).

3. Non-oxidized rods had less wear resistance than oxidized rods. None of the oxidized rods showed wear while 60 non-oxidized rods showed measurable wear.

Table A.2.2-2 PLUS7 Assembly Measurable Wear Scar

| | No. of rod with Measurable wear | No. of rod Sample | Ratio |
|------------------|---------------------------------|-------------------|-------------------|
| Oxidized rod | { } | { } | { } ^{TS} |
| Non-oxidized rod | | | |

Figure A.2.2-3 shows the wear distribution along grid elevations. Each mid grid had relatively even wear. Grid 2 has the least wear and Grid 8 has the most wear.

4.0 Summary and Conclusion

This test is for the long-term wear test of the PLUS7 fuel assembly and Guardian fuel assembly. The PLUS7 and Guardian fuel assemblies were tested in the VIPER loop residing side by side for 500 hours. The total loop axial flow was { }^{TS}.

This test was to verify the adequacy of the PLUS7 design. The vibration signals of the instrumented rods showed that the fuel assembly and fuel rods did not experience any abnormal flow-induced vibration. Every rod in the PLUS7 test assembly (including instrumented rods) was examined for grid-rod fretting wear, and all fretting wear scars were measured using the Accumeasure System 9000 tool to determine the fretting wear depth. Since all oxidized rods in { }^{TS} gap cells had no measurable wear, the PLUS7 test assembly met the test acceptance criteria.

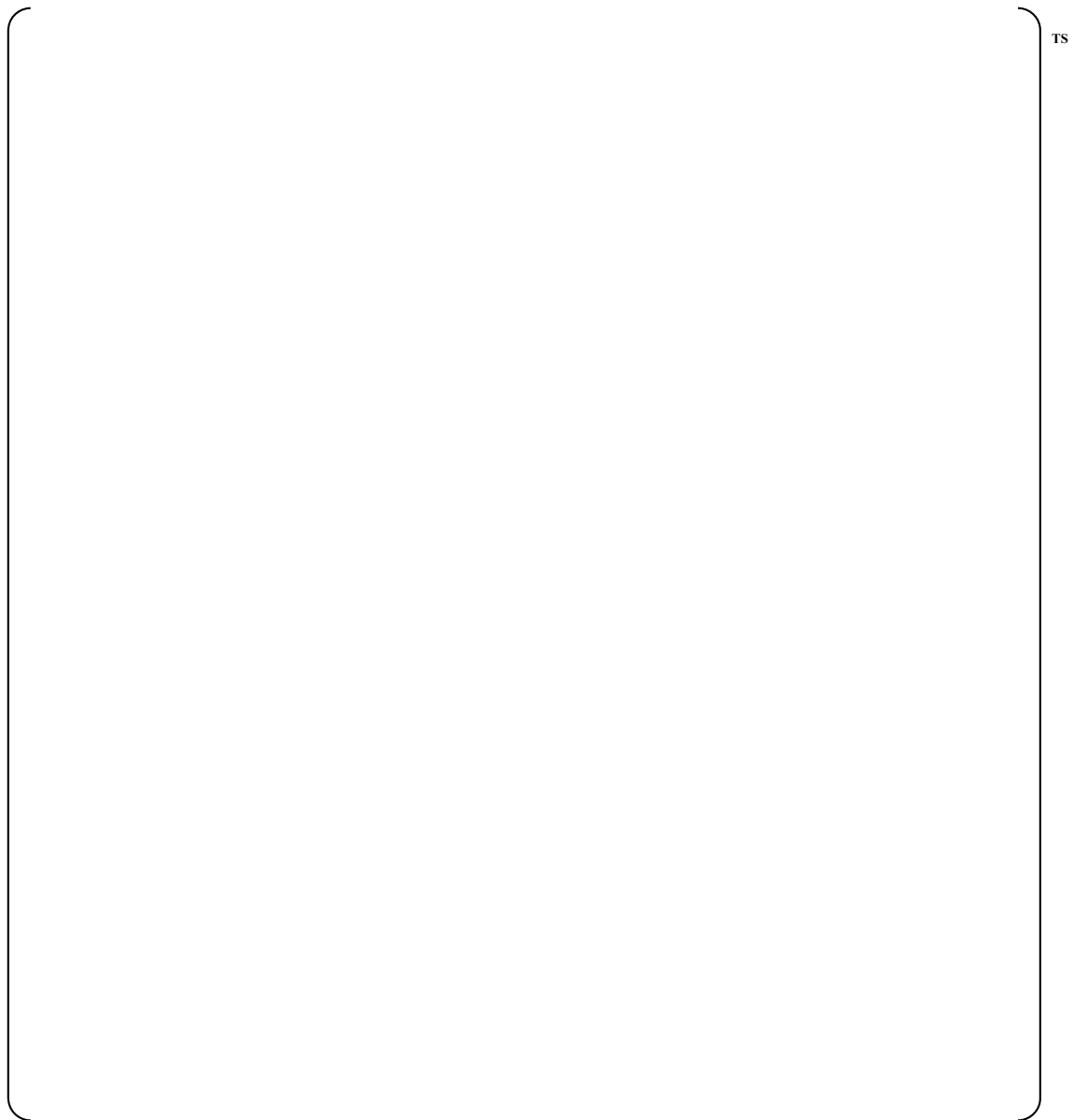


Figure A.2.2-1 Fretting Wear Scar Locations

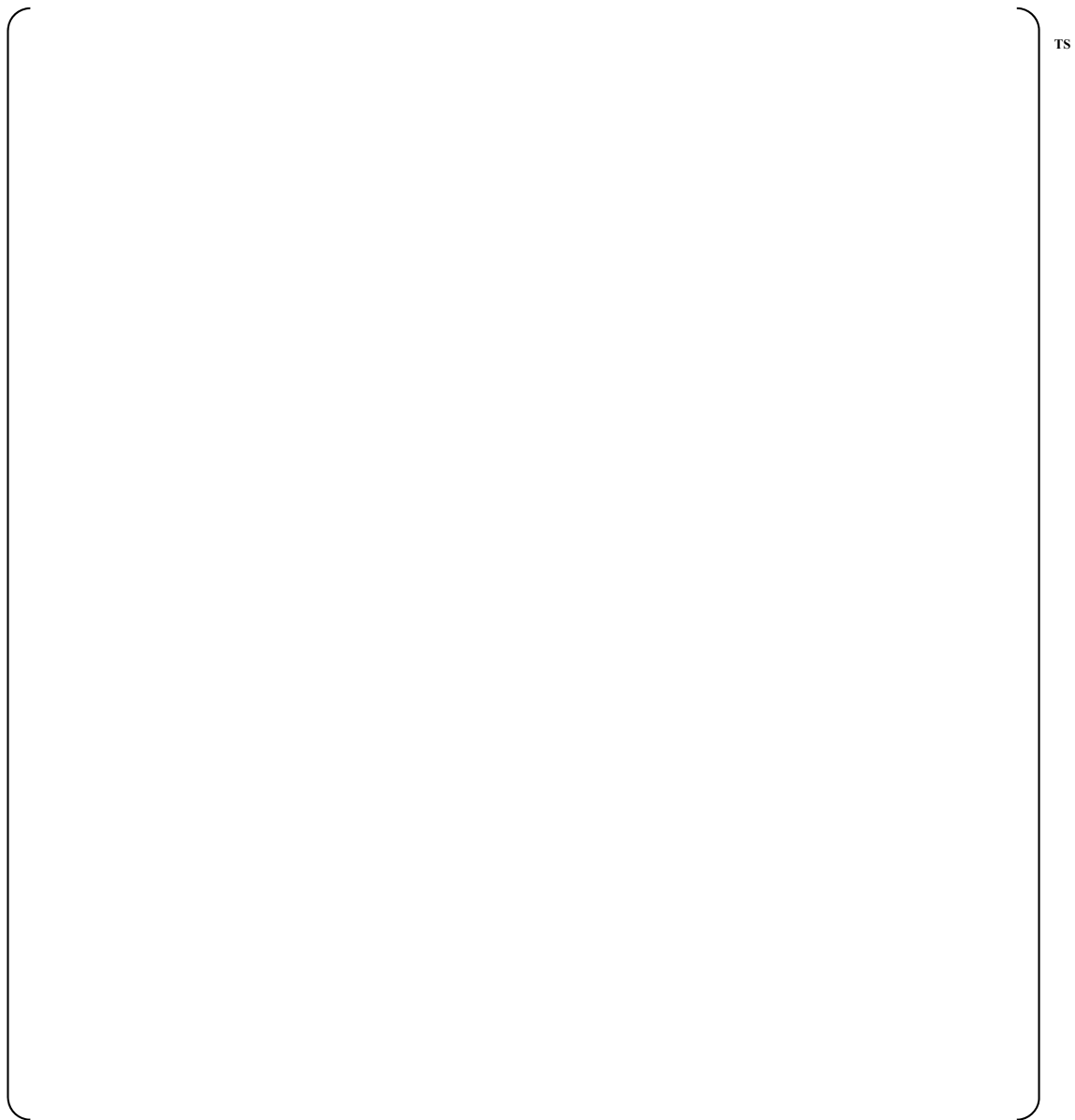


Figure A.2.2-2 Fretting Wear Scar Elevations



Figure A.2.2-3 PLUS7 Assembly Wear Scar Distribution Along Grid Elevations

A.2.3 Through-Grid Long Pulse Test

1.0 Introduction and Objectives

The through-grid buckling strength of the mid grid is required to show that seismic and LOCA loads are met. The specific test objectives for the through-grid long pulse test of the PLUS7 ZIRLO mid grid design at room temperatures are as follows:

- To obtain the data to determine the through-grid buckling strength
- To characterize the grid failure mode

2.0 Test Conditions

The through-grid long pulse tests were performed at room temperature. The grids were tested as a grid span section of fuel assembly, with drilled end plates supporting the short fuel rods and guide tubes. Each grid assembly was mounted with one vertical grid face contacting back plate that is rigidly fastened to the test cell wall. The load pulse was applied to grid assembly by the hydraulic actuator, which was controlled by the hydraulic control unit. The impact load was increased until the load decrease significantly and/or the grid has experienced observable permanent deformation. A schematic of the through-grid long pulse test arrangement is shown in Figure A.2.3-1.

3.0 Test Results

The through-grid buckling strength is determined by which the maximum load before the load begins to decrease with increasing deflection is conservatively selected as the grid strength. The lower 95% confidence value on the true mean of through-grid buckling strength is ()^{TS}. The impact force vs. run number and deformation vs. run number are shown in Figure A.2.3-2. The through-grid long pulse test results are summarized in Table A.2.3-1.

Table A.2.3-1 Through-Grid Long Pulse Test Results

| | Through-Grid Buckling Strength(lb_f) |
|--|---|
| Average | () ^{TS} |
| Standard Deviation | |
| Lower 95 % Confidence Value of True Mean | |

4.0 Summary and Conclusion

The impact force and deformation for the PLUS7 ZIRLO mid grids are shown in Figure A.2.3-2.

A summary of the through-grid long pulse test results is as follows:

- Through-Grid Buckling Strength for BOL condition:

The lower 95% confidence value of true mean is ()^{TS}

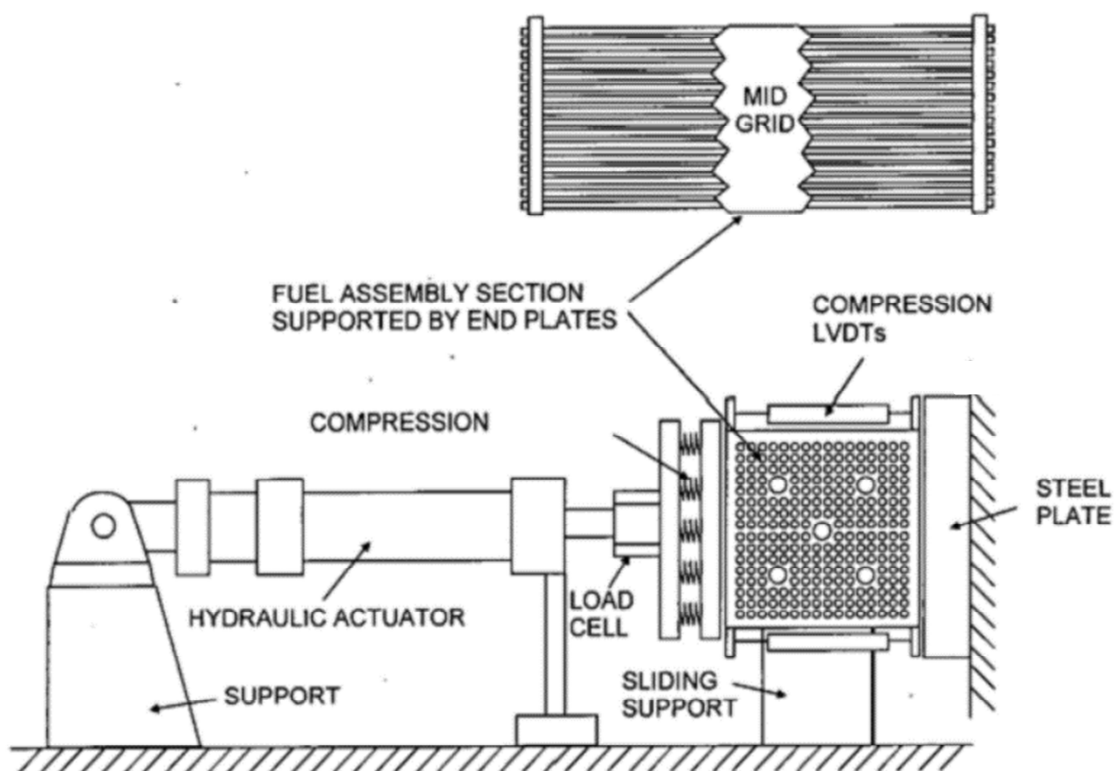


Figure A.2.3-1 Through-Grid Long Pulse Test Arrangement



TS

Figure A.2.3-2 Impact Force & Deformation versus Run Number

A.2.4 Top Nozzle Mechanical Test

1.0 Introduction and Objectives

The objectives of this test were to obtain displacements of the holddown plate as a function of axial loading.

The specific test objectives were as follows:

- To obtain the deflection characteristics of the holddown plate as a function of applied load
- To obtain the stiffness of the holddown spring

Loads applied in the test corresponded to the following:

- Shipping and handling load (> 4g)
- Holddown load (up to 0.05 inch above the holddown spring solid height)

2.0 Test Conditions

The PLUS7 top nozzle was tested in air at room temperature using an Instron Universal Testing Machine. The test arrangements used to perform the PLUS7 top nozzle test are shown in Figures A.2.4-1 through A.2.4-3.

3.0 Test Results

3.1 Shipping Load Test

The { }^{TS} load was applied on the top surface of the inner extension. The load was transmitted to directly the guide thimble through the inner extension. The maximum relative deflection on the holddown plate was { }^{TS} and the holddown plate elastically returned to its original shape when the loads were removed.

The deflection indication demonstrated that the PLUS7 top nozzle design met the design criterion that the dimensional stability be maintained.

3.2 Handling Load Test

The { }^{TS} load was applied on the bottom surface of the holddown plate by the handling tool. The maximum relative deflection on the holddown plate was { }^{TS} and the holddown plate elastically returned to its original shape when the loads were removed.

The deflection indication demonstrated that the PLUS7 top nozzle design met the design criterion that the dimensional stability be maintained.

3.3 Holddown Load Test

The holddown spring was deflected by { }^{TS} from the as-assembled condition for the first loading cycle. The holddown plate elastically returned to its original location when the loads were removed. The stiffness of the four assembled holddown springs for the first loading and unloading cycles were { }^{TS}, respectively. The average stiffness per one holddown spring for the first loading and unloading cycle was { }^{TS} and these

values met the drawing requirements of { }^{TS}. In the second loading and unloading cycle, the deflection of { }^{TS} was applied. The stiffness of the four assembled holddown springs for the second loading and unloading cycles were { }^{TS} respectively. The average stiffness per one holddown spring for the second loading and unloading cycle was { }^{TS} and { }^{TS} and these values met the drawing requirements. Figure A.2.4-4 shows the load deflection characteristics of the holddown spring.

4.0 Summary and Conclusion

The mechanical test of the PLUS7 top nozzle was performed to determine if the system met all the test objectives. The material deflections under load and permanent deformation after loading were characterized for load conditions of { }^{TS} shipping and handling and a holddown spring deflection of 0.05 inch above the spring solid height.

For the 4g shipping and handling load conditions, the deflection indications showed that deformation of the top nozzle remained elastic, and the dimensional stability was maintained. The holddown plate was slightly deformed when the { }^{TS} lifting load was applied but elastically returned to its original shape when the load was removed.

For the holddown load condition, the load deflection data and test observations demonstrated that the PLUS7 top nozzle met the design criteria for the structural integrity and holddown spring repeatability.

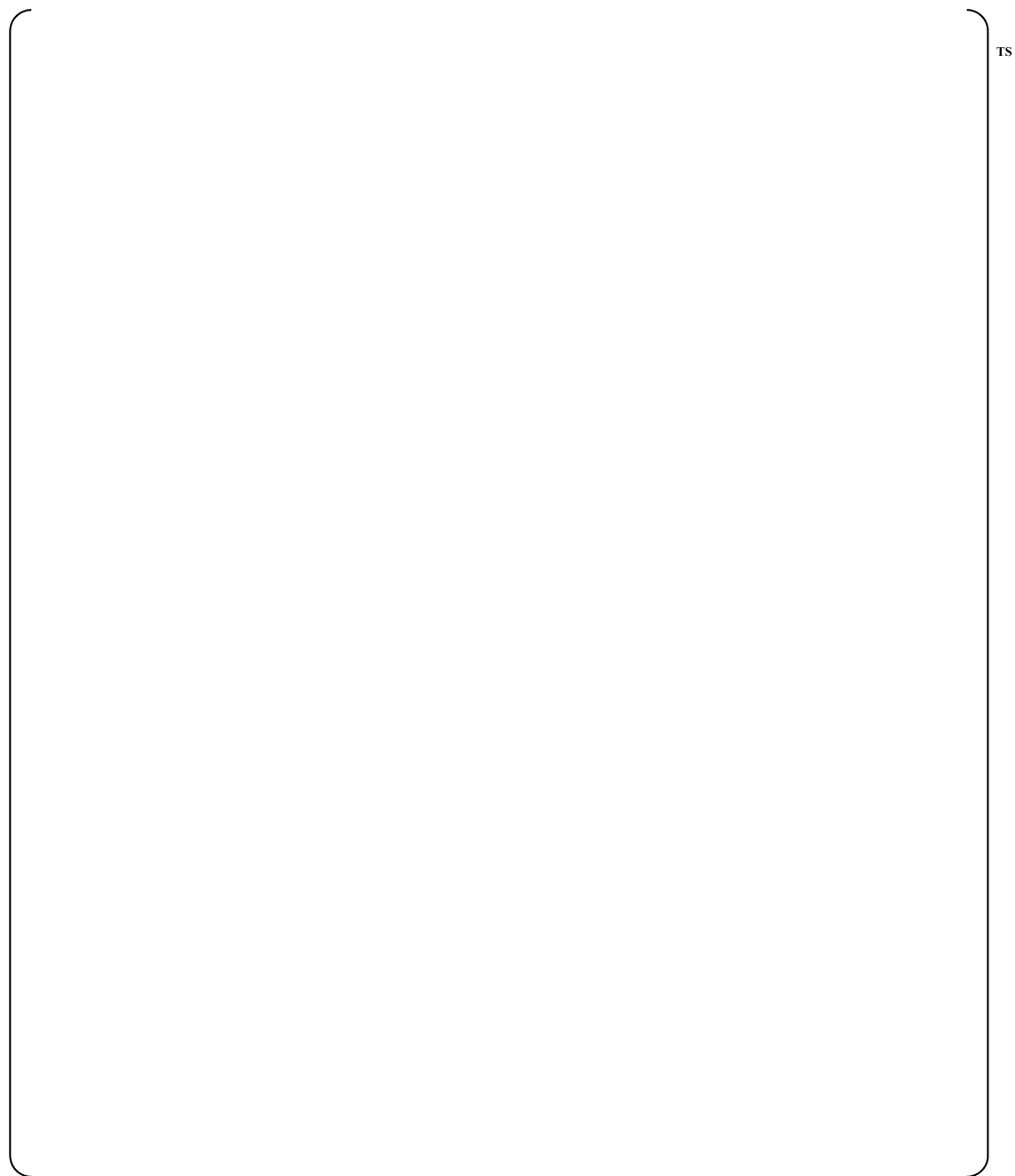


Figure A.2.4-1 Shipping Test Setup

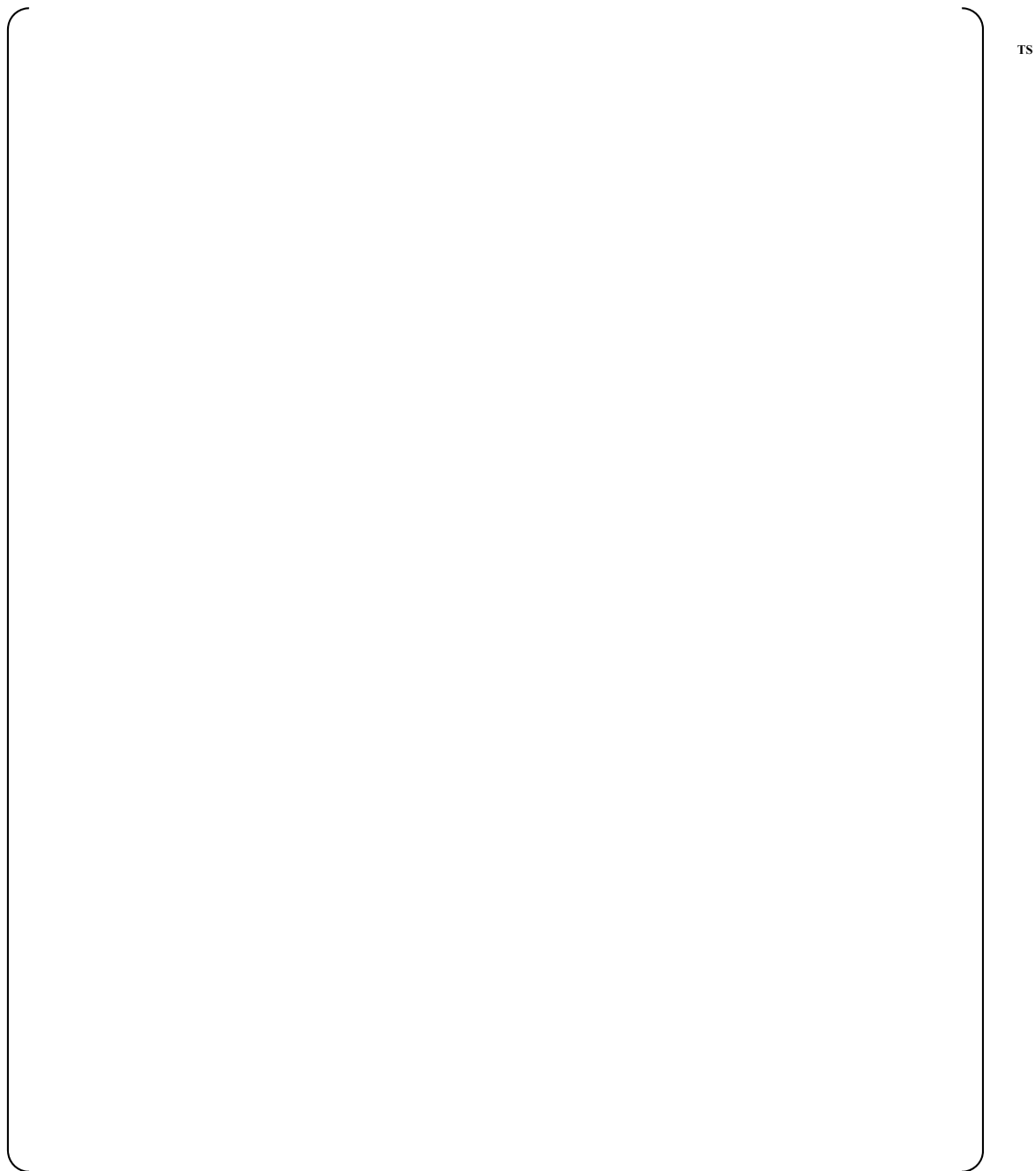


Figure A.2.4-2 Handling Test Setup

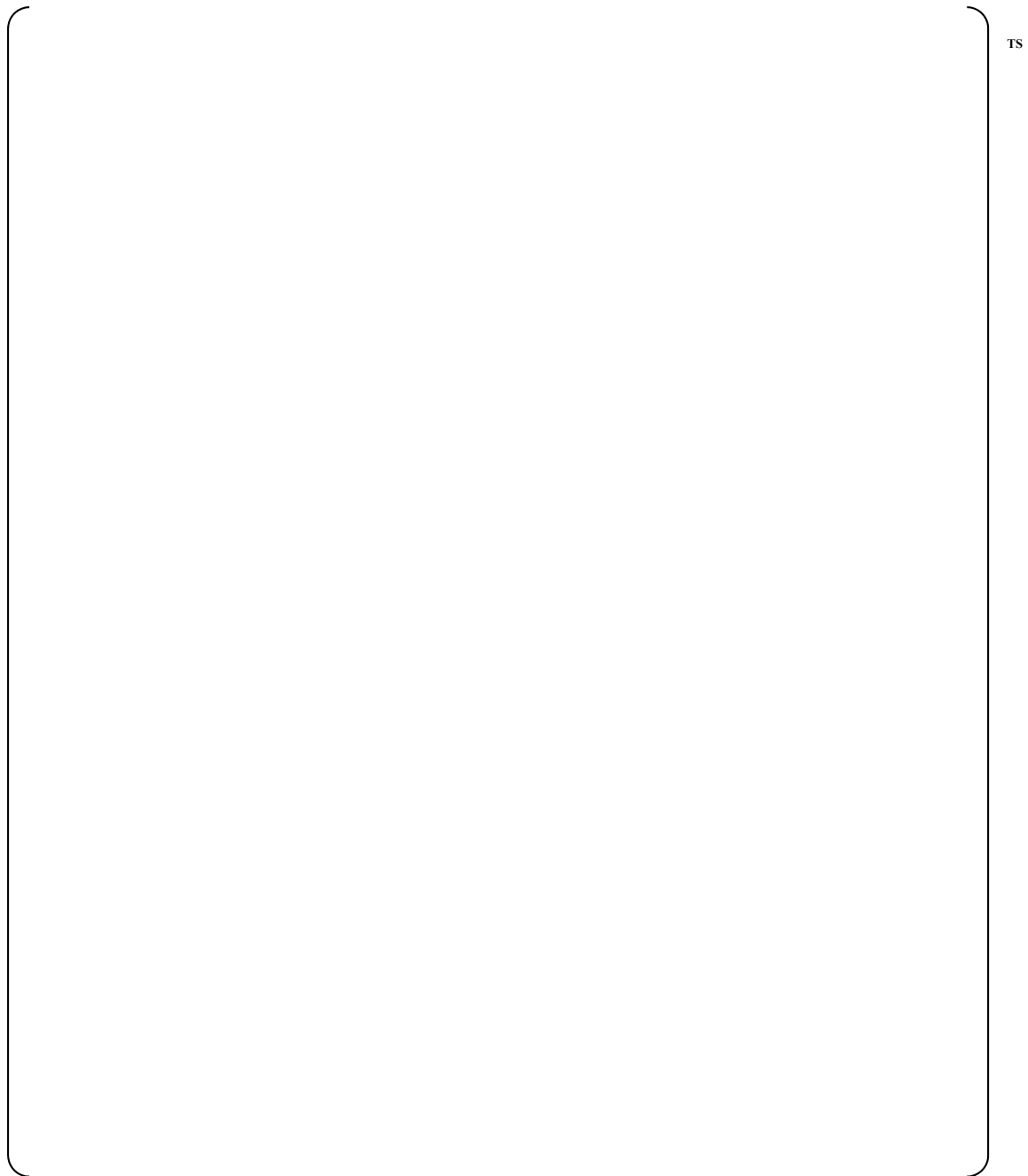


Figure A.2.4-3 Holddown Load Test Setup



Figure A.2.4-4 Holddown Spring Load Deflection Curve

A.2.5 DFBN Mechanical Test**1.0 Introduction and Objectives**

The objectives of this test were to obtain displacements of the adapter plate as a function of the axial loading.

The specific test objectives were as follows:

- To obtain the deflection characteristics of the bottom nozzle as a function of the applied load

Loads applied in the test corresponded to the following:

- Shipping and handling load (> 4g)
- LOCA load { }^{TS}

These axial loads were applied to the adapter plate of the DFBN at the guide thimble locations. The axial loading was applied through a set of Belleville washers to simulate the stiffness of the fuel assembly.

2.0 Test Conditions

The PLUS7 DFBN was tested in air at room temperature using an Instron Universal Testing Machine. The test arrangements used to perform the PLUS7 DFBN test are shown in Figures A.2.5-1 and A.2.5-2.

3.0 Test Results**3.1 Shipping and Handling Load Test**

The load cycles to { }^{TS} (> 4g shipping and handling load) was applied on the adapter plate of the DFBN. The largest measured elastic deflection was about { }^{TS}. Deflection traces for both load/unload cycles were fairly linear, and the distribution of deflections was consistent with the expected plate behavior. The maximum deflection on the DFBN was { }^{TS}. After the load cycles, all deflection indications returned to zero.

The deflection indications and flatness measurements demonstrated that the PLUS7 DFBN design met the design criterion that the dimensional stability be maintained.

3.2 LOCA Load Test

The deflection traces were linear up to a load of { }^{TS}. Residual deflections after the load were from { }^{TS}.

Observation during testing and visual inspection afterwards found no indication of loss of structural integrity (e.g., unrestrained or excessive deformation, cracking) in the DFBN assembly.

4.0 Summary and Conclusion

The material deflections under load and permanent deformation after loading were characterized for load cycles to J^{TS} ($> 4g$ shipping and handling load) and J^{TS} (LOCA load).

For the $4g$ shipping and handling load, the deflection indications and flatness measurements demonstrated that the PLUS7 DFBN design met the design criterion that the dimensional stability be maintained.

For the LOCA load, the load deflection data, flatness measurements, and test observations demonstrated that the PLUS7 DFBN met the design criterion that the structural integrity be maintained.

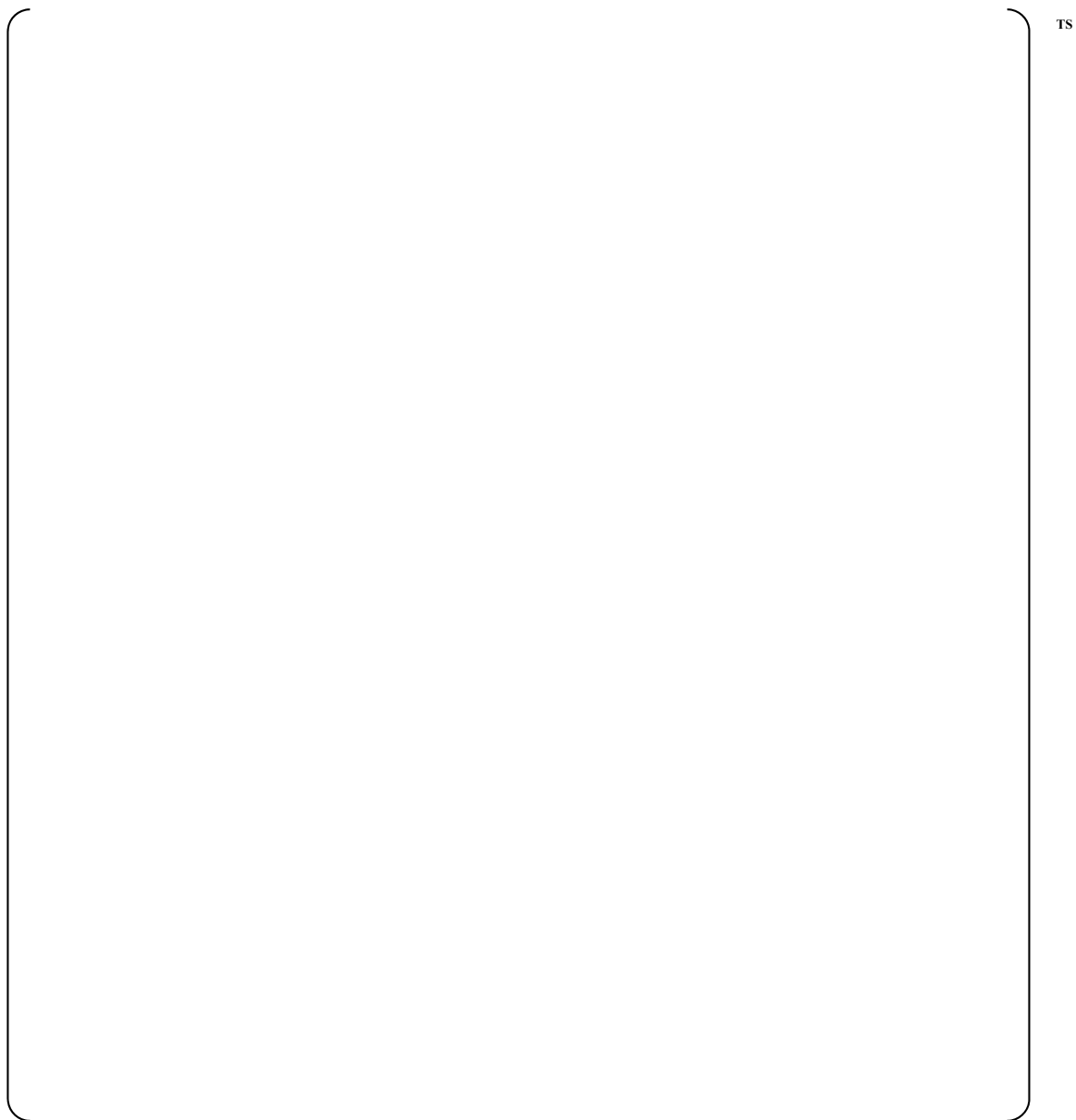


Figure A.2.5-1 Shipping and Handling Load Test Setup

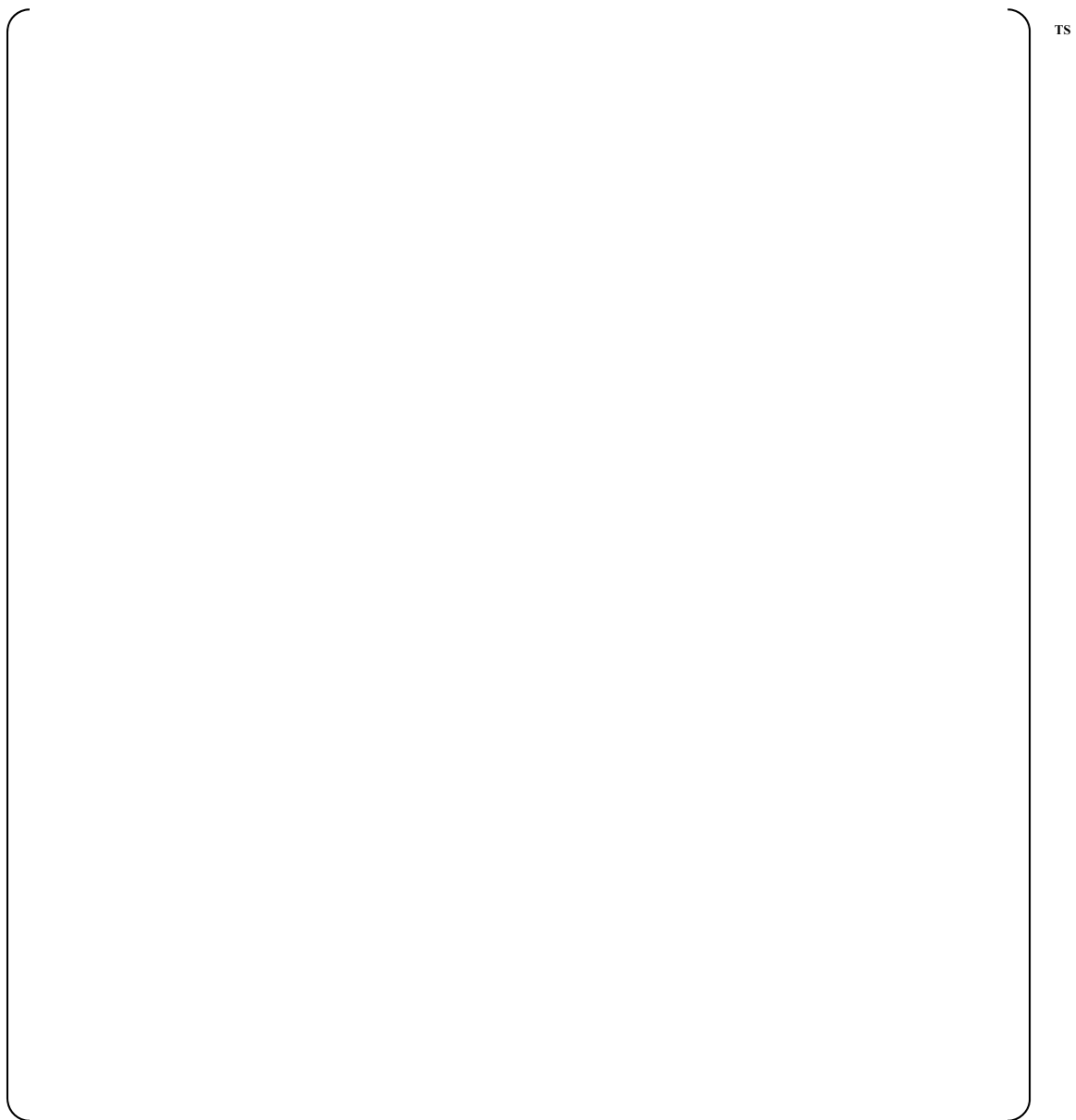


Figure A.2.5-2 LOCA Load Test Setup

A.2.6 Grid Hang-up Test

1.0 Introduction and Objectives

The grid hang-up test was performed as part of the confirmation tests for the PLUS7 fuel assembly grid design. The objective of the test was to perform full scale testing of the PLUS7 test assembly against the same PLUS7 fuel assembly and Guardian assembly it could interact with during fuel handling.

2.0 Test Conditions

A PLUS7 mechanical test assembly was used as the stationary fuel assembly. The stationary fuel assembly was bound on the strong back positioned vertically, and movable assemblies were connected to an overhead crane in turn as shown in Figure A.2.6-1. The top and bottom nozzles of the stationary fuel assembly next to a movable fuel assembly were bound on the strong back using two belts. The movable assemblies were pushed against the stationary assembly to enforce a required side load during the test.

The procedure was to position the grids of the movable assembly between the grids of the stationary assembly, to push the movable assembly against the stationary fuel assembly to enforce the required side load, and to raise or lower the movable assembly.

The location of the stationary assembly and the movable assembly during testing and the test definition are shown in Figure A.2.6-2. During the hang-up test, the movable assembly was raised and lowered three times in 19 cases per Figure 2.6-2. The PLUS7 to PLUS7 test was performed first and the PLUS7 to Guardian test followed. The crane speed was maintained at []^{TS}. All tests were performed in air at room temperature.

3.0 Test Results

PLUS7 vs. Guardian and PLUS7 vs. PLUS7 hang-up test revealed no irregularity during the raising or lowering of the movable assembly three times for each of the 19 cases.

4.0 Summary and Conclusion

The full scale grid hang-up tests of PLUS7-PLUS7 and PLUS7-Guardian fuel assemblies were performed for grid verification. The PLUS7 to Guardian fuel assemblies did not have any hang-up problems and the PLUS7 to PLUS7 fuel assemblies also did not have any hang-up problems.

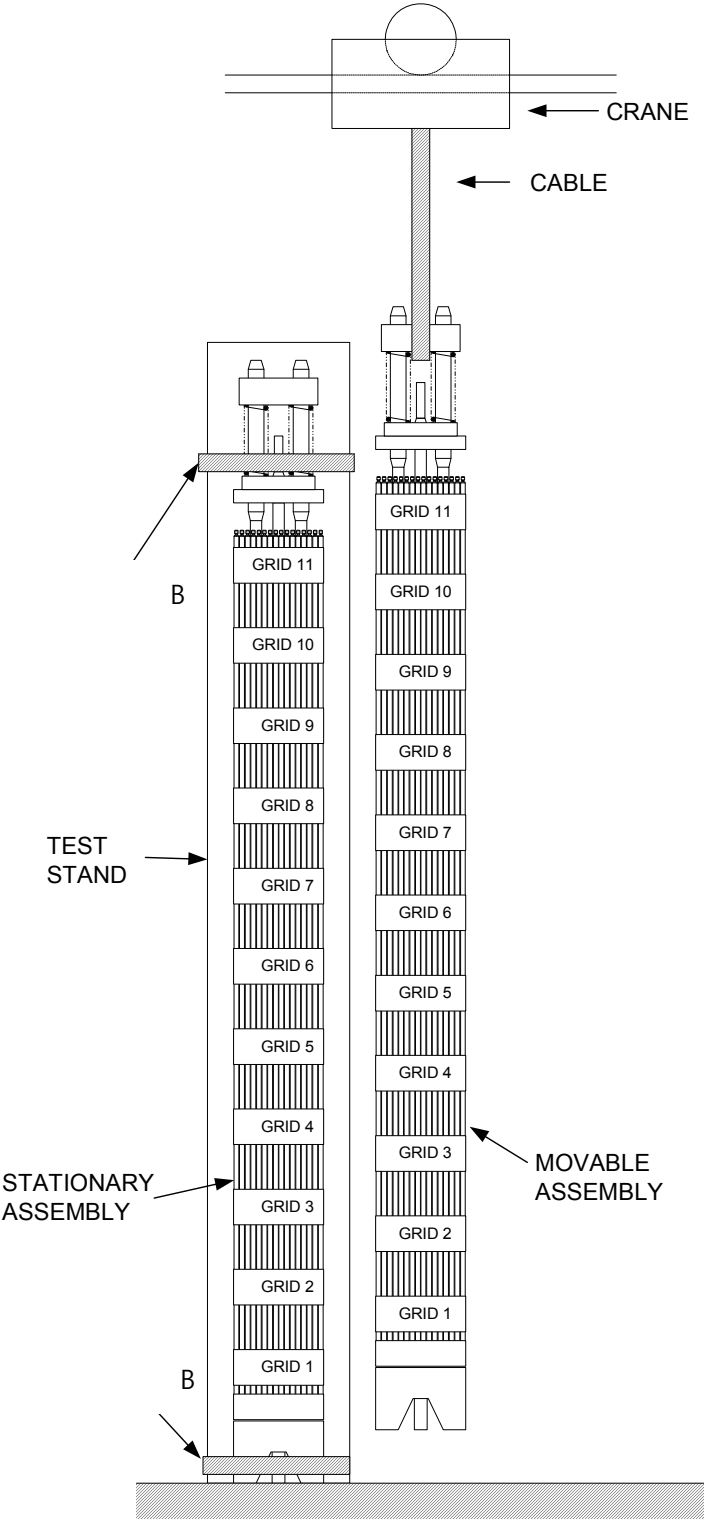


Figure A.2.6-1 Grid Hang-up Test Setup

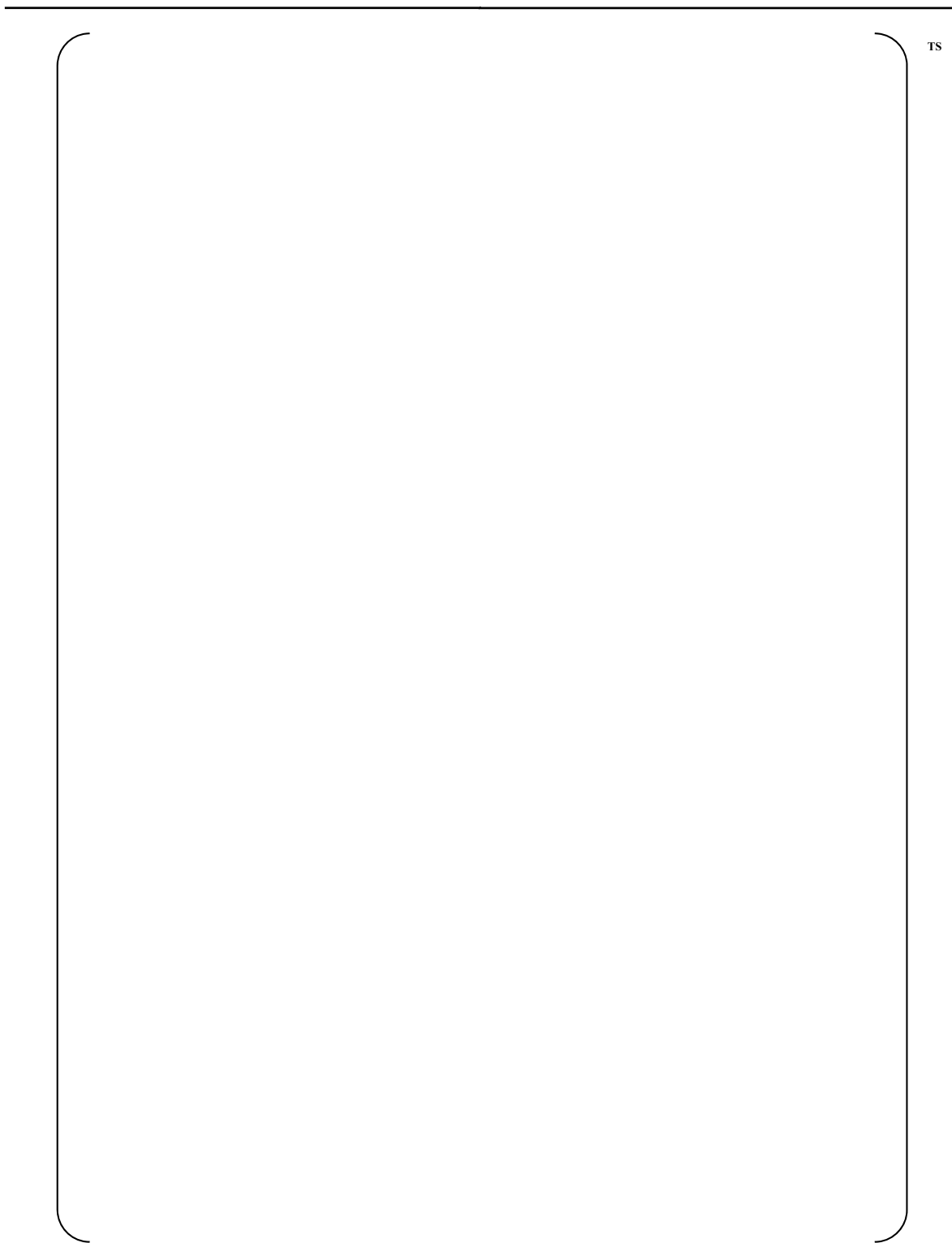


Figure A.2.6-2 Fuel Assembly Grid Hang-up Test Series

A.2.7 FACTS Hydraulic Test for PLUS7 Fuel Assembly

1.0 Introduction and Objectives

The purpose of this test is to determine the pressure loss coefficient of the PLUS7 fuel assembly. This test was performed by using the Combustion Engineering Nuclear Power (CENP) method based on the PLUS7 fuel assembly hydraulic test at the Westinghouse FACTS (Fuel Assembly Compatibility Test System).

2.0 Test Conditions and Methods

2.1 Conditions

The hydraulic tests were performed by varying the flow rate over a predetermined range at two temperatures, { }^{TS}. For the temperature of { }^{TS}, the flow ranged from { }^{TS} to the maximum achievable flow rate ({ }^{TS} for the fuel assembly with 40/20 DFBN, Debris Filter Bottom Nozzle with a { }^{TS} with increments of { }^{TS}. At the temperature of { }^{TS}, the flow ranged from { }^{TS} to the maximum achievable flow rate ({ }^{TS} for the fuel assembly with 40/20 DFBN) with increments of { }^{TS}. Given these flow rates and temperatures, the Reynolds number values ranged from approximately { }^{TS}.

2.2 Methods

The CENP method uses the following equation to calculate the pressure loss coefficient from the measured pressure drop test data.

$$\left[\frac{\Delta P}{L} \right]^{TS}$$

The resultant grid loss coefficients do not include the bare rod friction losses. The bare rod friction is predicted by the Colebrook equation shown below, assuming a { }^{TS} rod surface roughness.

$$\left[\frac{1}{f} \right]^{TS}$$

The measured pressure loss coefficients are reduced to the form:

$$\left[\frac{\Delta P}{L} \right]^{TS}$$

Where, A and B are constants which describe loss coefficient (K) as a function of the Reynolds number (Re). Additionally, the adjustments on the fitted data were performed to account for geometric differences and thermal expansion effects between the test and the reactor conditions.

3.0 Test Results

The pressure loss coefficients for each fuel assembly component based on the CENP methods are as shown in Table A.2.7-1.

Table A.2.7-1 Pressure Loss Coefficients

| | Correlation | Coefficients Re=500,000 |
|-------------------|-------------|----------------------------|
| Inlet | | TS |
| Mid grid | | |
| Outlet | | |
| Fuel rod friction | | |
| Fuel Assembly | | |

4.0 Summary and Conclusion

The FACTS test result for the PLUS7 fuel assembly was treated using the CENP method and the pressure loss coefficient for the PLUS7 fuel assembly was determined as shown in Table A.2.7-1.

A.2.8 Grid Spring Test

1.0 Introduction and Objectives

The spring tests of grids were performed to determine the cell stiffness and force values for use in the design calculations. Specifically, the objectives of these tests were to determine the load deflection characteristics and the unloading spring stiffness in the inner, outer and adjacent thimble cells of the test grids.

2.0 Test Conditions

A linear stepper motor and a strain gage equipped with an in-cell deflection measuring device (See Figures A.2.8-1 and A.2.8-2) were used for cell stiffness measurement. Fuel rod sections were inserted into the grid cells surrounding the specified test cells (See Figures A.2.8-3 through A.2.8-6). A spring force/deflection measurement tool, with a motor and a motor bracket, was used to cyclically load the grid cells. The grids were tested in air at room temperature.

3.0 Test Results

The grid spring load deflection tests of the PLUS7 ZIRLO mid grid, Inconel top/bottom grids and protective grid were performed in air at room temperature. The load deflection results are shown in Table A.2.8-1 and the inner cell load deflection curves are shown in Figure A.2.8-7.

Dashed vertical lines indicating nominal, maximum and minimum deflections are overlaid on the graph and reflect the expected range of deflections due to the manufacturing tolerance. Spring unloading curves are also shown for the adjacent minimum, nominal and maximum spring deflection values. Since some deflection for the grid cell is in the elastic range, its unloading curve follows the deflection curve.

4.0 Summary and Conclusion

The load deflection results for each grid are shown in Table A.2.8-1 and the load deflection curves are shown in Figure A.2.8-7.

Table A.2.8-1 Summary of Grid Spring Load Deflection Test Results

| Description | Inner Cell | |
|---|------------|----|
| ZIRLO Mid Grid Average Stiffness (lbf/in) Minimum Deflection Residual Load (lbf/in) Minimum Deflection Average Stiffness (lbf/in) Nominal Deflection Residual Load (lbf/in) Nominal Deflection Average Stiffness (lbf/in) Maximum Deflection Residual Load (lbf/in) Maximum Deflection Maximum Load(lbf/in) During Full Deflection | | TS |
| Inconel Top Grid Average Stiffness (lbf/in) Minimum Deflection Residual Load (lbf/in) Minimum Deflection Average Stiffness (lbf/in) Nominal Deflection Residual Load (lbf/in) Nominal Deflection Average Stiffness (lbf/in) Maximum Deflection Residual Load (lbf/in) Maximum Deflection Maximum Load(lbf/in) During Full Deflection | | |
| Inconel Bottom Grid Average Stiffness (lbf/in) Minimum Deflection Residual Load (lbf/in) Minimum Deflection Average Stiffness (lbf/in) Nominal Deflection Residual Load (lbf/in) Nominal Deflection Average Stiffness (lbf/in) Maximum Deflection Residual Load (lbf/in) Maximum Deflection Maximum Load(lbf/in) During Full Deflection | | |
| Protective Grid Average Stiffness (lbf/in) Minimum Deflection Residual Load (lbf/in) Minimum Deflection Average Stiffness (lbf/in) Nominal Deflection Residual Load (lbf/in) Nominal Deflection Average Stiffness (lbf/in) Maximum Deflection Residual Load (lbf/in) Maximum Deflection Maximum Load(lbf/in) During Full Deflection | | |



Figure A.2.8-1 Spring Test Apparatus Setup



Figure A.2.8-2 Load Deflection Tool



Figure A.2.8-3 ZIRLO Mid Grid Test Locations (Bottom View) **Figure A.2.8-4 Inconel Top Grid Test Locations (Bottom View)**



Figure A.2.8-5 Inconel Bottom Grid Test Locations (Top View) **Figure A.2.8-6 Protective Grid Test Locations (Bottom View)**



Figure A.2.8-7 ZIRLO Mid and Inconel Top/Bottom/Protective Grid Inner Cell Load Deflection

A.2.9 FACTS Lift-off Test for the PLUS7 Fuel Assembly

1.0 Introduction and Objectives

The objective of the lift-off tests of the PLUS7 fuel assembly is to determine the flow rates at which the fuel assembly lifts off under specified temperatures and holddown spring compressions. The test was performed with the Fuel Assembly Compatibility Test System (FACTS) as shown in Figure A.2.9-1 for the PLUS7 fuel assembly design with 40/20 []^{TS} Debris Filter Bottom Nozzle (DFBN).

2.0 Test Conditions

To ensure that the fuel assembly would lift-off during the tests, the holddown springs were compressed by []^{TS}. The lift-off tests were performed by increasing the flow rate from []^{TS} with increments of []^{TS}. When the flow rate reached []^{TS} the flow increased with an increment of []^{TS} for a better estimate of the flow rate that could lift-off the fuel assembly. The test conditions and APR1400 operating conditions are compared in Table A.2.9-1.

Table A.2.9-1 Comparison of the liftoff test condition ranges to the APR1400 operating condition ranges

| Liftoff Test Condition in FACTS Loop | | | APR1400 Operating Condition | |
|---|-------------------|-------------------|---|-------------------|
| Temperature (°F) | [] ^{TS} | [] ^{TS} | Average Temperature (°F) | [] ^{TS} |
| Corresponding Mechanical Design Flow in FACTS (gpm) | | | Mechanical Design Flow (gpm) per Assembly | [] ^{TS} |
| Test Flow Range (gpm) | | | | |

Two uni-axial accelerometers were mounted on the base of the pressure vessel to monitor the output impact signal. The output from the accelerometers was amplified and monitored through an oscilloscope and a visicorder.

Table A.2.9-2 Fuel Assembly and Specifications

| Component Descriptions | |
|---|--|
| Top Grid Material | Inconel 718 |
| Protective Grid Material | Inconel 718 |
| Bottom Grid Material | Inconel 718 |
| Protective Grid Inner Strap Heights | { } ^{TS} |
| Bottom Grid Inner Strap Heights | { } ^{TS} |
| Top Grid Inner Strap Heights | { } ^{TS} |
| Mid Grid Material | ZIRLO |
| Number of Mid grids | 9 |
| Mid Grid Inner Strap Heights | { } ^{TS} |
| Number of Rods | 236 |
| Rod OD | { } ^{TS} |
| Test Rod Length | { } ^{TS} |
| Number of Guide Thimble | 4 |
| Diameter of Guide Thimble Tubes | { } ^{TS} |
| Number of Instrument Tube | 1 |
| Diameter of Instrument Tube | { } ^{TS} |
| Dashpot Elevation (Top of Thimble Tube Smaller OD Elevation) | { } ^{TS} |
| Rod-to-Bottom Nozzle Gap | { } ^{TS} |
| Thimble Tube Plugging Device | None. However the flow is blocked by the standoff tubes |
| Test Condition | |
| { } ^{TS} | { } ^{TS} for the fuel assembly with 40/20 DFBN |
| { } ^{TS} | { } ^{TS} for the fuel assembly with 40/20 DFBN |

3.0 Test Results

The flow rates required to lift-off the PLUS7 fuel assembly with a 40/20 DFBN at temperatures of { }^{TS} were determined from the lift-off test. It was expected from similar tests that the fuel assembly would lift-off at a flow rate higher than { }^{TS}. No noticeable signal related to the assembly lift-off was detected until the flow rate reached { }^{TS}. The first noticeable accelerometer signal was detected at the flow rate of { }^{TS} and above this flow rate the signals became more noticeable. To find out the exact flow rate of the lift-off, the tests were performed with several different flow rates around the flow rate at which the first signal was detected. It was confirmed that the fuel assembly began to lift-off at { }^{TS}.

The same test procedure was followed for { }^{TS} case and the results confirmed that at a temperature of { }^{TS} the fuel assembly was lifted off at { }^{TS}. The test results are summarized in Table A.2.9-2. Figures A.2.9-2 and A.2.9-3 show the inlet loss coefficients and outlet loss coefficients versus the flow rate, respectively. In these figures, a sudden change in the slope of the loss coefficients indicates a lift-off.

Table A.2.9-3 Results of the Lift-off Tests Based on the Accelerometer Indications

| Holddown Spring Compression* | Temperature | Lift-off Flow Rate (gpm) |
|------------------------------|-------------|--------------------------|
| { } | | } ^{TS} |

* Holddown spring compression at room temperature

4.0 Summary and Conclusion

The FACTS lift-off tests confirmed that the PLUS7 fuel assembly with a holddown spring compression of { }^{TS} was lifted off at the flow rates of { }^{TS} at temperatures of { }^{TS}, respectively.



TS

Figure A.2.9-1 FACTS Flow Diagram



TS

Figure A.2.9-2 K11 (inlet) from The Lift-off Test



TS

Figure A.2.9-3 K8 (outlet) from The Lift-off Test

A.3.0 CONCLUSION

Hydraulic and Mechanical tests of the PLUS7 fuel assembly were conducted to verify their out-of-pile performance. All the tests were performed to ensure that the system met all the design criteria.

Appendix B

Commercial Operating Experience of KEPCO NF PWR Fuels

JULY 2017

**Copyright © 2017
All Rights Reserved**

TABLE OF CONTENTS

LIST OF TABLES B-3

B.1.0 COMMERCIAL OPERATING EXPERIENCE OF KEPCO NF PWR FUEL B-4

LIST OF TABLES

| | | |
|--------------|---|------|
| Table B.1-1 | Fuel Supplied by KNF for Kori Unit 1 | B-4 |
| Table B.1-2 | Fuel Supplied by KNF for Kori Unit 2 | B-5 |
| Table B.1-3 | Fuel Supplied by KNF for Kori Unit 3 | B-6 |
| Table B.1-4 | Fuel Supplied by KNF for Kori Unit 4 | B-7 |
| Table B.1-5 | Fuel Supplied by KNF for Yonggwang Unit 1 | B-8 |
| Table B.1-6 | Fuel Supplied by KNF for Yonggwang Unit 2 | B-9 |
| Table B.1-7 | Fuel Supplied by KNF for Ulchin Unit 1 | B-10 |
| Table B.1-8 | Fuel Supplied by KNF for Ulchin Unit 2 | B-11 |
| Table B.1-9 | Fuel Supplied by KNF for Yonggwang Unit 3 | B-12 |
| Table B.1-10 | Fuel Supplied by KNF for Yonggwang Unit 4 | B-13 |
| Table B.1-11 | Fuel Supplied by KNF for Yonggwang Unit 5 | B-13 |
| Table B.1-12 | Fuel Supplied by KNF for Yonggwang Unit 6 | B-14 |
| Table B.1-13 | Fuel Supplied by KNF for Ulchin Unit 3 | B-14 |
| Table B.1-14 | Fuel Supplied by KNF for Ulchin Unit 4 | B-15 |
| Table B.1-15 | Fuel Supplied by KNF for Ulchin Unit 5 | B-15 |
| Table B.1-16 | Fuel Supplied by KNF for Ulchin Unit 6 | B-16 |
| Table B.1-17 | Fuel Supplied by KNF for Shin-Kori Unit 1 | B-16 |

B.1.0 COMMERCIAL OPERATING EXPERIENCE OF KEPCO NF PWR FUEL

In Korea, the first nuclear power plant, Kori unit-1 (PWR), began commercial operation in April 1978. Currently there are 17 PWRs and four PHWRs in operation in Korea. KEPCO Nuclear Fuel (KNF) was established in 1982 and started to supply PWR and PHWR fuels from 1989 and 1997, respectively. PWR fuels supplied by KNF are as follows:

(1) 14x14 Fuel for Kori Unit 1

Kori unit 1 uses the fuel with a 14x14 lattice configuration and KNF has supplied this type of fuel assemblies since the 11th cycle of the unit as shown in Table B.1-1.

Table B.1-1 Fuel Supplied by KNF for Kori Unit 1

| Cycle | Date | Fuel Type | FAs | FRs | Clad Material |
|---|----------------------|------------------|------------|----------------|----------------------|
| 11 | 91/01 ~ 92/01 | KOFA | 48 | 8,592 | Zry-4 |
| 12 | 92/03 ~ 93/05 | KOFA | 48 | 8,592 | Zry-4 |
| 13 | 93/07 ~ 94/07 | KOFA | 44 | 7,876 | Zry-4 |
| 14 | 94/09 ~ 96/01 | KOFA | 44 | 7,876 | Zry-4 |
| 15 | 96/04 ~ 97/03 | KOFA | 44 | 7,876 | Zry-4 |
| 16 | 97/07 ~ 98/06 | KNF-OFA | 52 | 9,308 | Zry-4 (W)* |
| 17 | 98/09 ~ 99/09 | KNF-OFA | 40 | 7,160 | Zry-4 (W) |
| 18 | 99/11 ~ 00/10 | KNF-OFA | 40 | 7,160 | Zry-4 (S)** |
| 19 | 00/11 ~ 01/11 | KNF-OFA | 40 | 7,160 | Zry-4 (Z)*** |
| 20 | 01/12 ~ 03/01 | KNF-OFA | 40 | 7,160 | Zry-4 (Z) |
| 21 | 03/02 ~ 04/02 | KNF-OFA | 40 | 7,160 | Zry-4 (Z) |
| 22 | 04/03 ~ 05/03 | KNF-OFA | 40 | 7,160 | Zry-4 (Z) |
| 23 | 05/05 ~ 06/05 | KNF-OFA | 40 | 7,160 | Zry-4 (Z) |
| 24 | 06/06 ~ 07/06 | KNF-OFA | 40 | 7,160 | Zry-4 (Z) |
| 25 | 08/01 ~ 08/11 | KNF-OFA | 40 | 7,160 | Zry-4 (Z) |
| 26 | 08/12 ~ 09/12 | KNF-OFA | 41 | 7,339 | Zry-4 (Z) |
| 27 | 10/01 ~ 11/01 | KNF-OFA | 41 | 7,339 | Zry-4 (Z) |
| 28 | 11/02 ~ 12/02 | KNF-OFA | 41 | 7,339 | KNF ZIRLO |
| 29 | 12/03 ~ 13/04 | KNF-OFA | 45 | 8,055 | KNF ZIRLO |
| Total | 91/01 ~ 13/04 | - | 808 | 144,632 | - |
| * : Westinghouse – Imp. Zry-4, ** : ANF – PCA-2a *** : CEZUS – AFA-2G | | | | | |

(2) 16x16 Fuel for Kori Unit 2

Kori unit 2 uses the fuel with a 16x16 lattice configuration and KNF has supplied this type of fuel assemblies since the 7th cycle of the unit as shown in Table B.1-2.

Table B.1-2 Fuel Supplied by KNF for Kori Unit 2

| Cycle | Date | Fuel Type | FAs | FRs | Clad Material |
|---|----------------------|--------------|------------|----------------|---------------|
| 7 | 90/03 ~ 91/04 | KOFA | 48 | 11,280 | Zry-4 |
| 8 | 91/05 ~ 92/05 | KOFA | 48 | 11,280 | Zry-4 |
| 9 | 92/07 ~ 93/09 | KOFA | 50 | 12,220 | Zry-4 |
| 12 | 96/02 ~ 97/02 | KNF-STD | 44 | 10,340 | Zry-4 (W)* |
| 13 | 97/04 ~ 98/02 | KNF-STD | 36 | 8,460 | Zry-4 (W) |
| 14 | 98/03 ~ 99/03 | KNF-STD | 44 | 10,340 | Zry-4 (W) |
| 15 | 99/05 ~ 00/05 | KNF-STD | 44 | 10,340 | Zry-4 (S)** |
| 16 | 00/07 ~ 01/05 | KNF-STD | 40 | 9,400 | Zry-4 (Z)*** |
| 17 | 01/07 ~ 02/08 | KNF-STD | 48 | 11,280 | Zry-4 (Z) |
| 18 | 02/09 ~ 03/10 | KNF-STD | 48 | 11,280 | Zry-4 (Z) |
| 19 | 03/11 ~ 04/12 | KNF-STD | 48 | 11,280 | Zry-4 (Z) |
| 20 | 05/01 ~ 06/02 | KNF-STD | 40 | 9,400 | Zry-4 (Z) |
| | | 16ACE7 (LTA) | 4 | 940 | ZIRLO**** |
| 21 | 06/03 ~ 07/04 | KNF-STD | 52 | 12,220 | Zry-4 (Z) |
| 22 | 07/05 ~ 08/05 | KNF-STD | 40 | 9,400 | Zry-4 (Z) |
| 23 | 08/07 ~ 09/09 | 16ACE7 | 48 | 11,280 | ZIRLO |
| 24 | 09/09 ~ 10/10 | 16ACE7 | 48 | 11,280 | ZIRLO |
| 25 | 10/11 ~ 12/03 | 16ACE7 | 56 | 13,160 | KNF ZIRLO |
| 26 | 12/04 ~ 13/05 | 16ACE7 | 40 | 9,400 | KNF ZIRLO |
| Total | 90/03 ~ 13/05 | - | 826 | 194,580 | - |
| * : Westinghouse – Imp. Zry-4, ** : ANF – PCA-2a *** : CEZUS – AFA-2G, **** : Westinghouse | | | | | |

(3) 17x17 Fuel

Fuel with a 17x17 lattice configuration is used for Kori units 3&4, Yonggwang units 1&2 and Ulchin units 1&2, and the fuels of this type supplied by KNF are shown in Tables B.1-3 through B.1-8.

Table B.1-3 Fuel Supplied by KNF for Kori Unit 3

| Cycle | Date | Fuel Type | FAs | FRs | Clad Material |
|--------------|----------------------|--------------|------------|----------------|---------------|
| 5 | 90/01 ~ 90/12 | KOFA | 56 | 14,784 | Zry-4 |
| 6 | 91/02 ~ 91/12 | KOFA | 48 | 12,672 | Zry-4 |
| 7 | 92/02 ~ 92/12 | KOFA | 48 | 12,672 | Zry-4 |
| 8 | 93/02 ~ 94/03 | KOFA | 64 | 16,896 | Zry-4 |
| 11 | 97/04 ~ 98/05 | KNF-V5H | 56 | 14,784 | Zry-4 (W)* |
| 12 | 98/07 ~ 99/11 | KNF-V5H | 64 | 16,896 | Zry-4 (W) |
| 13 | 00/01 ~ 01/03 | KNF-V5H | 60 | 15,840 | Zry-4 (S)** |
| 14 | 01/04 ~ 02/09 | KNF-V5H | 68 | 17,952 | Zry-4 (Z)*** |
| 15 | 02/10 ~ 04/01 | KNF-V5H | 60 | 15,840 | ZIRLO**** |
| 16 | 04/03 ~ 05/06 | KNF-RFA | 60 | 15,840 | ZIRLO |
| 17 | 05/07 ~ 06/11 | KNF-RFA | 60 | 15,840 | ZIRLO |
| | | 17ACE7 (LTA) | 4 | 1,056 | ZIRLO |
| 18 | 07/01 ~ 08/04 | KNF-RFA | 64 | 16,896 | ZIRLO |
| 19 | 08/05 ~ 09/10 | KNF-RFA | 68 | 17,952 | ZIRLO |
| 20 | 09/12 ~ 11/04 | 17ACE7 | 68 | 17,952 | ZIRLO |
| 21 | 11/05 ~ 12/09 | 17ACE7 | 68 | 17,952 | KNF ZIRLO |
| 22 | 12/10 ~ 14/03 | 17ACE7 | 65 | 17,160 | KNF ZIRLO |
| Total | 90/01 ~ 14/03 | - | 981 | 258,984 | - |

* : Westinghouse – Imp. Zry-4, ** : ANF – PCA-2a
 *** : CEZUS – AFA-2G, **** : Westinghouse

Table B.1-4 Fuel Supplied by KNF for Kori Unit 4

| Cycle | Date | Fuel Type | FAs | FRs | Clad Material |
|--|----------------------|------------------|------------|----------------|----------------------|
| 5 | 90/07 ~ 91/04 | KOFA | 44 | 11,616 | Zry-4 |
| 6 | 91/05 ~ 92/04 | KOFA | 48 | 12,672 | Zry-4 |
| 7 | 92/06 ~ 93/07 | KOFA | 64 | 16,896 | Zry-4 |
| 8 | 93/09 ~ 94/12 | KOFA | 76 | 20,064 | Zry-4 |
| 10 | 96/06 ~ 97/09 | KNF-V5H | 60 | 15,840 | Zry-4 (W)* |
| 11 | 97/11 ~ 99/01 | KNF-V5H | 60 | 15,840 | Zry-4 (W) |
| 12 | 99/03 ~ 00/07 | KNF-V5H | 68 | 17,952 | Zry-4 (W) |
| 13 | 00/09 ~ 01/11 | KNF-V5H | 60 | 15,840 | Zry-4 (Z)** |
| 14 | 01/12 ~ 03/04 | KNF-V5H | 60 | 15,840 | Zry-4 (Z) |
| 15 | 03/05 ~ 04/09 | KNF-V5H | 60 | 15,840 | ZIRLO*** |
| 16 | 04/10 ~ 06/02 | KNF-RFA | 64 | 16,896 | ZIRLO |
| 17 | 06/04 ~ 07/06 | KNF-RFA | 64 | 16,896 | ZIRLO |
| 18 | 07/08 ~ 08/12 | KNF-RFA | 64 | 16,896 | ZIRLO |
| 19 | 09/02 ~ 10/05 | 17ACE7 | 64 | 16,896 | ZIRLO |
| 20 | 10/06 ~ 11/09 | 17ACE7 | 64 | 16,896 | KNF ZIRLO |
| 21 | 11/10 ~ 13/01 | 17ACE7 | 65 | 17,160 | KNF ZIRLO |
| Total | 90/07 ~ 13/01 | - | 985 | 260,040 | - |
| * : Westinghouse – Imp. Zry-4, ** : CEZUS – AFA-2G *** : Westinghouse | | | | | |

Table B.1-5 Fuel Supplied by KNF for Yonggwang Unit 1

| Cycle | Date | Fuel Type | FAs | FRs | Clad Material |
|--|----------------------|------------------|--------------|----------------|----------------------|
| 5 | 90/10 ~ 91/08 | KOFA | 52 | 13,728 | Zry-4 |
| 6 | 91/10 ~ 92/08 | KOFA | 48 | 12,672 | Zry-4 |
| 7 | 92/10 ~ 93/11 | KOFA | 64 | 16,896 | Zry-4 |
| 8 | 93/12 ~ 95/03 | KOFA | 76 | 20,064 | Zry-4 |
| 9 | 95/06 ~ 96/09 | KOFA | 76 | 20,064 | Zry-4 (W)* |
| 10 | 96/11 ~ 98/01 | KNF-V5H | 60 | 15,840 | Zry-4 (W) |
| 11 | 98/03 ~ 99/06 | KNF-V5H | 60 | 15,840 | Zry-4 (W) |
| 12 | 99/08 ~ 00/10 | KNF-V5H | 60 | 15,840 | Zry-4 (W) |
| 13 | 00/11 ~ 02/02 | KNF-V5H | 60 | 15,840 | Zry-4 (Z)** |
| 14 | 02/03 ~ 03/05 | KNF-V5H | 56 | 14,784 | ZIRLO*** |
| 15 | 03/06 ~ 04/10 | KNF-V5H | 60 | 15,840 | ZIRLO |
| 16 | 04/11 ~ 06/03 | KNF-RFA | 60 | 15,840 | ZIRLO |
| 17 | 06/04 ~ 07/09 | KNF-RFA | 64 | 16,896 | ZIRLO |
| 18 | 07/10 ~ 09/03 | KNF-RFA | 64 | 16,896 | ZIRLO |
| 19 | 09/04 ~ 10/09 | KNF-RFA | 68 | 17,952 | ZIRLO |
| 20 | 10/10 ~ 12/02 | 17ACE7 | 68 | 17,952 | KNF ZIRLO |
| 21 | 12/03 ~ 13/08 | 17ACE7 | 69 | 18,216 | KNF ZIRLO |
| Total | 90/10 ~ 13/08 | - | 1,065 | 281,160 | - |
| * : Westinghouse – Imp. Zry-4, ** : CEZUS – AFA-2G *** : Westinghouse | | | | | |

Table B.1-6 Fuel Supplied by KNF for Yonggwang Unit 2

| Cycle | Date | Fuel Type | FAs | FRs | Clad Material |
|--|----------------------|------------------|------------|----------------|----------------------|
| 4 | 90/06 ~ 91/02 | KOFA | 48 | 12,672 | Zry-4 |
| 5 | 91/04 ~ 92/03 | KOFA | 48 | 12,672 | Zry-4 |
| 6 | 92/05 ~ 93/03 | KOFA | 48 | 12,672 | Zry-4 |
| 7 | 93/04 ~ 94/05 | KOFA | 64 | 16,896 | Zry-4 |
| 10 | 97/05 ~ 98/09 | KNF-V5H | 64 | 16,896 | Zry-4 (W)* |
| 11 | 98/12 ~ 00/04 | KNF-V5H | 60 | 15,840 | Zry-4 (W) |
| 12 | 00/05 ~ 01/09 | KNF-V5H | 60 | 15,840 | Zry-4 (S)** |
| 13 | 01/10 ~ 03/01 | KNF-V5H | 60 | 15,840 | ZIRLO*** |
| 14 | 03/02 ~ 04/05 | KNF-V5H | 56 | 14,784 | ZIRLO |
| 15 | 04/07 ~ 05/11 | KNF-RFA | 60 | 15,840 | ZIRLO |
| 16 | 05/12 ~ 07/04 | KNF-RFA | 64 | 16,896 | ZIRLO |
| 17 | 07/05 ~ 08/09 | KNF-RFA | 64 | 16,896 | ZIRLO |
| 18 | 08/10 ~ 10/03 | KNF-RFA | 64 | 16,896 | ZIRLO |
| 19 | 10/04 ~ 11/08 | 17ACE7 | 68 | 17,952 | ZIRLO |
| 20 | 11/09 ~ 13/02 | 17ACE7 | 65 | 17,160 | KNF ZIRLO |
| Total | 90/06 ~ 13/02 | - | 893 | 235,752 | - |
| * : Westinghouse – Imp. Zry-4, ** : ANF – PCA-2a *** : Westinghouse | | | | | |

Table B.1-7 Fuel Supplied by KNF for Ulchin Unit 1

| Cycle | Date | Fuel Type | FAs | FRs | Clad Material |
|--|----------------------|------------------|--------------|----------------|----------------------|
| 3 | 91/01 ~ 92/02 | KOFA | 48 | 12,672 | Zry-4 |
| 4 | 92/04 ~ 93/02 | KOFA | 44 | 11,616 | Zry-4 |
| 5 | 93/03 ~ 94/01 | KOFA | 44 | 11,616 | Zry-4 |
| 6 | 94/03 ~ 95/03 | KOFA | 64 | 16,896 | Zry-4 |
| 7 | 95/05 ~ 96/04 | KOFA | 56 | 14,784 | Zry-4 |
| 8 | 96/06 ~ 97/10 | KNF-V5H | 60 | 15,840 | Zry-4 (W)* |
| 9 | 97/12 ~ 98/12 | KNF-V5H | 56 | 14,784 | Zry-4 (W) |
| 10 | 99/02 ~ 00/06 | KNF-V5H | 60 | 15,840 | Zry-4 (W) |
| 11 | 00/08 ~ 01/10 | KNF-V5H | 60 | 15,840 | Zry-4 (Z)** |
| 12 | 01/10 ~ 03/05 | KNF-V5H | 64 | 16,896 | ZIRLO*** |
| 13 | 03/07 ~ 04/10 | KNF-V5H | 60 | 15,840 | ZIRLO |
| 14 | 04/11 ~ 06/04 | KNF-RFA | 56 | 14,784 | ZIRLO |
| 15 | 06/05 ~ 07/09 | KNF-RFA | 64 | 16,896 | ZIRLO |
| 16 | 07/10 ~ 09/02 | KNF-RFA | 64 | 16,896 | ZIRLO |
| 17 | 09/03 ~ 10/08 | KNF-RFA | 68 | 17,952 | ZIRLO |
| 18 | 10/10 ~ 12/02 | KNF-RFA | 68 | 17,952 | ZIRLO |
| 19 | 12/05 ~ 13/09 | 17ACE7 | 65 | 17,160 | KNF ZIRLO |
| Total | 91/01 ~ 13/09 | - | 1,001 | 264,264 | - |
| * : Westinghouse – Imp. Zry-4, ** : CEZUS – AFA-2G *** : Westinghouse | | | | | |

Table B.1-8 Fuel Supplied by KNF for Ulchin Unit 2

| Cycle | Date | Fuel Type | FAs | FRs | Clad Material |
|---|----------------------|------------------|-------------|----------------|----------------------|
| 2 | 90/11 ~ 91/10 | KOFA | 44 | 11,616 | Zry-4 |
| 3 | 91/12 ~ 92/11 | KOFA | 48 | 12,672 | Zry-4 |
| 4 | 92/12 ~ 93/10 | KOFA | 48 | 12,672 | Zry-4 |
| 5 | 93/11 ~ 94/09 | KOFA | 48 | 12,672 | Zry-4 |
| 6 | 94/11 ~ 95/12 | KOFA | 64 | 16,896 | Zry-4 |
| 7 | 96/01 ~ 97/04 | KOFA | 76 | 20,064 | Zry-4 |
| 8 | 97/06 ~ 98/08 | KNF-V5H | 60 | 15,840 | Zry-4 (W)* |
| 9 | 98/10 ~ 00/01 | KNF-V5H | 60 | 15,840 | Zry-4 (W) |
| 10 | 00/03 ~ 01/05 | KNF-V5H | 60 | 15,840 | Zry-4 (S)** |
| 11 | 01/06 ~ 02/09 | KNF-V5H | 60 | 15,840 | Zry-4 (Z)*** |
| 12 | 02/11 ~ 04/05 | KNF-V5H | 64 | 16,896 | ZIRLO**** |
| 13 | 04/06 ~ 05/10 | KNF-RFA | 60 | 15,840 | ZIRLO |
| 14 | 05/12 ~ 07/04 | KNF-RFA | 64 | 16,896 | ZIRLO |
| 15 | 07/05 ~ 08/09 | KNF-RFA | 64 | 16,896 | ZIRLO |
| 16 | 08/10 ~ 10/03 | KNF-RFA | 64 | 16,896 | ZIRLO |
| 17 | 10/04 ~ 11/09 | KNF-RFA | 68 | 17,952 | KNF ZIRLO |
| 18 | 11/11 ~ 13/04 | 17ACE7 | 65 | 17,160 | KNF ZIRLO |
| Total | 90/11 ~ 13/04 | - | 1017 | 268,488 | - |
| * : Westinghouse – Imp. Zry-4, ** : ANF – PCA-2a, *** : CEZUS – AFA-2G, **** : Westinghouse | | | | | |

(4) 16x16 Fuel for OPR1000

Fuel with a 16x16 lattice configuration is used for OPR1000's including Yongggwang units 3 through 6, Ulchin units 3 through 6 and Shin-Kori unit 1. The fuels of this type supplied by KNF are shown in Tables B.1-9 through B.1-17.

Table B.1-9 Fuel Supplied by KNF for Yongggwang Unit 3

| Cycle | Date | Fuel Type | FAs | FRs | Clad Material |
|---|----------------------|------------|------------|----------------|---------------|
| 1 | 94/10 ~ 96/02 | KSFA | 177 | 41,772 | OPTIN* |
| 2 | 96/04 ~ 97/02 | KSFA | 48 | 11,328 | OPTIN |
| 3 | 97/05 ~ 98/03 | KSFA | 60 | 14,160 | OPTIN |
| 5 | 99/07 ~ 00/09 | KSFA | 64 | 15,104 | OPTIN |
| 6 | 00/11 ~ 02/03 | KSFA | 64 | 16,896 | OPTIN |
| 7 | 02/04 ~ 03/05 | K-Guardian | 56 | 13,216 | ZIRLO** |
| 8 | 03/06 ~ 04/10 | K-Guardian | 60 | 14,160 | ZIRLO |
| 9 | 04/11 ~ 06/01 | K-Guardian | 60 | 14,160 | ZIRLO |
| 10 | 06/02 ~ 07/04 | K-Guardian | 64 | 15,104 | ZIRLO |
| 11 | 07/06 ~ 08/10 | PLUS7 | 64 | 15,104 | ZIRLO |
| 12 | 08/11 ~ 10/02 | PLUS7 | 64 | 15,104 | ZIRLO |
| 13 | 10/03 ~ 11/05 | PLUS7 | 60 | 14,160 | KNF ZIRLO |
| 14 | 11/07 ~ 12/10 | PLUS7 | 69 | 16,284 | KNF ZIRLO |
| Total | 94/10 ~ 12/10 | - | 910 | 216,552 | - |
| * : Manufactured by SANDVIK, ** : ZIRLO manufactured by Westinghouse *** : ZIRLO manufactured by KNF | | | | | |

Table B.1-10 Fuel Supplied by KNF for Yonggwang Unit 4

| Cycle | Date | Fuel Type | FAs | FRs | Clad Material |
|--------------|----------------------|------------|------------|----------------|---------------|
| 1 | 95/07 ~ 96/11 | KSFA | 177 | 41,772 | OPTIN* |
| 2 | 97/01 ~ 97/10 | KSFA | 48 | 11,328 | OPTIN |
| 4 | 99/02 ~ 00/02 | KSFA | 56 | 13,216 | OPTIN |
| 5 | 00/03 ~ 01/05 | KSFA | 56 | 13,216 | OPTIN |
| 6 | 01/06 ~ 02/10 | K-Guardian | 60 | 14,160 | ZIRLO** |
| 7 | 02/11 ~ 04/04 | K-Guardian | 72 | 16,992 | ZIRLO |
| 8 | 04/05 ~ 05/08 | K-Guardian | 64 | 15,104 | ZIRLO |
| 9 | 05/09 ~ 07/01 | K-Guardian | 60 | 14,160 | ZIRLO |
| 10 | 07/02 ~ 08/05 | PLUS7 | 64 | 15,104 | ZIRLO |
| 11 | 08/06 ~ 09/10 | PLUS7 | 64 | 15,104 | ZIRLO |
| 12 | 09/11 ~ 11/01 | PLUS7 | 64 | 15,104 | M5*** |
| 13 | 11/03 ~ 12/04 | PLUS7 | 64 | 15,104 | KNF ZIRLO |
| 14 | 12/05 ~ 13/11 | PLUS7 | 64 | 15,104 | KNF ZIRLO |
| Total | 95/07 ~ 13/11 | - | 913 | 215,468 | - |

* : SANDVIK, ** : Westinghouse, *** : CEZUS

Table B.1-11 Fuel Supplied by KNF for Yonggwang Unit 5

| Cycle | Date | Fuel Type | FAs | FRs | Clad Material |
|--------------|----------------------|------------|------------|----------------|----------------------|
| 1 | 02/04 ~ 03/03 | KSFA | 177 | 41,772 | OPTIN* |
| 2 | 03/05 ~ 04/01 | K-Guardian | 48 | 11,328 | ZIRLO** |
| 3 | 04/04 ~ 05/05 | K-Guardian | 64 | 15,104 | ZIRLO |
| 4 | 05/06 ~ 06/11 | KSFA | 4 | 944 | OPTIN |
| | | K-Guardian | 60 | 14,160 | ZIRLO |
| 5 | 06/12 ~ 08/04 | PLUS7 | 68 | 16,048 | ZIRLO |
| 6 | 08/05 ~ 09/08 | PLUS7 | 64 | 15,104 | ZIRLO |
| 7 | 09/09 ~ 10/12 | PLUS7 | 64 | 15,104 | M5*** |
| 8 | 11/01 ~ 12/04 | PLUS7 | 64 | 15,104 | KNF ZIRLO, HANA-4, 6 |
| 9 | 12/05 ~ 13/11 | PLUS7 | 69 | 16,284 | KNF ZIRLO |
| Total | 02/04 ~ 13/11 | - | 682 | 160,952 | - |

* : SANDVIK, ** : Westinghouse, *** : CEZUS

Table B.1-12 Fuel Supplied by KNF for Yonggwang Unit 6

| Cycle | Date | Fuel Type | FAs | FRs | Clad Material |
|--------------------------------|----------------------|------------|------------|----------------|---------------|
| 1 | 02/12 ~ 03/11 | KSFA | 177 | 41,772 | OPTIN* |
| 2 | 04/04 ~ 05/01 | K-Guardian | 48 | 11,328 | ZIRLO** |
| 3 | 05/02 ~ 06/02 | K-Guardian | 64 | 15,104 | ZIRLO |
| 4 | 06/03 ~ 07/07 | K-Guardian | 64 | 15,104 | ZIRLO |
| 5 | 07/07 ~ 08/11 | PLUS7 | 64 | 15,104 | ZIRLO |
| 6 | 08/12 ~ 10/03 | PLUS7 | 64 | 15,104 | ZIRLO |
| 7 | 10/04 ~ 11/06 | PLUS7 | 60 | 14,160 | KNF ZIRLO |
| 8 | 11/07 ~ 12/11 | PLUS7 | 69 | 16,284 | KNF ZIRLO |
| Total | 02/12 ~ 12/11 | - | 610 | 143,960 | - |
| * : SANDVIK, ** : Westinghouse | | | | | |

Table B.1-13 Fuel Supplied by KNF for Ulchin Unit 3

| Cycle | Date | Fuel Type | FAs | FRs | Clad Material |
|---|----------------------|------------|------------|----------------|---------------|
| 1 | 98/01 ~ 99/06 | KSFA | 177 | 41,772 | OPTIN* |
| 2 | 99/08 ~ 00/05 | KSFA | 48 | 11,328 | OPTIN |
| 3 | 00/07 ~ 01/07 | KSFA | 64 | 15,104 | OPTIN |
| 4 | 01/07 ~ 02/11 | KSFA | 64 | 15,104 | ZIRLO** |
| 5 | 02/12 ~ 04/04 | K-Guardian | 60 | 14,160 | ZIRLO |
| | | PLUS7 | 4 | 944 | ZIRLO |
| 6 | 04/05 ~ 05/09 | K-Guardian | 68 | 16,048 | ZIRLO |
| 7 | 05/10 ~ 07/01 | K-Guardian | 68 | 16,048 | ZIRLO |
| 8 | 07/03 ~ 08/07 | PLUS7 | 64 | 15,104 | ZIRLO |
| 9 | 08/07 ~ 09/10 | PLUS7 | 64 | 15,104 | ZIRLO |
| 10 | 09/11 ~ 11/02 | PLUS7 | 64 | 15,104 | M5*** |
| 11 | 11/03 ~ 12/06 | PLUS7 | 64 | 15,104 | KNF ZIRLO |
| 12 | 12/10 ~ 14/04 | PLUS7 | 69 | 16,284 | KNF ZIRLO |
| Total | 98/01 ~ 14/04 | - | 878 | 207,208 | - |
| * : SANDVIK, ** : Westinghouse, *** : CEZUS | | | | | |

Table B.1-14 Fuel Supplied by KNF for Ulchin Unit 4

| Cycle | Date | Fuel Type | FAs | FRs | Clad Material |
|--------------|----------------------|------------|------------|----------------|---------------|
| 1 | 98/10 ~ 00/03 | KSFA | 177 | 41,772 | OPTIN* |
| 2 | 00/05 ~ 01/02 | KSFA | 48 | 11,328 | OPTIN |
| 3 | 01/03 ~ 02/04 | KSFA | 64 | 15,104 | OPTIN |
| 4 | 02/05 ~ 03/08 | K-Guardian | 60 | 14,160 | ZIRLO** |
| 5 | 03/09 ~ 05/01 | K-Guardian | 68 | 16,048 | ZIRLO |
| 6 | 05/02 ~ 06/05 | K-Guardian | 68 | 16,048 | ZIRLO |
| 7 | 06/06 ~ 07/09 | PLUS7 | 64 | 15,104 | ZIRLO |
| 8 | 07/11 ~ 09/02 | PLUS7 | 64 | 15,104 | ZIRLO |
| 9 | 09/03 ~ 10/05 | PLUS7 | 64 | 15,104 | M5*** |
| 10 | 10/06 ~ 11/09 | PLUS7 | 64 | 15,104 | M5, KNF ZIRLO |
| Total | 98/10 ~ 11/09 | - | 741 | 174,876 | - |

* : SANDVIK, ** : Westinghouse, *** : CEZUS

Table B.1-15 Fuel Supplied by KNF for Ulchin Unit 5

| Cycle | Date | Fuel Type | FAs | FRs | Clad Material |
|--------------|----------------------|------------|------------|----------------|---------------|
| 1 | 03/12 ~ 05/06 | K-Guardian | 177 | 41,772 | ZIRLO* |
| 2 | 05/08 ~ 06/09 | K-Guardian | 60 | 14,160 | ZIRLO |
| 3 | 06/10 ~ 07/11 | K-Guardian | 64 | 15,104 | ZIRLO |
| 4 | 07/12 ~ 09/05 | PLUS7 | 60 | 14,160 | ZIRLO |
| 5 | 09/05 ~ 10/09 | PLUS7 | 60 | 14,160 | M5** |
| | | | 4 | 944 | ZIRLO |
| 6 | 10/10 ~ 11/12 | PLUS7 | 60 | 14,160 | KNF ZIRLO |
| 7 | 11/12 ~ 13/05 | PLUS7 | 69 | 16,284 | KNF ZIRLO |
| Total | 03/12 ~ 13/05 | - | 554 | 130,744 | - |

* : Westinghouse, ** : CEZUS

Table B.1-16 Fuel Supplied by KNF for Ulchin Unit 6

| Cycle | Date | Fuel Type | FAs | FRs | Clad Material |
|-----------------|----------------------|------------|------------|----------------|-------------------|
| 1 | 04/11 ~ 06/03 | K-Guardian | 177 | 41,772 | ZIRLO* |
| 2 | 06/05 ~ 07/06 | K-Guardian | 60 | 14,160 | ZIRLO |
| 3 | 07/06 ~ 08/09 | PLUS7 | 64 | 15,104 | ZIRLO |
| 4 | 08/10 ~ 10/02 | PLUS7 | 64 | 15,104 | ZIRLO |
| 5 | 10/03 ~ 11/06 | PLUS7 | 64 | 15,104 | KNF ZIRLO |
| 6 | 11/06 ~ 12/10 | PLUS7 | 61 | 14,396 | KNF ZIRLO |
| | | HIPER | 8 | 1,888 | KNF ZIRLO, HANA-6 |
| 7 | 12/12 ~ 14/04 | PLUS7 | 69 | 16,284 | KNF ZIRLO |
| Total | 04/11 ~ 14/04 | - | 567 | 133,812 | - |
| *: Westinghouse | | | | | |

Table B.1-17 Fuel Supplied by KNF for Shin-Kori Unit 1

| Cycle | Date | Fuel Type | FAs | FRs | Clad Material |
|-----------------|----------------------|------------|------------|---------------|---------------|
| 1 | 10/07 ~ 12/01 | K-Guardian | 177 | 41,772 | ZIRLO* |
| 2 | 12/02 ~ 13/04 | PLUS7 | 60 | 14,160 | KNF ZIRLO |
| Total | 10/17 ~ 13/04 | - | 237 | 55,932 | - |
| *: Westinghouse | | | | | |

Appendix C

PLUS7 Scram Data Verification

JULY 2017

**Copyright © 2017
All Rights Reserved**

TABLE OF CONTENTS

LIST OF TABLES C-3

LIST OF FIGURES..... C-3

C.1.0 PURPOSE..... C-4

C.2.0 INTRODUCTION..... C-4

C.3.0 DESIGN CRITERIA C-4

C.4.0 VERIFICATION..... C-5

C.5.0 CONCLUSION C-9

LIST OF TABLES

| | | |
|-------------|---------------------------------|-----|
| Table C.4-1 | Summary of CEA Actual Test Data | C-6 |
| Table C.4-2 | Actual Test Data (CEA Types) | C-8 |

LIST OF FIGURES

| | | |
|--------------|--|-----|
| Figure C.3-1 | CEA Position Requirements during Reactor Scram | C-4 |
| Figure C.4-1 | Distribution of Actual Test Data | C-5 |
| Figure C.4-2 | Histogram of Actual Test Data | C-6 |
| Figure C.4-3 | Actual Test Raw Data from YGN-5 | C-7 |

C.1.0 PURPOSE

The purpose of this analysis is to verify that the CEA (Control Element Assembly) SCRAM analysis provides reasonable and conservative predictions of the CEA insertion time for the 90% insertion criterion during reactor operating conditions.

C.2.0 INTRODUCTION

The SCRAM analysis was developed to describe the CEA position, velocity and acceleration as a function of time and applicable reactor geometry during the rapid insertion of the CEAs into the reactor core to obtain a reactor “shutdown” condition.

C.3.0 DESIGN CRITERIA

Both full and part strength CEAs must be capable of traveling from a fully withdrawn position to the 90% insertion position within the time limits (4.0 seconds) as shown in Figure C.3-1. This criterion assures that the CEAs can be reliably inserted to shut down the reactor within the time limits.

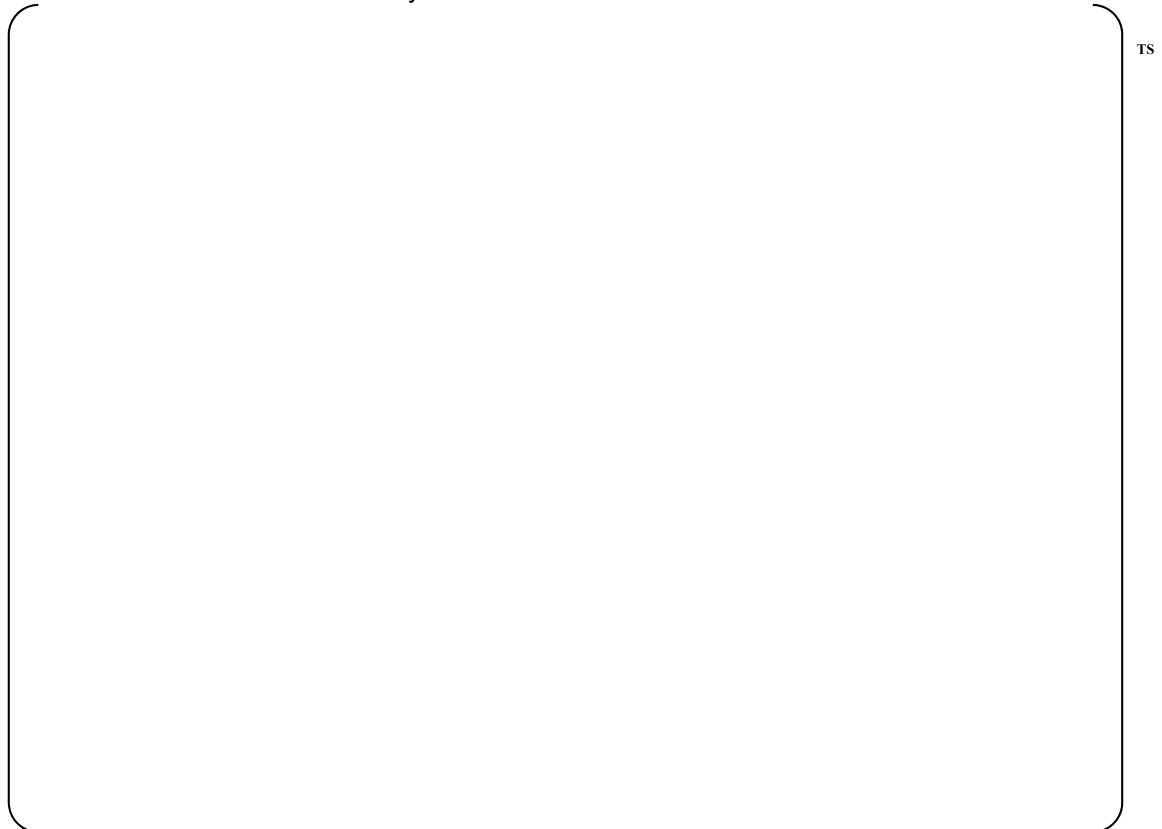


Figure C.3-1 CEA Position Requirements during Reactor Scram

C.4.0 VERIFICATION

Emphasis in this verification analysis is primarily directed towards comparison of the predicted insertion times with the actual test data. SCRAM analysis data were based on the OPR1000 plants loaded with PLUS7 fuel assemblies and the actual test data were collected at YGN-5 (an OPR 1000 plant) cycle 7 with PLUS7 full core as shown in Table C.4-2 and Figure C.4-3.

As indicated in Table C.4-1, Figure C.4-1 and Figure C.4-2 below, the actual test data do not exceed the data predicted from the SCRAM analysis. Therefore, it can be generally concluded that the SCRAM analysis provides a reasonably conservative prediction on the 90% insertion time.



Figure C.4-1 Distribution of Actual Test Data

Table C.4-1 Summary of CEA Actual Test Data

| CEA Type | Time to 90% Insertion (sec.) | | |
|-------------------------|------------------------------|---------------------|-----------------------------------|
| | Time Limits | Scram Analysis Data | Actual Test Data at YGN-5 Cycle 7 |
| 4-Finger Part Strength | | | TS |
| | | | |
| 4-Finger Full Strength | | | |
| | | | |
| 12-Finger Full Strength | | | |
| | | | |

※ SCRAM Analysis Data = Analysis Data + { } TS



Figure C.4-2 Histogram of Actual Test Data

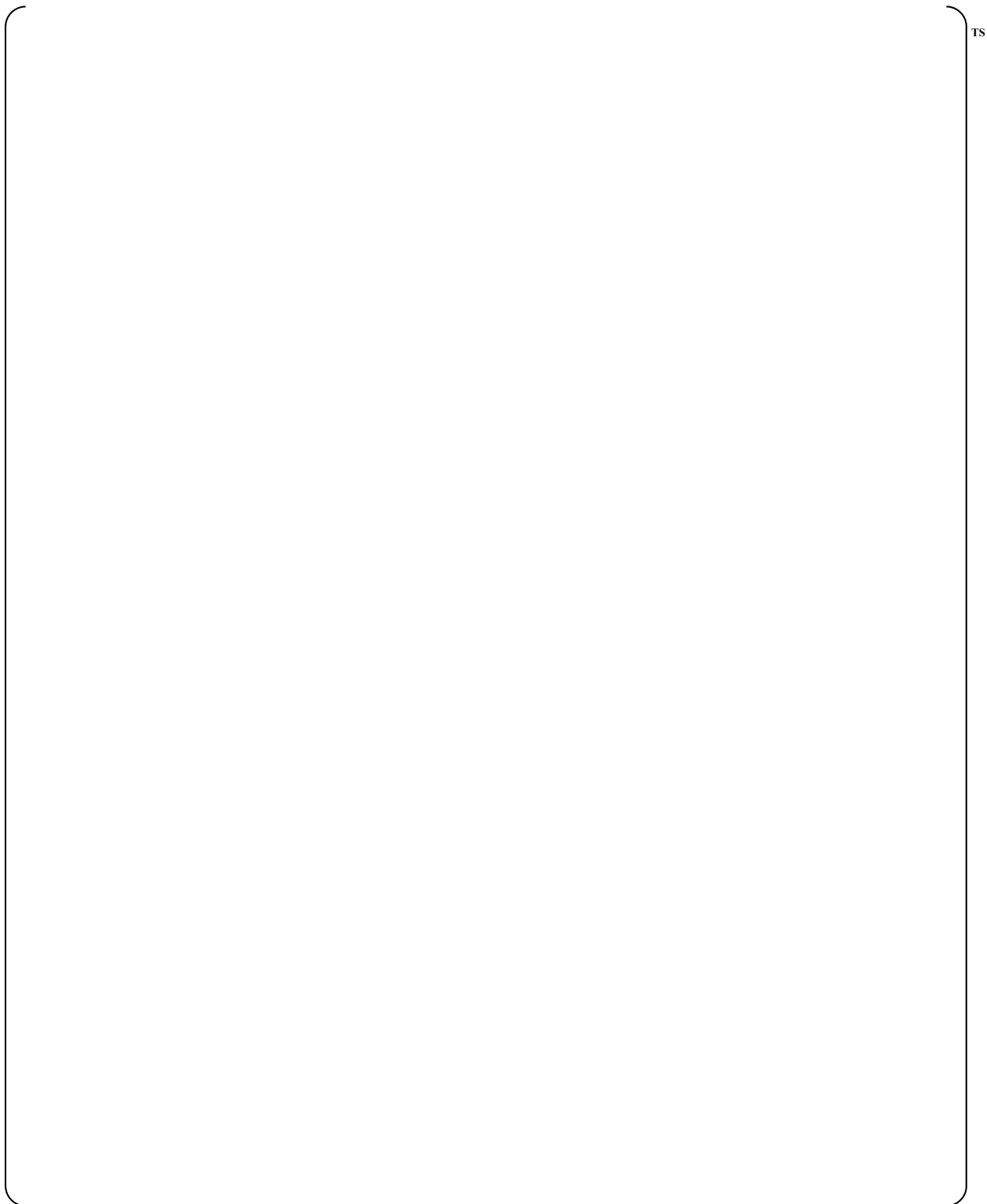


Figure C.4-3 Actual Test Raw Data from YGN-5

Table C.4-2 Actual Test Data (CEA Types)

TS

C.5.0 CONCLUSION

The results of the analysis show that the SCRAM analysis provides reasonably conservative predictions of the CEA insertion time for the 90% insertion criterion, compared with the actual test data from an operating plant.

Appendix D

PLUS7 Wear Performance Analysis

JULY 2017

**Copyright © 2017
All Rights Reserved**

TABLE OF CONTENTS

LIST OF FIGURES..... D-3

D.1.0 INTRODUCTION..... D-4

D.2.0 TEST CRITERIA..... D-5

D.3.0 WEAR CLACULATION AND EVALUATION..... D-5

D.4.0 CONCLUSION D-6

LIST OF FIGURES

Figure D.4-1 Days to the Critical Wear Volume Relative Wear Depths

D-6

D.1.0 INTRODUCTION

PLUS7 mid grids introduced conformal springs and dimples in order to minimize damage to fuel rods caused by fretting wear. A long-term wear test was performed to evaluate the fuel rod wear performance of PLUS7 grids that have area contact with fuel rods. The cells of the grids were adjusted to have some gaps between them and the fuel rods, and the wear test was performed for 500 hours in the VIPER (Vibration Investigation and Pressure-drop Experimental Research) hydraulic test facility of Westinghouse Co. in the USA. Based on the wear scar data from the wear test, fuel rods, springs, and dimples were modeled using the Solidworks to calculate wear volumes relative to wear depths. The required time to reach the critical wear volume which is related to its wear depth was predicted.

The cladding wear evaluation is summarized as follows:

(1) Out-of-pile tests

- Results of the VIPER long-term wear tests (See Appendix A.2.2)

- All fretting wear scars of the PLUS7 assembly were measured using the Accumeasure System 9000 tool to determine the fretting wear depth.
- No measurable wear scars were found in the pre-oxidized rods.

(2) Analysis

- Wear volume-to-depth calculations

- Fretting wear performance was evaluated by wear mark inspection.
- Analytical calculation based on geometric configuration.

D.2.0 TEST CRITERIA

Fuel rod wear of the test assembly, projected using the standard linear wear volume extrapolation, should not exceed a depth of []^{TS}.

- The depth of []^{TS} clad thickness is conservatively calculated considering fuel failure.

D.3.0 WEAR CALCULATION AND EVALUATION

The measurable wear scars were extrapolated to the critical volume (at []^{TS} clad thickness) appropriate for the grid support feature. This extrapolation assumed that the wear rate determined from the VIPER wear scars would be constant throughout the life of the assembly. This relative fretting performance of assembly grid designs were compared in the days to the critical wear volume. With a constant work rate, the following relationship exists:

$$\frac{\text{Days to Critical Wear Volume}}{\text{Critical Wear Volume}} = \frac{\left(500/24\right) \text{ days}}{\text{Wear Volume at } \left(500/24\right) \text{ days}}$$

Therefore, the days to the critical wear volume for each spring and dimple wear scar can be calculated by the following.

$$\text{Days to Critical Wear Volume} = \text{Critical Wear Volume} \times \frac{\left(500/24\right) \text{ days}}{\text{Wear Volume at } \left(500/24\right) \text{ days}}$$

For a 0.374 inch diameter fuel rod, with the []^{TS} nominal cladding thickness, the critical wear volume occurs at a wear depth equal to []^{TS} ([]^{TS} of the nominal cladding thickness).

D.4.0 CONCLUSION

- Since all oxidized rods had no measurable wear, the PLUS7 test assembly met the design criteria. Fretting wear did not occur when a realistic { }^{TS} gap existed between fuel rods and grids.
- Figure D.4-1 shows the days to the critical wear volume relative to wear depths that occurred during 500 hours of non-oxidized fuel rod. The conservatively evaluated time for the first fuel rod to reach the initial critical volume is { }^{TS}. Thus the PLUS7 test assembly meets the internal design criteria.



Figure D.4-1 Days to the Critical Wear Volume Relative to Wear Depths

Non-Proprietary

SECTION C

Non-Proprietary

Page intentionally left blank

**KHNP****KOREA HYDRO & NUCLEAR POWER CO., LTD**

70-1312-gil, Yuseong-daero, Yuseong-gu, Daejeon, 305-343, KOREA

Tel: +82-42-870-5740 / Fax: +82-42-870-5779

<http://www.khnp.co.kr>

June 26, 2014

Document Control Desk

U.S. Nuclear Regulatory Commission

Washington, DC 20555-0001

Attention: Mr. Jeffrey Ciocco

Division of New Reactor Licensing

Project No.0782

MKD/NW-14-0020L

Subject: KHNP Response to RAI 4-7542**Reference: 1) NRC Request for Additional Information 4-7542, dated May 27, 2014****2) KHNP Topical Report: PLUS7 Fuel Design for the APR1400, Revision 0, November 2012 (APR1400-F-M-TR-13001)**

KHNP is hereby submitting responses to the Request for Additional Information (RAI) 4-7542, dated May 27, 2014. This RAI response addresses all the ten (10) questions of the RAI 4-7542.

Enclosure 1 contains one copy of the associated affidavit. Enclosure 2 provides "KHNP Response to Request for Additional Information No 4-7542" (Proprietary), and Enclosure 3 provides "KHNP Response to Request for Additional Information No 4-7542" (Non-proprietary).

If additional information or clarification is required, please contact Yunho Kim, Director of KHNP Washington DC Center at yunhokim@khnp.co.kr or 703-388-0592.

Sincerely,

Myung-Ki Kim

Project Manager

Advanced Reactors Development Laboratory

Korea Hydro and Nuclear Power Co., Ltd

Enclosure:

1. Affidavit KAW-14-0020

2. KHNP Responses to Request for Additional Information No. 4-7542 (Proprietary)

3. KHNP Responses to Request for Additional Information No. 4-7542 (Non-Proprietary)

ENCLOSURE 1

Affidavit KAW-14-0020

I, Jae-yong Lee, state the following:

1. I am the Director of Korea Hydro & Nuclear Power Co., Ltd. (KHNP), and as such I am authorized to request withholding the information transmitted with this letter from public disclosure and to execute this affidavit.
2. I am familiar with the criteria applied by KHNP to determine whether certain information is proprietary, and with the policies established by KHNP to ensure the proper application of these criteria.
3. The information, KHNP Responses to Request for Additional Information No. 4-7542 (Proprietary), transmitted with this letter has been classified by KHNP as proprietary in accordance with the policies for the control and protection of proprietary and confidential information. The information regarded as proprietary is identified and marked consistent with the requirements of 10 CFR 2.390, § (b)(1)(i). Accordingly, the proprietary information is enclosed within brackets and the right-hand bracket carries a notation of “TS” to indicate that the trade secret nature of the information claimed to be proprietary is the basis for proposing that the information so identified be withheld from public disclosure.
4. Pursuant to the considerations set forth in 10 CFR Section 2.390(a), KHNP considers the information classified as proprietary to be “trade secret” information since it is design, analysis, or test information that would be difficult for a competitor to reproduce and hence provides an economic and competitive advantage to KHNP.
5. The need for designating the information as proprietary has been raised within KHNP. The information is being treated proprietary and confidential and has not been disclosed by KHNP to the public.
6. Nondisclosure of the proprietary information transmitted with this letter is vital to the competitiveness held by KHNP and, hence, disclosure of the proprietary information transmitted in with this letter would have negative commercial impacts on the competitive position of KHNP in the U.S. nuclear market.
7. In accordance with KHNP policy, proprietary information contained in this document may be, or may have been, made available on a limited basis to regulatory bodies, customers, potential customers, and their agents, suppliers, and licensees, and others under suitable agreements providing for nondisclosure and limited use of the information.



KHNP
KOREA HYDRO & NUCLEAR POWER CO., LTD

I declare that the foregoing statements are true and correct to the best of my knowledge, information and belief.

Executed on June 26, 2014.


Jae-yong Lee

Director

APR1400 Licensing Team

Korea Hydro & Nuclear Power Co., Ltd.

ENCLOSURE 3

“ KHNP Responses to Request for Additional Information No. 4-7542”
(Non-Proprietary)

June 2014

Enclosure 3

Docket No. PROJ 0782

KHNP Response to RAI 4-7542 on Topical Report
“PLUS7 Fuel Design for the APR1400”
APR1400-F-M-TR-13001-P Rev.0

June 2014

| |
|-------------------------|
| Non-Proprietary Version |
|-------------------------|

RESPONSE TO REQUEST FOR ADDITIONAL INFORMATION 4-7542

Date of RAI Issued: 05/27/2014

Response Date: 06/26/2014

Question 1

In Sections 1 and 4, discussions on in-pile tests reference Lead Test Assemblies (LTAs) and Commercial Surveillance Assemblies (CSAs). Staff is seeking clarification on the definitions of LTA and CSA. The following additional information is requested:

- Provide a definition of Lead Test Assembly, including any imposed limitations on location, number of LTAs, etc.
- Provide a definition for Commercial Surveillance Assembly, including any imposed limitations on location, number of CSAs, etc.

Response

PLUS7 is an advanced nuclear fuel, jointly developed with Westinghouse to improve fuel performance in both economy and safety. Complete details of the lead test assembly (LTA) and commercial surveillance assembly (CSA) programs to justify PLUS7 for commercial operation are provided in APR1400-F-M-TR-13001-P Rev.0.

In summary, the LTA program was implemented to justify fuel performance for 3 cycles of operation in a nuclear power plant. For this program, four LTAs were irradiated for three cycles from cycle 5 of Ulchin Unit 3. The only limitation imposed on the LTAs was that they operated in non-limiting locations in the core. Results of in-pile tests after each cycle showed that the in-reactor performance of the LTAs was well within their design criteria.

Following the successful LTA program, PLUS7 fuel was put into commercial operation in 2006 starting with cycle 5 of Yonggwang Unit 5. As a follow-up to the LTA program, the CSA program was initiated to evaluate PLUS7 fuel performance in limiting burn-up locations in the core. The CSA program consisted of 1) identifying four PLUS7 fuel assemblies operating in limiting burn-up core locations for two and three cycles of operation, 2) evaluating two of the limiting burn-up fuel assemblies after two cycles of operation and 3) evaluating two other limiting burn-up fuel assemblies after three cycles of operation. The only limitation on location of these fuel assemblies was that they were located in limiting burn-up locations in the core. The results of these evaluations showed that the in-reactor performance of the CSAs was within their design criteria even at the limiting burn-up locations in the core.

Question 2

Section 2.2.2.1 presents the criteria related to the fuel assembly stress limits for normal operation, AOOs, and postulated accidents. Provide additional information regarding the following:

- The minimum ultimate tensile strength at unirradiated conditions (S_u) is listed in the definitions, but is not found in the stress limit equations. How is S_u used in the Plus7 stress limit criteria.
- Is the S_m value, defined by the ASME Section III Stress Intensity for Class 1 Components, for all materials including zirconium alloys? Provide the values used and reference.

Response

The minimum ultimate tensile strength at unirradiated conditions (S_u) is not used directly in the stress limit equations, but it is used to determine S_m' which is the allowable design strength for the postulated accident conditions. The S_m' is a smaller value of $2.4 S_m$ and $0.7 S_u$, which is listed in the definitions of stress limit equation for the postulated accident conditions in section 2.2.2.1 of APR1400-F-M-TR-13001-P Rev.0.

According to the ASME Section III, the S_m , defined by the ASME Section II, Part D, is used for all materials including zirconium alloys. The S_m values for the austenitic steel components are calculated using the values defined in the Table 2A, ASME Section II, Part D and the S_m values for the ZIRLO components are calculated as follows:

- *Two-thirds of the minimum yield strength at temperature*

The S_m values used for the PLUS7 components and the references are in the Table 2-1.

Table 2-1 S_m values for the components at operating temperature

TS

Question 3

In Section 2.2.2.2 it is stated that the evaluation of the rod to top nozzle axial clearance is performed by calculation and confirmed by operating experience. The results of this evaluation are provided in Figure 4-6. The lack of a reference has caused staff to question how the calculation was performed. Provide a detailed description of how the rod to top nozzle axial clearance calculation is performed.

Response

In Figure 4-6 of APR1400-F-M-TR-13001-P Rev.0, the data indicate the rod to top nozzle axial clearances measured for the PLUS7 lead test assemblies (LTAs) and commercial surveillance assemblies (CSAs) during the pool side examinations (PSEs), and “95% lower prediction bound” is a line drawn by processing the measured data statistically.

The rod to top nozzle axial clearance was calculated considering dimensions of the PLUS7 components, thermal expansions, and irradiation growths of fuel rod and fuel assembly by the following equation:

$$\text{Rod to top nozzle axial clearance} = C - E + I_{GT} - I_{FR}$$

Where, C: Rod to top nozzle axial clearance (as-built),

E: Thermal expansion difference between fuel rod and guide tube,

I_{GT}: Irradiation growth of guide tube,

I_{FR}: Irradiation growth of fuel rod.

The calculated minimum clearance by using the above equation is [
]^{TS}.

Question 4

In Section 2.2.2.3, hydraulic stability is partially demonstrated through tests performed in the FACTS loop test facility. The range of flows chosen for the tests has caused staff to question the maximum design flow rate for the PLUS7 fuel assembly.

- What is the maximum design flow rate for the PLUS7 fuel assembly?
- Explain what is meant by “equivalent mechanical design flow in the FACTS test”, which was used in Section 2.0 of Appendix A.2.1. How does this value differ from in-reactor design flow?

Response

By considering the limiting reactor vessel flow rate, the total number of fuel assemblies (FAs) in core and total bypass flow, [

J^{TS} .

In addition, the flow in reactor is not equal to that in the fuel assembly compatibility test system (FACTS) due to the difference of FA channel size between the OPR1000 and FACTS facility. Therefore, the flow rate in FACTS was adjusted to be the same flow velocity as the reactor. Considering in-reactor mechanical design flow [J^{TS} , the channel size per FA in the OPR1000 and FACTS facility, block area in PLUS7 fuel and bypass flow in PLUS7 fuel, [J^{TS} . This is

“equivalent mechanical design flow in FACTS.”

In summary, [

J^{TS} . Also, the equivalent mechanical design flow in FACTS was adjusted considering in-reactor mechanical design flow for PLUS7 fuel, the difference of FA channel size between the OPR1000 and FACTS facility, etc.

Note:

TS

Question 5

The stress analyses for the bottom and top nozzles discussed in Sections 2.3.1.2 and 2.3.2.2 are based on an assumed load, which has caused staff to question the basis for the assumed load. Additionally, staff is seeking clarification of the calculation procedure for the stress analyses. Provide the following:

- Explain how the value for the assumed load during postulated accidents is conservative.
- Provide a summary of the calculation procedure for the stress analyses, including the codes utilized for the calculation, imposition of boundary conditions, and how adequate mesh refinement was determined.

Response

Since the load information of postulated accidents at a specific site was not available during the development of the PLUS7 fuel, the load during postulated accidents was conservatively assumed to be []^{TS}. By the comparison between the assumed load and loads during postulated accidents for the NRC DC project (Table 5-1), the assumed load is deemed to be conservative.

Table 5-1 Maximum Axial Loads for PLUS7 Fuel Assembly

TS

The following calculation procedure for the stress analyses is performed sequentially by using the ANSYS version 5.6.2, which consists of assumption, modeling, material properties, applied load and boundary condition, meshing and analysis.

Top nozzle

The PLUS7 top nozzle components, holddown plate and adapter plate, were modeled using three-dimensional solid elements []^{TS} consisting of 10 nodal points per element. The degree of freedom per []^{TS} element nodal point is U_x , U_y , U_z . The special option of ANSYS (called “smart element sizing”) was used for meshing the model. The one-eighth model was developed by utilizing symmetry in the geometry and loading conditions. To simplify and conservatively analyze the top nozzle, the chamfers or fillets were not modeled.

- The assumptions used in this analysis are summarized:
 - ✓ Nominal dimensions
 - ✓ Material properties at the specific temperature condition

In case of the holddown plate analysis, the assumed load during postulated accidents was applied as uniformly distributed loads at the interface between the holddown plate outer hub and the colandria tube as shown in Figure 5-1. In order to simulate the contact between spring and holddown plate, the contact area was restrained in the axial direction of the fuel assembly.

In case of the adapter plate analysis, the assumed load during postulated accidents was applied as uniformly distributed loads on the holddown spring seating surface as shown in Figure 5-2. The supported area by guide thimble flange was restrained in the axial direction of the fuel assembly.

Bottom nozzle

The PLUS7 bottom nozzle was modeled using the same three-dimensional solid elements []^{TS} as the top nozzle. The “smart element sizing” option was also used for meshing the model. The one-eighth model was developed by utilizing symmetry in the geometry and loading conditions. To simplify and conservatively analyze the bottom nozzle, the flow hole inlet chamfer on the bottom nozzle plate and the instrument guide were not modeled.

- The assumptions used in this analysis are summarized:
 - ✓ Nominal dimensions except the minimum thickness for the bottom nozzle plate
 - ✓ Material properties at the specific temperature condition

The assumed load during postulated accidents was applied to the bottom nozzle. Uniformly distributed loads were applied to the guide thimble location on the bottom nozzle plate as shown in Figure 5-3. The bottom surface of leg was restrained in the global U_x , U_y , U_z directions.

Meshing

A sensitivity study was performed to determine adequate mesh for stress analysis of the PLUS7 top and bottom nozzles by adjusting the element size.

By comparing P_m+P_b per each element size, adequate mesh size was determined as follows:

- In case of the holddown plate, the element sizes of []^{TS} were used and mesh was generated using the “smart element sizing” option. The sensitivity study shows that P_m+P_b at each size were within []^{TS} of each other. Therefore, element size for the holddown plate was selected to be []^{TS}.
- In case of the adapter plate, the element sizes of []^{TS} were used and mesh was generated using the “smart element sizing” option. The sensitivity study shows that P_m+P_b at each size were within []^{TS} of each other. Therefore, element size for the adapter plate was selected to be []^{TS}.
- In case of the bottom nozzle, the element sizes of []^{TS} were used and mesh was generated using the “smart element sizing” option. The sensitivity study shows that P_m+P_b at each size were within []^{TS} of each other. Therefore, element size for the bottom nozzle was selected to be []^{TS}.

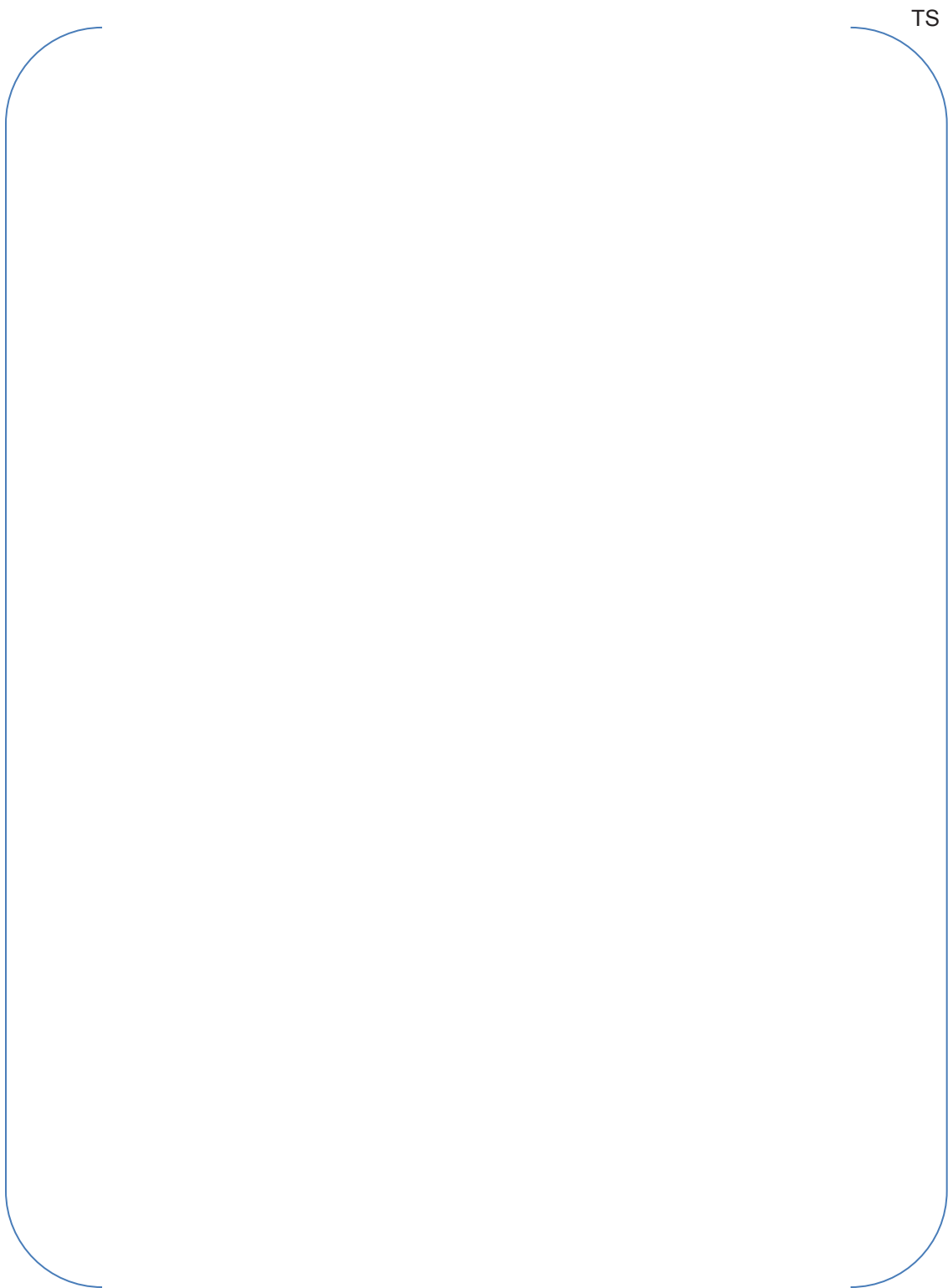


Figure 5-1 Boundary Conditions of Holddown Plate



Figure 5-2 Boundary Conditions of Adapter Plate



Figure 5-3 Boundary Conditions of Bottom Nozzle

Question 6

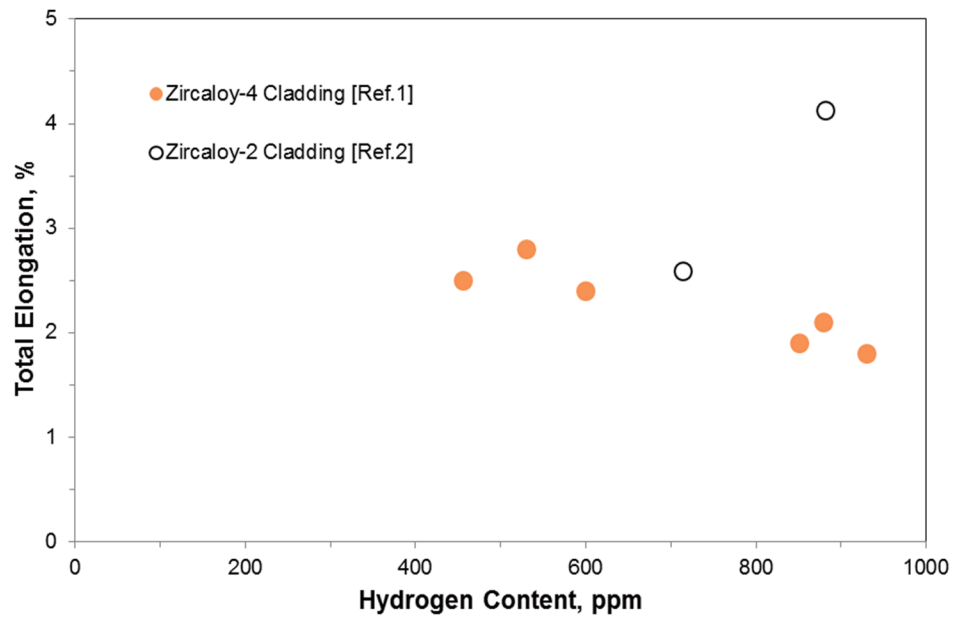
The proposed oxide limit in Section 3.2.4 of APR1400-F-M-TR-13001-P is 100 μm . Figure 4-44 indicates that cladding with 100 μm of oxide thickness would exceed the 600 ppm hydrogen content limit, which would lead to a loss of ductility. How does the use of a 100 μm oxide thickness limit support the 1% strain criterion?

Response

As proposed in Section 3.2.4 of APR1400-F-M-TR-13001-P Rev.0, the cladding hydrogen is currently limited to 600 ppm on a best estimate basis at end of life to preclude loss of ductility due to hydrogen embrittlement by the formation of zirconium hydride platelets. However, the specific limit value of 600 ppm was not determined by the firm basis on the specified ductility correlation for fuel cladding. It appears that the 600 ppm limit was chosen as a design limit because it was a conservative value for maintaining ductility, and was well above the hydrogen content values that existed when it was selected. The hydrogen-associated effect on ductility is also mainly explained by several combination factors such as temperature, hydride morphology, direction of principal stress, and strain rate, as well as the absolute level of hydrogen contents. Therefore, in consideration of historical determination and related factors, the exceeding a single limiting value of 600 ppm on a best estimate basis needs not to be concerned.

Furthermore, the main reason for the reduction in Zircaloy-4 strain capability is an irradiation hardening effect. The clad hydrogen content plays a lesser role since most of the hydrogen is in solution or precipitates as zirconium hydride platelets which are ductile at normal cladding operating temperatures. Therefore, the hydrogen does not have a significant impact on the cladding ductility at operating temperatures.

In conclusion, ductility is not significantly affected at operating temperatures and not susceptible up to hydrogen levels of 930 ppm shown in Figure 6-1. Therefore, as the 1% strain limit for cladding ductility was introduced to preclude excessive cladding deformation during normal operation and anticipated operational occurrences (AOOs), the 100 μm oxide thickness limit still supports the 1% strain criterion.



*Figure 6-1 Measured Total Elongation vs Hydrogen Content
(Irradiated fuel cladding & Tested at 300 °C or 350 °C)*

Note: References

[Ref.1] Yagnik S, "Ductility of Zircaloy-4 Fuel Cladding and Guide Tubes at High Fluences," Journal of ASTM International, Vol.2, No.5, May 2005.

[Ref.2] Yagnik S, "Effect of Hydrides on the Mechanical Properties of Zircaloy-2," Orlando, FL, 2004(b).

Question 7

Section A.2.1 describes the methodology to determine if there are flow induced vibration (FIV) resonances which could lead to fuel failures. It is stated that the vibration spectra is inspected for peaks. What is the criterion for determining if such resonances exist?

Response

The objective of the fuel assembly compatibility test system (FACTS) vibration test is to confirm that the PLUS7 design is not susceptible to high resonance flow-induced assembly vibration over a range of plant operation flow rate. The design acceptance criteria for the fuel assembly (FA) resonant vibration are as follows:

- *No resonant FA vibration phenomena will be observed within the reactor operating flow rate,*
- *The overall vibration amplitude, for frequencies in the range of 0 ~ 100 Hz, will be less than []^{TS} for reactor operating flow rates.*

As a result of the FACTS vibration test for the PLUS7 fuel, there was no indication of abnormal flow induced vibration response throughout the test flow range []^{TS} as shown in Figure A.2.1-2 of APR1400-F-M-TR-13001-P Rev.0. Data in this figure are the maximum vibration amplitude at each flow rate in the range of 0 ~ 100 Hz. Especially, the vibration amplitude of the FA is []^{TS} and the peak is not detected throughout the reactor operating flow range of []^{TS}. Therefore, the vibration characteristics of the PLUS7 fuel were verified through this test. In addition, there has been no issue of vibration on the PLUS7 fuel since the initial commercial supply.

Question 8

The FIV tests presented in Appendix A did not result in fretting wear-induced cladding failure caused by cross-flow or natural harmonics through the full range of flow rates. However, it is not stated that there were no indications of fretting wear associated with FIV. How much wall thinning occurred as a result of FIV and how was this incorporated into the stress analysis?

Response

Fuel rod fretting wear was evaluated through the vibration investigation and pressure drop experimental research (VIPER) long-term wear test and confirmed by the hot cell examination on the PLUS7 lead test assembly (LTA). The VIPER test results are summarized in the Appendix A.2.2 and the results of hot cell examination are described in Section 4.3.1 of APR1400-F-M-TR-13001-P Rev.0.

As a result of the VIPER test, the number of worn-rods and maximum wear depth of the each rod are described in Table A.2.2-2 and Figure A.2.2-1 of APR1400-F-M-TR-13001-P Rev.0, respectively. None of the []^{TS} oxidized rods had measurable wear depth while []^{TS} non-oxidized rods had measurable wear depth as shown in Table A.2.2-2 and Figure A.2.2-1 of APR1400-F-M-TR-13001-P Rev.0. Through the hot cell examination, spring contact area of fuel rod was sliced in 8 pieces with one (1) mm thickness to measure the wear depth. The results of cross section examinations showed that there was no measureable fretting wear depth as described in the Section 4.3.1 of APR1400-F-M-TR-13001-P Rev.0. Therefore, the evaluation shows that the PLUS7 fuel rod would not have fretting wear.

With regard to the stress analysis, fretting on the fuel rod clad surface will not have a significant effect on stresses. There should be only a small dependence of cladding stresses on fretting wear because this type of wear is local at grid contact locations, relatively shallow in depth, and on the clad outer surface, where stresses are lower than in other clad areas. As mentioned above, the flow induced vibration (FIV) test results indicate that there is no measurable wear depth on the surface of the PLUS7 fuel rod. The fretting wear therefore has a very small effect on the cladding stress evaluations. Nevertheless, the PLUS7 clad stress analysis was performed assuming the clad wall thinning effect due to []^{TS} which corresponds to the []^{TS}, and the calculation results show that the stresses in the cladding are within the allowable limits. This is a conservative approach because an actual clad wall thinning occurred by fretting wear is negligible compared to the reduction value assumed in the clad stress analysis.

Question 9

Figure 4-10 presents LTA and CSA predicted oxide thickness versus measured thickness. The staff noted a difference between the prediction accuracy for the LTA data versus the CSA data. While the CSA oxide thickness appears to be typically over predicted, which is conservative, the staff would like to understand the reason for the differences. Please provide a discussion which explains the differences between the CSA and LTA data presented in Figure 4-10 and an explanation of why the CSA oxide thickness appears to be over predicted while the LTA oxide thickness appears to follow a best estimate prediction.

Response

The current ZIRLO corrosion model is based on the []^{TS} corrosion model originally developed for Zircaloy-4 clad. Comparison of the measured cladding oxide thickness on ZIRLO rods to the measured cladding oxide thickness on Zircaloy-4 rods with similar power histories, indicated that the ZIRLO cladding corrosion rate was []^{TS} of the Zircaloy-4 cladding corrosion rate [Ref.1]. Thus, the ZIRLO corrosion model became []^{TS} times the []^{TS} Zircaloy-4 corrosion rate [Ref.1]. The pool side examination (PSE) for the PLUS7 lead test assemblies (LTAs) were conducted in 2007, which reflected the []^{TS} model prediction results. After that, based on the measured data from other domestic plants in addition to the PSE results for the PLUS7 LTAs, KEPCO NF found that the design corrosion model []^{TS} did not accurately predict oxide thickness on the surface of ZIRLO cladding. Thus, the []^{TS} model for ZIRLO cladding was replaced by []^{TS} model which conservatively predicts the oxide thickness for ZIRLO cladding irradiated in domestic plants [Ref.2]. The PSE for the PLUS7 commercial surveillance assemblies (CSAs) were conducted in 2011 and the predicted oxide thickness was calculated using the []^{TS} model.

Additionally, the predicted oxide thickness data for the PLUS7 LTAs were modified based on the []^{TS} model for standard comparison. The modified prediction results in Figure 9-1 conservatively bounds the measured oxide thickness data for the PLUS7 LTAs.



*Figure 9-1 Comparison of Measured and Predicted
Cladding Oxide Thickness for the PLUS7 LTAs and CSAs*

Note: References

[Ref. 1] VANTAGE+ Fuel Assembly Report Core Report, WCAP-12610-P-A, April 1995.

*[Ref. 2] Verification Report on Oxide Thickness Prediction Model of ZIRLO Cladding, KNF-
TR-MTL-07002, Rev.0, March 2007.*

Question 10

Figure 4-44 contains predicted and measured hydrogen content data for the CO3 LTA. Two of the three data points indicate an under prediction of hydrogen content. Provide predicted hydrogen content data for the Kori Unit 2 and Yonggwang Unit 4 data presented in Figure 4-44.

Response

The predicted hydrogen content data for the Kori Unit 2 and Yonggwang Unit 4 are presented in Figure 10-1. All the available data for the hydrogen content obtained from other domestic plants (Yonggwang Unit 2 & Kori Unit 3) are added to Figure 10-1. Based on this data, the predicted hydrogen contents appear to reasonably follow general trend of measured scattering data.



Figure 10-1 Comparison of Measured and Predicted Hydrogen Content vs Predicted Oxide Thickness

Non-Proprietary

SECTION D

Non-Proprietary

Page intentionally left blank

**KHNP****KOREA HYDRO & NUCLEAR POWER CO., LTD**

70-1312-gil, Yuseong-daero, Yuseong-gu, Daejeon, 305-343, KOREA

Tel: +82-42-870-5740 / Fax: +82-42-870-5779

<http://www.khnp.co.kr>

July 21, 2015

Document Control Desk

U.S. Nuclear Regulatory Commission

Washington, DC 20555-0001

Attention: Mr. Jeff Ciocco
Division of New Reactor Licensing

Docket No. 52-046
MKD/NW-15-0055L

Subject: Response to RAI 5-7954 on Topical Report “PLUS7 Fuel Design for the APR1400, APR1400-F-M-TR-13001, Rev. 0

Reference: NRC Request for Additional Information 5-7954, dated June 18, 2015

KHNP is hereby submitting the response to RAI 5-7954, dated June 18, 2015. The RAI response addresses questions 11, 12, 13, 14, 15, 17, 18, 19, 20, 21, 22, and 23.

The response to the remaining question 16 will be responded by September 16, 2015.

Enclosure 1 contains a copy of the associated affidavit. Enclosure 2 provides the response to RAI 5-7954 (Proprietary). Enclosure 3 provides the response to RAI 5-7954 (Non-Proprietary).

If additional information or clarification is required, please contact Yunho Kim, Director of KHNP Washington DC Center at yunho.kim@khnp.co.kr or 703-388-0592.

Sincerely,

Jae-yong Lee

Project Manager

Advanced Reactors Development Laboratory

Korea Hydro and Nuclear Power Co., Ltd

Enclosure

1. Affidavit KAW-15-0055
2. Response to RAI 5-7954 (Proprietary)
3. Response to RAI 5-7954 (Non-Proprietary)

Enclosure 1

Affidavit KAW-15-0055

I, Jae-yong Lee, state the following:

1. I am the General Manager of Korea Hydro & Nuclear Power Co., Ltd. (KHNP), and as such I am authorized to request withholding the information transmitted with this letter from public disclosure and to execute this affidavit.
2. I am familiar with the criteria applied by KHNP to determine whether certain information is proprietary, and with the policies established by KHNP to ensure the proper application of these criteria.
3. The information, Response to RAI 5-7954 (Proprietary), transmitted with this letter has been classified by KHNP as proprietary in accordance with the policies for the control and protection of proprietary and confidential information. The information regarded as proprietary is identified and marked consistent with the requirements of 10 CFR 2.390, § (b)(1)(i). Accordingly, the proprietary information is enclosed within brackets and the right-hand bracket carries a notation of “TS” to indicate that the trade secret nature of the information claimed to be proprietary is the basis for proposing that the information so identified be withheld from public disclosure.
4. Pursuant to the considerations set forth in 10 CFR Section 2.390(a), KHNP considers the information classified as proprietary to be “trade secret” information since it is design, analysis, or test information that would be difficult for a competitor to reproduce and hence provides an economic and competitive advantage to KHNP.
5. The need for designating the information as proprietary has been raised within KHNP. The information is being treated proprietary and confidential and has not been disclosed by KHNP to the public.
6. Nondisclosure of the proprietary information transmitted with this letter is vital to the competitiveness held by KHNP and, hence, disclosure of the proprietary information transmitted in with this letter would have negative commercial impacts on the competitive position of KHNP in the U.S. nuclear market.
7. In accordance with KHNP policy, proprietary information contained in this document may be, or may have been, made available on a limited basis to regulatory bodies, customers, potential customers, and their agents, suppliers, and licensees, and others under suitable agreements providing for nondisclosure and limited use of the information.



KHNP
KOREA HYDRO & NUCLEAR POWER CO., LTD

I declare that the foregoing statements are true and correct to the best of my knowledge, information and belief.

Executed on July 21, 2015.

Jae-yong Lee
General Manager
APR1400 Licensing Team
Central Research Institute
Korea Hydro & Nuclear Power Co., Ltd.

Enclosure 3

Response to RAI 5-7954

(Non-Proprietary)

July 21, 2015

RESPONSE TO REQUEST FOR ADDITIONAL INFORMATION

APR1400 Design Certification

Korea Electric Power Corporation / Korea Hydro & Nuclear Power Co., LTD

Docket No. PROJ 0782

RAI No.: 5-7954
SRP Section: 4.2 Fuel System Design
Application Section: PLUS7 Fuel Design for the APR1400
(APR1400-F-M-TR-13001-P)
Date of RAI Issued: 06/18/2015

Question No. 11

GDC 10 requires that the reactor core and associated coolant, control, and protection systems shall be designed with appropriate margin to assure that specified acceptable fuel design limits (SAFDLs) are not exceeded during any condition of normal operation, including the effects of anticipated operational occurrences (AOOs). SRP Section 4.2 (II)(1)(B)(v) provides guidance stating that the fuel failure criteria should address excessive fuel enthalpy.

This fuel failure criterion is addressed on Page 3-9 of APR1400-F-M-TR-13001-P for the PLUS7 fuel design. Section 3.4.4 of the topical report states that the code used to analyze this fuel failure mechanism (FATES3B) over predicts fuel thermal conductivity at high burnup. Therefore, it will also under predict fuel enthalpy. The staff notes that Section 3.4.4 provides a qualitative argument to state that the effects of burnup dependence of TCD are bounded by the reduced power capabilities at higher burnups. This raises concerns from the staff on the ability of the excessive fuel enthalpy analysis to demonstrate compliance with the excessive fuel enthalpy SAFDL given all core loading options available.

Please include a discussion, supported by analysis, within Section 3.2.10 and/or 3.4.4 of APR1400-F-M-TR-13001-P regarding the impacts of the fuel enthalpy under prediction and how excessive fuel enthalpy is precluded.

Response

A new section 3.4.5 has been added to discuss the impacts of fuel enthalpy.

“The impacts of TCD result in increasing the fuel enthalpy and the fuel centerline temperature. The impact on the fuel enthalpy due to TCD would be negligible for fresh fuel even though the maximum power peaking factors exist in the low burnup fuel in the APR1400 reload core designs. For the high burnup fuel which is affected by TCD, the fuel enthalpy and the fuel centerline temperature increase due to TCD are not significant because of the peaking factor

burndown effect at higher burnups. The detailed evaluation was performed for the impacts of TCD and submitted in TCD Technical Report in Reference 3-14.”

TCD Technical Report APR1400-F-A-NR-14002-P has been added as a reference and a pointer to it has been placed in the introduction of Section 3.4.

Impact on DCD

There is no impact on the DCD.

Impact on PRA

There is no impact on the PRA.

Impact on Technical Specifications

There is no impact on the Technical Specifications.

Impact on Technical/Topical/Environmental Report

PLUS7 fuel design topical report (APR1400-F-M-TR-13001-NP) will be revised as indicated on the attached markups.

Non Proprietary

PLUS7 FUEL DESIGN for the APR1400

APR1400-F-M-TR-13001-NP Rev.0

As shown in Figure 3-2, the predicted values are much higher than those of measured values for both H614 and H605 PLUS7 fuel assemblies. In addition, the means values and standard deviations of M/P are summarized in Table 3-9 for H615 and H605 assemblies.

- Comparison of operating conditions of OPR1000, Westinghouse Type Plants and APR1400

As explained in previous section, oxide thickness data to use the development of corrosion model multiplier and verification were measured at Ulchin unit 3, Yonggwang unit 2, Yonggwang unit 4 and Yonggwang unit 5. However, there are no available APR1400 plant specific corrosion data because the APR1400 plant was not started its first commercial operation yet.

It is, therefore, necessary to compare the operating conditions of Ulchin unit 3, Yonggwang unit 4 and Yonggwang unit 5 with those of APR1400 because the corrosion buildup on cladding material is mainly dependent on operating conditions in terms of coolant temperatures, mass flow rate, lithium concentration and core average power.

Table 3-10 shows the operating conditions of APR1400 and OPR1000 (Yonggwang unit 4 and Ulchin unit 3) as well as Westinghouse type plant of Yonggwang unit 2. As shown in Table 3-10, the coolant inlet temperature and outlet temperature of APR1400 plant are less than those of OPR1000 and Yonggwang unit 2 as well as the core average coolant mass flow rate of APR1400 plant is well within the range of OPR1000 and Yonggwang unit 2. In addition, the allowable maximum lithium concentration of APR1400 plant is the same as those of OPR1000 and Yonggwang unit 2. On the other hand, the core average linear heat rate of APR1400 plant is about four percent higher than that of OPR1000. However, it is expected that four percent increase of core average power does not give a significant effect on oxide buildup of cladding tube. Therefore, the applicability of PAD code with increased corrosion multiplier to PLUS7 fuel in APR1400 for corrosion evaluation was confirmed.

3.4 Impact of TCD on Fuel Rod Design Criteria

FATES3B does not explicitly model fuel thermal conductivity degradation (TCD) with burnup. FATES3B uses the burnup independent thermal conductivity of Lyons correlation. Compared with the thermal conductivity model with TCD effect, the Lyons model produces a relatively less conservative temperature distribution within fuel pellet.

Many of cladding-related criteria, such as cladding corrosion and hydrogen pickup, cladding collapse and fuel rod growth are not affected by TCD. Cladding temperature is not affected since the heat flux is not changed by TCD, so cladding corrosion and hydrogen criteria are unaffected. Fuel densification is not also affected by TCD, so cladding collapse criterion is not impacted by TCD. Fast neutron fluence does not change due to TCD, so fuel rod growth criterion is also not impacted by TCD.

The evaluations for the fuel rod design criteria that are affected by TCD are described as follows. The detailed evaluation results ~~will be provided in TCD Technical Report which is planned to submit to NRC.~~


 were described in TCD Technical Report in Reference 3-14.

3.4.1 Cladding Stress

As described in Section 3.2.1, KNF cladding stress criterion is established to prevent fuel damage from the excessive primary stress which results from the pressure difference between rod internal pressure and system pressure.

Non Proprietary

PLUS7 FUEL DESIGN for the APR1400

APR1400-F-M-TR-13001-NP Rev.0

Considering the amount of potential increase in rod internal pressure by TCD impact and design margin to the limit, it is judged that the cladding stress criteria are still met with consideration of TCD.

3.4.2 Cladding Strain and Fatigue

The cladding strain is affected by TCD due to the increased fuel thermal expansion. However, the increased thermal expansion can be offset with available design margin to the cladding strain and fatigue limits and conservatism in the input variables such as power history and assumed rod internal pressure. Therefore, cladding strain and fatigue criteria are still satisfied with consideration of TCD.

3.4.3 Fuel Rod Internal Pressure

The effect of increased fuel temperature due to TCD on fission gas release is inherently accounted for in the current performance code, FATES3B (References 3-1 through 3-4) because the model was calibrated to measured data for a full range of fuel rod burnup and operating conditions. Additionally, conservatism is considered in the original FATES3B calibration process and in fuel rod design analysis. However, the rod internal pressure may still increase with TCD due to the increased fuel thermal expansion, which reduces the total fuel rod void volume.

Evaluations show that the reduction of void volume due to increased thermal expansion is not significant in PLUS7 fuel rod design. In addition, the rod internal pressure limit calculation is inherently conservative in that actual gap reopening is predicted to occur at higher pressures.

In conclusion, the increased rod internal pressure can be offset with available design margin to the rod internal pressure limits. Therefore, rod internal pressure criteria are still satisfied considering the effects of TCD.

3.4.4 Overheating of Fuel Pellets

The power to melt limit depends on fuel burnup but the reduced power capability with burnup, which is caused by the depletion of the fissile material in the fuel and the buildup of fission products, offsets the TCD impact. Therefore, it is judged that there will be no safety concerns due to TCD. However, the power to melt values with burnup considering the impact of TCD are calculated and will be provided in the TCD Technical Report which will be submitted to NRC.

In summary, KNF fuel rod design criteria have been reviewed with respect to the potential impacts of TCD, and it is concluded that TCD can be accommodated such that approved fuel rod design criteria will remain satisfied for current fuel rod designs.

3.5 Conclusion

The PLUS7 fuel rod design is verified to maintain the rod integrity up to rod average burnup of 60,000 MWD/MTU based on the thermal performance and mechanical integrity evaluation results

3.4.5 Impacts of Fuel Enthalpy

The impacts of TCD result in increasing the fuel enthalpy and the fuel centerline temperature. The impact on the fuel enthalpy due to TCD would be negligible for fresh fuel even though the maximum power peaking factors exist in the low burnup fuel in the APR1400 reload core designs. For the high burnup fuel which is affected by TCD, the fuel enthalpy and the fuel centerline temperature increase due to TCD are not significant because of the peaking factor burndown effect at higher burnups. The detailed evaluation was performed for the impacts of TCD and submitted in TCD Technical Report in Reference 3-14.

Non Proprietary

PLUS7 FUEL DESIGN for the APR1400

APR1400-F-M-TR-13001-NP Rev.0

6. REFERENCES

- 2-1 CENPD-178-P, Revision 1-P, "Structural Analysis of Fuel Assemblies for Seismic and Loss of Coolant Accident Loading," Combustion Engineering Inc., August 1981.
- 3-1 CENPD-139-P-A, "C-E Fuel Evaluation Model Topical Report," Combustion Engineering Inc., July 1974.
- 3-2 CENPD-139, Supplement 1, Revision 01, "C-E Fuel Evaluation Model Topical Report," Combustion Engineering Inc., July 1974.
- 3-3 CEN-161(B)-P-A, "Improvements to Fuel Evaluation Model," August 1989.
- 3-4 CEN-161(B)-P Supplement 1-P-A, "Improvements to Fuel Evaluation Model," January 1992.
- 3-5 CENPD-404-P-A, "Implementation of ZIRLOTM Cladding Material in CE Nuclear Power Fuel Assembly Designs," November 2001.
- 3-6 CEN-372-P-A, "Fuel Rod Maximum Allowable Gas Pressure," May 1990.
- 3-7 CENPD-275-P, Revision 1-P-A, "C-E Methodology for Core Designs Containing Gadolinia-Urania Absorbers," May 1998.
- 3-8 CENPD-275-P, Revision 1-P, Supplement, 1-P-A, "C-E Methodology for Core Designs Containing Gadolinia-Urania Absorbers," April 1999.
- 3-9 CEN-193(B), Supplement 2-P, Partial Response to NRC Questions on CEN-161(B)-P, "Improvements to Fuel Evaluation Model," March 21, 1982.
- 3-10 WCAP-16500-P-A, Rev.0 "CE 16x16 Next Generation Fuel Core Reference Report," August 2007.
- 3-11 WCAP-15063-P-A, Rev.1, with Errata, "Westinghouse Improved Performance Analysis and Design Model (PAD4.0)," July 2000.
- 3-12 CENPD-187-P-A, CEPAN Method of Analyzing Creep Collapse of Oval Cladding, Combustion Engineering, Inc., April 1976 ; Supplement 1-P-A, June 1977.
- 3-13 EPRI NP-3966-CCM, "CEPAN Method of Analyzing Creep Collapse of Oval Cladding-Volume 5: Evaluation of Interpellet Gap Formation and Cladding Collapse in Modern PWR Fuel Rods," Combustion Engineering, Inc., April 1985.



3-14 APR1400-F-A-NR-14002-P, "The Effect of Thermal Conductivity Degradation on APR1400 Design and Safety Analysis," KEPKO NF, September 2014.

RESPONSE TO REQUEST FOR ADDITIONAL INFORMATION

APR1400 Design Certification

Korea Electric Power Corporation / Korea Hydro & Nuclear Power Co., LTD

Docket No. PROJ 0782

RAI No.: 5-7954
SRP Section: 4.2 Fuel System Design
Application Section: PLUS7 Fuel Design for the APR1400
(APR1400-F-M-TR-13001-P)
Date of RAI Issued: 06/18/2015

Question No. 12

GDC 10 requires that the reactor core and associated coolant, control, and protection systems shall be designed with appropriate margin to assure that specified acceptable fuel design limits (SAFDLs) are not exceeded during any condition of normal operation, including the effects of anticipated operational occurrences (AOOs). SRP Section 4.2 (II)(1)(B)(iv) provides guidance in regards to GDC 10 by stating that overheating of fuel pellets should be avoided by preventing centerline melting. This analysis should be performed for the maximum linear heat generation rate anywhere in the core, including all hot spots and should account for the effects of burnup and composition on the melting point.

Sections 3.4.4 of the PLUS7 fuel design topical report (APR1400-F-M-TR-13001-P) and 2.2.2 of the thermal conductivity degradation (TCD) technical report (APR1400-F-A-NR-13002-P) discuss overheating of the fuel pellets. The PLUS7 fuel design includes $\text{UO}_2\text{-Gd}_2\text{O}_3$ pellets. The impact of the $\text{UO}_2\text{-Gd}_2\text{O}_3$ pellet composition on the overheating of fuel pellets analysis is not discussed in either Section 3.4.4 of APR1400-F-M-TR-13001-P or Section 2.2.2 of APR1400-F-A-NR-13002-P. $\text{UO}_2\text{-Gd}_2\text{O}_3$ has a lower melting temperature and lower thermal conductivity than UO_2 which has caused the staff to question the ability of the fuel centerline melting analysis provided to demonstrate compliance with GDC 10.

Update the topical report, as applicable, to address fuel pellet overheating considering $\text{UO}_2\text{-Gd}_2\text{O}_3$ to ensure that no fuel centerline melting occurs for all fuel compositions and normal operation/AOO conditions.

Response

Figure 12-1 shows the normalized radial power fall-off curves for UO_2 and $\text{Gd}_2\text{O}_3\text{-UO}_2$ rods. As shown in Figure 12-1, the highest radial powers for $\text{Gd}_2\text{O}_3\text{-UO}_2$ rods are lower than those for UO_2 rods over all burnup ranges. Also, the radial powers decrease as burnup increases due to the reduced power capability caused by the depletion of the fissile material in the fuel and the buildup of fission products.

Figure 12-2 shows the calculated PTM (Power-to-Melt) values using the FRAPCON code for both UO_2 and $\text{Gd}_2\text{O}_3\text{-UO}_2$ rods, which are represented by black and red solid lines, respectively. Figure 12-2 also shows the highest attainable powers for UO_2 and $\text{Gd}_2\text{O}_3\text{-UO}_2$ rods in black and red dotted lines, respectively.

In Figure 12-2, each maximum attainable power of UO_2 and $\text{Gd}_2\text{O}_3\text{-UO}_2$ rods can be obtained from radial fall-off values, namely from the normalized radial power in Figure 12-1. Since the maximum attainable power for both UO_2 and $\text{Gd}_2\text{O}_3\text{-UO}_2$ rods is limited up to $[]^{\text{TS}}$ which is a SAFDL value for APR1400, it can be defined that the maximum attainable power of $[]^{\text{TS}}$ is only available with a normalized UO_2 rod radial power of $[]^{\text{TS}}$. In addition, attainable power after about $[]^{\text{TS}}$ in Figure 12-2 can be interpreted from the proportional decrease of normalized radial power fall-off curve in Figure 12-1.

Based on the same reasoning, the normalized radial power ratio of UO_2 and $\text{Gd}_2\text{O}_3\text{-UO}_2$ rods over all burnup ranges in Figure 12-1 was considered and the attainable power of $\text{Gd}_2\text{O}_3\text{-UO}_2$ rods in Figure 12-2 was derived.

As shown in Figure 12-2, the PTM values are well above the attainable powers for $\text{Gd}_2\text{O}_3\text{-UO}_2$ rods. Therefore, it can be concluded that there will be no melting of $\text{Gd}_2\text{O}_3\text{-UO}_2$ rods even when the rod power for UO_2 reaches the SAFDL value of $[]^{\text{TS}}$.

In conclusion, the lower power of $\text{Gd}_2\text{O}_3\text{-UO}_2$ burnable absorber fuel rods compared to UO_2 fuel rods allows for the UO_2 fuel rods to be the limiting case for centerline melt.

The text in Section 3.4.4 of the PLUS7 fuel design topical report (APR1400-F-M-TR-13001-P) will be revised to provide a discussion on $\text{Gd}_2\text{O}_3\text{-UO}_2$ melting.

TS

Figure 12-1 Rod Power Histories Used for PLUS7 Fuel

TS

Figure 12-2 Power to Melt and Maximum Attainable Powers for UO_2 and $\text{Gd}_2\text{O}_3\text{-UO}_2$ Rod as a Function of Burnup

Impact on DCD

There is no impact on the DCD.

Impact on PRA

There is no impact on the PRA.

Impact on Technical Specifications

There is no impact on the Technical Specifications.

Impact on Technical/Topical/Environmental Report

PLUS7 fuel design topical report (APR1400-F-M-TR-13001-NP) will be revised as indicated on the attached markups in response to Question 13.

RESPONSE TO REQUEST FOR ADDITIONAL INFORMATION

APR1400 Design Certification

Korea Electric Power Corporation / Korea Hydro & Nuclear Power Co., LTD

Docket No. PROJ 0782

RAI No.: 5-7954
SRP Section: 4.2 Fuel System Design
Application Section: PLUS7 Fuel Design for the APR1400
(APR1400-F-M-TR-13001-P)
Date of RAI Issued: 06/18/2015

Question No. 13

GDC 10 requires that the reactor core and associated coolant, control, and protection systems shall be designed with appropriate margin to assure that specified acceptable fuel design limits (SAFDLs) are not exceeded during any condition of normal operation, including the effects of anticipated operational occurrences (AOOs). SRP Section 4.2 (II)(1)(B)(iv) provides guidance in regards to GDC 10 by that overheating of fuel pellets should be avoided by preventing centerline melting. This analysis should be performed for the maximum linear heat generation rate anywhere in the core, including all hot spots and should account for the effects of burnup and composition on the melting point.

Section 2.2.2 of APR1400-F-A-NR-13002-P provides a scoping analysis using FRAPCON3.4 to investigate the impacts of burnup dependent TCD on the fuel centerline temperature analysis. The staff has concerns regarding the methodology and results presented in that the methodology is different than what is presented in APR1400-F-M-13001-P and the results do not support the stated conclusions. This in turn has caused the staff to question the ability of the fuel centerline melting analysis provided to demonstrate compliance with GDC 10.

Address the following concerns, as appropriate, to demonstrate compliance with GDC 10:

- a) Provide a basis for the assumed uncertainty of 9.7% on best estimate fuel centerline temperature used to calculate the conservative power to melt results.
- b) Section 2.2.2 of APR1400-F-A-NR-13002-P provides a SAFDL of 20 kW/ft. Figure 2-10 shows that the fuel would melt above 30 GWd/MTU assuming a conservative analysis. Update the topical report, as applicable, to ensure that the linear heat rate SAFDL is conservatively met.
- c) Provide a description and update the topical report, as necessary, to explain how the melt analysis will be performed on a cycle specific basis since FRAPCON-3.4 was used to perform the scoping analysis, or update the topical report methodology to not require FRAPCON-3.4 to

confirm compliance with GDC 10.

Response

- a) The assumed uncertainty of 9.7% in Section 2.2.2 of APR1400-F-A-NR-14002-P is a typo and the assumed uncertainty should be []^{TS}. The value comes from measured and predicted centerline temperature comparison for the UO₂ rod described in the FRAPCON manual [Reference 13-1]. The measured data is within []^{TS} level of lower and upper predicted limit in Figure 13-1. Therefore, the uncertainty of []^{TS} was conservatively determined by assuming a standard deviation of []^{TS} and multiplying by []^{TS}.

The text in Section 2.2.2 of APR1400-F-A-NR-14002-P will be revised to reflect the correction of uncertainty from 9.7% to []^{TS}.



Figure 13-1 Measured and Predicted Centerline Temperature for the UO₂ Assessment Cases throughout Life

- b) Divided by a SAFDL of 20 kW/ft, the conservative Power-To-Melt (PTM) values are normalized and plotted in Figure 13-2. As shown in Figure 13-2, the normalized Power-To-Melt (PTM) values indicate a gradual decline below a []^{TS} kW/ft from []^{TS}. The fuel will not melt because the descent ratio of actual fuel rod power (radial power fall-off) after 30 GWd/MTU will be much higher than that of the normalized PTM due to the reduced power capability caused by the depletion of the fissile material in the fuel and the buildup of fission products.

Furthermore, Figure 13-2 shows that the margin between Radial Power Fall-off and PTM tends to increase after 30 GWd/MTU. This analysis will be verified each cycle using the cycle specific radial power fall-off curve.



Figure 13-2 Normalized Power to Melt and Radial Power Fall-off Curve vs. Burnup

- c) A cycle specific radial fall-off curve based on the core loading pattern will be generated and bounded by conservative radial fall-off curve limits used in the FRAPCON analysis. This will ensure that the linear heat rate []^{TS} is valid.

The text of Section 3.4.4 of APR1400-F-M-TR-13001-P will be revised to explain how the melt analysis will be performed on a cycle specific basis.

References

[13-1] []^{TS}

Impact on DCD

There is no impact on the DCD.

Impact on PRA

There is no impact on the PRA.

Impact on Technical Specifications

There is no impact on the Technical Specifications.

Impact on Technical/Topical/Environmental Report

Topical Report APR1400-F-M-TR-13001-NP will be revised as indicated in Attachment 1.

Technical Report APR1400-F-A-NR-14002-NP will be revised as indicated in Attachment 2.

Non Proprietary

PLUS7 FUEL DESIGN for the APR1400

APR1400-F-M-TR-13001-NP Rev.0

Considering the amount of potential increase in rod internal pressure by TCD impact and design margin to the limit, it is judged that the cladding stress criteria are still met with consideration of TCD.

3.4.2 Cladding Strain and Fatigue

The cladding strain is affected by TCD due to the increased fuel thermal expansion. However, the increased thermal expansion can be offset with available design margin to the cladding strain and fatigue limits and conservatism in the input variables such as power history and assumed rod internal pressure. Therefore, cladding strain and fatigue criteria are still satisfied with consideration of TCD.

3.4.3 Fuel Rod Internal Pressure

The effect of increased fuel temperature due to TCD on fission gas release is inherently accounted for in the current performance code, FATES3B (References 3-1 through 3-4) because the model was calibrated to measured data for a full range of fuel rod burnup and operating conditions. Additionally, conservatism is considered in the original FATES3B calibration process and in fuel rod design analysis. However, the rod internal pressure may still increase with TCD due to the increased fuel thermal expansion, which reduces the total fuel rod void volume.

Evaluations show that the reduction of void volume due to increased thermal expansion is not significant in PLUS7 fuel rod design. In addition, the rod internal pressure limit calculation is inherently conservative in that actual gap reopening is predicted to occur at higher pressures.

In conclusion, the increased rod internal pressure can be offset with available design margin to the rod internal pressure limits. Therefore, rod internal pressure criteria are still satisfied considering the effects of TCD.

3.4.4 Overheating of Fuel Pellets

~~The power to melt limit depends on fuel burnup but the reduced power capability with burnup, which is caused by the depletion of the fissile material in the fuel and the buildup of fission products, offsets the TCD impact. Therefore, it is judged that there will be no safety concerns due to TCD. However, the power to melt values with burnup considering the impact of TCD are calculated and will be provided in the TCD Technical Report which will be submitted to NRC.~~

In summary, KNF fuel rod design criteria have been reviewed with respect to the potential impacts of TCD, and it is concluded that TCD can be accommodated such that approved fuel rod design criteria will remain satisfied for current fuel rod designs.

3.5 Conclusion

The PLUS7 fuel rod design is verified to maintain the rod integrity up to rod average burnup of 60,000 MWD/MTU based on the thermal performance and mechanical integrity evaluation results using by NRC approved design codes and methodologies.

The power to melt values with burnup considering the impact of TCD were calculated and provided in the TCD Technical Report (Reference 3-14). For UO₂ rod, the power to melt is decreased below a SAFDL of 20 kW/ft above 30 GWd/MTU but the reduced power capability with burnup, which is caused by the depletion of the fissile material in the fuel and the buildup of fission products, offsets the TCD impact. For Gd₂O₃-UO₂ rod, the attainable powers are below PTM of Gd₂O₃-UO₂ rod over all burnup range even when the power for UO₂ rod is reached at a SAFDL of 20 kW/ft. Therefore, it is judged that there will be no fuel centerline-melting due to TCD for UO₂ and Gd₂O₃-UO₂ rods.

This melt analysis will be verified each cycle by comparing the conservative radial fall-off curve limits used in the analysis of Reference 3-14 with a cycle specific radial fall-off curve to ensure that the linear heat rate SAFDL of 20 kW/ft is still valid.

Non-Proprietary

The Effect of TCD

APR1400-F-A-NR-14002-NP, Rev.0

2.2.2 Fuel centerline temperature

The power to fuel melting decreases as fuel rod burnup increases because the fuel melting temperature decreases. The local linear powers that preclude fuel centerline melting are calculated as a function of burnup using the FRAPCON3.4 fuel performance code [6] considering the thermal conductivity degradation effect for the transient accident analysis. The results are presented in Table 2-2 and Figure 2-10. The conservative power to fuel melting is calculated while considering an uncertainty of 9.7 % for the best estimated fuel centerline temperature. Based on the results of power to fuel melting with TCD, the linear heat rate specified acceptable fuel design limit (SAFDL) of 20.0 kW/ft was determined for the APR1400. It should be noted that an SAFDL of 20.0 kW/ft has been applied to the current APR1400 design control documents.

2.2.3 Cladding stress

The cladding stress criteria for a PLUS7 fuel rod loaded in the APR1400 are as follows [7].

- The primary tensile stress must not exceed []^{TS} of the material at the applicable temperature.
- The primary compressive stress must not exceed []^{TS} of the material at the applicable temperature.

It should be noted that the criteria of cladding stress are for primary stress not secondary stress. It is well known that the primary stress does not depend on the contact of the fuel pellet and cladding but on the pressure difference between the rod internal pressure and system pressure. The rod internal pressure is determined by the combination of fission gas release and total void volume. As explained in section 2.2.1, it was determined that the rod internal pressure predicted by FATES3B includes the effect of TCD.

Therefore, considering the conservatism of FATES3B with regard to the rod internal pressure and the design margin for cladding stresses, it is confirmed that the result of the cladding stress design criteria without TCD are still applicable to the results with TCD.

2.2.4 Cladding strain

The cladding strain was calculated using the convenient code FATES3B. Since the fission gas release data are provided by FATES3B, it is possible to evaluate the impact of TCD on cladding strain using codes in which the fuel thermal conductivity model, the Lyons correlation, is replaced with the modified NFI thermal conductivity model.

In order to assess the impact of TCD on the cladding strain, strain analysis was conducted using the cycle specific rod power history as well as the transient peak power as a function of rod burnup. The evaluation results show that the cladding plastic stain during normal operation and single AOO, and total strain (elastic plus plastic) during a single AOO, are []^{TS}, respectively, when TCD is accounted for; however, the design criteria are still satisfied with the consideration of TCD. A summary of the evaluation results is shown in Table 2-3.

2.2.5 Cladding fatigue

The cladding cumulative fatigue damage factor is determined as the sum of the fatigue damage factors resulting from the daily load following operation, reactor trips and startup/shutdown operation. The fatigue damage factor for the daily load following operation is calculated using the same convenient code, FATES3B, as was used for the cladding strain evaluation. On the other hand, the fatigue damage factors for reactor trips and startup/ shutdown are determined by hand calculation using a simple formula.

RESPONSE TO REQUEST FOR ADDITIONAL INFORMATION

APR1400 Design Certification

Korea Electric Power Corporation / Korea Hydro & Nuclear Power Co., LTD

Docket No. PROJ 0782

RAI No.: 5-7954
SRP Section: 4.2 Fuel System Design
Application Section: PLUS7 Fuel Design for the APR1400
(APR1400-F-M-TR-13001-P)
Date of RAI Issued: 06/18/2015

Question No. 14

GDC 10 requires that the reactor core and associated coolant, control, and protection systems shall be designed with appropriate margin to assure that specified acceptable fuel design limits (SAFDLs) are not exceeded during any condition of normal operation, including the effects of anticipated operational occurrences (AOOs). SRP Section 4.2 (II)(1)(B)(iv) provides guidance in regards to GDC 10 by stating that overheating of fuel pellets should be avoided by preventing centerline melting. This analysis should be performed for the maximum linear heat generation rate anywhere in the core, including all hot spots and should account for the effects of burnup and composition on the melting point.

Section 3.2.9 of the PLUS7 fuel design topical report, APR1400-F-M-TR-13001-P, provides the overheating of fuel pellets analysis for the APR1400 design. On Page 3-9, it is stated that the linear heat rate corresponding to the centerline melt of Gd_2O_3 - UO_2 burnable absorber fuel rods is always less than that of the UO_2 fuel rods. The lower thermal conductivity of Gd_2O_3 - UO_2 burnable absorber fuel rods causes the staff to question the claimed bounding nature.

Provide linear heat generation rate limits for UO_2 and Gd_2O_3 - UO_2 to support the position presented in APR1400-F-M-13001-P, or revise the topical report as necessary.

Response

Figure 14-1 shows the Power-to-Melt (PTM) for both UO_2 and Gd_2O_3 - UO_2 rods calculated by FATES3B code. It also shows the maximum attainable power for both UO_2 and Gd_2O_3 - UO_2 rods. As mentioned in the response to Question No.12, the attainable power of Gd_2O_3 - UO_2 rods in Figure 14-1 can be derived by considering the normalized radial power ratio of UO_2 and Gd_2O_3 - UO_2 rods shown in Figure 12-1. As shown in Figure 14-1, the attainable powers for Gd_2O_3 - UO_2 rods are well below the PTM values over all burnup ranges.

Therefore, it can be concluded that there will be no melting of $\text{Gd}_2\text{O}_3\text{-UO}_2$ rods even when the rod power for UO_2 rods reaches a SAFDL value of []^{TS}.

TS

Figure 14-1 Power to Melt and Maximum Attainable Power of $\text{Gd}_2\text{O}_3\text{-UO}_2$ Rod vs. Burnup

Impact on DCD

There is no impact on the DCD.

Impact on PRA

There is no impact on the PRA.

Impact on Technical Specifications

There is no impact on the Technical Specifications.

Impact on Technical/Topical/Environmental Report

There is no impact on any Technical, Topical, or Environmental Report.

RESPONSE TO REQUEST FOR ADDITIONAL INFORMATION

APR1400 Design Certification

Korea Electric Power Corporation / Korea Hydro & Nuclear Power Co., LTD

Docket No. PROJ 0782

RAI No.: 5-7954
SRP Section: 4.2 Fuel System Design
Application Section: PLUS7 Fuel Design for the APR1400
(APR1400-F-M-TR-13001-P)
Date of RAI Issued: 06/18/2015

Question No. 15

GDC 10 requires that the reactor core and associated coolant, control, and protection systems shall be designed with appropriate margin to assure that specified acceptable fuel design limits (SAFDLs) are not exceeded during any condition of normal operation, including the effects of anticipated operational occurrences (AOOs). SRP Section 4.2 (II)(1)(B)(vi) provides guidance in regards to GDC 10 by stating that rod internal gas pressures should be limited in order to (1) prevent cladding liftoff during normal operation, (2) prevent radial reorientation of hydrides in the cladding and (3) account for additional failures resulting from departure of nucleate boiling (DNB) caused by fuel rod overpressure during transients and postulated accidents. This analysis should be performed for the maximum linear heat generation rate anywhere in the core, including all hot spots and should account for the effects of burnup and composition on the melting point.

Section 3.2.5 of APR1400-F-M-TR-13001-P provides the APR1400 fuel rod internal pressure analysis. Page 3-17 of APR1400-F-M-TR-13001-P qualitatively discusses the impact of TCD on fuel rod internal pressure, stating that the impact of TCD on fuel rod internal pressure is negligible. While the stated overall calculated rod internal pressure is less than system pressure, the actual limit proposed by KHNP is not clear. This has caused the staff to question the specific rod internal pressure limit proposed by KHNP.

In order to assist the staff to perform confirmatory calculations to investigate the statements that TCD has a negligible effect on the rod internal pressure safety analyses, provide the rod internal pressure limit used for the PLUS7 fuel rod internal pressure safety analysis. If the limit is greater than system pressure, provide a basis and update the topical report, as applicable.

Response

As described in Section 3.2.5 of APR1400-F-M-TR-13001-P, the criterion for internal gas pressure is to prevent clad lift-off (No Clad Lift-Off, NCLO). When the internal gas pressure

exceeds the system pressure, the rod internal pressure should be less than the critical pressure limit, which could cause clad lift-off. The critical pressure limit for NCLO is the internal hot gas pressure, where the outward tensile creep rate of the cladding due to the differential pressure load would equal the fuel pellet swelling rate. Therefore, if rod internal pressure is less than system pressure, the NCLO criterion can be satisfied without critical pressure limit consideration.

The critical pressure limit depends on the power history. And it is determined by the FATES3B code calculation regarding creep and swelling rates. The FATES3B code automatically generates the critical pressure limit only when the internal gas pressure exceeds the system pressure. Generally, the calculated critical pressure limit would be []^{TS}.

Since the calculated maximum internal gas pressure of PLUS7 fuel rod did not exceed the system pressure as described in Section 3.2.5 of APR1400-F-M-TR-13001-P, clad lift-off did not occur and thus, satisfied NCLO criterion without a need to consider specific critical pressure limit.

Section 3.2.5 will be revised to provide a discussion on how the NCLO criterion is satisfied without a need to consider a critical pressure limit.

Impact on DCD

There is no impact on the DCD.

Impact on PRA

There is no impact on the PRA.

Impact on Technical Specifications

There is no impact on the Technical Specifications.

Impact on Technical/Topical/Environmental Report

Topical Report APR1400-F-M-TR-13001-P will be revised as indicated on the attached markups.

Non Proprietary

PLUS7 FUEL DESIGN for the APR1400

APR1400-F-M-TR-13001-NP Rev.0

3.2.4 Cladding Oxidation and Hydriding**(1) Basis**

Fuel system will not be damaged due to excessive oxidation under normal operation including AOOs.

(2) Criteria

The best estimate cladding oxide thickness shall be less than $\{ \quad \}^{TS}$

The clad hydrogen pickup is limited to $\{ \quad \}^{TS}$ at EOL to preclude loss of ductility due to hydrogen embrittlement by formation of zirconium hydride platelets.

(3) Evaluation

The cladding oxide thickness and hydrogen content of the PLUS7 fuel rod are evaluated by the same methodology and model as are used for Westinghouse PWR fuel rod designs. The best estimate oxide thickness and hydrogen content at the end of irradiation are calculated with NRC approved PAD code [3-11] during normal operation. Since cladding oxide thickness and hydrogen content do not increase during AOOs due to short time, it is not necessary to consider the AOOs for oxide thickness and hydrogen content.

The following parameters were used for evaluation.

- a) Nominal design inlet temperature, system pressure, and core mass velocity based on Thermal Design Flow Rate
- b) A crud thickness of $\{ \quad \}^{TS}$
- c) A ZrO_2 thermal conductivity of $\{ \quad \}^{TS}$

The maximum cladding thickness and hydrogen content up to rod average burnup of 60,000 MWD/MTU for APR1400 are 85.0 μm and 596.0 ppm, respectively. The criteria of cladding oxide thickness and hydrogen content are satisfied.

3.2.5 Fuel Rod Internal Pressure**(1) Basis**

Fuel system will not be damaged due to excessive rod internal pressure under normal operation.

(2) Criteria

The fuel rod internal hot gas pressure shall not the critical maximum pressure determined to cause an outward clad creep rate that is in excess of the fuel radial growth rate anywhere locally along the entire active fuel length of the fuel rod.

Reorientation of the hydrides in the radial direction in the cladding shall not occur

The radiological dose consequences of DNB failures shall remain within the specified limits.

Non Proprietary

PLUS7 FUEL DESIGN for the APR1400

APR1400-F-M-TR-13001-NP Rev.0

(3) Evaluation

FATES3B was used to calculate the rod internal pressure and corresponding critical limit according to the NRC approved methodology described in Reference 3-6. Where appropriate, the approved gadolinia methodology of References 3-7 and 3-8 has been applied. The critical limit is the internal hot gas pressure at which the outward tensile creep rate of the cladding exceeds the fuel pellet radial growth rate due to fuel swelling, thus creating any potentially damaging effects on the fuel rod due to detrimental thermal feedback effects within the fuel rod during normal operation.

Maximum rod internal pressure is calculated using conservative biasing of nominal fuel rod data including cladding outer diameter, cladding inner diameter, pellet outer diameter, active fuel length, fill gas pressure and will usually include additional conservatism in the power levels representing each successive cycle of projected residency in the reactor core. The input power history to the code is important for rod internal pressure calculation. The methodology and conservatism for determining the rod power history are described in Reference 3-9. The main parameters and rod power histories considered in representative fuel rod internal pressure calculation are summarized in Table 3-4 and Figure 3-1, respectively.

The evaluation shows that the maximum rod internal pressures are $\{ \quad \}^{TS}$ and $\{ \quad \}^{TS}$ for the UO_2 fuel rod and $Gd_2O_3-UO_2$ burnable absorber fuel rod, respectively. ~~Therefore, no clad lift-off criterion is satisfied since the calculated gas pressures are less than critical pressure limit.~~

DNB propagation evaluations for transients and DNB accidents are performed using the NRC approved methodology with INTEG code, which is a standalone computer code to predict fuel rod

Therefore, no clad lift-off (NCLO) criterion is satisfied since the calculated gas pressures are less than the system pressure. FATES3B code calculates the critical pressure limit to prevent clad lift-off only when the rod internal pressure exceeds the system pressure.

analysis methodology for any given plant. These inputs include time, heat flux, quality, mass flow, system pressure, rod internal pressure, and fuel rod initial geometry. To evaluate the potential for DNB propagation, the limiting DNB transients and internal pressure of $\{ \quad \}^{TS}$ are applied.

The results indicate that the clad strains induced by high temperature creep for limiting transients are less than $\{ \quad \}^{TS}$. This amount of strain does not induce DNB propagation to adjacent fuel rods.

Finally, hydride reorientation does not occur at internal pressure of $\{ \quad \}^{TS}$, which is well above the predicted rod internal pressure of $\{ \quad \}^{TS}$ on PLUS7 fuel (Reference 3-6).

3.2.6 Internal Hydriding**(1) Basis**

Fuel system will not be damaged due to excessive hydriding.

(2) Criteria

Primary hydriding is prevented by maintaining the level of moisture very low during the pellet manufacturing. The moisture content shall remain below the limit of 2.0 ppm (hydrogen from all sources for fuel pellets).

(3) Evaluation

RESPONSE TO REQUEST FOR ADDITIONAL INFORMATION

APR1400 Design Certification

Korea Electric Power Corporation / Korea Hydro & Nuclear Power Co., LTD

Docket No. PROJ 0782

RAI No.: 5-7954

SRP Section: 4.2 Fuel System Design

Application Section: PLUS7 Fuel Design for the APR1400
(APR1400-F-M-TR-13001-P)

Date of RAI Issued: 06/18/2015

Question No. 17

GDC 10 requires that the reactor core and associated coolant, control, and protection systems shall be designed with appropriate margin to assure that specified acceptable fuel design limits (SAFDLs) are not exceeded during any condition of normal operation, including the effects of anticipated operational occurrences (AOOs). SRP Section 4.2 (II)(3)(A)(i) provides review guidance related to the assessment of fuel system damage related to dimensional changes (including hydrogen uptake induced swelling) that should be presented and reviewed.

It is stated on Page 4-7 of APR1400-F-M-13001-P that a 13% hydrogen pickup fraction will be used for ZIRLO. This pickup fraction is lower than the staff expected based on previous experience and has caused the staff to question the basis for this hydrogen pickup fraction.

Please justify the use of a 13% hydrogen pickup fraction. Provide a figure based on Figure 4-44 with an overlay of calculated hydrogen pickup assuming 13%, 15%, and 17.5% pickup fractions. Also include the data shown in Figure 10-1 of the response to RAI 4-7542 on this figure.

Response

The differences and ratio between measured and predicted hydrogen contents using []^{TS} hydrogen pickup fraction are shown in Figure 17-1 and Figure 17-2, respectively. The average difference is []^{TS} in Figure 17-1 and the measured to predicted ratio is []^{TS} in Figure 17-2. The predicted values represent the best estimate tendency of measured hydrogen content. But under prediction tendency the measured hydrogen content, to some degree, ascends as oxide thickness increases. Therefore, a hydrogen pickup fraction of []^{TS} is newly suggested as shown in Figure 17-3 and Figure 17-4.

The hydrogen contents calculated by assuming []^{TS} were provided in Figure 17-5, Figure 17-6, and Figure 17-7. These Figures include the data shown in Figure 10-1 of the response to RAI 4-7542 and Figure 4-44 in Topical Report.

As suggested with the hydrogen pickup fraction of []^{TS}, the relevant oxide thickness and hydrogen content in Topical Report APR1400-F-M-13001-P were recalculated as follows.

The oxide thickness in Topical Report APR1400-F-M-13001-P was calculated using the imaginary power histories, which could conservatively cover all the power histories to be postulated. Because the imaginary power histories include unrealistic power histories, the oxide thickness and hydrogen pickup were very conservatively calculated.

Therefore, to remove the excessive conservatism, the oxide thickness and hydrogen content were re-evaluated with actual power histories based on nuclear physics data. It is noted that the []^{TS} hydrogen pickup fraction was used in the re-evaluation. As a result, the maximum oxide thickness of []^{TS} microns and a maximum hydrogen content of []^{TS} ppm were calculated. The results will be reflected into APR1400-F-M-13001-P as shown in the attachment.



Figure 17-1 Measured Hydrogen Contents Minus Hydrogen Contents Predicted by []^{TS}
Hydrogen Pickup Fraction vs. Predicted Oxide Thickness

TS

Figure 17-2 Measured to Predicted Hydrogen Contents Using []^{TS} Hydrogen Pickup Fraction vs. Predicted Oxide Thickness

TS

Figure 17-3 Measured Hydrogen Contents Minus Hydrogen Contents Predicted by []^{TS} Hydrogen Pickup Fraction vs. Predicted Oxide Thickness



Figure 17-4 Measured to Predicted Hydrogen Contents Using $[]^{TS}$ Hydrogen Pickup Fraction vs. Predicted Oxide Thickness

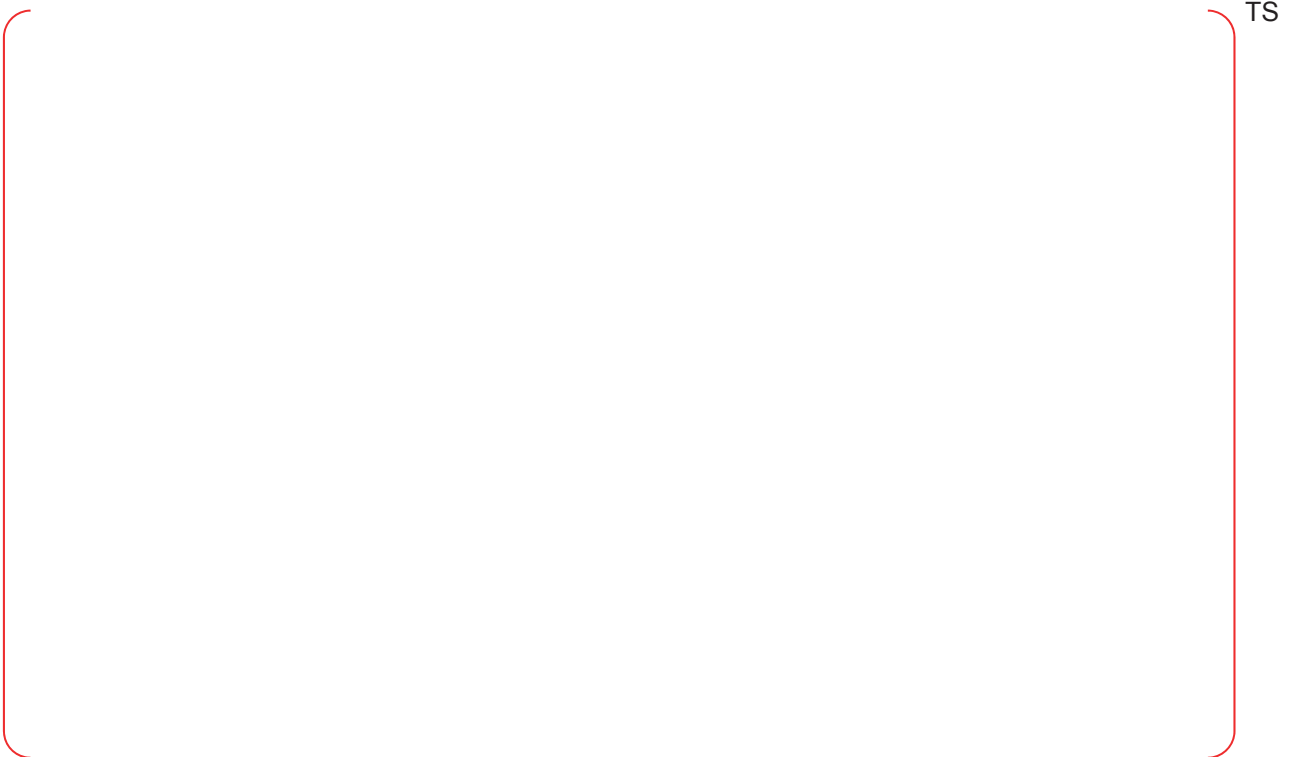


Figure 17-5 Comparison of Measured and Predicted Hydrogen Contents with $[]^{TS}$ Pickup Fraction vs. Predicted Oxide Thickness



Figure 17-6 Comparison of Measured and Predicted Hydrogen Contents with []^{TS} Pickup Fraction vs. Predicted Oxide Thickness



Figure 17-7 Comparison of Measured and Predicted Hydrogen Contents with []^{TS} Pickup Fraction vs. Predicted Oxide Thickness

Impact on DCD

There is no impact on the DCD.

Impact on PRA

There is no impact on the PRA.

Impact on Technical Specifications

There is no impact on the Technical Specifications.

Impact on Technical/Topical/Environmental Report

PLUS7 fuel design topical report (APR1400-F-M-TR-13001-NP) will be revised as indicated on the attached markups.

Non Proprietary

PLUS7 FUEL DESIGN for the APR1400

APR1400-F-M-TR-13001-NP Rev.0

3.2.4 Cladding Oxidation and Hydriding**(1) Basis**

Fuel system will not be damaged due to excessive oxidation under normal operation including AOOs.

(2) Criteria

The best estimate cladding oxide thickness shall be less than $\{ \quad \}^{TS}$

The clad hydrogen pickup is limited to $\{ \quad \}^{TS}$ at EOL to preclude loss of ductility due to hydrogen embrittlement by formation of zirconium hydride platelets.

(3) Evaluation

The cladding oxide thickness and hydrogen content of the PLUS7 fuel rod are evaluated by the same methodology and model as are used for Westinghouse PWR fuel rod designs. The best estimate oxide thickness and hydrogen content at the end of irradiation are calculated with NRC approved PAD code [3-11] during normal operation. Since cladding oxide thickness and hydrogen content do not increase during AOOs due to short time, it is not necessary to consider the AOOs for oxide thickness and hydrogen content.

The following parameters were used for evaluation.

- a) Nominal design inlet temperature, system pressure, and core mass velocity based on Thermal Design Flow Rate
- b) A crud thickness of $\{ \quad \}^{TS}$
- c) A ZrO_2 thermal conductivity of $\{ \quad \}^{TS}$

The maximum cladding thickness and hydrogen content up to rod average burnup of 60,000 MWD/MTU for APR1400 are ~~85.0~~ μm and ~~596.0~~ ppm, respectively. The criteria of cladding oxide thickness and hydrogen content are satisfied.

69.4

554.3

3.2.5 Fuel Rod Internal Pressure**(1) Basis**

Fuel system will not be damaged due to excessive rod internal pressure under normal operation.

(2) Criteria

The fuel rod internal hot gas pressure shall not the critical maximum pressure determined to cause an outward clad creep rate that is in excess of the fuel radial growth rate anywhere locally along the entire active fuel length of the fuel rod.

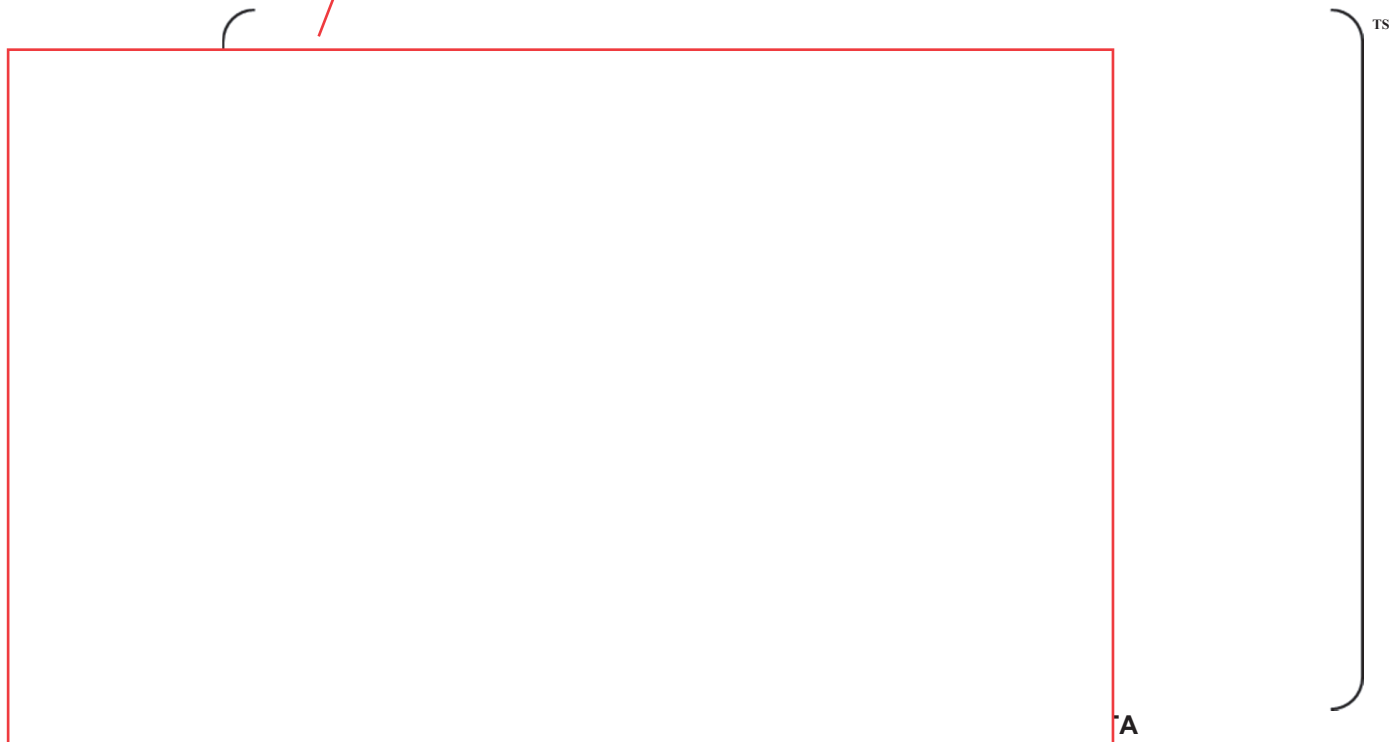
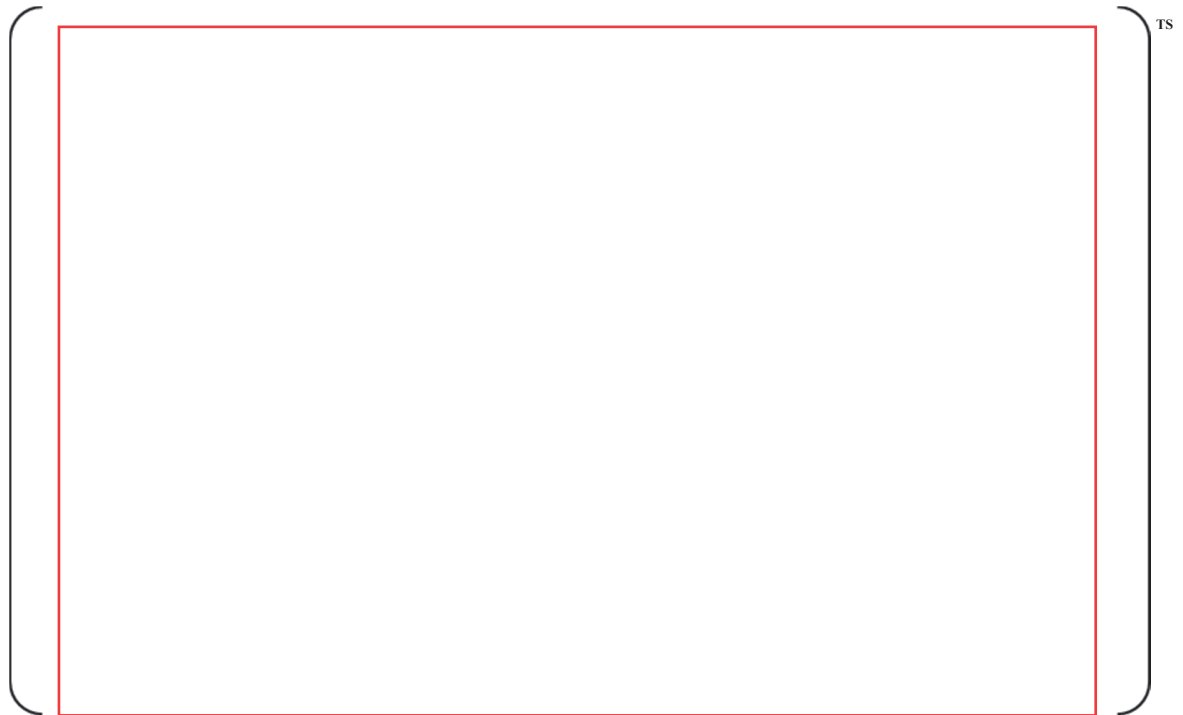
Reorientation of the hydrides in the radial direction in the cladding shall not occur

The radiological dose consequences of DNB failures shall remain within the specified limits.

Non Proprietary

PLUS7 FUEL DESIGN for the APR1400

APR1400-F-M-TR-13001-NP Rev.0



Non Proprietary

PLUS7 FUEL DESIGN for the APR1400

APR1400-F-M-TR-13001-NP Rev.0

Figure 4-44 shows the measured hydrogen contents in cladding as a function of oxide thickness. Figure 4-44 includes C03 fuel rod data and ZIRLO data irradiated in commercial reactors of Yonggwang unit 4, V.C. Summer, []^{TS}. The hydrogen contents of LTA fuel are within the ZIRLO cladding database.

The hydrogen content absorbed in cladding depends on the hydrogen pickup fraction and oxide layer thickness. The hydrogen pickup fraction is one of the material properties, which is []^{TS} for ZIRLO based on best estimate. This value is not dependent on the fuel types as well as the plant operating conditions. Therefore, the hydrogen content absorbed in ZIRLO cladding is based on oxide layer thickness generated by oxidation reaction.

Using the oxide thicknesses in Figure 4-9, the hydrogen contents averaged over the entire wall thickness is calculated using a hydrogen evolution model. The results are shown in Figure 4-45. For discharge burnup up to 60,000 MWD/MTU, the circumferential average hydrogen concentrations are less than []^{TS} for PLUS7 fuel in APR1400.

A photomicrograph of the etched C03 fuel rod cladding is shown in Figure 4-46. Figure 4-46 shows that the concentration of hydrides increases with increasing distance from the cladding inner surface due to the radial thermal gradient in the cladding. The cladding hydrogen contents exist mostly in the form of circumferential hydrides distributed in the outer region of the clad wall as shown in Figure 4-46.

4.3.6 Fission Gas Release

(1) Measurement Method

During the hot cell examination, A14 and C03 fuel rods of PLUS7 LTA irradiated in UCN-3 cycle 5 through cycle 7 were punctured and gases from these rods were collected and analyzed to determine the fractional fission gas release.

(2) Measurement Results and Evaluation

Table 4-8 shows the predicted values and measured data obtained in hot cell examination. As shown in Table 4-8, the fission gas released are []^{TS} for A14 and C03 fuel rods, respectively. In addition, the rod internal pressures were measured for A14 and C03 fuel rods. The measured rod internal pressures of []^{TS} are well within the database of PWR fuel rod internal pressure at the condition of room temperature.

4.4 Testing, Inspection, and Surveillance Plans

Testing and inspection of new fuel and post-irradiation surveillance are described in DCD tier 2, Section 4.2.

RESPONSE TO REQUEST FOR ADDITIONAL INFORMATION

APR1400 Design Certification

Korea Electric Power Corporation / Korea Hydro & Nuclear Power Co., LTD

Docket No. PROJ 0782

RAI No.: 5-7954
SRP Section: 4.2 Fuel System Design
Application Section: PLUS7 Fuel Design for the APR1400
(APR1400-F-M-TR-13001-P)
Date of RAI Issued: 06/18/2015

Question No. 18

GDC 10 requires that the reactor core and associated coolant, control, and protection systems shall be designed with appropriate margin to assure that specified acceptable fuel design limits (SAFDLs) are not exceeded during any condition of normal operation, including the effects of anticipated operational occurrences (AOOs).

To perform accurate confirmatory calculations to evaluate the application's conformance with GDC 10, NRC must use the correct input information for the APR1400 design, including rod geometry, reactor conditions, power history, and axial power profile.

Please provide the following sample calculations using FATES3B. For each case, include all appropriate input information including rod geometry, reactor conditions, power history, and axial power profile:

- a. Provide sample calculations of cladding strain under AOOs for a typical AOO overpower event. Provide calculations at rod average burnup of 0 GWd/MTU, 20 GWd/MTU, 40 GWd/MTU, and 60 GWd/MTU.
- b. Provide a sample calculation of rod internal pressure for a bounding power history up to a rod average burnup of 62 GWd/MTU. Provide pressure calculations as a function of time.
- c. Provide a sample calculation of power to melt at the following rod average burnup levels; 0 GWd/MTU, 10 GWd/MTU, 20 GWd/MTU, 30 GWd/MTU, 40 GWd/MTU, 50 GWd/MTU, 60 GWd/MTU.
- d. Provide a sample calculation of fuel stored energy for a bounding power history up to a rod average burnup of 62 GWd/MTU. Provide stored energy calculations as a function of time.

Response

Design input information including rod geometry, power history, axial power profile and reactor conditions are described in Tables 18-1 - 18-5. Sample calculations of transient strain, rod internal pressure, power to melt, and stored energy are below

Table 18-1 Fuel Rod Geometry

TS

Table 18-2 Generic Power Histories and Axial Power Profile for Transient Strain

TS

| |
|--|
| |
|--|

Table 18-3 Bounding Power Histories for Rod Internal Pressure,
Power to Melt and Stored Energy

TS

A large, empty rectangular frame with rounded corners, outlined in red. It occupies the majority of the page below the caption, indicating that the table content is either redacted or not present in this version of the document.

Table 18-4 Axial Power Profile for the Calculation of Rod Internal Pressure,
Power to Melt and Stored Energy

TS

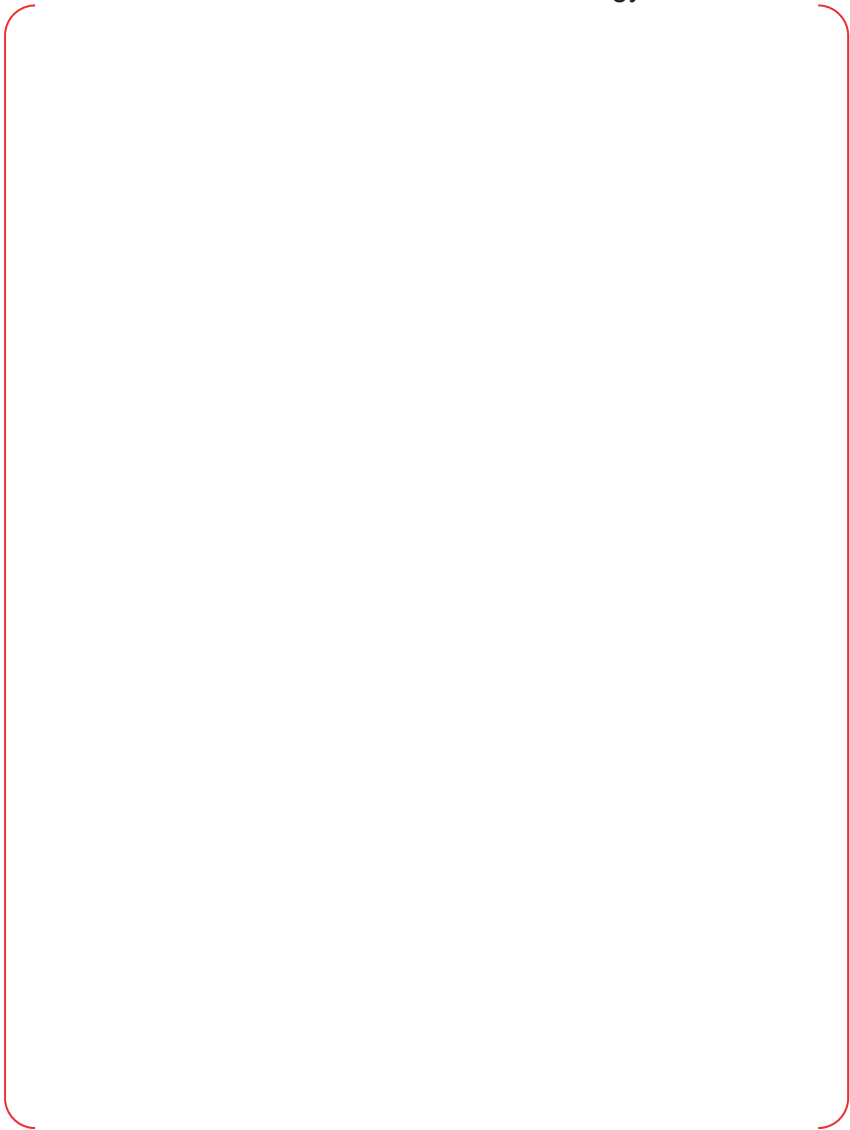


Table 18-5 Reactor Conditions

TS

Results of sample calculations for transient strain, rod internal pressure, power to melt and stored energy are as follows;

- a) Transient strain under AOO at rod average burnup of 0 GWd/MTU, 20 GWd/MTU, 40 GWd/MTU, and 60 GWd/MTU.



Re-examined total (elastic plus plastic) strain will be reflected in topical report as shown in the attached markup.

b) Rod Internal gas pressure up to fuel rod average burnup of 60 GWd/MTU TS

Rod internal pressure was calculated up to 60 GWd/MTU which is a license target burnup.

- c) Power to melt at 0 GWd/MTU, 10 GWd/MTU, 20 GWd/MTU, 30 GWd/MTU, 40 GWd/MTU, 50 GWd/MTU, 60GWd/MTU.

TS

d) Fuel stored energy for one fuel rod as a function of time

TS

Fuel stored energy was calculated up to 60 GWd/MTU which is a license target burnup.

Impact on DCD

There is no impact on the DCD.

Impact on PRA

There is no impact on the PRA.

Impact on Technical Specifications

There is no impact on the Technical Specifications.

Impact on Technical/Topical/Environmental Report

Topical Report APR1400-F-M-TR-13001-NP will be revised as indicated on the attached markups.

Non Proprietary

PLUS7 FUEL DESIGN for the APR1400

APR1400-F-M-TR-13001-NP Rev.0

normal operation involving fuel handling and storage, reactor servicing, power operation and reactor trip, heatup and cooldown, and minor fuel handling accident using the standard formulas.

The stress analyses for AOOs such as "Inadvertent Opening of an Atmospheric Dump Valve", "Uncontrolled CEA Withdrawal at Power", "Total Loss of Reactor Coolant Flow and "Loss of Condenser Vacuum" events were performed using the FATES3B code [3-1 through 3-4].

The results of the evaluation indicate that the primary tensile and compressive stresses in the cladding and end cap welds are within the allowable limits as shown in Table 3-3.

3.2.2 Cladding Strain**(1) Basis**

Fuel system will not be damaged due to excessive strain under normal operation including AOOs.

(2) Criteria

At any time during the fuel rod lifetime, the net unrecoverable circumferential tensile cladding strain shall not exceed $\{ \quad \}^{TS}$ based on the beginning-of-life (BOL) cladding dimensions. This criterion is applicable to normal operating conditions and following a single AOO.

The total (elastic plus plastic) circumferential cladding strain increment produced as a result of a single AOO shall not exceed $\{ \quad \}^{TS}$ relative to the pre-transient condition.

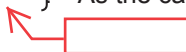
Ductility is a function of irradiation and hydride formation in the cladding wall. Because the waterside corrosion for ZIRLO is significantly lower and should result in less hydrogen uptake and less hydride formation, total stain capability of ZIRLO is projected to be in excess of $\{ \quad \}^{TS}$ at burnups of 60,000 MWD/MTU. Thus, a $\{ \quad \}^{TS}$ strain limit will continue to be applied as a strain criterion.

(3) Evaluation

The evaluation methodology for the fuel rod cladding strain is discussed in Reference 3-5, which was reviewed and approved by NRC for Westinghouse CE PWR fuel designs.

The first part of the strain limit concerns that the total plastic strain incurred as a result of cladding creep and cladding yielding during long term normal operation and the following short transient conditions. Cladding creep strain and plastic strain due to cladding yielding are driven by the stress in the cladding that results from differential pressure and interface with the fuel pellets. The method used to evaluate the strain accounts for power dependent and time dependent changes (e.g., fuel rod void volume, fission gas release and gas temperature, differential cladding, cladding creep and thermal expansion) that can produce strain in the fuel cladding. In addition, the strain analysis accounts for both long term, normal operating condition, and short term, transient condition.

For the present application, the predicted plastic strain using FATES3B code is $\{ \quad \}^{TS}$ and the total (elastic plus plastic) circumferential cladding strain increment produced as a result of a single AOO is $\{ \quad \}^{TS}$. As the calculated strains are less than $\{ \quad \}^{TS}$ the design criteria are satisfied.



RESPONSE TO REQUEST FOR ADDITIONAL INFORMATION

APR1400 Design Certification

Korea Electric Power Corporation / Korea Hydro & Nuclear Power Co., LTD

Docket No. PROJ 0782

RAI No.: 5-7954
SRP Section: 4.2 Fuel System Design
Application Section: PLUS7 Fuel Design for the APR1400
(APR1400-F-M-TR-13001-P)
Date of RAI Issued: 06/18/2015

Question No. 19

GDC 10 requires that the reactor core and associated coolant, control, and protection systems shall be designed with appropriate margin to assure that specified acceptable fuel design limits (SAFDLs) are not exceeded during any condition of normal operation, including the effects of anticipated operational occurrences (AOOs). SRP Section 4.2 (II)(3)(C)(i) provides guidance in regards to GDC 10 and the phenomenological models important to fuel temperature (stored energy) calculations. This fuel temperature calculation is important to the pellet swelling and clad creep models.

Table 4-8 on Page 4-12 of APR1400-F-M-TR-13001-P shows predicted and measured results from the puncture analysis. The staff notes that FGR is overpredicted but rod internal pressure is underpredicted. This has caused to the staff to question the validity of the void volume calculations and the potential subsequent impacts on the pellet swelling and clad creep models. Provide a discussion to explain why FGR is overpredicted but rod internal pressure is underpredicted, and update the topical report if applicable. If the pellet swelling or clad creep models are non-conservative, also address all other impacted analyses and update the topical report, if applicable.

Response

Generally, rod internal pressure is dependent on fission gas release as well as void volume. With regards to fission gas release, it can be easily inferred that the more fission gas release, the more rod internal pressure. However, Table 4-8 on Page 4-12 of APR-1400-F-M-TR-13001-P shows two comparison results in which fission gas release is overpredicted but rod internal pressure is underpredicted. The main reason for this unexpected behavior is attributed to the fact that FATES3B overpredicts the void volumes as shown in Table 4-8.

The measured values for void volume are compared with the predicted ones, which are shown in Figure 2-7 and Figure 2-8 of TCD technical report (APR1400-F-M-TR-13002-P). As can be

seen in those figures, the measured void volumes for some rods are greater than the volumes of the FATES3B predictions but for others the volumes are smaller than the volumes of the FATES3B predictions. Two data in Table 4-8 didn't result from the non-conservatism of the pellet swelling or ZIRLO clad creep models. They happened to fall into a case where the predicted void volume is greater than the measured one. Those models had already been verified and approved and their descriptions can be found in References 19-1 and 19-2. As explained in Section 2.1.3 of APR1400-F-M-TR-13002-P, in overall, over conservatism to predict void volume with an average value of []^{TS} is applied to the FATES3B code.

References

[19-1] []^{TS}
 [19-2] []^{TS}

Impact on DCD

There is no impact on the DCD.

Impact on PRA

There is no impact on the PRA.

Impact on Technical Specifications

There is no impact on the Technical Specifications.

Impact on Technical/Topical/Environmental Report

There is no impact on any Technical, Topical, or Environmental Report.

RESPONSE TO REQUEST FOR ADDITIONAL INFORMATION

APR1400 Design Certification

Korea Electric Power Corporation / Korea Hydro & Nuclear Power Co., LTD

Docket No. PROJ 0782

RAI No.: 5-7954

SRP Section: 4.2 Fuel System Design

Application Section: PLUS7 Fuel Design for the APR1400
(APR1400-F-M-TR-13001-P)

Date of RAI Issued: 06/18/2015

Question No. 20

GDC 10 requires that the reactor core and associated coolant, control, and protection systems shall be designed with appropriate margin to assure that specified acceptable fuel design limits (SAFDLs) are not exceeded during any condition of normal operation, including the effects of anticipated operational occurrences (AOOs). SRP Section 4.2 (II)(1)(B)(iv) provides guidance in regards to GDC 10 by stating that overheating of fuel pellets should be avoided by preventing centerline melting. This analysis should be performed for the maximum linear heat generation rate anywhere in the core, including all hot spots and should account for the effects of burnup and composition on the melting point.

Table 3-10 on Page 3-24 of APR1400-F-M-TR-13001-P lists various core inlet and outlet temperatures for plants. The staff notes that APR1400 is listed as having a higher core average linear heat rate while having essentially the same ΔT and core average mass flow as the other examples. This has caused the staff to question the accuracy of the core average linear heat rate calculations presented in Table 3-10.

Please describe the core average linear heat rate calculations in sufficient detail to explain how APR1400 calculates a higher linear heat rate and make the supporting calculations available for staff audit or submit them on the docket.

Response

To obtain the core average linear heat rate, the core thermal power []^{TS} of the APR1400 should be divided by number of fuel rods and flow path length of the active core. The number of fuel rods in a core is []^{TS}. And the flow path length of the active core is []^{TS}. Therefore, the core average linear heat rate can be acquired by following the calculation shown as equation 20-1. The parameters are also presented in the Table 4.1-1, 4.1-2 and 4.4-8 in Chapter 4 Reactor in DCD.

[]^{TS}

The core thermal power of the OPR1000 reactor type such as Yonggwang unit 4, Ulchin unit 3, and Yonggwang unit 5 is []^{TS}. And the core thermal power of Westinghouse type of Yonggwang unit 2 is []^{TS}. Therefore, the difference in thermal power is the main reason for the different linear heat rate presented in Table 3-10.

Impact on DCD

There is no impact on the DCD.

Impact on PRA

There is no impact on the PRA.

Impact on Technical Specifications

There is no impact on the Technical Specifications.

Impact on Technical/Topical/Environmental Report

There is no impact on any Technical, Topical, or Environmental Report.

RESPONSE TO REQUEST FOR ADDITIONAL INFORMATION

APR1400 Design Certification

Korea Electric Power Corporation / Korea Hydro & Nuclear Power Co., LTD

Docket No. PROJ 0782

RAI No.: 5-7954

SRP Section: 4.2 Fuel System Design

Application Section: PLUS7 Fuel Design for the APR1400
(APR1400-F-M-TR-13001-P)

Date of RAI Issued: 06/18/2015

Question No. 21

GDC 10 requires that the reactor core and associated coolant, control, and protection systems shall be designed with appropriate margin to assure that specified acceptable fuel design limits (SAFDLs) are not exceeded during any condition of normal operation, including the effects of anticipated operational occurrences (AOOs). SRP Section 4.2 provides review guidance related to the development of acceptance criteria based on test data, in part or in whole, for various phenomena (e.g. fretting wear, oxidation/hydriding/crud buildup, dimensional changes, PCI, cladding embrittlement, etc.).

Appendix A of APR1400-F-M-TR-13001-P provides a summary of PLUS7 fuel assembly tests. During the review, the staff noted that the test conditions were listed but not compared with the APR1400 operational ranges for all of the tests. This has made it difficult for the staff to complete the review of the adequacy of the testing.

Provide a table that compares the test condition ranges to the APR1400 condition ranges for the liftoff tests, assembly vibration tests, and buckling strength discussed in Appendix A so it can be determined that the test conditions bound the expected reactor conditions. Update the topical report as necessary.

Response

As described in Appendix A of APR1400-F-M-TR13001-P Rev.0, the liftoff test and assembly vibration test were conducted in the Fuel Assembly Compatibility Test System (FACTS), and the buckling strength test was conducted by using a dynamic grid crush test apparatus. These facilities are located at Westinghouse in Columbia, SC. The test conditions were compared with the APR1400 operational ranges as below:

1. The liftoff tests were performed by increasing the flow rate from []^{TS} and from []^{TS} by increments of []

[]^{TS}. When the flow rate reached []^{TS}, the flow increased by increments of []^{TS} for a better estimate of the flow rate that could liftoff the fuel assembly. The PLUS7 fuel assembly was lifted off at the flow rates of []^{TS}, respectively.

Compared with the in-reactor mechanical design flow of []^{TS} for the PLUS7 fuel assembly in the APR1400, the corresponding mechanical design flow in FACTS liftoff test was []^{TS}, and it was due to the difference in the fuel assembly channel size between the APR1400 and the FACTS loop. The conditions are compared in Table 21-1.

2. During fuel assembly vibration tests, the loop flow rate was increased from []^{TS} to the maximum achievable loop flow rate of []^{TS}. The corresponding mechanical design flow for the assembly vibration test in FACTS is []^{TS}. As shown in Table 21-2, the flow range in FACTS covers the mechanical design flow in APR1400.
3. The grid buckling strength test was conducted by using a dynamic crush grid test apparatus at []^{TS} which is conservative considering the average temperature of APR1400 reactor is []^{TS}. In addition, the pendulum weight of []^{TS} used in the grid buckling strength test was selected for the PLUS7 fuel assembly span weight of []^{TS}. The conditions are compared in Table 21-3.

Note:

TS

Table 21-1 Comparison of the liftoff test condition ranges to the APR1400 operating condition ranges



TS

Table 21-2 Comparison of the assembly vibration test condition ranges to the APR1400 operating condition ranges



TS

Table 21-3 Comparison of the buckling strength test condition ranges to the APR1400 operating condition ranges



TS

Impact on DCD

There is no impact on the DCD.

Impact on PRA

There is no impact on the PRA.

Impact on Technical Specifications

There is no impact on the Technical Specifications.

Impact on Technical/Topical/Environmental Report

PLUS7 fuel design topical report (APR1400-F-M-TR-13001-NP) will be revised as indicated on the attached markups.

Non Proprietary

PLUS7 FUEL DESIGN for the APR1400

APR1400-F-M-TR-13001-NP Rev.0

A.2.0 SUMMARY OF TESTS**A.2.1 Fuel Assembly Vibration Test (FACTS)****1.0 Introduction and Objectives**

The objective of this test is to confirm that the PLUS7 design is not susceptible to high resonance flow-induced assembly vibration over a range of plant operating flow rates. This is assessed by reviewing the vibration spectra from displacement transducers (see Figure A.2.1-1) and the instrumented fuel rod accelerometers for the presence of abnormal, flow-dependent, resonant vibration peaks. The absence of such peaks will be sufficient to determine the acceptability of the fuel assembly design.

2.0 Test Conditions

The test flow conditions were systematically varied in an effort to excite the vibration modes of the fuel assembly. Such a variation consisted of setting the loop at the required temperature of { }^{TS} and sweeping the loop flow rate from { }^{TS} to the maximum achievable flow rate. The flow rate was then returned to { }^{TS} at a same rate. The maximum achievable flow rate for this test was { }^{TS}. The PLUS7 fuel assembly will be placed at { }^{TS}. The equivalent mechanical design flow in the FACTS test is { }^{TS}. Although the FACTS loop could not reach the elevated test flow rate { }^{TS} the maximum achievable flow rate does bound all possible operating flow rates, representing over 117% of the best estimate flow { }^{TS} which is the flow rate at which PLUS7 fuel assembly will be placed. The maximum achievable flow rate is more than adequate to confirm that the PLUS7 design does not exhibit flow-induced resonant fuel assembly vibration.

3.0 Test Results

The test conditions and APR 1400 operating conditions are compared in Table A.2.1-1.

The flow sweep test was performed at { }^{TS}. In this test, the loop flow rate was increased in a constant manner from { }^{TS} to the maximum achievable loop flow rate of { }^{TS} in six minutes. Because the instrumented rod accelerometers were mounted at mid-grid elevations with as-built cell conditions, the accelerometer outputs represent the fuel assembly vibration.

Insert Table A.2.1-1 in Appendix 21-1

Figure A.2.1-2 shows that the assembly did not experience the high resonance flow-induced fuel assembly vibration. There was no indication of abnormal flow-induced vibration response throughout the test flow range.

4.0 Summary and Conclusion

A FACTS loop test was conducted to verify that the PLUS7 design did not exhibit high resonance flow-induced fuel assembly vibration. Displacement transducers and instrumented fuel rods at grid locations measured the fuel assembly vibration. There was no indication of abnormal flow-induced vibration response throughout the test flow range.

Non Proprietary

PLUS7 FUEL DESIGN for the APR1400

APR1400-F-M-TR-13001-NP Rev.0

A.2.3 Mid Grid Crush Test**1.0 Introduction and Objectives**

The dynamic crush strength of the mid grid is required to obtain the structural characteristics to show that both seismic and LOCA loads are met.

The specific test objectives for the dynamic crush test of the PLUS7 ZIRLO mid grid design at elevated temperatures were as follows:

- To obtain the impact force as a function of impact velocity
- To determine the grid ultimate load capability
- To characterize the grid failure mode
- To obtain the data to determine the grid dynamic stiffness

2.0 Test Conditions

The dynamic crush test was performed at operating temperature and the pendulum ~~inertial mass~~ ^{weight} was calculated as the weight of one span of PLUS7 fuel assembly.

The pendulum angle was increased by 1° from 7° until grid crushed.

Delete

- ~~Elevated temperature: 600°F ± 20°F~~
- ~~Pendulum inertial mass: { }^{TS}~~
- ~~Pendulum initial angle: 7°~~

The test conditions and APR 1400 operating conditions are compared in Table A.2.3-1.

Insert Table A.2.3-1 in Appendix 21-1

3.0 Test Results

Twelve grid crush tests were sequentially performed. The PLUS7 ZIRLO mid grid crush test results are summarized as follows: (Table.A.2.3-2)

A.2.3-2

Table A.2.3-1 PLUS7 ZIRLO Mid grid Crush Test Results

| | |
|--|--|
| | |
|--|--|

TS

4.0 Summary and Conclusion

The crush strength values for the PLUS7 ZIRLO mid grid tested with rod-in-cell are shown in Figure A.2.3-3.

A summary of the dynamic crush test results is as follows:

- Dynamic Crush Strength:

Non Proprietary

PLUS7 FUEL DESIGN for the APR1400

APR1400-F-M-TR-13001-NP Rev.0

A.2.9 FACTS Lift-off Test for the PLUS7 Fuel Assembly**1.0 Introduction and Objectives**

The objective of the lift-off tests of the PLUS7 fuel assembly is to determine the flow rates at which the fuel assembly lifts off under specified temperatures and holddown spring compressions. The test was performed with the Fuel Assembly Compatibility Test System (FACTS) as shown in Figure A.2.9-1 for the PLUS7 fuel assembly design with 40/20 ()^{TS} Debris Filter Bottom Nozzle (DFBN).

2.0 Test Conditions

The test conditions and APR 1400 operating conditions are compared in Table A.2.9-1.

To ensure that the fuel assembly would lift-off during the tests, the holddown springs were compressed by ()^{TS}. The lift-off tests were performed by increasing the flow rate from ()^{TS} with increments of ()^{TS}. When the flow rate reached ()^{TS} the flow increased with an increment of ()^{TS} for a better estimate of the flow rate that could lift-off the fuel assembly.

Two uni-axial accelerometers were mounted on the base of the pressure vessel to monitor the output impact signal. The output from the accelerometers was amplified and monitored through an oscilloscope and a visicorder.

Insert Table A.2.9-1 in Appendix 21-1

Table A.2.9-2

Table A.2.9-1 Fuel Assembly and Specifications

| Component Descriptions | |
|---|---|
| Top Grid Material | Inconel 718 |
| Protective Grid Material | Inconel 718 |
| Bottom Grid Material | Inconel 718 |
| Protective Grid Inner Strap Heights | () ^{TS} |
| Bottom Grid Inner Strap Heights | () ^{TS} |
| Top Grid Inner Strap Heights | () ^{TS} |
| Mid Grid Material | ZIRLO |
| Number of Mid grids | 9 |
| Mid Grid Inner Strap Heights | () ^{TS} |
| Number of Rods | 236 |
| Rod OD | () ^{TS} |
| Test Rod Length | () ^{TS} |
| Number of Guide Thimble | 4 |
| Diameter of Guide Thimble Tubes | () ^{TS} |
| Number of Instrument Tube | 1 |
| Diameter of Instrument Tube | () ^{TS} |
| Dashpot Elevation (Top of Thimble Tube Smaller OD Elevation) | () ^{TS} |
| Rod-to-Bottom Nozzle Gap | () ^{TS} |
| Thimble Tube Plugging Device | None. However the flow is blocked by the standoff tubes |
| Test Condition | |
| () ^{TS} | |

Non-Proprietary

PLUS7 FUEL DESIGN for the APR1400

APR1400-F-M-TR-12001-P Rev.0

Appendix 21-1

Table A.2.1-1 Comparison of the assembly vibration test condition range to the APR1400 operating condition ranges



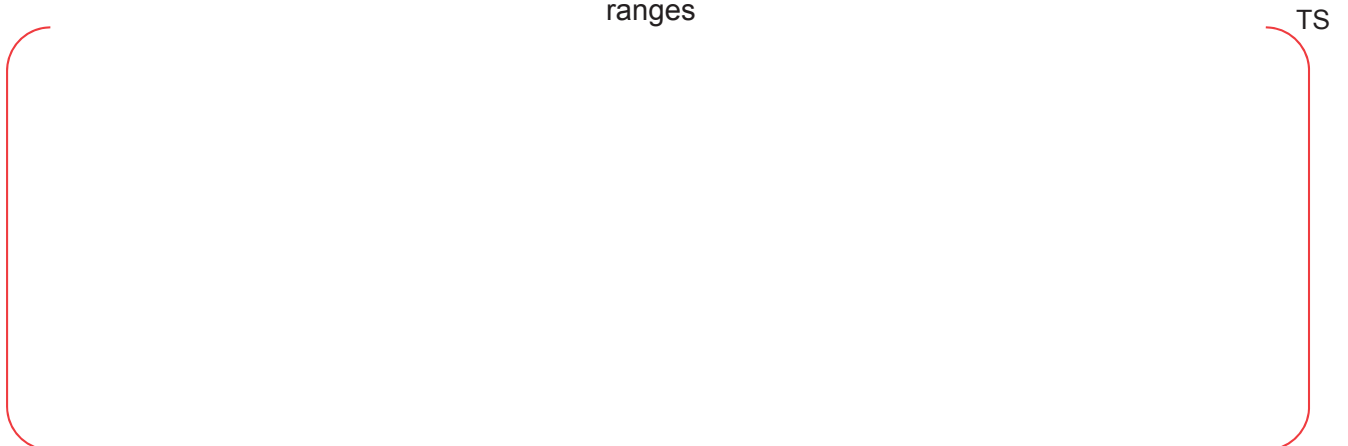
TS

Table A.2.3-1 Comparison of the buckling strength test condition range to the APR1400 operating condition ranges



TS

Table A.2.9-1 Comparison of the liftoff test condition range to the APR1400 operating condition ranges



TS

RESPONSE TO REQUEST FOR ADDITIONAL INFORMATION

APR1400 Design Certification

Korea Electric Power Corporation / Korea Hydro & Nuclear Power Co., LTD

Docket No. PROJ 0782

RAI No.: 5-7954
SRP Section: 4.2 Fuel System Design
Application Section: PLUS7 Fuel Design for the APR1400
(APR1400-F-M-TR-13001-P)
Date of RAI Issued: 06/18/2015

Question No. 22

GDC 10 requires that the reactor core and associated coolant, control, and protection systems shall be designed with appropriate margin to assure that specified acceptable fuel design limits (SAFDLs) are not exceeded during any condition of normal operation, including the effects of anticipated operational occurrences (AOOs). SRP Section 4.2 (II)(3)(A)(i) provides review guidance related to the assessment of fuel system damage by stating that stress limits must be presented and reviewed.

Section 2.2.2 of APR1400-F-M-TR-13001-P provides the structural integrity design basis, criteria, and evaluation. Within this section, it is stated that the evaluation of fuel assembly for seismic and LOCA loads will be addressed in the APR1400 DCD Section 4.2. The staff notes that APR1400 DCD Section 4.2 in turn points back to APR1400-F-M-TR-13001-P. Therefore, the staff is unable to ascertain if the proposed stress limits are violated by the analysis.

Provide the stress analysis results for the PLUS7 fuel design, and update the topical report as necessary.

Response

As described in Section 2.2.2 of APR1400-F-M-TR-13001-P, the evaluation of the fuel assembly for seismic and LOCA loads is addressed in Section 4.2 of APR1400 DCD tier 2. In addition, Section 4.2.3.5.3 of the DCD refers to technical report APR1400-Z-M-NR-14010-P (proprietary) and NP (non-proprietary) "Structural Analysis of Fuel Assemblies for Seismic and Loss of Coolant Accident Loading for the APR1400" in order to show the analysis results in detail. This technical report contains information on the test, model, analysis methodology, criteria, and stress analysis results for the fuel assembly during postulated accidents. Table 6-1 of Reference #35 (APR1400-Z-M-NR-14010) in DCD Section 4.2 provides the stress analysis results of the fuel assembly for seismic and LOCA loads.

Impact on DCD

There is no impact on the DCD.

Impact on PRA

There is no impact on the PRA.

Impact on Technical Specifications

There is no impact on the Technical Specifications.

Impact on Technical/Topical/Environmental Report

There is no impact on any Technical, Topical, or Environmental Report.

RESPONSE TO REQUEST FOR ADDITIONAL INFORMATION

APR1400 Design Certification

Korea Electric Power Corporation / Korea Hydro & Nuclear Power Co., LTD

Docket No. PROJ 0782

RAI No.: 5-7954
SRP Section: 4.2 Fuel System Design
Application Section: PLUS7 Fuel Design for the APR1400
(APR1400-F-M-TR-13001-P)
Date of RAI Issued: 06/18/2015

Question No. 23

GDC 10 requires that the reactor core and associated coolant, control, and protection systems shall be designed with appropriate margin to assure that specified acceptable fuel design limits (SAFDLs) are not exceeded during any condition of normal operation, including the effects of anticipated operational occurrences (AOOs). SRP Section 4.2 (II)(1)(B)(viii) and Appendix A provides review guidance related to mechanical fracturing based on seismic and LOCA applied loads. It is also stated specifically that control rod insertability must be maintained.

This topic is addressed in Section 2.2.2 of APR1400-F-M-TR-13001-P and also in the response to Question 2 of RAI 4-7542 (ML14177A220). The staff notes that for postulated accidents, the limits proposed in the topical report are based on ASME Section III Service Level D requirements. This service level could result in "faulted" conditions for the guide tubes. A faulted guide tube could affect the ability to insert RCCAs, and therefore challenge GDC 27.

Provide a discussion that covers the proposed stress-strain limits and what level of damage could occur to the components based on those limits. If damage could occur to the guide tubes, include a description of the tests and results that demonstrate control rod insertability. Update the topical report, as necessary, to capture these points.

Response

For control rod insertability, standard review plan (SRP) Section 4.2 Appendix A (IV-1) describes as follows: "Control rod insertability is a third criterion that must be satisfied. Loads from the worst-case LOCA that requires control rod insertion must be combined with the SSE loads, and control rod insertability must be demonstrated for that combined load. For a PWR, if combined loads on the grids remain below P(crit), as defined above, then significant deformation of the fuel assembly would not occur and lateral displacement of the guide tubes would not interfere with control rod insertion. If combined loads on the grids exceed P(crit), then additional analysis is needed to show that the deformation is not severe enough to prevent control rod insertion."

Based on the guideline above, control rod insertability for PLUS7 fuel is satisfied because buckling in the PLUS7 fuel assembly grid does not occur as a result of seismic and LOCA loads [Reference 23-1].

For the evaluation of guide tube stresses induced by the lateral displacements and the axial loads on the fuel assembly during seismic and LOCA events, Appendix F of ASME Section III is used as the general stress criteria: 1) the general primary membrane stress intensity P_m shall not exceed the lesser of $2.4S_m$ and $0.7S_u$, 2) the primary membrane plus primary bending stress intensity P_m+P_b shall not exceed 150% of the limit for P_m . [

]^{TS}.

In addition, the guide tube behavior related to the control rod insertability was evaluated through the PLUS7 fuel assembly lateral stiffness test [Appendix A.3 in Reference 23-1 and Section 3 in Reference 23-2]. [

]^{TS}. The maximum lateral displacement of guide tube as a result of seismic and LOCA analyses is []^{TS} based on the seismic and LOCA analysis described above. The location and numbering of strain gages attached to the guide tubes are presented in Figure 23-1.

In summary, the control rod insertability during seismic and LOCA events is maintained because the maximum guide tube stress based on the PLUS7 seismic/LOCA analysis and PLUS7 lateral stiffness test is below the yield strength ([]^{TS} ksi at temperature) as described above. The guide tube design stress limits during seismic and LOCA events could be adjusted if necessary.

References

[23-1] [

]^{TS}

[23-2] [

]^{TS}.

¹⁾ : the project name during PLUS7 fuel development

TS

Figure 23-1 PLUS7 Mechanical Test Fuel Assembly Strain Gage Location and Numbering
[Figure 3.2.3 in Reference 23-2]

Impact on DCD

There is no impact on the DCD.

Impact on PRA

There is no impact on the PRA.

Impact on Technical Specifications

There is no impact on the Technical Specifications.

Impact on Technical/Topical/Environmental Report

There is no impact on any Technical, Topical, or Environmental Report.

**KHNP****KOREA HYDRO & NUCLEAR POWER CO., LTD**

70-1312-gil, Yuseong-daero, Yuseong-gu, Daejeon, 305-343, KOREA

Tel: +82-42-870-5400 / Fax: +82-42-870-5449

<http://www.khnp.co.kr>

July 29, 2016
Document Control Desk
U.S. Nuclear Regulatory Commission
Washington, DC 20555-0001

Attention: Mr. Jeff Ciocco
Division of New Reactor Licensing

Docket No. 52-046
MKD/NW-16-0826L

Subject: Response to RAI 5-7954 for Question TR PLUS7 Fuel Design for the APR1400-16

Reference: NRC Request for Additional Information 5-7954, dated June 18, 2015

KHNP is hereby submitting the response to RAI 5-7954, dated June 18, 2015. The response addresses Question TR PLUS7 Fuel Design for the APR1400-16.

Enclosure 1 contains a copy of the associated affidavit. Enclosure 2 provides the response to RAI 5-7954 for Question TR PLUS7 Fuel Design for the APR1400-16 (Proprietary). Enclosure 3 provides the response to RAI 5-7954 for Question TR PLUS7 Fuel Design for the APR1400-16 (Non-Proprietary).

If additional information or clarification is required, please contact Daegeun Ahn, Director of KHNP Washington DC Center at ahn.daegeun@khnp.co.kr or 703-388-0592.

Sincerely,

Jae-yong Lee
Project Manager
Advanced Reactors Development Laboratory
Korea Hydro and Nuclear Power Co., Ltd

Enclosures:

1. Affidavit KAW-16-0826
2. Response to RAI 5-7954 for Question TR PLUS7 Fuel Design for the APR1400-16 (Proprietary)
3. Response to RAI 5-7954 for Question TR PLUS7 Fuel Design for the APR1400-16 (Non-Proprietary)

Enclosure 1

Affidavit KAW-16-0826

I, Yun-ho Kim, state the following:

1. I am the General Manager of Korea Hydro & Nuclear Power Co., Ltd. (KHNP), and as such I am authorized to request withholding the information transmitted with this letter from public disclosure and to execute this affidavit.
2. I am familiar with the criteria applied by KHNP to determine whether certain information is proprietary, and with the policies established by KHNP to ensure the proper application of these criteria.
3. The information, Response to RAI 5-7954 for Question TR PLUS7 Fuel Design for the APR1400-16 (Proprietary), transmitted with this letter has been classified by KHNP as proprietary in accordance with the policies for the control and protection of proprietary and confidential information. The information regarded as proprietary is identified and marked consistent with the requirements of 10 CFR 2.390, § (b)(1)(i). Accordingly, the proprietary information is enclosed within brackets and the right-hand bracket carries a notation of “TS” to indicate that the trade secret nature of the information claimed to be proprietary is the basis for proposing that the information so identified be withheld from public disclosure.
4. Pursuant to the considerations set forth in 10 CFR Section 2.390(a), KHNP considers the information classified as proprietary to be “trade secret” information since it is design, analysis, or test information that would be difficult for a competitor to reproduce and hence provides an economic and competitive advantage to KHNP.
5. The need for designating the information as proprietary has been raised within KHNP. The information is being treated proprietary and confidential and has not been disclosed by KHNP to the public.
6. Nondisclosure of the proprietary information transmitted with this letter is vital to the competitiveness held by KHNP and, hence, disclosure of the proprietary information transmitted in with this letter would have negative commercial impacts on the competitive position of KHNP in the U.S. nuclear market.
7. In accordance with KHNP policy, proprietary information contained in this document may be, or may have been, made available on a limited basis to regulatory bodies, customers, potential customers, and their agents, suppliers, and licensees, and others under suitable agreements providing for nondisclosure and limited use of the information.

I declare that the foregoing statements are true and correct to the best of my knowledge, information and belief.

Executed on July 29, 2016.



Yun-ho Kim
General Manager
APR1400 Licensing Team
Central Research Institute
Korea Hydro and Nuclear Power Co., Ltd

Enclosure 3

Response to RAI 5-7954 for Question TR PLUS7 Fuel Design for the
APR1400-16

(Non-Proprietary)

July 29, 2016

RESPONSE TO REQUEST FOR ADDITIONAL INFORMATION

APR1400 Design Certification

Korea Electric Power Corporation / Korea Hydro & Nuclear Power Co., LTD

Docket No. PROJ 0782

RAI No.: 5-7954

SRP Section: 4.2 Fuel System Design

Application Section: PLUS7 Fuel Design for the APR1400
(APR1400-F-M-TR-13001-P)

Date of RAI Issue: 06/18/2015

Question No. TR PLUS7 Fuel Design for the APR1400-16

GDC 10 requires that the reactor core and associated coolant, control, and protection systems shall be designed with appropriate margin to assure that specified acceptable fuel design limits (SAFDLs) are not exceeded during any condition of normal operation, including the effects of anticipated operational occurrences (AOOs). SRP Section 4.2 (II)(1)(A)(ii) provides guidance in regards to GDC 10 by stating that the cumulative number of strain fatigue cycles on the structural members should be significantly less than the design fatigue lifetime, which is based on appropriate data and includes a safety factor.

Pages 3-17 and 2-5 of the TCD report (APR1400-F-A-NR-13002-P) discuss cladding strain and fatigue. Section 3.4.2 states that the increased thermal expansion can be offset with available design margin in the cladding strain and fatigue limits. Sample calculations provided in the TCD report show that the fatigue damage factor will increase from 0.28 to 0.77 when TCD is considered. This has caused the staff to question the claim that increased thermal expansion can be offset with available design margin in the cladding strain and fatigue limits.

a) Discuss how the fatigue analysis will be performed on a cycle specific basis given this demonstration that FATES3B alone is inadequate to assess the fatigue damage fraction. Update the topical report, if necessary, to include the clarification.

b) The fatigue damage factors (FDF) presented in topical report APR1400-F-M-TR-13001-P and technical report APR1400-F-A-NR-13002-P (for the operating condition "without TCD") do not appear to match. Update the report(s) as necessary to reflect the correct FDF.

Response

a) According to Reference 16-1, a license condition that will impose more restrictive operation/design radial power fall-off (RFO) curve limits for St. Lucie 2 was accepted by NRC. This approach is applied to the licensing application of APR1400 Topical Reports.

Even though the FATES3B fuel performance code does not explicitly model Thermal Conductivity Degradation (TCD), FATES3B centerline temperature predictions are well matched to Halden measured data up to intermediate levels of rod average burnup []^{TS}. However, as the burnup goes beyond []^{TS}, the extent of underprediction gap linearly increases and finally reached []^{TS} at the rod average burnup of []^{TS} and then remains constant for higher burnup.

Based on these comparisons, a more restrictive (management) radial power fall-off (RFO) curve limit is determined by reducing the rod power from the analysis RFO power by an amount sufficient to reduce the fuel centerline temperature corresponds to []^{TS} over the burnup range from []^{TS} and []^{TS} for higher burnup. This temperature penalty will set aside margin to account for the burnup dependent effects of TCD. Figure 16-1 shows the derived management RFO curve limit accounting for the TCD penalty and the analysis RFO curve limit which is used for fuel performance analyses and temperature generation for safety analysis.

The management RFO curve limit will be validated on a cycle-by-cycle basis to confirm the applicability for a given subsequent cycle. This assures that the plant will be operated under the management RFO curve limit that accounts for the TCD penalty.

Fatigue analysis in the topical report is performed using higher rod power history (radial peaking factor) than the analysis RFO curve limit. Therefore, the fatigue analysis results presented in the topical report can be continually used for fatigue criterion confirmation if the management RFO curve limit is confirmed to be valid on a cycle specific basis. Section 3 in the PLUS7 topical report will be updated with mark-ups to provide a discussion on the derivation of both analysis and management RFO curve limits.

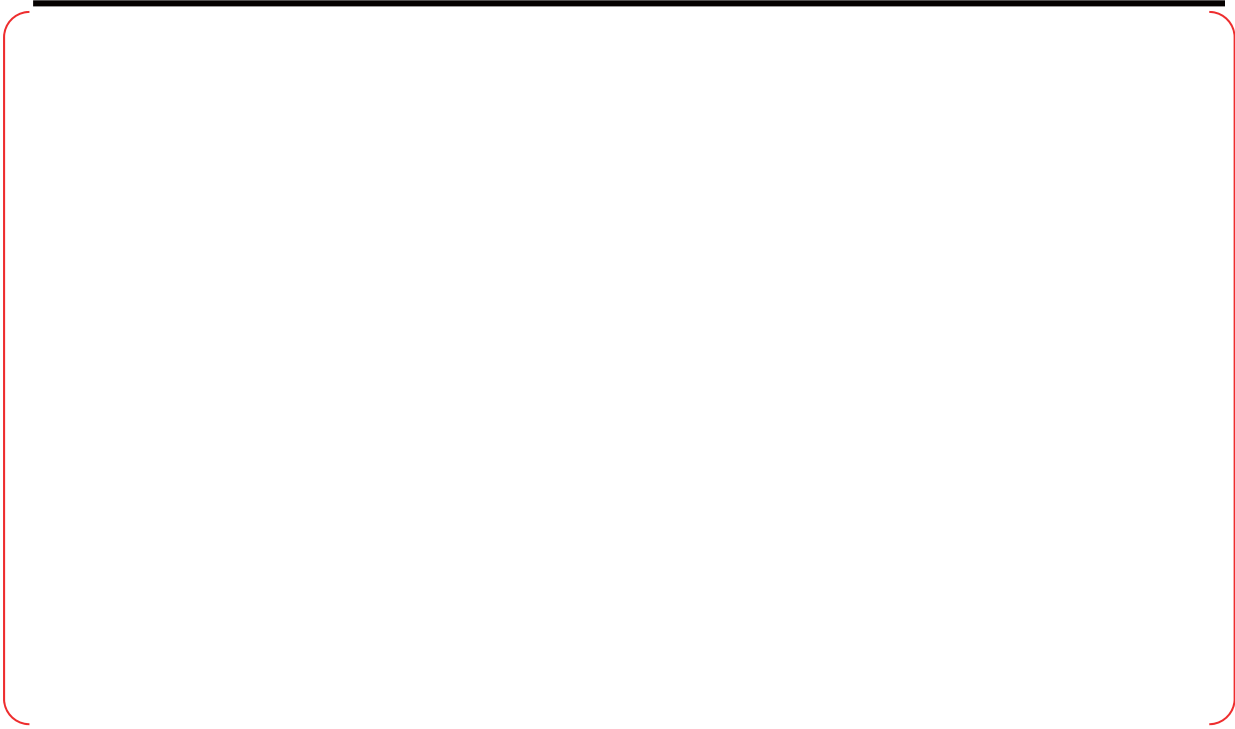


Figure 16-1 Radial Fall-Off Curve Limits

- b) The fatigue damage factors presented in topical report APR1400-F-M-TR-13001-P and technical report APR1400-F-A-NR-13002-P (for the operating condition without TCD) are []^{TS} and []^{TS}, respectively. The higher fatigue damage factor in topical report APR1400-F-M-TR-13001-P is mainly attributed to the excessive conservatism of power history assumed in the calculation. Rod power history (radial peaking factor) used in the fatigue analysis of the topical report is much higher than that of technical report as shown in Figure 16-2. The other conservatism in the fatigue analysis for the topical report is to assume higher End Of Life (EOL) rod average burnup of []^{TS}. In contrast, the fatigue analysis result (fatigue damage factor=[]^{TS}) presented in the technical report was obtained by assuming the EOL burnup of []^{TS} (the target licensing burnup) and reducing the excessive conservatism in the rod power history (radial peaking factor) as shown Figure 16-2.

Figure 16-2 Radial Peaking Factors used for Fatigue Analyses

Note) Figure 16-1 indicates that both RFO curves are conservatively regenerated to secure the applicability for a subsequent reload cycle. Thus, the radial peaking factor (rod power history) for fatigue analysis is also conservatively regenerated to bound the newly developed analysis RFO curve limit as shown in Figure 16-3. The fatigue result using the regenerated radial peaking factor in Figure 16-3 is []^{TS}. Both regenerated RFO curve limits in Figure 16-1 and the recalculated fatigue result will be reflected in topical report (APR1400-F-M-TR-13001-P). Affected contents due to the TCD penalty approach will be provided as mark-up and also reflected in the topical report.



Figure 16-3 Previous and Regenerated Radial Peaking Factors used for Fatigue Analyses

References

[16-1] Letter, ML#12198A202, "FINAL SAFETY EVALUATION REPORT ASSOCIATED WITH THE FLORIDA POWER AND LIGHT ST. LUCIE, UNIT 2, LICENSE AMENDMENT REQUEST FOR AN EXTENDED POWER UPRATE," July 23, 2012.

Impact on DCD

The effect on the Design Control Document (DCD) Tier 2 will be reviewed when the TCD penalty methodology results are applied. DCD Tier 2 will then be updated if necessary.

Impact on PRA

There is no impact on the PRA.

Impact on Technical Specifications

There is no impact on the Technical Specifications.

Impact on Technical/Topical/Environmental Report

The PLUS7 fuel design topical report (APR1400-F-M-TR-13001-NP) will be updated as indicated on the attached markups to include the TCD penalty approach. Technical Report APR1400-F-A-NR-14002-NP will be withdrawn.

Non Proprietary

PLUS7 FUEL DESIGN for the APR1400

APR1400-F-M-TR-13001-NP Rev.0

Fuel coolability applies to postulated accidents. To meet the requirements of GDC 27 and 35 as they relate to control rod insertability and core coolability for postulated accidents, fuel coolability should be provided for all severe damage mechanisms. Fuel coolability criteria involves cladding embrittlement, violent expulsion of fuel, generalized cladding melting, fuel rod ballooning and structural deformation.

In this section, evaluations have been done to verify that the fuel rod design bases and criteria can be met for the PLUS7 fuel design. The fuel rod design criteria for cladding stress, cladding strain, cladding fatigue, cladding corrosion/hydriding, rod internal pressure, cladding collapse, overheating of fuel pellets, pellet-to-cladding interaction have been evaluated using the NRC approved Westinghouse fuel rod performance codes and methodologies (References 3-1 through 3-9, 3-12, 3-13). The codes applied for evaluating each fuel rod design criterion are summarized in Table 3-2.

The design bases and limits for PLUS7 fuel rod are the same as NRC approved design bases and limits for Westinghouse CE PWR fuel designs (Reference 3-10).

The stress and loading limit for other than cladding, fretting wear, dimensional change, assembly lift-off, rod mechanical fracturing and structural deformation are described in Chapter 2. The criteria and evaluations related to safety analyses will be described in DCD Chapter 15 in detail.

3.2.1 Cladding Stress**(1) Basis**

FATES3B does not explicitly model fuel thermal conductivity degradation (TCD) with burnup. In order to preserve margin and conservatively offset the effects of TCD, a burnup dependent temperature penalty is suggested and approved (Reference 3-14). In detail, FATES3B centerline temperature predictions were well matched to Halden measured data up to intermediate levels of rod average burnup (35,000 MWD/MTU). However, temperature underprediction starts at 35,000 MWD/MTU burnup and increases linearly up to 200°F at 50,000 MWD/MTU rod average burnup, then remains constant for higher burnup. Based on these comparisons, a more restrictive (management) radial power fall-off (RFO) curve limit is determined by reducing the rod power from the analysis RFO power by an amount sufficient to reduce the fuel centerline temperature to correspond to 0 - 200°F over the burnup range from 35 to 50 GWD/MTU and 200°F for higher burnup. Figure 3-1 shows the derived management RFO curve limit accounting for TCD effect and analysis RFO curve limit which is used for fuel performance analyses and temperature generation for safety analyses. The management RFO curve limit will be validated on a cycle-by-cycle basis to confirm the applicability for a given reload cycle. This assures that the plant will be operated under the management RFO curve limit. Therefore, the calculation results from the analysis RFO curve limit can be maintained as applied to fuel rod design criteria confirmation and downstream safety analyses as long as the management RFO curve limit is valid on a cycle specific basis. The detailed evaluation results using the analysis RFO curve limit are described in this section.

The evaluation methodology for the fuel rod stress is discussed in Reference 3-5, which was reviewed and approved by the NRC for Westinghouse CE PWR fuel designs.

The rod internal pressures used to perform the stress analyses of the fuel rod designs accounts for power dependent and time dependent changes (e.g., fuel rod void volume, fission gas release and gas temperature, differential cladding pressure, cladding creep and thermal expansion) that can affect stresses in the fuel rod cladding. The rod external pressures are consistent with the event being analyzed and are biased in the conservative direction (maximum for compressive stresses, minimum for tensile stresses). The maximum tensile and compressive stresses were calculated for

Non Proprietary

PLUS7 FUEL DESIGN for the APR1400

APR1400-F-M-TR-13001-NP Rev.0

3.2.3 Cladding Fatigue**(1) Basis**

Fuel system will not be damaged due to excessive fatigue under normal operation.

(2) Criteria

For the number and type of transients which occur during normal operation, end-of-life (EOL) cumulative fatigue damage in the cladding must be less than $\left[\quad \right]^{TS}$.

A fatigue analysis for the ZIRLO cladding is performed using the Langer-O'Donnell fatigue design curve. A safety factor of 2 on the stress or a safety factor of 20 on the number of cycles is imposed on this curve conservatively. The fatigue damage is defined as the ratio of the number of calculated cycles in a given strain range to the permitted number of cycles determined by fatigue curve at strain range.

(3) Evaluation

The method used for fatigue analysis of fuel rod accounts for power dependent and time dependent changes (e.g., rod void volume, fission gas release and gas temperature, cladding creep and thermal expansion, and pellet swelling and thermal expansion) that can produce cyclic straining of the fuel cladding. With respect to determining changes in cladding and pellet diameters, the methodology used to evaluate the fatigue damage from power cycling is the same for the strain evaluation during normal operation, except that some of the parameters are biased in the opposite direction to provide results that are conservative for fatigue analysis.

The number of load cycles assumed in the fatigue evaluation is defined below for startup/shutdown, power variations and reactor trip during normal operation. The stress amplitudes for the cyclic loads are calculated using the FATES3B code.

a) Startup/shutdown

A startup/shutdown cycle is defined as the change from the 0% cold stand-by-state to the 0% hot stand-by state. $\left[\quad \right]^{TS}$ startups/shutdowns between 0% power and room temperature conditions are considered for fatigue evaluation.

b) Power variation during normal operation

Load follow operation is the most limiting condition of normal operation for fatigue evaluation. The power variation for load following is conservatively assumed to vary between 10% and 100% on a daily basis, and for each day.

c) Reactor Trip

The limiting condition for power change due to the AOOs is the reactor trip from 100 power to hot condition, conservatively. $\left[\quad \right]^{TS}$ reactor trips are considered for fatigue evaluation.

The total cumulative fatigue damage factor from power cycling, reactor trips and startups/shutdowns is $\left[\quad \right]^{TS}$ which is below the limit of $\left[\quad \right]^{TS}$. It was demonstrated that the fuel rod fatigue criterion was satisfied.

Non Proprietary

PLUS7 FUEL DESIGN for the APR1400

APR1400-F-M-TR-13001-NP Rev.0

(3) Evaluation

FATES3B was used to calculate the rod internal pressure and corresponding critical limit according to the NRC approved methodology described in Reference 3-6. Where appropriate, the approved gadolinia methodology of References 3-7 and 3-8 has been applied. The critical limit is the internal hot gas pressure at which the outward tensile creep rate of the cladding exceeds the fuel pellet radial growth rate due to fuel swelling, thus creating any potentially damaging effects on the fuel rod due to detrimental thermal feedback effects within the fuel rod during normal operation.

Maximum rod internal pressure is calculated using conservative biasing of nominal fuel rod data including cladding outer diameter, cladding inner diameter, pellet outer diameter, active fuel length, fill gas pressure and will usually include additional conservatisms in the power levels representing each successive cycle of projected residency in the reactor core. The input power history to the code is important for rod internal pressure calculation. The methodology and conservatism for determining the rod power history are described in Reference 3-9. The main parameters and rod power histories considered in representative fuel rod internal pressure calculation are summarized in Table 3-4 and Figure 3-1, respectively.

The evaluation shows that the maximum rod internal pressures are { }^{TS} and { }^{TS} for the UO₂ fuel rod and Gd₂O₃-UO₂ burnable absorber fuel rod, respectively. ~~Therefore, no clad lift-off criterion is satisfied since the calculated gas pressures are less than critical pressure limit.~~

DNB propagation evaluations for transients and DNB accidents are performed using the NRC approved methodology with INTEG code, which is a standalone computer code to predict fuel rod deformation and burst behavior under conditions of DNB (Reference 3-6).

~~Therefore, no clad lift-off (NCLO) criterion is satisfied since the calculated gas pressures are less than the system pressure. FATES3B code calculates the critical pressure limit to prevent clad lift-off only when the rod internal pressure exceeds the system pressure.~~

~~Analysis methodology for any given plant. These inputs include time, heat flux, quality, mass flow, system pressure, rod internal pressure, and fuel rod initial geometry. To evaluate the potential for DNB propagation, the limiting DNB transients and internal pressure of { }^{TS} are applied.~~

The results indicate that the clad strains induced by high temperature creep for limiting transients are less than { }^{TS}. This amount of strain does not induce DNB propagation to adjacent fuel rods.

Finally, hydride reorientation does not occur at internal pressure of { }^{TS}, which is well above the predicted rod internal pressure of { }^{TS} on PLUS7 fuel (Reference 3-6).

3.2.6 Internal Hydriding

(1) Basis

Fuel system will not be damaged due to excessive hydriding.

(2) Criteria

Primary hydriding is prevented by maintaining the level of moisture very low during the pellet manufacturing. The moisture content shall remain below the limit of 2.0 ppm (hydrogen from all sources for fuel pellets).

(3) Evaluation

Non Proprietary

PLUS7 FUEL DESIGN for the APR1400

APR1400-F-M-TR-13001-NP Rev.0

Fuel rod failure will not occur due to the overheating of cladding under normal operation including AOOs.

(2) Criteria

There should be a 95% probability at the 95% confidence level that a hot fuel rod in the reactor core will not experience a DNB during normal operation or AOOs. For postulated accidents, the rods that experience DNB are assumed to fail for radiological dose calculation purposes.

(3) Evaluation

The evaluation for overheating cladding is addressed in plant specific transient and accident analysis (Chapter 15 of DCD).

3.2.9 Overheating of Fuel Pellets

1) Basis

Fuel rod failure will not occur due to the overheating of fuel pellets under normal operation including AOOs. For postulated accidents, the total number of rods that experience centerline melting should be considered for radiological dose calculation.

(2) Criteria

During normal operating and AOOs, the fuel centerline temperature shall not exceed the melting temperature accounting for degradation due to burnup and addition of burnable absorbers.

The fuel rod is considered to be failed []^{TS} during postulated accidents. In the event of fuel failure, the radiological consequences of fuel failure must be accounted in the dose calculations.

The melting temperature of UO₂ is taken to be 5,080 °F (unirradiated) and to decrease []^{TS} per 10,000 MWD/MTU fuel burnup. For Gd₂O₃-UO₂ burnable absorber fuel rod, the melting temperature decreases additionally []^{TS} per weight percent of Gd₂O₃.

(3) Evaluation

The fuel centerline temperatures as a function of burnup are calculated using the NRC approved FATES3B code and methodology described in References 3-1 through 3-5 for UO₂ rod and References 3-7 and 3-8 for Gd₂O₃-UO₂ burnable absorber fuel rod.

The powers to fuel melting are calculated as a function of rod burnup. To preclude fuel melting, the peak local power experienced in normal operation and AOOs should be less than the power to fuel melting at all burnups.

The minimum design margin occurs at the end of cycle 1 because of the reduced power capability with burnup, which is caused by the depletion of the fissile material in the fuel and the buildup of fission products. The calculated power to fuel melting at the end of cycle 1 is []^{TS}, which is bounded by the local power density for trip setpoint of []^{TS}.



Non Proprietary

PLUS7 FUEL DESIGN for the APR1400

APR1400-F-M-TR-13001-NP Rev.0

- ZIRLO Corrosion Data Base

ZIRLO in-reactor corrosion data have been obtained from the BR-3 and North Anna fuel program. The BR-3 test fuel residence times extend to 47,500 hours, and the North Anna fuel has achieved a 10,150 EFPH residence time after one cycle of irradiation. Comparison of the corrosion data from the BR-3 ZIRLO rods with sibling Zr-4 rods show ZIRLO peak corrosion ranging from 66% to 83% of Zr-4 peak corrosion. Peak corrosion data from the one cycle North Anna rods range from 0.3 to 0.6 mil for the ZIRLO rods, and from 0.5 to 0.9 mil for the Zr-4 rods.

Based on these data, a corrosion multiplier of 0.75 relative to the Zr-4 corrosion model has been determined for use in ZIRLO fuel rod performance evaluations.

- Increase of Corrosion Model Multiplier

However, it was found that the model multiplier of 0.75 is less conservative for ZIRLO claddings irradiated in Yongggwang unit 2, Yongggwang unit 4 and Ulchin unit 3 through the Post Irradiation Examination Program.

Using the measured oxide layer thickness data of Yongggwang unit 2, Yongggwang unit 4 and Ulchin unit 3, the new corrosion model multiplier was determined to evaluate the best estimate predictions of oxide thickness. A total of 25 oxide thickness data with high burnup exceeding 50 MWD/kgU was used to determine best estimate corrosion model multiplier for Yongggwang unit 2, Yongggwang unit 4 and Ulchin unit 3. Those oxide thickness data consist of 6 fuel rods of V5H fuel irradiated in Yongggwang unit 2, 6 fuel rods of GUARDIAN fuel irradiated in Yongggwang unit 4 and 13 fuel rods of PLUS7 fuel irradiated in Ulchin unit 3 were used.

Through the process of statistical analyses and evaluations, the corrosion model multiplier of 0.92 was determined for best estimate oxide thickness prediction for ZIRLO cladding. Table 3-8 shows the comparison of measured oxide thickness and predicted oxide thickness using corrosion model multiplier of 0.92. The results of statistical analyses are as follows.

| | |
|-----------------------------|------|
| Number of Data : | 25 |
| Mean Value of M/P : | 0.89 |
| Standard Deviation of M/P : | 0.19 |

- Verification of Corrosion Model Multiplier

In order to verify the accuracy of corrosion model multiplier determined based on measured oxide thickness data from Yongggwang unit 2, Yongggwang unit 4 and Ulchin unit 3, the verification of modified corrosion model multiplier was performed using the measured oxide thickness data of PLUS7 fuel rods irradiated in Yongggwang unit 5. The 72 thrice burnt fuel rods with fuel rod average burnups of up to 58,000 MWD/MTU were selected for verification of corrosion model multiplier.

Figure 3-2 shows the comparison of measured oxide thickness and predicted oxide thickness. The predicted oxide thicknesses were generated using the corrosion model multiplier of 0.92.

3-3

3-3

Non Proprietary

PLUS7 FUEL DESIGN for the APR1400

APR1400-F-M-TR-13001-NP Rev.0

As shown in Figure 3-2, the predicted values are much higher than those of measured values for both H614 and H605 PLUS7 fuel assemblies. In addition, the means values and standard deviations of M/P are summarized in Table 3-9 for H615 and H605 assemblies.

- Comparison of operating conditions of OPR1000, Westinghouse Type Plants and APR1400

As explained in previous section, oxide thickness data to use the development of corrosion model multiplier and verification were measured at Ulchin unit 3, Yonggwang unit 2, Yonggwang unit 4 and Yonggwang unit 5. However, there are no available APR1400 plant specific corrosion data because the APR1400 plant was not started its first commercial operation yet.

It is, therefore, necessary to compare the operating conditions of Ulchin unit 3, Yonggwang unit 4 and Yonggwang unit 2 with those of APR1400 because the corrosion buildup on cladding material is mainly dependent on operating conditions in terms of coolant temperatures, mass flow rate, lithium concentration and core average power.

Table 3-10 shows the operating conditions of APR1400 and OPR1000 (Yonggwang unit 4 and Ulchin unit 3) as well as Westinghouse type plant of Yonggwang unit 2. As shown in Table 3-10, the coolant inlet temperature and outlet temperature of APR1400 plant are less than those of OPR1000 and Yonggwang unit 2 as well as the core average coolant mass flow rate of APR1400 plant is well within the range of OPR1000 and Yonggwang unit 2. In addition, the allowable maximum lithium concentration of APR1400 plant is the same as those of OPR1000 and Yonggwang unit 2. On the other hand, the core average linear heat rate of APR1400 plant is about four percent higher than that of OPR1000. However, it is expected that four percent increase of core average power does not give a significant effect on oxide buildup of cladding tube. Therefore, the applicability of PAD code with increased corrosion multiplier to PLUS7 fuel in APR1400 for corrosion evaluation was confirmed.

3.4 Impact of TCD on Fuel Rod Design Criteria

~~FATES3B does not explicitly model fuel thermal conductivity degradation (TCD) with burnup. FATES3B uses the burnup independent thermal conductivity of Lyons correlation. Compared with the thermal conductivity model with TCD effect, the Lyons model produces a relatively less conservative temperature distribution within fuel pellet.~~

~~Many of cladding-related criteria, such as cladding corrosion and hydrogen pickup, cladding collapse and fuel rod growth are not affected by TCD. Cladding temperature is not affected since the heat flux is not changed by TCD, so cladding corrosion and hydrogen criteria are unaffected. Fuel densification is not also affected by TCD, so cladding collapse criterion is not impacted by TCD. Fast neutron fluence does not change due to TCD, so fuel rod growth criterion is also not impacted by TCD.~~

~~The evaluations for the fuel rod design criteria that are affected by TCD are described as follows. The detailed evaluation results will be provided in TCD Technical Report which is planned to submit to NRC.~~

were described in TCD Technical Report in Reference 3-14.

3.4.1 Cladding Stress

~~As described in Section 3.2.1, KNE cladding stress criterion is established to prevent fuel damage from the excessive primary stress which results from the pressure difference between rod internal pressure and system pressure.~~

KHNP

3-16

Delete

Non Proprietary**Delete**

PLUS7 FUEL DESIGN for the APR1400

APR1400-F-M-TR-13001-NP Rev.0

~~Considering the amount of potential increase in rod internal pressure by TCD impact and design margin to the limit, it is judged that the cladding stress criteria are still met with consideration of TCD.~~

~~3.4.2 Cladding Strain and Fatigue~~

~~The cladding strain is affected by TCD due to the increased fuel thermal expansion. However, the increased thermal expansion can be offset with available design margin to the cladding strain and fatigue limits and conservatism in the input variables such as power history and assumed rod internal pressure. Therefore, cladding strain and fatigue criteria are still satisfied with consideration of TCD.~~

~~3.4.3 Fuel Rod Internal Pressure~~

~~The effect of increased fuel temperature due to TCD on fission gas release is inherently accounted for in the current performance code, FATES3B (References 3-1 through 3-4) because the model was calibrated to measured data for a full range of fuel rod burnup and operating conditions. Additionally, conservatism is considered in the original FATES3B calibration process and in fuel rod design analysis. However, the rod internal pressure may still increase with TCD due to the increased fuel thermal expansion, which reduces the total fuel rod void volume.~~

~~Evaluations show that the reduction of void volume due to increased thermal expansion is not significant in PLUS7 fuel rod design. In addition, the rod internal pressure limit calculation is inherently conservative in that actual gap reopening is predicted to occur at higher pressures.~~

~~In conclusion, the increased rod internal pressure can be offset with available design margin to the rod internal pressure limits. Therefore, rod internal pressure criteria are still satisfied considering the effects of TCD.~~

~~3.4.4 Overheating of Fuel Pellets~~

~~The power to melt limit depends on fuel burnup but the reduced power capability with burnup, which is caused by the depletion of the fissile material in the fuel and the buildup of fission products, offsets the TCD impact. Therefore, it is judged that there will be no safety concerns due to TCD. However, the power to melt values with burnup considering the impact of TCD are calculated and will be provided in the TCD Technical Report which will be submitted to NRC.~~

~~In summary, KNF fuel rod design criteria have been reviewed with respect to the potential impacts of TCD, and it is concluded that TCD can be accommodated such that approved fuel rod design criteria will remain satisfied for current fuel rod designs.~~

3.5 Conclusion

The PLUS7 fuel rod design is verified to maintain the rod integrity up to rod average burnup of 60,000 MWD/MTU based on the thermal performance and mechanical integrity evaluation results using by NRC approved design codes and methodologies.

Non Proprietary

PLUS7 FUEL DESIGN for the APR1400

APR1400-F-M-TR-13001-NP Rev.0

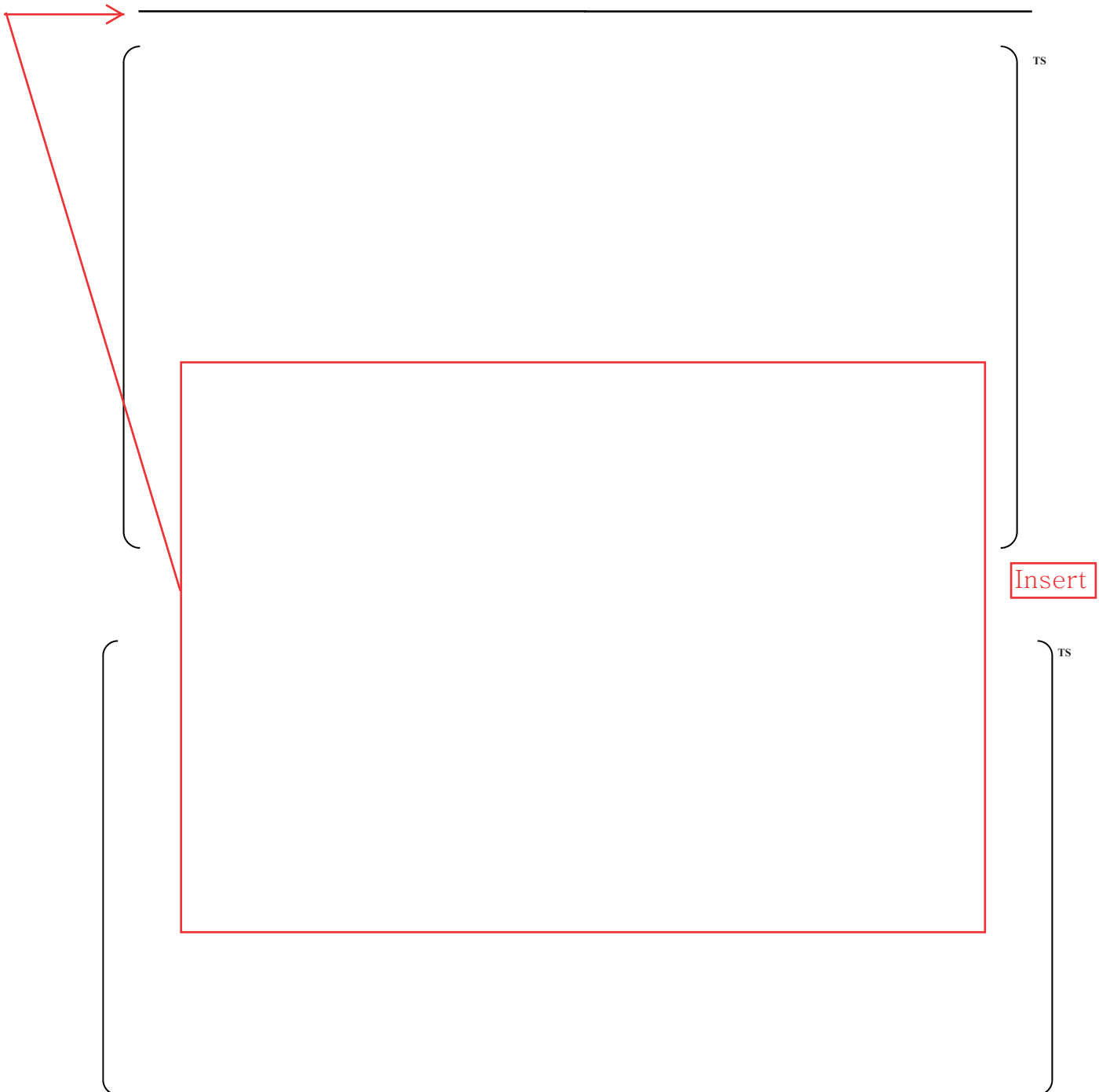


Figure 3-2 Comparison of Measured Oxide Layer Thickness and Predicted Oxide Layer Thickness for H615 and H605 Assemblies

Non Proprietary

PLUS7 FUEL DESIGN for the APR1400

APR1400-F-M-TR-13001-NP Rev.0

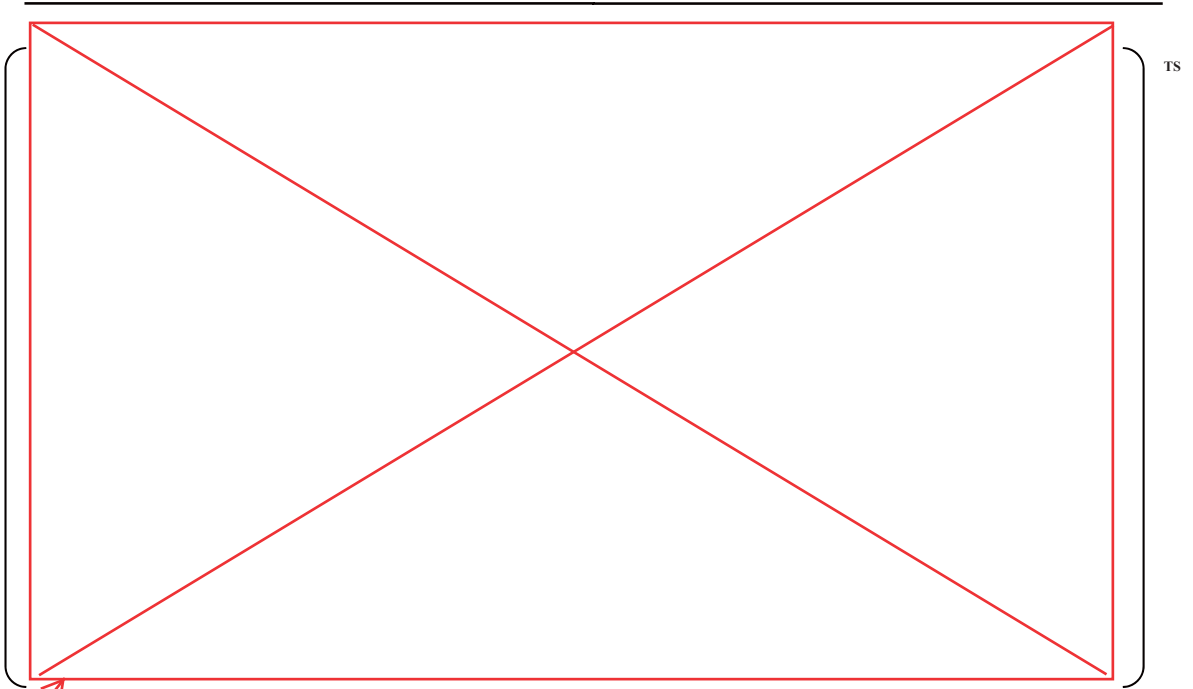


Figure 3-1 Rod Power History Used for PLUS7 Fuel Rod Performance Analysis

Replace

2

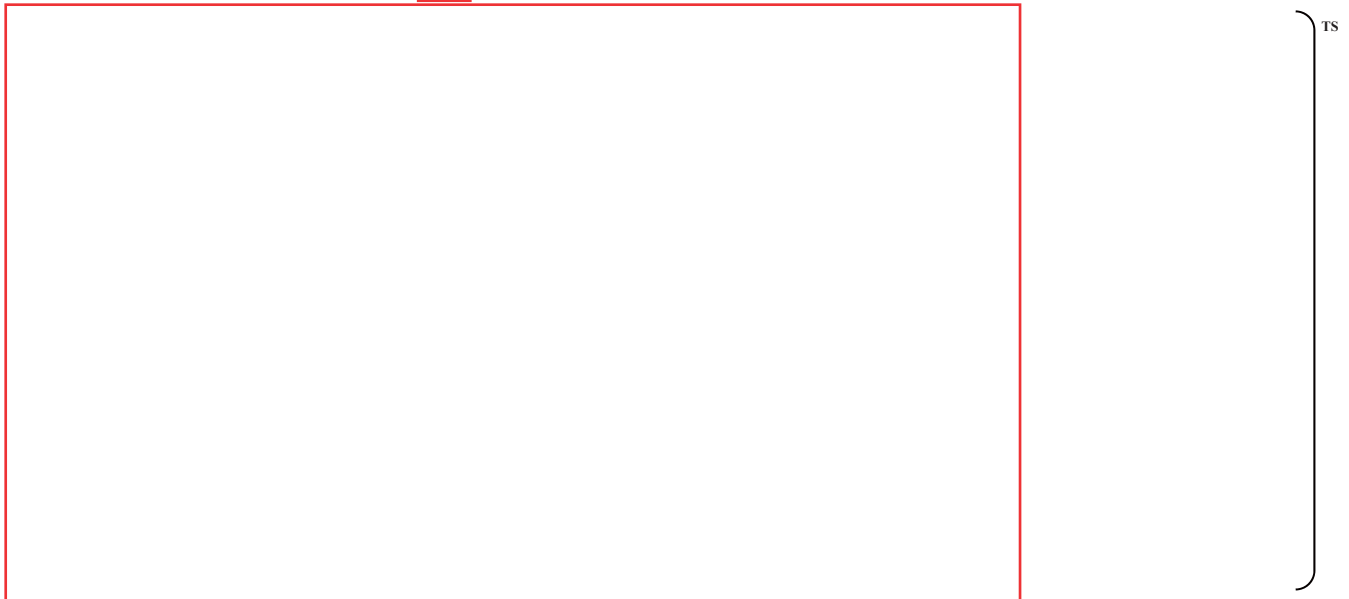


Figure 3-2 Comparison of Measured Oxide Layer Thickness and Predicted Oxide Layer Thickness for H615 and H605 Assemblies

3

Non Proprietary

PLUS7 FUEL DESIGN for the APR1400

APR1400-F-M-TR-13001-NP Rev.0

6. REFERENCES

- 2-1 CENPD-178-P, Revision 1-P, "Structural Analysis of Fuel Assemblies for Seismic and Loss of Coolant Accident Loading," Combustion Engineering Inc., August 1981.
- 3-1 CENPD-139-P-A, "C-E Fuel Evaluation Model Topical Report," Combustion Engineering Inc., July 1974.
- 3-2 CENPD-139, Supplement 1, Revision 01, "C-E Fuel Evaluation Model Topical Report," Combustion Engineering Inc., July 1974.
- 3-3 CEN-161(B)-P-A, "Improvements to Fuel Evaluation Model," August 1989.
- 3-4 CEN-161(B)-P Supplement 1-P-A, "Improvements to Fuel Evaluation Model," January 1992.
- 3-5 CENPD-404-P-A, "Implementation of ZIRLOTM Cladding Material in CE Nuclear Power Fuel Assembly Designs," November 2001.
- 3-6 CEN-372-P-A, "Fuel Rod Maximum Allowable Gas Pressure," May 1990.
- 3-7 CENPD-275-P, Revision 1-P-A, "C-E Methodology for Core Designs Containing Gadolinia-Urania Absorbers," May 1998.
- 3-8 CENPD-275-P, Revision 1-P, Supplement, 1-P-A, "C-E Methodology for Core Designs Containing Gadolinia-Urania Absorbers," April 1999.
- 3-9 CEN-193(B), Supplement 2-P, Partial Response to NRC Questions on CEN-161(B)-P, "Improvements to Fuel Evaluation Model," March 21, 1982.
- 3-10 WCAP-16500-P-A, Rev.0 "CE 16x16 Next Generation Fuel Core Reference Report," August 2007.
- 3-11 WCAP-15063-P-A, Rev.1, with Errata, "Westinghouse Improved Performance Analysis and Design Model (PAD4.0)," July 2000.
- 3-12 CENPD-187-P-A, CEPAN Method of Analyzing Creep Collapse of Oval Cladding, Combustion Engineering, Inc., April 1976 ; Supplement 1-P-A, June 1977.
- 3-13 EPRI NP-3966-CCM, "CEPAN Method of Analyzing Creep Collapse of Oval Cladding-Volume 5: Evaluation of Interpellet Gap Formation and Cladding Collapse in Modern PWR Fuel Rods," Combustion Engineering, Inc., April 1985.

3-14 APR1400-F-A-NR-14002-P, "The Effect of Thermal Conductivity Degradation on APR1400 Design and Safety Analysis." KEPCO NF, September 2014.

3-14 Letter, ML#12198A202, "FINAL SAFETY EVALUATION REPORT ASSOCIATED WITH THE FLORIDA POWER AND LIGHT ST. LUCIE, UNIT 2, LICENSE AMENDMENT REQUEST FOR AN EXTENDED POWER UPRATE," July 23, 2012.

**KHNP****KOREA HYDRO & NUCLEAR POWER CO., LTD**

70-1312-gil, Yuseong-daero, Yuseong-gu, Daejeon, 305-343, KOREA

Tel: +82-42-870-5400 / Fax: +82-42-870-5449

<http://www.khnp.co.kr>

August 11, 2017
Document Control Desk
U.S. Nuclear Regulatory Commission
Washington, DC 20555-0001

Attention: Mr. William Ward
Division of New Reactor Licensing

Docket No. 52-046
MKD/NW-17-0201L

Subject: Revised Response to RAI 5-7954 on Topical Report "PLUS7 Fuel Design for the APR1400"

References: 1) NRC Request for Additional Information 5-7954, dated June 18, 2015
2) KHNP Letter MKD/NW-15-0055L, Response to RAI 5-7954 on Topical Report "PLUS7 Fuel Design for the APR1400, APR1400-F-M-TR-13001, Rev. 0, dated July 21, 2015
3) KHNP Letter MKD/NW-16-0826L, Response to RAI 5-7954 for Question TR PLUS7 Fuel Design for the APR1400-16, dated July 29, 2016

KHNP is hereby submitting the response to RAI 5-7954, dated June 18, 2015. The revised response addresses Questions TR PLUS7 Fuel Design for the APR1400-11 ~ 14, 16, and 18.

Enclosure 1 contains a copy of the associated affidavit. Enclosure 2 provides the revised response to RAI 5-7954 on topical report "PLUS7 Fuel Design for the APR1400" (Proprietary). Enclosure 3 provides the revised response to RAI 5-7954 on topical report PLUS7 Fuel Design for the APR1400" (Non-Proprietary).

If additional information or clarification is required, please contact Daegeun Ahn, Director of KHNP Washington DC Center at ahn.daegeun@khnp.co.kr or 703-388-0592.

Sincerely,

Han-gon Kim
Project Manager
Advanced Reactors Development Laboratory
Korea Hydro & Nuclear Power Co., Ltd.

Enclosures:

1. Affidavit KAW-17-0201
2. Revised Response to RAI 5-7954 on Topical Report "PLUS7 Fuel Design for the APR1400" (Proprietary)
3. Revised Response to RAI 5-7954 on Topical Report "PLUS7 Fuel Design for the APR1400" (Non-Proprietary)

Enclosure 1

Affidavit KAW-17-0201

I, Yun-ho Kim, state the following:

1. I am the General Manager of Korea Hydro & Nuclear Power Co., Ltd. (KHNP), and as such I am authorized to request withholding the information transmitted with this letter from public disclosure and to execute this affidavit.
2. I am familiar with the criteria applied by KHNP to determine whether certain information is proprietary, and with the policies established by KHNP to ensure the proper application of these criteria.
3. The information, Revised Response to RAI 5-7954 on Topical Report “PLUS7 Fuel Design for the APR1400” (Proprietary), transmitted with this letter has been classified by KHNP as proprietary in accordance with the policies for the control and protection of proprietary and confidential information. The information regarded as proprietary is identified and marked consistent with the requirements of 10 CFR 2.390, § (b)(1)(i). Accordingly, the proprietary information is enclosed within brackets and the right-hand bracket carries a notation of “TS” to indicate that the trade secret nature of the information claimed to be proprietary is the basis for proposing that the information so identified be withheld from public disclosure.
4. Pursuant to the considerations set forth in 10 CFR Section 2.390(a), KHNP considers the information classified as proprietary to be “trade secret” information since it is design, analysis, or test information that would be difficult for a competitor to reproduce and hence provides an economic and competitive advantage to KHNP.
5. The need for designating the information as proprietary has been raised within KHNP. The information is being treated proprietary and confidential and has not been disclosed by KHNP to the public.
6. Nondisclosure of the proprietary information transmitted with this letter is vital to the competitiveness held by KHNP and, hence, disclosure of the proprietary information transmitted in with this letter would have negative commercial impacts on the competitive position of KHNP in the U.S. nuclear market.
7. In accordance with KHNP policy, proprietary information contained in this document may be, or may have been, made available on a limited basis to regulatory bodies, customers, potential customers, and their agents, suppliers, and licensees, and others under suitable agreements providing for nondisclosure and limited use of the information.

I declare that the foregoing statements are true and correct to the best of my knowledge,



KHNP
KOREA HYDRO & NUCLEAR POWER CO., LTD

information and belief.

Executed on August 11, 2017.

Yun-ho Kim

General Manager

APR1400 Licensing Team

Korea Hydro and Nuclear Power Co., Ltd

Enclosure 3

Revised Response to RAI 5-7954 on Topical Report “PLUS7 Fuel
Design for the APR1400”

(Non-Proprietary)

August 11, 2017

REVISED RESPONSE TO REQUEST FOR ADDITIONAL INFORMATION

APR1400 Topical Reports

Korea Electric Power Corporation / Korea Hydro & Nuclear Power Co., LTD

Docket No. PROJ 0782

RAI No.: 5-7954

SRP Section: TR PLUS7 Fuel Design for the APR1400

Application Section: PLUS7 Fuel Design for the APR1400
(APR1400-F-M-TR-13001-P)

Date of RAI Issue: 06/18/2015

Question No. TR PLUS7 Fuel Design for the APR1400-11

GDC 10 requires that the reactor core and associated coolant, control, and protection systems shall be designed with appropriate margin to assure that specified acceptable fuel design limits (SAFDLs) are not exceeded during any condition of normal operation, including the effects of anticipated operational occurrences (AOOs). SRP Section 4.2 (II)(1)(B)(v) provides guidance stating that the fuel failure criteria should address excessive fuel enthalpy.

This fuel failure criterion is addressed on Page 3-9 of APR1400-F-M-TR-13001-P for the PLUS7 fuel design. Section 3.4.4 of the topical report states that the code used to analyze this fuel failure mechanism (FATES3B) over predicts fuel thermal conductivity at high burnup. Therefore, it will also under predict fuel enthalpy. The staff notes that Section 3.4.4 provides a qualitative argument to state that the effects of burnup dependence of TCD are bounded by the reduced power capabilities at higher burnups. This raises concerns from the staff on the ability of the excessive fuel enthalpy analysis to demonstrate compliance with the excessive fuel enthalpy SAFDL given all core loading options available.

Please include a discussion, supported by analysis, within Section 3.2.10 and/or 3.4.4 of APR1400-F-M-TR-13001-P regarding the impacts of the fuel enthalpy under prediction and how excessive fuel enthalpy is precluded.

Response - (Rev.1)

A impact of fuel enthalpy will be updated and added in Section 3.6 of topical report (APR1400-F-M-TR-13001-P), which is currently described in Section 3.4.5.

“The impacts of TCD result in increasing the fuel enthalpy and the fuel centerline temperature. The impact on the fuel enthalpy due to TCD would be negligible for fresh fuel even though the maximum power peaking factors exist in the low burnup fuel in the APR1400 reload core designs. For the high burnup fuel which is affected by TCD, the fuel enthalpy and the fuel centerline temperature increase due to TCD are not significant because of the peaking factor burndown effect at higher burnups. The event specific evaluation considering the TCD penalty described in the Section 3.5 was performed and described in DCD Tier 2 Chapter 15.4.8.”

Impact on DCD

Effect on the Design Control Document (DCD) Tier 2 Chapter 15.4.8 for safety analyses will be updated because interface data results based on the thermal conductivity degradation (TCD) penalty methodology are applied.

In addition, for an extent of content review, TCD-affected chapters will be revised as indicated on the attached markups. The attached markups are classified as follow.

- References (Chapter 4.2.6) : Attachment 2
- Control Requirements (Chapter 4.3.2.4) : Attachment 3
- Containment Functional Design (Chapter 6.2.1) : Attachment 4
- Containment Functional Design (Chapter 6.2.1) : Attachment 5
- Criticality Safety of New Spent Fuel Storage (Chapter 9.1.1) : Attachment 6
- General Information for Safety Analysis (Chapter 15.0.0) and Spectrum of Control Element Assembly Ejection Accidents (15.4.8) : Attachment 7
- Loss-of-Coolant Accidents (Chapter 15.6.5) : Attachment 8

Impact on PRA

There is no impact on the PRA.

Impact on Technical Specifications

There is no impact on the Technical Specifications.

Impact on Technical/Topical/Environmental Reports

PLUS7 fuel design topical report (APR1400-F-M-TR-13001-P) will be revised as indicated on the attached markups (Attachment 1).

Criticality Analysis technical report (APR1400-Z-A-NR-14011-P) will be revised as indicated on the attached markups (Attachment 9).

Non Proprietary

PLUS7 FUEL DESIGN for the APR1400

APR1400-F-M-TR-13001-P Rev.0

Considering the amount of potential increase in rod internal pressure by TCD impact and design margin to the limit, it is judged that the cladding stress criteria are still met with consideration of TCD.

3.4.2 Cladding Strain and Fatigue

The cladding strain is affected by TCD due to the increased fuel thermal expansion. However, the increased thermal expansion can be offset with available design margin to the cladding strain and fatigue limits and conservatism in the input variables such as power history and assumed rod internal pressure. Therefore, cladding strain and fatigue criteria are still satisfied with consideration of TCD.

3.4.3 Fuel Rod Internal Pressure

The effect of increased fuel temperature due to TCD on fission gas release is inherently accounted for in the current performance code, FATES3B (References 3-1 through 3-4) because the model was calibrated to measured data for a full range of fuel rod burnup and operating conditions. Additionally, conservatism is considered in the original FATES3B calibration process and in fuel rod design analysis. However, the rod internal pressure may still increase with TCD due to the increased fuel thermal expansion, which reduces the total fuel rod void volume.

Evaluations show that the reduction of void volume due to increased thermal expansion is not significant in PLUS7 fuel rod design. In addition, the rod internal pressure limit calculation is inherently conservative in that actual gap reopening is predicted to occur at higher pressures.

In conclusion, the increased rod internal pressure can be offset with available design margin to the rod internal pressure limits. Therefore, rod internal pressure criteria are still satisfied considering the effects of TCD.

3.4.4 Overheating of Fuel Pellets

The power to melt limit depends on fuel burnup but the reduced power capability with burnup, which is caused by the depletion of the fissile material in the fuel and the buildup of fission products, offsets the TCD impact. Therefore, it is judged that there will be no safety concerns due to TCD. However, the power to melt values with burnup considering the impact of TCD are calculated and will be provided in the TCD Technical Report which will be submitted to NRC.

In summary, KNF fuel rod design criteria have been reviewed with respect to the potential impacts of TCD, and it is concluded that TCD can be accommodated such that approved fuel rod design criteria will remain satisfied for current fuel rod designs.

3.5 Conclusion

The PLUS7 fuel rod design is verified to maintain the rod integrity up to rod average burnup of 60,000 MWD/MTU based on the thermal performance and mechanical integrity evaluation results

3.4.5 Impacts of Fuel Enthalpy

The impacts of TCD result in increasing the fuel enthalpy and the fuel centerline temperature. The impact on the fuel enthalpy due to TCD would be negligible for fresh fuel even though the maximum power peaking factors exist in the low burnup fuel in the APR1400 reload core designs. For the high burnup fuel which is affected by TCD, the fuel enthalpy and the fuel centerline temperature increase due to TCD are not significant because of the peaking factor burndown effect at higher burnups. The detailed evaluation was performed for the impacts of TCD and submitted in TCD Technical Report in Reference 3-14.

KHNP

3-17

This Chapter 3.4.5 will be modified and moved to in the next newly added page.

3.5.2 Fuel Rod Interface Data for Safety Analyses

To generate the fuel rod interface data with TCD effect for safety analyses, the TCD penalty determined as a function of burnup is added to the temperatures calculated by FATES3B code and those TCD penalty-added centerline temperatures of hot and average rod should be provided to safety analyses team.

3.6 Impact of Fuel Enthalpy

The impacts of TCD result in increasing the fuel enthalpy and the fuel centerline temperature. The impact on the fuel enthalpy due to TCD would be negligible for fresh fuel even though the maximum power peaking factors exist in the low burnup fuel in the APR1400 reload core designs. For the high burnup fuel which is affected by TCD, the fuel enthalpy and the fuel centerline temperature increase due to TCD are not significant because of the peaking factor burndown effect at higher burnups. The event specific evaluation considering the TCD penalty described in the Section 3.5 was performed and described in DCD Tier 2 Chapter 15.4.8.

3.7 Conclusion

The PLUS7 fuel rod design criteria considering TCD effect is evaluated using NRC approved FATES3B code and verified acceptable up to rod average burnup of 60,000 MWd/MTU. In addition, the potential impact of TCD on the fuel rod design criteria was evaluated, and it is concluded that TCD can be accommodated. Fuel rod interface data accounting for TCD penalty are generated and transmitted to safety analyses team.

Chapter 3.4.5 for enthalpy is moved to new Chapter 3.6

Note: This page is newly added to reflect the TCD effect. This page is same with the Attachment 1 (7/11) in response to RAI 5-7954 Question 12.

4.2.6 References

1. 10 CFR Part 50, Appendix A, General Design Criterion for Nuclear Power Plants 10, "Reactor Design," U.S. Nuclear Regulatory Commission.
2. 10 CFR Part 50, Appendix A, General Design Criterion for Nuclear Power Plants 27, "Combined Reactivity Control Systems Capability," U.S. Nuclear Regulatory Commission.
3. 10 CFR Part 50, Appendix A, General Design Criterion for Nuclear Power Plants 35, "Emergency Core Cooling," U.S. Nuclear Regulatory Commission.
4. 10 CFR 50.46, "Acceptance criteria for emergency core cooling systems for light-water nuclear power reactors," U.S. Nuclear Regulatory Commission.
5. APR1400-F-M-TR-13001-P (Proprietary) & NP (Non-Proprietary), "PLUS7 Fuel Design for the APR1400, ~~Rev. 0, KHNP, August 2013.~~ Rev. 1 to be issued.
6. NUREG-0800, Standard Review Plan, Section 4.2, "Fuel System Design," Rev. 3, U.S. Nuclear Regulatory Commission, March 2007.
7. CENPD-404-P-A, "Implementation of ZIRLO™ Cladding Material in CE Nuclear Power Fuel Assembly Designs," Rev. 0, Combustion Engineering, Inc., November 2001.
8. WCAP-12610-P-A, "VANTAGE+ Fuel Assembly Reference Core Report," Westinghouse Electric Corporation, April 1995.
9. W. J. O'Donnell and B. F. Langer, "Fatigue Design Basis for Zircaloy Components," Nuc. Sci. Eng., Vol. 20, pp. 1-12, April 1964.
10. Conway, J. B., "The Thermal Expansion and Heat Capacity of UO₂ to 2200 °C," E-NMPD-TM-63-6-6.
11. Christensen, J. A., "Thermal Expansion and Change in Volume on Melting for Uranium Dioxide," HW-75148, October 1962.
12. Jones, J. M. and Murchison D. G., "Optical Properties of Uranium Oxides," Nature, Vol. 205, pp. 663-65, February 1965.

coefficient, is described in Subsection 4.3.2.3.2 and shown in Figures 4.3-31 and 4.3-32. The second factor ($\delta T_m / \delta p$) of the second term is a constant because the moderator temperature is controlled to be a linear function of power.

Because the fuel temperature coefficient ($\delta \rho / \delta T_f$) and moderator temperature coefficient ($\delta \rho / \delta T_m$) are functions of one or more independent variables (e.g., burnup, temperature, soluble boron content, xenon worth, CEA insertion), the total power coefficient, dp/dp , also depends on these variables.

The power coefficient tends to become more negative with burnup because the fuel and moderator temperature coefficients become more negative as shown in Figures 4.3-30 through 4.3-32. Insertion of the CEAs, while maintaining constant power, results in a more negative power coefficient because the soluble boron level is reduced and because of the spectral effects of the CEAs themselves. The full-power values of the overall power coefficient for the unrodded core at the beginning and end of the first cycle are shown in Table 4.3-4.

4.3.2.4 Control Requirements

The three basic types of control requirements that influence the design of this reactor are:

4.3.2.3.8 Impact of Thermal Conductivity Degradation on Reactivity Coefficients

The fuel temperature increase due to thermal conductivity degradation (TCD) could have impacts on the prediction results of the fuel temperature coefficients and the core average reactivity due to the change in reactivity feedback of fuel temperature. The least negative or the most negative fuel temperature coefficients are used for safety analysis on an event specific basis, which is limiting for the transient. The fuel temperature coefficients are calculated using the effective fuel temperature changes which are caused by power changes and the corresponding reactivity changes. The nodal average effective fuel temperature correlation as a function of the burnup and linear power density is determined based on the fuel temperatures generated by FATES (References 2 and 3) as described in Subsection 4.3.2.3.7. The prediction results of the reactivity parameters using the effective fuel temperature correlation combined with current nuclear cross section models of DIT (Subsection 4.3.3.1.1.3) have been validated through the operation of OPR1000 plants with designs similar to those of APR1400 in terms of fuel design, operating temperatures and linear power density.

The limiting reactivity parameters based on the fuel temperature correlation and the cross section data are used as input for the safety analysis with the biases and uncertainties which have been determined through the comparison of prediction data to the plant measurement data. Therefore, the reactivity parameters implicitly include the impact of TCD in APR1400 nuclear design since the effective fuel temperature correlations and the biases and uncertainties have been validated against plant measurements.

6.2.1.3.2 Energy Sources

The following sources of generated and stored energy in the RCS and secondary coolant system are considered:

- a. Primary coolant
- b. Secondary coolant
- c. Primary walls (including reactor internals)
- d. Secondary walls
- e. Safety injection water
- f. Core power
- g. Decay heat

The core stored energy may be increased by the thermal conductivity degradation (TCD). The containment peak pressure with the TCD effect is slightly higher by 0.63 psi than the case without TCD. The TCD effect on the LOCA is negligible. The detailed methodology descriptions and M/E and P/T results of the TCD effect analysis are provided in Section 3 of Reference 3.

For the conservative analysis, the assumptions about the energy sources are biased to maximize the stored energy.

For considering the stored energy in the coolant, the initial RCS water volumes are conservatively calculated based on the maximum manufacturing tolerances of the reactor vessel and steam generator tubes. Volume expansion of the loop components from cold to hot operating conditions is also considered for the primary and secondary coolant stored energy. The initial water volume in the pressurizer includes an allowance for level instrumentation error. This makes the maximized pressurizer water volume, which includes the maximized stored energy.

For considering the stored energy in the primary and secondary walls, the large specific heat and heat conductivity of carbon steel are conservatively assumed for all of the walls in the RCS.

~~The core stored energy may be increased slightly by thermal conductivity degradation (TCD). However, the effect of TCD on the M&E release is negligible. The results are described in Reference 5.~~

For considering the energy in the safety injection water, the liquid break flow is assumed to be mixed with the water in IRWST. The mixed water is taken and discharged into the

The total volume of fluid for two steam lines between the MSIVs and a steam generator is assumed to be the maximum in the analysis. The total volume of fluid between the MSIVs and the turbine stop valves is also assumed to be the maximum in the analysis. The analysis credits the energy stored in the steam and liquid in the affected steam generator.

There are two MFIVs in each feedwater line. The total volume of fluid between the upstream MFIV and each steam generator is assumed to be the maximum. The flashing of this fluid into the affected steam generator and then into the containment is considered in the analysis. These assumed volumes conservatively exceed the actual design values of the APR1400 volumes.

The sources of energy considered in the MSLB analysis include the stored energy in the (1) affected steam generator's metal, including the steam generator tube, (2) water in the affected steam generator, (3) feedwater transferred to the affected steam generator before the closure of the MFIV, and (4) steam from the unaffected steam generator before the closure of the MSIV. The energy sources that are considered also include the energy transferred from the primary coolant to the water in the affected steam generator during blowdown.

6.2.1.4.1 Mass and Energy Release Data

Mass and energy release data for the MSLB cases listed in Table 6.2.1-1 are given in Tables 6.2.1-9 through 6.2.1-18.

6.2.1.4.2 Single Failure Analysis

Non-class 1E electric power is conservatively assumed to be available because it allows the continuation of reactor coolant pump operation, which maximizes the rate of heat transfer to the affected steam generator, which maximizes the rate of an M&E release. With the availability of Non-class 1E electric power, a postulated diesel generator failure is unnecessary.

There is an MSIV in each main steam line. The MSIVs are designed to close based on a conservative calculation that maximizes the dynamic pressure loading on the valve for all possible flow rates and qualities. Each valve has dual control circuits to provide reasonable assurance of closure even with a single failure in the control system. Each valve is tested periodically. A single failure in the actuation signal does not prevent valve

The core stored energy may be increased by the thermal conductivity degradation (TCD). The containment peak pressure with the TCD effect is slightly higher by 0.33 psi than the case without TCD. The TCD effect on the MSLB is negligible. The detailed methodology descriptions and M/E and P/T results of the TCD effect analysis are provided in Section 3 of Reference 3

Table 6.2.1-4 (1 of 25)

Double-Ended Suction Leg Slot Break – Maximum SIS Flow
(0.9121 m² (9.8175 ft²) Total Break Area)

Part A. Mass and Energy Release Data
 (Blowdown Period)

| Time (sec) | Break Mass Flow Rate | | Break Enthalpy | |
|------------|----------------------|------------|----------------|---------|
| | kg/sec | lbm/sec | kcal/kg | Btu/lbm |
| 0.000 | 0.00 | 0.00 | 0.00 | 0.00 |
| 0.027 | 35,826.69 | 78,984.75 | 310.61 | 559.13 |
| 0.054 | 35,499.95 | 78,264.39 | 310.08 | 558.18 |
| 0.103 | 35,936.95 | 79,227.82 | 309.90 | 557.85 |
| 0.152 | 49,099.29 | 108,245.97 | 310.38 | 558.72 |
| 0.202 | 47,285.37 | 104,246.94 | 311.04 | 559.91 |
| 0.252 | 45,576.63 | 100,479.79 | 311.57 | 560.85 |
| 0.298 | 44,683.04 | 98,509.75 | 311.94 | 561.52 |
| 0.351 | 44,779.94 | 98,723.38 | 312.17 | 561.94 |
| 0.400 | 44,346.29 | 97,767.34 | 312.52 | 562.56 |
| 0.603 | 43,478.91 | 95,855.09 | 313.48 | 564.30 |
| 0.800 | 44,864.47 | 98,909.74 | 314.64 | 566.38 |
| 1.000 | 42,167.46 | 92,963.82 | 315.74 | 568.36 |
| 1.202 | 40,552.76 | 89,404.00 | 317.33 | 571.22 |
| 1.401 | 38,527.59 | 84,939.24 | 319.05 | 574.33 |
| 1.607 | 38,152.42 | 84,112.13 | 320.39 | 576.73 |
| 1.800 | 37,859.70 | 83,466.78 | 321.87 | 579.40 |
| 2.001 | 37,500.04 | 82,673.88 | 323.76 | 582.80 |
| 2.204 | 35,984.54 | 79,332.74 | 325.55 | 586.03 |
| 2.407 | 33,372.26 | 73,573.62 | 326.50 | 587.73 |
| 2.601 | 31,669.84 | 69,820.41 | 327.91 | 590.27 |
| 2.812 | 30,653.27 | 67,579.23 | 330.85 | 595.57 |
| 3.008 | 29,668.44 | 65,408.05 | 334.73 | 602.56 |
| 3.208 | 28,297.64 | 62,385.94 | 340.03 | 612.09 |
| 3.408 | 26,715.66 | 58,898.26 | 346.75 | 624.19 |

Replace these 25 pages of Table 6.2.1-4 with the following 25 pages of revised Table 6.2.1-4.

Table 6.2.1-4 (2 of 25)

Part A. Mass and Energy Release Data (Blowdown Period)

| Time (sec) | Break Mass Flow Rate | | Break Enthalpy | |
|------------|----------------------|-----------|----------------|---------|
| | kg/sec | lbm/sec | kcal/kg | Btu/lbm |
| 3.608 | 24,966.73 | 55,042.51 | 354.00 | 637.23 |
| 3.808 | 23,497.04 | 51,802.38 | 360.32 | 648.62 |
| 4.000 | 22,127.47 | 48,782.98 | 365.48 | 657.89 |
| 4.211 | 21,436.30 | 47,259.20 | 366.85 | 660.37 |
| 4.409 | 21,008.90 | 46,316.93 | 366.71 | 660.11 |
| 4.609 | 20,598.55 | 45,412.26 | 366.16 | 659.12 |
| 4.809 | 20,267.22 | 44,681.81 | 365.67 | 658.24 |
| 5.009 | 20,051.87 | 44,207.03 | 364.92 | 656.90 |
| 5.209 | 19,841.27 | 43,742.73 | 364.35 | 655.86 |
| 5.409 | 19,815.87 | 43,686.73 | 363.56 | 654.45 |
| 5.609 | 19,693.35 | 43,416.63 | 363.47 | 654.28 |
| 5.809 | 19,144.10 | 42,205.74 | 364.81 | 656.69 |
| 6.009 | 18,734.91 | 41,303.63 | 365.84 | 658.55 |
| 6.209 | 18,566.23 | 40,931.75 | 365.82 | 658.51 |
| 6.409 | 18,595.07 | 40,995.33 | 363.92 | 655.09 |
| 6.609 | 18,479.62 | 40,740.79 | 363.55 | 654.43 |
| 6.809 | 17,933.49 | 39,536.78 | 366.91 | 660.48 |
| 7.009 | 17,132.26 | 37,770.38 | 372.47 | 670.48 |
| 7.209 | 16,620.46 | 36,642.04 | 375.29 | 675.57 |
| 7.409 | 16,372.62 | 36,095.63 | 375.88 | 676.62 |
| 7.609 | 16,206.97 | 35,730.45 | 376.05 | 676.92 |
| 7.809 | 16,191.18 | 35,695.62 | 374.41 | 673.98 |
| 8.009 | 16,125.16 | 35,550.08 | 373.73 | 672.75 |
| 8.209 | 15,915.11 | 35,086.98 | 374.73 | 674.55 |
| 8.409 | 15,680.94 | 34,570.74 | 375.85 | 676.56 |
| 8.609 | 15,427.32 | 34,011.60 | 377.17 | 678.94 |
| 8.809 | 15,141.74 | 33,381.99 | 378.82 | 681.91 |
| 9.005 | 14,809.07 | 32,648.58 | 380.75 | 685.38 |

Replace these 25 pages of Table 6.2.1-4 with the following 25 pages of revised Table 6.2.1-4.

Table 6.2.1-4 (3 of 25)

Part A. Mass and Energy Release Data
(Blowdown Period)

| Time (sec) | Break Mass Flow Rate | | Break Enthalpy | |
|------------|----------------------|-----------|----------------|---------|
| | kg/sec | lbm/sec | kcal/kg | Btu/lbm |
| 9.204 | 14,527.77 | 32,028.41 | 382.90 | 689.26 |
| 9.400 | 14,196.28 | 31,297.60 | 385.45 | 693.86 |
| 9.608 | 13,797.32 | 30,418.04 | 387.37 | 697.31 |
| 9.801 | 13,391.38 | 29,523.09 | 391.81 | 705.30 |
| 10.004 | 13,129.00 | 28,944.65 | 395.88 | 712.62 |
| 10.205 | 12,765.77 | 28,143.85 | 399.12 | 718.46 |
| 10.404 | 12,429.45 | 27,402.39 | 401.76 | 723.21 |
| 10.603 | 11,985.20 | 26,422.98 | 406.03 | 730.90 |
| 10.799 | 11,582.15 | 25,534.40 | 412.05 | 741.74 |
| 11.004 | 11,140.57 | 24,560.87 | 417.73 | 751.96 |
| 11.205 | 10,637.22 | 23,451.17 | 423.35 | 762.07 |
| 11.406 | 10,190.47 | 22,466.27 | 428.61 | 771.53 |
| 11.601 | 9,728.82 | 21,448.50 | 433.53 | 780.39 |
| 11.804 | 9,042.09 | 19,934.50 | 445.87 | 802.61 |
| 12.006 | 8,756.29 | 19,304.41 | 452.29 | 814.16 |
| 12.205 | 8,377.30 | 18,468.88 | 457.85 | 824.18 |
| 12.406 | 8,013.92 | 17,667.76 | 463.75 | 834.79 |
| 12.599 | 7,657.53 | 16,882.05 | 469.08 | 844.38 |
| 12.806 | 7,397.99 | 16,309.86 | 475.41 | 855.78 |
| 13.005 | 7,153.35 | 15,770.51 | 476.56 | 857.85 |
| 13.213 | 6,944.67 | 15,310.45 | 475.99 | 856.84 |
| 13.413 | 6,730.23 | 14,837.69 | 477.18 | 858.98 |
| 13.613 | 6,534.48 | 14,406.13 | 479.25 | 862.71 |
| 13.813 | 6,358.64 | 14,018.47 | 480.50 | 864.96 |
| 14.013 | 6,188.02 | 13,642.32 | 481.42 | 866.61 |
| 14.203 | 5,966.42 | 13,153.78 | 482.94 | 869.34 |
| 14.409 | 5,852.22 | 12,902.00 | 478.07 | 860.57 |
| 14.616 | 5,895.97 | 12,998.45 | 457.84 | 824.16 |

Replace these 25 pages of Table 6.2.1-4
with the following 25 pages of revised
Table 6.2.1-4.

Table 6.2.1-4 (4 of 25)

Part A. Mass and Energy Release Data (Blowdown Period)

| Time (sec) | Break Mass Flow Rate | | Break Enthalpy | |
|------------|----------------------|-----------|----------------|---------|
| | kg/sec | lbm/sec | kcal/kg | Btu/lbm |
| 14.816 | 5,885.88 | 12,976.22 | 441.01 | 793.86 |
| 15.016 | 5,839.74 | 12,874.49 | 431.85 | 777.37 |
| 15.214 | 5,717.91 | 12,605.89 | 425.51 | 765.97 |
| 15.409 | 5,579.03 | 12,299.72 | 419.00 | 754.25 |
| 15.609 | 5,389.08 | 11,880.96 | 415.55 | 748.04 |
| 15.809 | 5,183.01 | 11,426.64 | 413.16 | 743.74 |
| 16.009 | 4,939.96 | 10,890.80 | 411.96 | 741.57 |
| 16.200 | 4,374.29 | 9,643.72 | 443.96 | 799.17 |
| 16.400 | 4,198.25 | 9,255.61 | 443.34 | 798.06 |
| 16.601 | 4,077.66 | 8,989.74 | 441.21 | 794.23 |
| 16.800 | 3,932.45 | 8,669.61 | 438.05 | 788.53 |
| 17.001 | 3,815.63 | 8,412.08 | 433.55 | 780.43 |
| 17.205 | 3,707.03 | 8,172.64 | 424.86 | 764.79 |
| 17.400 | 3,576.74 | 7,885.40 | 419.56 | 755.24 |
| 17.600 | 3,431.20 | 7,564.54 | 416.49 | 749.73 |
| 17.800 | 3,384.27 | 7,461.08 | 407.89 | 734.25 |
| 18.000 | 3,343.38 | 7,370.94 | 401.24 | 722.27 |
| 18.200 | 3,122.01 | 6,882.88 | 401.21 | 722.22 |
| 18.400 | 3,066.26 | 6,759.98 | 391.83 | 705.34 |
| 18.600 | 2,962.81 | 6,531.92 | 382.50 | 688.54 |
| 18.802 | 2,774.26 | 6,116.24 | 381.33 | 686.43 |
| 18.999 | 2,608.38 | 5,750.52 | 378.21 | 680.83 |
| 19.203 | 2,546.44 | 5,613.97 | 383.68 | 690.67 |

Integral Mass and Energy Release at End of Blowdown

| Time (sec) | Integral Mass | | Integral Energy | |
|------------|---------------|-------------|-----------------|-------------|
| | kg | lbm | Million kcal | Million Btu |
| 19.203 | 304,940.875 | 672,283.090 | 110.483 | 438.461 |

Replace these 25 pages of Table 6.2.1-4 with the following 25 pages of revised Table 6.2.1-4.

Table 6.2.1-4 (4 of 25)

Part A. Mass and Energy Release Data (Blowdown Period)

| Time (sec) | Break Mass Flow Rate | | Break Enthalpy | |
|------------|----------------------|-----------|----------------|---------|
| | kg/sec | lbm/sec | kcal/kg | Btu/lbm |
| 14.816 | 5,885.88 | 12,976.22 | 441.01 | 793.86 |
| 15.016 | 5,839.74 | 12,874.49 | 431.85 | 777.37 |
| 15.214 | 5,717.91 | 12,605.89 | 425.51 | 765.97 |
| 15.409 | 5,579.03 | 12,299.72 | 419.00 | 754.25 |
| 15.609 | 5,389.08 | 11,880.96 | 415.55 | 748.04 |
| 15.809 | 5,183.01 | 11,426.64 | 413.16 | 743.74 |
| 16.009 | 4,939.96 | 10,890.80 | 411.96 | 741.57 |
| 16.200 | 4,374.29 | 9,643.72 | 443.96 | 799.17 |
| 16.400 | 4,198.25 | 9,255.61 | 443.34 | 798.06 |
| 16.601 | 4,077.66 | 8,989.74 | 441.21 | 794.23 |
| 16.800 | 3,932.45 | 8,669.61 | 438.05 | 788.53 |
| 17.001 | 3,815.63 | 8,412.08 | 433.55 | 780.43 |
| 17.205 | 3,707.03 | 8,172.64 | 424.86 | 764.79 |
| 17.400 | 3,576.74 | 7,885.40 | 419.56 | 755.24 |
| 17.600 | 3,431.20 | 7,564.54 | 416.49 | 749.73 |
| 17.800 | 3,384.27 | 7,461.08 | 407.89 | 734.25 |
| 18.000 | 3,343.38 | 7,370.94 | 401.24 | 722.27 |
| 18.200 | 3,122.01 | 6,882.88 | 401.21 | 722.22 |
| 18.400 | 3,066.26 | 6,759.98 | 391.83 | 705.34 |
| 18.600 | 2,962.81 | 6,531.92 | 382.50 | 688.54 |
| 18.802 | 2,774.26 | 6,116.24 | 381.33 | 686.43 |
| 18.999 | 2,608.38 | 5,750.52 | 378.21 | 680.83 |
| 19.203 | 2,546.44 | 5,613.97 | 383.68 | 690.67 |

Integral Mass and Energy Release at End of Blowdown

| Time (sec) | Integral Mass | | Integral Energy | |
|------------|---------------|-------------|-----------------|-------------|
| | kg | lbm | Million kcal | Million Btu |
| 19.203 | 304,940.875 | 672,283.090 | 110.483 | 438.461 |

Replace these 25 pages of Table 6.2.1-4 with the following 25 pages of revised Table 6.2.1-4.

Table 6.2.1-4 (5 of 25)

Part A. Mass and Energy Release Data (Reflood and Post-reflood Period)

| Time (sec) | Break Mass Flow Rate | | Break Enthalpy | |
|------------|----------------------|----------|----------------|----------|
| | kg/sec | lbm/sec | kcal/kg | Btu/lbm |
| 19.20 | 0.00 | 0.00 | 0.00 | 0.00 |
| 19.30 | 66.99 | 147.69 | 705.17 | 1,269.37 |
| 19.40 | 89.74 | 197.84 | 704.39 | 1,267.98 |
| 21.40 | 188.20 | 414.92 | 706.66 | 1,272.06 |
| 23.40 | 443.15 | 976.98 | 709.46 | 1,277.10 |
| 25.40 | 653.90 | 1,441.61 | 708.54 | 1,275.45 |
| 27.90 | 854.83 | 1,884.59 | 706.02 | 1,270.91 |
| 28.00 | 861.36 | 1,898.99 | 705.91 | 1,270.71 |
| 28.10 | 503.31 | 1,109.62 | 705.80 | 1,270.51 |
| 28.20 | 506.33 | 1,116.27 | 705.69 | 1,270.32 |
| 32.20 | 495.32 | 1,091.99 | 703.65 | 1,266.65 |
| 36.20 | 482.35 | 1,063.40 | 701.74 | 1,263.20 |
| 40.20 | 469.72 | 1,035.56 | 699.87 | 1,259.84 |
| 44.20 | 457.41 | 1,008.43 | 698.06 | 1,256.59 |
| 48.20 | 445.46 | 982.07 | 696.27 | 1,253.35 |
| 52.20 | 433.85 | 956.47 | 694.47 | 1,250.12 |
| 56.20 | 422.51 | 931.49 | 692.72 | 1,246.97 |
| 60.20 | 411.46 | 907.12 | 691.01 | 1,243.89 |
| 63.60 | 402.29 | 886.90 | 689.57 | 1,241.30 |
| 63.70 | 402.03 | 886.32 | 689.52 | 1,241.21 |
| 63.80 | 692.50 | 1,526.72 | 689.49 | 1,241.15 |
| 63.90 | 691.55 | 1,524.61 | 689.45 | 1,241.08 |
| 65.60 | 673.65 | 1,485.15 | 688.93 | 1,240.14 |
| 67.30 | 658.82 | 1,452.46 | 688.38 | 1,239.16 |
| 69.00 | 646.15 | 1,424.53 | 687.82 | 1,238.14 |
| 70.70 | 635.81 | 1,401.72 | 687.22 | 1,237.07 |
| 72.40 | 626.95 | 1,382.20 | 686.79 | 1,236.29 |
| 74.10 | 619.36 | 1,365.47 | 686.15 | 1,235.13 |

Replace these 25 pages of Table 6.2.1-4 with the following 25 pages of revised Table 6.2.1-4.

Table 6.2.1-4 (6 of 25)

Part A. Mass and Energy Release Data (Reflood and Post-reflood Period)

| Time (sec) | Break Mass Flow Rate | | Break Enthalpy | |
|------------|----------------------|----------|----------------|----------|
| | kg/sec | lbm/sec | kcal/kg | Btu/lbm |
| 75.80 | 612.76 | 1,350.91 | 685.48 | 1,233.94 |
| 77.50 | 606.95 | 1,338.10 | 684.81 | 1,232.73 |
| 79.20 | 601.78 | 1,326.70 | 684.12 | 1,231.49 |
| 80.90 | 597.13 | 1,316.46 | 683.42 | 1,230.23 |
| 82.90 | 592.23 | 1,305.65 | 681.49 | 1,226.76 |
| 83.00 | 585.05 | 1,289.83 | 668.58 | 1,203.50 |
| 83.10 | 610.73 | 1,346.43 | 679.60 | 1,223.34 |
| 83.20 | 560.47 | 1,235.63 | 669.16 | 1,204.56 |
| 83.30 | 597.41 | 1,317.06 | 668.14 | 1,202.71 |
| 83.40 | 589.89 | 1,300.49 | 668.27 | 1,202.95 |
| 85.40 | 499.76 | 1,101.78 | 670.44 | 1,206.86 |
| 87.40 | 454.05 | 1,001.02 | 671.43 | 1,208.65 |
| 89.40 | 419.27 | 924.34 | 672.14 | 1,209.92 |
| 91.40 | 389.59 | 858.91 | 672.76 | 1,211.03 |
| 93.40 | 363.41 | 801.18 | 673.34 | 1,212.09 |
| 95.40 | 339.97 | 749.51 | 673.92 | 1,213.12 |
| 97.40 | 318.87 | 702.99 | 674.47 | 1,214.11 |
| 99.40 | 299.77 | 660.89 | 675.01 | 1,215.08 |
| 101.40 | 282.41 | 622.62 | 675.53 | 1,216.03 |
| 103.40 | 266.57 | 587.69 | 676.05 | 1,216.96 |
| 105.40 | 252.05 | 555.68 | 676.56 | 1,217.87 |
| 107.40 | 238.70 | 526.25 | 677.05 | 1,218.77 |
| 109.40 | 226.39 | 499.10 | 677.54 | 1,219.65 |
| 110.10 | 222.30 | 490.09 | 677.71 | 1,219.95 |
| 110.20 | 221.72 | 488.82 | 677.74 | 1,220.00 |
| 110.30 | 221.15 | 487.55 | 677.77 | 1,220.06 |
| 111.30 | 216.37 | 477.02 | 676.39 | 1,217.57 |
| 112.30 | 116.80 | 257.51 | 698.56 | 1,257.48 |

Replace these 25 pages of Table 6.2.1-4 with the following 25 pages of revised Table 6.2.1-4.

Table 6.2.1-4 (7 of 25)

Part A: Mass and Energy Release Data (Reflood and Post-reflood Period)

| Time (sec) | Break Mass Flow Rate | | Break Enthalpy | |
|---------------|----------------------|---------|----------------|----------|
| | kg/sec | lbm/sec | kcal/kg | Btu/lbm |
| 117.30 | 256.62 | 565.75 | 668.68 | 1,203.69 |
| 118.30 | 247.62 | 545.92 | 668.71 | 1,203.75 |
| 119.30 | 234.21 | 516.34 | 669.12 | 1,204.48 |
| 120.30 | 224.89 | 495.80 | 669.30 | 1,204.81 |
| 121.30 | 217.46 | 479.43 | 669.39 | 1,204.97 |
| 122.30 | 212.74 | 469.02 | 669.32 | 1,204.85 |
| 123.30 | 213.77 | 471.29 | 668.89 | 1,204.06 |
| 124.90 | 94.67 | 208.72 | 690.29 | 1,242.59 |
| 125.00 | 76.66 | 169.01 | 703.26 | 1,265.94 |

Integral Mass and Energy Release at the End of Reflood and Post-reflood

| Time (sec) | Integral Mass | | Integral Energy | |
|---------------|---------------|-----------|-----------------|-------------|
| | kg | lbm | Million kcal | Million Btu |
| 110.20 | 41,755.23 | 92,055.00 | 28.806 | 114.317 |
| 125.00 | 44,853.70 | 98,886.00 | 30.891 | 122.593 |

Replace these 25 pages of Table 6.2.1-4 with the following 25 pages of revised Table 6.2.1-4.

Table 6.2.1-4 (8 of 25)

Part A: Spillage Release Data (Reactor Vessel Side)
(Reflood and Post-Reflood Period)

| Time (sec) | Break Mass Flow Rate | | Break Enthalpy | |
|---------------|----------------------|----------|----------------|---------|
| | kg/sec | lbm/sec | kcal/kg | Btu/lbm |
| 19.20 | 0.00 | 0.00 | 0.00 | 0.00 |
| 19.30 | 0.00 | 0.00 | 0.00 | 0.00 |
| 28.00 | 0.00 | 0.00 | 0.00 | 0.00 |
| 28.10 | 701.48 | 1,546.51 | 390.64 | 703.18 |
| 28.20 | 1,438.30 | 3,170.92 | 217.00 | 390.63 |
| 32.20 | 1,274.95 | 2,810.80 | 233.78 | 420.83 |
| 36.20 | 1,151.76 | 2,539.21 | 247.58 | 445.66 |
| 40.20 | 1,053.60 | 2,322.81 | 259.77 | 467.61 |
| 44.20 | 974.39 | 2,148.18 | 270.30 | 486.57 |
| 48.20 | 909.86 | 2,005.91 | 279.16 | 502.52 |
| 52.20 | 856.97 | 1,889.30 | 286.34 | 515.44 |
| 56.20 | 813.57 | 1,793.62 | 291.82 | 525.30 |
| 60.20 | 777.94 | 1,715.08 | 295.65 | 532.21 |
| 63.60 | 752.70 | 1,659.42 | 297.70 | 535.90 |
| 63.70 | 752.01 | 1,657.91 | 297.75 | 535.98 |
| 63.80 | 0.00 | 0.00 | 0.00 | 0.00 |
| 124.90 | 0.00 | 0.00 | 0.00 | 0.00 |
| 125.00 | 0.00 | 0.00 | 0.00 | 0.00 |

Integral Mass and Energy (Reactor Vessel Side Spillage) at EOR and EOPR

| Time (sec) | Integral Mass | | Integral Energy | |
|---------------|---------------|-----------|-----------------|-------------|
| | kg | lbm | Million kcal | Million Btu |
| 110.20 | 35,368.68 | 77,975.00 | 9.360 | 37.144 |
| 125.00 | 35,368.68 | 77,975.00 | 9.360 | 37.144 |

Replace these 25 pages of Table 6.2.1-4 with the following 25 pages of revised Table 6.2.1-4.

Table 6.2.1-4 (9 of 25)

Part A: Spillage Release Data (Steam Generator Side)
(Reflood and Post-Reflood Period)

| Time (sec) | Break Mass Flow Rate | Break Enthalpy | | |
|---------------|----------------------|----------------|---------|---------|
| | kg/sec | lbm/sec | kcal/kg | Btu/lbm |
| 19.20 | 0.00 | 0.00 | 0.00 | 0.00 |
| 19.30 | 0.00 | 0.00 | 0.00 | 0.00 |
| 82.90 | 0.00 | 0.00 | 0.00 | 0.00 |
| 83.00 | 9.01 | 19.86 | 144.35 | 259.85 |
| 83.10 | 0.00 | 0.00 | 0.00 | 0.00 |
| 83.20 | 32.76 | 72.23 | 144.33 | 259.81 |
| 83.30 | 25.68 | 56.62 | 144.33 | 259.80 |
| 83.40 | 25.42 | 56.05 | 144.32 | 259.79 |
| 85.40 | 192.20 | 423.73 | 144.33 | 259.81 |
| 87.40 | 258.03 | 568.86 | 144.33 | 259.81 |
| 89.40 | 293.32 | 646.67 | 144.33 | 259.81 |
| 91.40 | 318.76 | 702.74 | 144.33 | 259.81 |
| 93.40 | 339.49 | 748.46 | 144.33 | 259.81 |
| 95.40 | 357.45 | 788.05 | 144.33 | 259.81 |
| 97.40 | 373.17 | 822.71 | 144.33 | 259.81 |
| 99.40 | 387.04 | 853.28 | 144.33 | 259.81 |
| 101.40 | 399.32 | 880.36 | 144.33 | 259.81 |
| 103.40 | 410.25 | 904.46 | 144.33 | 259.81 |
| 105.40 | 420.02 | 925.98 | 144.33 | 259.81 |
| 107.40 | 428.77 | 945.28 | 144.33 | 259.81 |
| 109.40 | 436.63 | 962.62 | 144.33 | 259.81 |
| 110.10 | 439.20 | 968.28 | 144.33 | 259.81 |
| 110.20 | 439.56 | 969.07 | 144.33 | 259.81 |
| 110.30 | 439.92 | 969.86 | 144.33 | 259.81 |
| 111.30 | 198.74 | 438.16 | 144.33 | 259.81 |
| 112.30 | 855.78 | 1,886.69 | 144.33 | 259.81 |
| 113.30 | 172.40 | 380.08 | 144.33 | 259.81 |
| 114.30 | 702.47 | 1,548.70 | 144.33 | 259.81 |
| 115.30 | 230.40 | 507.94 | 144.33 | 259.81 |
| 116.30 | 204.39 | 450.61 | 144.33 | 259.81 |

Replace these 25 pages of Table 6.2.1-4
with the following 25 pages of revised
Table 6.2.1-4.

Table 6.2.1-4 (10 of 25)

Part A: Spillage Release Data (Steam Generator Side)
(Reflood and Post-Reflood Period)

| Time (sec) | Break Mass Flow Rate | | Break Enthalpy | |
|---------------|----------------------|----------|----------------|---------|
| | kg/sec | lbm/sec | kcal/kg | Btu/lbm |
| 117.30 | 188.59 | 415.78 | 144.33 | 259.81 |
| 118.30 | 185.85 | 409.74 | 144.33 | 259.81 |
| 119.30 | 188.16 | 414.83 | 144.33 | 259.81 |
| 120.30 | 191.74 | 422.71 | 144.33 | 259.81 |
| 121.30 | 196.42 | 433.03 | 144.33 | 259.81 |
| 122.30 | 202.25 | 445.88 | 144.33 | 259.81 |
| 123.30 | 212.01 | 467.41 | 144.33 | 259.81 |
| 124.90 | 230.93 | 509.12 | 144.33 | 259.81 |
| 125.00 | 486.16 | 1,071.80 | 144.33 | 259.81 |

Integral Mass and Energy (Steam Generator Side Spillage) at EOR and EOPR

| Time (sec) | Integral Mass | | Integral Energy | |
|---------------|---------------|-----------|-----------------|-------------|
| | kg | lbm | Million kcal | Million Btu |
| 110.20 | 9,245.07 | 20,382.00 | 1.334 | 5.296 |
| 125.00 | 20,837.47 | 45,939.00 | 3.007 | 11.935 |

Replace these 25 pages of Table 6.2.1-4 with the following 25 pages of revised Table 6.2.1-4.

Table 6.2.1-4 (11 of 25)

Part A. Mass and Energy (Steam) Release Data (Decay heat Period)

| Time (sec) | Mass Flow Rate | | Break Enthalpy | |
|---------------|----------------|---------|----------------|---------|
| | kg/sec | lbm/sec | kcal/kg | Btu/lbm |
| 400.0 | 56.03 | 123.53 | 653.58 | 1176.45 |
| 599.9 | 52.8 | 116.41 | 653.25 | 1175.86 |
| 800.0 | 50.34 | 110.98 | 653.02 | 1175.44 |
| 999.0 | 48.23 | 106.33 | 652.84 | 1175.12 |
| 1503.3 | 44.15 | 97.33 | 652.53 | 1174.55 |
| 1996.8 | 41.12 | 90.65 | 652.32 | 1174.18 |
| 4002.6 | 33.89 | 74.72 | 651.91 | 1173.43 |
| 6001.4 | 30.28 | 66.76 | 651.69 | 1173.04 |
| 8000.6 | 28.11 | 61.98 | 651.56 | 1172.82 |
| 9990.3 | 26.62 | 58.68 | 651.48 | 1172.66 |
| 15005.7 | 24.3 | 53.58 | 651.33 | 1172.4 |
| 20011.4 | 22.88 | 50.45 | 651.16 | 1172.09 |
| 40036.7 | 19.95 | 43.98 | 650.42 | 1170.75 |
| 59963.5 | 18.43 | 40.64 | 649.67 | 1169.4 |
| 79990.5 | 17.48 | 38.53 | 649.08 | 1168.34 |
| 100002.0 | 14.51 | 31.98 | 647.91 | 1166.24 |
| 150010.0 | 12.81 | 28.25 | 646.49 | 1163.68 |
| 200018.5 | 11.71 | 25.81 | 645.78 | 1162.4 |
| 400053.2 | 9.2 | 20.29 | 644.5 | 1160.1 |
| 600094.9 | 7.86 | 17.32 | 643.87 | 1158.97 |
| 800141.2 | 6.98 | 15.4 | 643.5 | 1158.3 |
| 1000000.0 | 6.38 | 14.06 | 643.25 | 1157.86 |

Integral Mass and Energy(Steam) Release at 24hours after postulated accident

| Time (sec) | Integral Mass | | Integral Energy | |
|---------------|---------------|------------|-----------------|-------------|
| | kg | lbm | Million kcal | Million Btu |
| 85,095 | 1,892,545 | 4,172,349 | 1,233.798 | 4,896.105 |
| 1,000,000 | 10,026,920 | 22,105,576 | 6,481.549 | 25,720.864 |

Replace these 25 pages of Table 6.2.1-4 with the following 25 pages of revised Table 6.2.1-4.

Table 6.2.1-4 (12 of 25)

Part A. Mass and Energy (Spillage) Release Data (Decay heat Period)

| Time (sec) | Mass Flow Rate | | Break Enthalpy | |
|------------|----------------|---------|----------------|---------|
| | kg/sec | lbm/sec | kcal/kg | Btu/lbm |
| 400.0 | 177.29 | 390.85 | 61.98 | 111.56 |
| 599.9 | 185.21 | 408.32 | 72.56 | 130.6 |
| 800.0 | 190.95 | 420.98 | 77.0 | 138.6 |
| 999.0 | 195.36 | 430.69 | 79.87 | 143.77 |
| 1503.3 | 202.54 | 446.53 | 85.32 | 153.57 |
| 1996.8 | 206.56 | 455.38 | 89.73 | 161.51 |
| 4002.6 | 212.4 | 468.26 | 102.2 | 183.95 |
| 6001.4 | 214.62 | 473.15 | 109.38 | 196.89 |
| 8000.6 | 215.72 | 475.59 | 113.68 | 204.62 |
| 9990.3 | 216.58 | 477.47 | 116.26 | 209.27 |
| 15005.7 | 218.08 | 480.79 | 119.07 | 214.32 |
| 20011.4 | 219.29 | 483.45 | 119.55 | 215.19 |
| 40036.7 | 222.57 | 490.69 | 116.79 | 210.23 |
| 59963.5 | 224.82 | 495.64 | 112.91 | 203.24 |
| 79990.5 | 226.39 | 499.11 | 109.68 | 197.43 |
| 100002.0 | 230.12 | 507.33 | 104.29 | 187.72 |
| 150010.0 | 233.44 | 514.66 | 95.1 | 171.19 |
| 200018.5 | 235.28 | 518.7 | 90.4 | 162.72 |
| 400053.2 | 238.93 | 526.76 | 81.43 | 146.58 |
| 600094.9 | 240.83 | 530.93 | 76.5 | 137.7 |
| 800141.2 | 242.0 | 533.52 | 73.4 | 132.13 |
| 1000000.0 | 242.8 | 535.29 | 71.26 | 128.26 |

Integral Mass and Energy(Spillage) Release at 24 hours after postulated accident

| Time (sec) | Integral Mass | | Integral Energy | |
|------------|---------------|-------------|-----------------|-------------|
| | kg | lbm | Million kcal | Million Btu |
| 85,095 | 18,940,481 | 41,756,614 | 2,154.820 | 8,551.016 |
| 1,000,000 | 237,863,121 | 524,398,419 | 19,724.139 | 78,271.706 |

Replace these 25 pages of Table 6.2.1-4 with the following 25 pages of revised Table 6.2.1-4.

Table 6.2.1-4 (13 of 25)

Part B. reactor Vessel Pressure vs. Time
(Blowdown Period)

| Time (sec) | Reactor Vessel Pressure | |
|------------|-------------------------|----------|
| | kg/cm ² A | psia |
| 0.000 | 167.36 | 2,380.40 |
| 0.027 | 159.52 | 2,268.90 |
| 0.054 | 147.05 | 2,091.50 |
| 0.103 | 125.06 | 1,778.70 |
| 0.152 | 126.83 | 1,804.00 |
| 0.202 | 126.45 | 1,798.60 |
| 0.252 | 125.82 | 1,789.60 |
| 0.298 | 125.29 | 1,782.10 |
| 0.351 | 123.83 | 1,761.30 |
| 0.400 | 123.02 | 1,749.70 |
| 0.603 | 120.51 | 1,714.00 |
| 0.800 | 118.85 | 1,690.50 |
| 1.000 | 117.11 | 1,665.70 |
| 1.202 | 114.64 | 1,630.50 |
| 1.401 | 112.52 | 1,600.40 |
| 1.607 | 111.04 | 1,579.30 |
| 1.800 | 109.75 | 1,561.00 |
| 2.001 | 108.13 | 1,538.00 |
| 2.204 | 106.14 | 1,509.70 |
| 2.407 | 104.53 | 1,486.80 |
| 2.601 | 104.06 | 1,480.10 |
| 2.812 | 102.49 | 1,457.80 |
| 3.008 | 100.88 | 1,434.90 |
| 3.208 | 99.02 | 1,408.40 |
| 3.408 | 97.55 | 1,387.50 |

Replace these 25 pages of Table 6.2.1-4
with the following 25 pages of revised
Table 6.2.1-4.

Table 6.2.1-4 (14 of 25)

Part B. Reactor Vessel Pressure vs. Time
(Blowdown Period)

| Time (sec) | Reactor Vessel Pressure | |
|------------|-------------------------|----------|
| | kg/cm ² A | psia |
| 3.608 | 95.48 | 1,358.10 |
| 3.808 | 93.41 | 1,328.60 |
| 4.000 | 91.91 | 1,307.30 |
| 4.210 | 90.07 | 1,281.10 |
| 4.409 | 88.60 | 1,260.20 |
| 4.609 | 87.41 | 1,243.20 |
| 4.809 | 86.24 | 1,226.60 |
| 5.009 | 85.01 | 1,209.10 |
| 6.209 | 80.24 | 1,141.30 |
| 6.409 | 79.48 | 1,130.40 |
| 6.609 | 78.88 | 1,121.90 |
| 6.809 | 78.27 | 1,113.30 |
| 7.009 | 77.62 | 1,104.00 |
| 7.209 | 76.94 | 1,094.40 |
| 7.409 | 76.32 | 1,085.50 |
| 7.609 | 75.57 | 1,074.90 |
| 7.809 | 74.87 | 1,064.90 |
| 8.009 | 74.23 | 1,055.80 |
| 8.409 | 72.92 | 1,037.20 |
| 8.809 | 71.62 | 1,018.70 |
| 9.204 | 70.32 | 1,000.20 |
| 9.608 | 69.01 | 981.57 |
| 10.004 | 67.70 | 962.86 |
| 10.404 | 66.32 | 943.31 |
| 10.799 | 64.73 | 920.61 |
| 11.205 | 62.25 | 885.43 |

Replace these 25 pages of Table 6.2.1-4 with the following 25 pages of revised Table 6.2.1-4.

Table 6.2.1-4 (15 of 25)

Part B. Reactor Vessel Pressure vs. Time
(Blowdown Period)

| Time (sec) | Reactor Vessel Pressure | |
|------------|-------------------------|--------|
| | kg/cm ² A | psia |
| 11.601 | 59.92 | 852.22 |
| 12.006 | 58.14 | 826.88 |
| 12.205 | 55.99 | 796.34 |
| 12.406 | 55.20 | 785.18 |
| 12.599 | 53.98 | 767.78 |
| 12.806 | 52.89 | 752.32 |
| 13.005 | 51.83 | 737.15 |
| 13.213 | 50.66 | 720.49 |
| 13.413 | 49.62 | 705.72 |
| 13.613 | 48.60 | 691.24 |
| 14.816 | 40.78 | 579.98 |
| 15.016 | 39.48 | 561.58 |
| 15.214 | 37.97 | 540.09 |
| 15.409 | 36.72 | 522.26 |
| 15.609 | 35.32 | 502.42 |
| 15.809 | 34.01 | 483.72 |
| 16.009 | 32.71 | 465.30 |
| 16.200 | 31.56 | 448.93 |
| 16.400 | 30.45 | 433.14 |
| 16.601 | 29.23 | 415.81 |
| 16.800 | 28.03 | 398.63 |
| 17.001 | 26.77 | 380.75 |
| 17.205 | 25.49 | 362.53 |
| 17.400 | 24.24 | 344.80 |
| 17.600 | 23.00 | 327.17 |
| 17.800 | 21.78 | 309.80 |
| 18.000 | 20.54 | 292.11 |
| 18.200 | 19.37 | 275.52 |

Replace these 25 pages of Table 6.2.1-4
with the following 25 pages of revised
Table 6.2.1-4.

Table 6.2.1-4 (16 of 25)

Part B. Reactor Vessel Pressure vs. Time
(Reflood and Post-reflood Period)

| Time (sec) | Reactor Vessel Pressure | |
|------------|-------------------------|--------|
| | kg/cm ² A | psia |
| 18.400 | 18.22 | 259.10 |
| 18.600 | 17.10 | 243.28 |
| 18.802 | 15.99 | 227.49 |
| 18.999 | 14.94 | 212.46 |
| 19.203 | 15.92 | 226.38 |

Replace these 25 pages of Table 6.2.1-4
with the following 25 pages of revised
Table 6.2.1-4.

Table 6.2.1-4 (17 of 25)

Part B. Reactor Vessel Pressure vs. Time
(Reflood and Post-reflood Period)

| Time (sec) | Reactor Vessel Pressure | |
|------------|-------------------------|---------|
| | kg/cm ² A | psia |
| 19.20 | 4.080 | 58.000 |
| 19.30 | 4.120 | 58.590 |
| 19.40 | 4.180 | 59.510 |
| 21.40 | 4.530 | 64.410 |
| 23.40 | 6.230 | 88.590 |
| 25.40 | 8.150 | 115.870 |
| 27.90 | 10.220 | 145.340 |
| 28.00 | 10.290 | 146.340 |
| 28.10 | 10.360 | 147.320 |
| 28.20 | 10.410 | 148.060 |
| 32.20 | 10.140 | 144.220 |
| 36.20 | 9.860 | 140.200 |
| 40.20 | 9.590 | 136.350 |
| 44.20 | 9.330 | 132.690 |
| 48.20 | 9.080 | 129.180 |
| 52.20 | 8.850 | 125.830 |
| 56.20 | 8.620 | 122.630 |
| 60.20 | 8.410 | 119.570 |
| 63.60 | 8.230 | 117.070 |
| 63.70 | 8.230 | 117.000 |
| 63.80 | 8.220 | 116.890 |
| 63.90 | 8.210 | 116.740 |
| 65.60 | 8.030 | 114.210 |
| 67.30 | 7.880 | 112.120 |
| 69.00 | 7.760 | 110.340 |
| 70.70 | 7.650 | 108.870 |
| 72.40 | 7.570 | 107.640 |

Replace these 25 pages of Table 6.2.1-4 with the following 25 pages of revised Table 6.2.1-4.

Table 6.2.1-4 (18 of 25)

Part B. Reactor Vessel Pressure vs. Time
(Reflood and Post-reflood Period)

| Time (sec) | Reactor Vessel Pressure | |
|------------|-------------------------|---------|
| | kg/cm ² A | psia |
| 74.10 | 7.490 | 106.550 |
| 75.80 | 7.420 | 105.580 |
| 77.50 | 7.360 | 104.720 |
| 79.20 | 7.310 | 103.950 |
| 80.90 | 7.260 | 103.240 |
| 82.90 | 7.210 | 102.480 |
| 83.00 | 7.210 | 102.510 |
| 83.10 | 7.160 | 101.780 |
| 83.20 | 7.190 | 102.270 |
| 83.30 | 7.150 | 101.690 |
| 83.40 | 7.130 | 101.460 |
| 85.40 | 7.000 | 99.570 |
| 87.40 | 6.810 | 96.830 |
| 89.40 | 6.610 | 94.080 |
| 91.40 | 6.440 | 91.530 |
| 93.40 | 6.270 | 89.210 |
| 95.40 | 6.120 | 87.100 |
| 97.40 | 5.990 | 85.190 |
| 99.40 | 5.870 | 83.440 |
| 101.40 | 5.750 | 81.840 |
| 103.40 | 5.650 | 80.380 |
| 105.40 | 5.560 | 79.030 |
| 107.40 | 5.470 | 77.780 |
| 109.40 | 5.390 | 76.630 |
| 110.10 | 5.360 | 76.240 |
| 110.20 | 5.360 | 76.190 |
| 110.30 | 5.350 | 76.140 |

Replace these 25 pages of Table 6.2.1-4 with the following 25 pages of revised Table 6.2.1-4.

Table 6.2.1-4 (19 of 25)

Part B. Reactor Vessel Pressure vs. Time
(Reflood and Post-reflood period)

| Time (sec) | Reactor Vessel Pressure | |
|------------|-------------------------|--------|
| | kg/cm ² A | psia |
| 111.30 | 5.180 | 73.710 |
| 112.30 | 5.330 | 75.740 |
| 113.30 | 5.040 | 71.660 |
| 114.30 | 5.240 | 74.590 |
| 115.30 | 5.000 | 71.140 |
| 116.30 | 4.820 | 68.490 |
| 117.30 | 4.760 | 67.680 |
| 118.30 | 4.710 | 67.060 |
| 119.30 | 4.680 | 66.550 |
| 120.30 | 4.650 | 66.080 |
| 121.30 | 4.610 | 65.640 |
| 122.30 | 4.590 | 65.240 |
| 123.30 | 4.560 | 64.890 |
| 124.90 | 4.640 | 65.970 |
| 125.00 | 4.750 | 67.560 |

Replace these 25 pages of Table 6.2.1-4
with the following 25 pages of revised
Table 6.2.1-4.

Table 6.2.1-4 (20 of 25)

Part B. Reactor Vessel Pressure vs. Time (Decay heat Period)

| Time (sec) | Reactor Vessel Pressure | |
|------------|-------------------------|--------|
| | kg/cm ² A | psia |
| 200.0 | 4.272 | 60.757 |
| 400.0 | 3.975 | 56.537 |
| 599.9 | 3.855 | 54.836 |
| 800.0 | 3.774 | 53.674 |
| 999.0 | 3.711 | 52.79 |
| 1503.3 | 3.604 | 51.266 |
| 1996.8 | 3.537 | 50.303 |
| 4002.6 | 3.404 | 48.419 |
| 6001.4 | 3.337 | 47.46 |
| 8000.6 | 3.298 | 46.904 |
| 9990.3 | 3.272 | 46.54 |
| 15005.7 | 3.228 | 45.912 |
| 20011.4 | 3.178 | 45.203 |
| 40036.7 | 2.967 | 42.204 |
| 59963.5 | 2.768 | 39.374 |
| 79990.5 | 2.623 | 37.304 |
| 100002.0 | 2.356 | 33.507 |
| 150010.0 | 2.066 | 29.381 |
| 200018.5 | 1.934 | 27.505 |
| 400053.2 | 1.718 | 24.434 |
| 600094.9 | 1.62 | 23.042 |
| 800141.2 | 1.565 | 22.257 |
| 1000000.0 | 1.529 | 21.749 |

Replace these 25 pages of Table 6.2.1-4 with the following 25 pages of revised Table 6.2.1-4.

Table 6.2.1-4 (21 of 25)

Part C. Safety Injection Flow vs. Time (Blowdown Period)

| Time (sec) | Safety Injection Tank Flow | |
|------------|----------------------------|-----------|
| | kg/sec | lbm/sec |
| 0.000 | 0.00 | 0.00 |
| 0.027 | 0.00 | 0.00 |
| 13.813 | 0.00 | 0.00 |
| 14.013 | 0.00 | 0.00 |
| 14.203 | 1,281.21 | 2,824.60 |
| 14.409 | 1,690.48 | 3,726.90 |
| 14.616 | 1,989.35 | 4,385.80 |
| 14.816 | 2,357.62 | 5,197.70 |
| 15.016 | 2,555.71 | 5,634.40 |
| 15.214 | 2,769.58 | 6,105.90 |
| 15.409 | 2,934.41 | 6,469.30 |
| 15.609 | 3,097.38 | 6,828.60 |
| 15.809 | 3,236.55 | 7,135.40 |
| 16.009 | 3,362.73 | 7,413.60 |
| 16.200 | 3,451.73 | 7,609.80 |
| 16.400 | 3,536.73 | 7,797.20 |
| 16.601 | 3,639.88 | 8,024.60 |
| 16.800 | 3,738.76 | 8,242.60 |
| 17.001 | 3,845.63 | 8,478.20 |
| 17.205 | 3,957.26 | 8,724.30 |
| 17.400 | 4,061.17 | 8,953.40 |
| 17.600 | 4,159.33 | 9,169.80 |
| 17.800 | 4,253.59 | 9,377.60 |
| 18.000 | 4,351.61 | 9,593.70 |
| 18.200 | 4,434.98 | 9,777.50 |
| 18.400 | 4,517.85 | 9,960.20 |
| 18.600 | 4,594.41 | 10,129.00 |
| 18.802 | 4,668.35 | 10,292.00 |
| 18.999 | 4,740.47 | 10,451.00 |
| 19.203 | 4,496.26 | 9,912.60 |

Replace these 25 pages of Table 6.2.1-4 with the following 25 pages of revised Table 6.2.1-4.

Table 6.2.1-4 (22 of 25)

Part C. Safety Injection Flow vs. Time (Reflood and Post-reflood Period)

| Time (sec) | Safety Injection Tank Flow | | Safety Injection Pump Flow | |
|------------|----------------------------|----------|----------------------------|---------|
| | kg/sec | lbm/sec | kg/sec | lbm/sec |
| 19.203 | 3,140.51 | 6,923.66 | 328.55 | 724.33 |
| 19.303 | 3,128.73 | 6,897.71 | 328.55 | 724.33 |
| 21.303 | 2,898.47 | 6,390.06 | 328.12 | 723.38 |
| 23.303 | 2,609.51 | 5,753.00 | 325.77 | 718.20 |
| 25.303 | 2,312.95 | 5,099.22 | 323.05 | 712.21 |
| 27.303 | 2,031.18 | 4,478.00 | 320.57 | 706.73 |
| 28.003 | 1,939.29 | 4,275.41 | 319.82 | 705.09 |
| 28.103 | 1,926.52 | 4,247.28 | 319.72 | 704.87 |
| 31.603 | 1,750.66 | 3,859.57 | 319.86 | 705.18 |
| 35.103 | 1,619.26 | 3,569.87 | 320.22 | 705.97 |
| 38.603 | 1,509.04 | 3,326.87 | 320.56 | 706.72 |
| 42.103 | 1,415.35 | 3,120.33 | 320.89 | 707.45 |
| 45.603 | 1,334.88 | 2,942.92 | 321.21 | 708.15 |
| 49.103 | 1,265.14 | 2,789.18 | 321.51 | 708.82 |
| 52.603 | 1,204.31 | 2,655.06 | 321.81 | 709.47 |
| 56.103 | 1,150.94 | 2,537.40 | 322.09 | 710.09 |
| 59.603 | 1,103.87 | 2,433.64 | 322.36 | 710.68 |
| 63.603 | 1,056.60 | 2,329.42 | 322.66 | 711.34 |
| 63.703 | 1,055.50 | 2,326.99 | 322.66 | 711.35 |
| 63.803 | 478.11 | 1,054.06 | 322.67 | 711.37 |
| 63.903 | 478.29 | 1,054.45 | 322.68 | 711.39 |
| 68.403 | 493.13 | 1,087.18 | 323.27 | 712.68 |
| 72.903 | 496.10 | 1,093.72 | 323.63 | 713.49 |
| 77.403 | 493.39 | 1,087.74 | 323.89 | 714.05 |
| 81.903 | 487.90 | 1,075.64 | 324.08 | 714.48 |
| 86.403 | 497.54 | 1,096.88 | 324.53 | 715.47 |
| 90.903 | 515.58 | 1,136.65 | 325.14 | 716.81 |
| 95.403 | 527.71 | 1,163.41 | 325.65 | 717.93 |
| 99.903 | 534.86 | 1,179.17 | 326.05 | 718.83 |
| 104.403 | 538.52 | 1,187.24 | 326.39 | 719.57 |

Replace these 25 pages of Table 6.2.1-4 with the following 25 pages of revised Table 6.2.1-4.

Table 6.2.1-4 (23 of 25)

Part C. Safety Injection Flow vs. Time (Reflood and Post-reflood Period)

| Time (sec) | Safety Injection Tank Flow | | Safety Injection Pump Flow | |
|------------|----------------------------|----------|----------------------------|---------|
| | kg/sec | lbm/sec | kg/sec | lbm/sec |
| 108.903 | 539.70 | 1,189.84 | 326.67 | 720.18 |
| 110.203 | 539.68 | 1,189.80 | 326.74 | 720.34 |
| 111.903 | 555.69 | 1,225.09 | 327.15 | 721.24 |
| 113.603 | 545.69 | 1,203.05 | 327.04 | 721.01 |
| 115.303 | 559.32 | 1,233.09 | 327.41 | 721.81 |
| 117.003 | 553.48 | 1,220.23 | 327.38 | 721.75 |
| 118.703 | 477.62 | 1,052.97 | 326.05 | 718.82 |
| 120.403 | 563.38 | 1,242.05 | 327.75 | 722.58 |
| 122.103 | 544.49 | 1,200.40 | 327.46 | 721.93 |
| 123.803 | 567.37 | 1,250.85 | 328.01 | 723.13 |
| 125.003 | 552.37 | 1,217.77 | 327.76 | 722.60 |
| 129.503 | 546.45 | 1,204.72 | 327.86 | 722.82 |
| 134.003 | 506.57 | 1,116.79 | 327.31 | 721.61 |
| 138.503 | 544.21 | 1,199.79 | 328.23 | 723.62 |
| 143.003 | 534.02 | 1,177.31 | 328.22 | 723.61 |
| 147.503 | 520.87 | 1,148.33 | 328.16 | 723.47 |
| 152.003 | 520.46 | 1,147.43 | 328.32 | 723.83 |
| 156.503 | 512.85 | 1,130.66 | 328.35 | 723.89 |
| 160.503 | 504.46 | 1,112.16 | 328.34 | 723.87 |
| 183.903 | 465.15 | 1,025.47 | 328.40 | 724.00 |
| 207.303 | 430.33 | 948.71 | 328.44 | 724.10 |
| 230.703 | 399.46 | 880.66 | 328.48 | 724.18 |
| 254.103 | 371.43 | 818.87 | 328.51 | 724.24 |
| 277.503 | 344.67 | 759.87 | 328.52 | 724.26 |
| 300.903 | 319.54 | 704.46 | 328.52 | 724.27 |
| 324.303 | 296.19 | 652.99 | 328.52 | 724.27 |
| 347.703 | 274.34 | 604.83 | 328.52 | 724.28 |
| 367.903 | 256.51 | 565.52 | 328.53 | 724.28 |
| 368.003 | 256.43 | 565.33 | 328.53 | 724.28 |
| 368.103 | 0.00 | 0.00 | 328.53 | 724.28 |

Replace these 25 pages of Table 6.2.1-4 with the following 25 pages of revised Table 6.2.1-4.

Table 6.2.1-4 (24 of 25)

Part C. Safety Injection Flow vs. Time (Reflood and Post-reflood Period)

| Time (sec) | Safety Injection Tank Flow | | Safety Injection Pump Flow | |
|------------|----------------------------|---------|----------------------------|---------|
| | kg/sec | lbm/sec | kg/sec | lbm/sec |
| 368.203 | 0.00 | 0.00 | 328.53 | 724.28 |
| 398.203 | 0.00 | 0.00 | 328.54 | 724.32 |
| 428.203 | 0.00 | 0.00 | 328.54 | 724.32 |
| 458.203 | 0.00 | 0.00 | 328.54 | 724.32 |
| 488.203 | 0.00 | 0.00 | 328.54 | 724.32 |
| 499.903 | 0.00 | 0.00 | 328.54 | 724.31 |
| 500.003 | 0.00 | 0.00 | 328.54 | 724.31 |

Replace these 25 pages of Table 6.2.1-4 with the following 25 pages of revised Table 6.2.1-4.

Table 6.2.1-4 (25 of 25)

Part D. Chronology of Events

| Time (sec) | Event | Values |
|------------|---|--|
| 0.00 | Break occurs | - |
| 4.38 | Containment pressure Hi-Hi setpoint | 1.547 kg/cm ² G (22.0 psig) |
| 14.01 | Start safety injection tank (SIT) injection | - |
| 19.20 | End of blowdown | - |
| 19.21 | Start SI pump injection | - |
| | First peak containment pressure (Blowdown phase) | 3.126 kg/cm ² G (44.47 psig) |
| 63.70 | SIT flow is turned down to low flow by fluidic device in SIT | - |
| 101.91 | Peak containment temperature | 133.84 °C (272.91 °F) |
| 102.51 | Peak containment pressure | 3.512 kg/cm ² G (49.96 psig) |
| 110.20 | End of reflood | |
| 114.38 | Start containment spray actuation | |
| 125.0 | End of post reflood | - |
| 368.10 | Safety injection tank empty | - |
| 57,660.1 | Time of depressurization of the containment at 50% of peak pressure | 1.756 kg/cm ² G (24.97 psig) |

Replace these 25 pages of Table 6.2.1-4 with the following 25 pages of revised Table 6.2.1-4.

APR1400 DCD TIER 2

Table 6.2.1-4 (1 of 25)

Insert this page.

Double-Ended Suction Leg Slot Break – Maximum SIS Flow
(0.9121 m² (9.8175 ft²) Total Break Area)

Part A. Mass and Energy Release Data
 (Blowdown Period)

| Time (sec) | Break Mass Flow Rate | | Break Enthalpy | |
|------------|----------------------|------------|----------------|---------|
| | kg/sec | lbm/sec | kcal/kg | Btu/lbm |
| 0.000 | 0.00 | 0.00 | 0.00 | 0.00 |
| 0.027 | 35,826.69 | 78,984.75 | 310.61 | 559.13 |
| 0.054 | 35,499.95 | 78,264.39 | 310.08 | 558.18 |
| 0.103 | 35,936.95 | 79,227.82 | 309.90 | 557.85 |
| 0.152 | 49,099.29 | 108,245.97 | 310.38 | 558.72 |
| 0.202 | 47,285.37 | 104,246.94 | 311.04 | 559.91 |
| 0.252 | 45,576.63 | 100,479.79 | 311.57 | 560.85 |
| 0.298 | 44,683.04 | 98,509.75 | 311.94 | 561.52 |
| 0.351 | 44,779.94 | 98,723.38 | 312.17 | 561.94 |
| 0.400 | 44,346.29 | 97,767.34 | 312.52 | 562.56 |
| 0.603 | 43,478.91 | 95,855.09 | 313.48 | 564.30 |
| 0.800 | 44,864.47 | 98,909.74 | 314.64 | 566.38 |
| 1.000 | 42,167.46 | 92,963.82 | 315.74 | 568.36 |
| 1.202 | 40,552.76 | 89,404.00 | 317.33 | 571.22 |
| 1.401 | 38,527.59 | 84,939.24 | 319.05 | 574.33 |
| 1.607 | 38,152.42 | 84,112.13 | 320.39 | 576.73 |
| 1.800 | 37,859.70 | 83,466.78 | 321.87 | 579.40 |
| 2.001 | 37,500.04 | 82,673.88 | 323.76 | 582.80 |
| 2.204 | 35,984.54 | 79,332.74 | 325.55 | 586.03 |
| 2.407 | 33,372.26 | 73,573.62 | 326.50 | 587.73 |
| 2.601 | 31,669.84 | 69,820.41 | 327.91 | 590.27 |
| 2.812 | 30,653.27 | 67,579.23 | 330.85 | 595.57 |
| 3.008 | 29,668.44 | 65,408.05 | 334.73 | 602.56 |
| 3.208 | 28,297.64 | 62,385.94 | 340.03 | 612.09 |
| 3.408 | 26,715.66 | 58,898.26 | 346.75 | 624.19 |

APR1400 DCD TIER 2

Insert this page.

Table 6.2.1-4 (2 of 25)

Part A. Mass and Energy Release Data (Blowdown Period)

| Time (sec) | Break Mass Flow Rate | | Break Enthalpy | |
|------------|----------------------|-----------|----------------|---------|
| | kg/sec | lbm/sec | kcal/kg | Btu/lbm |
| 3.608 | 24,966.73 | 55,042.51 | 354.00 | 637.23 |
| 3.808 | 23,497.04 | 51,802.38 | 360.32 | 648.62 |
| 4.000 | 22,127.47 | 48,782.98 | 365.48 | 657.89 |
| 4.211 | 21,436.30 | 47,259.20 | 366.85 | 660.37 |
| 4.409 | 21,008.90 | 46,316.93 | 366.71 | 660.11 |
| 4.609 | 20,598.55 | 45,412.26 | 366.16 | 659.12 |
| 4.809 | 20,267.22 | 44,681.81 | 365.67 | 658.24 |
| 5.009 | 20,051.87 | 44,207.03 | 364.92 | 656.90 |
| 5.209 | 19,841.27 | 43,742.73 | 364.35 | 655.86 |
| 5.409 | 19,815.87 | 43,686.73 | 363.56 | 654.45 |
| 5.609 | 19,693.35 | 43,416.63 | 363.47 | 654.28 |
| 5.809 | 19,144.10 | 42,205.74 | 364.81 | 656.69 |
| 6.009 | 18,734.91 | 41,303.63 | 365.84 | 658.55 |
| 6.209 | 18,566.23 | 40,931.75 | 365.82 | 658.51 |
| 6.409 | 18,595.07 | 40,995.33 | 363.92 | 655.09 |
| 6.609 | 18,479.62 | 40,740.79 | 363.55 | 654.43 |
| 6.809 | 17,933.49 | 39,536.78 | 366.91 | 660.48 |
| 7.009 | 17,132.26 | 37,770.38 | 372.47 | 670.48 |
| 7.209 | 16,620.46 | 36,642.04 | 375.29 | 675.57 |
| 7.409 | 16,372.62 | 36,095.63 | 375.88 | 676.62 |
| 7.609 | 16,206.97 | 35,730.45 | 376.05 | 676.92 |
| 7.809 | 16,191.18 | 35,695.62 | 374.41 | 673.98 |
| 8.009 | 16,125.16 | 35,550.08 | 373.73 | 672.75 |
| 8.209 | 15,915.11 | 35,086.98 | 374.73 | 674.55 |
| 8.409 | 15,680.94 | 34,570.74 | 375.85 | 676.56 |
| 8.609 | 15,427.32 | 34,011.60 | 377.17 | 678.94 |
| 8.809 | 15,141.74 | 33,381.99 | 378.82 | 681.91 |
| 9.005 | 14,809.07 | 32,648.58 | 380.75 | 685.38 |

APR1400 DCD TIER 2

Table 6.2.1-4 (3 of 25)

Insert this page.

Part A. Mass and Energy Release Data
(Blowdown Period)

| Time (sec) | Break Mass Flow Rate | | Break Enthalpy | |
|------------|----------------------|-----------|----------------|---------|
| | kg/sec | lbm/sec | kcal/kg | Btu/lbm |
| 9.204 | 14,527.77 | 32,028.41 | 382.90 | 689.26 |
| 9.400 | 14,196.28 | 31,297.60 | 385.45 | 693.86 |
| 9.608 | 13,797.32 | 30,418.04 | 387.37 | 697.31 |
| 9.801 | 13,391.38 | 29,523.09 | 391.81 | 705.30 |
| 10.004 | 13,129.00 | 28,944.65 | 395.88 | 712.62 |
| 10.205 | 12,765.77 | 28,143.85 | 399.12 | 718.46 |
| 10.404 | 12,429.45 | 27,402.39 | 401.76 | 723.21 |
| 10.603 | 11,985.20 | 26,422.98 | 406.03 | 730.90 |
| 10.799 | 11,582.15 | 25,534.40 | 412.05 | 741.74 |
| 11.004 | 11,140.57 | 24,560.87 | 417.73 | 751.96 |
| 11.205 | 10,637.22 | 23,451.17 | 423.35 | 762.07 |
| 11.406 | 10,190.47 | 22,466.27 | 428.61 | 771.53 |
| 11.601 | 9,728.82 | 21,448.50 | 433.53 | 780.39 |
| 11.804 | 9,042.09 | 19,934.50 | 445.87 | 802.61 |
| 12.006 | 8,756.29 | 19,304.41 | 452.29 | 814.16 |
| 12.205 | 8,377.30 | 18,468.88 | 457.85 | 824.18 |
| 12.406 | 8,013.92 | 17,667.76 | 463.75 | 834.79 |
| 12.599 | 7,657.53 | 16,882.05 | 469.08 | 844.38 |
| 12.806 | 7,397.99 | 16,309.86 | 475.41 | 855.78 |
| 13.005 | 7,153.35 | 15,770.51 | 476.56 | 857.85 |
| 13.213 | 6,944.67 | 15,310.45 | 475.99 | 856.84 |
| 13.413 | 6,730.23 | 14,837.69 | 477.18 | 858.98 |
| 13.613 | 6,534.48 | 14,406.13 | 479.25 | 862.71 |
| 13.813 | 6,358.64 | 14,018.47 | 480.50 | 864.96 |
| 14.013 | 6,188.02 | 13,642.32 | 481.42 | 866.61 |
| 14.203 | 5,966.42 | 13,153.78 | 482.94 | 869.34 |
| 14.409 | 5,852.22 | 12,902.00 | 478.07 | 860.57 |
| 14.616 | 5,895.97 | 12,998.45 | 457.84 | 824.16 |

APR1400 DCD TIER 2

Table 6.2.1-4 (4 of 25)

Insert this page.

Part A. Mass and Energy Release Data (Blowdown Period)

| Time (sec) | Break Mass Flow Rate | | Break Enthalpy | |
|------------|----------------------|-----------|----------------|---------|
| | kg/sec | lbm/sec | kcal/kg | Btu/lbm |
| 14.816 | 5,885.88 | 12,976.22 | 441.01 | 793.86 |
| 15.016 | 5,839.74 | 12,874.49 | 431.85 | 777.37 |
| 15.214 | 5,717.91 | 12,605.89 | 425.51 | 765.97 |
| 15.409 | 5,579.03 | 12,299.72 | 419.00 | 754.25 |
| 15.609 | 5,389.08 | 11,880.96 | 415.55 | 748.04 |
| 15.809 | 5,183.01 | 11,426.64 | 413.16 | 743.74 |
| 16.009 | 4,939.96 | 10,890.80 | 411.96 | 741.57 |
| 16.200 | 4,374.29 | 9,643.72 | 443.96 | 799.17 |
| 16.400 | 4,198.25 | 9,255.61 | 443.34 | 798.06 |
| 16.601 | 4,077.66 | 8,989.74 | 441.21 | 794.23 |
| 16.800 | 3,932.45 | 8,669.61 | 438.05 | 788.53 |
| 17.001 | 3,815.63 | 8,412.08 | 433.55 | 780.43 |
| 17.205 | 3,707.03 | 8,172.64 | 424.86 | 764.79 |
| 17.400 | 3,576.74 | 7,885.40 | 419.56 | 755.24 |
| 17.600 | 3,431.20 | 7,564.54 | 416.49 | 749.73 |
| 17.800 | 3,384.27 | 7,461.08 | 407.89 | 734.25 |
| 18.000 | 3,343.38 | 7,370.94 | 401.24 | 722.27 |
| 18.200 | 3,122.01 | 6,882.88 | 401.21 | 722.22 |
| 18.400 | 3,066.26 | 6,759.98 | 391.83 | 705.34 |
| 18.600 | 2,962.81 | 6,531.92 | 382.50 | 688.54 |
| 18.802 | 2,774.26 | 6,116.24 | 381.33 | 686.43 |
| 18.999 | 2,608.38 | 5,750.52 | 378.21 | 680.83 |
| 19.203 | 2,546.44 | 5,613.97 | 383.68 | 690.67 |

Integral Mass and Energy Release at End of Blowdown

| Time (sec) | Integral Mass | | Integral Energy | |
|------------|---------------|-------------|-----------------|-------------|
| | kg | lbm | Million kcal | Million Btu |
| 19.203 | 304,940.875 | 672,283.090 | 110.483 | 438.461 |

APR1400 DCD TIER 2

Table 6.2.1-4 (5 of 25)

Insert this page.

Part A. Mass and Energy Release Data (Reflood and Post-reflood Period)

| Time (sec) | Break Mass Flow Rate | | Break Enthalpy | |
|------------|----------------------|----------|----------------|----------|
| | kg/sec | lbm/sec | kcal/kg | Btu/lbm |
| 19.20 | 0.00 | 0.00 | 0.00 | 0.00 |
| 19.30 | 66.99 | 147.69 | 705.17 | 1,269.37 |
| 21.30 | 171.80 | 378.76 | 706.28 | 1,271.37 |
| 23.30 | 431.79 | 951.94 | 709.45 | 1,277.08 |
| 25.30 | 644.37 | 1,420.61 | 708.62 | 1,275.58 |
| 27.90 | 854.79 | 1,884.51 | 706.03 | 1,270.92 |
| 28.00 | 861.33 | 1,898.91 | 705.91 | 1,270.72 |
| 28.10 | 503.29 | 1,109.58 | 705.80 | 1,270.51 |
| 28.20 | 506.30 | 1,116.21 | 705.69 | 1,270.32 |
| 32.20 | 495.28 | 1,091.91 | 703.65 | 1,266.65 |
| 36.20 | 482.31 | 1,063.31 | 701.74 | 1,263.21 |
| 40.20 | 469.68 | 1,035.47 | 699.88 | 1,259.86 |
| 44.20 | 457.37 | 1,008.34 | 698.07 | 1,256.60 |
| 48.20 | 445.42 | 981.98 | 696.28 | 1,253.37 |
| 52.20 | 433.80 | 956.38 | 694.48 | 1,250.14 |
| 56.20 | 422.47 | 931.40 | 692.73 | 1,246.99 |
| 60.20 | 411.42 | 907.03 | 691.02 | 1,243.90 |
| 63.50 | 402.51 | 887.39 | 689.63 | 1,241.40 |
| 63.60 | 402.24 | 886.80 | 689.59 | 1,241.33 |
| 63.70 | 692.87 | 1,527.52 | 689.54 | 1,241.25 |
| 63.80 | 691.90 | 1,525.38 | 689.51 | 1,241.19 |
| 65.80 | 671.17 | 1,479.69 | 688.89 | 1,240.08 |
| 67.80 | 654.55 | 1,443.05 | 688.24 | 1,238.91 |
| 69.80 | 640.80 | 1,412.73 | 687.56 | 1,237.68 |
| 71.80 | 629.79 | 1,388.46 | 686.84 | 1,236.39 |
| 73.80 | 620.54 | 1,368.06 | 686.28 | 1,235.37 |
| 75.80 | 612.73 | 1,350.84 | 685.50 | 1,233.98 |
| 77.80 | 606.01 | 1,336.02 | 684.71 | 1,232.54 |

APR1400 DCD TIER 2

Insert this page.

Table 6.2.1-4 (6 of 25)

Part A. Mass and Energy Release Data (Reflood and Post-reflood Period)

| Time (sec) | Break Mass Flow Rate | | Break Enthalpy | |
|------------|----------------------|----------|----------------|----------|
| | kg/sec | lbm/sec | kcal/kg | Btu/lbm |
| 79.80 | 600.13 | 1,323.06 | 683.90 | 1,231.09 |
| 81.80 | 594.92 | 1,311.59 | 683.06 | 1,229.59 |
| 82.80 | 592.54 | 1,306.34 | 682.63 | 1,228.81 |
| 82.90 | 592.31 | 1,305.83 | 682.59 | 1,228.73 |
| 83.00 | 592.08 | 1,305.32 | 670.61 | 1,207.17 |
| 83.10 | 603.96 | 1,331.50 | 682.16 | 1,227.96 |
| 83.20 | 567.57 | 1,251.29 | 668.96 | 1,204.20 |
| 83.30 | 598.90 | 1,320.36 | 668.10 | 1,202.64 |
| 83.40 | 590.50 | 1,301.83 | 668.25 | 1,202.93 |
| 83.50 | 578.55 | 1,275.49 | 668.53 | 1,203.43 |
| 85.70 | 492.65 | 1,086.12 | 670.60 | 1,207.15 |
| 88.20 | 440.02 | 970.09 | 671.72 | 1,209.16 |
| 90.70 | 400.10 | 882.07 | 672.54 | 1,210.64 |
| 93.20 | 366.44 | 807.86 | 673.27 | 1,211.96 |
| 95.70 | 337.16 | 743.32 | 673.98 | 1,213.24 |
| 98.20 | 311.46 | 686.66 | 674.67 | 1,214.48 |
| 100.70 | 288.73 | 636.55 | 675.33 | 1,215.67 |
| 103.20 | 268.49 | 591.92 | 675.98 | 1,216.84 |
| 105.70 | 250.35 | 551.94 | 676.61 | 1,217.97 |
| 108.20 | 234.02 | 515.92 | 677.23 | 1,219.08 |
| 110.10 | 222.64 | 490.84 | 677.70 | 1,219.94 |
| 110.20 | 222.06 | 489.57 | 677.73 | 1,219.98 |
| 110.30 | 221.49 | 488.31 | 677.75 | 1,220.02 |
| 110.80 | 139.75 | 308.09 | 693.37 | 1,248.13 |
| 111.30 | 208.44 | 459.53 | 677.28 | 1,219.18 |
| 111.80 | 338.59 | 746.46 | 666.99 | 1,200.64 |
| 112.30 | 312.96 | 689.96 | 667.70 | 1,201.92 |
| 112.80 | 309.68 | 682.73 | 667.52 | 1,201.60 |

APR1400 DCD TIER 2

Table 6.2.1-4 (7 of 25)

Insert this page.

Part A. Mass and Energy Release Data (Reflood and Post-reflood Period)

| Time (sec) | Break Mass Flow Rate | | Break Enthalpy | |
|------------|----------------------|----------|----------------|----------|
| | kg/sec | lbm/sec | kcal/kg | Btu/lbm |
| 113.30 | 305.80 | 674.18 | 667.40 | 1,201.40 |
| 113.80 | 299.76 | 660.86 | 667.43 | 1,201.44 |
| 114.30 | 315.71 | 696.02 | 666.56 | 1,199.87 |
| 114.80 | 520.38 | 1,147.24 | 661.81 | 1,191.34 |
| 115.30 | 141.91 | 312.86 | 686.46 | 1,235.69 |
| 116.30 | 294.07 | 648.32 | 667.46 | 1,201.49 |
| 117.30 | 308.31 | 679.70 | 666.17 | 1,199.18 |
| 118.30 | 522.76 | 1,152.50 | 661.27 | 1,190.36 |
| 119.30 | 460.22 | 1,014.61 | 661.77 | 1,191.25 |
| 120.30 | 450.21 | 992.55 | 661.68 | 1,191.09 |
| 121.30 | 383.23 | 844.88 | 662.84 | 1,193.18 |
| 122.30 | 233.34 | 514.44 | 669.40 | 1,205.00 |
| 123.30 | 108.99 | 240.29 | 689.49 | 1,241.15 |
| 124.00 | 174.91 | 385.62 | 672.43 | 1,210.44 |
| 124.10 | 75.66 | 166.80 | 701.12 | 1,262.09 |

Integral Mass and Energy Release at the End of Reflood and Post-reflood

| Time (sec) | Integral Mass | | Integral Energy | |
|------------|---------------|-----------|-----------------|-------------|
| | kg | lbm | Million kcal | Million Btu |
| 110.20 | 41,795.15 | 92,143.00 | 28.833 | 114.427 |
| 124.10 | 44,762.53 | 98,685.00 | 30.828 | 122.344 |

APR1400 DCD TIER 2

Table 6.2.1-4 (8 of 25)

Insert this page.

Part A: Spillage Release Data (Reactor Vessel Side)
(Reflood and Post-Reflood Period)

| Time (sec) | Break Mass Flow Rate | | Break Enthalpy | |
|---------------|----------------------|----------|----------------|---------|
| | kg/sec | lbm/sec | kcal/kg | Btu/lbm |
| 19.20 | 0.00 | 0.00 | 0.00 | 0.00 |
| 19.30 | 0.00 | 0.00 | 0.00 | 0.00 |
| 28.00 | 0.00 | 0.00 | 0.00 | 0.00 |
| 28.10 | 707.34 | 1,559.42 | 387.85 | 698.16 |
| 28.20 | 1,438.39 | 3,171.13 | 217.05 | 390.71 |
| 32.20 | 1,275.08 | 2,811.09 | 233.82 | 420.89 |
| 36.20 | 1,151.88 | 2,539.48 | 247.61 | 445.73 |
| 40.20 | 1,053.73 | 2,323.08 | 259.80 | 467.67 |
| 44.20 | 974.52 | 2,148.45 | 270.34 | 486.64 |
| 48.20 | 909.98 | 2,006.18 | 279.20 | 502.58 |
| 52.20 | 857.09 | 1,889.57 | 286.38 | 515.51 |
| 56.20 | 813.70 | 1,793.90 | 291.86 | 525.37 |
| 60.20 | 778.07 | 1,715.35 | 295.69 | 532.28 |
| 63.50 | 753.51 | 1,661.21 | 297.70 | 535.89 |
| 63.60 | 752.82 | 1,659.69 | 297.75 | 535.97 |
| 63.70 | 0.00 | 0.00 | 0.00 | 0.00 |
| 124.00 | 0.00 | 0.00 | 0.00 | 0.00 |
| 124.10 | 0.00 | 0.00 | 0.00 | 0.00 |

Integral Mass and Energy (Reactor Vessel Side Spillage) at EOR and EOPR

| Time (sec) | Integral Mass | | Integral Energy | |
|---------------|---------------|-----------|-----------------|-------------|
| | kg | lbm | Million kcal | Million Btu |
| 110.20 | 35,298.38 | 77,820.00 | 9.340 | 37.065 |
| 124.10 | 35,298.38 | 77,820.00 | 9.340 | 37.065 |

APR1400 DCD TIER 2

Table 6.2.1-4 (9 of 25)

Insert this page.

Double-Ended Suction Leg Slot Break – Maximum SIS Flow

Part A: Spillage Release Data (Steam Generator Side)
(Reflood and Post-Reflood Period)

| Time (sec) | Break Mass Flow Rate | | Break Enthalpy | |
|---------------|----------------------|----------|----------------|---------|
| | kg/sec | lbm/sec | kcal/kg | Btu/lbm |
| 19.20 | 0.00 | 0.00 | 0.00 | 0.00 |
| 19.30 | 0.00 | 0.00 | 0.00 | 0.00 |
| 83.10 | 0.00 | 0.00 | 0.00 | 0.00 |
| 83.20 | 22.00 | 48.51 | 144.32 | 259.80 |
| 83.30 | 18.01 | 39.71 | 144.32 | 259.79 |
| 83.40 | 21.11 | 46.54 | 144.34 | 259.82 |
| 83.50 | 33.94 | 74.83 | 144.32 | 259.80 |
| 85.70 | 204.32 | 450.45 | 144.33 | 259.81 |
| 88.20 | 273.47 | 602.91 | 144.33 | 259.81 |
| 90.70 | 310.46 | 684.44 | 144.33 | 259.81 |
| 93.20 | 337.17 | 743.33 | 144.33 | 259.81 |
| 95.70 | 359.59 | 792.77 | 144.33 | 259.81 |
| 98.20 | 378.61 | 834.69 | 144.33 | 259.81 |
| 100.70 | 394.89 | 870.59 | 144.33 | 259.81 |
| 103.20 | 408.94 | 901.56 | 144.33 | 259.81 |
| 105.70 | 421.13 | 928.43 | 144.33 | 259.81 |
| 108.20 | 431.76 | 951.88 | 144.33 | 259.81 |
| 110.10 | 438.96 | 967.74 | 144.33 | 259.81 |
| 110.20 | 439.32 | 968.53 | 144.33 | 259.81 |
| 110.30 | 439.67 | 969.32 | 144.33 | 259.81 |
| 110.80 | 916.90 | 2,021.42 | 144.33 | 259.81 |
| 111.30 | 202.95 | 447.42 | 144.33 | 259.81 |
| 111.80 | 198.76 | 438.20 | 144.33 | 259.81 |
| 112.30 | 199.61 | 440.06 | 144.33 | 259.81 |
| 112.80 | 186.16 | 410.42 | 144.33 | 259.81 |
| 113.30 | 177.92 | 392.24 | 144.33 | 259.81 |
| 113.80 | 173.72 | 383.00 | 144.33 | 259.81 |
| 114.30 | 179.28 | 395.25 | 144.33 | 259.81 |

APR1400 DCD TIER 2

Table 6.2.1-4 (10 of 25)

Insert this page.

Double-Ended Suction Leg Slot Break – Maximum SIS Flow

Part A: Spillage Release Data (Steam Generator Side)
(Reflood and Post-Reflood Period)

| Time (sec) | Break Mass Flow Rate | | Break Enthalpy | |
|---------------|----------------------|----------|----------------|---------|
| | kg/sec | lbm/sec | kcal/kg | Btu/lbm |
| 114.80 | 1,586.90 | 3,498.54 | 144.33 | 259.81 |
| 115.30 | 667.83 | 1,472.33 | 144.33 | 259.81 |
| 116.30 | 217.33 | 479.13 | 144.33 | 259.81 |
| 117.30 | 231.61 | 510.61 | 144.33 | 259.81 |
| 118.30 | 1,457.57 | 3,213.41 | 144.33 | 259.81 |
| 119.30 | 1,505.91 | 3,319.98 | 144.33 | 259.81 |
| 120.30 | 1,461.72 | 3,222.55 | 144.33 | 259.81 |
| 121.30 | 1,529.38 | 3,371.73 | 144.33 | 259.81 |
| 122.30 | 1,439.56 | 3,173.71 | 144.33 | 259.81 |
| 123.30 | 1,659.85 | 3,659.36 | 144.33 | 259.81 |
| 124.00 | 227.56 | 501.68 | 144.33 | 259.81 |
| 124.10 | 289.79 | 638.89 | 144.33 | 259.81 |

Integral Mass and Energy (Steam Generator Side Spillage) at EOR and EOPR

| Time (sec) | Integral Mass | | Integral Energy | |
|---------------|---------------|-----------|-----------------|-------------|
| | kg | lbm | Million kcal | Million Btu |
| 110.20 | 9,227.38 | 20,343.00 | 1.332 | 5.285 |
| 124.10 | 20,106.74 | 44,328.00 | 2.902 | 11.517 |

APR1400 DCD TIER 2

Table 6.2.1-4 (11 of 25)

Insert this page.

Part A. Mass and Energy (Steam) Release Data (Decay heat Period)

| Time (sec) | Mass Flow Rate | | Break Enthalpy | |
|---------------|----------------|---------|----------------|---------|
| | kg/sec | lbm/sec | kcal/kg | Btu/lbm |
| 400.0 | 55.75 | 122.91 | 653.47 | 1176.25 |
| 599.9 | 53.87 | 118.76 | 653.13 | 1175.63 |
| 800.0 | 51.05 | 112.55 | 652.88 | 1175.19 |
| 999.0 | 52.02 | 114.68 | 652.69 | 1174.83 |
| 1503.3 | 47.32 | 104.32 | 652.33 | 1174.19 |
| 1996.5 | 43.37 | 95.61 | 652.09 | 1173.75 |
| 4001.9 | 35.92 | 79.19 | 651.65 | 1172.97 |
| 5998.5 | 32.08 | 70.73 | 651.49 | 1172.69 |
| 7996.7 | 29.69 | 65.46 | 651.45 | 1172.61 |
| 9996.4 | 27.95 | 61.63 | 651.44 | 1172.6 |
| 15004.8 | 25.07 | 55.27 | 651.43 | 1172.57 |
| 20010.9 | 23.13 | 51.0 | 651.29 | 1172.32 |
| 40037.0 | 18.76 | 41.35 | 650.23 | 1170.41 |
| 59965.8 | 16.51 | 36.4 | 649.04 | 1168.26 |
| 79993.8 | 15.19 | 33.5 | 648.14 | 1166.64 |
| 100002.4 | 14.42 | 31.79 | 647.52 | 1165.54 |
| 150010.2 | 12.82 | 28.27 | 646.55 | 1163.8 |
| 200017.4 | 11.83 | 26.09 | 645.92 | 1162.65 |
| 400050.6 | 9.22 | 20.32 | 644.67 | 1160.41 |
| 600093.0 | 7.87 | 17.36 | 644.04 | 1159.27 |
| 800133.2 | 7.0 | 15.42 | 643.66 | 1158.58 |
| 1000000.0 | 6.39 | 14.08 | 643.4 | 1158.13 |

Integral Mass and Energy(Steam) Release at 24hours after postulated accident

| Time (sec) | Integral Mass | | Integral Energy | |
|---------------|---------------|------------|-----------------|-------------|
| | kg | lbm | Million kcal | Million Btu |
| 85,002 | 1,817,682 | 4,007,303 | 1,184.659 | 4,701.108 |
| 1,000,000 | 9,959,421 | 21,956,765 | 6,438.076 | 25,548.349 |

APR1400 DCD TIER 2

Table 6.2.1-4 (12 of 25)

Insert this page.

Part A. Mass and Energy (Spillage) Release Data (Decay heat Period)

| Time (sec) | Mass Flow Rate | | Break Enthalpy | |
|------------|----------------|---------|----------------|---------|
| | kg/sec | lbm/sec | kcal/kg | Btu/lbm |
| 400.0 | 139.86 | 308.35 | 30.25 | 54.45 |
| 599.9 | 182.87 | 403.15 | 58.95 | 106.11 |
| 800.0 | 189.1 | 416.89 | 64.66 | 116.38 |
| 999.0 | 193.44 | 426.46 | 67.28 | 121.1 |
| 1503.3 | 201.12 | 443.4 | 72.7 | 130.87 |
| 1996.5 | 205.83 | 453.78 | 78.0 | 140.4 |
| 4001.9 | 212.22 | 467.87 | 95.03 | 171.05 |
| 5998.5 | 214.23 | 472.29 | 105.04 | 189.07 |
| 7996.7 | 215.23 | 474.51 | 111.25 | 200.25 |
| 9996.4 | 215.94 | 476.06 | 115.23 | 207.41 |
| 15004.8 | 217.48 | 479.46 | 120.12 | 216.21 |
| 20010.9 | 218.93 | 482.65 | 121.57 | 218.82 |
| 40037.0 | 223.63 | 493.02 | 118.32 | 212.98 |
| 59965.8 | 227.02 | 500.49 | 112.16 | 201.89 |
| 79993.8 | 229.3 | 505.53 | 106.96 | 192.53 |
| 100002.4 | 230.78 | 508.77 | 103.18 | 185.72 |
| 150010.2 | 233.34 | 514.43 | 97.19 | 174.95 |
| 200017.4 | 235.07 | 518.23 | 93.04 | 167.47 |
| 400050.6 | 238.68 | 526.21 | 84.39 | 151.9 |
| 600093.0 | 240.58 | 530.39 | 79.5 | 143.1 |
| 800133.2 | 241.76 | 533.0 | 76.42 | 137.56 |
| 1000000.0 | 242.57 | 534.78 | 74.28 | 133.71 |

Integral Mass and Energy(Spillage) Release at 24 hours after postulated accident

| Time (sec) | Integral Mass | | Integral Energy | |
|------------|---------------|-------------|-----------------|-------------|
| | kg | lbm | Million kcal | Million Btu |
| 85,002 | 19,003,347 | 41,895,208 | 2,146.677 | 8,518.701 |
| 1,000,000 | 237,770,196 | 524,193,553 | 20,307.058 | 80,584.918 |

APR1400 DCD TIER 2

Table 6.2.1-4 (13 of 25)

Insert this page.

Part B. Reactor Vessel Pressure vs. Time
(Blowdown Period)

| Time (sec) | Reactor Vessel Pressure | |
|------------|-------------------------|----------|
| | kg/cm ² A | psia |
| 0.000 | 167.36 | 2,380.40 |
| 0.027 | 159.52 | 2,268.90 |
| 0.054 | 147.05 | 2,091.50 |
| 0.103 | 125.06 | 1,778.70 |
| 0.152 | 126.83 | 1,804.00 |
| 0.202 | 126.45 | 1,798.60 |
| 0.252 | 125.82 | 1,789.60 |
| 0.298 | 125.29 | 1,782.10 |
| 0.351 | 123.83 | 1,761.30 |
| 0.400 | 123.02 | 1,749.70 |
| 0.603 | 120.51 | 1,714.00 |
| 0.800 | 118.85 | 1,690.50 |
| 1.000 | 117.11 | 1,665.70 |
| 1.202 | 114.64 | 1,630.50 |
| 1.401 | 112.52 | 1,600.40 |
| 1.607 | 111.04 | 1,579.30 |
| 1.800 | 109.75 | 1,561.00 |
| 2.001 | 108.13 | 1,538.00 |
| 2.204 | 106.14 | 1,509.70 |
| 2.407 | 104.53 | 1,486.80 |
| 2.601 | 104.06 | 1,480.10 |
| 2.812 | 102.49 | 1,457.80 |
| 3.008 | 100.88 | 1,434.90 |
| 3.208 | 99.02 | 1,408.40 |
| 3.408 | 97.55 | 1,387.50 |

APR1400 DCD TIER 2

Table 6.2.1-4 (14 of 25)

Insert this page.

**Part B. Reactor Vessel Pressure vs. Time
(Blowdown Period)**

| Time (sec) | Reactor Vessel Pressure | |
|------------|-------------------------|----------|
| | kg/cm ² A | psia |
| 3.608 | 95.48 | 1,358.10 |
| 3.808 | 93.41 | 1,328.60 |
| 4.000 | 91.91 | 1,307.30 |
| 4.210 | 90.07 | 1,281.10 |
| 4.409 | 88.60 | 1,260.20 |
| 4.609 | 87.41 | 1,243.20 |
| 4.809 | 86.24 | 1,226.60 |
| 5.009 | 85.01 | 1,209.10 |
| 6.209 | 80.24 | 1,141.30 |
| 6.409 | 79.48 | 1,130.40 |
| 6.609 | 78.88 | 1,121.90 |
| 6.809 | 78.27 | 1,113.30 |
| 7.009 | 77.62 | 1,104.00 |
| 7.209 | 76.94 | 1,094.40 |
| 7.409 | 76.32 | 1,085.50 |
| 7.609 | 75.57 | 1,074.90 |
| 7.809 | 74.87 | 1,064.90 |
| 8.009 | 74.23 | 1,055.80 |
| 8.409 | 72.92 | 1,037.20 |
| 8.809 | 71.62 | 1,018.70 |
| 9.204 | 70.32 | 1,000.20 |
| 9.608 | 69.01 | 981.57 |
| 10.004 | 67.70 | 962.86 |
| 10.404 | 66.32 | 943.31 |
| 10.799 | 64.73 | 920.61 |
| 11.205 | 62.25 | 885.43 |

APR1400 DCD TIER 2

Table 6.2.1-4 (15 of 25)

Insert this page.

**Part B. Reactor Vessel Pressure vs. Time
(Blowdown Period)**

| Time (sec) | Reactor Vessel Pressure | |
|------------|-------------------------|--------|
| | kg/cm ² A | psia |
| 11.601 | 59.92 | 852.22 |
| 12.006 | 58.14 | 826.88 |
| 12.205 | 55.99 | 796.34 |
| 12.406 | 55.20 | 785.18 |
| 12.599 | 53.98 | 767.78 |
| 12.806 | 52.89 | 752.32 |
| 13.005 | 51.83 | 737.15 |
| 13.213 | 50.66 | 720.49 |
| 13.413 | 49.62 | 705.72 |
| 13.613 | 48.60 | 691.24 |
| 14.816 | 40.78 | 579.98 |
| 15.016 | 39.48 | 561.58 |
| 15.214 | 37.97 | 540.09 |
| 15.409 | 36.72 | 522.26 |
| 15.609 | 35.32 | 502.42 |
| 15.809 | 34.01 | 483.72 |
| 16.009 | 32.71 | 465.30 |
| 16.200 | 31.56 | 448.93 |
| 16.400 | 30.45 | 433.14 |
| 16.601 | 29.23 | 415.81 |
| 16.800 | 28.03 | 398.63 |
| 17.001 | 26.77 | 380.75 |
| 17.205 | 25.49 | 362.53 |
| 17.400 | 24.24 | 344.80 |
| 17.600 | 23.00 | 327.17 |
| 17.800 | 21.78 | 309.80 |
| 18.000 | 20.54 | 292.11 |
| 18.200 | 19.37 | 275.52 |

APR1400 DCD TIER 2

Table 6.2.1-4 (16 of 25)

Insert this page.

Part B. Reactor Vessel Pressure vs. Time
(Reflood and Post-reflood Period)

| Time (sec) | Reactor Vessel Pressure | |
|------------|-------------------------|--------|
| | kg/cm ² A | psia |
| 18.400 | 18.22 | 259.10 |
| 18.600 | 17.10 | 243.28 |
| 18.802 | 15.99 | 227.49 |
| 18.999 | 14.94 | 212.46 |
| 19.203 | 15.92 | 226.38 |

APR1400 DCD TIER 2

Table 6.2.1-4 (17 of 25)

Insert this page.

Part B. Reactor Vessel Pressure vs. Time
(Reflood and Post-reflood Period)

| Time (sec) | Reactor Vessel Pressure | |
|------------|-------------------------|---------|
| | kg/cm ² A | psia |
| 19.20 | 4.080 | 58.000 |
| 19.30 | 4.120 | 58.590 |
| 21.30 | 4.460 | 63.380 |
| 23.30 | 6.140 | 87.270 |
| 25.30 | 8.050 | 114.540 |
| 27.90 | 10.220 | 145.330 |
| 28.00 | 10.290 | 146.330 |
| 28.10 | 10.360 | 147.310 |
| 28.20 | 10.410 | 148.050 |
| 32.20 | 10.140 | 144.210 |
| 36.20 | 9.860 | 140.190 |
| 40.20 | 9.590 | 136.350 |
| 44.20 | 9.330 | 132.680 |
| 48.20 | 9.080 | 129.170 |
| 52.20 | 8.850 | 125.830 |
| 56.20 | 8.620 | 122.620 |
| 60.20 | 8.410 | 119.560 |
| 63.50 | 8.240 | 117.130 |
| 63.60 | 8.230 | 117.060 |
| 63.70 | 8.220 | 116.960 |
| 63.80 | 8.210 | 116.800 |
| 65.80 | 8.010 | 113.870 |
| 67.80 | 7.840 | 111.530 |
| 69.80 | 7.700 | 109.590 |
| 71.80 | 7.590 | 108.020 |
| 73.80 | 7.500 | 106.720 |
| 75.80 | 7.420 | 105.580 |
| 77.80 | 7.350 | 104.580 |

APR1400 DCD TIER 2

Table 6.2.1-4 (18 of 25)

Insert this page.

**Part B. Reactor Vessel Pressure vs. Time
(Reflood and Post-reflood Period)**

| Time (sec) | Reactor Vessel Pressure | |
|------------|-------------------------|---------|
| | kg/cm ² A | psia |
| 79.80 | 7.290 | 103.700 |
| 81.80 | 7.230 | 102.900 |
| 82.80 | 7.210 | 102.530 |
| 82.90 | 7.210 | 102.490 |
| 83.00 | 7.200 | 102.460 |
| 83.10 | 7.160 | 101.840 |
| 83.20 | 7.190 | 102.230 |
| 83.30 | 7.150 | 101.690 |
| 83.40 | 7.140 | 101.490 |
| 83.50 | 7.130 | 101.420 |
| 85.70 | 6.980 | 99.240 |
| 88.20 | 6.730 | 95.770 |
| 90.70 | 6.500 | 92.450 |
| 93.20 | 6.290 | 89.480 |
| 95.70 | 6.110 | 86.850 |
| 98.20 | 5.940 | 84.510 |
| 100.70 | 5.800 | 82.430 |
| 103.20 | 5.660 | 80.550 |
| 105.70 | 5.550 | 78.870 |
| 108.20 | 5.440 | 77.340 |
| 110.10 | 5.360 | 76.280 |
| 110.20 | 5.360 | 76.220 |
| 110.30 | 5.360 | 76.170 |
| 110.80 | 5.460 | 77.700 |
| 111.30 | 5.190 | 73.760 |
| 111.80 | 5.000 | 71.060 |
| 112.30 | 4.950 | 70.450 |
| 112.80 | 4.910 | 69.890 |

APR1400 DCD TIER 2

Table 6.2.1-4 (19 of 25)

Insert this page.

Part B. Reactor Vessel Pressure vs. Time
(Reflood and Post-reflood period)

| Time (sec) | Reactor Vessel Pressure | |
|------------|-------------------------|--------|
| | kg/cm ² A | psia |
| 113.30 | 4.880 | 69.430 |
| 113.80 | 4.850 | 69.020 |
| 114.30 | 4.830 | 68.660 |
| 114.80 | 4.790 | 68.120 |
| 115.30 | 5.060 | 72.010 |
| 116.30 | 4.820 | 68.600 |
| 117.30 | 4.750 | 67.530 |
| 118.30 | 4.640 | 65.930 |
| 119.30 | 4.620 | 65.660 |
| 120.30 | 4.580 | 65.090 |
| 121.30 | 4.590 | 65.340 |
| 122.30 | 4.680 | 66.520 |
| 123.30 | 4.750 | 67.620 |
| 124.00 | 4.570 | 65.070 |
| 124.10 | 4.680 | 66.570 |

APR1400 DCD TIER 2

Table 6.2.1-4 (20 of 25)

Insert this page.

Part B. Reactor Vessel Pressure vs. Time (Decay heat Period)

| Time (sec) | Reactor Vessel Pressure | |
|------------|-------------------------|--------|
| | kg/cm ² A | psia |
| 400.0 | 3.934 | 55.96 |
| 599.9 | 3.811 | 54.211 |
| 800.0 | 3.726 | 52.992 |
| 999.0 | 3.659 | 52.038 |
| 1503.3 | 3.538 | 50.326 |
| 1996.5 | 3.46 | 49.219 |
| 4001.9 | 3.323 | 47.267 |
| 5998.5 | 3.277 | 46.605 |
| 7996.7 | 3.263 | 46.417 |
| 9996.4 | 3.261 | 46.388 |
| 15004.8 | 3.256 | 46.307 |
| 20010.9 | 3.216 | 45.737 |
| 40037.0 | 2.916 | 41.473 |
| 59965.8 | 2.612 | 37.155 |
| 79993.8 | 2.404 | 34.199 |
| 100002.4 | 2.273 | 32.326 |
| 150010.2 | 2.078 | 29.554 |
| 200017.4 | 1.959 | 27.86 |
| 400050.6 | 1.746 | 24.829 |
| 600093.0 | 1.645 | 23.4 |
| 800133.2 | 1.588 | 22.586 |
| 1000000.0 | 1.551 | 22.055 |

APR1400 DCD TIER 2

Table 6.2.1-4 (21 of 25)

Insert this page.

Part C. Safety Injection Flow vs. Time (Blowdown Period)

| Time (sec) | Safety Injection Tank Flow | |
|------------|----------------------------|-----------|
| | kg/sec | lbm/sec |
| 0.000 | 0.00 | 0.00 |
| 0.027 | 0.00 | 0.00 |
| 13.813 | 0.00 | 0.00 |
| 14.013 | 0.00 | 0.00 |
| 14.203 | 1,281.21 | 2,824.60 |
| 14.409 | 1,690.48 | 3,726.90 |
| 14.616 | 1,989.35 | 4,385.80 |
| 14.816 | 2,357.62 | 5,197.70 |
| 15.016 | 2,555.71 | 5,634.40 |
| 15.214 | 2,769.58 | 6,105.90 |
| 15.409 | 2,934.41 | 6,469.30 |
| 15.609 | 3,097.38 | 6,828.60 |
| 15.809 | 3,236.55 | 7,135.40 |
| 16.009 | 3,362.73 | 7,413.60 |
| 16.200 | 3,451.73 | 7,609.80 |
| 16.400 | 3,536.73 | 7,797.20 |
| 16.601 | 3,639.88 | 8,024.60 |
| 16.800 | 3,738.76 | 8,242.60 |
| 17.001 | 3,845.63 | 8,478.20 |
| 17.205 | 3,957.26 | 8,724.30 |
| 17.400 | 4,061.17 | 8,953.40 |
| 17.600 | 4,159.33 | 9,169.80 |
| 17.800 | 4,253.59 | 9,377.60 |
| 18.000 | 4,351.61 | 9,593.70 |
| 18.200 | 4,434.98 | 9,777.50 |
| 18.400 | 4,517.85 | 9,960.20 |
| 18.600 | 4,594.41 | 10,129.00 |
| 18.802 | 4,668.35 | 10,292.00 |
| 18.999 | 4,740.47 | 10,451.00 |
| 19.203 | 4,496.26 | 9,912.60 |

APR1400 DCD TIER 2

Table 6.2.1-4 (22 of 25)

Insert this page.

Part C. Safety Injection Flow vs. Time (Reflood and Post-reflood Period)

| Time (sec) | Safety Injection Tank Flow | | Safety Injection Pump Flow | |
|------------|----------------------------|----------|----------------------------|---------|
| | kg/sec | lbm/sec | kg/sec | lbm/sec |
| 19.203 | 3,140.51 | 6,923.66 | 328.55 | 724.33 |
| 19.303 | 3,128.73 | 6,897.71 | 328.55 | 724.33 |
| 21.303 | 2,898.47 | 6,390.06 | 328.12 | 723.38 |
| 23.303 | 2,609.50 | 5,753.00 | 325.77 | 718.20 |
| 25.303 | 2,312.95 | 5,099.21 | 323.05 | 712.21 |
| 28.003 | 1,939.32 | 4,275.49 | 319.82 | 705.09 |
| 28.103 | 1,926.56 | 4,247.35 | 319.72 | 704.87 |
| 31.603 | 1,750.73 | 3,859.72 | 319.86 | 705.18 |
| 35.103 | 1,619.32 | 3,570.00 | 320.22 | 705.97 |
| 38.603 | 1,509.09 | 3,327.00 | 320.56 | 706.73 |
| 42.103 | 1,415.41 | 3,120.45 | 320.89 | 707.45 |
| 45.603 | 1,334.93 | 2,943.04 | 321.21 | 708.15 |
| 49.103 | 1,265.20 | 2,789.30 | 321.52 | 708.82 |
| 52.603 | 1,204.37 | 2,655.19 | 321.81 | 709.47 |
| 56.103 | 1,150.99 | 2,537.52 | 322.09 | 710.09 |
| 59.603 | 1,103.93 | 2,433.76 | 322.36 | 710.69 |
| 63.503 | 1,057.76 | 2,331.98 | 322.65 | 711.32 |
| 63.603 | 1,056.66 | 2,329.54 | 322.66 | 711.34 |
| 63.703 | 478.63 | 1,055.21 | 322.66 | 711.36 |
| 63.803 | 478.83 | 1,055.65 | 322.67 | 711.38 |
| 72.803 | 496.56 | 1,094.73 | 323.63 | 713.48 |
| 81.803 | 488.31 | 1,076.55 | 324.08 | 714.47 |
| 90.803 | 515.23 | 1,135.90 | 325.12 | 716.77 |
| 99.803 | 534.80 | 1,179.03 | 326.04 | 718.80 |
| 108.803 | 539.77 | 1,189.99 | 326.66 | 720.16 |
| 110.203 | 539.75 | 1,189.96 | 326.74 | 720.33 |
| 112.203 | 430.32 | 948.69 | 324.92 | 716.34 |
| 114.203 | 470.54 | 1,037.36 | 325.69 | 718.02 |

APR1400 DCD TIER 2

Table 6.2.1-4 (23of 25)

Insert this page.

Part C. Safety Injection Flow vs. Time (Reflood and Post-reflood Period)

| Time (sec) | Safety Injection Tank Flow | | Safety Injection Pump Flow | |
|------------|----------------------------|----------|----------------------------|---------|
| | kg/sec | lbm/sec | kg/sec | lbm/sec |
| 116.203 | 482.51 | 1,063.76 | 326.00 | 718.71 |
| 118.203 | 543.30 | 1,197.78 | 327.23 | 721.43 |
| 120.203 | 542.75 | 1,196.56 | 327.33 | 721.64 |
| 122.203 | 532.08 | 1,173.04 | 327.22 | 721.41 |
| 124.103 | 559.22 | 1,232.87 | 327.85 | 722.80 |
| 128.603 | 547.75 | 1,207.59 | 327.84 | 722.78 |
| 133.103 | 506.02 | 1,115.59 | 327.26 | 721.49 |
| 137.603 | 546.18 | 1,204.13 | 328.22 | 723.61 |
| 142.103 | 535.75 | 1,181.13 | 328.21 | 723.59 |
| 146.603 | 520.42 | 1,147.33 | 328.11 | 723.36 |
| 151.103 | 515.47 | 1,136.42 | 328.20 | 723.55 |
| 155.603 | 514.44 | 1,134.16 | 328.35 | 723.88 |
| 160.503 | 504.55 | 1,112.35 | 328.34 | 723.87 |
| 185.203 | 463.17 | 1,021.11 | 328.40 | 724.01 |
| 210.203 | 426.36 | 939.97 | 328.45 | 724.11 |
| 235.203 | 393.89 | 868.39 | 328.49 | 724.19 |
| 260.203 | 364.50 | 803.58 | 328.51 | 724.25 |
| 285.203 | 336.27 | 741.35 | 328.52 | 724.26 |
| 310.203 | 310.14 | 683.75 | 328.52 | 724.27 |
| 335.203 | 285.92 | 630.35 | 328.52 | 724.27 |
| 360.203 | 263.28 | 580.43 | 328.53 | 724.28 |
| 368.003 | 256.50 | 565.48 | 328.53 | 724.28 |
| 368.103 | 256.41 | 565.29 | 328.53 | 724.28 |
| 368.203 | 0.00 | 0.00 | 328.53 | 724.28 |
| 368.303 | 0.00 | 0.00 | 328.53 | 724.28 |
| 403.303 | 0.00 | 0.00 | 328.54 | 724.32 |
| 438.303 | 0.00 | 0.00 | 328.54 | 724.32 |
| 473.303 | 0.00 | 0.00 | 328.54 | 724.31 |

APR1400 DCD TIER 2

Table 6.2.1-4 (24 of 25)

Insert this page.

Part C. Safety Injection Flow vs. Time (Reflood and Post-reflood Period)

| Time (sec) | Safety Injection Tank Flow | | Safety Injection Pump Flow | |
|------------|----------------------------|---------|----------------------------|---------|
| | kg/sec | lbm/sec | kg/sec | lbm/sec |
| 508.303 | 0.00 | 0.00 | 328.54 | 724.31 |
| 543.303 | 0.00 | 0.00 | 328.53 | 724.30 |
| 578.303 | 0.00 | 0.00 | 328.53 | 724.29 |
| 600.003 | 0.00 | 0.00 | 328.53 | 724.29 |

APR1400 DCD TIER 2

Table 6.2.1-4 (25 of 25)

Insert this page.

Part D. Chronology of Events

| Time (sec) | Event | Values |
|------------|---|--|
| 0.00 | Break occurs | - |
| 4.36 | Containment pressure Hi-Hi setpoint | 1.547 kg/cm ² G (22.0 psig) |
| 14.01 | Start safety injection tank (SIT) injection | - |
| 19.01 | First peak containment pressure (Blowdown phase) | 3.073 kg/cm ² G (43.70 psig) |
| 19.20 | End of blowdown | - |
| | Start SI pump injection | - |
| 63.70 | SIT flow is turned down to low flow by fluidic device in SIT | - |
| 110.20 | End of reflood | |
| 114.36 | Start containment spray actuation | |
| 114.92 | Peak containment temperature | 133.07 °C (271.52 °F) |
| 114.92 | Peak containment pressure | 3.415 kg/cm ² G (48.57 psig) |
| 124.10 | End of post reflood | - |
| 368.20 | Safety injection tank empty | - |
| 50,852.2 | Time of depressurization of the containment at 50% of peak pressure | 1.706 kg/cm ² G (24.27 psig) |

Table 6.2.1-5 (1 of 27)

Double-Ended Suction Leg Slot Break – Minimum SIS Flow
(0.9121 m² (9.8175 ft²) Total Break Area)

Part A. Mass and Energy Release Data
 (Blowdown Period)

| Time (sec) | Break Mass Flow Rate | | Break Enthalpy | |
|------------|----------------------|------------|----------------|---------|
| | kg/sec | lbm/sec | kcal/kg | Btu/lbm |
| 0.000 | 0.00 | 0.00 | 0.00 | 0.00 |
| 0.027 | 35,826.69 | 78,984.75 | 310.61 | 559.13 |
| 0.054 | 35,499.95 | 78,264.39 | 310.08 | 558.18 |
| 0.103 | 35,936.95 | 79,227.82 | 309.90 | 557.85 |
| 0.152 | 49,099.29 | 108,245.97 | 310.38 | 558.72 |
| 0.202 | 47,285.37 | 104,246.94 | 311.04 | 559.91 |
| 0.252 | 45,576.63 | 100,479.79 | 311.57 | 560.85 |
| 0.298 | 44,683.04 | 98,509.75 | 311.94 | 561.52 |
| 0.351 | 44,779.94 | 98,723.38 | 312.17 | 561.94 |
| 0.400 | 44,346.29 | 97,767.34 | 312.52 | 562.56 |
| 0.603 | 43,478.91 | 95,855.09 | 313.48 | 564.30 |
| 0.800 | 44,864.47 | 98,909.74 | 314.64 | 566.38 |
| 1.000 | 42,167.46 | 92,963.82 | 315.74 | 568.36 |
| 1.202 | 40,552.76 | 89,404.00 | 317.33 | 571.22 |
| 1.401 | 38,527.59 | 84,939.24 | 319.05 | 574.33 |
| 1.607 | 38,152.42 | 84,112.13 | 320.39 | 576.73 |
| 1.800 | 37,859.70 | 83,466.78 | 321.87 | 579.40 |
| 2.001 | 37,500.04 | 82,673.88 | 323.76 | 582.80 |
| 2.204 | 35,984.54 | 79,332.74 | 325.55 | 586.03 |
| 2.407 | 33,372.26 | 73,573.62 | 326.50 | 587.73 |
| 2.601 | 31,669.84 | 69,820.41 | 327.91 | 590.27 |
| 2.812 | 30,653.27 | 67,579.23 | 330.85 | 595.57 |
| 3.008 | 29,668.44 | 65,408.05 | 334.73 | 602.56 |

Replace these 27 pages of Table 6.2.1–5
 with the following 26 pages of revised
 Table 6.2.1–5.

Table 6.2.1-5 (2 of 27)

Part A. Mass and Energy Release Data
(Blowdown Period)

| Time (sec) | Break Mass Flow Rate | | Break Enthalpy | |
|------------|----------------------|-----------|----------------|---------|
| | kg/sec | lbm/sec | kcal/kg | Btu/lbm |
| 3.208 | 28,297.64 | 62,385.94 | 340.03 | 612.09 |
| 3.408 | 26,715.66 | 58,898.26 | 346.75 | 624.19 |
| 3.608 | 24,966.73 | 55,042.51 | 354.00 | 637.23 |
| 3.808 | 23,497.04 | 51,802.38 | 360.32 | 648.62 |
| 4.000 | 22,127.47 | 48,782.98 | 365.48 | 657.89 |
| 4.211 | 21,436.30 | 47,259.20 | 366.85 | 660.37 |
| 4.409 | 21,008.90 | 46,316.93 | 366.71 | 660.11 |
| 4.609 | 20,598.55 | 45,412.26 | 366.16 | 659.12 |
| 4.809 | 20,267.22 | 44,681.81 | 365.67 | 658.24 |
| 5.009 | 20,051.87 | 44,207.03 | 364.92 | 656.90 |
| 5.209 | 19,841.27 | 43,742.73 | 364.35 | 655.86 |
| 5.409 | 19,815.87 | 43,686.73 | 363.56 | 654.45 |
| 5.609 | 19,693.35 | 43,416.63 | 363.47 | 654.28 |
| 5.809 | 19,144.10 | 42,205.74 | 364.81 | 656.69 |
| 6.009 | 18,734.91 | 41,303.63 | 365.84 | 658.55 |
| 6.209 | 18,566.23 | 40,931.75 | 365.82 | 658.51 |
| 6.409 | 18,595.07 | 40,995.33 | 363.92 | 655.09 |
| 6.609 | 18,479.62 | 40,740.79 | 363.55 | 654.43 |
| 6.809 | 17,933.49 | 39,536.78 | 366.91 | 660.48 |
| 7.009 | 17,132.26 | 37,770.38 | 372.47 | 670.48 |
| 7.209 | 16,620.46 | 36,642.04 | 375.29 | 675.57 |
| 7.409 | 16,372.62 | 36,095.63 | 375.88 | 676.62 |
| 7.609 | 16,206.97 | 35,730.45 | 376.05 | 676.92 |
| 7.809 | 16,191.18 | 35,695.62 | 374.41 | 673.98 |

Replace these 27 pages of Table 6.2.1-5
with the following 26 pages of revised
Table 6.2.1-5.

Table 6.2.1-5 (3 of 27)

Part A. Mass and Energy Release Data (Blowdown Period)

| Time (sec) | Break Mass Flow Rate | | Break Enthalpy | |
|------------|----------------------|-----------|----------------|---------|
| | kg/sec | lbm/sec | kcal/kg | Btu/lbm |
| 8.009 | 16,125.16 | 35,550.08 | 373.73 | 672.75 |
| 8.209 | 15,915.11 | 35,086.98 | 374.73 | 674.55 |
| 8.409 | 15,680.94 | 34,570.74 | 375.85 | 676.56 |
| 8.609 | 15,427.32 | 34,011.60 | 377.17 | 678.94 |
| 8.809 | 15,141.74 | 33,381.99 | 378.82 | 681.91 |
| 9.005 | 14,809.07 | 32,648.58 | 380.75 | 685.38 |
| 9.204 | 14,527.77 | 32,028.41 | 382.90 | 689.26 |
| 9.400 | 14,196.28 | 31,297.60 | 385.45 | 693.86 |
| 9.608 | 13,797.32 | 30,418.04 | 387.37 | 697.31 |
| 9.801 | 13,391.38 | 29,523.09 | 391.81 | 705.30 |
| 10.004 | 13,129.00 | 28,944.65 | 395.88 | 712.62 |
| 10.205 | 12,765.77 | 28,143.85 | 399.12 | 718.46 |
| 10.404 | 12,429.45 | 27,402.39 | 401.76 | 723.21 |
| 10.603 | 11,985.20 | 26,422.98 | 406.03 | 730.90 |
| 10.799 | 11,582.15 | 25,534.40 | 412.05 | 741.74 |
| 11.004 | 11,140.57 | 24,560.87 | 417.73 | 751.96 |
| 11.205 | 10,637.22 | 23,451.17 | 423.35 | 762.07 |
| 11.406 | 10,190.47 | 22,466.27 | 428.61 | 771.53 |
| 11.601 | 9,728.82 | 21,448.50 | 433.53 | 780.39 |
| 11.804 | 9,042.09 | 19,934.50 | 445.87 | 802.61 |
| 12.006 | 8,756.29 | 19,304.41 | 452.29 | 814.16 |
| 12.205 | 8,377.30 | 18,468.88 | 457.85 | 824.18 |
| 12.406 | 8,013.92 | 17,667.76 | 463.75 | 834.79 |
| 12.599 | 7,657.53 | 16,882.05 | 469.08 | 844.38 |
| 12.806 | 7,397.99 | 16,309.86 | 475.41 | 855.78 |
| 13.005 | 7,153.35 | 15,770.51 | 476.56 | 857.85 |
| 13.213 | 6,944.67 | 15,310.45 | 475.99 | 856.84 |

Replace these 27 pages of Table 6.2.1-5 with the following 26 pages of revised Table 6.2.1-5.

Table 6.2.1-5 (4 of 27)

Part A. Mass and Energy Release Data (Blowdown Period)

| Time (sec) | Break Mass Flow Rate | | Break Enthalpy | |
|------------|----------------------|-----------|----------------|---------|
| | kg/sec | lbm/sec | kcal/kg | Btu/lbm |
| 13.413 | 6,730.23 | 14,837.69 | 477.18 | 858.98 |
| 13.613 | 6,534.48 | 14,406.13 | 479.25 | 862.71 |
| 13.813 | 6,358.64 | 14,018.47 | 480.50 | 864.96 |
| 14.013 | 6,188.02 | 13,642.32 | 481.42 | 866.61 |
| 14.203 | 5,966.42 | 13,153.78 | 482.94 | 869.34 |
| 14.409 | 5,852.22 | 12,902.00 | 478.07 | 860.57 |
| 14.616 | 5,895.97 | 12,998.45 | 457.84 | 824.16 |
| 14.816 | 5,885.88 | 12,976.22 | 441.01 | 793.86 |
| 15.016 | 5,839.74 | 12,874.49 | 431.85 | 777.37 |
| 15.214 | 5,717.91 | 12,605.89 | 425.51 | 765.97 |
| 15.409 | 5,579.03 | 12,299.72 | 419.00 | 754.25 |
| 15.609 | 5,389.08 | 11,880.96 | 415.55 | 748.04 |
| 15.809 | 5,183.01 | 11,426.64 | 413.16 | 743.74 |
| 16.009 | 4,939.96 | 10,890.80 | 411.96 | 741.57 |
| 16.200 | 4,374.29 | 9,643.72 | 443.96 | 799.17 |
| 16.400 | 4,198.25 | 9,255.61 | 443.34 | 798.06 |
| 16.601 | 4,077.66 | 8,989.74 | 441.21 | 794.23 |
| 16.800 | 3,932.45 | 8,669.61 | 438.05 | 788.53 |
| 17.001 | 3,815.63 | 8,412.08 | 433.55 | 780.43 |
| 17.205 | 3,707.03 | 8,172.64 | 424.86 | 764.79 |
| 17.400 | 3,576.74 | 7,885.40 | 419.56 | 755.24 |
| 17.600 | 3,431.20 | 7,564.54 | 416.49 | 749.73 |
| 17.800 | 3,384.27 | 7,461.08 | 407.89 | 734.25 |
| 18.000 | 3,343.38 | 7,370.94 | 401.24 | 722.27 |
| 18.200 | 3,122.01 | 6,882.88 | 401.21 | 722.22 |
| 18.400 | 3,066.26 | 6,759.98 | 391.83 | 705.34 |
| 18.600 | 2,962.81 | 6,531.92 | 382.50 | 688.54 |

Replace these 27 pages of Table 6.2.1-5 with the following 26 pages of revised Table 6.2.1-5.

Table 6.2.1-5 (5 of 27)

Part A. Mass and Energy Release Data
(Blowdown Period)

| Time (sec) | Break Mass Flow Rate | | Break Enthalpy | |
|------------|----------------------|----------|----------------|---------|
| | kg/sec | lbm/sec | kcal/kg | Btu/lbm |
| 18.802 | 2,774.26 | 6,116.24 | 381.33 | 686.43 |
| 18.999 | 2,608.38 | 5,750.52 | 378.21 | 680.83 |
| 19.203 | 2,546.44 | 5,613.97 | 383.68 | 690.67 |

Integral Mass and Energy Release at End of Blowdown

| Time (sec) | Integral Mass | | Integral Energy | |
|------------|---------------|-------------|-----------------|-------------|
| | kg | lbm | Million kcal | Million Btu |
| 19.203 | 304,940.875 | 672,283.090 | 110.483 | 438.461 |

Replace these 27 pages of Table 6.2.1-5
with the following 26 pages of revised
Table 6.2.1-5.

Table 6.2.1-5 (6 of 27)

Part A. Mass and Energy Release Data
(Reflood and Post-reflood Period)

| Time (sec) | Break Mass Flow Rate | | Break Enthalpy | |
|------------|----------------------|----------|----------------|----------|
| | kg/sec | lbm/sec | kcal/kg | Btu/lbm |
| 19.20 | 0.00 | 0.00 | 0.00 | 0.00 |
| 19.30 | 65.68 | 144.80 | 705.18 | 1,269.39 |
| 19.40 | 87.02 | 191.85 | 704.39 | 1,267.97 |
| 21.40 | 170.74 | 376.42 | 706.26 | 1,271.34 |
| 23.40 | 419.58 | 925.02 | 709.42 | 1,277.03 |
| 25.40 | 619.99 | 1,366.86 | 708.76 | 1,275.85 |
| 27.40 | 778.07 | 1,715.35 | 707.06 | 1,272.79 |
| 28.70 | 857.72 | 1,890.96 | 705.73 | 1,270.38 |
| 28.80 | 863.10 | 1,902.81 | 705.62 | 1,270.19 |
| 28.90 | 503.65 | 1,110.37 | 705.52 | 1,270.00 |
| 29.00 | 505.52 | 1,114.49 | 705.44 | 1,269.86 |
| 31.60 | 498.21 | 1,098.37 | 704.10 | 1,267.45 |
| 34.20 | 489.69 | 1,079.58 | 702.84 | 1,265.19 |
| 36.80 | 481.32 | 1,061.13 | 701.61 | 1,262.97 |
| 39.40 | 473.10 | 1,043.01 | 700.39 | 1,260.78 |
| 42.00 | 465.01 | 1,025.18 | 699.21 | 1,258.65 |
| 44.60 | 457.06 | 1,007.65 | 698.04 | 1,256.54 |
| 47.20 | 449.25 | 990.44 | 696.87 | 1,254.44 |
| 49.80 | 441.62 | 973.60 | 695.70 | 1,252.32 |
| 52.40 | 434.10 | 957.04 | 694.53 | 1,250.23 |
| 55.00 | 426.71 | 940.73 | 693.39 | 1,248.18 |
| 57.60 | 419.43 | 924.69 | 692.26 | 1,246.14 |
| 60.20 | 412.26 | 908.89 | 691.15 | 1,244.15 |
| 62.80 | 405.21 | 893.35 | 690.05 | 1,242.17 |
| 63.50 | 403.34 | 889.22 | 689.76 | 1,241.64 |
| 63.60 | 403.08 | 888.64 | 689.71 | 1,241.55 |

Replace these 27 pages of Table 6.2.1-5
with the following 26 pages of revised
Table 6.2.1-5.

Table 6.2.1-5 (7 of 27)

Part A. Mass and Energy Release Data
(Reflood and Post-reflood Period)

| Time (sec) | Break Mass Flow Rate | | Break Enthalpy | |
|------------|----------------------|----------|----------------|----------|
| | kg/sec | lbm/sec | kcal/kg | Btu/lbm |
| 63.70 | 694.36 | 1,530.82 | 689.67 | 1,241.48 |
| 63.80 | 692.95 | 1,527.70 | 689.65 | 1,241.44 |
| 65.80 | 657.80 | 1,450.20 | 689.31 | 1,240.84 |
| 67.80 | 630.07 | 1,389.08 | 688.92 | 1,240.13 |
| 69.80 | 608.00 | 1,340.42 | 688.47 | 1,239.32 |
| 71.80 | 590.18 | 1,301.12 | 687.98 | 1,238.43 |
| 73.80 | 575.37 | 1,268.47 | 687.45 | 1,237.48 |
| 75.80 | 563.31 | 1,241.90 | 686.89 | 1,236.47 |
| 77.80 | 553.13 | 1,219.46 | 686.47 | 1,235.71 |
| 79.80 | 544.50 | 1,200.42 | 685.85 | 1,234.59 |
| 81.80 | 537.04 | 1,183.98 | 685.21 | 1,233.44 |
| 83.80 | 530.52 | 1,169.61 | 684.54 | 1,232.25 |
| 85.80 | 524.76 | 1,156.91 | 683.86 | 1,231.02 |
| 87.80 | 519.59 | 1,145.50 | 683.16 | 1,229.76 |
| 88.90 | 516.95 | 1,139.68 | 672.96 | 1,211.39 |
| 89.00 | 525.76 | 1,159.11 | 680.79 | 1,225.48 |
| 89.10 | 495.84 | 1,093.15 | 669.18 | 1,204.58 |
| 89.20 | 527.09 | 1,162.03 | 668.18 | 1,202.79 |
| 89.30 | 518.51 | 1,143.13 | 668.37 | 1,203.13 |
| 89.50 | 499.05 | 1,100.23 | 668.91 | 1,204.10 |
| 91.50 | 435.44 | 959.98 | 670.65 | 1,207.24 |
| 93.50 | 397.17 | 875.61 | 671.58 | 1,208.92 |
| 95.50 | 367.63 | 810.48 | 672.25 | 1,210.11 |
| 97.50 | 342.26 | 754.56 | 672.83 | 1,211.17 |
| 99.50 | 319.79 | 705.03 | 673.38 | 1,212.16 |
| 101.50 | 299.61 | 660.52 | 673.92 | 1,213.12 |
| 103.50 | 281.37 | 620.31 | 674.44 | 1,214.07 |
| 105.50 | 264.82 | 583.83 | 674.95 | 1,214.98 |

Replace these 27 pages of Table 6.2.1-5
with the following 26 pages of revised
Table 6.2.1-5.

Table 6.2.1-5 (8 of 27)

Mass and Energy Release Data (Reflood and Post-reflood Period)

| Time (sec) | Break Mass Flow Rate | | Break Enthalpy | |
|---------------|----------------------|----------|----------------|----------|
| | kg/sec | lbm/sec | kcal/kg | Btu/lbm |
| 117.10 | 192.98 | 425.46 | 677.72 | 1,219.97 |
| 117.20 | 192.50 | 424.39 | 677.75 | 1,220.02 |
| 118.20 | 160.97 | 354.88 | 682.73 | 1,228.99 |
| 119.20 | 433.91 | 956.61 | 663.25 | 1,193.93 |
| 120.20 | 94.59 | 208.53 | 701.96 | 1,263.60 |
| 121.20 | 173.41 | 382.31 | 677.72 | 1,219.96 |
| 122.20 | 132.67 | 292.49 | 686.52 | 1,235.80 |
| 123.20 | 515.95 | 1,137.48 | 661.26 | 1,190.33 |
| 124.20 | 506.65 | 1,116.98 | 660.92 | 1,189.72 |
| 125.20 | 394.68 | 870.13 | 662.55 | 1,192.66 |
| 126.20 | 128.13 | 282.47 | 683.18 | 1,229.79 |
| 127.50 | 101.43 | 223.61 | 688.12 | 1,238.68 |
| 127.60 | 76.44 | 168.52 | 702.72 | 1,264.96 |

Integral Mass and Energy Release at the End of Reflood and Post-reflood

| Time (sec) | Integral Mass | | Integral Energy | |
|---------------|---------------|-----------|-----------------|-------------|
| | kg | lbm | Million kcal | Million Btu |
| 117.10 | 43,315.58 | 95,495.00 | 29.90 | 118.66 |
| 127.60 | 45,246.51 | 99,752.00 | 31.20 | 123.84 |

Replace these 27 pages of Table 6.2.1-5 with the following 26 pages of revised Table 6.2.1-5.

Table 6.2.1-5 (9 of 27)

Part A: Spillage Release Data (Reactor Vessel Side)
(Reflood and Post-Reflood Period)

| Time (sec) | Break Mass Flow Rate | | Break Enthalpy | |
|---------------|----------------------|----------|----------------|---------|
| | kg/sec | lbm/sec | kcal/kg | Btu/lbm |
| 19.20 | 0.00 | 0.00 | 0.00 | 0.00 |
| 19.30 | 0.00 | 0.00 | 0.00 | 0.00 |
| 28.80 | 0.00 | 0.00 | 0.00 | 0.00 |
| 28.90 | 971.13 | 2,140.98 | 296.06 | 532.94 |
| 29.00 | 1,260.87 | 2,779.76 | 240.15 | 432.29 |
| 31.60 | 1,157.02 | 2,550.81 | 253.83 | 456.92 |
| 34.20 | 1,071.15 | 2,361.49 | 266.01 | 478.85 |
| 36.80 | 997.39 | 2,198.89 | 277.61 | 499.73 |
| 39.40 | 933.64 | 2,058.33 | 288.58 | 519.47 |
| 42.00 | 878.23 | 1,936.18 | 298.86 | 537.97 |
| 44.60 | 829.89 | 1,829.60 | 308.40 | 555.15 |
| 47.20 | 787.55 | 1,736.27 | 317.17 | 570.94 |
| 49.80 | 750.33 | 1,654.20 | 325.17 | 585.35 |
| 52.40 | 717.62 | 1,582.09 | 332.33 | 598.22 |
| 55.00 | 688.86 | 1,518.68 | 338.60 | 609.52 |
| 57.60 | 663.56 | 1,462.90 | 343.99 | 619.22 |
| 60.20 | 641.30 | 1,413.84 | 348.49 | 627.32 |
| 62.80 | 621.74 | 1,370.71 | 352.11 | 633.84 |
| 63.50 | 616.87 | 1,359.98 | 352.95 | 635.35 |
| 63.60 | 616.19 | 1,358.47 | 353.07 | 635.56 |
| 63.70 | 0.00 | 0.00 | 0.00 | 0.00 |
| 127.50 | 0.00 | 0.00 | 0.00 | 0.00 |
| 127.60 | 0.00 | 0.00 | 0.00 | 0.00 |

Integral Mass and Energy (Reactor Vessel Side Spillage) at EOR and EOPR

| Time (sec) | Integral Mass | | Integral Energy | |
|---------------|---------------|-----------|-----------------|-------------|
| | kg | lbm | Million kcal | Million Btu |
| 117.10 | 29,413.04 | 64,845.00 | 8.864 | 35.179 |
| 127.60 | 29,413.04 | 64,845.00 | 8.864 | 35.179 |

Replace these 27 pages of Table 6.2.1-5
with the following 26 pages of revised
Table 6.2.1-5.

Table 6.2.1-5 (10 of 27)

Part A: Spillage Release Data (Steam Generator Side)
(Reflood and Post-Reflood Period)

| Time (sec) | Break Mass Flow Rate | | Break Enthalpy | |
|---------------|----------------------|----------|----------------|---------|
| | kg/sec | lbm/sec | kcal/kg | Btu/lbm |
| 19.20 | 0.00 | 0.00 | 0.00 | 0.00 |
| 19.30 | 0.00 | 0.00 | 0.00 | 0.00 |
| 89.00 | 0.00 | 0.00 | 0.00 | 0.00 |
| 89.10 | 21.66 | 47.76 | 144.33 | 259.81 |
| 89.20 | 13.00 | 28.67 | 144.35 | 259.85 |
| 89.30 | 14.10 | 31.09 | 144.32 | 259.80 |
| 89.50 | 39.24 | 86.50 | 144.33 | 259.81 |
| 91.50 | 166.16 | 366.32 | 144.33 | 259.81 |
| 93.50 | 218.12 | 480.87 | 144.33 | 259.81 |
| 95.50 | 246.31 | 543.02 | 144.33 | 259.81 |
| 97.50 | 266.58 | 587.71 | 144.33 | 259.81 |
| 99.50 | 283.03 | 623.97 | 144.33 | 259.81 |
| 101.50 | 297.25 | 655.33 | 144.33 | 259.81 |
| 103.50 | 309.70 | 682.78 | 144.33 | 259.81 |
| 105.50 | 320.67 | 706.95 | 144.33 | 259.81 |
| 107.50 | 330.36 | 728.33 | 144.33 | 259.81 |
| 109.50 | 338.95 | 747.27 | 144.33 | 259.81 |
| 111.50 | 346.60 | 764.13 | 144.33 | 259.81 |
| 113.50 | 353.41 | 779.15 | 144.33 | 259.81 |
| 115.50 | 359.50 | 792.56 | 144.33 | 259.81 |
| 117.00 | 363.63 | 801.68 | 144.33 | 259.81 |
| 117.10 | 363.90 | 802.26 | 144.33 | 259.81 |
| 117.20 | 364.16 | 802.84 | 144.33 | 259.81 |
| 118.20 | 457.30 | 1,008.19 | 144.33 | 259.81 |
| 119.20 | 1,657.22 | 3,653.57 | 144.33 | 259.81 |
| 120.20 | 757.55 | 1,670.11 | 144.33 | 259.81 |
| 121.20 | 287.80 | 634.50 | 144.33 | 259.81 |
| 122.20 | 547.78 | 1,207.66 | 144.33 | 259.81 |
| 123.20 | 1,399.03 | 3,084.35 | 144.33 | 259.81 |
| 124.20 | 1,300.27 | 2,866.63 | 144.33 | 259.81 |

Replace these 27 pages of Table 6.2.1-5
with the following 26 pages of revised
Table 6.2.1-5.

Table 6.2.1-5 (11 of 27)

Part A: Spillage Release Data (Steam Generator Side)
(Reflood and Post-Reflood Period)

| Time (sec) | Break Mass Flow Rate | | Break Enthalpy | |
|---------------|----------------------|----------|----------------|---------|
| | kg/sec | lbm/sec | kcal/kg | Btu/lbm |
| 125.20 | 1,426.74 | 3,145.44 | 144.33 | 259.81 |
| 126.20 | 276.29 | 609.12 | 144.33 | 259.81 |
| 127.50 | 206.19 | 454.58 | 144.33 | 259.81 |
| 127.60 | 427.03 | 941.44 | 144.33 | 259.81 |

Integral Mass and Energy (Steam Generator Side Spillage) at EOR and EOPR

| Time (sec) | Integral Mass | | Integral Energy | |
|---------------|---------------|-----------|-----------------|-------------|
| | kg | lbm | Million kcal | Million Btu |
| 117.10 | 7,994.98 | 17,626.00 | 1.154 | 4.579 |
| 127.60 | 14,758.01 | 32,536.00 | 2.130 | 8.453 |

Replace these 27 pages of Table 6.2.1-5 with the following 26 pages of revised Table 6.2.1-5.

Table 6.2.1-5 (12 of 27)

Part A. Mass and Energy (Steam) Release Data
(Decay heat Period)

| Time (sec) | Mass Flow Rate | | Break Enthalpy | |
|------------|----------------|---------|----------------|---------|
| | kg/sec | lbm/sec | kcal/kg | Btu/lbm |
| 400.0 | 55.48 | 122.32 | 653.63 | 1176.53 |
| 599.9 | 52.38 | 115.47 | 653.29 | 1175.92 |
| 800.0 | 50.09 | 110.44 | 653.05 | 1175.49 |
| 999.0 | 48.07 | 105.97 | 652.87 | 1175.16 |
| 1503.6 | 44.06 | 97.14 | 652.54 | 1174.58 |
| 1997.0 | 41.06 | 90.52 | 652.33 | 1174.2 |
| 4002.9 | 33.87 | 74.66 | 651.91 | 1173.43 |
| 6001.3 | 30.26 | 66.72 | 651.68 | 1173.02 |
| 8001.1 | 28.1 | 61.95 | 651.54 | 1172.77 |
| 9990.4 | 26.6 | 58.65 | 651.45 | 1172.61 |
| 15005.4 | 24.29 | 53.55 | 651.28 | 1172.3 |
| 20011.0 | 22.87 | 50.42 | 651.09 | 1171.96 |
| 40037.0 | 19.93 | 43.94 | 650.3 | 1170.54 |
| 59962.5 | 18.41 | 40.6 | 649.52 | 1169.14 |
| 79990.4 | 17.46 | 38.49 | 648.93 | 1168.07 |
| 100001.8 | 14.49 | 31.94 | 647.76 | 1165.97 |
| 150010.3 | 12.8 | 28.22 | 646.35 | 1163.42 |
| 200017.9 | 11.69 | 25.78 | 645.64 | 1162.15 |
| 400054.9 | 9.2 | 20.27 | 644.38 | 1159.88 |
| 600095.6 | 7.85 | 17.31 | 643.76 | 1158.77 |
| 800137.2 | 6.98 | 15.38 | 643.39 | 1158.11 |
| 1000000.0 | 6.37 | 14.04 | 643.15 | 1157.67 |

Integral Mass and Energy Release(Steam) at 24 hours after postulated accident

| Time (sec) | Integral Mass | | Integral Energy | |
|---------------|---------------|------------|-----------------|-------------|
| | kg | lbm | Million kcal | Million Btu |
| 85,098 | 1,891,367 | 4,169,752 | 1,232.912 | 4,251.253 |
| 1,000,000 | 10,017,996 | 22,085,902 | 6,474.679 | 25,693.601 |

Replace these 27 pages of Table 6.2.1-5
with the following 26 pages of revised
Table 6.2.1-5.

Table 6.2.1-5 (13 of 27)

Part A. Mass and Energy (Spillage) Release Data
(Decay heat Period)

| Time (sec) | Mass Flow Rate | | Break Enthalpy | |
|------------|----------------|---------|----------------|---------|
| | kg/sec | lbm/sec | kcal/kg | Btu/lbm |
| 400.0 | 114.97 | 253.46 | 59.55 | 107.19 |
| 599.9 | 123.26 | 271.74 | 70.19 | 126.35 |
| 800.0 | 129.43 | 285.34 | 75.27 | 135.48 |
| 999.0 | 134.09 | 295.61 | 78.45 | 141.21 |
| 1503.6 | 141.61 | 312.19 | 84.11 | 151.39 |
| 1997.0 | 145.79 | 321.42 | 88.59 | 159.46 |
| 4002.9 | 152.06 | 335.24 | 101.15 | 182.07 |
| 6001.3 | 154.55 | 340.72 | 108.32 | 194.97 |
| 8001.1 | 155.89 | 343.69 | 112.55 | 202.59 |
| 9990.4 | 156.84 | 345.77 | 115.07 | 207.12 |
| 15005.4 | 158.47 | 349.36 | 117.71 | 211.87 |
| 20011.0 | 159.7 | 352.07 | 118.05 | 212.5 |
| 40037.0 | 162.88 | 359.09 | 114.98 | 206.96 |
| 59962.5 | 164.95 | 363.66 | 110.95 | 199.7 |
| 79990.4 | 166.37 | 366.79 | 107.64 | 193.76 |
| 100001.8 | 169.84 | 374.43 | 102.19 | 183.95 |
| 150010.3 | 172.74 | 380.83 | 92.98 | 167.36 |
| 200017.9 | 174.37 | 384.41 | 88.27 | 158.89 |
| 400054.9 | 177.64 | 391.62 | 79.29 | 142.71 |
| 600095.6 | 179.33 | 395.35 | 74.35 | 133.84 |
| 800137.2 | 180.38 | 397.67 | 71.26 | 128.26 |
| 1000000.0 | 181.1 | 399.26 | 69.1 | 124.38 |

Integral Mass and Energy Release (Spillage) at 24 hours and End of Analysis

| Time (sec) | Integral Mass | | Integral Energy | |
|------------|---------------|-------------|-----------------|-------------|
| | kg | lbm | Million kcal | Million Btu |
| 85,098 | 13,844,968 | 30,522,931 | 1,552.633 | 6,161.346 |
| 1,000,000 | 176,652,675 | 389,452,484 | 14,266.077 | 56,612.367 |

Replace these 27 pages of Table 6.2.1-5 with the following 26 pages of revised Table 6.2.1-5.

Table 6.2.1-5 (14 of 27)

Part B. Reactor Vessel Pressure vs. Time
(Blowdown Period)

| Time (sec) | Reactor Vessel Pressure | |
|------------|-------------------------|----------|
| | kg/cm ² A | psia |
| 0.000 | 167.36 | 2,380.40 |
| 0.027 | 159.52 | 2,268.90 |
| 0.054 | 147.05 | 2,091.50 |
| 0.103 | 125.06 | 1,778.70 |
| 0.152 | 126.83 | 1,804.00 |
| 0.202 | 126.45 | 1,798.60 |
| 0.252 | 125.82 | 1,789.60 |
| 0.298 | 125.29 | 1,782.10 |
| 0.351 | 123.83 | 1,761.30 |
| 0.400 | 123.02 | 1,749.70 |
| 0.603 | 120.51 | 1,714.00 |
| 0.800 | 118.85 | 1,690.50 |
| 1.000 | 117.11 | 1,665.70 |
| 1.202 | 114.64 | 1,630.50 |
| 1.401 | 112.52 | 1,600.40 |
| 1.607 | 111.04 | 1,579.30 |
| 1.800 | 109.75 | 1,561.00 |
| 2.001 | 108.13 | 1,538.00 |
| 2.204 | 106.14 | 1,509.70 |
| 2.407 | 104.53 | 1,486.80 |
| 2.601 | 104.06 | 1,480.10 |
| 2.812 | 102.49 | 1,457.80 |
| 3.008 | 100.88 | 1,434.90 |

Replace these 27 pages of Table 6.2.1-5
with the following 26 pages of revised
Table 6.2.1-5.

Table 6.2.1-5 (15 of 27)

Part B. Reactor Vessel Pressure vs. Time
(Blowdown Period)

| Time (sec) | Reactor Vessel Pressure | |
|------------|-------------------------|----------|
| | kg/cm ² A | psia |
| 3.208 | 99.02 | 1,408.40 |
| 3.408 | 97.55 | 1,387.50 |
| 3.608 | 95.48 | 1,358.10 |
| 3.808 | 93.41 | 1,328.60 |
| 4.000 | 91.91 | 1,307.30 |
| 4.210 | 90.07 | 1,281.10 |
| 4.409 | 88.60 | 1,260.20 |
| 4.609 | 87.41 | 1,243.20 |
| 4.809 | 86.24 | 1,226.60 |
| 5.009 | 85.01 | 1,209.10 |
| 5.209 | 84.51 | 1,202.00 |
| 5.409 | 83.78 | 1,191.60 |
| 5.609 | 82.37 | 1,171.60 |
| 5.809 | 81.56 | 1,160.00 |
| 6.009 | 80.92 | 1,151.00 |
| 6.209 | 80.24 | 1,141.30 |
| 6.409 | 79.48 | 1,130.40 |
| 6.609 | 78.88 | 1,121.90 |
| 6.809 | 78.27 | 1,113.30 |
| 7.009 | 77.62 | 1,104.00 |
| 7.209 | 76.94 | 1,094.40 |
| 7.409 | 76.32 | 1,085.50 |
| 7.609 | 75.57 | 1,074.90 |

Replace these 27 pages of Table 6.2.1-5
with the following 26 pages of revised
Table 6.2.1-5.

Table 6.2.1-5 (16 of 27)

Part B. Reactor Vessel Pressure vs. Time
(Blowdown Period)

| Time (sec) | Reactor Vessel Pressure | |
|------------|-------------------------|----------|
| | kg/cm ² A | psia |
| 7.809 | 74.87 | 1,064.90 |
| 8.009 | 74.23 | 1,055.80 |
| 8.409 | 72.92 | 1,037.20 |
| 8.809 | 71.62 | 1,018.70 |
| 9.204 | 70.32 | 1,000.20 |
| 9.608 | 69.01 | 981.57 |
| 10.004 | 67.70 | 962.86 |
| 10.404 | 66.32 | 943.31 |
| 10.799 | 64.73 | 920.61 |
| 11.205 | 62.25 | 885.43 |
| 11.601 | 59.92 | 852.22 |
| 12.006 | 58.14 | 826.88 |
| 12.205 | 55.99 | 796.34 |
| 12.406 | 55.20 | 785.18 |
| 12.599 | 53.98 | 767.78 |
| 12.806 | 52.89 | 752.32 |
| 13.005 | 51.83 | 737.15 |
| 13.213 | 50.66 | 720.49 |
| 13.413 | 49.62 | 705.72 |
| 13.613 | 48.60 | 691.24 |
| 13.813 | 47.57 | 676.65 |
| 14.013 | 46.53 | 661.87 |
| 14.203 | 45.07 | 641.07 |
| 14.409 | 43.74 | 622.06 |
| 14.616 | 42.39 | 602.96 |

Replace these 27 pages of Table 6.2.1-5
with the following 26 pages of revised
Table 6.2.1-5.

Table 6.2.1-5 (17 of 27)

Part B. Reactor Vessel Pressure vs. Time
(Blowdown Period)

| Time (sec) | Reactor Vessel Pressure | |
|------------|-------------------------|--------|
| | kg/cm ² A | psia |
| 14.816 | 40.78 | 579.98 |
| 15.016 | 39.48 | 561.58 |
| 15.214 | 37.97 | 540.09 |
| 15.409 | 36.72 | 522.26 |
| 15.609 | 35.32 | 502.42 |
| 15.809 | 34.01 | 483.72 |
| 16.009 | 32.71 | 465.30 |
| 16.200 | 31.56 | 448.93 |
| 16.400 | 30.45 | 433.14 |
| 16.601 | 29.23 | 415.81 |
| 16.800 | 28.03 | 398.63 |
| 17.001 | 26.77 | 380.75 |
| 17.205 | 25.49 | 362.53 |
| 17.400 | 24.24 | 344.80 |
| 17.600 | 23.00 | 327.17 |
| 17.800 | 21.78 | 309.80 |
| 18.000 | 20.54 | 292.11 |
| 18.200 | 19.37 | 275.52 |
| 18.400 | 18.22 | 259.10 |
| 18.600 | 17.10 | 243.28 |
| 18.802 | 15.99 | 227.49 |
| 18.999 | 14.94 | 212.46 |
| 19.203 | 15.92 | 226.38 |

Replace these 27 pages of Table 6.2.1-5
with the following 26 pages of revised
Table 6.2.1-5.

Table 6.2.1-5 (18 of 27)

Part B. Reactor Vessel Pressure vs. Time
(Reflood and Post-reflood Period)

| Time (sec) | Reactor Vessel Pressure | |
|------------|-------------------------|---------|
| | kg/cm ² A | psia |
| 19.20 | 4.080 | 58.000 |
| 19.30 | 4.120 | 58.560 |
| 19.40 | 4.180 | 59.420 |
| 21.40 | 4.450 | 63.310 |
| 23.40 | 6.040 | 85.850 |
| 25.40 | 7.810 | 111.150 |
| 27.40 | 9.400 | 133.710 |
| 28.70 | 10.240 | 145.660 |
| 28.80 | 10.300 | 146.480 |
| 28.90 | 10.350 | 147.280 |
| 29.00 | 10.380 | 147.670 |
| 31.60 | 10.200 | 145.140 |
| 34.20 | 10.020 | 142.470 |
| 36.80 | 9.840 | 139.890 |
| 39.40 | 9.660 | 137.380 |
| 42.00 | 9.490 | 134.950 |
| 44.60 | 9.320 | 132.590 |
| 47.20 | 9.160 | 130.300 |
| 49.80 | 9.000 | 128.070 |
| 52.40 | 8.850 | 125.910 |
| 55.00 | 8.700 | 123.810 |
| 57.60 | 8.560 | 121.770 |
| 60.20 | 8.420 | 119.790 |
| 62.80 | 8.290 | 117.870 |

Replace these 27 pages of Table 6.2.1-5
with the following 26 pages of revised
Table 6.2.1-5.

Table 6.2.1-5 (19 of 27)

Part B. Reactor Vessel Pressure vs. Time
(Reflood and Post-reflood Period)

| Time (sec) | Reactor Vessel Pressure | |
|------------|-------------------------|---------|
| | kg/cm ² A | psia |
| 63.50 | 8.250 | 117.360 |
| 63.60 | 8.250 | 117.290 |
| 63.70 | 8.240 | 117.190 |
| 63.80 | 8.220 | 116.960 |
| 65.80 | 7.880 | 112.150 |
| 67.80 | 7.620 | 108.430 |
| 69.80 | 7.420 | 105.510 |
| 71.80 | 7.250 | 103.160 |
| 73.80 | 7.120 | 101.230 |
| 75.80 | 7.010 | 99.650 |
| 77.80 | 6.910 | 98.340 |
| 79.80 | 6.830 | 97.200 |
| 81.80 | 6.760 | 96.210 |
| 83.80 | 6.700 | 95.340 |
| 85.80 | 6.650 | 94.560 |
| 87.80 | 6.600 | 93.860 |
| 88.90 | 6.570 | 93.500 |
| 89.00 | 6.540 | 93.080 |
| 89.10 | 6.560 | 93.360 |
| 89.20 | 6.530 | 92.870 |
| 89.30 | 6.520 | 92.700 |
| 89.50 | 6.510 | 92.600 |
| 91.50 | 6.400 | 90.960 |
| 93.50 | 6.240 | 88.740 |
| 95.50 | 6.080 | 86.530 |

Replace these 27 pages of Table 6.2.1-5
with the following 26 pages of revised
Table 6.2.1-5.

Table 6.2.1-5 (20 of 27)

Part B. Reactor Vessel Pressure vs. Time
(Reflood and Post-reflood Period)

| Time (sec) | Reactor Vessel Pressure | |
|------------|-------------------------|--------|
| | kg/cm ² A | psia |
| 97.50 | 5.940 | 84.480 |
| 99.50 | 5.810 | 82.620 |
| 101.50 | 5.690 | 80.930 |
| 103.50 | 5.580 | 79.390 |
| 105.50 | 5.480 | 77.990 |
| 107.50 | 5.390 | 76.710 |
| 109.50 | 5.310 | 75.540 |
| 111.50 | 5.240 | 74.460 |
| 113.50 | 5.170 | 73.470 |
| 115.50 | 5.100 | 72.560 |
| 117.00 | 5.060 | 71.920 |
| 117.10 | 5.050 | 71.880 |
| 117.20 | 5.050 | 71.840 |
| 118.20 | 5.070 | 72.160 |
| 119.20 | 4.800 | 68.340 |
| 120.20 | 5.040 | 71.630 |
| 121.20 | 4.870 | 69.290 |
| 122.20 | 4.950 | 70.360 |
| 123.20 | 4.580 | 65.160 |
| 124.20 | 4.500 | 64.060 |
| 125.20 | 4.550 | 64.780 |
| 126.20 | 4.740 | 67.360 |
| 127.50 | 4.650 | 66.080 |
| 127.60 | 4.730 | 67.270 |

Replace these 27 pages of Table 6.2.1-5
with the following 26 pages of revised
Table 6.2.1-5.

Table 6.2.1-5 (21 of 27)

Part B. Reactor Vessel Pressure vs. Time
(Decay heat Period)

| Time (sec) | Reactor Vessel Pressure | |
|------------|-------------------------|--------|
| | kg/cm ² A | psia |
| 200.0 | 4.422 | 62.894 |
| 400.0 | 4.562 | 64.889 |
| 599.9 | 4.378 | 62.273 |
| 800.0 | 4.248 | 60.419 |
| 999.0 | 4.149 | 59.012 |
| 1504.4 | 3.981 | 56.621 |
| 1997.8 | 3.876 | 55.135 |
| 4005.0 | 3.66 | 52.063 |
| 6003.6 | 3.544 | 50.41 |
| 8004.3 | 3.471 | 49.373 |
| 9995.6 | 3.42 | 48.648 |
| 15005.7 | 3.332 | 47.387 |
| 20011.7 | 3.252 | 46.247 |
| 40038.3 | 2.976 | 42.328 |
| 59965.1 | 2.751 | 39.127 |
| 79991.5 | 2.594 | 36.896 |
| 100002.3 | 2.347 | 33.387 |
| 150010.0 | 2.067 | 29.403 |
| 200018.4 | 1.936 | 27.533 |
| 400054.2 | 1.719 | 24.455 |
| 600092.3 | 1.621 | 23.059 |
| 800133.9 | 1.566 | 22.273 |
| 1000000.0 | 1.53 | 21.764 |

Replace these 27 pages of Table 6.2.1-5
with the following 26 pages of revised
Table 6.2.1-5.

Table 6.2.1-5 (22 of 27)

Part C. Safety Injection Flow vs. Time (Blowdown Period)

| Time (sec) | Safety Injection Tank Flow | |
|------------|----------------------------|----------|
| | kg/sec | lbm/sec |
| 0.000 | 0.00 | 0.00 |
| 0.027 | 0.00 | 0.00 |
| 13.813 | 0.00 | 0.00 |
| 14.013 | 0.00 | 0.00 |
| 14.203 | 1,281.21 | 2,824.60 |
| 14.409 | 1,690.48 | 3,726.90 |
| 14.616 | 1,989.35 | 4,385.80 |
| 14.816 | 2,357.62 | 5,197.70 |
| 15.016 | 2,555.71 | 5,634.40 |
| 15.214 | 2,769.58 | 6,105.90 |
| 15.409 | 2,934.41 | 6,469.30 |
| 15.609 | 3,097.38 | 6,828.60 |
| 15.809 | 3,236.55 | 7,135.40 |
| 16.009 | 3,362.73 | 7,413.60 |
| 16.200 | 3,451.73 | 7,609.80 |
| 16.400 | 3,536.73 | 7,797.20 |
| 16.601 | 3,639.88 | 8,024.60 |
| 16.800 | 3,738.76 | 8,242.60 |
| 17.001 | 3,845.63 | 8,478.20 |
| 17.205 | 3,957.26 | 8,724.30 |
| 17.400 | 4,061.17 | 8,953.40 |
| 17.600 | 4,159.33 | 9,169.80 |
| 17.800 | 4,253.59 | 9,377.60 |
| 18.000 | 4,351.61 | 9,593.70 |

Replace these 27 pages of Table 6.2.1-5 with the following 26 pages of revised Table 6.2.1-5.

Table 6.2.1-5 (23 of 27)

Part C. Safety Injection Flow vs. Time
(Blowdown Period)

| Time (sec) | Safety Injection Tank Flow | |
|------------|----------------------------|-----------|
| | kg/sec | lbm/sec |
| 18.200 | 4,434.98 | 9,777.50 |
| 18.400 | 4,517.85 | 9,960.20 |
| 18.600 | 4,594.41 | 10,129.00 |
| 18.802 | 4,668.35 | 10,292.00 |
| 18.999 | 4,740.47 | 10,451.00 |
| 19.203 | 4,496.26 | 9,912.60 |

Replace these 27 pages of Table 6.2.1-5 with the following 26 pages of revised Table 6.2.1-5.

Table 6.2.1-5 (24 of 27)

Part C. Safety Injection Flow vs. Time (Reflood and Post-reflood Period)

| Time (sec) | Safety Injection Tank Flow | | Safety Injection Pump Flow | |
|------------|----------------------------|----------|----------------------------|---------|
| | kg/sec | lbm/sec | kg/sec | lbm/sec |
| 19.203 | 3,140.51 | 6,923.67 | 193.78 | 427.22 |
| 19.303 | 3,128.73 | 6,897.71 | 193.78 | 427.22 |
| 20.303 | 3,010.38 | 6,636.79 | 193.69 | 427.01 |
| 21.303 | 2,903.09 | 6,400.25 | 193.60 | 426.81 |
| 22.303 | 2,763.24 | 6,091.93 | 193.01 | 425.52 |
| 23.303 | 2,622.04 | 5,780.65 | 192.34 | 424.05 |
| 24.303 | 2,479.59 | 5,466.59 | 191.63 | 422.48 |
| 25.303 | 2,337.51 | 5,153.36 | 190.91 | 420.88 |
| 26.303 | 2,200.04 | 4,850.28 | 190.21 | 419.35 |
| 27.303 | 2,068.76 | 4,560.86 | 189.58 | 417.95 |
| 28.803 | 1,886.53 | 4,159.11 | 188.76 | 416.16 |
| 28.903 | 1,875.13 | 4,133.97 | 188.72 | 416.05 |
| 32.003 | 1,727.89 | 3,809.36 | 188.81 | 416.26 |
| 35.103 | 1,613.41 | 3,556.98 | 189.00 | 416.67 |
| 38.203 | 1,515.40 | 3,340.89 | 189.17 | 417.06 |
| 41.303 | 1,430.60 | 3,153.95 | 189.34 | 417.43 |
| 44.403 | 1,356.61 | 2,990.84 | 189.51 | 417.80 |
| 47.503 | 1,291.61 | 2,847.52 | 189.67 | 418.15 |
| 50.603 | 1,234.14 | 2,720.82 | 189.82 | 418.48 |
| 53.703 | 1,183.10 | 2,608.31 | 189.97 | 418.81 |
| 56.803 | 1,137.59 | 2,507.96 | 190.11 | 419.13 |
| 59.903 | 1,096.84 | 2,418.13 | 190.25 | 419.43 |
| 63.003 | 1,060.23 | 2,337.42 | 190.38 | 419.72 |
| 63.503 | 1,054.67 | 2,325.16 | 190.40 | 419.77 |
| 63.603 | 1,053.57 | 2,322.73 | 190.41 | 419.78 |
| 63.703 | 477.23 | 1,052.13 | 190.41 | 419.79 |
| 63.803 | 477.37 | 1,052.43 | 190.42 | 419.80 |
| 69.003 | 514.32 | 1,133.89 | 191.02 | 421.12 |
| 74.203 | 524.77 | 1,156.93 | 191.34 | 421.84 |

Replace these 27 pages of Table 6.2.1-5 with the following 26 pages of revised Table 6.2.1-5.

Table 6.2.1-5 (25 of 27)

Part C. Safety Injection Flow vs. Time (Reflood and Post-reflood Period)

| Time (sec) | Safety Injection Tank Flow | | Safety Injection Pump Flow | |
|------------|----------------------------|----------|----------------------------|---------|
| | kg/sec | lbm/sec | kg/sec | lbm/sec |
| 79.403 | 523.95 | 1,155.12 | 191.54 | 422.28 |
| 84.603 | 518.32 | 1,142.70 | 191.68 | 422.59 |
| 89.803 | 514.40 | 1,134.07 | 191.83 | 422.91 |
| 95.003 | 525.84 | 1,159.28 | 192.13 | 423.58 |
| 100.203 | 536.06 | 1,181.81 | 192.42 | 424.21 |
| 105.403 | 540.89 | 1,192.47 | 192.65 | 424.71 |
| 110.603 | 542.02 | 1,194.95 | 192.82 | 425.11 |
| 115.803 | 540.61 | 1,191.84 | 192.97 | 425.42 |
| 117.103 | 539.96 | 1,190.41 | 193.00 | 425.49 |
| 118.103 | 537.26 | 1,184.47 | 193.00 | 425.49 |
| 119.103 | 521.88 | 1,150.56 | 192.86 | 425.18 |
| 120.103 | 547.83 | 1,207.75 | 193.17 | 425.88 |
| 121.103 | 543.93 | 1,199.17 | 193.16 | 425.85 |
| 122.103 | 536.73 | 1,183.29 | 193.11 | 425.73 |
| 123.103 | 533.91 | 1,177.07 | 193.11 | 425.73 |
| 124.103 | 538.11 | 1,186.34 | 193.18 | 425.89 |
| 125.103 | 541.68 | 1,194.20 | 193.25 | 426.04 |
| 126.103 | 544.03 | 1,199.39 | 193.30 | 426.16 |
| 127.603 | 543.15 | 1,197.44 | 193.33 | 426.23 |
| 147.903 | 526.95 | 1,161.73 | 193.65 | 426.93 |
| 168.203 | 479.60 | 1,057.35 | 193.58 | 426.77 |
| 188.503 | 449.96 | 992.00 | 193.64 | 426.90 |
| 208.803 | 427.63 | 942.77 | 193.73 | 427.09 |
| 229.103 | 399.77 | 881.35 | 193.73 | 427.11 |
| 249.403 | 374.31 | 825.21 | 193.74 | 427.13 |
| 269.703 | 350.80 | 773.39 | 193.75 | 427.14 |
| 290.003 | 328.92 | 725.15 | 193.75 | 427.15 |

Replace these 27 pages of Table 6.2.1-5 with the following 26 pages of revised Table 6.2.1-5.

Table 6.2.1-5 (26 of 27)

Part C. Safety Injection Flow vs. Time (Reflood and Post-reflood Period)

| Time (sec) | Safety Injection Tank Flow | | Safety Injection Pump Flow | |
|------------|----------------------------|---------|----------------------------|---------|
| | kg/sec | lbm/sec | kg/sec | lbm/sec |
| 310.303 | 308.41 | 679.94 | 193.76 | 427.16 |
| 330.603 | 289.07 | 637.28 | 193.76 | 427.17 |
| 350.903 | 270.71 | 596.82 | 193.76 | 427.18 |
| 368.103 | 255.85 | 564.05 | 193.77 | 427.18 |
| 368.203 | 255.76 | 563.86 | 193.77 | 427.18 |
| 368.303 | 0.00 | 0.00 | 193.77 | 427.18 |
| 368.403 | 0.00 | 0.00 | 193.77 | 427.18 |
| 398.403 | 0.00 | 0.00 | 193.78 | 427.21 |
| 428.403 | 0.00 | 0.00 | 193.78 | 427.21 |
| 458.403 | 0.00 | 0.00 | 193.76 | 427.16 |
| 488.403 | 0.00 | 0.00 | 193.74 | 427.13 |
| 499.903 | 0.00 | 0.00 | 193.75 | 427.14 |
| 500.003 | 0.00 | 0.00 | 193.74 | 427.12 |

Replace these 27 pages of Table 6.2.1-5 with the following 26 pages of revised Table 6.2.1-5.

Table 6.2.1-5 (27 of 27)

Part D. Chronology of Events

| Time (sec) | Event | Values |
|------------|--|---|
| 0.0 | Break occurs | - |
| 4.38 | Containment pressure Hi-Hi setpoint | 1.547kg/cm ² G (22.0 psig) |
| 14.01 | Start safety injection tank (SIT) injection | - |
| 19.20 | End of blowdown | - |
| | Start SI pump injection | - |
| 19.21 | First peak containment pressure (Blowdown phase) | 3.126kg/cm ² G (44.47 psig) |
| 63.70 | SIT flow is turned down to low flow by fluidic device in SIT | - |
| 104.21 | Peak containment temperature | 133.97 °C (273.14 °F) |
| 104.61 | Peak containment pressure | 3.524kg/cm ² G (50.12 psig) |
| 114.38 | Start containment spray actuation | - |
| 117.10 | End of reflood | - |
| 127.60 | End of post reflood | - |
| 368.30 | Safety injection tank empty | - |
| 53,253.9 | Time of depressurization of the containment at 50 % of peak pressure | 1.761kg/cm ² G (25.05 psig) |

Replace these 27 pages of Table 6.2.1-5 with the following 26 pages of revised Table 6.2.1-5.

APR1400 DCD TIER 2

Table 6.2.1-5 (1 of 26)

Insert this page.

Double-Ended Suction Leg Slot Break – Minimum SIS Flow
(0.9121 m² (9.8175 ft²) Total Break Area)

Part A. Mass and Energy Release Data
 (Blowdown Period)

| Time (sec) | Break Mass Flow Rate | | Break Enthalpy | |
|------------|----------------------|------------|----------------|---------|
| | kg/sec | lbm/sec | kcal/kg | Btu/lbm |
| 0.000 | 0.00 | 0.00 | 0.00 | 0.00 |
| 0.027 | 35,826.69 | 78,984.75 | 310.61 | 559.13 |
| 0.054 | 35,499.95 | 78,264.39 | 310.08 | 558.18 |
| 0.103 | 35,936.95 | 79,227.82 | 309.90 | 557.85 |
| 0.152 | 49,099.29 | 108,245.97 | 310.38 | 558.72 |
| 0.202 | 47,285.37 | 104,246.94 | 311.04 | 559.91 |
| 0.252 | 45,576.63 | 100,479.79 | 311.57 | 560.85 |
| 0.298 | 44,683.04 | 98,509.75 | 311.94 | 561.52 |
| 0.351 | 44,779.94 | 98,723.38 | 312.17 | 561.94 |
| 0.400 | 44,346.29 | 97,767.34 | 312.52 | 562.56 |
| 0.603 | 43,478.91 | 95,855.09 | 313.48 | 564.30 |
| 0.800 | 44,864.47 | 98,909.74 | 314.64 | 566.38 |
| 1.000 | 42,167.46 | 92,963.82 | 315.74 | 568.36 |
| 1.202 | 40,552.76 | 89,404.00 | 317.33 | 571.22 |
| 1.401 | 38,527.59 | 84,939.24 | 319.05 | 574.33 |
| 1.607 | 38,152.42 | 84,112.13 | 320.39 | 576.73 |
| 1.800 | 37,859.70 | 83,466.78 | 321.87 | 579.40 |
| 2.001 | 37,500.04 | 82,673.88 | 323.76 | 582.80 |
| 2.204 | 35,984.54 | 79,332.74 | 325.55 | 586.03 |
| 2.407 | 33,372.26 | 73,573.62 | 326.50 | 587.73 |
| 2.601 | 31,669.84 | 69,820.41 | 327.91 | 590.27 |
| 2.812 | 30,653.27 | 67,579.23 | 330.85 | 595.57 |
| 3.008 | 29,668.44 | 65,408.05 | 334.73 | 602.56 |
| 3.208 | 28,297.64 | 62,385.94 | 340.03 | 612.09 |
| 3.408 | 26,715.66 | 58,898.26 | 346.75 | 624.19 |

APR1400 DCD TIER 2

Table 6.2.1-5 (2 of 26)

Insert this page.

Part A. Mass and Energy Release Data
(Blowdown Period)

| Time (sec) | Break Mass Flow Rate | | Break Enthalpy | |
|------------|----------------------|-----------|----------------|---------|
| | kg/sec | lbm/sec | kcal/kg | Btu/lbm |
| 3.608 | 24,966.73 | 55,042.51 | 354.00 | 637.23 |
| 3.808 | 23,497.04 | 51,802.38 | 360.32 | 648.62 |
| 4.000 | 22,127.47 | 48,782.98 | 365.48 | 657.89 |
| 4.211 | 21,436.30 | 47,259.20 | 366.85 | 660.37 |
| 4.409 | 21,008.90 | 46,316.93 | 366.71 | 660.11 |
| 4.609 | 20,598.55 | 45,412.26 | 366.16 | 659.12 |
| 4.809 | 20,267.22 | 44,681.81 | 365.67 | 658.24 |
| 5.009 | 20,051.87 | 44,207.03 | 364.92 | 656.90 |
| 5.209 | 19,841.27 | 43,742.73 | 364.35 | 655.86 |
| 5.409 | 19,815.87 | 43,686.73 | 363.56 | 654.45 |
| 5.609 | 19,693.35 | 43,416.63 | 363.47 | 654.28 |
| 5.809 | 19,144.10 | 42,205.74 | 364.81 | 656.69 |
| 6.009 | 18,734.91 | 41,303.63 | 365.84 | 658.55 |
| 6.209 | 18,566.23 | 40,931.75 | 365.82 | 658.51 |
| 6.409 | 18,595.07 | 40,995.33 | 363.92 | 655.09 |
| 6.609 | 18,479.62 | 40,740.79 | 363.55 | 654.43 |
| 6.809 | 17,933.49 | 39,536.78 | 366.91 | 660.48 |
| 7.009 | 17,132.26 | 37,770.38 | 372.47 | 670.48 |
| 7.209 | 16,620.46 | 36,642.04 | 375.29 | 675.57 |
| 7.409 | 16,372.62 | 36,095.63 | 375.88 | 676.62 |
| 7.609 | 16,206.97 | 35,730.45 | 376.05 | 676.92 |
| 7.809 | 16,191.18 | 35,695.62 | 374.41 | 673.98 |
| 8.009 | 16,125.16 | 35,550.08 | 373.73 | 672.75 |
| 8.209 | 15,915.11 | 35,086.98 | 374.73 | 674.55 |
| 8.409 | 15,680.94 | 34,570.74 | 375.85 | 676.56 |
| 8.609 | 15,427.32 | 34,011.60 | 377.17 | 678.94 |
| 8.809 | 15,141.74 | 33,381.99 | 378.82 | 681.91 |
| 9.005 | 14,809.07 | 32,648.58 | 380.75 | 685.38 |

APR1400 DCD TIER 2

Table 6.2.1-5 (3 of 26)

Insert this page.

Part A. Mass and Energy Release Data (Blowdown Period)

| Time (sec) | Break Mass Flow Rate | | Break Enthalpy | |
|------------|----------------------|-----------|----------------|---------|
| | kg/sec | lbm/sec | kcal/kg | Btu/lbm |
| 9.204 | 14,527.77 | 32,028.41 | 382.90 | 689.26 |
| 9.400 | 14,196.28 | 31,297.60 | 385.45 | 693.86 |
| 9.608 | 13,797.32 | 30,418.04 | 387.37 | 697.31 |
| 9.801 | 13,391.38 | 29,523.09 | 391.81 | 705.30 |
| 10.004 | 13,129.00 | 28,944.65 | 395.88 | 712.62 |
| 10.205 | 12,765.77 | 28,143.85 | 399.12 | 718.46 |
| 10.404 | 12,429.45 | 27,402.39 | 401.76 | 723.21 |
| 10.603 | 11,985.20 | 26,422.98 | 406.03 | 730.90 |
| 10.799 | 11,582.15 | 25,534.40 | 412.05 | 741.74 |
| 11.004 | 11,140.57 | 24,560.87 | 417.73 | 751.96 |
| 11.205 | 10,637.22 | 23,451.17 | 423.35 | 762.07 |
| 11.406 | 10,190.47 | 22,466.27 | 428.61 | 771.53 |
| 11.601 | 9,728.82 | 21,448.50 | 433.53 | 780.39 |
| 11.804 | 9,042.09 | 19,934.50 | 445.87 | 802.61 |
| 12.006 | 8,756.29 | 19,304.41 | 452.29 | 814.16 |
| 12.205 | 8,377.30 | 18,468.88 | 457.85 | 824.18 |
| 12.406 | 8,013.92 | 17,667.76 | 463.75 | 834.79 |
| 12.599 | 7,657.53 | 16,882.05 | 469.08 | 844.38 |
| 12.806 | 7,397.99 | 16,309.86 | 475.41 | 855.78 |
| 13.005 | 7,153.35 | 15,770.51 | 476.56 | 857.85 |
| 13.213 | 6,944.67 | 15,310.45 | 475.99 | 856.84 |
| 13.413 | 6,730.23 | 14,837.69 | 477.18 | 858.98 |
| 13.613 | 6,534.48 | 14,406.13 | 479.25 | 862.71 |
| 13.813 | 6,358.64 | 14,018.47 | 480.50 | 864.96 |
| 14.013 | 6,188.02 | 13,642.32 | 481.42 | 866.61 |
| 14.203 | 5,966.42 | 13,153.78 | 482.94 | 869.34 |
| 14.409 | 5,852.22 | 12,902.00 | 478.07 | 860.57 |
| 14.616 | 5,895.97 | 12,998.45 | 457.84 | 824.16 |

APR1400 DCD TIER 2

Table 6.2.1-5 (4 of 26)

Insert this page.

Part A. Mass and Energy Release Data (Blowdown Period)

| Time (sec) | Break Mass Flow Rate | | Break Enthalpy | |
|------------|----------------------|-----------|----------------|---------|
| | kg/sec | lbm/sec | kcal/kg | Btu/lbm |
| 14.816 | 5,885.88 | 12,976.22 | 441.01 | 793.86 |
| 15.016 | 5,839.74 | 12,874.49 | 431.85 | 777.37 |
| 15.214 | 5,717.91 | 12,605.89 | 425.51 | 765.97 |
| 15.409 | 5,579.03 | 12,299.72 | 419.00 | 754.25 |
| 15.609 | 5,389.08 | 11,880.96 | 415.55 | 748.04 |
| 15.809 | 5,183.01 | 11,426.64 | 413.16 | 743.74 |
| 16.009 | 4,939.96 | 10,890.80 | 411.96 | 741.57 |
| 16.200 | 4,374.29 | 9,643.72 | 443.96 | 799.17 |
| 16.400 | 4,198.25 | 9,255.61 | 443.34 | 798.06 |
| 16.601 | 4,077.66 | 8,989.74 | 441.21 | 794.23 |
| 16.800 | 3,932.45 | 8,669.61 | 438.05 | 788.53 |
| 17.001 | 3,815.63 | 8,412.08 | 433.55 | 780.43 |
| 17.205 | 3,707.03 | 8,172.64 | 424.86 | 764.79 |
| 17.400 | 3,576.74 | 7,885.40 | 419.56 | 755.24 |
| 17.600 | 3,431.20 | 7,564.54 | 416.49 | 749.73 |
| 17.800 | 3,384.27 | 7,461.08 | 407.89 | 734.25 |
| 18.000 | 3,343.38 | 7,370.94 | 401.24 | 722.27 |
| 18.200 | 3,122.01 | 6,882.88 | 401.21 | 722.22 |
| 18.400 | 3,066.26 | 6,759.98 | 391.83 | 705.34 |
| 18.600 | 2,962.81 | 6,531.92 | 382.50 | 688.54 |
| 18.802 | 2,774.26 | 6,116.24 | 381.33 | 686.43 |
| 18.999 | 2,608.38 | 5,750.52 | 378.21 | 680.83 |
| 19.203 | 2,546.44 | 5,613.97 | 383.68 | 690.67 |

Integral Mass and Energy Release at End of Blowdown

| Time (sec) | Integral Mass | | Integral Energy | |
|------------|---------------|-------------|-----------------|-------------|
| | kg | lbm | Million kcal | Million Btu |
| 19.203 | 304,940.875 | 672,283.090 | 110.483 | 438.461 |

APR1400 DCD TIER 2

Table 6.2.1-5 (6 of 26)

Insert this page.

Part A. Mass and Energy Release Data
(Reflood and Post-reflood Period)

| Time (sec) | Break Mass Flow Rate | | Break Enthalpy | |
|------------|----------------------|----------|----------------|----------|
| | kg/sec | lbm/sec | kcal/kg | Btu/lbm |
| 19.20 | 0.00 | 0.00 | 0.00 | 0.00 |
| 19.30 | 65.68 | 144.80 | 705.18 | 1,269.39 |
| 21.30 | 153.65 | 338.75 | 705.84 | 1,270.58 |
| 23.30 | 408.73 | 901.11 | 709.40 | 1,276.99 |
| 25.30 | 610.92 | 1,346.85 | 708.84 | 1,275.98 |
| 27.30 | 771.18 | 1,700.16 | 707.16 | 1,272.97 |
| 28.70 | 857.72 | 1,890.95 | 705.73 | 1,270.39 |
| 28.80 | 863.09 | 1,902.80 | 705.63 | 1,270.20 |
| 28.90 | 503.65 | 1,110.36 | 705.52 | 1,270.01 |
| 29.00 | 505.52 | 1,114.48 | 705.43 | 1,269.85 |
| 31.50 | 498.53 | 1,099.07 | 704.15 | 1,267.54 |
| 34.00 | 490.32 | 1,080.97 | 702.94 | 1,265.37 |
| 36.50 | 482.26 | 1,063.21 | 701.75 | 1,263.23 |
| 39.00 | 474.34 | 1,045.74 | 700.58 | 1,261.12 |
| 41.50 | 466.54 | 1,028.55 | 699.43 | 1,259.05 |
| 44.00 | 458.87 | 1,011.63 | 698.31 | 1,257.03 |
| 46.50 | 451.32 | 994.99 | 697.19 | 1,255.02 |
| 49.00 | 443.93 | 978.71 | 696.06 | 1,252.97 |
| 51.50 | 436.67 | 962.70 | 694.93 | 1,250.95 |
| 54.00 | 429.52 | 946.93 | 693.83 | 1,248.96 |
| 56.50 | 422.47 | 931.40 | 692.74 | 1,247.00 |
| 59.00 | 415.53 | 916.10 | 691.67 | 1,245.07 |
| 61.50 | 408.70 | 901.04 | 690.60 | 1,243.16 |
| 63.50 | 403.32 | 889.17 | 689.76 | 1,241.64 |
| 63.60 | 403.06 | 888.59 | 689.71 | 1,241.56 |
| 63.70 | 694.31 | 1,530.70 | 689.67 | 1,241.49 |
| 63.80 | 692.89 | 1,527.56 | 689.65 | 1,241.44 |
| 65.80 | 657.75 | 1,450.09 | 689.31 | 1,240.84 |

APR1400 DCD TIER 2

Table 6.2.1-5 (7 of 26)

Insert this page.

Part A. Mass and Energy Release Data
(Reflood and Post-reflood Period)

| Time (sec) | Break Mass Flow Rate | | Break Enthalpy | |
|------------|----------------------|----------|----------------|----------|
| | kg/sec | lbm/sec | kcal/kg | Btu/lbm |
| 67.80 | 630.03 | 1,388.98 | 688.93 | 1,240.14 |
| 69.80 | 607.97 | 1,340.35 | 688.47 | 1,239.32 |
| 71.80 | 590.15 | 1,301.06 | 687.98 | 1,238.43 |
| 73.80 | 575.34 | 1,268.42 | 687.45 | 1,237.48 |
| 75.80 | 563.30 | 1,241.86 | 686.89 | 1,236.47 |
| 77.80 | 553.12 | 1,219.42 | 686.47 | 1,235.72 |
| 79.80 | 544.48 | 1,200.39 | 685.85 | 1,234.60 |
| 81.80 | 537.03 | 1,183.95 | 685.21 | 1,233.45 |
| 83.80 | 530.51 | 1,169.58 | 684.55 | 1,232.26 |
| 85.80 | 524.75 | 1,156.88 | 683.87 | 1,231.03 |
| 87.80 | 519.58 | 1,145.48 | 683.17 | 1,229.77 |
| 88.90 | 516.94 | 1,139.66 | 680.75 | 1,225.41 |
| 89.00 | 501.38 | 1,105.35 | 669.07 | 1,204.39 |
| 89.10 | 539.58 | 1,189.58 | 669.56 | 1,205.28 |
| 89.20 | 525.22 | 1,157.91 | 669.36 | 1,204.92 |
| 91.20 | 442.86 | 976.35 | 670.45 | 1,206.88 |
| 93.20 | 402.33 | 887.00 | 671.46 | 1,208.70 |
| 95.20 | 371.88 | 819.87 | 672.15 | 1,209.93 |
| 97.20 | 346.00 | 762.80 | 672.74 | 1,211.00 |
| 99.20 | 323.14 | 712.41 | 673.29 | 1,212.00 |
| 101.20 | 302.63 | 667.19 | 673.83 | 1,212.96 |
| 103.20 | 284.11 | 626.36 | 674.36 | 1,213.92 |
| 105.20 | 267.32 | 589.35 | 674.86 | 1,214.82 |
| 107.20 | 252.04 | 555.65 | 675.36 | 1,215.72 |
| 109.20 | 238.07 | 524.86 | 675.86 | 1,216.62 |
| 111.20 | 225.27 | 496.64 | 676.34 | 1,217.48 |
| 113.20 | 213.50 | 470.69 | 676.82 | 1,218.34 |
| 115.20 | 202.65 | 446.76 | 677.28 | 1,219.18 |

APR1400 DCD TIER 2

Table 6.2.1-5 (8 of 26)

Insert this page.

**Part A. Mass and Energy Release Data
(Reflood and Post-reflood Period)**

| Time (sec) | Break Mass Flow Rate | | Break Enthalpy | |
|------------|----------------------|----------|----------------|----------|
| | kg/sec | lbm/sec | kcal/kg | Btu/lbm |
| 117.00 | 193.58 | 426.78 | 677.69 | 1,219.91 |
| 117.10 | 193.10 | 425.71 | 677.71 | 1,219.95 |
| 117.20 | 192.61 | 424.64 | 677.74 | 1,220.00 |
| 118.20 | 161.00 | 354.95 | 682.73 | 1,228.99 |
| 119.20 | 457.69 | 1,009.03 | 662.72 | 1,192.96 |
| 120.20 | 93.04 | 205.13 | 701.15 | 1,262.15 |
| 121.20 | 179.98 | 396.78 | 676.68 | 1,218.10 |
| 122.20 | 125.93 | 277.64 | 688.34 | 1,239.07 |
| 123.20 | 103.57 | 228.33 | 701.55 | 1,262.86 |
| 124.20 | 164.79 | 363.31 | 676.72 | 1,218.17 |
| 125.20 | 98.24 | 216.58 | 696.31 | 1,253.43 |
| 126.20 | 228.01 | 502.68 | 668.50 | 1,203.37 |
| 127.30 | 104.72 | 230.88 | 687.00 | 1,236.67 |
| 127.40 | 76.26 | 168.12 | 702.43 | 1,264.45 |

Integral Mass and Energy Release at the End of Reflood and Post-reflood

| Time (sec) | Integral Mass | | Integral Energy | |
|------------|---------------|-----------|-----------------|-------------|
| | kg | lbm | Million kcal | Million Btu |
| 117.10 | 43,319.21 | 95,503.00 | 29.902 | 118.668 |
| 127.40 | 45,185.28 | 99,617.00 | 31.164 | 123.677 |

APR1400 DCD TIER 2

Table 6.2.1-5 (9 of 26)

Insert this page.

Double-Ended Suction Leg Slot Break – Minimum SIS Flow

Part A: Spillage Release Data (Reactor Vessel Side)
(Reflood and Post-Reflood Period)

| Time (sec) | Break Mass Flow Rate | | Break Enthalpy | |
|---------------|----------------------|----------|----------------|---------|
| | kg/sec | lbm/sec | kcal/kg | Btu/lbm |
| 19.20 | 0.00 | 0.00 | 0.00 | 0.00 |
| 19.30 | 0.00 | 0.00 | 0.00 | 0.00 |
| 28.80 | 0.00 | 0.00 | 0.00 | 0.00 |
| 28.90 | 974.95 | 2,149.41 | 295.13 | 531.26 |
| 29.00 | 1,260.90 | 2,779.82 | 240.18 | 432.36 |
| 31.50 | 1,160.65 | 2,558.81 | 253.38 | 456.10 |
| 34.00 | 1,077.34 | 2,375.15 | 265.12 | 477.24 |
| 36.50 | 1,005.41 | 2,216.56 | 276.33 | 497.42 |
| 39.00 | 942.92 | 2,078.80 | 286.96 | 516.55 |
| 41.50 | 888.36 | 1,958.51 | 296.96 | 534.55 |
| 44.00 | 840.53 | 1,853.07 | 306.29 | 551.35 |
| 46.50 | 798.49 | 1,760.37 | 314.90 | 566.86 |
| 49.00 | 761.34 | 1,678.47 | 322.82 | 581.11 |
| 51.50 | 728.54 | 1,606.16 | 329.96 | 593.97 |
| 54.00 | 699.55 | 1,542.26 | 336.31 | 605.39 |
| 56.50 | 673.93 | 1,485.78 | 341.83 | 615.34 |
| 59.00 | 651.29 | 1,435.86 | 346.54 | 623.80 |
| 61.50 | 631.28 | 1,391.74 | 350.42 | 630.79 |
| 63.50 | 616.95 | 1,360.14 | 352.96 | 635.37 |
| 63.60 | 616.26 | 1,358.63 | 353.08 | 635.58 |
| 63.70 | 0.00 | 0.00 | 0.00 | 0.00 |
| 127.30 | 0.00 | 0.00 | 0.00 | 0.00 |
| 127.40 | 0.00 | 0.00 | 0.00 | 0.00 |

Integral Mass and Energy (Reactor Vessel Side Spillage) at EOR and EOPR

| Time (sec) | Integral Mass | | Integral Energy | |
|---------------|---------------|-----------|-----------------|-------------|
| | kg | lbm | Million kcal | Million Btu |
| 117.10 | 29,415.77 | 64,851.00 | 8.866 | 35.184 |
| 127.40 | 29,415.77 | 64,851.00 | 8.866 | 35.184 |

APR1400 DCD TIER 2

Table 6.2.1-5 (10 of 26)

Insert this page.

Double-Ended Suction Leg Slot Break – Minimum SIS Flow

Part A: Spillage Release Data (Steam Generator Side)
(Reflood and Post-Reflood Period)

| Time (sec) | Break Mass Flow Rate | | Break Enthalpy | |
|---------------|----------------------|----------|----------------|---------|
| | kg/sec | lbm/sec | kcal/kg | Btu/lbm |
| 19.20 | 0.00 | 0.00 | 0.00 | 0.00 |
| 19.30 | 0.00 | 0.00 | 0.00 | 0.00 |
| 88.90 | 0.00 | 0.00 | 0.00 | 0.00 |
| 89.00 | 19.23 | 42.40 | 144.33 | 259.81 |
| 89.10 | 0.00 | 0.00 | 0.00 | 0.00 |
| 89.20 | 0.00 | 0.00 | 0.00 | 0.00 |
| 91.20 | 153.69 | 338.84 | 144.33 | 259.81 |
| 93.20 | 212.24 | 467.91 | 144.33 | 259.81 |
| 95.20 | 242.61 | 534.86 | 144.33 | 259.81 |
| 97.20 | 263.70 | 581.36 | 144.33 | 259.81 |
| 99.20 | 280.56 | 618.53 | 144.33 | 259.81 |
| 101.20 | 295.09 | 650.56 | 144.33 | 259.81 |
| 103.20 | 307.79 | 678.56 | 144.33 | 259.81 |
| 105.20 | 318.96 | 703.19 | 144.33 | 259.81 |
| 107.20 | 328.83 | 724.96 | 144.33 | 259.81 |
| 109.20 | 337.58 | 744.25 | 144.33 | 259.81 |
| 111.20 | 345.36 | 761.40 | 144.33 | 259.81 |
| 113.20 | 352.29 | 776.68 | 144.33 | 259.81 |
| 115.20 | 358.49 | 790.33 | 144.33 | 259.81 |
| 117.00 | 363.49 | 801.36 | 144.33 | 259.81 |
| 117.10 | 363.75 | 801.94 | 144.33 | 259.81 |
| 117.20 | 364.02 | 802.52 | 144.33 | 259.81 |
| 118.20 | 458.10 | 1,009.94 | 144.33 | 259.81 |
| 119.20 | 1,667.46 | 3,676.14 | 144.33 | 259.81 |
| 120.20 | 630.97 | 1,391.05 | 144.33 | 259.81 |
| 121.20 | 251.18 | 553.75 | 144.33 | 259.81 |
| 122.20 | 547.89 | 1,207.89 | 144.33 | 259.81 |
| 123.20 | 1,696.67 | 3,740.53 | 144.33 | 259.81 |

APR1400 DCD TIER 2

Table 6.2.1-5 (11 of 26)

Insert this page.

Double-Ended Suction Leg Slot Break – Minimum SIS Flow

Part A: Spillage Release Data (Steam Generator Side)
(Reflood and Post-Reflood Period)

| Time (sec) | Break Mass Flow Rate | | Break Enthalpy | |
|---------------|----------------------|----------|----------------|---------|
| | kg/sec | lbm/sec | kcal/kg | Btu/lbm |
| 124.20 | 159.80 | 352.30 | 144.33 | 259.81 |
| 125.20 | 667.76 | 1,472.17 | 144.33 | 259.81 |
| 126.20 | 177.11 | 390.47 | 144.33 | 259.81 |
| 127.30 | 202.32 | 446.04 | 144.33 | 259.81 |
| 127.40 | 407.88 | 899.23 | 144.33 | 259.81 |

Integral Mass and Energy (Steam Generator Side Spillage) at EOR and EOPR

| Time (sec) | Integral Mass | | Integral Energy | |
|---------------|---------------|-----------|-----------------|-------------|
| | kg | lbm | Million kcal | Million Btu |
| 117.10 | 7,988.17 | 17,611.00 | 1.153 | 4.576 |
| 127.40 | 14,672.73 | 32,348.00 | 2.118 | 8.404 |

APR1400 DCD TIER 2

Table 6.2.1-5 (12 of 26)

Insert this page.

**Part A. Mass and Energy (Steam) Release Data
(Decay heat Period)**

| Time (sec) | Mass Flow Rate | | Break Enthalpy | |
|------------|----------------|---------|----------------|---------|
| | kg/sec | lbm/sec | kcal/kg | Btu/lbm |
| 400.0 | 53.18 | 117.24 | 653.52 | 1176.34 |
| 599.9 | 52.95 | 116.73 | 653.17 | 1175.7 |
| 800.0 | 53.42 | 117.78 | 652.91 | 1175.24 |
| 999.0 | 51.55 | 113.65 | 652.71 | 1174.88 |
| 1503.4 | 44.29 | 97.64 | 652.34 | 1174.21 |
| 1996.6 | 43.25 | 95.36 | 652.09 | 1173.76 |
| 4001.4 | 35.86 | 79.07 | 651.62 | 1172.91 |
| 5997.8 | 32.04 | 70.63 | 651.44 | 1172.6 |
| 7995.9 | 29.65 | 65.36 | 651.38 | 1172.49 |
| 9995.2 | 27.91 | 61.54 | 651.36 | 1172.45 |
| 15006.5 | 25.03 | 55.19 | 651.32 | 1172.37 |
| 20012.2 | 23.1 | 50.92 | 651.16 | 1172.08 |
| 40037.9 | 18.73 | 41.29 | 650.03 | 1170.06 |
| 59965.8 | 16.48 | 36.34 | 648.82 | 1167.87 |
| 79994.6 | 15.17 | 33.44 | 647.91 | 1166.24 |
| 100002.1 | 14.39 | 31.73 | 647.3 | 1165.14 |
| 150009.3 | 12.78 | 28.19 | 646.34 | 1163.41 |
| 200016.7 | 11.68 | 25.75 | 645.71 | 1162.28 |
| 400050.3 | 9.21 | 20.29 | 644.49 | 1160.08 |
| 600092.2 | 7.86 | 17.33 | 643.86 | 1158.96 |
| 800132.9 | 6.99 | 15.4 | 643.49 | 1158.29 |
| 1000000.0 | 6.38 | 14.06 | 643.24 | 1157.84 |

Integral Mass and Energy Release(Steam) at 24 hours after postulated accident

| Time (sec) | Integral Mass | | Integral Energy | |
|---------------|---------------|------------|-----------------|-------------|
| | kg | lbm | Million kcal | Million Btu |
| 85,002 | 1,815,167 | 4,001,758 | 1,182.816 | 4,251.110 |
| 1,000,000 | 9,945,179 | 21,925,367 | 6,427.148 | 25,504.982 |

APR1400 DCD TIER 2

Table 6.2.1-5 (13 of 26)

Insert this page.

**Part A. Mass and Energy (Spillage) Release Data
(Decay heat Period)**

| Time (sec) | Mass Flow Rate | | Break Enthalpy | |
|------------|----------------|---------|----------------|---------|
| | kg/sec | lbm/sec | kcal/kg | Btu/lbm |
| 400.0 | 89.79 | 197.96 | 22.92 | 41.25 |
| 599.9 | 119.91 | 264.37 | 54.01 | 97.22 |
| 800.0 | 127.09 | 280.18 | 62.23 | 112.02 |
| 999.0 | 131.84 | 290.65 | 65.57 | 118.02 |
| 1503.4 | 139.7 | 307.98 | 71.03 | 127.85 |
| 1996.6 | 144.5 | 318.56 | 76.01 | 136.83 |
| 4001.4 | 151.65 | 334.32 | 93.07 | 167.52 |
| 5997.8 | 154.02 | 339.55 | 103.12 | 185.62 |
| 7995.9 | 155.27 | 342.32 | 109.29 | 196.73 |
| 9995.2 | 156.19 | 344.35 | 113.2 | 203.76 |
| 15006.5 | 157.96 | 348.23 | 117.89 | 212.21 |
| 20012.2 | 159.47 | 351.58 | 119.17 | 214.51 |
| 40037.9 | 164.04 | 361.66 | 115.5 | 207.9 |
| 59965.8 | 167.15 | 368.5 | 109.13 | 196.43 |
| 79994.6 | 169.19 | 373.0 | 103.82 | 186.88 |
| 100002.1 | 170.49 | 375.86 | 99.99 | 179.99 |
| 150009.3 | 172.75 | 380.86 | 93.96 | 169.13 |
| 200016.7 | 174.3 | 384.27 | 89.8 | 161.64 |
| 400050.3 | 177.54 | 391.41 | 81.13 | 146.03 |
| 600092.2 | 179.23 | 395.14 | 76.22 | 137.2 |
| 800132.9 | 180.29 | 397.47 | 73.14 | 131.65 |
| 1000000.0 | 181.01 | 399.06 | 70.99 | 127.78 |

Integral Mass and Energy Release (Spillage) at 24 hours and End of Analysis

| Time (sec) | Integral Mass | | Integral Energy | |
|------------|---------------|-------------|-----------------|-------------|
| | kg | lbm | Million kcal | Million Btu |
| 85,002 | 13,914,308 | 30,675,799 | 1,534.970 | 6,091.252 |
| 1,000,000 | 176,691,103 | 389,537,202 | 14,512.222 | 57,589.151 |

APR1400 DCD TIER 2

Table 6.2.1-5 (14 of 26)

Insert this page.

Part B. Reactor Vessel Pressure vs. Time
(Blowdown Period)

| Time (sec) | Reactor Vessel Pressure | |
|------------|-------------------------|----------|
| | kg/cm ² A | psia |
| 0.000 | 167.36 | 2,380.40 |
| 0.027 | 159.52 | 2,268.90 |
| 0.054 | 147.05 | 2,091.50 |
| 0.103 | 125.06 | 1,778.70 |
| 0.152 | 126.83 | 1,804.00 |
| 0.202 | 126.45 | 1,798.60 |
| 0.252 | 125.82 | 1,789.60 |
| 0.298 | 125.29 | 1,782.10 |
| 0.351 | 123.83 | 1,761.30 |
| 0.400 | 123.02 | 1,749.70 |
| 0.603 | 120.51 | 1,714.00 |
| 0.800 | 118.85 | 1,690.50 |
| 1.000 | 117.11 | 1,665.70 |
| 1.202 | 114.64 | 1,630.50 |
| 1.401 | 112.52 | 1,600.40 |
| 1.607 | 111.04 | 1,579.30 |
| 1.800 | 109.75 | 1,561.00 |
| 2.001 | 108.13 | 1,538.00 |
| 2.204 | 106.14 | 1,509.70 |
| 2.407 | 104.53 | 1,486.80 |
| 2.601 | 104.06 | 1,480.10 |
| 2.812 | 102.49 | 1,457.80 |
| 3.008 | 100.88 | 1,434.90 |

APR1400 DCD TIER 2

Table 6.2.1-5 (15 of 26)

Insert this page.

Part B. Reactor Vessel Pressure vs. Time
(Blowdown Period)

| Time (sec) | Reactor Vessel Pressure | |
|------------|-------------------------|----------|
| | kg/cm ² A | psia |
| 3.208 | 99.02 | 1,408.40 |
| 3.408 | 97.55 | 1,387.50 |
| 3.608 | 95.48 | 1,358.10 |
| 3.808 | 93.41 | 1,328.60 |
| 4.000 | 91.91 | 1,307.30 |
| 4.210 | 90.07 | 1,281.10 |
| 4.409 | 88.60 | 1,260.20 |
| 4.609 | 87.41 | 1,243.20 |
| 4.809 | 86.24 | 1,226.60 |
| 5.009 | 85.01 | 1,209.10 |
| 5.209 | 84.51 | 1,202.00 |
| 5.409 | 83.78 | 1,191.60 |
| 5.609 | 82.37 | 1,171.60 |
| 5.809 | 81.56 | 1,160.00 |
| 6.009 | 80.92 | 1,151.00 |
| 6.209 | 80.24 | 1,141.30 |
| 6.409 | 79.48 | 1,130.40 |
| 6.609 | 78.88 | 1,121.90 |
| 6.809 | 78.27 | 1,113.30 |
| 7.009 | 77.62 | 1,104.00 |
| 7.209 | 76.94 | 1,094.40 |
| 7.409 | 76.32 | 1,085.50 |
| 7.609 | 75.57 | 1,074.90 |

APR1400 DCD TIER 2

Table 6.2.1-5 (16 of 26)

Insert this page.

**Part B. Reactor Vessel Pressure vs. Time
(Blowdown Period)**

| Time (sec) | Reactor Vessel Pressure | |
|------------|-------------------------|----------|
| | kg/cm ² A | psia |
| 7.809 | 74.87 | 1,064.90 |
| 8.009 | 74.23 | 1,055.80 |
| 8.409 | 72.92 | 1,037.20 |
| 8.809 | 71.62 | 1,018.70 |
| 9.204 | 70.32 | 1,000.20 |
| 9.608 | 69.01 | 981.57 |
| 10.004 | 67.70 | 962.86 |
| 10.404 | 66.32 | 943.31 |
| 10.799 | 64.73 | 920.61 |
| 11.205 | 62.25 | 885.43 |
| 11.601 | 59.92 | 852.22 |
| 12.006 | 58.14 | 826.88 |
| 12.205 | 55.99 | 796.34 |
| 12.406 | 55.20 | 785.18 |
| 12.599 | 53.98 | 767.78 |
| 12.806 | 52.89 | 752.32 |
| 13.005 | 51.83 | 737.15 |
| 13.213 | 50.66 | 720.49 |
| 13.413 | 49.62 | 705.72 |
| 13.613 | 48.60 | 691.24 |
| 13.813 | 47.57 | 676.65 |
| 14.013 | 46.53 | 661.87 |
| 14.203 | 45.07 | 641.07 |
| 14.409 | 43.74 | 622.06 |
| 14.616 | 42.39 | 602.96 |

APR1400 DCD TIER 2

Table 6.2.1-5 (17 of 26)

Insert this page.

Part B. Reactor Vessel Pressure vs. Time
(Blowdown Period)

| Time (sec) | Reactor Vessel Pressure | |
|------------|-------------------------|--------|
| | kg/cm ² A | psia |
| 14.816 | 40.78 | 579.98 |
| 15.016 | 39.48 | 561.58 |
| 15.214 | 37.97 | 540.09 |
| 15.409 | 36.72 | 522.26 |
| 15.609 | 35.32 | 502.42 |
| 15.809 | 34.01 | 483.72 |
| 16.009 | 32.71 | 465.30 |
| 16.200 | 31.56 | 448.93 |
| 16.400 | 30.45 | 433.14 |
| 16.601 | 29.23 | 415.81 |
| 16.800 | 28.03 | 398.63 |
| 17.001 | 26.77 | 380.75 |
| 17.205 | 25.49 | 362.53 |
| 17.400 | 24.24 | 344.80 |
| 17.600 | 23.00 | 327.17 |
| 17.800 | 21.78 | 309.80 |
| 18.000 | 20.54 | 292.11 |
| 18.200 | 19.37 | 275.52 |
| 18.400 | 18.22 | 259.10 |
| 18.600 | 17.10 | 243.28 |
| 18.802 | 15.99 | 227.49 |
| 18.999 | 14.94 | 212.46 |
| 19.203 | 15.92 | 226.38 |

APR1400 DCD TIER 2

Table 6.2.1-5 (18 of 26)

Part B. Reactor Vessel Pressure vs. Time
(Reflood and Post-reflood Period)

Insert this page.

| Time (sec) | Reactor Vessel Pressure | |
|------------|-------------------------|---------|
| | kg/cm ² A | psia |
| 19.20 | 4.080 | 58.000 |
| 19.30 | 4.120 | 58.560 |
| 21.30 | 4.380 | 62.330 |
| 23.30 | 5.950 | 84.620 |
| 25.30 | 7.730 | 109.920 |
| 27.30 | 9.330 | 132.690 |
| 28.70 | 10.240 | 145.660 |
| 28.80 | 10.300 | 146.480 |
| 28.90 | 10.350 | 147.280 |
| 29.00 | 10.380 | 147.670 |
| 31.50 | 10.210 | 145.240 |
| 34.00 | 10.030 | 142.670 |
| 36.50 | 9.860 | 140.180 |
| 39.00 | 9.690 | 137.760 |
| 41.50 | 9.520 | 135.410 |
| 44.00 | 9.360 | 133.120 |
| 46.50 | 9.200 | 130.900 |
| 49.00 | 9.050 | 128.740 |
| 51.50 | 8.900 | 126.650 |
| 54.00 | 8.760 | 124.610 |
| 56.50 | 8.620 | 122.620 |
| 59.00 | 8.490 | 120.690 |
| 61.50 | 8.350 | 118.820 |
| 63.50 | 8.250 | 117.350 |
| 63.60 | 8.250 | 117.280 |
| 63.70 | 8.240 | 117.180 |
| 63.80 | 8.220 | 116.950 |
| 65.80 | 7.880 | 112.150 |

APR1400 DCD TIER 2

Table 6.2.1-5 (19 of 26)

Insert this page.

Part B. Reactor Vessel Pressure vs. Time
(Reflood and Post-reflood Period)

| Time (sec) | Reactor Vessel Pressure | |
|------------|-------------------------|---------|
| | kg/cm ² A | psia |
| 67.80 | 7.620 | 108.430 |
| 69.80 | 7.420 | 105.500 |
| 71.80 | 7.250 | 103.160 |
| 73.80 | 7.120 | 101.230 |
| 75.80 | 7.010 | 99.650 |
| 77.80 | 6.910 | 98.340 |
| 79.80 | 6.830 | 97.200 |
| 81.80 | 6.760 | 96.210 |
| 83.80 | 6.700 | 95.340 |
| 85.80 | 6.650 | 94.560 |
| 87.80 | 6.600 | 93.860 |
| 88.90 | 6.570 | 93.500 |
| 89.00 | 6.580 | 93.610 |
| 89.10 | 6.530 | 92.940 |
| 89.20 | 6.520 | 92.770 |
| 91.20 | 6.420 | 91.270 |
| 93.20 | 6.260 | 89.090 |
| 95.20 | 6.110 | 86.860 |
| 97.20 | 5.960 | 84.790 |
| 99.20 | 5.830 | 82.900 |
| 101.20 | 5.710 | 81.180 |
| 103.20 | 5.600 | 79.620 |
| 105.20 | 5.500 | 78.200 |
| 107.20 | 5.410 | 76.910 |
| 109.20 | 5.320 | 75.720 |
| 111.20 | 5.250 | 74.630 |
| 113.20 | 5.180 | 73.630 |
| 115.20 | 5.110 | 72.700 |

APR1400 DCD TIER 2

Table 6.2.1-5 (20 of 26)

Insert this page.

Part B. Reactor Vessel Pressure vs. Time
(Reflood and Post-reflood Period)

| Time (sec) | Reactor Vessel Pressure | |
|------------|-------------------------|--------|
| | kg/cm ² A | psia |
| 117.00 | 5.060 | 71.930 |
| 117.10 | 5.050 | 71.890 |
| 117.20 | 5.050 | 71.850 |
| 118.20 | 5.070 | 72.170 |
| 119.20 | 4.790 | 68.090 |
| 120.20 | 4.970 | 70.730 |
| 121.20 | 4.860 | 69.140 |
| 122.20 | 4.950 | 70.400 |
| 123.20 | 5.180 | 73.730 |
| 124.20 | 4.740 | 67.440 |
| 125.20 | 4.880 | 69.460 |
| 126.20 | 4.600 | 65.460 |
| 127.30 | 4.640 | 66.060 |
| 127.40 | 4.720 | 67.120 |

APR1400 DCD TIER 2

Table 6.2.1-5 (21 of 26)

Part B. Reactor Vessel Pressure vs. Time
(Decay heat Period)

Insert this page.

| Time (sec) | Reactor Vessel Pressure | |
|------------|-------------------------|--------|
| | kg/cm ² A | psia |
| 200.0 | 4.245 | 60.375 |
| 400.0 | 3.954 | 56.235 |
| 599.9 | 3.824 | 54.394 |
| 800.0 | 3.735 | 53.129 |
| 999.0 | 3.666 | 52.149 |
| 1503.4 | 3.542 | 50.386 |
| 1996.6 | 3.461 | 49.227 |
| 4001.4 | 3.313 | 47.128 |
| 5997.8 | 3.261 | 46.381 |
| 7995.9 | 3.243 | 46.128 |
| 9995.2 | 3.237 | 46.044 |
| 15006.5 | 3.223 | 45.843 |
| 20012.2 | 3.176 | 45.18 |
| 40037.9 | 2.864 | 40.736 |
| 59965.8 | 2.56 | 36.415 |
| 79994.6 | 2.355 | 33.497 |
| 100002.1 | 2.226 | 31.664 |
| 150009.3 | 2.037 | 28.97 |
| 200016.7 | 1.922 | 27.332 |
| 400050.3 | 1.716 | 24.402 |
| 600092.2 | 1.619 | 23.025 |
| 800132.9 | 1.564 | 22.239 |
| 1000000.0 | 1.527 | 21.725 |

APR1400 DCD TIER 2

Table 6.2.1-5 (22 of 26)

Insert this page.

Part C. Safety Injection Flow vs. Time (Blowdown Period)

| Time (sec) | Safety Injection Tank Flow | |
|------------|----------------------------|-----------|
| | kg/sec | lbm/sec |
| 0.000 | 0.00 | 0.00 |
| 0.027 | 0.00 | 0.00 |
| 13.813 | 0.00 | 0.00 |
| 14.013 | 0.00 | 0.00 |
| 14.203 | 1,281.21 | 2,824.60 |
| 14.409 | 1,690.48 | 3,726.90 |
| 14.616 | 1,989.35 | 4,385.80 |
| 14.816 | 2,357.62 | 5,197.70 |
| 15.016 | 2,555.71 | 5,634.40 |
| 15.214 | 2,769.58 | 6,105.90 |
| 15.409 | 2,934.41 | 6,469.30 |
| 15.609 | 3,097.38 | 6,828.60 |
| 15.809 | 3,236.55 | 7,135.40 |
| 16.009 | 3,362.73 | 7,413.60 |
| 16.200 | 3,451.73 | 7,609.80 |
| 16.400 | 3,536.73 | 7,797.20 |
| 16.601 | 3,639.88 | 8,024.60 |
| 16.800 | 3,738.76 | 8,242.60 |
| 17.001 | 3,845.63 | 8,478.20 |
| 17.205 | 3,957.26 | 8,724.30 |
| 17.400 | 4,061.17 | 8,953.40 |
| 17.600 | 4,159.33 | 9,169.80 |
| 17.800 | 4,253.59 | 9,377.60 |
| 18.000 | 4,351.61 | 9,593.70 |
| 18.200 | 4,434.98 | 9,777.50 |
| 18.400 | 4,517.85 | 9,960.20 |
| 18.600 | 4,594.41 | 10,129.00 |
| 18.802 | 4,668.35 | 10,292.00 |
| 18.999 | 4,740.47 | 10,451.00 |
| 19.203 | 4,496.26 | 9,912.60 |

APR1400 DCD TIER 2

Table 6.2.1-5 (23 of 26)

Insert this page.

Part C. Safety Injection Flow vs. Time (Reflood and Post-reflood Period)

| Time (sec) | Safety Injection Tank Flow | | Safety Injection Pump Flow | |
|------------|----------------------------|----------|----------------------------|---------|
| | kg/sec | lbm/sec | kg/sec | lbm/sec |
| 19.203 | 3,140.51 | 6,923.67 | 193.78 | 427.22 |
| 19.303 | 3,128.73 | 6,897.71 | 193.78 | 427.22 |
| 22.303 | 2,763.24 | 6,091.92 | 193.01 | 425.52 |
| 25.303 | 2,337.52 | 5,153.37 | 190.91 | 420.88 |
| 28.803 | 1,886.53 | 4,159.10 | 188.76 | 416.16 |
| 28.903 | 1,875.12 | 4,133.96 | 188.72 | 416.05 |
| 31.903 | 1,731.93 | 3,818.27 | 188.81 | 416.25 |
| 37.903 | 1,524.29 | 3,360.50 | 189.16 | 417.02 |
| 43.903 | 1,367.93 | 3,015.78 | 189.48 | 417.74 |
| 49.903 | 1,246.55 | 2,748.19 | 189.79 | 418.41 |
| 55.903 | 1,150.32 | 2,536.03 | 190.07 | 419.04 |
| 58.903 | 1,109.54 | 2,446.13 | 190.21 | 419.33 |
| 63.503 | 1,054.71 | 2,325.24 | 190.40 | 419.77 |
| 63.603 | 1,053.61 | 2,322.82 | 190.41 | 419.78 |
| 63.703 | 477.25 | 1,052.17 | 190.41 | 419.79 |
| 63.803 | 477.41 | 1,052.51 | 190.42 | 419.80 |
| 68.803 | 513.56 | 1,132.21 | 191.00 | 421.08 |
| 73.803 | 524.49 | 1,156.32 | 191.32 | 421.80 |
| 78.803 | 524.35 | 1,156.01 | 191.52 | 422.24 |
| 83.803 | 519.37 | 1,145.03 | 191.66 | 422.55 |
| 88.803 | 512.06 | 1,128.91 | 191.77 | 422.78 |
| 93.803 | 522.57 | 1,152.08 | 192.05 | 423.41 |
| 98.803 | 533.86 | 1,176.97 | 192.35 | 424.06 |
| 103.803 | 539.82 | 1,190.11 | 192.58 | 424.57 |
| 108.803 | 541.92 | 1,194.74 | 192.77 | 424.98 |
| 113.803 | 541.35 | 1,193.49 | 192.92 | 425.31 |
| 117.103 | 539.92 | 1,190.32 | 193.00 | 425.49 |
| 118.103 | 537.20 | 1,184.34 | 193.00 | 425.49 |

APR1400 DCD TIER 2

Table 6.2.1-5 (24 of 26)

Insert this page.

Part C. Safety Injection Flow vs. Time (Reflood and Post-reflood Period)

| Time (sec) | Safety Injection Tank Flow | | Safety Injection Pump Flow | |
|------------|----------------------------|----------|----------------------------|---------|
| | kg/sec | lbm/sec | kg/sec | lbm/sec |
| 119.103 | 524.95 | 1,157.33 | 192.89 | 425.26 |
| 120.103 | 548.19 | 1,208.55 | 193.18 | 425.89 |
| 121.103 | 544.24 | 1,199.86 | 193.16 | 425.85 |
| 122.103 | 537.26 | 1,184.46 | 193.11 | 425.75 |
| 123.103 | 536.28 | 1,182.30 | 193.13 | 425.78 |
| 124.103 | 549.66 | 1,211.79 | 193.31 | 426.18 |
| 125.103 | 535.70 | 1,181.03 | 193.18 | 425.89 |
| 126.103 | 481.43 | 1,061.38 | 192.64 | 424.70 |
| 127.403 | 543.72 | 1,198.69 | 193.33 | 426.23 |
| 147.403 | 490.64 | 1,081.67 | 193.27 | 426.08 |
| 167.403 | 479.18 | 1,056.41 | 193.56 | 426.73 |
| 187.403 | 459.38 | 1,012.76 | 193.71 | 427.06 |
| 207.403 | 429.67 | 947.27 | 193.72 | 427.09 |
| 227.403 | 402.01 | 886.30 | 193.73 | 427.11 |
| 247.403 | 376.72 | 830.54 | 193.74 | 427.13 |
| 267.403 | 353.37 | 779.06 | 193.75 | 427.14 |
| 287.403 | 331.63 | 731.13 | 193.75 | 427.15 |
| 307.403 | 311.25 | 686.20 | 193.76 | 427.16 |
| 327.403 | 292.03 | 643.81 | 193.76 | 427.17 |
| 347.403 | 273.79 | 603.61 | 193.76 | 427.18 |
| 368.103 | 255.83 | 564.00 | 193.77 | 427.18 |
| 368.203 | 255.74 | 563.81 | 193.77 | 427.18 |
| 368.303 | 0.00 | 0.00 | 193.77 | 427.18 |
| 368.403 | 0.00 | 0.00 | 193.77 | 427.18 |
| 403.403 | 0.00 | 0.00 | 193.78 | 427.21 |
| 438.403 | 0.00 | 0.00 | 193.77 | 427.20 |
| 473.403 | 0.00 | 0.00 | 193.75 | 427.15 |
| 508.403 | 0.00 | 0.00 | 193.75 | 427.14 |

APR1400 DCD TIER 2

Table 6.2.1-5 (25 of 26)

Insert this page.

Part C. Safety Injection Flow vs. Time (Reflood and Post-reflood Period)

| Time (sec) | Safety Injection Tank Flow | | Safety Injection Pump Flow | |
|------------|----------------------------|---------|----------------------------|---------|
| | kg/sec | lbm/sec | kg/sec | lbm/sec |
| 543.403 | 0.00 | 0.00 | 193.74 | 427.13 |
| 578.403 | 0.00 | 0.00 | 193.74 | 427.12 |
| 600.003 | 0.00 | 0.00 | 193.73 | 427.11 |

APR1400 DCD TIER 2

Table 6.2.1-5 (26 of 26)

Insert this page.

Part D. Chronology of Events

| Time (sec) | Event | Values |
|------------|--|---|
| 0.0 | Break occurs | — |
| 4.36 | Containment pressure Hi-Hi setpoint | 1.547kgf/cm ² g (22.0psig) |
| 14.01 | Start safety injection tank (SIT) injection | — |
| 19.01 | First peak containment pressure (Blowdown phase) | 3.073kgf/cm ² g (43.70psig) |
| 19.20 | End of blowdown | — |
| | Start SI pump injection | — |
| 63.70 | SIT flow is turned down to low flow by fluidic device in SIT | — |
| 114.31 | Peak containment temperature | 133.15°C (271.67°F) |
| 114.31 | Peak containment pressure | 3.422kgf/cm ² g (48.68psig) |
| 114.36 | Start containment spray actuation | — |
| 117.10 | End of reflood | — |
| 127.40 | End of post-reflood | — |
| 368.30 | Safety injection tank empty | — |
| 47,148.1 | Time of depressurization of the containment at 50 % of peak pressure | 1.710kgf/cm ² g (24.33psig) |

Table 6.2.1-6 (1 of 25)

Double-Ended Discharge Leg Slot Break – Maximum SIS Flow
(0.9121 m² (9.8175 ft²) Break Area)

Part A. Mass and Energy Release Data (Blowdown Period)

| Time (sec) | Break Mass Flow Rate | | Break Enthalpy | |
|------------|----------------------|------------|----------------|---------|
| | kg/sec | lbm/sec | kcal/kg | Btu/lbm |
| 0.000 | 0.00 | 0.00 | 0.00 | 0.00 |
| 0.026 | 35,570.66 | 78,420.29 | 309.67 | 557.44 |
| 0.051 | 36,255.06 | 79,929.15 | 309.62 | 557.34 |
| 0.102 | 52,155.38 | 114,983.53 | 310.08 | 558.17 |
| 0.150 | 54,241.46 | 119,582.56 | 310.69 | 559.27 |
| 0.205 | 53,118.19 | 117,106.18 | 311.20 | 560.19 |
| 0.251 | 53,000.48 | 116,846.67 | 311.46 | 560.66 |
| 0.303 | 52,555.82 | 115,866.36 | 311.68 | 561.06 |
| 0.355 | 51,903.33 | 114,427.86 | 311.78 | 561.23 |
| 0.455 | 51,283.34 | 113,060.99 | 311.86 | 561.38 |
| 0.548 | 50,839.80 | 112,083.15 | 311.87 | 561.40 |
| 0.655 | 50,335.08 | 110,970.43 | 311.89 | 561.44 |
| 0.751 | 49,799.01 | 109,788.59 | 311.92 | 561.50 |
| 0.850 | 49,295.77 | 108,679.14 | 311.98 | 561.60 |
| 0.952 | 48,985.60 | 107,995.33 | 312.09 | 561.80 |
| 1.256 | 45,974.67 | 101,357.32 | 312.52 | 562.57 |
| 1.500 | 44,806.61 | 98,782.18 | 313.10 | 563.62 |
| 1.749 | 42,469.15 | 93,628.95 | 313.84 | 564.95 |
| 2.001 | 40,547.50 | 89,392.40 | 314.75 | 566.58 |
| 2.253 | 39,075.65 | 86,147.52 | 315.77 | 568.41 |
| 2.513 | 37,917.46 | 83,594.12 | 316.79 | 570.25 |
| 2.753 | 37,135.87 | 81,871.00 | 317.79 | 572.06 |
| 3.013 | 35,641.45 | 78,576.37 | 318.70 | 573.69 |
| 3.253 | 34,354.67 | 75,739.48 | 319.39 | 574.94 |
| 3.513 | 33,446.63 | 73,737.59 | 320.70 | 577.29 |

Replace these 25 pages of Table 6.2.1–6 with the following 23 pages of revised Table 6.2.1–6.

Table 6.2.1-6 (2 of 25)

Part A. Mass and Energy Release Data
(Blowdown Period)

| Time (sec) | Break Mass Flow Rate | | Break Enthalpy | |
|------------|----------------------|-----------|----------------|----------|
| | kg/sec | lbm/sec | kcal/kg | Btu/lbm |
| 3.753 | 32,136.20 | 70,848.55 | 322.26 | 580.11 |
| 4.013 | 30,679.12 | 67,636.23 | 324.09 | 583.39 |
| 4.513 | 28,504.55 | 62,842.10 | 327.42 | 589.38 |
| 5.013 | 26,227.90 | 57,822.93 | 331.03 | 595.89 |
| 5.513 | 24,545.92 | 54,114.76 | 337.02 | 606.67 |
| 6.013 | 21,825.68 | 48,117.64 | 349.22 | 628.64 |
| 6.513 | 17,987.35 | 39,655.52 | 376.16 | 677.13 |
| 7.013 | 13,886.23 | 30,614.05 | 428.08 | 770.59 |
| 7.505 | 12,225.23 | 26,952.15 | 454.34 | 817.86 |
| 8.014 | 11,663.92 | 25,714.69 | 459.62 | 827.36 |
| 8.513 | 11,152.79 | 24,587.83 | 461.97 | 831.59 |
| 9.013 | 10,759.50 | 23,720.77 | 463.01 | 833.46 |
| 9.513 | 9,894.04 | 21,812.74 | 479.71 | 863.53 |
| 10.013 | 8,931.05 | 19,689.70 | 504.97 | 908.99 |
| 10.513 | 8,006.74 | 17,651.93 | 528.35 | 951.08 |
| 11.013 | 6,975.26 | 15,377.90 | 556.89 | 1,002.46 |
| 11.513 | 5,926.46 | 13,065.67 | 588.71 | 1,059.75 |
| 12.013 | 5,345.95 | 11,785.86 | 593.54 | 1,068.43 |
| 12.513 | 6,618.02 | 14,590.32 | 460.05 | 828.14 |
| 13.013 | 7,205.45 | 15,885.38 | 405.88 | 730.62 |
| 13.513 | 7,216.60 | 15,909.95 | 378.11 | 680.64 |
| 14.009 | 7,049.69 | 15,541.99 | 356.91 | 642.47 |
| 14.507 | 6,840.23 | 15,080.21 | 336.96 | 606.56 |
| 15.017 | 6,604.21 | 14,559.86 | 319.10 | 574.41 |
| 15.257 | 6,493.95 | 14,316.78 | 311.68 | 561.06 |
| 15.503 | 6,334.92 | 13,966.18 | 305.12 | 549.25 |
| 15.753 | 6,086.67 | 13,418.88 | 297.94 | 536.33 |
| 16.008 | 6,015.11 | 13,261.12 | 289.68 | 521.46 |

Replace these 25 pages of Table 6.2.1-6
with the following 23 pages of revised
Table 6.2.1-6.

Table 6.2.1-6 (3 of 25)

Part A. Mass and Energy Release Data
(Blowdown Period)

| Time (sec) | Break Mass Flow Rate | | Break Enthalpy | |
|------------|----------------------|-----------|----------------|---------|
| | kg/sec | lbm/sec | kcal/kg | Btu/lbm |
| 16.257 | 5,794.29 | 12,774.28 | 281.39 | 506.53 |
| 16.505 | 5,416.53 | 11,941.46 | 273.92 | 493.08 |
| 16.753 | 4,955.88 | 10,925.90 | 268.62 | 483.55 |
| 17.007 | 4,447.82 | 9,805.81 | 263.22 | 473.82 |
| 17.251 | 3,984.08 | 8,783.44 | 258.14 | 464.68 |
| 17.500 | 3,606.06 | 7,950.04 | 253.32 | 456.00 |
| 17.750 | 3,263.42 | 7,194.64 | 248.40 | 447.14 |
| 18.000 | 3,088.10 | 6,808.13 | 245.86 | 442.57 |
| 18.249 | 1,743.93 | 3,844.73 | 240.28 | 432.53 |
| 18.509 | 1,671.14 | 3,684.24 | 240.44 | 432.82 |
| 18.752 | 1,508.29 | 3,325.24 | 243.71 | 438.70 |
| 19.002 | 1,297.66 | 2,860.86 | 243.27 | 437.91 |
| 19.254 | 1,091.70 | 2,406.81 | 244.26 | 439.70 |
| 19.508 | 882.79 | 1,946.23 | 247.16 | 444.92 |
| 19.752 | 678.35 | 1,495.51 | 254.14 | 457.48 |

Integral Mass and Energy Release at End of Blowdown

| Time (sec) | Integral Mass | | Integral Energy | |
|------------|---------------|------------|-----------------|-------------|
| | kg | lbm | Million kcal | Million Btu |
| 19.752 | 322,456.13 | 710,897.80 | 112.812 | 447.702 |

Replace these 25 pages of Table 6.2.1-6 with the following 23 pages of revised Table 6.2.1-6.

Table 6.2.1-6 (4 of 25)

Part A. Mass and Energy Release Data
(Reflood and Post-reflood Period)

| Time (sec) | Break Mass Flow Rate | | Break Enthalpy | |
|---------------|----------------------|---------|----------------|----------|
| | kg/sec | lbm/sec | kcal/kg | Btu/lbm |
| 19.75 | 0.00 | 0.00 | 0.00 | 0.00 |
| 19.85 | 51.63 | 113.82 | 727.51 | 1,309.58 |
| 19.95 | 61.91 | 136.49 | 727.37 | 1,309.35 |
| 21.95 | 100.88 | 222.40 | 726.81 | 1,308.34 |
| 23.95 | 248.28 | 547.36 | 725.99 | 1,306.87 |
| 25.95 | 348.64 | 768.62 | 725.22 | 1,305.47 |
| 27.95 | 431.74 | 951.82 | 724.39 | 1,303.97 |
| 28.05 | 435.52 | 960.16 | 724.35 | 1,303.91 |
| 28.15 | 254.78 | 561.70 | 724.30 | 1,303.82 |
| 28.25 | 256.67 | 565.87 | 724.27 | 1,303.77 |
| 32.25 | 254.36 | 560.78 | 724.01 | 1,303.29 |
| 36.25 | 251.36 | 554.15 | 723.67 | 1,302.68 |
| 40.25 | 248.11 | 546.99 | 723.33 | 1,302.06 |
| 44.25 | 245.14 | 540.45 | 722.98 | 1,301.45 |
| 48.25 | 242.37 | 534.33 | 722.63 | 1,300.80 |
| 49.15 | 241.76 | 533.00 | 722.54 | 1,300.65 |
| 49.25 | 241.70 | 532.85 | 722.53 | 1,300.64 |
| 49.35 | 416.51 | 918.25 | 722.53 | 1,300.63 |
| 49.45 | 416.37 | 917.95 | 722.52 | 1,300.60 |
| 79.45 | 385.27 | 849.39 | 719.51 | 1,295.20 |
| 109.45 | 356.63 | 786.23 | 716.19 | 1,289.22 |
| 139.45 | 328.46 | 724.14 | 712.76 | 1,283.03 |
| 169.45 | 300.46 | 662.41 | 709.36 | 1,276.92 |
| 199.65 | 272.34 | 600.41 | 706.12 | 1,271.10 |
| 199.75 | 272.25 | 600.21 | 706.11 | 1,271.07 |
| 199.85 | 272.15 | 600.00 | 706.10 | 1,271.06 |
| 209.55 | 272.59 | 600.97 | 704.76 | 1,268.65 |
| 218.85 | 273.05 | 601.98 | 703.47 | 1,266.32 |

Replace these 25 pages of Table 6.2.1-6
with the following 23 pages of revised
Table 6.2.1-6.

Table 6.2.1-6 (5 of 25)

Part A. Mass and Energy Release Data
(Reflood and Post-reflood Period)

| Time (sec) | Break Mass Flow Rate | | Break Enthalpy | |
|------------|----------------------|---------|----------------|----------|
| | kg/sec | lbm/sec | kcal/kg | Btu/lbm |
| 228.15 | 273.65 | 603.30 | 702.14 | 1,263.92 |
| 237.45 | 274.33 | 604.80 | 700.76 | 1,261.45 |
| 246.95 | 275.11 | 606.51 | 699.28 | 1,258.78 |
| 247.05 | 274.94 | 606.15 | 685.99 | 1,234.85 |
| 247.15 | 282.99 | 623.89 | 684.93 | 1,232.95 |
| 247.45 | 275.60 | 607.59 | 685.73 | 1,234.39 |
| 247.75 | 283.60 | 625.24 | 678.22 | 1,220.86 |
| 248.35 | 274.91 | 606.07 | 669.86 | 1,205.82 |
| 248.45 | 274.77 | 605.77 | 668.92 | 1,204.13 |
| 251.95 | 243.76 | 537.41 | 653.81 | 1,176.93 |
| 255.65 | 217.27 | 478.99 | 653.81 | 1,176.93 |
| 259.15 | 203.58 | 448.83 | 653.82 | 1,176.95 |
| 262.65 | 195.38 | 430.74 | 653.82 | 1,176.94 |
| 266.15 | 190.04 | 418.96 | 653.81 | 1,176.92 |
| 269.65 | 186.24 | 410.59 | 653.81 | 1,176.93 |
| 273.15 | 183.33 | 404.18 | 653.82 | 1,176.94 |
| 276.65 | 180.96 | 398.94 | 653.81 | 1,176.93 |
| 280.15 | 178.87 | 394.35 | 653.81 | 1,176.92 |
| 281.05 | 178.37 | 393.23 | 653.81 | 1,176.93 |
| 281.15 | 178.31 | 393.10 | 653.82 | 1,176.95 |
| 281.25 | 178.25 | 392.98 | 653.82 | 1,176.94 |
| 283.65 | 177.23 | 390.72 | 653.81 | 1,176.93 |
| 285.15 | 176.78 | 389.74 | 653.81 | 1,176.93 |
| 285.25 | 175.29 | 386.44 | 653.82 | 1,176.94 |
| 285.35 | 176.58 | 389.29 | 653.82 | 1,176.93 |
| 288.85 | 142.66 | 314.52 | 653.82 | 1,176.95 |
| 292.35 | 164.56 | 362.79 | 653.81 | 1,176.93 |
| 295.85 | 339.62 | 748.74 | 653.81 | 1,176.93 |

Replace these 25 pages of Table 6.2.1-6
with the following 23 pages of revised
Table 6.2.1-6.

Table 6.2.1-6 (6 of 25)

Part A: Mass and Energy Release Data (Reflood and Post-reflood Period)

| Time (sec) | Break Mass Flow Rate | | Break Enthalpy | |
|---------------|----------------------|---------|----------------|----------|
| | kg/sec | lbm/sec | kcal/kg | Btu/lbm |
| 313.35 | 109.25 | 240.86 | 653.81 | 1,176.93 |
| 316.85 | 206.98 | 456.31 | 653.82 | 1,176.94 |
| 320.35 | 102.22 | 225.36 | 653.83 | 1,176.96 |
| 323.85 | 98.81 | 217.83 | 653.82 | 1,176.95 |
| 327.35 | 184.79 | 407.40 | 653.81 | 1,176.93 |
| 330.85 | 93.68 | 206.52 | 653.81 | 1,176.93 |
| 334.35 | 92.15 | 203.15 | 653.82 | 1,176.95 |
| 337.85 | 124.24 | 273.90 | 653.81 | 1,176.93 |
| 341.35 | 130.69 | 288.13 | 653.81 | 1,176.93 |
| 344.85 | 111.96 | 246.84 | 653.81 | 1,176.93 |
| 348.35 | 72.51 | 159.86 | 653.81 | 1,176.93 |
| 351.85 | 72.00 | 158.74 | 653.80 | 1,176.90 |
| 355.35 | 116.68 | 257.24 | 653.81 | 1,176.92 |
| 358.85 | 62.06 | 136.83 | 653.80 | 1,176.91 |
| 360.15 | 61.54 | 135.67 | 653.82 | 1,176.94 |
| 360.25 | 60.92 | 134.31 | 653.81 | 1,176.92 |

Integral Mass and Energy Release at the End of Reflood and Post-reflood

| Time (sec) | Integral Mass | | Integral Energy | |
|---------------|---------------|------------|-----------------|-------------|
| | kg | lbm | Million kcal | Million Btu |
| 199.75 | 58,868.73 | 129,784.00 | 42.157 | 167.303 |
| 360.25 | 89,568.60 | 197,466.00 | 62.874 | 249.519 |

Replace these 25 pages of Table 6.2.1-6 with the following 23 pages of revised Table 6.2.1-6.

Table 6.2.1-6 (7 of 25)

Part A: Spillage Release Data (Reactor Vessel Side)
(Reflood and Post-Reflood Period)

| Time (sec) | Break Mass Flow Rate | | Break Enthalpy | |
|---------------|----------------------|----------|----------------|---------|
| | kg/sec | lbm/sec | kcal/kg | Btu/lbm |
| 19.75 | 0.00 | 0.00 | 0.00 | 0.00 |
| 19.85 | 0.00 | 0.00 | 0.00 | 0.00 |
| 28.05 | 0.00 | 0.00 | 0.00 | 0.00 |
| 28.15 | 465.09 | 1,025.35 | 317.38 | 571.31 |
| 28.25 | 2,031.84 | 4,479.47 | 111.51 | 200.73 |
| 32.25 | 1,881.58 | 4,148.19 | 115.85 | 208.55 |
| 36.25 | 1,752.17 | 3,862.90 | 119.91 | 215.84 |
| 40.25 | 1,649.04 | 3,635.52 | 123.34 | 222.02 |
| 44.25 | 1,558.85 | 3,436.70 | 126.67 | 228.02 |
| 48.25 | 1,479.16 | 3,261.00 | 129.90 | 233.84 |
| 49.15 | 1,462.46 | 3,224.20 | 130.61 | 235.12 |
| 49.25 | 1,460.64 | 3,220.17 | 130.69 | 235.26 |
| 49.35 | 458.73 | 1,011.34 | 50.40 | 90.72 |
| 49.45 | 458.43 | 1,010.68 | 50.40 | 90.73 |
| 79.45 | 405.29 | 893.52 | 50.78 | 91.41 |
| 109.45 | 372.58 | 821.40 | 51.13 | 92.04 |
| 139.45 | 355.00 | 782.64 | 51.47 | 92.65 |
| 169.45 | 347.92 | 767.04 | 51.82 | 93.28 |
| 199.65 | 348.35 | 767.98 | 52.17 | 93.91 |
| 199.75 | 348.36 | 768.00 | 52.17 | 93.91 |
| 199.85 | 436.54 | 962.41 | 52.17 | 93.91 |
| 209.55 | 421.82 | 929.96 | 52.30 | 94.14 |
| 218.85 | 408.81 | 901.28 | 52.42 | 94.36 |
| 228.15 | 396.07 | 873.19 | 52.54 | 94.58 |
| 237.45 | 383.64 | 845.78 | 52.66 | 94.80 |
| 246.95 | 371.23 | 818.43 | 52.79 | 95.04 |
| 247.05 | 362.82 | 799.88 | 52.80 | 95.04 |
| 247.15 | 322.92 | 711.93 | 52.80 | 95.04 |
| 247.45 | 346.30 | 763.46 | 52.80 | 95.05 |
| 247.75 | 334.13 | 736.63 | 52.81 | 95.06 |
| 248.35 | 342.38 | 754.83 | 52.81 | 95.05 |

Replace these 25 pages of Table 6.2.1-6
with the following 23 pages of revised
Table 6.2.1-6.

Table 6.2.1-6 (8 of 25)

Part A: Spillage Release Data (Reactor Vessel Side)
(Reflood and Post-Reflood Period)

| Time (sec) | Break Mass Flow Rate | | Break Enthalpy | |
|---------------|----------------------|---------|----------------|---------|
| | kg/sec | lbm/sec | kcal/kg | Btu/lbm |
| 248.45 | 339.48 | 748.43 | 52.81 | 95.06 |
| 251.95 | 285.14 | 628.62 | 52.84 | 95.12 |
| 255.65 | 217.96 | 480.53 | 52.91 | 95.24 |
| 259.15 | 170.21 | 375.26 | 52.97 | 95.35 |
| 262.65 | 134.28 | 296.03 | 53.04 | 95.47 |
| 266.15 | 105.35 | 232.26 | 53.11 | 95.60 |
| 269.65 | 80.04 | 176.45 | 53.18 | 95.73 |
| 273.15 | 56.26 | 124.04 | 53.25 | 95.86 |
| 276.65 | 32.68 | 72.05 | 53.33 | 96.00 |
| 280.15 | 8.06 | 17.77 | 53.42 | 96.17 |
| 281.05 | 1.42 | 3.13 | 53.35 | 96.04 |
| 281.15 | 0.67 | 1.48 | 53.30 | 95.95 |
| 281.25 | 0.00 | 0.00 | 0.00 | 0.00 |
| 360.15 | 0.00 | 0.00 | 0.00 | 0.00 |
| 360.25 | 0.00 | 0.00 | 0.00 | 0.00 |

Integral Mass and Energy (Reactor Vessel Side Spillage) at EOR and EOPR

| Time (sec) | Integral Mass | | Integral Energy | |
|---------------|---------------|------------|-----------------|-------------|
| | kg | lbm | Million kcal | Million Btu |
| 199.75 | 92,597.23 | 204,143.00 | 7.278 | 28.883 |
| 360.25 | 116,570.82 | 256,996.00 | 8.538 | 33.885 |

Replace these 25 pages of Table 6.2.1-6
with the following 23 pages of revised
Table 6.2.1-6.

Table 6.2.1-6 (9 of 25)

Part A: Spillage Release Data (Steam Generator Side)
(Reflood and Post-Reflood Period)

| Time (sec) | Break Mass Flow Rate | | Break Enthalpy | |
|---------------|----------------------|----------|----------------|---------|
| | kg/sec | lbm/sec | kcal/kg | Btu/lbm |
| 19.75 | 0.00 | 0.00 | 0.00 | 0.00 |
| 19.85 | 0.00 | 0.00 | 0.00 | 0.00 |
| 199.75 | 0.00 | 0.00 | 0.00 | 0.00 |
| 237.45 | 0.00 | 0.00 | 0.00 | 0.00 |
| 246.95 | 0.00 | 0.00 | 0.00 | 0.00 |
| 247.05 | 1.56 | 3.44 | 144.40 | 259.94 |
| 247.15 | 1.34 | 2.95 | 144.12 | 259.42 |
| 247.45 | 11.85 | 26.13 | 144.31 | 259.78 |
| 247.75 | 14.31 | 31.54 | 144.32 | 259.78 |
| 248.35 | 25.15 | 55.44 | 144.33 | 259.81 |
| 248.45 | 26.33 | 58.04 | 144.33 | 259.82 |
| 251.95 | 105.95 | 233.57 | 144.33 | 259.81 |
| 255.65 | 195.79 | 431.64 | 144.33 | 259.81 |
| 259.15 | 255.18 | 562.58 | 144.33 | 259.81 |
| 262.65 | 297.37 | 655.60 | 144.33 | 259.81 |
| 266.15 | 329.09 | 725.53 | 144.33 | 259.81 |
| 269.65 | 355.09 | 782.85 | 144.33 | 259.81 |
| 273.15 | 378.24 | 833.87 | 144.33 | 259.81 |
| 276.65 | 400.35 | 882.62 | 144.33 | 259.81 |
| 280.15 | 422.94 | 932.43 | 144.33 | 259.81 |
| 281.05 | 429.00 | 945.79 | 144.33 | 259.81 |
| 281.15 | 429.68 | 947.29 | 144.33 | 259.81 |
| 281.25 | 430.37 | 948.80 | 144.33 | 259.81 |
| 283.65 | 443.10 | 976.88 | 144.33 | 259.81 |
| 285.15 | 445.06 | 981.20 | 144.33 | 259.81 |
| 285.25 | 447.57 | 986.72 | 144.33 | 259.81 |
| 285.35 | 454.00 | 1,000.91 | 144.33 | 259.81 |
| 288.85 | 393.41 | 867.32 | 144.33 | 259.81 |
| 292.35 | 317.04 | 698.95 | 144.33 | 259.81 |
| 295.85 | 590.86 | 1,302.64 | 144.33 | 259.81 |
| 299.35 | 708.55 | 1,562.09 | 144.33 | 259.81 |

Replace these 25 pages of Table 6.2.1-6 with the following 23 pages of revised Table 6.2.1-6.

Table 6.2.1-6 (10 of 25)

Part A: Spillage Release Data (Steam Generator Side)
(Reflood and Post-Reflood Period)

| Time (sec) | Break Mass Flow Rate | | Break Enthalpy | |
|---------------|----------------------|----------|----------------|---------|
| | kg/sec | lbm/sec | kcal/kg | Btu/lbm |
| 302.85 | 258.24 | 569.32 | 144.33 | 259.81 |
| 306.35 | 616.82 | 1,359.86 | 144.33 | 259.81 |
| 309.85 | 685.57 | 1,511.42 | 144.33 | 259.81 |
| 313.35 | 272.19 | 600.09 | 144.33 | 259.81 |
| 316.85 | 646.62 | 1,425.56 | 144.33 | 259.81 |
| 320.35 | 670.59 | 1,478.41 | 144.33 | 259.81 |
| 323.85 | 282.38 | 622.54 | 144.33 | 259.81 |
| 327.35 | 667.62 | 1,471.85 | 144.33 | 259.81 |
| 330.85 | 732.92 | 1,615.81 | 144.33 | 259.81 |
| 334.35 | 311.70 | 687.18 | 144.33 | 259.81 |
| 337.85 | 825.46 | 1,819.83 | 144.33 | 259.81 |
| 341.35 | 305.77 | 674.11 | 144.33 | 259.81 |
| 344.85 | 184.18 | 406.04 | 144.33 | 259.81 |
| 348.35 | 922.54 | 2,033.86 | 144.33 | 259.81 |
| 351.85 | 685.61 | 1,511.51 | 144.33 | 259.81 |
| 355.35 | 84.80 | 186.95 | 144.33 | 259.81 |
| 358.85 | 774.68 | 1,707.88 | 144.33 | 259.81 |
| 360.15 | 772.81 | 1,703.77 | 144.33 | 259.81 |
| 360.25 | 755.90 | 1,666.49 | 144.33 | 259.81 |

Integral Mass and Energy (Steam Generator Side Spillage) at EOR and EOPR

| Time (sec) | Integral Mass | | Integral Energy | |
|---------------|---------------|------------|-----------------|-------------|
| | kg | lbm | Million kcal | Million Btu |
| 199.75 | 0.00 | 0.00 | 0.000 | 0.000 |
| 360.25 | 50,583.00 | 111,517.00 | 7.301 | 28.973 |

Replace these 25 pages of Table 6.2.1-6 with the following 23 pages of revised Table 6.2.1-6.

Table 6.2.1-6 (11 of 25)

Part A. Mass and Energy (Steam) Release Data (Decay heat Period)

| Time (sec) | Mass Flow Rate | | Break Enthalpy | |
|------------|----------------|---------|----------------|---------|
| | kg/sec | lbm/sec | kcal/kg | Btu/lbm |
| 600.0 | 48.45 | 106.81 | 654.62 | 1178.31 |
| 800.0 | 46.52 | 102.56 | 654.29 | 1177.73 |
| 999.0 | 45.45 | 100.21 | 654.04 | 1177.27 |
| 1504.4 | 42.95 | 94.7 | 653.6 | 1176.47 |
| 1997.8 | 40.53 | 89.36 | 653.31 | 1175.96 |
| 4005.0 | 33.76 | 74.43 | 652.69 | 1174.85 |
| 6003.6 | 30.18 | 66.54 | 652.34 | 1174.22 |
| 8004.3 | 27.99 | 61.7 | 652.12 | 1173.81 |
| 9995.6 | 26.46 | 58.33 | 651.96 | 1173.53 |
| 15005.7 | 24.1 | 53.13 | 651.67 | 1173.01 |
| 20011.7 | 22.65 | 49.93 | 651.41 | 1172.54 |
| 40038.3 | 19.66 | 43.35 | 650.45 | 1170.81 |
| 59965.1 | 18.13 | 39.97 | 649.6 | 1169.27 |
| 79991.5 | 17.17 | 37.84 | 648.96 | 1168.13 |
| 100002.3 | 14.49 | 31.95 | 647.87 | 1166.17 |
| 150010.0 | 12.81 | 28.25 | 646.5 | 1163.7 |
| 200018.4 | 11.71 | 25.81 | 645.79 | 1162.42 |
| 400054.2 | 9.2 | 20.29 | 644.51 | 1160.12 |
| 600092.3 | 7.86 | 17.32 | 643.88 | 1158.98 |
| 800133.9 | 6.98 | 15.4 | 643.51 | 1158.32 |
| 1000000.0 | 6.38 | 14.06 | 643.26 | 1157.87 |

Integral Mass and Energy Release (Steam) at 24 hours and End of Analysis

| Time (sec) | Integral Mass | | Integral Energy | |
|------------|---------------|------------|-----------------|-------------|
| | kg | lbm | Million kcal | Million Btu |
| 85,100 | 1,898,431 | 4,185,325 | 1,240.804 | 4,344.599 |
| 1,000,000 | 10,032,626 | 22,118,155 | 6,488.479 | 25,748.366 |

Replace these 25 pages of Table 6.2.1-6 with the following 23 pages of revised Table 6.2.1-6.

Table 6.2.1-6 (12 of 25)

Part A. Mass and Energy (Spillage) Release Data (Decay heat Period)

| Time (sec) | Mass Flow Rate | | Break Enthalpy | |
|------------|----------------|---------|----------------|---------|
| | kg/sec | lbm/sec | kcal/kg | Btu/lbm |
| 600.0 | 159.63 | 351.93 | 79.76 | 143.57 |
| 800.0 | 170.72 | 376.37 | 80.0 | 144.0 |
| 999.0 | 180.69 | 398.34 | 82.58 | 148.64 |
| 1504.4 | 197.28 | 434.93 | 88.1 | 158.59 |
| 1997.8 | 204.81 | 451.53 | 92.57 | 166.62 |
| 4005.0 | 211.71 | 466.74 | 105.06 | 189.11 |
| 6003.6 | 213.95 | 471.68 | 112.15 | 201.86 |
| 8004.3 | 215.14 | 474.3 | 116.3 | 209.34 |
| 9995.6 | 216.08 | 476.37 | 118.72 | 213.7 |
| 15005.7 | 217.77 | 480.09 | 121.08 | 217.95 |
| 20011.7 | 219.11 | 483.06 | 121.14 | 218.05 |
| 40038.3 | 222.74 | 491.06 | 117.19 | 210.94 |
| 59965.1 | 225.14 | 496.35 | 112.7 | 202.85 |
| 79991.5 | 226.79 | 499.98 | 109.13 | 196.43 |
| 100002.3 | 230.19 | 507.49 | 104.02 | 187.24 |
| 150010.0 | 233.44 | 514.65 | 95.14 | 171.25 |
| 200018.4 | 235.27 | 518.69 | 90.45 | 162.8 |
| 400054.2 | 238.93 | 526.75 | 81.46 | 146.63 |
| 600092.3 | 240.82 | 530.93 | 76.51 | 137.73 |
| 800133.9 | 242.0 | 533.52 | 73.42 | 132.15 |
| 1000000.0 | 242.8 | 535.29 | 71.26 | 128.27 |

Integral Mass and Energy Release(Spillage) at 24 hours and End of Analysis

| Time (sec) | Integral Mass | | Integral Energy | |
|------------|---------------|-------------|-----------------|-------------|
| | kg | lbm | Million kcal | Million Btu |
| 85,100 | 18,926,678 | 41,726,182 | 2,161.914 | 8,579.170 |
| 1,000,000 | 237,848,696 | 524,366,617 | 19,733.144 | 78,307.442 |

Replace these 25 pages of Table 6.2.1-6 with the following 23 pages of revised Table 6.2.1-6.

Table 6.2.1-6 (13 of 25)

Part B. Reactor Vessel Pressure vs. Time
(Blowdown Period)

| Time (sec) | Reactor Vessel Pressure | |
|------------|-------------------------|----------|
| | kg/cm ² A | psia |
| 0.000 | 167.360 | 2,380.40 |
| 0.026 | 147.360 | 2,096.00 |
| 0.051 | 131.970 | 1,877.00 |
| 0.102 | 124.440 | 1,770.00 |
| 0.150 | 126.550 | 1,799.90 |
| 0.205 | 123.280 | 1,753.50 |
| 0.251 | 124.390 | 1,769.20 |
| 0.303 | 122.240 | 1,738.60 |
| 0.355 | 121.610 | 1,729.70 |
| 0.455 | 119.600 | 1,701.10 |
| 0.548 | 118.700 | 1,688.30 |
| 0.655 | 117.750 | 1,674.80 |
| 0.751 | 116.290 | 1,654.00 |
| 0.850 | 115.400 | 1,641.40 |
| 0.952 | 114.580 | 1,629.70 |
| 1.256 | 107.300 | 1,526.10 |
| 1.500 | 106.660 | 1,517.00 |
| 1.749 | 101.420 | 1,442.50 |
| 2.001 | 99.780 | 1,419.20 |
| 2.253 | 96.330 | 1,370.10 |
| 2.513 | 95.120 | 1,352.90 |
| 2.753 | 93.450 | 1,329.20 |
| 3.013 | 91.670 | 1,303.90 |

Replace these 25 pages of Table 6.2.1-6
with the following 23 pages of revised
Table 6.2.1-6.

Table 6.2.1-6 (14 of 25)

Part B. Reactor Vessel Pressure vs. Time
(Blowdown Period)

| Time (sec) | Reactor Vessel Pressure | |
|------------|-------------------------|----------|
| | kg/cm ² A | psia |
| 3.253 | 90.120 | 1,281.80 |
| 3.513 | 88.880 | 1,264.20 |
| 3.753 | 87.480 | 1,244.20 |
| 4.013 | 86.210 | 1,226.20 |
| 4.513 | 84.160 | 1,197.00 |
| 5.013 | 82.180 | 1,168.90 |
| 5.513 | 80.350 | 1,142.80 |
| 6.013 | 78.810 | 1,120.90 |
| 6.513 | 76.680 | 1,090.70 |
| 7.013 | 74.800 | 1,063.90 |
| 7.505 | 71.970 | 1,023.70 |
| 8.014 | 70.510 | 1,002.90 |
| 8.513 | 68.090 | 968.43 |
| 9.013 | 66.110 | 940.35 |
| 9.513 | 64.050 | 910.98 |
| 10.013 | 61.900 | 880.49 |
| 10.513 | 58.870 | 837.39 |
| 11.013 | 55.490 | 789.25 |
| 11.513 | 50.790 | 722.45 |
| 12.013 | 46.480 | 661.04 |
| 12.513 | 41.990 | 597.21 |
| 13.013 | 38.250 | 544.01 |
| 13.513 | 34.690 | 493.40 |

Replace these 25 pages of Table 6.2.1-6
with the following 23 pages of revised
Table 6.2.1-6.

Table 6.2.1-6 (15 of 25)

Part B. Reactor Vessel Pressure vs. Time
(Blowdown Period)

| Time (sec) | Reactor Vessel Pressure | |
|------------|-------------------------|--------|
| | kg/cm ² A | psia |
| 14.009 | 31.030 | 441.40 |
| 14.507 | 27.720 | 394.32 |
| 15.017 | 24.580 | 349.64 |
| 15.257 | 23.270 | 330.97 |
| 15.503 | 21.850 | 310.76 |
| 15.753 | 20.290 | 288.64 |
| 16.008 | 18.750 | 266.73 |
| 16.257 | 17.220 | 244.90 |
| 16.505 | 15.700 | 223.25 |
| 16.753 | 14.160 | 201.46 |
| 17.007 | 12.680 | 180.32 |
| 17.251 | 11.370 | 161.79 |
| 17.500 | 10.200 | 145.11 |
| 17.750 | 9.100 | 129.40 |
| 18.000 | 8.150 | 115.88 |
| 18.249 | 7.340 | 104.41 |
| 18.509 | 6.610 | 94.06 |
| 18.752 | 6.050 | 86.09 |
| 19.002 | 5.560 | 79.01 |
| 19.254 | 5.120 | 72.85 |
| 19.508 | 4.730 | 67.23 |
| 19.752 | 4.410 | 62.76 |

Replace these 25 pages of Table 6.2.1-6
with the following 23 pages of revised
Table 6.2.1-6.

Table 6.2.1-6 (16 of 25)

Part B. Reactor Vessel Pressure vs. Time
(Reflood and Post-reflood Period)

| Time (sec) | Reactor Vessel Pressure | |
|------------|-------------------------|--------|
| | kg/cm ² A | psia |
| 19.75 | 4.080 | 58.000 |
| 19.85 | 4.090 | 58.170 |
| 19.95 | 4.110 | 58.390 |
| 21.95 | 4.150 | 59.030 |
| 23.95 | 4.500 | 63.980 |
| 25.95 | 4.870 | 69.300 |
| 27.95 | 5.250 | 74.630 |
| 28.05 | 5.270 | 74.890 |
| 28.15 | 5.280 | 75.150 |
| 28.25 | 5.300 | 75.380 |
| 32.25 | 5.280 | 75.060 |
| 36.25 | 5.250 | 74.670 |
| 40.25 | 5.220 | 74.270 |
| 44.25 | 5.200 | 73.900 |
| 48.25 | 5.170 | 73.550 |
| 49.15 | 5.170 | 73.480 |
| 49.25 | 5.170 | 73.470 |
| 49.35 | 5.160 | 73.460 |
| 49.45 | 5.160 | 73.450 |
| 79.45 | 5.010 | 71.260 |
| 109.45 | 4.880 | 69.360 |
| 139.45 | 4.750 | 67.620 |
| 169.45 | 4.640 | 66.020 |
| 199.65 | 4.540 | 64.570 |
| 199.75 | 4.540 | 64.570 |
| 199.85 | 4.540 | 64.560 |

Replace these 25 pages of Table 6.2.1-6
with the following 23 pages of revised
Table 6.2.1-6.

Table 6.2.1-6 (17 of 25)

Part B. Reactor Vessel Pressure vs. Time
(Reflood and Post-reflood Period)

| Time (sec) | Reactor Vessel Pressure | |
|------------|-------------------------|--------|
| | kg/cm ² A | psia |
| 209.55 | 4.540 | 64.550 |
| 218.85 | 4.540 | 64.540 |
| 228.15 | 4.540 | 64.530 |
| 237.45 | 4.540 | 64.520 |
| 246.95 | 4.540 | 64.520 |
| 247.05 | 4.540 | 64.570 |
| 247.15 | 4.530 | 64.490 |
| 247.45 | 4.530 | 64.490 |
| 247.75 | 4.530 | 64.380 |
| 248.35 | 4.520 | 64.260 |
| 248.45 | 4.520 | 64.230 |
| 251.95 | 4.490 | 63.840 |
| 255.65 | 4.490 | 63.920 |
| 259.15 | 4.500 | 63.980 |
| 262.65 | 4.500 | 64.010 |
| 266.15 | 4.500 | 64.040 |
| 269.65 | 4.510 | 64.080 |
| 273.15 | 4.510 | 64.120 |
| 276.65 | 4.510 | 64.170 |
| 280.15 | 4.520 | 64.240 |
| 281.05 | 4.520 | 64.250 |
| 281.15 | 4.520 | 64.260 |
| 281.25 | 4.520 | 64.260 |
| 283.65 | 4.520 | 64.290 |
| 285.15 | 4.520 | 64.290 |
| 285.25 | 4.520 | 64.300 |

Replace these 25 pages of Table 6.2.1-6
with the following 23 pages of revised
Table 6.2.1-6.

Table 6.2.1-6 (18 of 25)

Part B. Reactor Vessel Pressure vs. Time
(Reflood and Post-reflood Period)

| Time (sec) | Reactor Vessel Pressure | |
|------------|-------------------------|--------|
| | kg/cm ² A | psia |
| 285.35 | 4.520 | 64.310 |
| 288.85 | 4.520 | 64.270 |
| 292.35 | 4.440 | 63.220 |
| 295.85 | 4.340 | 61.780 |
| 299.35 | 4.520 | 64.280 |
| 302.85 | 4.370 | 62.190 |
| 306.35 | 4.300 | 61.170 |
| 309.85 | 4.440 | 63.170 |
| 313.35 | 4.320 | 61.470 |
| 316.85 | 4.280 | 60.860 |
| 320.35 | 4.390 | 62.410 |
| 323.85 | 4.280 | 60.820 |
| 327.35 | 4.260 | 60.600 |
| 330.85 | 4.350 | 61.920 |
| 334.35 | 4.270 | 60.780 |
| 337.85 | 4.280 | 60.830 |
| 341.35 | 4.230 | 60.160 |
| 344.85 | 4.220 | 60.030 |
| 348.35 | 4.260 | 60.640 |
| 351.85 | 4.320 | 61.500 |
| 355.35 | 4.150 | 59.080 |
| 358.85 | 4.210 | 59.900 |
| 360.15 | 4.210 | 59.870 |
| 360.25 | 4.210 | 59.820 |
| 380.166 | 4.64 | 66.03 |
| 400.166 | 4.60 | 65.43 |

Replace these 25 pages of Table 6.2.1-6
with the following 23 pages of revised
Table 6.2.1-6.

Table 6.2.1-6 (19 of 25)

Part B. Reactor Vessel Pressure vs. Time
(Reflood and Post-reflood Period)

| Time (sec) | Reactor Vessel Pressure | |
|------------|-------------------------|-------|
| | kg/cm ² A | psia |
| 420.166 | 4.56 | 64.89 |
| 440.166 | 4.53 | 64.39 |
| 460.166 | 4.50 | 63.93 |
| 480.166 | 4.47 | 63.50 |
| 500.166 | 4.44 | 63.11 |
| 520.166 | 4.41 | 62.73 |
| 540.166 | 4.39 | 62.38 |
| 560.166 | 4.36 | 62.04 |
| 580.166 | 4.34 | 61.72 |
| 600.166 | 4.32 | 61.41 |
| 620.166 | 4.30 | 61.12 |
| 640.166 | 4.28 | 60.83 |
| 660.166 | 4.26 | 60.55 |
| 680.166 | 4.24 | 60.28 |
| 700.166 | 4.22 | 60.03 |
| 720.166 | 4.20 | 59.77 |
| 740.166 | 4.19 | 59.53 |
| 760.166 | 4.17 | 59.29 |
| 780.166 | 4.15 | 59.06 |
| 800.166 | 4.14 | 58.84 |
| 820.263 | 4.12 | 58.62 |
| 840.348 | 4.11 | 58.41 |
| 860.348 | 4.09 | 58.20 |
| 880.348 | 4.08 | 58.00 |
| 900.348 | 4.06 | 57.81 |
| 920.348 | 4.05 | 57.62 |

Replace these 25 pages of Table 6.2.1-6
with the following 23 pages of revised
Table 6.2.1-6.

Table 6.2.1-6 (20 of 25)

Part B. Reactor Vessel Pressure vs. Time
(Decay heat Period)

| Time (sec) | Reactor Vessel Pressure | |
|------------|-------------------------|--------|
| | kg/cm ² A | psia |
| 600.0 | 4.378 | 62.273 |
| 800.0 | 4.248 | 60.419 |
| 999.0 | 4.149 | 59.012 |
| 1504.4 | 3.981 | 56.621 |
| 1997.8 | 3.876 | 55.135 |
| 4005.0 | 3.66 | 52.063 |
| 6003.6 | 3.544 | 50.41 |
| 8004.3 | 3.471 | 49.373 |
| 9995.6 | 3.42 | 48.648 |
| 15005.7 | 3.332 | 47.387 |
| 20011.7 | 3.252 | 46.247 |
| 40038.3 | 2.976 | 42.328 |
| 59965.1 | 2.751 | 39.127 |
| 79991.5 | 2.594 | 36.896 |
| 100002.3 | 2.347 | 33.387 |
| 150010.0 | 2.067 | 29.403 |
| 200018.4 | 1.936 | 27.533 |
| 400054.2 | 1.719 | 24.455 |
| 600092.3 | 1.621 | 23.059 |
| 800133.9 | 1.566 | 22.273 |
| 1000000.0 | 1.53 | 21.764 |

Replace these 25 pages of Table 6.2.1-6
with the following 23 pages of revised
Table 6.2.1-6.

Table 6.2.1-6 (21 of 25)

Part C. Safety Injection Flow vs. Time (Blowdown Period)

| Time (sec) | Safety Injection Tank Flow | |
|------------|----------------------------|-----------|
| | kg/sec | lbm/sec |
| 0.000 | 0.00 | 0.00 |
| 0.026 | 0.00 | 0.00 |
| 11.513 | 0.00 | 0.00 |
| 12.013 | 0.00 | 0.00 |
| 12.513 | 2,164.62 | 4,772.20 |
| 13.013 | 2,786.54 | 6,143.30 |
| 13.513 | 3,212.60 | 7,082.60 |
| 14.009 | 3,589.48 | 7,913.50 |
| 14.507 | 3,867.31 | 8,526.00 |
| 15.017 | 4,094.01 | 9,025.80 |
| 15.257 | 4,166.59 | 9,185.80 |
| 15.503 | 4,261.98 | 9,396.10 |
| 15.753 | 4,377.01 | 9,649.70 |
| 16.008 | 4,487.23 | 9,892.70 |
| 16.257 | 4,598.95 | 10,139.00 |
| 16.505 | 4,710.99 | 10,386.00 |
| 16.753 | 4,823.48 | 10,634.00 |
| 17.007 | 4,925.99 | 10,860.00 |
| 17.251 | 5,008.54 | 11,042.00 |
| 17.500 | 5,074.31 | 11,187.00 |
| 17.750 | 5,130.56 | 11,311.00 |
| 18.000 | 5,170.47 | 11,399.00 |
| 18.249 | 5,196.33 | 11,456.00 |

Replace these 25 pages of Table 6.2.1-6 with the following 23 pages of revised Table 6.2.1-6.

Table 6.2.1-6 (22 of 25)

Part C. Safety Injection Flow vs. Time (Blowdown Period)

| Time (sec) | Safety Injection Tank Flow | |
|------------|----------------------------|-----------|
| | kg/sec | lbm/sec |
| 18.509 | 5,209.93 | 11,486.00 |
| 18.752 | 5,210.84 | 11,488.00 |
| 19.002 | 5,203.58 | 11,472.00 |
| 19.254 | 5,192.24 | 11,447.00 |
| 19.508 | 5,176.37 | 11,412.00 |
| 19.752 | 5,157.32 | 11,370.00 |

Replace these 25 pages of Table 6.2.1-6 with the following 23 pages of revised Table 6.2.1-6.

Table 6.2.1-6 (23 of 25)

Part C. Safety Injection Flow vs. Time (Reflood and Post-reflood Period)

| Time (sec) | Safety Injection Tank Flow | | Safety Injection Pump Flow | |
|------------|----------------------------|----------|----------------------------|---------|
| | kg/sec | lbm/sec | kg/sec | lbm/sec |
| 19.752 | 2,681.58 | 5,911.91 | 328.55 | 724.33 |
| 19.852 | 2,674.22 | 5,895.68 | 328.55 | 724.33 |
| 20.852 | 2,600.14 | 5,732.36 | 328.48 | 724.18 |
| 21.852 | 2,534.94 | 5,588.61 | 328.48 | 724.19 |
| 22.852 | 2,461.80 | 5,427.38 | 328.26 | 723.70 |
| 23.852 | 2,390.82 | 5,270.89 | 328.01 | 723.15 |
| 24.852 | 2,322.43 | 5,120.10 | 327.75 | 722.58 |
| 25.852 | 2,256.38 | 4,974.49 | 327.49 | 721.99 |
| 26.852 | 2,192.52 | 4,833.71 | 327.22 | 721.39 |
| 27.852 | 2,130.98 | 4,698.04 | 326.95 | 720.81 |
| 28.052 | 2,118.95 | 4,671.50 | 326.90 | 720.69 |
| 28.152 | 2,112.96 | 4,658.30 | 326.87 | 720.64 |
| 30.152 | 2,028.39 | 4,471.86 | 326.84 | 720.56 |
| 32.152 | 1,954.64 | 4,309.26 | 326.86 | 720.60 |
| 34.152 | 1,887.04 | 4,160.23 | 326.87 | 720.63 |
| 36.152 | 1,825.19 | 4,023.89 | 326.89 | 720.68 |
| 38.152 | 1,767.99 | 3,897.78 | 326.91 | 720.73 |
| 40.152 | 1,714.78 | 3,780.47 | 326.93 | 720.77 |
| 42.152 | 1,665.10 | 3,670.93 | 326.95 | 720.81 |
| 44.152 | 1,618.54 | 3,568.28 | 326.97 | 720.85 |
| 46.152 | 1,574.76 | 3,471.78 | 326.99 | 720.89 |
| 48.152 | 1,533.49 | 3,380.78 | 327.01 | 720.93 |
| 49.152 | 1,513.71 | 3,337.18 | 327.01 | 720.95 |
| 49.252 | 1,511.76 | 3,332.89 | 327.01 | 720.95 |
| 49.352 | 684.62 | 1,509.33 | 327.02 | 720.95 |
| 49.452 | 684.26 | 1,508.55 | 327.02 | 720.95 |
| 64.552 | 631.76 | 1,392.80 | 327.13 | 721.21 |
| 79.652 | 587.39 | 1,294.99 | 327.24 | 721.44 |
| 94.752 | 549.31 | 1,211.03 | 327.34 | 721.65 |
| 109.852 | 516.17 | 1,137.97 | 327.43 | 721.86 |
| 124.952 | 487.00 | 1,073.66 | 327.52 | 722.06 |
| 140.052 | 461.07 | 1,016.49 | 327.60 | 722.24 |
| 155.152 | 437.80 | 965.19 | 327.68 | 722.42 |

Replace these 25 pages of Table 6.2.1-6 with the following 23 pages of revised Table 6.2.1-6.

Table 6.2.1-6 (24 of 25)

Part C. Safety Injection Flow vs. Time (Reflood and Post-reflood Period)

| Time (sec) | Safety Injection Tank Flow | | Safety Injection Pump Flow | |
|------------|----------------------------|---------|----------------------------|---------|
| | kg/sec | lbm/sec | kg/sec | lbm/sec |
| 170.252 | 416.76 | 918.81 | 327.76 | 722.60 |
| 185.352 | 397.61 | 876.57 | 327.84 | 722.76 |
| 199.752 | 380.82 | 839.56 | 327.90 | 722.91 |
| 215.252 | 359.30 | 792.11 | 327.91 | 722.91 |
| 230.352 | 339.44 | 748.35 | 327.91 | 722.92 |
| 245.452 | 320.62 | 706.84 | 327.91 | 722.92 |
| 260.552 | 307.17 | 677.21 | 327.96 | 723.03 |
| 275.652 | 288.52 | 636.08 | 327.94 | 723.00 |
| 290.752 | 270.34 | 596.00 | 327.93 | 722.96 |
| 305.852 | 285.85 | 630.20 | 328.24 | 723.64 |
| 320.952 | 273.03 | 601.92 | 328.25 | 723.68 |
| 336.052 | 264.44 | 583.00 | 328.31 | 723.80 |
| 351.152 | 252.48 | 556.64 | 328.33 | 723.84 |
| 360.252 | 248.68 | 548.24 | 328.37 | 723.93 |
| 362.252 | 256.00 | 564.38 | 328.45 | 724.11 |
| 364.252 | 246.05 | 542.46 | 328.37 | 723.95 |
| 366.252 | 246.46 | 543.36 | 328.39 | 723.99 |
| 368.252 | 246.43 | 543.29 | 328.41 | 724.02 |
| 370.252 | 245.72 | 541.73 | 328.42 | 724.04 |
| 371.852 | 243.99 | 537.91 | 328.42 | 724.03 |
| 371.952 | 244.19 | 538.36 | 328.42 | 724.04 |
| 372.052 | 0.00 | 0.00 | 328.42 | 724.05 |
| 372.152 | 0.00 | 0.00 | 328.42 | 724.05 |
| 402.352 | 0.00 | 0.00 | 328.49 | 724.20 |
| 432.552 | 0.00 | 0.00 | 328.51 | 724.24 |
| 462.752 | 0.00 | 0.00 | 328.47 | 724.16 |
| 492.952 | 0.00 | 0.00 | 328.47 | 724.15 |
| 523.152 | 0.00 | 0.00 | 328.45 | 724.10 |
| 553.352 | 0.00 | 0.00 | 328.45 | 724.11 |
| 583.552 | 0.00 | 0.00 | 328.47 | 724.15 |
| 599.852 | 0.00 | 0.00 | 328.47 | 724.16 |
| 599.952 | 0.00 | 0.00 | 328.47 | 724.16 |

Replace these 25 pages of Table 6.2.1-6 with the following 23 pages of revised Table 6.2.1-6.

Table 6.2.1-6 (25 of 25)

Part D. Chronology of Events

| Time (sec) | Event | Values |
|------------|--|--|
| 0.0 | Break occurs | - |
| 3.76 | Containment pressure Hi-Hi setpoint | 1.547kg/cm ² G (22.0 psig) |
| 12.01 | Start safety injection tank (SIT) injection | - |
| 17.71 | First peak containment pressure (Blowdown phase) | 3.123kg/cm ² G (44.42 psig) |
| 19.75 | End of blowdown | - |
| | Start SI pump injection | - |
| 49.35 | SIT flow is turned down to low flow by fluidic device in SIT | - |
| 113.76 | Start containment spray actuation | - |
| 199.75 | End of reflood | - |
| 323.82 | Peak containment temperature | 134.59 °C (274.27 °F) |
| 324.12 | Peak containment pressure | 3.592kg/cm ² G (51.09 psig) |
| 360.25 | End of post reflood | - |
| 372.05 | Safety injection tank empty | - |
| 52,355.4 | Time of depressurization of the containment at 50 % of peak pressure | 1.795kg/cm ² G (25.54 psig) |

Replace these 25 pages of Table 6.2.1-6 with the following 23 pages of revised Table 6.2.1-6.

APR1400 DCD TIER 2

Table 6.2.1-6 (1 of 23)

Insert this page.

Double-Ended Discharge Leg Slot Break – Maximum SIS Flow
(0.9121 m² (9.8175 ft²) Break Area)

Part A. Mass and Energy Release Data (Blowdown Period)

| Time (sec) | Break Mass Flow Rate | | Break Enthalpy | |
|------------|----------------------|------------|----------------|---------|
| | kg/sec | lbm/sec | kcal/kg | Btu/lbm |
| 0.000 | 0.00 | 0.00 | 0.00 | 0.00 |
| 0.026 | 35,570.66 | 78,420.29 | 309.67 | 557.44 |
| 0.051 | 36,255.06 | 79,929.15 | 309.62 | 557.34 |
| 0.102 | 52,155.38 | 114,983.53 | 310.08 | 558.17 |
| 0.150 | 54,241.46 | 119,582.56 | 310.69 | 559.27 |
| 0.205 | 53,118.19 | 117,106.18 | 311.20 | 560.19 |
| 0.251 | 53,000.48 | 116,846.67 | 311.46 | 560.66 |
| 0.303 | 52,555.82 | 115,866.36 | 311.68 | 561.06 |
| 0.355 | 51,903.33 | 114,427.86 | 311.78 | 561.23 |
| 0.455 | 51,283.34 | 113,060.99 | 311.86 | 561.38 |
| 0.548 | 50,839.80 | 112,083.15 | 311.87 | 561.40 |
| 0.655 | 50,335.08 | 110,970.43 | 311.89 | 561.44 |
| 0.751 | 49,799.01 | 109,788.59 | 311.92 | 561.50 |
| 0.850 | 49,295.77 | 108,679.14 | 311.98 | 561.60 |
| 0.952 | 48,985.60 | 107,995.33 | 312.09 | 561.80 |
| 1.256 | 45,974.67 | 101,357.32 | 312.52 | 562.57 |
| 1.500 | 44,806.61 | 98,782.18 | 313.10 | 563.62 |
| 1.749 | 42,469.15 | 93,628.95 | 313.84 | 564.95 |
| 2.001 | 40,547.50 | 89,392.40 | 314.75 | 566.58 |
| 2.253 | 39,075.65 | 86,147.52 | 315.77 | 568.41 |
| 2.513 | 37,917.46 | 83,594.12 | 316.79 | 570.25 |
| 2.753 | 37,135.87 | 81,871.00 | 317.79 | 572.06 |
| 3.013 | 35,641.45 | 78,576.37 | 318.70 | 573.69 |
| 3.253 | 34,354.67 | 75,739.48 | 319.39 | 574.94 |
| 3.513 | 33,446.63 | 73,737.59 | 320.70 | 577.29 |

APR1400 DCD TIER 2

Table 6.2.1-6 (2 of 23)

Insert this page.

Part A. Mass and Energy Release Data
(Blowdown Period)

| Time (sec) | Break Mass Flow Rate | | Break Enthalpy | |
|------------|----------------------|-----------|----------------|----------|
| | kg/sec | lbm/sec | kcal/kg | Btu/lbm |
| 3.753 | 32,136.20 | 70,848.55 | 322.26 | 580.11 |
| 4.013 | 30,679.12 | 67,636.23 | 324.09 | 583.39 |
| 4.513 | 28,504.55 | 62,842.10 | 327.42 | 589.38 |
| 5.013 | 26,227.90 | 57,822.93 | 331.03 | 595.89 |
| 5.513 | 24,545.92 | 54,114.76 | 337.02 | 606.67 |
| 6.013 | 21,825.68 | 48,117.64 | 349.22 | 628.64 |
| 6.513 | 17,987.35 | 39,655.52 | 376.16 | 677.13 |
| 7.013 | 13,886.23 | 30,614.05 | 428.08 | 770.59 |
| 7.505 | 12,225.23 | 26,952.15 | 454.34 | 817.86 |
| 8.014 | 11,663.92 | 25,714.69 | 459.62 | 827.36 |
| 8.513 | 11,152.79 | 24,587.83 | 461.97 | 831.59 |
| 9.013 | 10,759.50 | 23,720.77 | 463.01 | 833.46 |
| 9.513 | 9,894.04 | 21,812.74 | 479.71 | 863.53 |
| 10.013 | 8,931.05 | 19,689.70 | 504.97 | 908.99 |
| 10.513 | 8,006.74 | 17,651.93 | 528.35 | 951.08 |
| 11.013 | 6,975.26 | 15,377.90 | 556.89 | 1,002.46 |
| 11.513 | 5,926.46 | 13,065.67 | 588.71 | 1,059.75 |
| 12.013 | 5,345.95 | 11,785.86 | 593.54 | 1,068.43 |
| 12.513 | 6,618.02 | 14,590.32 | 460.05 | 828.14 |
| 13.013 | 7,205.45 | 15,885.38 | 405.88 | 730.62 |
| 13.513 | 7,216.60 | 15,909.95 | 378.11 | 680.64 |
| 14.009 | 7,049.69 | 15,541.99 | 356.91 | 642.47 |
| 14.507 | 6,840.23 | 15,080.21 | 336.96 | 606.56 |
| 15.017 | 6,604.21 | 14,559.86 | 319.10 | 574.41 |
| 15.257 | 6,493.95 | 14,316.78 | 311.68 | 561.06 |
| 15.503 | 6,334.92 | 13,966.18 | 305.12 | 549.25 |
| 15.753 | 6,086.67 | 13,418.88 | 297.94 | 536.33 |
| 16.008 | 6,015.11 | 13,261.12 | 289.68 | 521.46 |

APR1400 DCD TIER 2

Table 6.2.1-6 (3 of 23)

Insert this page.

**Part A. Mass and Energy Release Data
(Blowdown Period)**

| Time (sec) | Break Mass Flow Rate | | Break Enthalpy | |
|------------|----------------------|-----------|----------------|---------|
| | kg/sec | lbm/sec | kcal/kg | Btu/lbm |
| 16.257 | 5,794.29 | 12,774.28 | 281.39 | 506.53 |
| 16.505 | 5,416.53 | 11,941.46 | 273.92 | 493.08 |
| 16.753 | 4,955.88 | 10,925.90 | 268.62 | 483.55 |
| 17.007 | 4,447.82 | 9,805.81 | 263.22 | 473.82 |
| 17.251 | 3,984.08 | 8,783.44 | 258.14 | 464.68 |
| 17.500 | 3,606.06 | 7,950.04 | 253.32 | 456.00 |
| 17.750 | 3,263.42 | 7,194.64 | 248.40 | 447.14 |
| 18.000 | 3,088.10 | 6,808.13 | 245.86 | 442.57 |
| 18.249 | 1,743.93 | 3,844.73 | 240.28 | 432.53 |
| 18.509 | 1,671.14 | 3,684.24 | 240.44 | 432.82 |
| 18.752 | 1,508.29 | 3,325.24 | 243.71 | 438.70 |
| 19.002 | 1,297.66 | 2,860.86 | 243.27 | 437.91 |
| 19.254 | 1,091.70 | 2,406.81 | 244.26 | 439.70 |
| 19.508 | 882.79 | 1,946.23 | 247.16 | 444.92 |
| 19.752 | 678.35 | 1,495.51 | 254.14 | 457.48 |

Integral Mass and Energy Release at End of Blowdown

| Time (sec) | Integral Mass | | Integral Energy | |
|------------|---------------|------------|-----------------|-------------|
| | kg | lbm | Million kcal | Million Btu |
| 19.752 | 322,456.13 | 710,897.80 | 112.812 | 447.702 |

APR1400 DCD TIER 2

Table 6.2.1-6 (4 of 23)

Part A. Mass and Energy Release Data
(Reflood and Post-reflood Period)

Insert this page.

| Time (sec) | Break Mass Flow Rate | | Break Enthalpy | |
|---------------|----------------------|---------|----------------|----------|
| | kg/sec | lbm/sec | kcal/kg | Btu/lbm |
| 19.75 | 0.00 | 0.00 | 0.00 | 0.00 |
| 19.85 | 51.63 | 113.82 | 727.51 | 1,309.58 |
| 21.85 | 89.85 | 198.09 | 726.94 | 1,308.56 |
| 23.85 | 242.56 | 534.76 | 726.05 | 1,306.96 |
| 25.85 | 344.08 | 758.58 | 725.26 | 1,305.55 |
| 27.85 | 427.92 | 943.40 | 724.43 | 1,304.06 |
| 27.95 | 431.74 | 951.82 | 724.39 | 1,303.97 |
| 28.05 | 435.52 | 960.17 | 724.34 | 1,303.90 |
| 28.15 | 254.78 | 561.70 | 724.31 | 1,303.82 |
| 32.15 | 254.41 | 560.89 | 724.01 | 1,303.29 |
| 36.15 | 251.35 | 554.13 | 723.68 | 1,302.70 |
| 40.15 | 248.10 | 546.98 | 723.34 | 1,302.09 |
| 44.15 | 245.14 | 540.45 | 723.00 | 1,301.47 |
| 49.15 | 241.70 | 532.86 | 722.55 | 1,300.67 |
| 49.25 | 241.64 | 532.72 | 722.53 | 1,300.63 |
| 49.35 | 416.40 | 918.00 | 722.53 | 1,300.63 |
| 49.45 | 416.26 | 917.69 | 722.53 | 1,300.62 |
| 79.45 | 385.18 | 849.17 | 719.52 | 1,295.21 |
| 109.45 | 356.54 | 786.03 | 716.20 | 1,289.23 |
| 139.45 | 328.38 | 723.95 | 712.77 | 1,283.06 |
| 169.45 | 300.39 | 662.24 | 709.37 | 1,276.94 |
| 199.65 | 272.27 | 600.26 | 706.14 | 1,271.13 |
| 199.75 | 272.18 | 600.06 | 706.13 | 1,271.10 |
| 199.85 | 272.09 | 599.86 | 706.11 | 1,271.07 |
| 208.85 | 272.49 | 600.74 | 704.88 | 1,268.85 |
| 217.85 | 272.92 | 601.68 | 703.64 | 1,266.63 |
| 226.85 | 273.49 | 602.94 | 702.34 | 1,264.29 |
| 235.85 | 274.13 | 604.36 | 701.02 | 1,261.91 |

APR1400 DCD TIER 2

Table 6.2.1-6 (5 of 23)

Insert this page.

Part A. Mass and Energy Release Data
(Reflood and Post-reflood Period)

| Time (sec) | Break Mass Flow Rate | | Break Enthalpy | |
|------------|----------------------|---------|----------------|----------|
| | kg/sec | lbm/sec | kcal/kg | Btu/lbm |
| 247.05 | 275.03 | 606.34 | 699.34 | 1,258.88 |
| 247.15 | 275.04 | 606.36 | 699.28 | 1,258.78 |
| 247.25 | 276.03 | 608.55 | 687.42 | 1,237.43 |
| 247.35 | 282.31 | 622.40 | 685.00 | 1,233.07 |
| 247.55 | 277.59 | 611.99 | 685.49 | 1,233.94 |
| 247.75 | 274.71 | 605.64 | 681.38 | 1,226.55 |
| 247.85 | 275.67 | 607.75 | 676.04 | 1,216.94 |
| 247.95 | 281.82 | 621.31 | 676.93 | 1,218.54 |
| 248.15 | 277.49 | 611.77 | 674.26 | 1,213.73 |
| 248.55 | 275.19 | 606.70 | 670.23 | 1,206.49 |
| 251.55 | 250.35 | 551.93 | 653.82 | 1,176.94 |
| 254.55 | 224.96 | 495.96 | 653.82 | 1,176.94 |
| 257.55 | 209.96 | 462.88 | 653.81 | 1,176.93 |
| 260.55 | 200.52 | 442.08 | 653.82 | 1,176.94 |
| 263.55 | 194.31 | 428.39 | 653.81 | 1,176.92 |
| 266.55 | 189.94 | 418.75 | 653.82 | 1,176.94 |
| 269.55 | 186.67 | 411.54 | 653.82 | 1,176.94 |
| 272.55 | 184.08 | 405.84 | 653.82 | 1,176.95 |
| 275.55 | 181.94 | 401.11 | 653.82 | 1,176.94 |
| 278.55 | 180.07 | 396.99 | 653.81 | 1,176.93 |
| 281.55 | 178.36 | 393.22 | 653.82 | 1,176.94 |
| 281.85 | 178.20 | 392.86 | 653.81 | 1,176.93 |
| 281.95 | 178.14 | 392.74 | 653.81 | 1,176.92 |
| 285.25 | 176.72 | 389.60 | 653.82 | 1,176.94 |
| 288.85 | 188.61 | 415.82 | 653.81 | 1,176.92 |
| 292.35 | 264.19 | 582.44 | 653.82 | 1,176.94 |
| 295.85 | 131.97 | 290.94 | 653.82 | 1,176.94 |
| 299.35 | 125.73 | 277.18 | 653.81 | 1,176.92 |

APR1400 DCD TIER 2

Table 6.2.1-6 (6 of 23)

Insert this page.

Part A. Mass and Energy Release Data
(Reflood and Post-reflood Period)

| Time (sec) | Break Mass Flow Rate | | Break Enthalpy | |
|------------|----------------------|---------|----------------|----------|
| | kg/sec | lbm/sec | kcal/kg | Btu/lbm |
| 302.85 | 279.60 | 616.42 | 653.82 | 1,176.94 |
| 306.35 | 118.19 | 260.57 | 653.82 | 1,176.94 |
| 309.85 | 113.51 | 250.25 | 653.80 | 1,176.91 |
| 316.85 | 106.51 | 234.82 | 653.80 | 1,176.91 |
| 323.85 | 182.26 | 401.82 | 653.81 | 1,176.93 |
| 327.35 | 127.56 | 281.22 | 653.83 | 1,176.95 |
| 330.85 | 167.85 | 370.05 | 653.82 | 1,176.94 |
| 334.35 | 91.46 | 201.63 | 653.80 | 1,176.91 |
| 337.85 | 88.43 | 194.95 | 653.81 | 1,176.92 |
| 341.35 | 92.06 | 202.96 | 653.80 | 1,176.91 |
| 344.85 | 83.38 | 183.83 | 653.83 | 1,176.96 |
| 348.35 | 134.97 | 297.57 | 653.82 | 1,176.94 |
| 351.85 | 69.91 | 154.13 | 653.82 | 1,176.94 |
| 358.85 | 104.80 | 231.05 | 653.81 | 1,176.92 |
| 361.05 | 61.57 | 135.73 | 653.84 | 1,176.97 |
| 361.15 | 60.94 | 134.36 | 653.80 | 1,176.91 |

Integral Mass and Energy Release at the End of Reflood and Post-reflood

| Time (sec) | Integral Mass | | Integral Energy | |
|------------|---------------|------------|-----------------|-------------|
| | kg | lbm | Million kcal | Million Btu |
| 199.75 | 58,854.21 | 129,752.00 | 42.147 | 167.264 |
| 361.15 | 89,721.91 | 197,804.00 | 62.976 | 249.926 |

APR1400 DCD TIER 2

Table 6.2.1-6 (7 of 23)

Insert this page.

Part A: Spillage Release Data (Reactor Vessel Side)
(Reflood and Post-Reflood Period)

| Time (sec) | Break Mass Flow Rate | | Break Enthalpy | |
|---------------|----------------------|----------|----------------|---------|
| | kg/sec | lbm/sec | kcal/kg | Btu/lbm |
| 19.75 | 0.00 | 0.00 | 0.00 | 0.00 |
| 19.85 | 0.00 | 0.00 | 0.00 | 0.00 |
| 28.05 | 0.00 | 0.00 | 0.00 | 0.00 |
| 28.15 | 472.02 | 1,040.63 | 313.51 | 564.35 |
| 32.15 | 1,885.03 | 4,155.81 | 115.83 | 208.51 |
| 36.15 | 1,755.25 | 3,869.69 | 119.87 | 215.77 |
| 40.15 | 1,651.70 | 3,641.39 | 123.31 | 221.97 |
| 44.15 | 1,561.18 | 3,441.83 | 126.65 | 227.99 |
| 49.15 | 1,462.64 | 3,224.58 | 130.68 | 235.24 |
| 49.25 | 1,460.81 | 3,220.55 | 130.76 | 235.38 |
| 49.35 | 458.93 | 1,011.78 | 50.59 | 91.07 |
| 49.45 | 458.62 | 1,011.10 | 50.60 | 91.08 |
| 79.45 | 405.45 | 893.86 | 51.04 | 91.88 |
| 109.45 | 372.72 | 821.71 | 51.40 | 92.53 |
| 139.45 | 355.12 | 782.92 | 51.74 | 93.15 |
| 169.45 | 348.04 | 767.29 | 52.09 | 93.77 |
| 199.65 | 348.45 | 768.20 | 52.45 | 94.42 |
| 199.75 | 348.46 | 768.22 | 52.46 | 94.42 |
| 199.85 | 436.62 | 962.58 | 52.46 | 94.43 |
| 208.85 | 422.90 | 932.33 | 52.58 | 94.64 |
| 217.85 | 410.29 | 904.53 | 52.70 | 94.86 |
| 226.85 | 397.92 | 877.26 | 52.82 | 95.09 |
| 235.85 | 385.85 | 850.65 | 52.95 | 95.32 |
| 247.05 | 371.20 | 818.35 | 53.12 | 95.61 |
| 247.15 | 371.07 | 818.07 | 53.12 | 95.62 |
| 247.25 | 365.02 | 804.74 | 53.12 | 95.62 |
| 247.35 | 330.49 | 728.62 | 53.12 | 95.63 |
| 247.55 | 354.12 | 780.71 | 53.12 | 95.62 |

APR1400 DCD TIER 2

Table 6.2.1-6 (8 of 23)

Insert this page.

Part A: Spillage Release Data (Reactor Vessel Side)
(Reflood and Post-Reflood Period)

| Time (sec) | Break Mass Flow Rate | | Break Enthalpy | |
|---------------|----------------------|---------|----------------|---------|
| | kg/sec | lbm/sec | kcal/kg | Btu/lbm |
| 247.75 | 343.98 | 758.36 | 53.12 | 95.63 |
| 247.85 | 327.60 | 722.23 | 53.13 | 95.63 |
| 247.95 | 331.23 | 730.25 | 53.13 | 95.64 |
| 248.15 | 337.66 | 744.42 | 53.13 | 95.64 |
| 248.55 | 341.87 | 753.69 | 53.13 | 95.64 |
| 251.55 | 298.11 | 657.23 | 53.15 | 95.68 |
| 254.55 | 240.41 | 530.01 | 53.20 | 95.77 |
| 257.55 | 194.40 | 428.59 | 53.26 | 95.87 |
| 260.55 | 158.35 | 349.11 | 53.31 | 95.97 |
| 263.55 | 129.76 | 286.08 | 53.37 | 96.07 |
| 266.55 | 105.70 | 233.02 | 53.43 | 96.18 |
| 269.55 | 84.17 | 185.57 | 53.50 | 96.30 |
| 272.55 | 63.91 | 140.89 | 53.56 | 96.42 |
| 275.55 | 44.03 | 97.06 | 53.63 | 96.54 |
| 278.55 | 23.78 | 52.43 | 53.71 | 96.68 |
| 281.55 | 2.45 | 5.41 | 53.80 | 96.84 |
| 281.85 | 0.24 | 0.52 | 53.31 | 95.96 |
| 281.95 | 0.00 | 0.00 | 0.00 | 0.00 |
| 361.05 | 0.00 | 0.00 | 0.00 | 0.00 |
| 361.15 | 0.00 | 0.00 | 0.00 | 0.00 |

Integral Mass and Energy (Reactor Vessel Side Spillage) at EOR and EOPR

| Time (sec) | Integral Mass | | Integral Energy | |
|---------------|---------------|------------|-----------------|-------------|
| | kg | lbm | Million kcal | Million Btu |
| 199.75 | 92,620.36 | 204,194.00 | 7.297 | 28.958 |
| 361.15 | 116,739.56 | 257,368.00 | 8.572 | 34.019 |

APR1400 DCD TIER 2

Table 6.2.1-6 (9 of 23)

Insert this page.

Double-Ended Discharge Leg Slot Break – Maximum SIS Flow

Part A: Spillage Release Data (Steam Generator Side)
(Reflood and Post-Reflood Period)

| Time (sec) | Break Mass Flow Rate | | Break Enthalpy | |
|---------------|----------------------|----------|----------------|---------|
| | kg/sec | lbm/sec | kcal/kg | Btu/lbm |
| 19.75 | 0.00 | 0.00 | 0.00 | 0.00 |
| 19.85 | 0.00 | 0.00 | 0.00 | 0.00 |
| 247.25 | 0.00 | 0.00 | 0.00 | 0.00 |
| 247.35 | 0.27 | 0.60 | 143.14 | 257.67 |
| 247.55 | 6.84 | 15.08 | 144.35 | 259.85 |
| 247.75 | 14.54 | 32.05 | 144.32 | 259.80 |
| 247.85 | 18.17 | 40.05 | 144.33 | 259.81 |
| 247.95 | 15.25 | 33.62 | 144.33 | 259.80 |
| 248.15 | 19.28 | 42.50 | 144.33 | 259.81 |
| 248.55 | 24.63 | 54.30 | 144.33 | 259.81 |
| 251.55 | 87.07 | 191.95 | 144.33 | 259.81 |
| 254.55 | 166.29 | 366.61 | 144.33 | 259.80 |
| 257.55 | 225.39 | 496.90 | 144.33 | 259.81 |
| 260.55 | 269.33 | 593.78 | 144.33 | 259.81 |
| 263.55 | 302.35 | 666.57 | 144.33 | 259.81 |
| 266.55 | 328.54 | 724.31 | 144.33 | 259.81 |
| 269.55 | 350.67 | 773.11 | 144.33 | 259.81 |
| 272.55 | 370.56 | 816.95 | 144.33 | 259.81 |
| 275.55 | 389.38 | 858.43 | 144.33 | 259.81 |
| 278.55 | 408.08 | 899.66 | 144.33 | 259.81 |
| 281.55 | 427.53 | 942.55 | 144.33 | 259.81 |
| 281.85 | 429.55 | 947.00 | 144.33 | 259.81 |
| 281.95 | 430.23 | 948.49 | 144.33 | 259.81 |
| 285.25 | 446.99 | 985.44 | 144.33 | 259.81 |
| 288.85 | 335.87 | 740.46 | 144.33 | 259.81 |
| 292.35 | 664.77 | 1,465.57 | 144.33 | 259.81 |
| 295.85 | 716.25 | 1,579.08 | 144.33 | 259.81 |
| 299.35 | 253.29 | 558.42 | 144.33 | 259.81 |

APR1400 DCD TIER 2

Table 6.2.1-6 (10 of 23)

Insert this page.

Double-Ended Discharge Leg Slot Break – Maximum SIS Flow

Part A: Spillage Release Data (Steam Generator Side)
(Reflood and Post-Reflood Period)

| Time (sec) | Break Mass Flow Rate | | Break Enthalpy | |
|---------------|----------------------|----------|----------------|---------|
| | kg/sec | lbm/sec | kcal/kg | Btu/lbm |
| 302.85 | 601.89 | 1,326.94 | 144.33 | 259.81 |
| 306.35 | 689.89 | 1,520.96 | 144.33 | 259.81 |
| 309.85 | 268.46 | 591.85 | 144.33 | 259.81 |
| 316.85 | 676.02 | 1,490.38 | 144.33 | 259.81 |
| 323.85 | 661.56 | 1,458.49 | 144.33 | 259.81 |
| 327.35 | 491.92 | 1,084.50 | 144.33 | 259.81 |
| 330.85 | 703.73 | 1,551.46 | 144.33 | 259.81 |
| 334.35 | 721.57 | 1,590.79 | 144.33 | 259.81 |
| 337.85 | 822.95 | 1,814.30 | 144.33 | 259.81 |
| 341.35 | 270.22 | 595.73 | 144.33 | 259.81 |
| 344.85 | 979.30 | 2,159.00 | 144.33 | 259.81 |
| 348.35 | 175.60 | 387.14 | 144.33 | 259.81 |
| 351.85 | 894.29 | 1,971.58 | 144.33 | 259.81 |
| 358.85 | 79.43 | 175.12 | 144.33 | 259.82 |
| 361.05 | 778.31 | 1,715.89 | 144.33 | 259.81 |
| 361.15 | 762.02 | 1,679.97 | 144.33 | 259.81 |

Integral Mass and Energy (Steam Generator Side Spillage) at EOR and EOPR

| Time (sec) | Integral Mass | | Integral Energy | |
|---------------|---------------|------------|-----------------|-------------|
| | kg | lbm | Million kcal | Million Btu |
| 199.75 | 0.00 | 0.00 | 0.000 | 0.000 |
| 361.15 | 50,774.41 | 111,939.00 | 7.328 | 29.083 |

APR1400 DCD TIER 2

Table 6.2.1-6 (11 of 23)

Insert this page.

Part A. Mass and Energy (Steam) Release Data (Decay heat Period)

| Time (sec) | Mass Flow Rate | | Break Enthalpy | |
|------------|----------------|---------|----------------|---------|
| | kg/sec | lbm/sec | kcal/kg | Btu/lbm |
| 599.9 | 49.19 | 108.44 | 654.62 | 1178.31 |
| 800.0 | 47.54 | 104.8 | 654.27 | 1177.68 |
| 999.0 | 45.96 | 101.33 | 653.99 | 1177.18 |
| 1504.3 | 43.37 | 95.62 | 653.48 | 1176.26 |
| 1998.2 | 42.11 | 92.85 | 653.14 | 1175.65 |
| 4004.1 | 35.98 | 79.32 | 652.44 | 1174.39 |
| 6001.5 | 31.31 | 69.02 | 652.1 | 1173.78 |
| 8002.0 | 28.47 | 62.76 | 651.92 | 1173.46 |
| 9990.5 | 27.25 | 60.07 | 651.81 | 1173.27 |
| 15005.7 | 24.71 | 54.47 | 651.64 | 1172.96 |
| 20010.7 | 22.83 | 50.34 | 651.43 | 1172.58 |
| 40037.9 | 18.79 | 41.43 | 650.31 | 1170.57 |
| 59965.8 | 16.59 | 36.58 | 649.13 | 1168.44 |
| 79995.5 | 15.22 | 33.56 | 648.21 | 1166.78 |
| 100002.2 | 14.42 | 31.79 | 647.58 | 1165.64 |
| 150010.3 | 12.82 | 28.27 | 646.58 | 1163.85 |
| 200017.3 | 11.76 | 25.92 | 645.94 | 1162.68 |
| 400052.4 | 9.22 | 20.32 | 644.69 | 1160.44 |
| 600091.6 | 7.87 | 17.36 | 644.05 | 1159.29 |
| 800140.2 | 7.0 | 15.43 | 643.67 | 1158.6 |
| 1000000.0 | 6.39 | 14.08 | 643.41 | 1158.14 |

Integral Mass and Energy Release (Steam) at 24 hours and End of Analysis

| Time (sec) | Integral Mass | | Integral Energy | |
|------------|---------------|------------|-----------------|-------------|
| | kg | lbm | Million kcal | Million Btu |
| 85,003 | 1,836,057 | 4,047,812 | 1,199.868 | 4,345.004 |
| 1,000,000 | 9,978,494 | 21,998,813 | 6,453.868 | 25,611.019 |

APR1400 DCD TIER 2

Table 6.2.1-6 (12 of 23)

Insert this page.

Part A. Mass and Energy (Spillage) Release Data (Decay heat Period)

| Time (sec) | Mass Flow Rate | | Break Enthalpy | |
|------------|----------------|---------|----------------|---------|
| | kg/sec | lbm/sec | kcal/kg | Btu/lbm |
| 599.9 | 156.7 | 345.47 | 70.16 | 126.3 |
| 800.0 | 167.5 | 369.28 | 69.41 | 124.94 |
| 999.0 | 177.63 | 391.61 | 71.42 | 128.55 |
| 1504.3 | 195.51 | 431.02 | 76.83 | 138.3 |
| 1998.2 | 204.27 | 450.34 | 82.1 | 147.78 |
| 4004.1 | 212.04 | 467.47 | 98.59 | 177.46 |
| 6001.5 | 214.08 | 471.97 | 108.1 | 194.58 |
| 8002.0 | 215.15 | 474.33 | 113.87 | 204.97 |
| 9990.5 | 215.95 | 476.08 | 117.44 | 211.39 |
| 15005.7 | 217.53 | 479.57 | 121.59 | 218.85 |
| 20010.7 | 218.96 | 482.73 | 122.55 | 220.59 |
| 40037.9 | 223.5 | 492.74 | 118.78 | 213.8 |
| 59965.8 | 226.84 | 500.09 | 112.68 | 202.83 |
| 79995.5 | 229.18 | 505.26 | 107.43 | 193.37 |
| 100002.2 | 230.71 | 508.63 | 103.49 | 186.28 |
| 150010.3 | 233.32 | 514.37 | 97.33 | 175.2 |
| 200017.3 | 235.05 | 518.2 | 93.13 | 167.63 |
| 400052.4 | 238.68 | 526.19 | 84.43 | 151.97 |
| 600091.6 | 240.58 | 530.38 | 79.52 | 143.13 |
| 800140.2 | 241.76 | 532.99 | 76.43 | 137.58 |
| 1000000.0 | 242.57 | 534.77 | 74.29 | 133.73 |

Integral Mass and Energy Release(Spillage) at 24 hours and End of Analysis

| Time (sec) | Integral Mass | | Integral Energy | |
|------------|---------------|-------------|-----------------|-------------|
| | kg | lbm | Million kcal | Million Btu |
| 85,003 | 18,976,330 | 41,835,646 | 2,162.840 | 8,582.842 |
| 1,000,000 | 237,735,477 | 524,117,011 | 20,332.246 | 80,684.869 |

APR1400 DCD TIER 2

Table 6.2.1-6 (13 of 23)

Insert this page.

Part B. Reactor Vessel Pressure vs. Time
(Blowdown Period)

| Time (sec) | Reactor Vessel Pressure | |
|------------|-------------------------|----------|
| | kg/cm ² A | psia |
| 0.000 | 167.360 | 2,380.40 |
| 0.026 | 147.360 | 2,096.00 |
| 0.051 | 131.970 | 1,877.00 |
| 0.102 | 124.440 | 1,770.00 |
| 0.150 | 126.550 | 1,799.90 |
| 0.205 | 123.280 | 1,753.50 |
| 0.251 | 124.390 | 1,769.20 |
| 0.303 | 122.240 | 1,738.60 |
| 0.355 | 121.610 | 1,729.70 |
| 0.455 | 119.600 | 1,701.10 |
| 0.548 | 118.700 | 1,688.30 |
| 0.655 | 117.750 | 1,674.80 |
| 0.751 | 116.290 | 1,654.00 |
| 0.850 | 115.400 | 1,641.40 |
| 0.952 | 114.580 | 1,629.70 |
| 1.256 | 107.300 | 1,526.10 |
| 1.500 | 106.660 | 1,517.00 |
| 1.749 | 101.420 | 1,442.50 |
| 2.001 | 99.780 | 1,419.20 |
| 2.253 | 96.330 | 1,370.10 |
| 2.513 | 95.120 | 1,352.90 |
| 2.753 | 93.450 | 1,329.20 |
| 3.013 | 91.670 | 1,303.90 |

APR1400 DCD TIER 2

Table 6.2.1-6 (14 of 23)

Insert this page.

Part B. Reactor Vessel Pressure vs. Time
(Blowdown Period)

| Time (sec) | Reactor Vessel Pressure | |
|------------|-------------------------|----------|
| | kg/cm ² A | psia |
| 3.253 | 90.120 | 1,281.80 |
| 3.513 | 88.880 | 1,264.20 |
| 3.753 | 87.480 | 1,244.20 |
| 4.013 | 86.210 | 1,226.20 |
| 4.513 | 84.160 | 1,197.00 |
| 5.013 | 82.180 | 1,168.90 |
| 5.513 | 80.350 | 1,142.80 |
| 6.013 | 78.810 | 1,120.90 |
| 6.513 | 76.680 | 1,090.70 |
| 7.013 | 74.800 | 1,063.90 |
| 7.505 | 71.970 | 1,023.70 |
| 8.014 | 70.510 | 1,002.90 |
| 8.513 | 68.090 | 968.43 |
| 9.013 | 66.110 | 940.35 |
| 9.513 | 64.050 | 910.98 |
| 10.013 | 61.900 | 880.49 |
| 10.513 | 58.870 | 837.39 |
| 11.013 | 55.490 | 789.25 |
| 11.513 | 50.790 | 722.45 |
| 12.013 | 46.480 | 661.04 |
| 12.513 | 41.990 | 597.21 |
| 13.013 | 38.250 | 544.01 |
| 13.513 | 34.690 | 493.40 |

APR1400 DCD TIER 2

Table 6.2.1-6 (15 of 23)

Insert this page.

Part B. Reactor Vessel Pressure vs. Time
(Blowdown Period)

| Time (sec) | Reactor Vessel Pressure | |
|------------|-------------------------|--------|
| | kg/cm ² A | psia |
| 14.009 | 31.030 | 441.40 |
| 14.507 | 27.720 | 394.32 |
| 15.017 | 24.580 | 349.64 |
| 15.257 | 23.270 | 330.97 |
| 15.503 | 21.850 | 310.76 |
| 15.753 | 20.290 | 288.64 |
| 16.008 | 18.750 | 266.73 |
| 16.257 | 17.220 | 244.90 |
| 16.505 | 15.700 | 223.25 |
| 16.753 | 14.160 | 201.46 |
| 17.007 | 12.680 | 180.32 |
| 17.251 | 11.370 | 161.79 |
| 17.500 | 10.200 | 145.11 |
| 17.750 | 9.100 | 129.40 |
| 18.000 | 8.150 | 115.88 |
| 18.249 | 7.340 | 104.41 |
| 18.509 | 6.610 | 94.06 |
| 18.752 | 6.050 | 86.09 |
| 19.002 | 5.560 | 79.01 |
| 19.254 | 5.120 | 72.85 |
| 19.508 | 4.730 | 67.23 |
| 19.752 | 4.410 | 62.76 |

APR1400 DCD TIER 2

Table 6.2.1-6 (16 of 23)

Insert this page.

Part B. Reactor Vessel Pressure vs. Time
(Reflood and Post-reflood Period)

| Time (sec) | Reactor Vessel Pressure | |
|------------|-------------------------|--------|
| | kg/cm ² A | psia |
| 19.75 | 4.080 | 58.000 |
| 19.85 | 4.090 | 58.170 |
| 21.85 | 4.140 | 58.820 |
| 23.85 | 4.480 | 63.720 |
| 25.85 | 4.850 | 69.030 |
| 27.85 | 5.230 | 74.370 |
| 27.95 | 5.250 | 74.630 |
| 28.05 | 5.270 | 74.890 |
| 28.15 | 5.280 | 75.150 |
| 32.15 | 5.280 | 75.060 |
| 36.15 | 5.250 | 74.670 |
| 40.15 | 5.220 | 74.270 |
| 44.15 | 5.200 | 73.900 |
| 49.15 | 5.170 | 73.470 |
| 49.25 | 5.160 | 73.460 |
| 49.35 | 5.160 | 73.450 |
| 49.45 | 5.160 | 73.440 |
| 79.45 | 5.010 | 71.250 |
| 109.45 | 4.880 | 69.350 |
| 139.45 | 4.750 | 67.610 |
| 169.45 | 4.640 | 66.020 |
| 199.65 | 4.540 | 64.570 |
| 199.75 | 4.540 | 64.570 |
| 199.85 | 4.540 | 64.560 |
| 208.85 | 4.540 | 64.550 |
| 217.85 | 4.540 | 64.530 |
| 226.85 | 4.540 | 64.530 |
| 235.85 | 4.540 | 64.520 |

APR1400 DCD TIER 2

Table 6.2.1-6 (17 of 23)

Insert this page.

Part B. Reactor Vessel Pressure vs. Time
(Reflood and Post-reflood Period)

| Time (sec) | Reactor Vessel Pressure | |
|------------|-------------------------|--------|
| | kg/cm ² A | psia |
| 247.05 | 4.540 | 64.510 |
| 247.15 | 4.540 | 64.510 |
| 247.25 | 4.540 | 64.550 |
| 247.35 | 4.530 | 64.490 |
| 247.55 | 4.530 | 64.480 |
| 247.75 | 4.530 | 64.490 |
| 247.85 | 4.540 | 64.510 |
| 247.95 | 4.530 | 64.410 |
| 248.15 | 4.530 | 64.380 |
| 248.55 | 4.520 | 64.270 |
| 251.55 | 4.490 | 63.830 |
| 254.55 | 4.490 | 63.890 |
| 257.55 | 4.500 | 63.940 |
| 260.55 | 4.500 | 63.980 |
| 263.55 | 4.500 | 64.010 |
| 266.55 | 4.500 | 64.030 |
| 269.55 | 4.500 | 64.060 |
| 272.55 | 4.510 | 64.100 |
| 275.55 | 4.510 | 64.140 |
| 278.55 | 4.510 | 64.190 |
| 281.55 | 4.520 | 64.240 |
| 281.85 | 4.520 | 64.250 |
| 281.95 | 4.520 | 64.250 |
| 285.25 | 4.520 | 64.290 |
| 288.85 | 4.470 | 63.520 |
| 292.35 | 4.460 | 63.480 |
| 295.85 | 4.550 | 64.720 |
| 299.35 | 4.390 | 62.480 |

APR1400 DCD TIER 2

Table 6.2.1-6 (18 of 23)

Insert this page.

Part B. Reactor Vessel Pressure vs. Time
(Reflood and Post-reflood Period)

| Time (sec) | Reactor Vessel Pressure | |
|------------|-------------------------|--------|
| | kg/cm ² A | psia |
| 302.85 | 4.310 | 61.290 |
| 306.35 | 4.460 | 63.450 |
| 309.85 | 4.340 | 61.750 |
| 316.85 | 4.400 | 62.640 |
| 323.85 | 4.270 | 60.710 |
| 327.35 | 4.290 | 61.040 |
| 330.85 | 4.260 | 60.640 |
| 334.35 | 4.360 | 62.000 |
| 337.85 | 4.320 | 61.390 |
| 341.35 | 4.250 | 60.520 |
| 344.85 | 4.310 | 61.270 |
| 348.35 | 4.200 | 59.740 |
| 351.85 | 4.250 | 60.440 |
| 358.85 | 4.150 | 59.040 |
| 361.05 | 4.210 | 59.880 |
| 361.15 | 4.210 | 59.830 |

APR1400 DCD TIER 2

Table 6.2.1-6 (19 of 23)

Part B. Reactor Vessel Pressure vs. Time
(Decay heat Period)

Insert this page.

| Time (sec) | Reactor Vessel Pressure | |
|------------|-------------------------|--------|
| | kg/cm ² A | psia |
| 599.9 | 4.379 | 62.286 |
| 800.0 | 4.238 | 60.277 |
| 999.0 | 4.128 | 58.716 |
| 1504.3 | 3.937 | 55.991 |
| 1998.2 | 3.816 | 54.273 |
| 4004.1 | 3.576 | 50.857 |
| 6001.5 | 3.465 | 49.282 |
| 8002.0 | 3.408 | 48.471 |
| 9990.5 | 3.375 | 47.997 |
| 15005.7 | 3.321 | 47.238 |
| 20010.7 | 3.257 | 46.33 |
| 40037.9 | 2.939 | 41.798 |
| 59965.8 | 2.635 | 37.483 |
| 79995.5 | 2.422 | 34.445 |
| 100002.2 | 2.284 | 32.481 |
| 150010.3 | 2.083 | 29.631 |
| 200017.3 | 1.963 | 27.914 |
| 400052.4 | 1.748 | 24.86 |
| 600091.6 | 1.647 | 23.425 |
| 800140.2 | 1.589 | 22.608 |
| 1000000.0 | 1.552 | 22.075 |

APR1400 DCD TIER 2

Table 6.2.1-6 (20 of 23)

Insert this page.

Part C. Safety Injection Flow vs. Time (Blowdown Period)

| Time (sec) | Safety Injection Tank Flow | |
|------------|----------------------------|-----------|
| | kg/sec | lbm/sec |
| 0.000 | 0.00 | 0.00 |
| 0.026 | 0.00 | 0.00 |
| 11.513 | 0.00 | 0.00 |
| 12.013 | 0.00 | 0.00 |
| 12.513 | 2,164.62 | 4,772.20 |
| 13.013 | 2,786.54 | 6,143.30 |
| 13.513 | 3,212.60 | 7,082.60 |
| 14.009 | 3,589.48 | 7,913.50 |
| 14.507 | 3,867.31 | 8,526.00 |
| 15.017 | 4,094.01 | 9,025.80 |
| 15.257 | 4,166.59 | 9,185.80 |
| 15.503 | 4,261.98 | 9,396.10 |
| 15.753 | 4,377.01 | 9,649.70 |
| 16.008 | 4,487.23 | 9,892.70 |
| 16.257 | 4,598.95 | 10,139.00 |
| 16.505 | 4,710.99 | 10,386.00 |
| 16.753 | 4,823.48 | 10,634.00 |
| 17.007 | 4,925.99 | 10,860.00 |
| 17.251 | 5,008.54 | 11,042.00 |
| 17.500 | 5,074.31 | 11,187.00 |
| 17.750 | 5,130.56 | 11,311.00 |
| 18.000 | 5,170.47 | 11,399.00 |
| 18.249 | 5,196.33 | 11,456.00 |
| 18.509 | 5,209.93 | 11,486.00 |
| 18.752 | 5,210.84 | 11,488.00 |
| 19.002 | 5,203.58 | 11,472.00 |
| 19.254 | 5,192.24 | 11,447.00 |
| 19.508 | 5,176.37 | 11,412.00 |
| 19.752 | 5,157.32 | 11,370.00 |

APR1400 DCD TIER 2

Table 6.2.1-6 (21 of 23)

Insert this page.

Part C. Safety Injection Flow vs. Time (Reflood and Post-reflood Period)

| Time (sec) | Safety Injection Tank Flow | | Safety Injection Pump Flow | |
|------------|----------------------------|----------|----------------------------|---------|
| | kg/sec | lbm/sec | kg/sec | lbm/sec |
| 19.752 | 2,681.58 | 5,911.91 | 328.55 | 724.33 |
| 19.852 | 2,674.22 | 5,895.68 | 328.55 | 724.33 |
| 20.852 | 2,600.14 | 5,732.36 | 328.48 | 724.18 |
| 21.852 | 2,534.94 | 5,588.61 | 328.48 | 724.19 |
| 22.852 | 2,461.80 | 5,427.38 | 328.26 | 723.70 |
| 23.852 | 2,390.82 | 5,270.89 | 328.01 | 723.15 |
| 24.852 | 2,322.43 | 5,120.10 | 327.75 | 722.58 |
| 25.852 | 2,256.38 | 4,974.49 | 327.49 | 721.99 |
| 26.852 | 2,192.52 | 4,833.71 | 327.22 | 721.39 |
| 28.052 | 2,118.95 | 4,671.50 | 326.90 | 720.69 |
| 28.152 | 2,112.96 | 4,658.30 | 326.87 | 720.64 |
| 32.152 | 1,954.65 | 4,309.28 | 326.86 | 720.60 |
| 36.152 | 1,825.27 | 4,024.06 | 326.89 | 720.68 |
| 40.152 | 1,714.85 | 3,780.62 | 326.94 | 720.77 |
| 44.152 | 1,618.59 | 3,568.41 | 326.97 | 720.85 |
| 46.152 | 1,574.82 | 3,471.89 | 326.99 | 720.89 |
| 48.152 | 1,533.54 | 3,380.89 | 327.01 | 720.93 |
| 49.152 | 1,513.76 | 3,337.28 | 327.01 | 720.95 |
| 49.252 | 1,511.81 | 3,332.99 | 327.02 | 720.95 |
| 49.352 | 684.64 | 1,509.38 | 327.02 | 720.95 |
| 49.452 | 684.29 | 1,508.60 | 327.02 | 720.96 |
| 64.452 | 632.10 | 1,393.54 | 327.13 | 721.21 |
| 79.452 | 587.96 | 1,296.23 | 327.24 | 721.44 |
| 94.452 | 550.04 | 1,212.63 | 327.33 | 721.65 |
| 109.452 | 517.01 | 1,139.82 | 327.43 | 721.86 |
| 124.452 | 487.93 | 1,075.70 | 327.52 | 722.05 |
| 139.452 | 462.06 | 1,018.67 | 327.60 | 722.24 |
| 154.452 | 438.84 | 967.48 | 327.68 | 722.42 |

APR1400 DCD TIER 2

Table 6.2.1-6 (22 of 23)

Insert this page.

Part C. Safety Injection Flow vs. Time (Reflood and Post-reflood Period)

| Time (sec) | Safety Injection Tank Flow | | Safety Injection Pump Flow | |
|------------|----------------------------|---------|----------------------------|---------|
| | kg/sec | lbm/sec | kg/sec | lbm/sec |
| 169.452 | 417.84 | 921.18 | 327.76 | 722.59 |
| 184.452 | 398.71 | 879.01 | 327.83 | 722.75 |
| 199.752 | 380.82 | 839.58 | 327.90 | 722.91 |
| 214.752 | 359.98 | 793.62 | 327.91 | 722.92 |
| 229.752 | 340.22 | 750.07 | 327.91 | 722.92 |
| 244.752 | 321.48 | 708.74 | 327.91 | 722.92 |
| 259.752 | 308.27 | 679.63 | 327.96 | 723.04 |
| 274.752 | 289.79 | 638.88 | 327.95 | 723.00 |
| 289.752 | 274.57 | 605.33 | 327.96 | 723.03 |
| 304.752 | 286.79 | 632.26 | 328.23 | 723.64 |
| 319.752 | 276.38 | 609.32 | 328.28 | 723.73 |
| 334.752 | 261.16 | 575.76 | 328.27 | 723.71 |
| 349.752 | 255.90 | 564.17 | 328.35 | 723.88 |
| 361.152 | 247.85 | 546.42 | 328.37 | 723.93 |
| 365.152 | 243.88 | 537.67 | 328.36 | 723.92 |
| 369.152 | 251.53 | 554.53 | 328.46 | 724.14 |
| 371.852 | 243.62 | 537.08 | 328.41 | 724.03 |
| 371.952 | 244.35 | 538.70 | 328.42 | 724.04 |
| 372.052 | 0.00 | 0.00 | 328.44 | 724.09 |
| 372.152 | 0.00 | 0.00 | 328.46 | 724.13 |
| 461.952 | 0.00 | 0.00 | 328.49 | 724.21 |
| 551.752 | 0.00 | 0.00 | 328.45 | 724.11 |
| 596.652 | 0.00 | 0.00 | 328.47 | 724.15 |
| 599.952 | 0.00 | 0.00 | 328.47 | 724.15 |

APR1400 DCD TIER 2

Table 6.2.1-6 (23 of 23)

Insert this page.

Part D. Chronology of Events

| Time (sec) | Event | Values |
|------------|--|---|
| 0.0 | Break occurs | — |
| 3.73 | Containment pressure Hi-Hi setpoint | 1.547kgf/cm ² g (22.0psig) |
| 12.01 | Start safety injection tank (SIT) injection | — |
| 16.81 | First peak containment pressure (Blowdown phase) | 3.106kgf/cm ² g (44.18psig) |
| 19.75 | End of blowdown | — |
| | Start SI pump injection | — |
| 49.35 | SIT flow is turned down to low flow by fluidic device in SIT | — |
| 113.73 | Start containment spray actuation | — |
| 199.75 | End of reflood | — |
| 325.73 | Peak containment temperature | 134.96°C (274.93°F) |
| 325.73 | Peak containment pressure | 3.600kgf/cm ² g (51.21psig) |
| 361.15 | End of post-reflood | — |
| 372.05 | Safety injection tank empty | — |
| 46,346.5 | Time of depressurization of the containment at 50 % of peak pressure | 1.799kgf/cm ² g (25.59psig) |

Table 6.2.1-7 (1 of 23)

Double-Ended Discharge Leg Slot Break – Minimum SIS Flow
(0.9121 m² (9.8175 ft²) Break Area)

Part A. Mass and Energy Release Data
 (Blowdown Period)

| Time (sec) | Break Mass Flow Rate | | Break Enthalpy | |
|------------|----------------------|------------|----------------|---------|
| | kg/sec | lbm/sec | kcal/kg | Btu/lbm |
| 0.000 | 0.00 | 0.00 | 0.00 | 0.00 |
| 0.026 | 35,570.66 | 78,420.29 | 309.67 | 557.44 |
| 0.051 | 36,255.06 | 79,929.15 | 309.62 | 557.34 |
| 0.102 | 52,155.38 | 114,983.53 | 310.08 | 558.17 |
| 0.150 | 54,241.46 | 119,582.56 | 310.69 | 559.27 |
| 0.205 | 53,118.19 | 117,106.18 | 311.20 | 560.19 |
| 0.251 | 53,000.48 | 116,846.67 | 311.46 | 560.66 |
| 0.303 | 52,555.82 | 115,866.36 | 311.68 | 561.06 |
| 0.355 | 51,903.33 | 114,427.86 | 311.78 | 561.23 |
| 0.455 | 51,283.34 | 113,060.99 | 311.86 | 561.38 |
| 0.548 | 50,839.80 | 112,083.15 | 311.87 | 561.40 |
| 0.655 | 50,335.08 | 110,970.43 | 311.89 | 561.44 |
| 0.751 | 49,799.01 | 109,788.59 | 311.92 | 561.50 |
| 0.850 | 49,295.77 | 108,679.14 | 311.98 | 561.60 |
| 0.952 | 48,985.60 | 107,995.33 | 312.09 | 561.80 |
| 1.256 | 45,974.67 | 101,357.32 | 312.52 | 562.57 |
| 1.500 | 44,806.61 | 98,782.18 | 313.10 | 563.62 |
| 1.749 | 42,469.15 | 93,628.95 | 313.84 | 564.95 |
| 2.001 | 40,547.50 | 89,392.40 | 314.75 | 566.58 |
| 2.253 | 39,075.65 | 86,147.52 | 315.77 | 568.41 |
| 2.513 | 37,917.46 | 83,594.12 | 316.79 | 570.25 |
| 2.753 | 37,135.87 | 81,871.00 | 317.79 | 572.06 |
| 3.013 | 35,641.45 | 78,576.37 | 318.70 | 573.69 |
| 3.253 | 34,354.67 | 75,739.48 | 319.39 | 574.94 |
| 3.513 | 33,446.63 | 73,737.59 | 320.70 | 577.29 |

Replace these 23 pages of Table 6.2.1–7 with the following 23 pages of revised Table 6.2.1–7.

Table 6.2.1-7 (2 of 23)

Part A. Mass and Energy Release Data
(Blowdown Period)

| Time (sec) | Break Mass Flow Rate | | Break Enthalpy | |
|------------|----------------------|-----------|----------------|----------|
| | kg/sec | lbm/sec | kcal/kg | Btu/lbm |
| 3.753 | 32,136.20 | 70,848.55 | 322.26 | 580.11 |
| 4.013 | 30,679.12 | 67,636.23 | 324.09 | 583.39 |
| 4.513 | 28,504.55 | 62,842.10 | 327.42 | 589.38 |
| 5.013 | 26,227.90 | 57,822.93 | 331.03 | 595.89 |
| 5.513 | 24,545.92 | 54,114.76 | 337.02 | 606.67 |
| 6.013 | 21,825.68 | 48,117.64 | 349.22 | 628.64 |
| 6.513 | 17,987.35 | 39,655.52 | 376.16 | 677.13 |
| 7.013 | 13,886.23 | 30,614.05 | 428.08 | 770.59 |
| 7.505 | 12,225.23 | 26,952.15 | 454.34 | 817.86 |
| 8.014 | 11,663.92 | 25,714.69 | 459.62 | 827.36 |
| 8.513 | 11,152.79 | 24,587.83 | 461.97 | 831.59 |
| 9.013 | 10,759.50 | 23,720.77 | 463.01 | 833.46 |
| 9.513 | 9,894.04 | 21,812.74 | 479.71 | 863.53 |
| 10.013 | 8,931.05 | 19,689.70 | 504.97 | 908.99 |
| 10.513 | 8,006.74 | 17,651.93 | 528.35 | 951.08 |
| 11.013 | 6,975.26 | 15,377.90 | 556.89 | 1,002.46 |
| 11.513 | 5,926.46 | 13,065.67 | 588.71 | 1,059.75 |
| 12.013 | 5,345.95 | 11,785.86 | 593.54 | 1,068.43 |
| 12.513 | 6,618.02 | 14,590.32 | 460.05 | 828.14 |
| 13.013 | 7,205.45 | 15,885.38 | 405.88 | 730.62 |
| 13.513 | 7,216.60 | 15,909.95 | 378.11 | 680.64 |
| 14.009 | 7,049.69 | 15,541.99 | 356.91 | 642.47 |
| 14.507 | 6,840.23 | 15,080.21 | 336.96 | 606.56 |
| 15.017 | 6,604.21 | 14,559.86 | 319.10 | 574.41 |
| 15.257 | 6,493.95 | 14,316.78 | 311.68 | 561.06 |
| 15.503 | 6,334.92 | 13,966.18 | 305.12 | 549.25 |
| 15.753 | 6,086.67 | 13,418.88 | 297.94 | 536.33 |
| 16.008 | 6,015.11 | 13,261.12 | 289.68 | 521.46 |

Replace these 23 pages of Table 6.2.1-7
with the following 23 pages of revised
Table 6.2.1-7.

Table 6.2.1-7 (3 of 23)

Part A. Mass and Energy Release Data
(Blowdown Period)

| Time (sec) | Break Mass Flow Rate | | Break Enthalpy | |
|------------|----------------------|-----------|----------------|---------|
| | kg/sec | lbm/sec | kcal/kg | Btu/lbm |
| 16.257 | 5,794.29 | 12,774.28 | 281.39 | 506.53 |
| 16.505 | 5,416.53 | 11,941.46 | 273.92 | 493.08 |
| 16.753 | 4,955.88 | 10,925.90 | 268.62 | 483.55 |
| 17.007 | 4,447.82 | 9,805.81 | 263.22 | 473.82 |
| 17.251 | 3,984.08 | 8,783.44 | 258.14 | 464.68 |
| 17.500 | 3,606.06 | 7,950.04 | 253.32 | 456.00 |
| 17.750 | 3,263.42 | 7,194.64 | 248.40 | 447.14 |
| 18.000 | 3,088.10 | 6,808.13 | 245.86 | 442.57 |
| 18.249 | 1,743.93 | 3,844.73 | 240.28 | 432.53 |
| 18.509 | 1,671.14 | 3,684.24 | 240.44 | 432.82 |
| 18.752 | 1,508.29 | 3,325.24 | 243.71 | 438.70 |
| 19.002 | 1,297.66 | 2,860.86 | 243.27 | 437.91 |
| 19.254 | 1,091.70 | 2,406.81 | 244.26 | 439.70 |
| 19.508 | 882.79 | 1,946.23 | 247.16 | 444.92 |
| 19.752 | 678.35 | 1,495.51 | 254.14 | 457.48 |

Integral Mass and Energy Release at End of Blowdown

| Time (sec) | Integral Mass | | Integral Energy | |
|------------|---------------|------------|-----------------|-------------|
| | kg | lbm | Million kcal | Million Btu |
| 19.752 | 322,456.13 | 710,897.80 | 112.812 | 447.702 |

Replace these 23 pages of Table 6.2.1-7 with the following 23 pages of revised Table 6.2.1-7.

Table 6.2.1-7 (4 of 23)

Part A. Mass and Energy Release Data
(Reflood and Post-reflood Period)

| Time (sec) | Break Mass Flow Rate | | Break Enthalpy | |
|------------|----------------------|---------|----------------|----------|
| | kg/sec | lbm/sec | kcal/kg | Btu/lbm |
| 19.75 | 0.00 | 0.00 | 0.00 | 0.00 |
| 19.85 | 50.46 | 111.24 | 727.54 | 1,309.65 |
| 21.85 | 76.60 | 168.87 | 727.13 | 1,308.90 |
| 23.85 | 229.76 | 506.53 | 726.02 | 1,306.92 |
| 25.85 | 328.08 | 723.29 | 725.39 | 1,305.78 |
| 27.85 | 408.58 | 900.77 | 724.62 | 1,304.39 |
| 28.55 | 433.51 | 955.72 | 724.34 | 1,303.89 |
| 28.65 | 436.93 | 963.28 | 724.30 | 1,303.82 |
| 28.75 | 255.41 | 563.08 | 724.26 | 1,303.74 |
| 28.85 | 256.64 | 565.80 | 724.24 | 1,303.70 |
| 32.85 | 254.15 | 560.31 | 723.97 | 1,303.22 |
| 36.85 | 250.94 | 553.22 | 723.64 | 1,302.63 |
| 40.85 | 247.75 | 546.19 | 723.30 | 1,302.02 |
| 44.85 | 244.83 | 539.75 | 722.95 | 1,301.39 |
| 48.85 | 242.08 | 533.70 | 722.60 | 1,300.75 |
| 49.15 | 241.88 | 533.26 | 722.57 | 1,300.70 |
| 49.25 | 241.81 | 533.11 | 722.57 | 1,300.69 |
| 49.35 | 416.74 | 918.76 | 722.56 | 1,300.68 |
| 49.45 | 416.61 | 918.47 | 722.55 | 1,300.66 |
| 79.45 | 385.62 | 850.16 | 719.55 | 1,295.26 |
| 109.45 | 357.04 | 787.14 | 716.22 | 1,289.27 |
| 139.45 | 328.90 | 725.11 | 712.79 | 1,283.09 |
| 169.45 | 300.92 | 663.41 | 709.38 | 1,276.96 |
| 199.45 | 272.98 | 601.83 | 706.15 | 1,271.14 |
| 199.95 | 272.52 | 600.80 | 706.10 | 1,271.06 |
| 200.05 | 272.43 | 600.60 | 706.09 | 1,271.03 |
| 200.15 | 272.33 | 600.39 | 706.08 | 1,271.02 |
| 211.85 | 272.82 | 601.47 | 704.49 | 1,268.15 |

Replace these 23 pages of Table 6.2.1-7
with the following 23 pages of revised
Table 6.2.1-7.

Table 6.2.1-7 (5 of 23)

Part A. Mass and Energy Release Data
(Reflood and Post-reflood Period)

| Time (sec) | Break Mass Flow Rate | | Break Enthalpy | |
|------------|----------------------|---------|----------------|----------|
| | kg/sec | lbm/sec | kcal/kg | Btu/lbm |
| 223.55 | 273.53 | 603.03 | 702.81 | 1,265.13 |
| 235.25 | 274.36 | 604.86 | 701.10 | 1,262.04 |
| 246.95 | 275.52 | 607.42 | 699.28 | 1,258.78 |
| 247.05 | 274.49 | 605.15 | 686.09 | 1,235.04 |
| 247.15 | 283.36 | 624.71 | 684.93 | 1,232.94 |
| 247.75 | 284.27 | 626.72 | 678.18 | 1,220.79 |
| 248.25 | 276.02 | 608.52 | 670.85 | 1,207.60 |
| 249.35 | 270.10 | 595.48 | 659.76 | 1,187.64 |
| 253.35 | 231.38 | 510.10 | 653.82 | 1,176.93 |
| 257.35 | 209.44 | 461.74 | 653.81 | 1,176.92 |
| 261.35 | 197.72 | 435.89 | 653.82 | 1,176.94 |
| 262.15 | 196.06 | 432.25 | 653.81 | 1,176.93 |
| 262.25 | 195.87 | 431.82 | 653.81 | 1,176.93 |
| 265.35 | 191.26 | 421.65 | 653.82 | 1,176.94 |
| 269.35 | 187.01 | 412.29 | 653.81 | 1,176.92 |
| 273.35 | 183.06 | 403.57 | 653.81 | 1,176.93 |
| 274.85 | 182.19 | 401.66 | 653.81 | 1,176.93 |
| 274.95 | 180.99 | 399.01 | 653.81 | 1,176.93 |
| 286.65 | 131.77 | 290.50 | 653.81 | 1,176.93 |
| 298.35 | 116.00 | 255.74 | 653.81 | 1,176.93 |
| 310.05 | 102.25 | 225.42 | 653.80 | 1,176.91 |
| 321.75 | 92.51 | 203.95 | 653.82 | 1,176.94 |
| 333.45 | 84.57 | 186.45 | 653.80 | 1,176.91 |
| 345.15 | 77.90 | 171.73 | 653.82 | 1,176.95 |
| 356.85 | 71.98 | 158.70 | 653.82 | 1,176.95 |
| 368.55 | 92.48 | 203.88 | 653.80 | 1,176.92 |
| 374.35 | 80.39 | 177.22 | 653.80 | 1,176.91 |
| 374.45 | 80.48 | 177.43 | 653.80 | 1,176.91 |

Replace these 23 pages of Table 6.2.1-7
with the following 23 pages of revised
Table 6.2.1-7.

Table 6.2.1-7 (6 of 23)

Part A: Mass and Energy Release Data (Reflood and Post-reflood Period)

| Time (sec) | Break Mass Flow Rate | | Break Enthalpy | |
|---------------|----------------------|---------|----------------|----------|
| | kg/sec | lbm/sec | kcal/kg | Btu/lbm |
| 396.95 | 65.09 | 143.50 | 653.80 | 1,176.90 |
| 401.45 | 64.25 | 141.65 | 653.82 | 1,176.94 |
| 405.85 | 63.82 | 140.70 | 653.82 | 1,176.95 |
| 420.95 | 64.11 | 141.33 | 653.82 | 1,176.94 |
| 436.05 | 65.64 | 144.71 | 653.83 | 1,176.96 |
| 451.15 | 67.51 | 148.83 | 653.82 | 1,176.95 |
| 466.25 | 69.38 | 152.95 | 653.82 | 1,176.95 |
| 481.35 | 71.13 | 156.82 | 653.79 | 1,176.90 |
| 496.45 | 72.73 | 160.35 | 653.80 | 1,176.90 |
| 511.55 | 74.18 | 163.53 | 653.82 | 1,176.95 |
| 527.25 | 75.52 | 166.50 | 653.80 | 1,176.90 |
| 529.25 | 76.85 | 169.42 | 653.83 | 1,176.96 |
| 529.45 | 74.65 | 164.57 | 653.80 | 1,176.90 |
| 532.45 | 68.85 | 151.79 | 653.79 | 1,176.90 |
| 535.45 | 64.72 | 142.68 | 653.79 | 1,176.90 |
| 538.45 | 61.84 | 136.33 | 653.81 | 1,176.92 |
| 541.45 | 59.72 | 131.67 | 653.82 | 1,176.95 |
| 544.45 | 58.10 | 128.10 | 653.80 | 1,176.90 |
| 547.45 | 56.81 | 125.25 | 653.82 | 1,176.95 |
| 549.05 | 56.22 | 123.95 | 653.84 | 1,176.98 |
| 549.15 | 56.19 | 123.88 | 653.80 | 1,176.91 |

Integral Mass and Energy Release at the End of Reflood and Post-reflood

| Time (sec) | Integral Mass | | Integral Energy | |
|---------------|---------------|------------|-----------------|-------------|
| | kg | lbm | Million kcal | Million Btu |
| 200.05 | 59,016.59 | 130,110.00 | 42.263 | 167.725 |
| 549.15 | 102,624.29 | 226,249.00 | 71.416 | 283.419 |

Replace these 23 pages of Table 6.2.1-7 with the following 23 pages of revised Table 6.2.1-7.

Table 6.2.1-7 (7 of 23)

Part A: Spillage Release Data (Reactor Vessel Side)
(Reflood and Post-Reflood Period)

| Time (sec) | Break Mass Flow Rate | | Break Enthalpy | |
|---------------|----------------------|----------|----------------|---------|
| | kg/sec | lbm/sec | kcal/kg | Btu/lbm |
| 19.75 | 0.00 | 0.00 | 0.00 | 0.00 |
| 19.85 | 0.00 | 0.00 | 0.00 | 0.00 |
| 28.65 | 0.00 | 0.00 | 0.00 | 0.00 |
| 28.75 | 982.13 | 2,165.23 | 176.82 | 318.29 |
| 28.85 | 1,872.03 | 4,127.14 | 116.76 | 210.18 |
| 32.85 | 1,726.42 | 3,806.13 | 121.70 | 219.07 |
| 36.85 | 1,601.07 | 3,529.78 | 126.34 | 227.42 |
| 40.85 | 1,500.09 | 3,307.16 | 130.44 | 234.81 |
| 44.85 | 1,411.63 | 3,112.13 | 134.47 | 242.06 |
| 48.85 | 1,333.32 | 2,939.49 | 138.42 | 249.17 |
| 49.15 | 1,327.80 | 2,927.32 | 138.71 | 249.70 |
| 49.25 | 1,325.98 | 2,923.29 | 138.81 | 249.88 |
| 49.35 | 324.19 | 714.71 | 50.19 | 90.35 |
| 49.45 | 323.91 | 714.10 | 50.19 | 90.35 |
| 79.45 | 270.47 | 596.28 | 50.46 | 90.83 |
| 109.45 | 237.59 | 523.79 | 50.72 | 91.30 |
| 139.45 | 219.90 | 484.79 | 50.98 | 91.76 |
| 169.45 | 212.74 | 469.02 | 51.24 | 92.24 |
| 199.45 | 213.10 | 469.81 | 51.52 | 92.74 |
| 199.95 | 213.16 | 469.93 | 51.52 | 92.75 |
| 200.05 | 213.17 | 469.96 | 51.52 | 92.75 |
| 200.15 | 301.41 | 664.49 | 51.52 | 92.75 |
| 211.85 | 283.93 | 625.97 | 51.64 | 92.97 |
| 223.55 | 267.62 | 590.00 | 51.77 | 93.19 |
| 235.25 | 251.83 | 555.19 | 51.90 | 93.42 |
| 246.95 | 235.25 | 518.65 | 52.03 | 93.66 |
| 247.05 | 227.58 | 501.74 | 52.03 | 93.67 |
| 247.15 | 186.57 | 411.32 | 52.04 | 93.67 |
| 247.75 | 198.69 | 438.03 | 52.04 | 93.68 |
| 248.25 | 208.42 | 459.50 | 52.04 | 93.68 |

Replace these 23 pages of Table 6.2.1-7
with the following 23 pages of revised
Table 6.2.1-7.

Table 6.2.1-7 (8 of 23)

Part A: Spillage Release Data (Reactor Vessel Side)
(Reflood and Post-Reflood Period)

| Time (sec) | Break Mass Flow Rate | | Break Enthalpy | |
|---------------|----------------------|---------|----------------|---------|
| | kg/sec | lbm/sec | kcal/kg | Btu/lbm |
| 249.35 | 199.33 | 439.46 | 52.04 | 93.68 |
| 253.35 | 121.35 | 267.54 | 52.09 | 93.76 |
| 257.35 | 55.69 | 122.77 | 52.15 | 93.87 |
| 261.35 | 8.28 | 18.26 | 52.22 | 94.01 |
| 262.15 | 0.44 | 0.98 | 52.32 | 94.18 |
| 262.25 | 0.00 | 0.00 | 0.00 | 0.00 |
| 549.05 | 0.00 | 0.00 | 0.00 | 0.00 |
| 549.15 | 0.00 | 0.00 | 0.00 | 0.00 |

Integral Mass and Energy (Reactor Vessel Side Spillage) at EOR and EOPR

| Time (sec) | Integral Mass | | Integral Energy | |
|---------------|---------------|------------|-----------------|-------------|
| | kg | lbm | Million kcal | Million Btu |
| 200.05 | 68,418.16 | 150,837.00 | 5.952 | 23.619 |
| 549.15 | 82,592.84 | 182,087.00 | 6.686 | 26.533 |

Replace these 23 pages of Table 6.2.1-7
with the following 23 pages of revised
Table 6.2.1-7.

Table 6.2.1-7 (9 of 23)

Part A: Spillage Release Data (Steam Generator Side)
(Reflood and Post-Reflood Period)

| Time (sec) | Break Mass Flow Rate | | Break Enthalpy | |
|---------------|----------------------|----------|----------------|---------|
| | kg/sec | lbm/sec | kcal/kg | Btu/lbm |
| 19.75 | 0.00 | 0.00 | 0.00 | 0.00 |
| 19.85 | 0.00 | 0.00 | 0.00 | 0.00 |
| 246.95 | 0.00 | 0.00 | 0.00 | 0.00 |
| 247.05 | 2.51 | 5.53 | 144.38 | 259.89 |
| 247.15 | 1.81 | 3.99 | 144.26 | 259.67 |
| 247.75 | 14.24 | 31.40 | 144.31 | 259.77 |
| 248.25 | 23.79 | 52.44 | 144.33 | 259.81 |
| 249.35 | 38.51 | 84.91 | 144.33 | 259.81 |
| 253.35 | 145.68 | 321.17 | 144.33 | 259.80 |
| 257.35 | 230.21 | 507.52 | 144.33 | 259.81 |
| 261.35 | 287.14 | 633.04 | 144.33 | 259.81 |
| 262.15 | 296.14 | 652.89 | 144.33 | 259.81 |
| 262.25 | 297.23 | 655.28 | 144.33 | 259.81 |
| 265.35 | 320.26 | 706.05 | 144.33 | 259.81 |
| 269.35 | 333.38 | 734.97 | 144.33 | 259.81 |
| 273.35 | 339.04 | 747.47 | 144.33 | 259.81 |
| 274.85 | 336.76 | 742.44 | 144.33 | 259.81 |
| 274.95 | 340.46 | 750.60 | 144.33 | 259.81 |
| 286.65 | 305.12 | 672.68 | 144.33 | 259.81 |
| 298.35 | 569.95 | 1,256.53 | 144.33 | 259.81 |
| 310.05 | 527.14 | 1,162.15 | 144.33 | 259.81 |
| 321.75 | 506.43 | 1,116.49 | 144.33 | 259.81 |
| 333.45 | 491.70 | 1,084.01 | 144.33 | 259.81 |
| 345.15 | 479.51 | 1,057.15 | 144.33 | 259.81 |
| 356.85 | 469.28 | 1,034.58 | 144.33 | 259.81 |
| 368.55 | 355.57 | 783.90 | 144.33 | 259.81 |
| 374.35 | 146.61 | 323.22 | 144.33 | 259.81 |
| 374.45 | 144.26 | 318.05 | 144.33 | 259.81 |
| 378.95 | 136.87 | 301.74 | 144.33 | 259.81 |
| 383.45 | 135.81 | 299.41 | 144.33 | 259.81 |

Replace these 23 pages of Table 6.2.1-7
with the following 23 pages of revised
Table 6.2.1-7.

Table 6.2.1-7 (10 of 23)

Part A: Spillage Release Data (Steam Generator Side)
(Reflood and Post-Reflood Period)

| Time (sec) | Break Mass Flow Rate | | Break Enthalpy | |
|---------------|----------------------|---------|----------------|---------|
| | kg/sec | lbm/sec | kcal/kg | Btu/lbm |
| 387.95 | 135.90 | 299.60 | 144.33 | 259.81 |
| 392.45 | 132.30 | 291.68 | 144.33 | 259.80 |
| 396.95 | 130.69 | 288.12 | 144.33 | 259.81 |
| 401.45 | 129.71 | 285.97 | 144.33 | 259.81 |
| 405.85 | 128.89 | 284.15 | 144.33 | 259.81 |
| 420.95 | 126.41 | 278.68 | 144.33 | 259.81 |
| 436.05 | 124.27 | 273.96 | 144.33 | 259.81 |
| 451.15 | 122.39 | 269.82 | 144.33 | 259.81 |
| 466.25 | 120.73 | 266.17 | 144.33 | 259.80 |
| 481.35 | 119.26 | 262.93 | 144.33 | 259.81 |
| 496.45 | 117.96 | 260.06 | 144.33 | 259.81 |
| 511.55 | 116.81 | 257.53 | 144.33 | 259.81 |
| 527.25 | 115.76 | 255.21 | 144.33 | 259.81 |
| 529.25 | 117.75 | 259.60 | 144.33 | 259.81 |
| 529.45 | 121.82 | 268.57 | 144.33 | 259.81 |
| 532.45 | 131.37 | 289.62 | 144.33 | 259.81 |
| 535.45 | 135.70 | 299.17 | 144.33 | 259.81 |
| 538.45 | 138.36 | 305.04 | 144.33 | 259.80 |
| 541.45 | 139.91 | 308.44 | 144.33 | 259.81 |
| 544.45 | 140.79 | 310.38 | 144.33 | 259.80 |
| 547.45 | 141.29 | 311.49 | 144.33 | 259.81 |
| 549.05 | 141.47 | 311.90 | 144.33 | 259.81 |
| 549.15 | 141.48 | 311.92 | 144.33 | 259.81 |

Integral Mass and Energy (Steam Generator Side Spillage) at EOR and EOPR

| Time (sec) | Integral Mass | | Integral Energy | |
|---------------|---------------|------------|-----------------|-------------|
| | kg | lbm | Million kcal | Million Btu |
| 200.05 | 0.00 | 0.00 | 0.000 | 0.000 |
| 549.15 | 65,190.41 | 143,721.00 | 9.409 | 37.340 |

Replace these 23 pages of Table 6.2.1-7
with the following 23 pages of revised
Table 6.2.1-7.

Table 6.2.1-7 (11 of 23)

Part A. Mass and energy (Steam) Release Data (Decay heat Period)

| Time (sec) | Mass Flow Rate | | Break Enthalpy | |
|------------|----------------|---------|----------------|---------|
| | kg/sec | lbm/sec | Kcal/kg | Btu/lbm |
| 600.0 | 55.35 | 122.03 | 654.84 | 1178.71 |
| 800.0 | 46.77 | 103.1 | 654.53 | 1178.15 |
| 999.0 | 44.74 | 98.63 | 654.26 | 1177.67 |
| 1504.8 | 42.52 | 93.75 | 653.79 | 1176.82 |
| 1999.1 | 40.33 | 88.91 | 653.49 | 1176.28 |
| 3996.9 | 33.7 | 74.3 | 652.84 | 1175.11 |
| 5996.1 | 30.12 | 66.41 | 652.46 | 1174.43 |
| 7996.5 | 27.93 | 61.56 | 652.21 | 1173.98 |
| 9998.0 | 26.38 | 58.16 | 652.02 | 1173.64 |
| 15005.8 | 24.01 | 52.94 | 651.69 | 1173.04 |
| 20012.3 | 22.56 | 49.73 | 651.39 | 1172.49 |
| 40038.8 | 19.56 | 43.12 | 650.32 | 1170.58 |
| 59966.9 | 18.02 | 39.72 | 649.42 | 1168.96 |
| 79995.6 | 17.05 | 37.6 | 648.76 | 1167.78 |
| 100001.6 | 14.47 | 31.91 | 647.71 | 1165.87 |
| 150008.6 | 12.8 | 28.22 | 646.35 | 1163.43 |
| 200016.7 | 11.7 | 25.78 | 645.65 | 1162.17 |
| 400050.2 | 9.2 | 20.27 | 644.39 | 1159.9 |
| 600089.4 | 7.85 | 17.31 | 643.77 | 1158.78 |
| 800134.1 | 6.98 | 15.38 | 643.4 | 1158.12 |
| 1000000.0 | 6.37 | 14.04 | 643.16 | 1157.69 |

Integral Mass and Energy Release(Steam) at 24 hours and End of Analysis

| Time (sec) | Integral Mass | | Integral Energy | |
|------------|---------------|------------|-----------------|-------------|
| | kg | lbm | Million kcal | Million Btu |
| 85,005 | 1,891,405 | 4,169,834 | 1,236.108 | 4,349.405 |
| 1,000,000 | 10,019,578 | 22,089,388 | 6,478.911 | 25,710.395 |

Replace these 23 pages of Table 6.2.1-7 with the following 23 pages of revised Table 6.2.1-7.

Table 6.2.1-7 (12 of 23)

Part A. Mass and Energy (Spillage) Release Data (Decay heat Period)

| Time (sec) | Mass Flow Rate | | Break Enthalpy | |
|------------|----------------|---------|----------------|---------|
| | kg/sec | lbm/sec | kcal/kg | Btu/lbm |
| 600.0 | 106.14 | 233.99 | 119.94 | 215.89 |
| 800.0 | 105.26 | 232.05 | 87.54 | 157.57 |
| 999.0 | 114.45 | 252.31 | 84.04 | 151.27 |
| 1504.8 | 133.83 | 295.05 | 88.24 | 158.84 |
| 1999.1 | 143.24 | 315.8 | 92.7 | 166.87 |
| 3996.9 | 151.34 | 333.66 | 105.03 | 189.05 |
| 5996.1 | 153.88 | 339.25 | 111.96 | 201.53 |
| 7996.5 | 155.33 | 342.45 | 115.94 | 208.69 |
| 9998.0 | 156.38 | 344.77 | 118.21 | 212.78 |
| 15005.8 | 158.21 | 348.8 | 120.22 | 216.39 |
| 20012.3 | 159.6 | 351.85 | 120.0 | 216.0 |
| 40038.8 | 163.14 | 359.66 | 115.4 | 207.73 |
| 59966.9 | 165.37 | 364.57 | 110.6 | 199.08 |
| 79995.6 | 166.86 | 367.87 | 106.87 | 192.37 |
| 100001.6 | 169.92 | 374.62 | 101.81 | 183.26 |
| 150008.6 | 172.74 | 380.83 | 93.0 | 167.39 |
| 200016.7 | 174.36 | 384.4 | 88.32 | 158.97 |
| 400050.2 | 177.63 | 391.61 | 79.32 | 142.77 |
| 600089.4 | 179.33 | 395.35 | 74.37 | 133.87 |
| 800134.1 | 180.38 | 397.67 | 71.27 | 128.28 |
| 1000000.0 | 181.1 | 399.26 | 69.11 | 124.4 |

Integral Mass and Energy Release (Spillage) at 24 hours and End of Analysis

| Time (sec) | Integral Mass | | Integral Energy | |
|------------|---------------|-------------|-----------------|-------------|
| | kg | lbm | Million kcal | Million Btu |
| 85,005 | 13,803,866 | 30,432,316 | 1,556.366 | 6,176.160 |
| 1,000,000 | 176,628,783 | 389,399,810 | 14,272.280 | 56,636.983 |

Replace these 23 pages of Table 6.2.1-7 with the following 23 pages of revised Table 6.2.1-7.

Table 6.2.1-7 (13 of 23)

Part B. Reactor Vessel Pressure vs. Time
(Blowdown Period)

| Time (sec) | Reactor Vessel Pressure | |
|------------|-------------------------|----------|
| | kg/cm ² A | psia |
| 0.000 | 167.360 | 2,380.40 |
| 0.026 | 147.360 | 2,096.00 |
| 0.051 | 131.970 | 1,877.00 |
| 0.102 | 124.440 | 1,770.00 |
| 0.150 | 126.550 | 1,799.90 |
| 0.205 | 123.280 | 1,753.50 |
| 0.251 | 124.390 | 1,769.20 |
| 0.303 | 122.240 | 1,738.60 |
| 0.355 | 121.610 | 1,729.70 |
| 0.455 | 119.600 | 1,701.10 |
| 0.548 | 118.700 | 1,688.30 |
| 0.655 | 117.750 | 1,674.80 |
| 0.751 | 116.290 | 1,654.00 |
| 0.850 | 115.400 | 1,641.40 |
| 0.952 | 114.580 | 1,629.70 |
| 1.256 | 107.300 | 1,526.10 |
| 1.500 | 106.660 | 1,517.00 |
| 1.749 | 101.420 | 1,442.50 |
| 2.001 | 99.780 | 1,419.20 |
| 2.253 | 96.330 | 1,370.10 |
| 2.513 | 95.120 | 1,352.90 |
| 2.753 | 93.450 | 1,329.20 |
| 3.013 | 91.670 | 1,303.90 |
| 3.253 | 90.120 | 1,281.80 |
| 3.513 | 88.880 | 1,264.20 |
| 3.753 | 87.480 | 1,244.20 |
| 4.013 | 86.210 | 1,226.20 |

Replace these 23 pages of Table 6.2.1-7 with the following 23 pages of revised Table 6.2.1-7.

Table 6.2.1-7 (14 of 23)

Part B. Reactor Vessel Pressure vs. Time
(Blowdown Period)

| Time (sec) | Reactor Vessel Pressure | |
|------------|-------------------------|----------|
| | kg/cm ² A | psia |
| 4.513 | 84.160 | 1,197.00 |
| 5.013 | 82.180 | 1,168.90 |
| 5.513 | 80.350 | 1,142.80 |
| 6.013 | 78.810 | 1,120.90 |
| 6.513 | 76.680 | 1,090.70 |
| 7.013 | 74.800 | 1,063.90 |
| 7.505 | 71.970 | 1,023.70 |
| 8.014 | 70.510 | 1,002.90 |
| 8.513 | 68.090 | 968.43 |
| 9.013 | 66.110 | 940.35 |
| 9.513 | 64.050 | 910.98 |
| 10.013 | 61.900 | 880.49 |
| 10.513 | 58.870 | 837.39 |
| 11.013 | 55.490 | 789.25 |
| 11.513 | 50.790 | 722.45 |
| 12.013 | 46.480 | 661.04 |
| 12.513 | 41.990 | 597.21 |
| 13.013 | 38.250 | 544.01 |
| 13.513 | 34.690 | 493.40 |
| 14.009 | 31.030 | 441.40 |
| 14.507 | 27.720 | 394.32 |
| 15.017 | 24.580 | 349.64 |
| 15.257 | 23.270 | 330.97 |
| 15.503 | 21.850 | 310.76 |
| 15.753 | 20.290 | 288.64 |
| 16.008 | 18.750 | 266.73 |
| 16.257 | 17.220 | 244.90 |

Replace these 23 pages of Table 6.2.1-7 with the following 23 pages of revised Table 6.2.1-7.

Table 6.2.1-7 (15 of 23)

Part B. Reactor Vessel Pressure vs. Time
(Blowdown Period)

| Time (sec) | Reactor Vessel Pressure | |
|---------------|-------------------------|--------|
| | kg/cm ² A | psia |
| 16.505 | 15.700 | 223.25 |
| 16.753 | 14.160 | 201.46 |
| 17.007 | 12.680 | 180.32 |
| 17.251 | 11.370 | 161.79 |
| 17.500 | 10.200 | 145.11 |
| 17.750 | 9.100 | 129.40 |
| 18.000 | 8.150 | 115.88 |
| 18.249 | 7.340 | 104.41 |
| 18.509 | 6.610 | 94.06 |
| 18.752 | 6.050 | 86.09 |
| 19.002 | 5.560 | 79.01 |
| 19.254 | 5.120 | 72.85 |
| 19.508 | 4.730 | 67.23 |
| 19.752 | 4.410 | 62.76 |

Replace these 23 pages of Table 6.2.1-7
with the following 23 pages of revised
Table 6.2.1-7.

Table 6.2.1-7 (16 of 23)

Part B. Reactor Vessel Pressure vs. Time
(Reflood and Post-reflood Period)

| Time (sec) | Reactor Vessel Pressure | |
|------------|-------------------------|--------|
| | kg/cm ² A | psia |
| 19.75 | 4.080 | 58.000 |
| 19.85 | 4.090 | 58.160 |
| 21.85 | 4.120 | 58.600 |
| 23.85 | 4.440 | 63.150 |
| 25.85 | 4.790 | 68.100 |
| 27.85 | 5.140 | 73.070 |
| 28.55 | 5.260 | 74.750 |
| 28.65 | 5.270 | 74.990 |
| 28.75 | 5.290 | 75.230 |
| 28.85 | 5.300 | 75.360 |
| 32.85 | 5.280 | 75.030 |
| 36.85 | 5.250 | 74.620 |
| 40.85 | 5.220 | 74.220 |
| 44.85 | 5.190 | 73.860 |
| 48.85 | 5.170 | 73.520 |
| 49.15 | 5.170 | 73.500 |
| 49.25 | 5.170 | 73.490 |
| 49.35 | 5.170 | 73.470 |
| 49.45 | 5.160 | 73.460 |
| 79.45 | 5.010 | 71.280 |
| 109.45 | 4.880 | 69.380 |
| 139.45 | 4.760 | 67.640 |
| 169.45 | 4.640 | 66.050 |
| 199.45 | 4.540 | 64.600 |
| 199.95 | 4.540 | 64.580 |
| 200.05 | 4.540 | 64.580 |
| 200.15 | 4.540 | 64.570 |
| 211.85 | 4.540 | 64.550 |

Replace these 23 pages of Table 6.2.1-7
with the following 23 pages of revised
Table 6.2.1-7.

Table 6.2.1-7 (17 of 23)

Part B. Reactor Vessel Pressure vs. Time
(Reflood and Post-reflood Period)

| Time (sec) | Reactor Vessel Pressure | |
|------------|-------------------------|--------|
| | kg/cm ² A | psia |
| 223.55 | 4.540 | 64.540 |
| 235.25 | 4.540 | 64.530 |
| 246.95 | 4.540 | 64.530 |
| 247.05 | 4.540 | 64.590 |
| 247.15 | 4.530 | 64.500 |
| 247.75 | 4.530 | 64.380 |
| 248.25 | 4.520 | 64.290 |
| 249.35 | 4.500 | 64.010 |
| 253.35 | 4.490 | 63.890 |
| 257.35 | 4.500 | 63.970 |
| 261.35 | 4.500 | 64.020 |
| 262.15 | 4.500 | 64.030 |
| 262.25 | 4.500 | 64.030 |
| 265.35 | 4.500 | 64.020 |
| 269.35 | 4.500 | 63.940 |
| 273.35 | 4.490 | 63.830 |
| 274.85 | 4.480 | 63.770 |
| 274.95 | 4.480 | 63.780 |
| 286.65 | 4.440 | 63.100 |
| 298.35 | 4.430 | 62.970 |
| 310.05 | 4.350 | 61.820 |
| 321.75 | 4.300 | 61.180 |
| 333.45 | 4.270 | 60.760 |
| 345.15 | 4.250 | 60.430 |
| 356.85 | 4.230 | 60.160 |
| 368.55 | 4.190 | 59.560 |

Replace these 23 pages of Table 6.2.1-7
with the following 23 pages of revised
Table 6.2.1-7.

Table 6.2.1-7 (18 of 23)

Part B. Reactor Vessel Pressure vs. Time
(Reflood and Post-reflood Period)

| Time (sec) | Reactor Vessel Pressure | |
|------------|-------------------------|--------|
| | kg/cm ² A | psia |
| 374.35 | 4.160 | 59.150 |
| 374.45 | 4.160 | 59.140 |
| 378.95 | 4.150 | 59.020 |
| 383.45 | 4.140 | 58.940 |
| 387.95 | 4.140 | 58.870 |
| 392.45 | 4.140 | 58.820 |
| 396.95 | 4.130 | 58.790 |
| 401.45 | 4.130 | 58.770 |
| 405.85 | 4.130 | 58.760 |
| 420.95 | 4.130 | 58.760 |
| 436.05 | 4.130 | 58.780 |
| 451.15 | 4.130 | 58.810 |
| 466.25 | 4.140 | 58.840 |
| 481.35 | 4.140 | 58.870 |
| 496.45 | 4.140 | 58.900 |
| 511.55 | 4.140 | 58.920 |
| 527.25 | 4.140 | 58.940 |
| 529.25 | 4.150 | 58.970 |
| 529.45 | 4.150 | 58.990 |
| 532.45 | 4.140 | 58.950 |
| 535.45 | 4.140 | 58.910 |
| 538.45 | 4.140 | 58.880 |
| 541.45 | 4.140 | 58.860 |
| 544.45 | 4.140 | 58.840 |
| 547.45 | 4.140 | 58.820 |
| 549.05 | 4.130 | 58.810 |
| 549.15 | 4.130 | 58.810 |

Replace these 23 pages of Table 6.2.1-7
with the following 23 pages of revised
Table 6.2.1-7.

Table 6.2.1-7 (19 of 23)

Part B. Reactor Vessel Pressure vs. Time
(Decay heat Period)

| Time (sec) | Reactor Vessel Pressure | |
|------------|-------------------------|--------|
| | kg/cm ² A | psia |
| 600.0 | 4.469 | 63.57 |
| 800.0 | 4.342 | 61.763 |
| 999.0 | 4.236 | 60.256 |
| 1504.8 | 4.054 | 57.658 |
| 1999.1 | 3.941 | 56.058 |
| 3996.9 | 3.71 | 52.769 |
| 5996.1 | 3.582 | 50.952 |
| 7996.5 | 3.5 | 49.785 |
| 9998.0 | 3.441 | 48.944 |
| 15005.8 | 3.336 | 47.454 |
| 20012.3 | 3.244 | 46.137 |
| 40038.8 | 2.941 | 41.831 |
| 59966.9 | 2.707 | 38.504 |
| 79995.6 | 2.548 | 36.239 |
| 100001.6 | 2.311 | 32.871 |
| 150008.6 | 2.04 | 29.01 |
| 200016.7 | 1.912 | 27.189 |
| 400050.2 | 1.7 | 24.18 |
| 600089.4 | 1.604 | 22.821 |
| 800134.1 | 1.551 | 22.053 |
| 1000000.0 | 1.516 | 21.556 |

Replace these 23 pages of Table 6.2.1-7 with the following 23 pages of revised Table 6.2.1-7.

Table 6.2.1-7 (20 of 23)

Part C Safety Injection Flow vs. Time
(Blowdown Period)

| Time (sec) | Safety Injection Tank Flow | |
|---------------|----------------------------|-----------|
| | kg/sec | kg/sec |
| 0.000 | 0.00 | 0.00 |
| 0.026 | 0.00 | 0.00 |
| 11.513 | 0.00 | 0.00 |
| 12.013 | 0.00 | 0.00 |
| 12.513 | 2,164.62 | 4,772.20 |
| 13.013 | 2,786.54 | 6,143.30 |
| 13.513 | 3,212.60 | 7,082.60 |
| 14.009 | 3,589.48 | 7,913.50 |
| 14.507 | 3,867.31 | 8,526.00 |
| 15.017 | 4,094.01 | 9,025.80 |
| 15.257 | 4,166.59 | 9,185.80 |
| 15.503 | 4,261.98 | 9,396.10 |
| 15.753 | 4,377.01 | 9,649.70 |
| 16.008 | 4,487.23 | 9,892.70 |
| 16.257 | 4,598.95 | 10,139.00 |
| 16.505 | 4,710.99 | 10,386.00 |
| 16.753 | 4,823.48 | 10,634.00 |
| 17.007 | 4,925.99 | 10,860.00 |
| 17.251 | 5,008.54 | 11,042.00 |
| 17.500 | 5,074.31 | 11,187.00 |
| 17.750 | 5,130.56 | 11,311.00 |
| 18.000 | 5,170.47 | 11,399.00 |
| 18.249 | 5,196.33 | 11,456.00 |
| 18.509 | 5,209.93 | 11,486.00 |
| 18.752 | 5,210.84 | 11,488.00 |
| 19.002 | 5,203.58 | 11,472.00 |
| 19.254 | 5,192.24 | 11,447.00 |
| 19.508 | 5,176.37 | 11,412.00 |
| 19.752 | 5,157.32 | 11,370.00 |

Replace these 23 pages of Table 6.2.1-7
with the following 23 pages of revised
Table 6.2.1-7.

Table 6.2.1-7 (21 of 23)

Part C Safety Injection Flow vs. Time
(Reflood and Post-reflood Period)

| Time (sec) | Safety Injection Tank Flow | | Safety Injection Pump Flow | |
|---------------|----------------------------|----------|----------------------------|---------|
| | kg/sec | lbm/sec | kg/sec | lbm/sec |
| 19.752 | 2,681.59 | 5,911.91 | 193.78 | 427.22 |
| 19.852 | 2,674.22 | 5,895.68 | 193.78 | 427.22 |
| 21.052 | 2,587.00 | 5,703.38 | 193.75 | 427.14 |
| 22.252 | 2,507.16 | 5,527.36 | 193.72 | 427.07 |
| 23.452 | 2,421.47 | 5,338.45 | 193.56 | 426.74 |
| 24.652 | 2,339.70 | 5,158.17 | 193.40 | 426.38 |
| 25.852 | 2,261.52 | 4,985.83 | 193.23 | 426.00 |
| 27.052 | 2,186.62 | 4,820.69 | 193.06 | 425.63 |
| 28.252 | 2,115.08 | 4,662.97 | 192.89 | 425.26 |
| 28.652 | 2,091.94 | 4,611.97 | 192.84 | 425.14 |
| 28.752 | 2,086.21 | 4,599.33 | 192.82 | 425.11 |
| 32.752 | 1,933.08 | 4,261.74 | 192.82 | 425.10 |
| 36.752 | 1,807.06 | 3,983.91 | 192.84 | 425.15 |
| 40.752 | 1,699.06 | 3,745.80 | 192.87 | 425.20 |
| 44.752 | 1,604.69 | 3,537.75 | 192.89 | 425.25 |
| 49.152 | 1,513.30 | 3,336.27 | 192.91 | 425.29 |
| 49.252 | 1,511.35 | 3,331.98 | 192.91 | 425.30 |
| 49.352 | 684.43 | 1,508.92 | 192.91 | 425.30 |
| 49.452 | 684.07 | 1,508.12 | 192.91 | 425.30 |
| 64.552 | 631.57 | 1,392.37 | 192.98 | 425.44 |
| 79.652 | 587.21 | 1,294.58 | 193.04 | 425.57 |
| 94.752 | 549.13 | 1,210.63 | 193.09 | 425.70 |
| 109.852 | 516.00 | 1,137.58 | 193.15 | 425.81 |
| 124.952 | 486.83 | 1,073.28 | 193.20 | 425.93 |
| 140.052 | 460.90 | 1,016.12 | 193.24 | 426.03 |
| 155.152 | 437.64 | 964.84 | 193.29 | 426.14 |
| 170.252 | 416.61 | 918.48 | 193.34 | 426.24 |
| 185.352 | 397.46 | 876.26 | 193.38 | 426.33 |
| 200.052 | 380.35 | 838.53 | 193.42 | 426.41 |
| 215.152 | 359.39 | 792.32 | 193.42 | 426.42 |

Replace these 23 pages of Table 6.2.1-7 with the following 23 pages of revised Table 6.2.1-7.

Table 6.2.1-7 (22 of 23)

Part C. Safety Injection Flow vs. Time (Reflood and Post-reflood Period)

| Time (sec) | Safety Injection Tank Flow | | Safety Injection Pump Flow | |
|------------|----------------------------|---------|----------------------------|---------|
| | kg/sec | lbm/sec | kg/sec | lbm/sec |
| 230.252 | 339.53 | 748.53 | 193.42 | 426.42 |
| 245.352 | 320.69 | 706.99 | 193.42 | 426.42 |
| 260.452 | 307.12 | 677.08 | 193.45 | 426.48 |
| 275.552 | 292.22 | 644.23 | 193.46 | 426.51 |
| 290.652 | 283.59 | 625.22 | 193.51 | 426.61 |
| 305.752 | 293.28 | 646.57 | 193.65 | 426.94 |
| 320.852 | 276.64 | 609.88 | 193.64 | 426.91 |
| 335.952 | 260.17 | 573.58 | 193.63 | 426.89 |
| 351.052 | 259.70 | 572.54 | 193.70 | 427.05 |
| 351.152 | 256.89 | 566.36 | 193.69 | 427.02 |
| 369.452 | 242.77 | 535.23 | 193.70 | 427.04 |
| 369.552 | 238.51 | 525.83 | 193.68 | 426.99 |
| 369.652 | 0.00 | 0.00 | 193.68 | 427.00 |
| 369.752 | 0.00 | 0.00 | 193.70 | 427.03 |
| 384.852 | 0.00 | 0.00 | 193.73 | 427.11 |
| 399.952 | 0.00 | 0.00 | 193.74 | 427.12 |
| 415.052 | 0.00 | 0.00 | 193.74 | 427.13 |
| 430.152 | 0.00 | 0.00 | 193.74 | 427.13 |
| 445.252 | 0.00 | 0.00 | 193.74 | 427.12 |
| 460.352 | 0.00 | 0.00 | 193.74 | 427.12 |
| 475.452 | 0.00 | 0.00 | 193.74 | 427.11 |
| 490.552 | 0.00 | 0.00 | 193.73 | 427.11 |
| 505.652 | 0.00 | 0.00 | 193.73 | 427.11 |
| 520.752 | 0.00 | 0.00 | 193.73 | 427.11 |
| 535.852 | 0.00 | 0.00 | 193.73 | 427.11 |
| 549.152 | 0.00 | 0.00 | 193.74 | 427.12 |
| 564.252 | 0.00 | 0.00 | 193.74 | 427.13 |
| 579.352 | 0.00 | 0.00 | 193.74 | 427.13 |
| 599.852 | 0.00 | 0.00 | 193.74 | 427.13 |
| 599.952 | 0.00 | 0.00 | 193.74 | 427.13 |

Replace these 23 pages of Table 6.2.1-7 with the following 23 pages of revised Table 6.2.1-7.

Table 6.2.1-7 (23 of 23)

Part D. Chronology of Events

| Time (sec) | Event | Values |
|------------|--|---|
| 0.0 | Break occurs | - |
| 3.76 | Containment pressure Hi-Hi setpoint | 1.547kg/cm ² G (22.0 psig) |
| 12.01 | Start safety injection tank (SIT) injection | - |
| 17.71 | First peak containment pressure (Blowdown phase) | 3.123kg/cm ² G (44.42 psig) |
| 19.75 | End of blowdown | - |
| | Start SI pump injection | - |
| 49.35 | SIT flow is turned down to low flow by fluidic device in SIT | - |
| 113.76 | Start containment spray actuation | - |
| 200.05 | End of reflood | - |
| 320.42 | Peak containment temperature | 134.52 °C (274.13 °F) |
| 321.92 | Peak containment pressure | 3.583kg/cm ² G (50.97 psig) |
| 369.65 | Safety injection tank empty | - |
| 549.15 | End of post reflood | - |
| 49,051.8 | Time of depressurization of the containment at 50 % of peak pressure | 1.791kg/cm ² G (25.47 psig) |

Replace these 23 pages of Table 6.2.1-7 with the following 23 pages of revised Table 6.2.1-7.

APR1400 DCD TIER 2

Table 6.2.1-7 (1 of 23)

Insert this page.

Double-Ended Discharge Leg Slot Break – Minimum SIS Flow
(0.9121 m² (9.8175 ft²) Break Area)

Part A. Mass and Energy Release Data
 (Blowdown Period)

| Time (sec) | Break Mass Flow Rate | | Break Enthalpy | |
|------------|----------------------|------------|----------------|---------|
| | kg/sec | lbm/sec | kcal/kg | Btu/lbm |
| 0.000 | 0.00 | 0.00 | 0.00 | 0.00 |
| 0.026 | 35,570.66 | 78,420.29 | 309.67 | 557.44 |
| 0.051 | 36,255.06 | 79,929.15 | 309.62 | 557.34 |
| 0.102 | 52,155.38 | 114,983.53 | 310.08 | 558.17 |
| 0.150 | 54,241.46 | 119,582.56 | 310.69 | 559.27 |
| 0.205 | 53,118.19 | 117,106.18 | 311.20 | 560.19 |
| 0.251 | 53,000.48 | 116,846.67 | 311.46 | 560.66 |
| 0.303 | 52,555.82 | 115,866.36 | 311.68 | 561.06 |
| 0.355 | 51,903.33 | 114,427.86 | 311.78 | 561.23 |
| 0.455 | 51,283.34 | 113,060.99 | 311.86 | 561.38 |
| 0.548 | 50,839.80 | 112,083.15 | 311.87 | 561.40 |
| 0.655 | 50,335.08 | 110,970.43 | 311.89 | 561.44 |
| 0.751 | 49,799.01 | 109,788.59 | 311.92 | 561.50 |
| 0.850 | 49,295.77 | 108,679.14 | 311.98 | 561.60 |
| 0.952 | 48,985.60 | 107,995.33 | 312.09 | 561.80 |
| 1.256 | 45,974.67 | 101,357.32 | 312.52 | 562.57 |
| 1.500 | 44,806.61 | 98,782.18 | 313.10 | 563.62 |
| 1.749 | 42,469.15 | 93,628.95 | 313.84 | 564.95 |
| 2.001 | 40,547.50 | 89,392.40 | 314.75 | 566.58 |
| 2.253 | 39,075.65 | 86,147.52 | 315.77 | 568.41 |
| 2.513 | 37,917.46 | 83,594.12 | 316.79 | 570.25 |
| 2.753 | 37,135.87 | 81,871.00 | 317.79 | 572.06 |
| 3.013 | 35,641.45 | 78,576.37 | 318.70 | 573.69 |
| 3.253 | 34,354.67 | 75,739.48 | 319.39 | 574.94 |
| 3.513 | 33,446.63 | 73,737.59 | 320.70 | 577.29 |

APR1400 DCD TIER 2

Table 6.2.1-7 (2 of 23)

Insert this page.

**Part A. Mass and Energy Release Data
(Blowdown Period)**

| Time (sec) | Break Mass Flow Rate | | Break Enthalpy | |
|------------|----------------------|-----------|----------------|----------|
| | kg/sec | lbm/sec | kcal/kg | Btu/lbm |
| 3.753 | 32,136.20 | 70,848.55 | 322.26 | 580.11 |
| 4.013 | 30,679.12 | 67,636.23 | 324.09 | 583.39 |
| 4.513 | 28,504.55 | 62,842.10 | 327.42 | 589.38 |
| 5.013 | 26,227.90 | 57,822.93 | 331.03 | 595.89 |
| 5.513 | 24,545.92 | 54,114.76 | 337.02 | 606.67 |
| 6.013 | 21,825.68 | 48,117.64 | 349.22 | 628.64 |
| 6.513 | 17,987.35 | 39,655.52 | 376.16 | 677.13 |
| 7.013 | 13,886.23 | 30,614.05 | 428.08 | 770.59 |
| 7.505 | 12,225.23 | 26,952.15 | 454.34 | 817.86 |
| 8.014 | 11,663.92 | 25,714.69 | 459.62 | 827.36 |
| 8.513 | 11,152.79 | 24,587.83 | 461.97 | 831.59 |
| 9.013 | 10,759.50 | 23,720.77 | 463.01 | 833.46 |
| 9.513 | 9,894.04 | 21,812.74 | 479.71 | 863.53 |
| 10.013 | 8,931.05 | 19,689.70 | 504.97 | 908.99 |
| 10.513 | 8,006.74 | 17,651.93 | 528.35 | 951.08 |
| 11.013 | 6,975.26 | 15,377.90 | 556.89 | 1,002.46 |
| 11.513 | 5,926.46 | 13,065.67 | 588.71 | 1,059.75 |
| 12.013 | 5,345.95 | 11,785.86 | 593.54 | 1,068.43 |
| 12.513 | 6,618.02 | 14,590.32 | 460.05 | 828.14 |
| 13.013 | 7,205.45 | 15,885.38 | 405.88 | 730.62 |
| 13.513 | 7,216.60 | 15,909.95 | 378.11 | 680.64 |
| 14.009 | 7,049.69 | 15,541.99 | 356.91 | 642.47 |
| 14.507 | 6,840.23 | 15,080.21 | 336.96 | 606.56 |
| 15.017 | 6,604.21 | 14,559.86 | 319.10 | 574.41 |
| 15.257 | 6,493.95 | 14,316.78 | 311.68 | 561.06 |
| 15.503 | 6,334.92 | 13,966.18 | 305.12 | 549.25 |
| 15.753 | 6,086.67 | 13,418.88 | 297.94 | 536.33 |
| 16.008 | 6,015.11 | 13,261.12 | 289.68 | 521.46 |

APR1400 DCD TIER 2

Table 6.2.1-7 (3 of 23)

Insert this page.

**Part A. Mass and Energy Release Data
(Blowdown Period)**

| Time (sec) | Break Mass Flow Rate | | Break Enthalpy | |
|------------|----------------------|-----------|----------------|---------|
| | kg/sec | lbm/sec | kcal/kg | Btu/lbm |
| 16.257 | 5,794.29 | 12,774.28 | 281.39 | 506.53 |
| 16.505 | 5,416.53 | 11,941.46 | 273.92 | 493.08 |
| 16.753 | 4,955.88 | 10,925.90 | 268.62 | 483.55 |
| 17.007 | 4,447.82 | 9,805.81 | 263.22 | 473.82 |
| 17.251 | 3,984.08 | 8,783.44 | 258.14 | 464.68 |
| 17.500 | 3,606.06 | 7,950.04 | 253.32 | 456.00 |
| 17.750 | 3,263.42 | 7,194.64 | 248.40 | 447.14 |
| 18.000 | 3,088.10 | 6,808.13 | 245.86 | 442.57 |
| 18.249 | 1,743.93 | 3,844.73 | 240.28 | 432.53 |
| 18.509 | 1,671.14 | 3,684.24 | 240.44 | 432.82 |
| 18.752 | 1,508.29 | 3,325.24 | 243.71 | 438.70 |
| 19.002 | 1,297.66 | 2,860.86 | 243.27 | 437.91 |
| 19.254 | 1,091.70 | 2,406.81 | 244.26 | 439.70 |
| 19.508 | 882.79 | 1,946.23 | 247.16 | 444.92 |
| 19.752 | 678.35 | 1,495.51 | 254.14 | 457.48 |

Integral Mass and Energy Release at End of Blowdown

| Time (sec) | Integral Mass | | Integral Energy | |
|------------|---------------|------------|-----------------|-------------|
| | kg | lbm | Million kcal | Million Btu |
| 19.752 | 322,456.13 | 710,897.80 | 112.812 | 447.702 |

APR1400 DCD TIER 2

Table 6.2.1-7 (4 of 23)

Insert this page.

Part A. Mass and Energy Release Data
(Reflood and Post-reflood Period)

| Time (sec) | Break Mass Flow Rate | | Break Enthalpy | |
|------------|----------------------|---------|----------------|----------|
| | kg/sec | lbm/sec | kcal/kg | Btu/lbm |
| 19.75 | 0.00 | 0.00 | 0.00 | 0.00 |
| 19.85 | 50.46 | 111.24 | 727.54 | 1,309.65 |
| 21.85 | 76.60 | 168.87 | 727.13 | 1,308.90 |
| 23.85 | 229.76 | 506.53 | 726.03 | 1,306.93 |
| 27.85 | 408.58 | 900.77 | 724.62 | 1,304.39 |
| 28.55 | 433.51 | 955.72 | 724.34 | 1,303.89 |
| 28.65 | 436.93 | 963.28 | 724.30 | 1,303.82 |
| 28.75 | 255.41 | 563.08 | 724.26 | 1,303.75 |
| 28.85 | 256.64 | 565.79 | 724.24 | 1,303.71 |
| 32.85 | 254.15 | 560.31 | 723.97 | 1,303.23 |
| 36.85 | 250.99 | 553.34 | 723.64 | 1,302.63 |
| 40.85 | 247.78 | 546.27 | 723.30 | 1,302.02 |
| 44.85 | 244.85 | 539.80 | 722.96 | 1,301.40 |
| 49.15 | 241.90 | 533.30 | 722.57 | 1,300.69 |
| 49.25 | 241.83 | 533.15 | 722.56 | 1,300.68 |
| 49.35 | 416.76 | 918.81 | 722.56 | 1,300.68 |
| 49.45 | 416.63 | 918.52 | 722.55 | 1,300.66 |
| 79.45 | 385.59 | 850.08 | 719.55 | 1,295.26 |
| 109.45 | 356.98 | 787.02 | 716.23 | 1,289.28 |
| 139.45 | 328.85 | 724.99 | 712.79 | 1,283.09 |
| 169.45 | 300.87 | 663.30 | 709.38 | 1,276.96 |
| 199.95 | 272.47 | 600.70 | 706.10 | 1,271.06 |
| 200.05 | 272.38 | 600.49 | 706.10 | 1,271.05 |
| 200.15 | 272.29 | 600.29 | 706.08 | 1,271.02 |
| 210.15 | 272.75 | 601.31 | 704.70 | 1,268.53 |
| 220.15 | 273.26 | 602.43 | 703.31 | 1,266.04 |
| 230.15 | 273.93 | 603.91 | 701.86 | 1,263.41 |
| 246.95 | 275.25 | 606.82 | 699.31 | 1,258.82 |

APR1400 DCD TIER 2

Table 6.2.1-7 (5 of 23)

Insert this page.

Part A. Mass and Energy Release Data
(Reflood and Post-reflood Period)

| Time (sec) | Break Mass Flow Rate | | Break Enthalpy | |
|------------|----------------------|---------|----------------|----------|
| | kg/sec | lbm/sec | kcal/kg | Btu/lbm |
| 247.05 | 275.64 | 607.68 | 699.27 | 1,258.75 |
| 247.15 | 273.77 | 603.57 | 686.19 | 1,235.21 |
| 247.25 | 283.48 | 624.98 | 684.90 | 1,232.90 |
| 247.65 | 274.30 | 604.73 | 680.04 | 1,224.14 |
| 248.55 | 274.81 | 605.85 | 668.64 | 1,203.62 |
| 253.05 | 234.50 | 516.98 | 653.81 | 1,176.93 |
| 257.55 | 209.07 | 460.93 | 653.82 | 1,176.94 |
| 262.05 | 196.51 | 433.23 | 653.82 | 1,176.94 |
| 262.35 | 195.92 | 431.93 | 653.81 | 1,176.93 |
| 262.45 | 195.72 | 431.50 | 653.82 | 1,176.94 |
| 266.55 | 190.02 | 418.93 | 653.81 | 1,176.93 |
| 271.05 | 185.57 | 409.12 | 653.82 | 1,176.94 |
| 274.85 | 183.11 | 403.69 | 653.82 | 1,176.95 |
| 274.95 | 182.83 | 403.08 | 653.82 | 1,176.95 |
| 289.95 | 129.09 | 284.60 | 653.81 | 1,176.93 |
| 304.95 | 107.41 | 236.81 | 653.80 | 1,176.91 |
| 319.95 | 93.97 | 207.17 | 653.82 | 1,176.94 |
| 334.95 | 83.80 | 184.75 | 653.82 | 1,176.94 |
| 349.95 | 75.45 | 166.35 | 653.80 | 1,176.90 |
| 364.95 | 68.51 | 151.05 | 653.80 | 1,176.91 |
| 374.35 | 78.66 | 173.41 | 653.83 | 1,176.96 |
| 374.45 | 78.72 | 173.54 | 653.82 | 1,176.94 |
| 379.45 | 74.06 | 163.28 | 653.82 | 1,176.94 |
| 384.45 | 70.18 | 154.72 | 653.81 | 1,176.93 |
| 389.45 | 67.24 | 148.23 | 653.83 | 1,176.96 |
| 394.45 | 65.53 | 144.46 | 653.82 | 1,176.95 |
| 399.45 | 64.47 | 142.13 | 653.79 | 1,176.90 |
| 405.85 | 63.85 | 140.77 | 653.83 | 1,176.95 |

APR1400 DCD TIER 2

Table 6.2.1-7 (6 of 23)

Insert this page.

Part A. Mass and Energy Release Data
(Reflood and Post-reflood Period)

| Time (sec) | Break Mass Flow Rate | | Break Enthalpy | |
|------------|----------------------|---------|----------------|----------|
| | kg/sec | lbm/sec | kcal/kg | Btu/lbm |
| 425.85 | 64.75 | 142.76 | 653.80 | 1,176.90 |
| 445.85 | 67.12 | 147.97 | 653.83 | 1,176.96 |
| 465.85 | 69.62 | 153.49 | 653.82 | 1,176.94 |
| 485.85 | 71.92 | 158.56 | 653.83 | 1,176.96 |
| 505.85 | 73.95 | 163.04 | 653.81 | 1,176.93 |
| 528.45 | 76.44 | 168.52 | 653.83 | 1,176.96 |
| 528.55 | 76.52 | 168.70 | 653.81 | 1,176.93 |
| 529.45 | 77.17 | 170.13 | 653.83 | 1,176.96 |
| 532.95 | 68.66 | 151.38 | 653.83 | 1,176.96 |
| 536.45 | 64.15 | 141.42 | 653.83 | 1,176.97 |
| 539.95 | 61.13 | 134.78 | 653.82 | 1,176.94 |
| 543.45 | 58.98 | 130.04 | 653.84 | 1,176.98 |
| 546.95 | 57.37 | 126.47 | 653.84 | 1,176.98 |
| 550.15 | 56.20 | 123.89 | 653.80 | 1,176.90 |
| 550.25 | 56.16 | 123.81 | 653.84 | 1,176.97 |

Integral Mass and Energy Release at the End of Reflood and Post-reflood

| Time (sec) | Integral Mass | | Integral Energy | |
|------------|---------------|------------|-----------------|-------------|
| | kg | lbm | Million kcal | Million Btu |
| 200.05 | 59,010.25 | 130,096.00 | 42.259 | 167.709 |
| 550.25 | 102,740.41 | 226,505.00 | 71.493 | 283.724 |

APR1400 DCD TIER 2

Table 6.2.1-7 (7 of 23)

Insert this page.

Double-Ended Discharge Leg Slot Break – Minimum SIS Flow

Part A: Spillage Release Data (Reactor Vessel Side)
(Reflood and Post-Reflood Period)

| Time (sec) | Break Mass Flow Rate | | Break Enthalpy | |
|---------------|----------------------|----------|----------------|---------|
| | kg/sec | lbm/sec | kcal/kg | Btu/lbm |
| 19.75 | 0.00 | 0.00 | 0.00 | 0.00 |
| 19.85 | 0.00 | 0.00 | 0.00 | 0.00 |
| 28.65 | 0.00 | 0.00 | 0.00 | 0.00 |
| 28.75 | 986.45 | 2,174.76 | 176.31 | 317.37 |
| 28.85 | 1,872.03 | 4,127.15 | 116.81 | 210.27 |
| 32.85 | 1,726.42 | 3,806.12 | 121.75 | 219.17 |
| 36.85 | 1,600.83 | 3,529.25 | 126.42 | 227.57 |
| 40.85 | 1,499.94 | 3,306.81 | 130.52 | 234.94 |
| 44.85 | 1,411.52 | 3,111.89 | 134.53 | 242.18 |
| 49.15 | 1,327.73 | 2,927.16 | 138.77 | 249.79 |
| 49.25 | 1,325.90 | 2,923.13 | 138.86 | 249.97 |
| 49.35 | 324.11 | 714.55 | 50.28 | 90.51 |
| 49.45 | 323.83 | 713.93 | 50.28 | 90.51 |
| 79.45 | 270.52 | 596.39 | 50.58 | 91.04 |
| 109.45 | 237.67 | 523.97 | 50.85 | 91.53 |
| 139.45 | 219.98 | 484.98 | 51.11 | 92.00 |
| 169.45 | 212.82 | 469.20 | 51.39 | 92.50 |
| 199.95 | 213.23 | 470.09 | 51.68 | 93.03 |
| 200.05 | 213.24 | 470.12 | 51.68 | 93.03 |
| 200.15 | 301.46 | 664.62 | 51.68 | 93.03 |
| 210.15 | 286.33 | 631.25 | 51.79 | 93.23 |
| 220.15 | 272.37 | 600.47 | 51.90 | 93.43 |
| 230.15 | 258.72 | 570.38 | 52.02 | 93.64 |
| 246.95 | 236.57 | 521.54 | 52.22 | 94.01 |
| 247.05 | 234.20 | 516.32 | 52.23 | 94.01 |
| 247.15 | 226.72 | 499.84 | 52.23 | 94.01 |
| 247.25 | 183.93 | 405.49 | 52.23 | 94.02 |
| 247.65 | 208.32 | 459.26 | 52.23 | 94.02 |

APR1400 DCD TIER 2

Table 6.2.1-7 (8 of 23)

Insert this page.

Double-Ended Discharge Leg Slot Break – Minimum SIS Flow

Part A: Spillage Release Data (Reactor Vessel Side)
(Reflood and Post-Reflood Period)

| Time (sec) | Break Mass Flow Rate | | Break Enthalpy | |
|---------------|----------------------|---------|----------------|---------|
| | kg/sec | lbm/sec | kcal/kg | Btu/lbm |
| 248.55 | 204.47 | 450.78 | 52.23 | 94.03 |
| 253.05 | 129.18 | 284.79 | 52.28 | 94.10 |
| 257.55 | 54.73 | 120.65 | 52.34 | 94.22 |
| 262.05 | 3.19 | 7.03 | 52.41 | 94.34 |
| 262.35 | 0.37 | 0.82 | 52.44 | 94.39 |
| 262.45 | 0.00 | 0.00 | 0.00 | 0.00 |
| 550.15 | 0.00 | 0.00 | 0.00 | 0.00 |
| 550.25 | 0.00 | 0.00 | 0.00 | 0.00 |

Integral Mass and Energy (Reactor Vessel Side Spillage) at EOR and EOPR

| Time (sec) | Integral Mass | | Integral Energy | |
|---------------|---------------|------------|-----------------|-------------|
| | kg | lbm | Million kcal | Million Btu |
| 200.05 | 68,427.23 | 150,857.00 | 5.959 | 23.647 |
| 550.25 | 82,632.76 | 182,175.00 | 6.697 | 26.578 |

APR1400 DCD TIER 2

Table 6.2.1-7 (9 of 23)

Insert this page.

Double-Ended Discharge Leg Slot Break – Minimum SIS Flow

Part A: Spillage Release Data (Steam Generator Side)
(Reflood and Post-Reflood Period)

| Time (sec) | Break Mass Flow Rate | | Break Enthalpy | |
|---------------|----------------------|----------|----------------|---------|
| | kg/sec | lbm/sec | kcal/kg | Btu/lbm |
| 19.75 | 0.00 | 0.00 | 0.00 | 0.00 |
| 19.85 | 0.00 | 0.00 | 0.00 | 0.00 |
| 247.05 | 0.00 | 0.00 | 0.00 | 0.00 |
| 247.15 | 3.46 | 7.62 | 144.30 | 259.75 |
| 247.25 | 2.26 | 4.98 | 144.22 | 259.62 |
| 247.65 | 16.02 | 35.31 | 144.34 | 259.83 |
| 248.55 | 26.69 | 58.85 | 144.32 | 259.80 |
| 253.05 | 135.10 | 297.85 | 144.33 | 259.81 |
| 257.55 | 231.30 | 509.93 | 144.33 | 259.81 |
| 262.05 | 293.00 | 645.95 | 144.33 | 259.81 |
| 262.35 | 296.25 | 653.13 | 144.33 | 259.81 |
| 262.45 | 297.32 | 655.49 | 144.33 | 259.81 |
| 266.55 | 324.40 | 715.19 | 144.33 | 259.81 |
| 271.05 | 335.42 | 739.47 | 144.33 | 259.81 |
| 274.85 | 340.94 | 751.64 | 144.33 | 259.81 |
| 274.95 | 337.42 | 743.89 | 144.33 | 259.81 |
| 289.95 | 317.89 | 700.84 | 144.33 | 259.81 |
| 304.95 | 539.76 | 1,189.97 | 144.33 | 259.81 |
| 319.95 | 508.57 | 1,121.21 | 144.33 | 259.81 |
| 334.95 | 490.80 | 1,082.03 | 144.33 | 259.81 |
| 349.95 | 474.51 | 1,046.11 | 144.33 | 259.81 |
| 364.95 | 463.03 | 1,020.81 | 144.33 | 259.81 |
| 374.35 | 144.86 | 319.36 | 144.33 | 259.81 |
| 374.45 | 145.27 | 320.26 | 144.33 | 259.81 |
| 379.45 | 136.41 | 300.73 | 144.33 | 259.80 |
| 384.45 | 135.43 | 298.57 | 144.33 | 259.81 |
| 389.45 | 134.49 | 296.50 | 144.33 | 259.81 |
| 394.45 | 131.00 | 288.81 | 144.33 | 259.80 |

APR1400 DCD TIER 2

Table 6.2.1-7 (10 of 23)

Insert this page.

Double-Ended Discharge Leg Slot Break – Minimum SIS Flow

Part A: Spillage Release Data (Steam Generator Side)
(Reflood and Post-Reflood Period)

| Time (sec) | Break Mass Flow Rate | | Break Enthalpy | |
|---------------|----------------------|---------|----------------|---------|
| | kg/sec | lbm/sec | kcal/kg | Btu/lbm |
| 399.45 | 129.78 | 286.11 | 144.33 | 259.81 |
| 405.85 | 128.56 | 283.43 | 144.33 | 259.81 |
| 425.85 | 125.37 | 276.39 | 144.33 | 259.80 |
| 445.85 | 122.71 | 270.53 | 144.33 | 259.81 |
| 465.85 | 120.46 | 265.57 | 144.33 | 259.81 |
| 485.85 | 118.55 | 261.35 | 144.33 | 259.80 |
| 505.85 | 116.91 | 257.75 | 144.33 | 259.81 |
| 528.45 | 116.80 | 257.50 | 144.33 | 259.81 |
| 528.55 | 116.86 | 257.63 | 144.33 | 259.80 |
| 529.45 | 117.40 | 258.83 | 144.33 | 259.81 |
| 532.95 | 131.60 | 290.13 | 144.33 | 259.80 |
| 536.45 | 136.29 | 300.47 | 144.33 | 259.81 |
| 539.95 | 138.88 | 306.19 | 144.33 | 259.81 |
| 543.45 | 140.24 | 309.18 | 144.33 | 259.81 |
| 546.95 | 140.95 | 310.74 | 144.33 | 259.81 |
| 550.15 | 141.31 | 311.54 | 144.33 | 259.80 |
| 550.25 | 141.32 | 311.55 | 144.33 | 259.81 |

Integral Mass and Energy (Steam Generator Side Spillage) at EOR and EOPR

| Time (sec) | Integral Mass | | Integral Energy | |
|---------------|---------------|------------|-----------------|-------------|
| | kg | lbm | Million kcal | Million Btu |
| 200.05 | 0.00 | 0.00 | 0.000 | 0.000 |
| 550.25 | 65,224.88 | 143,797.00 | 9.414 | 37.360 |

APR1400 DCD TIER 2

Table 6.2.1-7 (11 of 23)

Insert this page.

Part A. Mass and energy (Steam) Release Data (Decay heat Period)

| Time (sec) | Mass Flow Rate | | Break Enthalpy | |
|------------|----------------|---------|----------------|---------|
| | kg/sec | lbm/sec | Kcal/kg | Btu/lbm |
| 599.9 | 58.09 | 128.07 | 654.83 | 1178.7 |
| 800.0 | 47.19 | 104.04 | 654.5 | 1178.1 |
| 999.0 | 45.77 | 100.91 | 654.2 | 1177.55 |
| 1503.0 | 42.8 | 94.36 | 653.64 | 1176.55 |
| 1997.0 | 40.8 | 89.95 | 653.27 | 1175.89 |
| 4004.0 | 33.75 | 74.41 | 652.49 | 1174.49 |
| 6002.6 | 30.57 | 67.4 | 652.1 | 1173.78 |
| 8002.3 | 29.06 | 64.06 | 651.88 | 1173.39 |
| 9993.7 | 26.78 | 59.03 | 651.75 | 1173.14 |
| 15005.5 | 24.45 | 53.9 | 651.52 | 1172.73 |
| 20011.6 | 22.7 | 50.04 | 651.28 | 1172.3 |
| 40038.2 | 18.78 | 41.39 | 650.11 | 1170.2 |
| 59966.1 | 16.6 | 36.6 | 648.92 | 1168.06 |
| 79996.1 | 15.21 | 33.53 | 648.0 | 1166.4 |
| 100002.3 | 14.4 | 31.74 | 647.36 | 1165.24 |
| 150010.2 | 12.95 | 28.54 | 646.37 | 1163.46 |
| 200018.3 | 11.73 | 25.86 | 645.73 | 1162.31 |
| 400053.1 | 9.21 | 20.3 | 644.5 | 1160.1 |
| 600094.4 | 7.86 | 17.33 | 643.88 | 1158.98 |
| 800133.6 | 6.99 | 15.4 | 643.5 | 1158.31 |
| 1000000.0 | 6.38 | 14.06 | 643.25 | 1157.85 |

Integral Mass and Energy Release(Steam) at 24 hours and End of Analysis

| Time (sec) | Integral Mass | | Integral Energy | |
|------------|---------------|------------|-----------------|-------------|
| | kg | lbm | Million kcal | Million Btu |
| 85,002 | 1,832,345 | 4,039,630 | 1,197.195 | 4,349.710 |
| 1,000,000 | 9,963,099 | 21,964,874 | 6,442.147 | 25,564.503 |

APR1400 DCD TIER 2

Table 6.2.1-7 (12 of 23)

Insert this page.

Part A. Mass and Energy (Spillage) Release Data (Decay heat Period)

| Time (sec) | Mass Flow Rate | | Break Enthalpy | |
|------------|----------------|---------|----------------|---------|
| | kg/sec | lbm/sec | kcal/kg | Btu/lbm |
| 599.9 | 39.67 | 87.46 | 115.23 | 207.42 |
| 800.0 | 101.57 | 223.93 | 77.33 | 139.19 |
| 999.0 | 110.18 | 242.9 | 72.24 | 130.04 |
| 1503.0 | 131.13 | 289.1 | 75.81 | 136.46 |
| 1997.0 | 142.18 | 313.44 | 80.72 | 145.29 |
| 4004.0 | 151.81 | 334.68 | 97.18 | 174.92 |
| 6002.6 | 154.2 | 339.96 | 106.64 | 191.94 |
| 8002.3 | 155.49 | 342.8 | 112.26 | 202.08 |
| 9993.7 | 156.43 | 344.86 | 115.67 | 208.21 |
| 15005.5 | 158.2 | 348.78 | 119.44 | 214.99 |
| 20011.6 | 159.66 | 351.98 | 120.13 | 216.23 |
| 40038.2 | 163.94 | 361.43 | 115.89 | 208.6 |
| 59966.1 | 166.96 | 368.08 | 109.69 | 197.43 |
| 79996.1 | 169.07 | 372.74 | 104.36 | 187.85 |
| 100002.3 | 170.43 | 375.74 | 100.34 | 180.62 |
| 150010.2 | 172.73 | 380.81 | 94.12 | 169.41 |
| 200018.3 | 174.29 | 384.24 | 89.89 | 161.8 |
| 400053.1 | 177.54 | 391.4 | 81.16 | 146.1 |
| 600094.4 | 179.23 | 395.14 | 76.24 | 137.24 |
| 800133.6 | 180.29 | 397.47 | 73.15 | 131.68 |
| 1000000.0 | 181.01 | 399.06 | 71.0 | 127.8 |

Integral Mass and Energy Release (Spillage) at 24 hours and End of Analysis

| Time (sec) | Integral Mass | | Integral Energy | |
|------------|---------------|-------------|-----------------|-------------|
| | kg | lbm | Million kcal | Million Btu |
| 85,002 | 13,876,652 | 30,592,781 | 1,546.831 | 6,138.321 |
| 1,000,000 | 176,647,364 | 389,440,774 | 14,531.359 | 57,665.089 |

APR1400 DCD TIER 2

Table 6.2.1-7 (13 of 23)

Insert this page.

**Part B. Reactor Vessel Pressure vs. Time
(Blowdown Period)**

| Time (sec) | Reactor Vessel Pressure | |
|------------|-------------------------|----------|
| | kg/cm ² A | psia |
| 0.000 | 167.360 | 2,380.40 |
| 0.026 | 147.360 | 2,096.00 |
| 0.051 | 131.970 | 1,877.00 |
| 0.102 | 124.440 | 1,770.00 |
| 0.150 | 126.550 | 1,799.90 |
| 0.205 | 123.280 | 1,753.50 |
| 0.251 | 124.390 | 1,769.20 |
| 0.303 | 122.240 | 1,738.60 |
| 0.355 | 121.610 | 1,729.70 |
| 0.455 | 119.600 | 1,701.10 |
| 0.548 | 118.700 | 1,688.30 |
| 0.655 | 117.750 | 1,674.80 |
| 0.751 | 116.290 | 1,654.00 |
| 0.850 | 115.400 | 1,641.40 |
| 0.952 | 114.580 | 1,629.70 |
| 1.256 | 107.300 | 1,526.10 |
| 1.500 | 106.660 | 1,517.00 |
| 1.749 | 101.420 | 1,442.50 |
| 2.001 | 99.780 | 1,419.20 |
| 2.253 | 96.330 | 1,370.10 |
| 2.513 | 95.120 | 1,352.90 |
| 2.753 | 93.450 | 1,329.20 |
| 3.013 | 91.670 | 1,303.90 |
| 3.253 | 90.120 | 1,281.80 |
| 3.513 | 88.880 | 1,264.20 |
| 3.753 | 87.480 | 1,244.20 |
| 4.013 | 86.210 | 1,226.20 |

APR1400 DCD TIER 2

Table 6.2.1-7 (14 of 23)

Insert this page.

**Part B. Reactor Vessel Pressure vs. Time
(Blowdown Period)**

| Time (sec) | Reactor Vessel Pressure | |
|------------|-------------------------|----------|
| | kg/cm ² A | psia |
| 4.513 | 84.160 | 1,197.00 |
| 5.013 | 82.180 | 1,168.90 |
| 5.513 | 80.350 | 1,142.80 |
| 6.013 | 78.810 | 1,120.90 |
| 6.513 | 76.680 | 1,090.70 |
| 7.013 | 74.800 | 1,063.90 |
| 7.505 | 71.970 | 1,023.70 |
| 8.014 | 70.510 | 1,002.90 |
| 8.513 | 68.090 | 968.43 |
| 9.013 | 66.110 | 940.35 |
| 9.513 | 64.050 | 910.98 |
| 10.013 | 61.900 | 880.49 |
| 10.513 | 58.870 | 837.39 |
| 11.013 | 55.490 | 789.25 |
| 11.513 | 50.790 | 722.45 |
| 12.013 | 46.480 | 661.04 |
| 12.513 | 41.990 | 597.21 |
| 13.013 | 38.250 | 544.01 |
| 13.513 | 34.690 | 493.40 |
| 14.009 | 31.030 | 441.40 |
| 14.507 | 27.720 | 394.32 |
| 15.017 | 24.580 | 349.64 |
| 15.257 | 23.270 | 330.97 |
| 15.503 | 21.850 | 310.76 |
| 15.753 | 20.290 | 288.64 |
| 16.008 | 18.750 | 266.73 |
| 16.257 | 17.220 | 244.90 |

APR1400 DCD TIER 2

Table 6.2.1-7 (15 of 23)

Insert this page.

Part B. Reactor Vessel Pressure vs. Time
(Blowdown Period)

| Time (sec) | Reactor Vessel Pressure | |
|---------------|-------------------------|--------|
| | kg/cm ² A | psia |
| 16.505 | 15.700 | 223.25 |
| 16.753 | 14.160 | 201.46 |
| 17.007 | 12.680 | 180.32 |
| 17.251 | 11.370 | 161.79 |
| 17.500 | 10.200 | 145.11 |
| 17.750 | 9.100 | 129.40 |
| 18.000 | 8.150 | 115.88 |
| 18.249 | 7.340 | 104.41 |
| 18.509 | 6.610 | 94.06 |
| 18.752 | 6.050 | 86.09 |
| 19.002 | 5.560 | 79.01 |
| 19.254 | 5.120 | 72.85 |
| 19.508 | 4.730 | 67.23 |
| 19.752 | 4.410 | 62.76 |

APR1400 DCD TIER 2

Table 6.2.1-7 (16 of 23)

Insert this page.

Part B. Reactor Vessel Pressure vs. Time
(Reflood and Post-reflood Period)

| Time (sec) | Reactor Vessel Pressure | |
|------------|-------------------------|--------|
| | kg/cm ² A | psia |
| 19.75 | 4.080 | 58.000 |
| 19.85 | 4.090 | 58.160 |
| 21.85 | 4.120 | 58.600 |
| 23.85 | 4.440 | 63.150 |
| 27.85 | 5.140 | 73.070 |
| 28.55 | 5.260 | 74.750 |
| 28.65 | 5.270 | 74.990 |
| 28.75 | 5.290 | 75.230 |
| 28.85 | 5.300 | 75.360 |
| 32.85 | 5.280 | 75.030 |
| 36.85 | 5.250 | 74.630 |
| 40.85 | 5.220 | 74.230 |
| 44.85 | 5.190 | 73.860 |
| 49.15 | 5.170 | 73.500 |
| 49.25 | 5.170 | 73.490 |
| 49.35 | 5.170 | 73.480 |
| 49.45 | 5.170 | 73.470 |
| 79.45 | 5.010 | 71.280 |
| 109.45 | 4.880 | 69.380 |
| 139.45 | 4.760 | 67.640 |
| 169.45 | 4.640 | 66.050 |
| 199.95 | 4.540 | 64.580 |
| 200.05 | 4.540 | 64.570 |
| 200.15 | 4.540 | 64.570 |
| 210.15 | 4.540 | 64.550 |
| 220.15 | 4.540 | 64.540 |
| 230.15 | 4.540 | 64.530 |
| 246.95 | 4.540 | 64.520 |

APR1400 DCD TIER 2

Table 6.2.1-7 (17 of 23)

Insert this page.

Part B. Reactor Vessel Pressure vs. Time
(Reflood and Post-reflood Period)

| Time (sec) | Reactor Vessel Pressure | |
|------------|-------------------------|--------|
| | kg/cm ² A | psia |
| 247.05 | 4.540 | 64.540 |
| 247.15 | 4.540 | 64.600 |
| 247.25 | 4.530 | 64.500 |
| 247.65 | 4.540 | 64.510 |
| 248.55 | 4.520 | 64.230 |
| 253.05 | 4.490 | 63.880 |
| 257.55 | 4.500 | 63.970 |
| 262.05 | 4.500 | 64.020 |
| 262.35 | 4.500 | 64.030 |
| 262.45 | 4.500 | 64.030 |
| 266.55 | 4.500 | 64.000 |
| 271.05 | 4.490 | 63.890 |
| 274.85 | 4.480 | 63.780 |
| 274.95 | 4.480 | 63.770 |
| 289.95 | 4.430 | 63.020 |
| 304.95 | 4.370 | 62.190 |
| 319.95 | 4.310 | 61.260 |
| 334.95 | 4.270 | 60.710 |
| 349.95 | 4.240 | 60.310 |
| 364.95 | 4.220 | 60.000 |
| 374.35 | 4.160 | 59.120 |
| 374.45 | 4.160 | 59.110 |
| 379.45 | 4.150 | 58.990 |
| 384.45 | 4.140 | 58.910 |
| 389.45 | 4.140 | 58.850 |
| 394.45 | 4.130 | 58.800 |
| 399.45 | 4.130 | 58.780 |
| 405.85 | 4.130 | 58.760 |

APR1400 DCD TIER 2

Table 6.2.1-7 (18 of 23)

Insert this page.

Part B. Reactor Vessel Pressure vs. Time
(Reflood and Post-reflood Period)

| Time (sec) | Reactor Vessel Pressure | |
|------------|-------------------------|--------|
| | kg/cm ² A | psia |
| | | |
| 425.85 | 4.130 | 58.770 |
| 445.85 | 4.130 | 58.810 |
| 465.85 | 4.140 | 58.850 |
| 485.85 | 4.140 | 58.880 |
| 505.85 | 4.140 | 58.920 |
| 528.45 | 4.150 | 58.960 |
| 528.55 | 4.150 | 58.970 |
| 529.45 | 4.150 | 58.980 |
| 532.95 | 4.140 | 58.950 |
| 536.45 | 4.140 | 58.910 |
| 539.95 | 4.140 | 58.880 |
| 543.45 | 4.140 | 58.850 |
| 546.95 | 4.140 | 58.820 |
| 550.15 | 4.130 | 58.810 |
| 550.25 | 4.130 | 58.810 |

APR1400 DCD TIER 2

Table 6.2.1-7 (19 of 23)

Insert this page.

Part B. Reactor Vessel Pressure vs. Time (Decay heat Period)

| Time (sec) | Reactor Vessel Pressure | |
|------------|-------------------------|--------|
| | kg/cm ² A | psia |
| 599.9 | 4.469 | 63.56 |
| 800.0 | 4.33 | 61.585 |
| 999.0 | 4.21 | 59.883 |
| 1503.0 | 3.998 | 56.858 |
| 1997.0 | 3.863 | 54.947 |
| 4004.0 | 3.593 | 51.105 |
| 6002.6 | 3.465 | 49.282 |
| 8002.3 | 3.396 | 48.297 |
| 9993.7 | 3.353 | 47.693 |
| 15005.5 | 3.284 | 46.71 |
| 20011.6 | 3.211 | 45.67 |
| 40038.2 | 2.884 | 41.019 |
| 59966.1 | 2.585 | 36.768 |
| 79996.1 | 2.374 | 33.772 |
| 100002.3 | 2.238 | 31.83 |
| 150010.2 | 2.042 | 29.05 |
| 200018.3 | 1.925 | 27.387 |
| 400053.1 | 1.718 | 24.433 |
| 600094.4 | 1.621 | 23.05 |
| 800133.6 | 1.565 | 22.261 |
| 1000000.0 | 1.529 | 21.745 |

APR1400 DCD TIER 2

Table 6.2.1-7 (20 of 23)

Insert this page.

Part C. Safety Injection Flow vs. Time
(Blowdown Period)

| Time (sec) | Safety Injection Tank Flow | |
|---------------|----------------------------|-----------|
| | kg/sec | kg/sec |
| 0.000 | 0.00 | 0.00 |
| 0.026 | 0.00 | 0.00 |
| 11.513 | 0.00 | 0.00 |
| 12.013 | 0.00 | 0.00 |
| 12.513 | 2,164.62 | 4,772.20 |
| 13.013 | 2,786.54 | 6,143.30 |
| 13.513 | 3,212.60 | 7,082.60 |
| 14.009 | 3,589.48 | 7,913.50 |
| 14.507 | 3,867.31 | 8,526.00 |
| 15.017 | 4,094.01 | 9,025.80 |
| 15.257 | 4,166.59 | 9,185.80 |
| 15.503 | 4,261.98 | 9,396.10 |
| 15.753 | 4,377.01 | 9,649.70 |
| 16.008 | 4,487.23 | 9,892.70 |
| 16.257 | 4,598.95 | 10,139.00 |
| 16.505 | 4,710.99 | 10,386.00 |
| 16.753 | 4,823.48 | 10,634.00 |
| 17.007 | 4,925.99 | 10,860.00 |
| 17.251 | 5,008.54 | 11,042.00 |
| 17.500 | 5,074.31 | 11,187.00 |
| 17.750 | 5,130.56 | 11,311.00 |
| 18.000 | 5,170.47 | 11,399.00 |
| 18.249 | 5,196.33 | 11,456.00 |
| 18.509 | 5,209.93 | 11,486.00 |
| 18.752 | 5,210.84 | 11,488.00 |
| 19.002 | 5,203.58 | 11,472.00 |
| 19.254 | 5,192.24 | 11,447.00 |
| 19.508 | 5,176.37 | 11,412.00 |
| 19.752 | 5,157.32 | 11,370.00 |

APR1400 DCD TIER 2

Table 6.2.1-7 (21 of 23)

Insert this page.

Part C Safety Injection Flow vs. Time
(Reflood and Post-reflood Period)

| Time (sec) | Safety Injection Tank Flow | | Safety Injection Pump Flow | |
|---------------|----------------------------|----------|----------------------------|---------|
| | kg/sec | lbm/sec | kg/sec | lbm/sec |
| 19.752 | 2,681.59 | 5,911.91 | 193.78 | 427.22 |
| 19.852 | 2,674.22 | 5,895.68 | 193.78 | 427.22 |
| 20.852 | 2,600.43 | 5,733.00 | 193.75 | 427.14 |
| 21.852 | 2,535.24 | 5,589.28 | 193.75 | 427.15 |
| 22.852 | 2,463.84 | 5,431.85 | 193.64 | 426.91 |
| 23.852 | 2,393.77 | 5,277.40 | 193.51 | 426.62 |
| 24.852 | 2,326.43 | 5,128.93 | 193.37 | 426.32 |
| 25.852 | 2,261.52 | 4,985.83 | 193.23 | 426.00 |
| 26.852 | 2,198.87 | 4,847.70 | 193.09 | 425.69 |
| 27.852 | 2,138.56 | 4,714.74 | 192.95 | 425.38 |
| 28.652 | 2,091.94 | 4,611.97 | 192.84 | 425.14 |
| 28.752 | 2,086.21 | 4,599.33 | 192.82 | 425.11 |
| 32.752 | 1,933.08 | 4,261.74 | 192.82 | 425.10 |
| 36.752 | 1,807.01 | 3,983.81 | 192.84 | 425.15 |
| 40.152 | 1,714.27 | 3,779.35 | 192.86 | 425.19 |
| 40.252 | 1,711.71 | 3,773.70 | 192.86 | 425.19 |
| 40.352 | 1,709.16 | 3,768.07 | 192.86 | 425.20 |
| 40.452 | 1,706.61 | 3,762.46 | 192.87 | 425.20 |
| 55.452 | 662.09 | 1,459.67 | 192.94 | 425.36 |
| 70.452 | 613.39 | 1,352.30 | 193.00 | 425.50 |
| 85.452 | 571.93 | 1,260.91 | 193.06 | 425.62 |
| 100.452 | 536.11 | 1,181.94 | 193.11 | 425.74 |
| 115.452 | 504.77 | 1,112.84 | 193.16 | 425.86 |
| 130.452 | 477.06 | 1,051.74 | 193.21 | 425.97 |
| 145.452 | 452.31 | 997.19 | 193.26 | 426.07 |
| 160.452 | 430.04 | 948.08 | 193.31 | 426.17 |
| 175.452 | 409.83 | 903.53 | 193.35 | 426.27 |
| 190.452 | 391.38 | 862.84 | 193.39 | 426.36 |

APR1400 DCD TIER 2

Table 6.2.1-7 (22 of 23)

Insert this page.

Part C. Safety Injection Flow vs. Time (Reflood and Post-reflood Period)

| Time (sec) | Safety Injection Tank Flow | | Safety Injection Pump Flow | |
|------------|----------------------------|---------|----------------------------|---------|
| | kg/sec | lbm/sec | kg/sec | lbm/sec |
| 200.052 | 380.36 | 838.55 | 193.42 | 426.41 |
| 215.052 | 359.53 | 792.64 | 193.42 | 426.42 |
| 230.052 | 339.79 | 749.12 | 193.42 | 426.42 |
| 245.052 | 321.06 | 707.83 | 193.42 | 426.42 |
| 260.052 | 307.68 | 678.33 | 193.45 | 426.49 |
| 275.052 | 292.86 | 645.64 | 193.46 | 426.51 |
| 290.052 | 283.60 | 625.24 | 193.50 | 426.61 |
| 305.052 | 275.80 | 608.03 | 193.55 | 426.71 |
| 320.052 | 269.80 | 594.82 | 193.60 | 426.82 |
| 335.052 | 260.71 | 574.76 | 193.63 | 426.89 |
| 350.052 | 250.88 | 553.10 | 193.65 | 426.94 |
| 365.052 | 240.70 | 530.64 | 193.67 | 426.98 |
| 369.352 | 241.72 | 532.91 | 193.70 | 427.03 |
| 369.452 | 238.88 | 526.63 | 193.68 | 427.00 |
| 369.552 | 0.00 | 0.00 | 193.71 | 427.05 |
| 369.652 | 0.00 | 0.00 | 193.71 | 427.05 |
| 439.652 | 0.00 | 0.00 | 193.74 | 427.12 |
| 509.652 | 0.00 | 0.00 | 193.73 | 427.11 |
| 550.252 | 0.00 | 0.00 | 193.74 | 427.12 |
| 580.252 | 0.00 | 0.00 | 193.74 | 427.13 |
| 595.252 | 0.00 | 0.00 | 193.74 | 427.13 |
| 599.952 | 0.00 | 0.00 | 193.74 | 427.13 |

APR1400 DCD TIER 2

Table 6.2.1-7 (23 of 23)

Insert this page.

Part D. Chronology of Events

| Time (sec) | Event | Values |
|------------|--|---|
| 0.0 | Break occurs | — |
| 3.73 | Containment pressure Hi-Hi setpoint | 1.547kgf/cm ² g (22.0psig) |
| 12.01 | Start safety injection tank (SIT) injection | — |
| 16.81 | First peak containment pressure (Blowdown phase) | 3.106kgf/cm ² g (44.18psig) |
| 19.75 | End of blowdown | — |
| | Start SI pump injection | — |
| 49.35 | SIT flow is turned down to low flow by fluidic device in SIT | — |
| 113.73 | Start containment spray actuation | — |
| 200.05 | End of reflood | — |
| 323.43 | Peak containment temperature | 134.88°C (274.78°F) |
| 325.53 | Peak containment pressure | 3.591kgf/cm ² g (51.08psig) |
| 369.55 | Safety injection tank empty | — |
| 550.25 | End of post-reflood | — |
| 43,242.4 | Time of depressurization of the containment at 50 % of peak pressure | 1.795kgf/cm ² g (25.53psig) |

Table 6.2.1-8 (1 of 13)

Double-Ended Hot Leg Slot Break (1.7877 m² (19.2423 ft²) Break Area)Part A. Mass and Energy Release Data
(Blowdown Period)

| Time (sec) | Break Mass Flow Rate | | Break Enthalpy | |
|------------|----------------------|------------|----------------|---------|
| | kg/sec | lbm/sec | kcal/kg | Btu/lbm |
| 0.000 | 0.00 | 0.00 | 0.00 | 0.00 |
| 0.025 | 76,463.94 | 168,575.00 | 358.81 | 645.90 |
| 0.051 | 71,583.69 | 157,815.84 | 357.26 | 643.11 |
| 0.100 | 78,379.65 | 172,798.45 | 358.80 | 645.88 |
| 0.151 | 78,075.82 | 172,128.63 | 359.59 | 647.29 |
| 0.199 | 73,247.67 | 161,484.31 | 359.42 | 646.99 |
| 0.257 | 69,096.98 | 152,333.56 | 359.43 | 647.00 |
| 0.301 | 65,747.36 | 144,948.88 | 359.52 | 647.17 |
| 0.353 | 63,219.10 | 139,374.98 | 359.76 | 647.61 |
| 0.504 | 59,599.23 | 131,394.50 | 360.43 | 648.81 |
| 0.652 | 55,612.68 | 122,605.60 | 361.40 | 650.56 |
| 0.799 | 52,805.95 | 116,417.80 | 362.99 | 653.42 |
| 0.962 | 50,268.79 | 110,824.29 | 365.52 | 657.97 |
| 1.207 | 46,410.82 | 102,318.88 | 368.49 | 663.32 |
| 1.407 | 45,069.94 | 99,362.73 | 367.67 | 661.85 |
| 1.609 | 44,404.87 | 97,896.49 | 365.84 | 658.54 |
| 1.801 | 44,178.17 | 97,396.70 | 363.00 | 653.45 |
| 2.001 | 44,303.25 | 97,672.45 | 359.42 | 646.99 |
| 2.201 | 44,546.16 | 98,207.98 | 355.69 | 640.28 |
| 2.401 | 44,650.70 | 98,438.45 | 352.16 | 633.93 |
| 2.601 | 44,567.73 | 98,255.53 | 349.42 | 628.99 |
| 2.801 | 44,137.88 | 97,307.87 | 347.62 | 625.76 |
| 3.001 | 43,037.65 | 94,882.27 | 347.97 | 626.38 |
| 3.201 | 41,113.16 | 90,639.48 | 350.58 | 631.09 |
| 3.401 | 39,506.41 | 87,097.19 | 353.52 | 636.36 |
| 3.601 | 37,945.09 | 83,655.05 | 356.60 | 641.92 |

Replace these 13 pages of Table 6.2.1–8 with the following 13 pages of revised Table 6.2.1–8.

Table 6.2.1-8 (2 of 13)

Part A. Mass and Energy Release Data
(Blowdown Period)

| Time (sec) | Break Mass Flow Rate | | Break Enthalpy | |
|------------|----------------------|-----------|----------------|---------|
| | kg/sec | lbm/sec | kcal/kg | Btu/lbm |
| 3.801 | 36,414.18 | 80,279.95 | 359.80 | 647.68 |
| 4.001 | 34,945.21 | 77,041.40 | 363.09 | 653.60 |
| 4.201 | 33,502.52 | 73,860.79 | 366.44 | 659.62 |
| 4.401 | 32,343.39 | 71,305.35 | 369.61 | 665.33 |
| 4.601 | 31,165.54 | 68,708.63 | 372.35 | 670.27 |
| 4.801 | 30,087.66 | 66,332.29 | 374.66 | 674.43 |
| 5.001 | 29,021.42 | 63,981.62 | 377.05 | 678.73 |
| 5.201 | 27,888.46 | 61,483.85 | 380.01 | 684.05 |
| 5.401 | 26,727.17 | 58,923.64 | 383.79 | 690.86 |
| 5.601 | 25,533.29 | 56,291.55 | 388.42 | 699.19 |
| 5.801 | 24,260.05 | 53,484.53 | 393.87 | 709.01 |
| 6.001 | 22,940.05 | 50,574.42 | 400.19 | 720.38 |
| 6.201 | 21,641.55 | 47,711.69 | 407.47 | 733.50 |
| 6.401 | 20,399.99 | 44,974.52 | 415.69 | 748.28 |
| 6.601 | 19,210.83 | 42,352.85 | 424.88 | 764.82 |
| 6.801 | 18,114.06 | 39,934.88 | 432.47 | 778.48 |
| 7.001 | 17,563.30 | 38,720.65 | 430.48 | 774.91 |
| 7.201 | 16,242.88 | 35,809.61 | 437.89 | 788.25 |
| 7.401 | 14,396.00 | 31,737.90 | 455.32 | 819.62 |
| 7.601 | 12,483.44 | 27,521.41 | 478.78 | 861.85 |
| 7.803 | 10,519.83 | 23,192.38 | 513.73 | 924.78 |
| 8.001 | 9,057.38 | 19,968.20 | 516.31 | 929.41 |
| 8.200 | 7,756.37 | 17,099.95 | 517.49 | 931.53 |
| 8.401 | 6,774.16 | 14,934.54 | 514.89 | 926.86 |
| 8.601 | 5,921.37 | 13,054.45 | 514.69 | 926.49 |
| 8.804 | 5,272.76 | 11,624.50 | 512.13 | 921.89 |
| 9.005 | 4,728.00 | 10,423.51 | 510.89 | 919.66 |
| 9.204 | 4,450.27 | 9,811.23 | 539.71 | 971.54 |

Replace these 13 pages of Table 6.2.1-8
with the following 13 pages of revised
Table 6.2.1-8.

Table 6.2.1-8 (3 of 13)

Part A. Mass and Energy Release Data
(Blowdown Period)

| Time (sec) | Break Mass Flow Rate | | Break Enthalpy | |
|------------|----------------------|-----------|----------------|----------|
| | kg/sec | lbm/sec | kcal/kg | Btu/lbm |
| 9.400 | 4,558.87 | 10,050.63 | 548.54 | 987.43 |
| 9.612 | 4,586.78 | 10,112.17 | 561.64 | 1,011.01 |
| 9.803 | 4,595.26 | 10,130.86 | 565.36 | 1,017.71 |
| 10.011 | 4,721.83 | 10,409.92 | 550.48 | 990.93 |
| 10.200 | 4,458.70 | 9,829.80 | 554.50 | 998.15 |
| 10.400 | 4,287.29 | 9,451.91 | 559.17 | 1,006.56 |
| 10.600 | 4,142.66 | 9,133.05 | 563.27 | 1,013.94 |
| 10.801 | 3,967.56 | 8,747.02 | 566.89 | 1,020.45 |
| 11.001 | 3,801.78 | 8,381.54 | 567.80 | 1,022.10 |
| 11.200 | 3,576.19 | 7,884.19 | 571.65 | 1,029.04 |
| 11.400 | 3,267.58 | 7,203.82 | 583.08 | 1,049.61 |
| 11.600 | 2,999.69 | 6,613.22 | 584.05 | 1,051.36 |
| 11.800 | 2,566.36 | 5,657.89 | 583.09 | 1,049.62 |
| 12.000 | 2,058.34 | 4,537.88 | 594.79 | 1,070.68 |
| 12.200 | 1,698.88 | 3,745.40 | 586.91 | 1,056.50 |
| 12.400 | 1,546.84 | 3,410.21 | 592.55 | 1,066.65 |
| 12.601 | 1,399.98 | 3,086.44 | 601.69 | 1,083.10 |
| 12.801 | 1,205.75 | 2,658.24 | 605.21 | 1,089.44 |
| 13.001 | 1,000.25 | 2,205.19 | 605.09 | 1,089.22 |
| 13.201 | 848.41 | 1,870.43 | 606.60 | 1,091.93 |
| 13.401 | 761.90 | 1,679.71 | 601.78 | 1,083.26 |

Integral Mass and Energy Release at End of Blowdown

| Time (sec) | Integral Mass | | Integral Energy | |
|------------|---------------|------------|-----------------|-------------|
| | kg | lbm | Million kcal | Million Btu |
| 13.401 | 301,079.78 | 663,770.75 | 115.563 | 458.618 |

Replace these 13 pages of Table 6.2.1-8 with the following 13 pages of revised Table 6.2.1-8.

Table 6.2.1-8 (4 of 13)

Part A. Mass and Energy (Steam) Release Data (Decay heat Period)

| Time (sec) | Mass Flow Rate | | Break Enthalpy | |
|------------|----------------|---------|----------------|---------|
| | kg/sec | lbm/sec | kcal/kg | Btu/lbm |
| 100.0 | 88.02 | 194.05 | 653.21 | 1175.79 |
| 150.0 | 79.66 | 175.61 | 652.8 | 1175.03 |
| 200.0 | 71.28 | 157.14 | 652.5 | 1174.49 |
| 400.0 | 57.85 | 127.55 | 651.89 | 1173.41 |
| 599.9 | 53.39 | 117.7 | 651.61 | 1172.9 |
| 800.0 | 50.81 | 112.03 | 651.43 | 1172.58 |
| 999.0 | 48.82 | 107.62 | 651.3 | 1172.34 |
| 1502.9 | 44.86 | 98.89 | 651.1 | 1171.97 |
| 1996.0 | 41.77 | 92.09 | 650.98 | 1171.77 |
| 4000.6 | 34.25 | 75.52 | 650.82 | 1171.47 |
| 5996.5 | 30.61 | 67.48 | 650.76 | 1171.38 |
| 8004.8 | 28.46 | 62.75 | 650.76 | 1171.37 |
| 9994.5 | 27.0 | 59.52 | 650.78 | 1171.41 |
| 15005.2 | 24.75 | 54.57 | 650.84 | 1171.52 |
| 20010.6 | 23.36 | 51.5 | 650.83 | 1171.49 |
| 40034.6 | 20.51 | 45.22 | 650.45 | 1170.81 |
| 59960.8 | 19.02 | 41.94 | 649.87 | 1169.76 |
| 79987.5 | 18.08 | 39.86 | 649.37 | 1168.86 |
| 100002.4 | 14.53 | 32.04 | 648.05 | 1166.49 |
| 150008.7 | 12.82 | 28.25 | 646.51 | 1163.72 |
| 200017.4 | 11.71 | 25.81 | 645.78 | 1162.41 |

Integral Mass and Energy Release(Steam) at 24 hours and End of Analysis

| Time (sec) | Integral Mass | | Integral Energy | |
|------------|---------------|------------|-----------------|-------------|
| | kg | lbm | Million kcal | Million Btu |
| 85,095 | 2,207,211 | 4,866,067 | 1,356.127 | 4,601.320 |
| 1,000,000 | 10,343,406 | 22,803,307 | 6,605.165 | 26,211.413 |

Replace these 13 pages of Table 6.2.1-8 with the following 13 pages of revised Table 6.2.1-8.

Table 6.2.1-8 (5 of 13)

Part A. Mass and Energy (Spillage) Release Data
(Decay heat Period)

| Time (sec) | Mass Flow Rate | | Break Enthalpy | |
|------------|----------------|---------|----------------|---------|
| | kg/sec | lbm/sec | kcal/kg | Btu/lbm |
| 100.0 | 152.41 | 336.0 | 52.39 | 94.31 |
| 150.0 | 153.7 | 338.86 | 55.19 | 99.34 |
| 200.0 | 155.53 | 342.88 | 57.44 | 103.39 |
| 400.0 | 164.58 | 362.84 | 63.66 | 114.59 |
| 599.9 | 173.9 | 383.39 | 68.08 | 122.55 |
| 800.0 | 182.31 | 401.92 | 71.59 | 128.87 |
| 999.0 | 189.19 | 417.1 | 74.17 | 133.51 |
| 1502.9 | 200.74 | 442.57 | 79.33 | 142.8 |
| 1996.0 | 206.6 | 455.48 | 83.61 | 150.5 |
| 4000.6 | 213.52 | 470.73 | 96.13 | 173.04 |
| 5996.5 | 215.7 | 475.53 | 103.73 | 186.72 |
| 8004.8 | 216.67 | 477.68 | 108.56 | 195.4 |
| 9994.5 | 217.37 | 479.21 | 111.66 | 200.99 |
| 15005.2 | 218.52 | 481.76 | 115.65 | 208.17 |
| 20010.6 | 219.47 | 483.84 | 117.08 | 210.75 |
| 40034.6 | 222.13 | 489.72 | 116.57 | 209.83 |
| 59960.8 | 224.11 | 494.09 | 113.73 | 204.72 |
| 79987.5 | 225.55 | 497.26 | 111.06 | 199.9 |
| 100002.4 | 229.89 | 506.83 | 105.21 | 189.38 |
| 150008.7 | 233.41 | 514.59 | 95.25 | 171.44 |
| 200017.4 | 235.27 | 518.69 | 90.43 | 162.78 |

Integral Mass and Energy Release(Spillage) at 24 hours and End of Analysis

| Time (sec) | Integral Mass | | Integral Energy | |
|---------------|---------------|-------------|-----------------|-------------|
| | kg | kg | kg | Million Btu |
| 85,095 | 18,992,294 | 41,870,842 | 2,135.757 | 8,475.369 |
| 1,000,000 | 237,904,035 | 524,488,617 | 19,713.765 | 78,230.541 |

Replace these 13 pages of Table 6.2.1-8
with the following 13 pages of revised
Table 6.2.1-8.

Table 6.2.1-8 (6 of 13)

Part B. Reactor Vessel Pressure vs. Time
(Blowdown Period)

| Time (sec) | Reactor Vessel Pressure | |
|------------|-------------------------|----------|
| | kg/cm ² A | psia |
| 0.000 | 167.36 | 2,380.40 |
| 0.025 | 157.69 | 2,242.90 |
| 0.051 | 128.16 | 1,822.80 |
| 0.100 | 126.19 | 1,794.90 |
| 0.151 | 126.33 | 1,796.80 |
| 0.199 | 121.45 | 1,727.40 |
| 0.257 | 119.94 | 1,706.00 |
| 0.301 | 117.60 | 1,672.60 |
| 0.353 | 115.03 | 1,636.10 |
| 0.504 | 110.53 | 1,572.10 |
| 0.652 | 106.06 | 1,508.50 |
| 0.799 | 100.47 | 1,429.00 |
| 0.962 | 96.25 | 1,369.00 |
| 1.207 | 89.49 | 1,272.80 |
| 1.407 | 85.42 | 1,214.90 |
| 1.609 | 82.23 | 1,169.60 |
| 1.801 | 79.81 | 1,135.10 |
| 2.001 | 78.39 | 1,115.00 |
| 2.201 | 77.66 | 1,104.60 |
| 2.401 | 77.06 | 1,096.10 |
| 2.601 | 76.44 | 1,087.30 |
| 2.801 | 75.50 | 1,073.90 |
| 3.001 | 74.51 | 1,059.80 |

Replace these 13 pages of Table 6.2.1-8
with the following 13 pages of revised
Table 6.2.1-8.

Table 6.2.1-8 (7 of 13)

Part B. Reactor Vessel Pressure vs. Time
(Blowdown Period)

| Time (sec) | Reactor Vessel Pressure | |
|------------|-------------------------|----------|
| | kg/cm ² A | psia |
| 3.201 | 73.27 | 1,042.10 |
| 3.401 | 72.02 | 1,024.40 |
| 3.601 | 70.64 | 1,004.80 |
| 3.801 | 69.17 | 983.77 |
| 4.001 | 67.77 | 963.96 |
| 4.201 | 66.44 | 945.06 |
| 4.401 | 65.12 | 926.21 |
| 4.601 | 63.76 | 906.90 |
| 4.801 | 62.38 | 887.28 |
| 5.001 | 60.97 | 867.18 |
| 5.201 | 59.55 | 847.04 |
| 5.401 | 58.14 | 826.93 |
| 5.601 | 56.70 | 806.40 |
| 5.801 | 55.25 | 785.87 |
| 6.001 | 53.82 | 765.55 |
| 6.201 | 52.40 | 745.33 |
| 6.401 | 50.96 | 724.79 |
| 6.601 | 49.52 | 704.34 |
| 6.801 | 48.05 | 683.40 |
| 7.001 | 45.37 | 645.30 |
| 7.201 | 41.69 | 593.00 |
| 7.401 | 38.67 | 550.08 |

Replace these 13 pages of Table 6.2.1-8 with the following 13 pages of revised Table 6.2.1-8.

Table 6.2.1-8 (8 of 13)

Part B. Reactor Vessel Pressure vs. Time
(Blowdown Period)

| Time (sec) | Reactor Vessel Pressure | |
|------------|-------------------------|--------|
| | kg/cm ² A | psia |
| 7.601 | 35.75 | 508.47 |
| 7.803 | 32.78 | 466.21 |
| 8.001 | 30.09 | 428.04 |
| 8.200 | 26.95 | 383.33 |
| 8.401 | 23.75 | 337.83 |
| 8.601 | 20.81 | 295.97 |
| 8.804 | 18.33 | 260.76 |
| 9.005 | 17.98 | 255.67 |
| 9.204 | 18.84 | 267.94 |
| 9.401 | 19.52 | 277.67 |
| 9.612 | 19.81 | 281.76 |
| 9.803 | 19.68 | 279.86 |
| 10.011 | 19.09 | 271.49 |
| 10.200 | 18.81 | 267.47 |
| 10.400 | 18.31 | 260.39 |
| 10.600 | 17.56 | 249.70 |
| 10.801 | 16.73 | 237.92 |
| 11.001 | 15.78 | 224.49 |
| 11.200 | 14.74 | 209.70 |
| 11.400 | 13.50 | 191.99 |
| 11.600 | 11.92 | 169.59 |
| 11.800 | 10.23 | 145.44 |
| 12.000 | 8.82 | 125.49 |

Replace these 13 pages of Table 6.2.1-8 with the following 13 pages of revised Table 6.2.1-8.

Table 6.2.1-8 (9 of 13)

Part B. Reactor Vessel Pressure vs. Time
(Blowdown Period)

| Time (sec) | Reactor Vessel Pressure | |
|------------|-------------------------|--------|
| | kg/cm ² A | psia |
| 12.200 | 7.82 | 111.16 |
| 12.400 | 6.98 | 99.29 |
| 12.601 | 6.26 | 88.97 |
| 12.801 | 5.63 | 80.01 |
| 13.001 | 5.09 | 72.37 |
| 13.201 | 4.63 | 65.89 |
| 13.401 | 7.89 | 112.17 |

Replace these 13 pages of Table 6.2.1-8 with the following 13 pages of revised Table 6.2.1-8.

Table 6.2.1-8 (10 of 13)

Part B. Reactor Vessel Pressure vs. Time
(Decay heat Period)

| Time (sec) | Reactor Vessel Pressure | |
|------------|-------------------------|--------|
| | kg/cm ² A | psia |
| 100.0 | 3.84 | 54.621 |
| 150.0 | 3.694 | 52.541 |
| 200.0 | 3.593 | 51.099 |
| 400.0 | 3.399 | 48.342 |
| 599.9 | 3.312 | 47.113 |
| 800.0 | 3.258 | 46.336 |
| 999.0 | 3.219 | 45.783 |
| 1502.9 | 3.158 | 44.923 |
| 1996.0 | 3.125 | 44.448 |
| 4000.6 | 3.078 | 43.785 |
| 5996.5 | 3.063 | 43.568 |
| 8004.8 | 3.063 | 43.566 |
| 9994.5 | 3.069 | 43.648 |
| 15005.2 | 3.086 | 43.887 |
| 20010.6 | 3.081 | 43.826 |
| 40034.6 | 2.976 | 42.323 |
| 59960.8 | 2.82 | 40.111 |
| 79987.5 | 2.693 | 38.302 |
| 100002.4 | 2.385 | 33.928 |
| 150008.7 | 2.07 | 29.44 |
| 200017.4 | 1.935 | 27.521 |

Replace these 13 pages of Table 6.2.1-8
with the following 13 pages of revised
Table 6.2.1-8.

Table 6.2.1-8 (11 of 13)

Part C. Safety Injection Flow vs. Time
(Blowdown Period)

| Time (sec) | Reactor Vessel Pressure | |
|------------|-------------------------|-----------|
| | kg/cm ² A | psia |
| 0.000 | 0.00 | 0.00 |
| 0.025 | 0.00 | 0.00 |
| 6.601 | 0.00 | 0.00 |
| 6.801 | 0.00 | 0.00 |
| 7.001 | 1,242.61 | 2,739.50 |
| 7.201 | 2,386.97 | 5,262.40 |
| 7.401 | 3,000.72 | 6,615.50 |
| 7.601 | 3,470.51 | 7,651.20 |
| 7.803 | 3,860.91 | 8,511.90 |
| 8.001 | 4,188.27 | 9,233.60 |
| 8.200 | 4,536.81 | 10,002.00 |
| 8.401 | 4,857.95 | 10,710.00 |
| 8.601 | 5,136.45 | 11,324.00 |
| 8.804 | 5,340.12 | 11,773.00 |
| 9.005 | 5,259.83 | 11,596.00 |
| 9.204 | 5,021.24 | 11,070.00 |
| 9.401 | 4,802.61 | 10,588.00 |
| 9.612 | 4,643.40 | 10,237.00 |
| 9.803 | 4,558.58 | 10,050.00 |
| 10.011 | 4,543.16 | 10,016.00 |
| 10.200 | 4,476.89 | 9,869.90 |
| 10.400 | 4,460.51 | 9,833.80 |
| 10.600 | 4,480.11 | 9,877.00 |
| 10.801 | 4,517.62 | 9,959.70 |
| 11.001 | 4,571.73 | 10,079.00 |

Replace these 13 pages of Table 6.2.1-8
with the following 13 pages of revised
Table 6.2.1-8.

Table 6.2.1-8 (12 of 13)

Part C. Safety Injection Flow vs. Time
(Blowdown Period)

| Time (sec) | Reactor Vessel Pressure | |
|------------|-------------------------|-----------|
| | kg/cm ² A | psia |
| 11.200 | 4,638.86 | 10,227.00 |
| 11.400 | 4,736.84 | 10,443.00 |
| 11.600 | 4,895.14 | 10,792.00 |
| 11.800 | 5,061.61 | 11,159.00 |
| 12.000 | 5,183.63 | 11,428.00 |
| 12.200 | 5,234.88 | 11,541.00 |
| 12.400 | 5,273.89 | 11,627.00 |
| 12.601 | 5,301.56 | 11,688.00 |
| 12.801 | 5,321.06 | 11,731.00 |
| 13.001 | 5,327.87 | 11,746.00 |
| 13.201 | 5,325.60 | 11,741.00 |
| 13.401 | 4,832.55 | 10,654.00 |

Replace these 13 pages of Table 6.2.1-8 with the following 13 pages of revised Table 6.2.1-8.

Table 6.2.1-8 (13 of 13)

Part D. Chronology of Events

| Time (sec) | Event | Values |
|------------|--|--|
| 0.0 | Break occurs | - |
| 2.51 | Containment pressure Hi-Hi setpoint | 1.547 kg/cm ² G (22.0 psig) |
| 6.80 | Start SI pump injection | - |
| 13.01 | Peak containment temperature | 132.99 °C (271.38 °F) |
| | Peak containment pressure | 3.394 kg/cm ² G (48.28 psig) |
| 13.40 | End of blowdown | - |
| 73,578.8 | Time of depressurization of the containment at 50% of peak pressure | 1.697 kg/cm ² G (24.14 psig) |

Replace these 13 pages of Table 6.2.1-8
with the following 13 pages of revised
Table 6.2.1-8.

APR1400 DCD TIER 2

Table 6.2.1-8 (1 of 13)

Insert this page.

Double-Ended Hot Leg Slot Break (1.7877 m² (19.2423 ft²) Break Area)Part A. Mass and Energy Release Data
(Blowdown Period)

| Time (sec) | Break Mass Flow Rate | | Break Enthalpy | |
|------------|----------------------|------------|----------------|---------|
| | kg/sec | lbm/sec | kcal/kg | Btu/lbm |
| 0.000 | 0.00 | 0.00 | 0.00 | 0.00 |
| 0.025 | 76,463.94 | 168,575.00 | 358.81 | 645.90 |
| 0.051 | 71,583.69 | 157,815.84 | 357.26 | 643.11 |
| 0.100 | 78,379.65 | 172,798.45 | 358.80 | 645.88 |
| 0.151 | 78,075.82 | 172,128.63 | 359.59 | 647.29 |
| 0.199 | 73,247.67 | 161,484.31 | 359.42 | 646.99 |
| 0.257 | 69,096.98 | 152,333.56 | 359.43 | 647.00 |
| 0.301 | 65,747.36 | 144,948.88 | 359.52 | 647.17 |
| 0.353 | 63,219.10 | 139,374.98 | 359.76 | 647.61 |
| 0.504 | 59,599.23 | 131,394.50 | 360.43 | 648.81 |
| 0.652 | 55,612.68 | 122,605.60 | 361.40 | 650.56 |
| 0.799 | 52,805.95 | 116,417.80 | 362.99 | 653.42 |
| 0.962 | 50,268.79 | 110,824.29 | 365.52 | 657.97 |
| 1.207 | 46,410.82 | 102,318.88 | 368.49 | 663.32 |
| 1.407 | 45,069.94 | 99,362.73 | 367.67 | 661.85 |
| 1.609 | 44,404.87 | 97,896.49 | 365.84 | 658.54 |
| 1.801 | 44,178.17 | 97,396.70 | 363.00 | 653.45 |
| 2.001 | 44,303.25 | 97,672.45 | 359.42 | 646.99 |
| 2.201 | 44,546.16 | 98,207.98 | 355.69 | 640.28 |
| 2.401 | 44,650.70 | 98,438.45 | 352.16 | 633.93 |
| 2.601 | 44,567.73 | 98,255.53 | 349.42 | 628.99 |
| 2.801 | 44,137.88 | 97,307.87 | 347.62 | 625.76 |
| 3.001 | 43,037.65 | 94,882.27 | 347.97 | 626.38 |
| 3.201 | 41,113.16 | 90,639.48 | 350.58 | 631.09 |
| 3.401 | 39,506.41 | 87,097.19 | 353.52 | 636.36 |
| 3.601 | 37,945.09 | 83,655.05 | 356.60 | 641.92 |

APR1400 DCD TIER 2

Table 6.2.1-8 (2 of 13)

Insert this page.

**Part A. Mass and Energy Release Data
(Blowdown Period)**

| Time (sec) | Break Mass Flow Rate | | Break Enthalpy | |
|------------|----------------------|-----------|----------------|---------|
| | kg/sec | lbm/sec | kcal/kg | Btu/lbm |
| 3.801 | 36,414.18 | 80,279.95 | 359.80 | 647.68 |
| 4.001 | 34,945.21 | 77,041.40 | 363.09 | 653.60 |
| 4.201 | 33,502.52 | 73,860.79 | 366.44 | 659.62 |
| 4.401 | 32,343.39 | 71,305.35 | 369.61 | 665.33 |
| 4.601 | 31,165.54 | 68,708.63 | 372.35 | 670.27 |
| 4.801 | 30,087.66 | 66,332.29 | 374.66 | 674.43 |
| 5.001 | 29,021.42 | 63,981.62 | 377.05 | 678.73 |
| 5.201 | 27,888.46 | 61,483.85 | 380.01 | 684.05 |
| 5.401 | 26,727.17 | 58,923.64 | 383.79 | 690.86 |
| 5.601 | 25,533.29 | 56,291.55 | 388.42 | 699.19 |
| 5.801 | 24,260.05 | 53,484.53 | 393.87 | 709.01 |
| 6.001 | 22,940.05 | 50,574.42 | 400.19 | 720.38 |
| 6.201 | 21,641.55 | 47,711.69 | 407.47 | 733.50 |
| 6.401 | 20,399.99 | 44,974.52 | 415.69 | 748.28 |
| 6.601 | 19,210.83 | 42,352.85 | 424.88 | 764.82 |
| 6.801 | 18,114.06 | 39,934.88 | 432.47 | 778.48 |
| 7.001 | 17,563.30 | 38,720.65 | 430.48 | 774.91 |
| 7.201 | 16,242.88 | 35,809.61 | 437.89 | 788.25 |
| 7.401 | 14,396.00 | 31,737.90 | 455.32 | 819.62 |
| 7.601 | 12,483.44 | 27,521.41 | 478.78 | 861.85 |
| 7.803 | 10,519.83 | 23,192.38 | 513.73 | 924.78 |
| 8.001 | 9,057.38 | 19,968.20 | 516.31 | 929.41 |
| 8.200 | 7,756.37 | 17,099.95 | 517.49 | 931.53 |
| 8.401 | 6,774.16 | 14,934.54 | 514.89 | 926.86 |
| 8.601 | 5,921.37 | 13,054.45 | 514.69 | 926.49 |
| 8.804 | 5,272.76 | 11,624.50 | 512.13 | 921.89 |
| 9.005 | 4,728.00 | 10,423.51 | 510.89 | 919.66 |
| 9.204 | 4,450.27 | 9,811.23 | 539.71 | 971.54 |

APR1400 DCD TIER 2

Table 6.2.1-8 (3 of 13)

Part A. Mass and Energy Release Data
(Blowdown Period)

Insert this page.

| Time (sec) | Break Mass Flow Rate | | Break Enthalpy | |
|------------|----------------------|-----------|----------------|----------|
| | kg/sec | lbm/sec | kcal/kg | Btu/lbm |
| 9.400 | 4,558.87 | 10,050.63 | 548.54 | 987.43 |
| 9.612 | 4,586.78 | 10,112.17 | 561.64 | 1,011.01 |
| 9.803 | 4,595.26 | 10,130.86 | 565.36 | 1,017.71 |
| 10.011 | 4,721.83 | 10,409.92 | 550.48 | 990.93 |
| 10.200 | 4,458.70 | 9,829.80 | 554.50 | 998.15 |
| 10.400 | 4,287.29 | 9,451.91 | 559.17 | 1,006.56 |
| 10.600 | 4,142.66 | 9,133.05 | 563.27 | 1,013.94 |
| 10.801 | 3,967.56 | 8,747.02 | 566.89 | 1,020.45 |
| 11.001 | 3,801.78 | 8,381.54 | 567.80 | 1,022.10 |
| 11.200 | 3,576.19 | 7,884.19 | 571.65 | 1,029.04 |
| 11.400 | 3,267.58 | 7,203.82 | 583.08 | 1,049.61 |
| 11.600 | 2,999.69 | 6,613.22 | 584.05 | 1,051.36 |
| 11.800 | 2,566.36 | 5,657.89 | 583.09 | 1,049.62 |
| 12.000 | 2,058.34 | 4,537.88 | 594.79 | 1,070.68 |
| 12.200 | 1,698.88 | 3,745.40 | 586.91 | 1,056.50 |
| 12.400 | 1,546.84 | 3,410.21 | 592.55 | 1,066.65 |
| 12.601 | 1,399.98 | 3,086.44 | 601.69 | 1,083.10 |
| 12.801 | 1,205.75 | 2,658.24 | 605.21 | 1,089.44 |
| 13.001 | 1,000.25 | 2,205.19 | 605.09 | 1,089.22 |
| 13.201 | 848.41 | 1,870.43 | 606.60 | 1,091.93 |
| 13.401 | 761.90 | 1,679.71 | 601.78 | 1,083.26 |

Integral Mass and Energy Release at End of Blowdown

| Time (sec) | Integral Mass | | Integral Energy | |
|------------|---------------|------------|-----------------|-------------|
| | kg | lbm | Million kcal | Million Btu |
| 13.401 | 301,079.78 | 663,770.75 | 115.563 | 458.618 |

APR1400 DCD TIER 2

Table 6.2.1-8 (4 of 13)

Insert this page.

Part A. Mass and Energy (Steam) Release Data (Decay heat Period)

| Time (sec) | Mass Flow Rate | | Break Enthalpy | |
|------------|----------------|---------|----------------|---------|
| | kg/sec | lbm/sec | kcal/kg | Btu/lbm |
| 100.0 | 75.71 | 166.91 | 652.75 | 1174.95 |
| 150.0 | 74.58 | 164.41 | 652.48 | 1174.46 |
| 200.0 | 70.85 | 156.19 | 652.28 | 1174.1 |
| 400.0 | 62.6 | 138.0 | 651.84 | 1173.32 |
| 599.9 | 58.54 | 129.06 | 651.61 | 1172.9 |
| 799.7 | 55.92 | 123.29 | 651.45 | 1172.61 |
| 999.7 | 53.82 | 118.66 | 651.33 | 1172.4 |
| 1502.6 | 49.8 | 109.8 | 651.15 | 1172.07 |
| 1995.5 | 46.7 | 102.95 | 651.05 | 1171.9 |
| 3998.7 | 38.73 | 85.39 | 651.04 | 1171.86 |
| 6003.4 | 34.46 | 75.98 | 651.14 | 1172.05 |
| 7999.8 | 31.67 | 69.81 | 651.26 | 1172.27 |
| 9998.5 | 29.56 | 65.17 | 651.37 | 1172.46 |
| 15005.2 | 25.95 | 57.22 | 651.48 | 1172.66 |
| 20010.8 | 23.52 | 51.86 | 651.37 | 1172.46 |
| 40038.3 | 18.48 | 40.75 | 650.16 | 1170.29 |
| 59967.1 | 16.31 | 35.95 | 648.91 | 1168.04 |
| 79994.9 | 15.14 | 33.39 | 648.05 | 1166.49 |
| 100002.1 | 14.41 | 31.78 | 647.48 | 1165.47 |
| 150008.9 | 12.82 | 28.27 | 646.54 | 1163.77 |
| 200017.1 | 11.72 | 25.83 | 645.91 | 1162.63 |

Integral Mass and Energy Release(Steam) at 24 hours and End of Analysis

| Time (sec) | Integral Mass | | Integral Energy | |
|------------|---------------|------------|-----------------|-------------|
| | kg | lbm | Million kcal | Million Btu |
| 85,004 | 2,116,106 | 4,665,215 | 1,296.566 | 4,601.320 |
| 1,000,000 | 10,257,523 | 22,613,968 | 6,549.709 | 25,991.346 |

APR1400 DCD TIER 2

Table 6.2.1-8 (5 of 13)

Insert this page.

**Part A. Mass and Energy (Spillage) Release Data
(Decay heat Period)**

| Time (sec) | Mass Flow Rate | | Break Enthalpy | |
|------------|----------------|---------|----------------|---------|
| | kg/sec | lbm/sec | kcal/kg | Btu/lbm |
| 100.0 | 100.3 | 221.11 | 11.37 | 20.46 |
| 150.0 | 124.9 | 275.37 | 28.5 | 51.31 |
| 200.0 | 148.07 | 326.44 | 38.74 | 69.74 |
| 400.0 | 160.74 | 354.37 | 53.24 | 95.84 |
| 599.9 | 169.23 | 373.09 | 57.48 | 103.46 |
| 799.7 | 177.05 | 390.33 | 60.29 | 108.53 |
| 999.7 | 183.68 | 404.94 | 62.5 | 112.5 |
| 1502.6 | 195.73 | 431.52 | 67.75 | 121.95 |
| 1995.5 | 202.6 | 446.66 | 73.03 | 131.45 |
| 3998.7 | 210.65 | 464.4 | 90.48 | 162.86 |
| 6003.4 | 212.9 | 469.36 | 101.4 | 182.53 |
| 7999.8 | 214.07 | 471.94 | 108.5 | 195.31 |
| 9998.5 | 214.97 | 473.94 | 113.27 | 203.88 |
| 15005.2 | 216.8 | 477.95 | 119.51 | 215.12 |
| 20010.8 | 218.54 | 481.8 | 121.6 | 218.88 |
| 40038.3 | 223.9 | 493.62 | 118.16 | 212.69 |
| 59967.1 | 227.33 | 501.18 | 111.55 | 200.78 |
| 79994.9 | 229.46 | 505.88 | 106.43 | 191.57 |
| 100002.1 | 230.84 | 508.91 | 102.9 | 185.22 |
| 150008.9 | 233.36 | 514.47 | 97.11 | 174.79 |
| 200017.1 | 235.07 | 518.25 | 93.0 | 167.39 |

Integral Mass and Energy Release(Spillage) at 24 hours and End of Analysis

| Time (sec) | Integral Mass | | Integral Energy | |
|---------------|---------------|-------------|-----------------|-------------|
| | kg | kg | kg | Million Btu |
| 85,004 | 18,898,645 | 41,664,380 | 2,118.550 | 8,407.087 |
| 1,000,000 | 237,669,568 | 523,971,705 | 20,273.753 | 80,452.751 |

APR1400 DCD TIER 2

Table 6.2.1-8 (6 of 13)

Insert this page.

Part B. Reactor Vessel Pressure vs. Time
(Blowdown Period)

| Time (sec) | Reactor Vessel Pressure | |
|------------|-------------------------|----------|
| | kg/cm ² A | psia |
| 0.000 | 167.36 | 2,380.40 |
| 0.025 | 157.69 | 2,242.90 |
| 0.051 | 128.16 | 1,822.80 |
| 0.100 | 126.19 | 1,794.90 |
| 0.151 | 126.33 | 1,796.80 |
| 0.199 | 121.45 | 1,727.40 |
| 0.257 | 119.94 | 1,706.00 |
| 0.301 | 117.60 | 1,672.60 |
| 0.353 | 115.03 | 1,636.10 |
| 0.504 | 110.53 | 1,572.10 |
| 0.652 | 106.06 | 1,508.50 |
| 0.799 | 100.47 | 1,429.00 |
| 0.962 | 96.25 | 1,369.00 |
| 1.207 | 89.49 | 1,272.80 |
| 1.407 | 85.42 | 1,214.90 |
| 1.609 | 82.23 | 1,169.60 |
| 1.801 | 79.81 | 1,135.10 |
| 2.001 | 78.39 | 1,115.00 |
| 2.201 | 77.66 | 1,104.60 |
| 2.401 | 77.06 | 1,096.10 |
| 2.601 | 76.44 | 1,087.30 |
| 2.801 | 75.50 | 1,073.90 |
| 3.001 | 74.51 | 1,059.80 |

APR1400 DCD TIER 2

Table 6.2.1-8 (7 of 13)

Insert this page.

Part B. Reactor Vessel Pressure vs. Time
(Blowdown Period)

| Time (sec) | Reactor Vessel Pressure | |
|------------|-------------------------|----------|
| | kg/cm ² A | psia |
| 3.201 | 73.27 | 1,042.10 |
| 3.401 | 72.02 | 1,024.40 |
| 3.601 | 70.64 | 1,004.80 |
| 3.801 | 69.17 | 983.77 |
| 4.001 | 67.77 | 963.96 |
| 4.201 | 66.44 | 945.06 |
| 4.401 | 65.12 | 926.21 |
| 4.601 | 63.76 | 906.90 |
| 4.801 | 62.38 | 887.28 |
| 5.001 | 60.97 | 867.18 |
| 5.201 | 59.55 | 847.04 |
| 5.401 | 58.14 | 826.93 |
| 5.601 | 56.70 | 806.40 |
| 5.801 | 55.25 | 785.87 |
| 6.001 | 53.82 | 765.55 |
| 6.201 | 52.40 | 745.33 |
| 6.401 | 50.96 | 724.79 |
| 6.601 | 49.52 | 704.34 |
| 6.801 | 48.05 | 683.40 |
| 7.001 | 45.37 | 645.30 |
| 7.201 | 41.69 | 593.00 |
| 7.401 | 38.67 | 550.08 |

APR1400 DCD TIER 2

Table 6.2.1-8 (8 of 13)

Insert this page.

**Part B. Reactor Vessel Pressure vs. Time
(Blowdown Period)**

| Time (sec) | Reactor Vessel Pressure | |
|------------|-------------------------|--------|
| | kg/cm ² A | psia |
| 7.601 | 35.75 | 508.47 |
| 7.803 | 32.78 | 466.21 |
| 8.001 | 30.09 | 428.04 |
| 8.200 | 26.95 | 383.33 |
| 8.401 | 23.75 | 337.83 |
| 8.601 | 20.81 | 295.97 |
| 8.804 | 18.33 | 260.76 |
| 9.005 | 17.98 | 255.67 |
| 9.204 | 18.84 | 267.94 |
| 9.401 | 19.52 | 277.67 |
| 9.612 | 19.81 | 281.76 |
| 9.803 | 19.68 | 279.86 |
| 10.011 | 19.09 | 271.49 |
| 10.200 | 18.81 | 267.47 |
| 10.400 | 18.31 | 260.39 |
| 10.600 | 17.56 | 249.70 |
| 10.801 | 16.73 | 237.92 |
| 11.001 | 15.78 | 224.49 |
| 11.200 | 14.74 | 209.70 |
| 11.400 | 13.50 | 191.99 |
| 11.600 | 11.92 | 169.59 |
| 11.800 | 10.23 | 145.44 |
| 12.000 | 8.82 | 125.49 |

APR1400 DCD TIER 2

Table 6.2.1-8 (9 of 13)

Part B. Reactor Vessel Pressure vs. Time
(Blowdown Period)

Insert this page.

| Time (sec) | Reactor Vessel Pressure | |
|------------|-------------------------|--------|
| | kg/cm ² A | psia |
| 12.200 | 7.82 | 111.16 |
| 12.400 | 6.98 | 99.29 |
| 12.601 | 6.26 | 88.97 |
| 12.801 | 5.63 | 80.01 |
| 13.001 | 5.09 | 72.37 |
| 13.201 | 4.63 | 65.89 |
| 13.401 | 7.89 | 112.17 |

APR1400 DCD TIER 2

Table 6.2.1-8 (10 of 13)

Insert this page.

Part B. Reactor Vessel Pressure vs. Time
(Decay heat Period)

| Time (sec) | Reactor Vessel Pressure | |
|------------|-------------------------|--------|
| | kg/cm ² A | psia |
| 100.0 | 3.678 | 52.31 |
| 150.0 | 3.587 | 51.019 |
| 200.0 | 3.522 | 50.094 |
| 400.0 | 3.383 | 48.118 |
| 599.9 | 3.311 | 47.098 |
| 799.7 | 3.264 | 46.422 |
| 999.7 | 3.229 | 45.922 |
| 1502.6 | 3.174 | 45.144 |
| 1995.5 | 3.146 | 44.75 |
| 3998.7 | 3.141 | 44.671 |
| 6003.4 | 3.171 | 45.103 |
| 7999.8 | 3.207 | 45.619 |
| 9998.5 | 3.238 | 46.051 |
| 15005.2 | 3.271 | 46.529 |
| 20010.8 | 3.238 | 46.059 |
| 40038.3 | 2.897 | 41.21 |
| 59967.1 | 2.583 | 36.735 |
| 79994.9 | 2.386 | 33.93 |
| 100002.1 | 2.264 | 32.199 |
| 150008.9 | 2.075 | 29.514 |
| 200017.1 | 1.957 | 27.838 |

APR1400 DCD TIER 2

Table 6.2.1-8 (11 of 13)

Insert this page.

Part C. Safety Injection Flow vs. Time (Blowdown Period)

| Time (sec) | Reactor Vessel Pressure | |
|------------|-------------------------|-----------|
| | kg/cm ² A | psia |
| 0.000 | 0.00 | 0.00 |
| 0.025 | 0.00 | 0.00 |
| 6.601 | 0.00 | 0.00 |
| 6.801 | 0.00 | 0.00 |
| 7.001 | 1,242.61 | 2,739.50 |
| 7.201 | 2,386.97 | 5,262.40 |
| 7.401 | 3,000.72 | 6,615.50 |
| 7.601 | 3,470.51 | 7,651.20 |
| 7.803 | 3,860.91 | 8,511.90 |
| 8.001 | 4,188.27 | 9,233.60 |
| 8.200 | 4,536.81 | 10,002.00 |
| 8.401 | 4,857.95 | 10,710.00 |
| 8.601 | 5,136.45 | 11,324.00 |
| 8.804 | 5,340.12 | 11,773.00 |
| 9.005 | 5,259.83 | 11,596.00 |
| 9.204 | 5,021.24 | 11,070.00 |
| 9.401 | 4,802.61 | 10,588.00 |
| 9.612 | 4,643.40 | 10,237.00 |
| 9.803 | 4,558.58 | 10,050.00 |
| 10.011 | 4,543.16 | 10,016.00 |
| 10.200 | 4,476.89 | 9,869.90 |
| 10.400 | 4,460.51 | 9,833.80 |
| 10.600 | 4,480.11 | 9,877.00 |
| 10.801 | 4,517.62 | 9,959.70 |
| 11.001 | 4,571.73 | 10,079.00 |

APR1400 DCD TIER 2

Table 6.2.1-8 (12 of 13)

Insert this page.

Part C. Safety Injection Flow vs. Time (Blowdown Period)

| Time (sec) | Reactor Vessel Pressure | |
|------------|-------------------------|-----------|
| | kg/cm ² A | psia |
| 11.200 | 4,638.86 | 10,227.00 |
| 11.400 | 4,736.84 | 10,443.00 |
| 11.600 | 4,895.14 | 10,792.00 |
| 11.800 | 5,061.61 | 11,159.00 |
| 12.000 | 5,183.63 | 11,428.00 |
| 12.200 | 5,234.88 | 11,541.00 |
| 12.400 | 5,273.89 | 11,627.00 |
| 12.601 | 5,301.56 | 11,688.00 |
| 12.801 | 5,321.06 | 11,731.00 |
| 13.001 | 5,327.87 | 11,746.00 |
| 13.201 | 5,325.60 | 11,741.00 |
| 13.401 | 4,832.55 | 10,654.00 |

APR1400 DCD TIER 2

Table 6.2.1-8 (13 of 13)

Insert this page.

Part D. Chronology of Events

| Time (sec) | Event | Values |
|------------|---|--|
| 0.0 | Break occurs | - |
| 2.50 | Containment pressure Hi-Hi setpoint | 1.547 kg/cm ² G (22.0 psig) |
| 6.80 | Start SI pump injection | - |
| 12.01 | Peak containment temperature | 132.29 °C (270.13 °F) |
| 12.31 | Peak containment pressure | 3.333 kg/cm ² G (47.41 psig) |
| 13.40 | End of blowdown | - |
| 51,655.0 | Time of depressurization of the containment at 50% of peak pressure | 1.665 kg/cm ² G (23.69 psig) |

Table 6.2.1-9 (11 of 11)

Part C. Chronology of Events

| Time (sec) | Events | Values |
|-----------------|---|---|
| 0.0 | Break occurs | - |
| 3.89 | Containment pressure reaches reactor trip analysis setpoint and main steam isolation signal analysis setpoint | 0.422 kg/cm ² G (6.0 psig) |
| 4.05 | High containment pressure reactor trip signal | - |
| 5.20 | Reactor trip breakers open, turbine admission valves closed | - |
| 5.30 | Main steam isolation valves closed | - |
| 10.40 | Main feedwater isolation valves closed | - |
| 15.40 | Containment pressure hi-hi setpoint | 1.547 kg/cm ² G (22.0 psig) |
| 125.51 | Start containment spray injection | - |
| | Peak containment temperature | 164.85 °C (328.72 °F) |
| 345.41 | Peak containment pressure | 3.140kg/cm ² G (44.66 psig) |
| 1,800.0 | End of blowdown | - |
| 3,503.2 | Time of depressurization of the containment at 50% of peak pressure | 1.569kg/cm ² G (22.31 psig) |

Table 6.2.1-10 (11 of 11)

Part C. Chronology of Events

| Time (sec) | Events | Values |
|-----------------|---|--|
| 0.0 | Break occurs | - |
| 3.89 | Containment pressure reaches reactor trip analysis setpoint and main steam isolation signal analysis setpoint | 0.422 kg/cm ² G (6.0 psig) |
| 4.05 | High containment pressure reactor trip signal | - |
| 5.20 | Reactor trip breakers open, turbine admission valves closed | - |
| 5.30 | Main steam isolation valves closed | - |
| 10.40 | Main feedwater isolation valves closed | - |
| 15.40 | Containment pressure Hi-Hi setpoint | 1.547 kg/cm ² G (22.0 psig) |
| 21.71 | Start containment spray injection | - |
| 111.71 | Peak containment temperature | 167.45 °C (333.41 °F) |
| 323.52 | Peak containment pressure | 3.137kg/cm ² G (44.62 psig) |
| 1,800.0 | End of blowdown | - |
| 2,799.4 | Time of depressurization of the containment at 50% of peak pressure | 1.568kg/cm ² G (22.31 psig) |

Table 6.2.1-11 (11 of 11)

Part C. Chronology of Events

| Time (sec) | Events | Values |
|-----------------|---|---|
| 0.0 | Break occurs | - |
| 3.71 | Containment pressure reaches reactor trip analysis setpoint and main steam isolation signal analysis setpoint | 0.422 kg/cm ² G (6.0 psig) |
| 3.85 | High containment pressure reactor trip signal | - |
| 5.00 | High containment pressure reactor trip signal | - |
| 5.10 | Reactor trip breakers open, turbine admission valves closed | - |
| 10.20 | Main steam isolation valves closed | - |
| 15.20 | Main feedwater isolation valves closed | - |
| 36.31 | Containment pressure Hi-Hi setpoint | 1.547 kg/cm ² G (22.0 psig) |
| 126.31 | Start containment spray injection | - |
| 126.31 | Peak containment temperature | 163.52 °C (326.34 °F) |
| 436.91 | Peak containment pressure | 3.281kg/cm ² G (46.67psig) |
| 1,800.0 | End of blowdown | - |
| 3,608.4 | Time of depressurization of the containment at 50% of peak pressure | 1.639kg/cm ² G (23.31psig) |

Table 6.2.1-12 (11 of 11)

Part C. Chronology of Events

| Time (sec) | Events | Values |
|-----------------|---|---|
| 0.0 | Break occurs | - |
| 3.71 | Containment pressure reaches reactor trip analysis setpoint and main steam isolation signal analysis setpoint | 0.422 kg/cm ² G (6.0 psig) |
| 3.85 | High containment pressure reactor trip signal | - |
| 5.00 | Reactor trip breakers open, turbine admission valves closed | - |
| 5.10 | Main steam isolation valves closed | - |
| 10.20 | Main feedwater isolation valves closed | - |
| 15.20 | Containment pressure Hi-Hi setpoint | 1.547 kg/cm ² G (22.0 psig) |
| 22.21 | Start containment spray injection | - |
| 112.21 | Peak containment temperature | 165.28 °C (329.51 °F) |
| 399.31 | Peak containment pressure | 3.206kg/cm ² G (45.60 psig) |
| 1,800.0 | End of blowdown | - |
| 2,944.8 | Time of depressurization of the containment at 50% of peak pressure | 1.598kg/cm ² G (22.72 psig) |

Table 6.2.1-13 (11 of 11)

Part C. Chronology of Events

| Time (sec) | Events | Values |
|-----------------|---|---|
| 0.0 | Break occurs | - |
| 3.61 | Containment pressure reaches reactor trip analysis setpoint and main steam isolation signal analysis setpoint | 0.422 kg/cm ² G (6.0 psig) |
| 3.75 | High containment pressure reactor trip signal | - |
| 4.90 | Reactor trip breakers open, turbine admission valves closed | - |
| 5.00 | Reactor trip breakers open, turbine admission valves closed | - |
| 10.10 | Main steam isolation valves closed | - |
| 15.10 | Main feedwater isolation valves closed | - |
| 37.51 | Containment pressure Hi-Hi setpoint | 1.547 kg/cm ² G (22.0 psig) |
| 127.51 | Start containment spray injection | - |
| 127.51 | Peak containment temperature | 161.90 °C (323.43 °F) |
| 457.61 | Peak containment pressure | 3.115kg/cm ² G (44.31 psig) |
| 1,800.0 | End of blowdown | - |
| 3,629.4 | Time of depressurization of the containment at 50% of peak pressure | 1.554kg/cm ² G (22.10 psig) |

Table 6.2.1-14 (11 of 11)

Part C. Chronology of Events

| Time (sec) | Events | Values |
|-----------------|---|---|
| 0.0 | Break occurs | - |
| 3.61 | Containment pressure reaches reactor trip analysis setpoint and main steam isolation signal analysis setpoint | 0.422 kg/cm ² G (6.0 psig) |
| 3.75 | | |
| 4.90 | High containment pressure reactor trip signal | - |
| 5.00 | Reactor trip breakers open, turbine admission valves closed | - |
| 10.10 | Main steam isolation valves closed | - |
| 15.10 | Main feedwater isolation valves closed | - |
| 22.51 | Peak containment temperature | 163.77 °C (326.79 °F) |
| 22.61 | Containment pressure Hi-Hi setpoint | 1.547 kg/cm ² G (22.0 psig) |
| 112.61 | Start containment spray injection | - |
| 414.11 | Peak containment pressure | 3.036kg/cm ² G (43.18 psig) |
| 1,800.0 | End of blowdown | - |
| 2,965.3 | Time of depressurization of the containment at 50% of peak pressure | 1.517kg/cm ² G (21.58 psig) |

Table 6.2.1-15 (11 of 11)

Part C. Chronology of Events

| | Time (sec) | Events | Values |
|-------|------------|---|---|
| 3.70 | 0.0 | Break occurs | - |
| 4.85 | 5.57 | Containment pressure reaches reactor trip analysis setpoint and main steam isolation signal analysis setpoint | 0.422 k/cm ² G (6.0 psig) |
| 4.95 | 5.20 | High containment pressure reactor trip signal | - |
| | 5.30 | Reactor trip breakers open, turbine admission valves closed | - |
| 10.05 | 10.40 | Main steam isolation valves closed | - |
| 15.05 | 15.40 | Main feedwater isolation valves closed | - |
| | 43.31 | Containment pressure Hi-Hi setpoint | 1.547 kg/cm ² G (22.0 psig) |
| | 97.81 | Peak containment temperature | 157.37 °C (315.27 °F) |
| | 133.31 | Start containment spray injection | - |
| | 769.04 | Peak containment pressure | 2.980kg/cm ² G (42.38 psig) |
| | 1,800.0 | End of blowdown | - |
| | 3,787.2 | Time of depressurization of the containment at 50% of peak pressure | 1.486kg/cm ² G (21.13 psig) |

Table 6.2.1-16 (11 of 11)

Part C. Chronology of Events

| Time (sec) | Events | Values |
|-----------------|---|---|
| 0.0 | Break occurs | - |
| 3.57 | Containment pressure reaches reactor trip analysis setpoint and main steam isolation signal analysis setpoint | 0.422 kg/cm ² G (6.0 psig) |
| 3.70 | High containment pressure reactor trip signal | - |
| 4.85 | Reactor trip breakers open, turbine admission valves closed | - |
| 4.95 | Main steam isolation valves closed | - |
| 10.05 | Main feedwater isolation valves closed | - |
| 15.05 | Peak containment temperature | 162.43 °C (324.38 °F) |
| 22.91 | Containment pressure Hi-Hi setpoint | 1.547kg/cm ² G (22.0 psig) |
| 25.71 | Start containment spray injection | - |
| 115.71 | Peak containment pressure | 2.792kg/cm ² G (39.71 psig) |
| 585.71 | End of blowdown | - |
| 1,800.0 | Time of depressurization of the containment at 50% of peak pressure | 1.393kg/cm ² G (19.81 psig) |
| 3,242.4 | | |

Table 6.2.1-17 (11 of 11)

Part C. Chronology of Events

| | Time (sec) | Events | Values |
|-------|------------------|---|---|
| | 0.0 | Break occurs | - |
| 4.65 | 4.53 | Containment pressure reaches reactor trip analysis setpoint and main steam isolation signal analysis setpoint | 0.422 kg/cm ² G (6.0 psig) |
| 5.80 | 5.20 | High containment pressure reactor trip signal | - |
| 5.90 | 5.30 | Reactor trip breakers open, turbine admission valves closed | - |
| 11.00 | 10.40 | Main steam isolation valves closed | - |
| 16.00 | 15.40 | Main feedwater isolation valves closed | - |
| | 43.21 | Containment pressure Hi-Hi setpoint | 1.547 kg/cm ² G (22.0 psig) |
| | 133.21 | Start containment spray injection | - |
| | 133.21 | Peak containment temperature | 161.83 °C (323.30 °F) |
| | 767.04 | Peak containment pressure | 3.208kg/cm ² G (45.63 psig) |
| | 1,800.0 | End of blowdown | - |
| | 3,829.3 | Time of depressurization of the containment at 50% of peak pressure | 1.601kg/cm ² G (22.77 psig) |

Table 6.2.1-18 (11 of 11)

Part C. Chronology of Events

| Time (sec) | Events | Values |
|-----------------|---|--|
| 0.0 | Break occurs | - |
| 4.53 | Containment pressure reaches reactor trip analysis setpoint and main steam isolation signal analysis setpoint | 0.422 kg/cm ² G (6.0 psig) |
| 5.80 | High containment pressure reactor trip signal | - |
| 5.90 | Reactor trip breakers open, turbine admission valves closed | - |
| 11.00 | Main steam isolation valves closed | - |
| 16.00 | Main feedwater isolation valves closed | - |
| 29.11 | Containment pressure Hi-Hi setpoint | 1.547 kg/cm ² G (22.0 psig) |
| 119.11 | Start containment spray injection | - |
| 119.11 | Peak containment temperature | 163.22 °C (325.79 °F) |
| 381.91 | Peak containment pressure | 3.051 kg/cm ² G (43.40 psig) |
| 1,800.0 | End of blowdown | - |
| 3,253.5 | Time of depressurization of the containment at 50% of peak pressure | 1.522 kg/cm ² G (21.65 psig) |

4.65

Table 6.2.1-37 (1 of 30)

Replace with next page

Stored Energy Sources

Part A. Loss-of-Coolant Accident

Case: Double-Ended Suction Leg Slot Break with Maximum ECCS Flow

Unit of Energy: ⁽¹⁾ 10⁶ kcal (10⁶ Btu)

| Description of Stored Energy | Prior to LOCA | At Peak Pressure Prior to EOB | At EOB | At Peak Pressure After EOB | At End of Reflood | At End of Post-Reflood | At 1 Day |
|--|-----------------------|-------------------------------|----------------------|----------------------------|---------------------|------------------------|----------------------------------|
| 1. Reactor coolant system water internal energy | 103.036 (408.906) | 5.639 (22.378) | 5.639 (22.378) | 10.642 (42.234) | 10.72 (42.541) | 10.503 (41.681) | 6.98 (27.69) |
| 2. Safety injection tank water internal energy | 10.53 (41.788) | 9.657 (38.325) | 9.657 (38.325) | 4.917 (19.514) | 4.779 (18.964) | 4.346 (17.247) | 0.0 (0.0) |
| 3. Energy stored in core | 7.65 (30.361) | 3.615 (14.346) | 3.615 (14.346) | 1.153 (4.577) | 1.151 (4.567) | 0.964 (3.827) | 55.40 ⁽²⁾ (219.83) |
| 4. Energy stored in RV internals | 10.584 (42.003) | 8.941 (35.482) | 8.941 (35.482) | 7.243 (28.744) | 7.178 (28.485) | 6.961 (27.626) | |
| 5. Energy stored in RV metal | 22.625 (89.789) | 22.049 (87.501) | 22.049 (87.501) | 21.637 (85.869) | 21.611 (85.767) | 21.529 (85.439) | |
| 6. Energy Stored in PZR, Primary Pipes, Valves and Pumps | 39.834 (158.082) | 35.358 (140.319) | 35.358 (140.319) | 33.904 (134.552) | 33.829 (134.252) | 33.6 (133.344) | |
| 7. Energy stored in SG secondary tubes | 10.688 (42.416) | 9.738 (38.647) | 9.738 (38.647) | 6.829 (27.102) | 6.779 (26.904) | 6.639 (26.348) | 0.0 (0.0) |
| 8. Energy stored in SG secondary walls | 37.688 (149.569) | 37.777 (149.919) | 37.777 (149.919) | 34.948 (138.692) | 34.845 (138.284) | 34.554 (137.13) | |
| 9. Secondary Coolant Internal Energy in SG 1(Affected) | 34.395 (136.5) | 35.788 (142.028) | 35.788 (142.028) | 20.843 (82.718) | 20.623 (81.844) | 19.891 (78.939) | 0.0 (0.0) |
| 10. Secondary Coolant Internal Energy in SG 2 (Unaffected) | 34.395 (136.5) | 37.935 (150.548) | 37.935 (150.548) | 31.214 (123.874) | 31.02 (123.105) | 30.602 (121.447) | |
| 11. Secondary Coolant Internal Energy in Steam Line | 9.076 (36.02) | 9.076 (36.02) | 9.076 (36.02) | 9.076 (36.02) | 9.076 (36.02) | 9.076 (36.02) | |
| 12. Total NSSS Stored Energy | 320.502 (1271.934) | 215.572 (855.513) | 215.572 (855.513) | 182.408 (723.897) | 181.61 (720.732) | 178.666 (709.048) | 62.37 (247.52) |

APR1400 DCD TIER 2

Table 6.2.1-37 (1 of 30)

Stored Energy Sources

Part A. Loss-of-Coolant Accident

Case: Double-Ended Suction Leg Slot Break with Maximum ECCS Flow

Unit of Energy:⁽¹⁾ 10⁶ kcal (10⁶ Btu)

| Description of Stored Energy | Prior to LOCA | At Peak Pressure Prior to EOB | At EOB | At End of Reflood | At Peak Pressure After EOB | At End of Post-Reflood | At 1 Day |
|--|----------------------|-------------------------------|----------------------|---------------------|----------------------------|------------------------|----------------------------------|
| 1. Reactor coolant system water internal energy | 103.036 (408.906) | 5.639 (22.378) | 5.639 (22.378) | 10.725 (42.563) | 10.645 (42.244) | 10.523 (41.761) | 6.33 (25.13) |
| 2. Safety injection tank water internal energy | 10.53 (41.788) | 9.657 (38.325) | 9.657 (38.325) | 4.756 (18.873) | 4.625 (18.355) | 4.354 (17.279) | 0.0 (0.0) |
| 3. Energy stored in core | 7.65 (30.361) | 3.615 (14.346) | 3.615 (14.346) | 1.154 (4.578) | 1.049 (4.161) | 0.97 (3.851) | 56.50 ⁽²⁾ (224.22) |
| 4. Energy stored in RV internals | 10.584 (42.003) | 8.941 (35.482) | 8.941 (35.482) | 7.176 (28.48) | 7.106 (28.2) | 6.974 (27.675) | |
| 5. Energy stored in RV metal | 22.625 (89.789) | 22.049 (87.501) | 22.049 (87.501) | 21.61 (85.762) | 21.584 (85.659) | 21.533 (85.455) | |
| 6. Energy Stored in PZR, Primary Pipes, Valves and Pumps | 39.834 (158.082) | 35.358 (140.319) | 35.358 (140.319) | 33.831 (134.26) | 33.755 (133.961) | 33.615 (133.405) | |
| 7. Energy stored in SG secondary tubes | 10.688 (42.416) | 9.738 (38.647) | 9.738 (38.647) | 6.78 (26.906) | 6.706 (26.612) | 6.641 (26.356) | 0.0 (0.0) |
| 8. Energy stored in SG secondary walls | 37.688 (149.569) | 37.777 (149.919) | 37.777 (149.919) | 34.845 (138.286) | 34.748 (137.901) | 34.57 (137.194) | |
| 9. Secondary Coolant Internal Energy in SG 1(Affected) | 34.395 (136.5) | 35.786 (142.018) | 35.788 (142.028) | 20.625 (81.853) | 20.347 (80.747) | 19.923 (79.066) | 0.0 (0.0) |
| 10. Secondary Coolant Internal Energy in SG 2 (Unaffected) | 34.395 (136.5) | 37.935 (150.548) | 37.935 (150.548) | 31.021 (123.11) | 30.864 (122.486) | 30.628 (121.549) | |
| 11. Secondary Coolant Internal Energy in Steam Line | 9.076 (36.02) | 9.076 (36.02) | 9.076 (36.02) | 9.076 (36.02) | 9.076 (36.02) | 9.076 (36.02) | |
| 12. Total NSSS Stored Energy | 320.502 (1271.93) | 215.57 (855.503) | 215.572 (855.513) | 181.6 (720.692) | 180.505 (716.347) | 178.808 (709.612) | 62.84 (249.35) |

Replace with next page

Table 6.2.1-37 (2 of 30)

Part A. Loss-of-Coolant Accident

Case: Double-Ended Suction Leg Slot Break with Maximum ECCS Flow

Unit of Energy:⁽¹⁾ 10⁶ kcal (10⁶ Btu)

| Description of Stored Energy | Prior to LOCA | At Peak Pressure Prior to EOB | At EOB | At Peak Pressure After EOB | At End of Reflood | At End of Post-Reflood | At 1 Day |
|--|-------------------|-------------------------------|---------------------|----------------------------|----------------------|------------------------|----------------------|
| 13. Feedwater to SG 1 (Affected) | 0.0 (0.0) | 3.316 (13.158) | 3.316 (13.158) | 3.316 (13.158) | 3.316 (13.158) | 3.316 (13.158) | 0.0 (0.0) |
| 14. Feedwater to SG 2 (Unaffected) | 0.0 (0.0) | 3.316 (13.158) | 3.316 (13.158) | 3.316 (13.158) | 3.316 (13.158) | 3.316 (13.158) | 0.0 (0.0) |
| 15. Steam flow to turbine | 0.0 (0.0) | 0.02 (0.078) | 0.02 (0.078) | 0.02 (0.078) | 0.02 (0.078) | 0.02 (0.078) | 0.0 (0.0) |
| 16. Energy from decay heat after shutdown | 0.0 (0.0) | 2.108 (8.367) | 2.108 (8.367) | 6.061 (24.053) | 6.255 (24.823) | 6.842 (27.153) | 762.91 (3027.49) |
| 17. Steam energy release through break | 0.0 (0.0) | 110.483 (438.46) | 110.483 (438.46) | 138.521 (549.732) | 139.289 (552.777) | 141.374 (561.053) | 1358.12 (5389.44) |
| 18. Liquid energy release by spillage | 0.0 (0.0) | 0.0 (0.0) | 0.0 (0.0) | 10.396 (41.256) | 10.694 (42.439) | 12.367 (49.079) | 2185.61 (8673.21) |
| 19. Total energy release | 0.0 (0.0) | 110.483 (438.46) | 110.483 (438.46) | 148.917 (590.988) | 149.983 (595.216) | 153.741 (610.132) | 3543.73 (14062.7) |
| 20. Energy Content of RCB Atmosphere | 66.56 (264.15) | 156.30 (620.27) | 156.30 (620.27) | 168.15 (667.28) | 168.06 (666.90) | 167.51 (664.74) | 110.34 (437.88) |
| 21. Energy Content of RCB Internal Structures ⁽³⁾ | 0.00 (0.00) | 5.98 (23.73) | 5.98 (23.73) | 25.26 (100.23) | 26.29 (104.32) | 28.26 (112.13) | 186.96 (741.93) |
| 22. Energy Content of IRWST Water | 48.01 (190.51) | 49.52 (196.50) | 49.52 (196.50) | 64.96 (257.77) | 66.02 (261.99) | 68.48 (271.76) | 146.95 (583.14) |
| 23. Energy Removed by CSHXs | 0.00 (0.00) | 0.00 (0.00) | 0.00 (0.00) | 0.00 (0.00) | 0.00 (0.00) | 0.02 (0.09) | 746.77 (2963.43) |

(1) The provided energy data is based on the temperature: 0 °C (32 °F), if not specified.

(2) All the RCS metal components are incorporated into a heat structure to model metal sensible energy release after EOPR.

(3) The initial energy content in RCB internal structures is assumed to zero (0) Btu.

APR1400 DCD TIER 2

Table 6.2.1-37 (2 of 30)

Part A. Loss-of-Coolant Accident

Case: Double-Ended Suction Leg Slot Break with Maximum ECCS Flow

Unit of Energy:⁽¹⁾ 10⁶ kcal (10⁶ Btu)

| Description of Stored Energy | Prior to LOCA | At Peak Pressure Prior to EOB | At EOB | At End of Reflood | At Peak Pressure After EOB | At End of Post-Reflood | At 1 Day |
|--|--------------------|-------------------------------|---------------------|----------------------|----------------------------|------------------------|----------------------|
| 13. Feedwater to SG 1 (Affected) | 0.0 (0.0) | 3.316 (13.158) | 3.316 (13.158) | 3.316 (13.158) | 3.316 (13.158) | 3.316 (13.158) | 0.0 (0.0) |
| 14. Feedwater to SG 2 (Unaffected) | 0.0 (0.0) | 3.316 (13.158) | 3.316 (13.158) | 3.316 (13.158) | 3.316 (13.158) | 3.316 (13.158) | 0.0 (0.0) |
| 15. Steam flow to turbine | 0.0 (0.0) | 0.015 (0.061) | 0.02 (0.078) | 0.02 (0.078) | 0.02 (0.078) | 0.02 (0.078) | 0.0 (0.0) |
| 16. Energy from decay heat after shutdown | 0.0 (0.0) | 2.108 (8.367) | 2.108 (8.367) | 6.255 (24.823) | 6.443 (25.57) | 6.807 (27.013) | 762.91 (3027.48) |
| 17. Steam energy release through break | 0.0 (0.0) | 110.287 (437.68) | 110.483 (438.46) | 139.317 (552.887) | 140.11 (556.035) | 141.311 (560.804) | 1307.92 (5190.23) |
| 18. Liquid energy release by spillage | 0.0 (0.0) | 0.0 (0.0) | 0.0 (0.0) | 10.671 (42.35) | 11.24 (44.605) | 12.242 (48.582) | 2179.24 (8647.93) |
| 19. Total energy release | 0.0 (0.0) | 110.287 (437.68) | 110.483 (438.46) | 149.988 (595.238) | 151.349 (600.641) | 153.553 (609.386) | 3487.16 (13838.2) |
| 20. Energy Content of RCB Atmosphere | 65.49 (259.87) | 152.57 (605.44) | 152.57 (605.44) | 162.36 (644.31) | 162.58 (645.15) | 162.47 (644.72) | 103.47 (410.61) |
| 21. Energy Content of RCB Internal Structures ⁽³⁾ | 0.00 (0.00) | 8.66 (34.36) | 8.79 (34.88) | 29.65 (117.67) | 30.18 (119.75) | 31.10 (123.42) | 177.92 (706.05) |
| 22. Energy Content of IRWST Water | 114.72 (455.24) | 117.22 (465.15) | 117.25 (465.28) | 126.87 (503.47) | 127.27 (505.06) | 127.99 (507.91) | 142.87 (566.94) |
| 23. Energy Removed by CSHXs | 0.00 (0.00) | 0.00 (0.00) | 0.00 (0.00) | 0.00 (0.00) | 0.00 (0.00) | 0.01 (0.06) | 728.16 (2889.56) |

(1) The provided energy data is based on the temperature: 0 °C (32 °F), if not specified.

(2) All the RCS metal components are incorporated into a heat structure to model metal sensible energy release after EOPR.

(3) The initial energy content in RCB internal structures is assumed to zero (0) Btu.

Replace with next page

Table 6.2.1-37 (3 of 30)

Part A. Loss-of-Coolant Accident

Case: Double-Ended Suction Leg Slot Break with Minimum ECCS Flow

Unit of Energy: ⁽¹⁾ 10⁶ kcal (10⁶ Btu)

| Description of Stored Energy | Prior to LOCA | At Peak Pressure Prior to EOB | At EOB | At Peak Pressure After EOB | At End of Reflood | At End of Post-Reflood | At 1 Day |
|--|-----------------------|-------------------------------|----------------------|----------------------------|----------------------|------------------------|----------------------------------|
| 1. Reactor Coolant System Water Internal Energy | 103.036 (408.906) | 5.639 (22.378) | 5.639 (22.378) | 10.613 (42.119) | 10.77 (42.741) | 10.716 (42.527) | 6.52 (25.86) |
| 2. Safety Injection Tank Water Internal Energy | 10.53 (41.788) | 9.657 (38.325) | 9.657 (38.325) | 4.88 (19.365) | 4.602 (18.264) | 4.305 (17.085) | 0.0 (0.0) |
| 3. Energy Stored in Core | 7.65 (30.361) | 3.615 (14.346) | 3.615 (14.346) | 1.24 (4.921) | 1.24 (4.921) | 1.093 (4.338) | 55.38 ⁽²⁾ (219.78) |
| 4. Energy Stored in RV Internals | 10.584 (42.003) | 8.941 (35.482) | 8.941 (35.482) | 7.291 (28.937) | 7.181 (28.499) | 7.048 (27.972) | |
| 5. Energy Stored in RV Metal | 22.625 (89.789) | 22.049 (87.501) | 22.049 (87.501) | 21.635 (85.862) | 21.586 (85.664) | 21.531 (85.445) | |
| 6. Energy Stored in PZR, Primary Pipes, Valves and Pumps | 39.834 (158.082) | 35.358 (140.319) | 35.358 (140.319) | 33.901 (134.539) | 33.755 (133.961) | 33.606 (133.367) | |
| 7. Energy Stored in SG Secondary Tubes | 10.688 (42.416) | 9.738 (38.647) | 9.738 (38.647) | 6.825 (27.087) | 6.736 (26.731) | 6.652 (26.399) | 0.0 (0.0) |
| 8. Energy Stored in SG Secondary Walls | 37.688 (149.569) | 37.777 (149.919) | 37.777 (149.919) | 34.929 (138.618) | 34.73 (137.829) | 34.543 (137.086) | 0.0 (0.0) |
| 9. Secondary Coolant Internal Energy in SG 1(Affected) | 34.395 (136.5) | 35.788 (142.028) | 35.788 (142.028) | 20.719 (82.224) | 20.311 (80.607) | 19.921 (79.059) | |
| 10. Secondary Coolant Internal Energy in SG 2 (Unaffected) | 34.395 (136.5) | 37.935 (150.548) | 37.935 (150.548) | 31.309 (124.253) | 30.961 (122.872) | 30.683 (121.767) | |
| 11. Secondary Coolant Internal Energy in Steam Line | 9.076 (36.02) | 9.076 (36.02) | 9.076 (36.02) | 9.076 (36.02) | 9.076 (36.02) | 9.076 (36.02) | 61.90 (245.64) |
| 12. Total NSSS Stored Energy | 320.502 (1271.934) | 215.572 (855.513) | 215.572 (855.513) | 182.42 (723.945) | 180.949 (718.109) | 179.174 (711.066) | |

APR1400 DCD TIER 2

Table 6.2.1-37 (3 of 30)

Part A. Loss-of-Coolant Accident

Case: Double-Ended Suction Leg Slot Break with Minimum ECCS Flow

Unit of Energy: ⁽¹⁾ 10⁶ kcal (10⁶ Btu)

| Description of Stored Energy | Prior to LOCA | At Peak Pressure Prior to EOB | At EOB | At Peak Pressure After EOB | At End of Reflood | At End of Post-Reflood | At 1 Day |
|--|----------------------|-------------------------------|----------------------|----------------------------|----------------------|------------------------|----------------------------------|
| 1. Reactor Coolant System Water Internal Energy | 103.036 (408.906) | 5.639 (22.378) | 5.639 (22.378) | 10.728 (42.574) | 10.774 (42.757) | 10.721 (42.548) | 5.78 (22.93) |
| 2. Safety Injection Tank Water Internal Energy | 10.53 (41.788) | 9.657 (38.325) | 9.657 (38.325) | 4.664 (18.508) | 4.584 (18.193) | 4.296 (17.049) | 0.0 (0.0) |
| 3. Energy Stored in Core | 7.65 (30.361) | 3.615 (14.346) | 3.615 (14.346) | 1.241 (4.925) | 1.242 (4.929) | 1.096 (4.351) | 56.45 ⁽²⁾ (224.00) |
| 4. Energy Stored in RV Internals | 10.584 (42.003) | 8.941 (35.482) | 8.941 (35.482) | 7.214 (28.629) | 7.184 (28.509) | 7.052 (27.988) | |
| 5. Energy Stored in RV Metal | 22.625 (89.789) | 22.049 (87.501) | 22.049 (87.501) | 21.6 (85.723) | 21.586 (85.666) | 21.532 (85.452) | |
| 6. Energy Stored in PZR, Primary Pipes, Valves and Pumps | 39.834 (158.082) | 35.358 (140.319) | 35.358 (140.319) | 33.797 (134.125) | 33.756 (133.962) | 33.61 (133.385) | |
| 7. Energy Stored in SG Secondary Tubes | 10.688 (42.416) | 9.738 (38.647) | 9.738 (38.647) | 6.759 (26.823) | 6.736 (26.731) | 6.654 (26.405) | 0.0 (0.0) |
| 8. Energy Stored in SG Secondary Walls | 37.688 (149.569) | 37.777 (149.919) | 37.777 (149.919) | 34.784 (138.043) | 34.73 (137.83) | 34.548 (137.106) | |
| 9. Secondary Coolant Internal Energy in SG 1(Affected) | 34.395 (136.5) | 35.786 (142.018) | 35.788 (142.028) | 20.413 (81.011) | 20.312 (80.61) | 19.945 (79.153) | 0.0 (0.0) |
| 10. Secondary Coolant Internal Energy in SG 2 (Unaffected) | 34.395 (136.5) | 37.935 (150.548) | 37.935 (150.548) | 31.054 (123.24) | 30.962 (122.873) | 30.684 (121.772) | |
| 11. Secondary Coolant Internal Energy in Steam Line | 9.076 (36.02) | 9.076 (36.02) | 9.076 (36.02) | 9.076 (36.02) | 9.076 (36.02) | 9.076 (36.02) | |
| 12. Total NSSS Stored Energy | 320.502 (1271.93) | 215.57 (855.503) | 215.572 (855.513) | 181.33 (719.62) | 180.942 (718.081) | 179.215 (711.228) | 62.22 (246.92) |

Replace with next page

Table 6.2.1-37 (4 of 30)

Part A. Loss-of-Coolant Accident

Case: Double-Ended Suction Leg Slot Break with Minimum ECCS Flow

Unit of Energy: ⁽¹⁾ 10⁶ kcal (10⁶ Btu)

| Description of Stored Energy | Prior to LOCA | At Peak Pressure Prior to EOB | At EOB | At Peak Pressure After EOB | At End of Reflood | At End of Post-Reflood | At 1 Day |
|--|-------------------|-------------------------------|---------------------|----------------------------|----------------------|------------------------|----------------------|
| 13. Feedwater to SG 1 (Affected) | 0.0 (0.0) | 3.316 (13.158) | 3.316 (13.158) | 3.316 (13.158) | 3.316 (13.158) | 3.316 (13.158) | 0.0 (0.0) |
| 14. Feedwater to SG 2 (Unaffected) | 0.0 (0.0) | 3.316 (13.158) | 3.316 (13.158) | 3.316 (13.158) | 3.316 (13.158) | 3.316 (13.158) | 0.0 (0.0) |
| 15. Steam Flow to Turbine | 0.0 (0.0) | 0.02 (0.078) | 0.02 (0.078) | 0.02 (0.078) | 0.02 (0.078) | 0.02 (0.078) | 0.0 (0.0) |
| 16. Energy from Decay Heat after Shutdown | 0.0 (0.0) | 2.108 (8.367) | 2.108 (8.367) | 6.138 (24.359) | 6.531 (25.917) | 6.944 (27.556) | 762.93 (3027.55) |
| 17. Steam Energy Release through Break | 0.0 (0.0) | 110.483 (438.46) | 110.483 (438.46) | 138.925 (551.335) | 140.383 (557.119) | 141.687 (562.295) | 1357.18 (5385.73) |
| 18. Liquid Energy Release by Spillage | 0.0 (0.0) | 0.0 (0.0) | 0.0 (0.0) | 9.526 (37.803) | 10.018 (39.759) | 10.994 (43.632) | 1574.79 (6249.27) |
| 19. Total Energy Release | 0.0 (0.0) | 110.483 (438.46) | 110.483 (438.46) | 148.451 (589.138) | 150.401 (596.878) | 152.682 (605.927) | 2931.97 (11635.0) |
| 20. Energy Content of RCB Atmosphere | 66.56 (264.15) | 156.30 (620.27) | 156.30 (620.27) | 168.50 (668.68) | 168.18 (667.40) | 167.58 (665.02) | 109.29 (433.68) |
| 21. Energy Content of RCB Internal Structures ⁽³⁾ | 0.00 (0.00) | 5.98 (23.73) | 5.98 (23.73) | 25.60 (101.61) | 27.28 (108.25) | 28.61 (113.55) | 184.93 (733.85) |
| 22. Energy Content of IRWST Water | 48.01 (190.51) | 49.52 (196.50) | 49.52 (196.50) | 64.12 (254.45) | 65.72 (260.80) | 67.20 (266.66) | 144.02 (571.53) |
| 23. Energy Removed by CSHXs | 0.00 (0.00) | 0.00 (0.00) | 0.00 (0.00) | 0.00 (0.00) | 0.01 (0.02) | 0.03 (0.11) | 734.26 (2913.77) |

- (1) The provided energy data is based on the temperature: 0 °C (32 °F), if not specified.
- (2) All the RCS metal components are incorporated into a heat structure to model metal sensible energy release after EOPR.
- (3) The initial energy content in RCB internal structures is assumed to zero (0) Btu.

APR1400 DCD TIER 2

Table 6.2.1-37 (4 of 30)

Part A. Loss-of-Coolant Accident

Case: Double-Ended Suction Leg Slot Break with Minimum ECCS Flow

Unit of Energy: ⁽¹⁾ 10⁶ kcal (10⁶ Btu)

| Description of Stored Energy | Prior to LOCA | At Peak Pressure Prior to EOB | At EOB | At Peak Pressure After EOB | At End of Reflood | At End of Post-Reflood | At 1 Day |
|--|--------------------|-------------------------------|---------------------|----------------------------|----------------------|------------------------|----------------------|
| 13. Feedwater to SG 1 (Affected) | 0.0 (0.0) | 3.316 (13.158) | 3.316 (13.158) | 3.316 (13.158) | 3.316 (13.158) | 3.316 (13.158) | 0.0 (0.0) |
| 14. Feedwater to SG 2 (Unaffected) | 0.0 (0.0) | 3.316 (13.158) | 3.316 (13.158) | 3.316 (13.158) | 3.316 (13.158) | 3.316 (13.158) | 0.0 (0.0) |
| 15. Steam Flow to Turbine | 0.0 (0.0) | 0.015 (0.061) | 0.02 (0.078) | 0.02 (0.078) | 0.02 (0.078) | 0.02 (0.078) | 0.0 (0.0) |
| 16. Energy from Decay Heat after Shutdown | 0.0 (0.0) | 2.108 (8.367) | 2.108 (8.367) | 6.419 (25.475) | 6.531 (25.917) | 6.936 (27.525) | 762.93 (3027.55) |
| 17. Steam Energy Release through Break | 0.0 (0.0) | 110.287 (437.68) | 110.483 (438.46) | 140.006 (555.624) | 140.385 (557.128) | 141.647 (562.137) | 1306.04 (5182.78) |
| 18. Liquid Energy Release by Spillage | 0.0 (0.0) | 0.0 (0.0) | 0.0 (0.0) | 9.873 (39.183) | 10.019 (39.76) | 10.984 (43.589) | 1558.28 (6183.77) |
| 19. Total Energy Release | 0.0 (0.0) | 110.287 (437.68) | 110.483 (438.46) | 149.879 (594.806) | 150.404 (596.888) | 152.631 (605.725) | 2864.32 (11366.5) |
| 20. Energy Content of RCB Atmosphere | 65.49 (259.87) | 152.57 (605.44) | 152.57 (605.44) | 162.74 (645.79) | 162.79 (646.00) | 162.54 (645.00) | 102.05 (404.97) |
| 21. Energy Content of RCB Internal Structures ⁽³⁾ | 0.00 (0.00) | 8.66 (34.36) | 8.79 (34.88) | 30.43 (120.75) | 30.13 (119.57) | 31.45 (124.79) | 174.66 (693.09) |
| 22. Energy Content of IRWST Water | 114.72 (455.24) | 117.22 (465.15) | 117.25 (465.28) | 126.62 (502.46) | 126.47 (501.85) | 127.28 (505.10) | 138.89 (551.14) |
| 23. Energy Removed by CSHXs | 0.00 (0.00) | 0.00 (0.00) | 0.00 (0.00) | 0.00 (0.01) | 0.00 (0.00) | 0.02 (0.07) | 707.89 (2809.13) |

- (1) The provided energy data is based on the temperature: 0 °C (32 °F), if not specified.
- (2) All the RCS metal components are incorporated into a heat structure to model metal sensible energy release after EOPR.
- (3) The initial energy content in RCB internal structures is assumed to zero (0) Btu.

Replace with next page

Table 6.2.1-37 (5 of 30)

Part A. Loss-of-Coolant Accident

Case: Double-Ended Discharge Leg Slot Break with Maximum ECCS Flow

Unit of Energy: ⁽¹⁾ 10⁶ kcal (10⁶ Btu)

| Description of Stored Energy | Prior to LOCA | At Peak Pressure Prior to EOB | At EOB | At End of Reflood | At Peak Pressure After EOR | At End of Post-Reflood | At 1 Day |
|--|-----------------------|-------------------------------|----------------------|----------------------|----------------------------|------------------------|----------------------------------|
| 1. Reactor coolant system water internal energy | 103.036 (408.906) | 3.127 (12.41) | 3.262 (12.944) | 10.159 (40.316) | 9.16 (36.353) | 8.235 (32.682) | 4.01 (15.90) |
| 2. Safety injection tank water internal energy | 10.53 (41.788) | 9.405 (37.323) | 8.962 (35.565) | 0.0 (0.0) | 0.0 (0.0) | 0.0 (0.0) | 0.0 (0.0) |
| 3. Energy stored in core | 7.65 (30.361) | 3.376 (13.398) | 3.448 (13.683) | 1.518 (6.023) | 0.969 (3.846) | 1.164 (4.62) | 50.12 ⁽²⁾ (198.90) |
| 4. Energy stored in RV internals | 10.584 (42.003) | 8.75 (34.724) | 8.66 (34.369) | 6.775 (26.887) | 6.075 (24.108) | 5.876 (23.32) | |
| 5. Energy stored in RV metal | 22.625 (89.789) | 22.063 (87.558) | 21.959 (87.145) | 21.165 (83.994) | 20.619 (81.83) | 20.449 (81.152) | |
| 6. Energy Stored in PZR, Primary Pipes, Valves, and Pumps | 39.834 (158.082) | 35.918 (142.544) | 35.828 (142.186) | 32.979 (130.881) | 31.322 (124.303) | 30.962 (122.873) | |
| 7. Energy stored in SG secondary tubes | 10.688 (42.416) | 9.863 (39.143) | 9.878 (39.2) | 6.551 (25.998) | 5.438 (21.582) | 5.314 (21.091) | 0.0 (0.0) |
| 8. Energy stored in SG secondary walls | 37.688 (149.569) | 37.871 (150.294) | 37.824 (150.109) | 34.305 (136.143) | 32.334 (128.319) | 31.948 (126.789) | |
| 9. Secondary coolant internal energy in SG 1 (Affected) | 34.395 (136.5) | 36.967 (146.708) | 36.983 (146.768) | 22.816 (90.547) | 19.525 (77.487) | 19.408 (77.023) | 0.0 (0.0) |
| 10. Secondary Coolant Internal Energy in SG 2 (Unaffected) | 34.395 (136.5) | 37.839 (150.168) | 37.834 (150.148) | 27.195 (107.924) | 22.316 (88.562) | 21.515 (85.384) | |
| 11. Secondary Coolant Internal Energy in Steam Line | 9.076 (36.02) | 9.076 (36.02) | 9.076 (36.02) | 9.076 (36.02) | 9.076 (36.02) | 9.076 (36.02) | |
| 12. Total NSSS Stored Energy | 320.502 (1271.934) | 214.256 (850.29) | 213.714 (848.137) | 172.539 (684.733) | 156.835 (622.411) | 153.948 (610.953) | 54.13 (214.80) |

APR1400 DCD TIER 2

Table 6.2.1-37 (5 of 30)

Part A. Loss-of-Coolant Accident

Case: Double-Ended Discharge Leg Slot Break with Maximum ECCS Flow

Unit of Energy: ⁽¹⁾ 10⁶ kcal (10⁶ Btu)

| Description of Stored Energy | Prior to LOCA | At Peak Pressure Prior to EOB | At EOB | At End of Reflood | At Peak Pressure After EOR | At End of Post-Reflood | At 1 Day |
|--|----------------------|-------------------------------|----------------------|----------------------|----------------------------|------------------------|----------------------------------|
| 1. Reactor coolant system water internal energy | 103.036 (408.906) | 3.127 (12.41) | 3.262 (12.944) | 10.168 (40.353) | 9.132 (36.243) | 8.181 (32.467) | 3.28 (13.03) |
| 2. Safety injection tank water internal energy | 10.53 (41.788) | 9.405 (37.323) | 8.962 (35.565) | 1.987 (7.885) | 0.0 (0.0) | 0.0 (0.0) | 0.0 (0.0) |
| 3. Energy stored in core | 7.65 (30.361) | 3.376 (13.398) | 3.448 (13.683) | 1.518 (6.023) | 0.973 (3.859) | 1.222 (4.851) | 51.43 ⁽²⁾ (204.07) |
| 4. Energy stored in RV internals | 10.584 (42.003) | 8.75 (34.724) | 8.66 (34.369) | 6.774 (26.883) | 6.065 (24.068) | 5.877 (23.324) | |
| 5. Energy stored in RV metal | 22.625 (89.789) | 22.063 (87.558) | 21.959 (87.145) | 21.164 (83.992) | 20.611 (81.795) | 20.445 (81.136) | |
| 6. Energy Stored in PZR, Primary Pipes, Valves, and Pumps | 39.834 (158.082) | 35.918 (142.544) | 35.828 (142.186) | 32.98 (130.884) | 31.303 (124.226) | 30.955 (122.846) | |
| 7. Energy stored in SG secondary tubes | 10.688 (42.416) | 9.863 (39.143) | 9.878 (39.2) | 6.553 (26.007) | 5.431 (21.555) | 5.311 (21.078) | 0.0 (0.0) |
| 8. Energy stored in SG secondary walls | 37.688 (149.569) | 37.871 (150.294) | 37.824 (150.109) | 34.308 (136.153) | 32.314 (128.239) | 31.941 (126.758) | |
| 9. Secondary coolant internal energy in SG 1 (Affected) | 34.395 (136.5) | 36.967 (146.708) | 36.983 (146.768) | 22.826 (90.587) | 19.518 (77.46) | 19.409 (77.025) | 0.0 (0.0) |
| 10. Secondary Coolant Internal Energy in SG 2 (Unaffected) | 34.395 (136.5) | 37.847 (150.198) | 37.834 (150.148) | 27.202 (107.953) | 22.272 (88.388) | 21.496 (85.308) | |
| 11. Secondary Coolant Internal Energy in Steam Line | 9.076 (36.02) | 9.076 (36.02) | 9.076 (36.02) | 9.076 (36.02) | 9.076 (36.02) | 9.076 (36.02) | |
| 12. Total NSSS Stored Energy | 320.502 (1271.93) | 214.264 (850.32) | 213.714 (848.137) | 174.556 (692.739) | 156.695 (621.854) | 153.913 (610.815) | 54.71 (217.10) |

Replace with next page

Table 6.2.1-37 (6 of 30)

Part A. Loss-of-Coolant Accident**Case: Double-Ended Discharge Leg Slot Break with Maximum ECCS Flow****Unit of Energy:⁽¹⁾ 10⁶ kcal (10⁶ Btu)**

| Description of Stored Energy | Prior to LOCA | At Peak Pressure Prior to EOB | At EOB | At End of Reflood | At Peak Pressure After EOR | At End of Post-Reflood | At 1 Day |
|--|-------------------|-------------------------------|--------------------|----------------------|----------------------------|------------------------|----------------------|
| 13. Feedwater to SG 1 (Affected) | 0.0 (0.0) | 3.316 (13.158) | 3.316 (13.158) | 3.316 (13.158) | 3.316 (13.158) | 3.316 (13.158) | 0.0 (0.0) |
| 14. Feedwater to SG 2 (Unaffected) | 0.0 (0.0) | 3.316 (13.158) | 3.316 (13.158) | 3.316 (13.158) | 3.316 (13.158) | 3.316 (13.158) | 0.0 (0.0) |
| 15. Steam flow to turbine | 0.0 (0.0) | 0.075 (0.299) | 0.073 (0.289) | 0.073 (0.289) | 0.073 (0.289) | 0.073 (0.289) | 0.0 (0.0) |
| 16. Energy from decay heat after shutdown | 0.0 (0.0) | 1.702 (6.753) | 1.804 (7.159) | 9.283 (36.84) | 13.449 (53.373) | 14.601 (57.945) | 763.68 (3030.54) |
| 17. Steam energy release through break | 0.0 (0.0) | 112.156 (445.1) | 112.811 (447.7) | 154.968 (615.003) | 173.309 (687.788) | 175.685 (697.219) | 1367.16 (5425.32) |
| 18. Liquid energy release by spillage | 0.0 (0.0) | 0.0 (0.0) | 0.0 (0.0) | 9.303 (36.919) | 12.684 (50.336) | 14.869 (59.008) | 2192.47 (8700.43) |
| 19. Total energy release | 0.0 (0.0) | 112.156 (445.1) | 112.811 (447.7) | 164.271 (651.922) | 185.993 (738.124) | 190.554 (756.228) | 3559.63 (14125.7) |
| 20. Energy Content of RCB Atmosphere | 66.56 (264.15) | 156.18 (619.79) | 155.66 (617.69) | 164.37 (652.26) | 170.21 (675.43) | 169.80 (673.81) | 109.36 (433.97) |
| 21. Energy Content of RCB Internal Structures ⁽³⁾ | 0.00 (0.00) | 5.73 (22.72) | 6.55 (25.99) | 33.90 (134.52) | 41.76 (165.73) | 43.35 (172.02) | 186.94 (741.83) |
| 22. Energy Content of IRWST Water | 48.01 (190.51) | 49.46 (196.28) | 49.81 (197.67) | 75.61 (300.06) | 88.15 (349.80) | 92.75 (368.07) | 155.03 (615.20) |
| 23. Energy Removed by CSHXs | 0.00 (0.00) | 0.00 (0.00) | 0.00 (0.00) | 0.19 (0.75) | 0.52 (2.08) | 0.64 (2.54) | 753.46 (2989.97) |

(1) The provided energy data is based on the temperature: 0 °C (32 °F), if not specified.

(2) All the RCS metal components are incorporated into a heat structure to model metal sensible energy release after EOPR.

(3) The initial energy content in RCB internal structures is assumed to zero (0) Btu.

APR1400 DCD TIER 2

Table 6.2.1-37 (6 of 30)

Part A. Loss-of-Coolant Accident

Case: Double-Ended Discharge Leg Slot Break with Maximum ECCS Flow

Unit of Energy:⁽¹⁾ 10⁶ kcal (10⁶ Btu)

| Description of Stored Energy | Prior to LOCA | At Peak Pressure Prior to EOB | At EOB | At End of Reflood | At Peak Pressure After EOR | At End of Post-Reflood | At 1 Day |
|--|--------------------|-------------------------------|--------------------|----------------------|----------------------------|------------------------|----------------------|
| 13. Feedwater to SG 1 (Affected) | 0.0 (0.0) | 3.316 (13.158) | 3.316 (13.158) | 3.316 (13.158) | 3.316 (13.158) | 3.316 (13.158) | 0.0 (0.0) |
| 14. Feedwater to SG 2 (Unaffected) | 0.0 (0.0) | 3.316 (13.158) | 3.316 (13.158) | 3.316 (13.158) | 3.316 (13.158) | 3.316 (13.158) | 0.0 (0.0) |
| 15. Steam flow to turbine | 0.0 (0.0) | 0.078 (0.308) | 0.073 (0.289) | 0.073 (0.289) | 0.073 (0.289) | 0.073 (0.289) | 0.0 (0.0) |
| 16. Energy from decay heat after shutdown | 0.0 (0.0) | 1.702 (6.753) | 1.804 (7.159) | 9.283 (36.84) | 13.51 (53.614) | 14.629 (58.057) | 763.92 (3031.46) |
| 17. Steam energy release through break | 0.0 (0.0) | 111.249 (441.5) | 112.811 (447.7) | 154.959 (614.964) | 173.491 (688.512) | 175.788 (697.626) | 1340.32 (5318.83) |
| 18. Liquid energy release by spillage | 0.0 (0.0) | 0.0 (0.0) | 0.0 (0.0) | 7.297 (28.958) | 12.73 (50.519) | 14.858 (58.966) | 2186.81 (8677.96) |
| 19. Total energy release | 0.0 (0.0) | 111.249 (441.5) | 112.811 (447.7) | 162.255 (643.922) | 186.221 (739.031) | 190.646 (756.593) | 3527.13 (13996.8) |
| 20. Energy Content of RCB Atmosphere | 65.49 (259.87) | 153.52 (609.24) | 152.20 (603.99) | 161.12 (639.37) | 168.17 (667.35) | 167.90 (666.30) | 103.83 (412.05) |
| 21. Energy Content of RCB Internal Structures ⁽³⁾ | 0.00 (0.00) | 7.26 (28.80) | 9.20 (36.51) | 35.47 (140.75) | 42.53 (168.76) | 43.96 (174.46) | 179.82 (713.59) |
| 22. Energy Content of IRWST Water | 114.72 (455.24) | 117.20 (465.09) | 117.73 (467.20) | 129.31 (513.16) | 134.26 (532.81) | 136.42 (541.36) | 152.18 (603.92) |
| 23. Energy Removed by CSHXs | 0.00 (0.00) | 0.00 (0.00) | 0.00 (0.00) | 0.13 (0.51) | 0.35 (1.39) | 0.42 (1.68) | 738.25 (2929.60) |

(1) The provided energy data is based on the temperature: 0 °C (32 °F), if not specified.

(2) All the RCS metal components are incorporated into a heat structure to model metal sensible energy release after EOPR.

(3) The initial energy content in RCB internal structures is assumed to zero (0) Btu.

Replace with next page

Table 6.2.1-37 (7 of 30)

Part A. Loss-of-Coolant Accident

Case: Double-Ended Discharge Leg Slot Break with Minimum ECCS Flow

Unit of Energy: ⁽¹⁾ 10⁶ kcal (10⁶ Btu)

| Description of Stored Energy | Prior to LOCA | At Peak Pressure Prior to EOB | At EOB | At End of Reflood | At Peak Pressure After EOR | At End of Post-Reflood | At 1 Day |
|--|-----------------------|-------------------------------|----------------------|----------------------|----------------------------|------------------------|----------------------------------|
| 1. Reactor Coolant System Water Internal Energy | 103.036 (408.906) | 3.127 (12.41) | 3.262 (12.944) | 10.142 (40.249) | 9.463 (37.556) | 10.495 (41.649) | 5.63 (22.34) |
| 2. Safety Injection Tank Water Internal Energy | 10.53 (41.788) | 9.405 (37.323) | 8.962 (35.565) | 2.106 (8.356) | 0.0 (0.0) | 0.0 (0.0) | 0.0 (0.0) |
| 3. Energy Stored in Core | 7.65 (30.361) | 3.376 (13.398) | 3.448 (13.683) | 1.518 (6.023) | 1.205 (4.781) | 1.471 (5.839) | 47.90 ⁽²⁾ (190.06) |
| 4. Energy Stored in RV Internals | 10.584 (42.003) | 8.75 (34.724) | 8.66 (34.369) | 6.774 (26.882) | 6.136 (24.351) | 5.784 (22.953) | |
| 5. Energy Stored in RV Metal | 22.625 (89.789) | 22.063 (87.558) | 21.959 (87.145) | 21.164 (83.989) | 20.644 (81.926) | 19.792 (78.545) | |
| 6. Energy Stored in PZR, Primary Pipes, Valves, and Pumps | 39.834 (158.082) | 35.918 (142.544) | 35.828 (142.186) | 32.978 (130.874) | 31.375 (124.512) | 29.766 (118.13) | |
| 7. Energy Stored in SG Secondary Tubes | 10.688 (42.416) | 9.863 (39.143) | 9.878 (39.2) | 6.548 (25.988) | 5.474 (21.724) | 5.013 (19.895) | 0.0 (0.0) |
| 8. Energy Stored in SG Secondary Walls | 37.688 (149.569) | 37.871 (150.294) | 37.824 (150.109) | 34.303 (136.135) | 32.396 (128.564) | 30.472 (120.93) | 0.0 (0.0) |
| 9. Secondary Coolant Internal Energy in SG 1(Affected) | 34.395 (136.5) | 36.967 (146.708) | 36.983 (146.768) | 22.806 (90.506) | 19.473 (77.281) | 19.33 (76.711) | |
| 10. Secondary Coolant Internal Energy in SG 2 (Unaffected) | 34.395 (136.5) | 37.839 (150.168) | 37.834 (150.148) | 27.187 (107.895) | 22.615 (89.748) | 19.433 (77.123) | |
| 11. Secondary Coolant Internal Energy in Steam Line | 9.076 (36.02) | 9.076 (36.02) | 9.076 (36.02) | 9.076 (36.02) | 9.076 (36.02) | 9.076 (36.02) | |
| 12. Total NSSS Stored Energy | 320.502 (1271.934) | 214.256 (850.29) | 213.714 (848.137) | 174.601 (692.918) | 157.856 (626.464) | 150.632 (597.794) | 53.52 (212.40) |

APR1400 DCD TIER 2

Table 6.2.1-37 (7 of 30)

Part A. Loss-of-Coolant Accident

Case: Double-Ended Discharge Leg Slot Break with Minimum ECCS Flow

Unit of Energy: ⁽¹⁾ 10⁶ kcal (10⁶ Btu)

| Description of Stored Energy | Prior to LOCA | At Peak Pressure Prior to EOB | At EOB | At End of Reflood | At Peak Pressure After EOR | At End of Post-Reflood | At 1 Day |
|--|----------------------|-------------------------------|----------------------|---------------------|----------------------------|------------------------|----------------------------------|
| 1. Reactor Coolant System Water Internal Energy | 103.036 (408.906) | 3.127 (12.41) | 3.262 (12.944) | 10.148 (40.274) | 9.368 (37.179) | 10.521 (41.755) | 5.07 (20.12) |
| 2. Safety Injection Tank Water Internal Energy | 10.53 (41.788) | 9.405 (37.323) | 8.962 (35.565) | 2.085 (8.273) | 0.0 (0.0) | 0.0 (0.0) | 0.0 (0.0) |
| 3. Energy Stored in Core | 7.65 (30.361) | 3.376 (13.398) | 3.448 (13.683) | 1.518 (6.023) | 1.215 (4.821) | 1.472 (5.84) | 49.27 ⁽²⁾ (195.50) |
| 4. Energy Stored in RV Internals | 10.584 (42.003) | 8.75 (34.724) | 8.66 (34.369) | 6.775 (26.886) | 6.101 (24.213) | 5.783 (22.951) | |
| 5. Energy Stored in RV Metal | 22.625 (89.789) | 22.063 (87.558) | 21.959 (87.145) | 21.164 (83.992) | 20.617 (81.82) | 19.789 (78.535) | |
| 6. Energy Stored in PZR, Primary Pipes, Valves, and Pumps | 39.834 (158.082) | 35.918 (142.544) | 35.828 (142.186) | 32.978 (130.875) | 31.309 (124.254) | 29.758 (118.096) | |
| 7. Energy Stored in SG Secondary Tubes | 10.688 (42.416) | 9.863 (39.143) | 9.878 (39.2) | 6.549 (25.99) | 5.452 (21.636) | 5.013 (19.895) | 0.0 (0.0) |
| 8. Energy Stored in SG Secondary Walls | 37.688 (149.569) | 37.871 (150.294) | 37.824 (150.109) | 34.304 (136.137) | 32.329 (128.301) | 30.465 (120.904) | |
| 9. Secondary Coolant Internal Energy in SG 1(Affected) | 34.395 (136.5) | 36.967 (146.708) | 36.983 (146.768) | 22.809 (90.518) | 19.454 (77.204) | 19.329 (76.71) | 0.0 (0.0) |
| 10. Secondary Coolant Internal Energy in SG 2 (Unaffected) | 34.395 (136.5) | 37.847 (150.198) | 37.834 (150.148) | 27.19 (107.903) | 22.471 (89.178) | 19.433 (77.121) | |
| 11. Secondary Coolant Internal Energy in Steam Line | 9.076 (36.02) | 9.076 (36.02) | 9.076 (36.02) | 9.076 (36.02) | 9.076 (36.02) | 9.076 (36.02) | |
| 12. Total NSSS Stored Energy | 320.502 (1271.93) | 214.264 (850.32) | 213.714 (848.137) | 174.594 (692.89) | 157.393 (624.624) | 150.64 (597.827) | 54.34 (215.63) |

Replace with next page

Table 6.2.1-37 (8 of 30)

Part A. Loss-of-Coolant Accident

Case: Double-Ended Discharge Leg Slot Break with Minimum ECCS Flow

Unit of Energy: ⁽¹⁾ 10⁶ kcal (10⁶ Btu)

| Description of Stored Energy | Prior to LOCA | At Peak Pressure Prior to EOB | At EOB | At End of Reflood | At Peak Pressure After EOR | At End of Post-Reflood | At 1 Day |
|--|-------------------|-------------------------------|--------------------|----------------------|----------------------------|------------------------|----------------------|
| 13. Feedwater to SG 1 (Affected) | 0.0 (0.0) | 3.316 (13.158) | 3.316 (13.158) | 3.316 (13.158) | 3.316 (13.158) | 3.316 (13.158) | 0.0 (0.0) |
| 14. Feedwater to SG 2 (Unaffected) | 0.0 (0.0) | 3.316 (13.158) | 3.316 (13.158) | 3.316 (13.158) | 3.316 (13.158) | 3.316 (13.158) | 0.0 (0.0) |
| 15. Steam Flow to Turbine | 0.0 (0.0) | 0.075 (0.299) | 0.073 (0.289) | 0.073 (0.289) | 0.073 (0.289) | 0.073 (0.289) | 0.0 (0.0) |
| 16. Energy from Decay Heat after Shutdown | 0.0 (0.0) | 1.702 (6.753) | 1.804 (7.159) | 9.293 (36.882) | 13.311 (52.826) | 20.24 (80.324) | 764.41 (3033.40) |
| 17. Steam Energy Release through Break | 0.0 (0.0) | 112.156 (445.1) | 112.811 (447.7) | 155.075 (615.425) | 172.783 (685.701) | 184.227 (731.119) | 1363.41 (5410.44) |
| 18. Liquid Energy Release by Spillage | 0.0 (0.0) | 0.0 (0.0) | 0.0 (0.0) | 5.952 (23.619) | 9.996 (39.668) | 13.702 (54.378) | 1580.06 (6270.20) |
| 19. Total Energy Release | 0.0 (0.0) | 112.156 (445.1) | 112.811 (447.7) | 161.026 (639.045) | 182.779 (725.369) | 197.93 (785.497) | 2943.47 (11680.6) |
| 20. Energy Content of RCB Atmosphere | 66.56 (264.15) | 156.18 (619.79) | 155.66 (617.69) | 164.48 (652.71) | 170.01 (674.67) | 166.63 (661.23) | 108.00 (428.56) |
| 21. Energy Content of RCB Internal Structures ⁽³⁾ | 0.00 (0.00) | 5.73 (22.72) | 6.55 (25.99) | 33.95 (134.73) | 41.51 (164.74) | 48.81 (193.69) | 184.63 (732.67) |
| 22. Energy Content of IRWST Water | 48.01 (190.51) | 49.46 (196.28) | 49.81 (197.67) | 74.29 (294.80) | 84.99 (337.25) | 102.52 (406.84) | 152.30 (604.37) |
| 23. Energy Removed by CSHXs | 0.00 (0.00) | 0.00 (0.00) | 0.00 (0.00) | 0.19 (0.76) | 0.51 (2.02) | 1.34 (5.33) | 742.38 (2945.99) |

(1) The provided energy data is based on the temperature: 0 °C (32 °F), if not specified.

(2) All the RCS metal components are incorporated into a heat structure to model metal sensible energy release after EOPR.

(3) The initial energy content in RCB internal structures is assumed to zero (0) Btu.

APR1400 DCD TIER 2

Table 6.2.1-37 (8 of 30)

Part A. Loss-of-Coolant Accident

Case: Double-Ended Discharge Leg Slot Break with Minimum ECCS Flow

Unit of Energy:⁽¹⁾ 10⁶ kcal (10⁶ Btu)

| Description of Stored Energy | Prior to LOCA | At Peak Pressure Prior to EOB | At EOB | At End of Reflood | At Peak Pressure After EOR | At End of Post-Reflood | At 1 Day |
|--|--------------------|-------------------------------|--------------------|----------------------|----------------------------|------------------------|----------------------|
| 13. Feedwater to SG 1 (Affected) | 0.0 (0.0) | 3.316 (13.158) | 3.316 (13.158) | 3.316 (13.158) | 3.316 (13.158) | 3.316 (13.158) | 0.0 (0.0) |
| 14. Feedwater to SG 2 (Unaffected) | 0.0 (0.0) | 3.316 (13.158) | 3.316 (13.158) | 3.316 (13.158) | 3.316 (13.158) | 3.316 (13.158) | 0.0 (0.0) |
| 15. Steam Flow to Turbine | 0.0 (0.0) | 0.078 (0.308) | 0.073 (0.289) | 0.073 (0.289) | 0.073 (0.289) | 0.073 (0.289) | 0.0 (0.0) |
| 16. Energy from Decay Heat after Shutdown | 0.0 (0.0) | 1.702 (6.753) | 1.804 (7.159) | 9.293 (36.882) | 13.503 (53.589) | 20.272 (80.449) | 764.41 (3033.43) |
| 17. Steam Energy Release through Break | 0.0 (0.0) | 111.249 (441.5) | 112.811 (447.7) | 155.071 (615.409) | 173.281 (687.679) | 184.304 (731.424) | 1322.78 (5249.22) |
| 18. Liquid Energy Release by Spillage | 0.0 (0.0) | 0.0 (0.0) | 0.0 (0.0) | 5.959 (23.647) | 10.186 (40.422) | 13.558 (53.806) | 1570.25 (6231.24) |
| 19. Total Energy Release | 0.0 (0.0) | 111.249 (441.5) | 112.811 (447.7) | 161.029 (639.056) | 183.467 (728.101) | 197.862 (785.23) | 2893.03 (11480.5) |
| 20. Energy Content of RCB Atmosphere | 65.49 (259.87) | 153.52 (609.24) | 152.20 (603.99) | 161.22 (639.78) | 167.89 (666.24) | 164.73 (653.72) | 102.45 (406.57) |
| 21. Energy Content of RCB Internal Structures ⁽³⁾ | 0.00 (0.00) | 7.26 (28.80) | 9.20 (36.51) | 35.51 (140.92) | 42.53 (168.76) | 49.22 (195.32) | 176.69 (701.15) |
| 22. Energy Content of IRWST Water | 114.72 (455.24) | 117.20 (465.09) | 117.73 (467.20) | 129.20 (512.70) | 133.80 (530.94) | 141.05 (559.72) | 148.66 (589.94) |
| 23. Energy Removed by CSHXs | 0.00 (0.00) | 0.00 (0.00) | 0.00 (0.00) | 0.13 (0.51) | 0.35 (1.38) | 0.87 (3.43) | 718.66 (2851.86) |

(1) The provided energy data is based on the temperature: 0 °C (32 °F), if not specified.

(2) All the RCS metal components are incorporated into a heat structure to model metal sensible energy release after EOPR.

(3) The initial energy content in RCB internal structures is assumed to zero (0) Btu.

Replace with next page

Table 6.2.1-37 (9 of 30)

Part A. Loss-of-Coolant Accident

Case: Double-Ended Hot Leg Slot Break

Unit of Energy:⁽¹⁾ 10⁶ kcal (10⁶ Btu)

| Description of Stored Energy | Prior to LOCA | At Peak Pressure at EOB | At EOB | At 1 Day |
|--|-----------------------|----------------------------|---------------------|----------------------------------|
| 1. Reactor coolant system water internal energy | 103.036 (408.906) | 5.591 (22.19) | 5.591 (22.19) | 3.49 (13.87) |
| 2. Safety injection tank water internal energy | 10.53 (41.788) | 9.086 (36.058) | 9.086 (36.058) | 0.0 (0.0) |
| 3. Energy stored in core | 7.65 (30.361) | 3.551 (14.091) | 3.551 (14.091) | 62.29 ⁽²⁾ (247.19) |
| 4. Energy stored in RV internals | 10.584 (42.003) | 8.485 (33.675) | 8.485 (33.675) | |
| 5. Energy stored in RV metal | 22.625 (89.789) | 21.957 (87.138) | 21.957 (87.138) | |
| 6. Energy stored in PZR, primary piping, valves, and pumps | 39.834 (158.082) | 35.076 (139.201) | 35.076 (139.201) | |
| 7. Energy stored in SG secondary tubes | 10.688 (42.416) | 9.421 (37.389) | 9.421 (37.389) | 0.0 (0.0) |
| 8. Energy stored in SG secondary walls | 37.688 (149.569) | 37.107 (147.263) | 37.107 (147.263) | |
| 9. Secondary coolant internal energy in SG 1 (Affected) | 34.395 (136.5) | 34.455 (136.738) | 34.455 (136.738) | 0.0 (0.0) |
| 10. Secondary coolant internal energy in SG 2 (Unaffected) | 34.395 (136.5) | 36.753 (145.858) | 36.753 (145.858) | |
| 11. Secondary coolant internal energy in steam line | 9.076 (36.02) | 9.076 (36.02) | 9.076 (36.02) | |
| 12. Total NSSS stored energy | 320.502 (1271.934) | 210.56 (835.621) | 210.56 (835.621) | 65.78 (261.06) |

APR1400 DCD TIER 2

Table 6.2.1-37 (9 of 30)

Part A. Loss-of-Coolant Accident

Case: Double-Ended Hot Leg Slot Break

Unit of Energy:⁽¹⁾ 10⁶ kcal (10⁶ Btu)

| Description of Stored Energy | Prior to LOCA | At Peak Pressure at EOB | At EOB | At 1 Day |
|---|----------------------|----------------------------|---------------------|----------------------------------|
| 1. Reactor coolant system water internal energy | 103.036 (408.906) | 5.591 (22.19) | 5.591 (22.19) | 1.98 (7.86) |
| 2. Safety injection tank water internal energy | 10.53 (41.788) | 9.086 (36.058) | 9.086 (36.058) | 0.0 (0.0) |
| 3. Energy stored in core | 7.65 (30.361) | 3.551 (14.091) | 3.551 (14.091) | 62.68 ⁽²⁾ (248.75) |
| 4. Energy stored in RV internals | 10.584 (42.003) | 8.485 (33.675) | 8.485 (33.675) | |
| 5. Energy stored in RV metal | 22.625 (89.789) | 21.957 (87.138) | 21.957 (87.138) | |
| 6. Energy stored in PZR, primary piping, valves, and pumps | 39.834 (158.082) | 35.076 (139.201) | 35.076 (139.201) | |
| 7. Energy stored in SG secondary tubes | 10.688 (42.416) | 9.421 (37.389) | 9.421 (37.389) | 0.0 (0.0) |
| 8. Energy stored in SG secondary walls | 37.688 (149.569) | 37.107 (147.263) | 37.107 (147.263) | |
| 9. Secondary coolant internal energy in SG 1 (Affected) | 34.395 (136.5) | 34.455 (136.738) | 34.455 (136.738) | 0.0 (0.0) |
| 10. Secondary coolant internal energy in SG 2 (Unaffected) | 34.395 (136.5) | 36.733 (145.778) | 36.753 (145.858) | |
| 11. Secondary coolant internal energy in steam line | 9.076 (36.02) | 9.076 (36.02) | 9.076 (36.02) | |
| 12. Total NSSS stored energy | 320.502 (1271.93) | 210.54 (835.541) | 210.56 (835.621) | 64.66 (256.61) |

Replace with next page

Table 6.2.1-37 (10 of 30)

Part A. Loss-of-Coolant Accident
 Case: Double-Ended Hot Leg Slot Break
 Unit of Energy:⁽¹⁾ 10⁶ kcal (10⁶ Btu)

| Description of Stored Energy | Prior to LOCA | At Peak Pressure at EOB | At EOB | At 1 Day |
|--|-------------------|-------------------------|---------------------|----------------------|
| 13. Feedwater to SG 1 (Affected) | 0.0 (0.0) | 3.316 (13.158) | 3.316 (13.158) | 0.0 (0.0) |
| 14. Feedwater to SG 2 (Unaffected) | 0.0 (0.0) | 3.316 (13.158) | 3.316 (13.158) | 0.0 (0.0) |
| 15. Steam flow to turbine | 0.0 (0.0) | 0.0 (0.0) | 0.0 (0.0) | 0.0 (0.0) |
| 16. Energy generated from decay heat after shutdown | 0.0 (0.0) | 1.978 (7.848) | 1.978 (7.848) | 762.37 (3025.34) |
| 17. Steam energy release through break | 0.0 (0.0) | 115.563 (458.62) | 115.563 (458.62) | 1370.47 (5438.44) |
| 18. Liquid energy release by spillage | 0.0 (0.0) | 0.0 (0.0) | 0.0 (0.0) | 2152.03 (8539.93) |
| 19. Total energy release | 0.0 (0.0) | 115.563 (458.62) | 115.563 (458.62) | 3522.49 (13978.4) |
| 20. Energy content of RCB atmosphere | 66.56 (264.15) | 164.18 (651.53) | 164.08 (651.13) | 112.52 (446.53) |
| 21. Energy content of RCB internal structures ⁽³⁾ | 0.00 (0.00) | 4.92 (19.52) | 5.11 (20.27) | 188.20 (746.86) |
| 22. Energy content of IRWST water | 48.01 (190.51) | 48.97 (194.33) | 49.03 (194.57) | 147.18 (584.06) |
| 23. Energy removed by CSHXs | 0.00 (0.00) | 0.00 (0.00) | 0.00 (0.00) | 737.55 (2926.82) |

- (1) The provided energy data is based on the temperature: 0 °C (32 °F), if not specified.
 (2) All the RCS metal components are incorporated into a heat structure to model metal sensible energy release after EOPR.
 (3) The initial energy content in RCB internal structures is assumed to zero (0) Btu.

Table 6.2.1-37 (11 of 30)

Part B. Main Steam Line Break

Conditions: Main Steam Line Break, 102 % Power – Loss of One CSS Train

Unit of Energy:⁽¹⁾ 10⁶ kcal (10⁶ Btu)

| Energy Description (Time) | Prior to MSLB | At Peak Pressure | End of Blowdown |
|--|------------------------|----------------------|----------------------|
| 1. Reactor coolant system water internal energy | 101.996 (404.777) | 68.753 (272.852) | 60.080 (238.43) |
| 2. Energy stored in core | 8.525 (33.831) | 2.788 (11.064) | 2.475 (9.822) |
| 3. Energy stored in pressurizer, primary piping, valves, and pumps | 59.117 (234.611) | 43.958 (174.449) | 39.776 (157.853) |
| 4. Energy stored in SG tubes | 10.340 (41.036) | 7.553 (29.973) | 6.752 (26.794) |
| 5. Energy stored in SG secondary walls | 41.159 (163.341) | 37.368 (148.298) | 36.924 (146.534) |
| 6. Secondary coolant internal energy in Steam Generator | 34.546 (137.1) | 23.448 (93.055) | 21.258 (84.364) |
| 7. Secondary coolant internal energy in Steam Generator 2 | 34.546 (137.1) | 1.371 (5.442) | 0.430 (1.706) |
| 8. Secondary coolant internal energy in steamline | 9.105 (36.132) | 7.251 (28.775) | 7.251 (28.775) |
| 9. Total NSSS Stored Energy | 299.334 (1,187.929) | 192.490 (763.909) | 174.944 (694.278) |
| 10. Feedwater To Steam Generator 1 | 0.000 (0.000) | 0.000 (0.000) | 0.000 (0.000) |
| 11. Feedwater To Steam Generator 2 | 0.000 (0.000) | 18.696 (74.198) | 23.181 (91.997) |
| 12. Steam Flow To Turbine | 0.000 (0.000) | 6.425 (25.500) | 6.425 (25.500) |
| 13. Energy Generated During Shutdown From Decay Heat | 0.000 (0.000) | 21.576 (85.624) | 58.285 (231.309) |
| 14. Break Flow | 0.000 (0.000) | 140.378 (557.100) | 198.938 (789.5) |

Replace with Part "A1" of next page

APR1400 DCD TIER 2

Table 6.2.1-37 (11 of 30)

Part B. Main Steam Line Break

Conditions: Main Steam Line Break, 102 % Power – Loss of One CSS Train

Unit of Energy:⁽¹⁾ 10⁶ kcal (10⁶ Btu)

| Energy Description (Time) | Prior to MSLB | At Peak Pressure | End of Blowdown |
|--|------------------------|----------------------|----------------------|
| 1. Reactor coolant system water internal energy | 101.996 (404.777) | 68.802 (273.046) | 60.080 (238.43) |
| 2. Energy stored in core | 8.525 (33.831) | 2.790 (11.071) | 2.475 (9.822) |
| 3. Energy stored in pressurizer, primary piping, valves, and pumps | 59.117 (234.611) | 43.981 (174.541) | 39.776 (157.853) |
| 4. Energy stored in SG tubes | 10.340 (41.036) | 7.557 (29.990) | 6.752 (26.794) |
| 5. Energy stored in SG secondary walls | 41.159 (163.341) | 37.373 (148.318) | 36.924 (146.534) |
| 6. Secondary coolant internal energy in Steam Generator | 34.546 (137.1) | 23.463 (93.114) | 21.258 (84.364) |
| 7. Secondary coolant internal energy in Steam Generator 2 | 34.546 (137.1) | 1.427 (5.661) | 0.430 (1.706) |
| 8. Secondary coolant internal energy in steamline | 9.105 (36.132) | 7.251 (28.775) | 7.251 (28.775) |
| 9. Total NSSS Stored Energy | 299.334 (1,187.929) | 192.643 (764.516) | 174.944 (694.278) |
| 10. Feedwater To Steam Generator 1 | 0.000 (0.000) | 0.000 (0.000) | 0.000 (0.000) |
| 11. Feedwater To Steam Generator 2 | 0.000 (0.000) | 18.684 (74.147) | 23.181 (91.997) |
| 12. Steam Flow To Turbine | 0.000 (0.000) | 6.425 (25.500) | 6.425 (25.500) |
| 13. Energy Generated During Shutdown From Decay Heat | 0.000 (0.000) | 21.496 (85.308) | 58.285 (231.309) |
| 14. Break Flow | 0.000 (0.000) | 140.151 (556.200) | 198.938 (789.5) |

Part "A1"

Table 6.2.1-37 (13 of 30)

Part B. Main Steam Line Break

Conditions: Main Steam Line Break, 102 % Power – MSIV Failure

Unit of Energy: ⁽¹⁾ 10⁶ kcal (10⁶ Btu)

| Energy Description (Time) | Prior to MSLB | At Peak Pressure | End of Blowdown |
|--|------------------------|----------------------|----------------------|
| 1. Reactor coolant system water internal energy | 101.996 (404.777) | 69.270 (274.903) | 60.086 (238.456) |
| 2. Energy stored in core | 8.525 (33.831) | 2.807 (11.141) | 2.475 (9.823) |
| 3. Energy stored in pressurizer, primary piping, valves, and pumps | 59.117 (234.611) | 44.204 (175.426) | 39.779 (157.866) |
| 4. Energy stored in SG tubes | 10.340 (41.036) | 7.597 (30.149) | 6.752 (26.797) |
| 5. Energy stored in SG secondary walls | 41.159 (163.341) | 37.420 (148.503) | 36.923 (146.53) |
| 6. Secondary coolant internal energy in Steam Generator | 34.546 (137.1) | 23.602 (93.668) | 21.259 (84.37) |
| 7. Secondary coolant internal energy in Steam Generator 2 | 34.546 (137.1) | 1.955 (7.757) | 0.433 (1.718) |
| 8. Secondary coolant internal energy in steamline | 9.105 (36.132) | 0.594 (2.358) | 0.512 (2.033) |
| 9. Total NSSS Stored Energy | 299.334 (1,187.929) | 187.449 (743.905) | 168.220 (667.592) |
| 10. Feedwater to Steam Generator 1 | 0.000 (0.000) | 0.000 (0.000) | 0.000 (0.000) |
| 11. Feedwater to Steam Generator 2 | 0.000 (0.000) | 18.573 (73.709) | 23.183 (92.002) |
| 12. Steam Flow to Turbine | 0.000 (0.000) | 6.425 (25.500) | 6.425 (25.500) |
| 13. Energy Generated During Shutdown From Decay Heat | 0.000 (0.000) | 20.854 (82.760) | 58.285 (231.309) |
| 14. Break Flow | 0.000 (0.000) | 144.662 (574.100) | 205.666 (816.200) |

Replace with Part "A2" of next page

APR1400 DCD TIER 2

Table 6.2.1-37 (13 of 30)

Part B. Main Steam Line Break

Conditions: Main Steam Line Break, 102 % Power – MSIV Failure

Unit of Energy: ⁽¹⁾ 10⁶ kcal (10⁶ Btu)

| Energy Description (Time) | Prior to MSLB | At Peak Pressure | End of Blowdown |
|--|------------------------|----------------------|----------------------|
| 1. Reactor coolant system water internal energy | 101.996 (404.777) | 69.411 (275.461) | 60.086 (238.456) |
| 2. Energy stored in core | 8.525 (33.831) | 2.812 (11.161) | 2.475 (9.823) |
| 3. Energy stored in pressurizer, primary piping, valves, and pumps | 59.117 (234.611) | 44.271 (175.683) | 39.779 (157.866) |
| 4. Energy stored in SG tubes | 10.340 (41.036) | 7.609 (30.197) | 6.752 (26.797) |
| 5. Energy stored in SG secondary walls | 41.159 (163.341) | 37.434 (148.558) | 36.923 (146.53) |
| 6. Secondary coolant internal energy in Steam Generator | 34.546 (137.1) | 23.643 (93.828) | 21.259 (84.37) |
| 7. Secondary coolant internal energy in Steam Generator 2 | 34.546 (137.1) | 2.112 (8.381) | 0.433 (1.718) |
| 8. Secondary coolant internal energy in steamline | 9.105 (36.132) | 0.598 (2.372) | 0.512 (2.033) |
| 9. Total NSSS Stored Energy | 299.334 (1,187.929) | 187.889 (745.651) | 168.220 (667.592) |
| 10. Feedwater to Steam Generator 1 | 0.000 (0.000) | 0.000 (0.000) | 0.000 (0.000) |
| 11. Feedwater to Steam Generator 2 | 0.000 (0.000) | 18.573 (73.709) | 23.183 (92.002) |
| 12. Steam Flow to Turbine | 0.000 (0.000) | 6.425 (25.500) | 6.425 (25.500) |
| 13. Energy Generated During Shutdown From Decay Heat | 0.000 (0.000) | 20.692 (82.117) | 58.285 (231.309) |
| 14. Break Flow | 0.000 (0.000) | 144.032 (571.600) | 205.666 (816.200) |

Part "A2"

Table 6.2.1-37 (15 of 30)

Part B. Main Steam Line Break

Conditions: Main Steam Line Break, 75 % Power – Loss of One CSS Train

Unit of Energy: ⁽¹⁾ 10⁶ kcal (10⁶ Btu)

| Energy Description (Time) | Prior to MSLB | At Peak Pressure | End of Blowdown |
|--|------------------------|----------------------|----------------------|
| 1. Reactor coolant system water internal energy | 100.913 (400.480) | 63.604 (252.417) | 55.498 (220.247) |
| 2. Energy stored in core | 7.141 (28.342) | 2.536 (10.063) | 2.349 (9.324) |
| 3. Energy stored in pressurizer, primary piping, valves, and pumps | 58.598 (232.552) | 41.223 (163.597) | 37.316 (148.092) |
| 4. Energy stored in SG tubes | 10.282 (40.804) | 7.026 (27.883) | 6.278 (24.915) |
| 5. Energy stored in SG secondary walls | 41.281 (163.826) | 36.120 (143.346) | 35.615 (141.34) |
| 6. Secondary coolant internal energy in Steam Generator | 37.732 (149.74) | 24.168 (95.913) | 21.651 (85.924) |
| 7. Secondary coolant internal energy in Steam Generator 2 | 37.732 (149.74) | 1.277 (5.067) | 0.550 (2.183) |
| 8. Secondary coolant internal energy in steamline | 9.314 (36.962) | 7.059 (28.014) | 7.059 (28.014) |
| 9. Total NSSS stored energy | 302.992 (1,202.446) | 183.013 (726.300) | 166.316 (660.038) |
| 10. Feedwater to Steam Generator 1 | 0.000 (0.000) | 0.000 (0.000) | 0.000 (0.000) |
| 11. Feedwater to Steam Generator 2 | 0.000 (0.000) | 18.842 (74.777) | 23.016 (91.341) |
| 12. Steam Flow to Turbine | 0.000 (0.000) | 4.770 (18.93) | 4.770 (18.93) |
| 13. Energy Generated during Shutdown From Decay Heat | 0.000 (0.000) | 17.818 (70.711) | 51.595 (204.759) |
| 14. Break Flow | 0.000 (0.000) | 151.591 (601.600) | 206.170 (818.2) |

Replace with Part "A3" of next page

APR1400 DCD TIER 2

Table 6.2.1-37 (15 of 30)

Part B. Main Steam Line Break

Conditions: Main Steam Line Break, 75 % Power – Loss of One CSS Train

Unit of Energy:⁽¹⁾ 10⁶ kcal (10⁶ Btu)

| Energy Description (Time) | Prior to MSLB | At Peak Pressure | End of Blowdown |
|--|------------------------|----------------------|----------------------|
| 1. Reactor coolant system water internal energy | 100.913 (400.480) | 63.705 (252.819) | 55.498 (220.247) |
| 2. Energy stored in core | 7.141 (28.342) | 2.539 (10.077) | 2.349 (9.324) |
| 3. Energy stored in pressurizer, primary piping, valves, and pumps | 58.598 (232.552) | 41.272 (163.790) | 37.316 (148.092) |
| 4. Energy stored in SG tubes | 10.282 (40.804) | 7.035 (27.919) | 6.278 (24.915) |
| 5. Energy stored in SG secondary walls | 41.281 (163.826) | 36.130 (143.384) | 35.615 (141.34) |
| 6. Secondary coolant internal energy in Steam Generator | 37.732 (149.74) | 24.200 (96.040) | 21.651 (85.924) |
| 7. Secondary coolant internal energy in Steam Generator 2 | 37.732 (149.74) | 1.353 (5.371) | 0.550 (2.183) |
| 8. Secondary coolant internal energy in steamline | 9.314 (36.962) | 7.059 (28.014) | 7.059 (28.014) |
| 9. Total NSSS stored energy | 302.992 (1,202.446) | 183.294 (727.415) | 166.316 (660.038) |
| 10. Feedwater to Steam Generator 1 | 0.000 (0.000) | 0.000 (0.000) | 0.000 (0.000) |
| 11. Feedwater to Steam Generator 2 | 0.000 (0.000) | 18.822 (74.696) | 23.016 (91.341) |
| 12. Steam Flow to Turbine | 0.000 (0.000) | 4.770 (18.930) | 4.770 (18.93) |
| 13. Energy Generated during Shutdown From Decay Heat | 0.000 (0.000) | 17.706 (70.269) | 51.595 (204.759) |
| 14. Break Flow | 0.000 (0.000) | 151.188 (600.000) | 206.170 (818.2) |

Part "A3"

Table 6.2.1-37 (17 of 30)

Part B. Main Steam Line Break

Conditions: Main Steam Line Break, 75 % Power – MSIV Failure

Unit of Energy:⁽¹⁾ 10⁶ kcal (10⁶ Btu)

| Energy Description (Time) | Prior to MSLB | At Peak Pressure | End of Blowdown |
|--|------------------------|----------------------|----------------------|
| 1. Reactor coolant system water internal energy | 100.913 (400.48) | 64.621 (256.454) | 55.499 (220.251) |
| 2. Energy stored in core | 7.141 (28.342) | 2.570 (10.199) | 2.350 (9.326) |
| 3. Energy stored in pressurizer, primary piping, valves, and pumps | 58.598 (232.552) | 41.710 (165.530) | 37.317 (148.093) |
| 4. Energy stored in SG tubes | 10.282 (40.804) | 7.117 (28.243) | 6.278 (24.916) |
| 5. Energy stored in SG secondary walls | 41.281 (163.826) | 36.220 (143.741) | 35.613 (141.332) |
| 6. Secondary coolant internal energy in Steam Generator | 37.732 (149.74) | 24.487 (97.177) | 21.651 (85.924) |
| 7. Secondary coolant internal energy in Steam Generator 2 | 37.732 (149.74) | 2.086 (8.277) | 0.554 (2.198) |
| 8. Secondary coolant internal energy in steamline | 9.314 (36.962) | 0.585 (2.320) | 0.511 (2.028) |
| 9. Total NSSS Stored Energy | 302.992 (1,202.446) | 179.395 (711.940) | 159.773 (634.068) |
| 10. Feedwater to Steam Generator 1 | 0.000 (0.000) | 0.000 (0.000) | 0.000 (0.000) |
| 11. Feedwater to Steam Generator 2 | 0.000 (0.000) | 18.659 (74.051) | 23.018 (91.349) |
| 12. Steam Flow to Turbine | 0.000 (0.000) | 4.770 (18.93) | 4.770 (18.93) |
| 13. Energy Generated During Shutdown From Decay Heat | 0.000 (0.000) | 16.863 (66.920) | 51.579 (204.693) |
| 14. Break Flow | 0.000 (0.000) | 154.136 (611.700) | 212.696 (844.1) |


 Replace with Part "A4" of next page

APR1400 DCD TIER 2

Table 6.2.1-37 (17 of 30)

Part B. Main Steam Line Break

Conditions: Main Steam Line Break, 75 % Power – MSIV Failure

Unit of Energy: ⁽¹⁾ 10⁶ kcal (10⁶ Btu)

| Energy Description (Time) | Prior to MSLB | At Peak Pressure | End of Blowdown |
|--|------------------------|----------------------|----------------------|
| 1. Reactor coolant system water internal energy | 100.913 (400.48) | 64.767 (257.032) | 55.499 (220.251) |
| 2. Energy stored in core | 7.141 (28.342) | 2.575 (10.218) | 2.350 (9.326) |
| 3. Energy stored in pressurizer, primary piping, valves, and pumps | 58.598 (232.552) | 41.780 (165.807) | 37.317 (148.093) |
| 4. Energy stored in SG tubes | 10.282 (40.804) | 7.130 (28.294) | 6.278 (24.916) |
| 5. Energy stored in SG secondary walls | 41.281 (163.826) | 36.234 (143.798) | 35.613 (141.332) |
| 6. Secondary coolant internal energy in Steam Generator | 37.732 (149.74) | 24.531 (97.354) | 21.651 (85.924) |
| 7. Secondary coolant internal energy in Steam Generator 2 | 37.732 (149.74) | 2.207 (8.758) | 0.554 (2.198) |
| 8. Secondary coolant internal energy in steamline | 9.314 (36.962) | 0.587 (2.328) | 0.511 (2.028) |
| 9. Total NSSS Stored Energy | 302.992 (1,202.446) | 179.810 (713.590) | 159.773 (634.068) |
| 10. Feedwater to Steam Generator 1 | 0.000 (0.000) | 0.000 (0.000) | 0.000 (0.000) |
| 11. Feedwater to Steam Generator 2 | 0.000 (0.000) | 18.636 (73.959) | 23.018 (91.349) |
| 12. Steam Flow to Turbine | 0.000 (0.000) | 4.770 (18.930) | 4.770 (18.93) |
| 13. Energy Generated During Shutdown From Decay Heat | 0.000 (0.000) | 16.749 (66.468) | 51.579 (204.693) |
| 14. Break Flow | 0.000 (0.000) | 153.607 (609.600) | 212.696 (844.1) |

Part "A4"

Table 6.2.1-37 (19 of 30)

Part B. Main Steam Line Break

Conditions: Main Steam Line Break, 50 % Power – Loss of One CSS Train

Unit of Energy: ⁽¹⁾ 10⁶ kcal (10⁶ Btu)

| Energy Description (Time) | Prior to MSLB | At Peak Pressure | End of Blowdown |
|--|------------------------|----------------------|----------------------|
| 1. Reactor coolant system water internal energy | 100.044 (397.031) | 66.464 (263.766) | 57.907 (229.808) |
| 2. Energy stored in core | 5.859 (23.252) | 2.540 (10.080) | 2.378 (9.437) |
| 3. Energy stored in pressurizer, primary piping, valves, and pumps | 58.094 (230.549) | 42.306 (167.894) | 38.184 (151.537) |
| 4. Energy stored in SG tubes | 10.221 (40.563) | 7.227 (28.682) | 6.446 (25.58) |
| 5. Energy stored in SG secondary walls | 41.397 (164.287) | 35.946 (142.655) | 35.184 (139.63) |
| 6. Secondary coolant internal energy in Steam Generator | 40.766 (161.781) | 26.976 (107.055) | 23.758 (94.285) |
| 7. Secondary coolant internal energy in Steam Generator 2 | 40.766 (161.781) | 3.726 (14.787) | 0.581 (2.307) |
| 8. Secondary coolant internal energy in steamline | 9.489 (37.658) | 6.963 (27.632) | 6.963 (27.632) |
| 9. Total NSSS Stored Energy | 306.635 (1,216.902) | 192.148 (762.552) | 171.401 (680.216) |
| 10. Feedwater to Steam Generator 1 | 0.000 (0.000) | 0.000 (0.000) | 0.000 (0.000) |
| 11. Feedwater to Steam Generator 2 | 0.000 (0.000) | 13.844 (54.942) | 18.421 (73.106) |
| 12. Steam Flow to Turbine | 0.000 (0.000) | 3.177 (12.61) | 3.177 (12.61) |
| 13. Energy Generated During Shutdown From Decay Heat | 0.000 (0.000) | 10.380 (41.192) | 50.537 (200.561) |
| 14. Break Flow | 0.000 (0.000) | 135.439 (537.500) | 200.702 (796.5) |

Replace with Part "A5" of next page

APR1400 DCD TIER 2

Table 6.2.1-37 (19 of 30)

Part B. Main Steam Line Break

Conditions: Main Steam Line Break, 50 % Power – Loss of One CSS Train

Unit of Energy: ⁽¹⁾ 10⁶ kcal (10⁶ Btu)

| Energy Description (Time) | Prior to MSLB | At Peak Pressure | End of Blowdown |
|--|------------------------|----------------------|----------------------|
| 1. Reactor coolant system water internal energy | 100.044 (397.031) | 63.091 (250.383) | 57.907 (229.808) |
| 2. Energy stored in core | 5.859 (23.252) | 2.432 (9.651) | 2.378 (9.437) |
| 3. Energy stored in pressurizer, primary piping, valves, and pumps | 58.094 (230.549) | 40.688 (161.472) | 38.184 (151.537) |
| 4. Energy stored in SG tubes | 10.221 (40.563) | 6.923 (27.474) | 6.446 (25.58) |
| 5. Energy stored in SG secondary walls | 41.397 (164.287) | 35.585 (141.223) | 35.184 (139.63) |
| 6. Secondary coolant internal energy in Steam Generator | 40.766 (161.781) | 25.824 (102.486) | 23.758 (94.285) |
| 7. Secondary coolant internal energy in Steam Generator 2 | 40.766 (161.781) | 1.295 (5.138) | 0.581 (2.307) |
| 8. Secondary coolant internal energy in steamline | 9.489 (37.658) | 6.963 (27.632) | 6.963 (27.632) |
| 9. Total NSSS Stored Energy | 306.635 (1,216.902) | 182.801 (725.459) | 171.401 (680.216) |
| 10. Feedwater to Steam Generator 1 | 0.000 (0.000) | 0.000 (0.000) | 0.000 (0.000) |
| 11. Feedwater to Steam Generator 2 | 0.000 (0.000) | 14.318 (56.822) | 18.421 (73.106) |
| 12. Steam Flow to Turbine | 0.000 (0.000) | 3.177 (12.610) | 3.177 (12.61) |
| 13. Energy Generated During Shutdown From Decay Heat | 0.000 (0.000) | 12.044 (47.797) | 50.537 (200.561) |
| 14. Break Flow | 0.000 (0.000) | 146.627 (581.900) | 200.702 (796.5) |

Part "A5"

Table 6.2.1-37 (21 of 30)

Part B. Main Steam Line Break

Conditions: Main Steam Line Break, 50 % Power – MSIV Failure

Unit of Energy:⁽¹⁾ 10⁶ kcal (10⁶ Btu)

| Energy Description (Time) | Prior to MSLB | At Peak Pressure | End of Blowdown |
|--|------------------------|----------------------|----------------------|
| 1. Reactor coolant system water internal energy | 100.044 (397.031) | 64.500 (255.973) | 57.907 (229.808) |
| 2. Energy stored in core | 5.859 (23.252) | 2.477 (9.831) | 2.378 (9.437) |
| 3. Energy stored in pressurizer, primary piping, valves, and pumps | 58.094 (230.549) | 41.363 (164.152) | 38.184 (151.537) |
| 4. Energy stored in SG tubes | 10.221 (40.563) | 7.050 (27.978) | 6.446 (25.58) |
| 5. Energy stored in SG secondary walls | 41.397 (164.287) | 35.732 (141.805) | 35.182 (139.622) |
| 6. Secondary coolant internal energy in Steam Generator | 40.766 (161.781) | 26.311 (104.418) | 23.758 (94.285) |
| 7. Secondary coolant internal energy in Steam Generator 2 | 40.766 (161.781) | 2.214 (8.785) | 0.585 (2.321) |
| 8. Secondary coolant internal energy in steamline | 9.489 (37.658) | 0.569 (2.258) | 0.512 (2.033) |
| 9. Total NSSS Stored Energy | 306.635 (1,216.902) | 180.216 (715.201) | 164.952 (654.622) |
| 10. Feedwater to Steam Generator 1 | 0.000 (0.000) | 0.000 (0.000) | 0.000 (0.000) |
| 11. Feedwater to Steam Generator 2 | 0.000 (0.000) | 14.098 (55.948) | 18.423 (73.113) |
| 12. Steam Flow to Turbine | 0.000 (0.000) | 3.177 (12.61) | 3.177 (12.61) |
| 13. Energy Generated During Shutdown From Decay Heat | 0.000 (0.000) | 11.225 (44.546) | 50.527 (200.521) |
| 14. Break Flow | 0.000 (0.000) | 148.391 (588.900) | 207.153 (822.1) |

Replace with Part "A6" of next page

APR1400 DCD TIER 2

Table 6.2.1-37 (21 of 30)

Part B. Main Steam Line Break

Conditions: Main Steam Line Break, 50 % Power – MSIV Failure

Unit of Energy:⁽¹⁾ 10⁶ kcal (10⁶ Btu)

| Energy Description (Time) | Prior to MSLB | At Peak Pressure | End of Blowdown |
|--|------------------------|----------------------|----------------------|
| 1. Reactor coolant system water internal energy | 100.044 (397.031) | 64.732 (256.893) | 57.907 (229.808) |
| 2. Energy stored in core | 5.859 (23.252) | 2.485 (9.861) | 2.378 (9.437) |
| 3. Energy stored in pressurizer, primary piping, valves, and pumps | 58.094 (230.549) | 41.474 (164.593) | 38.184 (151.537) |
| 4. Energy stored in SG tubes | 10.221 (40.563) | 7.071 (28.061) | 6.446 (25.58) |
| 5. Energy stored in SG secondary walls | 41.397 (164.287) | 35.757 (141.903) | 35.182 (139.622) |
| 6. Secondary coolant internal energy in Steam Generator | 40.766 (161.781) | 26.391 (104.733) | 23.758 (94.285) |
| 7. Secondary coolant internal energy in Steam Generator 2 | 40.766 (161.781) | 2.380 (9.446) | 0.585 (2.321) |
| 8. Secondary coolant internal energy in steamline | 9.489 (37.658) | 0.572 (2.269) | 0.512 (2.033) |
| 9. Total NSSS Stored Energy | 306.635 (1,216.902) | 180.861 (717.758) | 164.952 (654.622) |
| 10. Feedwater to Steam Generator 1 | 0.000 (0.000) | 0.000 (0.000) | 0.000 (0.000) |
| 11. Feedwater to Steam Generator 2 | 0.000 (0.000) | 14.066 (55.821) | 18.423 (73.113) |
| 12. Steam Flow to Turbine | 0.000 (0.000) | 3.177 (12.610) | 3.177 (12.61) |
| 13. Energy Generated During Shutdown From Decay Heat | 0.000 (0.000) | 11.111 (44.095) | 50.527 (200.521) |
| 14. Break Flow | 0.000 (0.000) | 147.610 (584.800) | 207.153 (822.1) |

Part "A6"

Table 6.2.1-37 (23 of 30)

Part B. Main Steam Line Break

Conditions: Main Steam Line Break, 20 % Power – Loss of One CSS Train

Unit of Energy: ⁽¹⁾ 10⁶ kcal (10⁶ Btu)

| Energy Description (Time) | Prior to MSLB | At Peak Pressure | End of Blowdown |
|--|------------------------|----------------------|----------------------|
| 1. Reactor coolant system water internal energy | 98.468 (390.776) | 60.071 (238.395) | 60.175 (238.807) |
| 2. Energy stored in core | 4.317 (17.134) | 2.511 (9.964) | 2.396 (9.51) |
| 3. Energy stored in pressurizer, primary piping, valves, and pumps | 57.458 (228.027) | 39.035 (154.913) | 39.103 (155.184) |
| 4. Energy stored in SG tubes | 10.141 (40.244) | 6.610 (26.232) | 6.623 (26.283) |
| 5. Energy stored in SG secondary walls | 41.473 (164.587) | 33.969 (134.810) | 33.974 (134.829) |
| 6. Secondary coolant internal energy in Steam Generator | 46.168 (183.222) | 27.922 (110.809) | 27.689 (109.884) |
| 7. Secondary coolant internal energy in Steam Generator 2 | 46.168 (183.222) | 1.232 (4.889) | 0.836 (3.316) |
| 8. Secondary coolant internal energy in steamline | 9.606 (38.121) | 6.744 (26.765) | 6.744 (26.765) |
| 9. Total NSSS Stored Energy | 313.799 (1,245.332) | 178.093 (706.776) | 177.540 (704.578) |
| 10. Feedwater to Steam Generator 1 | 0.000 (0.000) | 0.000 (0.000) | 0.000 (0.000) |
| 11. Feedwater to Steam Generator 2 | 0.000 (0.000) | 8.447 (33.523) | 11.593 (46.006) |
| 12. Steam Flow to Turbine | 0.000 (0.000) | 1.123 (4.457) | 1.123 (4.457) |
| 13. Energy Generated During Shutdown From Decay Heat | 0.000 (0.000) | 15.343 (60.889) | 53.033 (210.464) |
| 14. Break Flow | 0.000 (0.000) | 158.168 (627.700) | 199.493 (791.7) |

Replace with Part "A7" of next page

APR1400 DCD TIER 2

Table 6.2.1-37 (23 of 30)

Part B. Main Steam Line Break

Conditions: Main Steam Line Break, 20 % Power – Loss of One CSS Train

Unit of Energy: ⁽¹⁾ 10⁶ kcal (10⁶ Btu)

| Energy Description (Time) | Prior to MSLB | At Peak Pressure | End of Blowdown |
|--|------------------------|----------------------|----------------------|
| 1. Reactor coolant system water internal energy | 98.468 (390.776) | 59.752 (237.129) | 60.175 (238.807) |
| 2. Energy stored in core | 4.317 (17.134) | 2.565 (10.180) | 2.396 (9.51) |
| 3. Energy stored in pressurizer, primary piping, valves, and pumps | 57.458 (228.027) | 38.872 (154.267) | 39.103 (155.184) |
| 4. Energy stored in SG tubes | 10.141 (40.244) | 6.579 (26.108) | 6.623 (26.283) |
| 5. Energy stored in SG secondary walls | 41.473 (164.587) | 33.939 (134.691) | 33.974 (134.829) |
| 6. Secondary coolant internal energy in Steam Generator | 46.168 (183.222) | 27.797 (110.314) | 27.689 (109.884) |
| 7. Secondary coolant internal energy in Steam Generator 2 | 46.168 (183.222) | 1.349 (5.355) | 0.836 (3.316) |
| 8. Secondary coolant internal energy in steamline | 9.606 (38.121) | 6.744 (26.765) | 6.744 (26.765) |
| 9. Total NSSS Stored Energy | 313.799 (1,245.332) | 177.598 (704.809) | 177.540 (704.578) |
| 10. Feedwater to Steam Generator 1 | 0.000 (0.000) | 0.000 (0.000) | 0.000 (0.000) |
| 11. Feedwater to Steam Generator 2 | 0.000 (0.000) | 8.335 (33.077) | 11.593 (46.006) |
| 12. Steam Flow to Turbine | 0.000 (0.000) | 1.123 (4.457) | 1.123 (4.457) |
| 13. Energy Generated During Shutdown From Decay Heat | 0.000 (0.000) | 13.126 (52.092) | 53.033 (210.464) |
| 14. Break Flow | 0.000 (0.000) | 156.354 (620.500) | 199.493 (791.7) |

Part "A7"

Table 6.2.1-37 (25 of 30)

Part B. Main Steam Line Break

Conditions: Main Steam Line Break, 20 % Power – MSIV Failure

Unit of Energy: ⁽¹⁾ 10⁶ kcal (10⁶ Btu)

| Energy Description (Time) | Prior to MSLB | At Peak Pressure | End of Blowdown |
|--|------------------------|----------------------|----------------------|
| 1. Reactor coolant system water internal energy | 98.468 (390.776) | 60.927 (241.794) | 60.175 (238.807) |
| 2. Energy stored in core | 4.317 (17.134) | 2.274 (9.023) | 2.396 (9.51) |
| 3. Energy stored in pressurizer, primary piping, valves, and pumps | 57.458 (228.027) | 39.478 (156.669) | 39.103 (155.184) |
| 4. Energy stored in SG tubes | 10.141 (40.244) | 6.688 (26.541) | 6.623 (26.283) |
| 5. Energy stored in SG secondary walls | 41.473 (164.587) | 34.207 (135.751) | 33.975 (134.832) |
| 6. Secondary coolant internal energy in Steam Generator | 46.168 (183.222) | 28.626 (113.606) | 27.689 (109.884) |
| 7. Secondary coolant internal energy in Steam Generator 2 | 46.168 (183.222) | 2.815 (11.170) | 0.840 (3.333) |
| 8. Secondary coolant internal energy in steamline | 9.606 (38.121) | 0.531 (2.106) | 0.512 (2.034) |
| 9. Total NSSS Stored Energy | 313.799 (1,245.332) | 175.545 (696.661) | 171.313 (679.867) |
| 10. Feedwater to Steam Generator 1 | 0.000 (0.000) | 0.000 (0.000) | 0.000 (0.000) |
| 11. Feedwater to Steam Generator 2 | 0.000 (0.000) | 7.592 (30.128) | 11.592 (46.005) |
| 12. Steam Flow to Turbine | 0.000 (0.000) | 1.123 (4.457) | 1.123 (4.457) |
| 13. Energy Generated During Shutdown From Decay Heat | 0.000 (0.000) | 5.268 (20.907) | 53.031 (210.456) |
| 14. Break Flow | 0.000 (0.000) | 149.827 (594.600) | 205.716 (816.4) |

Replace with Part "A8" of next page

APR1400 DCD TIER 2

Table 6.2.1-37 (25 of 30)

Part B. Main Steam Line Break

Conditions: Main Steam Line Break, 20 % Power – MSIV Failure

Unit of Energy:⁽¹⁾ 10⁶ kcal (10⁶ Btu)

| Energy Description (Time) | Prior to MSLB | At Peak Pressure | End of Blowdown |
|--|------------------------|----------------------|----------------------|
| 1. Reactor coolant system water internal energy | 98.468 (390.776) | 60.855 (241.509) | 60.175 (238.807) |
| 2. Energy stored in core | 4.317 (17.134) | 2.271 (9.014) | 2.396 (9.51) |
| 3. Energy stored in pressurizer, primary piping, valves, and pumps | 57.458 (228.027) | 39.443 (156.532) | 39.103 (155.184) |
| 4. Energy stored in SG tubes | 10.141 (40.244) | 6.681 (26.515) | 6.623 (26.283) |
| 5. Energy stored in SG secondary walls | 41.473 (164.587) | 34.198 (135.718) | 33.975 (134.832) |
| 6. Secondary coolant internal energy in Steam Generator | 46.168 (183.222) | 28.599 (113.496) | 27.689 (109.884) |
| 7. Secondary coolant internal energy in Steam Generator 2 | 46.168 (183.222) | 2.784 (11.049) | 0.840 (3.333) |
| 8. Secondary coolant internal energy in steamline | 9.606 (38.121) | 0.530 (2.104) | 0.512 (2.034) |
| 9. Total NSSS Stored Energy | 313.799 (1,245.332) | 175.362 (695.938) | 171.313 (679.867) |
| 10. Feedwater to Steam Generator 1 | 0.000 (0.000) | 0.000 (0.000) | 0.000 (0.000) |
| 11. Feedwater to Steam Generator 2 | 0.000 (0.000) | 7.605 (30.182) | 11.592 (46.005) |
| 12. Steam Flow to Turbine | 0.000 (0.000) | 1.123 (4.457) | 1.123 (4.457) |
| 13. Energy Generated During Shutdown From Decay Heat | 0.000 (0.000) | 5.282 (20.963) | 53.031 (210.456) |
| 14. Break Flow | 0.000 (0.000) | 150.054 (597.500) | 205.716 (816.4) |

Part "A8"

Table 6.2.1-37 (27 of 30)

Part B. Main Steam Line Break

Conditions: Main Steam Line Break, 0 % Power – Loss of One CSS Train

Unit of Energy: ⁽¹⁾ 10⁶ kcal (10⁶ Btu)

| Energy Description (Time) | Prior to MSLB | At Peak Pressure | End of Blowdown |
|--|------------------------|----------------------|----------------------|
| 1. Reactor coolant system water internal energy | 98.364 (390.366) | 62.225 (246.945) | 62.455 (247.856) |
| 2. Energy stored in core | 3.289 (13.054) | 2.501 (9.923) | 2.422 (9.611) |
| 3. Energy stored in pressurizer, primary piping, valves, and pumps | 61.107 (242.509) | 42.204 (167.491) | 42.349 (168.066) |
| 4. Energy stored in SG tubes | 10.082 (40.012) | 6.705 (26.608) | 6.723 (26.682) |
| 5. Energy stored in SG secondary walls | 41.907 (166.312) | 34.756 (137.932) | 34.769 (137.985) |
| 6. Secondary coolant internal energy in Steam Generator | 49.521 (196.526) | 30.304 (120.264) | 30.069 (119.332) |
| 7. Secondary coolant internal energy in Steam Generator 2 | 49.521 (196.526) | 0.471 (1.870) | 0.321 (1.272) |
| 8. Secondary coolant internal energy in steamline | 10.084 (40.019) | 8.007 (31.777) | 8.007 (31.777) |
| 9. Total NSSS Stored Energy | 323.876 (1,285.323) | 187.174 (742.811) | 187.116 (742.581) |
| 10. Feedwater to Steam Generator 1 | 0.000 (0.000) | 0.000 (0.000) | 0.000 (0.000) |
| 11. Feedwater to Steam Generator 2 | 0.000 (0.000) | 7.573 (30.054) | 10.697 (42.451) |
| 12. Steam Flow to Turbine | 0.000 (0.000) | 0.002 (0.007) | 0.002 (0.007) |
| 13. Energy Generated During Shutdown From Decay Heat | 0.000 (0.000) | 23.131 (91.798) | 64.154 (254.598) |
| 14. Break Flow | 0.000 (0.000) | 167.189 (663.500) | 208.186 (826.2) |

Replace with Part "A9" of next page

APR1400 DCD TIER 2

Table 6.2.1-37 (27 of 30)

Part B. Main Steam Line Break

Conditions: Main Steam Line Break, 0 % Power – Loss of One CSS Train

Unit of Energy:⁽¹⁾ 10⁶ kcal (10⁶ Btu)

| Energy Description (Time) | Prior to MSLB | At Peak Pressure | End of Blowdown |
|--|------------------------|----------------------|----------------------|
| 1. Reactor coolant system water internal energy | 98.364 (390.366) | 62.201 (246.851) | 62.455 (247.856) |
| 2. Energy stored in core | 3.289 (13.054) | 2.501 (9.924) | 2.422 (9.611) |
| 3. Energy stored in pressurizer, primary piping, valves, and pumps | 61.107 (242.509) | 42.198 (167.465) | 42.349 (168.066) |
| 4. Energy stored in SG tubes | 10.082 (40.012) | 6.698 (26.581) | 6.723 (26.682) |
| 5. Energy stored in SG secondary walls | 41.907 (166.312) | 34.756 (137.933) | 34.769 (137.985) |
| 6. Secondary coolant internal energy in Steam Generator | 49.521 (196.526) | 30.304 (120.262) | 30.069 (119.332) |
| 7. Secondary coolant internal energy in Steam Generator 2 | 49.521 (196.526) | 0.534 (2.121) | 0.321 (1.272) |
| 8. Secondary coolant internal energy in steamline | 10.084 (40.019) | 8.007 (31.777) | 8.007 (31.777) |
| 9. Total NSSS Stored Energy | 323.876 (1,285.323) | 187.199 (742.913) | 187.116 (742.581) |
| 10. Feedwater to Steam Generator 1 | 0.000 (0.000) | 0.000 (0.000) | 0.000 (0.000) |
| 11. Feedwater to Steam Generator 2 | 0.000 (0.000) | 7.566 (30.024) | 10.697 (42.451) |
| 12. Steam Flow to Turbine | 0.000 (0.000) | 0.002 (0.007) | 0.002 (0.007) |
| 13. Energy Generated During Shutdown From Decay Heat | 0.000 (0.000) | 22.990 (91.237) | 64.154 (254.598) |
| 14. Break Flow | 0.000 (0.000) | 167.038 (662.900) | 208.186 (826.2) |

Part "A9"

Table 6.2.1-37 (29 of 30)

Part B. Main Steam Line Break

Conditions: Main Steam Line Break, 0 % Power – MSIV Failure

Unit of Energy: ⁽¹⁾ 10⁶ kcal (10⁶ Btu)

| Energy Description (Time) | Prior to MSLB | At Peak Pressure | End of Blowdown |
|--|------------------------|----------------------|----------------------|
| 1. Reactor coolant system water internal energy | 98.364 (390.366) | 61.677 (244.768) | 62.455 (247.856) |
| 2. Energy stored in core | 3.289 (13.054) | 2.207 (8.759) | 2.422 (9.611) |
| 3. Energy stored in pressurizer, primary piping, valves, and pumps | 57.017 (226.277) | 39.267 (155.835) | 39.627 (157.263) |
| 4. Energy stored in SG tubes | 10.082 (40.012) | 6.646 (26.373) | 6.723 (26.682) |
| 5. Energy stored in SG secondary walls | 41.907 (166.312) | 34.724 (137.803) | 34.716 (137.772) |
| 6. Secondary coolant internal energy in Steam Generator | 49.521 (196.526) | 30.436 (120.786) | 30.059 (119.291) |
| 7. Secondary coolant internal energy in Steam Generator 2 | 49.521 (196.526) | 1.411 (5.600) | 0.324 (1.284) |
| 8. Secondary coolant internal energy in steamline | 10.084 (40.019) | 0.656 (2.605) | 0.522 (2.072) |
| 9. Total NSSS Stored Energy | 319.786 (1,269.092) | 177.023 (702.530) | 176.848 (701.832) |
| 10. Feedwater to Steam Generator 1 | 0.000 (0.000) | 0.000 (0.000) | 0.000 (0.000) |
| 11. Feedwater to Steam Generator 2 | 0.000 (0.000) | 3.368 (13.367) | 9.377 (37.212) |
| 12. Steam Flow to Turbine | 0.000 (0.000) | 0.002 (0.007) | 0.002 (0.007) |
| 13. Energy Generated During Shutdown From Decay Heat | 0.000 (0.000) | 0.006 (0.025) | 66.378 (263.425) |
| 14. Break Flow | 0.000 (0.000) | 146.048 (579.600) | 216.073 (857.5) |

Replace with Part "A10" of next page

APR1400 DCD TIER 2

Table 6.2.1-37 (29 of 30)

Part B. Main Steam Line Break

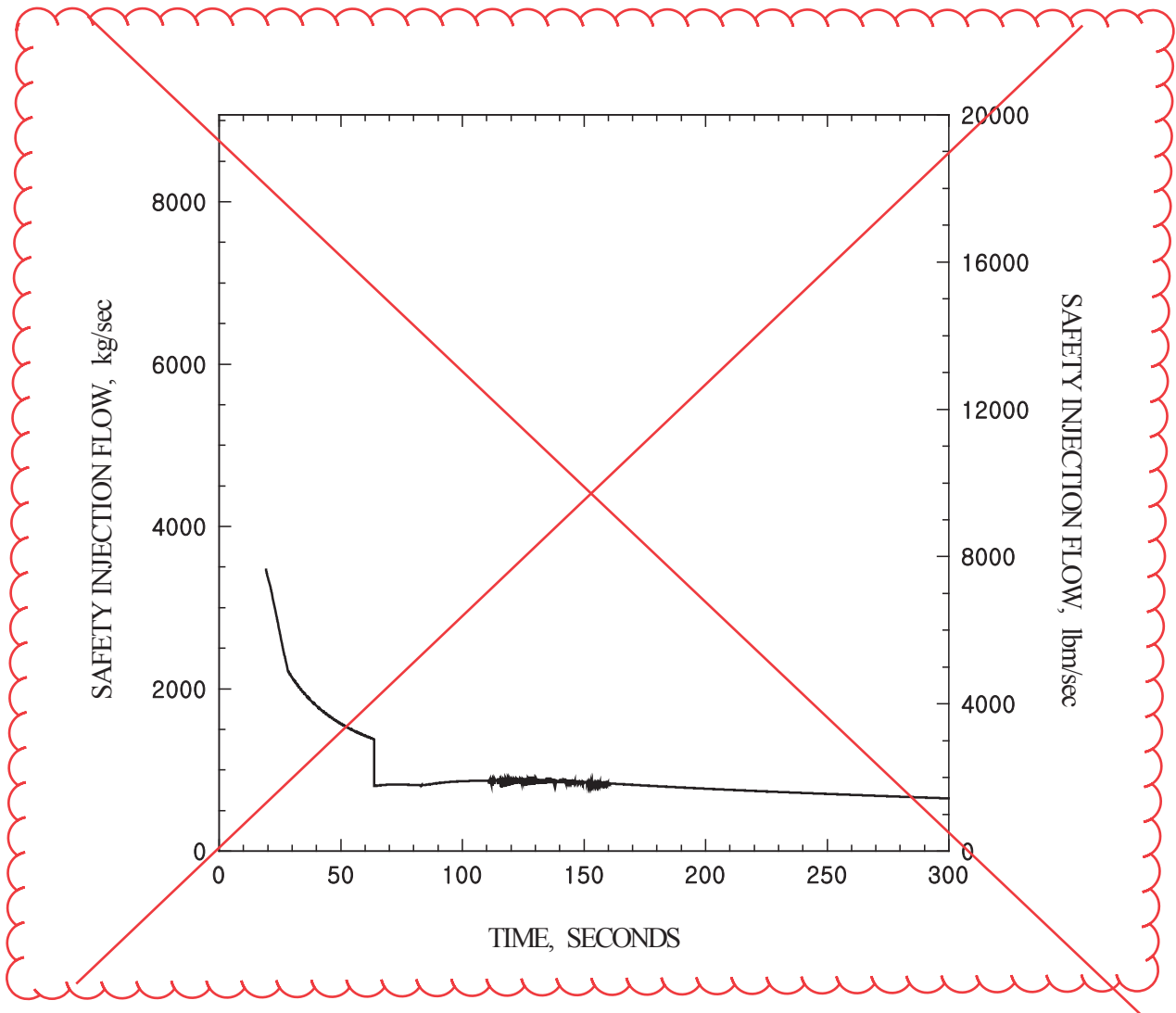
Conditions: Main Steam Line Break, 0 % Power – MSIV Failure

Unit of Energy: ⁽¹⁾ 10⁶ kcal (10⁶ Btu)

| Energy Description (Time) | Prior to MSLB | At Peak Pressure | End of Blowdown |
|--|------------------------|----------------------|----------------------|
| 1. Reactor coolant system water internal energy | 98.364 (390.366) | 61.770 (245.138) | 62.455 (247.856) |
| 2. Energy stored in core | 3.289 (13.054) | 2.210 (8.771) | 2.422 (9.611) |
| 3. Energy stored in pressurizer, primary piping, valves, and pumps | 57.017 (226.277) | 39.312 (156.012) | 39.627 (157.263) |
| 4. Energy stored in SG tubes | 10.082 (40.012) | 6.654 (26.406) | 6.723 (26.682) |
| 5. Energy stored in SG secondary walls | 41.907 (166.312) | 34.735 (137.849) | 34.716 (137.772) |
| 6. Secondary coolant internal energy in Steam Generator | 49.521 (196.526) | 30.480 (120.960) | 30.059 (119.291) |
| 7. Secondary coolant internal energy in Steam Generator 2 | 49.521 (196.526) | 1.482 (5.880) | 0.324 (1.284) |
| 8. Secondary coolant internal energy in steamline | 10.084 (40.019) | 0.661 (2.622) | 0.522 (2.072) |
| 9. Total NSSS Stored Energy | 319.786 (1,269.092) | 177.303 (703.638) | 176.848 (701.832) |
| 10. Feedwater to Steam Generator 1 | 0.000 (0.000) | 0.000 (0.000) | 0.000 (0.000) |
| 11. Feedwater to Steam Generator 2 | 0.000 (0.000) | 3.362 (13.343) | 9.377 (37.212) |
| 12. Steam Flow to Turbine | 0.000 (0.000) | 0.002 (0.007) | 0.002 (0.007) |
| 13. Energy Generated During Shutdown From Decay Heat | 0.000 (0.000) | 0.006 (0.024) | 66.378 (263.425) |
| 14. Break Flow | 0.000 (0.000) | 145.745 (579.400) | 216.073 (857.5) |

Part "A10"

Replace with next page



**Figure 6.2.1-33 Double-Ended Suction Leg Slot Break;
Maximum SI Pump Flow vs. Time**

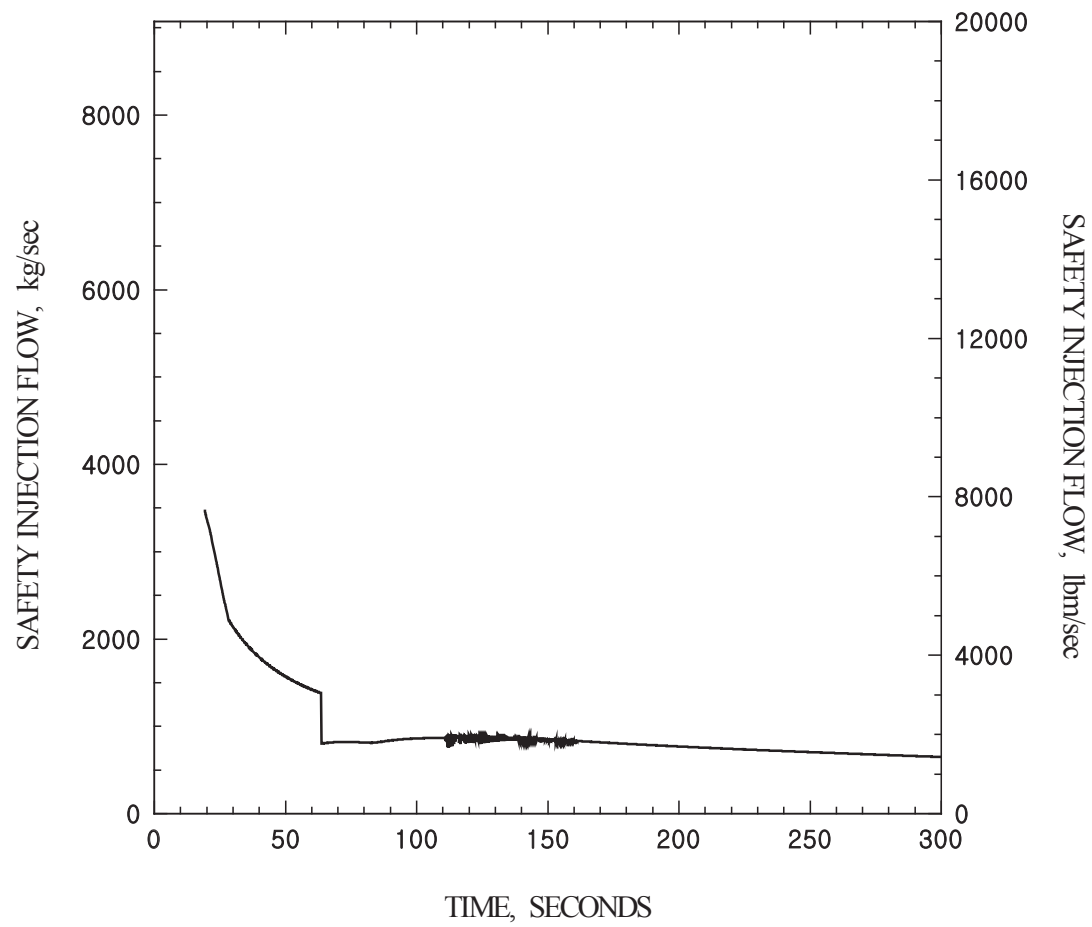
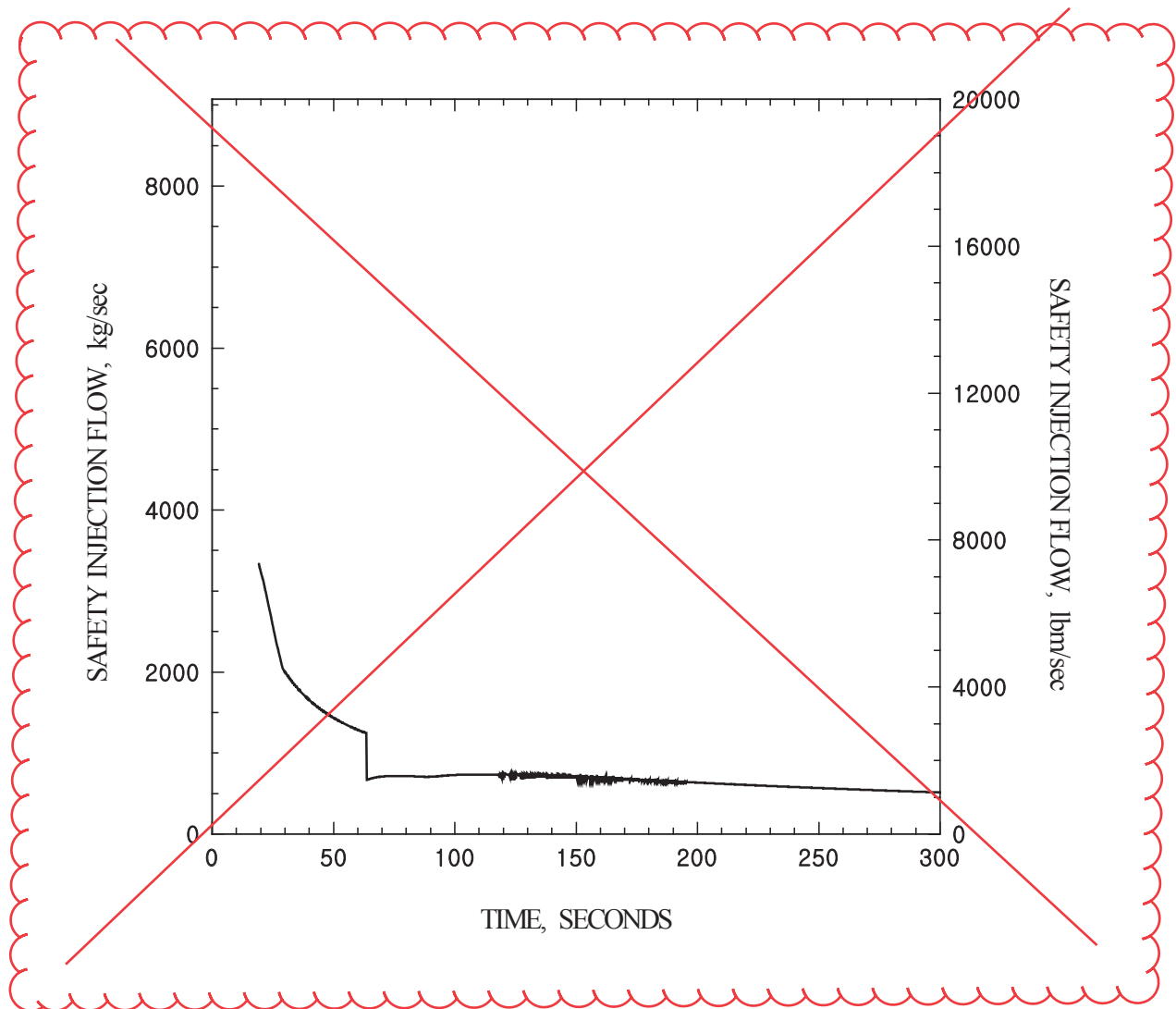


Figure 6.2.1-33 Double-Ended Suction Leg Slot Break;
Maximum SI Pump Flow vs. Time

Replace with next page



**Figure 6.2.1-34 Double-Ended Suction Leg Slot Break;
Minimum SI Pump Flow vs. Time**

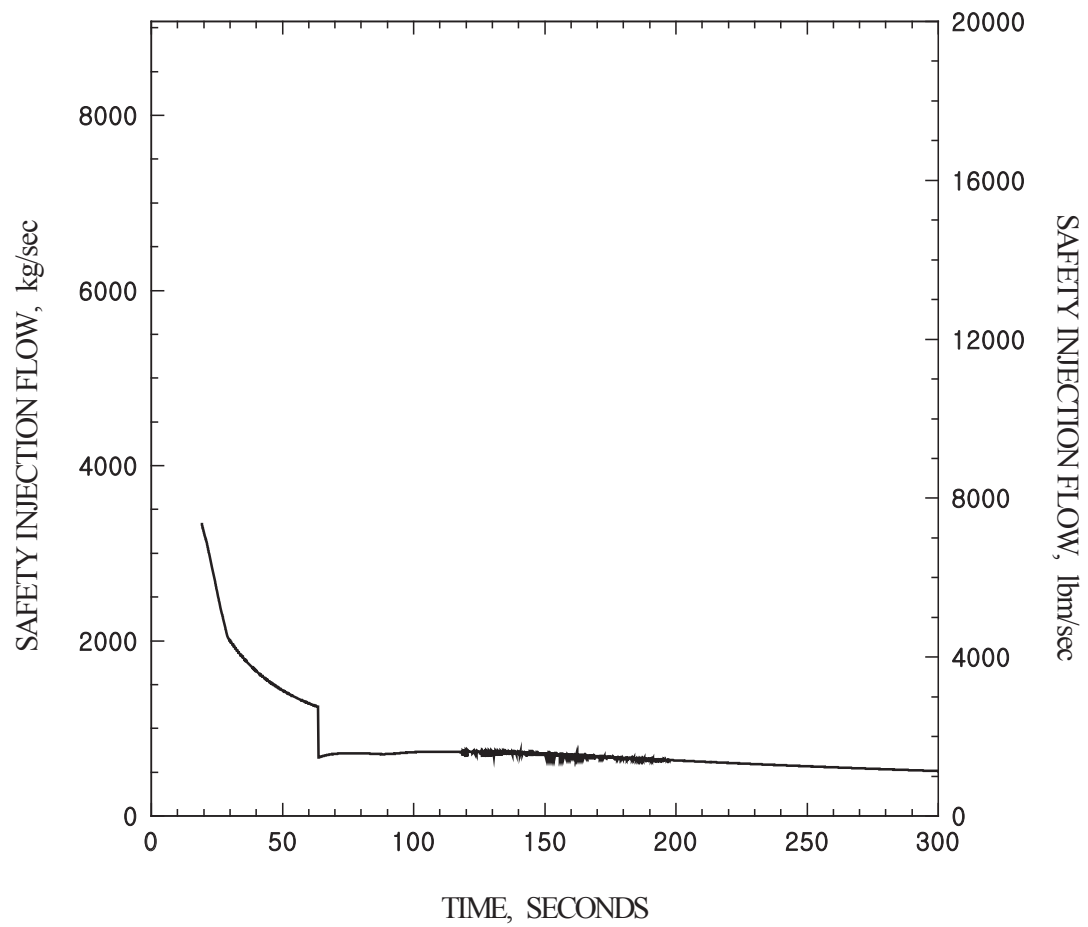
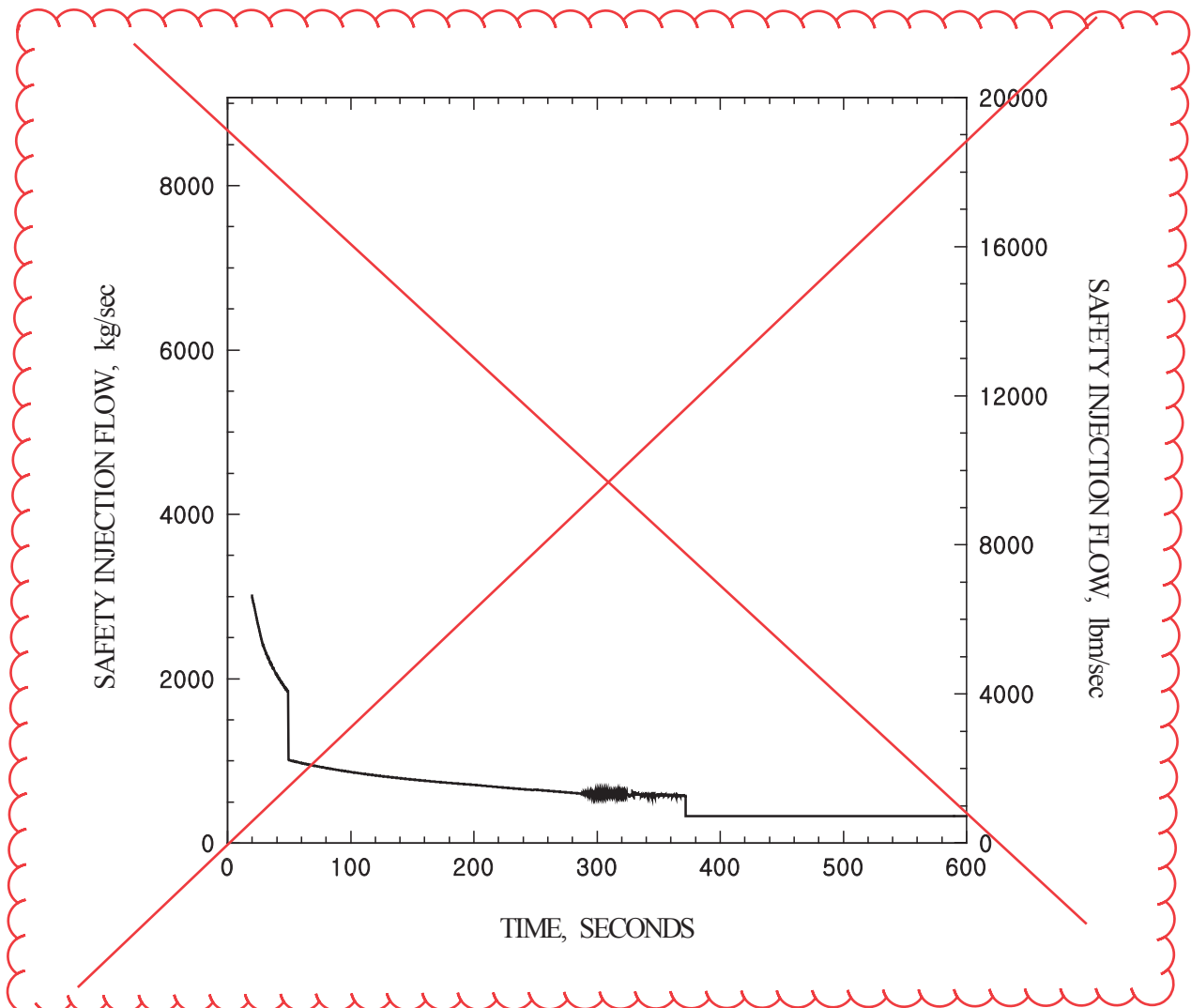


Figure 6.2.1-34 Double-Ended Suction Leg Slot Break;
Minimum SI Pump Flow vs. Time

Replace with next page



**Figure 6.2.1-35 Double-Ended Discharge Leg Slot Break;
Maximum SI Pump Flow vs. Time**

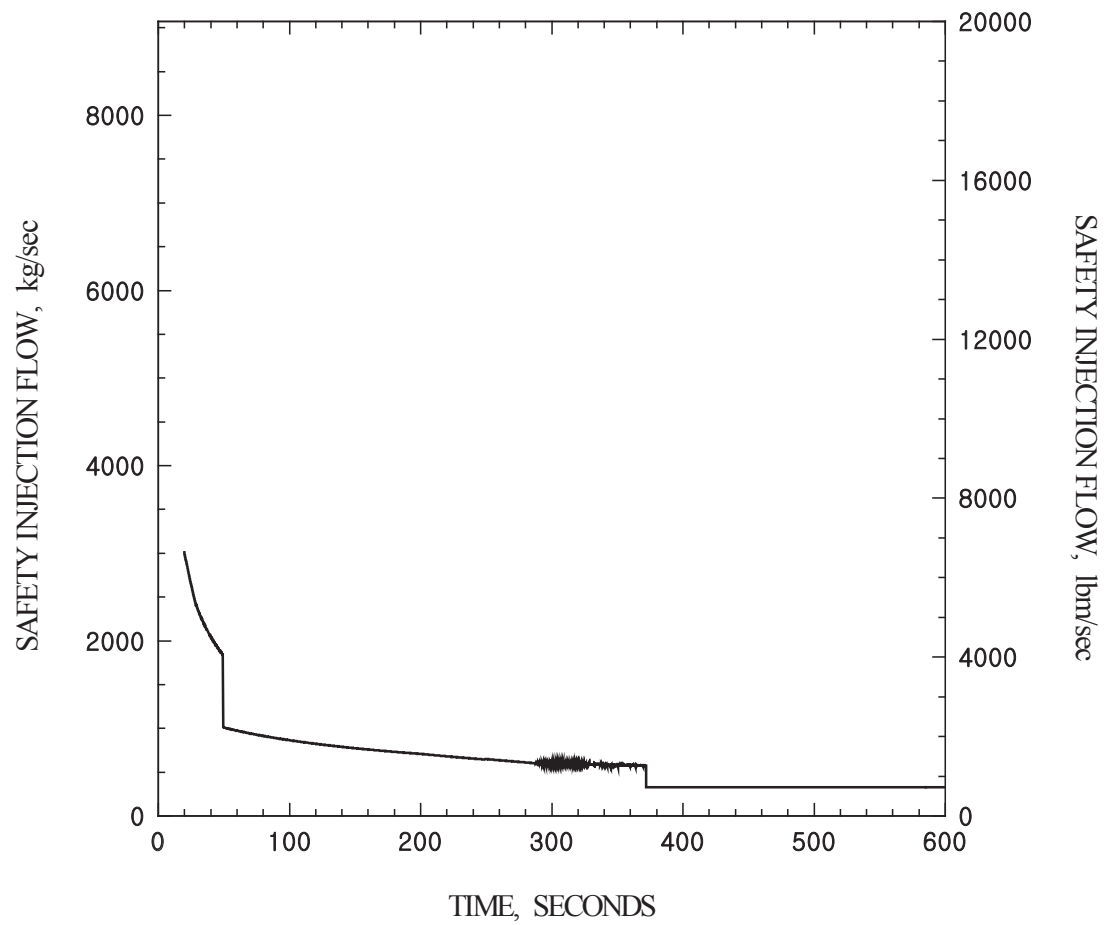
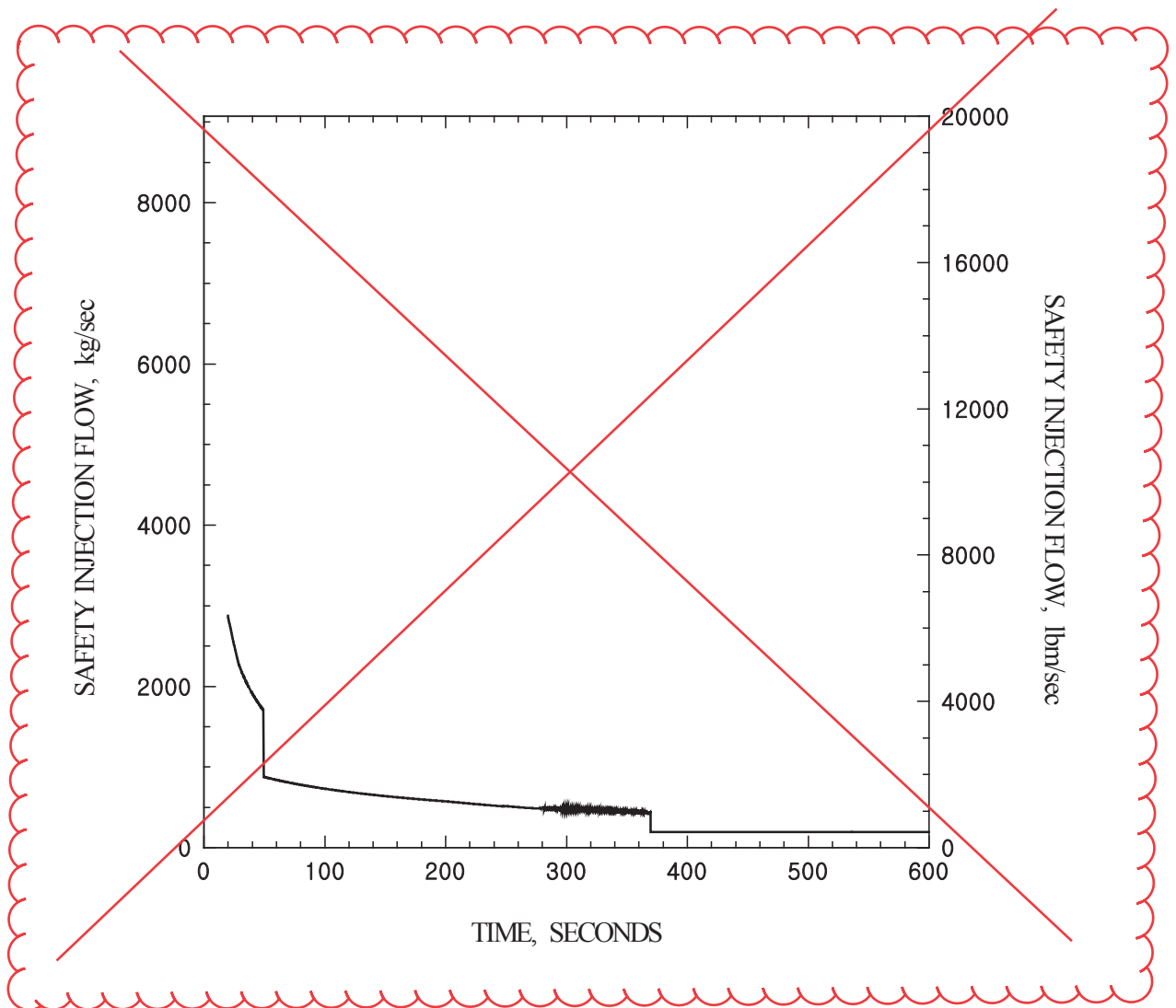


Figure 6.2.1-35 Double-Ended Discharge Leg Slot Break;
Maximum SI Pump Flow vs. Time

Replace with next page



**Figure 6.2.1-36 Double-Ended Discharge Leg Slot Break;
Minimum SI Pump Flow vs. Time**

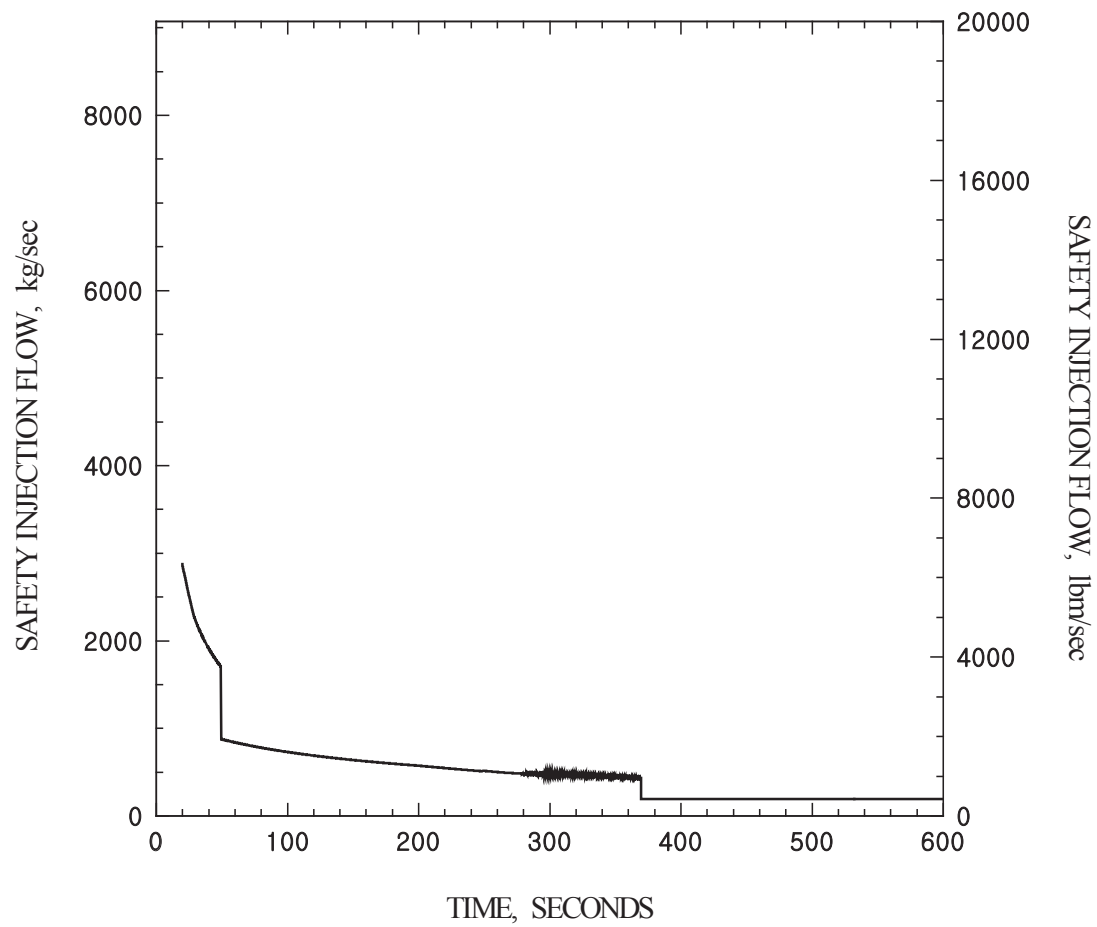


Figure 6.2.1-36 Double-Ended Discharge Leg Slot Break;
Minimum SI Pump Flow vs. Time

Pressure values in the affected and unaffected steam generators for each MSLB case listed in Table 6.2.1-1 are given in Tables 6.2.1-9 through 6.2.1-18.

The chronologies of events for the MSLB cases listed in Table 6.2.1-1 are given in Tables 6.2.1-9 through 6.2.1-18.

Feedwater flow to the affected steam generator for each MSLB case listed in Table 6.2.1-1 is shown in Figures 6.2.1-38 through 6.2.1-47.

6.2.1.5 Minimum Containment Pressure Analysis for Performance Capability Studies of the Emergency Core Cooling System

This subsection presents the analysis on the minimum containment pressure that is used in the ECCS performance analysis, which is presented in Subsection 15.6.5.

6.2.1.5.1 Analytical Models

The calculations reported in this subsection are performed using the realistic evaluation methodology for large break LOCA of the APR1400 described in Reference 16 and are in accordance with NRC RG 1.157 (Reference 17). In the code-accuracy-based realistic evaluation method (CAREM), the RELAP5/MOD3.3/K computer program, a modified version of RELAP5/MOD3.3 (Reference 18), is used for the analysis of the ECCS thermal-hydraulic transient calculation and the cladding temperature calculation. A part of the RELAP/MOD3.3 code's reflood model has been modified to improve the prediction of rods quenching time and to correct coding errors. The minimum containment back pressure and temperature calculations are performed using the CONTEMPT4/MOD5 code (Reference 19).

RELAP5/MOD3.3 is one of the best-estimate safety analysis codes to date. The code has been widely applied in the analysis of system transients of pressurized water reactors, including a postulated large break loss of coolant accident (LBLOCA). The film boiling heat transfer model of the reflood package of RELAP5/MOD3.3 has been modified based on independent assessment calculations against the FLECHT-SEASET data.

Containment back pressure depends on mass and energy release rates, and thermal-hydraulic phenomena depend on the containment back pressure. CONTEMPT4/MOD5 is a containment analysis code that is used especially for calculating containment back pressures in case of a LOCA. It includes fan and spray cooling system

models and passive heat sink models that are essential for the calculation of the containment back pressures following a LOCA. It is equipped with the conservation equations of mass, momentum, and energy and can calculate the mass and energy transfer due to the pressure difference between compartments. It also includes state equation of non-condensable gas and can calculate humidity. Heat conduction can be modeled with diverse boundary heat transfer conditions.

RELAP5/~~MOD3.3~~ ^{MOD3.3/K} and CONTEMPT4/MOD5 are merged to exchange the containment back pressure calculated by the CONTEMPT4 and the mass and energy release rate calculated by the RELAP5/MOD3.3/K in every time step.

6.2.1.5.2 Mass and Energy Release Data

^{insert: with the burnup of 27,000 MWd/MTU}

^{insert: considering TCD effect}

The mass and energy released to the containment for a limiting LBLOCA, 100 percent double-ended guillotine break at the pump discharge leg ($1.0 \times \text{DEG/PD}$), are listed as a function of time in Table 6.2.1-39. The quantity of safety injection fluid that spills from the break is described in Subsection 6.2.1.5.6. The analytical models applied in Subsection 15.6.5 best estimate analysis calculate the mass and energy released to the containment. This results are used to the calculation of minimum containment pressure.

6.2.1.5.3 Initial Containment Internal Conditions

The minimum containment temperature, minimum containment pressure, and maximum humidity encountered under limiting normal operating conditions are used for the analysis. The initial containment internal conditions that are used in the analysis are as follows:

| | |
|-------------------------|---|
| Containment temperature | 10 °C (50 °F) (minimum value) |
| IRWST water temperature | 10 °C (50 °F) (minimum value) |
| Containment pressure | 1.024 kg/cm ² A (14.56 psia) (minimum value) |
| Relative humidity | 90 percent (maximum value) |

Each condition is a specified conservative value to minimize the containment pressure, consistent with Branch Technical Position 6-2 (Reference 20).

6.2.1.5.4 Containment Volume

The maximum net free containment volume that is used for the analysis is 97,155 m³ (3,431,000 ft³). The maximum net free volume is determined from the gross containment

volume minus the volumes of internal structures such as walls and floors, structural steel, major equipment, and piping with a consideration of uncertainty.

6.2.1.5.5 Active Heat Sinks

In order to conservatively consider the heat removal capacity of the containment active heat sinks, the containment sprays and cooling fans are modeled to actuate immediately with the maximum capacity at the time of the postulated LOCA.

The containment atmosphere cooling systems designed as the non-safety-related system are also modeled to actuate immediately at the time of the postulated LOCA. In addition, the minimum temperature of the stored water for the spray cooling system and the cooling water supplied to the fan coolers, based on technical specification limits, are assumed.

The operating parameters for the containment sprays that are used in the analysis are as follows:

| | | | |
|--|---|--|--|
| Flow rate (total, 4 pumps) | 2 | 37,853 | 10,000 |
| | | 75,706 L/min (20,000 gpm) | |
| Temperature | | 10.0 °C (50 °F) | |

The heat removal capacity of reactor containment fan cooler (RCFC) is shown in Figure 6.2.1-48.

6.2.1.5.6 Steam-Water Mixing

The spillage of subcooled ECCS water into the containment provides an additional heat sink as the subcooled ECCS water mixes with the steam in the containment by the steam-water mixing. The spilled SIS water from the broken cold leg is determined by the thermal-hydraulic behavior of the core cooling system. It is considered in the analysis model of CONTEMPT4/MOD5.

6.2.1.5.7 Passive Heat Sinks

The passive heat sinks included in the containment evaluation model are established by identifying structures and components within the containment that are influenced the pressure response. The surface areas and thicknesses of all exposed containment passive heat sink, as well as the thermal properties used for the passive heat sinks, are listed in Table 6.2.1-23. The passive heat sink data are conservatively assumed with minimum

paint thickness and maximum structure thickness. Containment air wall is not considered, conservatively.

6.2.1.5.8 Heat Transfer to Passive Heat Sinks

The conservative condensing heat transfer coefficients for heat transfer to the exposed passive heat sinks during the blowdown and post-blowdown phases of the LOCA are applied. The variations in the condensing heat transfer coefficients between the containment atmosphere and the passive heat sinks are calculated as a function of time and are shown quantitatively in Figure 6.2.1-49. The condensation heat transfer coefficient at the surface of thermal structure is calculated by using Tagami and Uchida correlations shown as below:

$$h_{TAGAMI} = 0.607 \times \left(\frac{U}{V \times tp} \right)^{0.62} \text{ in SI unit}$$

Where:

U = Total released energy from the primary system during the blowdown period

V = Free volume in the containment

tp = time at the end of blowdown

The heat transfer coefficient during the blowdown period increases linearly from the initial values to a peak value h_{\max} and decreases exponentially as shown below. The Uchida heat transfer coefficient is given as the mass ratio function of air and steam:

$$h = h_{stag} + (h_{\max} - h_{stag})e^{-0.025(t-t_p)}$$

$$h_{stag} = 1.2 h_{UCHIDA}$$

Where:

h_{\max} = Four times of calculated condensing heat transfer coefficient at the end of blowdown

6.2.1.5.9 Other Parameters

The minimum containment pressure analysis assumes that the 20.3 cm (8 in) diameter purge system is operating from the time of the LOCA initiation until the isolation valves close, which is after a containment isolation actuation signal. It is conservatively assumed that only dry air is purged from the containment and the maximum mass of air purged is 272.2 kg (600 lbs) for the minimum containment pressure analysis.

6.2.1.5.10 Results insert: with the burnup of 27,000 MWd/MTU

For the limiting large break LOCA, 100 percent double-ended guillotine break at the pump discharge leg, the minimum containment pressure response to be used in the ECCS performance analysis is shown in Figure 6.2.1-50. The responses of the containment atmosphere and IRWST temperatures are shown in Figures 6.2.1-51 and 6.2.1-52, respectively.

The transient containment response is used in the ECCS performance analysis presented in Subsection 15.6.5.

6.2.1.6 Test and Inspections

This section describes the preoperational testing, in-service testing, and inspection of the containment. The primary objective of testing and inspection is to verify the structural integrity and leak-tight integrity of the containment. The testing and inspection requirements for the containment are described in Subsections 3.8.1.7, 3.8.2.7, 6.2.4, and 6.2.6. Section 14.2, the initial test program, also includes preoperational testing requirements.

Requirements for the structural integrity test are described in Subsection 14.2.12.1.119. The structural integrity test is performed in accordance with ASME Section III, Division 2, CC-6000, to verify the structural integrity of the containment including the liner, concrete structures, all electrical and piping penetrations, equipment hatch, personnel airlocks, and post-tensioning. The pressure will be brought up to 115 percent of the containment design pressure in approximately five or more equal increments. In addition, all ASME Class MC components are tested for their structural acceptance and leak rate at the same time of the structural integrity test. The in-service testing and inspection requirements and methods used for the ASME Class MC components and structural integrity test is described in Subsections 3.8.1.7 and 3.8.2.7.

16. APR1400-F-A-TR-12004-P (Proprietary) & NP (Non-Proprietary), “Realistic Evaluation Methodology for Large-Break LOCA of the APR1400,” Rev. 0, KHNP, December 2012
- July 2017
- Rev. 1
17. Regulatory Guide 1.157, “Best-estimate Calculations of Emergency Core Cooling System Performance,” U.S. Nuclear Regulatory Commission, May 1989.
18. NUREG/CR-5535, “RELAP5/MOD3.3 Code Manual,” Rev. 3, U.S. Nuclear Regulatory Commission, March 2006.
19. NUREG/CR-3716, “A Multi-compartment Containment System Analysis Program,” U.S. Nuclear Regulatory Commission, March 1984.
- NUREG/CR-4001, “An Improvement to CONTEMPT4/MOD5 Multi-compartment System Analysis Program for Ice Containment Analysis,” U.S. Nuclear Regulatory Commission, September 1984.
20. NUREG-0800, Standard Review Plan, BTP 6-2, “Minimum Containment Pressure Model for PWR ECCS Performance Evaluation,” U.S. Nuclear Regulatory Commission, March 2007.
21. Regulatory Guide 1.163, “Performance-Based Containment Leak Test Program,” U.S. Nuclear Regulatory Commission, September 1995.
22. ASTM E799-2003(R2009), “Standard Practice for Determining Data Criteria and Processing for Liquid Drop Size Analysis,” American Society for Testing and Material, 2003.
23. ASME Boiler and Pressure Vessel Code, Section XI, “Rules for Inservice Inspection of Nuclear Power Plant Components,” The American Society of Mechanical Engineers.
24. ASME OM Code, “Code for Operation and Maintenance of Nuclear Power Plants,” The American Society of Mechanical Engineers.
25. 10 CFR Part 50, Appendix A, General Design Criterion 56, “Primary Containment Isolation,” U.S. Nuclear Regulatory Commission.
26. Regulatory Guide 1.11, “Instrument Lines Penetrating the Primary Reactor Containment,” Rev. 1, U.S. Nuclear Regulatory Commission, March 2010.

Table 6.2.1-23 (5 of 7)

Part C. Heat Sink Physical Data for ECCS Performance Analysis

| Heat Sinks | Layer | Material | Thickness | | Surface Area | |
|----------------------|-------|--------------|-----------|----------|----------------|-----------------|
| | | | m | ft | m ² | ft ² |
| Containment cylinder | 1 | E Paint | 0.0000762 | 0.00025 | 7,804.3 | 84,005 |
| | 2 | Z Paint | 0.0000762 | 0.00025 | | |
| | 3 | Carbon Steel | 0.008778 | 0.0288 | | |
| | 4 | Concrete | 1.355994 | 4.4488 | | |
| Dome | 1 | E Paint | 0.0000762 | 0.00025 | 3,316.3 | 35,696.4 |
| | 2 | Z Paint | 0.0000762 | 0.00025 | | |
| | 3 | Carbon Steel | 0.007894 | 0.0259 | | |
| | 4 | Concrete | 1.0668 | 3.5 | | |
| Basemat | 1 | E Paint | 0.000668 | 0.002192 | 1,410.9 | 15,186.3 |
| | 2 | Concrete | 0.9144 | 3 | | |
| | 3 | Carbon Steel | 0.00635 | 0.020833 | | |
| | 4 | Concrete | 3.6576 | 12 | | |
| Embedment Concrete | 1 | E Paint | 0.0000762 | 0.00025 | 726.1 | 7,815.6 |
| | 2 | Z Paint | 0.0000762 | 0.00025 | | |
| | 3 | Carbon Steel | 0.026335 | 0.0864 | | |
| | 4 | Concrete | 0.780776 | 2.5616 | | |

Table 6.2.1-23 (6 of 7)

Part C. Heat Sink Physical Data for ECCS Performance Analysis (Continued)

| Heat Sinks | Layer | Material | Thickness | | Surface Area | |
|------------------------|-------|-----------------|------------|----------|----------------|-----------------|
| | | | m | ft | m ² | ft ² |
| Unembedment Concrete | 1 | E Paint | 0.000389 | 0.001275 | 11,120.7 | 119,702 |
| | 2 | Concrete | 0.77254 | 2.534579 | | |
| Refueling Pool | 1 | Stainless Steel | 0.005243 | 0.0172 | 1,153.6 | 12,417.7 |
| IRWST Outside | 1 | E Paint | 0.000668 | 0.002192 | 2,017.4 | 21,714.6 |
| | 2 | Concrete | 0.4572 | 1.5 | | |
| IRWST Inside | 1 | Stainless Steel | 0.00633984 | 0.0208 | 1,038.8 | 11,181.7 |
| | 2 | Concrete | 0.4572 | 1.5 | | |
| Polar Crane and Bridge | 1 | E Paint | 0.0000762 | 0.00025 | 8,291.6 | 89,250 |
| | 2 | Z Paint | 0.0000762 | 0.00025 | | |
| | 3 | Carbon Steel | 0.012192 | 0.04 | | |
| SIT | 1 | E Paint | 0.000152 | 0.0005 | 526.8 | 5,670 |
| | 2 | Carbon Steel | 0.048798 | 0.1601 | | |
| Misc. steel G-A | 1 | E Paint | 0.0000762 | 0.00025 | 10,212.1 | 109,922 |
| | 2 | Z Paint | 0.0000762 | 0.00025 | | |
| | 3 | Carbon Steel | 0.016712 | 0.054831 | | |
| Misc. steel G-B | 1 | Z Paint | 0.0000762 | 0.00025 | 7,062.1 | 76,015.5 |
| | 3 | Carbon Steel | 0.004175 | 0.013698 | | |
| Misc. steel G-C | 1 | E Paint | 0.0000762 | 0.00025 | 3,361.5 | 36,182.7 |
| | 2 | Z Paint | 0.0000762 | 0.00025 | | |
| | 3 | Carbon Steel | 0.00518099 | 0.016998 | | |
| Misc. steel G-D | 1 | Z Paint | 0.0000762 | 0.00025 | 3,664.1 | 39,439.6 |
| | 2 | Carbon Steel | 0.004 | 0.013124 | | |
| Misc. steel G-E | 1 | Z Paint | 0.0000762 | 0.00025 | 21,557.5 | 232,042 |
| | 2 | Carbon Steel | 0.001644 | 0.005393 | | |

Table 6.2.1-23 (7 of 7)

Part C. Heat Sink Physical Data for ECCS Performance Analysis (Continued)

| Heat Sinks | Layer | Material | Thickness | | Surface Area | |
|-----------------|-------|-----------------|------------|----------|----------------|-----------------|
| | | | m | ft | m ² | ft ² |
| Misc. steel G-F | 1 | E Paint | 0.0000762 | 0.00025 | 1,589.3 | 17,106.9 |
| | 2 | Z Paint | 0.0000762 | 0.00025 | | |
| | 3 | Carbon Steel | 0.00672846 | 0.022075 | | |
| Misc. steel G-G | 1 | Stainless Steel | 0.00627888 | 0.020600 | 1,872.0 | 20,149.6 |
| Misc. steel G-J | 1 | Z Paint | 0.0000762 | 0.00025 | 1,738.6 | 18,713.6 |
| | 2 | Carbon Steel | 0.009216 | 0.030235 | | |
| Misc. steel G-K | 1 | Stainless Steel | 0.072558 | 0.23805 | 1,269.3 | 13,662.7 |

| | |
|------------------------------|--|
| Thermal Conductivity of: | |
| Steel | 40.6 kcal/m-hr-°C (27.3 Btu/ft-hr-°F) |
| Concrete | 1.94 kcal/m-hr-°C (1.3 Btu/ft-hr-°F) |
| Paint (epoxy) | 0.31 kcal/m-hr-°C (0.21 Btu/ft-hr-°F) |
| Paint (inorganic zinc) | 1.49 kcal/m-hr-°C (1.0 Btu/ft-hr-°F) |
| Volumetric Heat Capacity of: | |
| Steel | 942 kcal/m ³ -°C (58.8 Btu/ft ³ -°F) |
| Concrete | 517 kcal/m ³ -°C (32.3 Btu/ft ³ -°F) |
| Paint (epoxy) | 585 kcal/m ³ -°C (36.5 Btu/ft ³ -°F) |
| Paint (inorganic zinc) | 1,250 kcal/m ³ -°C (78.0 Btu/ft ³ -°F) |

Insert

- (1) The surface area uses its maximum value within the ranges of margin estimated from the geometry uncertainty of each structure.
- (2) The thickness of each structure are determined based on the surface area exposed to the containment atmosphere and the net volume occupied by the structure.
- (3) The thickness of the painting material on the structure is considered as its averaging nominal value.

A detailed description of how to calculate the thickness and surface area is provided in Reference 3.

Replace with next page A-1

Table 6.2.1-39 (1 of 4)

Blowdown and Reflood Mass and Energy Release for the Minimum Containment Pressure Analysis

| Time (sec) | Mass Flow | | Enthalpy | | Integral of Mass Flow | | Integral of Energy | |
|---------------|------------|------------|------------|------------|-----------------------|------------|--------------------|------------|
| | (kg/sec) | (lbm/sec) | (kcal/kg) | (Btu/lbm) | (kg) | (lbm) | (kcal) | (Btu) |
| 0.0 | 0.0000E+00 | 0.0000E+00 | 0.0000E+00 | 0.0000E+00 | 0.0000E+00 | 0.0000E+00 | 0.0000E+00 | 0.0000E+00 |
| 0.5 | 3.9083E+04 | 8.6164E+04 | 3.0484E+02 | 5.4870E+02 | 1.9481E+04 | 4.2948E+04 | 5.9366E+06 | 2.3558E+07 |
| 1.0 | 3.7229E+04 | 8.2876E+04 | 3.0525E+02 | 5.4944E+02 | 3.8697E+04 | 8.5313E+04 | 1.1798E+07 | 4.6818E+07 |
| 1.5 | 3.4198E+04 | 7.5395E+04 | 3.0599E+02 | 5.5078E+02 | 5.6465E+04 | 1.2448E+05 | 1.7227E+07 | 6.8364E+07 |
| 2.0 | 3.2051E+04 | 7.0661E+04 | 3.0712E+02 | 5.5282E+02 | 7.3059E+04 | 1.6107E+05 | 2.2314E+07 | 8.8548E+07 |
| 2.5 | 2.9526E+04 | 6.5093E+04 | 3.0870E+02 | 5.5566E+02 | 8.8435E+04 | 1.9497E+05 | 2.7047E+07 | 1.0733E+08 |
| 3.0 | 2.6495E+04 | 5.8411E+04 | 3.1044E+02 | 5.5879E+02 | 1.0245E+05 | 2.2587E+05 | 3.1385E+07 | 1.2455E+08 |
| 3.5 | 2.4309E+04 | 5.3593E+04 | 3.1248E+02 | 5.6246E+02 | 1.1511E+05 | 2.5378E+05 | 3.5328E+07 | 1.4019E+08 |
| 4.0 | 2.2818E+04 | 5.0305E+04 | 3.1483E+02 | 5.6670E+02 | 1.2688E+05 | 2.7972E+05 | 3.9020E+07 | 1.5484E+08 |
| 4.5 | 2.1564E+04 | 4.7541E+04 | 3.1670E+02 | 5.7006E+02 | 1.3793E+05 | 3.0408E+05 | 4.2509E+07 | 1.6869E+08 |
| 5.0 | 2.0493E+04 | 4.5180E+04 | 3.1844E+02 | 5.7320E+02 | 1.4841E+05 | 3.2719E+05 | 4.5840E+07 | 1.8191E+08 |
| 5.5 | 1.9184E+04 | 4.2294E+04 | 3.2188E+02 | 5.7939E+02 | 1.5834E+05 | 3.4908E+05 | 4.9016E+07 | 1.9451E+08 |
| 6.0 | 1.8037E+04 | 3.9764E+04 | 3.2567E+02 | 5.8620E+02 | 1.6764E+05 | 3.6959E+05 | 5.2028E+07 | 2.0646E+08 |
| 6.5 | 1.7038E+04 | 3.7562E+04 | 3.2853E+02 | 5.9136E+02 | 1.7640E+05 | 3.8891E+05 | 5.4895E+07 | 2.1784E+08 |
| 7.0 | 1.6036E+04 | 3.5353E+04 | 3.3182E+02 | 5.9727E+02 | 1.8467E+05 | 4.0713E+05 | 5.7624E+07 | 2.2867E+08 |
| 7.5 | 1.5212E+04 | 3.3536E+04 | 3.3461E+02 | 6.0229E+02 | 1.9247E+05 | 4.2433E+05 | 6.0225E+07 | 2.3899E+08 |
| 8.0 | 1.4582E+04 | 3.2149E+04 | 3.3657E+02 | 6.0582E+02 | 1.9991E+05 | 4.4073E+05 | 6.2721E+07 | 2.4890E+08 |
| 8.5 | 1.4003E+04 | 3.0871E+04 | 3.3755E+02 | 6.0760E+02 | 2.0705E+05 | 4.5647E+05 | 6.5131E+07 | 2.5846E+08 |

A-1

Table 6.2.1-39 (1 of 4)

Blowdown and Reflood Mass and Energy Release for the Minimum Containment Pressure Analysis

| Time (sec) | Mass Flow | | Enthalpy | | Integral of Mass Flow | | Integral of Energy | |
|---------------|------------|------------|------------|------------|-----------------------|------------|--------------------|------------|
| | (kg/sec) | (lbm/sec) | (kcal/kg) | (Btu/lbm) | (kg) | (lbm) | (kcal) | (Btu) |
| 0.0 | 0.0000E+00 | 0.0000E+00 | 0.0000E+00 | 0.0000E+00 | 0.0000E+00 | 0.0000E+00 | 0.0000E+00 | 0.0000E+00 |
| 0.5 | 3.8724E+04 | 8.5372E+04 | 3.0481E+02 | 5.4866E+02 | 1.9481E+04 | 4.2948E+04 | 5.9366E+06 | 2.3558E+07 |
| 1.0 | 3.6719E+04 | 8.0951E+04 | 3.0522E+02 | 5.4940E+02 | 3.8697E+04 | 8.5313E+04 | 1.1798E+07 | 4.6818E+07 |
| 1.5 | 3.4041E+04 | 7.5047E+04 | 3.0599E+02 | 5.5078E+02 | 5.6465E+04 | 1.2448E+05 | 1.7227E+07 | 6.8364E+07 |
| 2.0 | 3.1857E+04 | 7.0232E+04 | 3.0710E+02 | 5.5278E+02 | 7.3059E+04 | 1.6107E+05 | 2.2314E+07 | 8.8548E+07 |
| 2.5 | 2.9010E+04 | 6.3957E+04 | 3.0871E+02 | 5.5567E+02 | 8.8435E+04 | 1.9497E+05 | 2.7047E+07 | 1.0733E+08 |
| 3.0 | 2.6322E+04 | 5.8031E+04 | 3.1038E+02 | 5.5868E+02 | 1.0245E+05 | 2.2587E+05 | 3.1385E+07 | 1.2455E+08 |
| 3.5 | 2.4281E+04 | 5.3531E+04 | 3.1241E+02 | 5.6235E+02 | 1.1511E+05 | 2.5378E+05 | 3.5328E+07 | 1.4019E+08 |
| 4.0 | 2.2928E+04 | 5.0548E+04 | 3.1473E+02 | 5.6652E+02 | 1.2688E+05 | 2.7972E+05 | 3.9020E+07 | 1.5484E+08 |
| 4.5 | 2.1645E+04 | 4.7720E+04 | 3.1615E+02 | 5.6907E+02 | 1.3793E+05 | 3.0408E+05 | 4.2509E+07 | 1.6869E+08 |
| 5.0 | 2.0561E+04 | 4.5329E+04 | 3.1811E+02 | 5.7260E+02 | 1.4841E+05 | 3.2719E+05 | 4.5840E+07 | 1.8191E+08 |
| 5.5 | 1.9289E+04 | 4.2526E+04 | 3.2143E+02 | 5.7857E+02 | 1.5834E+05 | 3.4908E+05 | 4.9016E+07 | 1.9451E+08 |
| 6.0 | 1.8132E+04 | 3.9975E+04 | 3.2525E+02 | 5.8545E+02 | 1.6764E+05 | 3.6959E+05 | 5.2028E+07 | 2.0646E+08 |
| 6.5 | 1.7101E+04 | 3.7700E+04 | 3.2825E+02 | 5.9084E+02 | 1.7640E+05 | 3.8891E+05 | 5.4895E+07 | 2.1784E+08 |
| 7.0 | 1.6093E+04 | 3.5480E+04 | 3.3151E+02 | 5.9672E+02 | 1.8467E+05 | 4.0713E+05 | 5.7624E+07 | 2.2867E+08 |
| 7.5 | 1.5240E+04 | 3.3598E+04 | 3.3453E+02 | 6.0215E+02 | 1.9247E+05 | 4.2433E+05 | 6.0225E+07 | 2.3899E+08 |
| 8.0 | 1.4614E+04 | 3.2218E+04 | 3.3647E+02 | 6.0565E+02 | 1.9991E+05 | 4.4073E+05 | 6.2721E+07 | 2.4890E+08 |
| 8.5 | 1.4153E+04 | 3.1202E+04 | 3.3747E+02 | 6.0745E+02 | 2.0705E+05 | 4.5647E+05 | 6.5131E+07 | 2.5846E+08 |

Replace with next page A-2

Table 6.2.1-39 (2 of 4)

| Time (sec) | Mass Flow | | Enthalpy | | Integral of Mass Flow | | Integral of Energy | |
|---------------|------------|------------|------------|------------|-----------------------|------------|--------------------|------------|
| | (kg/sec) | (lbm/sec) | (kcal/kg) | (Btu/lbm) | (kg) | (lbm) | (kcal) | (Btu) |
| 9.0 | 1.3295E+04 | 2.9310E+04 | 3.4122E+02 | 6.1420E+02 | 2.1383E+05 | 4.7141E+05 | 6.7437E+07 | 2.6761E+08 |
| 9.5 | 1.2034E+04 | 2.6531E+04 | 3.5498E+02 | 6.3897E+02 | 2.2013E+05 | 4.8530E+05 | 6.9627E+07 | 2.7630E+08 |
| 10.0 | 1.1140E+04 | 2.4560E+04 | 3.6620E+02 | 6.5916E+02 | 2.2592E+05 | 4.9807E+05 | 7.1714E+07 | 2.8458E+08 |
| 11.0 | 9.7376E+03 | 2.1468E+04 | 3.8751E+02 | 6.9752E+02 | 2.3643E+05 | 5.2124E+05 | 7.5655E+07 | 3.0022E+08 |
| 12.0 | 8.3059E+03 | 1.8311E+04 | 4.1727E+02 | 7.5109E+02 | 2.4544E+05 | 5.4110E+05 | 7.9270E+07 | 3.1457E+08 |
| 13.0 | 7.0495E+03 | 1.5541E+04 | 4.4490E+02 | 8.0082E+02 | 2.5319E+05 | 5.5818E+05 | 8.2584E+07 | 3.2772E+08 |
| 14.0 | 5.6965E+03 | 1.2559E+04 | 4.8057E+02 | 8.6502E+02 | 2.5955E+05 | 5.7221E+05 | 8.5525E+07 | 3.3939E+08 |
| 15.0 | 4.6371E+03 | 1.0223E+04 | 5.0858E+02 | 9.1544E+02 | 2.6470E+05 | 5.8357E+05 | 8.8068E+07 | 3.4948E+08 |
| 16.0 | 4.2699E+03 | 9.4135E+03 | 4.6259E+02 | 8.3266E+02 | 2.6917E+05 | 5.9341E+05 | 9.0244E+07 | 3.5812E+08 |
| 17.0 | 4.2033E+03 | 9.2667E+03 | 3.8856E+02 | 6.9941E+02 | 2.7347E+05 | 6.0289E+05 | 9.2034E+07 | 3.6522E+08 |
| 18.0 | 3.9604E+03 | 8.7312E+03 | 3.4041E+02 | 6.1274E+02 | 2.7755E+05 | 6.1190E+05 | 9.3514E+07 | 3.7109E+08 |
| 19.0 | 3.6815E+03 | 8.1162E+03 | 3.1006E+02 | 5.5811E+02 | 2.8146E+05 | 6.2052E+05 | 9.4767E+07 | 3.7607E+08 |
| 20.0 | 3.3936E+03 | 7.4816E+03 | 2.8308E+02 | 5.0955E+02 | 2.8507E+05 | 6.2848E+05 | 9.5825E+07 | 3.8026E+08 |
| 21.0 | 3.1712E+03 | 6.9912E+03 | 2.5108E+02 | 4.5195E+02 | 2.8836E+05 | 6.3572E+05 | 9.6706E+07 | 3.8376E+08 |
| 22.0 | 3.5105E+03 | 7.7394E+03 | 2.1884E+02 | 3.9391E+02 | 2.9193E+05 | 6.4359E+05 | 9.7537E+07 | 3.8706E+08 |
| 23.0 | 3.1260E+03 | 6.8917E+03 | 1.9468E+02 | 3.5043E+02 | 2.9524E+05 | 6.5089E+05 | 9.8226E+07 | 3.8979E+08 |
| 24.0 | 2.3483E+03 | 5.1770E+03 | 1.9237E+02 | 3.4627E+02 | 2.9799E+05 | 6.5696E+05 | 9.8754E+07 | 3.9189E+08 |
| 25.0 | 1.9377E+03 | 4.2719E+03 | 1.7847E+02 | 3.2125E+02 | 3.0006E+05 | 6.6152E+05 | 9.9149E+07 | 3.9346E+08 |
| 26.0 | 1.9829E+03 | 4.3715E+03 | 1.3967E+02 | 2.5141E+02 | 3.0202E+05 | 6.6584E+05 | 9.9457E+07 | 3.9468E+08 |
| 27.0 | 1.7744E+03 | 3.9119E+03 | 1.1880E+02 | 2.1384E+02 | 3.0376E+05 | 6.6968E+05 | 9.9691E+07 | 3.9561E+08 |

A-2

Table 6.2.1-39 (2 of 4)

| Time (sec) | Mass Flow | | Enthalpy | | Integral of Mass Flow | | Integral of Energy | |
|---------------|------------|------------|------------|------------|-----------------------|------------|--------------------|------------|
| | (kg/sec) | (lbm/sec) | (kcal/kg) | (Btu/lbm) | (kg) | (lbm) | (kcal) | (Btu) |
| 9.0 | 1.3205E+04 | 2.9113E+04 | 3.4232E+02 | 6.1617E+02 | 2.1383E+05 | 4.7141E+05 | 6.7437E+07 | 2.6761E+08 |
| 9.5 | 1.2105E+04 | 2.6688E+04 | 3.5269E+02 | 6.3484E+02 | 2.2013E+05 | 4.8530E+05 | 6.9627E+07 | 2.7630E+08 |
| 10.0 | 1.1219E+04 | 2.4734E+04 | 3.6500E+02 | 6.5699E+02 | 2.2592E+05 | 4.9807E+05 | 7.1714E+07 | 2.8458E+08 |
| 11.0 | 9.8545E+03 | 2.1725E+04 | 3.8504E+02 | 6.9308E+02 | 2.3643E+05 | 5.2124E+05 | 7.5655E+07 | 3.0022E+08 |
| 12.0 | 8.3606E+03 | 1.8432E+04 | 4.1553E+02 | 7.4795E+02 | 2.4544E+05 | 5.4110E+05 | 7.9270E+07 | 3.1457E+08 |
| 13.0 | 7.0900E+03 | 1.5631E+04 | 4.4297E+02 | 7.9734E+02 | 2.5319E+05 | 5.5818E+05 | 8.2584E+07 | 3.2772E+08 |
| 14.0 | 5.7429E+03 | 1.2661E+04 | 4.7810E+02 | 8.6058E+02 | 2.5955E+05 | 5.7221E+05 | 8.5525E+07 | 3.3939E+08 |
| 15.0 | 4.6607E+03 | 1.0275E+04 | 5.0738E+02 | 9.1328E+02 | 2.6470E+05 | 5.8357E+05 | 8.8068E+07 | 3.4948E+08 |
| 16.0 | 4.5045E+03 | 9.9308E+03 | 4.3551E+02 | 7.8392E+02 | 2.6917E+05 | 5.9341E+05 | 9.0244E+07 | 3.5812E+08 |
| 17.0 | 4.5892E+03 | 1.0117E+04 | 3.4965E+02 | 6.2937E+02 | 2.7347E+05 | 6.0289E+05 | 9.2034E+07 | 3.6522E+08 |
| 18.0 | 6.2080E+03 | 1.3686E+04 | 2.6115E+02 | 4.7008E+02 | 2.7755E+05 | 6.1190E+05 | 9.3514E+07 | 3.7109E+08 |
| 19.0 | 5.3897E+03 | 1.1882E+04 | 2.4960E+02 | 4.4928E+02 | 2.8146E+05 | 6.2052E+05 | 9.4767E+07 | 3.7607E+08 |
| 20.0 | 5.0298E+03 | 1.1089E+04 | 2.1821E+02 | 3.9278E+02 | 2.8507E+05 | 6.2848E+05 | 9.5825E+07 | 3.8026E+08 |
| 21.0 | 4.5887E+03 | 1.0072E+04 | 1.9425E+02 | 3.4965E+02 | 2.8836E+05 | 6.3572E+05 | 9.6706E+07 | 3.8376E+08 |
| 22.0 | 4.0662E+03 | 8.9645E+03 | 1.7118E+02 | 3.0812E+02 | 2.9193E+05 | 6.4359E+05 | 9.7537E+07 | 3.8706E+08 |
| 23.0 | 3.3917E+03 | 7.4775E+03 | 1.5942E+02 | 2.8695E+02 | 2.9524E+05 | 6.5089E+05 | 9.8226E+07 | 3.8979E+08 |
| 24.0 | 2.8318E+03 | 6.2430E+03 | 1.4577E+02 | 2.6238E+02 | 2.9799E+05 | 6.5696E+05 | 9.8754E+07 | 3.9189E+08 |
| 25.0 | 2.2366E+03 | 4.9309E+03 | 1.3316E+02 | 2.3969E+02 | 3.0006E+05 | 6.6152E+05 | 9.9149E+07 | 3.9346E+08 |
| 26.0 | 2.2567E+03 | 4.9752E+03 | 1.1145E+02 | 2.0062E+02 | 3.0202E+05 | 6.6584E+05 | 9.9457E+07 | 3.9468E+08 |
| 27.0 | 1.7760E+03 | 3.9153E+03 | 7.5469E+01 | 1.3584E+02 | 3.0376E+05 | 6.6968E+05 | 9.9691E+07 | 3.9561E+08 |

Replace with next page A-3

Table 6.2.1-39 (3 of 4)

| Time (sec) | Mass Flow | | Enthalpy | | Integral of Mass Flow | | Integral of Energy | |
|---------------|-------------|-------------|------------|------------|-----------------------|------------|--------------------|------------|
| | (kg/sec) | (lbm/sec) | (kcal/kg) | (Btu/lbm) | (kg) | (lbm) | (kcal) | (Btu) |
| 28.0 | 5.6570E+02 | 1.2472E+03 | 1.0175E+02 | 1.8315E+02 | 3.0503E+05 | 6.7249E+05 | 9.9830E+07 | 3.9616E+08 |
| 29.0 | -9.8747E+01 | -2.1770E+02 | 3.4733E+02 | 6.2520E+02 | 3.0511E+05 | 6.7265E+05 | 9.9824E+07 | 3.9613E+08 |
| 30.0 | -2.8582E+01 | -6.3013E+01 | 1.3609E+02 | 2.4497E+02 | 3.0507E+05 | 6.7256E+05 | 9.9811E+07 | 3.9608E+08 |
| 35.0 | 2.2727E+02 | 5.0104E+02 | 9.4225E+01 | 1.6961E+02 | 3.0599E+05 | 6.7460E+05 | 9.9938E+07 | 3.9659E+08 |
| 40.0 | 4.0079E+02 | 8.8360E+02 | 1.4478E+02 | 2.6060E+02 | 3.0759E+05 | 6.7813E+05 | 1.0014E+08 | 3.9737E+08 |
| 45.0 | 4.1072E+02 | 9.0548E+02 | 1.4478E+02 | 2.6061E+02 | 3.0931E+05 | 6.8191E+05 | 1.0040E+08 | 3.9840E+08 |
| 50.0 | 2.3177E+03 | 5.1096E+03 | 8.2609E+01 | 1.4870E+02 | 3.1563E+05 | 6.9585E+05 | 1.0100E+08 | 4.0081E+08 |
| 55.0 | 1.6683E+03 | 3.6780E+03 | 8.2492E+01 | 1.4848E+02 | 3.2501E+05 | 7.1652E+05 | 1.0177E+08 | 4.0384E+08 |
| 60.0 | 2.0347E+03 | 4.4857E+03 | 8.2038E+01 | 1.4767E+02 | 3.3385E+05 | 7.3602E+05 | 1.0249E+08 | 4.0673E+08 |
| 65.0 | 1.5550E+03 | 3.4282E+03 | 9.3659E+01 | 1.6859E+02 | 3.4338E+05 | 7.5703E+05 | 1.0330E+08 | 4.0994E+08 |
| 70.0 | 1.1052E+03 | 2.4365E+03 | 9.7418E+01 | 1.7535E+02 | 3.4738E+05 | 7.6628E+05 | 1.0374E+08 | 4.1166E+08 |
| 75.0 | 1.0596E+03 | 2.3359E+03 | 9.9657E+01 | 1.7938E+02 | 3.5262E+05 | 7.7739E+05 | 1.0424E+08 | 4.1364E+08 |
| 80.0 | 7.8015E+02 | 1.7199E+03 | 1.0732E+02 | 1.9318E+02 | 3.5648E+05 | 7.8590E+05 | 1.0465E+08 | 4.1529E+08 |
| 85.0 | 2.3990E+02 | 5.2888E+02 | 1.9546E+02 | 3.5183E+02 | 3.6095E+05 | 7.9577E+05 | 1.0512E+08 | 4.1717E+08 |
| 90.0 | 8.0717E+02 | 1.7795E+03 | 1.0951E+02 | 1.9713E+02 | 3.6243E+05 | 7.9903E+05 | 1.0539E+08 | 4.1822E+08 |
| 95.0 | 6.5211E+02 | 1.4377E+03 | 1.1473E+02 | 2.0651E+02 | 3.6588E+05 | 8.0663E+05 | 1.0579E+08 | 4.1982E+08 |
| 100.0 | 1.7141E+03 | 3.7789E+03 | 9.6159E+01 | 1.7309E+02 | 3.7052E+05 | 8.1686E+05 | 1.0629E+08 | 4.2178E+08 |
| 110.0 | 1.3707E+03 | 3.0219E+03 | 9.3458E+01 | 1.6822E+02 | 3.8066E+05 | 8.3921E+05 | 1.0730E+08 | 4.2582E+08 |
| 120.0 | 1.1553E+03 | 2.5469E+03 | 1.0026E+02 | 1.8046E+02 | 3.9104E+05 | 8.6210E+05 | 1.0835E+08 | 4.2998E+08 |

A-3

Table 6.2.1-39 (3 of 4)

| Time (sec) | Mass Flow | | Enthalpy | | Integral of Mass Flow | | Integral of Energy | |
|---------------|-------------|-------------|-------------|-------------|-----------------------|------------|--------------------|------------|
| | (kg/sec) | (lbm/sec) | (kcal/kg) | (Btu/lbm) | (kg) | (lbm) | (kcal) | (Btu) |
| 28.0 | 1.3825E+03 | 3.0478E+03 | 7.4008E+01 | 1.3321E+02 | 3.0503E+05 | 6.7249E+05 | 9.9830E+07 | 3.9616E+08 |
| 29.0 | -4.6888E+01 | -1.0337E+02 | 2.9049E+02 | 5.2288E+02 | 3.0511E+05 | 6.7265E+05 | 9.9824E+07 | 3.9613E+08 |
| 30.0 | -9.2798E+00 | -2.0459E+01 | -3.7440E+02 | -6.7393E+02 | 3.0507E+05 | 6.7256E+05 | 9.9811E+07 | 3.9608E+08 |
| 35.0 | 8.2544E+02 | 1.8198E+03 | 7.0693E+01 | 1.2725E+02 | 3.0599E+05 | 6.7460E+05 | 9.9938E+07 | 3.9659E+08 |
| 40.0 | 1.5654E+03 | 3.4512E+03 | 6.5703E+01 | 1.1826E+02 | 3.0759E+05 | 6.7813E+05 | 1.0014E+08 | 3.9737E+08 |
| 45.0 | 2.2241E+03 | 4.9033E+03 | 6.8862E+01 | 1.2395E+02 | 3.0912E+05 | 6.8149E+05 | 1.0037E+08 | 3.9829E+08 |
| 50.0 | 7.7318E+02 | 1.7046E+03 | 9.6668E+01 | 1.7400E+02 | 3.1457E+05 | 6.9352E+05 | 1.0091E+08 | 4.0045E+08 |
| 55.0 | 7.2726E+02 | 1.6033E+03 | 1.0195E+02 | 1.8351E+02 | 3.2410E+05 | 7.1452E+05 | 1.0169E+08 | 4.0355E+08 |
| 60.0 | 5.4934E+02 | 1.2111E+03 | 1.1092E+02 | 1.9966E+02 | 3.3289E+05 | 7.3389E+05 | 1.0241E+08 | 4.0641E+08 |
| 65.0 | 9.7930E+02 | 2.1590E+03 | 1.0144E+02 | 1.8259E+02 | 3.4263E+05 | 7.5537E+05 | 1.0323E+08 | 4.0966E+08 |
| 70.0 | 9.4834E+02 | 2.0907E+03 | 1.0456E+02 | 1.8820E+02 | 3.4706E+05 | 7.6514E+05 | 1.0369E+08 | 4.1146E+08 |
| 75.0 | 9.2547E+02 | 2.0403E+03 | 1.0588E+02 | 1.9058E+02 | 3.5208E+05 | 7.7621E+05 | 1.0418E+08 | 4.1343E+08 |
| 80.0 | 1.6133E+03 | 3.5567E+03 | 9.9377E+01 | 1.7888E+02 | 3.5606E+05 | 7.8498E+05 | 1.0461E+08 | 4.1511E+08 |
| 85.0 | 2.1460E+03 | 4.7310E+03 | 9.6351E+01 | 1.7343E+02 | 3.6080E+05 | 7.9543E+05 | 1.0510E+08 | 4.1706E+08 |
| 90.0 | 1.0122E+02 | 2.2316E+02 | 2.5144E+02 | 4.5258E+02 | 3.6243E+05 | 7.9903E+05 | 1.0539E+08 | 4.1822E+08 |
| 95.0 | 9.6142E+02 | 2.1196E+03 | 9.9371E+01 | 1.7887E+02 | 3.6588E+05 | 8.0663E+05 | 1.0579E+08 | 4.1982E+08 |
| 100.0 | 6.8324E+02 | 1.5063E+03 | 1.0617E+02 | 1.9111E+02 | 3.7052E+05 | 8.1686E+05 | 1.0629E+08 | 4.2178E+08 |
| 110.0 | 1.2417E+03 | 2.7374E+03 | 1.0184E+02 | 1.8332E+02 | 3.8016E+05 | 8.3811E+05 | 1.0726E+08 | 4.2562E+08 |
| 120.0 | 7.2970E+02 | 1.6087E+03 | 1.0815E+02 | 1.9466E+02 | 3.9050E+05 | 8.6091E+05 | 1.0830E+08 | 4.2976E+08 |

Replace with next page A-4

Table 6.2.1-39 (4 of 4)

| Time (sec) | Mass Flow | | Enthalpy | | Integral of Mass Flow | | Integral of Energy | |
|---------------|------------|------------|------------|------------|-----------------------|------------|--------------------|------------|
| | (kg/sec) | (lbm/sec) | (kcal/kg) | (Btu/lbm) | (kg) | (lbm) | (kcal) | (Btu) |
| 130.0 | 8.9815E+02 | 1.9801E+03 | 1.0577E+02 | 1.9039E+02 | 4.0040E+05 | 8.8274E+05 | 1.0933E+08 | 4.3384E+08 |
| 140.0 | 1.1298E+03 | 2.4908E+03 | 1.0262E+02 | 1.8471E+02 | 4.1093E+05 | 9.0594E+05 | 1.1043E+08 | 4.3821E+08 |
| 150.0 | 9.5167E+02 | 2.0981E+03 | 1.0889E+02 | 1.9600E+02 | 4.1912E+05 | 9.2399E+05 | 1.1132E+08 | 4.4175E+08 |
| 160.0 | 1.1363E+03 | 2.5051E+03 | 1.0489E+02 | 1.8881E+02 | 4.3166E+05 | 9.5164E+05 | 1.1261E+08 | 4.4686E+08 |
| 170.0 | 9.1526E+02 | 2.0178E+03 | 1.0773E+02 | 1.9391E+02 | 4.4223E+05 | 9.7495E+05 | 1.1373E+08 | 4.5131E+08 |
| 180.0 | 4.4847E+02 | 9.8870E+02 | 1.2333E+02 | 2.2199E+02 | 4.4953E+05 | 9.9104E+05 | 1.1454E+08 | 4.5453E+08 |
| 190.0 | 4.9428E+02 | 1.0897E+03 | 1.7914E+02 | 3.2245E+02 | 4.5528E+05 | 1.0037E+06 | 1.1524E+08 | 4.5732E+08 |
| 200.0 | 5.4523E+02 | 1.2020E+03 | 1.8537E+02 | 3.3366E+02 | 4.6069E+05 | 1.0157E+06 | 1.1622E+08 | 4.6121E+08 |
| 210.0 | 5.2823E+02 | 1.1645E+03 | 1.8529E+02 | 3.3352E+02 | 4.6557E+05 | 1.0264E+06 | 1.1717E+08 | 4.6496E+08 |
| 220.0 | 5.1639E+02 | 1.1384E+03 | 1.7528E+02 | 3.1550E+02 | 4.7111E+05 | 1.0386E+06 | 1.1813E+08 | 4.6879E+08 |
| 230.0 | 3.4466E+02 | 7.5985E+02 | 2.1803E+02 | 3.9246E+02 | 4.7535E+05 | 1.0480E+06 | 1.1894E+08 | 4.7201E+08 |
| 240.0 | 1.3835E+02 | 3.0501E+02 | 3.4640E+02 | 6.2352E+02 | 4.7706E+05 | 1.0517E+06 | 1.1950E+08 | 4.7422E+08 |
| 250.0 | 1.1657E+02 | 2.5700E+02 | 3.5294E+02 | 6.3529E+02 | 4.7832E+05 | 1.0545E+06 | 1.1994E+08 | 4.7596E+08 |
| 260.0 | 1.1309E+02 | 2.4933E+02 | 3.2035E+02 | 5.7663E+02 | 4.7943E+05 | 1.0576E+06 | 1.2031E+08 | 4.7745E+08 |
| 270.0 | 1.0166E+02 | 2.2411E+02 | 3.5015E+02 | 6.3027E+02 | 4.8051E+05 | 1.0593E+06 | 1.2068E+08 | 4.7889E+08 |
| 280.0 | 1.0073E+02 | 2.2206E+02 | 3.5595E+02 | 6.4071E+02 | 4.8152E+05 | 1.0616E+06 | 1.2104E+08 | 4.8031E+08 |
| 290.0 | 1.0174E+02 | 2.2430E+02 | 3.5329E+02 | 6.3591E+02 | 4.8252E+05 | 1.0638E+06 | 1.2139E+08 | 4.8172E+08 |
| 300.0 | 9.5467E+01 | 2.1047E+02 | 3.4684E+02 | 6.2431E+02 | 4.8351E+05 | 1.0660E+06 | 1.2174E+08 | 4.8310E+08 |

A-4

Table 6.2.1-39 (4 of 4)

| Time (sec) | Mass Flow | | Enthalpy | | Integral of Mass Flow | | Integral of Energy | |
|---------------|------------|------------|------------|------------|-----------------------|------------|--------------------|------------|
| | (kg/sec) | (lbm/sec) | (kcal/kg) | (Btu/lbm) | (kg) | (lbm) | (kcal) | (Btu) |
| 130.0 | 4.4106E+02 | 9.7237E+02 | 1.5443E+02 | 2.7797E+02 | 3.9996E+05 | 8.8177E+05 | 1.0928E+08 | 4.3366E+08 |
| 140.0 | 8.9698E+02 | 1.9775E+03 | 1.2583E+02 | 2.2650E+02 | 4.1034E+05 | 9.0465E+05 | 1.1037E+08 | 4.3797E+08 |
| 150.0 | 9.1549E+02 | 2.0183E+03 | 1.2770E+02 | 2.2987E+02 | 4.1868E+05 | 9.2304E+05 | 1.1127E+08 | 4.4156E+08 |
| 160.0 | 7.0149E+02 | 1.5465E+03 | 1.4420E+02 | 2.5956E+02 | 4.3109E+05 | 9.5039E+05 | 1.1255E+08 | 4.4663E+08 |
| 170.0 | 5.7435E+02 | 1.2662E+03 | 1.3331E+02 | 2.3997E+02 | 4.4180E+05 | 9.7401E+05 | 1.1368E+08 | 4.5113E+08 |
| 180.0 | 2.9484E+02 | 6.5000E+02 | 2.9684E+02 | 5.3431E+02 | 4.4929E+05 | 9.9051E+05 | 1.1451E+08 | 4.5442E+08 |
| 190.0 | 4.5837E+02 | 1.0105E+03 | 1.7477E+02 | 3.1459E+02 | 4.5507E+05 | 1.0033E+06 | 1.1520E+08 | 4.5717E+08 |
| 200.0 | 4.3574E+02 | 9.6065E+02 | 1.8588E+02 | 3.3459E+02 | 4.6043E+05 | 1.0151E+06 | 1.1617E+08 | 4.6101E+08 |
| 210.0 | 1.8636E+02 | 4.1085E+02 | 3.1251E+02 | 5.6252E+02 | 4.6531E+05 | 1.0258E+06 | 1.1712E+08 | 4.6478E+08 |
| 220.0 | 1.2309E+02 | 2.7136E+02 | 3.9496E+02 | 7.1094E+02 | 4.7086E+05 | 1.0381E+06 | 1.1809E+08 | 4.6862E+08 |
| 230.0 | 1.0636E+02 | 2.3449E+02 | 4.5244E+02 | 8.1440E+02 | 4.7498E+05 | 1.0471E+06 | 1.1887E+08 | 4.7171E+08 |
| 240.0 | 1.0104E+02 | 2.2275E+02 | 4.7516E+02 | 8.5528E+02 | 4.7692E+05 | 1.0514E+06 | 1.1945E+08 | 4.7403E+08 |
| 250.0 | 1.3263E+02 | 2.9240E+02 | 3.6438E+02 | 6.5588E+02 | 4.7826E+05 | 1.0544E+06 | 1.1992E+08 | 4.7588E+08 |
| 260.0 | 1.3883E+02 | 3.0606E+02 | 3.7319E+02 | 6.7175E+02 | 4.7937E+05 | 1.0568E+06 | 1.2030E+08 | 4.7737E+08 |
| 270.0 | 1.3114E+02 | 2.8912E+02 | 3.6650E+02 | 6.5970E+02 | 4.8046E+05 | 1.0592E+06 | 1.2066E+08 | 4.7882E+08 |
| 280.0 | 1.2790E+02 | 2.8198E+02 | 3.6663E+02 | 6.5994E+02 | 4.8146E+05 | 1.0614E+06 | 1.2102E+08 | 4.8024E+08 |
| 290.0 | 1.3176E+02 | 2.9047E+02 | 3.7484E+02 | 6.7471E+02 | 4.8247E+05 | 1.0637E+06 | 1.2137E+08 | 4.8165E+08 |
| 300.0 | 1.3813E+02 | 3.0452E+02 | 3.6063E+02 | 6.4913E+02 | 4.8341E+05 | 1.0657E+06 | 1.2170E+08 | 4.8296E+08 |

Replace with next page B

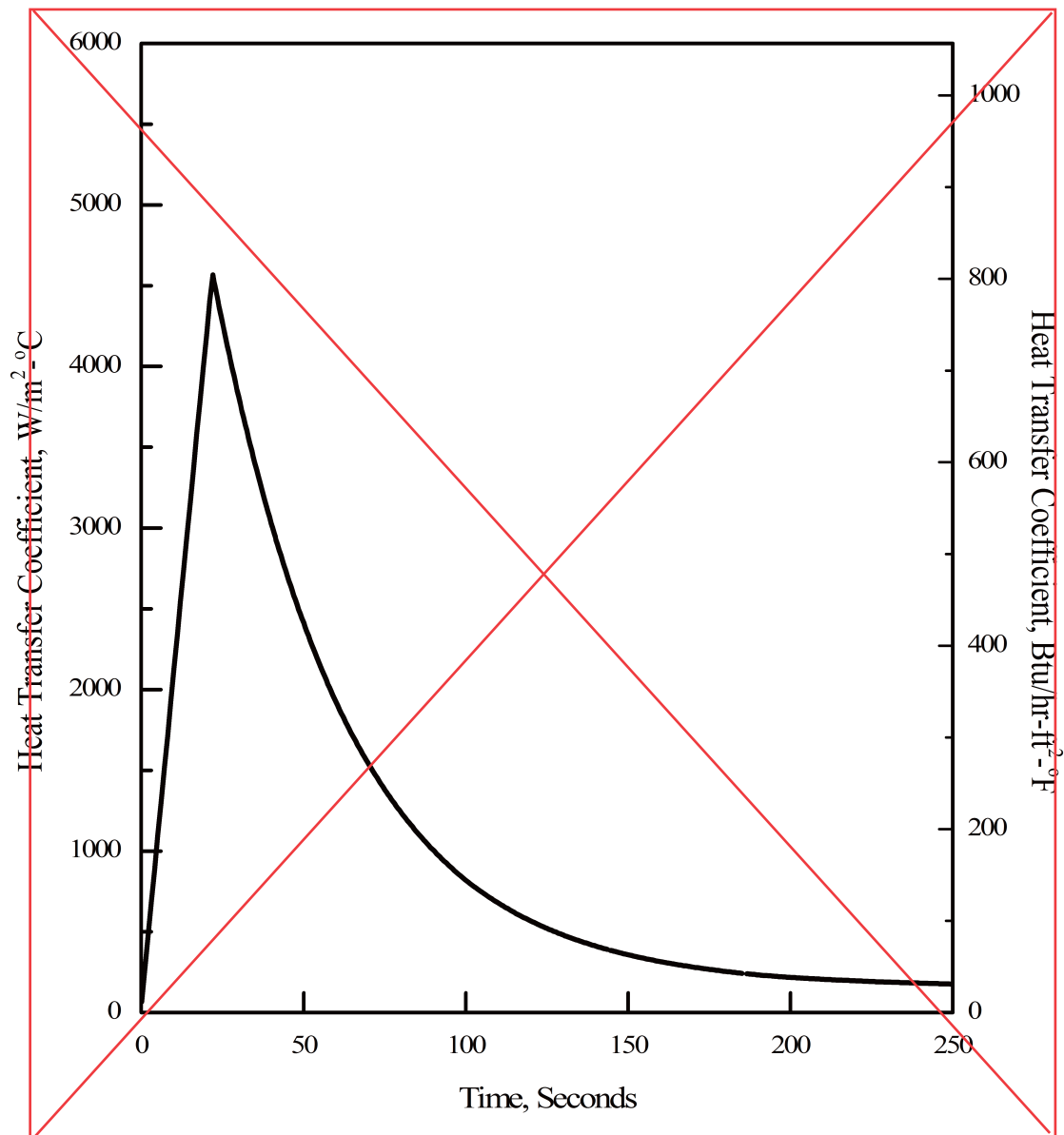
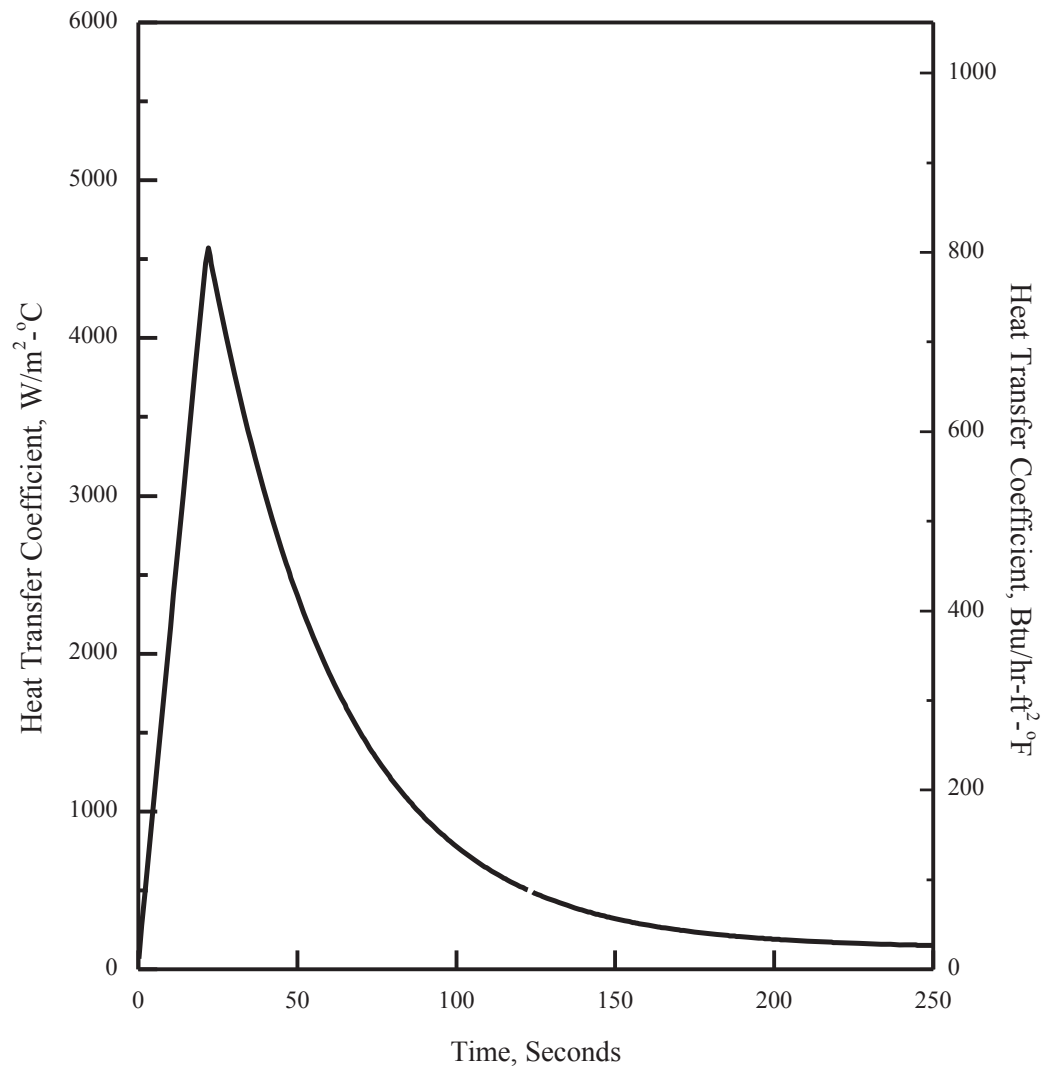
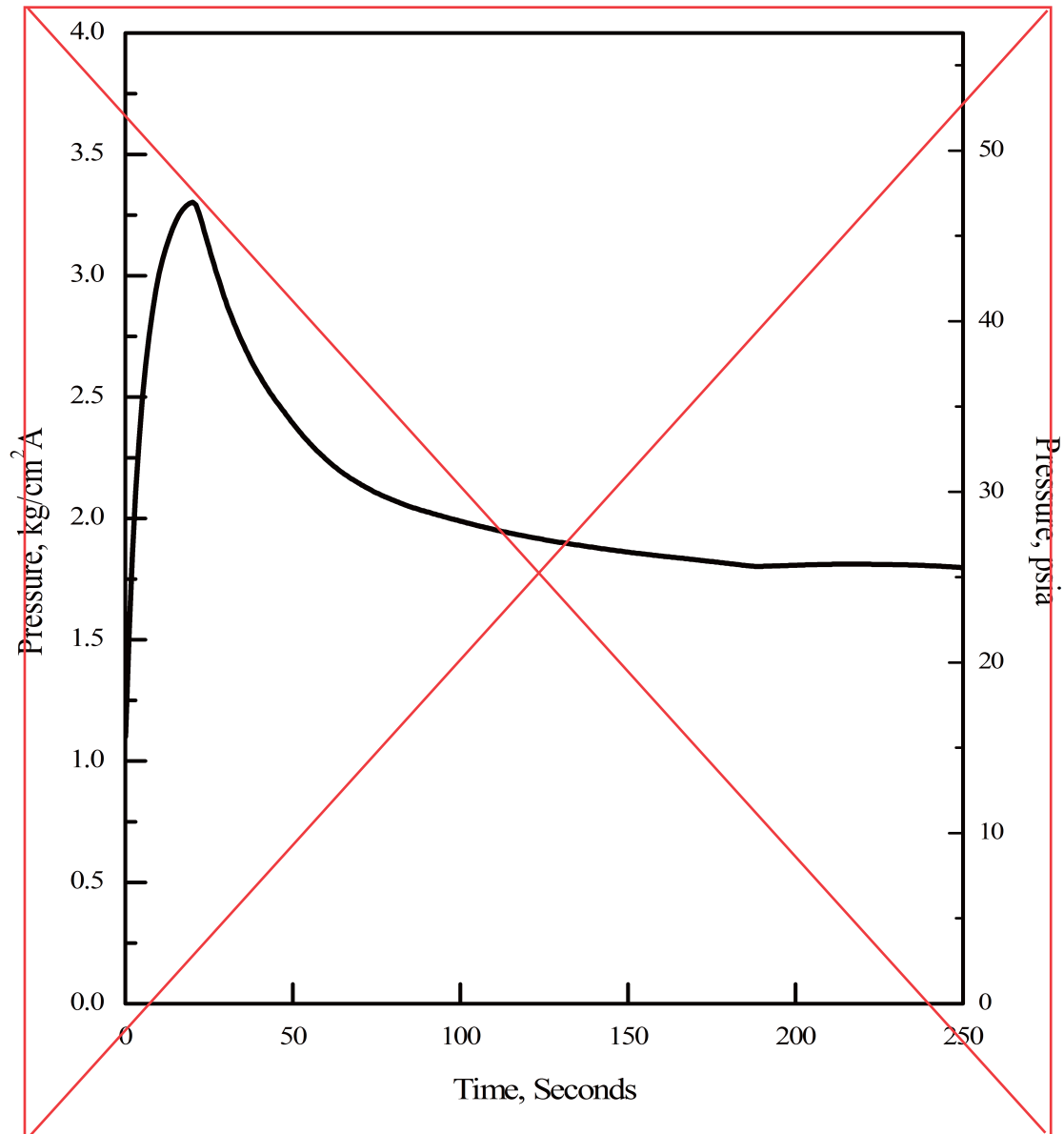


Figure 6.2.1-49 ECCS Performance Analysis
(Condensation Heat Transfer Coefficient for Passive Heat Removal Source)

B

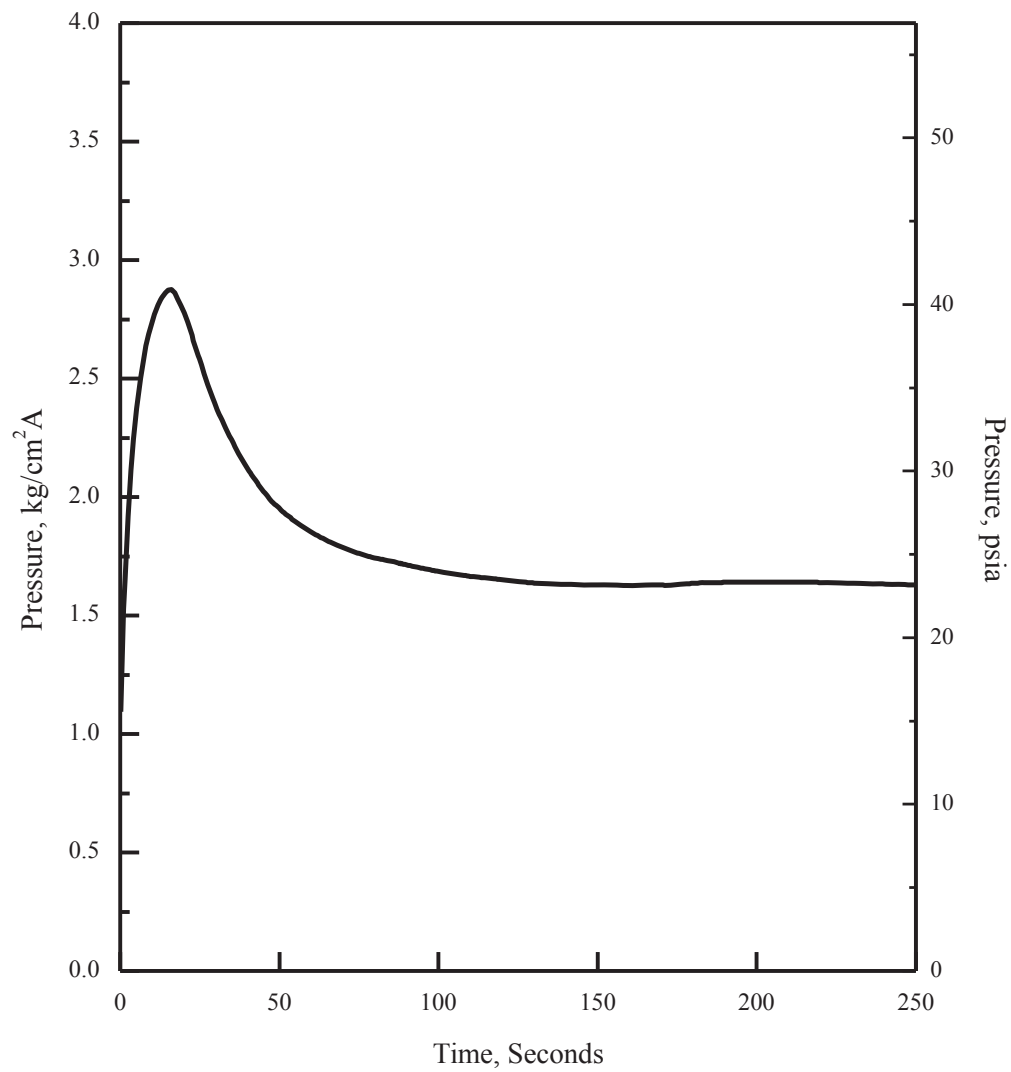


Replace with next page C

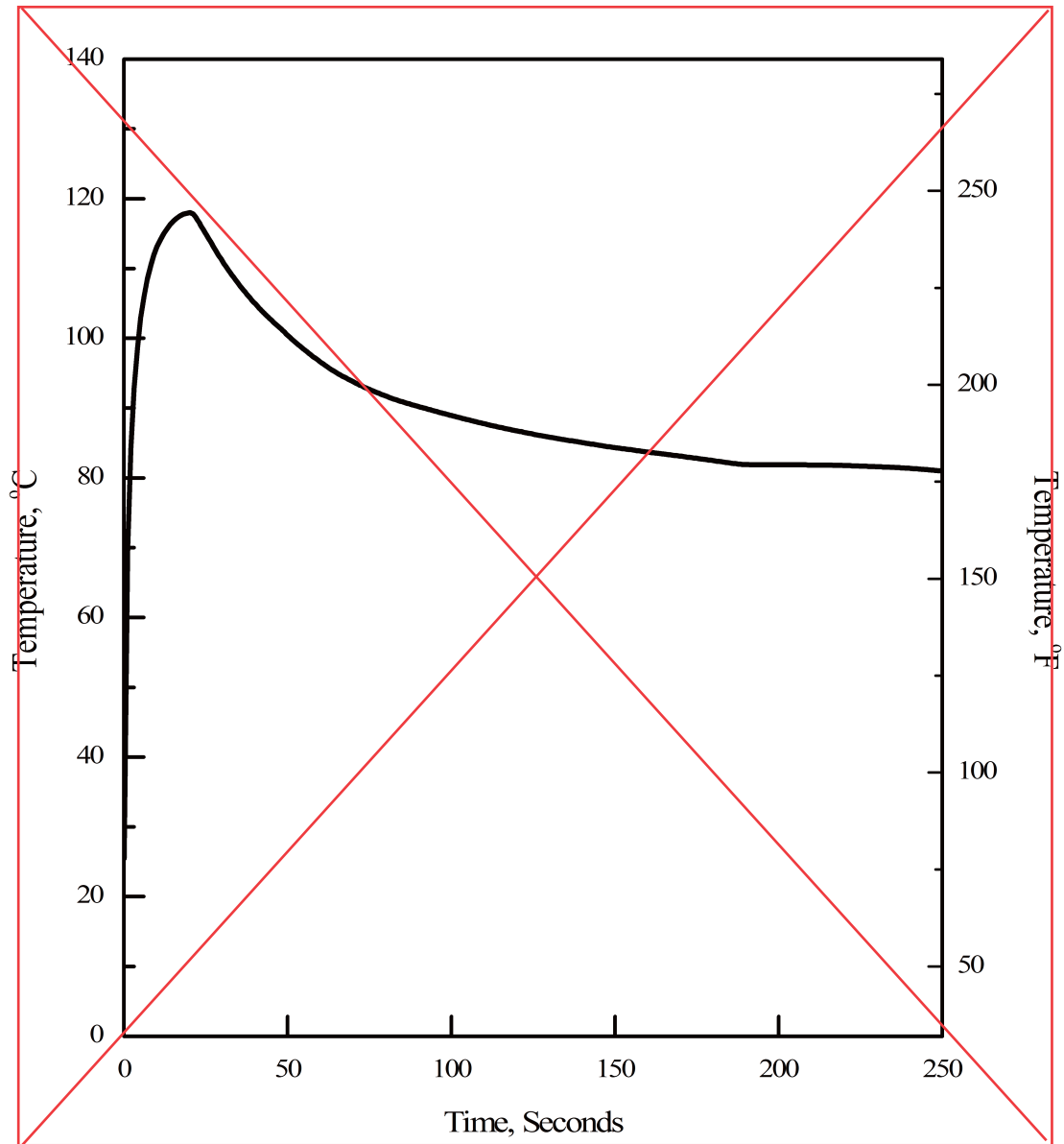


**Figure 6.2.1-50 1.0 x Double-Ended Guillotine Break in Pump Discharge Leg
(Min. Containment Pressure for ECCS Performance Analysis)**

C

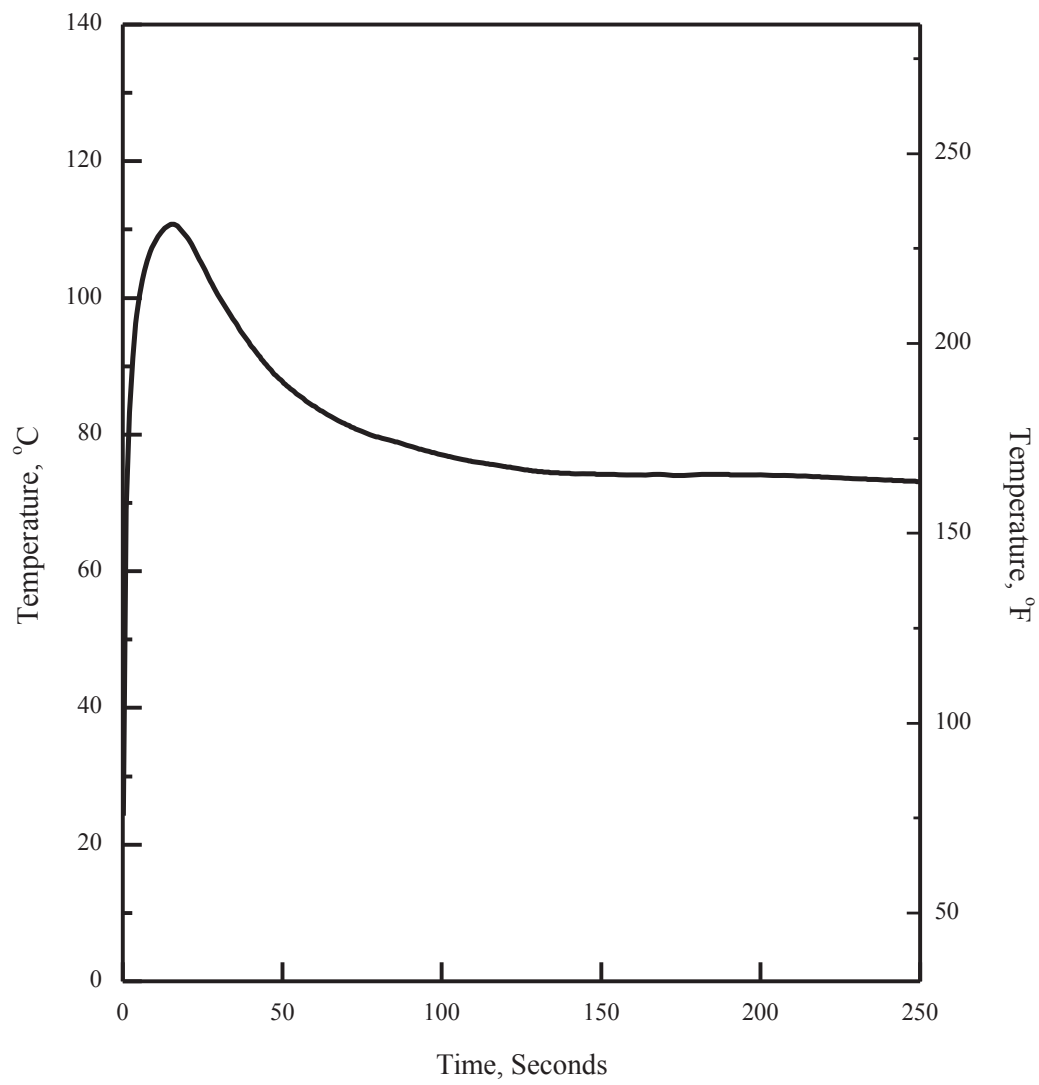


Replace with next page D

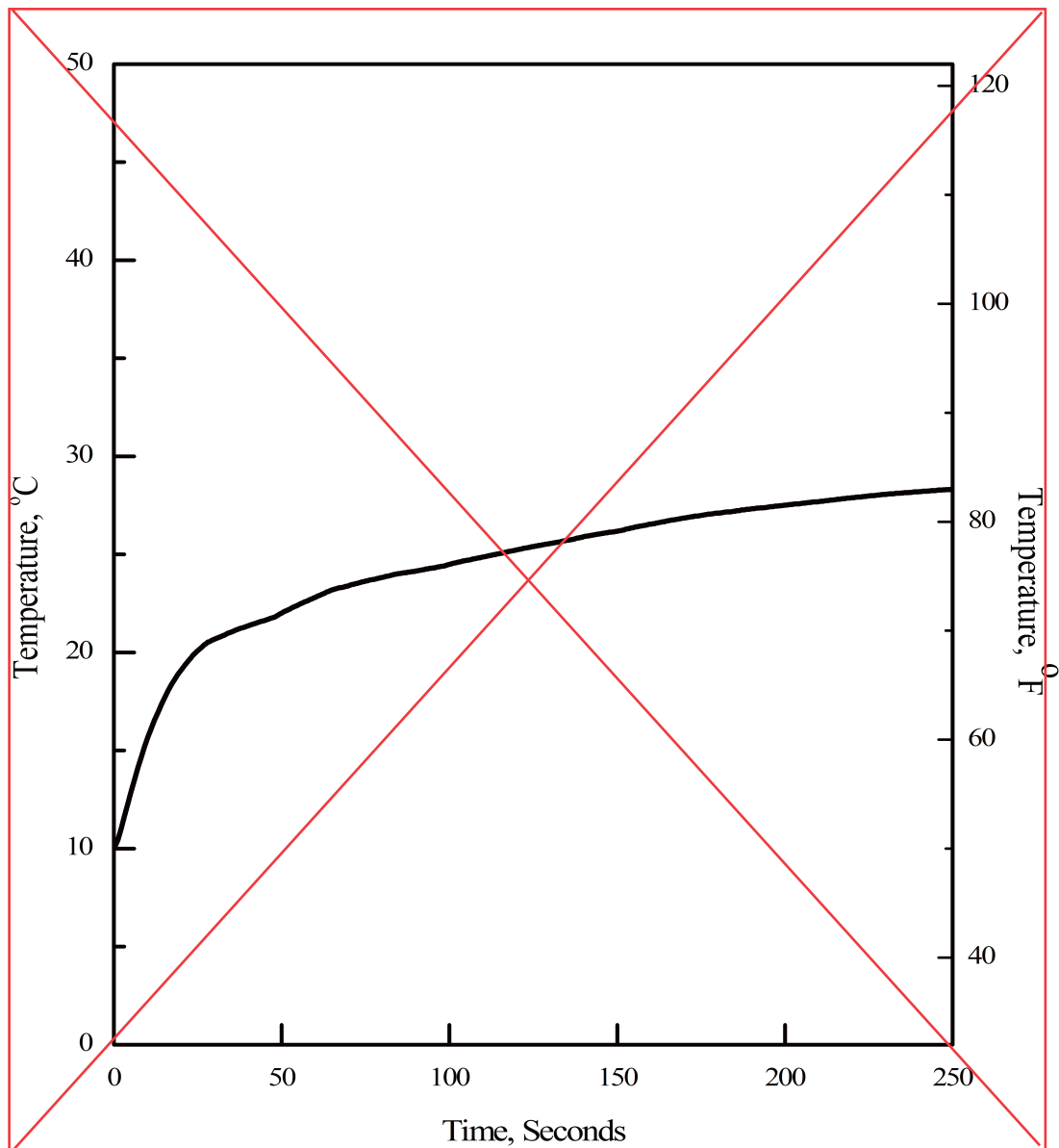


**Figure 6.2.1-51 1.0 x Double-Ended Guillotine Break in Pump Discharge Leg
(Containment Atmosphere Temperature)**

D

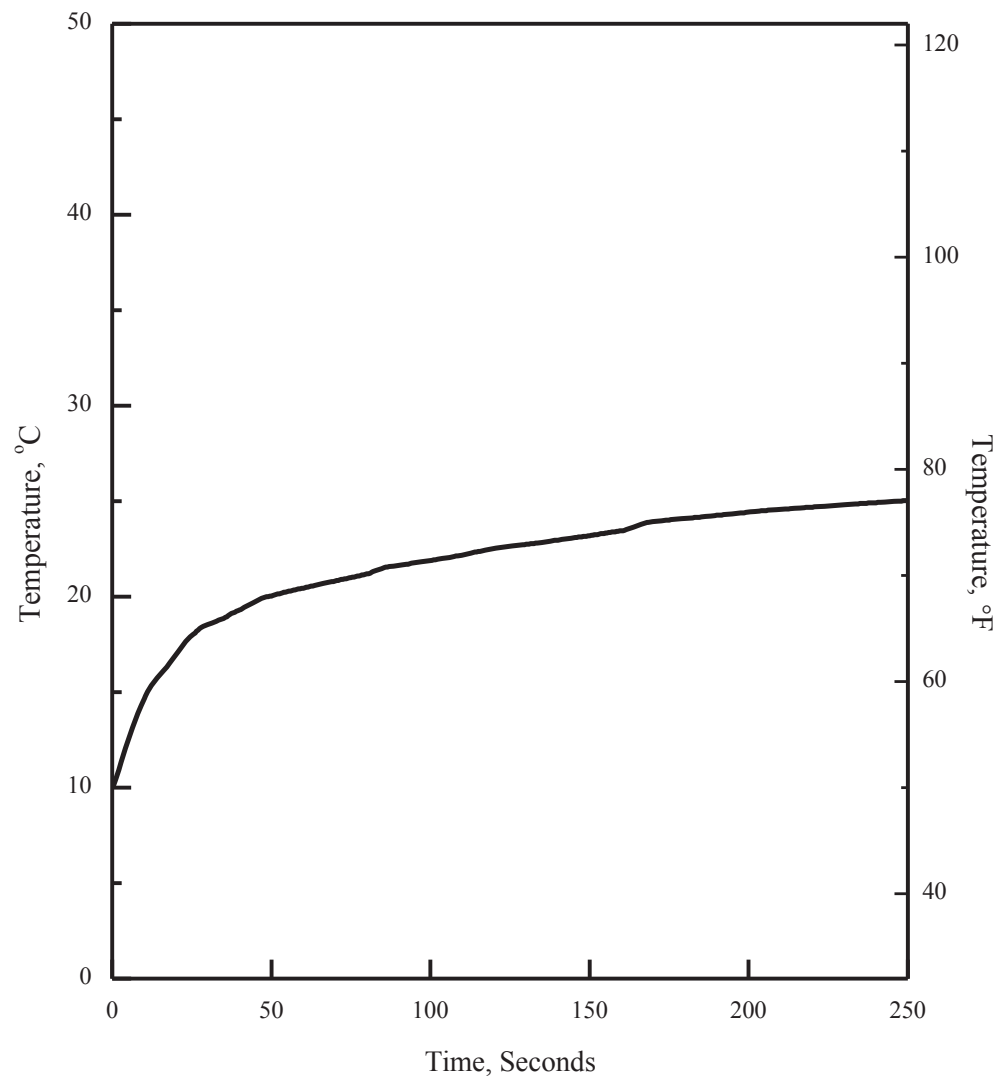


Replace with next page E



**Figure 6.2.1-52 1.0 x Double-Ended Guillotine Break In Pump Discharge Leg
(In-containment Refueling Water Storage Tank)**

E



fuel maximum reactivity assumption, worst-case moderator density, and tolerances and uncertainties of the fuel and racks are considered to maximize the calculated K_{eff} for normal conditions and postulated accidents.

The design of the new fuel storage racks is such that K_{eff} (with all biases and uncertainties) must not exceed 0.95 with full density unborated water and 0.98 with optimum moderation in the new fuel rack, at a 95 percent probability and 95 percent confidence level. For the spent fuel storage racks, credit is taken for the presence of soluble boron in the SFP. Therefore, the maximum K_{eff} including all biases and uncertainties must ~~not~~ exceed 0.95 with borated water, and must remain below 1.0 with full density unborated water, at a 95 percent probability and 95 percent confidence level.

not

The criticality safety evaluation for the new and spent fuel storage racks is performed in accordance with the following acceptance criteria and relevant guidance: 10 CFR Part 50 Appendix A, General Design Criterion (GDC) 62 (Reference 1), 10 CFR Part 50.68 (Reference 2), NRC guidance (Reference 3), and NUREG/CR-6698 (Reference 4). The 10 CFR Part 50.68 (b) items (2) and (3) for new fuel storage racks and item (4) for spent fuel storage racks are applied as the criticality safety design criteria. Criticality analysis codes are validated in accordance with NUREG/CR-6698.

9.1.1.2 Facilities Description


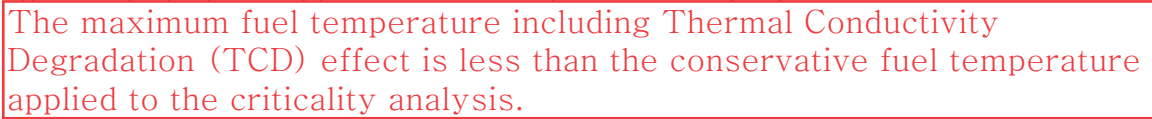
The description of new and spent fuel storage facilities is presented in Subsection 9.1.2.2.

9.1.1.3 Safety Evaluation

Prevention of an inadvertent criticality is provided by the adequate design of fuel handling and storage facilities and by administrative control procedures, considering the double contingency principle. The main methods for criticality control are (1) limiting the size of the array of fuel assemblies and (2) limiting the assembly neutron interaction by fixing the minimum separation and/or providing neutron poisons. In addition, rack cells are maintained in a safe geometry with no deformation in any design basis event. Flooding in the new fuel storage racks and boron dilution in the SFP water are minimized. Fuel mishandling is prevented by the fuel handling procedures.

For criticality safety design, the following analyses are performed to evaluate the degree of subcriticality and to verify conformance with the following design criteria (Reference 10):

condition, an infinite array of fresh fuel assemblies is modeled in the criticality calculation. Criticality for damaged fuel assemblies is separately evaluated and the effects of gap between racks are also evaluated.

- b. For the region II analyses, an infinite array of 2×2 fuel assemblies with various U-235 enrichments, from 2.0 to 5.0 wt%, is used for the criticality calculation. The moderator of pure water is at the temperature (density) within the design limits that yields the largest reactivity. The full density of unborated water is assumed to be 1.0 g/cm^3 (62.4 lbm/ft^3).
- c. Credit is taken for the neutron absorption in the neutron absorbing materials, and only 75 percent of B-10 areal density in the neutron absorbing materials is credited in the analysis. These assumptions provide additional margin in the event that deformation, degradation, or damage to the neutron absorber occur.
- d. Credit is taken for the soluble boron in the SFP. The SFP soluble boron concentration is assumed to be the same or less than the minimum concentration provided in the LCO 3.7.15.
- e. No cooling time is assumed to avoid fission product accumulation and Xe-135 is not included in the criticality calculation to conservatively evaluate the K_{eff} .
- f. The nuclear characteristics of the spent fuel are affected by the core operation parameters, such as fuel temperature, coolant temperature, soluble boron concentration in the coolant, and axial burnup profile. Thus, the most severe operating conditions are conservatively assumed in the fuel burnup calculation.
- g. No CEAs or burnable poison rods in the fuel assembly, and no neutron absorption
- h. The maximum fuel temperature including Thermal Conductivity Degradation (TCD) effect is less than the conservative fuel temperature applied to the criticality analysis.
the SFP filled with water.
- i. The bias and bias uncertainty obtained from benchmark calculation are reflected in the calculated K_{eff} . Uncertainties from mechanical tolerances and variations in the design parameters are added to the total uncertainty. For region II analyses, the effects of axial burnup profile and burnable poison rods, and uncertainty from the depletion calculation methodology are considered in the calculation K_{eff} .

APR1400 DCD TIER 2

In Non-LOCA analysis, maximum gap conductance used in CESEC-III code is not affected by TCD because the highest gap conductance value is obtained without gas generation. And minimum gap conductance used in CESEC-III code is not affected because the lowest gap conductance value is obtained at low burnup where fission gas release is negligible. The fuel temperature coefficient reflecting a large uncertainty can cover the TCD. Also, Doppler feedback effect in CESEC-III code is still conservative because of the conservative gap conductance assumption.

In DNB analyses, CETOP/TORC code is not affected by TCD due to the use of "dummy" rods to define the heat flux boundary. A dummy rod does not consider the conduction heat transfer within the fuel rods.

Most of stored energy is eliminated before the core uncover during a blowdown phase in small break LOCA (SBLOCA). Hence, the initial stored energy effects caused by TCD are negligible in SBLOCA.

The impacts of TCD for a CEA ejection accident and LBLOCA are considered by reflecting TCD penalty in initializing the fuel centerline and average temperature. The TCD penalty is provided in Reference 78.

each design basis event.

The setpoints presented in Table 15.0-2 are determined based on the methodology presented above. The main methodology for determining uncertainties and the detailed uncertainty values are provided in Reference 51, which is based on NRC RG 1.105, Rev. 3, "Setpoints for Safety-Related Instrumentation." The setpoint methodology for plant protection system is provided in Reference 77.

15.0.0.10 Thermal Conductivity Degradation

The effects of thermal conductivity degradation (TCD) on non-LOCA and LOCA evaluations, except for a CEA ejection accident and LBLOCA, are negligible. ~~The effects are provided in Reference 78.~~

The results of the evaluation of a CEA ejection accident and LBLOCA are provided in Subsections 15.4.8.3 and 15.6.5.3, respectively.

15.0.1 Radiological Consequence Analysis Using Alternative Source Terms

This subsection is not applicable to the APR1400 because it is prepared to review the application for the initial implementation of an alternative source terms (AST)

APR1400-F-M-TR-13001-P, "PLUS7 Fuel Design for the APR1400," Rev. 1, KHNP, To be issued

78. ~~APR1400-F-A-NR-14002-P, "The Effect of Thermal Conductivity Degradation on APR1400 Design and Safety Analyses," Rev. 0, KHNP, September 2014.~~
79. NUREG-1462, "Final Safety Evaluation Report Related to the Certification of the System 80+ Design Docket No. 52-002," Rev. 0, U.S. Nuclear Regulatory Commission, 1994.
80. APR1400-Z-A-NR-14014-P, "ATWS Evaluation," Rev. 0, KHNP, November 2014.
81. APR1400-F-M-TR-13001-P (Proprietary), "PLUS7 Fuel Design for the APR1400," Rev. 0, KHNP, August 2013.

APR1400 DCD TIER 2

The reactor coolant pressure stays below 110 percent of the design pressure so that the integrity of the reactor coolant pressure boundary is maintained.

15.4.8 Spectrum of Control Element Assembly Ejection Accidents

15.4.8.1 Identification of Causes and Frequency Classification

A control element assembly (CEA) ejection (CEAE) event is postulated to occur as a result of a mechanical failure that causes an instantaneous circumferential rupture of the control element drive mechanism (CEDM) housing or its associated nozzle. This results in the reactor coolant system pressure ejecting the CEA and drive shaft to the fully withdrawn position.

The CEDM housings are capable of withstanding throughout their design life all normal operating loads including the steady-state and transient operating conditions specified for the reactor vessel. The occurrence of such a failure is considered to be incredible, and this event is classified as a PA as defined in Subsection 15.0.0.1.

The CEA ejection accident applies the following acceptance criteria:

- a. The maximum reactor pressure during any portion of the assumed excursion is less than the value that result in stresses that exceed the “Service Limit C” as defined in the ASME Code.
- b. The total number of failed fuel rods that are considered in the radiological assessment is equal to the sum of all of the fuel rods failing each of the criteria below:
 - 1) The high cladding temperature failure criterion for zero-power conditions is a peak radial average fuel enthalpy greater than 711.8 kJ/kg (170 cal/g) for fuel rods with an internal rod pressure at or below system pressure, or 628.0 kJ/kg (150 cal/g) for fuel rods with an internal rod pressure exceeding system pressure. For intermediate and full-power conditions, fuel cladding failure is presumed if local heat flux exceeds thermal design limits.
 - 2) The pellet cladding mechanical interaction (PCMI) failure criterion is a change in radial average fuel enthalpy greater than the corrosion-dependent limit depicted in Figure B-1 of NUREG-0800 (SRP 4.2, Appendix B).

APR1400 DCD TIER 2

In addition to the fuel failure and boundary criteria above, the following criteria from NUREG-0800 (SRP, Section 4.2, Appendix B) apply to core coolability.

- a. Peak radial average fuel enthalpy remains below 963.0 kJ/kg (230 cal/g).
- b. Peak fuel temperature remains below incipient melting conditions.
- c. Mechanical energy generated as a result of (1) non-molten fuel-to-coolant interaction and (2) fuel rod burst must be addressed with respect to reactor pressure boundary, reactor internals, and fuel assembly structural integrity.
- d. There is no loss of coolable geometry due to (1) fuel pellet and cladding fragmentation and dispersal or (2) fuel rod ballooning.

15.4.8.2 Sequence of Events and Systems Operation

The sequence of events during the fuel performance aspect of the CEAE initiated from various power conditions is presented in Table 15.4.8-1.

The postulated mechanical failure of the CEDM causes the ejection of a CEA, which adds positive reactivity to the core resulting in a rapid increase in reactor core power for a short period of time. This power excursion is terminated by the combination of delayed neutron and Doppler feedback effects. Closely following the CEAE, reactor shutdown is initiated by a core protection calculator (CPC) or reactor protection system (RPS) variable overpower trip (VOPT) on high neutron power. The reactor power decreases rapidly as the shutdown CEAs drop into the reactor core. A loss of offsite power (LOOP) is assumed to be coincident with a turbine trip.

The analysis assumes that operator action is delayed until 30 minutes after event initiation. Plant cooldown is accomplished by using the auxiliary feedwater (AFW) system in conjunction with the atmospheric dump valves (ADV) until shutdown cooling entry conditions are reached.

This event results in a turbine trip when initiated from at-power conditions. A turbine trip could cause a disturbance to the utility grid, which could cause a loss of offsite power, which could cause a RCP coastdown. The RCS pressure increase caused by turbine trip and LOOP can mitigate fuel failure due to DNB, but the change of RCS pressure is not conservatively considered for DNBR calculation.

APR1400 DCD TIER 2

None of single failures listed in Table 15.0-4 has any effect on this event. The limiting single failure for this event is one train failure of the RPS. Other trains provide adequate protection. Details on the RPS are provided in Section 7.2.

15.4.8.3 Core and System Performance**15.4.8.3.1 Evaluation Model**

The core response to a CEAE is simulated using the method of analysis referenced in Subsection 15.0.2. The evaluation model is used to determine the peak fuel rod temperature and fuel rod enthalpy, which are required for the evaluation of the high cladding temperature failure, the pellet cladding mechanical interaction (PCMI) failure, and the core coolability. The DNBR is calculated using the CETOP and STRIKIN-II computer programs described in Subsection 15.0.2 with the KCE-1 CHF correlation. A matrix relating the initial and ejected CEA radial peaking factors is obtained from ROCS code, which is a three-dimensional, two-group diffusion core calculation code based on the nodal expansion method, as described in Subsection 4.3.3.1. This matrix is used to calculate the number of fuel pins experiencing DNB. Further conservatism is introduced by assuming that clad failure occurs when fuel rods undergo DNB.

The nuclear steam supply system (NSSS) response to a CEA ejection is simulated using the CESEC-III computer program described in Subsection 15.0.2.2.1.

Except for radiological release from containment, the analysis of the NSSS response to a CEA ejection does not consider the leakage and the RCS depressurization that would be caused by the rupture of the primary pressure boundary. This approach does not affect the fuel failure calculation, but it does increase the calculated secondary steam release. Not considering the leakage and the RCS depressurization maximizes the resultant doses from secondary steam release.

15.4.8.3.2 Input Parameters and Initial Conditions

The initial conditions for the principal process variables are varied within the reactor operating space given in Table 15.0-3 to determine the set of conditions that produce the most adverse consequences following a CEA ejection. The initial pressurizer and steam generator water level, as controlled within the operating space, have an insignificant effect on the consequences of the CEA ejection analysis. Table 15.4.8-2 shows the parameters used in the CEA ejection analysis for peak fuel rod temperature and fuel rod enthalpy

APR1400 DCD TIER 2

analysis. The following assumptions, which encompass conditions characteristic of the beginning of cycle (BOC) and end of cycle (EOC), are used to calculate conservative transient results.

- a. A spectrum of initial reactor power level is considered as follows: (1) hot full power (HFP), (2) 50 percent power, (3) 20 percent power, and (4) hot zero power (HZIP).
- b. Thermal-hydraulic parameters (maximum reactor coolant inlet temperatures, minimum reactor coolant system pressure, and minimum reactor coolant flow fraction) are set to maximize the net energy increase in the fuel of hot channel. For DNBR analysis, the most adverse combination of initial conditions (core inlet temperature, reactor coolant system pressure, and core flow) at a power operating limit by COLSS are selected by parametric studies to minimize the DNBR for HFP and 50 percent power case. COLSS is described in Subsection 7.7.1.4.
- c. It is conservative to use minimum delayed neutron fraction and minimum neutron lifetime at EOC to make the power increase faster and further.
- d. The most positive moderator temperature coefficient (MTC) at BOC is used with varying power level to maximize the positive feedback during the transient.
- e. The least negative fuel temperature coefficient (FTC) is used to minimize Doppler feedback during the power excursion. Doppler reactivity weighting factor is assumed to be 1.0 for conservatism.
- f. In the three-dimensional modeling, the most reactive CEA ejection is selected with consideration for power dependent rod insertion limit. The magnitude of the enthalpy rise increases with increasing ejected worth.
- g. A maximum three-dimensional post-ejected peaking factor is used to maximize the net energy content in the hottest fuel. And, the maximum ratio of the three-dimensional post-ejected to pre-ejected peaking factor is used to maximize the prompt enthalpy rise in the hottest fuel.
- h. Scram curves corresponding to bottom peaked axial shape are used to minimize the initial negative reactivity insertion. The minimum net scram worth with the most reactive rod stuck out and a CEA ejected is used from HFP to HZIP.

APR1400 DCD TIER 2

- i. A top-peaked axial power distribution is set to maximize the energy content in the hottest fuel pellet.
- j. The maximum delay time is 0.55 second (including time to open the reactor trip switchgear) for the VOPT and 0.5 second for CEA holding coil decay time.

15.4.8.3.3 Results

For peak fuel rod temperature and fuel rod enthalpy analysis, the results are summarized in Table 15.4.8-3. For the HZP case, the fuel radial average enthalpy of hot spot is well below the high cladding temperature failure criterion. The prompt fuel enthalpy rise is less than 251.2 kJ/kg (60 cal/g), which is the lowest criterion of the PCMI failure depicted in Figure B-1 of SRP 4.2 and the oxide to wall thickness ratio is less than 0.2 (the maximum cladding oxide thickness is less than 100 μm , Reference 81). The PCMI

k. For TCD effects, the TCD penalty described in Reference 78 was reflected in initializing the fuel centerline and average temperature.

and the HZP case. The non-prompt scenarios that do not exhibit a prompt critical or narrow pulse power excursion, such as the HFP case and the 50 percent power case, would be not concerned with PCMI cladding failure.

In the results, there are no fuel failures due to the high fuel enthalpy and PCMI. From a core coolability perspective, the peak fuel radial average enthalpy and the fuel centerline temperature meet the criterion. The maximum fuel cladding temperature is not high enough to cause fuel rupture or significant rod ballooning. Therefore, there is no loss of core coolable geometry. The interim criteria for reactivity-initiated accident (RIA) described in NUREG-0800 (SRP 4.2 Appendix B) are met.

Delete

~~The centerline temperature is increased by 157.2 °C (315 °F) in case of considering the thermal conductivity degradation (TCD) effect (Reference 78). However, the maximum centerline temperature is below the melting temperature and met the criterion.~~

Following a postulated CEA ejection event, 10.0 percent of the fuel is calculated to undergo DNB. As all fuel pins that undergo DNB are conservatively assumed to suffer clad failure, 10.0 percent of fuel failure is used in the offsite dose evaluation in Subsection 15.4.8.5. The case initiated from HFP initial conditions is expected to result in the greatest potential for offsite dose consequences.

APR1400 DCD TIER 2

Table 15.4.8-1 contains the sequence of events that occur during a CEA ejection for enthalpy case. Figures 15.4.8-1 through 15.4.8-12 show the core power, heat flux, clad and fuel temperatures, and reactivity effects for HFP and HZP cases.

The limiting secondary system releases for the CEAE event are based on a full-power DNBR analysis, with the sequence of events summarized in Table 15.4.8-1. These steam releases are applied to the CEAE radiological consequence assessment presented in Subsection 15.4.8.5. The dynamic behaviors of important NSSS parameters following CEA ejection are presented in Figures 15.4.8-13 and 15.4.8-14.

15.4.8.4 Barrier Performance

15.4.8.4.1 Evaluation Model

The evaluation model is identical to that of core performance as described in Subsection 15.4.8.3.1. The CESEC-III code is used to analyze the RCS pressure transient following CEA ejection.

15.4.8.4.2 Input Parameters and Initial Conditions

The input parameters are similar to the core and system performance analysis described in Subsection 15.4.8.3.2. The initial conditions and NSSS characteristics assumed in this analysis are determined to maximize the primary and secondary system pressures. The input parameters of full-power conditions are used with the difference of the initial pressurizer pressure. The initial pressurizer pressure for this case is 163.46 kg/cm²A (2,325 psia).

15.4.8.4.3 Results

The peak RCS pressure for this event is 177.55 kg/cm²A (2,525.34 psia). The peak RCS pressure includes the pressure difference between the cold leg at the RCP discharge and the surge line. This value is less than the value that results in stresses that exceed the Service Limit C. The peak main steam system pressure reaches 90.17 kg/cm²A (1,282.52 psia). The main steam system pressure is not challenged by this event.

The dynamic behaviors of important NSSS parameters following CEA ejection are presented in Figures 15.4.8-15 through 15.4.8-18.

APR1400 DCD TIER 2**15.4.8.5 Radiological Consequences**

The radiological consequences are performed to determine EAB, LPZ, MCR, and TSC doses due to CEA ejection accident using the AST methodology, the TEDE dose criteria, the guidance in SRP 15.0.3, and the plant-specific bounding design information applicable to the APR1400.

The following two release cases are considered:

- a. Containment leakage release: activity released from the fuel is assumed to be released instantaneously and homogeneously throughout the containment atmosphere and available for release to the environment.
- b. Secondary system release: activity released from the fuel is assumed to be completely dissolved in the primary coolant and available for release to the environment through the secondary system.

15.4.8.5.1 Evaluation Model

Figure 15A-4 in Appendix 15A shows the leakage paths and transport of the activity released to environment, MCR, and TSC during a CEA ejection event.

Containment Leakage Case

For this case, the activity released from the failed fuel is assumed to be instantaneously and homogeneously distributed in the containment following a CEA ejection. This analysis also releases 100 percent of the iodine, alkali metals and noble gases initially present in the RCS. The activity in the containment is subject to be released by the design leak rate specified in the Technical Specifications.

Secondary System Release Case

The offsite power is lost so that the main steam condenser is not available. Following the CEA ejection event, the reactor is shut down and the plant is cooled down by discharging secondary coolant through the two SGs using the combination of one or more ADVs and MSSVs.

The SG tubes are expected to be uncovered during the first 30 minutes of the CEA ejection event because the MSSVs are open to cool down the RCS. During this period, the P-T-S

APR1400 DCD TIER 2

leakage flashing fraction averages 15.0 percent. After 30 minutes, the SG tubes remain covered during the CEA ejection. During the first 30 minutes, the unflashed P-T-S leakage mixes with the SG secondary coolant, and after 30 minutes all of the P-T-S leakage mixes with the SG secondary coolant. The partition coefficients of 100 for iodine and 200 for alkali metal are assumed for the secondary liquid release from the SG.

15.4.8.5.2 Input Parameters and Initial Conditions

The design basis CEA ejection accident is analyzed using a conservative set of assumptions and APR1400 design inputs. The CEA ejection analysis is performed using the guidance in NRC RG 1.183, Appendix H.

Per NRC RG 1.183, Appendix H, Section 1, for the CEA ejection accident, the release from the failed fuel is based on the number of fuel rods to undergo DNB and the assumption that 10 percent of the core inventory of the noble gases and iodines and 12 percent of the core inventory of the alkali metals are in the fuel gap. The expected number of fuel rods in DNB is 10 percent of the core. The failed fuel is modeled with a radial peaking factor of 1.80. Fuel melt is not expected to occur during the CEA ejection. The CEA ejection releases more iodine and noble gases from fuel gap than the other non-LOCA events as specified in NRC RG 1.183, Table 3. The assumed inventory of fission products in the reactor core and available for release to the reactor coolant is based on the maximum power level of 4,062.66 MWt corresponding to current fuel enrichment and fuel burnup, which is 1.02 times the APR1400 licensed thermal power of 3,983 MWt with the cycle burnup of 56.4 GWD/MTU.

The secondary coolant iodine concentration is limited to 3.7×10^3 Bq/g (0.1 μ Ci/g) DE I-131. The RCS DE I-131 isotopic concentration profile is multiplied by a factor of 0.1, representing 10 percent of primary coolant concentration to determine the secondary coolant iodine concentration. The secondary coolant iodine concentration is multiplied by the total coolant mass in both steam generators to calculate the total secondary coolant iodine inventory.

The chemical forms of iodine released from the steam generators to the environment are 97 percent elemental and 3 percent organic. These iodine chemical forms apply to iodine releases from the P-T-S leakage and from the secondary liquid.

Input parameter values used for CEA ejection radiological consequence evaluation are presented in Table 15.4.8-4.

APR1400 DCD TIER 2

A reduction in the amount of radioactive material available for leakage from the containment that is due to natural deposition, containment sprays, recirculating filter systems, or other engineered safety features can be taken into account. This analysis credits aerosol removal by natural deposition. No credit is taken for elemental iodine or aerosol removal by containment sprays.

The primary containment leaks at a Technical Specification peak pressure leak rate of 0.1 percent by volume for the first 24 hours. This leak rate is reduced to 0.05 weight percent after 24 hours.

The P-T-S leakage is at the RCS operational leakage limit of 1.14 L/min (0.3 gpm) through any one SG as specified in the Technical Specification. The P-T-S leak exists until shutdown cooling is in operation and releases from the steam generators have been terminated at 8.0 hours. The primary coolant density used in converting the volumetric P-T-S leak rates to mass leak rates is 1.0 g/cm³ (62.4 lbm/ft³). All noble gas radionuclides released from the primary system via the P-T-S leaks are released to the environment without reduction or mitigation.

The χ/Q values used in the analysis for EAB, LPZ, MCR, and TSC are described in Subsection 2.3.4 and are provided in Tables 2.3-1 through 2.3-12; breathing rates are given in Table 15A-12.

15.4.8.5.3 Results

The radiological consequences due to a CEA ejection are presented in Table 15.4.8-5. The results of the CEA ejection analyses indicate that the EAB and LPZ doses are within their allowable dose limit, which is 25 percent of the 10 CFR 50.34(a)(1) value, as specified in SRP 15.0.3. The MCR and TSC doses are also within the dose limit in GDC 19.

15.4.8.6 Conclusions

For the spectrum of CEA ejection evaluated, none of the power excursions causes the fuel temperatures to reach the limiting fuel melting temperature or the fuel enthalpy limits. For the events that exceeded the DNBR limit, the number of fuel failures was less than the value allowed for the radiological release limit. The peak RCS pressure remains below 110 percent of the RCS design pressure. The stresses due to the primary pressure response during the transients do not exceed Service Limit C as defined in the ASME Code.

APR1400 DCD TIER 2

The doses at the EAB, LPZ, MCR, and TSC are within their allowable dose criteria.

15.4.9 Combined License Information

No COL information is required with regard to Section 15.4.

APR1400 DCD TIER 2

Table 15.4.8-1 (1 of 3)

Sequence of Events for the CEA Ejection

| Power | Time (sec) | Event | Setpoint or Value |
|-------|------------|---|--|
| HFP | 0.00 | Mechanical failure | Maximum clad surface temperature in the hot spot, °C (°F) |
| | 0.03 | Core power reaches variable overpower reactor trip analysis setpoint, % of design power | 127.5 |
| | 0.05 | CEA fully ejected | - |
| | 0.07 | Maximum core power, % of design power | 156.3 |
| | 1.08 | CEAs begin to drop into core | 526.8 (980.3) |
| | 3.30 | Maximum radial average fuel enthalpy in the hot spot, kJ/kg (cal/gm) | 522.1 (124.7) |
| | 3.43 | Maximum clad surface temperature in the hot spot, °C (°F) | 567.2 (1,053.0) |
| 50% | 3.67 | Maximum fuel centerline temperature in the hot spot, °C (°F) | 2,490.2 (4,514.3) |
| | 0.00 | Mechanical failure | Maximum radial average fuel enthalpy in the hot spot, kJ/kg (cal/gm) |
| | 0.03 | Core power reaches variable overpower reactor trip analysis setpoint, % of design power | 75.0 |
| | 0.05 | CEA fully ejected | Maximum radial average fuel enthalpy in the hot spot, kJ/kg (cal/gm) |
| | 0.08 | Maximum core power, % of design power | 515.4 (123.1) |
| | 1.08 | CEAs begin to drop into core | 569.2 (1,056.5) |
| | 3.20 | Maximum clad surface temperature in the hot spot, °C (°F) | 524.1 (975.3) |
| | 3.31 | Maximum radial average fuel enthalpy in the hot spot, kJ/kg (cal/gm) | 504.1 (120.4) |
| | 3.72 | Maximum fuel centerline temperature in the hot spot, °C (°F) | 2,370.9 (4,299.6) |
| | | Maximum clad surface temperature in the hot spot, °C (°F) | 2,423.6 (4,394.5) |

APR1400 DCD TIER 2

Maximum clad surface temperature in the hot spot,
°C (°F)

Table 15.4.8-1 (2 of 3)

| Power | Time (sec) | Event | Maximum radial average fuel enthalpy in the hot spot, kJ/kg (cal/gm) | |
|-------|------------|---|---|-------------------|
| 20% | 0.00 | Mechanical failure of CEDM | | |
| | 0.04 | Core power reaches variable overpower reactor trip analysis setpoint, % of design power | 45.0 | |
| | 0.05 | CEA fully ejected | - | |
| | 0.10 | Maximum core power, % of design power | 140.3 | |
| | 2.32 | 1.09 CEAs begin to drop into core | - | 348.2 (658.7) |
| | 3.26 | 3.30 Maximum radial average fuel enthalpy in the hot spot, kJ/kg (cal/gm) | 473.5 (113.1) | 500.4 (119.6) |
| | 3.87 | 3.62 Maximum clad surface temperature in the hot spot, °C (°F) | 586.7 (1,088.1) | 2,388.8 (4,331.8) |
| | | 3.67 Maximum fuel centerline temperature in the hot spot, °C (°F) | 2,331.3 (4,228.4) | |
| HZIP | 0.00 | Mechanical failure of CEDM causes CEA to eject | - | |
| | 0.21 | Core power reaches variable overpower reactor trip analysis setpoint, % of design power | 25.0 | |
| | 0.05 | CEA fully ejected | - | |
| | 0.32 | Maximum core power, % of design power | 141.3 | |
| | 2.61 | 1.26 CEAs begin to drop into core | - | (656.4) |
| | 3.09 | 2.48 Maximum clad surface temperature in the hot spot, °C (°F) | 346.9 (656.5) | 319.1 (76.2) |
| | 3.74 | 3.04 Maximum radial average fuel enthalpy in the hot spot, kJ/kg (cal/gm) | 314.8 (75.2) | 1,526.5 (2,779.7) |
| | | 3.67 Maximum fuel centerline temperature in the hot spot, °C (°F) | 1,501.5 (2,734.7) | |

APR1400 DCD TIER 2

Table 15.4.8-1 (3 of 3)

| Time (sec) | Event (System Response at HFP) | Setpoint or Value |
|------------|---|-------------------|
| 0.00 | Mechanical failure of CEDM causes CEA to eject | - |
| 0.04 | Core power reaches variable overpower reactor trip analysis setpoint, % of design power | 127.5 |
| 0.05 | CEA fully ejected | - |
| 0.16 | Maximum core power, % of design power | 151.7 |
| 0.49 | Reactor trip signal | - |
| 0.59 | Reactor trip breakers open | - |
| 1.09 | CEAs begin to drop into core | - |
| 3.10 | Maximum RCS pressure, kg/cm ² A (psia) | 177.5 (2,524.7) |
| 3.59 | Turbine trip/generator trip/loss of offsite power | - |
| 7.20 | Main steam safety valves open, kg/cm ² A (psia) | 86.9 (1,235.7) |
| 11.50 | Maximum steam generator pressure, kg/cm ² A (psia) | 90.1 (1,281.9) |
| 1,800.00 | Operator begins plant cooldown | - |

APR1400 DCD TIER 2

Table 15.4.8-2

Assumptions and Initial Conditions for the CEA Ejection Analysis

| Parameter | Cases | | | |
|---|----------------|----------------|----------------|----------------|
| | HZP | 20% | 50% | HFP |
| Core power level, MWt | 1.00 | 796.60 | 1991.50 | 4,062.66 |
| Delayed neutron fraction, β | 0.00412 | 0.00412 | 0.00412 | 0.00412 |
| Moderator temperature coefficient, $10^{-4} \Delta\rho / ^\circ\text{C}$ ($10^{-4} \Delta\rho / ^\circ\text{F}$) | 0.90 (0.50) | 0.72 (0.40) | 0.45 (0.25) | 0.00 (0.00) |
| Doppler temperature coefficient, $\Delta\rho / \sqrt{\text{K}}$ | -0.00130 | -0.00130 | -0.00130 | -0.00130 |
| Ejected CEA worth, $10^{-2} \Delta\rho$ | 0.4469 | 0.3711 | 0.2578 | 0.1459 |
| Post-ejected 3-d power peaking factor | 11.49 | 10.79 | 6.49 | 4.32 |
| Ratio of the 3-d post-ejected to pre-ejected power peaking factor | 3.93 | 3.90 | 3.49 | 3.17 |
| Total CEA worth available for insertion on reactor trip, $10^{-2} \Delta\rho$ | -5.0 | -5.0 | -5.0 | -5.0 |
| Postulated CEA Ejection time, sec | 0.05 | 0.05 | 0.05 | 0.05 |
| Core inlet coolant temperature, $^\circ\text{C}$ ($^\circ\text{F}$) | 295 (563) | 295 (563) | 295 (563) | 295 (563) |
| Core mass flow rate, 10^6 kg/hr (10^6 lbm/hr) | 69.64 (153.52) | 69.64 (153.52) | 69.64 (153.52) | 69.64 (153.52) |
| Pressurizer pressure, $\text{kg/cm}^2\text{A}$ (psia) | 152.9 (2,175) | 152.9 (2,175) | 152.9 (2,175) | 152.9 (2,175) |

APR1400 I & II

Table

Results of the CEA Ejection Analysis

| Parameter | Power | | | |
|--|--|--|--|--|
| | HZP | 20% | 50% | HFP |
| Maximum radial average fuel enthalpy at hot spot, kJ/kg (cal/gm) | 314.8 (75.2) | 473.5 (113.1) | 504.1 (120.4) | 522.1 (124.7) |
| Maximum fuel centerline temperature, °C (°F) | 1,501.5 (2,734.7) | 2,331.3 (4,228.4) | 2,370.9 (4,299.6) | 2,490.2 (4,514.3) |
| Maximum prompt enthalpy rise, ⁽¹⁾ kJ/kg (cal/gm) | 90.9 (21.7) | 138.6 (33.1) | 160.8 (38.4) | 118.9 (28.4) |
| Maximum cladding surface temperature, °C (°F) | 347.0 (656.6) | 586.7 (1,088.1) | 569.2 (1,056.5) | 567.2 (1,053.0) |

(1) Maximum energy deposition during the prompt power pulse width. For HFP and 50 percent power case, the prompt enthalpy rise is the value at 1.0 second.

346.9
(656.4)

348.2
(658.7)

524.1
(975.3)

526.8
(980.3)

139.0
(33.2)

162.0
(38.7)

122.3
(29.2)

APR1400 DCD TIER 2

Table 15.4.8-4 (1 of 3)

Parameters Used in Evaluating the Radiological Consequences of the CEA Ejection

| Parameter | Value |
|--|--|
| Source Terms | |
| Reactor Core Power Level | 4,062.66 MWt |
| Percent of Fuel Assumed to Undergo DNB | 10 % |
| Initial RCS Iodine Specific Activity | 3.7×10^4 Bq/g (1.0 μ Ci/g) DE I-131 |
| Initial RCS Noble Gases Specific Activity | 2.15×10^7 Bq/g (580 μ Ci/g) DE Xe-133 |
| Initial RCS Alkali Metal Specific Activity | RCS concentrations with 1% fuel defect |
| Initial Secondary Liquid Iodine Specific Activity | 3.7×10^3 Bq/g (0.1 μ Ci/g) DE I-131 |
| Radial Peaking Factor | 1.80 |
| RCS Initial Mass | 267,620 kg (590,000 lbm) |
| Containment Leakage Transport Model | |
| Containment Net Free Volume | 8.86×10^4 m ³ (3.13×10^6 ft ³) |
| Reactor Coolant Mass Released to Containment | 2.68×10^5 kg (5.90×10^5 lbm) |
| Credit for Radioactive Decay during Hold up in Containment In Transit to Dose Points | Applicable Not Applicable |
| Iodine Chemical Form Aerosol (CsI) Elemental Organic | 95.0 % 4.85 % 0.15 % |
| Containment Aerosol Natural Deposition Removal | Powers model with a 10-percentile probability |
| Containment Leak Rate | 0.1 %/day (0 ~ 24 hr) 0.05 %/day (24 ~ 720 hr) |

APR1400 DCD TIER 2

Table 15.4.8-4 (2 of 3)

| Parameter | Value |
|---|---|
| Secondary System Release Transport Model | |
| Primary-To-Secondary Leak Rate through SGs | 2.27 L/min (0.6 gpm) through all SGs 1.14 L/min (0.3 gpm) through any one SG |
| Steam Generator Liquid Mass | 104,326 kg (230,000 lbm) |
| Primary-To-Secondary Leak Duration | 8 hr |
| Steam Mass Released from Both Intact SGs to Environment | |
| 0 ~ 0.5 hr | 118,660 kg (261,600 lbm) |
| 0.5 ~ 2 hr | 650,737 kg (1,434,630 lbm) |
| 2 ~ 8 hr | 624,538 kg (1,376,870 lbm) |
| Primary-To-Secondary Leak Flashing Fraction | 15.0 % average for 1,800 sec after onset of accident |
| SG Liquid Iodine Partition Coefficient | 100 |
| SG Liquid Alkali Metal Partition Coefficient | 200 |
| Chemical Form of Iodine Released from SG | |
| Elemental | 97 % |
| Organic Iodine | 3 % |

APR1400 DCD TIER 2

Table 15.4.8-4 (3 of 3)

| Parameter | Value |
|---|---|
| MCR and TSC Model Parameters | |
| Envelope Volume | 5,663 m ³ (200,000 ft ³) |
| Normal Ventilation Flow Rate (unfiltered) | 105 m ³ /min (3,700 cfm) |
| Emergency Ventilation Makeup Rate (filtered) | 105 m ³ /min (3,700 cfm) |
| Emergency Ventilation Recirculation Flow Rate (filtered) | 122 m ³ /min (4,300 cfm) |
| Emergency HVAC Delay Time | 5 min |
| Emergency Ventilation Charcoal Filter Efficiency (elemental and organic iodine removal) | 99 % |
| Emergency Ventilation HEPA Filter Efficiency (particulate removal) | 99 % |
| Unfiltered Inleakage | 2.83 m ³ /min (100 cfm) |
| Occupancy Factors | |
| 0 ~ 24 hr | 100 % |
| 24 ~ 96 hr | 60 % |
| 96 ~ 720 hr | 40 % |
| Onsite χ/Q_s | See Tables 2.3.2 ~ 2.3.12 |
| Offsite Model Parameters | |
| χ/Q_s | See Table 2.3-1 |
| Breathing Rate | See Table 15A-12 |
| Dose Conversion Factors | See Table 15A-11 |

APR1400 DCD TIER 2

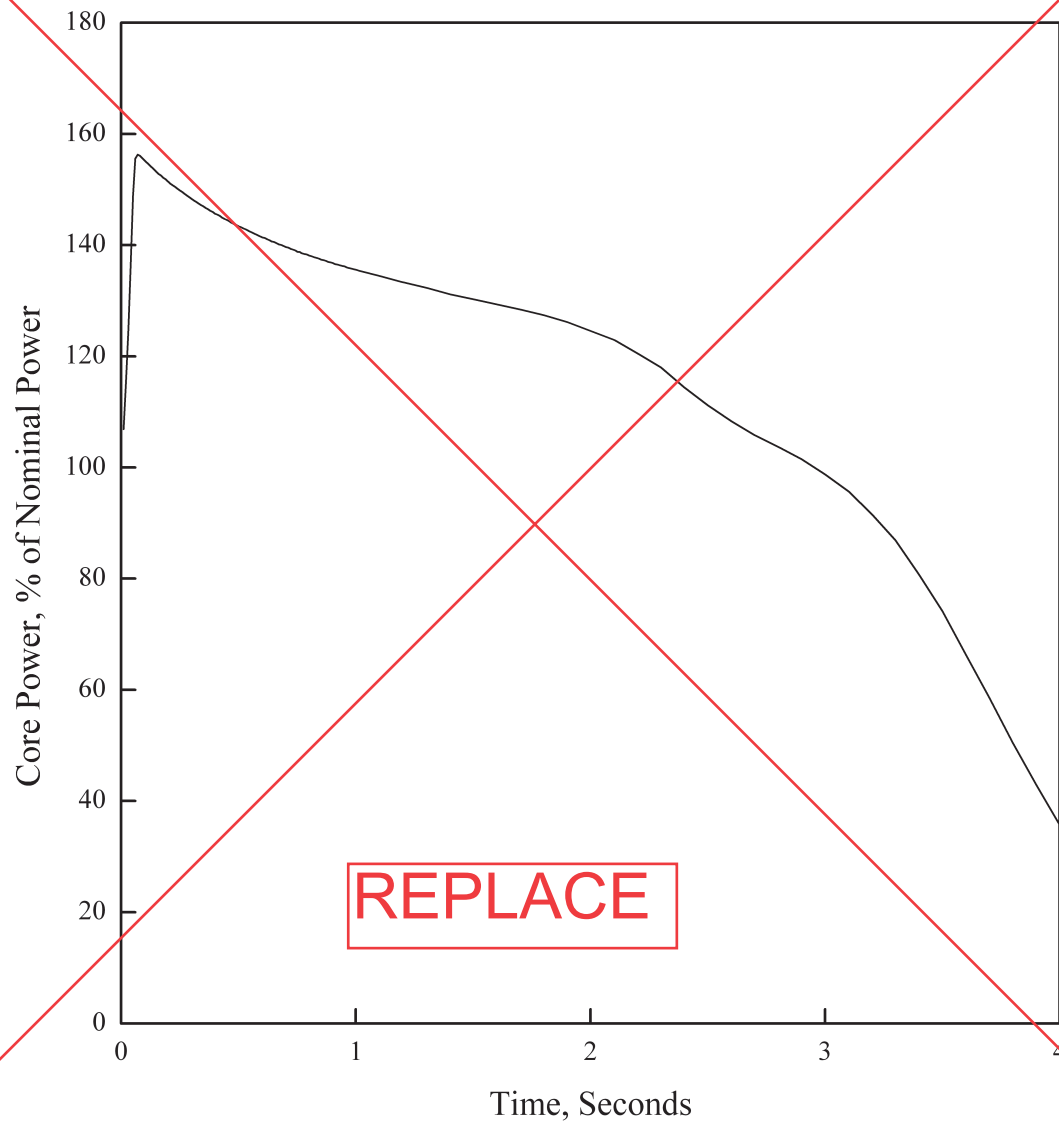
Table 15.4.8-5

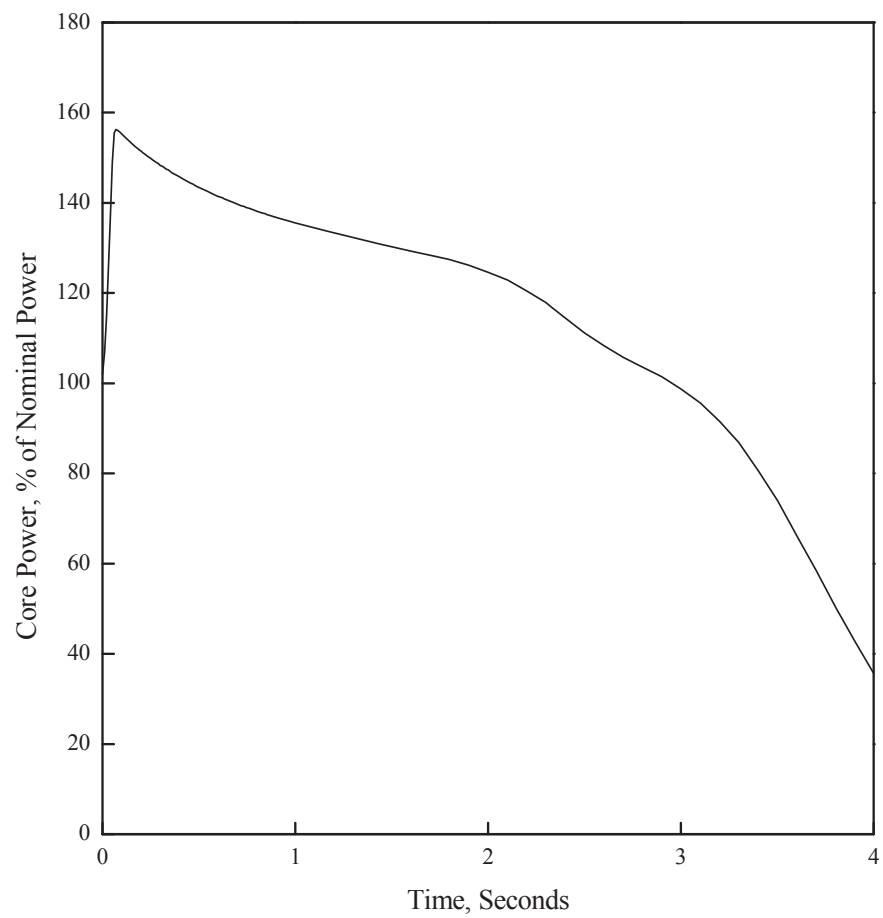
Radiological Consequences of the CEA EjectionContainment Leakage Case

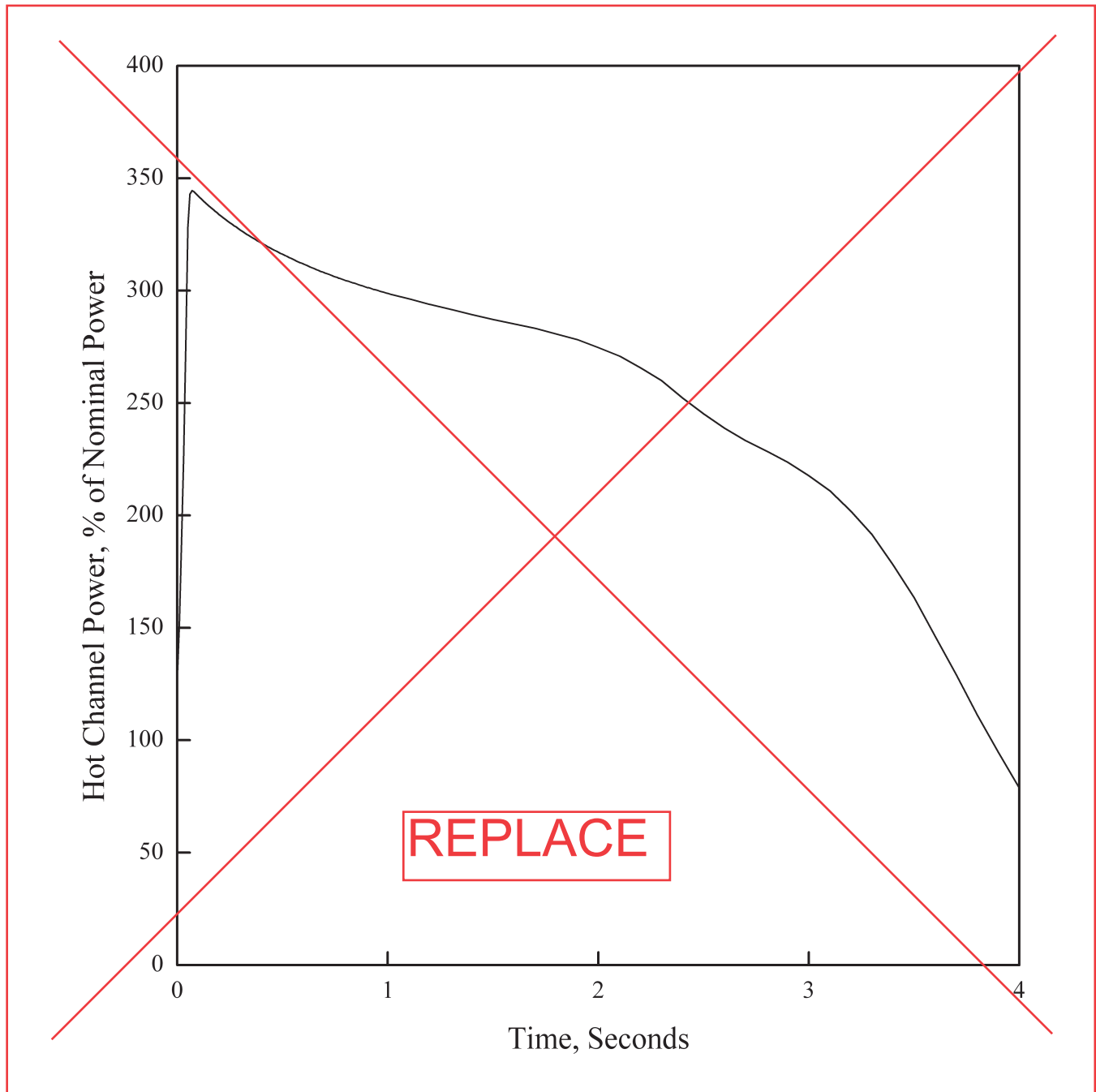
| Post-CEA Ejection Activity Release Path | TEDE Dose (mSv) | | |
|--|-----------------|----------|----------|
| | MCR and TSC | EAB | LPZ |
| Containment Leakage | 1.62E+01 | 5.86E+01 | 5.55E+01 |
| External Cloud | 6.22E+00 | 0.00E+00 | 0.00E+00 |
| Emergency Ventilation Filter Shine | 1.29E+01 | 0.00E+00 | 0.00E+00 |
| Total | 3.53E+01 | 5.86E+01 | 5.55E+01 |
| Allowable TEDE Limit | 5.00E+01 | 6.30E+01 | 6.30E+01 |

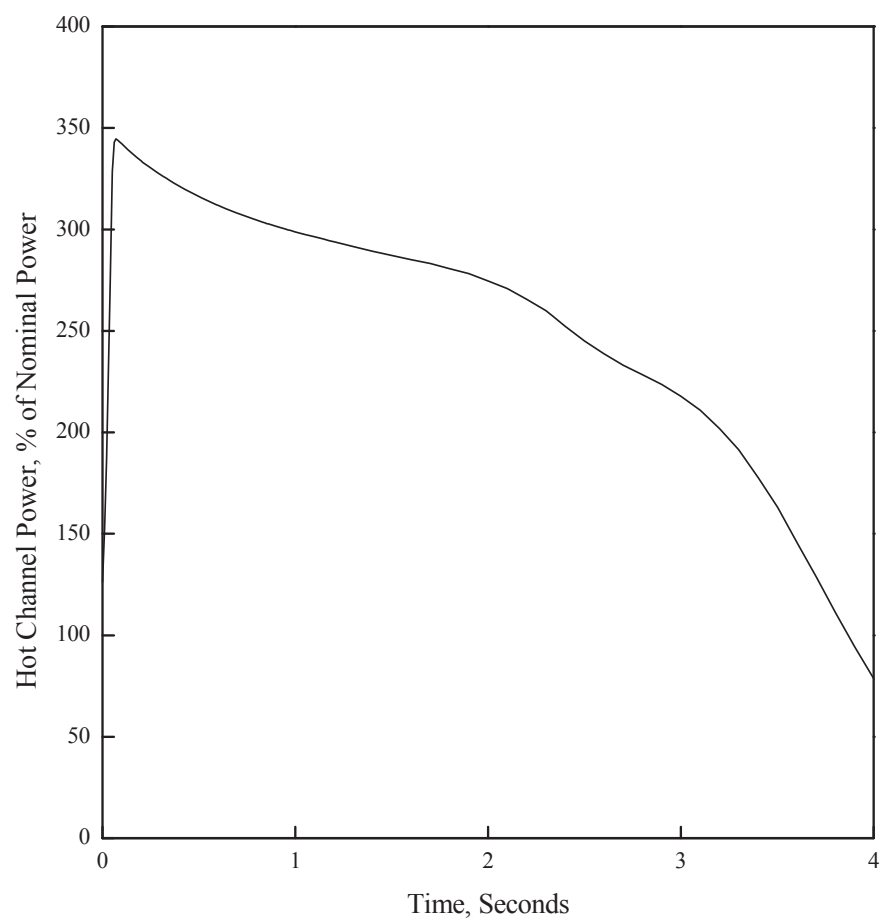
Steam System Release Case

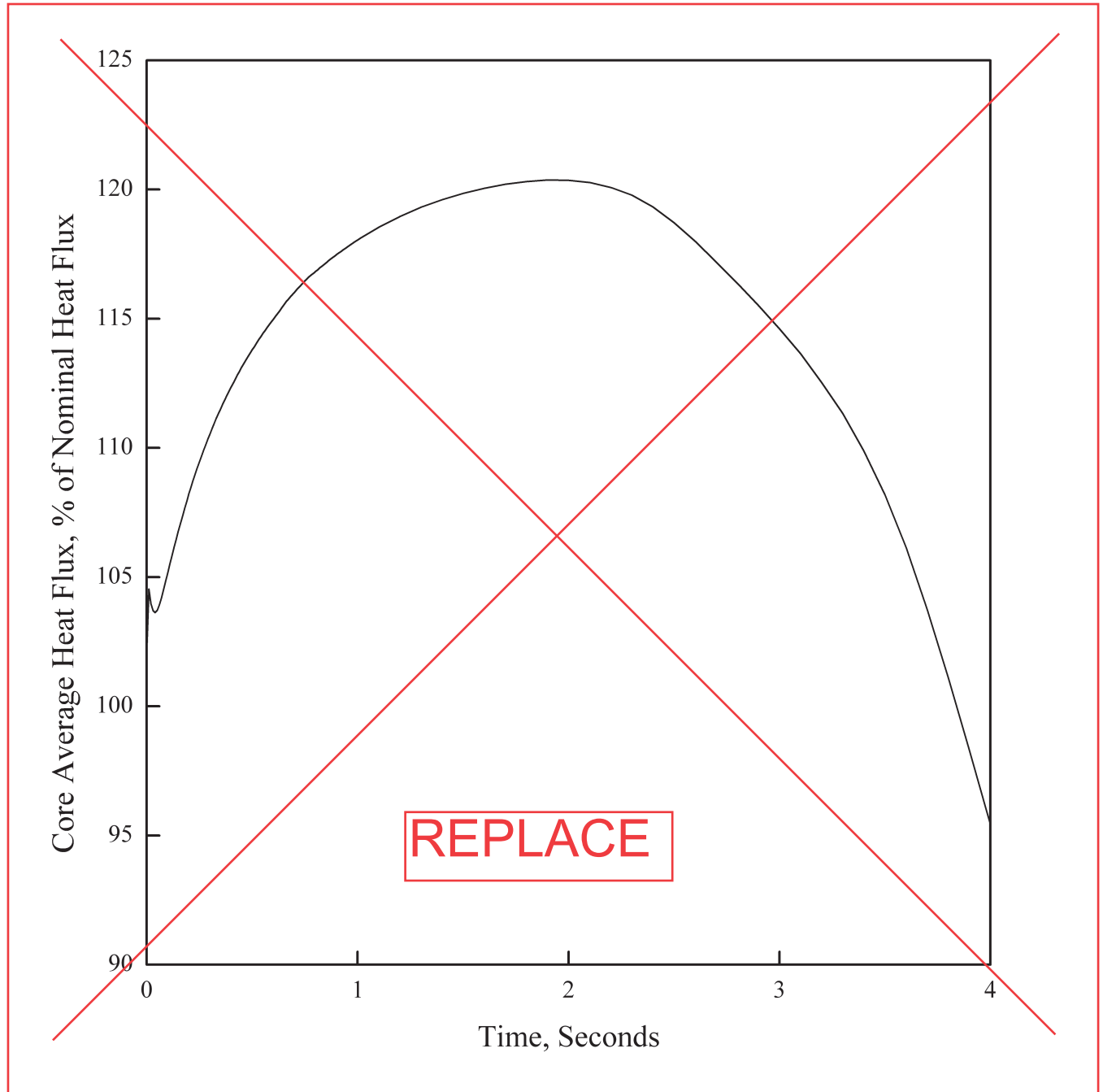
| Post-CEA Ejection Activity Release Path | TEDE Dose (mSv) | | |
|--|-----------------|----------|----------|
| | MCR and TSC | EAB | LPZ |
| P-T-S Iodine Release | 2.60E+00 | 1.46E+01 | 1.01E+01 |
| P-T-S Noble Gas Release | 6.55E+00 | 2.04E+01 | 8.79E+00 |
| P-T-S Alkali Metal Release | 8.32E-01 | 4.92E+00 | 2.90E+00 |
| Secondary Liquid Iodine Release | 1.83E-02 | 1.22E-01 | 4.65E-02 |
| External Cloud | 6.22E+00 | 0.00E+00 | 0.00E+00 |
| Emergency Ventilation Filter Shine | 1.29E+01 | 0.00E+00 | 0.00E+00 |
| Total | 2.91E+01 | 4.00E+01 | 2.18E+01 |
| Allowable TEDE Limit | 5.00E+01 | 6.30E+01 | 6.30E+01 |

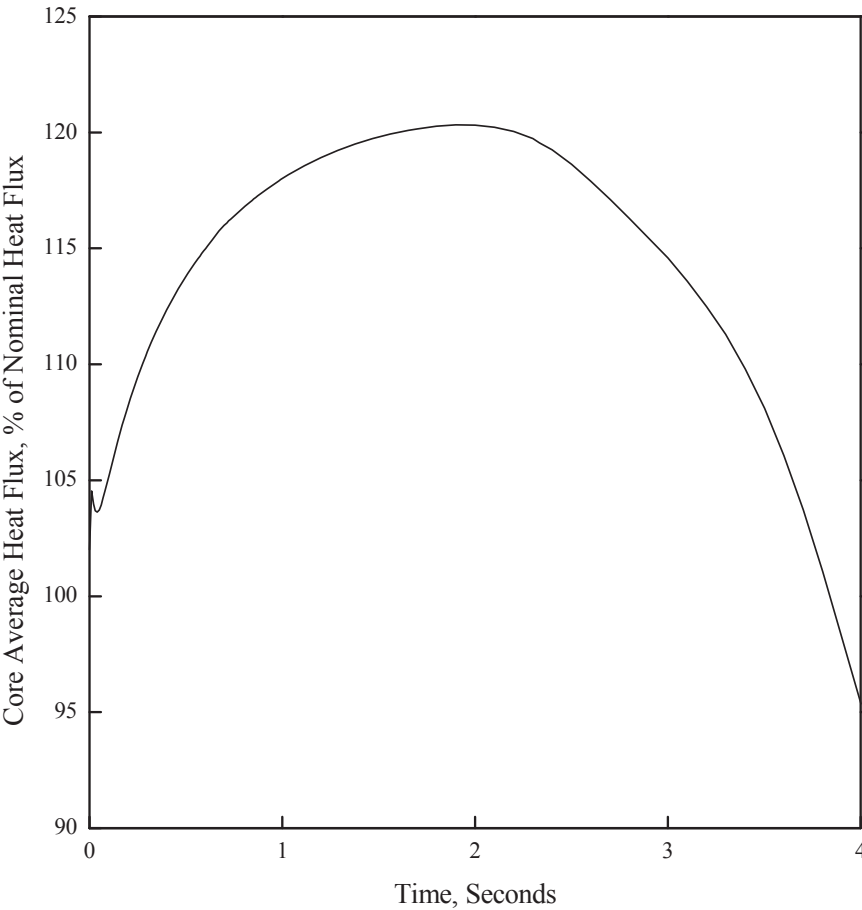
APR1400 DCD TIER 2**Figure 15.4.8-1 CEA Ejection: Core Power vs. Time (HFP)**

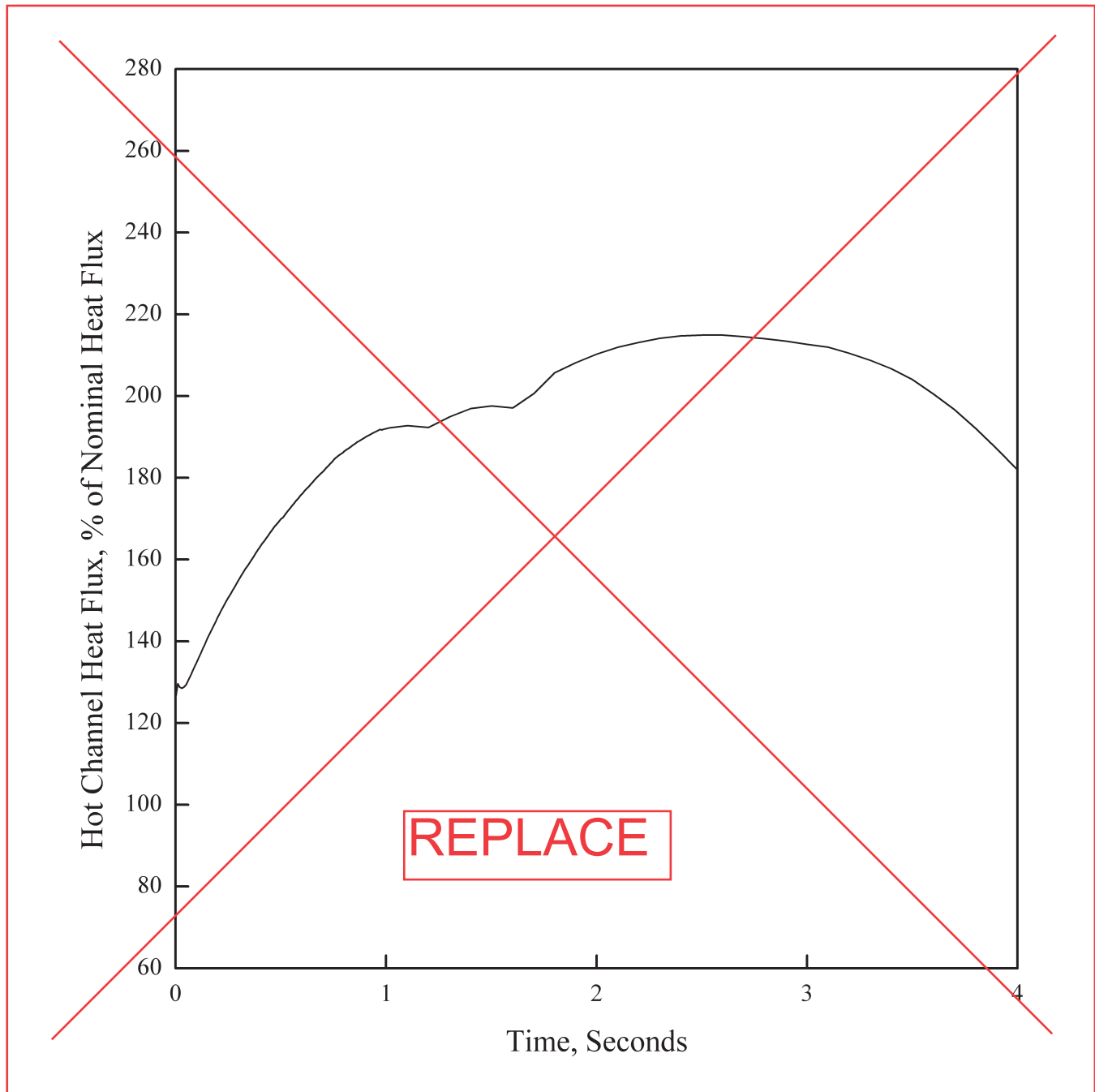


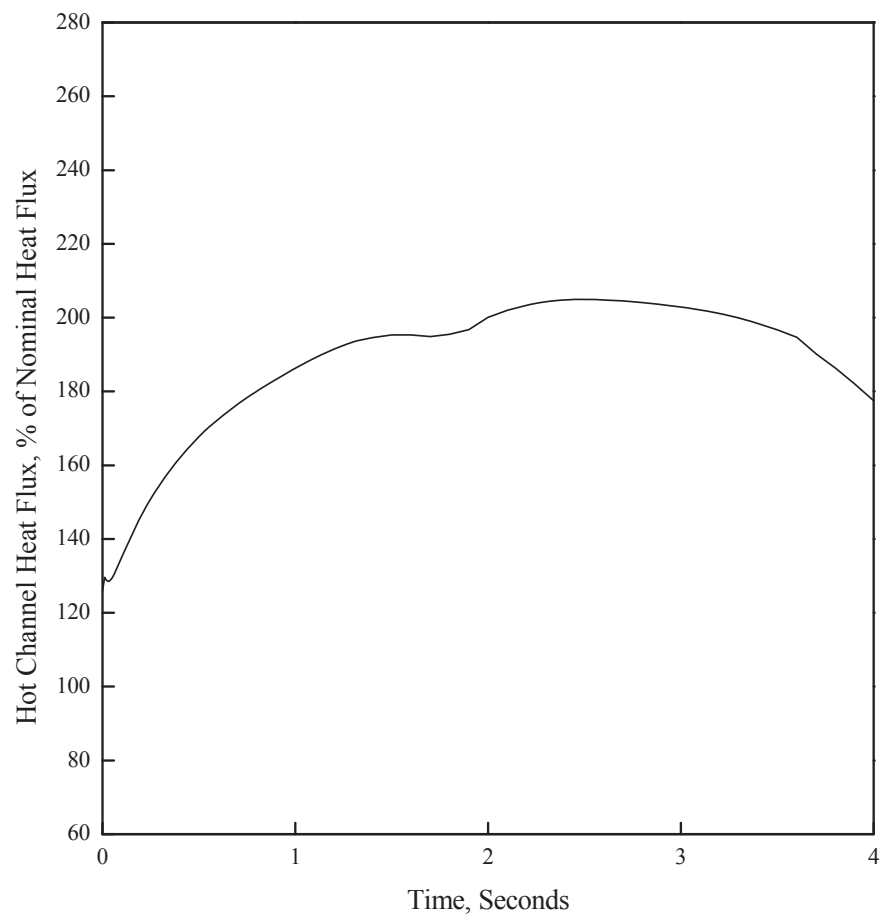
APR1400 DCD TIER 2**Figure 15.4.8-2 CEA Ejection: Hot Channel Power vs. Time (HFP)**



APR1400 DCD TIER 2**Figure 15.4.8-3 CEA Ejection: Core Average Heat Flux vs. Time (HFP)**



APR1400 DCD TIER 2**Figure 15.4.8-4 CEA Ejection: Hot Channel Heat Flux vs. Time (HFP)**



APR1400 DCD TIER 2

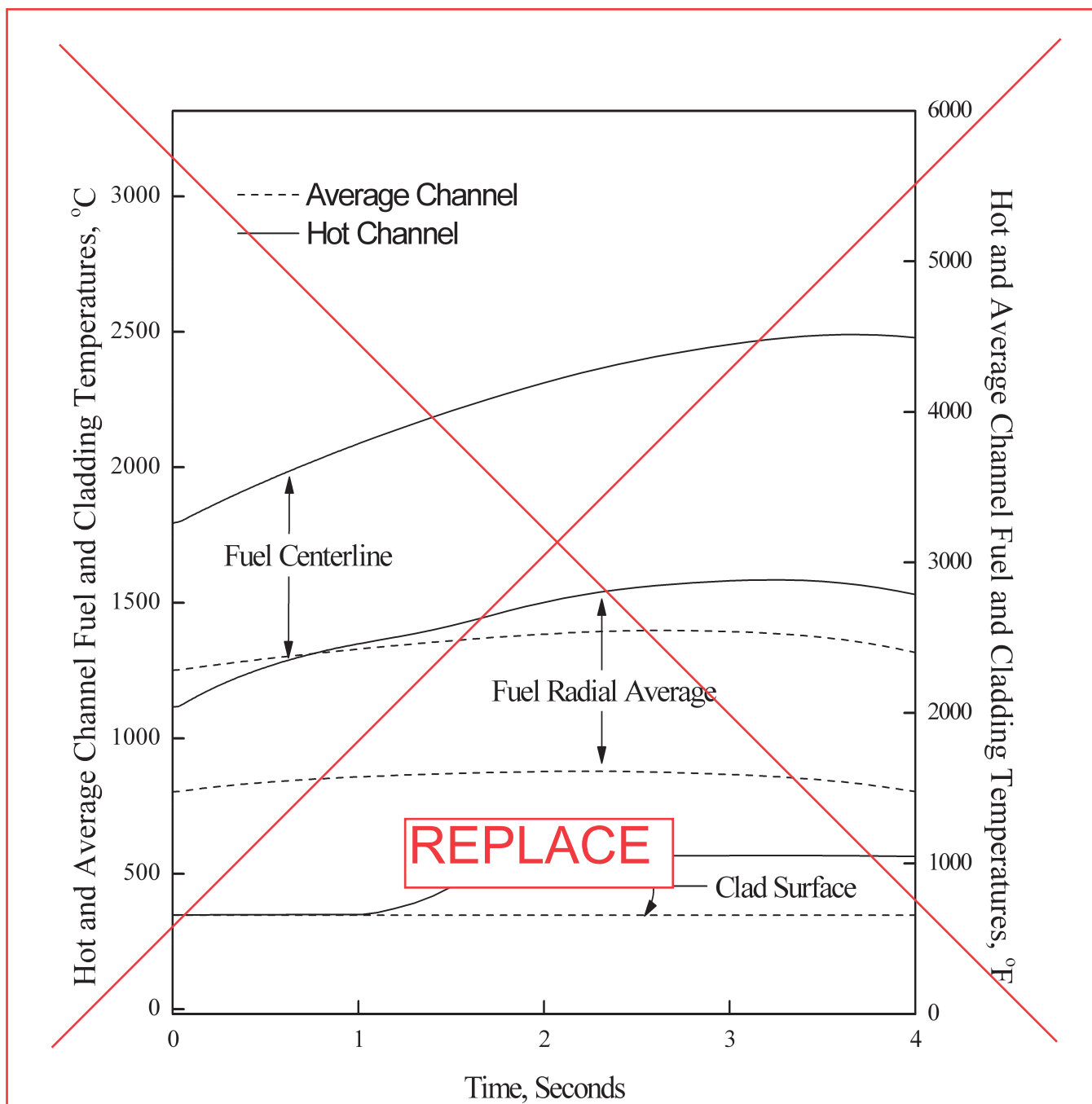


Figure 15.4.8-5 CEA Ejection: Hot and Average Channel Fuel and Cladding Temperatures vs. Time (HFP)

APR1400 DCD TIER 2

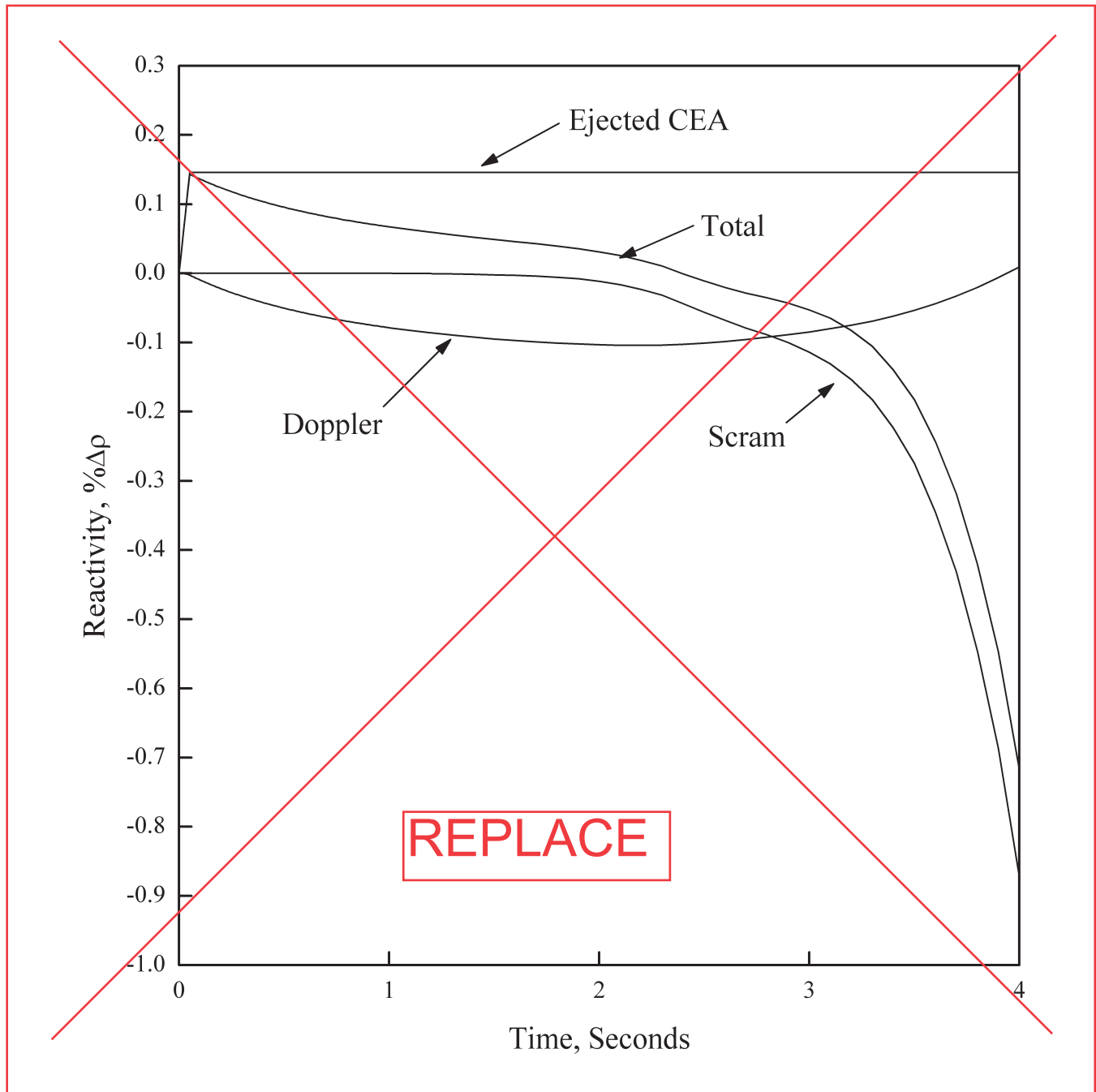
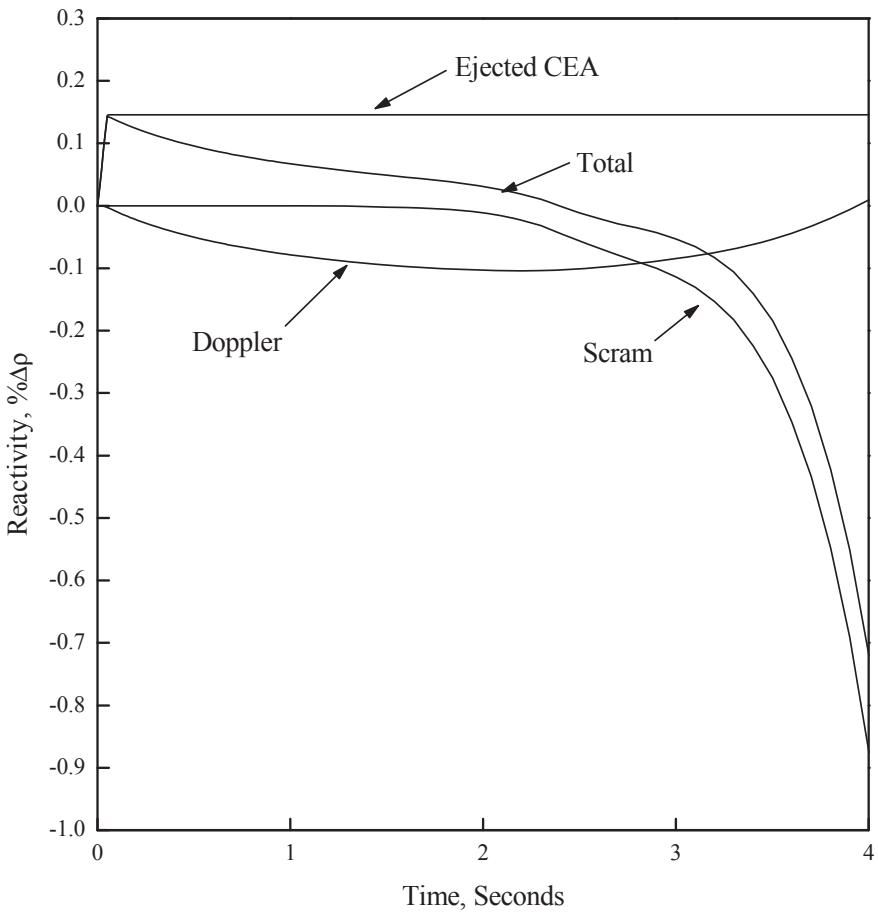
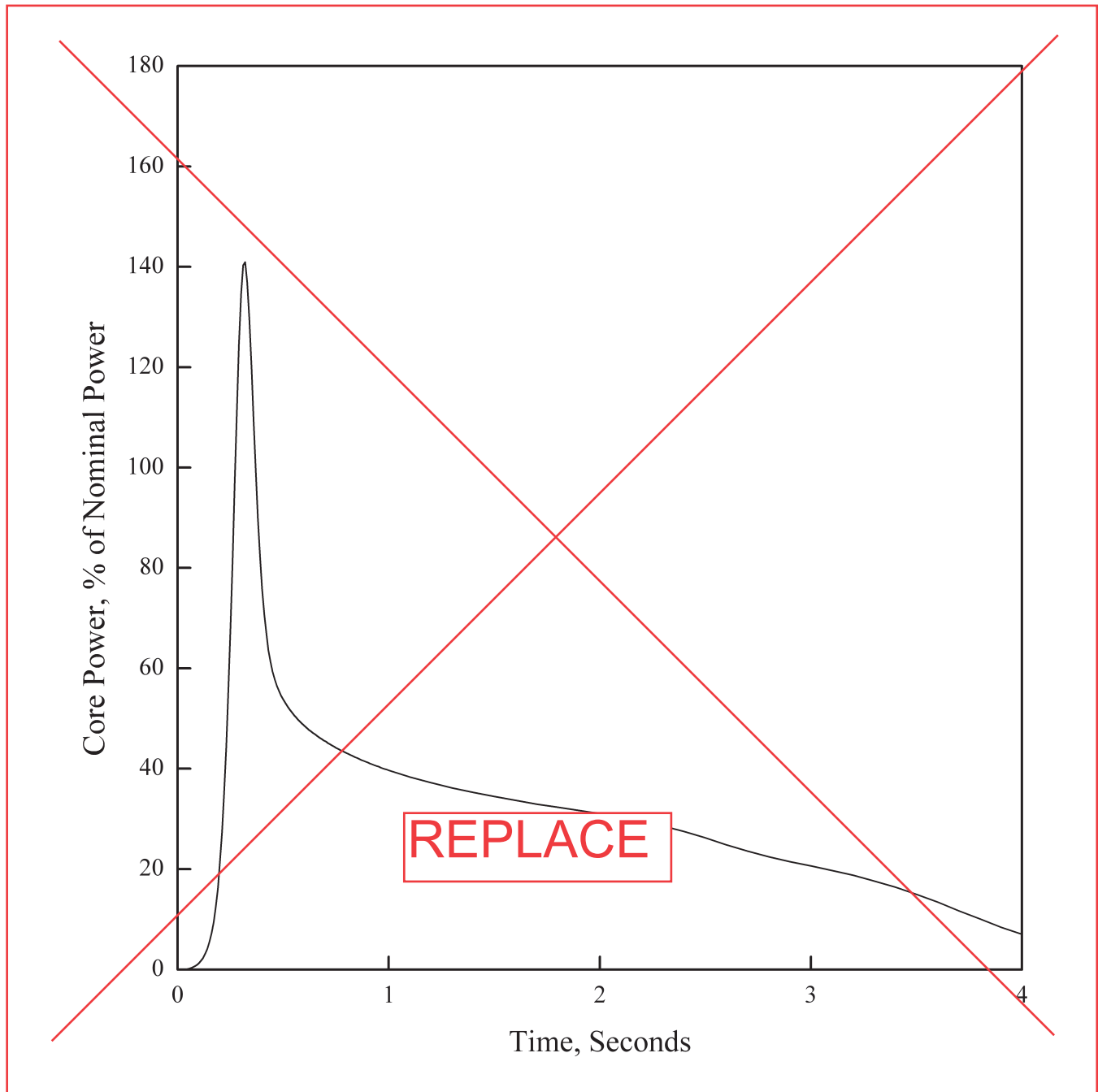
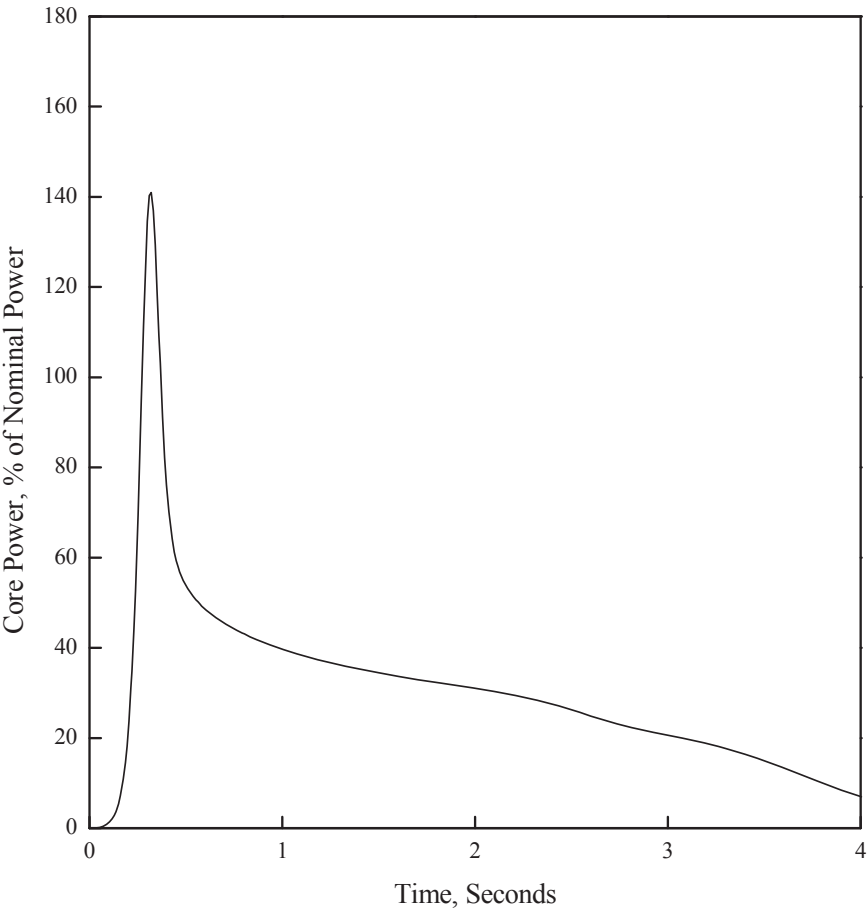
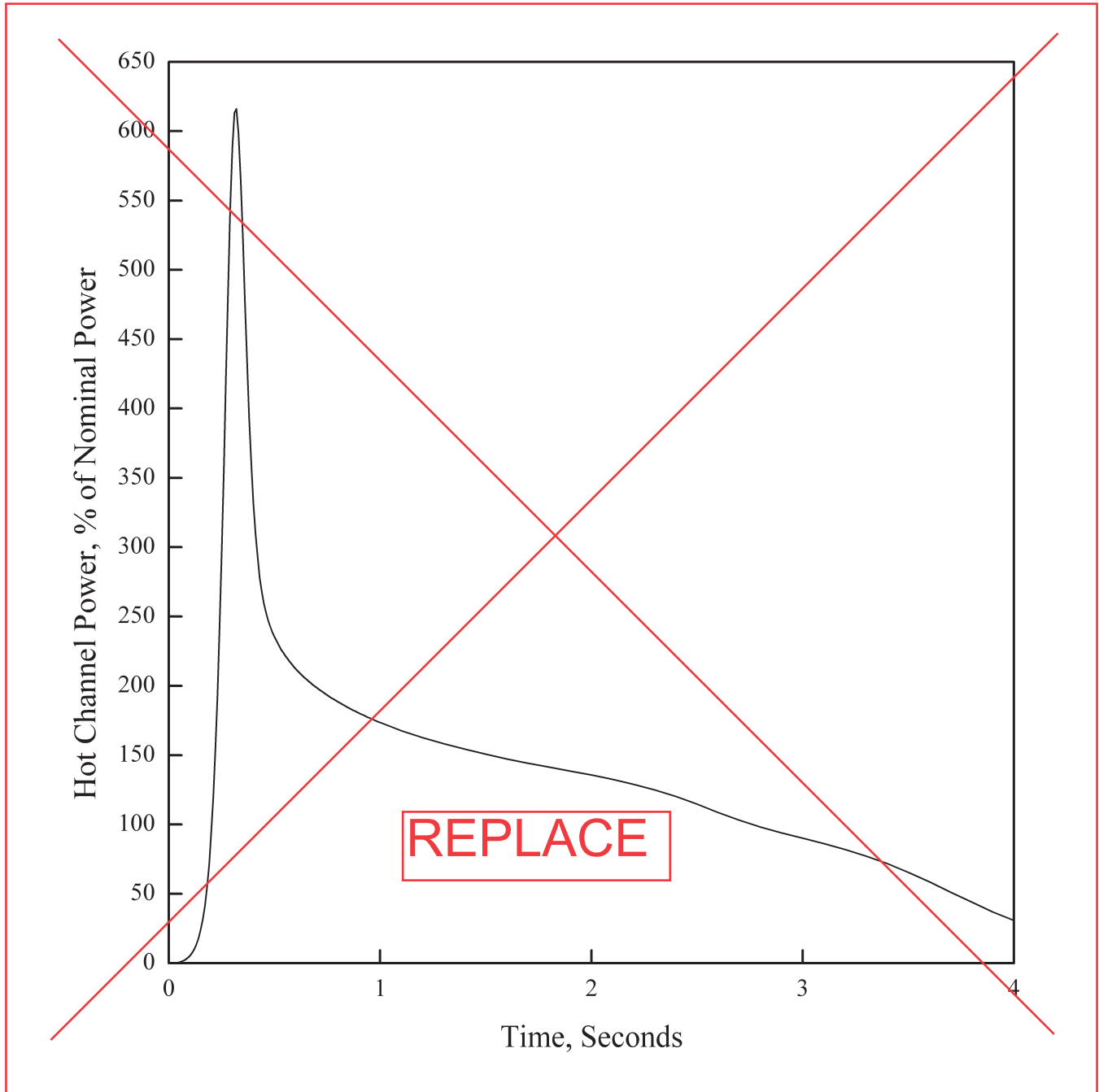


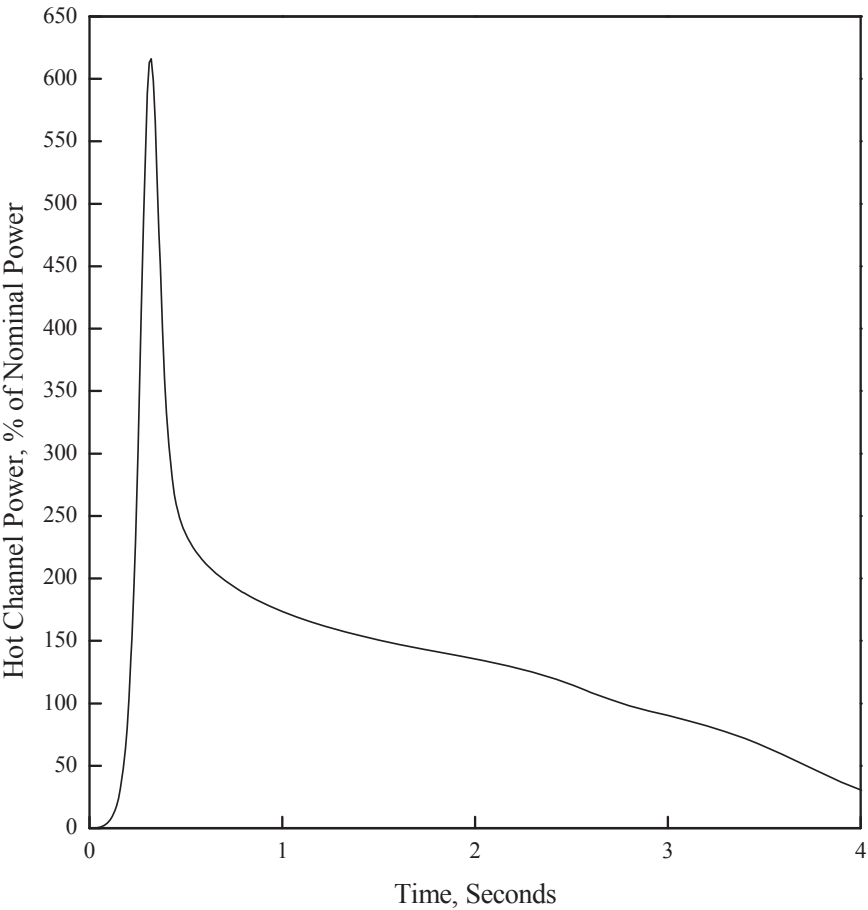
Figure 15.4.8-6 CEA Ejection: Reactivity vs. Time (HFP)

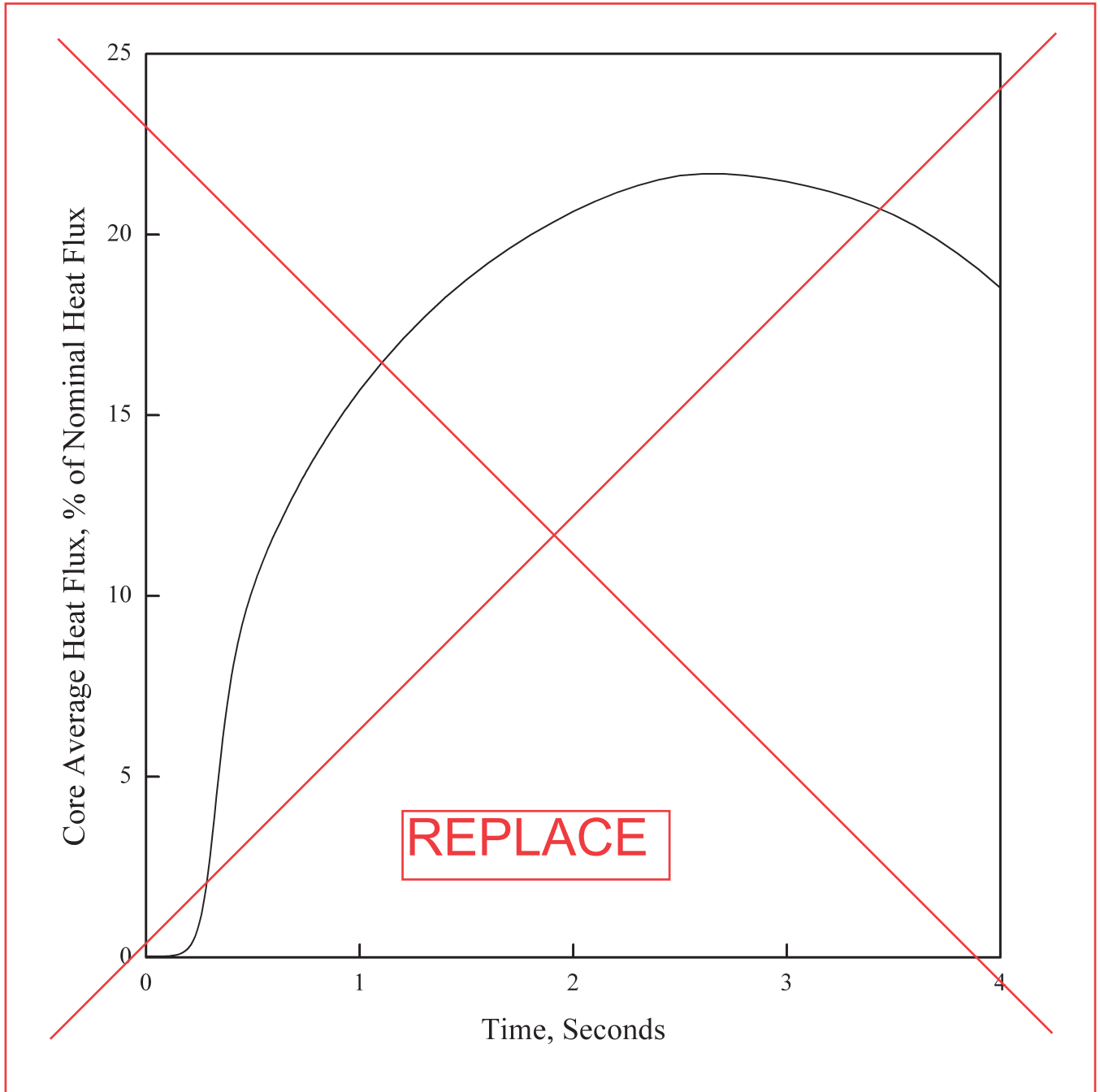


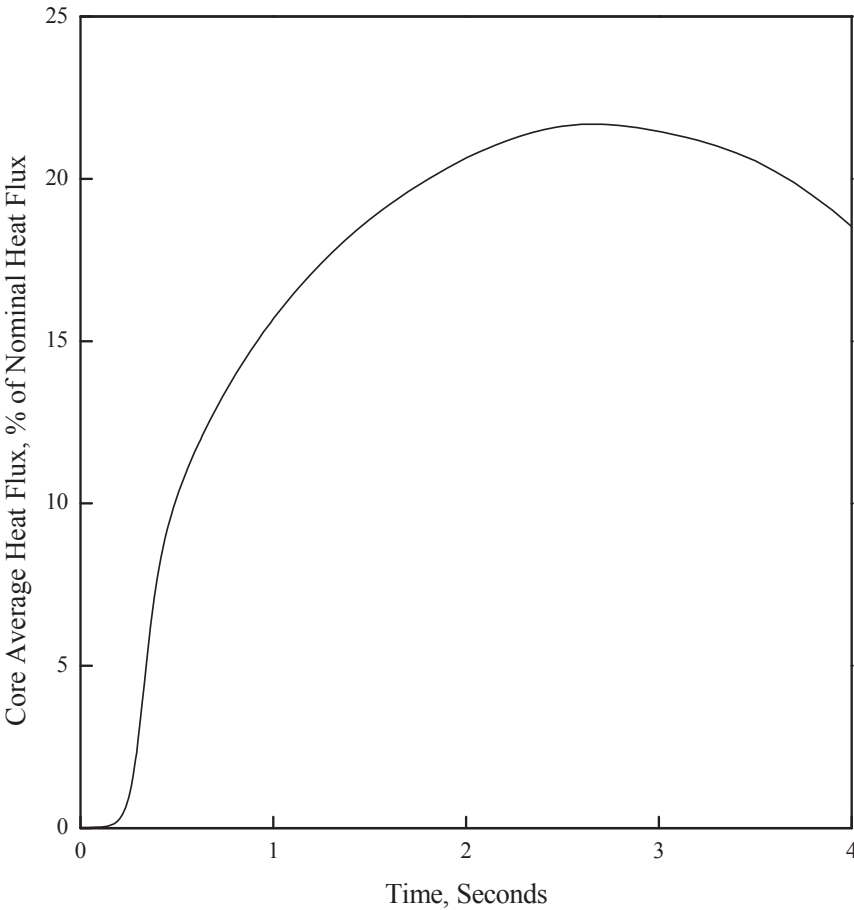
APR1400 DCD TIER 2**Figure 15.4.8-7 CEA Ejection: Core Power vs. Time (HYP)**

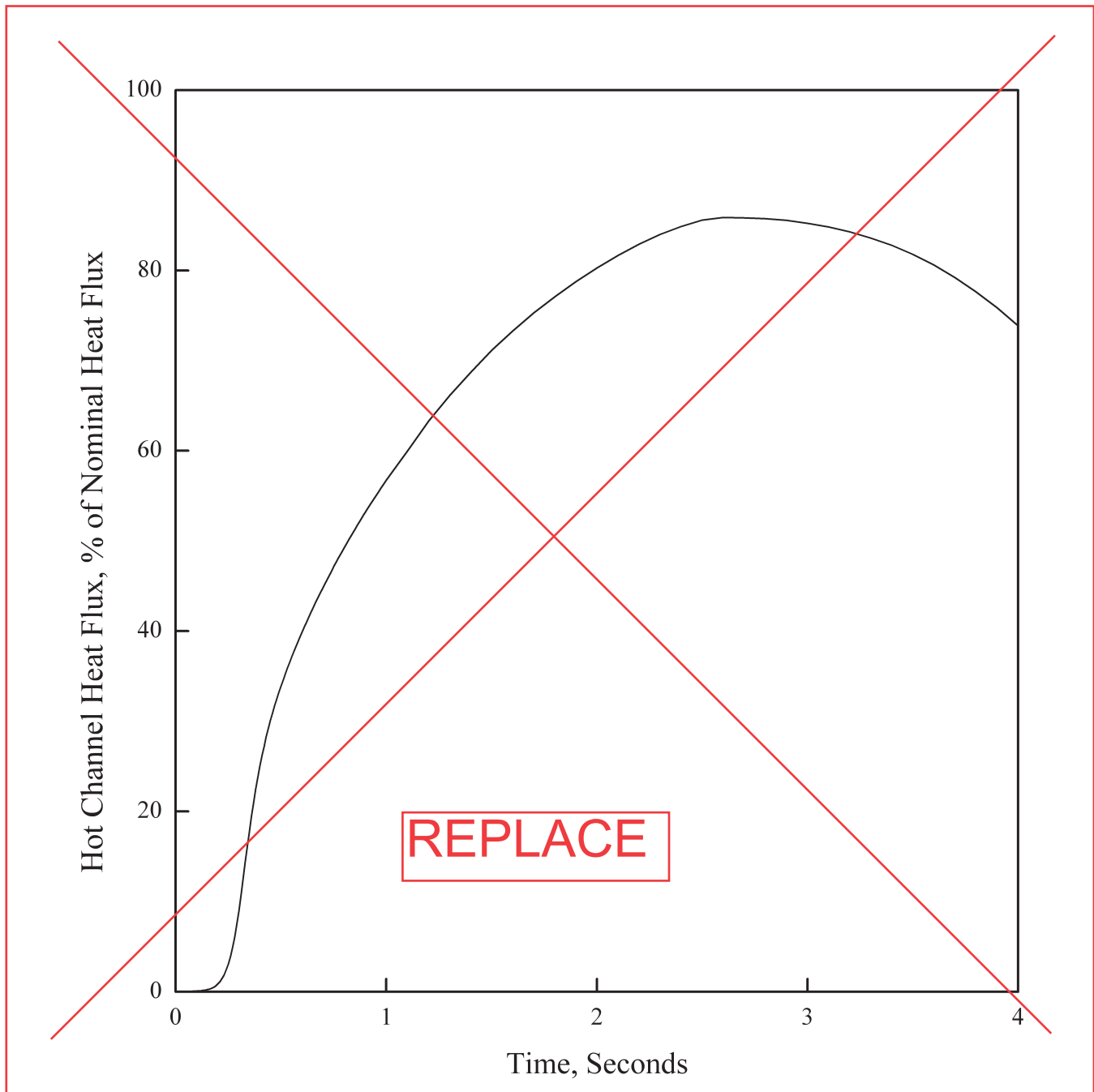


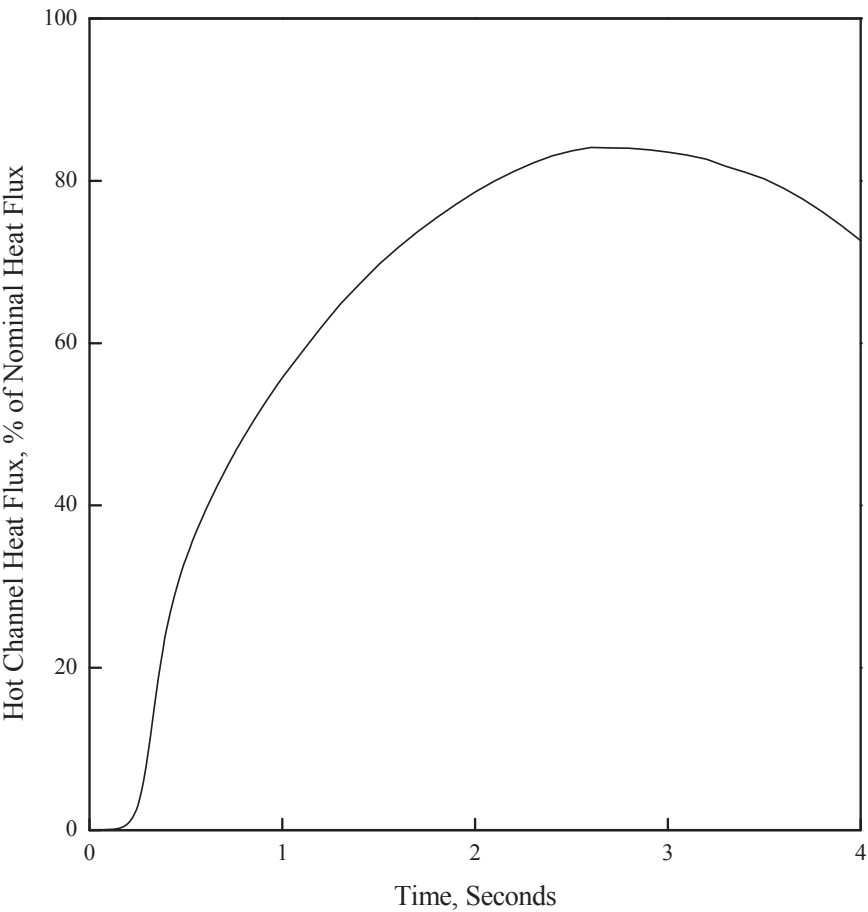
APR1400 DCD TIER 2**Figure 15.4.8-8 CEA Ejection: Hot Channel Power vs. Time (HZP)**



APR1400 DCD TIER 2**Figure 15.4.8-9 CEA Ejection: Core Average Heat Flux vs. Time (HZP)**



APR1400 DCD TIER 2**Figure 15.4.8-10 CEA Ejection: Hot Channel Heat Flux vs. Time (HWP)**



APR1400 DCD TIER 2

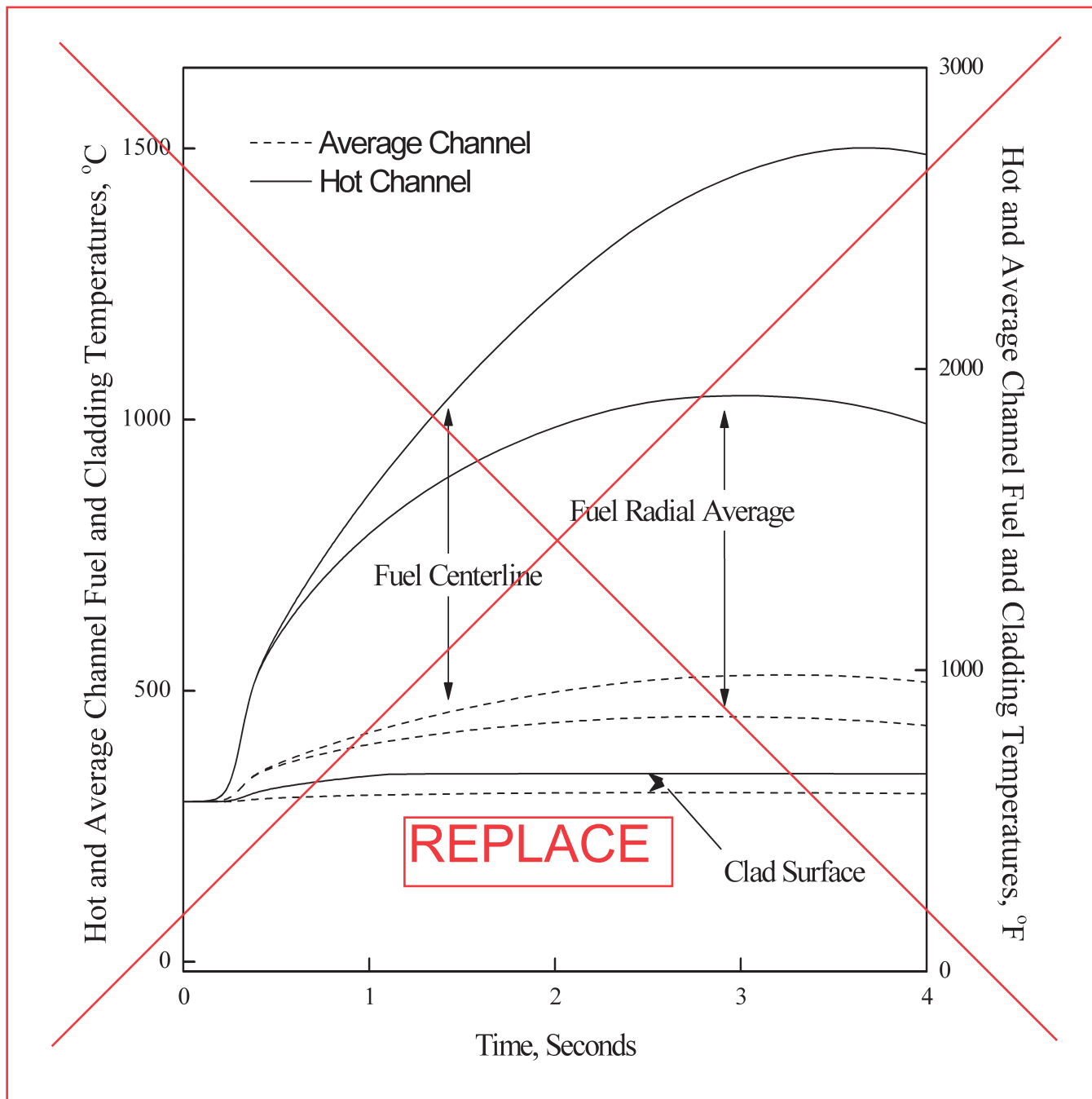
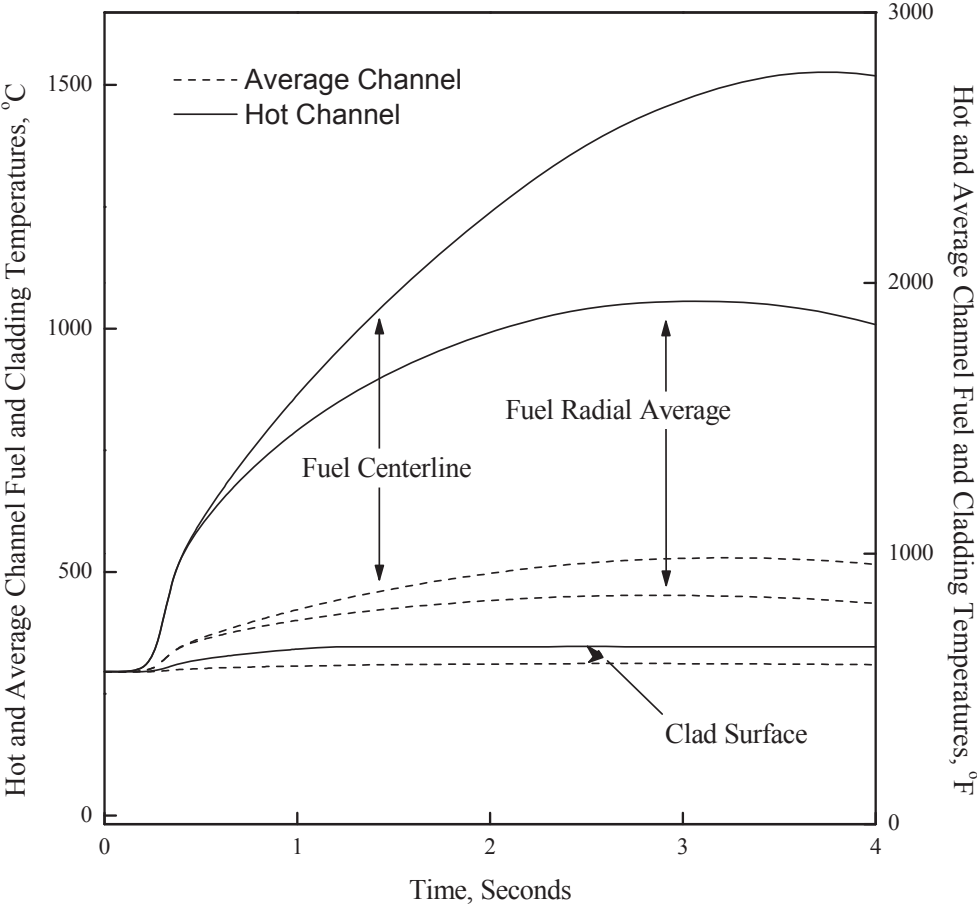


Figure 15.4.8-11 CEA Ejection: Hot and Average Channel Fuel and Cladding Temperatures vs. Time (HZP)



APR1400 DCD TIER 2

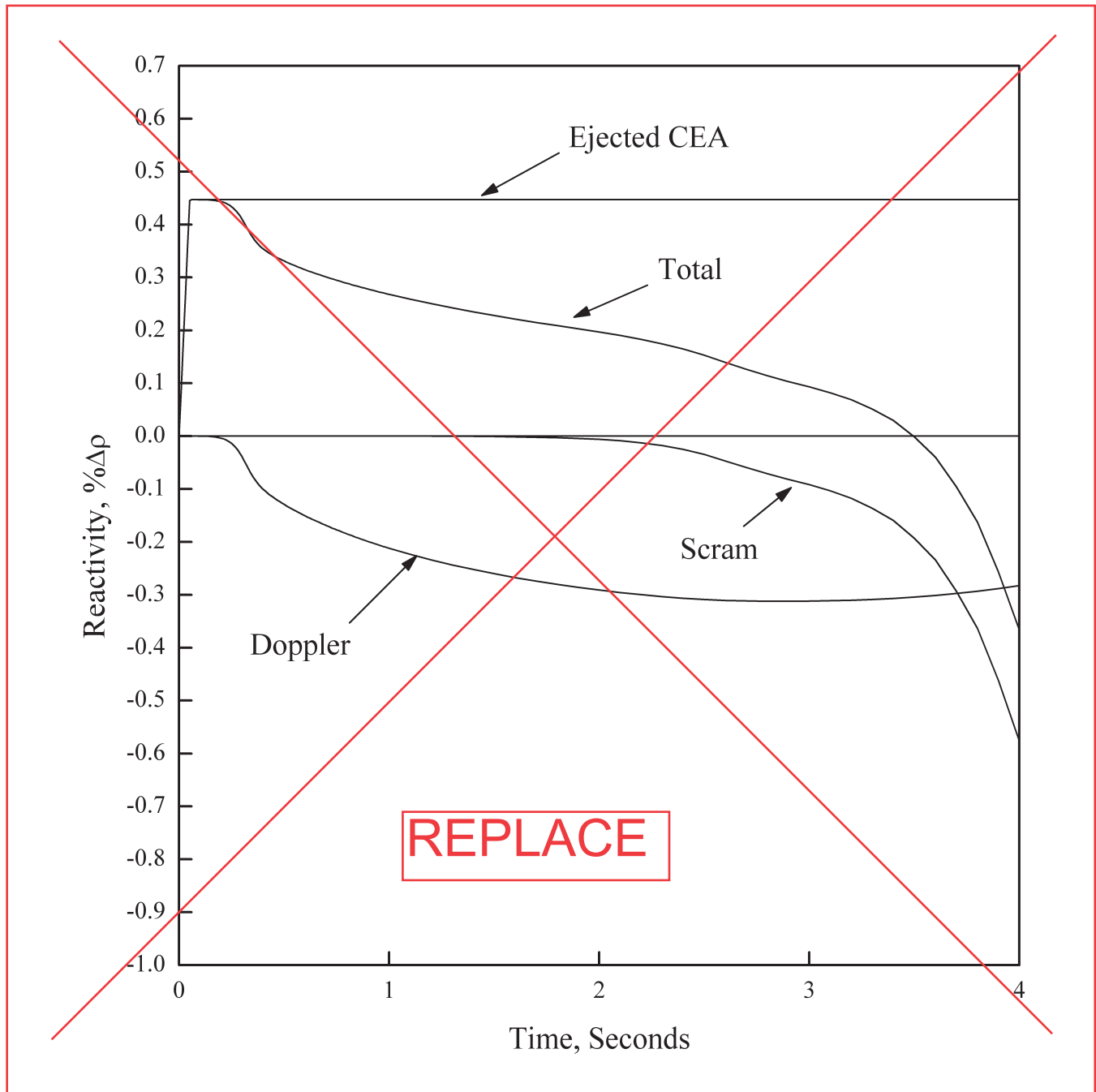
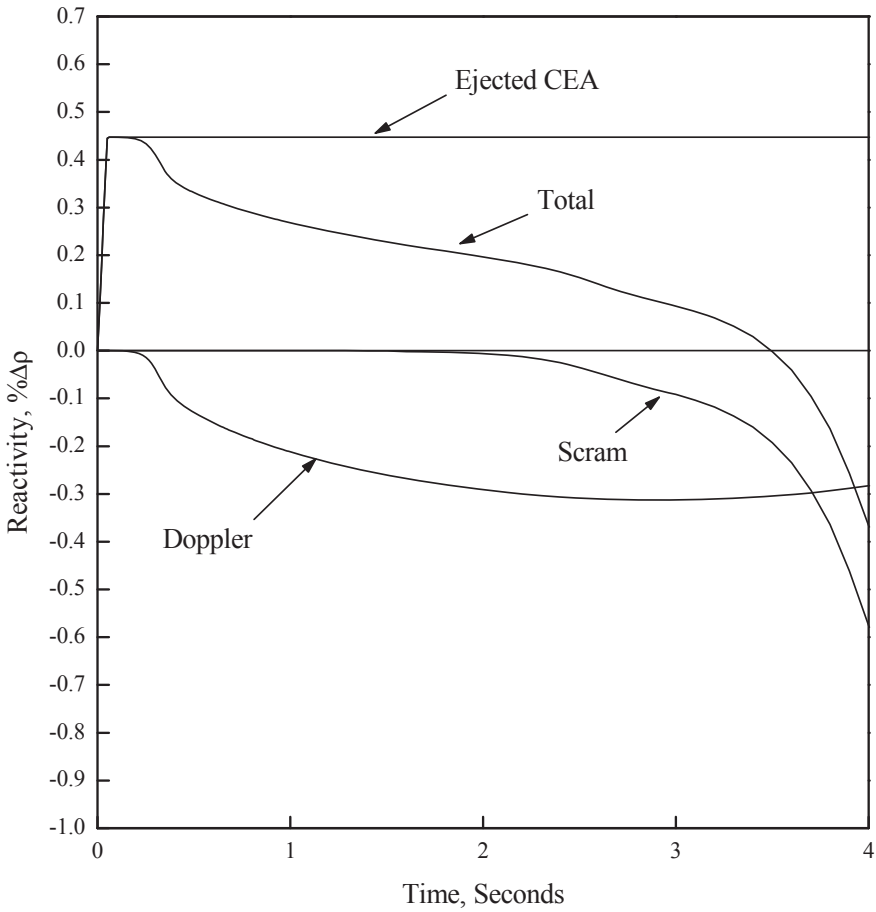
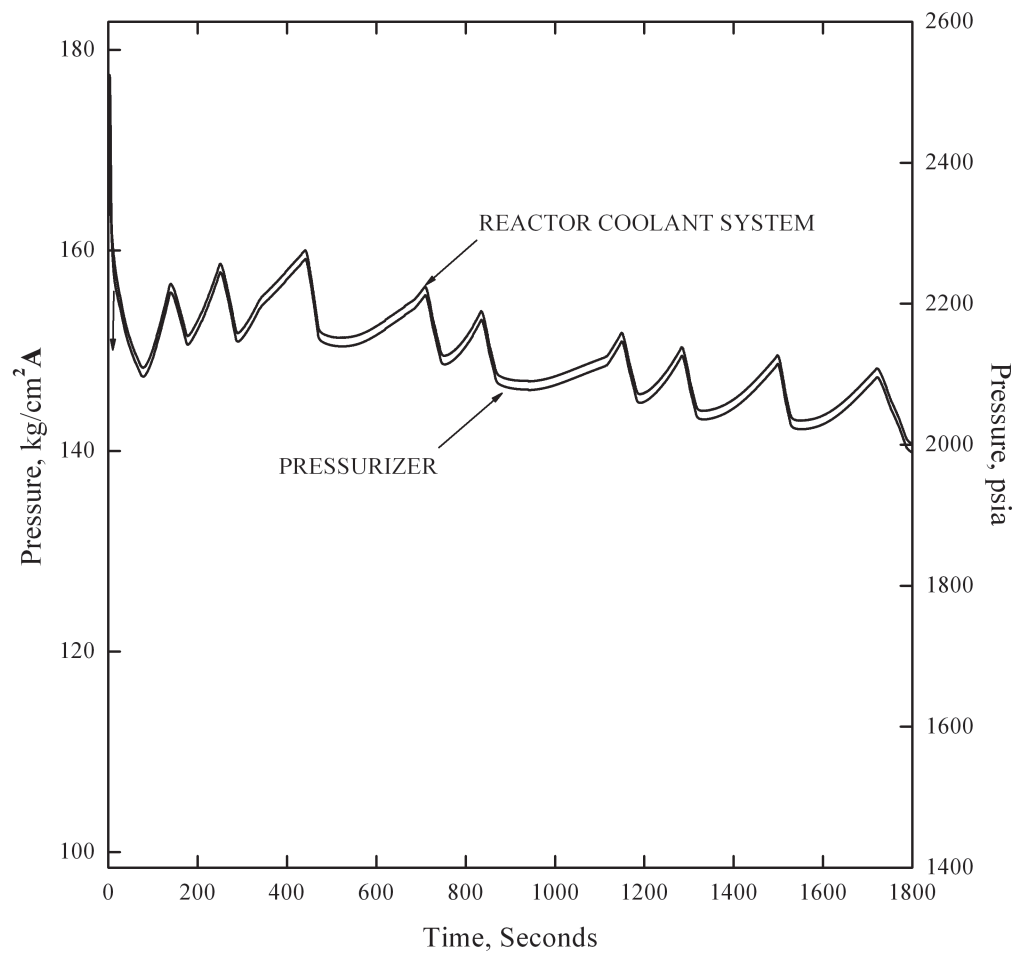


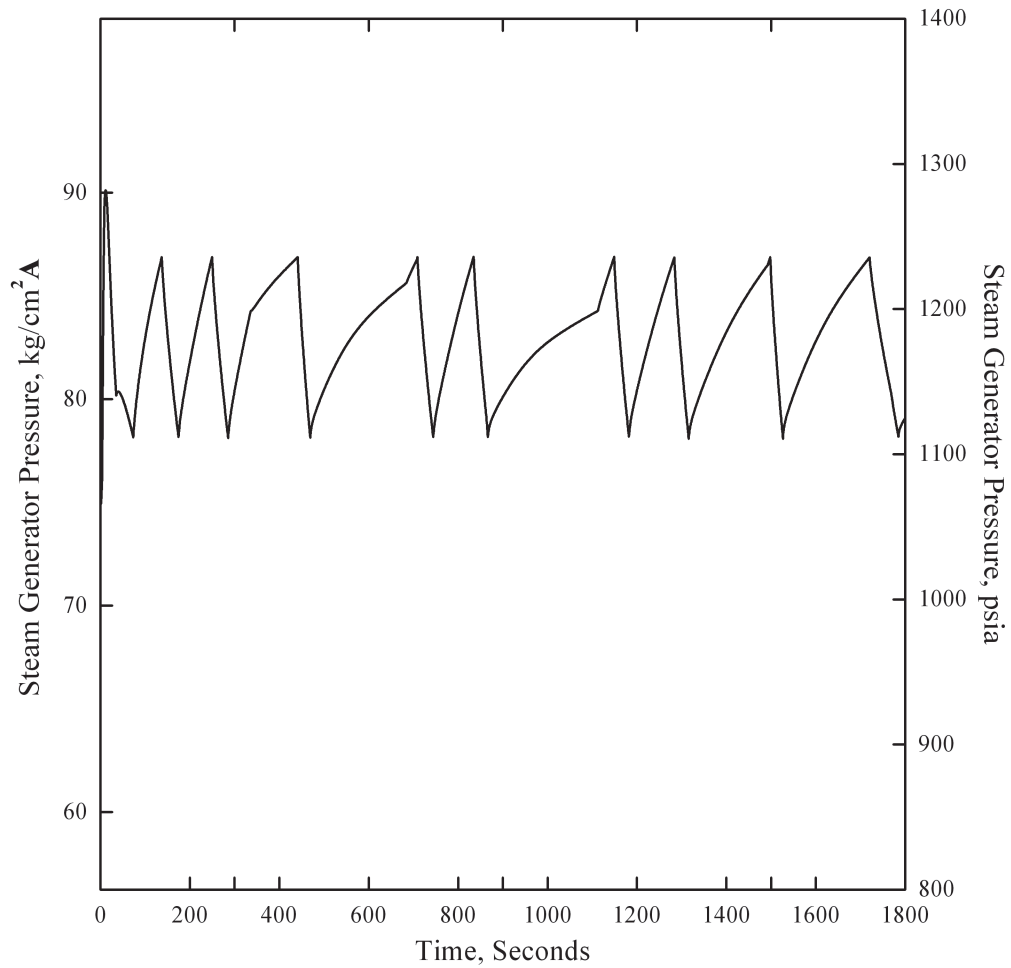
Figure 15.4.8-12 CEA Ejection: Reactivity vs. Time (HZP)

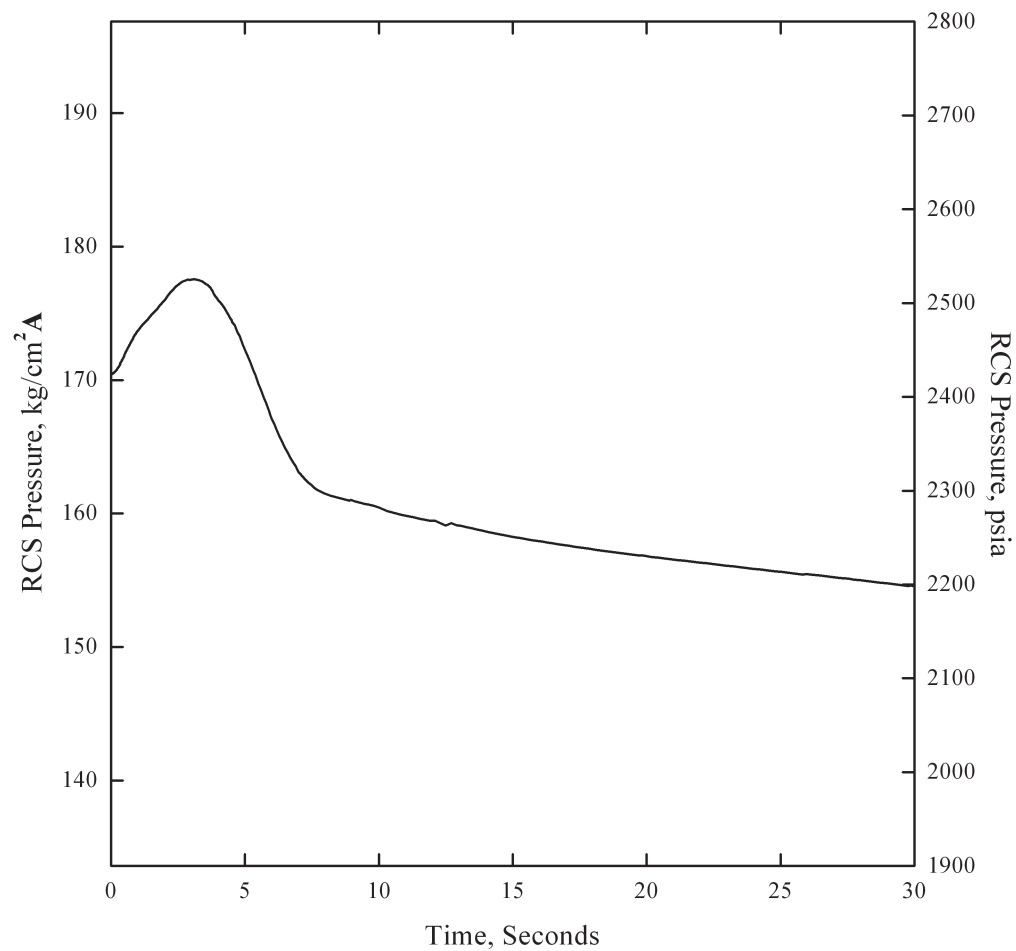


APR1400 DCD TIER 2

* The pressure difference between cold leg at the RCP discharge and the surge line is not included.

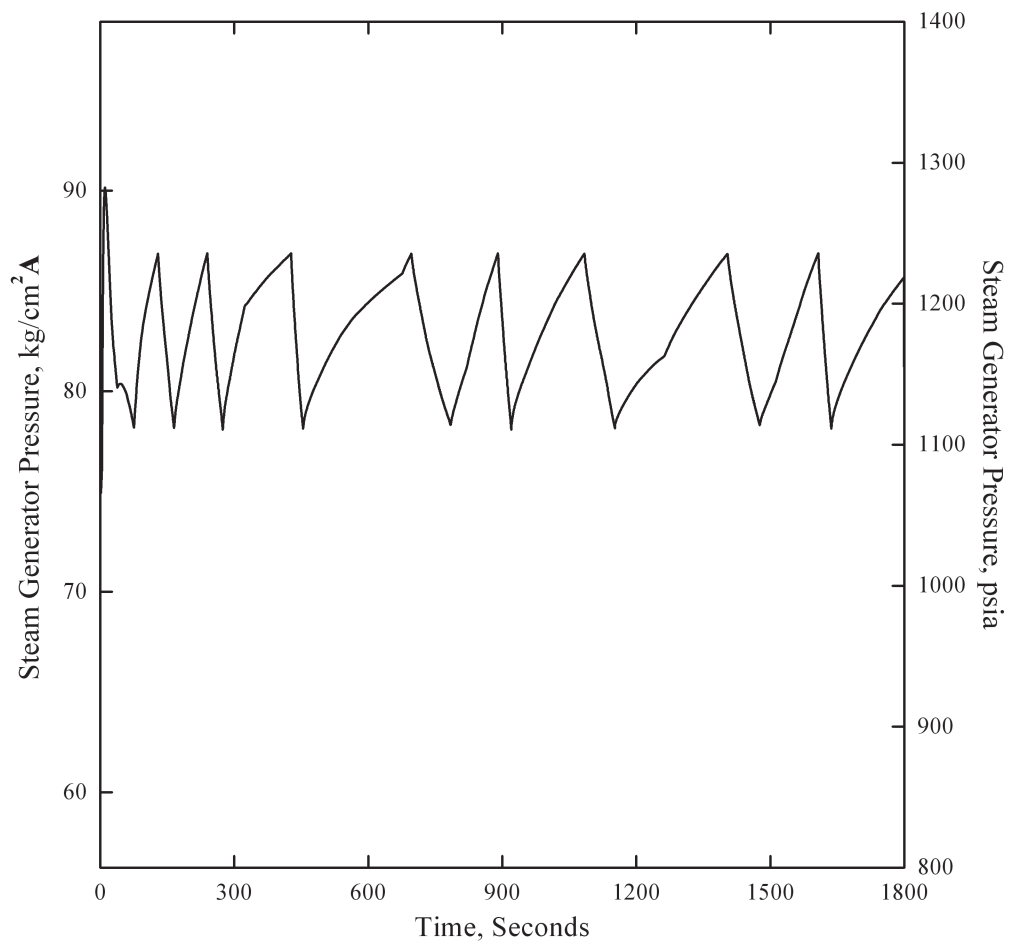
Figure 15.4.8-13 CEA Ejection: RCS and Pressurizer Pressures vs. Time

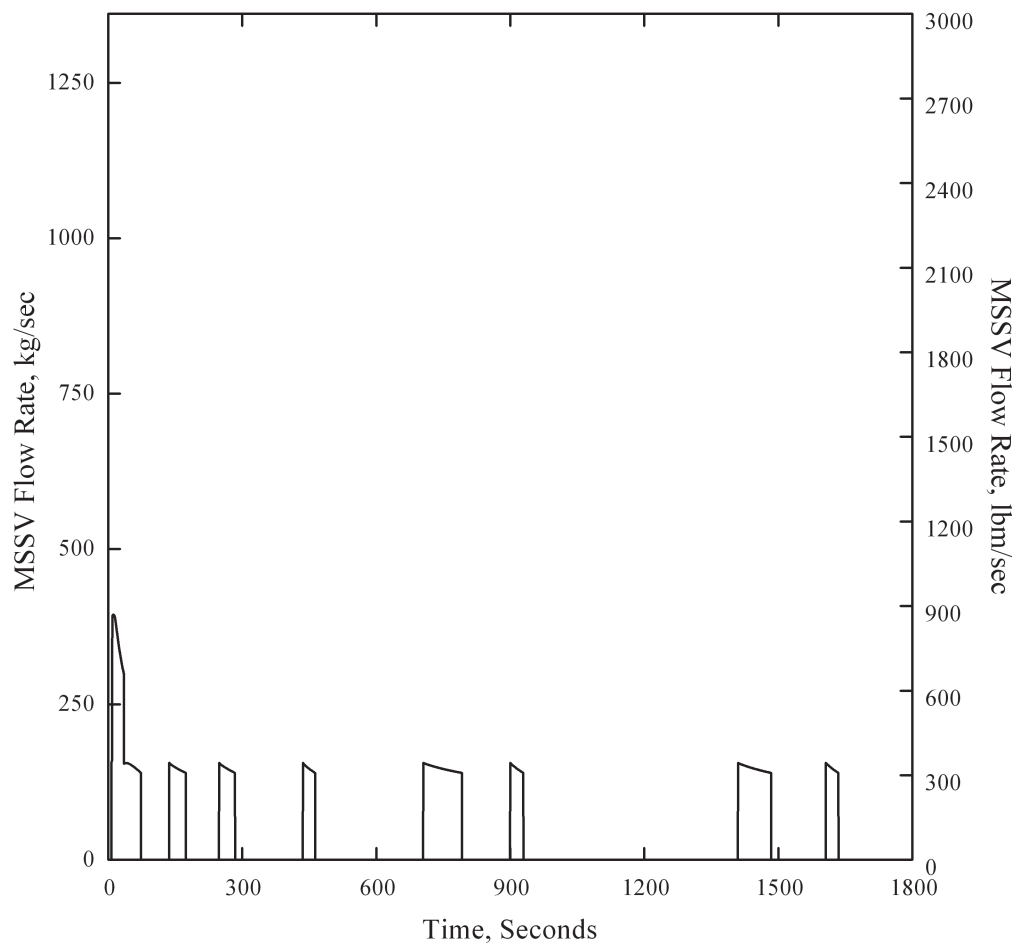
APR1400 DCD TIER 2**Figure 15.4.8-14 CEA Ejection: Steam Generator Pressure vs. Time**

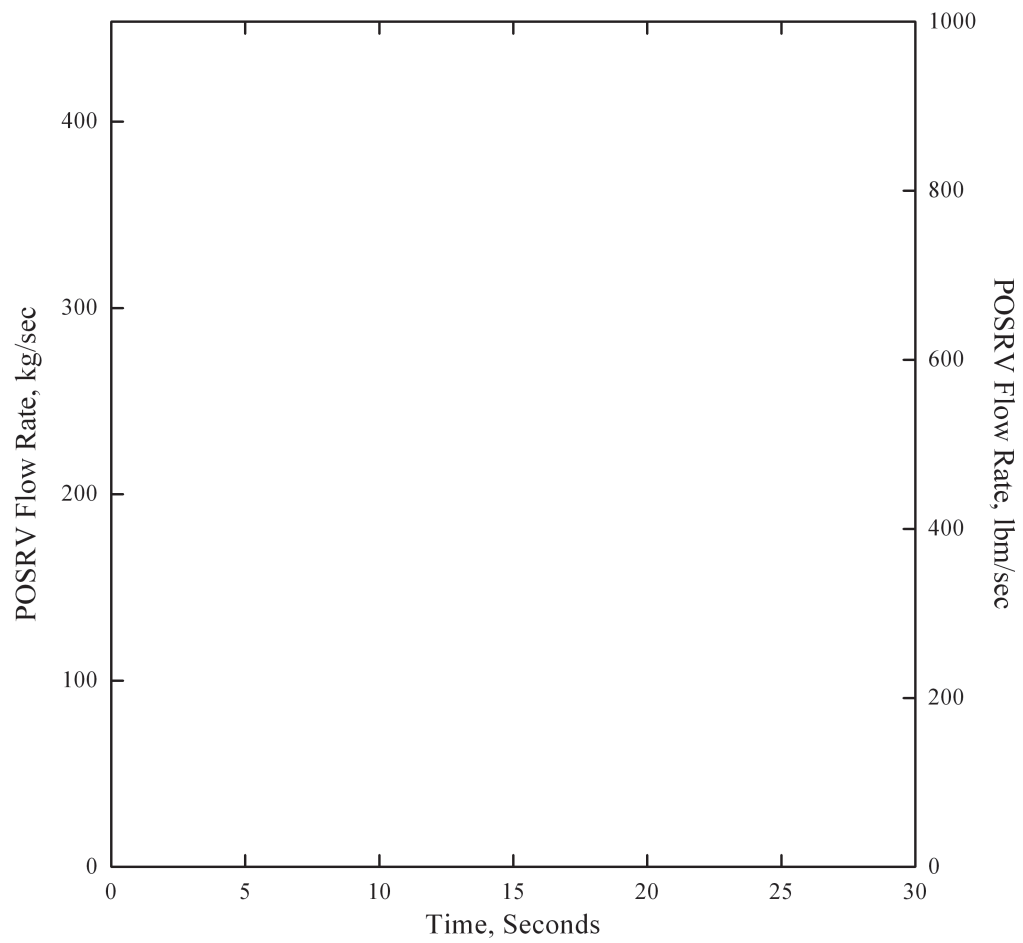
APR1400 DCD TIER 2

*The pressure difference between cold leg at the RCP discharge and the surge line is included.

Figure 15.4.8-15 CEA Ejection: RCS Pressure vs. Time (Peak Pressure Case)

APR1400 DCD TIER 2**Figure 15.4.8-16 CEA Ejection: Steam Generator Pressure vs. Time (Peak Pressure Case)**


APR1400 DCD TIER 2**Figure 15.4.8-17 CEA Ejection: MSSV Flow Rate vs. Time (Peak Pressure Case)**

APR1400 DCD TIER 2**Figure 15.4.8-18 CEA Ejection: POSRV Flow Rate vs. Time (Peak Pressure Case)**

| | | |
|---------------------------|---|--------------------|
| Table 15.6.3-3 | Sequence of Events for a Steam Generator Tube Rupture with a Loss of Offsite Power | 15.6-58 |
| Table 15.6.3-4 | Assumptions and Initial Conditions for the Steam Generator Tube Rupture with a Loss of Offsite Power | 15.6-59 |
| Table 15.6.3-5 | Parameters Used in Evaluating the Radiological Consequences of the Steam Generator Tube Rupture with a Loss of Offsite Power..... | 15.6-60 |
| Table 15.6.3-6 | Radiological Consequences of the Steam Generator Tube Rupture with a Loss of Offsite Power..... | 15.6-63 |
| Table 15.6.5-1 | Uncertainty Parameter Ranges and Distributions | 15.6-64 |
| Table 15.6.5-2 | General System Parameters and Initial Conditions for Large Break ECCS Performance | 15.6-65 |
| Table 15.6.5-3 | Summary of Fuel Rod Performance for Break Spectrum of Large Break LOCA..... | 15.6-67 |
| Table 15.6.5-4 | Sequence of Events for Representative Large Break LOCA..... | 15.6-68 |
| Table 15.6.5-5 | Summary of SRS and Bias Evaluation Results..... | 15.6-69 |
| Table 15.6.5-6 | Safety Injection Pumps Minimum Delivered Flow to RCS (Assuming Two SI Pump Trains Failed) | 15.6-70 |
| Table 15.6.5-7 | General System Parameters and Initial Conditions; Small Break ECCS Performance Analysis..... | 15.6-71 |
| Table 15.6.5-8 | Small Break Spectrum | 15.6-72 |
| Table 15.6.5-9 | Variables Plotted as a Function of Time for Each Small Break in the Spectrum..... | 15.6-73 |
| Table 15.6.5-10 | Peak Cladding Temperature and Oxidation Percentage for the Small Break Spectrum | 15.6-74 |
| Table 15.6.5-11 | Times of Interest for the Small Break Spectrum (Seconds after Break) | 15.6-75 |
| Table 15.6.5-12 | General System Parameters and Initial Conditions Long-Term Cooling SIS Performance..... | 15.6-76 |
| Table 15.6.5-13 | Major Input Parameters Used in Radiological Consequences Analysis for Large Break LOCA | 15.6-77 |
| Table 15.6.5-14 | Radiological Consequences of a Large Break LOCA | 15.6-81 |

delete

insert: TCD thermal conductivity degradation



| | |
|-------|--------------------------------------|
| TBV | turbine bypass valve |
| TEDE | total effective dose equivalent |
| TSC | technical support center |
| TS | technical specification |
| UGS | upper guide structure |
| USEPA | U.S. Environmental Protection Agency |
| USI | Unresolved Safety Issue |
| VOPT | variable overpower trip |

APR1400 DCD TIER 2

53. NUREG-1465, "Accident Source Terms for Light Water Nuclear Power Plants," U.S. Nuclear Regulatory Commission, February 1995.
54. Regulatory Guide 1.183, "Alternative Radiological Source Terms for Evaluating Design Basis Accidents at Nuclear Power Reactors," U.S. Nuclear Regulatory Commission, July 2000.
55. USEPA, Federal Guidance Report No. 11, EPA 520/1-88-020, "Limiting Values of Radionuclide Intake and Air Concentration and Dose Conversion Factors for Inhalation, Submersion, and Ingestion," September 1993.
56. USEPA, Federal Guidance Report No. 12, EPA 402-R-93-081, "External Exposure to Radionuclides in Air, Water, and Soil," September 1993.
57. 10 CFR 50.34, "Contents of Applications; Technical Information," U.S. Nuclear Regulatory Commission, January 10, 1997.
58. 10 CFR Part 50, Appendix A, "General Design Criteria for Nuclear Power Plants," U.S. Nuclear Regulatory Commission, January 24, 2000.
59. NUREG/CR-6604, "RADTRAD: A Simplified Model for RADionuclide Transport and Removal and Dose Estimation," SNL, December 1997.
60. NUREG-0800, Standard Review Plan, BTP 11-5, "Postulated Radioactive Release Due to Waste Gas System Leak or Failure," Rev.3, U.S. Nuclear Regulatory Commission, March 2007.
61. NUREG-0800, Standard Review Plan, BTP 11-6, "Postulated Radioactive Release Due to Liquid-Containing Tank Failure," Rev.3, U.S. Nuclear Regulatory Commission, March 2007.
62. 10CFR50.46, "Acceptance Criteria for Emergency Core Cooling Systems for Light Water-Cooled Nuclear Power Reactors," U.S. Nuclear Regulatory Commission.
63. APR1400-F-A-TR-12004-P (Proprietary), "Realistic Evaluation Methodology for Large-Break LOCA," KHNP, insert: , Rev. 1 December 2012 July 2017
64. Regulatory Guide 1.157, "Best-estimate Calculations of Emergency Core Cooling System Performance," U.S. Nuclear Regulatory Commission, May 1989.

APR1400 DCD TIER 2

65. NUREG/CR-5535, "RELAP5/MOD3 Code Manual Vol. 6, Validation of Numerical Techniques in RELAP5/MOD3.0," Rev.P3, U.S. Nuclear Regulatory Commission, March 2006.
66. NUREG/CR-3716, BNL-NUREG-51754, "CONTEMPT4/MOD4, A Multicompartment Containment System Analysis Program," U.S. Nuclear Regulatory Commission, March 1984.
- NUREG/CR-4001, BNL-NUREG-51894, "CONTEMPT4/MOD5: An improvement to CONTEMPT4/MOD4 multi-compartment containment system analysis program for ice containment analysis," Brookhaven National Laboratory, 1984.
67. APR1400-F-A-NR-14001-P, "Small Break LOCA Evaluation Model," KHNP, September 2014.
68. Letter, O. D. Parr (NRC) to F. M. Stern (C-E), June 13, 1975.
69. CENPD-133P (Proprietary), "CEFLASH-4AS, A Computer Program for Reactor Blowdown Analysis of the Small Break Loss-of-Coolant Accident," Supplement 1, Combustion Engineering, Inc., August 1974.
- CENPD-133 (Proprietary), "CEFLASH-4AS, A Computer Program for the Reactor Blowdown Analysis of the Small Break Loss-of-Coolant Accident," Supplement 3-P, Combustion Engineering, Inc., January 1977.
70. CENPD-134P (Proprietary), "COMPERC-II, A Program for Emergency Refill-Reflood of the Core," Combustion Engineering, Inc., August 1974
- CENPD-134P (Proprietary), "COMPERC-II, A Program for Emergency Refill-Reflood of the Core (Modifications)," Supplement 1, Combustion Engineering, Inc., February 1975.
- CENPD-134 "COMPERC-II, A Program for Emergency Refill-Reflood of the Core," Supplement 2, Combustion Engineering, Inc., June 1985.
71. CENPD-135P (Proprietary), "STRIKIN-II, A Cylindrical Geometry Fuel Rod Heat Transfer Program," Combustion Engineering, Inc., August 1974.

APR1400 DCD TIER 2

CENPD-135P (Proprietary), "STRIKIN-II, A Cylindrical Geometry Fuel Rod Heat Transfer Program (Modifications)," Supplement 2, Combustion Engineering, Inc., February 1975.

CENPD-135 (Proprietary), "STRIKIN-II, A Cylindrical Geometry Fuel Rod Heat Transfer Program," Supplement 4-P, Combustion Engineering, Inc., August 1976.

CENPD-135 (Proprietary), "STRIKIN-II, A Cylindrical Geometry Fuel Rod Heat Transfer Program," Supplement 5-P, Combustion Engineering, Inc., April 1977.

72. CENPD-138P (Proprietary), "PARCH, A FORTRAN-IV Digital Program to Evaluate Pool Boiling, Axial Rod and Coolant Heatup," Combustion Engineering, Inc., August 1974.

CENPD-138P (Proprietary), "PARCH, A FORTRAN-IV Digital Program to Evaluate Pool Boiling, Axial Rod and Coolant Heatup (Modifications)," Supplement 1, Combustion Engineering, Inc., February 1975.

73. APR1400-F-A-NR-14003-P, "Post-LOCA Long Term Cooling Evaluation Model," KHNP, September 2014.

74. CENPD-139-P-A (Proprietary), "C-E Fuel Evaluation Model," Combustion Engineering, Inc., July 1974.

CEN-161 (B)-P-A (Proprietary), "Improvements to Fuel Evaluation Model," Combustion Engineering, Inc., August 1989.

CEN-161 (B)-P (Proprietary) "Improvements to Fuel Evaluation Model," Supplement 1-P-A, Combustion Engineering, Inc., January 1992.

75. CEN-268, "Justification of Trip Two/Leave Two Reactor Coolant Pump Trip Strategy," Rev. 1, Combustion Engineering, Inc., May 1987.
76. APR1400-Z-A-NR-14006-P, "Non-LOCA Safety Analysis Methodology," Rev. 1, KHNP, February 2017.
77. APR1400-Z-J-NR-14005-P, "Setpoint Methodology for Plant Protection System," Rev. 1, KHNP, February 2017.

APR1400 DCD TIER 2

delete

~~78. APR1400-F-A-NR-14002-P, "The Effect of Thermal Conductivity Degradation on APR1400 Design and Safety Analyses," Rev. 0, KHNP, September 2014.~~

78

79. NUREG-1462, "Final Safety Evaluation Report Related to the Certification of the System 80+ Design Docket No. 52-002," Rev. 0, U.S. Nuclear Regulatory Commission, 1994.

79

80. APR1400-Z-A-NR-14014-P, "ATWS Evaluation," Rev. 0, KHNP, November 2014.

80

81. APR1400-F-M-TR-13001-P (Proprietary), "PLUS7 Fuel Design for the APR1400," Rev. 0, KHNP, August 2013.

APR1400 DCD TIER 2

allowable dose criteria limits, which are 100 percent and 10 percent of the 10 CFR 50.34(a)(1) value, respectively. The MCR and TSC doses are also within the dose limit in GDC 19.

15.6.3.2.6 Conclusions

The radiological consequences for the SGTR accident with a LOOP are within the allowable criteria. The RCS and secondary system pressures are below the 110 percent of the design pressure limits, thus providing reasonable assurance of the integrity of these systems. The minimum DNBR is above the DNBR SAFDL value of 1.29. The acceptance criterion regarding fuel performance is met.

For the limiting SGTR event with respect to SG overfill considerations (SGTR with a LOOP), the maximum liquid inventories do not result in an overfill and consequent introduction of liquid water into the steam lines, providing reasonable assurance of the integrity of these steam lines.

After 30 minutes, the operator uses the plant emergency procedure for the SGTR to cool down the plant to shutdown cooling entry conditions.

15.6.4 Radiological Consequences of Main Steam Line Failure Outside Containment (Boiling Water Reactor)

Not applicable to the APR1400.

15.6.5 Loss-of-Coolant Accidents Resulting from the Spectrum of Postulated Piping Breaks within the Reactor Coolant Pressure Boundary

15.6.5.1 Identification of Causes and Frequency Classification

Loss-of-coolant accidents (LOCAs) are hypothetical accidents that result from the loss of reactor coolant at a rate that exceeds the capability of the reactor coolant makeup system. The cause is breaks in the pipes in the reactor coolant pressure boundary up to and including a break equivalent in size to the double-ended rupture of the largest pipe in the RCS.

In the accident analyses for the APR1400, large break and small break LOCAs are both classified as postulated accidents (PAs). They are not expected to occur during the life of the plant but are postulated as a conservative design basis.

APR1400 DCD TIER 215.6.5.2 Sequence of Events and Systems Operation

insert: and burnup to consider thermal conductivity degradation (TCD) effects

15.6.5.2.1 Description of Large Break Loss-of-Coolant Accident

insert: with various burnup cases

A cold leg break between the outlet of the reactor coolant pump (RCP) and the corresponding reactor vessel (RV) inlet nozzle is found to be the most limiting with respect to the peak cladding temperature (PCT) in a large break LOCA. The large break LOCA analysis assumes a Loss Of Offsite Power (LOOP). The RCPs lose power and coast down after the LOOP. In order to determine the limiting break size, a guillotine break spectrum of a 100, 80, and 60 percent break area is studied. The blowdown PCT is a maximum when the break area is 100 percent of the cold leg cross-sectional area. The reflood PCT is a maximum when the break area is 80 percent. However, because the reflood PCT is not as high as the blowdown PCT, the 100 percent break size is chosen as the limiting guillotine break case.

insert: with the burnup of 27,000 MWd/MTU

delete

In the 100 percent guillotine break, the total break area is two times the cold leg cross-sectional area. A 200 percent slot break shows lower PCT in the blowdown phase and the transient is found to be faster by about 4 seconds than that of the 100 percent guillotine break. The PCT of the reflood phase is lower than that of the guillotine break, and the fuel quenching is somewhat earlier. The 100 percent double-ended guillotine break in a cold leg is determined to be the limiting case.

delete

insert: with the burnup of 27,000 MWd/MTU

The scenario is divided into four phases that characterize the events during the transient. The phases are blowdown, refill, early reflood, and late reflood and are defined by the inventory of the reactor pressure vessel and the flow condition of safety injection tank with fluidic device (SIT-FD).

A blowdown is defined as the phase from the opening time of the break to the start time of the SIT-FD injection. The refill phase is defined as the phase from the start time of the SIT-FD injection to the time when the mixture level in the reactor vessel lower plenum reaches the bottom of the active core. The definitions of these two phases are the same as those of the conventional large break LOCA scenario in PWRs.

Unlike the conventional scenario, the reflood phase is divided into early reflood and late reflood phases based on the time in which the SIT-FD becomes empty. The division is intended to address any possibility of core heatup during the late reflood phase in detail because the APR1400 does not have a low-pressure safety injection pump.

APR1400 DCD TIER 2Blowdown Phase

The blowdown phase starts when the break opens and ends when an SIT-FD injection is initiated; blowdown lasts for approximately 15 seconds. During blowdown, the primary coolant is rapidly expelled into the containment through the break. The reactor coolant changes from a subcooled liquid to a two-phase mixture or pure steam due to fluid flashing. By roughly 6 seconds, the core region begins to dry out.

The initial break flow is very high, reflecting the subcooled critical flow at the break. Mass flow from the reactor vessel side of the break is larger than that from the pump side due to the higher hydraulic resistances of the pump and the Steam Generator(SG). As the break flow develops in the reverse direction from the core to the break as well as in the positive direction, the core flow rapidly stagnates and then reverses shortly after the break occurs.

As the primary system depressurizes, flashing occurs first in the hot regions of the system, such as the upper plenum, hot leg, pressurizer, and core, and then proceeds to the relatively cold regions, such as the lower plenum, downcomer, and cold legs. Extensive voiding occurs in all areas of the reactor pressure vessel. Nucleate boiling develops in the core. Fission power that is calculated by a kinetics model drops to the level of decay heat due to the voiding in the core. The flashing also reduces the primary system depressurization rate.

When the critical heat flux (CHF) condition is reached in the core, heat transfer changes from nucleate boiling to post-CHF heat transfer regimes (i.e., transition boiling, film boiling, and forced convection to vapor), and much of the core dries out. Fuel rod cladding temperatures increase rapidly due to the degrading rod-to-fluid heat transfer. The cladding temperature increase during the early blowdown phase is terminated by several processes:

- a. First, as the core rapidly voids, the core power immediately decreases via void reactivity insertion.
- b. Second, the flow at the core reverses after stagnation.
- c. Third, the large coolant inventory of the upper guide structures (UGSs) and upper head moves toward the top of the core by two paths, through the UGS drainage

APR1400 DCD TIER 2

holes in the UGS bottom plate between the UGS and upper plenum and through the guide tube pipes that terminate in the upper inactive core.

As the low pressurizer pressure setpoint is reached, the reactor is tripped. Reactor coolant pumps (RCPs) are modeled to trip and coast down from the beginning of the accident assuming a LOOP. As the primary system pressure continues to decrease, flashing develops in the cold regions of the system. The resultant voiding occurring in the RCP degrades its pumping performance. The break flow rate decreases rapidly as the flow regime changes from subcooled to saturated critical flow at the break.

delete

~~Four SIT FDs begin to deliver flow into the four direct vessel injection (DVI) lines when the primary system pressure falls below its actuation setpoint. The coolant flows through the DVI nozzles into the upper annulus and then begins to refill the reactor pressure vessel. Because the reactor coolant system is still depressurizing, some of the coolant entering the upper annulus is swept out to the break along with entrained liquid from the lower plenum and the downcomer. Although the break flow remains high, the coolant is delivered downward into the downcomer and increases the downcomer water level. Then the coolant injected by the SIT FD eventually reaches the lower plenum.~~

Refill Phase

The refill phase begins when the SIT-FD injection flow is initiated and ends when the water level in the lower plenum reaches the core inlet.

mixture

bottom of the active core

Emergency core cooling (ECC) water in the reactor vessel downcomer can flow down by insert A from next page, swept out to the break by the pressure differential and upward-escaping steam flow that levitates the liquid. Reactor vessel walls and internals are considered as the large metal structures at temperatures above saturation. When subcooled ECC water comes into contact with the metal structures in the downcomer, steam is generated by nucleate boiling, reducing the gravitational head of the fluid in the downcomer. The process of liquid penetration and sweep-out repeats in the downcomer and direct-contact condensation of steam on the subcooled ECC water continues in the upper annulus.

The depressurization of the system wanes as the differential pressure between the RCS and the containment reduces. Owing to the gradual reduction of flashing and break flow, the rate of liquid penetration into the lower plenum increases. With a decreasing steam flow rate, a small amount of the ECC injection is bypassed, and most of it flows downward to

| |
|---|
| A |
|---|

Four SIT-FDs begin to deliver flow into the four DVI lines when the primary system pressure falls below their actuation set-point. The coolant flows through the DVI nozzles into the upper annulus and then begins to refill the reactor pressure vessel. The reactor coolant system keeps depressurizing because some of the coolant entering the upper annulus is swept out to the break along with entrained liquid from the lower plenum and the downcomer. Although the break flow remains high, sufficient flow in the excess of the bypass is delivered downward into the downcomer and increases the downcomer water level. Eventually, the coolant injected by the SIT-FDs reaches the lower plenum.

APR1400 DCD TIER 2

fill the downcomer and the lower plenum. At this stage, **mixture** **water** levels in the downcomer and the lower plenum increase rapidly.

Heatup, which is almost adiabatic, continues in the core during this phase because there is no inventory to cool the core.

The refill phase ends when the **liquid** **mixture** level in the lower plenum reaches the bottom of the active core.

insert: and remains full thereafter and conditions are established for continuous core reflooding.

Early Reflood Phase

The early reflood phase begins when the lower plenum **mixture level in the** **is completely filled with water** and ends when the SIT-FD water is depleted. Near the beginning of the early reflood phase, the safety injection pumps (SIPs) begin to inject water. Initially, the core reflood is quite rapid because of the following:

reaches the bottom of the active core

- The downcomer remains filled with water by the ECC injection.
- The high flow injection of SIT-FD continues.
- There is little loop steam flow and hydraulic resistance in the loop is therefore low.
- There is no severe steam binding.

insert: control port of

The maximum SIT-FD injection flow is reached during this phase. High flow injection through the standpipe becomes unavailable, and only the flow through the fluidic-device becomes injected. During the high-flow injection, the downcomer and core liquid levels increase rapidly. As the downcomer liquid level approaches the level of the cold legs, much of the coolant spills out of the break, and the vessel side break flow tends to increase. When the water level in the SIT-FD decreases to below the top of the standpipe, the low-flow injection begins. Water levels in the downcomer and core decrease slightly, but the levels increase again within approximately **10** seconds, maintaining downcomer water level **around** **above** the level of the cold legs. The combined SIP and SIT-FD flows are injected to maintain the water level in the downcomer and to retard core heatup.

5

In the core, heat transfer regimes encompass the entire spectrum. The regimes include single-phase liquid convection, nucleate boiling, transition boiling, film boiling, and single-phase vapor convection.

APR1400 DCD TIER 2

Local quenching could occur due to droplet de-entrainment at the fuel alignment plate and spacer grids. Vapor velocities and liquid entrainment in the central region of the core are higher due to the higher power of this region. The entrained liquid could have a cooling effect on the upper region of the core. Some of the entrained liquid is de-entrained at the fuel alignment plate, and the remainder is carried into the upper plenum, forming a two-phase pool. Liquid from the pool can re-enter the low-powered regions of the core through the fuel alignment plate due to the lower vapor velocities in those regions. A three-dimensional flow pattern can therefore occur: water flows from low-powered to high-powered regions in the core, while the flow is in the opposite direction in the upper plenum. Liquid from the upper plenum pool may be further entrained and carried over into the hot legs and SGs.

As reflooding progresses upward from the lower core region, more liquid is entrained to the upper plenum, and the level of the two-phase mixture in the pool can reach the hot leg. When the entrained liquid reaches the U-tubes of the SGs, it is vaporized by reverse heat transfer from the secondary side to the primary side. Due to the vaporization in the U-tubes, hot side pressure increases and causes steam binding, which deteriorates the reflooding of the core. Because the steam generation rate in the core decreases due to the lower reflood rate, liquid entrainment and the steam binding effect decrease, causing the reflood rate to increase again. Through this cyclical process, the entire core eventually becomes reflooded. The increase of core pressure due to the steam binding causes manometric oscillations between levels in the downcomer and the core.

The early reflood phase ends when SIT-FDs are emptied.

Late Reflood Phase

The late reflood phase begins when the SIT-FDs are emptied. ECC water is supplied only by the Safety Injection Pumps(SIPs) during this phase.

during this phase

Water level in the downcomer decreases somewhat as the SIT flow stops at the beginning of the late reflood phase and falls below the level of the cold legs. Then the core water level becomes stabilized. Liquid levels in the downcomer and core become balanced ~~within approximately 20 seconds.~~ Due to the decreased flow of coolant into the downcomer, liquid temperature in the downcomer can increase to a near saturation temperature under the influence of the residual heat of the metal structures (i.e., vessel walls in the downcomer). Boiling can occur on the surface of the walls depending on the

APR1400 DCD TIER 2

conditions. ECC water is provided by the four SIPs, the possibility of downcomer boiling is suppressed, and the core is found to remain amenable to cooling.

insert: is quenched and

Because the entire core remains in a quenched state during this phase, steam generation in the core is not significant enough to cause any severe ECC water bypass during this phase.

does not

Only safety-related systems or components are credited to mitigate the accident, as follows:

- a. Normally operating plant instrumentation and controls

Steady-state conditions of a large break LOCA analysis are calculated at the normal operating plant conditions (e.g., power, flow rate, pressure, temperature).

- b. Reactor protection system (RPS)

The reactor trip signal is generated from the low pressurizer pressure during the large break LOCA. The trip signal also generates the turbine trip and RCP trip automatically. Coastdown of the RCP progresses after the RCP trip. However, because the CEA insertion is not used for large break LOCA analysis, the negative reactivity of CEA is not credited. For the small break LOCA analysis, the CEA insertion is credited including the signal delay.

- c. Engineered safety feature actuation system (ESFAS)

An ESFAS is generated from the low pressurizer pressure or high-containment pressure during the large break LOCA. Low pressurizer pressure is credited only in the LOCA analysis and actuates the containment isolation actuation signal (CIAS) and safety injection actuation signal (SIAS).

- d. Safety injection system (SIS)

During the LOCA, the SIS provides the direct vessel injection. The discharge of each SIP and SIT is piped directly to a reactor vessel nozzle where the flow is directed into the reactor vessel downcomer region. Storage of fluid for the SIS is accomplished by the IRWST, which contains borated fluid.

- e. Containment spray system (CSS)

APR1400 DCD TIER 2

The CSS is designed to reduce containment pressure and temperature from a main steam line break or LOCA and to remove fission products from the containment atmosphere following a LOCA. The CSS uses the IRWST and has two independent trains. During the large break LOCA, CSS is automatically actuated on a high-high containment pressure signal. Maximum containment spray capacity is assumed to calculate the minimum containment pressure, which is described in Subsection 6.2.1.5.

15.6.5.2.2 Description of Small Break Loss-of-Coolant Accident

Small Break LOCA shows the significantly different behaviors depending on the break size and location. For a smaller break size, a SIP can maintain the RCS coolant inventory, since the reactor operator utilizes the Steam Generator (SG) to depressurize and cool down the system. For a larger break size, the blowdown break flow cannot be compensated by the SIP.

Small Break LOCA behavior can be changed with break location. The scenario of DVI line break, which is known to be the most limiting case of Small Break LOCA, can be generally subdivided into five phases: blowdown, natural circulation, loop seal clearing, core boil-off, and core recovery. The duration and occurrence of each phase are varied with break size and system characteristics.

Blowdown Phase

The break drastically depressurizes the RCS. When the RCS pressure reaches a reactor trip set-point on low pressurizer pressure, the reactor is tripped by the insertion of control rods. Once the RCS is depressurized to the low-low pressurizer pressure, safety injection signal is actuated. And safety injection water is delivered into the RCS after a delay until the injection pump is started. During the blowdown phase, the RCS is mostly filled with fluid in liquid phase and subcooled or saturated coolant is discharged into the containment building through the break. When the RCS is further depressurized to reach a quasi-equilibrium state with the secondary side of SG, the blow-down phase is finished.

Natural Circulation phase

The thermal quasi-equilibrium state can last for hundreds of seconds depending on the break size. Since the Reactor Coolant Pump (RCP) is shut down due to the assumption of Loss-Of-Offsite Power (LOOP), there is no forced circulation flow during this phase. The heat transfer from the primary to the secondary side is carried out by either single or two-

APR1400 DCD TIER 2

phase natural circulation. The coolant is gradually drained from the upper side of reactor coolant system. The phase separation proceeds from the upper side of U tube in SG to the reactor core upper head and then to the reactor upper plenum. The reactor core decay heat is removed via the break and SGs. The loop seal is filled with the coolant not to form the effective flow path for steam so that the steam generated in the reactor core cannot be effectively discharged.

Loop Seal Clearing phase

This phase covers from the termination of natural circulation flow until the loop seal clearing. When the coolant level in the SG side of loop seal becomes lower than the top of horizontal portion of pump suction leg, the loop seal is cleared and the steam isolated in the system is discharged through the break. Before the loop seal is cleared, the two-phase mixture level in the core can be significantly decreased to cause the reactor core uncover within short period of time. After the loop seal clearing, the pressure imbalance in the RCS disappears. The core level recovers up to the cold leg elevation.

Core Boil-Off phase

After the loop seal is cleared, the coolant in the reactor core starts to boil due to the decay heat so that the core mixture level decreases gradually. Consequently, the core uncover could happen again. At this time the cladding temperature can reach its peak value. When the safety injection flow becomes larger than the break flow as RCS pressure decreases, the core mixture level starts to recover.

Core Recovery phase

Core recovery continues from the moment when the core is at its lowest level until it is filled with SI flow. The core can be sufficiently cooled for the prolonged time in this phase by the recovered water level.

15.6.5.2.3 Description of Post Loss-of-Coolant Accident Long-Term Cooling

Immediately following a LOCA, safety injection is initiated to mitigate the short-term consequences of the event by replenishing the lost coolant. Safety injection is characterized by the automatic actuation of SIPs and the passive operation of SITs. Responses by operators are not required in the short term after a LOCA.

APR1400 DCD TIER 2

The post-LOCA long-term phase is defined as beginning when the core is reflooded and ending when the plant is secured. During the long term, operator action is needed to provide reasonable assurance that the core cooling is maintained until the plant is brought to a cold shutdown condition.

The basic function of long-term cooling (LTC) is to maintain the core at safe temperature levels while avoiding the precipitation of boric acid in the RCS. The capability of performing this basic function is reasonably assured until such time that the fuel assemblies are removed from the reactor vessel.

The analysis procedures account for single-failures to provide reasonable assurance that the performance objectives are met even with this assumption. There is a behavioral difference between large and small break LOCAs in the long term. This difference is that the RCS will remain at high pressure for small breaks and the safety injection flow rate will be too low for effective cooling; thus, small breaks require cooling of the RCS by the SGs until shutdown cooling (SDC) can be initiated. Large breaks, on the other hand, are adequately cooled by the safety injection flow because this flow is large due to the low RCS pressure; however, large breaks use simultaneous hot leg and direct vessel injection to flush boric acid from the vessel. As a consequence, the LTC large break and small break analyses are different.

15.6.5.3 Core and System Performance

15.6.5.3.1 Evaluation Model

The acceptance criteria for the emergency core cooling system (ECCS) for light water-cooled reactors are provided in 10 CFR 50.46 (Reference 62). The analyses presented in this section demonstrate that the APR1400 design satisfies these criteria.

Analyses are performed for a complete spectrum of break sizes. The most limiting break, which limits the peak linear heat generation rate (PLHGR), is identified as the 1.0 (break area) × double-ended guillotine at the pump discharge (DEG/PD) break. The results of the analyses demonstrate that for a PLHGR of 446.2 W/cm (13.6 kW/ft), the APR1400 SIS design meets the acceptance criteria of Reference 62. Requirements are as follows:

- a. Criterion 1 – Peak Cladding Temperature

APR1400 DCD TIER 2

The calculated maximum fuel element cladding temperature shall not exceed 1,204 °C (2,200 °F).

b. Criterion 2 – Maximum Cladding Oxidation

The calculated total oxidation of the cladding anywhere shall not exceed 0.17 times (17 percent) of the total cladding thickness before oxidation.

c. Criterion 3 – Maximum Hydrogen Generation

The calculated total amount of hydrogen generated from the chemical reaction of the cladding with water or steam shall not exceed 0.01 times (1 percent) the hypothetical amount that would be generated if all of the metal in the cladding cylinders surrounding the fuel, excluding the cladding surrounding the plenum volume, were to react.

d. Criterion 4 – Coolable Geometry

Calculated changes in core geometry shall be such that the core remains amenable to cooling.

e. Criterion 5 – Long-Term Cooling

After any calculated successful initial operation of the ECCS, the calculated core temperature shall be maintained at an acceptably low value, and decay heat shall be removed for the extended period of time required by the long-lived radioactivity remaining in the core.

Large Break Loss-of-Coolant Accident Evaluation Model

The large break LOCA analysis is performed using the CAREM (Reference 63) realistic evaluation methodology for the criteria of 10 CFR 50.46 (Reference 62). This methodology is based on the models and assumptions described in NRC RG 1.157 (Reference 64).

insert: RELAP5/MOD3.3/K Code, a modified version of RELAP5/MOD3.3

In CAREM, the RELAP5/MOD3.3 Code (Reference 65) is used for the calculation of ECCS thermal-hydraulics behavior and cladding temperature. Containment back pressure and temperature calculations are performed by the CONTEMPT4/MOD5 Code (Reference 66). Containment back pressure is affected by the mass and energy release

APR1400 DCD TIER 2

rate, and thermal-hydraulics phenomena is dependent on the containment back pressure. RELAP5/MOD3.3 and CONTEMPT4/MOD5 are merged to exchange their results in every time step.

insert: /K

CAREM quantifies the overall calculation uncertainty by propagating the uncertainty of each parameter. The ranges of uncertainty parameters are determined by auxiliary calculations and literature survey and confirmed by checking experimental data. To quantify the PCT at a 95 percent probability with a 95 percent confidence level, 124 times random sampling calculations are performed adopting non-parametric statistics. This methodology extrapolates the code accuracy to quantify the uncertainty that is applied to plant calculations.

181

A total of 124 input vectors are generated by random sampling, and simple random sampling (SRS) analyses are performed with the application of each input vector. The code uncertainty parameters and their ranges are determined by the evaluation of the code accuracy and confirmation of data covering processes. PCT is determined by applying Wilks' Formula to the SRS results in a 95 percent tolerance limit at a 95 percent confidence level.

181

Cases in which the reflood peak clad temperature differences within 100K compared with the highest reflood peak are selected for scale bias calculations, extracting the highest two cases from 124 cases of SRS. Code biases in the prediction of ECC water bypass and steam binding are evaluated separately. Steam binding bias is evaluated by combining the results of two bias evaluations of droplet de-entrainment in the upper plenum of the reactor vessel and droplet evaporation in the steam generator U-tube. The final values of the third PCT considering the uncertainties of the automatic time step control function and data reading frequency of RELAP5/MOD3.3/K are suggested for the comparison of LOCA criteria.

181

Small Break Loss-of-Coolant Accident Evaluation Model

The calculations presented in this section are performed using the small break evaluation model, which is described in Reference 67 and approved by the Nuclear Regulatory Commission (NRC) in Reference 68. The CEFLASH-4AS (Reference 69) computer program is used to determine the primary system hydraulic parameters during the blowdown phase, and the COMPERC-II (Reference 70) computer program is used to determine the system behavior during the reflood phase. Fuel rod temperatures and clad

APR1400 DCD TIER 2

oxidation percentages are calculated using the STRIKIN-II (Reference 71) and PARCH (Reference 72) computer programs. The interface between these programs is described in detail in Reference 67.

The small break evaluation model already met the requirements of TMI action item II.K.3.30 and II.K.3.31. Details are respectively described in Reference 23 and Section 15.6.5.3.

Post Loss-of-Coolant Accident Long-Term Cooling Evaluation Model

Long-term cooling (LTC) initiates when the core is quenched after a LOCA and terminates when the plant is secured. The objectives of LTC are to maintain the core at safe temperature levels and to avoid the precipitation of boric acid in the core region. To accomplish these objectives, an LTC analysis was performed using the codes and methods documented in Reference 73.

The LTC plan uses one of two procedures depending on the break area. The shutdown cooling system (SCS) is used if the break is sufficiently small that reasonable assurance of a successful operation of the SCS is provided. For large break LOCAs, a simultaneous hot leg and direct vessel injection is used to maintain core cooling and boric acid flushing. The plant operator initiates the appropriate procedure based on the indicated RCS pressure.

Figure 15.6.5-34 shows the LTC sequence of events and the schedule for operator actions for the LTC plan. The operator's first action is to initiate cooldown within 1 hour post-LOCA by releasing steam from the SGs. The steam is released through the turbine bypass system if available or through the atmospheric dump valves. Between 1 and 3 hours post-LOCA, the operator isolates or vents the safety injection tanks (SITs) to avoid injecting a large quantity of nitrogen (noncondensable) gas into the RCS. Between 1 and 4 hours post-LOCA, pressurizer depressurization is initiated. Between 2 and 3 hours post-LOCA, the discharge lines of SIP 3 and 4 are realigned to the hot legs to divide the SIP flow between the hot leg and direct vessel injection connections.

If the RCS pressure is above 31.6 kg/cm²A (450 psia) between 8 to 9 hours post-LOCA, the RCS is filled, which provides reasonable assurance that proper suction is available for entering shutdown cooling. Cooling of the RCS continues until the indicated RCS temperature is lower than the maximum SDC entry temperature including instrument uncertainty. The operator then throttles the SIPs until the RCS pressure is reduced to

APR1400 DCD TIER 2

shutdown cooling entry pressure, including instrument uncertainty, and initiates shutdown cooling.

A prerequisite to throttling or terminating SI flow is that the RCS is in a subcooled condition for the indicated RCS pressure. While reducing RCS pressure to initiate SCS operation, the operator maintains subcooling of the RCS consistent with the emergency operating procedures.

If the SCS is inoperable, the alternative for decay heat removal is the continued use of the SGs. This requires the continued availability of auxiliary feedwater and the atmospheric dump valves or the turbine bypass system. If the SCS becomes operable later, it is put into operation. This path is indicated by the dashed lines in Figure 15.6.5-34.

If the indicated RCS pressure falls below 31.6 kg/cm²A (450 psia) at 8 to 9 hours, the break may be too large for absolute assurance that proper suction is available for the shutdown cooling mode. In this event, a simultaneous hot leg and direct vessel injection by itself cools the core and also flushes the reactor vessel indefinitely.

15.6.5.3.2 Input Parameters and Initial Conditions

Large Break Loss-of-Coolant Accident

The SIS consists of four safety injection pumps (SIPs) and four safety injection tanks (SITs). Automatic operation of the SIPs is actuated by a low pressurizer pressure signal or a high containment pressure signal. Flow is initiated from the SITs by the opening of a check valve when the reactor vessel downcomer pressure drops below the SIT pressure. A fixed internal device in the SIT regulates the flow rate with changing level and pressure. SI flow is delivered by DVI connections.

The most limiting single failure for a large break LOCA is the loss of one SIP train. However, two of the four SIPs are conservatively assumed to be available. The available SIP injection located near the broken cold leg with another available injection located on the opposite side of broken cold leg is used for the large break LOCA analysis.

The operating parameters and ranges for the plant uncertainty evaluation determined in large break LOCA analysis are listed in Table 15.6.5-1. Core and system parameters are prepared by using measurement uncertainty ranges or determined to cover the minimum and maximum ranges of the design data or the limit of the Technical Specifications.

described in Reference 63

Burnup sensitivity study to determine the limiting burnup is introduced by considering TCD effects. In addition, since determination of the limiting break size could be affected by burnup, break size sensitivity with various burnup cases are evaluated.

The large break LOCA analysis accounts for 10 percent tube plugging of the steam generator tubes that may occur during the life of the plant.

~~The accidents are assumed to occur at the initial burnup for the large break LOCA analysis. The stored energy is the maximum value because the fuel elements show the most densification at the initial burnup (BOC), and the burnup yields the highest cladding temperature in the large break LOCA.~~

Subsection 6.2.1.5 presents the minimum containment pressure analysis that is performed in the analysis of ECCS performance. The analysis identifies the containment parameters used in the large break analysis. The values for the containment parameters are chosen to minimize containment pressure to minimize the core reflood rate.

insert: with the burnup of 27,000 MWd/MTU

The worst break in the large break LOCA analysis is the double-ended guillotine at the pump discharge leg (Reference 63). To determine the limiting break area, a guillotine break spectrum of 100 percent, 80 percent, and 60 percent break areas is analyzed, and the limiting break area is applied for 124 cases of SRS calculation.

Small Break Loss-of-Coolant Accident

181

insert: with various burnup

The safety injection system (SIS) consists of four direct vessel injection lines, each supplying flow from one SIT and one SIP. Offsite power is conservatively assumed to be lost upon reactor trip, and the SIPs therefore await diesel generator startup and load sequencing before they can start. The total time delay assumed is 40 seconds from when the SIAS setpoint is reached to when the full SI flow is delivered to the RCS. For breaks in the DVI line, all safety injection flow delivered to the broken line is assumed to spill out of the break.

An analysis of the possible single failures that can occur within the SIS shows that the worst single failure for the small break spectrum is the failure of one SIP train. However, two of the four SIPs are conservatively assumed to be available, thereby minimizing the safety injection available to cool the core.

Based on the above assumptions, the following safety injection flows are credited for the small break LOCA analysis:

- a. For a break in the pump discharge leg, the SI flow credited is full flow from two SIPs and four SITs.

APR1400 DCD TIER 2

- b. For a break in a DVI line, the SI flow credited is full flow from one SIP and three SITs. The flow from the remaining active SIP and from one SIT is assumed to spill out of the break.

Table 15.6.5-6 presents the SIP flow rates assumed at each of the four injection points as a function of RCS pressure.

The significant core and system parameters used in the small break LOCA calculations are presented in Table 15.6.5-7. PLHGR of 492.1 W/cm (15.0 kW/ft) is assumed to occur about 15 percent from the top of the active core. A conservative beginning-of-life moderator temperature coefficient of $0.0 \times 10^{-4} \Delta\rho/^{\circ}\text{C}$ ($0.0 \times 10^{-4} \Delta\rho/^{\circ}\text{F}$) was used in all small break LOCA calculations.

The initial steady-state fuel rod conditions are obtained from the FATES3 (Reference 74) computer program. The small break LOCA analysis uses a hot rod average burnup, which maximizes the amount of stored energy in the fuel.

The small break LOCA analysis uses the containment parameters of the initial containment pressure and the maximum containment volume. Containment parameters do not influence the small break LOCA analysis because the break flow stays critical.

Post Loss-of-Coolant Accident Long-Term Cooling

The major assumptions used in performing the LTC analysis are as follows:

- a. No offsite power is available.
- b. The worst single failure is the loss of two SIP trains with additional conservativeness. This results in the following:
 - 1) Two SIPs are operable.
 - 2) One motor-driven auxiliary feedwater pump is operable.
- c. One atmospheric dump valve on each SG is available to cool down the RCS.
- d. RCS cooldown begins at 2 hours post-LOCA.
- e. The SITs are vented or isolated before establishing shutdown cooling conditions for the small break LTC procedure.

APR1400 DCD TIER 2

- f. The pressurizer is depressurized to establish shutdown cooling conditions for the small break LTC procedure.
- g. RCS cooldown is terminated when the hot leg temperature is below the maximum shutdown cooling entry temperature including instrument uncertainty.
- h. Pump flow rates and initial water source inventories used in the large break LOCA boric acid precipitation analysis are selected to maximize the boric acid concentration in the core.
- i. A boric acid precipitation limit of 29.3 weight percent (Reference 73) is used in the large break LOCA boric acid precipitation analysis. This limit is based on a conservative containment pressure of 1.03 kg/cm²A (14.7 psia).

Significant core and system parameters used in the post-LOCA long-term cooling analysis are presented in Table 15.6.5-12.

The IRWST sump strainer related to GSI-191 is designed to provide reasonable assurance that debris quantities are maintained within the bounds of a post-LOCA long-term cooling analysis. See Subsection 6.8.4.5 for further information.

15.6.5.3.3 Results

Large Break Loss-of-Coolant Accident Analysis Results

Major input variables used in the performance evaluation of the SIS in a large break LOCA are summarized in Table 15.6.5-2. The important results such as the PCT, PCT location, and time results for large break LOCA spectrum analyses are listed in Table 15.6.5-3. Major times of interest are listed in Table 15.6.5-4. The transient behaviors of the NSSS parameters are shown in Figures 15.6.5-2 through 15.6.5-23.

The most limiting break area is a 100 percent of double-ended guillotine at the pump discharge break. Hence, a SRS calculation is performed for a 100 percent double-ended guillotine break at the pump discharge leg.

The cladding temperature behavior result obtained from 124 times SRS calculations is shown in Figure 15.6.5-23. In the 124 times calculations, the highest two PCT cases are excluded. The third highest PCT is 991.3 °C (1,816.4 °F) and maximum cladding oxidation is 3 percent with exceeding the 95 percent at 95 percent confidence level.

The third highest PCT is occurred during reflood phase and the PCTs are increased by the biases. The total PCT bias is evaluated as +9.8 °C and the peak local oxidation and hot rod hydrogen generation are confirmed not to increase by the scale bias calculations. Therefore the final PCT (w/ BIAS) is 1,019.7 °C (1,867.5 °F) and the maximum cladding oxidation (w/ BIAS) is 6.30 percent as shown in Table 15.6.5-4.

The cases in which the clad temperature differences in the second peak are within 100 °C (180 °F) compared with the highest second peak are selected for scale bias calculations. Code biases in the prediction of ECC water bypass and steam binding are evaluated separately. Steam binding bias is evaluated by combining the results of two separate bias evaluations of droplet de-entrainment in the upper plenum of the reactor vessel and droplet evaporation in the steam generator U-tube. Even though reflood cladding temperatures are increased by the biases, they do not exceed the blowdown PCT of 991.3 °C (1,816.4 °F). Total PCT bias is evaluated as +0 °C, as shown in Table 15.6.5-5. The maximum cladding oxidation with bias evaluation is 3 percent as shown in Table 15.6.5-5.

Uncertainties from sources other than code models or plant operation conditions, such as automatic time step control function and data reading frequency of RELAP5/MOD3.3/K, are considered of maximum 10 °C (18 °F). The hot rod average oxidation is calculated lower than one percent. The final PCT, maximum cladding oxidation, and core-wide hydrogen generation combining all the biases are as follows:

$$\begin{aligned}\text{Peak cladding temperature} &= 991.3\text{ °C} + 10\text{ °C} \\ &= 1,001.3\text{ °C (1,834.3 °F)} \\ &= 1,274.5\text{ K} < 1,477.15\text{ K (2,200 °F)}\end{aligned}$$

$$\text{Maximum cladding oxidation} = 3.09\% < 17\%$$

$$\text{Maximum hydrogen generation} \ll 1\%$$

The highest cladding temperature in the large break LOCA analysis is 1,001.3 °C (1,834.3 °F), which is 202.7 °C (365.7 °F) lower than the acceptance criterion of 1,204 °C (2,200 °F).

The final PCT considering the effect of thermal conductivity degradation is still satisfied the acceptance criteria. Details are given in Reference 78. The PCT increase is ended when the core is maintaining a coolable geometry. The heat generated from the fuel is able to be removed properly for a long period.

Based on the results of this analysis, it is concluded that the APR1400 ECCS satisfies the all SRP acceptance criteria of References 62 and 64 (Subsection 15.0.5) for a complete spectrum of large break LOCAs and is adequate to perform its intended function of maintaining the integrity of the core, thereby limiting radiation release to the environment.

APR1400 DCD TIER 2Small Break Loss-of-Coolant Accident Analysis Results

The nine breaks analyzed at 4,062.66 MWt, 102 percent of nominal, include reactor coolant pump discharge leg breaks ranging in size from 465 cm² (0.5 ft²) to 46.5 cm² (0.05 ft²) and DVI line breaks from 372 cm² (0.4 ft²) to 18.6 cm² (0.02 ft²). One break, equal in area to a fully open POSRV, 27.9 cm² (0.03 ft²), is postulated to occur in the top of the pressurizer. Table 15.6.5-8 lists the various break sizes and locations examined for this analysis.

The transient behavior of important NSSS parameters is shown in the figures listed in Table 15.6.5-9. Table 15.6.5-10 summarizes the important results of this analysis. Times of interest for the various breaks analyzed are presented in Table 15.6.5-11. A plot of PCT versus break size is presented in Figure 15.6.5-33. The 372 ft² (0.4 ft²) DVI break results in the highest cladding temperature 624 °C (1,156 °F) of the small breaks analyzed, which is 580 °C (1,044 °F) lower than the acceptance criteria of 1,204 °C (2,200 °F). Of the pump discharge leg and DVI line break locations, the DVI line break is limiting due to the assumed loss of all safety injection flow to the broken line.

For the DVI line break location, as the break size becomes progressively smaller than 372 cm² (0.4 ft²), the inner vessel two phase level follows a definite pattern:

- a. The time of initial core uncover is later.
- b. The depth of core uncover is less.
- c. The rate of level decrease and increase becomes slower.

This trend continues until the core does not uncover at all. These trends predictably affect the PCT.

As the break size decreases, both the later time of the initial core uncover and the shallower depth of uncover tend to mitigate the temperature transient. This trend continues until the core does not uncover as typified by the 18.6 cm² (0.02 ft²) break. By analyzing several break sizes over this range, the behavior of PCT versus break size is adequately determined.

The above behavior of core uncover with break size results from the design characteristics of the SIS. For DVI break sizes below 93 cm² (0.1 ft²), the RCS pressure remains above the SIT pressure and coolant flow injection to the reactor vessel is accomplished entirely by

APR1400 DCD TIER 2

one SIP. For break sizes greater than 93 cm^2 (0.1 ft^2), the transient is terminated by the action of both the SITs and SIPs.

For the cold leg breaks, the additional SIS flow resulting from being able to credit two SIPs precludes core uncover to break sizes up to 93 cm^2 (0.1 ft^2). In addition, the core uncover for break sizes greater than 93 cm^2 (0.1 ft^2) is delayed, and the depth and duration of uncover decreased relative to DVI breaks, which credit only one SIP. This more favorable behavior results in lower cladding temperatures relative to breaks in a DVI line.

In addition to the break locations described above, the rupture of an in-core instrument tube is considered. A break equal in size to a completely severed instrument tube (2.8 cm^2 [0.003 ft^2]) is postulated to occur in the reactor vessel bottom head.

Following rupture, the primary system depressurizes until a reactor scram signal and safety injection actuation signal (SIAS) are generated due to low pressurizer pressure at $109.3 \text{ kg/cm}^2\text{A}$ ($1,555 \text{ psia}$). The assumed LOOP causes the primary coolant pumps and the feedwater pumps to coast down. After the 40-second delay, required to actuate the emergency diesel and the SIPs following the SIAS, safety injection flow is initiated to the RCS. Four SITs are available but do not inject due to the high RCS pressure.

The primary side depressurization continues accompanied by a rise in secondary side pressure until the secondary side pressure reaches the lowest setpoint of the steam generator safety valves. The primary system pressure continues to fall until it is just slightly greater than the secondary side pressure. At this point, the flow from the two operating SIPs (63 kg/sec [139 lbm/sec]) exceeds the leak flow (12 kg/sec [26 lbm/sec]). Therefore, the RCS fills. The decay heat generated in the core is removed in the SGs by steam flow through the secondary side safety valves. The core remains covered and cooled in this condition.

Based on the results of this analysis, it is concluded that the APR1400 ECCS satisfies the all SRP acceptance criteria of References 1 and 62 (Subsection 15.0.5) for small break LOCAs.

Post Loss-of-Coolant Accident Long-term Cooling Evaluation Results

An evaluation of the various break locations showed that the double-ended ($9,104.5 \text{ cm}^2$ [9.8 ft^2]) cold leg break was confirmed to be the limiting break geometry for the boric acid precipitation analysis (Reference 73). The long-term loop seal refilling with a slot break at the top of the cold leg does not significantly affect the boric acid precipitation analysis.

APR1400 DCD TIER 2

For a cold leg break, the core flushing flow is the difference between the hot leg injection flow rate and the core boiloff rate. The initiation of a simultaneous hot leg and direct vessel SIP injection flow at 3 hours post-LOCA provides a substantial and time-increasing core flushing flow as shown in Figure 15.6.5-35. Figure 15.6.5-36 shows that with no core flushing flow, boric acid does not begin to precipitate until 3.2 hours post-LOCA. The margin provided for the prevention of boric acid precipitation by the core flushing flow of 113.6 L/min (30 gpm) is also shown in Figure 15.6.5-36. The analyses also show that all hot leg steam entrainment of injection water is terminated in less than 3 hours post-LOCA. When the operator initiates simultaneous hot leg and direct vessel injection by 3 hours, there is no potential for the hot leg entrainment and boric acid precipitation.

The left branch of the LTC plan in Figure 15.6.5-34 applies to the break areas for which the RCS refills. The LTC analysis predicts that the RCS will refill at various times depending on break area, as shown in Figure 15.6.5-37. As shown, for a break area as large as 37.2 cm² (0.04 ft²), the RCS refills within 8 hours. The LTC analysis determines that more than 14 hours is required to exhaust all of the auxiliary feedwater during cooldown of the RCS. To allow a substantial time margin to avoid exhausting the auxiliary feedwater, a period of 8 to 9 hours is selected for the operator to decide whether the small break LTC procedure is appropriate. These results demonstrate that breaks as large as 37.2 cm² (0.04 ft²) are able to use SCS for the long-term cooling and flushing of the core. The LTC analysis determines that the large break procedures can flush the core for break areas down to 3.7 cm² (0.004 ft²). The overlap in break areas for which either the large break or small break procedures can be used is illustrated in Figure 15.6.5-38.

The operator chooses the appropriate procedure on the basis of the indicated RCS pressure between 8 and 9 hours. Figure 15.6.5-38 lists the RCS pressure at 8 hours for a wide range of break areas, and Figure 15.6.5-39 presents this information graphically. The decision pressure is selected as 31.6 kg/cm²A (450 psia) so that, with consideration of the maximum RCS pressure measurement error up to ± 21.1 kg/cm² (± 300 psia), reasonable assurance is provided that the operator selects the proper procedure for any break area.

The natural circulation cooldown analysis that is performed as part of the LTC analysis determines that the SCS entry temperature of 193 °C (380 °F) is reached at approximately 6.7 hours after the start of the LOCA. The analysis simulates a conservatively slow cooldown rate and consequently, a maximum value for the earliest time that the SCS entry temperature is reached. The analysis takes credit only for safety grade systems, namely, the safety injection system, the auxiliary feedwater system, and the atmospheric dump

APR1400 DCD TIER 2

valves. Reaching the SCS entry temperature at 6.7 hours leaves sufficient time for the operator to depressurize the RCS to the SCS entry pressure and initiate shutdown cooling.

Based on the results of this analysis, it is concluded that the APR1400 ECCS satisfies the all SRP acceptance criteria of References 1 and 62 (Subsection 15.0.5) for LTC.

15.6.5.4 Barrier Performance

In Section 6.2, the barrier performance is described in detail, and the containment vessel pressure that affects the performance of the barriers is evaluated.

15.6.5.5 Radiological Consequence

The radiological consequences for large break LOCAs are performed to determine the post-LOCA doses at the EAB, LPZ, MCR, and TSC using the AST guidance in NRC RG 1.183, plant-specific design inputs, and TEDE dose criteria for the following post-LOCA release paths:

- a. Containment leakage
- b. Engineered safety feature (ESF) leakage
- c. Low volume purge release
- d. Back leakage to the IRWST leakage

The following regulatory requirement and guidance are applied as the acceptance criteria for the receptors at EAB, LPZ, MCR, and TSC:

- a. NRC RG 1.183
- b. 10 CFR 50.34
- c. Standard Review Plan, Subsection 15.0.3

15.6.5.5.1 Evaluation Model

For the design basis LOCA, all fuel assemblies in the core are assumed to be affected, and the maximum core fission product inventory is used. The maximum core fission product inventories are listed in Appendix 15A, Table 15A-1. The remaining isotopes are not

APR1400 DCD TIER 2

Table 15.6.5-1

Uncertainty Parameter Ranges and Distributions

| No. | Parameter | Distribution | Parameter Ranges | | Component |
|-----|-----------------------------|--------------|------------------|----------|----------------|
| | | | Min. | Max | |
| 1 | Fq | Uniform | 1.94 | 2.41 | Fuel |
| 2 | Gap conductance | Uniform | 0.75 | 1.50 | |
| 3 | Fuel conductivity | Normal | 0.8455 | 1.1545 | |
| 4 | Core power | Normal | 0.9691 | 1.0309 | |
| 5 | Decay heat | Normal | 0.89803 | 1.10197 | |
| 6 | Burst temperature dial | Uniform | 0.90 | 1.10 | |
| 7 | Burst strain dial | Uniform | 0.30 | 1.70 | |
| 8 | Oxidization dial | Normal | 0.961 | 1.039 | |
| 9 | Groeneveld CHF dial | Normal | -0.17111 | 2.17111 | Core |
| 10 | Chen nucleate boiling dial | Normal | 0.382 | 1.618 | |
| 11 | Zuber CHF dial | Normal | 0.5365 | 1.4635 | |
| 12 | Dittus Boelter, liquid dial | Normal | 0.606025 | 1.393975 | |
| 13 | Dittus Boelter, vapor dial | Normal | 0.606025 | 1.393975 | |
| 14 | Bromley dial | Normal | 0.42835 | 1.57165 | |
| 15 | Weber number dial | Uniform | 1.350 | 7.0 | |
| 16 | F. Rohsenow dial | Uniform | 0.5 | 1.5 | |
| 17 | Weismann dial | Uniform | 0.40 | 1.60 | |
| 18 | 1-Phase Cd | Normal | 0.7821 | 0.9979 | |
| 19 | 2-Phase Cd | Normal | 0.7026 | 1.4374 | |
| 20 | Pump K-factor | Uniform | 0.239 | 0.577 | Loop |
| 21 | Pump head multiplier | Uniform | 0.0 | 1.0 | |
| 22 | Pump torque multiplier | Uniform | 0.0 | 1.0 | |
| 23 | Pressurizer pressure, bar | Normal | 152.47 | 157.80 | Pressurizer |
| 24 | SIT pressure, bar | Uniform | 40.31 | 44.59 | SIT/Cold Leg |
| 25 | SIT water volume, m3 | Uniform | 50.69 | 54.57 | |
| 26 | SIT water temp, K | Uniform | 283.0 | 321.9 | |
| 27 | SIP flow multiplier | Uniform | -0.5 | 0.5 | |
| 28 | IRWST water temp, K | Uniform | 283.0 | 321.9 | |
| 29 | Thermal Conductivity | Uniform | 1.0 | 2.0 | Downcomer Wall |
| 30 | Heat Capacity | Uniform | 1.0 | 1.5 | |

APR1400 DCD TIER 2

Table 15.6.5-2 (1 of 2)

General System Parameters and Initial Conditions for Large Break ECCS Performance

| Plant Parameters | Reference Conditions |
|---|----------------------|
| Core | |
| 1. Core power, MWt | 3,983 |
| 2. Power peaking factor | 2.258 ← 2.184 |
| 3. Fuel type | 16 × 16 |
| 4. Power output pattern | Figure 15.6.5-1 |
| 5. Decay heat | ANS79 model |
| Reactor Coolant System | |
| 1. Initial core flow rate, kg/hr | 73.3×10^6 |
| Pressurizer | |
| 1. Pressure, bar | 155.1 |
| Steam Generator | |
| 1. Feedwater temperature, K | 505.23 |
| 2. Tube plugging rate, % | 10 |
| Safety Injection System | |
| 1. Safety injection tank coolant volume, m ³ | 52.63 ← 52.61 |
| 2. Safety injection tank gas pressure, bar | 42.45 ← 43.07 |
| 3. Safety injection tank coolant temperature, K | 302.5 ← 302.59 |
| 4. FD K-factor for high injection flow (including piping K) | 25 ← 10 |
| 5. FD K-factor for low injection flow (including piping K) | 120 ← 80 |
| 6. IRWST temperature, K | 302.5 ← 302.59 |

APR1400 DCD TIER 2

Table 15.6.5-2 (2 of 2)

| Plant Parameters | Reference Conditions |
|---|----------------------|
| Containment Building | |
| 1. Initial pressure, bar | 0.98 |
| 2. Initial temperature, K | 283.15 |
| 3. Net Free volume, m ³ | 97,239 |
| 4. Number of spray | 2 |
| 5. Delay time for spray actuation, sec | 0 |
| 6. Spray flow rate (2 pumps), L/min (gpm) | 37,853 |

Replace with next page C

APR1400 DCD TIER 2

Table 15.6.5-3

Summary of Fuel Rod Performance for Break Spectrum of Large Break LOCA

| Variable | | 100 % Break | 80 % Break | 60 % Break |
|--------------------------------------|-----------------|-------------|------------|------------|
| Blowdown | PCT, °C | 892.0 | 870.0 | 768.9 |
| | PCT Location, m | 2.57 | 2.57 | 2.76 |
| | PCT Time, sec | 6.5 | 36.5 | 36.5 |
| Reflood | PCT, °C | 798.9 | 869.5 | 762.5 |
| | PCT Location, m | 2.57 | 2.76 | 2.76 |
| | PCT Time, sec | 36.5 | 64.0 | 71.5 |
| Peak Local Oxidation, % | | 1.50 | 1.92 | 1.24 |
| Peak Zr-H ₂ O location, m | | 2.57 | 2.76 | 2.76 |
| Maximum Hydrogen Generation, % | | < 1.0 | < 1.0 | < 1.0 |
| Hot Fuel Rod Rupture | | N/A | N/A | N/A |

C

Table 15.6.5-2

Summary of Fuel Rod Performance for Break Spectrum of Large Break LOCA

| Variable | | 100 % Break | 80 % Break | 60 % Break |
|--------------------------------------|-----------------|-------------|------------|------------|
| Burn-Up | | 27,000 | 27,000 | 0 |
| Blowdown | PCT, °C | 896.8 | 847.7 | 633.4 |
| | PCT Location, m | 2.76 | 2.76 | 2.76 |
| | PCT Time, sec | 7.2 | 9.2 | 2.7 |
| Reflood | PCT, °C | 846.8 | 887.3 | 796.4 |
| | PCT Location, m | 2.57 | 2.76 | 2.76 |
| | PCT Time, sec | 92.5 | 80.5 | 87.5 |
| Peak Local Oxidation, % | | 2.661 | 2.860 | 0.560 |
| Peak Zr-H ₂ O location, m | | 2.19 | 2.57 | 2.76 |
| Maximum Hydrogen Generation, % | | < 1.0 | < 1.0 | < 1.0 |
| Hot Fuel Rod Rupture | | 28.8 | 27.8 | N/A |

Replace with next page D

APR1400 DCD TIER 2

Table 15.6.5-4

Sequence of Events for Representative Large Break LOCA

| EVENT | 100 % Break (sec) | 80 % Break (sec) | 60 % Break (sec) |
|--|----------------------|---------------------|---------------------|
| Break Occurs | 0 | 0 | 0 |
| Reactor Trip signal Occurs | 6.2 | 6.2 | 7.3 |
| SI Injection signal Occurs | 6.2 | 6.2 | 7.3 |
| SIT Discharge Begins | | | |
| SIT 1 (Broken Cold Leg Side) | 14.4 | 16.2 | 22.2 |
| SIT 2 (Broken Loop Intact Cold Leg Side) | 14.4 | 16.2 | 22.2 |
| SIT 3 (Intact Loop Intact Cold Leg Side 1) | 14.4 | 16.2 | 22.2 |
| SIT 4 (Intact Loop Intact Cold Leg Side 2) | 14.4 | 16.2 | 22.2 |
| Pumped SI Injection | 46.2 | 46.2 | 46.4 |
| Core Water Level Recovery | 44.2 | 40.6 | 45.5 |
| SIT Empty Time | | | |
| SIT 1 (Broken Cold Leg Side) | 201.5 | 207.5 | 206.7 |
| SIT 2 (Broken Loop Intact Cold Leg Side) | 201.5 | 207.5 | 206.8 |
| SIT 3 (Intact Loop Intact Cold Leg Side 1) | 201.5 | 207.5 | 206.7 |
| SIT 4 (Intact Loop Intact Cold Leg Side 2) | 201.5 | 207.5 | 206.6 |

D

Table 15.6.5-3

Sequence of Event for Representative Large Break LOCA

| EVENT | 100 % Break(sec) | 80 % Break(sec) | 60 % Break(sec) |
|--|---------------------|--------------------|--------------------|
| Break Occurs | 0 | 0 | 0 |
| Reactor Trip signal Occurs | 9.51 | 9.57 | 9.77 |
| SI Injection signal Occurs | 9.51 | 9.57 | 9.77 |
| SIT Discharge Begins | | | |
| SIT 1 (Broken Cold Leg Side) | 14.8 | 16.6 | 20.1 |
| SIT 2 (Broken Loop Intact Cold Leg Side) | 14.8 | 16.6 | 20.1 |
| SIT 3 (Intact Loop Intact Cold Leg Side 1) | 14.8 | 16.6 | 20.1 |
| SIT 4 (Intact Loop Intact Cold Leg Side 2) | 14.8 | 16.6 | 20.1 |
| Pumped SI Injection | 48.36 | 48.42 | 48.62 |
| Core Water Level Recovery | 32.5 | 35.5 | 43.0 |
| SIT Empty Time | | | |
| SIT 1 (Broken Cold Leg Side) | 171.4 | 178.7 | 177.9 |
| SIT 2 (Broken Loop Intact Cold Leg Side) | 171.5 | 178.8 | 177.9 |
| SIT 3 (Intact Loop Intact Cold Leg Side 1) | 171.4 | 178.7 | 177.9 |
| SIT 4 (Intact Loop Intact Cold Leg Side 2) | 171.5 | 178.7 | 177.9 |

Replace with next page E

APR1400 DCD TIER 2

Table 15.6.5-5

Summary of SRS and Bias Evaluation Results

| Peak Cladding Temperature (PCT) | | Value, °C |
|---|----------------------------|----------------------|
| SRS Results | Highest PCT | 991.3 |
| | Highest Reflood PCT | 982.9 |
| Scale BIAS Evaluation Results | Final BIAS Reflood PCT | 982.9 |
| | Max. BIAS Case Reflood PCT | 982.9 |
| | – ECC Bypass BIAS | +0.0 |
| | – Steam Binding BIAS | +0.0 |
| Final PCT (w/ BIAS) | | 991.3 ⁽¹⁾ |
| Max. Cladding Oxidation | | Value, % |
| SRS Results | Max. Cladding Oxidation | 3.00 |
| Scale BIAS Evaluation Results | Final BIAS Oxidation | 3.09 |
| | Max. BIAS Case Oxidation | 2.56 |
| | – ECC Bypass BIAS | +0.14 |
| | – Steam Binding BIAS | +0.39 |
| Final Max. Cladding Oxidation (w/ BIAS) | | 3.09 |

- (1) The final PCT with considering thermal conductivity degradation effect is still satisfied the acceptance criteria.

E

Table 15.6.5-4

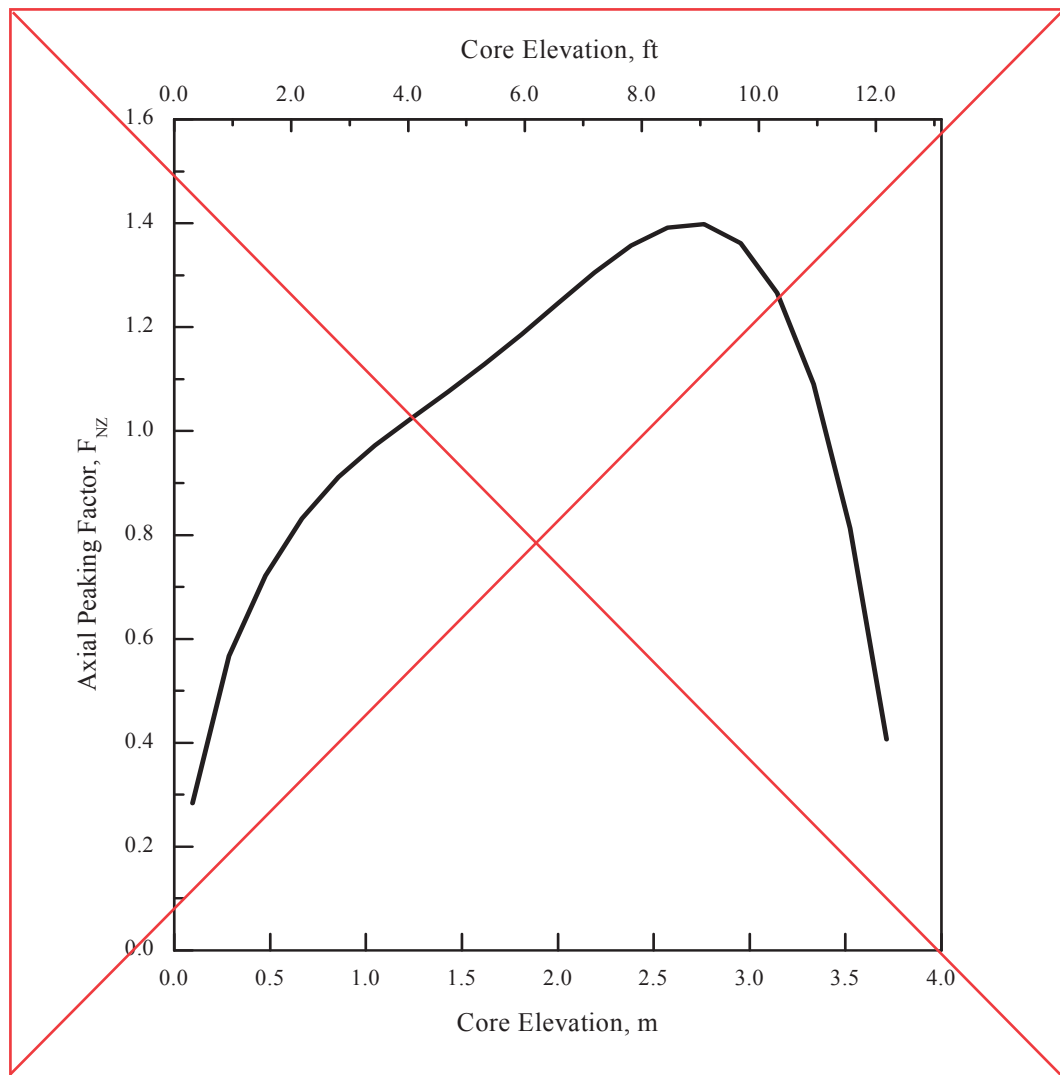
Summary of SRS and Bias Evaluation Results

| Peak Cladding Temperature (PCT) | | Value, °C |
|---|------------------------------------|-----------------------|
| SRS Results | Highest PCT | 1,009.9 |
| | Highest Reflood PCT | 1,009.9 |
| Scale BIAS Evaluation Results | Final BIAS Reflood PCT | 1,019.7 |
| | Max. BIAS Case Reflood PCT | 1,009.9 |
| | - ECC Bypass BIAS | +9.8 |
| | - Steam Binding BIAS | +0.0 |
| Final PCT (w/ BIAS) | | 1,019.7 ¹⁾ |
| Max. Cladding Oxidation | | Value, % |
| SRS Results | Max. Cladding Oxidation | 6.30 |
| Scale BIAS Evaluation Results | Final BIAS Max. Cladding Oxidation | 6.30 |
| | Max. BIAS Case Cladding Oxidation | 6.30 |
| | - ECC Bypass BIAS | +0.0 |
| | - Steam Binding BIAS | +0.0 |
| Final Max. Cladding Oxidation (w/ BIAS) | | 6.30 |

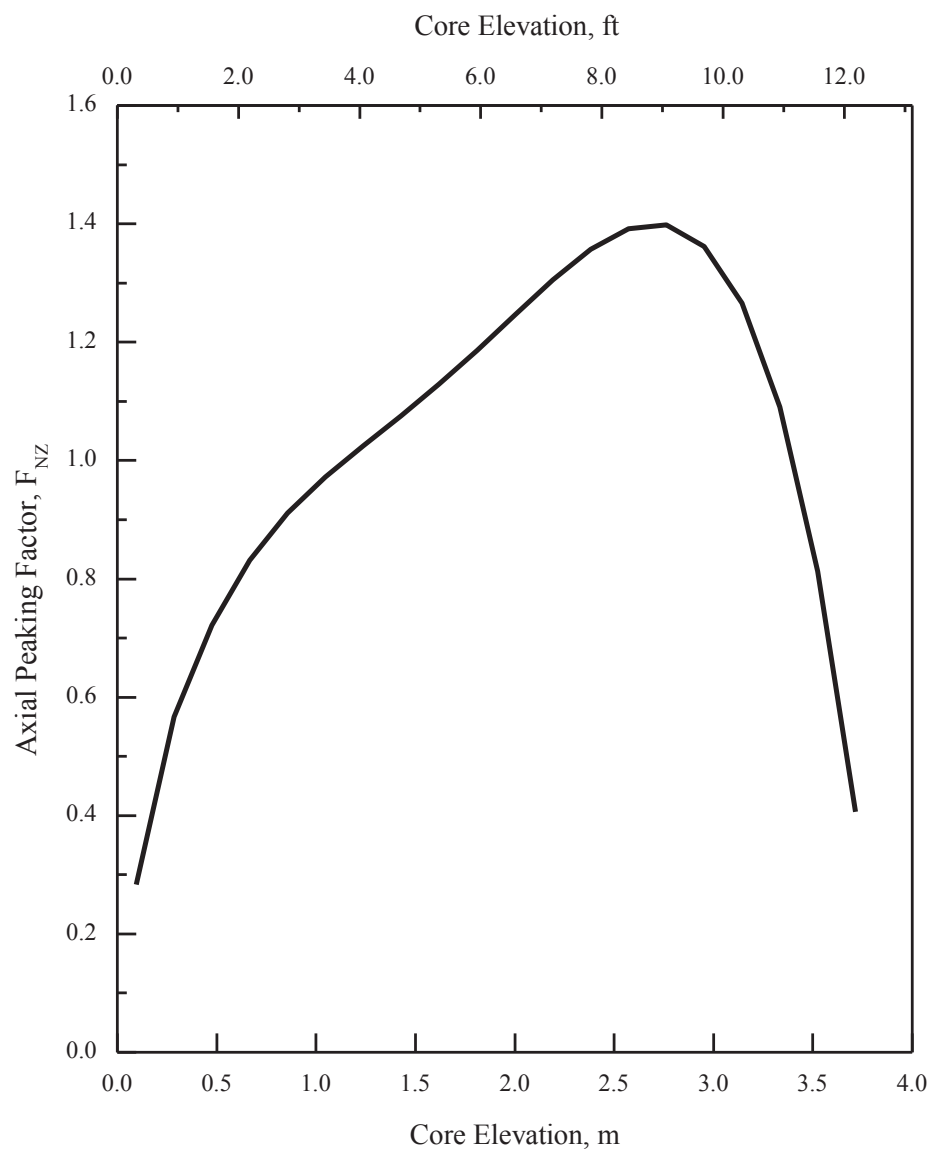
(1) The final PCT with considering thermal conductivity degradation effect is still satisfied the acceptance criteria.

APR1400 DCD TIER 2

Replace with next page F

**Figure 15.6.5-1 Axial Power Distribution at Large Break**

F



APR1400 DCD TIER 2

Replace with next page G

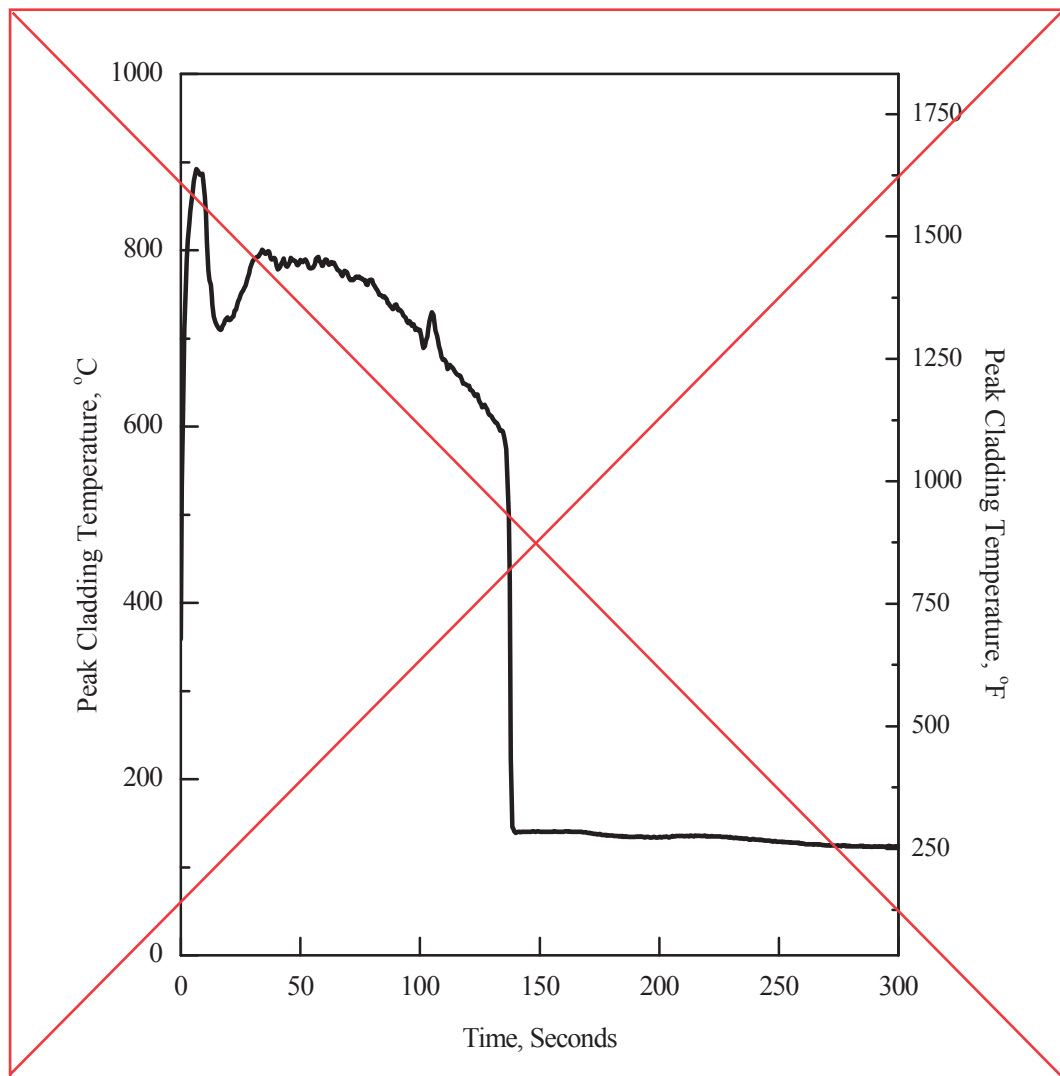
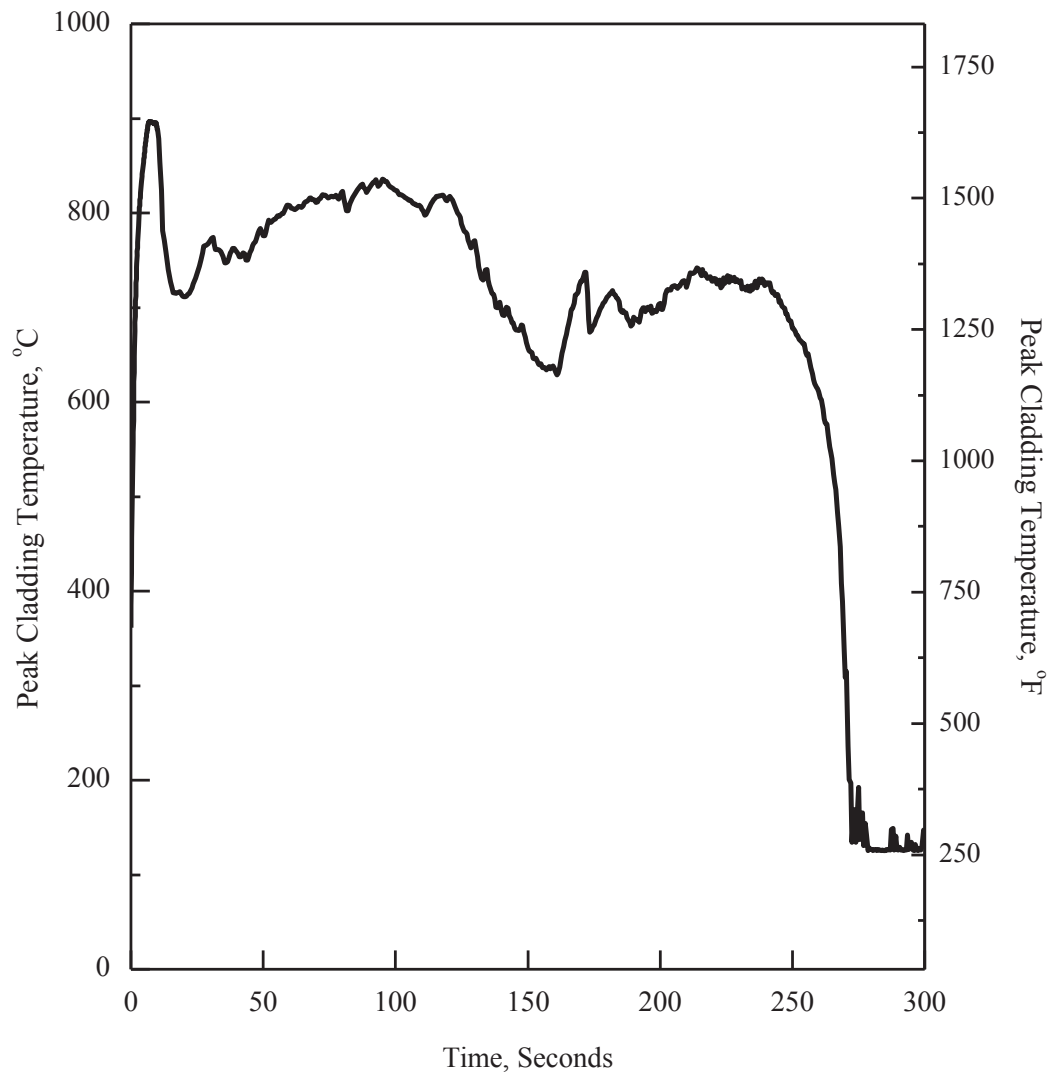


Figure 15.6.5-2 1.0 × Double-ended Guillotine Break in Pump Discharge Leg (Peak Cladding Temperature)

G



APR1400 DCD TIER 2

Replace with next page H

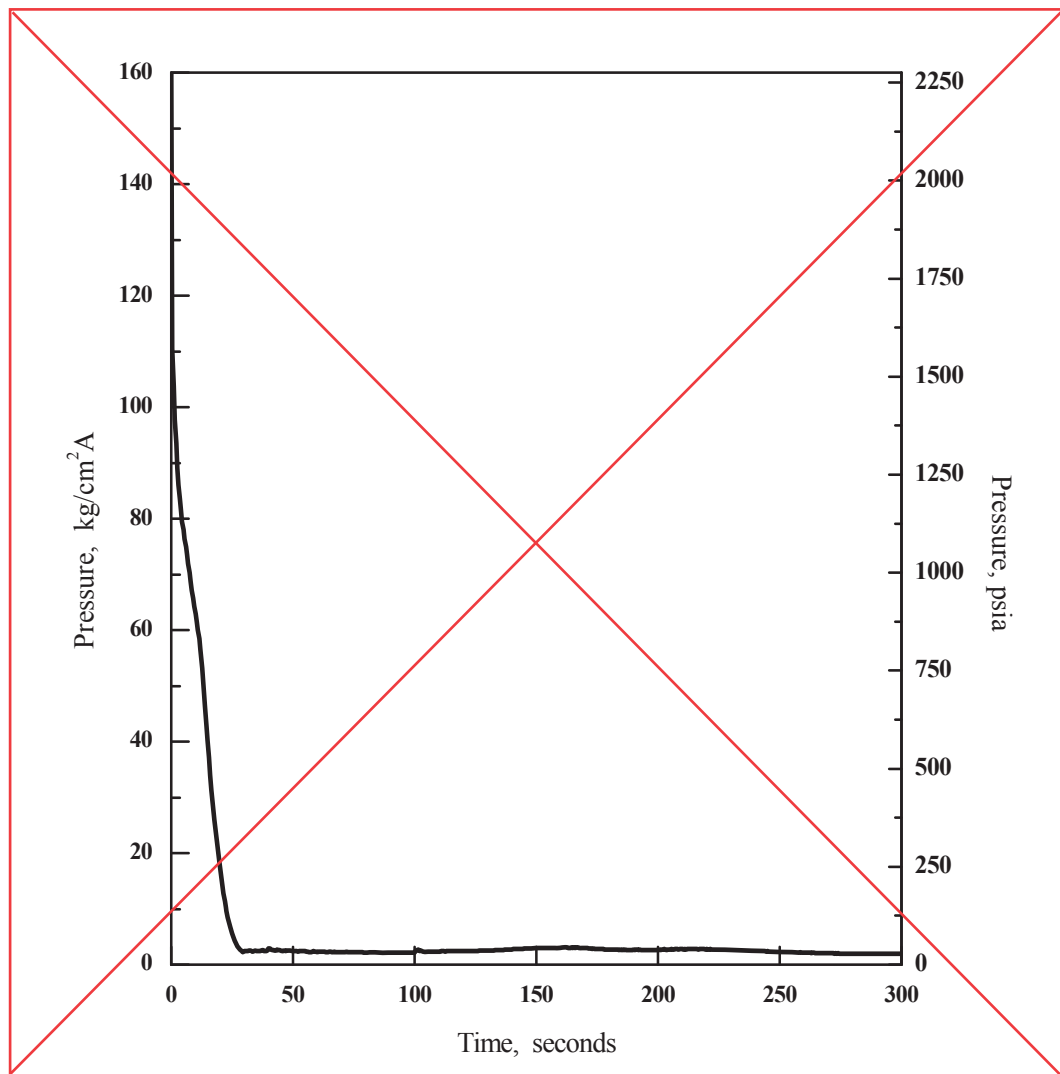
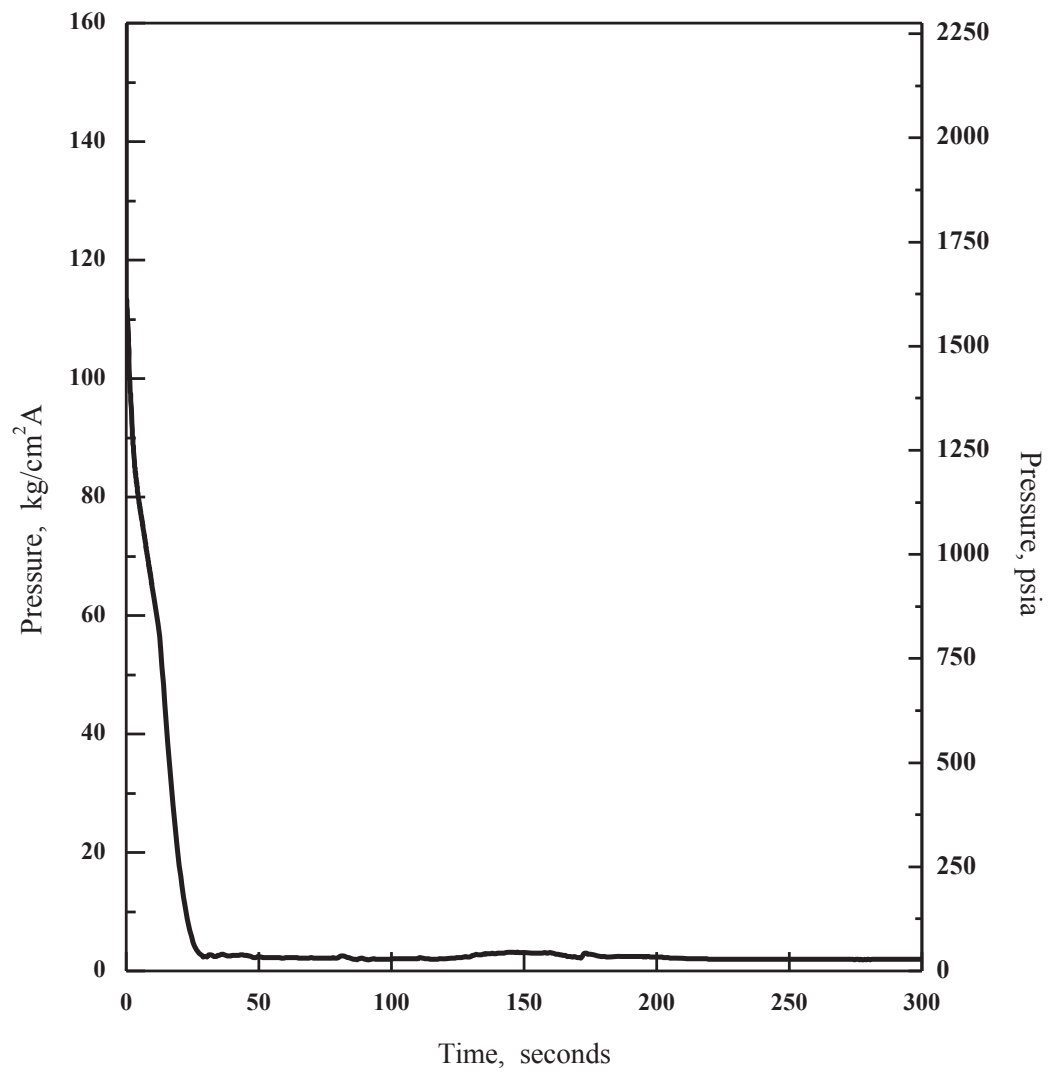


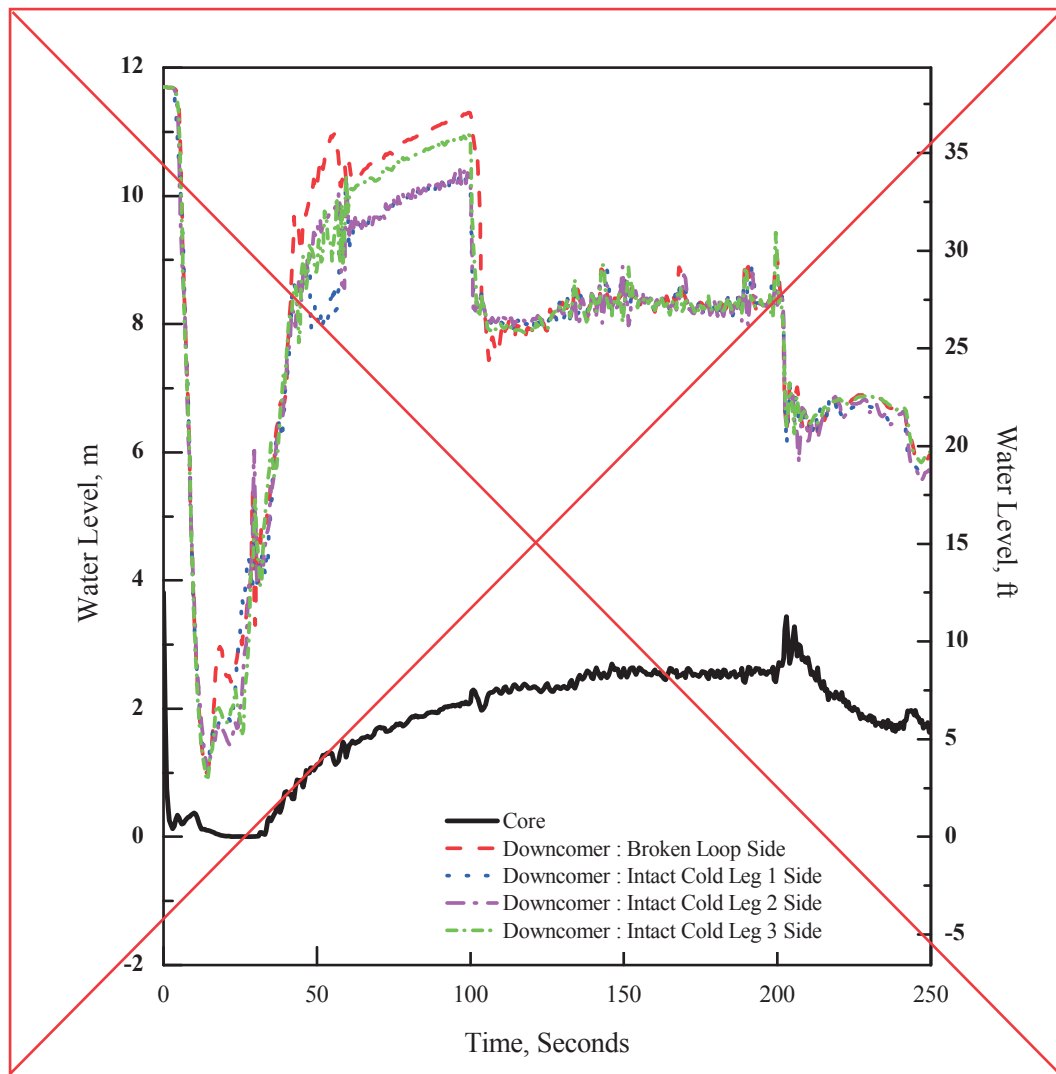
Figure 15.6.5-3 1.0 x Double-ended Guillotine Break in Pump Discharge Leg (Core Pressure)

H



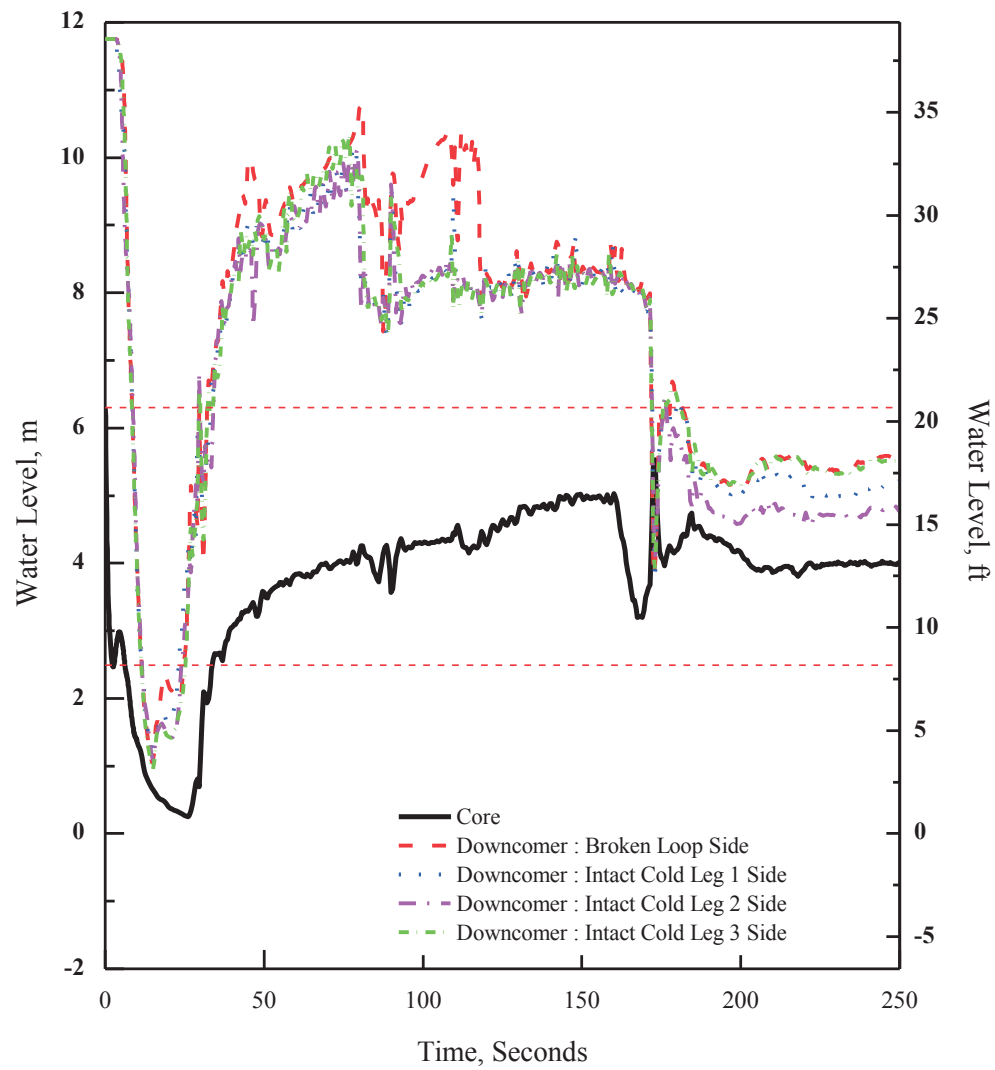
APR1400 DCD TIER 2

Replace with next page I



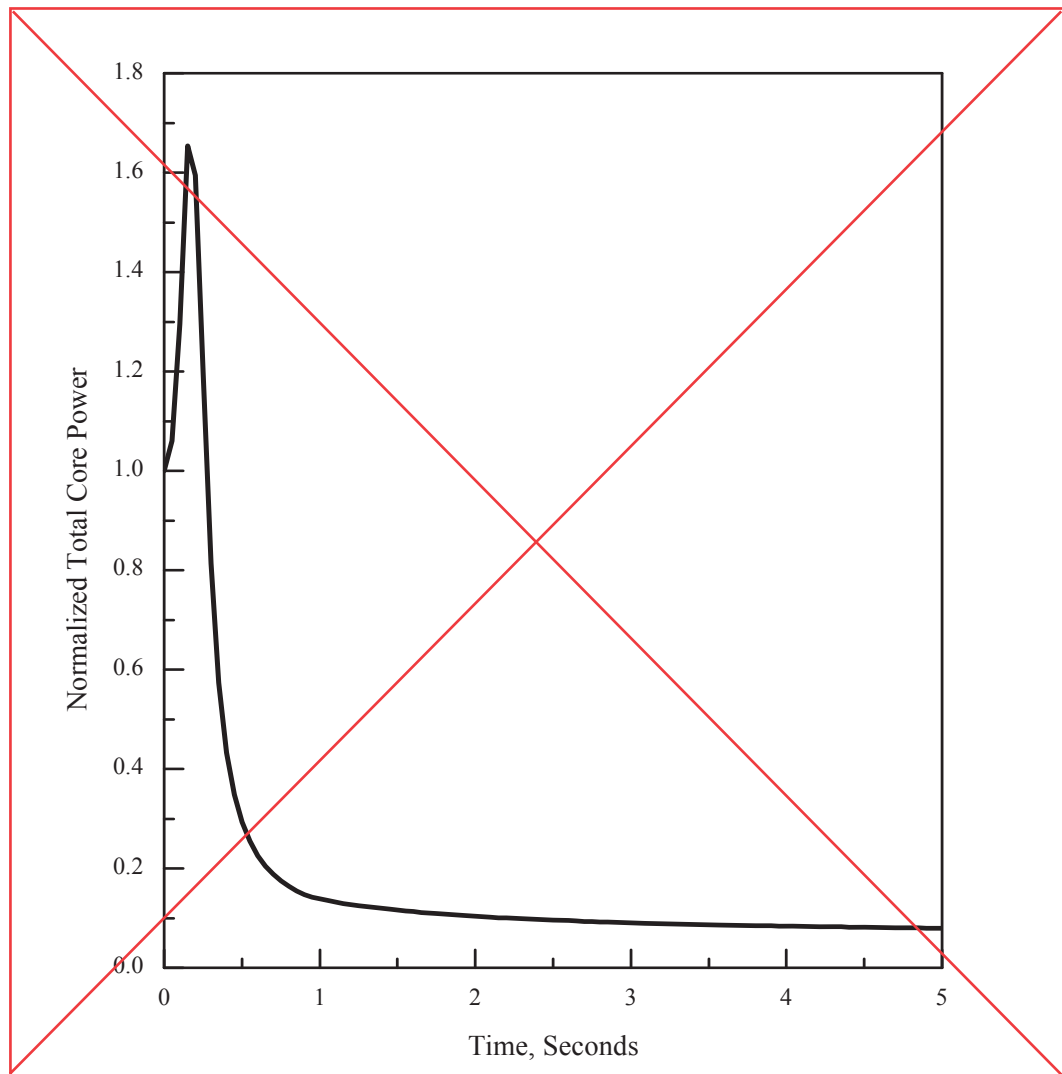
**Figure 15.6.5-4 1.0 × Double-ended Guillotine Break in Pump Discharge Leg
(Water Level in Core and Downcommer)**

I



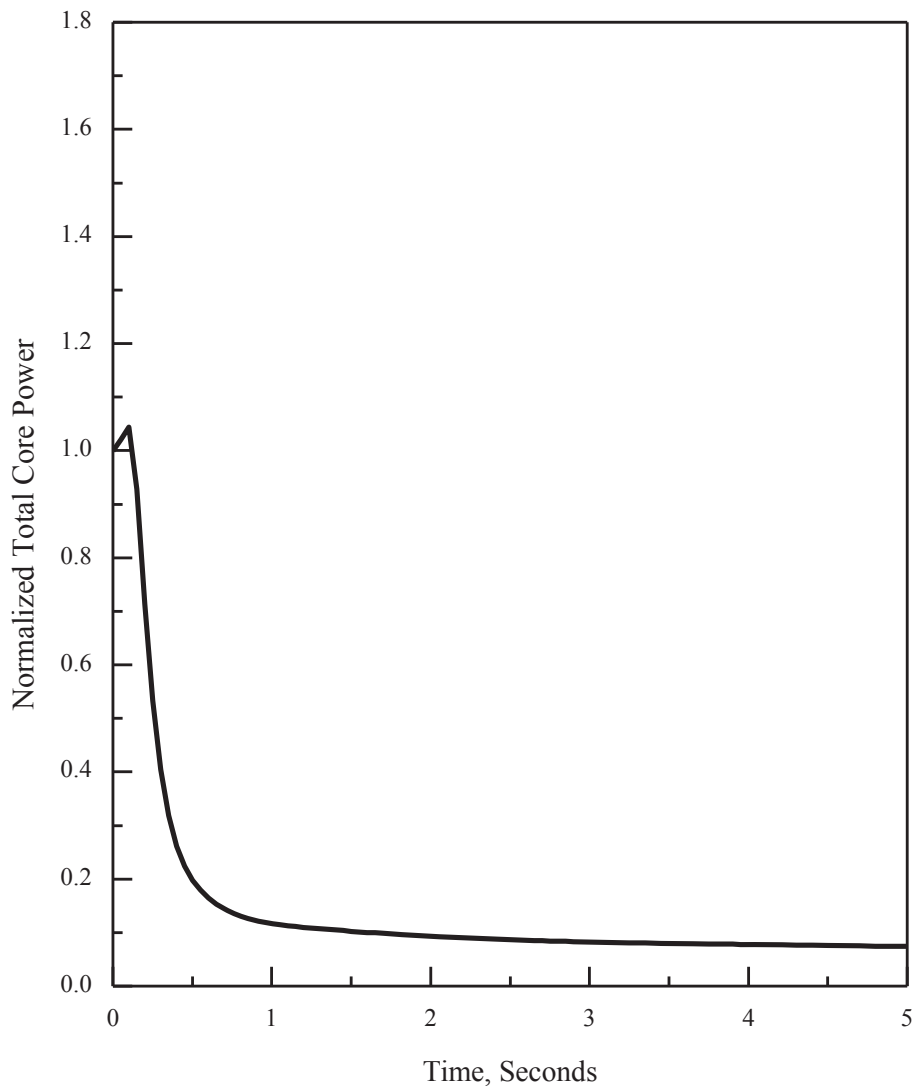
APR1400 DCD TIER 2

Replace with next page J



**Figure 15.6.5-5 1.0 × Double-ended Guillotine Break in Pump Discharge Leg
(Normalized Core Power)**

J



APR1400 DCD TIER 2

Replace with next page K

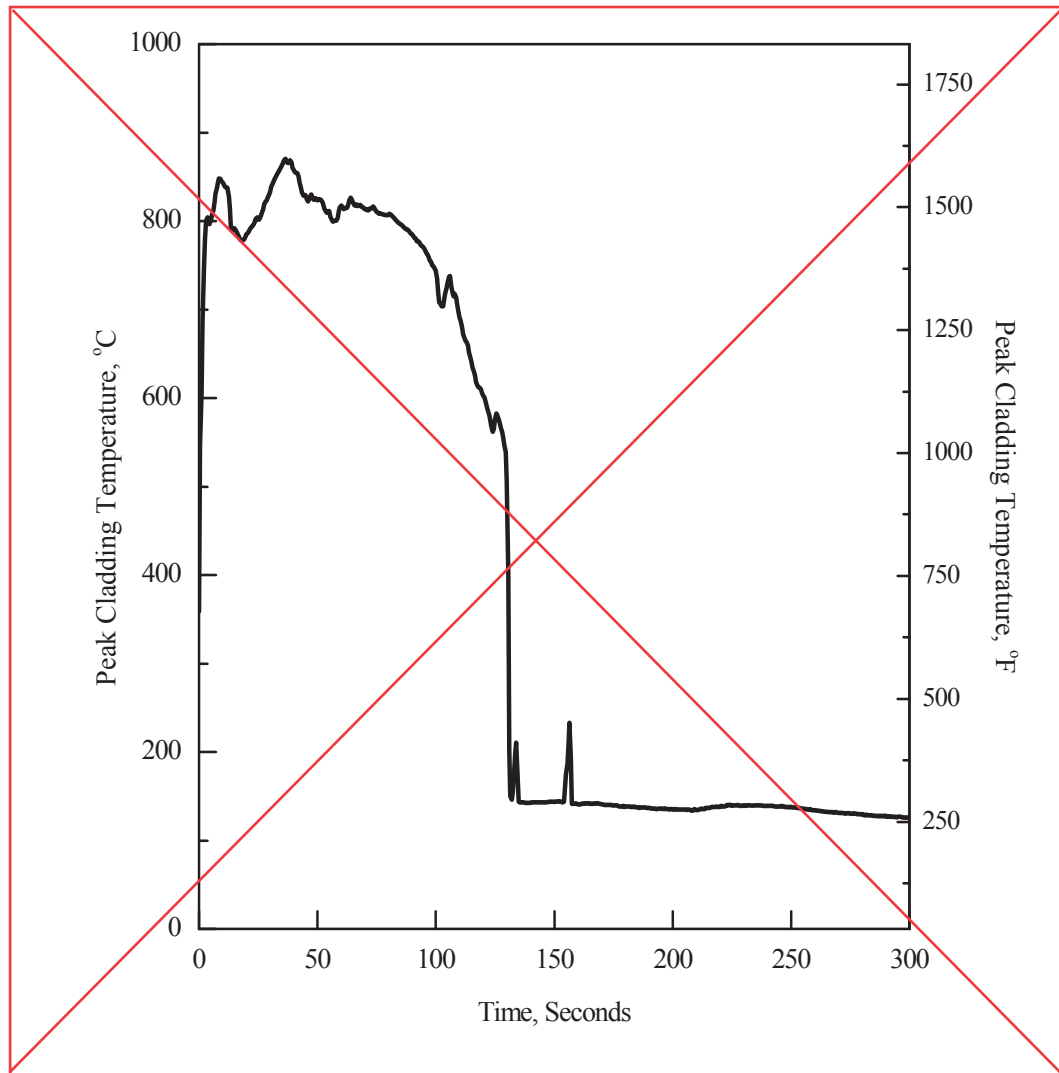
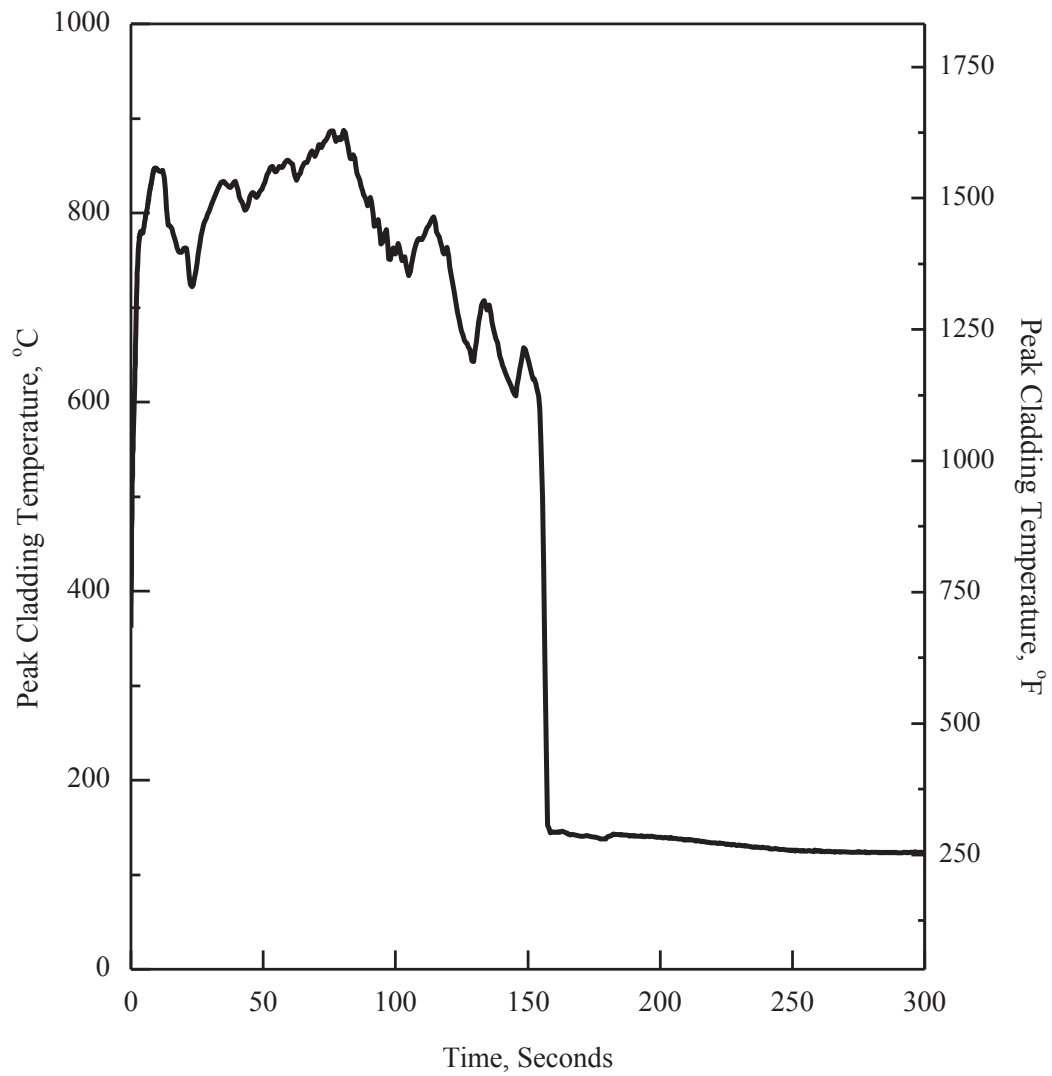


Figure 15.6.5-6 0.8 × Double-ended Guillotine Break in Pump Discharge Leg (Peak Cladding Temperature)

K



APR1400 DCD TIER 2

Replace with next page L

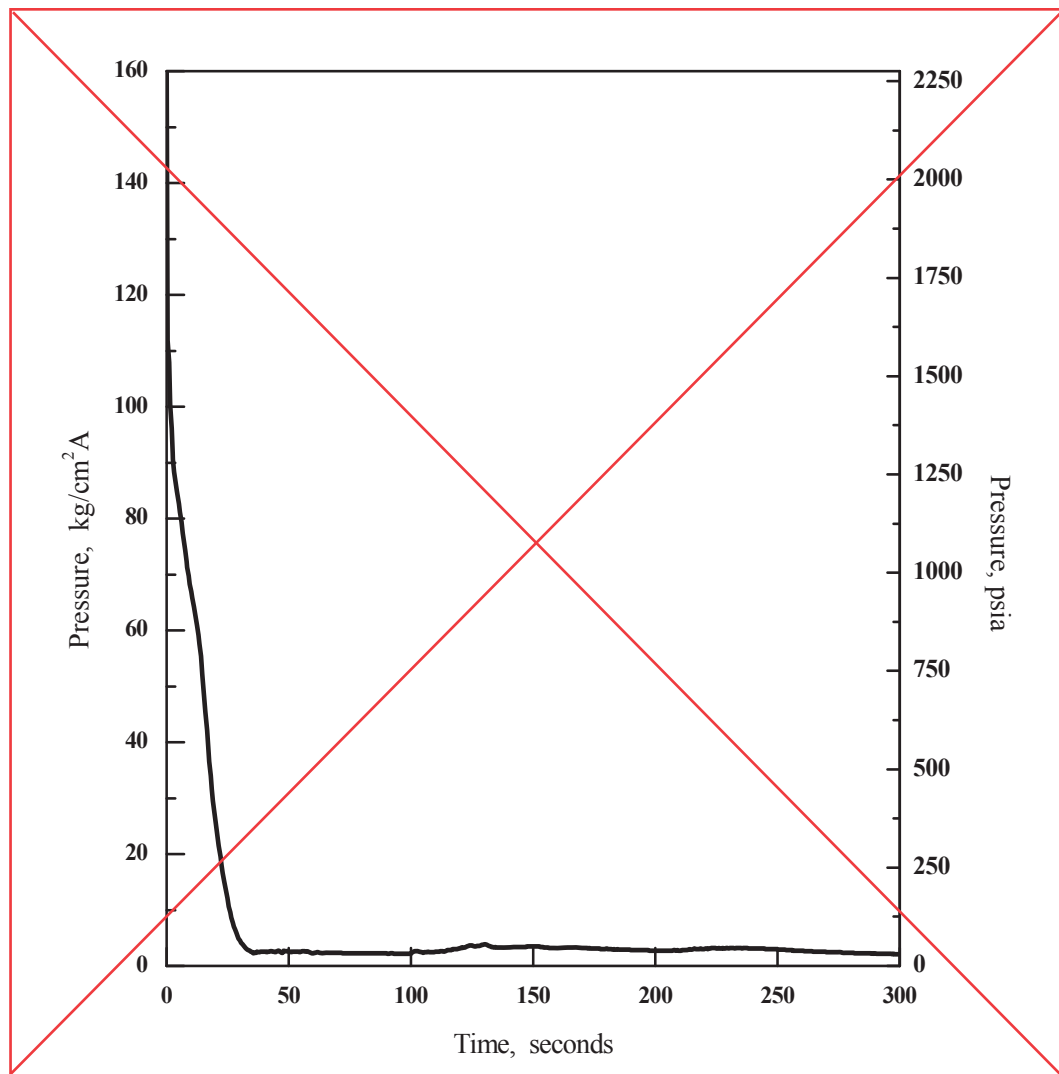
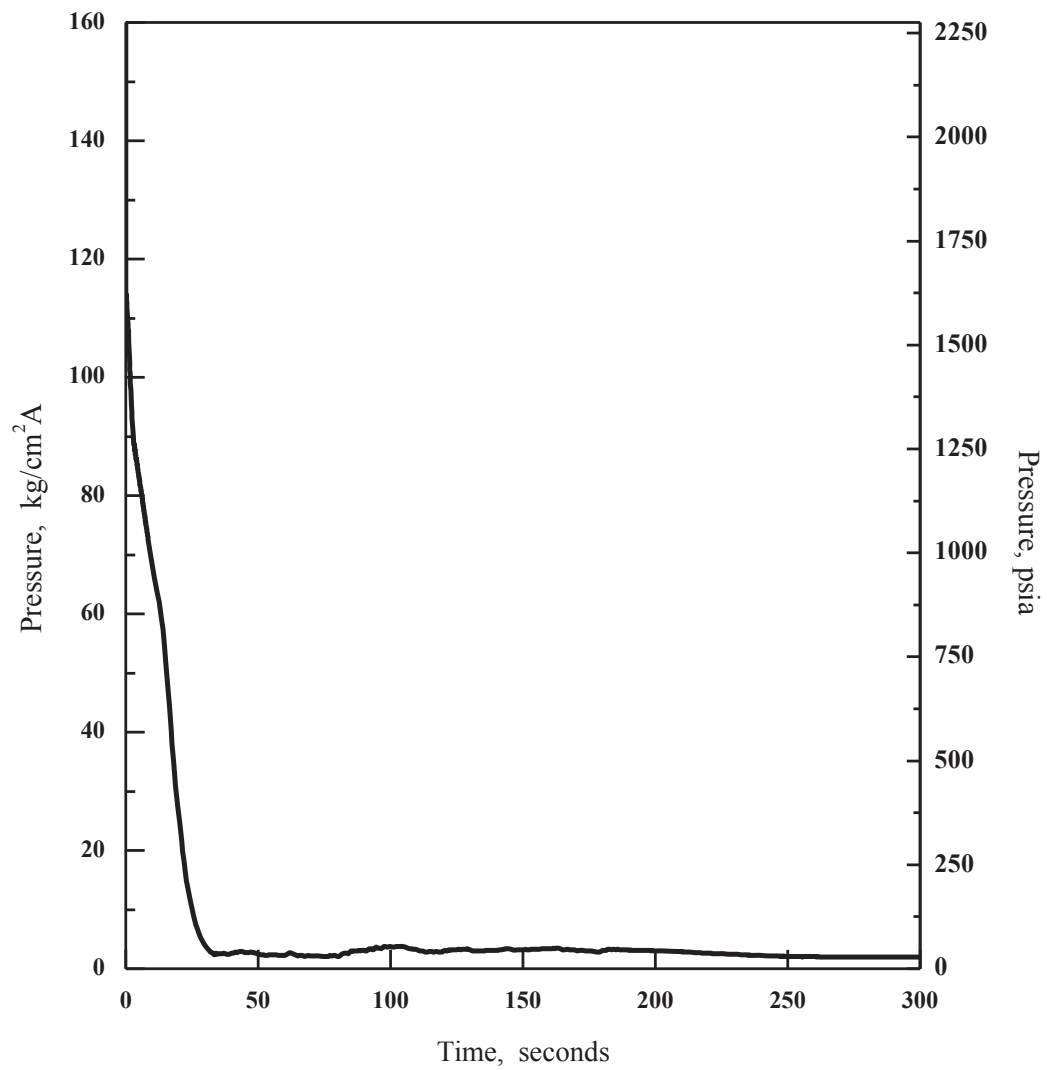


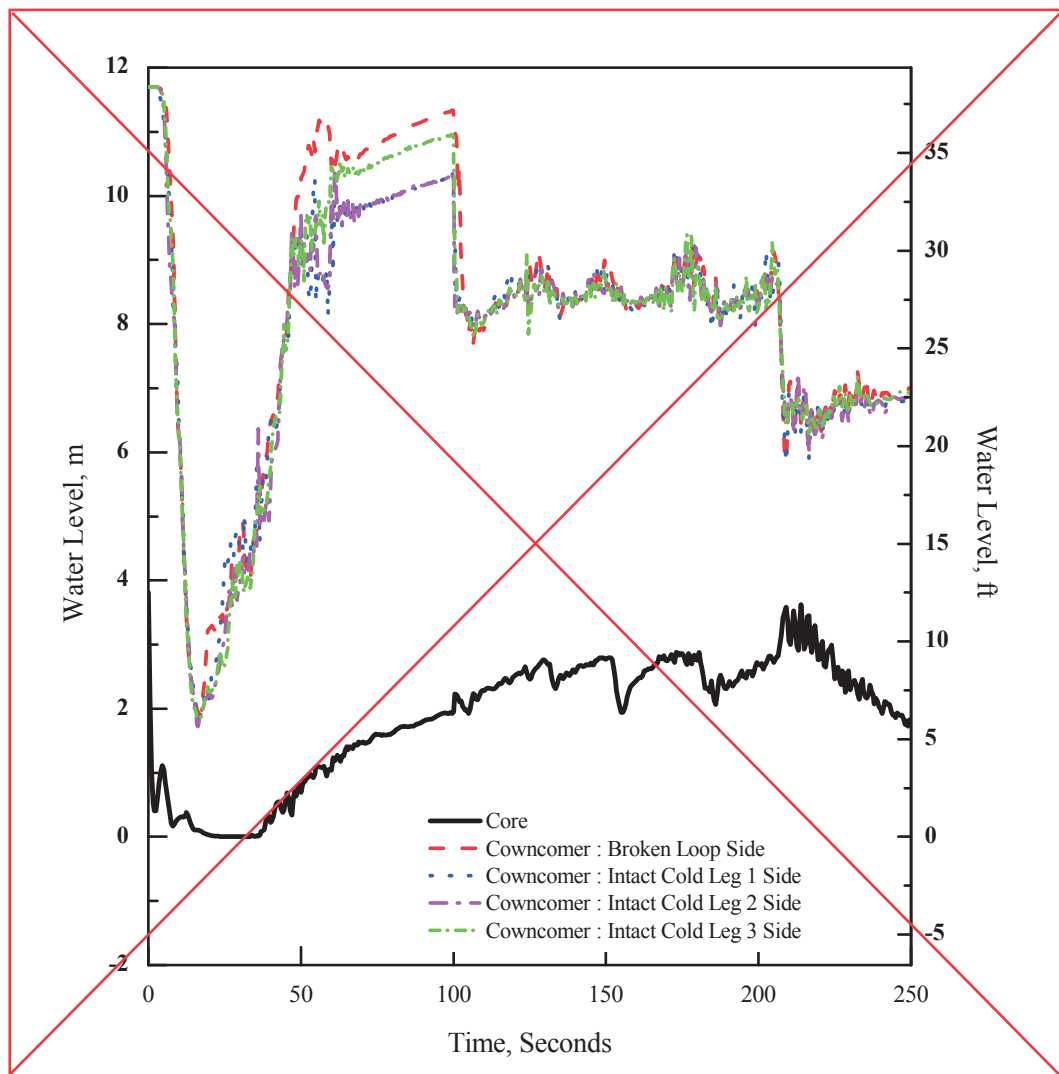
Figure 15.6.5-7 0.8 x Double-ended Guillotine Break in Pump Discharge Leg
(Core Pressure)

L



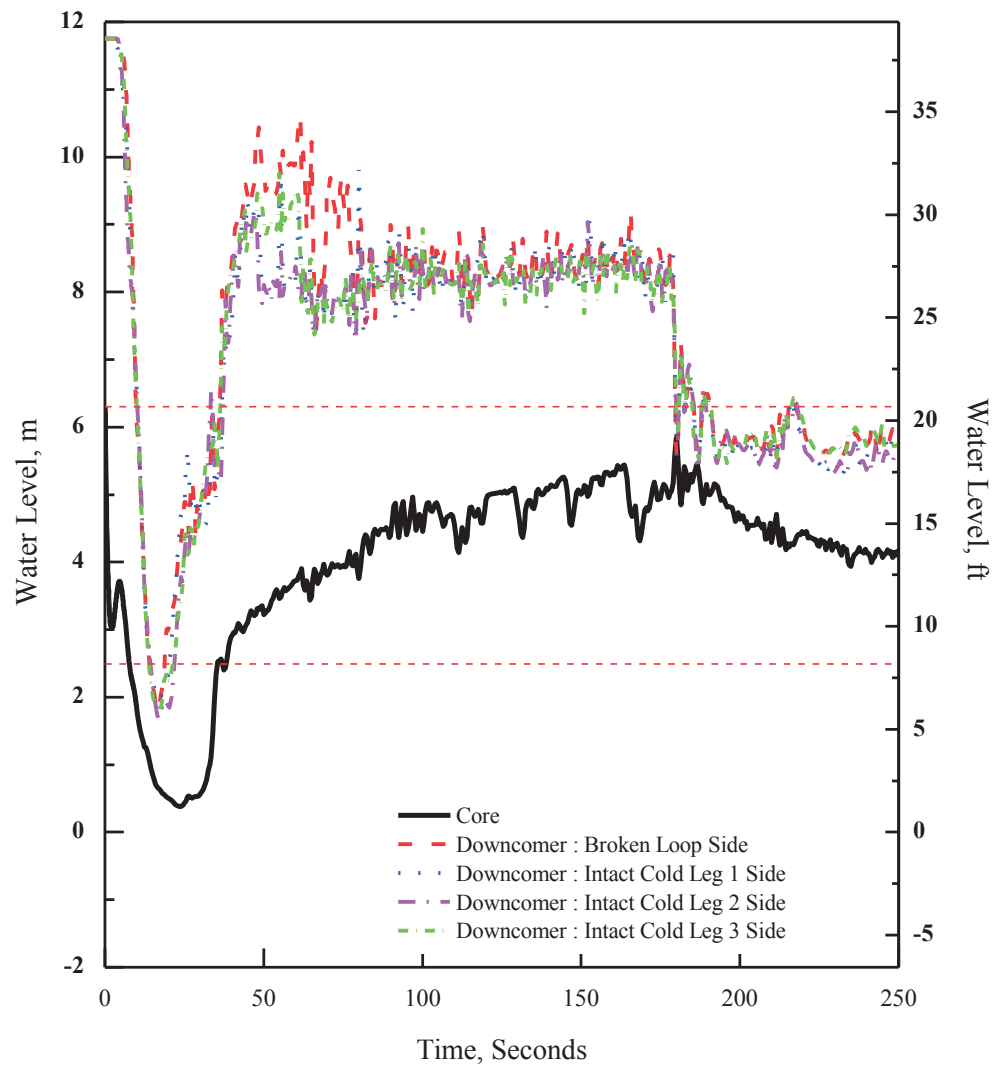
APR1400 DCD TIER 2

Replace with next page M



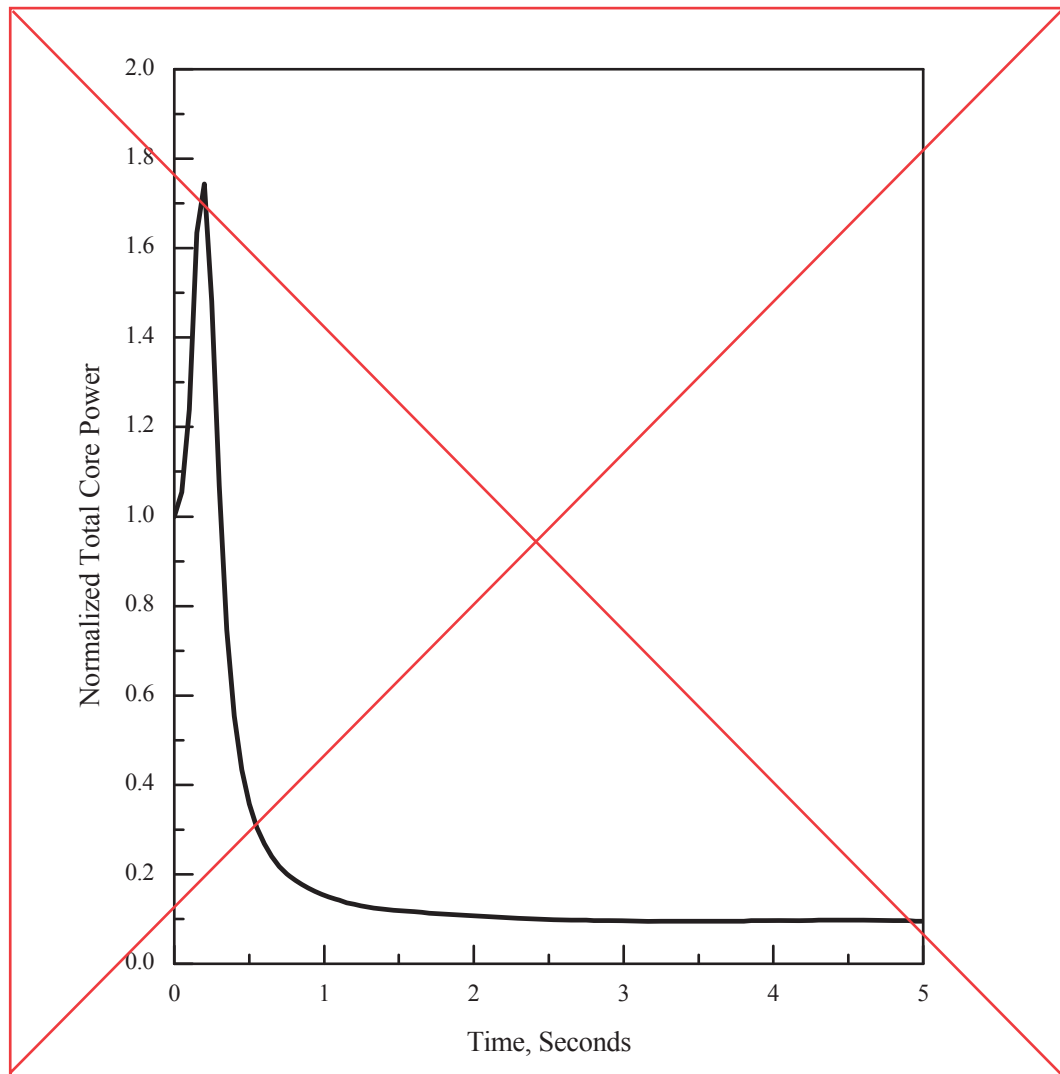
**Figure 15.6.5-8 0.8 × Double-ended Guillotine Break in Pump Discharge Leg
(Water Level in Core and Downcommer)**

M



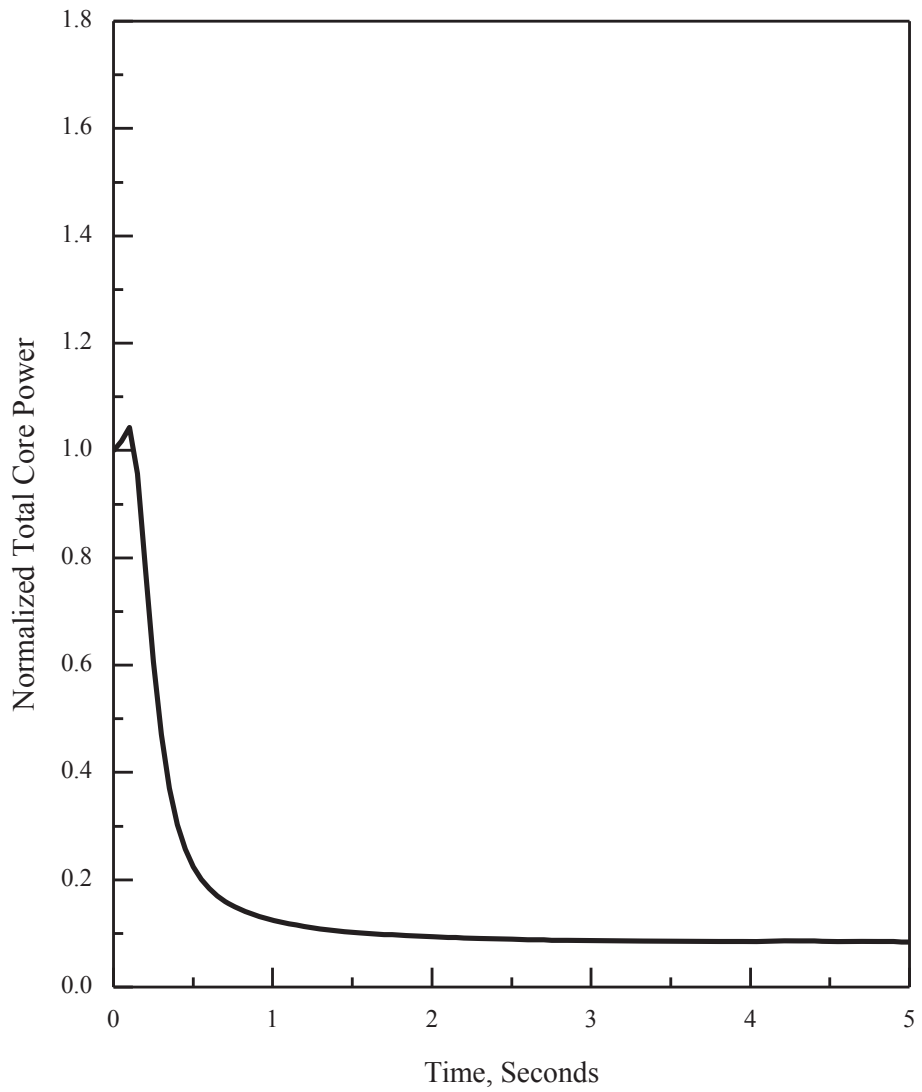
APR1400 DCD TIER 2

Replace with next page N



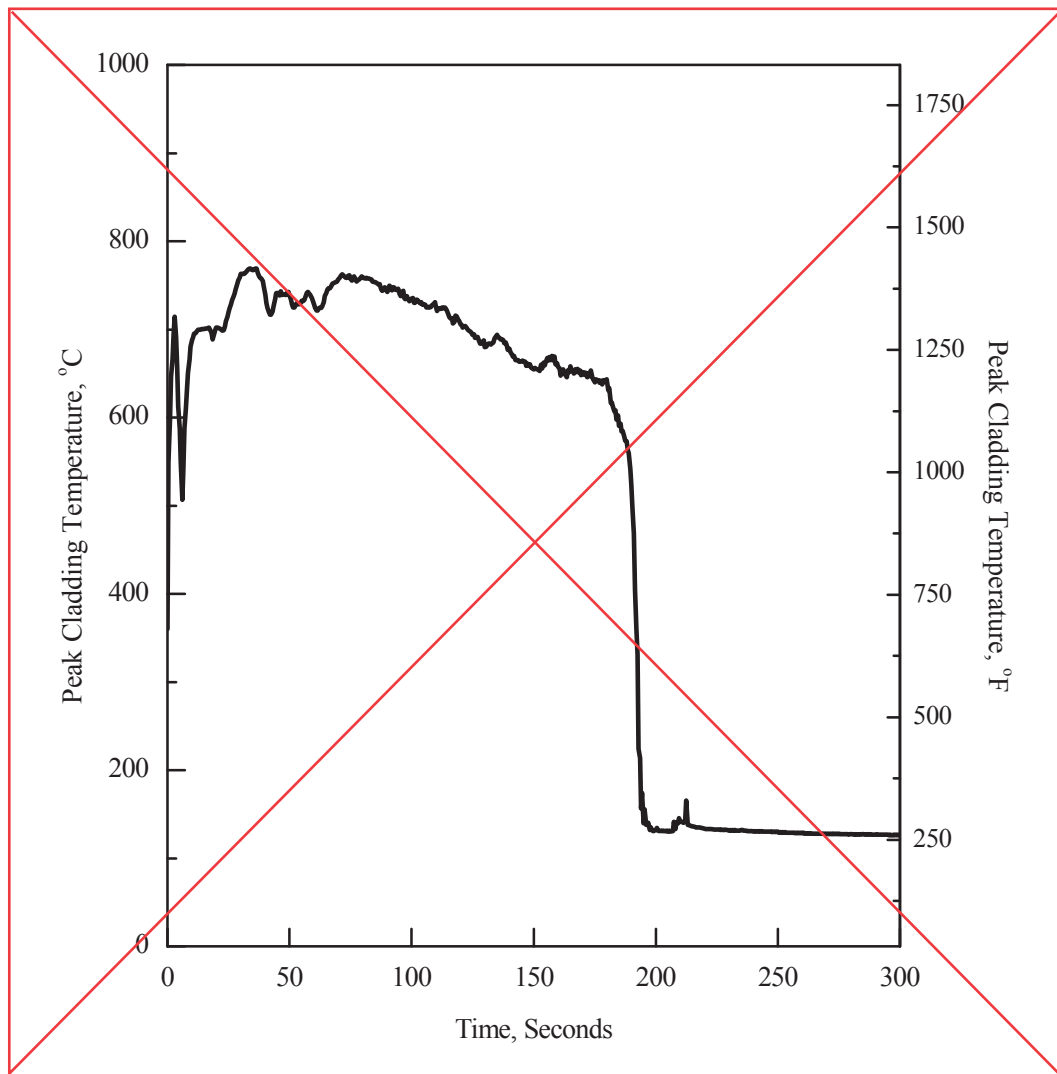
**Figure 15.6.5-9 0.8 × Double-ended Guillotine Break in Pump Discharge Leg
(Normalized Core Power)**

N



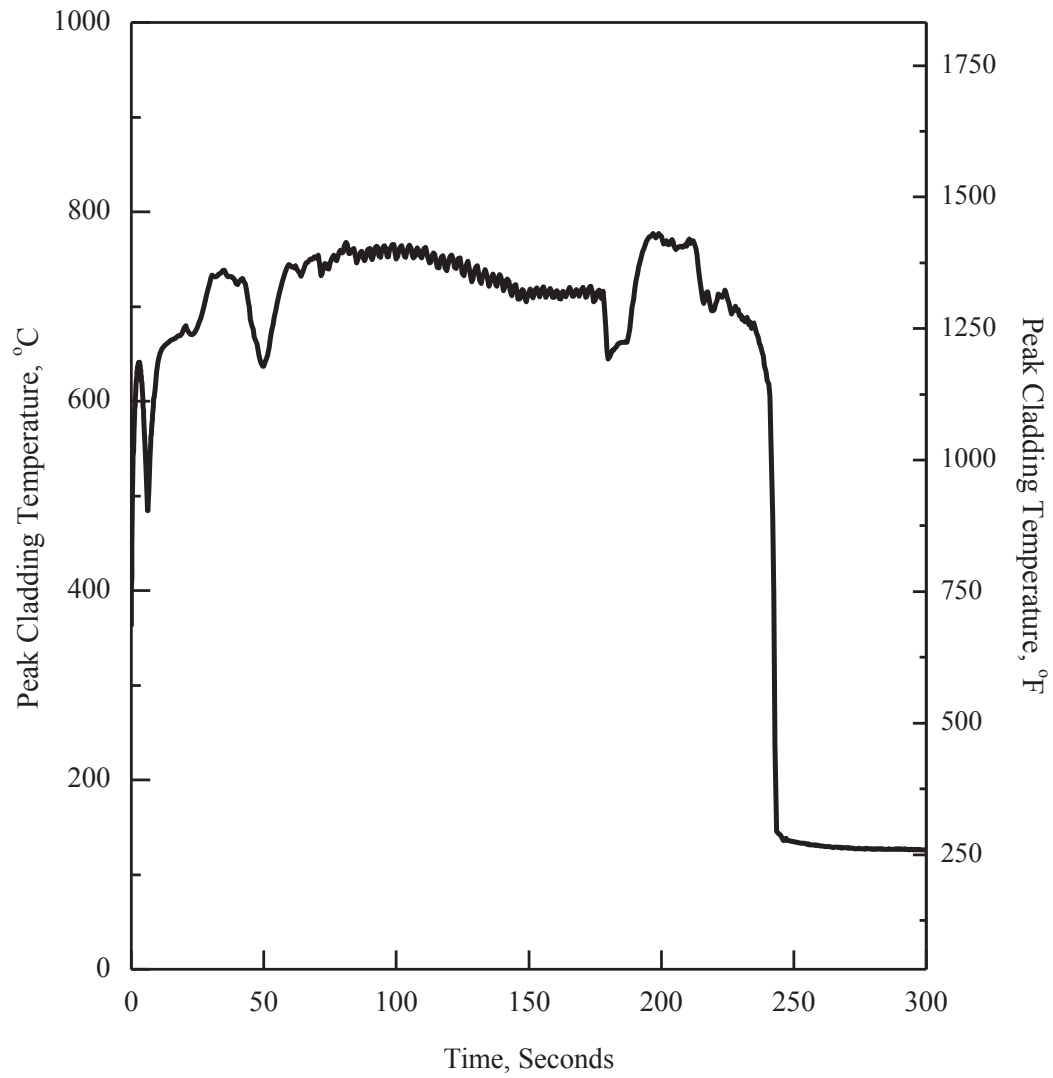
APR1400 DCD TIER 2

Replace with next page O



**Figure 15.6.5-10 0.6 × Double-ended Guillotine Break in Pump Discharge Leg
(Peak Cladding Temperature)**

O



APR1400 DCD TIER 2

Replace with next page P

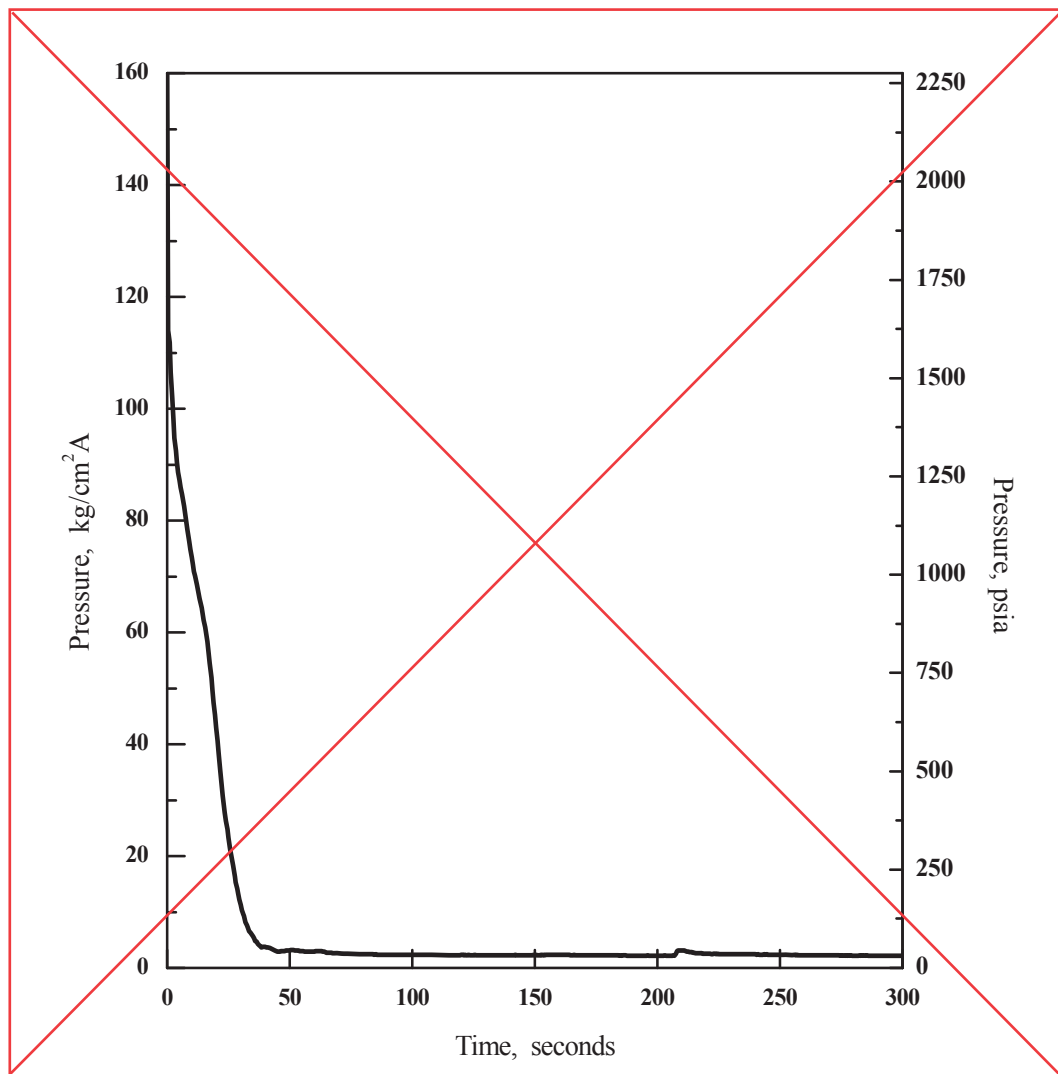
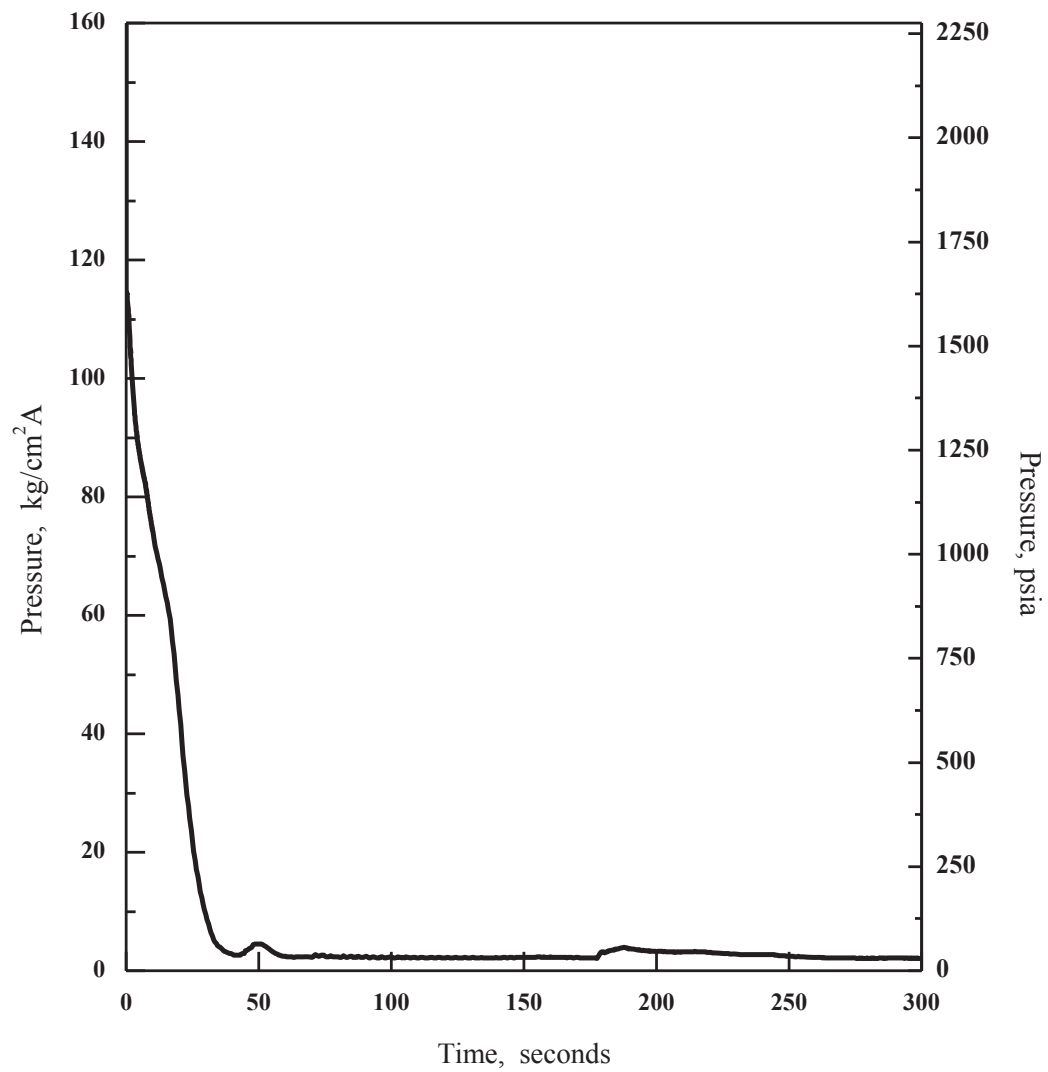


Figure 15.6.5-11 0.6 × Double-ended Guillotine Break in Pump Discharge Leg
(Core Pressure)

P



APR1400 DCD TIER 2

Replace with next page Q

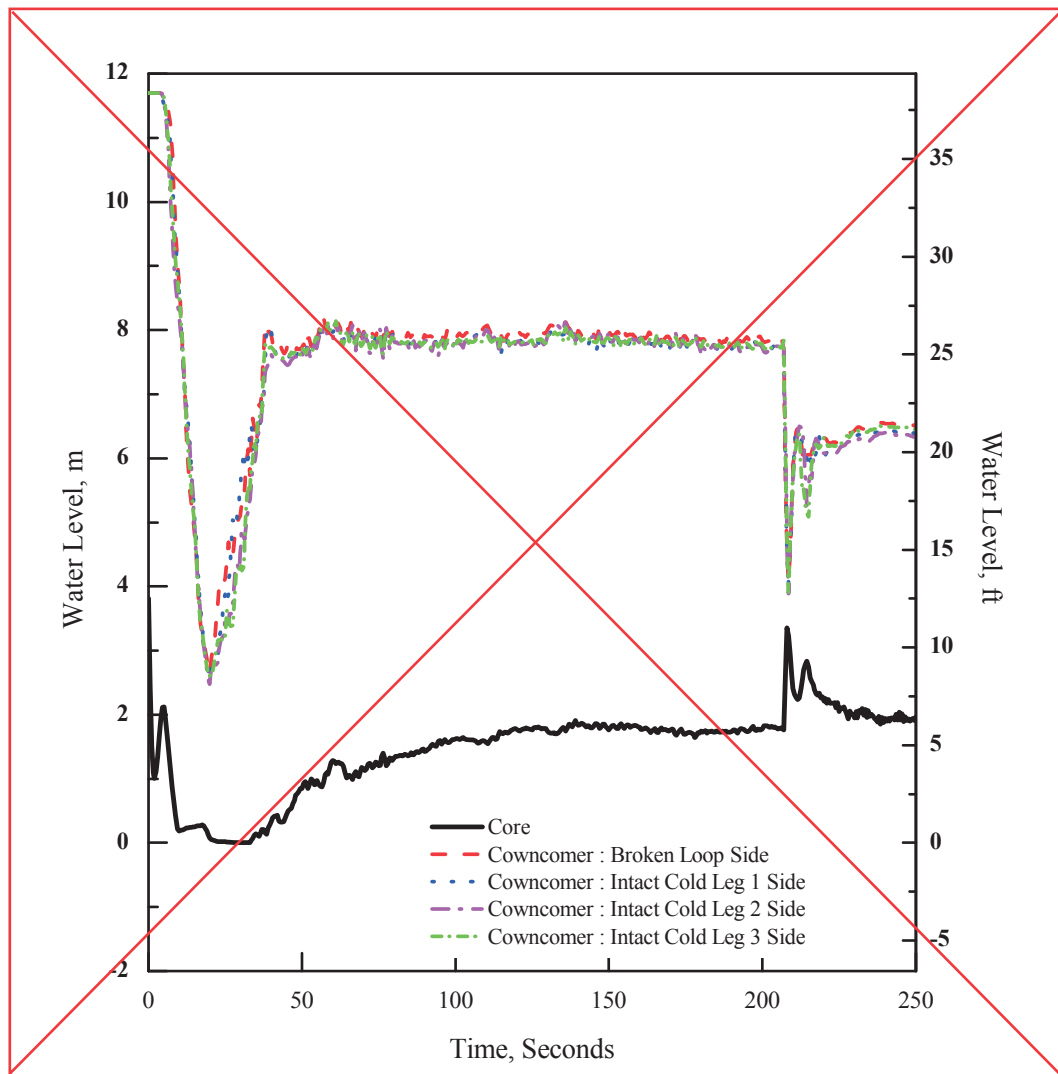
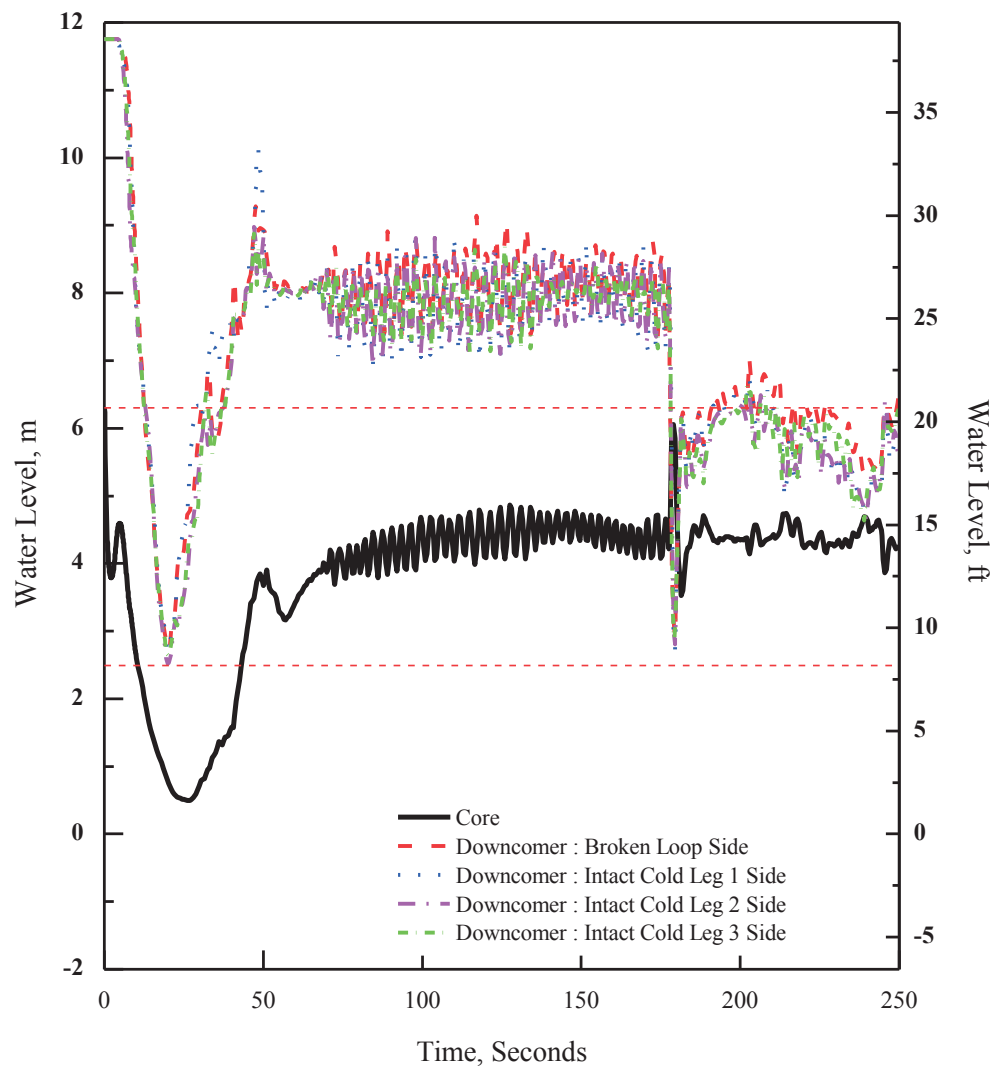


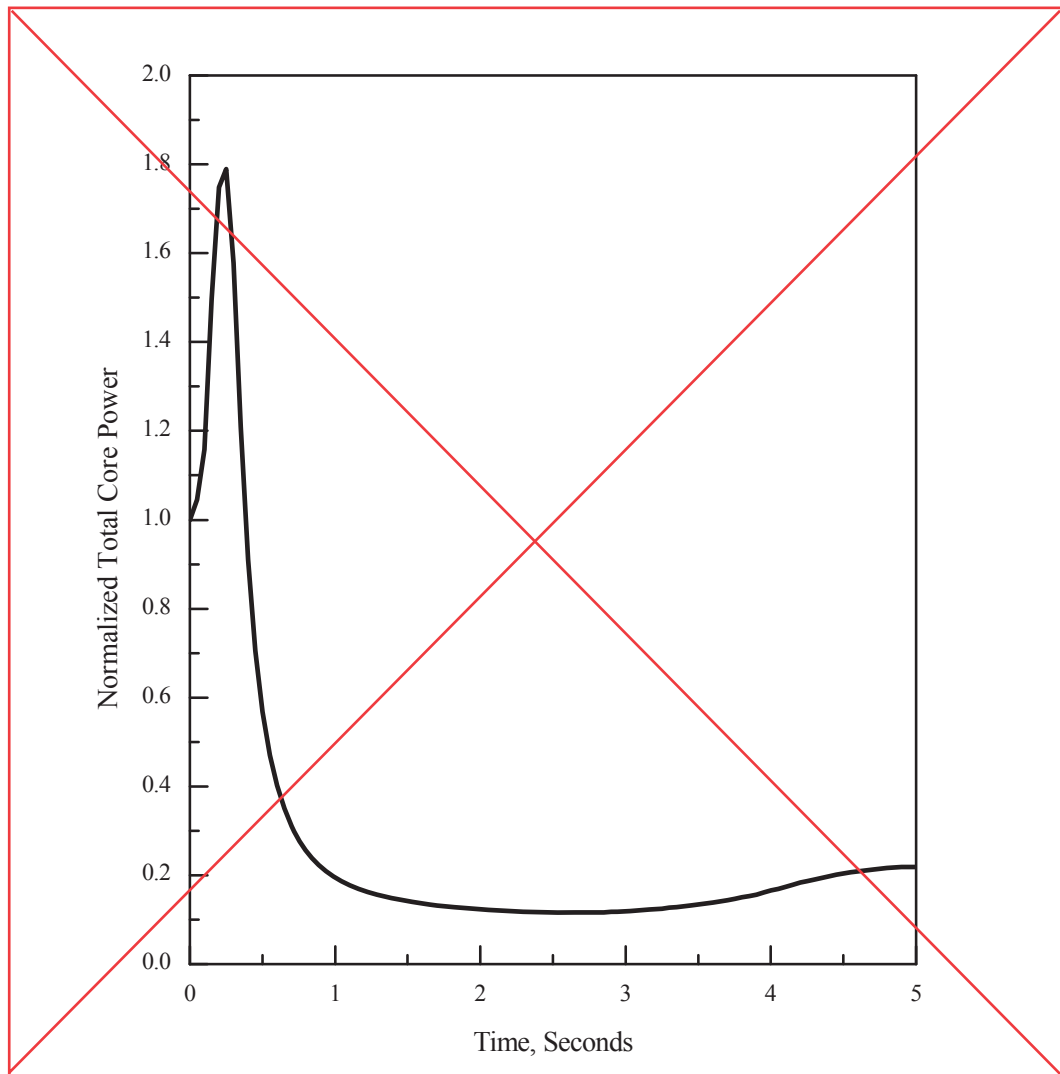
Figure 15.6.5-12 0.6 × Double-ended Guillotine Break in Pump Discharge Leg
(Water Level in Core and Downcommer)

Q



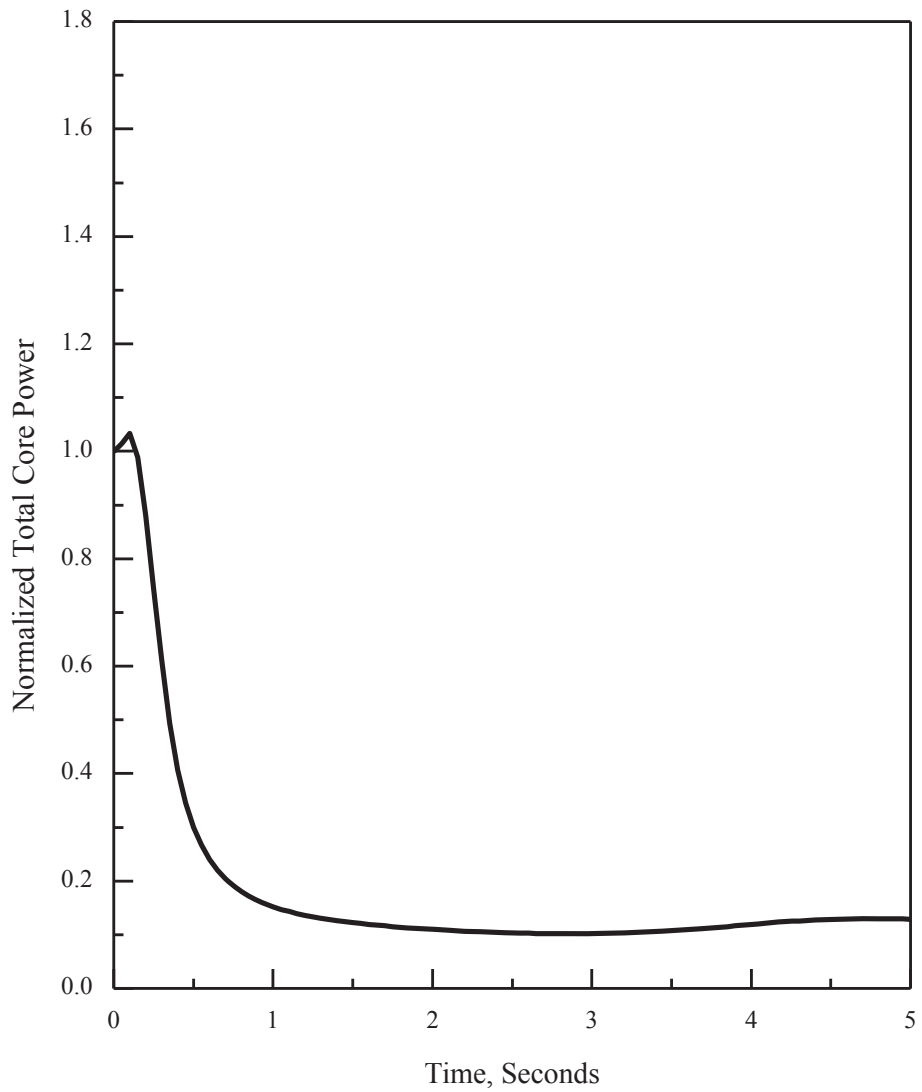
APR1400 DCD TIER 2

Replace with next page R



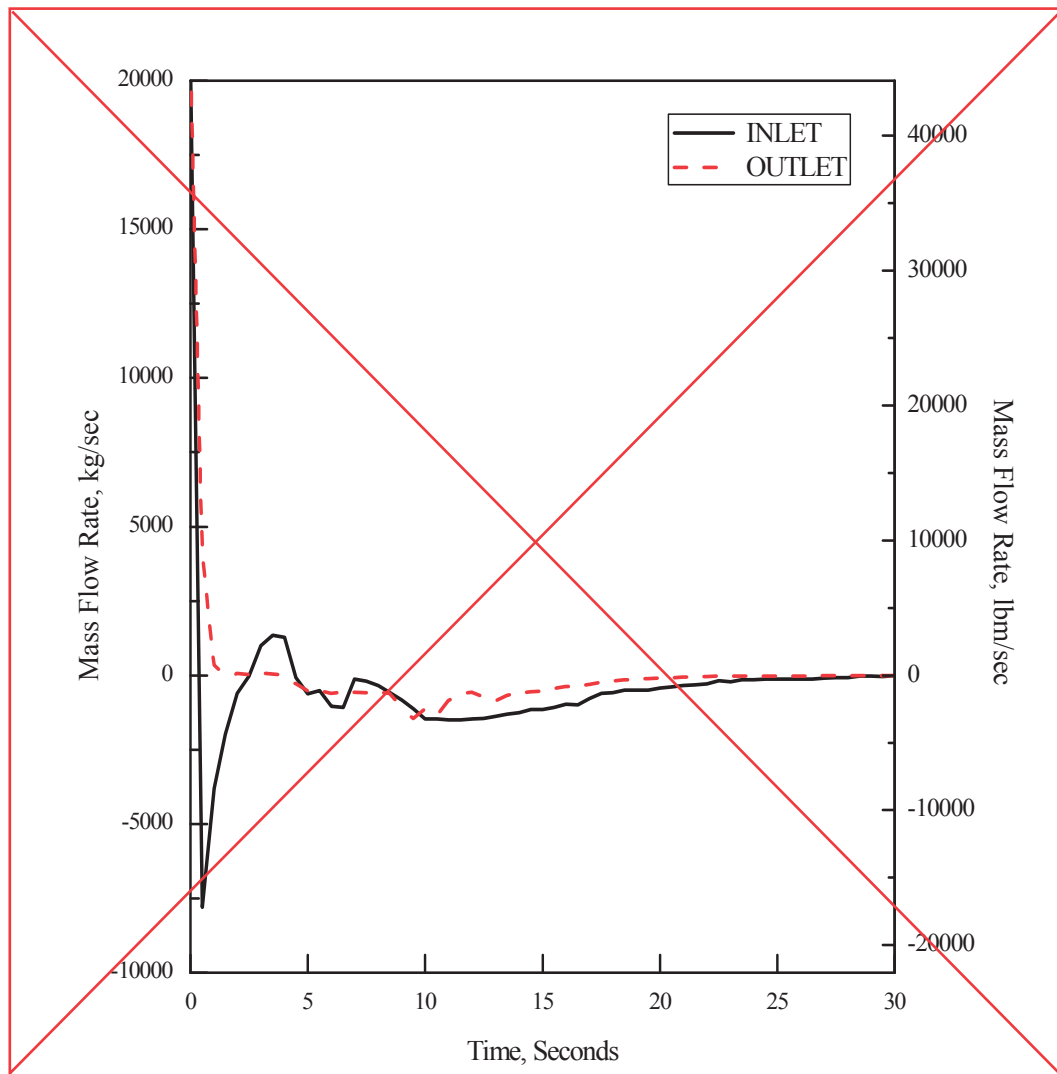
**Figure 15.6.5-13 0.6 × Double-ended Guillotine Break in Pump Discharge Leg
(Normalized Core Power)**

| |
|---|
| R |
|---|



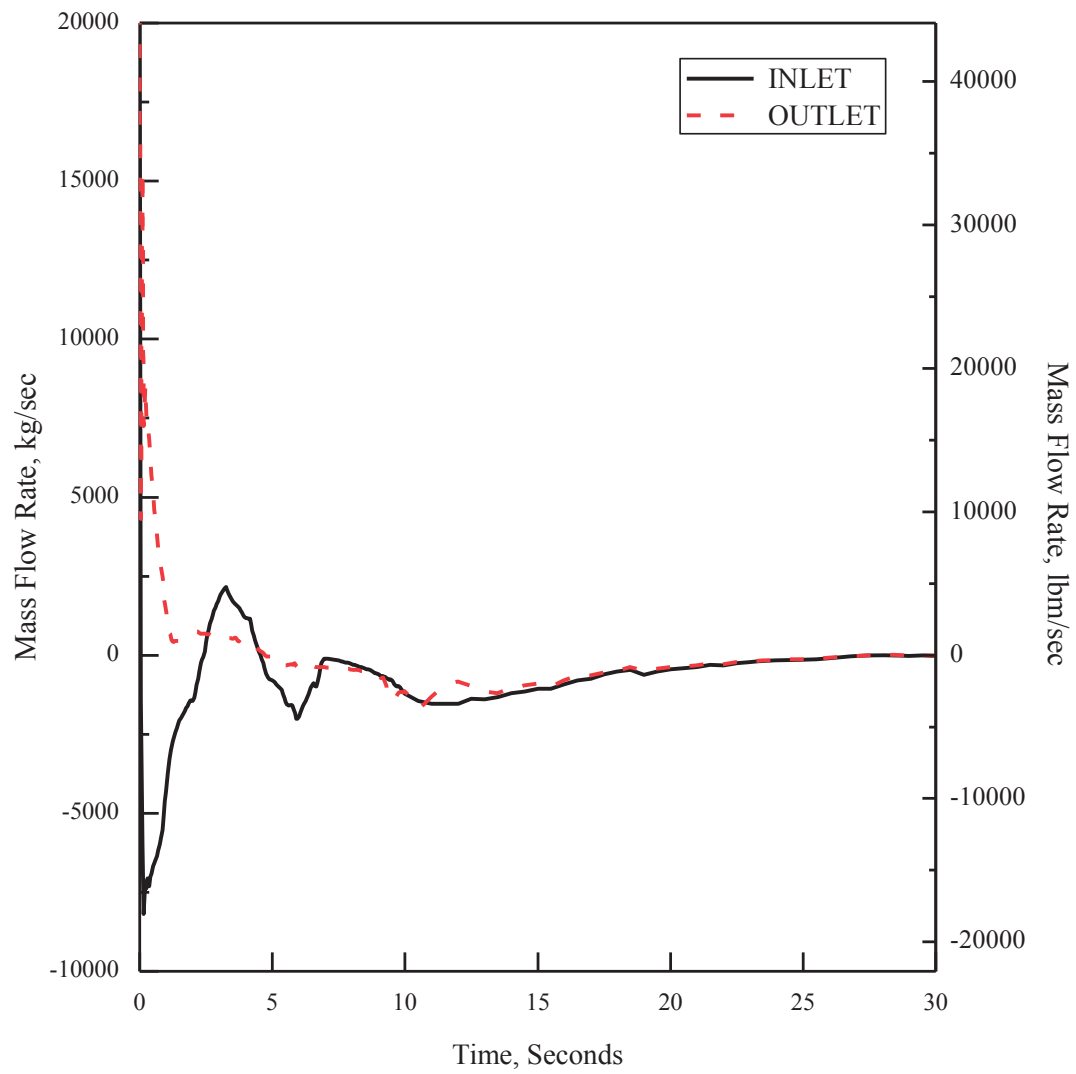
APR1400 DCD TIER 2

Replace with next page S



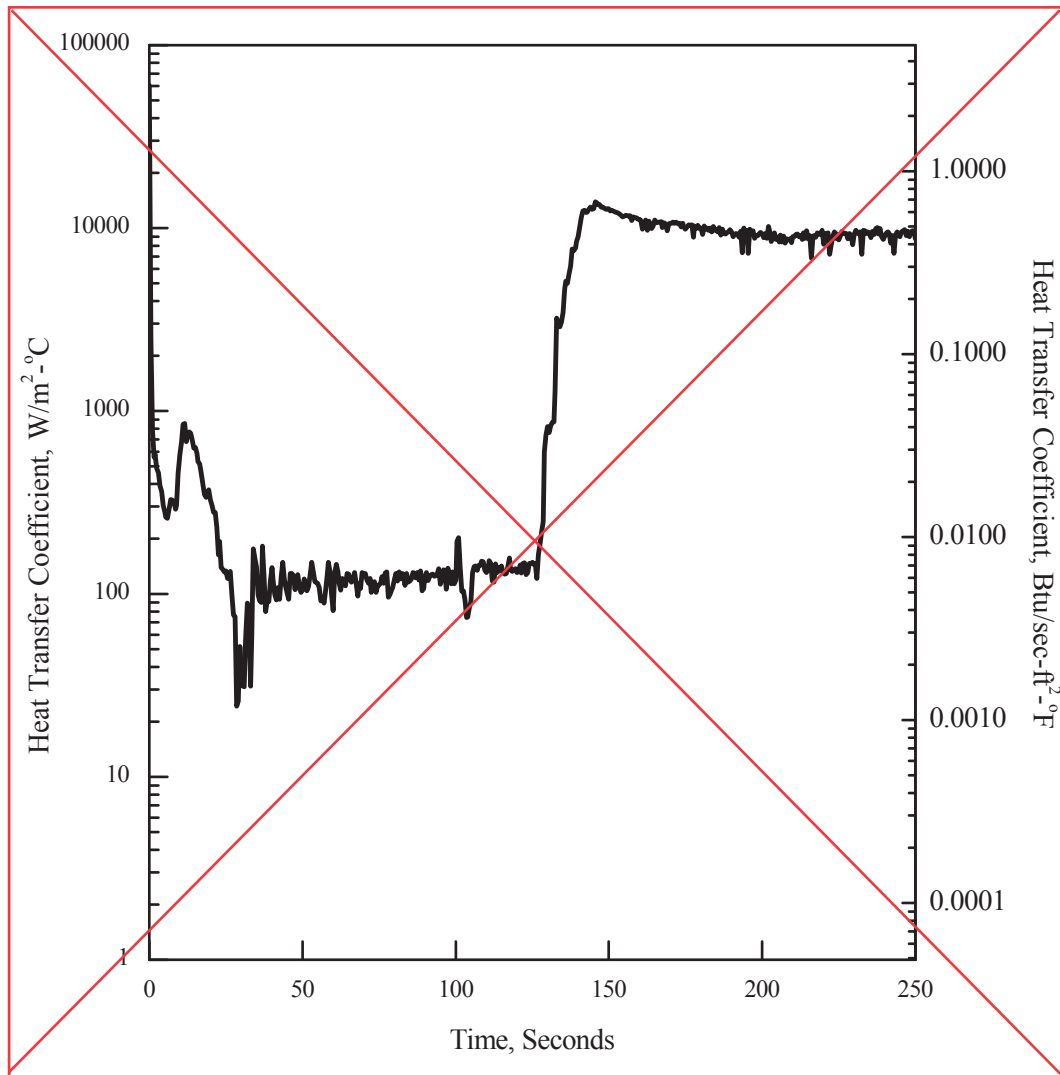
**Figure 15.6.5-14 1.0 × Double-ended Guillotine Break in Pump Discharge Leg
(Core Inlet and Outlet Mass Flow)**

S



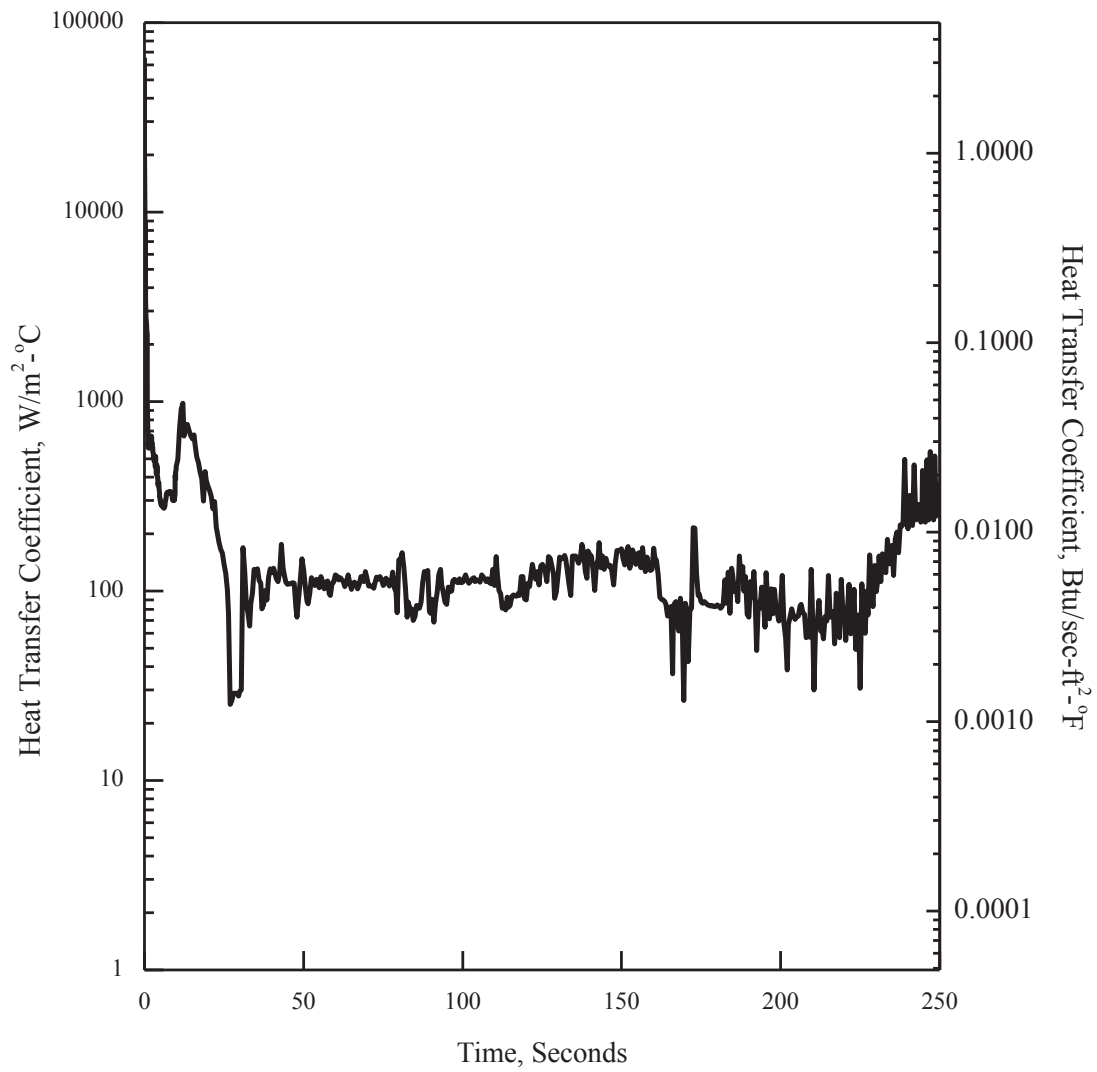
APR1400 DCD TIER 2

Replace with next page T



**Figure 15.6.5-15 1.0 × Double-ended Guillotine Break in Pump Discharge Leg
(Hot Spot Heat Transfer Coefficient)**

T



APR1400 DCD TIER 2

Replace with next page U

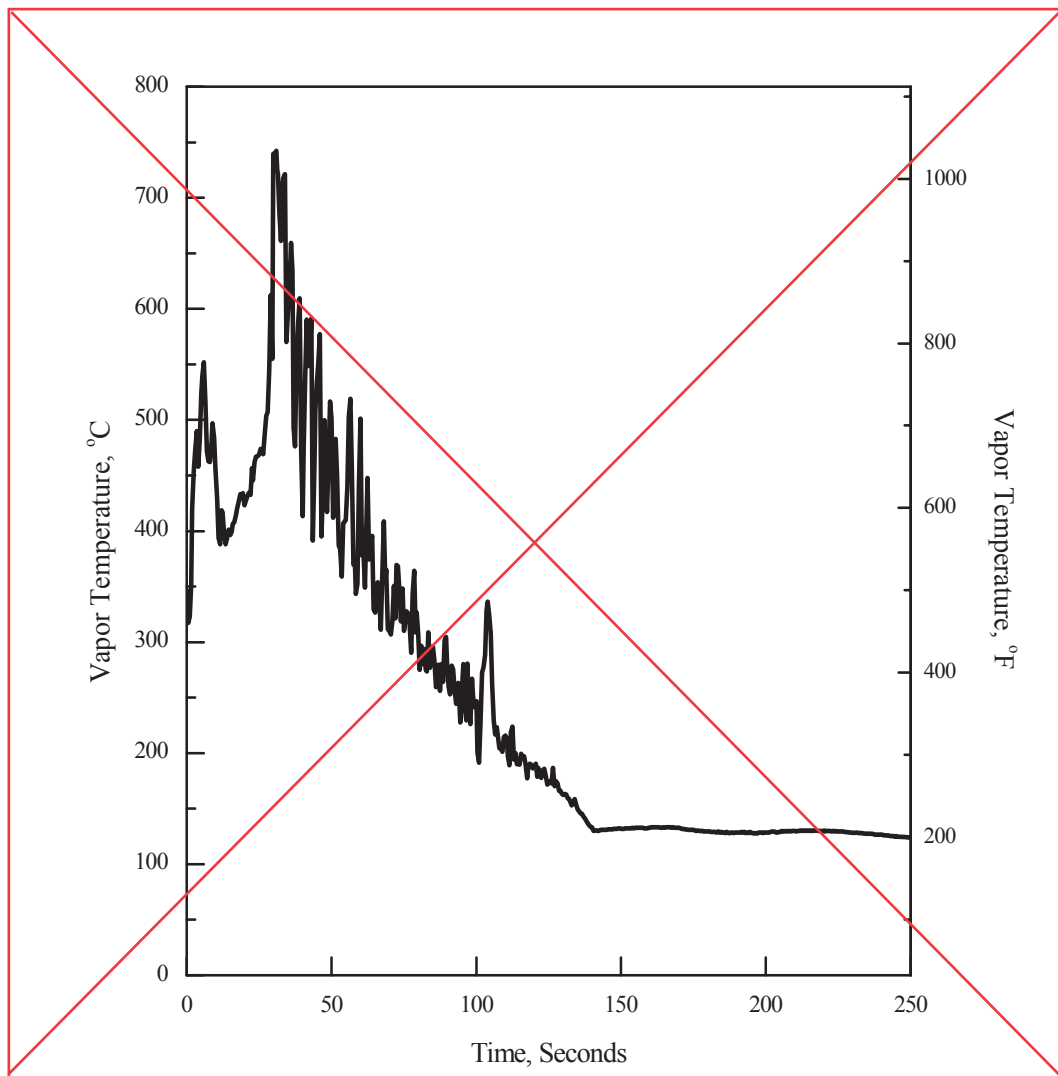
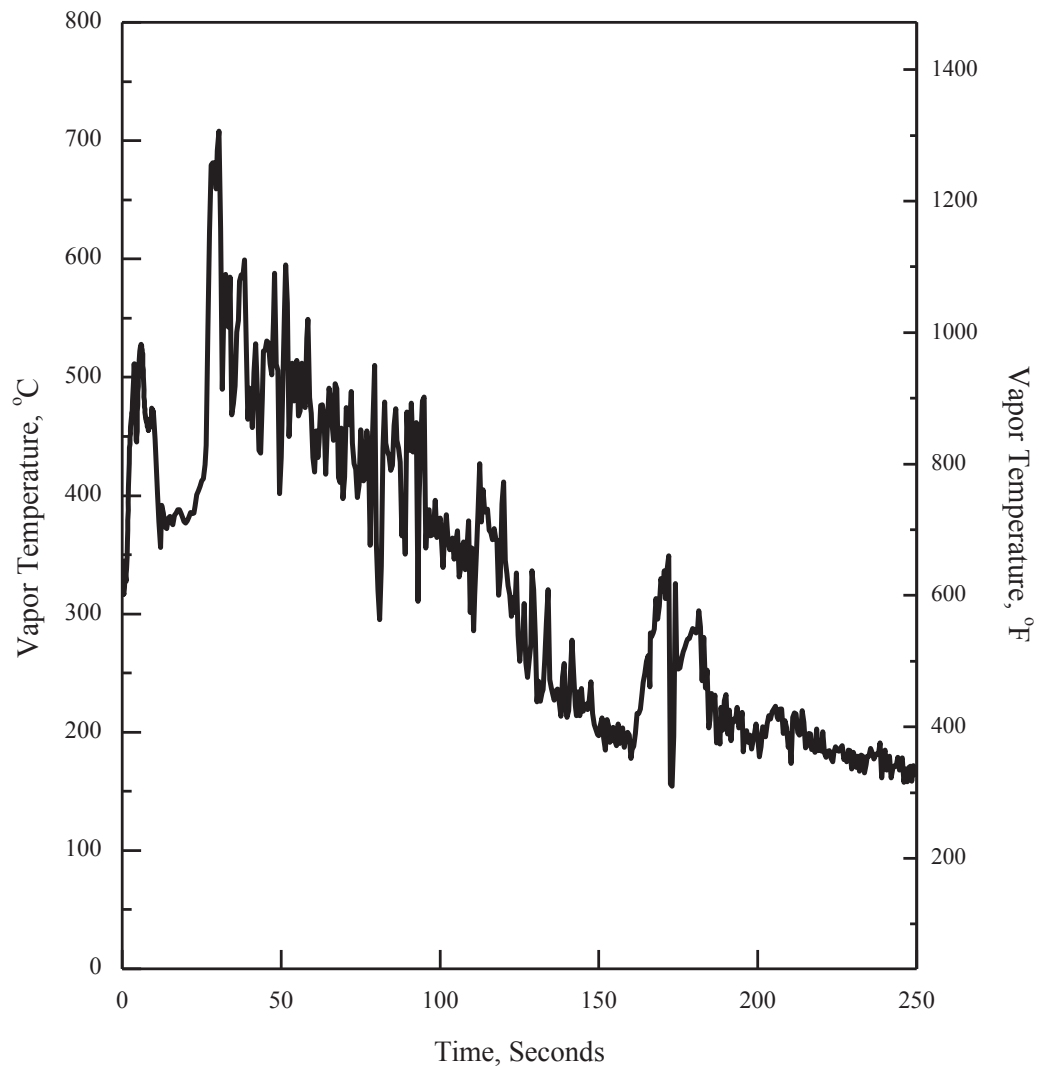


Figure 15.6.5-16 1.0 × Double-ended Guillotine Break in Pump Discharge Leg (Hot Spot Vapor Temperature)

U



APR1400 DCD TIER 2

Replace with next page V

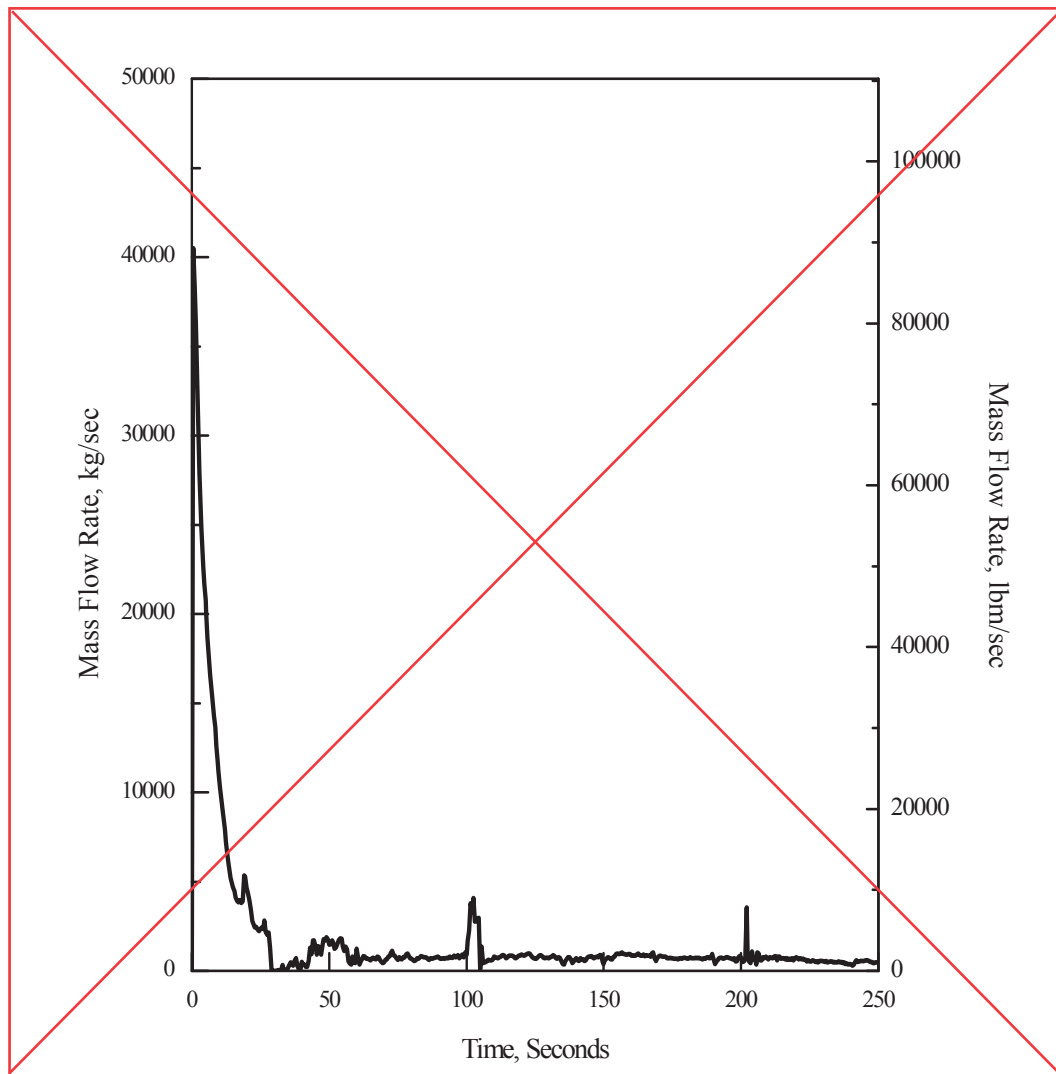
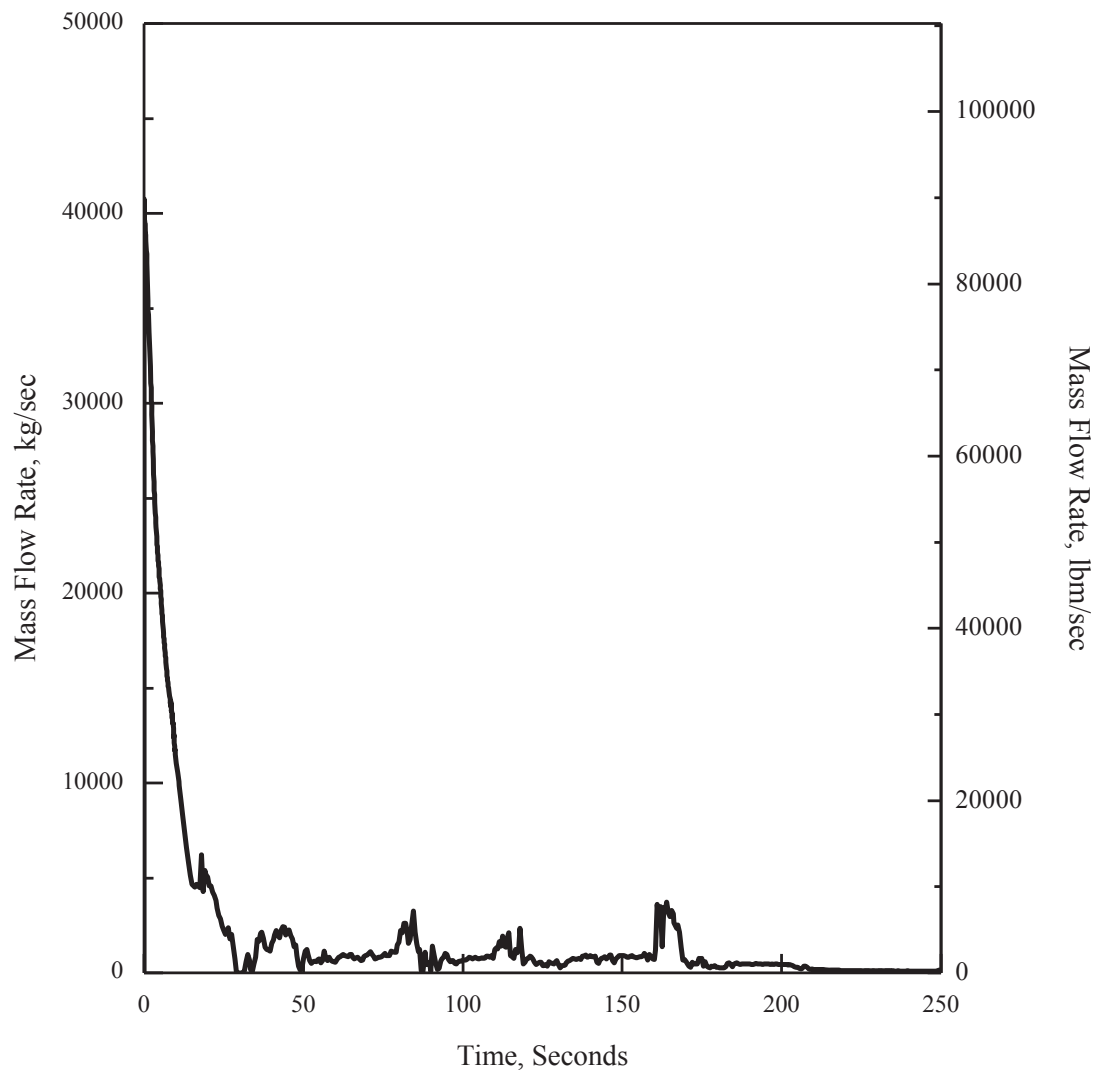


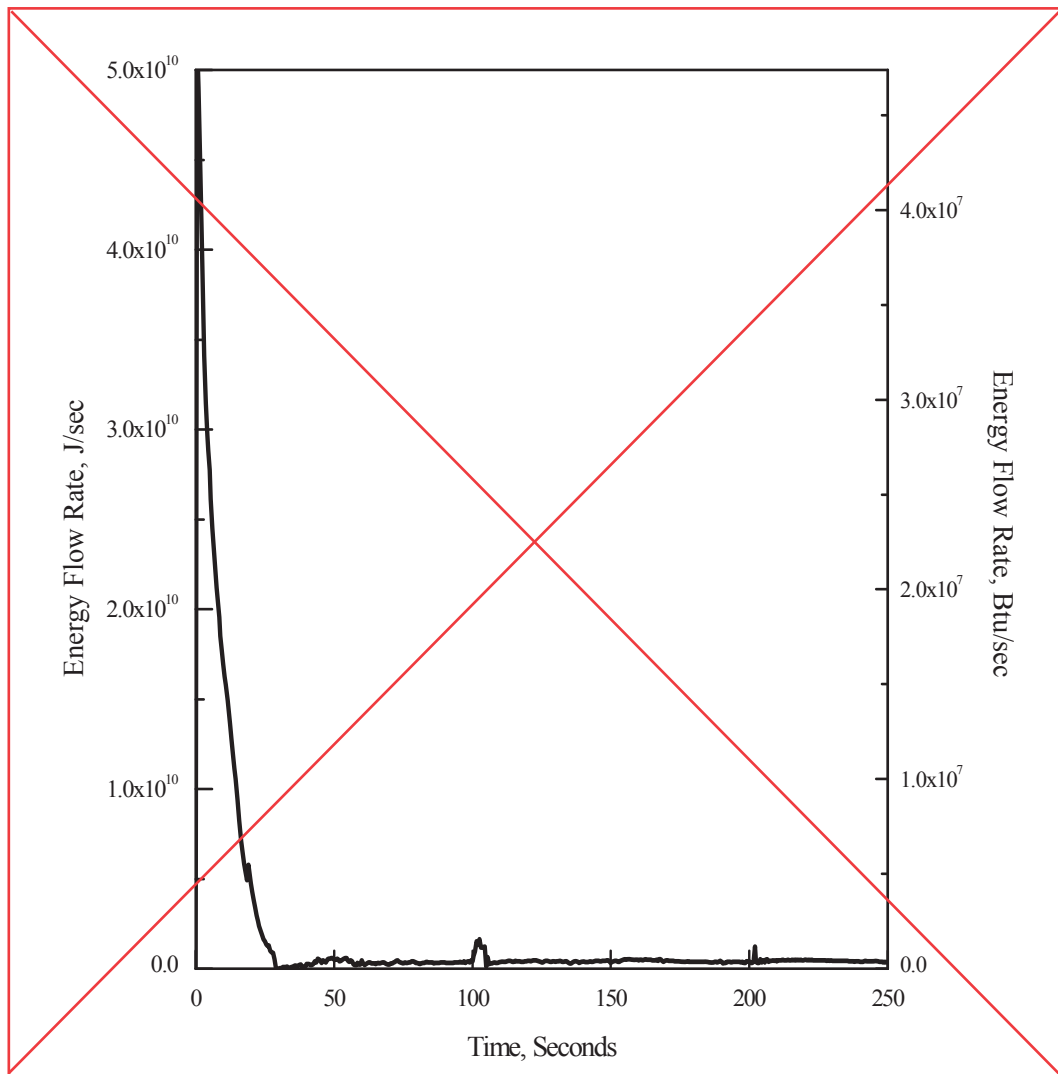
Figure 15.6.5-17 1.0 x Double-ended Guillotine Break in Pump Discharge Leg (Break Flow)

V



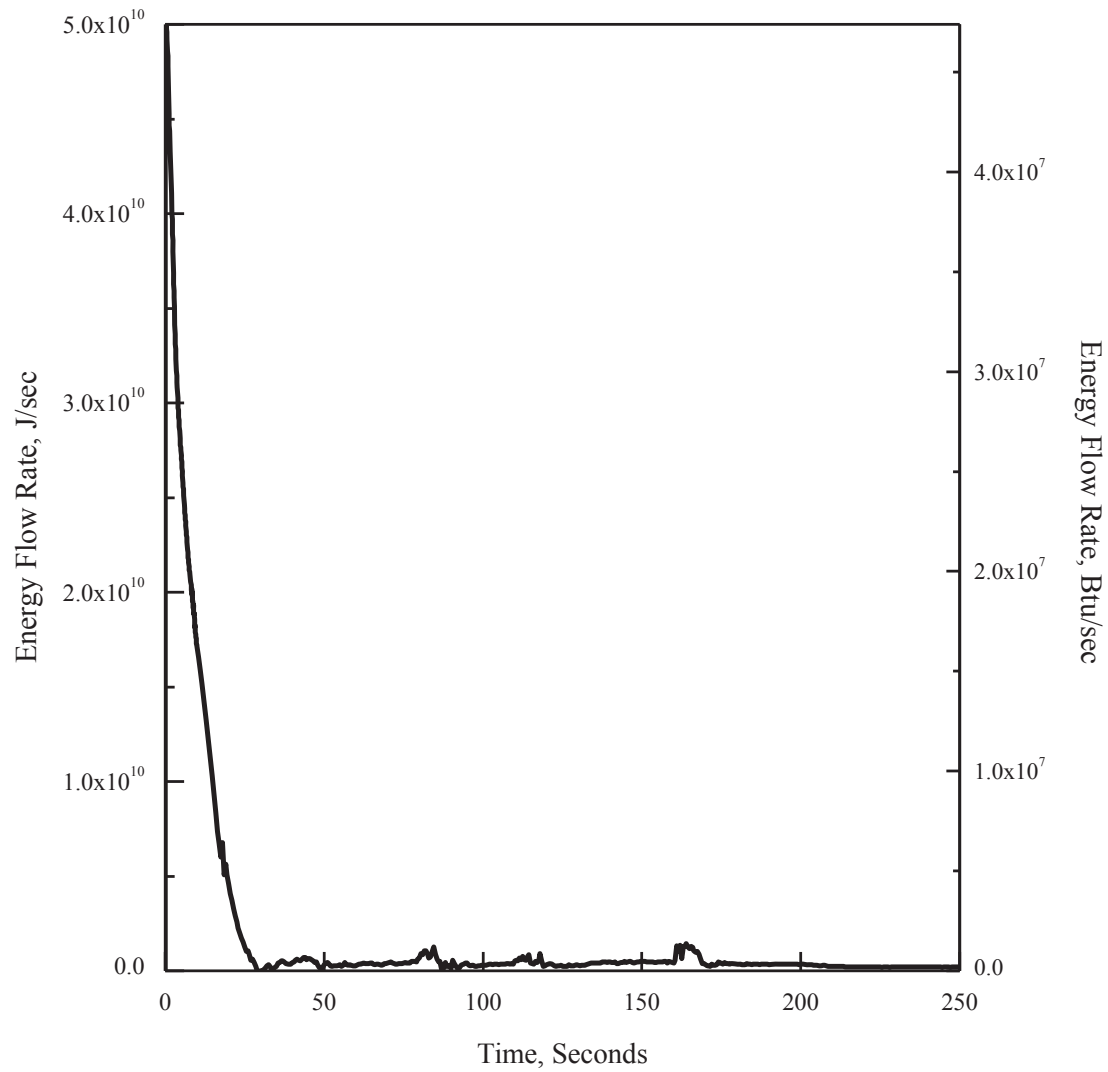
APR1400 DCD TIER 2

Replace with next page W



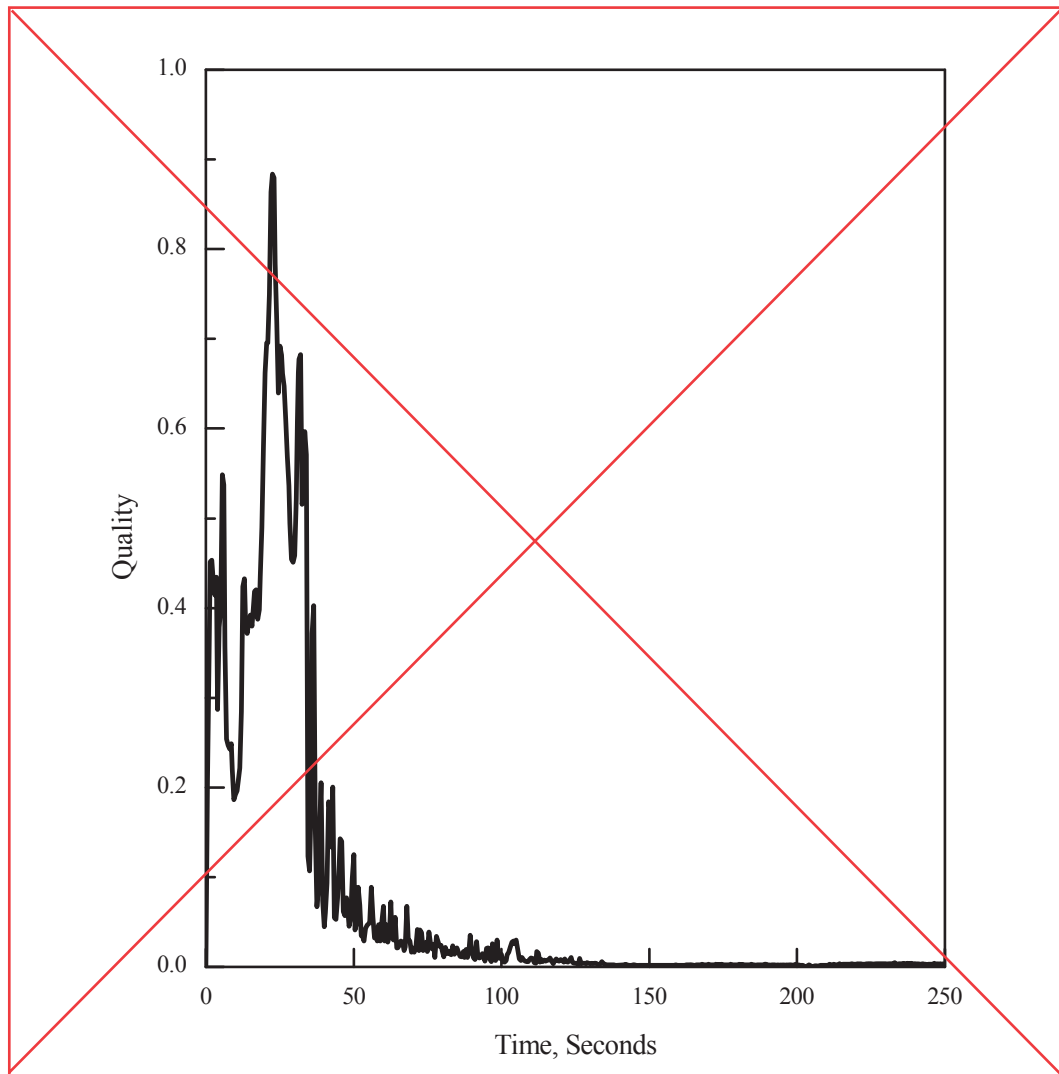
**Figure 15.6.5-18 1.0 × Double-ended Guillotine Break in Pump Discharge Leg
(Break Energy Flow)**

W



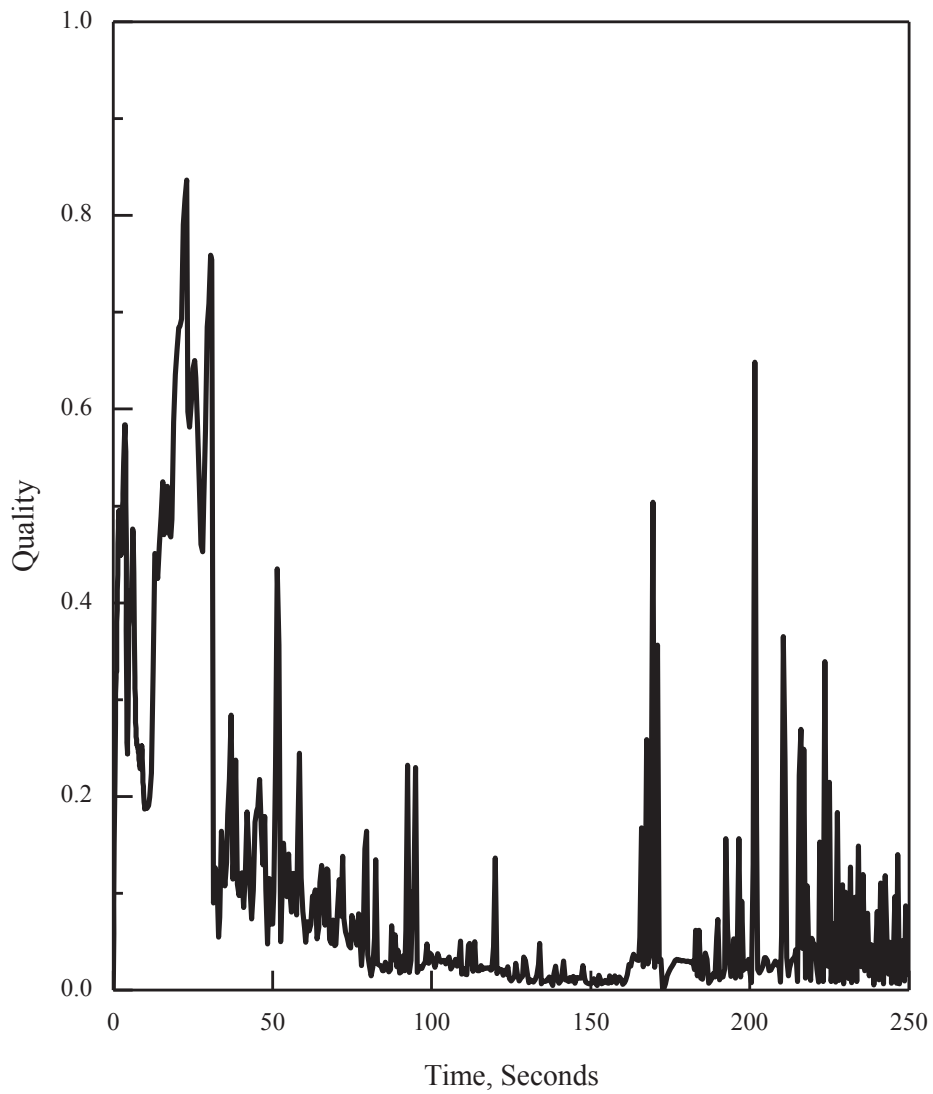
APR1400 DCD TIER 2

Replace with next page X



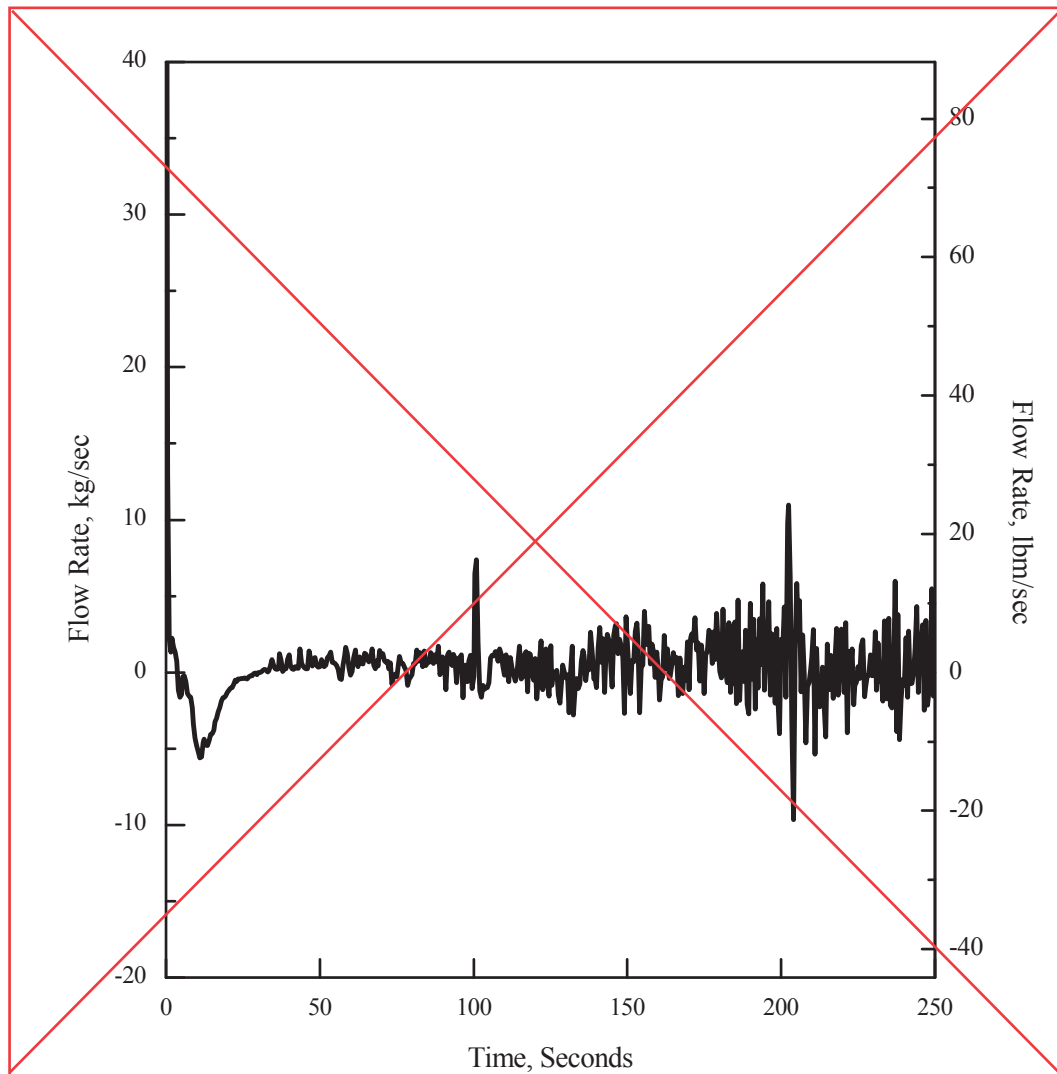
**Figure 15.6.5-19 1.0 x Double-ended Guillotine Break in Pump Discharge Leg
(Hot Assembly Quality)**

X



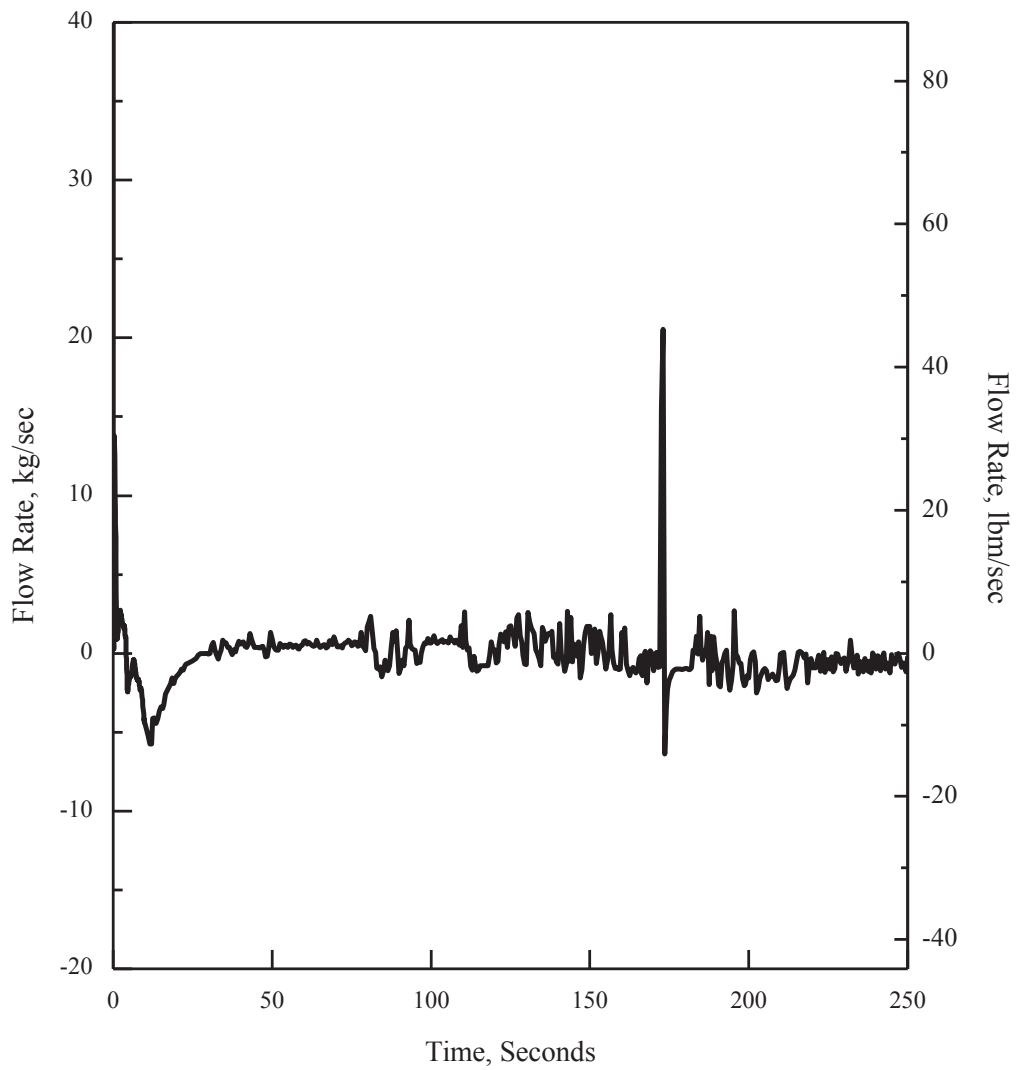
APR1400 DCD TIER 2

Replace with next page Y



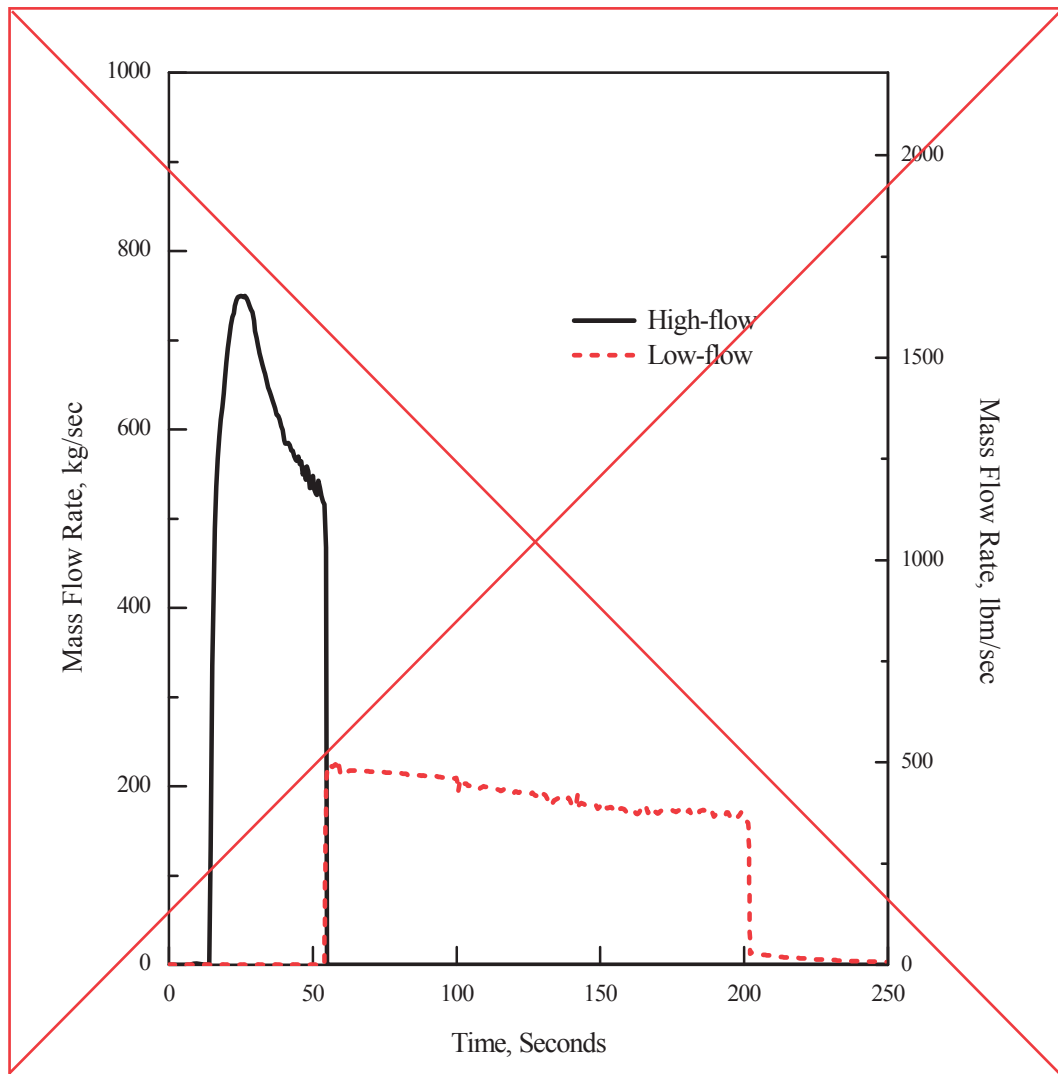
**Figure 15.6.5-20 1.0 x Double-ended Guillotine Break in Pump Discharge Leg
(Hot Assembly Mass Flow Rate)**

Y



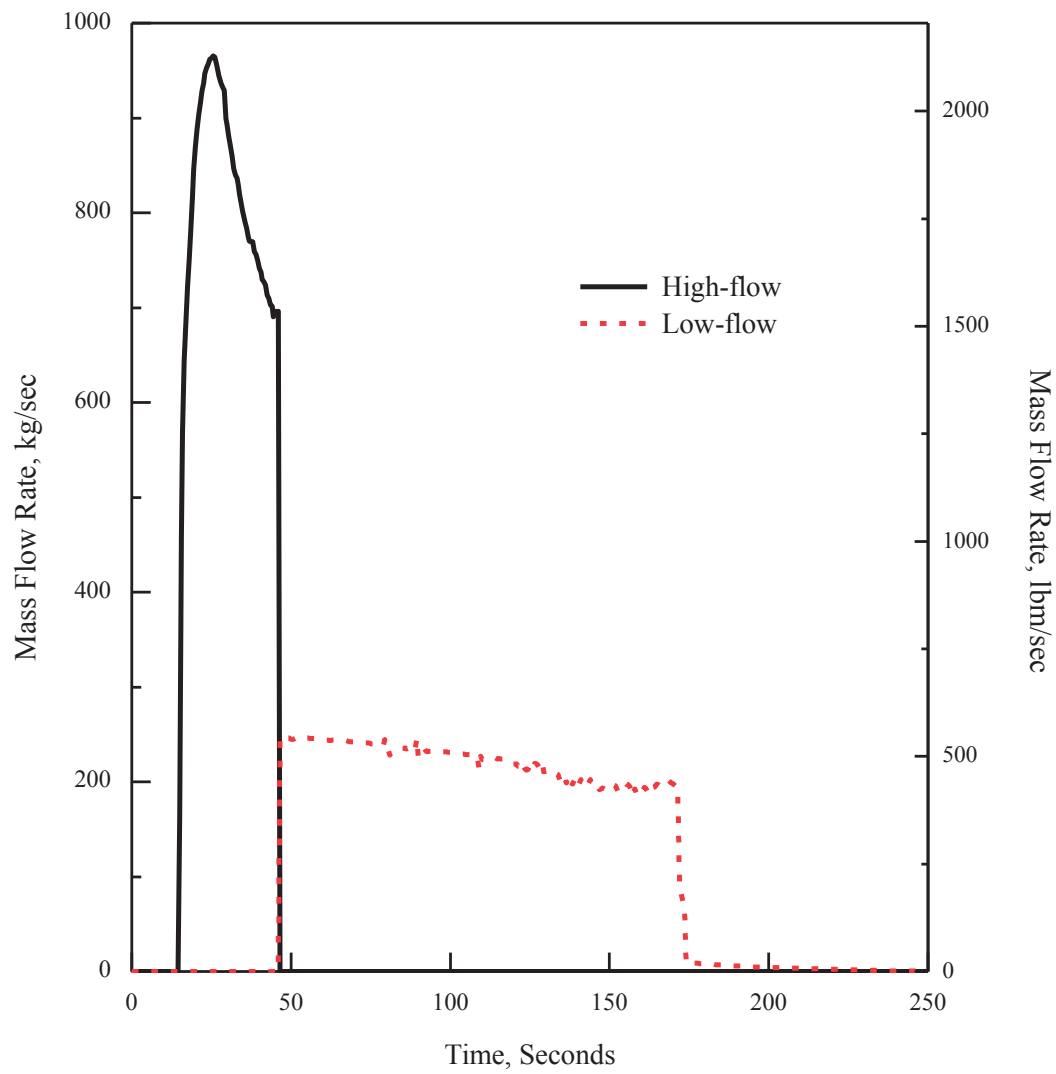
APR1400 DCD TIER 2

Replace with next page Z



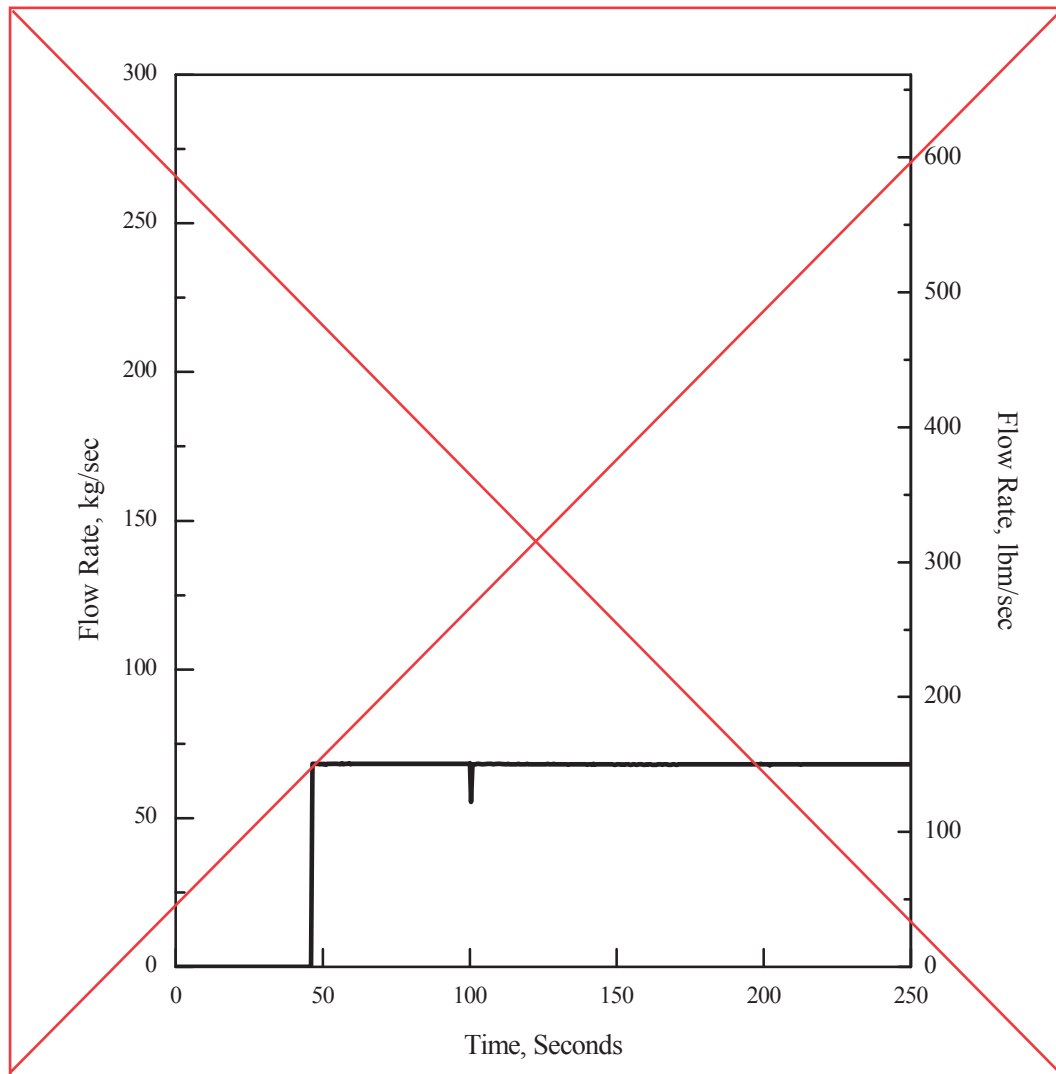
**Figure 15.6.5-21 1.0 × Double-ended Guillotine Break in Pump Discharge Leg
(Safety Injection Tank Flow)**

Z



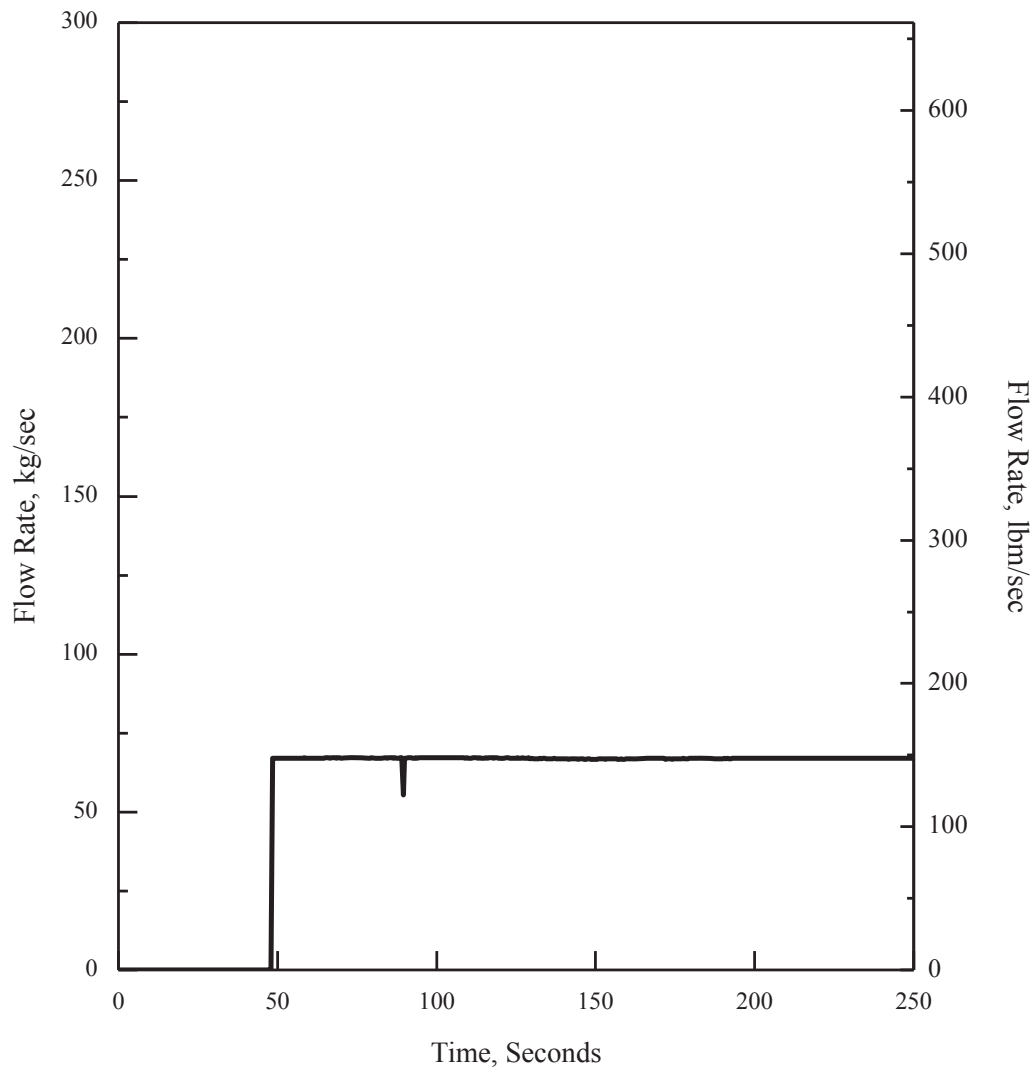
APR1400 DCD TIER 2

Replace with next page AA



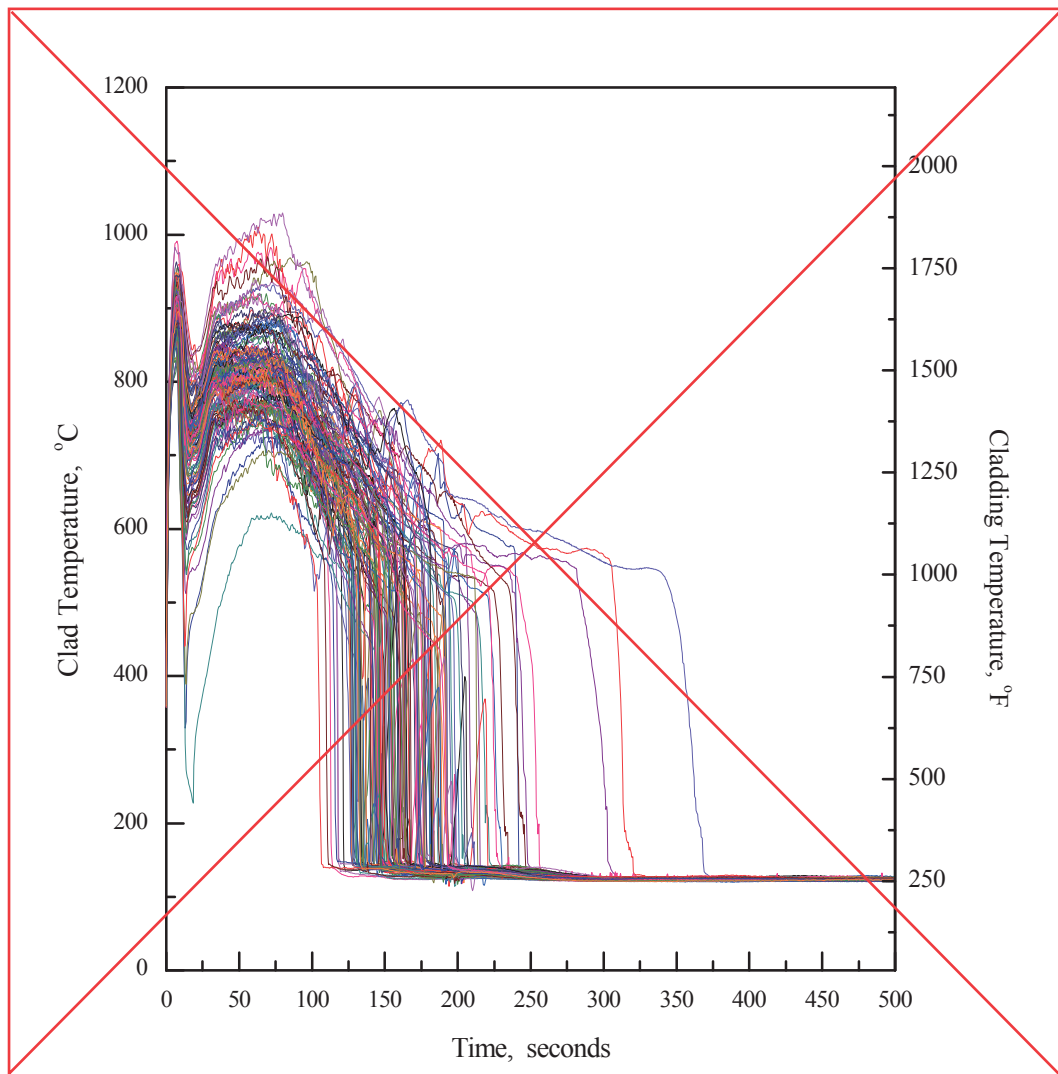
**Figure 15.6.5-22 1.0 × Double-ended Guillotine Break in Pump Discharge Leg
(SI Pump Flow Rate)**

AA

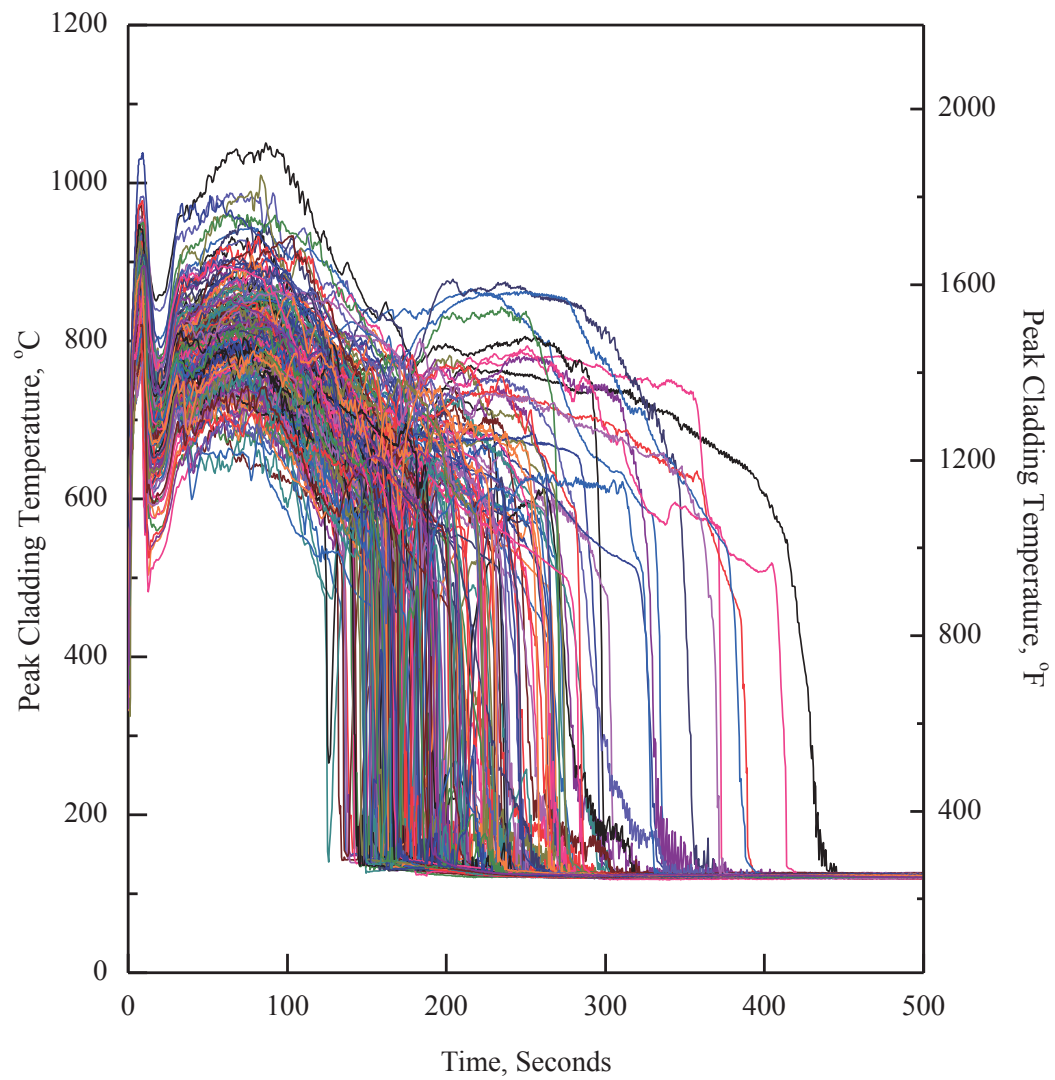


APR1400 DCD TIER 2

Replace with next page AB

**Figure 15.6.5-23 SRS Peak Cladding Temperature**

AB



Non-Proprietary

Criticality Analysis of NFR and SFR

APR1400-Z-A-NR-14011-NP, Rev.1

3.5 Criticality Analysis for Spent Fuel Pool Region II

The spent fuel pool region II is designed to accommodate the fuel assemblies with the minimum burnup which satisfies the criticality acceptance criteria. The criticality analysis is performed using the CSAS5/KENO-V.a sequence and the ORIGEN-ARP with cross section libraries generated using the TRITON and the ENDF/B-VII 238 energy group library.

In order to determine the loading curve, the criticality analyses are performed to find the minimum burnup which produced a k_{eff} less than 1.0 at the each initial enrichment of fuel assemblies.

Figures 3.5-8 and 3.5-9 provide the top and side views of SFP region II. As can be seen from the Figure 3.5-8, spent fuel storage racks in SFP region II are based on a high density rack design and at least one neutron absorber plate is placed between adjacent fuel assemblies to maintain sub-criticality.

Design data for fuel storage cells of SFP region II are provided in Figures 3.5-8, 3.5-9 and Table 3.1-2, and information for rack interfaces within and between the SFP regions are provided in Subsection 3.6.

3.5.1 Depletion Calculations

As discussed in Subsection 3.3.2, the depletion calculations are performed using the ORIGEN-ARP with cross section libraries generated using the TRITON sequence. For the generation of the cross section libraries using the TRITON sequence, bounding reactor parameters described in the Subsection 3.5.1.1 are used. The isotopic concentrations are generated by the ORIGEN-ARP at each 2.25 GWd/MTU intervals from 0 to 72 GWd/MTU for the initial enrichments from 2.0 to 5.0 wt% U-235 with 0.5 wt% increments of U-235 enrichment.

Zero cooling time is taken for conservatism so that the fuel assembly is not allowed to decay after depleted to a desired assembly-average burnup.

3.5.1.1 Bounding Reactor Parameters for the Depletion Calculation

The bounding reactor parameters are a fuel temperature, a fuel enrichment, a power level, a moderator temperature, a soluble boron concentration, and a power level.

The applied fuel temperature is higher than the maximum fuel temperature of []^{TS} including Thermal Conductivity Degradation (TCD) effect.

- a. Fuel temperature: Higher fuel temperature causes Doppler broadening and it results in increased plutonium production. Therefore, the maximum fuel temperature of []^{TS} is applied to the depletion calculations.
- b. Fuel density: To maximize fissile material, the maximum fuel density is applied to the depletion calculation.
- c. Moderator temperature: Higher moderator temperature causes energy spectrum hardening. Therefore, the minimum moderator temperature is applied to the depletion calculation.
- d. Soluble boron concentration: Higher soluble boron concentration causes energy spectrum hardening. Therefore, the maximum soluble boron concentration is applied to the depletion calculation.
- e. Power level: The sensitivity analysis is performed for the power level, and it is found that there is no trend with respect to power level as shown in Table 3.5-2. So, the maximum power level corresponding to the maximum fuel temperature is used as a bounding reactor parameter.

REVISED RESPONSE TO REQUEST FOR ADDITIONAL INFORMATION

APR1400 Topical Reports

Korea Electric Power Corporation / Korea Hydro & Nuclear Power Co., LTD

Docket No. PROJ 0782

RAI No.: 5-7954

SRP Section: TR PLUS7 Fuel Design for the APR1400

Application Section: PLUS7 Fuel Design for the APR1400
(APR1400-F-M-TR-13001-P)

Date of RAI Issue: 06/18/2015

Question No. TR PLUS7 Fuel Design for the APR1400-12

GDC 10 requires that the reactor core and associated coolant, control, and protection systems shall be designed with appropriate margin to assure that specified acceptable fuel design limits (SAFDLs) are not exceeded during any condition of normal operation, including the effects of anticipated operational occurrences (AOOs). SRP Section 4.2 (II)(1)(B)(iv) provides guidance in regards to GDC 10 by stating that overheating of fuel pellets should be avoided by preventing centerline melting. This analysis should be performed for the maximum linear heat generation rate anywhere in the core, including all hot spots and should account for the effects of burnup and composition on the melting point.

Sections 3.4.4 of the PLUS7 fuel design topical report (APR1400-F-M-TR-13001-P) and 2.2.2 of the thermal conductivity degradation (TCD) technical report (APR1400-F-A-NR-13002-P) discuss overheating of the fuel pellets. The PLUS7 fuel design includes $\text{UO}_2\text{-Gd}_2\text{O}_3$ pellets. The impact of the $\text{UO}_2\text{-Gd}_2\text{O}_3$ pellet composition on the overheating of fuel pellets analysis is not discussed in either Section 3.4.4 of APR1400-F-M-TR-13001-P or Section 2.2.2 of APR1400-F-A-NR-13002-P. $\text{UO}_2\text{-Gd}_2\text{O}_3$ has a lower melting temperature and lower thermal conductivity than UO_2 which has caused the staff to question the ability of the fuel centerline melting analysis provided to demonstrate compliance with GDC 10.

Update the topical report, as applicable, to address fuel pellet overheating considering $\text{UO}_2\text{-Gd}_2\text{O}_3$ to ensure that no fuel centerline melting occurs for all fuel compositions and normal operation/AOO conditions.

Response - (Rev.1)

Figure 12-1 shows the normalized radial power fall-off curves for UO_2 and $\text{Gd}_2\text{O}_3\text{-UO}_2$ rods. As shown in Figure 12-1, the highest radial powers for $\text{Gd}_2\text{O}_3\text{-UO}_2$ rods are lower than those for UO_2 rods over all burnup ranges. Also, the radial powers decrease as burnup increases due to the reduced power capability caused by the depletion of the fissile material in the fuel and the buildup of fission products.

Figure 12-2 shows the calculated PTM (Power-to-Melt) values using the [FATES3B code considering TCD penalty](#) for both UO_2 and $\text{Gd}_2\text{O}_3\text{-UO}_2$ rods, which are represented by black and red solid lines, respectively. Figure 12-2 also shows the highest attainable powers for UO_2 and $\text{Gd}_2\text{O}_3\text{-UO}_2$ rods in black and red dotted lines, respectively.

In Figure 12-2, each maximum attainable power of UO_2 and $\text{Gd}_2\text{O}_3\text{-UO}_2$ rods can be obtained from radial fall-off values, namely from the normalized radial power in Figure 12-1. Since the maximum attainable powers for both UO_2 and $\text{Gd}_2\text{O}_3\text{-UO}_2$ rods is limited up to $[]^{\text{TS}}$ which is a SAFDL value for APR1400, it can be defined that the maximum attainable power of $[]^{\text{TS}}$ is only available with a normalized UO_2 rod radial power of $[]^{\text{TS}}$. In addition, attainable power after about $[]^{\text{TS}}$ in Figure 12-2 can be interpreted from the proportional decrease of normalized radial power fall-off curve in Figure 12-1.

Based on the same reasoning, the normalized radial power ratio of UO_2 and $\text{Gd}_2\text{O}_3\text{-UO}_2$ rods over all burnup ranges in Figure 12-1 was considered and the attainable power of $\text{Gd}_2\text{O}_3\text{-UO}_2$ rod in Figure 12-2 was derived.

As shown in Figure 12-2, the PTM values are well above the attainable powers for UO_2 and $\text{Gd}_2\text{O}_3\text{-UO}_2$ rods along whole range of burnup. Therefore, it can be concluded that there will be no melting for UO_2 and $\text{Gd}_2\text{O}_3\text{-UO}_2$ rods. The TCD penalty methodology will be described in Section 3.5 of the PLUS7 fuel design topical report (APR1400-F-M-TR-13001-P) and, accordingly, the current Section 3.4.4 of the PLUS7 topical report will be changed to 3.4.5 with the update to reflect TCD effect on PTM analysis. In addition, the discussion on $\text{Gd}_2\text{O}_3\text{-UO}_2$ melting will be added to the text in Section 3.4.5.

The TCD technical report (APR1400-F-A-NR-14002-P) will be withdrawn.

TS

Figure 12-1 Rod Power Histories Used for PLUS7 Fuel

TS

Figure 12-2 Power to Melt and Maximum Attainable Powers for UO_2 and $\text{Gd}_2\text{O}_3\text{-UO}_2$ Rods as a Function of Burnup

Impact on DCD

There is no impact on the DCD.

Impact on PRA

There is no impact on the PRA.

Impact on Technical Specifications

There is no impact on the Technical Specifications.

Impact on Technical/Topical/Environmental Reports

PLUS7 fuel design topical report (APR1400-F-M-TR-13001-P) will be revised as indicated on the attached markups (Attachment 1).

Furthermore, to reflect the minor changes including editorial error, PLUS7 fuel design topical report (APR1400-F-M-TR-13001-P) will be revised as indicated on the attached markups (Attachment 2).

There is no impact on the TCD technical report (APR1400-F-A-NR-14002-P), and technical report will be withdrawn.

Non Proprietary

PLUS7 FUEL DESIGN for the APR1400

APR1400-F-M-TR-13001-P Rev.0

| | | |
|-----------|---|------------|
| 3.2.8 | Overheating of Cladding | 3-7 |
| 3.2.9 | Overheating of Fuel Pellets | 3-8 |
| 3.2.10 | Excessive Fuel Enthalpy | 3-8 |
| 3.2.11 | Pellet-to-Cladding Interaction | 3-9 |
| 3.2.12 | Bursting | 3-9 |
| 3.2.13 | Cladding Embrittlement | 3-10 |
| 3.2.13.1 | Cladding Stress | 3-16 |
| 3.2.13.2 | Cladding Strain | 3-17 |
| 3.2.13.3 | Cladding Fatigue | 3-17 |
| 3.2.13.4 | Fuel Rod Internal Pressure | 3-17 |
| 3.2.13.5 | Overheating of Fuel Pellets | 3-17 |
| 3.3 | Impact of TCD on Safety Analysis | 3-18 |
| 3.3.1 | Determination of TCD penalty | 3-18 |
| 3.3.2 | Fuel Rod Interface Data for Safety Analyses | 3-19 |
| 3.3.3 | Impact of Fuel Enthalpy | 3-19 |
| 3.3.3 | Applicability of CEPANFL Code to PLUS7 Fuel Rod Design | 3-14 |
| 3.3.4 | Applicability of PAD Code to PLUS7 Fuel Rod Design | 3-15 |
| 3.4 | Impact on Thermal Conductivity Degradation (TCD) on Fuel Rod Design Criteria .. | 3-16 |
| 3.5 | Conclusion | 3-17 |
| 4. | PLUS7 FUEL EXPERIENCE | 4-1 |
| 4.1 | Core | 4-1 |
| 4.2 | Pool-Side Examinations | 4-1 |
| 4.2.1 | Fuel Assembly Irradiation Growth | 4-2 |
| 4.2.2 | Fuel Assembly Bow and Twist | 4-2 |
| 4.2.3 | Rod-to-Top Nozzle Axial Clearance (Shoulder Gap) | 4-3 |
| 4.2.4 | Fuel Rod Bow | 4-3 |
| 4.2.5 | Grid Width | 4-3 |
| 4.2.6 | Cladding Oxide Thickness | 4-4 |
| 4.2.7 | Fuel Rod Outer Diameter | 4-4 |
| 4.3 | Hot-Cell Examinations | 4-5 |
| 4.3.1 | Fuel Rod Fretting Wear | 4-5 |
| 4.3.2 | Cladding Oxide Thickness | 4-5 |
| 4.3.3 | CRUD Thickness | 4-5 |
| 4.3.4 | Fuel Rod Outer Diameter | 4-6 |
| 4.3.5 | Cladding Hydrogen Contents and Hydride Orientation | 4-6 |
| 4.3.6 | Fission Gas Release | 4-7 |
| 4.4 | Testing, Inspection and Surveillance Plans | 4-7 |

Non Proprietary

PLUS7 FUEL DESIGN for the APR1400

APR1400-F-M-TR-13001-P Rev.0

LIST OF FIGURES

| | | |
|-------------|--|------|
| Figure 2-1 | PLUS7 Fuel Assembly Configuration | 2-20 |
| Figure 2-2 | Comparison of Fuel Rod Designs | 2-21 |
| Figure 2-3 | Mid Grid Designs | 2-22 |
| Figure 2-4 | Spring and Dimple Configurations of PLUS7 Mid Grid | 2-23 |
| Figure 2-5 | Comparison of Top and Bottom Grids | 2-24 |
| Figure 2-6 | Debris Filtering Design of PLUS7 | 2-25 |
| Figure 2-7 | Reconstitutable Design of PLUS7 Top Nozzle | 2-26 |
| Figure 2-8 | Comparison of Bottom Nozzles | 2-27 |
| Figure 2-9 | Comparison of Guide Thimbles | 2-28 |
| Figure 2-10 | Vibration Test Results of PLUS7 Fuel Assembly | 2-29 |
| Figure 2-11 | PLUS7 Bottom Nozzle | 2-30 |
| Figure 2-12 | 1/8 Bottom Nozzle Finite Element Model | 2-30 |
| Figure 2-13 | PLUS7 Top Nozzle | 2-31 |
| Figure 2-14 | PLUS7 Top Nozzle/Guide Thimble Joint & Connection | 2-32 |
| Figure 2-15 | 1/8 Top Nozzle Adapter Plate Finite Element Model | 2-33 |
| Figure 2-16 | 1/8 Top Nozzle Holddown Plate Finite Element Model | 2-33 |
| Figure 2-17 | PLUS7 Guide Thimble and Instrument Tube | 2-34 |
| Figure 2-18 | CEA Drop Time | 2-35 |
| Figure 2-19 | PLUS7 Top and Bottom Grid | 2-36 |
| Figure 2-20 | PLUS7 Protective Grid | 2-36 |
| Figure 2-21 | PLUS7 Mid Grid | 2-37 |
| Figure 2-22 | PLUS7 Grid/Guide Thimble and Instrument Tube Joint & Connection | 2-38 |
| Figure 2-23 | PLUS7 Bottom Grid/Guide Thimble and Instrument Tube Joint & Connection | 2-39 |
| Figure 2-24 | PLUS7 Bottom Nozzle and P-Grid/Guide Thimble Joint & Connection | 2-40 |
| Figure 3-1 | Rod Power History Used for PLUS7 Fuel Rod Performance Analysis | 3-25 |
| Figure 3-2 | Comparison of Measured Oxide Layer Thickness and Predicted Oxide Layer Thickness for H615 and H605 Assemblies | 3-25 |
| Figure 4-1 | Development & Commercial Supply Status of PLUS7 | 4-13 |

| | | |
|------------|--|------|
| Figure 3-3 | Power to Melt and Maximum Attainable Powers for UO ₂ and Gd ₂ O ₃ -UO ₂ Rods | 3-28 |
| Figure 3-4 | Comparison of Predicted and Measured Fuel Centerline Temperatures as a Function of Burnup vs. Determined TCD Penalty (red line) | 3-28 |

Insert

Non Proprietary

3-3

PLUS7 FUEL DESIGN for the APR1400

APR1400-F-M-TR-13001-P Rev.0

3-2

As shown in Figure 3-2, the predicted values are much higher than those of measured values for both H614 and H605 PLUS7 fuel assemblies. In addition, the means values and standard deviations of M/P are summarized in Table 3-9 for H615 and H605 assemblies.

- Comparison of operating conditions of OPR1000, Westinghouse Type Plants and APR1400

3.4 Impact of Thermal Conductivity Degradation (TCD) on Fuel Rod Design Criteria

As explained in (blank)

multiple (blank)
and Yonggwang (blank)
because (blank)

It is, the (blank)

Yonggwang (blank)

mainly (blank)
concentrated (blank)

Table 3-9

Ulchin unit 2

the core (blank)

OPR1000 (blank)

plant is (blank)

maximum (blank)

Yonggwang unit 2. On the other hand, the core average linear heat rate of APR1400 plant is about four percent higher than that of OPR1000. However, it is expected that four percent increase of core average power does not give a significant effect on oxide buildup of cladding tube. Therefore, the applicability of PAD code with increased corrosion multiplier to PLUS7 fuel in APR1400 for corrosion evaluation was confirmed.

3.4 Impact of TCD on Fuel Rod Design Criteria

FATES3B does not explicitly model fuel thermal conductivity degradation (TCD) with burnup.

3.4.1 Cladding Stress

FATES3B (blank)

the thermal (blank)

conservative (blank)

Many of (blank)

collapse (blank)

the heat flux (blank)

Fuel densification (blank)

TCD. Fast (blank)

impacted (blank)

As described in Section 3.2.1, cladding stress criterion is established to prevent fuel damage from the excessive primary stress which results from the pressure difference between rod internal pressure and system pressure. In Section 3.4.4, it was evaluated that the rod internal pressure predicted by FATES3B includes the effect of TCD.

Therefore, considering the conservatism of FATES3B with regarding the rod internal pressure and design margin for cladding stress, it is judged that the cladding stress design criterion is still met with consideration of TCD.

The evaluations for the fuel rod design criteria that are affected by TCD are described as follows.

The detailed evaluation results will be provided in TCD Technical Report which is planned to submit to NRC.

were described in TCD Technical Report in Reference 3-14.

3.4.1 Cladding Stress

As described in Section 3.2.1, KNE cladding stress criterion is established to prevent fuel damage from the excessive primary stress which results from the pressure difference between rod internal pressure and system pressure.

KHNP

3-16

Delete

Non Proprietary Delete

PLUS7 FUEL DESIGN for the APR1400

APR1400-F-M-TR-13001-P Rev.0

This page will be replaced with next page A, B, and C

~~Considering the amount of potential increase in rod internal pressure by TCD impact and design margin to the limit, it is judged that the cladding stress criteria are still met with consideration of TCD.~~

~~3.4.2 Cladding Strain and Fatigue~~

~~The cladding strain is affected by TCD due to the increased fuel thermal expansion. However, the increased thermal expansion can be offset with available design margin to the cladding strain and fatigue limits and conservatism in the input variables such as power history and assumed rod internal pressure. Therefore, cladding strain and fatigue criteria are still satisfied with consideration of TCD.~~

~~3.4.3 Fuel Rod Internal Pressure~~

~~The effect of increased fuel temperature due to TCD on fission gas release is inherently accounted for in the current performance code, FATES3B (References 3-1 through 3-4) because the model was calibrated to measured data for a full range of fuel rod burnup and operating conditions. Additionally, conservatism is considered in the original FATES3B calibration process and in fuel rod design analysis. However, the rod internal pressure may still increase with TCD due to the increased fuel thermal expansion, which reduces the total fuel rod void volume.~~

~~Evaluations show that the reduction of void volume due to increased thermal expansion is not significant in PLUS7 fuel rod design. In addition, the rod internal pressure limit calculation is inherently conservative in that actual gap reopening is predicted to occur at higher pressures.~~

~~In conclusion, the increased rod internal pressure can be offset with available design margin to the rod internal pressure limits. Therefore, rod internal pressure criteria are still satisfied considering the effects of TCD.~~

~~3.4.4 Overheating of Fuel Pellets~~

~~The power to melt limit depends on fuel burnup but the reduced power capability with burnup, which is caused by the depletion of the fissile material in the fuel and the buildup of fission products, offsets the TCD impact. Therefore, it is judged that there will be no safety concerns due to TCD. However, the power to melt values with burnup considering the impact of TCD are calculated and will be provided in the TCD Technical Report which will be submitted to NRC.~~

~~In summary, KNE fuel rod design criteria have been reviewed with respect to the potential impacts of TCD, and it is concluded that TCD can be accommodated such that approved fuel rod design criteria will remain satisfied for current fuel rod designs.~~

~~3.5 Conclusion~~

~~The PLUS7 fuel rod design is verified to maintain the rod integrity up to rod average burnup of 60,000 MWD/MTU based on the thermal performance and mechanical integrity evaluation results using by NRC approved design codes and methodologies.~~

A

3.4.2 Cladding Strain

The cladding strain considering the effect of TCD was calculated using the convenient codes of FATES3B which fuel thermal conductivity model, Lyons correlation, is replaced with the modified NFI thermal conductivity model. According to the evaluation results considering the TCD effect, the cladding plastic strain during normal operation and following a single AOO is []^{TS}, and, total (elastic plus plastic) circumferential strain increment produced as a result of a single AOO is []^{TS}. Because the calculated strains are less than []^{TS}, the strain design criteria are still satisfied with the consideration of TCD.

3.4.3 Cladding Fatigue

The fatigue damage factor for the daily load following operation was calculated using the same convenient code of FATES3B as used for cladding strain evaluation. In this calculation, more conservative radial peaking factor (RPF) than the cycle specific RPF curve was used. On the other hand, the fatigue damage factors for reactor trips and startups/shutdowns are determined by hand calculation using a simple formula. The total cumulative fatigue damage factor from daily load following operation, reactor trips and startups/shutdowns was []^{TS} which is below the limit of []^{TS}. Therefore, it was confirmed that the cladding fatigue criterion is still satisfied with the consideration of TCD.

And then, to confirm the applicability for a given subsequent cycle, the conservative RPF used in the calculation will be validated on a cycle-by-cycle basis.

3.4.4 Fuel Rod Internal Pressure

The fuel rod internal gas pressure is determined by the combination of fission gas release and fuel rod void volume. The effect of increased fuel temperature due to TCD on fission gas release is inherently accounted for in the current performance code, FATES3B (References 3-1 through 3-4), because the model was calibrated to measured data for a full range of fuel rod burnup and operating conditions. Additionally, conservatism is considered in the original FATES3B calibration process and in design methodology. In contrast, the rod internal pressure may be increased due to the TCD-induced fuel thermal expansion, which reduces the total fuel rod void volume. However, the potential increase of rod internal pressure due to reduction of void volume can be sufficiently offset with the inherent conservatism of FATES3B and available design margin to the design limit. It is also noted that the rod internal pressure is conservatively calculated assuming the RPF curve and biased input to generate higher rod internal gas pressure. Therefore, it can be concluded that rod internal pressure criteria are still satisfied considering the effects of TCD.

3.4.5 Overheating of Fuel Pellets

The power to melt (PTM) decreases as fuel rod burnup increases because the fuel melting temperature is decreased. The local linear powers that preclude fuel centerline melting are calculated for UO₂ and Gd₂O₃-UO₂ rods as a function of burnup using FATES3B code considering the TCD effect. In this calculation, as explained in section 3.5.1, TCD effects was considered by adding a penalty on fuel centerline temperature that linearly increases from []^{TS} over the burnup range from []^{TS} and remains constant for higher range of burnup. The calculated power to fuel melting considering the TCD penalty is presented in Figure 3-3. As shown in Figure 3-3, the PTM limit with TCD penalty for UO₂ rod is decreased below a SAFDL of []^{TS} above []^{TS} but the fuel will not melt because the decreasing rate of the maximum attainable rod power will be much higher than that of the PTM due to the reduced power capability caused by the depletion of the fissile material in the fuel and the buildup of fission products. In Figure 3-3, each maximum attainable power of UO₂ and Gd₂O₃-UO₂ rods can be obtained from radial fall-off values, namely from the normalized radial power in Figure 3-1. Since the maximum attainable power for both UO₂ and Gd₂O₃-UO₂ rods is limited up to []^{TS} which is a SAFDL value for APR1400, it can be defined that the maximum attainable power of []^{TS} is only available with

Chapter 3.4.4 is moved to new Chapter 3.4.5

Note: Chapter 3.4.5 is for the Response to RAI 5-7954 Question12, 13, and 14

B

Chapter 3.4.4 is moved to new Chapter 3.4.5

a normalized UO_2 rod radial power of []^{TS}. In addition, the maximum attainable power after about []^{TS} in Figure 3-3 is derived from the proportional decrease of normalized radial power fall-off curve in Figure 3-1. Based on the same reasoning, the maximum attainable powers of $\text{Gd}_2\text{O}_3\text{-UO}_2$ rods are obtained by considering the normalized radial power ratio of UO_2 and $\text{Gd}_2\text{O}_3\text{-UO}_2$ rods over all burnup ranges shown in Figure 3-1.

As shown in Figure 3-3, the PTM values are well above the attainable powers for UO_2 and $\text{Gd}_2\text{O}_3\text{-UO}_2$ rods along whole range of burnup. Therefore, it can be concluded that there will be no melting for UO_2 and $\text{Gd}_2\text{O}_3\text{-UO}_2$ rods. In addition, fuel melting of $\text{Gd}_2\text{O}_3\text{-UO}_2$ rods will not be occurred even when the rod power for UO_2 rod reaches the SAFDL value of []^{TS}. Therefore, the lower power of $\text{Gd}_2\text{O}_3\text{-UO}_2$ rod compared to UO_2 rod ensures that UO_2 rod remains limiting for centerline melt. This melting analysis will be performed on a cycle specific basis with FATES3B code considering the TCD penalty. This will ensure that the linear heat rate SAFDL of []^{TS} is valid.

In summary, the fuel rod design criteria have been reviewed with respect to the potential impacts of TCD, and it is concluded that TCD can be accommodated to the fuel rod design criteria that satisfied for current APR1400 fuel rod designs.

3.5 Impact of TCD on Safety Analyses

As previously described, the FATES3B code uses the fuel pellet thermal conductivity model which does not consider the TCD effects. Therefore, it is necessary to evaluate the non-conservatism of the FATES3B code on the generation of fuel rod interface data for safety analyses. In this section, the degree of non-conservatism in the FATES3B temperature prediction (TCD penalty values) is determined based on the comparison results with the measured temperature data from Halden test reactor.

3.5.1 Determination of TCD Penalty

The verification of the TCD penalty of FATES3B code for fuel centerline temperature was completed using the measured Halden test reactor data. Halden data with the power range of []^{TS} and burnup range of []^{TS} are applied to the comparison and include the comparable conditions of APR1400.

- Hot Rod Fuel Temperature Penalty

The deviation of M-P (measured minus predicted) at an upper bound basis which is indicated as red line in Figure 3-4 is linearly increased from []^{TS} at []^{TS} to []^{TS} to []^{TS} and remains constant for above []^{TS}. The upper bound deviation line in Figure 3-4 bounds over []^{TS} of all M-P comparison data. Therefore, the deviation line in red of Figure 3-4 represents as reasonable centerline temperature penalty due to TCD for FATES3B prediction. The fuel volume-averaged temperature is assumed as []^{TS} of the fuel centerline temperature with TCD penalty.

- Average Rod Fuel Centerline Temperature Penalty

The centerline temperature penalty is linearly increased from []^{TS} at []^{TS} to []^{TS} to []^{TS} and remains constant for above []^{TS}. This best-estimated penalty was determined based on the comparison of FATES3B and Halden test data which are similar to the APR1400 core average power.

For the mass and energy calculations used in the containment pressure analysis, 95 % upper bounded penalty was determined as the linear increasing of centerline temperature from []^{TS} at []^{TS} to []^{TS} to []^{TS} and remaining constant for above []^{TS}.

Added new Chapter 3.5 for TCD methodology

Note: Chapter 3.5 is for the Response to RAI 5-7954 Question12 and 14.

| |
|---|
| C |
|---|

3.5.2 Fuel Rod Interface Data for Safety Analyses

To generate the fuel rod interface data with TCD effect for safety analyses, the TCD penalty determined as a function of burnup is added to the temperatures calculated by FATES3B code and those TCD penalty-added centerline temperatures of hot and average rod should be provided to safety analyses team.

3.6 Impact of Fuel Enthalpy

The impacts of TCD result in increasing the fuel enthalpy and the fuel centerline temperature. The impact on the fuel enthalpy due to TCD would be negligible for fresh fuel even though the maximum power peaking factors exist in the low burnup fuel in the APR1400 reload core designs. For the high burnup fuel which is affected by TCD, the fuel enthalpy and the fuel centerline temperature increase due to TCD are not significant because of the peaking factor burndown effect at higher burnups. The event specific evaluation considering the TCD penalty described in the Section 3.5 was performed and described in DCD Tier 2 Chapter 15.4.8.

3.7 Conclusion

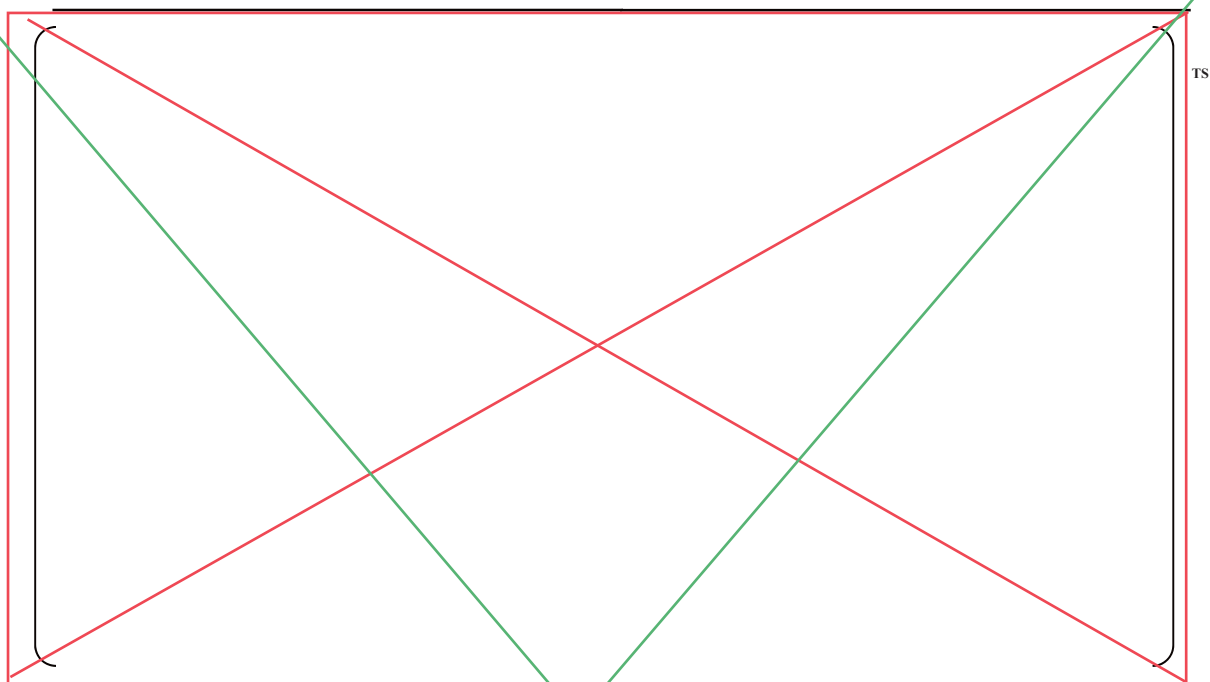
The PLUS7 fuel rod design criteria considering TCD effect is evaluated using NRC approved FATES3B code and verified acceptable up to rod average burnup of 60,000 MWd/MTU. In addition, the potential impact of TCD on the fuel rod design criteria was evaluated, and it is concluded that TCD can be accommodated. Fuel rod interface data accounting for TCD penalty are generated and transmitted to safety analyses team.

This page will be replaced with next page D and E

Non Proprietary

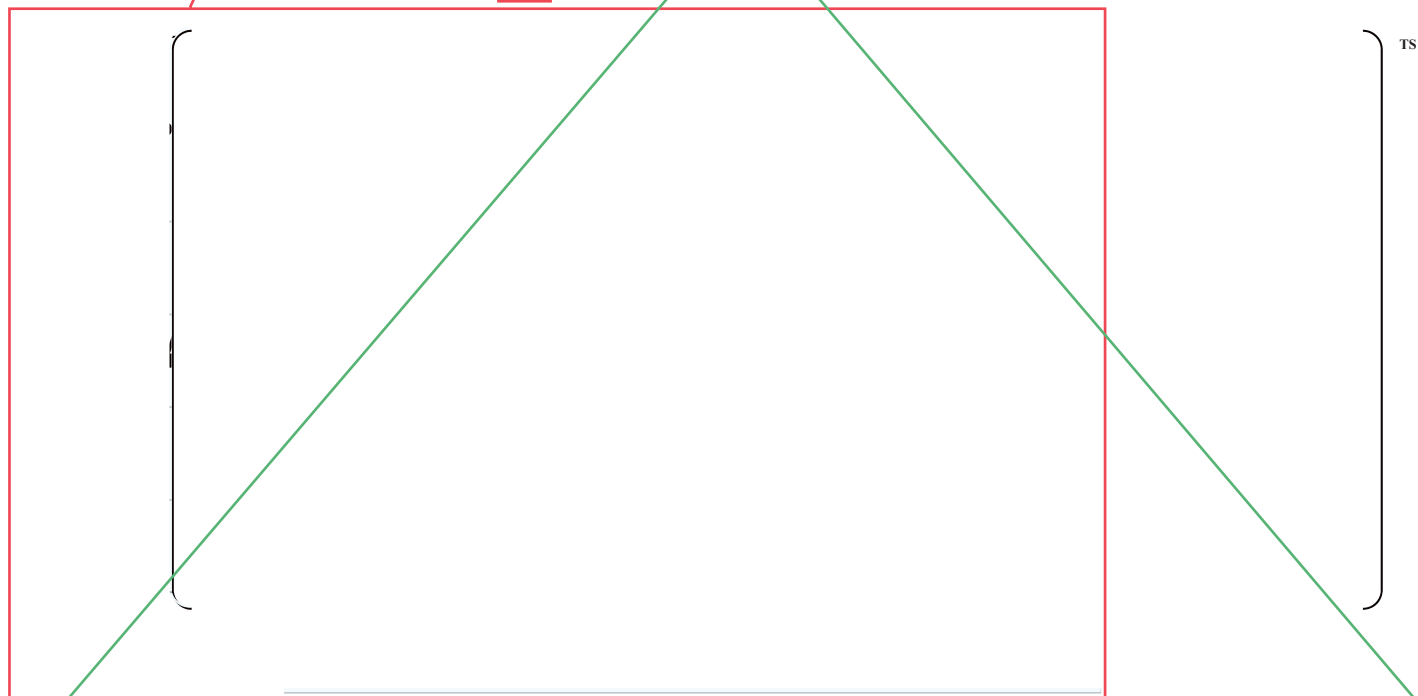
PLUS7 FUEL DESIGN for the APR1400

APR1400-F-M-TR-13001-P Rev.0

**Figure 3-4 Rod Power History Used for PLUS7 Fuel Rod Performance Analysis**

Replace

2

**Figure 3-2 Comparison of Measured Oxide Layer Thickness and Predicted Oxide Layer Thickness for H615 and H605 Assemblies**

3

D

TS

Figure 3-1 Rod Power History Used for PLUS7 Fuel Rod Performance Analysis

Note: Figure 3-1 is for the Response to RAI 5-7954 Question12.

TS

Figure 3-2 Comparison of Measured Oxide Layer Thickness and Predicted Oxide Layer Thickness for H615 and H605 Assemblies

E

TS

Figure 3-3 Power to Melt and Maximum Attainable Powers for UO_2 and $\text{Gd}_2\text{O}_3\text{-UO}_2$ Rods

TS

Figure 3-4 Comparison of Predicted and Measured Fuel Centerline Temperatures as a Function of Burnup vs. Determined TCD Penalty (red line)

Note: Figure 3-3 is for the Response to RAI 5-7954 Question12.

TR PLUS7 Fuel Design for the APR1400-Rev.0

TR PLUS7 Fuel Design for the APR1400-Rev.0

Non Proprietary

TR PLUS7 Fuel Design for the APR1400-Rev.1

PLUS7 FUEL DESIGN for the APR1400

APR1400-F-M-TR-13001-P Rev.0

6. REFERENCES

- 2-1 CENPD-178-P, Revision 1-P, "Structural Analysis of Fuel Assemblies for Seismic and Loss of Coolant Accident Loading," Combustion Engineering Inc., August 1981.
- 3-1 CENPD-139-P-A, "C-E Fuel Evaluation Model Topical Report," Combustion Engineering Inc., July 1974.
- 3-2 CENPD-139, Supplement 1, Revision 01, "C-E Fuel Evaluation Model Topical Report," Combustion Engineering Inc., July 1974.
- 3-3 CEN-161(B)-P-A, "Improvements to Fuel Evaluation Model," August 1989.
- 3-4 CEN-161(B)-P Supplement 1-P-A, "Improvements to Fuel Evaluation Model," January 1992.
- 3-5 CENPD-404-P-A, "Implementation of ZIRLO™ Cladding Material in CE Nuclear Power Fuel Assembly Designs," November 2001.
- 3-6 CEN-372-P-A, "Fuel Rod Maximum Allowable Gas Pressure," May 1990.
- 3-7 CENPD-275-P, Revision 1-P-A, "C-E Methodology for Core Designs Containing Gadolinia-Urania Absorbers," May 1998.
- 3-8 CENPD-275-P, Revision 1-P, Supplement, 1-P-A, "C-E Methodology for Core Designs Containing Gadolinia-Urania Absorbers," April 1999.
- 3-9 CEN-193(B), Supplement 2-P, Partial Response to NRC Questions on CEN-161(B)-P, "Improvements to Fuel Evaluation Model," March 21, 1982.
- 3-10 WCAP-16500-P-A, Rev.0 "CE 16x16 Next Generation Fuel Core Reference Report," August 2007.
- 3-11 WCAP-15063-P-A, Rev.1, with Errata, "Westinghouse Improved Performance Analysis and Design Model (PAD4.0)," July 2000.
- 3-12 CENPD-187-P-A, CEPAN Method of Analyzing Creep Collapse of Oval Cladding, Combustion Engineering, Inc., April 1976 ; Supplement 1-P-A, June 1977.
- 3-13 EPRI NP-3966-CCM, "CEPAN Method of Analyzing Creep Collapse of Oval Cladding-Volume 5: Evaluation of Interpellet Gap Formation and Cladding Collapse in Modern PWR Fuel Rods," Combustion Engineering, Inc., April 1985.

3-14 APR1400-F-A-NR-14002-P, "The Effect of Thermal Conductivity Degradation on APR1400 Design and Safety Analysis," KEPCO NF, September 2014.

3-14 Letter, ML#12198A202, "FINAL SAFETY EVALUATION REPORT ASSOCIATED WITH THE FLORIDA POWER AND LIGHT ST. LUCIE, UNIT 2, LICENSE AMENDMENT REQUEST FOR AN EXTENDED POWER UPRATE," July 23, 2012.

remove

Non Proprietary

PLUS7 FUEL DESIGN for the APR1400


APR1400-F-M-TR-13001-NP Rev.0

D.1.0 INTRODUCTION

PLUS7 mid grids introduced conformal springs and dimples in order to minimize damage to fuel rods caused by fretting wear. A long-term wear test was performed to evaluate the fuel rod wear performance of PLUS7 grids that have area contact with fuel rods. The cells of the grids were adjusted to have some gaps between them and the fuel rods, and the wear test was performed for 500 hours in the VIPER (Vibration Investigation and Pressure-drop Experimental Research) hydraulic test facility of Westinghouse Co. in the USA. Based on the wear scar data from the wear test, fuel rods, springs, and dimples were modeled using the Solidworks to calculate wear volumes relative to wear depths. The required time to reach the critical wear volume which is related to its wear depth was predicted.

The cladding wear evaluation is summarized as follows:

(1) Out-of-pile tests

- Results of the VIPER long-term wear tests (See Appendix A.2.3)

- All fretting wear scars of the PLUS7 assembly were measured using the Accumeasure System 9000 tool to determine the fretting wear depth.
- No measurable wear scars were found in the pre-oxidized rods.

(2) Analysis

- Wear volume-to-depth calculations

- Fretting wear performance was evaluated by wear mark inspection.
- Analytical calculation based on geometric configuration.

Non Proprietary

PLUS7 FUEL DESIGN for the APR1400

APR1400-F-M-TR-13001-NP Rev.0

Fuel rod failure will not occur due to the overheating of cladding under normal operation including AOOs.

(2) Criteria

There should be a 95% probability at the 95% confidence level that a hot fuel rod in the reactor core will not experience a DNB during normal operation or AOOs. For postulated accidents, the rods that experience DNB are assumed to fail for radiological dose calculation purposes.

(3) Evaluation

The evaluation for overheating cladding is addressed in plant specific transient and accident analysis (Chapter 15 of DCD).

3.2.9 Overheating of Fuel Pellets**1) Basis**

Fuel rod failure will not occur due to the overheating of fuel pellets under normal operation including AOOs. For postulated accidents, the total number of rods that experience centerline melting should be considered for radiological dose calculation.

(2) Criteria

During normal operating and AOOs, the fuel centerline temperature shall not exceed the melting temperature accounting for degradation due to burnup and addition of burnable absorbers.

The fuel rod is considered to be failed []^{TS} during postulated accidents. In the event of fuel failure, the radiological consequences of fuel failure must be accounted in the dose calculations.

The melting temperature of UO₂ is taken to be 5,080 °F (unirradiated) and to decrease []^{TS} per 10,000 MWD/MTU fuel burnup. For Gd₂O₃-UO₂ burnable absorber fuel rod, the melting temperature decreases additionally []^{TS} per weight percent of Gd₂O₃.

(3) Evaluation

The fuel centerline temperatures as a function of burnup are calculated using the NRC approved FATES3B code and methodology described in References 3-1 through 3-5 for UO₂ rod and References 3-7 and 3-8 for Gd₂O₃-UO₂ burnable absorber fuel rod.

The powers to fuel melting are calculated as a function of rod burnup. To preclude fuel melting, the peak local power experienced in normal operation and AOOs should be less than the power to fuel melting at all burnups.

The minimum design margin occurs at the end of cycle 1 because of the reduced power capability with burnup, which is caused by the depletion of the fissile material in the fuel and the buildup of fission products. The calculated power to fuel melting at the end of cycle 1 is []^{TS}, which is bounded by the local power density for trip setpoint of []^{TS}.




Non Proprietary

PLUS7 FUEL DESIGN for the APR1400

APR1400-F-M-TR-13001-NP Rev.0

Table 3-4 Main Design Parameters Used for PLUS7 Fuel Rod Performance Analysis

| | | |
|---|--|----|
| | | TS |
|  | | |

Non Proprietary

PLUS7 FUEL DESIGN for the APR1400

APR1400-F-M-TR-13001-NP Rev.0

Table 3-5 Description of Data Base Used for FATES3B Verification

TS

| |
|--|
| |
|--|



REVISED RESPONSE TO REQUEST FOR ADDITIONAL INFORMATION

APR1400 Topical Reports

Korea Electric Power Corporation / Korea Hydro & Nuclear Power Co., LTD

Docket No. PROJ 0782

RAI No.: 5-7954

SRP Section: TR PLUS7 Fuel Design for the APR1400

Application Section: PLUS7 Fuel Design for the APR1400
(APR1400-F-M-TR-13001-P)

Date of RAI Issue: 06/18/2015

Question No. TR PLUS7 Fuel Design for the APR1400-13

GDC 10 requires that the reactor core and associated coolant, control, and protection systems shall be designed with appropriate margin to assure that specified acceptable fuel design limits (SAFDLs) are not exceeded during any condition of normal operation, including the effects of anticipated operational occurrences (AOOs). SRP Section 4.2 (II)(1)(B)(iv) provides guidance in regards to GDC 10 by that overheating of fuel pellets should be avoided by preventing centerline melting. This analysis should be performed for the maximum linear heat generation rate anywhere in the core, including all hot spots and should account for the effects of burnup and composition on the melting point.

Section 2.2.2 of APR1400-F-A-NR-13002-P provides a scoping analysis using FRAPCON3.4 to investigate the impacts of burnup dependent TCD on the fuel centerline temperature analysis. The staff has concerns regarding the methodology and results presented in that the methodology is different than what is presented in APR1400-F-M-13001-P and the results do not support the stated conclusions. This in turn has caused the staff to question the ability of the fuel centerline melting analysis provided to demonstrate compliance with GDC 10.

Address the following concerns, as appropriate, to demonstrate compliance with GDC 10:

- a) Provide a basis for the assumed uncertainty of 9.7% on best estimate fuel centerline temperature used to calculate the conservative power to melt results.
- b) Section 2.2.2 of APR1400-F-A-NR-13002-P provides a SAFDL of 20 kW/ft. Figure 2-10 shows that the fuel would melt above 30 GWd/MTU assuming a conservative analysis. Update the topical report, as applicable, to ensure that the linear heat rate SAFDL is conservatively met.
- c) Provide a description and update the topical report, as necessary, to explain how the melt analysis will be performed on a cycle specific basis since FRAPCON-3.4 was used to perform the scoping analysis, or update the topical report methodology to not require FRAPCON-3.4 to confirm compliance with GDC 10.

Response - (Rev.1)

- a) The assumed uncertainty of 9.7% in Section 2.2.2 of APR1400-F-A-NR-14002-P is a typo and the assumed uncertainty should be []^{TS}. The value comes from measured and predicted centerline temperature comparison for the UO₂ rod described in the FRAPCON manual [Reference 13-1]. The measured data is within []^{TS} level of lower and upper predicted limit in Figure 13-1. Therefore, the uncertainty of []^{TS} was conservatively determined by assuming a standard deviation of []^{TS} and multiplying by []^{TS}.

The text in Section 2.2.2 of APR1400-F-A-NR-14002-P will **not** be revised to reflect the correction of uncertainty from 9.7% to []^{TS} because the TCD technical report (APR1400-F-A-NR-14002-P) will be withdrawn.

TS

Figure 13-1 Measured and Predicted Centerline Temperature for the UO₂ Assessment Cases throughout Life

- b) Divided by a SAFDL of 20 kW/ft, the conservative Power-To-Melt (PTM) values are normalized and plotted in Figure 13-2. As shown in Figure 13-2, the normalized Power-To-Melt (PTM) values indicate a gradual decline below a []^{TS} kW/ft from []^{TS}. The fuel will not melt because the descent ratio of actual fuel rod power (radial power fall-off) after []^{TS} will be much higher than that of the normalized PTM due to the reduced power capability caused by the depletion of the fissile material in the fuel and the buildup of fission products. Furthermore, Figure 13-2 shows that the margin between Radial Power Fall-off and PTM tends to increase after []^{TS}.

Since TCD technical report (APR1400-F-A-NR-14002-P) will be withdrawn, PTM calculations using FATES3B code with TCD penalty will be performed to ensure that a SAFDL of []^{TS} is conservatively met. And also, the current Section 3.4.4 of the PLUS7 topical report (APR1400-F-M-TR-13001-P) will be changed to 3.4.5 with the update to reflect TCD effect on PTM analysis.

TS

Figure 13-2 Normalized Power to Melt and Radial Power Fall-off Curve vs. Burnup

- c) A cycle specific analysis will be performed using a cycle specific radial fall-off curve based on the core loading pattern with FATES3B code considering the TCD penalty. This will ensure that the linear heat rate []^{TS} is valid.

The current Section 3.4.4 of the PLUS7 topical report (APR1400-F-M-TR-13001-P) will be changed to 3.4.5 with the update to explain how the melt analysis will be performed on a cycle specific basis with the TCD.

References

[13-1] []^{TS}

Impact on DCD

There is no impact on the DCD.

Impact on PRA

There is no impact on the PRA.

Impact on Technical Specifications

There is no impact on the Technical Specifications.

Impact on Technical/Topical/Environmental Reports

Topical Report APR1400-F-M-TR-13001-P will be revised as indicated on the attached markups in response to Question 12.

Technical Report APR1400-F-A-NR-14002-P will not be revised because the TCD Technical report (APR1400-F-A-NR-14002-P) will be withdrawn.

REVISED RESPONSE TO REQUEST FOR ADDITIONAL INFORMATION

APR1400 Topical Reports

Korea Electric Power Corporation / Korea Hydro & Nuclear Power Co., LTD

Docket No. PROJ 0782

RAI No.: 5-7954

SRP Section: TR PLUS7 Fuel Design for the APR1400

Application Section: PLUS7 Fuel Design for the APR1400
(APR1400-F-M-TR-13001-P)

Date of RAI Issue: 06/18/2015

Question No. TR PLUS7 Fuel Design for the APR1400-14

GDC 10 requires that the reactor core and associated coolant, control, and protection systems shall be designed with appropriate margin to assure that specified acceptable fuel design limits (SAFDLs) are not exceeded during any condition of normal operation, including the effects of anticipated operational occurrences (AOOs). SRP Section 4.2 (II)(1)(B)(iv) provides guidance in regards to GDC 10 by stating that overheating of fuel pellets should be avoided by preventing centerline melting. This analysis should be performed for the maximum linear heat generation rate anywhere in the core, including all hot spots and should account for the effects of burnup and composition on the melting point.

Section 3.2.9 of the PLUS7 fuel design topical report, APR1400-F-M-TR-13001-P, provides the overheating of fuel pellets analysis for the APR1400 design. On Page 3-9, it is stated that the linear heat rate corresponding to the centerline melt of Gd_2O_3 - UO_2 burnable absorber fuel rods is always less than that of the UO_2 fuel rods. The lower thermal conductivity of Gd_2O_3 - UO_2 burnable absorber fuel rods causes the staff to question the claimed bounding nature.

Provide linear heat generation rate limits for UO_2 and Gd_2O_3 - UO_2 to support the position presented in APR1400-F-M-13001-P, or revise the topical report as necessary.

Response - (Rev.1)

In the response to Question 12, Figure 12-2 shows the Power-to-Melt (PTM) for both UO_2 and $\text{Gd}_2\text{O}_3\text{-UO}_2$ rods calculated by FATES3B code with TCD penalty. It also shows the maximum attainable powers for both UO_2 and $\text{Gd}_2\text{O}_3\text{-UO}_2$ rods. As mentioned in the response to Question No.12, the attainable power of $\text{Gd}_2\text{O}_3\text{-UO}_2$ rod in Figure 12-2 can be derived by considering the normalized radial power ratio of UO_2 and $\text{Gd}_2\text{O}_3\text{-UO}_2$ rods shown in Figure 12-1. As shown in Figure 12-2, the attainable powers for $\text{Gd}_2\text{O}_3\text{-UO}_2$ rod are well below the PTM values over all burnup ranges.

Based on the Figure 12-2, it can be concluded that there will be no melting of $\text{Gd}_2\text{O}_3\text{-UO}_2$ rod even when the rod power for UO_2 rod reaches a SAFDL value of []^{TS}. Therefore, the lower power of $\text{Gd}_2\text{O}_3\text{-UO}_2$ rod compared to UO_2 rod ensures that UO_2 rod remains limiting for centerline melt.

The TCD penalty methodology will be described in Section 3.5 of the PLUS7 fuel design topical report (APR1400-F-M-TR-13001-P) and, accordingly, the current Section 3.4.4 will be changed to 3.4.5 with the update to reflect TCD effect on PTM analysis. In addition, the discussion on $\text{Gd}_2\text{O}_3\text{-UO}_2$ melting will be added to the text in Section 3.4.5.

Impact on DCD

There is no impact on the DCD.

Impact on PRA

There is no impact on the PRA.

Impact on Technical Specifications

There is no impact on the Technical Specifications.

Impact on Technical/Topical/Environmental Reports

Topical Report APR1400-F-M-TR-13001-P will be revised as indicated on the attached markups in response to Question 12.

REVISED RESPONSE TO REQUEST FOR ADDITIONAL INFORMATION

APR1400 Topical Reports

Korea Electric Power Corporation / Korea Hydro & Nuclear Power Co., LTD

Docket No. PROJ 0782

RAI No.: 5-7954

SRP Section: TR PLUS7 Fuel Design for the APR1400

Application Section: PLUS7 Fuel Design for the APR1400
(APR1400-F-M-TR-13001-P)

Date of RAI Issue: 06/18/2015

Question No. TR PLUS7 Fuel Design for the APR1400-16

GDC 10 requires that the reactor core and associated coolant, control, and protection systems shall be designed with appropriate margin to assure that specified acceptable fuel design limits (SAFDLs) are not exceeded during any condition of normal operation, including the effects of anticipated operational occurrences (AOOs). SRP Section 4.2 (II)(1)(A)(ii) provides guidance in regards to GDC 10 by stating that the cumulative number of strain fatigue cycles on the structural members should be significantly less than the design fatigue lifetime, which is based on appropriate data and includes a safety factor.

Pages 3-17 and 2-5 of the TCD report (APR1400-F-A-NR-13002-P) discuss cladding strain and fatigue. Section 3.4.2 states that the increased thermal expansion can be offset with available design margin in the cladding strain and fatigue limits. Sample calculations provided in the TCD report show that the fatigue damage factor will increase from 0.28 to 0.77 when TCD is considered. This has caused the staff to question the claim that increased thermal expansion can be offset with available design margin in the cladding strain and fatigue limits.

a) Discuss how the fatigue analysis will be performed on a cycle specific basis given this demonstration that FATES3B alone is inadequate to assess the fatigue damage fraction. Update the topical report, if necessary, to include the clarification.

b) The fatigue damage factors (FDF) presented in topical report APR1400-F-M-TR-13001-P and technical report APR1400-F-A-NR-13002-P (for the operating condition "without TCD") do not appear to match. Update the report(s) as necessary to reflect the correct FDF.

Response - (Rev.1)

- a) Fatigue analysis in the technical report (APR1400-F-A-NR-13002-P) is performed using more conservative radial peaking factor (RPF, marked as blue-dotted line in Figure 16-1) than the cycle specific RPF curve. And the calculated fatigue damage factor accounting for TCD effect is $[\quad]^{TS}$ which is below the limit of $[\quad]^{TS}$. Thus, it is confirmed that the cladding fatigue criterion is still satisfied with the consideration of TCD.

Since technical report will be withdrawn, this result on the fatigue damage factor will be described in Section 3.4.3, which is currently indicated in Section 3.4.2, of topical report APR1400-F-M-TR-13001-P. The conservative RPF (marked as blue-dotted line in Figure 16-1) will be validated on a cycle-by-cycle basis to confirm the applicability for a given subsequent cycle.

Therefore, the fatigue analysis result presented in the topical report can be continually used for fatigue criterion confirmation if the conservative RPF is confirmed to be valid on a cycle specific basis.

- b) The fatigue damage factors presented in topical report APR1400-F-M-TR-13001-P and technical report APR1400-F-A-NR-13002-P (for the operating condition without TCD) are $[\quad]^{TS}$ and $[\quad]^{TS}$, respectively. The higher fatigue damage factor in topical report APR1400-F-M-TR-13001-P is mainly attributed to the excessive conservatism of power history assumed in the calculation. Rod power history (radial peaking factor) used in the fatigue analysis of the topical report is much higher than that of technical report as shown in Figure 16-1. The other conservatism in the fatigue analysis for the topical report is to assume higher End Of Life (EOL) rod average burnup of $[\quad]^{TS}$. In contrast, the fatigue analysis result (fatigue damage factor= $[\quad]^{TS}$) presented in technical report was obtained by assuming the EOL burnup of $[\quad]^{TS}$ (the target licensing burnup) and reducing the excessive conservatism in the rod power history (radial peaking factor) as shown Figure 16-1.

TS



Figure 16-1 Radial Peaking Factors (RPF) used for Fatigue Analyses

References

“Deleted”

Impact on DCD

There is no impact on the DCD.

Impact on PRA

There is no impact on the PRA.

Impact on Technical Specifications

There is no impact on the Technical Specifications.

Impact on Technical/Topical/Environmental Reports

Topical Report APR1400-F-M-TR-13001-P will be revised as indicated on the attached markups.
Technical Report APR1400-F-A-NR-14002-P will be withdrawn.

TR PLUS7 Fuel Design for the APR1400_Rev.0 - 16

TR PLUS7 Fuel Design for the APR1400_Rev.1 - 16

Proprietary

Delete

PLUS7 FUEL DESIGN for the APR1400

APR1400-F-M-TR-13001-P Rev.0

~~Considering the amount of potential increase in rod internal pressure by TCD impact and design margin to the limit, it is judged that the cladding stress criteria are still met with consideration of TCD.~~

~~3.4.2 Cladding Strain and Fatigue~~

~~The cladding strain is affected by TCD due to the increased fuel thermal expansion. However, the increased thermal expansion can be offset with available design margin to the cladding strain and fatigue limits and conservatism in the input variables such as power history and assumed rod internal pressure. Therefore, cladding strain and fatigue criteria are still satisfied with consideration of TCD.~~

~~3.4.3 Fuel Rod Internal Pressure~~

3.4.3 Cladding Fatigue

(blank)

The fatigue damage factor for the daily load following operation was calculated using the same convenient code of FATES3B as used for cladding strain evaluation. In this calculation, more conservative radial peaking factor (RPF) than the cycle specific RPF curve was used. On the other hand, the fatigue damage factors for reactor trips and startups/shutdowns are determined by hand calculation using a simple formula. The total cumulative fatigue damage factor from daily load following operation, reactor trips and startups/shutdowns was []^{TS} which is below the limit of []^{TS}. Therefore, it was confirmed that the cladding fatigue criterion is still satisfied with the consideration of TCD.

(blank)

And then, to confirm the applicability for a given subsequent cycle, the conservative RPF used in the calculation will be validated on a cycle-by-cycle basis.

~~In conclusion, the increased rod internal pressure can be offset with available design margin to the rod internal pressure limits. Therefore, rod internal pressure criteria are still satisfied considering the effects of TCD.~~

~~3.4.4 Overheating of Fuel Pellets~~

~~The power to melt limit depends on fuel burnup but the reduced power capability with burnup, which is caused by the depletion of the fissile material in the fuel and the buildup of fission products, offsets the TCD impact. Therefore, it is judged that there will be no safety concerns due to TCD. However, the power to melt values with burnup considering the impact of TCD are calculated and will be provided in the TCD Technical Report which will be submitted to NRC.~~

~~In summary, KNE fuel rod design criteria have been reviewed with respect to the potential impacts of TCD, and it is concluded that TCD can be accommodated such that approved fuel rod design criteria will remain satisfied for current fuel rod designs.~~

3.5 Conclusion

The PLUS7 fuel rod design is verified to maintain the rod integrity up to rod average burnup of 60,000 MWD/MTU based on the thermal performance and mechanical integrity evaluation results using by NRC approved design codes and methodologies.

REVISED RESPONSE TO REQUEST FOR ADDITIONAL INFORMATION

APR1400 Topical Reports

Korea Electric Power Corporation / Korea Hydro & Nuclear Power Co., LTD

Docket No. PROJ 0782

RAI No.: 5-7954

SRP Section: TR PLUS7 Fuel Design for the APR1400

Application Section: PLUS7 Fuel Design for the APR1400
(APR1400-F-M-TR-13001-P)

Date of RAI Issue: 06/18/2015

Question No. TR PLUS7 Fuel Design for the APR1400-18

GDC 10 requires that the reactor core and associated coolant, control, and protection systems shall be designed with appropriate margin to assure that specified acceptable fuel design limits (SAFDLs) are not exceeded during any condition of normal operation, including the effects of anticipated operational occurrences (AOOs).

To perform accurate confirmatory calculations to evaluate the application's conformance with GDC 10, NRC must use the correct input information for the APR1400 design, including rod geometry, reactor conditions, power history, and axial power profile.

Please provide the following sample calculations using FATES3B. For each case, include all appropriate input information including rod geometry, reactor conditions, power history, and axial power profile:

- a. Provide sample calculations of cladding strain under AOOs for a typical AOO overpower event. Provide calculations at rod average burnup of 0 GWd/MTU, 20 GWd/MTU, 40 GWd/MTU, and 60 GWd/MTU.
- b. Provide a sample calculation of rod internal pressure for a bounding power history up to a rod average burnup of 62 GWd/MTU. Provide pressure calculations as a function of time.
- c. Provide a sample calculation of power to melt at the following rod average burnup levels; 0 GWd/MTU, 10 GWd/MTU, 20 GWd/MTU, 30 GWd/MTU, 40 GWd/MTU, 50 GWd/MTU, 60 GWd/MTU.
- d. Provide a sample calculation of fuel stored energy for a bounding power history up to a rod average burnup of 62 GWd/MTU. Provide stored energy calculations as a function of time.

Response - (Rev.1)

Design input information including rod geometry, power history, axial power profile and reactor conditions are described in Tables 18-1 - 18-5. Sample calculations of transient strain, rod internal pressure, power to melt, and stored energy are below

Table 18-1 Fuel Rod Geometry

TS

| |
|--|
| |
|--|

Table 18-2 Generic Power Histories and Axial Power Profile for Transient Strain

TS



Table 18-3 Bounding Power Histories for Rod Internal Pressure, Power to Melt and Stored Energy

TS

Table 18-4 Axial Power Profile for the Calculation of Rod Internal Pressure,
Power to Melt and Stored Energy

TS

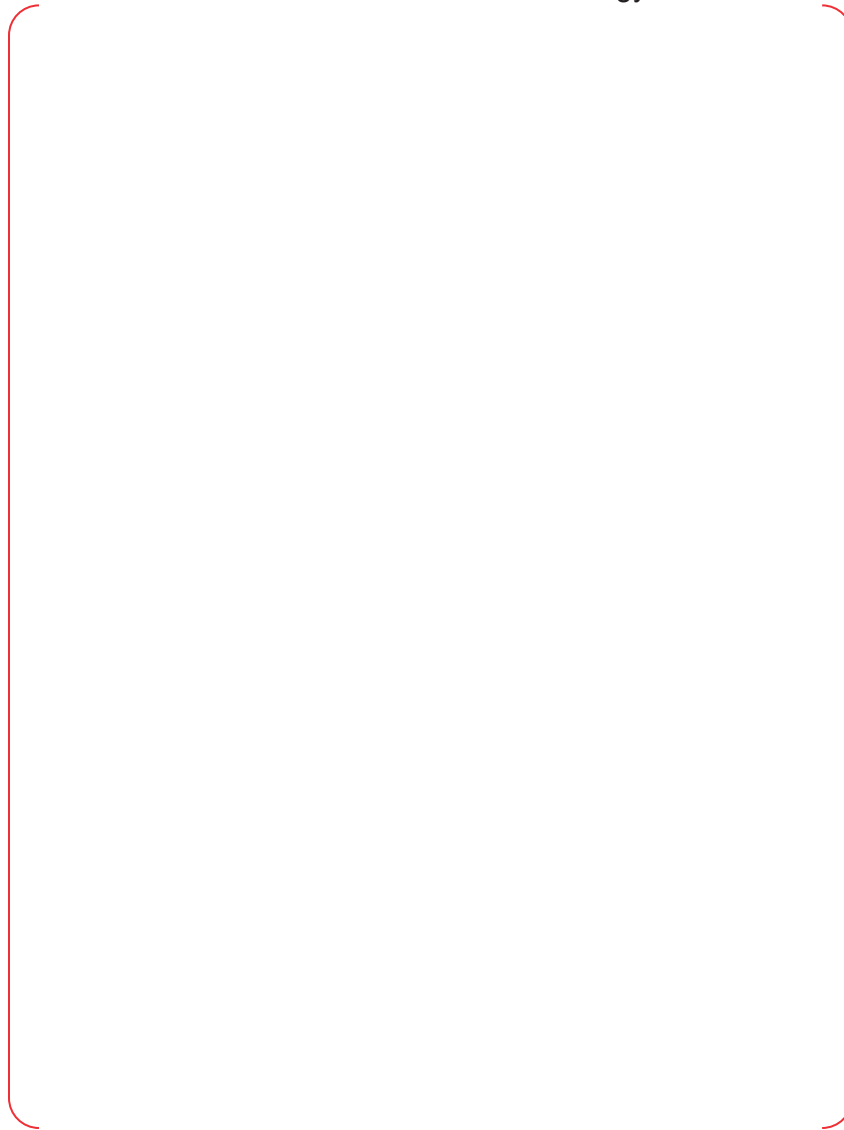


Table 18-5 Reactor Conditions

TS

Results of sample calculations for transient strain, rod internal pressure, power to melt and stored energy are as follows;

- a) Transient strain under AOO at rod average burnup of 0 GWd/MTU, 20 GWd/MTU, 40 GWd/MTU, and 60 GWd/MTU.

TS

Re-examined total (elastic plus plastic) strain will be reflected in topical report as shown in the attached markup.

b) Rod Internal gas pressure up to fuel rod average burnup of 60 GWd/MTU

TS

Rod internal pressure was calculated up to 60 GWd/MTU which is a license target burnup.

- c) Power to melt at 0 GWd/MTU, 10 GWd/MTU, 20 GWd/MTU, 30 GWd/MTU, 40 GWd/MTU, 50 GWd/MTU, 60GWd/MTU._



Power to melt was updated to reflect thermal conductivity degradation (TCD) effect in accordance with Section 3.4.5 of the PLUS7 fuel design topical report (APR1400-F-M-TR-13001-P)

d) Fuel stored energy for one fuel rod as a function of time

TS

Fuel stored energy was calculated with TCD penalty in accordance with Section 3.5 of the PLUS7 fuel design topical report (APR1400-F-M-TR-13001-P) up to 60 GWd/MTU which is a license target burnup.

Impact on DCD

There is no impact on the DCD.

Impact on PRA

There is no impact on the PRA.

Impact on Technical Specifications

There is no impact on the Technical Specifications.

Impact on Technical/Topical/Environmental Reports

Topical Report APR1400-F-M-TR-13001-P will be revised as indicated on the attached markups.

Non Proprietary

PLUS7 FUEL DESIGN for the APR1400

APR1400-F-M-TR-13001-NP Rev.0

normal operation involving fuel handling and storage, reactor servicing, power operation and reactor trip, heatup and cooldown, and minor fuel handling accident using the standard formulas.

The stress analyses for AOOs such as "Inadvertent Opening of an Atmospheric Dump Valve", "Uncontrolled CEA Withdrawal at Power", "Total Loss of Reactor Coolant Flow and "Loss of Condenser Vacuum" events were performed using the FATES3B code [3-1 through 3-4].

The results of the evaluation indicate that the primary tensile and compressive stresses in the cladding and end cap welds are within the allowable limits as shown in Table 3-3.

3.2.2 Cladding Strain**(1) Basis**

Fuel system will not be damaged due to excessive strain under normal operation including AOOs.

(2) Criteria

At any time during the fuel rod lifetime, the net unrecoverable circumferential tensile cladding strain shall not exceed $\left[\quad \right]^{TS}$, based on the beginning-of-life (BOL) cladding dimensions. This criterion is applicable to normal operating conditions and following a single AOO.

The total (elastic plus plastic) circumferential cladding strain increment produced as a result of a single AOO shall not exceed $\left[\quad \right]^{TS}$ relative to the pre-transient condition.

Ductility is a function of irradiation and hydride formation in the cladding wall. Because the waterside corrosion for ZIRLO is significantly lower and should result in less hydrogen uptake and less hydride formation, total strain capability of ZIRLO is projected to be in excess of $\left[\quad \right]^{TS}$ at burnups of 60,000 MWD/MTU. Thus, a $\left[\quad \right]^{TS}$ strain limit will continue to be applied as a strain criterion.

(3) Evaluation

The evaluation methodology for the fuel rod cladding strain is discussed in Reference 3-5, which was reviewed and approved by NRC for Westinghouse CE PWR fuel designs.

The first part of the strain limit concerns that the total plastic strain incurred as a result of cladding creep and cladding yielding during long term normal operation and the following short transient conditions. Cladding creep strain and plastic strain due to cladding yielding are driven by the stress in the cladding that results from differential pressure and interface with the fuel pellets. The method used to evaluate the strain accounts for power dependent and time dependent changes (e.g., fuel rod void volume, fission gas release and gas temperature, differential cladding, cladding creep and thermal expansion) that can produce strain in the fuel cladding. In addition, the strain analysis accounts for both long term, normal operating condition, and short term, transient condition.

For the present application, the predicted plastic strain using FATES3B code is $\left[\quad \right]^{TS}$ and the total (elastic plus plastic) circumferential cladding strain increment produced as a result of a single AOO is $\left[\quad \right]^{TS}$. As the calculated strains are less than $\left[\quad \right]^{TS}$ the design criteria are satisfied.



**KHNP****KOREA HYDRO & NUCLEAR POWER CO., LTD**

70-1312-gil, Yuseong-daero, Yuseong-gu, Daejeon, 305-343, KOREA

Tel: +82-42-870-5400 / Fax: +82-42-870-5449

<http://www.khnp.co.kr>

October 16, 2017
Document Control Desk
U.S. Nuclear Regulatory Commission
Washington, DC 20555-0001

Attention: Mr. William Ward
Division of New Reactor Licensing

Docket No. 52-046
MKD/NW-17-0323L

Subject: Revised Response to RAI 5-7954 on Topical Report “PLUS7 Fuel Design for the APR1400” (Rev.2)

- References:** 1) NRC Request for Additional Information 5-7954, dated June 18, 2015
2) KHNP Letter MKD/NW-15-0055L, Response to RAI 5-7954 on Topical Report “PLUS7 Fuel Design for the APR1400, APR1400-F-M-TR-13001, Rev. 0, dated July 21, 2015
3) KHNP Letter MKD/NW-16-0826L, Response to RAI 5-7954 for Question TR PLUS7 Fuel Design for the APR1400-16, dated July 29, 2016
4) KHNP Letter MKD/NW-17-0201L, Revised Response to RAI 5-7954 on Topical Report “PLUS7 Fuel Design for the APR1400”, dated August 11, 2017

KHNP is hereby submitting the response to RAI 5-7954, dated June 18, 2015. The revised response addresses Question TR PLUS7 Fuel Design for the APR1400-11.

Enclosure 1 contains a copy of the associated affidavit. Enclosure 2 provides the revised response to RAI 5-7954 on topical report “PLUS7 Fuel Design for the APR1400” (Rev.2) (Proprietary). Enclosure 3 provides the revised response to RAI 5-7954 on topical report PLUS7 Fuel Design for the APR1400” (Non-Proprietary).

If additional information or clarification is required, please contact Daegeun Ahn, Director of KHNP Washington DC Center at ahn.daegeun@khnp.co.kr or 703-388-0592.

Sincerely,

Han-gon Kim
Project Manager
Advanced Reactors Development Laboratory
Korea Hydro & Nuclear Power Co., Ltd.



KHNP
KOREA HYDRO & NUCLEAR POWER CO., LTD

Enclosures:

1. Affidavit KAW-17-0323
2. Revised Response to RAI 5-7954 on Topical Report “PLUS7 Fuel Design for the APR1400”
(Rev.2) (Proprietary)
3. Revised Response to RAI 5-7954 on Topical Report “PLUS7 Fuel Design for the APR1400”
(Rev.2) (Non-Proprietary)

Enclosure 1

Affidavit KAW-17-0323

I, Yun-ho Kim, state the following:

1. I am the General Manager of Korea Hydro & Nuclear Power Co., Ltd. (KHNP), and as such I am authorized to request withholding the information transmitted with this letter from public disclosure and to execute this affidavit.
2. I am familiar with the criteria applied by KHNP to determine whether certain information is proprietary, and with the policies established by KHNP to ensure the proper application of these criteria.
3. The information, Revised Response to RAI 5-7954 on Topical Report “PLUS7 Fuel Design for the APR1400” (Rev.2) (Proprietary), transmitted with this letter has been classified by KHNP as proprietary in accordance with the policies for the control and protection of proprietary and confidential information. The information regarded as proprietary is identified and marked consistent with the requirements of 10 CFR 2.390, § (b)(1)(i). Accordingly, the proprietary information is enclosed within brackets and the right-hand bracket carries a notation of “TS” to indicate that the trade secret nature of the information claimed to be proprietary is the basis for proposing that the information so identified be withheld from public disclosure.
4. Pursuant to the considerations set forth in 10 CFR Section 2.390(a), KHNP considers the information classified as proprietary to be “trade secret” information since it is design, analysis, or test information that would be difficult for a competitor to reproduce and hence provides an economic and competitive advantage to KHNP.
5. The need for designating the information as proprietary has been raised within KHNP. The information is being treated proprietary and confidential and has not been disclosed by KHNP to the public.
6. Nondisclosure of the proprietary information transmitted with this letter is vital to the competitiveness held by KHNP and, hence, disclosure of the proprietary information transmitted in with this letter would have negative commercial impacts on the competitive position of KHNP in the U.S. nuclear market.
7. In accordance with KHNP policy, proprietary information contained in this document may be, or may have been, made available on a limited basis to regulatory bodies, customers, potential customers, and their agents, suppliers, and licensees, and others under suitable agreements providing for nondisclosure and limited use of the information.



KHNP
KOREA HYDRO & NUCLEAR POWER CO., LTD

I declare that the foregoing statements are true and correct to the best of my knowledge, information and belief.

Executed on October 16, 2017.

Yun-ho Kim
General Manager
APR1400 Licensing Team
Korea Hydro and Nuclear Power Co., Ltd

Enclosure 3

Revised Response to RAI 5-7954 on Topical Report “PLUS7 Fuel
Design for the APR1400” (Rev.2)

(Non-Proprietary)

October 16, 2017

REVISED RESPONSE TO REQUEST FOR ADDITIONAL INFORMATION

APR1400 Topical Reports

Korea Electric Power Corporation / Korea Hydro & Nuclear Power Co., LTD

Docket No. PROJ 0782

RAI No.: 5-7954

SRP Section: TR PLUS7 Fuel Design for the APR1400

Application Section: PLUS7 Fuel Design for the APR1400
(APR1400-F-M-TR-13001-P)

Date of RAI Issue: 06/18/2015

Question No. TR PLUS7 Fuel Design for the APR1400-11

GDC 10 requires that the reactor core and associated coolant, control, and protection systems shall be designed with appropriate margin to assure that specified acceptable fuel design limits (SAFDLs) are not exceeded during any condition of normal operation, including the effects of anticipated operational occurrences (AOOs). SRP Section 4.2 (II)(1)(B)(v) provides guidance stating that the fuel failure criteria should address excessive fuel enthalpy.

This fuel failure criterion is addressed on Page 3-9 of APR1400-F-M-TR-13001-P for the PLUS7 fuel design. Section 3.4.4 of the topical report states that the code used to analyze this fuel failure mechanism (FATES3B) over predicts fuel thermal conductivity at high burnup. Therefore, it will also under predict fuel enthalpy. The staff notes that Section 3.4.4 provides a qualitative argument to state that the effects of burnup dependence of TCD are bounded by the reduced power capabilities at higher burnups. This raises concerns from the staff on the ability of the excessive fuel enthalpy analysis to demonstrate compliance with the excessive fuel enthalpy SAFDL given all core loading options available.

Please include a discussion, supported by analysis, within Section 3.2.10 and/or 3.4.4 of APR1400-F-M-TR-13001-P regarding the impacts of the fuel enthalpy under prediction and how excessive fuel enthalpy is precluded.

Response - (Rev.2)

A impact of fuel enthalpy will be updated and added in Section 3.6 of topical report (APR1400-F-M-TR-13001-P), which is currently described in Section 3.4.5.

“The impacts of TCD result in increasing the fuel enthalpy and the fuel centerline temperature. The impact on the fuel enthalpy due to TCD would be negligible for fresh fuel even though the maximum power peaking factors exist in the low burnup fuel in the APR1400 reload core designs. For the high burnup fuel which is affected by TCD, the fuel enthalpy and the fuel centerline temperature increase due to TCD are not significant because of the peaking factor burndown effect at higher burnups. The event specific evaluation considering the TCD penalty described in the Section 3.5 was performed and described in DCD Tier 2 Chapter 15.4.8.”

Impact on DCD

Effect on the Design Control Document (DCD) Tier 2 Chapter 15.4.8 for safety analyses will be updated because interface data results based on the thermal conductivity degradation (TCD) penalty methodology are applied.

In addition, for an extent of content review, TCD-affected chapters will be revised as indicated on the attached markups. The attached markups are classified as follow.

- References (Chapter 4.2.6) : Attachment 2
- Control Requirements (Chapter 4.3.2.4) : Attachment 3
- Containment Functional Design (Chapter 6.2.1) : Attachment 4
- Containment Functional Design (Chapter 6.2.1) : Attachment 5
- Criticality Safety of New Spent Fuel Storage (Chapter 9.1.1) : Attachment 6
- General Information for Safety Analysis (Chapter 15.0.0) and Spectrum of Control Element Assembly Ejection Accidents (15.4.8) : Attachment 7
- Loss-of-Coolant Accidents (Chapter 15.6.5) : Attachment 8

Impact on PRA

There is no impact on the PRA.

Impact on Technical Specifications

There is no impact on the Technical Specifications.

Impact on Technical/Topical/Environmental Reports

PLUS7 fuel design topical report (APR1400-F-M-TR-13001-P) will be revised as indicated on the attached markups (Attachment 1).

Criticality Analysis technical report (APR1400-Z-A-NR-14011-P) will be revised as indicated on the attached markups (Attachment 9).

Non Proprietary

PLUS7 FUEL DESIGN for the APR1400

APR1400-F-M-TR-13001-P Rev.0

Considering the amount of potential increase in rod internal pressure by TCD impact and design margin to the limit, it is judged that the cladding stress criteria are still met with consideration of TCD.

3.4.2 Cladding Strain and Fatigue

The cladding strain is affected by TCD due to the increased fuel thermal expansion. However, the increased thermal expansion can be offset with available design margin to the cladding strain and fatigue limits and conservatism in the input variables such as power history and assumed rod internal pressure. Therefore, cladding strain and fatigue criteria are still satisfied with consideration of TCD.

3.4.3 Fuel Rod Internal Pressure

The effect of increased fuel temperature due to TCD on fission gas release is inherently accounted for in the current performance code, FATES3B (References 3-1 through 3-4) because the model was calibrated to measured data for a full range of fuel rod burnup and operating conditions. Additionally, conservatism is considered in the original FATES3B calibration process and in fuel rod design analysis. However, the rod internal pressure may still increase with TCD due to the increased fuel thermal expansion, which reduces the total fuel rod void volume.

Evaluations show that the reduction of void volume due to increased thermal expansion is not significant in PLUS7 fuel rod design. In addition, the rod internal pressure limit calculation is inherently conservative in that actual gap reopening is predicted to occur at higher pressures.

In conclusion, the increased rod internal pressure can be offset with available design margin to the rod internal pressure limits. Therefore, rod internal pressure criteria are still satisfied considering the effects of TCD.

3.4.4 Overheating of Fuel Pellets

The power to melt limit depends on fuel burnup but the reduced power capability with burnup, which is caused by the depletion of the fissile material in the fuel and the buildup of fission products, offsets the TCD impact. Therefore, it is judged that there will be no safety concerns due to TCD. However, the power to melt values with burnup considering the impact of TCD are calculated and will be provided in the TCD Technical Report which will be submitted to NRC.

In summary, KNF fuel rod design criteria have been reviewed with respect to the potential impacts of TCD, and it is concluded that TCD can be accommodated such that approved fuel rod design criteria will remain satisfied for current fuel rod designs.

3.5 Conclusion

The PLUS7 fuel rod design is verified to maintain the rod integrity up to rod average burnup of 60,000 MWD/MTU based on the thermal performance and mechanical integrity evaluation results

3.4.5 Impacts of Fuel Enthalpy

The impacts of TCD result in increasing the fuel enthalpy and the fuel centerline temperature. The impact on the fuel enthalpy due to TCD would be negligible for fresh fuel even though the maximum power peaking factors exist in the low burnup fuel in the APR1400 reload core designs. For the high burnup fuel which is affected by TCD, the fuel enthalpy and the fuel centerline temperature increase due to TCD are not significant because of the peaking factor burndown effect at higher burnups. The detailed evaluation was performed for the impacts of TCD and submitted in TCD Technical Report in Reference 3-14.

KHNP

3-17

This Chapter 3.4.5 will be modified and moved to in the next newly added page.

3.5.2 Fuel Rod Interface Data for Safety Analyses

To generate the fuel rod interface data with TCD effect for safety analyses, the TCD penalty determined as a function of burnup is added to the temperatures calculated by FATES3B code and those TCD penalty-added centerline temperatures of hot and average rod should be provided to safety analyses team.

3.6 Impact of Fuel Enthalpy

The impacts of TCD result in increasing the fuel enthalpy and the fuel centerline temperature. The impact on the fuel enthalpy due to TCD would be negligible for fresh fuel even though the maximum power peaking factors exist in the low burnup fuel in the APR1400 reload core designs. For the high burnup fuel which is affected by TCD, the fuel enthalpy and the fuel centerline temperature increase due to TCD are not significant because of the peaking factor burndown effect at higher burnups. The event specific evaluation considering the TCD penalty described in the Section 3.5 was performed and described in DCD Tier 2 Chapter 15.4.8.

3.7 Conclusion

The PLUS7 fuel rod design criteria considering TCD effect is evaluated using NRC approved FATES3B code and verified acceptable up to rod average burnup of 60,000 MWd/MTU. In addition, the potential impact of TCD on the fuel rod design criteria was evaluated, and it is concluded that TCD can be accommodated. Fuel rod interface data accounting for TCD penalty are generated and transmitted to safety analyses team.

Chapter 3.4.5 for enthalpy is moved to new Chapter 3.6

Note: This page is newly added to reflect the TCD effect. This page is same with the Attachment 1 (7/11) in response to RAI 5-7954 Question 12.

4.2.6 References

1. 10 CFR Part 50, Appendix A, General Design Criterion for Nuclear Power Plants 10, "Reactor Design," U.S. Nuclear Regulatory Commission.
2. 10 CFR Part 50, Appendix A, General Design Criterion for Nuclear Power Plants 27, "Combined Reactivity Control Systems Capability," U.S. Nuclear Regulatory Commission.
3. 10 CFR Part 50, Appendix A, General Design Criterion for Nuclear Power Plants 35, "Emergency Core Cooling," U.S. Nuclear Regulatory Commission.
4. 10 CFR 50.46, "Acceptance criteria for emergency core cooling systems for light-water nuclear power reactors," U.S. Nuclear Regulatory Commission.
5. APR1400-F-M-TR-13001-P (Proprietary) & NP (Non-Proprietary), "PLUS7 Fuel Design for the APR1400, ~~Rev. 0, KHNP, August 2013.~~ Rev. 1 to be issued.
6. NUREG-0800, Standard Review Plan, Section 4.2, "Fuel System Design," Rev. 3, U.S. Nuclear Regulatory Commission, March 2007.
7. CENPD-404-P-A, "Implementation of ZIRLO™ Cladding Material in CE Nuclear Power Fuel Assembly Designs," Rev. 0, Combustion Engineering, Inc., November 2001.
8. WCAP-12610-P-A, "VANTAGE+ Fuel Assembly Reference Core Report," Westinghouse Electric Corporation, April 1995.
9. W. J. O'Donnell and B. F. Langer, "Fatigue Design Basis for Zircaloy Components," Nuc. Sci. Eng., Vol. 20, pp. 1-12, April 1964.
10. Conway, J. B., "The Thermal Expansion and Heat Capacity of UO₂ to 2200 °C," E-NMPD-TM-63-6-6.
11. Christensen, J. A., "Thermal Expansion and Change in Volume on Melting for Uranium Dioxide," HW-75148, October 1962.
12. Jones, J. M. and Murchison D. G., "Optical Properties of Uranium Oxides," Nature, Vol. 205, pp. 663-65, February 1965.

coefficient, is described in Subsection 4.3.2.3.2 and shown in Figures 4.3-31 and 4.3-32. The second factor ($\delta T_m / \delta p$) of the second term is a constant because the moderator temperature is controlled to be a linear function of power.

Because the fuel temperature coefficient ($\delta \rho / \delta T_f$) and moderator temperature coefficient ($\delta \rho / \delta T_m$) are functions of one or more independent variables (e.g., burnup, temperature, soluble boron content, xenon worth, CEA insertion), the total power coefficient, dp/dp , also depends on these variables.

The power coefficient tends to become more negative with burnup because the fuel and moderator temperature coefficients become more negative as shown in Figures 4.3-30 through 4.3-32. Insertion of the CEAs, while maintaining constant power, results in a more negative power coefficient because the soluble boron level is reduced and because of the spectral effects of the CEAs themselves. The full-power values of the overall power coefficient for the unrodded core at the beginning and end of the first cycle are shown in Table 4.3-4.

4.3.2.4 Control Requirements

The three basic types of control requirements that influence the design of this reactor are:

4.3.2.3.8 Impact of Thermal Conductivity Degradation on Reactivity Coefficients

The fuel temperature increase due to thermal conductivity degradation (TCD) could have impacts on the prediction results of the fuel temperature coefficients and the core average reactivity due to the change in reactivity feedback of fuel temperature. The least negative or the most negative fuel temperature coefficients are used for safety analysis on an event specific basis, which is limiting for the transient. The fuel temperature coefficients are calculated using the effective fuel temperature changes which are caused by power changes and the corresponding reactivity changes. The nodal average effective fuel temperature correlation as a function of the burnup and linear power density is determined based on the fuel temperatures generated by FATES (References 2 and 3) as described in Subsection 4.3.2.3.7. The prediction results of the reactivity parameters using the effective fuel temperature correlation combined with current nuclear cross section models of DIT (Subsection 4.3.3.1.1.3) have been validated through the operation of OPR1000 plants with designs similar to those of APR1400 in terms of fuel design, operating temperatures and linear power density.

The limiting reactivity parameters based on the fuel temperature correlation and the cross section data are used as input for the safety analysis with the biases and uncertainties which have been determined through the comparison of prediction data to the plant measurement data. Therefore, the reactivity parameters implicitly include the impact of TCD in APR1400 nuclear design since the effective fuel temperature correlations and the biases and uncertainties have been validated against plant measurements.

6.2.1.3.2 Energy Sources

The following sources of generated and stored energy in the RCS and secondary coolant system are considered:

- a. Primary coolant
- b. Secondary coolant
- c. Primary walls (including reactor internals)
- d. Secondary walls
- e. Safety injection water
- f. Core power
- g. Decay heat

The core stored energy may be increased by the thermal conductivity degradation (TCD). The containment peak pressure with the TCD effect is slightly higher by 0.63 psi than the case without TCD. The TCD effect on the LOCA is negligible. The detailed methodology descriptions and M/E and P/T results of the TCD effect analysis are provided in Section 3 of Reference 3.

For the conservative analysis, the assumptions about the energy sources are biased to maximize the stored energy.

For considering the stored energy in the coolant, the initial RCS water volumes are conservatively calculated based on the maximum manufacturing tolerances of the reactor vessel and steam generator tubes. Volume expansion of the loop components from cold to hot operating conditions is also considered for the primary and secondary coolant stored energy. The initial water volume in the pressurizer includes an allowance for level instrumentation error. This makes the maximized pressurizer water volume, which includes the maximized stored energy.

For considering the stored energy in the primary and secondary walls, the large specific heat and heat conductivity of carbon steel are conservatively assumed for all of the walls in the RCS.

~~The core stored energy may be increased slightly by thermal conductivity degradation (TCD). However, the effect of TCD on the M&E release is negligible. The results are described in Reference 5.~~

For considering the energy in the safety injection water, the liquid break flow is assumed to be mixed with the water in IRWST. The mixed water is taken and discharged into the

The total volume of fluid for two steam lines between the MSIVs and a steam generator is assumed to be the maximum in the analysis. The total volume of fluid between the MSIVs and the turbine stop valves is also assumed to be the maximum in the analysis. The analysis credits the energy stored in the steam and liquid in the affected steam generator.

There are two MFIVs in each feedwater line. The total volume of fluid between the upstream MFIV and each steam generator is assumed to be the maximum. The flashing of this fluid into the affected steam generator and then into the containment is considered in the analysis. These assumed volumes conservatively exceed the actual design values of the APR1400 volumes.

The sources of energy considered in the MSLB analysis include the stored energy in the (1) affected steam generator's metal, including the steam generator tube, (2) water in the affected steam generator, (3) feedwater transferred to the affected steam generator before the closure of the MFIV, and (4) steam from the unaffected steam generator before the closure of the MSIV. The energy sources that are considered also include the energy transferred from the primary coolant to the water in the affected steam generator during blowdown.

6.2.1.4.1 Mass and Energy Release Data

Mass and energy release data for the MSLB cases listed in Table 6.2.1-1 are given in Tables 6.2.1-9 through 6.2.1-18.

6.2.1.4.2 Single Failure Analysis

Non-class 1E electric power is conservatively assumed to be available because it allows the continuation of reactor coolant pump operation, which maximizes the rate of heat transfer to the affected steam generator, which maximizes the rate of an M&E release. With the availability of Non-class 1E electric power, a postulated diesel generator failure is unnecessary.

There is an MSIV in each main steam line. The MSIVs are designed to close based on a conservative calculation that maximizes the dynamic pressure loading on the valve for all possible flow rates and qualities. Each valve has dual control circuits to provide reasonable assurance of closure even with a single failure in the control system. Each valve is tested periodically. A single failure in the actuation signal does not prevent valve

The core stored energy may be increased by the thermal conductivity degradation (TCD). The containment peak pressure with the TCD effect is slightly higher by 0.33 psi than the case without TCD. The TCD effect on the MSLB is negligible. The detailed methodology descriptions and M/E and P/T results of the TCD effect analysis are provided in Section 3 of Reference 3

Pressure values in the affected and unaffected steam generators for each MSLB case listed in Table 6.2.1-1 are given in Tables 6.2.1-9 through 6.2.1-18.

The chronologies of events for the MSLB cases listed in Table 6.2.1-1 are given in Tables 6.2.1-9 through 6.2.1-18.

Feedwater flow to the affected steam generator for each MSLB case listed in Table 6.2.1-1 is shown in Figures 6.2.1-38 through 6.2.1-47.

6.2.1.5 Minimum Containment Pressure Analysis for Performance Capability Studies of the Emergency Core Cooling System

This subsection presents the analysis on the minimum containment pressure that is used in the ECCS performance analysis, which is presented in Subsection 15.6.5.

6.2.1.5.1 Analytical Models

The calculations reported in this subsection are performed using the realistic evaluation methodology for large break LOCA of the APR1400 described in Reference 16 and are in accordance with NRC RG 1.157 (Reference 17). In the code-accuracy-based realistic evaluation method (CAREM), the RELAP5/MOD3.3/K computer program, a modified version of RELAP5/MOD3.3 (Reference 18), is used for the analysis of the ECCS thermal-hydraulic transient calculation and the cladding temperature calculation. A part of the RELAP/MOD3.3 code's reflood model has been modified to improve the prediction of rods quenching time and to correct coding errors. The minimum containment back pressure and temperature calculations are performed using the CONTEMPT4/MOD5 code (Reference 19).

RELAP5/MOD3.3 is one of the best-estimate safety analysis codes to date. The code has been widely applied in the analysis of system transients of pressurized water reactors, including a postulated large break loss of coolant accident (LBLOCA). The film boiling heat transfer model of the reflood package of RELAP5/MOD3.3 has been modified based on independent assessment calculations against the FLECHT-SEASET data.

Containment back pressure depends on mass and energy release rates, and thermal-hydraulic phenomena depend on the containment back pressure. CONTEMPT4/MOD5 is a containment analysis code that is used especially for calculating containment back pressures in case of a LOCA. It includes fan and spray cooling system

models and passive heat sink models that are essential for the calculation of the containment back pressures following a LOCA. It is equipped with the conservation equations of mass, momentum, and energy and can calculate the mass and energy transfer due to the pressure difference between compartments. It also includes state equation of non-condensable gas and can calculate humidity. Heat conduction can be modeled with diverse boundary heat transfer conditions.

RELAP5/~~MOD3.3~~ ^{MOD3.3/K} and CONTEMPT4/MOD5 are merged to exchange the containment back pressure calculated by the CONTEMPT4 and the mass and energy release rate calculated by the RELAP5/MOD3.3/K in every time step.

6.2.1.5.2 Mass and Energy Release Data

^{insert: with the burnup of 27,000 MWd/MTU}

^{insert: considering TCD effect}

The mass and energy released to the containment for a limiting LBLOCA, 100 percent double-ended guillotine break at the pump discharge leg ($1.0 \times \text{DEG/PD}$), are listed as a function of time in Table 6.2.1-39. The quantity of safety injection fluid that spills from the break is described in Subsection 6.2.1.5.6. The analytical models applied in Subsection 15.6.5 best estimate analysis calculate the mass and energy released to the containment. This results are used to the calculation of minimum containment pressure.

6.2.1.5.3 Initial Containment Internal Conditions

The minimum containment temperature, minimum containment pressure, and maximum humidity encountered under limiting normal operating conditions are used for the analysis. The initial containment internal conditions that are used in the analysis are as follows:

| | |
|-------------------------|---|
| Containment temperature | 10 °C (50 °F) (minimum value) |
| IRWST water temperature | 10 °C (50 °F) (minimum value) |
| Containment pressure | 1.024 kg/cm ² A (14.56 psia) (minimum value) |
| Relative humidity | 90 percent (maximum value) |

Each condition is a specified conservative value to minimize the containment pressure, consistent with Branch Technical Position 6-2 (Reference 20).

6.2.1.5.4 Containment Volume

The maximum net free containment volume that is used for the analysis is 97,155 m³ (3,431,000 ft³). The maximum net free volume is determined from the gross containment

volume minus the volumes of internal structures such as walls and floors, structural steel, major equipment, and piping with a consideration of uncertainty.

6.2.1.5.5 Active Heat Sinks

In order to conservatively consider the heat removal capacity of the containment active heat sinks, the containment sprays and cooling fans are modeled to actuate immediately with the maximum capacity at the time of the postulated LOCA.

The containment atmosphere cooling systems designed as the non-safety-related system are also modeled to actuate immediately at the time of the postulated LOCA. In addition, the minimum temperature of the stored water for the spray cooling system and the cooling water supplied to the fan coolers, based on technical specification limits, are assumed.

The operating parameters for the containment sprays that are used in the analysis are as follows:

| | | | |
|--|---|--|--|
| Flow rate (total, 4 pumps) | 2 | 37,853 | 10,000 |
| | | 75,706 L/min (20,000 gpm) | |
| Temperature | | 10.0 °C (50 °F) | |

The heat removal capacity of reactor containment fan cooler (RCFC) is shown in Figure 6.2.1-48.

6.2.1.5.6 Steam-Water Mixing

The spillage of subcooled ECCS water into the containment provides an additional heat sink as the subcooled ECCS water mixes with the steam in the containment by the steam-water mixing. The spilled SIS water from the broken cold leg is determined by the thermal-hydraulic behavior of the core cooling system. It is considered in the analysis model of CONTEMPT4/MOD5.

6.2.1.5.7 Passive Heat Sinks

The passive heat sinks included in the containment evaluation model are established by identifying structures and components within the containment that are influenced the pressure response. The surface areas and thicknesses of all exposed containment passive heat sink, as well as the thermal properties used for the passive heat sinks, are listed in Table 6.2.1-23. The passive heat sink data are conservatively assumed with minimum

paint thickness and maximum structure thickness. Containment air wall is not considered, conservatively.

6.2.1.5.8 Heat Transfer to Passive Heat Sinks

The conservative condensing heat transfer coefficients for heat transfer to the exposed passive heat sinks during the blowdown and post-blowdown phases of the LOCA are applied. The variations in the condensing heat transfer coefficients between the containment atmosphere and the passive heat sinks are calculated as a function of time and are shown quantitatively in Figure 6.2.1-49. The condensation heat transfer coefficient at the surface of thermal structure is calculated by using Tagami and Uchida correlations shown as below:

$$h_{TAGAMI} = 0.607 \times \left(\frac{U}{V \times tp} \right)^{0.62} \text{ in SI unit}$$

Where:

U = Total released energy from the primary system during the blowdown period

V = Free volume in the containment

tp = time at the end of blowdown

The heat transfer coefficient during the blowdown period increases linearly from the initial values to a peak value h_{\max} and decreases exponentially as shown below. The Uchida heat transfer coefficient is given as the mass ratio function of air and steam:

$$h = h_{stag} + (h_{\max} - h_{stag})e^{-0.025(t-t_p)}$$

$$h_{stag} = 1.2 h_{UCHIDA}$$

Where:

h_{\max} = Four times of calculated condensing heat transfer coefficient at the end of blowdown

6.2.1.5.9 Other Parameters

The minimum containment pressure analysis assumes that the 20.3 cm (8 in) diameter purge system is operating from the time of the LOCA initiation until the isolation valves close, which is after a containment isolation actuation signal. It is conservatively assumed that only dry air is purged from the containment and the maximum mass of air purged is 272.2 kg (600 lbs) for the minimum containment pressure analysis.

6.2.1.5.10 Results

insert: with the burnup of 27,000 MWd/MTU



For the limiting large break LOCA, 100 percent double-ended guillotine break at the pump discharge leg, the minimum containment pressure response to be used in the ECCS performance analysis is shown in Figure 6.2.1-50. The responses of the containment atmosphere and IRWST temperatures are shown in Figures 6.2.1-51 and 6.2.1-52, respectively.

The transient containment response is used in the ECCS performance analysis presented in Subsection 15.6.5.

6.2.1.6 Test and Inspections

This section describes the preoperational testing, in-service testing, and inspection of the containment. The primary objective of testing and inspection is to verify the structural integrity and leak-tight integrity of the containment. The testing and inspection requirements for the containment are described in Subsections 3.8.1.7, 3.8.2.7, 6.2.4, and 6.2.6. Section 14.2, the initial test program, also includes preoperational testing requirements.

Requirements for the structural integrity test are described in Subsection 14.2.12.1.119. The structural integrity test is performed in accordance with ASME Section III, Division 2, CC-6000, to verify the structural integrity of the containment including the liner, concrete structures, all electrical and piping penetrations, equipment hatch, personnel airlocks, and post-tensioning. The pressure will be brought up to 115 percent of the containment design pressure in approximately five or more equal increments. In addition, all ASME Class MC components are tested for their structural acceptance and leak rate at the same time of the structural integrity test. The in-service testing and inspection requirements and methods used for the ASME Class MC components and structural integrity test is described in Subsections 3.8.1.7 and 3.8.2.7.


16. APR1400-F-A-TR-12004-P (Proprietary) & NP (Non-Proprietary), “Realistic Evaluation Methodology for Large-Break LOCA of the APR1400,” Rev. 0, KHNP, December 2012 
17. Regulatory Guide 1.157, “Best-estimate Calculations of Emergency Core Cooling System Performance,” U.S. Nuclear Regulatory Commission, May 1989.
18. NUREG/CR-5535, “RELAP5/MOD3.3 Code Manual,” Rev. 3, U.S. Nuclear Regulatory Commission, March 2006.
19. NUREG/CR-3716, “A Multi-compartment Containment System Analysis Program,” U.S. Nuclear Regulatory Commission, March 1984.
- NUREG/CR-4001, “An Improvement to CONTEMPT4/MOD5 Multi-compartment System Analysis Program for Ice Containment Analysis,” U.S. Nuclear Regulatory Commission, September 1984.
20. NUREG-0800, Standard Review Plan, BTP 6-2, “Minimum Containment Pressure Model for PWR ECCS Performance Evaluation,” U.S. Nuclear Regulatory Commission, March 2007.
21. Regulatory Guide 1.163, “Performance-Based Containment Leak Test Program,” U.S. Nuclear Regulatory Commission, September 1995.
22. ASTM E799-2003(R2009), “Standard Practice for Determining Data Criteria and Processing for Liquid Drop Size Analysis,” American Society for Testing and Material, 2003.
23. ASME Boiler and Pressure Vessel Code, Section XI, “Rules for Inservice Inspection of Nuclear Power Plant Components,” The American Society of Mechanical Engineers.
24. ASME OM Code, “Code for Operation and Maintenance of Nuclear Power Plants,” The American Society of Mechanical Engineers.
25. 10 CFR Part 50, Appendix A, General Design Criterion 56, “Primary Containment Isolation,” U.S. Nuclear Regulatory Commission.
26. Regulatory Guide 1.11, “Instrument Lines Penetrating the Primary Reactor Containment,” Rev. 1, U.S. Nuclear Regulatory Commission, March 2010.

Table 6.2.1-23 (5 of 7)

Part C. Heat Sink Physical Data for ECCS Performance Analysis

| Heat Sinks | Layer | Material | Thickness | | Surface Area | |
|----------------------|-------|--------------|-----------|----------|----------------|-----------------|
| | | | m | ft | m ² | ft ² |
| Containment cylinder | 1 | E Paint | 0.0000762 | 0.00025 | 7,804.3 | 84,005 |
| | 2 | Z Paint | 0.0000762 | 0.00025 | | |
| | 3 | Carbon Steel | 0.008778 | 0.0288 | | |
| | 4 | Concrete | 1.355994 | 4.4488 | | |
| Dome | 1 | E Paint | 0.0000762 | 0.00025 | 3,316.3 | 35,696.4 |
| | 2 | Z Paint | 0.0000762 | 0.00025 | | |
| | 3 | Carbon Steel | 0.007894 | 0.0259 | | |
| | 4 | Concrete | 1.0668 | 3.5 | | |
| Basemat | 1 | E Paint | 0.000668 | 0.002192 | 1,410.9 | 15,186.3 |
| | 2 | Concrete | 0.9144 | 3 | | |
| | 3 | Carbon Steel | 0.00635 | 0.020833 | | |
| | 4 | Concrete | 3.6576 | 12 | | |
| Embedment Concrete | 1 | E Paint | 0.0000762 | 0.00025 | 726.1 | 7,815.6 |
| | 2 | Z Paint | 0.0000762 | 0.00025 | | |
| | 3 | Carbon Steel | 0.026335 | 0.0864 | | |
| | 4 | Concrete | 0.780776 | 2.5616 | | |

Table 6.2.1-23 (6 of 7)

Part C. Heat Sink Physical Data for ECCS Performance Analysis (Continued)

| Heat Sinks | Layer | Material | Thickness | | Surface Area | |
|------------------------|-------|-----------------|------------|----------|----------------|-----------------|
| | | | m | ft | m ² | ft ² |
| Unembedment Concrete | 1 | E Paint | 0.000389 | 0.001275 | 11,120.7 | 119,702 |
| | 2 | Concrete | 0.77254 | 2.534579 | | |
| Refueling Pool | 1 | Stainless Steel | 0.005243 | 0.0172 | 1,153.6 | 12,417.7 |
| IRWST Outside | 1 | E Paint | 0.000668 | 0.002192 | 2,017.4 | 21,714.6 |
| | 2 | Concrete | 0.4572 | 1.5 | | |
| IRWST Inside | 1 | Stainless Steel | 0.00633984 | 0.0208 | 1,038.8 | 11,181.7 |
| | 2 | Concrete | 0.4572 | 1.5 | | |
| Polar Crane and Bridge | 1 | E Paint | 0.0000762 | 0.00025 | 8,291.6 | 89,250 |
| | 2 | Z Paint | 0.0000762 | 0.00025 | | |
| | 3 | Carbon Steel | 0.012192 | 0.04 | | |
| SIT | 1 | E Paint | 0.000152 | 0.0005 | 526.8 | 5,670 |
| | 2 | Carbon Steel | 0.048798 | 0.1601 | | |
| Misc. steel G-A | 1 | E Paint | 0.0000762 | 0.00025 | 10,212.1 | 109,922 |
| | 2 | Z Paint | 0.0000762 | 0.00025 | | |
| | 3 | Carbon Steel | 0.016712 | 0.054831 | | |
| Misc. steel G-B | 1 | Z Paint | 0.0000762 | 0.00025 | 7,062.1 | 76,015.5 |
| | 3 | Carbon Steel | 0.004175 | 0.013698 | | |
| Misc. steel G-C | 1 | E Paint | 0.0000762 | 0.00025 | 3,361.5 | 36,182.7 |
| | 2 | Z Paint | 0.0000762 | 0.00025 | | |
| | 3 | Carbon Steel | 0.00518099 | 0.016998 | | |
| Misc. steel G-D | 1 | Z Paint | 0.0000762 | 0.00025 | 3,664.1 | 39,439.6 |
| | 2 | Carbon Steel | 0.004 | 0.013124 | | |
| Misc. steel G-E | 1 | Z Paint | 0.0000762 | 0.00025 | 21,557.5 | 232,042 |
| | 2 | Carbon Steel | 0.001644 | 0.005393 | | |

Table 6.2.1-23 (7 of 7)

Part C. Heat Sink Physical Data for ECCS Performance Analysis (Continued)

| Heat Sinks | Layer | Material | Thickness | | Surface Area | |
|-----------------|-------|-----------------|------------|----------|----------------|-----------------|
| | | | m | ft | m ² | ft ² |
| Misc. steel G-F | 1 | E Paint | 0.0000762 | 0.00025 | 1,589.3 | 17,106.9 |
| | 2 | Z Paint | 0.0000762 | 0.00025 | | |
| | 3 | Carbon Steel | 0.00672846 | 0.022075 | | |
| Misc. steel G-G | 1 | Stainless Steel | 0.00627888 | 0.020600 | 1,872.0 | 20,149.6 |
| Misc. steel G-J | 1 | Z Paint | 0.0000762 | 0.00025 | 1,738.6 | 18,713.6 |
| | 2 | Carbon Steel | 0.009216 | 0.030235 | | |
| Misc. steel G-K | 1 | Stainless Steel | 0.072558 | 0.23805 | 1,269.3 | 13,662.7 |

| | |
|------------------------------|--|
| Thermal Conductivity of: | |
| Steel | 40.6 kcal/m-hr-°C (27.3 Btu/ft-hr-°F) |
| Concrete | 1.94 kcal/m-hr-°C (1.3 Btu/ft-hr-°F) |
| Paint (epoxy) | 0.31 kcal/m-hr-°C (0.21 Btu/ft-hr-°F) |
| Paint (inorganic zinc) | 1.49 kcal/m-hr-°C (1.0 Btu/ft-hr-°F) |
| Volumetric Heat Capacity of: | |
| Steel | 942 kcal/m ³ -°C (58.8 Btu/ft ³ -°F) |
| Concrete | 517 kcal/m ³ -°C (32.3 Btu/ft ³ -°F) |
| Paint (epoxy) | 585 kcal/m ³ -°C (36.5 Btu/ft ³ -°F) |
| Paint (inorganic zinc) | 1,250 kcal/m ³ -°C (78.0 Btu/ft ³ -°F) |

Insert

- (1) The surface area uses its maximum value within the ranges of margin estimated from the geometry uncertainty of each structure.
- (2) The thickness of each structure are determined based on the surface area exposed to the containment atmosphere and the net volume occupied by the structure.
- (3) The thickness of the painting material on the structure is considered as its averaging nominal value.

A detailed description of how to calculate the thickness and surface area is provided in Reference 3.

Replace with next page A-1

Table 6.2.1-39 (1 of 4)

Blowdown and Reflood Mass and Energy Release for the Minimum Containment Pressure Analysis

| Time (sec) | Mass Flow | | Enthalpy | | Integral of Mass Flow | | Integral of Energy | |
|---------------|------------|------------|------------|------------|-----------------------|------------|--------------------|------------|
| | (kg/sec) | (lbm/sec) | (kcal/kg) | (Btu/lbm) | (kg) | (lbm) | (kcal) | (Btu) |
| 0.0 | 0.0000E+00 | 0.0000E+00 | 0.0000E+00 | 0.0000E+00 | 0.0000E+00 | 0.0000E+00 | 0.0000E+00 | 0.0000E+00 |
| 0.5 | 3.9083E+04 | 8.6164E+04 | 3.0484E+02 | 5.4870E+02 | 1.9481E+04 | 4.2948E+04 | 5.9366E+06 | 2.3558E+07 |
| 1.0 | 3.7229E+04 | 8.2876E+04 | 3.0525E+02 | 5.4944E+02 | 3.8697E+04 | 8.5313E+04 | 1.1798E+07 | 4.6818E+07 |
| 1.5 | 3.4198E+04 | 7.5395E+04 | 3.0599E+02 | 5.5078E+02 | 5.6465E+04 | 1.2448E+05 | 1.7227E+07 | 6.8364E+07 |
| 2.0 | 3.2051E+04 | 7.0661E+04 | 3.0712E+02 | 5.5282E+02 | 7.3059E+04 | 1.6107E+05 | 2.2314E+07 | 8.8548E+07 |
| 2.5 | 2.9526E+04 | 6.5093E+04 | 3.0870E+02 | 5.5566E+02 | 8.8435E+04 | 1.9497E+05 | 2.7047E+07 | 1.0733E+08 |
| 3.0 | 2.6495E+04 | 5.8411E+04 | 3.1044E+02 | 5.5879E+02 | 1.0245E+05 | 2.2587E+05 | 3.1385E+07 | 1.2455E+08 |
| 3.5 | 2.4309E+04 | 5.3593E+04 | 3.1248E+02 | 5.6246E+02 | 1.1511E+05 | 2.5378E+05 | 3.5328E+07 | 1.4019E+08 |
| 4.0 | 2.2818E+04 | 5.0305E+04 | 3.1483E+02 | 5.6670E+02 | 1.2688E+05 | 2.7972E+05 | 3.9020E+07 | 1.5484E+08 |
| 4.5 | 2.1564E+04 | 4.7541E+04 | 3.1670E+02 | 5.7006E+02 | 1.3793E+05 | 3.0408E+05 | 4.2509E+07 | 1.6869E+08 |
| 5.0 | 2.0493E+04 | 4.5180E+04 | 3.1844E+02 | 5.7320E+02 | 1.4841E+05 | 3.2719E+05 | 4.5840E+07 | 1.8191E+08 |
| 5.5 | 1.9184E+04 | 4.2294E+04 | 3.2188E+02 | 5.7939E+02 | 1.5834E+05 | 3.4908E+05 | 4.9016E+07 | 1.9451E+08 |
| 6.0 | 1.8037E+04 | 3.9764E+04 | 3.2567E+02 | 5.8620E+02 | 1.6764E+05 | 3.6959E+05 | 5.2028E+07 | 2.0646E+08 |
| 6.5 | 1.7038E+04 | 3.7562E+04 | 3.2853E+02 | 5.9136E+02 | 1.7640E+05 | 3.8891E+05 | 5.4895E+07 | 2.1784E+08 |
| 7.0 | 1.6036E+04 | 3.5353E+04 | 3.3182E+02 | 5.9727E+02 | 1.8467E+05 | 4.0713E+05 | 5.7624E+07 | 2.2867E+08 |
| 7.5 | 1.5212E+04 | 3.3536E+04 | 3.3461E+02 | 6.0229E+02 | 1.9247E+05 | 4.2433E+05 | 6.0225E+07 | 2.3899E+08 |
| 8.0 | 1.4582E+04 | 3.2149E+04 | 3.3657E+02 | 6.0582E+02 | 1.9991E+05 | 4.4073E+05 | 6.2721E+07 | 2.4890E+08 |
| 8.5 | 1.4003E+04 | 3.0871E+04 | 3.3755E+02 | 6.0760E+02 | 2.0705E+05 | 4.5647E+05 | 6.5131E+07 | 2.5846E+08 |

A-1

Table 6.2.1-39 (1 of 4)

Blowdown and Reflood Mass and Energy Release for the Minimum Containment Pressure Analysis

| Time (sec) | Mass Flow | | Enthalpy | | Integral of Mass Flow | | Integral of Energy | |
|---------------|------------|------------|------------|------------|-----------------------|------------|--------------------|------------|
| | (kg/sec) | (lbm/sec) | (kcal/kg) | (Btu/lbm) | (kg) | (lbm) | (kcal) | (Btu) |
| 0.0 | 0.0000E+00 | 0.0000E+00 | 0.0000E+00 | 0.0000E+00 | 0.0000E+00 | 0.0000E+00 | 0.0000E+00 | 0.0000E+00 |
| 0.5 | 3.8724E+04 | 8.5372E+04 | 3.0481E+02 | 5.4866E+02 | 1.9481E+04 | 4.2948E+04 | 5.9366E+06 | 2.3558E+07 |
| 1.0 | 3.6719E+04 | 8.0951E+04 | 3.0522E+02 | 5.4940E+02 | 3.8697E+04 | 8.5313E+04 | 1.1798E+07 | 4.6818E+07 |
| 1.5 | 3.4041E+04 | 7.5047E+04 | 3.0599E+02 | 5.5078E+02 | 5.6465E+04 | 1.2448E+05 | 1.7227E+07 | 6.8364E+07 |
| 2.0 | 3.1857E+04 | 7.0232E+04 | 3.0710E+02 | 5.5278E+02 | 7.3059E+04 | 1.6107E+05 | 2.2314E+07 | 8.8548E+07 |
| 2.5 | 2.9010E+04 | 6.3957E+04 | 3.0871E+02 | 5.5567E+02 | 8.8435E+04 | 1.9497E+05 | 2.7047E+07 | 1.0733E+08 |
| 3.0 | 2.6322E+04 | 5.8031E+04 | 3.1038E+02 | 5.5868E+02 | 1.0245E+05 | 2.2587E+05 | 3.1385E+07 | 1.2455E+08 |
| 3.5 | 2.4281E+04 | 5.3531E+04 | 3.1241E+02 | 5.6235E+02 | 1.1511E+05 | 2.5378E+05 | 3.5328E+07 | 1.4019E+08 |
| 4.0 | 2.2928E+04 | 5.0548E+04 | 3.1473E+02 | 5.6652E+02 | 1.2688E+05 | 2.7972E+05 | 3.9020E+07 | 1.5484E+08 |
| 4.5 | 2.1645E+04 | 4.7720E+04 | 3.1615E+02 | 5.6907E+02 | 1.3793E+05 | 3.0408E+05 | 4.2509E+07 | 1.6869E+08 |
| 5.0 | 2.0561E+04 | 4.5329E+04 | 3.1811E+02 | 5.7260E+02 | 1.4841E+05 | 3.2719E+05 | 4.5840E+07 | 1.8191E+08 |
| 5.5 | 1.9289E+04 | 4.2526E+04 | 3.2143E+02 | 5.7857E+02 | 1.5834E+05 | 3.4908E+05 | 4.9016E+07 | 1.9451E+08 |
| 6.0 | 1.8132E+04 | 3.9975E+04 | 3.2525E+02 | 5.8545E+02 | 1.6764E+05 | 3.6959E+05 | 5.2028E+07 | 2.0646E+08 |
| 6.5 | 1.7101E+04 | 3.7700E+04 | 3.2825E+02 | 5.9084E+02 | 1.7640E+05 | 3.8891E+05 | 5.4895E+07 | 2.1784E+08 |
| 7.0 | 1.6093E+04 | 3.5480E+04 | 3.3151E+02 | 5.9672E+02 | 1.8467E+05 | 4.0713E+05 | 5.7624E+07 | 2.2867E+08 |
| 7.5 | 1.5240E+04 | 3.3598E+04 | 3.3453E+02 | 6.0215E+02 | 1.9247E+05 | 4.2433E+05 | 6.0225E+07 | 2.3899E+08 |
| 8.0 | 1.4614E+04 | 3.2218E+04 | 3.3647E+02 | 6.0565E+02 | 1.9991E+05 | 4.4073E+05 | 6.2721E+07 | 2.4890E+08 |
| 8.5 | 1.4153E+04 | 3.1202E+04 | 3.3747E+02 | 6.0745E+02 | 2.0705E+05 | 4.5647E+05 | 6.5131E+07 | 2.5846E+08 |

Replace with next page A-2

Table 6.2.1-39 (2 of 4)

| Time (sec) | Mass Flow | | Enthalpy | | Integral of Mass Flow | | Integral of Energy | |
|---------------|------------|------------|------------|------------|-----------------------|------------|--------------------|------------|
| | (kg/sec) | (lbm/sec) | (kcal/kg) | (Btu/lbm) | (kg) | (lbm) | (kcal) | (Btu) |
| 9.0 | 1.3295E+04 | 2.9310E+04 | 3.4122E+02 | 6.1420E+02 | 2.1383E+05 | 4.7141E+05 | 6.7437E+07 | 2.6761E+08 |
| 9.5 | 1.2034E+04 | 2.6531E+04 | 3.5498E+02 | 6.3897E+02 | 2.2013E+05 | 4.8530E+05 | 6.9627E+07 | 2.7630E+08 |
| 10.0 | 1.1140E+04 | 2.4560E+04 | 3.6620E+02 | 6.5916E+02 | 2.2592E+05 | 4.9807E+05 | 7.1714E+07 | 2.8458E+08 |
| 11.0 | 9.7376E+03 | 2.1468E+04 | 3.8751E+02 | 6.9752E+02 | 2.3643E+05 | 5.2124E+05 | 7.5655E+07 | 3.0022E+08 |
| 12.0 | 8.3059E+03 | 1.8311E+04 | 4.1727E+02 | 7.5109E+02 | 2.4544E+05 | 5.4110E+05 | 7.9270E+07 | 3.1457E+08 |
| 13.0 | 7.0495E+03 | 1.5541E+04 | 4.4490E+02 | 8.0082E+02 | 2.5319E+05 | 5.5818E+05 | 8.2584E+07 | 3.2772E+08 |
| 14.0 | 5.6965E+03 | 1.2559E+04 | 4.8057E+02 | 8.6502E+02 | 2.5955E+05 | 5.7221E+05 | 8.5525E+07 | 3.3939E+08 |
| 15.0 | 4.6371E+03 | 1.0223E+04 | 5.0858E+02 | 9.1544E+02 | 2.6470E+05 | 5.8357E+05 | 8.8068E+07 | 3.4948E+08 |
| 16.0 | 4.2699E+03 | 9.4135E+03 | 4.6259E+02 | 8.3266E+02 | 2.6917E+05 | 5.9341E+05 | 9.0244E+07 | 3.5812E+08 |
| 17.0 | 4.2033E+03 | 9.2667E+03 | 3.8856E+02 | 6.9941E+02 | 2.7347E+05 | 6.0289E+05 | 9.2034E+07 | 3.6522E+08 |
| 18.0 | 3.9604E+03 | 8.7312E+03 | 3.4041E+02 | 6.1274E+02 | 2.7755E+05 | 6.1190E+05 | 9.3514E+07 | 3.7109E+08 |
| 19.0 | 3.6815E+03 | 8.1162E+03 | 3.1006E+02 | 5.5811E+02 | 2.8146E+05 | 6.2052E+05 | 9.4767E+07 | 3.7607E+08 |
| 20.0 | 3.3936E+03 | 7.4816E+03 | 2.8308E+02 | 5.0955E+02 | 2.8507E+05 | 6.2848E+05 | 9.5825E+07 | 3.8026E+08 |
| 21.0 | 3.1712E+03 | 6.9912E+03 | 2.5108E+02 | 4.5195E+02 | 2.8836E+05 | 6.3572E+05 | 9.6706E+07 | 3.8376E+08 |
| 22.0 | 3.5105E+03 | 7.7394E+03 | 2.1884E+02 | 3.9391E+02 | 2.9193E+05 | 6.4359E+05 | 9.7537E+07 | 3.8706E+08 |
| 23.0 | 3.1260E+03 | 6.8917E+03 | 1.9468E+02 | 3.5043E+02 | 2.9524E+05 | 6.5089E+05 | 9.8226E+07 | 3.8979E+08 |
| 24.0 | 2.3483E+03 | 5.1770E+03 | 1.9237E+02 | 3.4627E+02 | 2.9799E+05 | 6.5696E+05 | 9.8754E+07 | 3.9189E+08 |
| 25.0 | 1.9377E+03 | 4.2719E+03 | 1.7847E+02 | 3.2125E+02 | 3.0006E+05 | 6.6152E+05 | 9.9149E+07 | 3.9346E+08 |
| 26.0 | 1.9829E+03 | 4.3715E+03 | 1.3967E+02 | 2.5141E+02 | 3.0202E+05 | 6.6584E+05 | 9.9457E+07 | 3.9468E+08 |
| 27.0 | 1.7744E+03 | 3.9119E+03 | 1.1880E+02 | 2.1384E+02 | 3.0376E+05 | 6.6968E+05 | 9.9691E+07 | 3.9561E+08 |

A-2

Table 6.2.1-39 (2 of 4)

| Time (sec) | Mass Flow | | Enthalpy | | Integral of Mass Flow | | Integral of Energy | |
|---------------|------------|------------|------------|------------|-----------------------|------------|--------------------|------------|
| | (kg/sec) | (lbm/sec) | (kcal/kg) | (Btu/lbm) | (kg) | (lbm) | (kcal) | (Btu) |
| 9.0 | 1.3205E+04 | 2.9113E+04 | 3.4232E+02 | 6.1617E+02 | 2.1383E+05 | 4.7141E+05 | 6.7437E+07 | 2.6761E+08 |
| 9.5 | 1.2105E+04 | 2.6688E+04 | 3.5269E+02 | 6.3484E+02 | 2.2013E+05 | 4.8530E+05 | 6.9627E+07 | 2.7630E+08 |
| 10.0 | 1.1219E+04 | 2.4734E+04 | 3.6500E+02 | 6.5699E+02 | 2.2592E+05 | 4.9807E+05 | 7.1714E+07 | 2.8458E+08 |
| 11.0 | 9.8545E+03 | 2.1725E+04 | 3.8504E+02 | 6.9308E+02 | 2.3643E+05 | 5.2124E+05 | 7.5655E+07 | 3.0022E+08 |
| 12.0 | 8.3606E+03 | 1.8432E+04 | 4.1553E+02 | 7.4795E+02 | 2.4544E+05 | 5.4110E+05 | 7.9270E+07 | 3.1457E+08 |
| 13.0 | 7.0900E+03 | 1.5631E+04 | 4.4297E+02 | 7.9734E+02 | 2.5319E+05 | 5.5818E+05 | 8.2584E+07 | 3.2772E+08 |
| 14.0 | 5.7429E+03 | 1.2661E+04 | 4.7810E+02 | 8.6058E+02 | 2.5955E+05 | 5.7221E+05 | 8.5525E+07 | 3.3939E+08 |
| 15.0 | 4.6607E+03 | 1.0275E+04 | 5.0738E+02 | 9.1328E+02 | 2.6470E+05 | 5.8357E+05 | 8.8068E+07 | 3.4948E+08 |
| 16.0 | 4.5045E+03 | 9.9308E+03 | 4.3551E+02 | 7.8392E+02 | 2.6917E+05 | 5.9341E+05 | 9.0244E+07 | 3.5812E+08 |
| 17.0 | 4.5892E+03 | 1.0117E+04 | 3.4965E+02 | 6.2937E+02 | 2.7347E+05 | 6.0289E+05 | 9.2034E+07 | 3.6522E+08 |
| 18.0 | 6.2080E+03 | 1.3686E+04 | 2.6115E+02 | 4.7008E+02 | 2.7755E+05 | 6.1190E+05 | 9.3514E+07 | 3.7109E+08 |
| 19.0 | 5.3897E+03 | 1.1882E+04 | 2.4960E+02 | 4.4928E+02 | 2.8146E+05 | 6.2052E+05 | 9.4767E+07 | 3.7607E+08 |
| 20.0 | 5.0298E+03 | 1.1089E+04 | 2.1821E+02 | 3.9278E+02 | 2.8507E+05 | 6.2848E+05 | 9.5825E+07 | 3.8026E+08 |
| 21.0 | 4.5887E+03 | 1.0072E+04 | 1.9425E+02 | 3.4965E+02 | 2.8836E+05 | 6.3572E+05 | 9.6706E+07 | 3.8376E+08 |
| 22.0 | 4.0662E+03 | 8.9645E+03 | 1.7118E+02 | 3.0812E+02 | 2.9193E+05 | 6.4359E+05 | 9.7537E+07 | 3.8706E+08 |
| 23.0 | 3.3917E+03 | 7.4775E+03 | 1.5942E+02 | 2.8695E+02 | 2.9524E+05 | 6.5089E+05 | 9.8226E+07 | 3.8979E+08 |
| 24.0 | 2.8318E+03 | 6.2430E+03 | 1.4577E+02 | 2.6238E+02 | 2.9799E+05 | 6.5696E+05 | 9.8754E+07 | 3.9189E+08 |
| 25.0 | 2.2366E+03 | 4.9309E+03 | 1.3316E+02 | 2.3969E+02 | 3.0006E+05 | 6.6152E+05 | 9.9149E+07 | 3.9346E+08 |
| 26.0 | 2.2567E+03 | 4.9752E+03 | 1.1145E+02 | 2.0062E+02 | 3.0202E+05 | 6.6584E+05 | 9.9457E+07 | 3.9468E+08 |
| 27.0 | 1.7760E+03 | 3.9153E+03 | 7.5469E+01 | 1.3584E+02 | 3.0376E+05 | 6.6968E+05 | 9.9691E+07 | 3.9561E+08 |

Replace with next page A-3

Table 6.2.1-39 (3 of 4)

| Time (sec) | Mass Flow | | Enthalpy | | Integral of Mass Flow | | Integral of Energy | |
|---------------|-------------|-------------|------------|------------|-----------------------|------------|--------------------|------------|
| | (kg/sec) | (lbm/sec) | (kcal/kg) | (Btu/lbm) | (kg) | (lbm) | (kcal) | (Btu) |
| 28.0 | 5.6570E+02 | 1.2472E+03 | 1.0175E+02 | 1.8315E+02 | 3.0503E+05 | 6.7249E+05 | 9.9830E+07 | 3.9616E+08 |
| 29.0 | -9.8747E+01 | -2.1770E+02 | 3.4733E+02 | 6.2520E+02 | 3.0511E+05 | 6.7265E+05 | 9.9824E+07 | 3.9613E+08 |
| 30.0 | -2.8582E+01 | -6.3013E+01 | 1.3609E+02 | 2.4497E+02 | 3.0507E+05 | 6.7256E+05 | 9.9811E+07 | 3.9608E+08 |
| 35.0 | 2.2727E+02 | 5.0104E+02 | 9.4225E+01 | 1.6961E+02 | 3.0599E+05 | 6.7460E+05 | 9.9938E+07 | 3.9659E+08 |
| 40.0 | 4.0079E+02 | 8.8360E+02 | 1.4478E+02 | 2.6060E+02 | 3.0759E+05 | 6.7813E+05 | 1.0014E+08 | 3.9737E+08 |
| 45.0 | 4.1072E+02 | 9.0548E+02 | 1.4478E+02 | 2.6061E+02 | 3.0931E+05 | 6.8191E+05 | 1.0040E+08 | 3.9840E+08 |
| 50.0 | 2.3177E+03 | 5.1096E+03 | 8.2609E+01 | 1.4870E+02 | 3.1563E+05 | 6.9585E+05 | 1.0100E+08 | 4.0081E+08 |
| 55.0 | 1.6683E+03 | 3.6780E+03 | 8.2492E+01 | 1.4848E+02 | 3.2501E+05 | 7.1652E+05 | 1.0177E+08 | 4.0384E+08 |
| 60.0 | 2.0347E+03 | 4.4857E+03 | 8.2038E+01 | 1.4767E+02 | 3.3385E+05 | 7.3602E+05 | 1.0249E+08 | 4.0673E+08 |
| 65.0 | 1.5550E+03 | 3.4282E+03 | 9.3659E+01 | 1.6859E+02 | 3.4338E+05 | 7.5703E+05 | 1.0330E+08 | 4.0994E+08 |
| 70.0 | 1.1052E+03 | 2.4365E+03 | 9.7418E+01 | 1.7535E+02 | 3.4738E+05 | 7.6628E+05 | 1.0374E+08 | 4.1166E+08 |
| 75.0 | 1.0596E+03 | 2.3359E+03 | 9.9657E+01 | 1.7938E+02 | 3.5262E+05 | 7.7739E+05 | 1.0424E+08 | 4.1364E+08 |
| 80.0 | 7.8015E+02 | 1.7199E+03 | 1.0732E+02 | 1.9318E+02 | 3.5648E+05 | 7.8590E+05 | 1.0465E+08 | 4.1529E+08 |
| 85.0 | 2.3990E+02 | 5.2888E+02 | 1.9546E+02 | 3.5183E+02 | 3.6095E+05 | 7.9577E+05 | 1.0512E+08 | 4.1717E+08 |
| 90.0 | 8.0717E+02 | 1.7795E+03 | 1.0951E+02 | 1.9713E+02 | 3.6243E+05 | 7.9903E+05 | 1.0539E+08 | 4.1822E+08 |
| 95.0 | 6.5211E+02 | 1.4377E+03 | 1.1473E+02 | 2.0651E+02 | 3.6588E+05 | 8.0663E+05 | 1.0579E+08 | 4.1982E+08 |
| 100.0 | 1.7141E+03 | 3.7789E+03 | 9.6159E+01 | 1.7309E+02 | 3.7052E+05 | 8.1686E+05 | 1.0629E+08 | 4.2178E+08 |
| 110.0 | 1.3707E+03 | 3.0219E+03 | 9.3458E+01 | 1.6822E+02 | 3.8066E+05 | 8.3921E+05 | 1.0730E+08 | 4.2582E+08 |
| 120.0 | 1.1553E+03 | 2.5469E+03 | 1.0026E+02 | 1.8046E+02 | 3.9104E+05 | 8.6210E+05 | 1.0835E+08 | 4.2998E+08 |

A-3

Table 6.2.1-39 (3 of 4)

| Time (sec) | Mass Flow | | Enthalpy | | Integral of Mass Flow | | Integral of Energy | |
|---------------|-------------|-------------|-------------|-------------|-----------------------|------------|--------------------|------------|
| | (kg/sec) | (lbm/sec) | (kcal/kg) | (Btu/lbm) | (kg) | (lbm) | (kcal) | (Btu) |
| 28.0 | 1.3825E+03 | 3.0478E+03 | 7.4008E+01 | 1.3321E+02 | 3.0503E+05 | 6.7249E+05 | 9.9830E+07 | 3.9616E+08 |
| 29.0 | -4.6888E+01 | -1.0337E+02 | 2.9049E+02 | 5.2288E+02 | 3.0511E+05 | 6.7265E+05 | 9.9824E+07 | 3.9613E+08 |
| 30.0 | -9.2798E+00 | -2.0459E+01 | -3.7440E+02 | -6.7393E+02 | 3.0507E+05 | 6.7256E+05 | 9.9811E+07 | 3.9608E+08 |
| 35.0 | 8.2544E+02 | 1.8198E+03 | 7.0693E+01 | 1.2725E+02 | 3.0599E+05 | 6.7460E+05 | 9.9938E+07 | 3.9659E+08 |
| 40.0 | 1.5654E+03 | 3.4512E+03 | 6.5703E+01 | 1.1826E+02 | 3.0759E+05 | 6.7813E+05 | 1.0014E+08 | 3.9737E+08 |
| 45.0 | 2.2241E+03 | 4.9033E+03 | 6.8862E+01 | 1.2395E+02 | 3.0912E+05 | 6.8149E+05 | 1.0037E+08 | 3.9829E+08 |
| 50.0 | 7.7318E+02 | 1.7046E+03 | 9.6668E+01 | 1.7400E+02 | 3.1457E+05 | 6.9352E+05 | 1.0091E+08 | 4.0045E+08 |
| 55.0 | 7.2726E+02 | 1.6033E+03 | 1.0195E+02 | 1.8351E+02 | 3.2410E+05 | 7.1452E+05 | 1.0169E+08 | 4.0355E+08 |
| 60.0 | 5.4934E+02 | 1.2111E+03 | 1.1092E+02 | 1.9966E+02 | 3.3289E+05 | 7.3389E+05 | 1.0241E+08 | 4.0641E+08 |
| 65.0 | 9.7930E+02 | 2.1590E+03 | 1.0144E+02 | 1.8259E+02 | 3.4263E+05 | 7.5537E+05 | 1.0323E+08 | 4.0966E+08 |
| 70.0 | 9.4834E+02 | 2.0907E+03 | 1.0456E+02 | 1.8820E+02 | 3.4706E+05 | 7.6514E+05 | 1.0369E+08 | 4.1146E+08 |
| 75.0 | 9.2547E+02 | 2.0403E+03 | 1.0588E+02 | 1.9058E+02 | 3.5208E+05 | 7.7621E+05 | 1.0418E+08 | 4.1343E+08 |
| 80.0 | 1.6133E+03 | 3.5567E+03 | 9.9377E+01 | 1.7888E+02 | 3.5606E+05 | 7.8498E+05 | 1.0461E+08 | 4.1511E+08 |
| 85.0 | 2.1460E+03 | 4.7310E+03 | 9.6351E+01 | 1.7343E+02 | 3.6080E+05 | 7.9543E+05 | 1.0510E+08 | 4.1706E+08 |
| 90.0 | 1.0122E+02 | 2.2316E+02 | 2.5144E+02 | 4.5258E+02 | 3.6243E+05 | 7.9903E+05 | 1.0539E+08 | 4.1822E+08 |
| 95.0 | 9.6142E+02 | 2.1196E+03 | 9.9371E+01 | 1.7887E+02 | 3.6588E+05 | 8.0663E+05 | 1.0579E+08 | 4.1982E+08 |
| 100.0 | 6.8324E+02 | 1.5063E+03 | 1.0617E+02 | 1.9111E+02 | 3.7052E+05 | 8.1686E+05 | 1.0629E+08 | 4.2178E+08 |
| 110.0 | 1.2417E+03 | 2.7374E+03 | 1.0184E+02 | 1.8332E+02 | 3.8016E+05 | 8.3811E+05 | 1.0726E+08 | 4.2562E+08 |
| 120.0 | 7.2970E+02 | 1.6087E+03 | 1.0815E+02 | 1.9466E+02 | 3.9050E+05 | 8.6091E+05 | 1.0830E+08 | 4.2976E+08 |

Replace with next page A-4

Table 6.2.1-39 (4 of 4)

| Time (sec) | Mass Flow | | Enthalpy | | Integral of Mass Flow | | Integral of Energy | |
|---------------|------------|------------|------------|------------|-----------------------|------------|--------------------|------------|
| | (kg/sec) | (lbm/sec) | (kcal/kg) | (Btu/lbm) | (kg) | (lbm) | (kcal) | (Btu) |
| 130.0 | 8.9815E+02 | 1.9801E+03 | 1.0577E+02 | 1.9039E+02 | 4.0040E+05 | 8.8274E+05 | 1.0933E+08 | 4.3384E+08 |
| 140.0 | 1.1298E+03 | 2.4908E+03 | 1.0262E+02 | 1.8471E+02 | 4.1093E+05 | 9.0594E+05 | 1.1043E+08 | 4.3821E+08 |
| 150.0 | 9.5167E+02 | 2.0981E+03 | 1.0889E+02 | 1.9600E+02 | 4.1912E+05 | 9.2399E+05 | 1.1132E+08 | 4.4175E+08 |
| 160.0 | 1.1363E+03 | 2.5051E+03 | 1.0489E+02 | 1.8881E+02 | 4.3166E+05 | 9.5164E+05 | 1.1261E+08 | 4.4686E+08 |
| 170.0 | 9.1526E+02 | 2.0178E+03 | 1.0773E+02 | 1.9391E+02 | 4.4223E+05 | 9.7495E+05 | 1.1373E+08 | 4.5131E+08 |
| 180.0 | 4.4847E+02 | 9.8870E+02 | 1.2333E+02 | 2.2199E+02 | 4.4953E+05 | 9.9104E+05 | 1.1454E+08 | 4.5453E+08 |
| 190.0 | 4.9428E+02 | 1.0897E+03 | 1.7914E+02 | 3.2245E+02 | 4.5528E+05 | 1.0037E+06 | 1.1524E+08 | 4.5732E+08 |
| 200.0 | 5.4523E+02 | 1.2020E+03 | 1.8537E+02 | 3.3366E+02 | 4.6069E+05 | 1.0157E+06 | 1.1622E+08 | 4.6121E+08 |
| 210.0 | 5.2823E+02 | 1.1645E+03 | 1.8529E+02 | 3.3352E+02 | 4.6557E+05 | 1.0264E+06 | 1.1717E+08 | 4.6496E+08 |
| 220.0 | 5.1639E+02 | 1.1384E+03 | 1.7528E+02 | 3.1550E+02 | 4.7111E+05 | 1.0386E+06 | 1.1813E+08 | 4.6879E+08 |
| 230.0 | 3.4466E+02 | 7.5985E+02 | 2.1803E+02 | 3.9246E+02 | 4.7535E+05 | 1.0480E+06 | 1.1894E+08 | 4.7201E+08 |
| 240.0 | 1.3835E+02 | 3.0501E+02 | 3.4640E+02 | 6.2352E+02 | 4.7706E+05 | 1.0517E+06 | 1.1950E+08 | 4.7422E+08 |
| 250.0 | 1.1657E+02 | 2.5700E+02 | 3.5294E+02 | 6.3529E+02 | 4.7832E+05 | 1.0545E+06 | 1.1994E+08 | 4.7596E+08 |
| 260.0 | 1.1309E+02 | 2.4933E+02 | 3.2035E+02 | 5.7663E+02 | 4.7943E+05 | 1.0576E+06 | 1.2031E+08 | 4.7745E+08 |
| 270.0 | 1.0166E+02 | 2.2411E+02 | 3.5015E+02 | 6.3027E+02 | 4.8051E+05 | 1.0593E+06 | 1.2068E+08 | 4.7889E+08 |
| 280.0 | 1.0073E+02 | 2.2206E+02 | 3.5595E+02 | 6.4071E+02 | 4.8152E+05 | 1.0616E+06 | 1.2104E+08 | 4.8031E+08 |
| 290.0 | 1.0174E+02 | 2.2430E+02 | 3.5329E+02 | 6.3591E+02 | 4.8252E+05 | 1.0638E+06 | 1.2139E+08 | 4.8172E+08 |
| 300.0 | 9.5467E+01 | 2.1047E+02 | 3.4684E+02 | 6.2431E+02 | 4.8351E+05 | 1.0660E+06 | 1.2174E+08 | 4.8310E+08 |

A-4

Table 6.2.1-39 (4 of 4)

| Time (sec) | Mass Flow | | Enthalpy | | Integral of Mass Flow | | Integral of Energy | |
|---------------|------------|------------|------------|------------|-----------------------|------------|--------------------|------------|
| | (kg/sec) | (lbm/sec) | (kcal/kg) | (Btu/lbm) | (kg) | (lbm) | (kcal) | (Btu) |
| 130.0 | 4.4106E+02 | 9.7237E+02 | 1.5443E+02 | 2.7797E+02 | 3.9996E+05 | 8.8177E+05 | 1.0928E+08 | 4.3366E+08 |
| 140.0 | 8.9698E+02 | 1.9775E+03 | 1.2583E+02 | 2.2650E+02 | 4.1034E+05 | 9.0465E+05 | 1.1037E+08 | 4.3797E+08 |
| 150.0 | 9.1549E+02 | 2.0183E+03 | 1.2770E+02 | 2.2987E+02 | 4.1868E+05 | 9.2304E+05 | 1.1127E+08 | 4.4156E+08 |
| 160.0 | 7.0149E+02 | 1.5465E+03 | 1.4420E+02 | 2.5956E+02 | 4.3109E+05 | 9.5039E+05 | 1.1255E+08 | 4.4663E+08 |
| 170.0 | 5.7435E+02 | 1.2662E+03 | 1.3331E+02 | 2.3997E+02 | 4.4180E+05 | 9.7401E+05 | 1.1368E+08 | 4.5113E+08 |
| 180.0 | 2.9484E+02 | 6.5000E+02 | 2.9684E+02 | 5.3431E+02 | 4.4929E+05 | 9.9051E+05 | 1.1451E+08 | 4.5442E+08 |
| 190.0 | 4.5837E+02 | 1.0105E+03 | 1.7477E+02 | 3.1459E+02 | 4.5507E+05 | 1.0033E+06 | 1.1520E+08 | 4.5717E+08 |
| 200.0 | 4.3574E+02 | 9.6065E+02 | 1.8588E+02 | 3.3459E+02 | 4.6043E+05 | 1.0151E+06 | 1.1617E+08 | 4.6101E+08 |
| 210.0 | 1.8636E+02 | 4.1085E+02 | 3.1251E+02 | 5.6252E+02 | 4.6531E+05 | 1.0258E+06 | 1.1712E+08 | 4.6478E+08 |
| 220.0 | 1.2309E+02 | 2.7136E+02 | 3.9496E+02 | 7.1094E+02 | 4.7086E+05 | 1.0381E+06 | 1.1809E+08 | 4.6862E+08 |
| 230.0 | 1.0636E+02 | 2.3449E+02 | 4.5244E+02 | 8.1440E+02 | 4.7498E+05 | 1.0471E+06 | 1.1887E+08 | 4.7171E+08 |
| 240.0 | 1.0104E+02 | 2.2275E+02 | 4.7516E+02 | 8.5528E+02 | 4.7692E+05 | 1.0514E+06 | 1.1945E+08 | 4.7403E+08 |
| 250.0 | 1.3263E+02 | 2.9240E+02 | 3.6438E+02 | 6.5588E+02 | 4.7826E+05 | 1.0544E+06 | 1.1992E+08 | 4.7588E+08 |
| 260.0 | 1.3883E+02 | 3.0606E+02 | 3.7319E+02 | 6.7175E+02 | 4.7937E+05 | 1.0568E+06 | 1.2030E+08 | 4.7737E+08 |
| 270.0 | 1.3114E+02 | 2.8912E+02 | 3.6650E+02 | 6.5970E+02 | 4.8046E+05 | 1.0592E+06 | 1.2066E+08 | 4.7882E+08 |
| 280.0 | 1.2790E+02 | 2.8198E+02 | 3.6663E+02 | 6.5994E+02 | 4.8146E+05 | 1.0614E+06 | 1.2102E+08 | 4.8024E+08 |
| 290.0 | 1.3176E+02 | 2.9047E+02 | 3.7484E+02 | 6.7471E+02 | 4.8247E+05 | 1.0637E+06 | 1.2137E+08 | 4.8165E+08 |
| 300.0 | 1.3813E+02 | 3.0452E+02 | 3.6063E+02 | 6.4913E+02 | 4.8341E+05 | 1.0657E+06 | 1.2170E+08 | 4.8296E+08 |

Replace with next page B

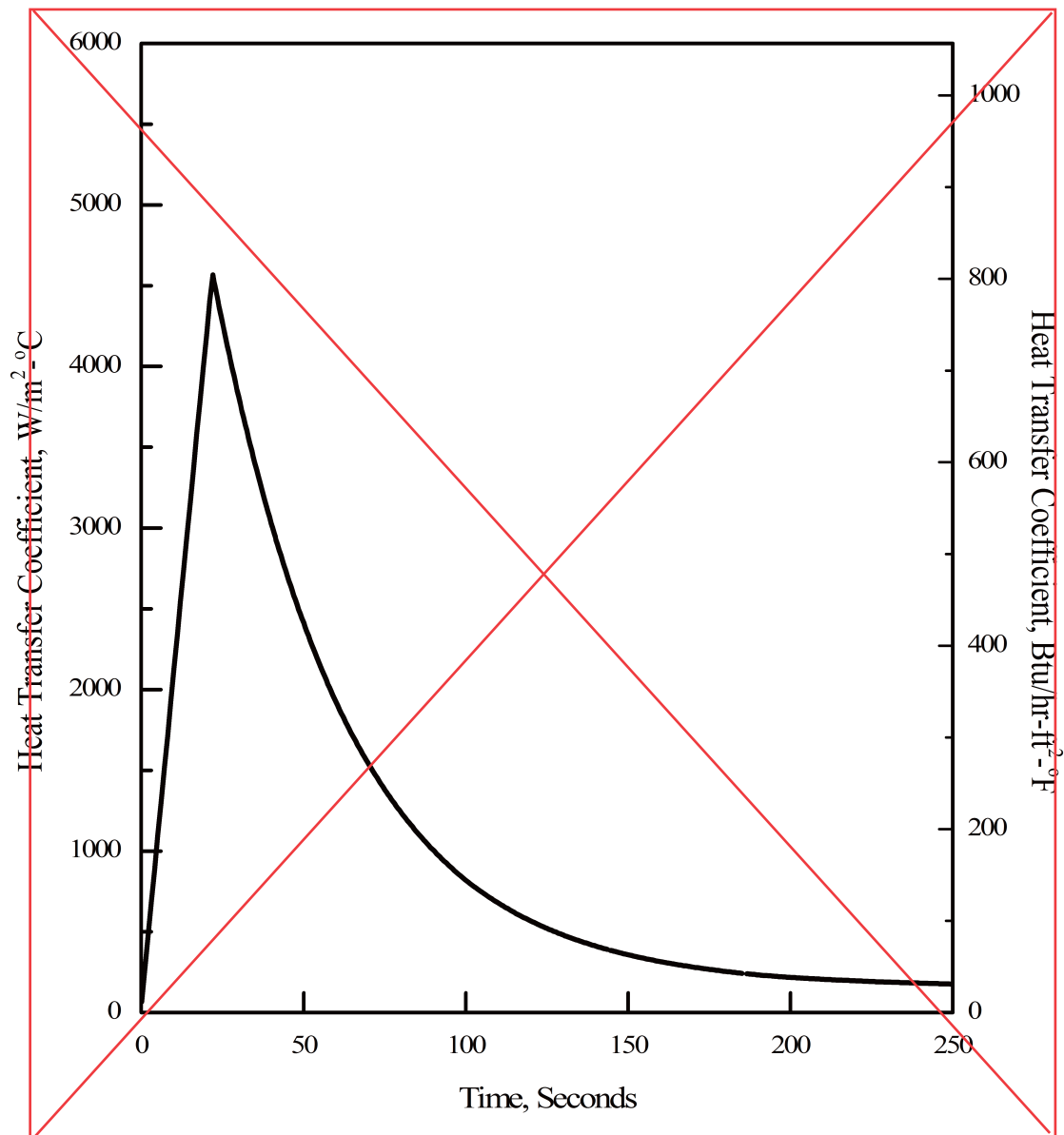
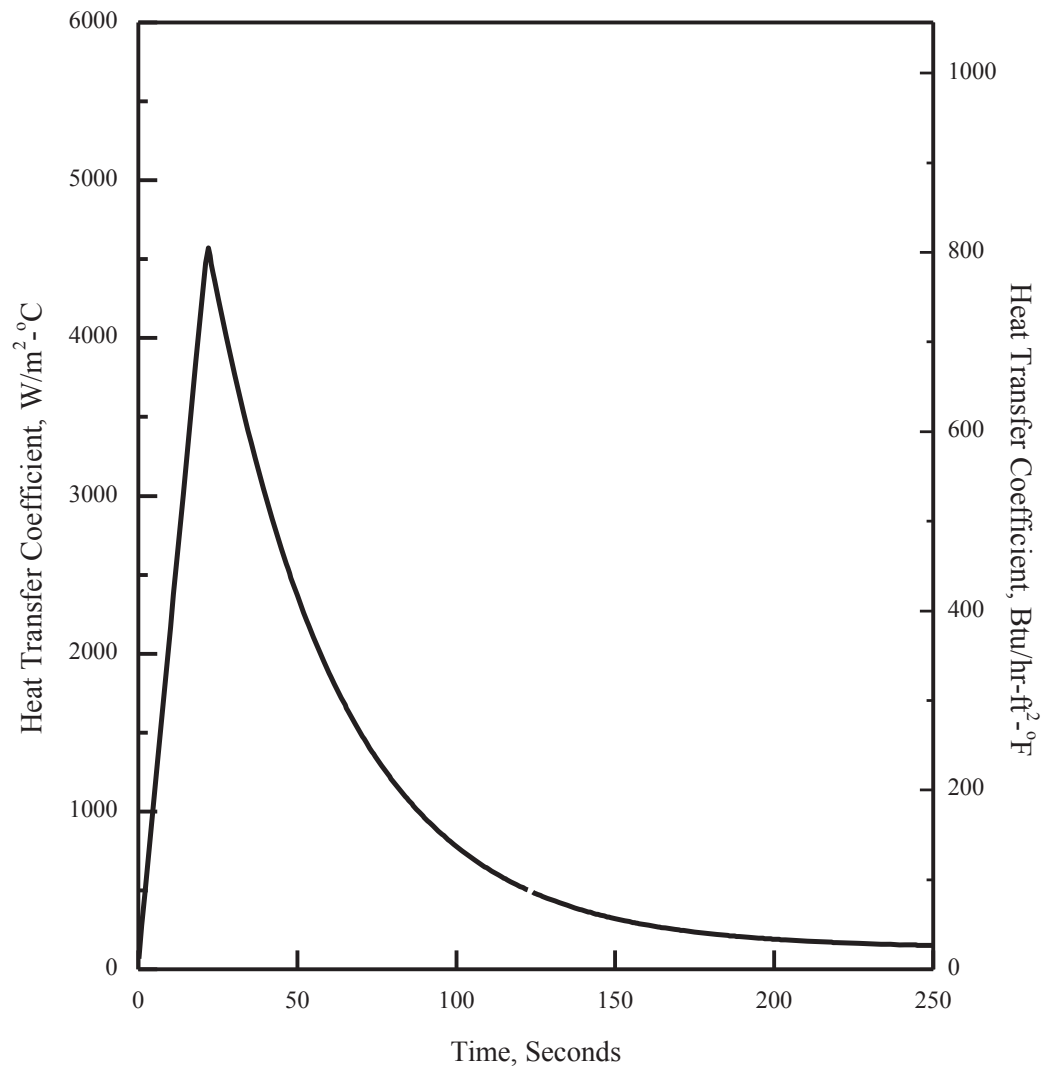
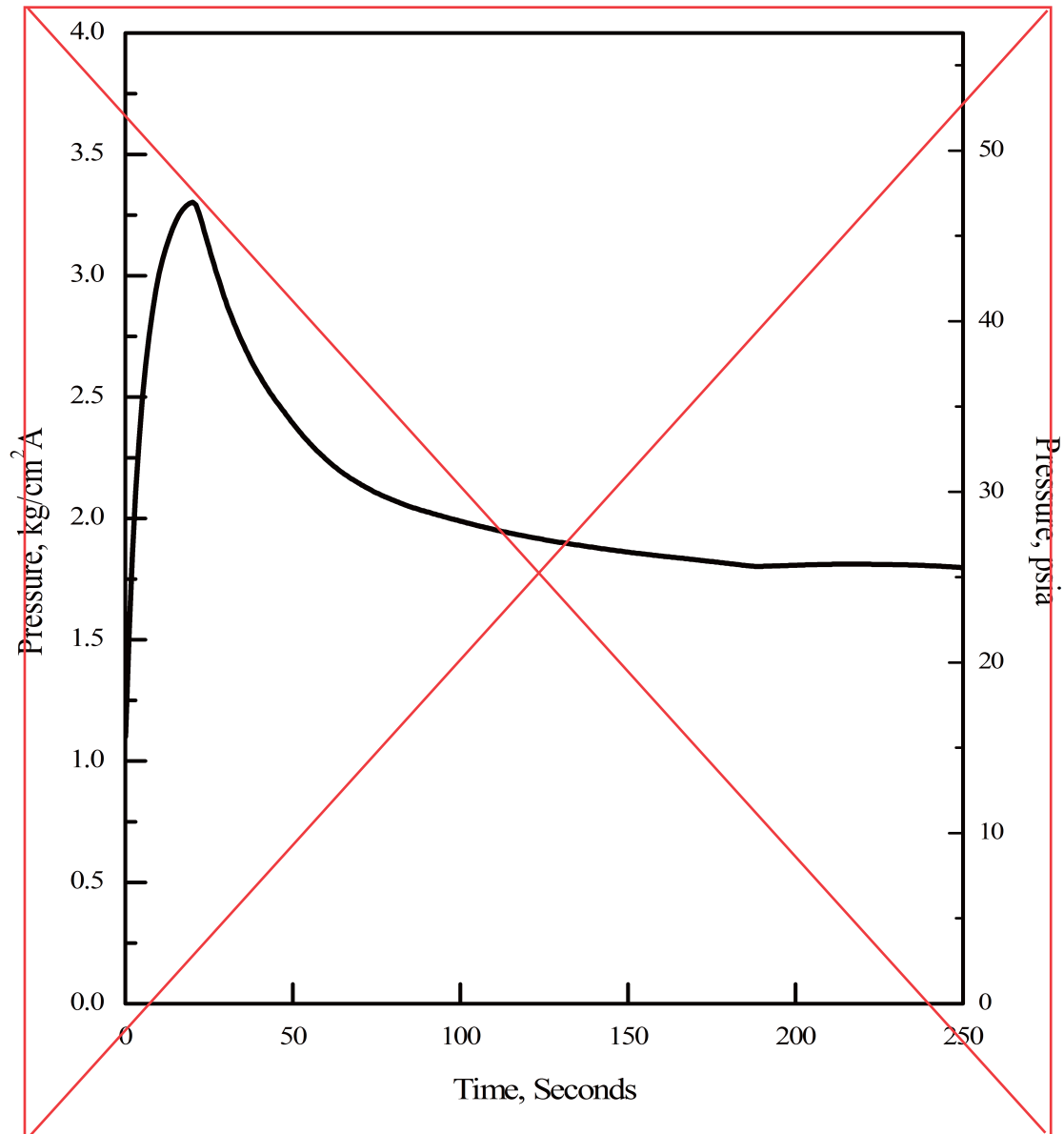


Figure 6.2.1-49 ECCS Performance Analysis
(Condensation Heat Transfer Coefficient for Passive Heat Removal Source)

B

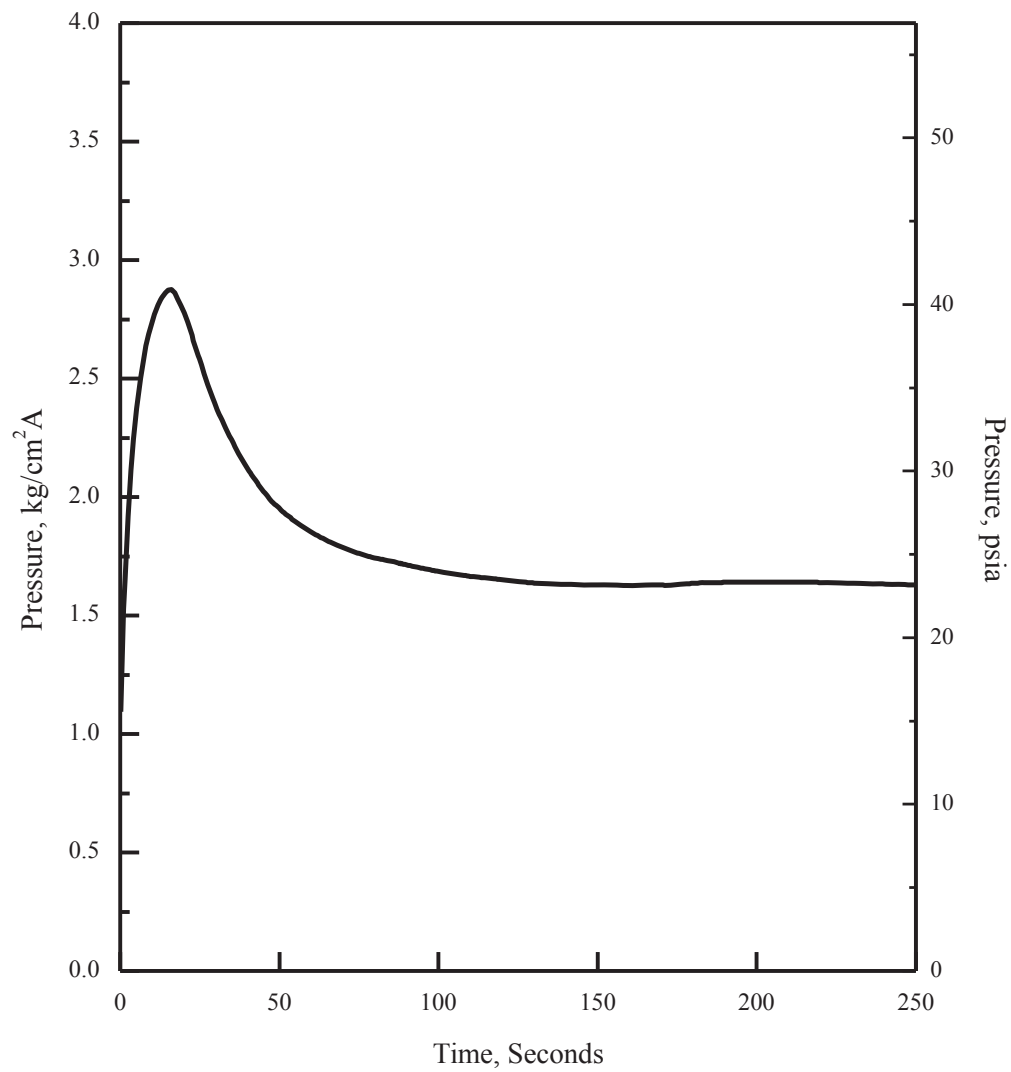


Replace with next page C

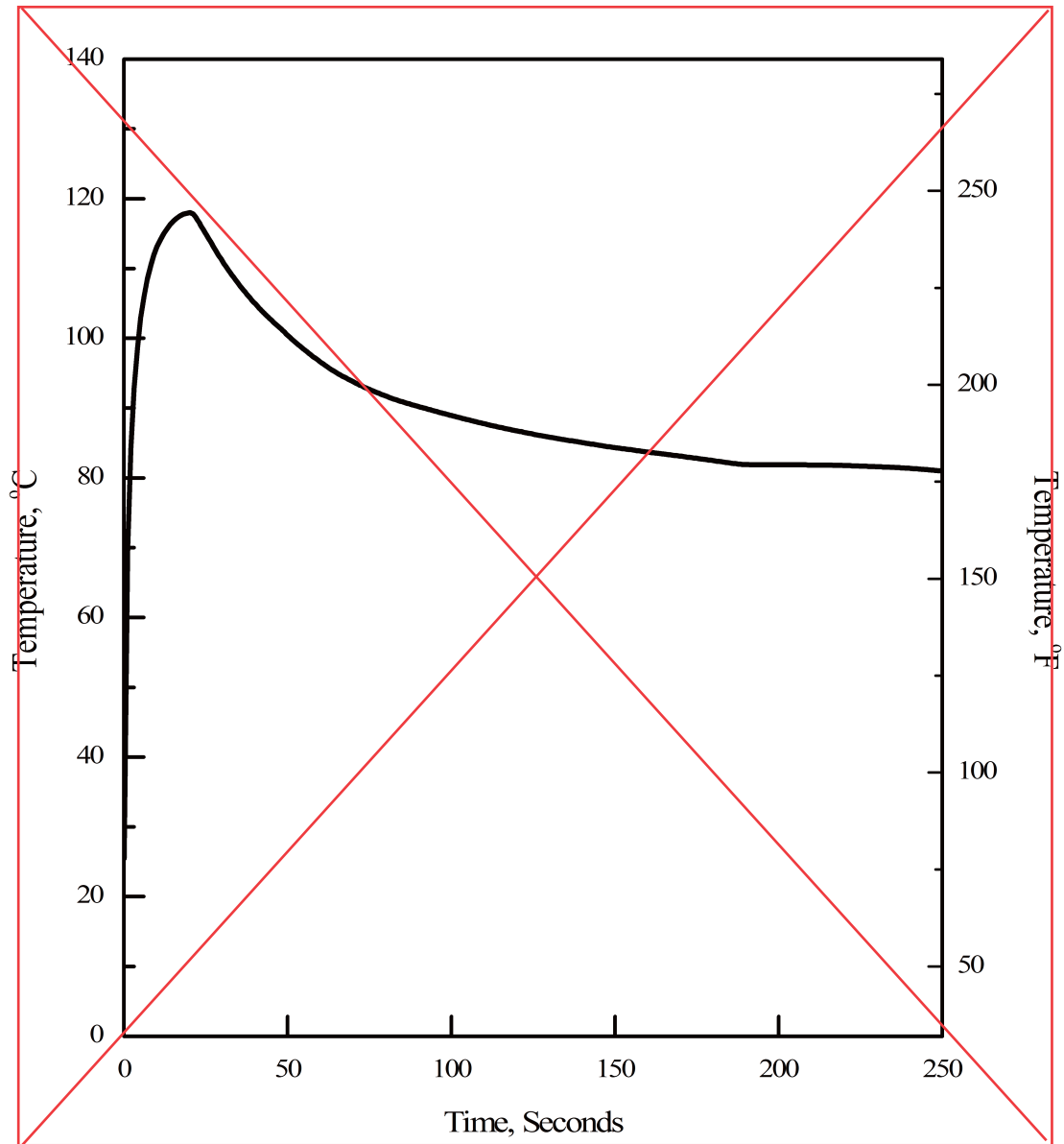


**Figure 6.2.1-50 1.0 x Double-Ended Guillotine Break in Pump Discharge Leg
(Min. Containment Pressure for ECCS Performance Analysis)**

C

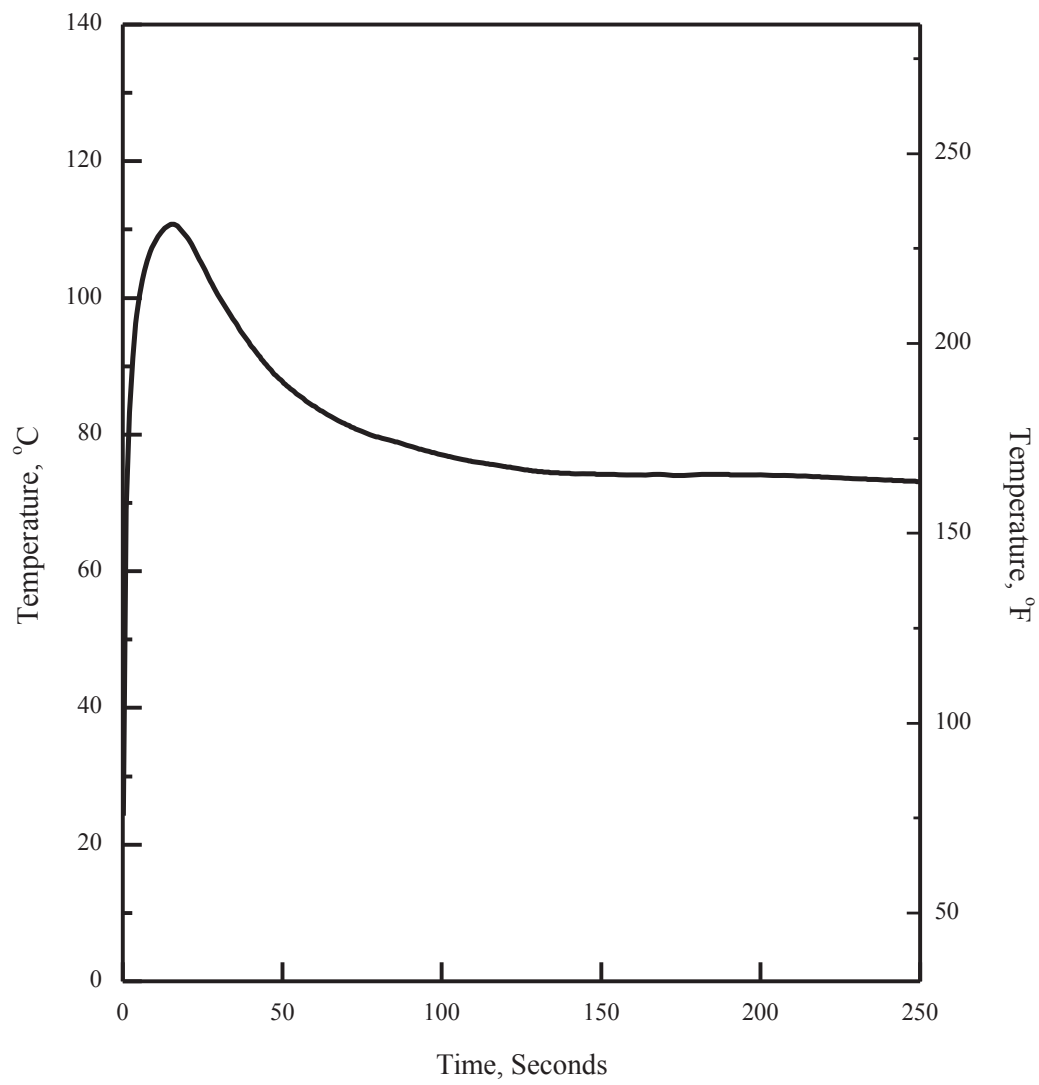


Replace with next page D

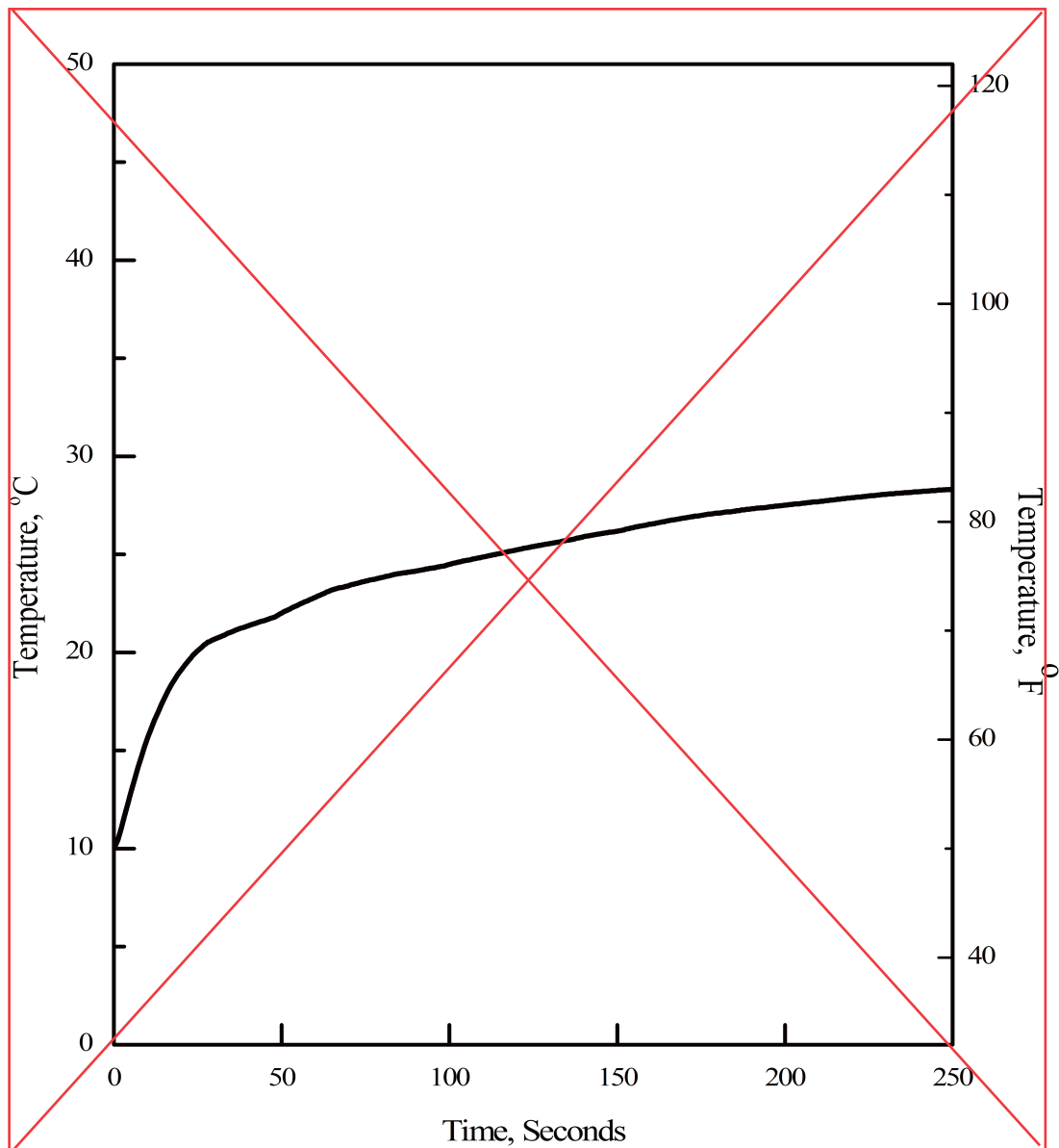


**Figure 6.2.1-51 1.0 x Double-Ended Guillotine Break in Pump Discharge Leg
(Containment Atmosphere Temperature)**

| |
|---|
| D |
|---|

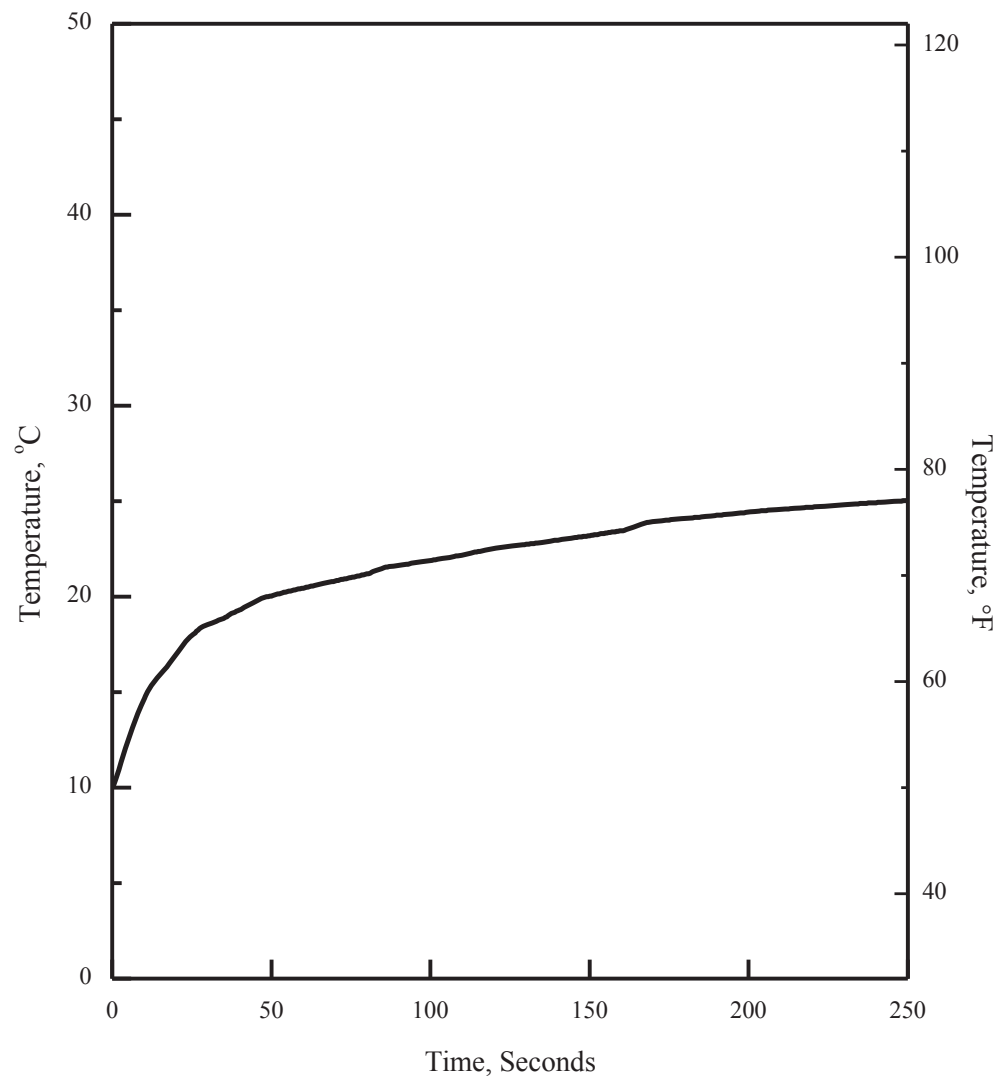


Replace with next page E



**Figure 6.2.1-52 1.0 x Double-Ended Guillotine Break In Pump Discharge Leg
(In-containment Refueling Water Storage Tank)**

| |
|---|
| E |
|---|



fuel maximum reactivity assumption, worst-case moderator density, and tolerances and uncertainties of the fuel and racks are considered to maximize the calculated K_{eff} for normal conditions and postulated accidents.

The design of the new fuel storage racks is such that K_{eff} (with all biases and uncertainties) must not exceed 0.95 with full density unborated water and 0.98 with optimum moderation in the new fuel rack, at a 95 percent probability and 95 percent confidence level. For the spent fuel storage racks, credit is taken for the presence of soluble boron in the SFP. Therefore, the maximum K_{eff} including all biases and uncertainties must ~~not~~ exceed 0.95 with borated water, and must remain below 1.0 with full density unborated water, at a 95 percent probability and 95 percent confidence level.

not

The criticality safety evaluation for the new and spent fuel storage racks is performed in accordance with the following acceptance criteria and relevant guidance: 10 CFR Part 50 Appendix A, General Design Criterion (GDC) 62 (Reference 1), 10 CFR Part 50.68 (Reference 2), NRC guidance (Reference 3), and NUREG/CR-6698 (Reference 4). The 10 CFR Part 50.68 (b) items (2) and (3) for new fuel storage racks and item (4) for spent fuel storage racks are applied as the criticality safety design criteria. Criticality analysis codes are validated in accordance with NUREG/CR-6698.

9.1.1.2 Facilities Description


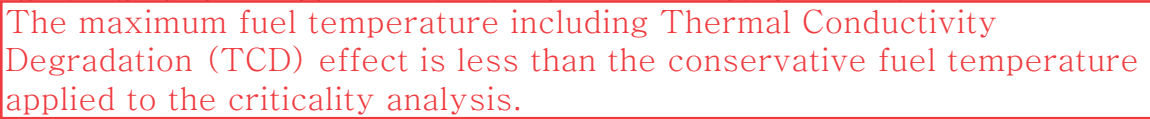
The description of new and spent fuel storage facilities is presented in Subsection 9.1.2.2.

9.1.1.3 Safety Evaluation

Prevention of an inadvertent criticality is provided by the adequate design of fuel handling and storage facilities and by administrative control procedures, considering the double contingency principle. The main methods for criticality control are (1) limiting the size of the array of fuel assemblies and (2) limiting the assembly neutron interaction by fixing the minimum separation and/or providing neutron poisons. In addition, rack cells are maintained in a safe geometry with no deformation in any design basis event. Flooding in the new fuel storage racks and boron dilution in the SFP water are minimized. Fuel mishandling is prevented by the fuel handling procedures.

For criticality safety design, the following analyses are performed to evaluate the degree of subcriticality and to verify conformance with the following design criteria (Reference 10):

condition, an infinite array of fresh fuel assemblies is modeled in the criticality calculation. Criticality for damaged fuel assemblies is separately evaluated and the effects of gap between racks are also evaluated.

- b. For the region II analyses, an infinite array of 2×2 fuel assemblies with various U-235 enrichments, from 2.0 to 5.0 wt%, is used for the criticality calculation. The moderator of pure water is at the temperature (density) within the design limits that yields the largest reactivity. The full density of unborated water is assumed to be 1.0 g/cm^3 (62.4 lbm/ft^3).
- c. Credit is taken for the neutron absorption in the neutron absorbing materials, and only 75 percent of B-10 areal density in the neutron absorbing materials is credited in the analysis. These assumptions provide additional margin in the event that deformation, degradation, or damage to the neutron absorber occur.
- d. Credit is taken for the soluble boron in the SFP. The SFP soluble boron concentration is assumed to be the same or less than the minimum concentration provided in the LCO 3.7.15.
- e. No cooling time is assumed to avoid fission product accumulation and Xe-135 is not included in the criticality calculation to conservatively evaluate the K_{eff} .
- f. The nuclear characteristics of the spent fuel are affected by the core operation parameters, such as fuel temperature, coolant temperature, soluble boron concentration in the coolant, and axial burnup profile. Thus, the most severe operating conditions are conservatively assumed in the fuel burnup calculation.
- g. No CEAs or burnable poison rods in the fuel assembly, and no neutron absorption
- h. The maximum fuel temperature including Thermal Conductivity Degradation (TCD) effect is less than the conservative fuel temperature applied to the criticality analysis.
- i. the SFP filled with water.
- i. The bias and bias uncertainty obtained from benchmark calculation are reflected in the calculated K_{eff} . Uncertainties from mechanical tolerances and variations in the design parameters are added to the total uncertainty. For region II analyses, the effects of axial burnup profile and burnable poison rods, and uncertainty from the depletion calculation methodology are considered in the calculation K_{eff} .

APR1400 DCD TIER 2

In Non-LOCA analysis, maximum gap conductance used in CESEC-III code is not affected by TCD because the highest gap conductance value is obtained without gas generation. And minimum gap conductance used in CESEC-III code is not affected because the lowest gap conductance value is obtained at low burnup where fission gas release is negligible. The fuel temperature coefficient reflecting a large uncertainty can cover the TCD. Also, Doppler feedback effect in CESEC-III code is still conservative because of the conservative gap conductance assumption.

In DNB analyses, CETOP/TORC code is not affected by TCD due to the use of "dummy" rods to define the heat flux boundary. A dummy rod does not consider the conduction heat transfer within the fuel rods.

Most of stored energy is eliminated before the core uncover during a blowdown phase in small break LOCA (SBLOCA). Hence, the initial stored energy effects caused by TCD are negligible in SBLOCA.

The impacts of TCD for a CEA ejection accident and LBLOCA are considered by reflecting TCD penalty in initializing the fuel centerline and average temperature. The TCD penalty is provided in Reference 78.

each design basis event.

The setpoints presented in Table 15.0-2 are determined based on the methodology presented above. The main methodology for determining uncertainties and the detailed uncertainty values are provided in Reference 51, which is based on NRC RG 1.105, Rev. 3, "Setpoints for Safety-Related Instrumentation." The setpoint methodology for plant protection system is provided in Reference 77.

15.0.0.10 Thermal Conductivity Degradation

The effects of thermal conductivity degradation (TCD) on non-LOCA and LOCA evaluations, except for a CEA ejection accident and LBLOCA, are negligible. ~~The effects are provided in Reference 78.~~

The results of the evaluation of a CEA ejection accident and LBLOCA are provided in Subsections 15.4.8.3 and 15.6.5.3, respectively.

15.0.1 Radiological Consequence Analysis Using Alternative Source Terms

This subsection is not applicable to the APR1400 because it is prepared to review the application for the initial implementation of an alternative source terms (AST)

APR1400-F-M-TR-13001-P, "PLUS7 Fuel Design for the APR1400," Rev. 1, KHNP, To be issued

78. ~~APR1400-F-A-NR-14002-P, "The Effect of Thermal Conductivity Degradation on APR1400 Design and Safety Analyses," Rev. 0, KHNP, September 2014.~~
79. NUREG-1462, "Final Safety Evaluation Report Related to the Certification of the System 80+ Design Docket No. 52-002," Rev. 0, U.S. Nuclear Regulatory Commission, 1994.
80. APR1400-Z-A-NR-14014-P, "ATWS Evaluation," Rev. 0, KHNP, November 2014.
81. APR1400-F-M-TR-13001-P (Proprietary), "PLUS7 Fuel Design for the APR1400," Rev. 0, KHNP, August 2013.

APR1400 DCD TIER 2

The reactor coolant pressure stays below 110 percent of the design pressure so that the integrity of the reactor coolant pressure boundary is maintained.

15.4.8 Spectrum of Control Element Assembly Ejection Accidents

15.4.8.1 Identification of Causes and Frequency Classification

A control element assembly (CEA) ejection (CEAE) event is postulated to occur as a result of a mechanical failure that causes an instantaneous circumferential rupture of the control element drive mechanism (CEDM) housing or its associated nozzle. This results in the reactor coolant system pressure ejecting the CEA and drive shaft to the fully withdrawn position.

The CEDM housings are capable of withstanding throughout their design life all normal operating loads including the steady-state and transient operating conditions specified for the reactor vessel. The occurrence of such a failure is considered to be incredible, and this event is classified as a PA as defined in Subsection 15.0.0.1.

The CEA ejection accident applies the following acceptance criteria:

- a. The maximum reactor pressure during any portion of the assumed excursion is less than the value that result in stresses that exceed the “Service Limit C” as defined in the ASME Code.
- b. The total number of failed fuel rods that are considered in the radiological assessment is equal to the sum of all of the fuel rods failing each of the criteria below:
 - 1) The high cladding temperature failure criterion for zero-power conditions is a peak radial average fuel enthalpy greater than 711.8 kJ/kg (170 cal/g) for fuel rods with an internal rod pressure at or below system pressure, or 628.0 kJ/kg (150 cal/g) for fuel rods with an internal rod pressure exceeding system pressure. For intermediate and full-power conditions, fuel cladding failure is presumed if local heat flux exceeds thermal design limits.
 - 2) The pellet cladding mechanical interaction (PCMI) failure criterion is a change in radial average fuel enthalpy greater than the corrosion-dependent limit depicted in Figure B-1 of NUREG-0800 (SRP 4.2, Appendix B).

APR1400 DCD TIER 2

In addition to the fuel failure and boundary criteria above, the following criteria from NUREG-0800 (SRP, Section 4.2, Appendix B) apply to core coolability.

- a. Peak radial average fuel enthalpy remains below 963.0 kJ/kg (230 cal/g).
- b. Peak fuel temperature remains below incipient melting conditions.
- c. Mechanical energy generated as a result of (1) non-molten fuel-to-coolant interaction and (2) fuel rod burst must be addressed with respect to reactor pressure boundary, reactor internals, and fuel assembly structural integrity.
- d. There is no loss of coolable geometry due to (1) fuel pellet and cladding fragmentation and dispersal or (2) fuel rod ballooning.

15.4.8.2 Sequence of Events and Systems Operation

The sequence of events during the fuel performance aspect of the CEAE initiated from various power conditions is presented in Table 15.4.8-1.

The postulated mechanical failure of the CEDM causes the ejection of a CEA, which adds positive reactivity to the core resulting in a rapid increase in reactor core power for a short period of time. This power excursion is terminated by the combination of delayed neutron and Doppler feedback effects. Closely following the CEAE, reactor shutdown is initiated by a core protection calculator (CPC) or reactor protection system (RPS) variable overpower trip (VOPT) on high neutron power. The reactor power decreases rapidly as the shutdown CEAs drop into the reactor core. A loss of offsite power (LOOP) is assumed to be coincident with a turbine trip.

The analysis assumes that operator action is delayed until 30 minutes after event initiation. Plant cooldown is accomplished by using the auxiliary feedwater (AFW) system in conjunction with the atmospheric dump valves (ADV) until shutdown cooling entry conditions are reached.

This event results in a turbine trip when initiated from at-power conditions. A turbine trip could cause a disturbance to the utility grid, which could cause a loss of offsite power, which could cause a RCP coastdown. The RCS pressure increase caused by turbine trip and LOOP can mitigate fuel failure due to DNB, but the change of RCS pressure is not conservatively considered for DNBR calculation.

APR1400 DCD TIER 2

None of single failures listed in Table 15.0-4 has any effect on this event. The limiting single failure for this event is one train failure of the RPS. Other trains provide adequate protection. Details on the RPS are provided in Section 7.2.

15.4.8.3 Core and System Performance**15.4.8.3.1 Evaluation Model**

The core response to a CEAE is simulated using the method of analysis referenced in Subsection 15.0.2. The evaluation model is used to determine the peak fuel rod temperature and fuel rod enthalpy, which are required for the evaluation of the high cladding temperature failure, the pellet cladding mechanical interaction (PCMI) failure, and the core coolability. The DNBR is calculated using the CETOP and STRIKIN-II computer programs described in Subsection 15.0.2 with the KCE-1 CHF correlation. A matrix relating the initial and ejected CEA radial peaking factors is obtained from ROCS code, which is a three-dimensional, two-group diffusion core calculation code based on the nodal expansion method, as described in Subsection 4.3.3.1. This matrix is used to calculate the number of fuel pins experiencing DNB. Further conservatism is introduced by assuming that clad failure occurs when fuel rods undergo DNB.

The nuclear steam supply system (NSSS) response to a CEA ejection is simulated using the CESEC-III computer program described in Subsection 15.0.2.2.1.

Except for radiological release from containment, the analysis of the NSSS response to a CEA ejection does not consider the leakage and the RCS depressurization that would be caused by the rupture of the primary pressure boundary. This approach does not affect the fuel failure calculation, but it does increase the calculated secondary steam release. Not considering the leakage and the RCS depressurization maximizes the resultant doses from secondary steam release.

15.4.8.3.2 Input Parameters and Initial Conditions

The initial conditions for the principal process variables are varied within the reactor operating space given in Table 15.0-3 to determine the set of conditions that produce the most adverse consequences following a CEA ejection. The initial pressurizer and steam generator water level, as controlled within the operating space, have an insignificant effect on the consequences of the CEA ejection analysis. Table 15.4.8-2 shows the parameters used in the CEA ejection analysis for peak fuel rod temperature and fuel rod enthalpy

APR1400 DCD TIER 2

analysis. The following assumptions, which encompass conditions characteristic of the beginning of cycle (BOC) and end of cycle (EOC), are used to calculate conservative transient results.

- a. A spectrum of initial reactor power level is considered as follows: (1) hot full power (HFP), (2) 50 percent power, (3) 20 percent power, and (4) hot zero power (HZIP).
- b. Thermal-hydraulic parameters (maximum reactor coolant inlet temperatures, minimum reactor coolant system pressure, and minimum reactor coolant flow fraction) are set to maximize the net energy increase in the fuel of hot channel. For DNBR analysis, the most adverse combination of initial conditions (core inlet temperature, reactor coolant system pressure, and core flow) at a power operating limit by COLSS are selected by parametric studies to minimize the DNBR for HFP and 50 percent power case. COLSS is described in Subsection 7.7.1.4.
- c. It is conservative to use minimum delayed neutron fraction and minimum neutron lifetime at EOC to make the power increase faster and further.
- d. The most positive moderator temperature coefficient (MTC) at BOC is used with varying power level to maximize the positive feedback during the transient.
- e. The least negative fuel temperature coefficient (FTC) is used to minimize Doppler feedback during the power excursion. Doppler reactivity weighting factor is assumed to be 1.0 for conservatism.
- f. In the three-dimensional modeling, the most reactive CEA ejection is selected with consideration for power dependent rod insertion limit. The magnitude of the enthalpy rise increases with increasing ejected worth.
- g. A maximum three-dimensional post-ejected peaking factor is used to maximize the net energy content in the hottest fuel. And, the maximum ratio of the three-dimensional post-ejected to pre-ejected peaking factor is used to maximize the prompt enthalpy rise in the hottest fuel.
- h. Scram curves corresponding to bottom peaked axial shape are used to minimize the initial negative reactivity insertion. The minimum net scram worth with the most reactive rod stuck out and a CEA ejected is used from HFP to HZIP.

APR1400 DCD TIER 2

- i. A top-peaked axial power distribution is set to maximize the energy content in the hottest fuel pellet.
- j. The maximum delay time is 0.55 second (including time to open the reactor trip switchgear) for the VOPT and 0.5 second for CEA holding coil decay time.

15.4.8.3.3 Results

For peak fuel rod temperature and fuel rod enthalpy analysis, the results are summarized in Table 15.4.8-3. For the HZP case, the fuel radial average enthalpy of hot spot is well below the high cladding temperature failure criterion. The prompt fuel enthalpy rise is less than 251.2 kJ/kg (60 cal/g), which is the lowest criterion of the PCMI failure depicted in Figure B-1 of SRP 4.2 and the oxide to wall thickness ratio is less than 0.2 (the maximum cladding oxide thickness is less than 100 μm , Reference 81). The PCMI

k. For TCD effects, the TCD penalty described in Reference 78 was reflected in initializing the fuel centerline and average temperature.

and the HZP case. The non-prompt scenarios that do not exhibit a prompt critical or narrow pulse power excursion, such as the HFP case and the 50 percent power case, would be not concerned with PCMI cladding failure.

In the results, there are no fuel failures due to the high fuel enthalpy and PCMI. From a core coolability perspective, the peak fuel radial average enthalpy and the fuel centerline temperature meet the criterion. The maximum fuel cladding temperature is not high enough to cause fuel rupture or significant rod ballooning. Therefore, there is no loss of core coolable geometry. The interim criteria for reactivity-initiated accident (RIA) described in NUREG-0800 (SRP 4.2 Appendix B) are met.

Delete

~~The centerline temperature is increased by 157.2 °C (315 °F) in case of considering the thermal conductivity degradation (TCD) effect (Reference 78). However, the maximum centerline temperature is below the melting temperature and met the criterion.~~

Following a postulated CEA ejection event, 10.0 percent of the fuel is calculated to undergo DNB. As all fuel pins that undergo DNB are conservatively assumed to suffer clad failure, 10.0 percent of fuel failure is used in the offsite dose evaluation in Subsection 15.4.8.5. The case initiated from HFP initial conditions is expected to result in the greatest potential for offsite dose consequences.

APR1400 DCD TIER 2

Table 15.4.8-1 contains the sequence of events that occur during a CEA ejection for enthalpy case. Figures 15.4.8-1 through 15.4.8-12 show the core power, heat flux, clad and fuel temperatures, and reactivity effects for HFP and HZP cases.

The limiting secondary system releases for the CEAE event are based on a full-power DNBR analysis, with the sequence of events summarized in Table 15.4.8-1. These steam releases are applied to the CEAE radiological consequence assessment presented in Subsection 15.4.8.5. The dynamic behaviors of important NSSS parameters following CEA ejection are presented in Figures 15.4.8-13 and 15.4.8-14.

15.4.8.4 Barrier Performance

15.4.8.4.1 Evaluation Model

The evaluation model is identical to that of core performance as described in Subsection 15.4.8.3.1. The CESEC-III code is used to analyze the RCS pressure transient following CEA ejection.

15.4.8.4.2 Input Parameters and Initial Conditions

The input parameters are similar to the core and system performance analysis described in Subsection 15.4.8.3.2. The initial conditions and NSSS characteristics assumed in this analysis are determined to maximize the primary and secondary system pressures. The input parameters of full-power conditions are used with the difference of the initial pressurizer pressure. The initial pressurizer pressure for this case is 163.46 kg/cm²A (2,325 psia).

15.4.8.4.3 Results

The peak RCS pressure for this event is 177.55 kg/cm²A (2,525.34 psia). The peak RCS pressure includes the pressure difference between the cold leg at the RCP discharge and the surge line. This value is less than the value that results in stresses that exceed the Service Limit C. The peak main steam system pressure reaches 90.17 kg/cm²A (1,282.52 psia). The main steam system pressure is not challenged by this event.

The dynamic behaviors of important NSSS parameters following CEA ejection are presented in Figures 15.4.8-15 through 15.4.8-18.

APR1400 DCD TIER 2**15.4.8.5 Radiological Consequences**

The radiological consequences are performed to determine EAB, LPZ, MCR, and TSC doses due to CEA ejection accident using the AST methodology, the TEDE dose criteria, the guidance in SRP 15.0.3, and the plant-specific bounding design information applicable to the APR1400.

The following two release cases are considered:

- a. Containment leakage release: activity released from the fuel is assumed to be released instantaneously and homogeneously throughout the containment atmosphere and available for release to the environment.
- b. Secondary system release: activity released from the fuel is assumed to be completely dissolved in the primary coolant and available for release to the environment through the secondary system.

15.4.8.5.1 Evaluation Model

Figure 15A-4 in Appendix 15A shows the leakage paths and transport of the activity released to environment, MCR, and TSC during a CEA ejection event.

Containment Leakage Case

For this case, the activity released from the failed fuel is assumed to be instantaneously and homogeneously distributed in the containment following a CEA ejection. This analysis also releases 100 percent of the iodine, alkali metals and noble gases initially present in the RCS. The activity in the containment is subject to be released by the design leak rate specified in the Technical Specifications.

Secondary System Release Case

The offsite power is lost so that the main steam condenser is not available. Following the CEA ejection event, the reactor is shut down and the plant is cooled down by discharging secondary coolant through the two SGs using the combination of one or more ADVs and MSSVs.

The SG tubes are expected to be uncovered during the first 30 minutes of the CEA ejection event because the MSSVs are open to cool down the RCS. During this period, the P-T-S

APR1400 DCD TIER 2

leakage flashing fraction averages 15.0 percent. After 30 minutes, the SG tubes remain covered during the CEA ejection. During the first 30 minutes, the unflashed P-T-S leakage mixes with the SG secondary coolant, and after 30 minutes all of the P-T-S leakage mixes with the SG secondary coolant. The partition coefficients of 100 for iodine and 200 for alkali metal are assumed for the secondary liquid release from the SG.

15.4.8.5.2 Input Parameters and Initial Conditions

The design basis CEA ejection accident is analyzed using a conservative set of assumptions and APR1400 design inputs. The CEA ejection analysis is performed using the guidance in NRC RG 1.183, Appendix H.

Per NRC RG 1.183, Appendix H, Section 1, for the CEA ejection accident, the release from the failed fuel is based on the number of fuel rods to undergo DNB and the assumption that 10 percent of the core inventory of the noble gases and iodines and 12 percent of the core inventory of the alkali metals are in the fuel gap. The expected number of fuel rods in DNB is 10 percent of the core. The failed fuel is modeled with a radial peaking factor of 1.80. Fuel melt is not expected to occur during the CEA ejection. The CEA ejection releases more iodine and noble gases from fuel gap than the other non-LOCA events as specified in NRC RG 1.183, Table 3. The assumed inventory of fission products in the reactor core and available for release to the reactor coolant is based on the maximum power level of 4,062.66 MWt corresponding to current fuel enrichment and fuel burnup, which is 1.02 times the APR1400 licensed thermal power of 3,983 MWt with the cycle burnup of 56.4 GWD/MTU.

The secondary coolant iodine concentration is limited to 3.7×10^3 Bq/g (0.1 μ Ci/g) DE I-131. The RCS DE I-131 isotopic concentration profile is multiplied by a factor of 0.1, representing 10 percent of primary coolant concentration to determine the secondary coolant iodine concentration. The secondary coolant iodine concentration is multiplied by the total coolant mass in both steam generators to calculate the total secondary coolant iodine inventory.

The chemical forms of iodine released from the steam generators to the environment are 97 percent elemental and 3 percent organic. These iodine chemical forms apply to iodine releases from the P-T-S leakage and from the secondary liquid.

Input parameter values used for CEA ejection radiological consequence evaluation are presented in Table 15.4.8-4.

APR1400 DCD TIER 2

A reduction in the amount of radioactive material available for leakage from the containment that is due to natural deposition, containment sprays, recirculating filter systems, or other engineered safety features can be taken into account. This analysis credits aerosol removal by natural deposition. No credit is taken for elemental iodine or aerosol removal by containment sprays.

The primary containment leaks at a Technical Specification peak pressure leak rate of 0.1 percent by volume for the first 24 hours. This leak rate is reduced to 0.05 weight percent after 24 hours.

The P-T-S leakage is at the RCS operational leakage limit of 1.14 L/min (0.3 gpm) through any one SG as specified in the Technical Specification. The P-T-S leak exists until shutdown cooling is in operation and releases from the steam generators have been terminated at 8.0 hours. The primary coolant density used in converting the volumetric P-T-S leak rates to mass leak rates is 1.0 g/cm³ (62.4 lbm/ft³). All noble gas radionuclides released from the primary system via the P-T-S leaks are released to the environment without reduction or mitigation.

The χ/Q values used in the analysis for EAB, LPZ, MCR, and TSC are described in Subsection 2.3.4 and are provided in Tables 2.3-1 through 2.3-12; breathing rates are given in Table 15A-12.

15.4.8.5.3 Results

The radiological consequences due to a CEA ejection are presented in Table 15.4.8-5. The results of the CEA ejection analyses indicate that the EAB and LPZ doses are within their allowable dose limit, which is 25 percent of the 10 CFR 50.34(a)(1) value, as specified in SRP 15.0.3. The MCR and TSC doses are also within the dose limit in GDC 19.

15.4.8.6 Conclusions

For the spectrum of CEA ejection evaluated, none of the power excursions causes the fuel temperatures to reach the limiting fuel melting temperature or the fuel enthalpy limits. For the events that exceeded the DNBR limit, the number of fuel failures was less than the value allowed for the radiological release limit. The peak RCS pressure remains below 110 percent of the RCS design pressure. The stresses due to the primary pressure response during the transients do not exceed Service Limit C as defined in the ASME Code.

APR1400 DCD TIER 2

The doses at the EAB, LPZ, MCR, and TSC are within their allowable dose criteria.

15.4.9 Combined License Information

No COL information is required with regard to Section 15.4.

APR1400 DCD TIER 2

Table 15.4.8-1 (1 of 3)

Sequence of Events for the CEA Ejection

| Power | Time (sec) | Event | Setpoint or Value |
|-------|------------|---|--|
| HFP | 0.00 | Mechanical failure | Maximum clad surface temperature in the hot spot, °C (°F) |
| | 0.03 | Core power reaches variable overpower reactor trip analysis setpoint, % of design power | 127.5 |
| | 0.05 | CEA fully ejected | - |
| | 0.07 | Maximum core power, % of design power | 156.3 |
| | 1.08 | CEAs begin to drop into core | 526.8 (980.3) |
| | 3.30 | Maximum radial average fuel enthalpy in the hot spot, kJ/kg (cal/gm) | 522.1 (124.7) |
| | 3.43 | Maximum clad surface temperature in the hot spot, °C (°F) | 567.2 (1,053.0) |
| 50% | 3.67 | Maximum fuel centerline temperature in the hot spot, °C (°F) | 2,490.2 (4,514.3) |
| | 0.00 | Mechanical failure | Maximum radial average fuel enthalpy in the hot spot, kJ/kg (cal/gm) |
| | 0.03 | Core power reaches variable overpower reactor trip analysis setpoint, % of design power | 75.0 |
| | 0.05 | CEA fully ejected | Maximum radial average fuel enthalpy in the hot spot, kJ/kg (cal/gm) |
| | 0.08 | Maximum core power, % of design power | 515.4 (123.1) |
| | 1.08 | CEAs begin to drop into core | 569.2 (1,056.5) |
| | 3.20 | Maximum clad surface temperature in the hot spot, °C (°F) | 524.1 (975.3) |
| | 3.31 | Maximum radial average fuel enthalpy in the hot spot, kJ/kg (cal/gm) | 504.1 (120.4) |
| | 3.72 | Maximum fuel centerline temperature in the hot spot, °C (°F) | 2,370.9 (4,299.6) |
| | | Maximum clad surface temperature in the hot spot, °C (°F) | 2,423.6 (4,394.5) |

APR1400 DCD TIER 2

Maximum clad surface temperature in the hot spot,
°C (°F)

Table 15.4.8-1 (2 of 3)

| Power | Time (sec) | Event | Maximum radial average fuel enthalpy in the hot spot, kJ/kg (cal/gm) | |
|-------|------------|---|---|-------------------|
| 20% | 0.00 | Mechanical failure of CEDM | | |
| | 0.04 | Core power reaches variable overpower reactor trip analysis setpoint, % of design power | 45.0 | |
| | 0.05 | CEA fully ejected | - | |
| | 0.10 | Maximum core power, % of design power | 140.3 | |
| | 2.32 | 1.09 CEAs begin to drop into core | - | 348.2 (658.7) |
| | 3.26 | 3.30 Maximum radial average fuel enthalpy in the hot spot, kJ/kg (cal/gm) | 473.5 (113.1) | 500.4 (119.6) |
| | 3.87 | 3.62 Maximum clad surface temperature in the hot spot, °C (°F) | 586.7 (1,088.1) | 2,388.8 (4,331.8) |
| | | 3.67 Maximum fuel centerline temperature in the hot spot, °C (°F) | 2,331.3 (4,228.4) | |
| HZP | 0.00 | Mechanical failure of CEDM causes CEA to eject | - | |
| | 0.21 | Core power reaches variable overpower reactor trip analysis setpoint, % of design power | 25.0 | |
| | 0.05 | CEA fully ejected | - | |
| | 0.32 | Maximum core power, % of design power | 141.3 | |
| | 2.61 | 1.26 CEAs begin to drop into core | - | (656.4) |
| | 3.09 | 2.48 Maximum clad surface temperature in the hot spot, °C (°F) | 346.9 (656.5) | 319.1 (76.2) |
| | 3.74 | 3.04 Maximum radial average fuel enthalpy in the hot spot, kJ/kg (cal/gm) | 314.8 (75.2) | 1,526.5 (2,779.7) |
| | | 3.67 Maximum fuel centerline temperature in the hot spot, °C (°F) | 1,501.5 (2,734.7) | |

APR1400 DCD TIER 2

Table 15.4.8-1 (3 of 3)

| Time (sec) | Event (System Response at HFP) | Setpoint or Value |
|------------|---|-------------------|
| 0.00 | Mechanical failure of CEDM causes CEA to eject | - |
| 0.04 | Core power reaches variable overpower reactor trip analysis setpoint, % of design power | 127.5 |
| 0.05 | CEA fully ejected | - |
| 0.16 | Maximum core power, % of design power | 151.7 |
| 0.49 | Reactor trip signal | - |
| 0.59 | Reactor trip breakers open | - |
| 1.09 | CEAs begin to drop into core | - |
| 3.10 | Maximum RCS pressure, kg/cm ² A (psia) | 177.5 (2,524.7) |
| 3.59 | Turbine trip/generator trip/loss of offsite power | - |
| 7.20 | Main steam safety valves open, kg/cm ² A (psia) | 86.9 (1,235.7) |
| 11.50 | Maximum steam generator pressure, kg/cm ² A (psia) | 90.1 (1,281.9) |
| 1,800.00 | Operator begins plant cooldown | - |

APR1400 DCD TIER 2

Table 15.4.8-2

Assumptions and Initial Conditions for the CEA Ejection Analysis

| Parameter | Cases | | | |
|---|----------------|----------------|----------------|----------------|
| | HZP | 20% | 50% | HFP |
| Core power level, MWt | 1.00 | 796.60 | 1991.50 | 4,062.66 |
| Delayed neutron fraction, β | 0.00412 | 0.00412 | 0.00412 | 0.00412 |
| Moderator temperature coefficient, $10^{-4} \Delta\rho / ^\circ\text{C}$ ($10^{-4} \Delta\rho / ^\circ\text{F}$) | 0.90 (0.50) | 0.72 (0.40) | 0.45 (0.25) | 0.00 (0.00) |
| Doppler temperature coefficient, $\Delta\rho / \sqrt{\text{K}}$ | -0.00130 | -0.00130 | -0.00130 | -0.00130 |
| Ejected CEA worth, $10^{-2} \Delta\rho$ | 0.4469 | 0.3711 | 0.2578 | 0.1459 |
| Post-ejected 3-d power peaking factor | 11.49 | 10.79 | 6.49 | 4.32 |
| Ratio of the 3-d post-ejected to pre-ejected power peaking factor | 3.93 | 3.90 | 3.49 | 3.17 |
| Total CEA worth available for insertion on reactor trip, $10^{-2} \Delta\rho$ | -5.0 | -5.0 | -5.0 | -5.0 |
| Postulated CEA Ejection time, sec | 0.05 | 0.05 | 0.05 | 0.05 |
| Core inlet coolant temperature, $^\circ\text{C}$ ($^\circ\text{F}$) | 295 (563) | 295 (563) | 295 (563) | 295 (563) |
| Core mass flow rate, 10^6 kg/hr (10^6 lbm/hr) | 69.64 (153.52) | 69.64 (153.52) | 69.64 (153.52) | 69.64 (153.52) |
| Pressurizer pressure, $\text{kg/cm}^2\text{A}$ (psia) | 152.9 (2,175) | 152.9 (2,175) | 152.9 (2,175) | 152.9 (2,175) |

APR1400 I & II

Table

Results of the CEA Ejection Analysis

| Parameter | Power | | | |
|--|--|--|--|--|
| | HZP | 20% | 50% | HFP |
| Maximum radial average fuel enthalpy at hot spot, kJ/kg (cal/gm) | 314.8 (75.2) | 473.5 (113.1) | 504.1 (120.4) | 522.1 (124.7) |
| Maximum fuel centerline temperature, °C (°F) | 1,501.5 (2,734.7) | 2,331.3 (4,228.4) | 2,370.9 (4,299.6) | 2,490.2 (4,514.3) |
| Maximum prompt enthalpy rise, ⁽¹⁾ kJ/kg (cal/gm) | 90.9 (21.7) | 138.6 (33.1) | 160.8 (38.4) | 118.9 (28.4) |
| Maximum cladding surface temperature, °C (°F) | 347.0 (656.6) | 586.7 (1,088.1) | 569.2 (1,056.5) | 567.2 (1,053.0) |

(1) Maximum energy deposition during the prompt power pulse width. For HFP and 50 percent power case, the prompt enthalpy rise is the value at 1.0 second.

346.9
(656.4)

348.2
(658.7)

524.1
(975.3)

526.8
(980.3)

139.0
(33.2)

162.0
(38.7)

122.3
(29.2)

APR1400 DCD TIER 2

Table 15.4.8-4 (1 of 3)

Parameters Used in Evaluating the Radiological Consequences of the CEA Ejection

| Parameter | Value |
|--|--|
| Source Terms | |
| Reactor Core Power Level | 4,062.66 MWt |
| Percent of Fuel Assumed to Undergo DNB | 10 % |
| Initial RCS Iodine Specific Activity | 3.7×10^4 Bq/g (1.0 μ Ci/g) DE I-131 |
| Initial RCS Noble Gases Specific Activity | 2.15×10^7 Bq/g (580 μ Ci/g) DE Xe-133 |
| Initial RCS Alkali Metal Specific Activity | RCS concentrations with 1% fuel defect |
| Initial Secondary Liquid Iodine Specific Activity | 3.7×10^3 Bq/g (0.1 μ Ci/g) DE I-131 |
| Radial Peaking Factor | 1.80 |
| RCS Initial Mass | 267,620 kg (590,000 lbm) |
| Containment Leakage Transport Model | |
| Containment Net Free Volume | 8.86×10^4 m ³ (3.13×10^6 ft ³) |
| Reactor Coolant Mass Released to Containment | 2.68×10^5 kg (5.90×10^5 lbm) |
| Credit for Radioactive Decay during Hold up in Containment In Transit to Dose Points | Applicable Not Applicable |
| Iodine Chemical Form Aerosol (CsI) Elemental Organic | 95.0 % 4.85 % 0.15 % |
| Containment Aerosol Natural Deposition Removal | Powers model with a 10-percentile probability |
| Containment Leak Rate | 0.1 %/day (0 ~ 24 hr) 0.05 %/day (24 ~ 720 hr) |

APR1400 DCD TIER 2

Table 15.4.8-4 (2 of 3)

| Parameter | Value |
|---|---|
| Secondary System Release Transport Model | |
| Primary-To-Secondary Leak Rate through SGs | 2.27 L/min (0.6 gpm) through all SGs 1.14 L/min (0.3 gpm) through any one SG |
| Steam Generator Liquid Mass | 104,326 kg (230,000 lbm) |
| Primary-To-Secondary Leak Duration | 8 hr |
| Steam Mass Released from Both Intact SGs to Environment | |
| 0 ~ 0.5 hr | 118,660 kg (261,600 lbm) |
| 0.5 ~ 2 hr | 650,737 kg (1,434,630 lbm) |
| 2 ~ 8 hr | 624,538 kg (1,376,870 lbm) |
| Primary-To-Secondary Leak Flashing Fraction | 15.0 % average for 1,800 sec after onset of accident |
| SG Liquid Iodine Partition Coefficient | 100 |
| SG Liquid Alkali Metal Partition Coefficient | 200 |
| Chemical Form of Iodine Released from SG | |
| Elemental | 97 % |
| Organic Iodine | 3 % |

APR1400 DCD TIER 2

Table 15.4.8-4 (3 of 3)

| Parameter | Value |
|---|---|
| MCR and TSC Model Parameters | |
| Envelope Volume | 5,663 m ³ (200,000 ft ³) |
| Normal Ventilation Flow Rate (unfiltered) | 105 m ³ /min (3,700 cfm) |
| Emergency Ventilation Makeup Rate (filtered) | 105 m ³ /min (3,700 cfm) |
| Emergency Ventilation Recirculation Flow Rate (filtered) | 122 m ³ /min (4,300 cfm) |
| Emergency HVAC Delay Time | 5 min |
| Emergency Ventilation Charcoal Filter Efficiency (elemental and organic iodine removal) | 99 % |
| Emergency Ventilation HEPA Filter Efficiency (particulate removal) | 99 % |
| Unfiltered Inleakage | 2.83 m ³ /min (100 cfm) |
| Occupancy Factors | |
| 0 ~ 24 hr | 100 % |
| 24 ~ 96 hr | 60 % |
| 96 ~ 720 hr | 40 % |
| Onsite χ/Q_s | See Tables 2.3.2 ~ 2.3.12 |
| Offsite Model Parameters | |
| χ/Q_s | See Table 2.3-1 |
| Breathing Rate | See Table 15A-12 |
| Dose Conversion Factors | See Table 15A-11 |

APR1400 DCD TIER 2

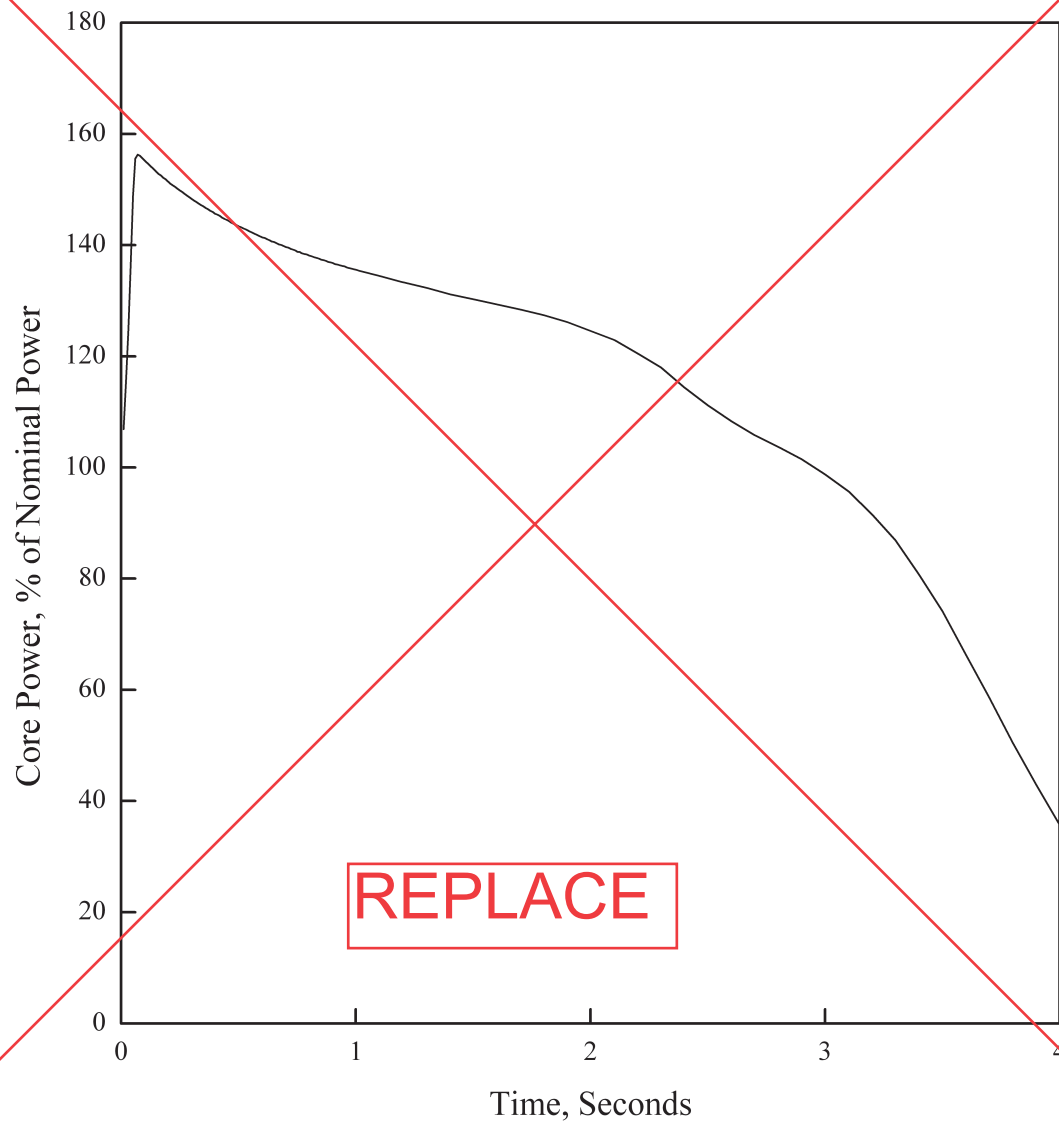
Table 15.4.8-5

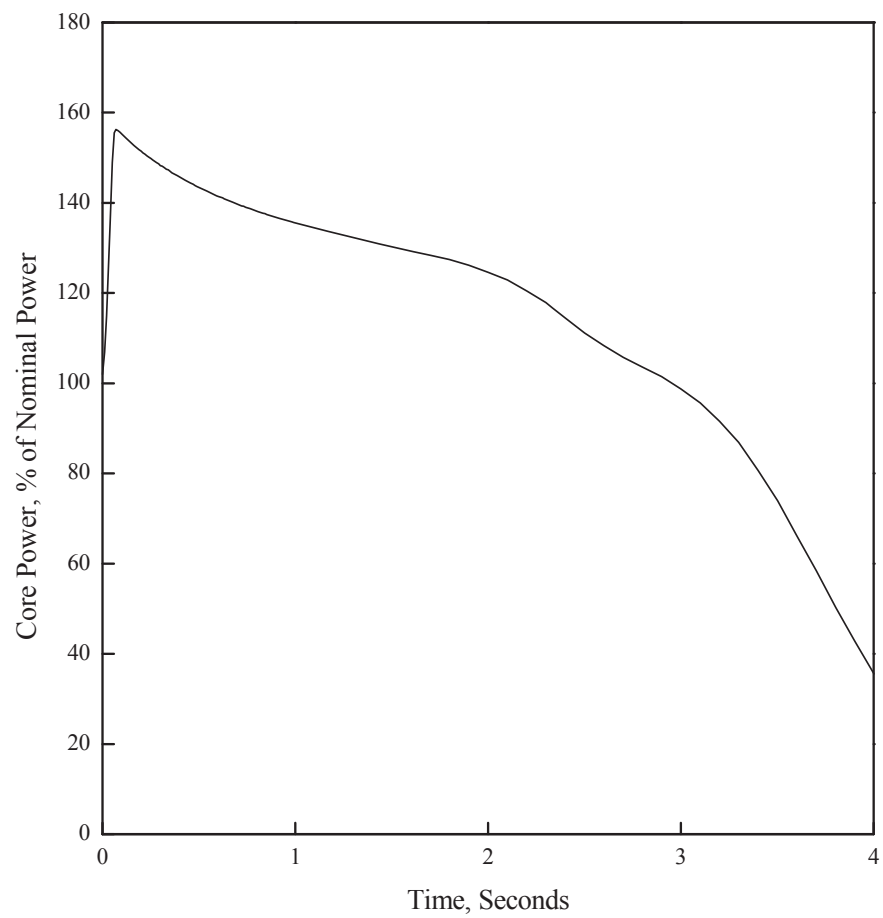
Radiological Consequences of the CEA EjectionContainment Leakage Case

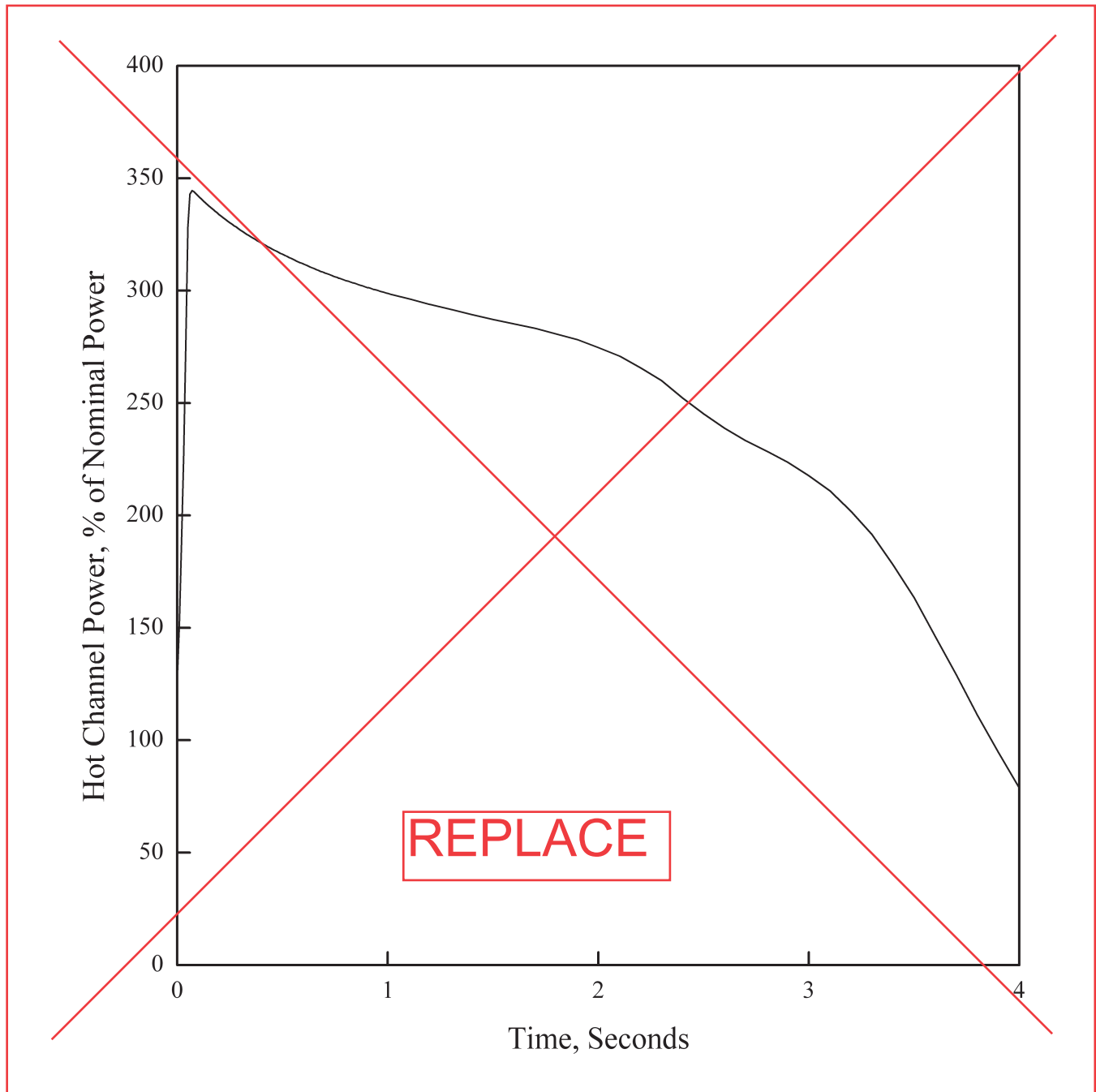
| Post-CEA Ejection Activity Release Path | TEDE Dose (mSv) | | |
|--|-----------------|----------|----------|
| | MCR and TSC | EAB | LPZ |
| Containment Leakage | 1.62E+01 | 5.86E+01 | 5.55E+01 |
| External Cloud | 6.22E+00 | 0.00E+00 | 0.00E+00 |
| Emergency Ventilation Filter Shine | 1.29E+01 | 0.00E+00 | 0.00E+00 |
| Total | 3.53E+01 | 5.86E+01 | 5.55E+01 |
| Allowable TEDE Limit | 5.00E+01 | 6.30E+01 | 6.30E+01 |

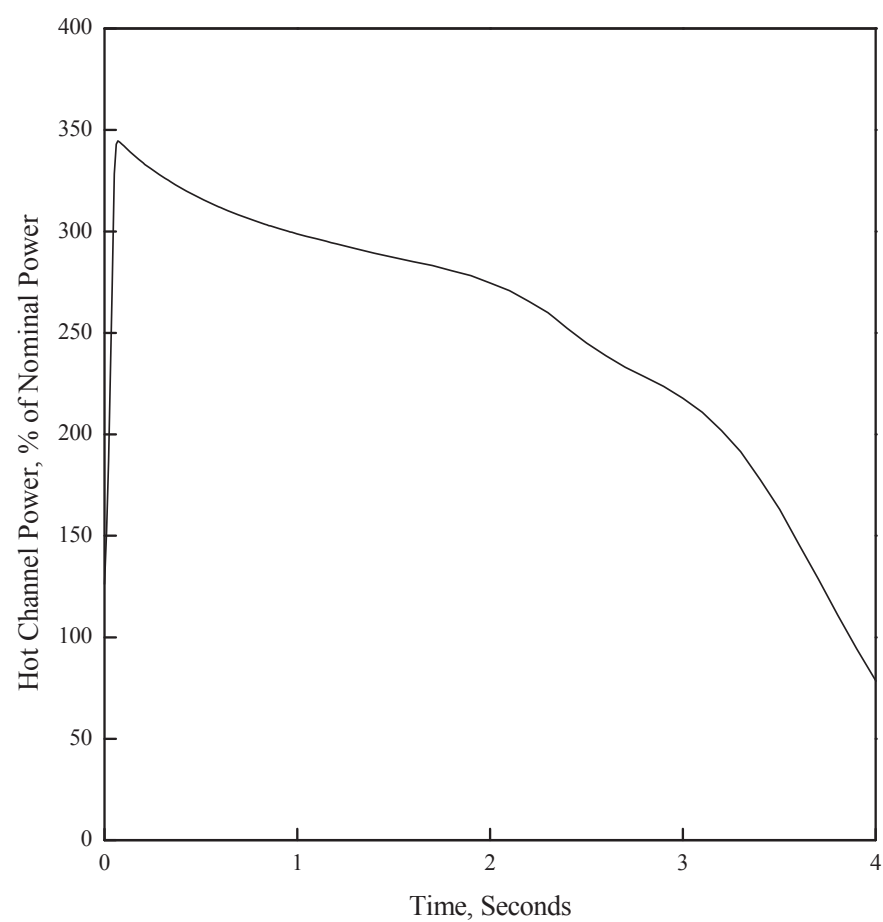
Steam System Release Case

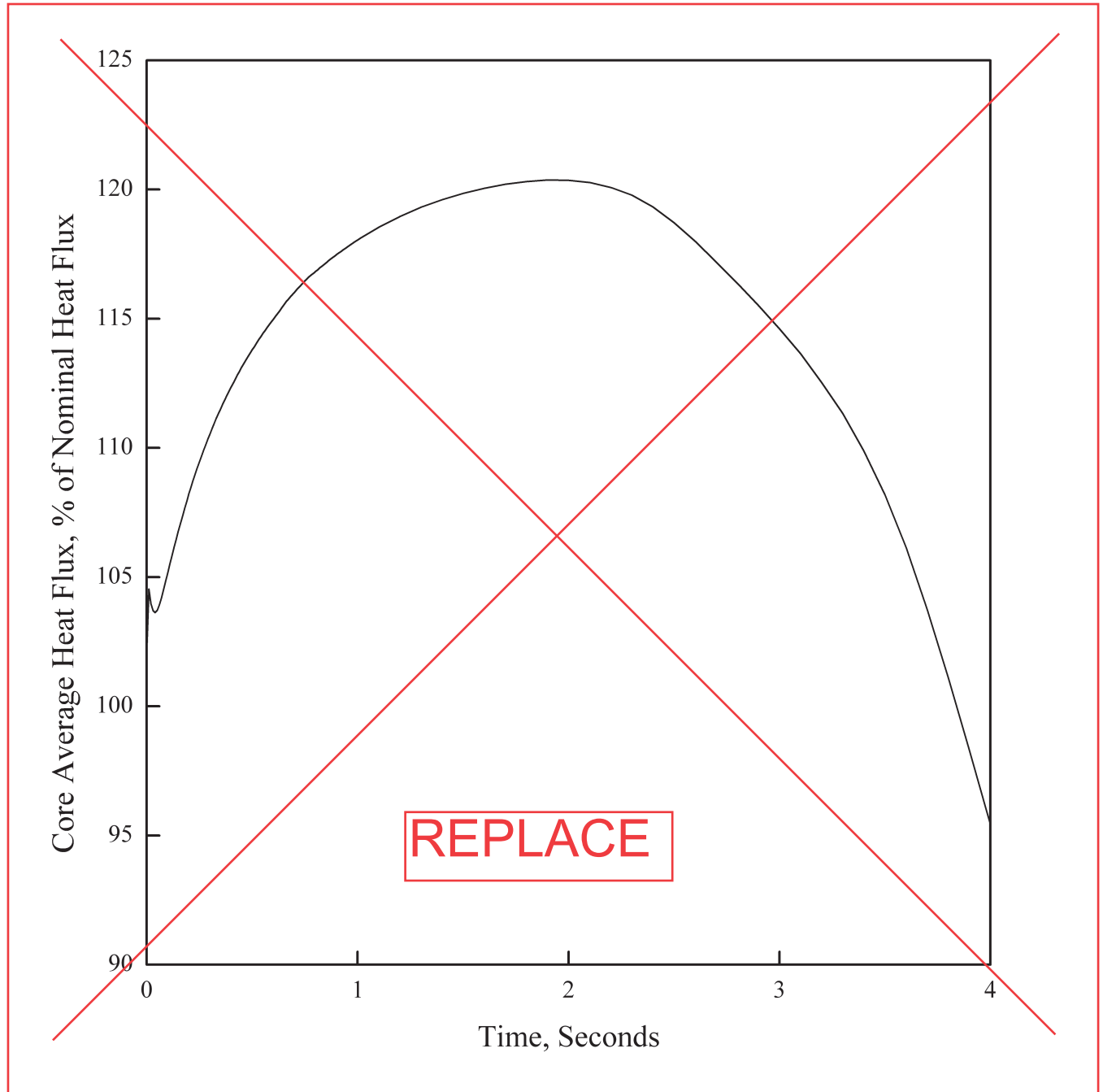
| Post-CEA Ejection Activity Release Path | TEDE Dose (mSv) | | |
|--|-----------------|----------|----------|
| | MCR and TSC | EAB | LPZ |
| P-T-S Iodine Release | 2.60E+00 | 1.46E+01 | 1.01E+01 |
| P-T-S Noble Gas Release | 6.55E+00 | 2.04E+01 | 8.79E+00 |
| P-T-S Alkali Metal Release | 8.32E-01 | 4.92E+00 | 2.90E+00 |
| Secondary Liquid Iodine Release | 1.83E-02 | 1.22E-01 | 4.65E-02 |
| External Cloud | 6.22E+00 | 0.00E+00 | 0.00E+00 |
| Emergency Ventilation Filter Shine | 1.29E+01 | 0.00E+00 | 0.00E+00 |
| Total | 2.91E+01 | 4.00E+01 | 2.18E+01 |
| Allowable TEDE Limit | 5.00E+01 | 6.30E+01 | 6.30E+01 |

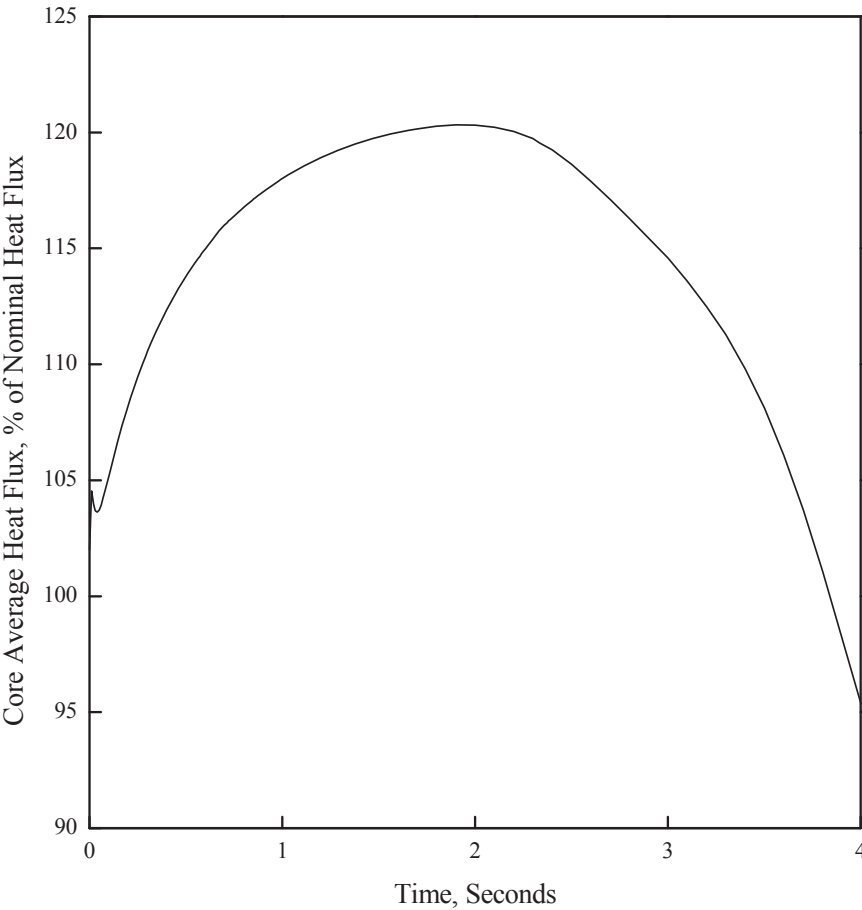
APR1400 DCD TIER 2**Figure 15.4.8-1 CEA Ejection: Core Power vs. Time (HFP)**

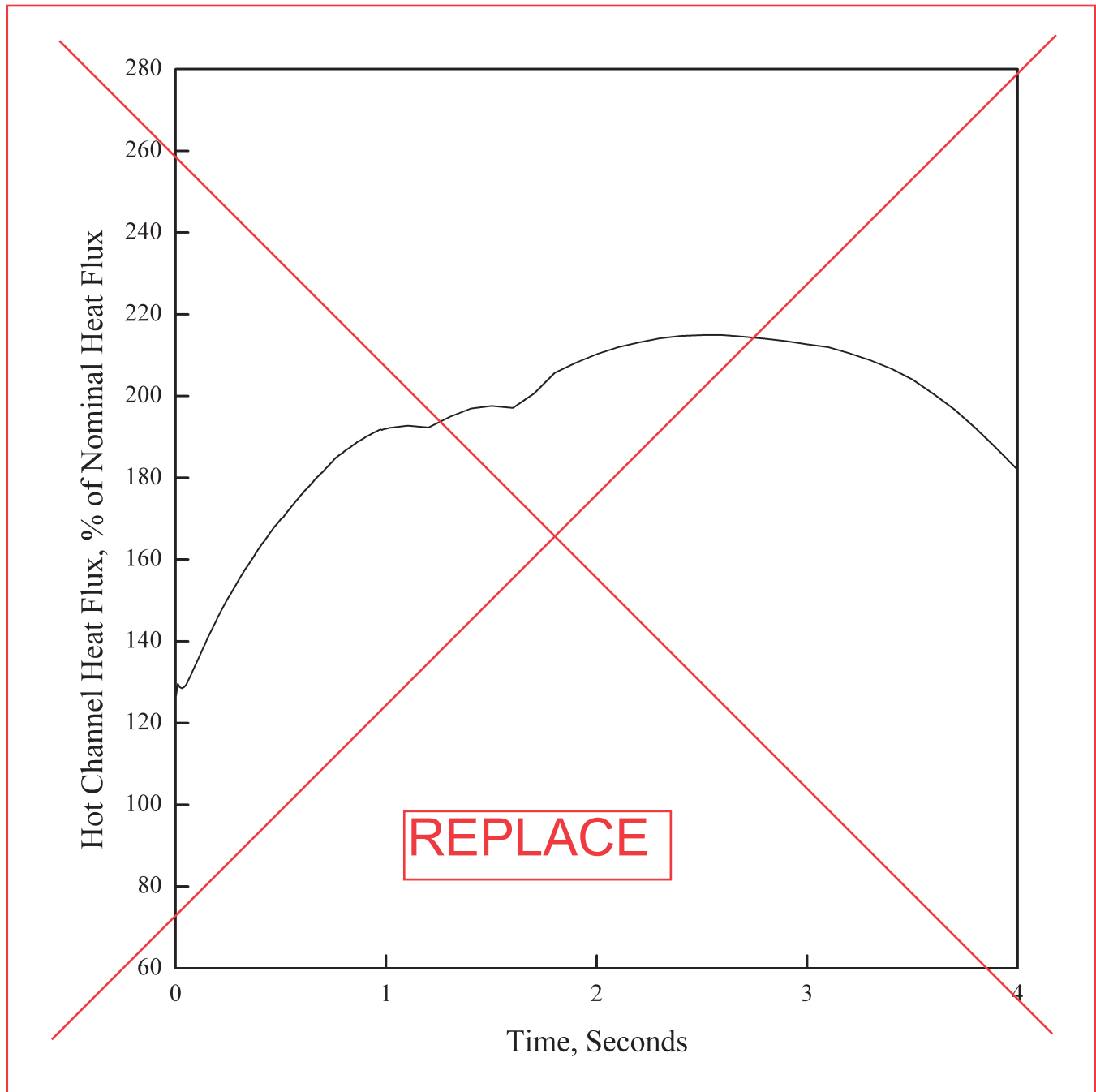


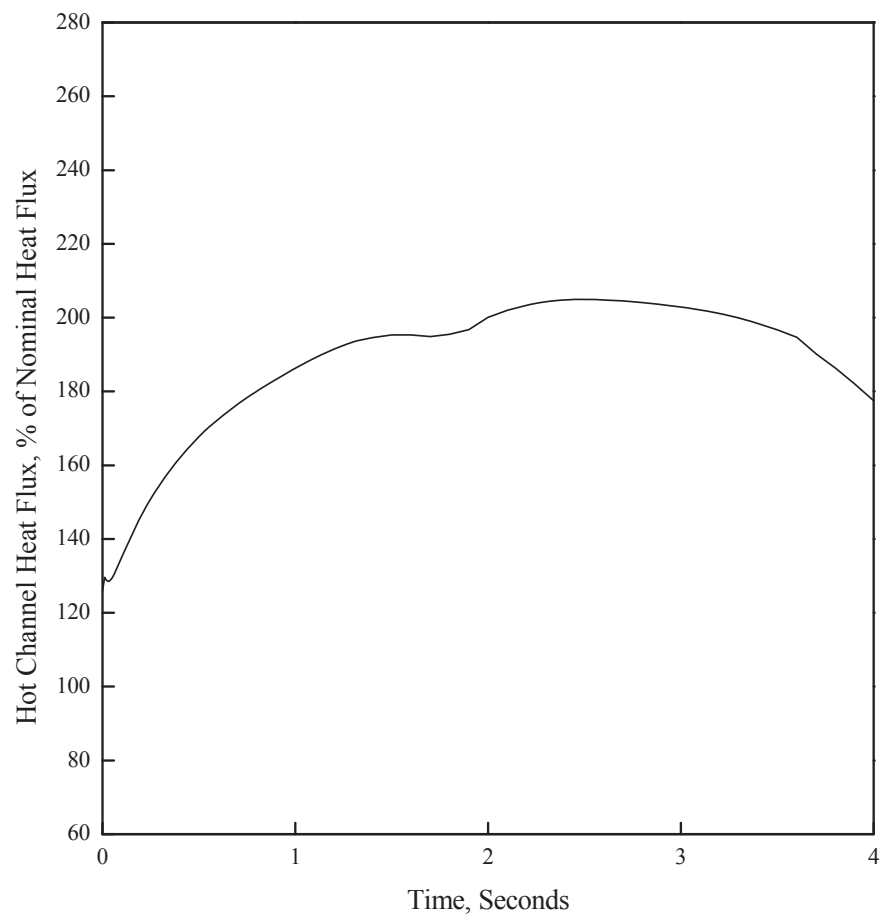
APR1400 DCD TIER 2**Figure 15.4.8-2 CEA Ejection: Hot Channel Power vs. Time (HFP)**



APR1400 DCD TIER 2**Figure 15.4.8-3 CEA Ejection: Core Average Heat Flux vs. Time (HFP)**



APR1400 DCD TIER 2**Figure 15.4.8-4 CEA Ejection: Hot Channel Heat Flux vs. Time (HFP)**



APR1400 DCD TIER 2

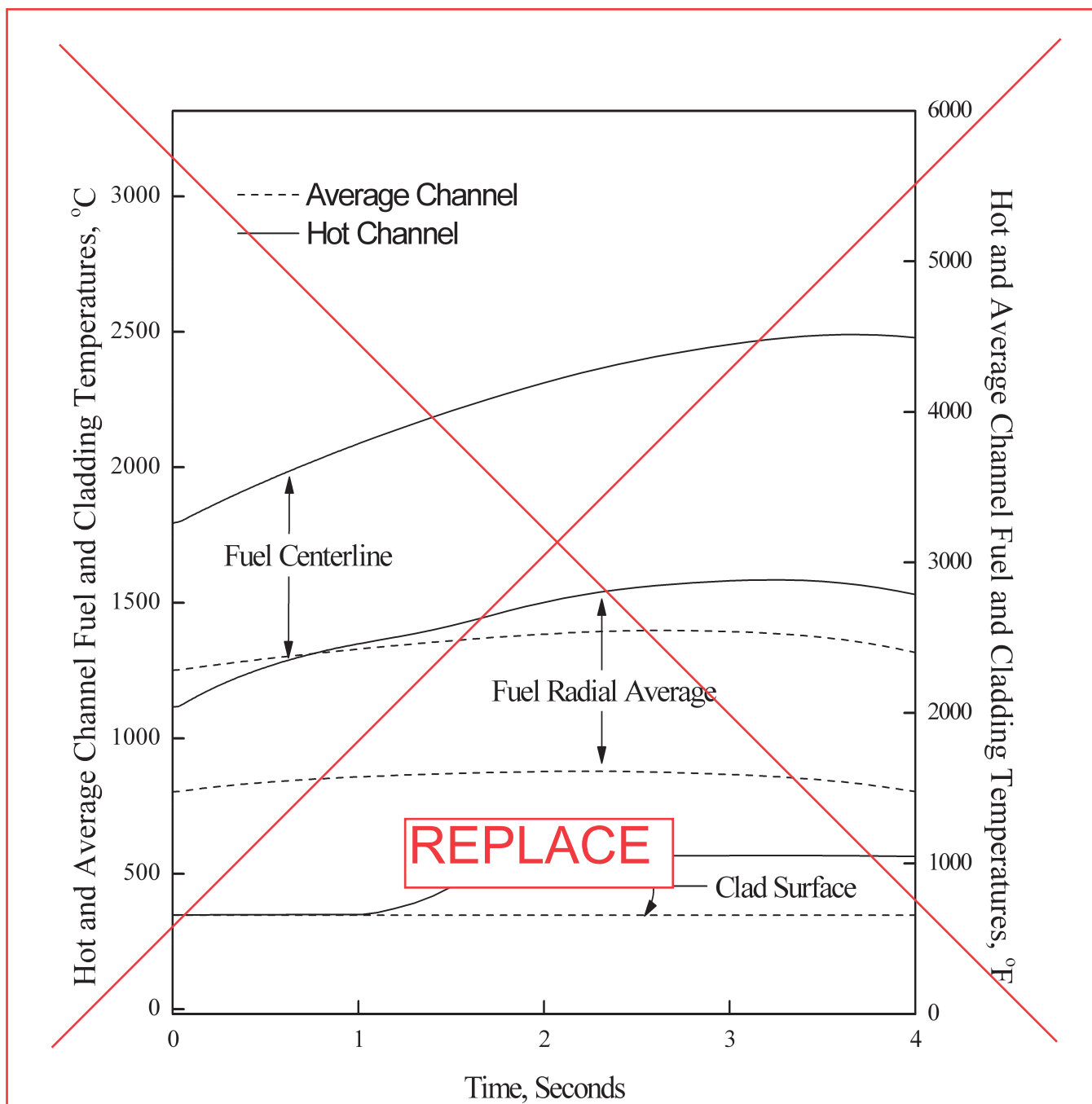


Figure 15.4.8-5 CEA Ejection: Hot and Average Channel Fuel and Cladding Temperatures vs. Time (HFP)

APR1400 DCD TIER 2

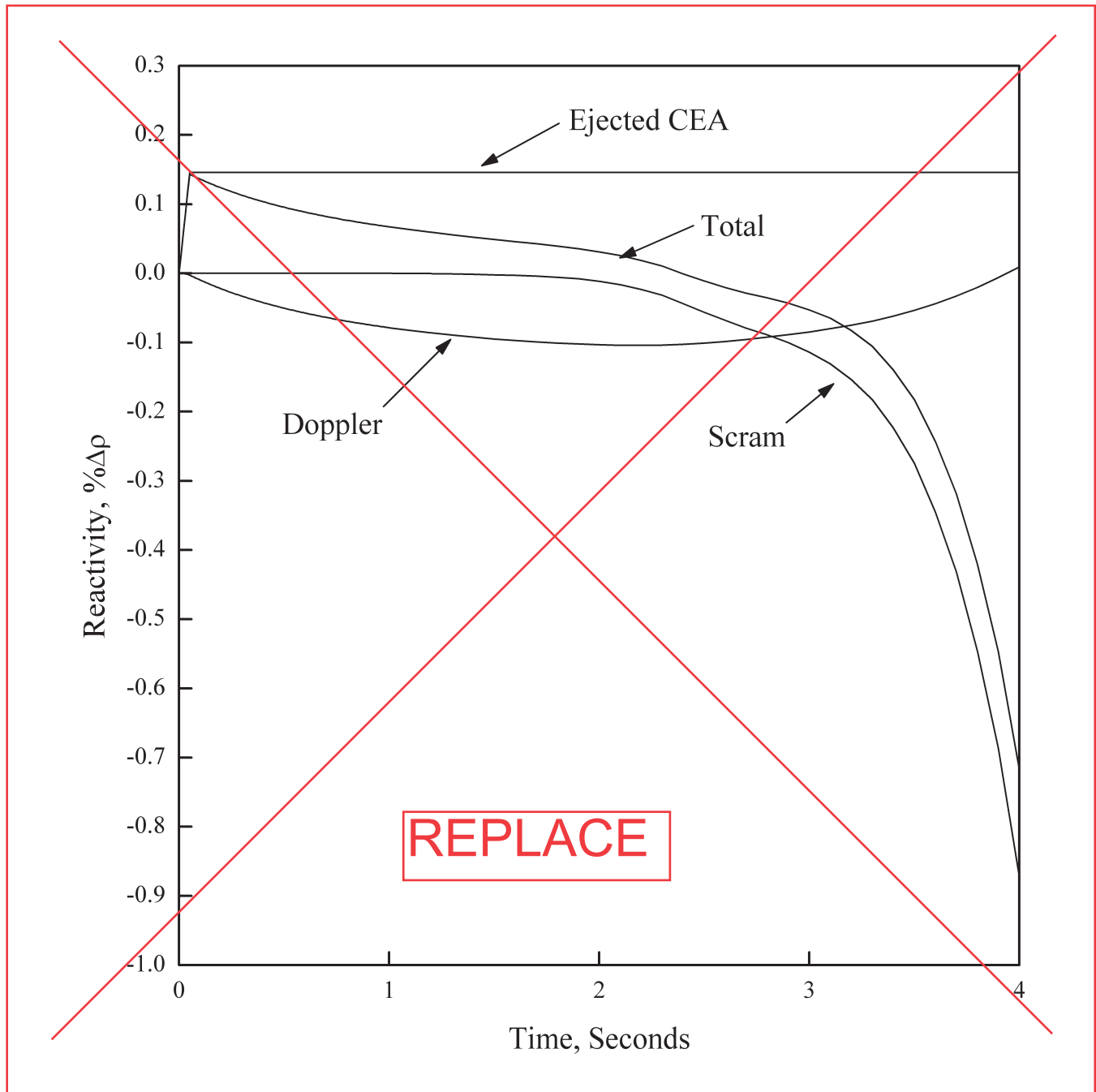
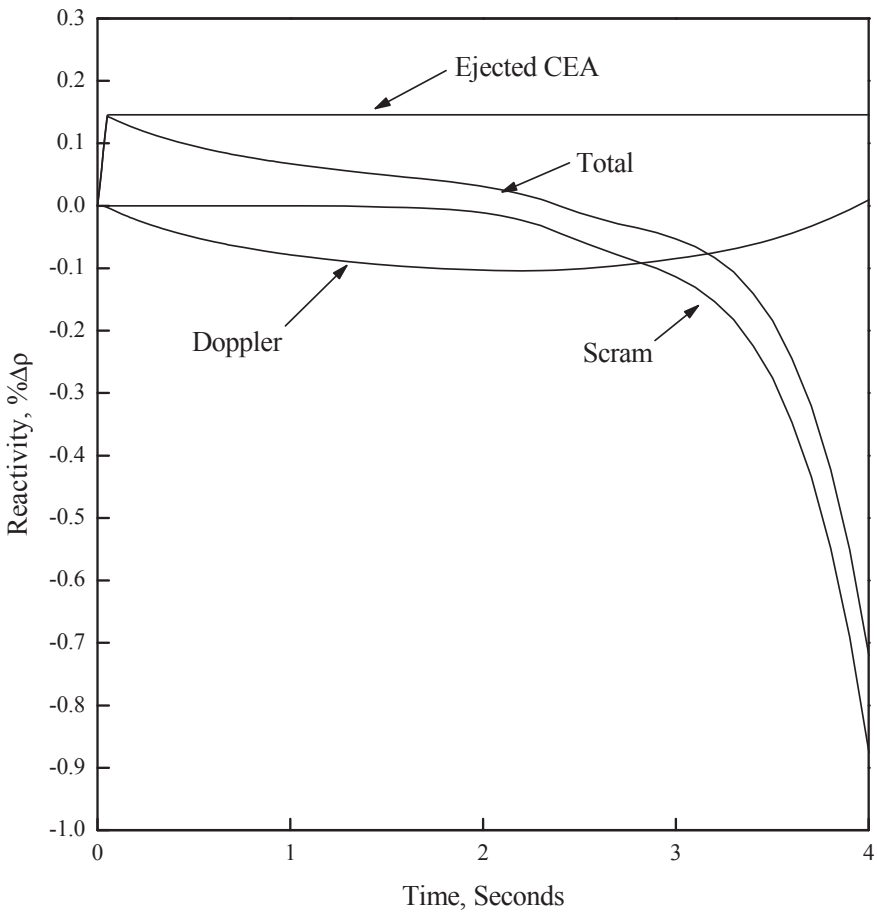
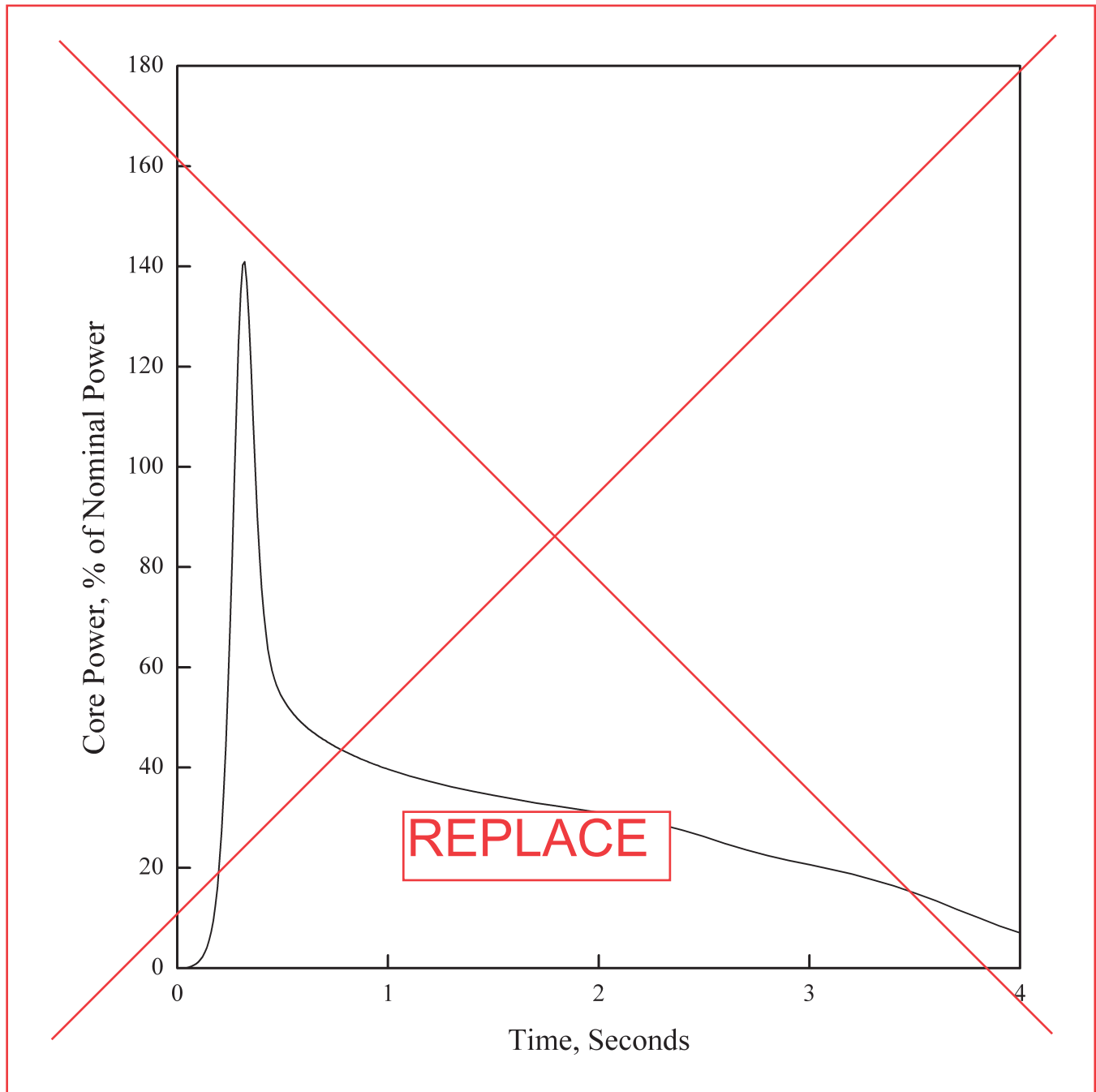
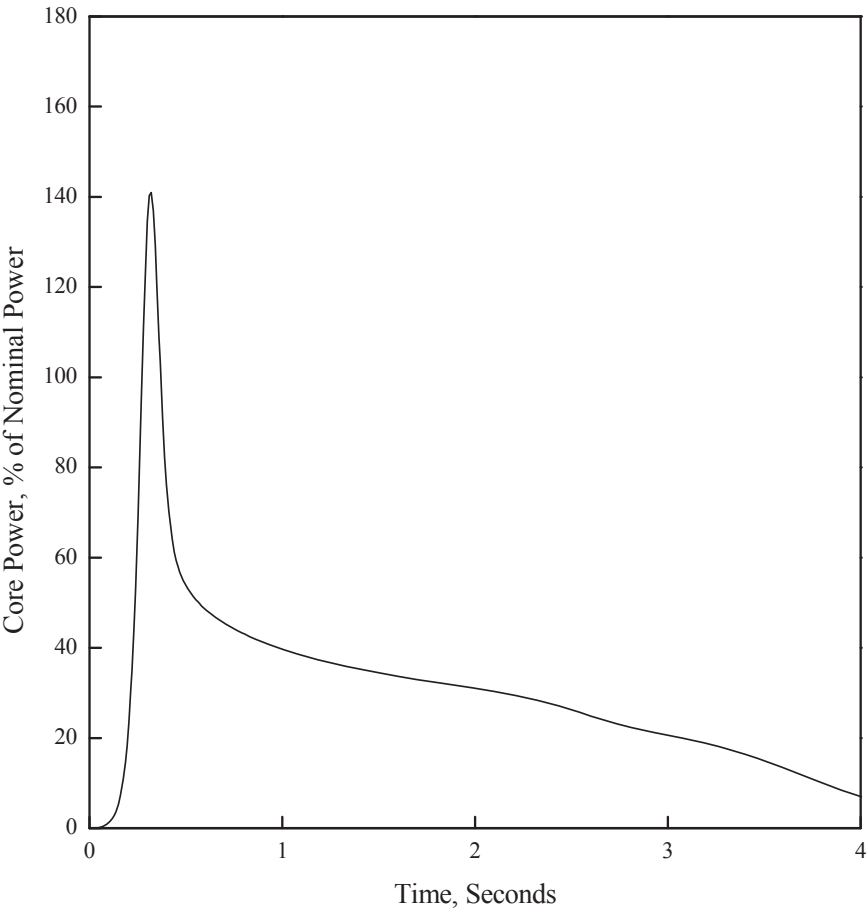
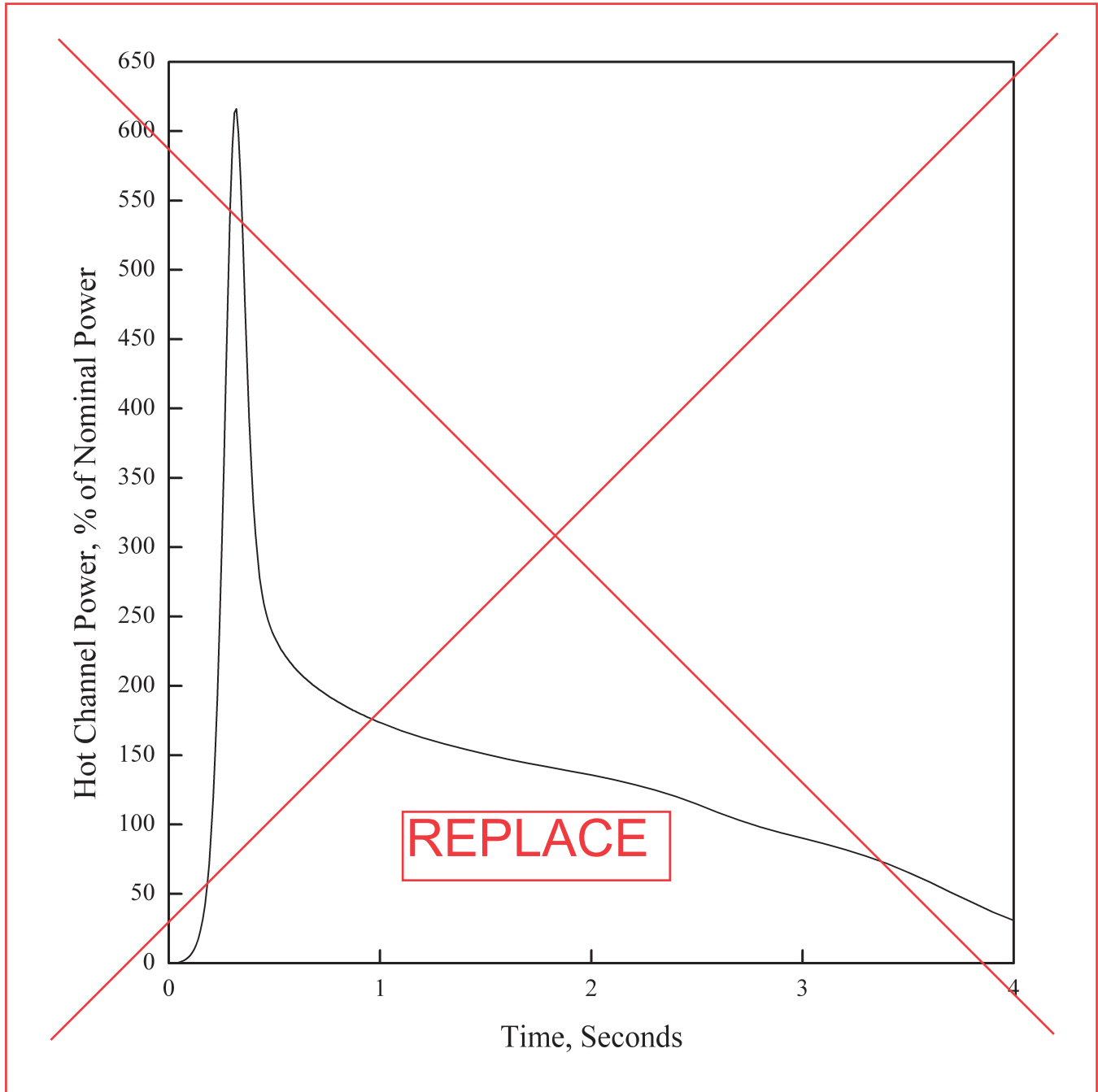


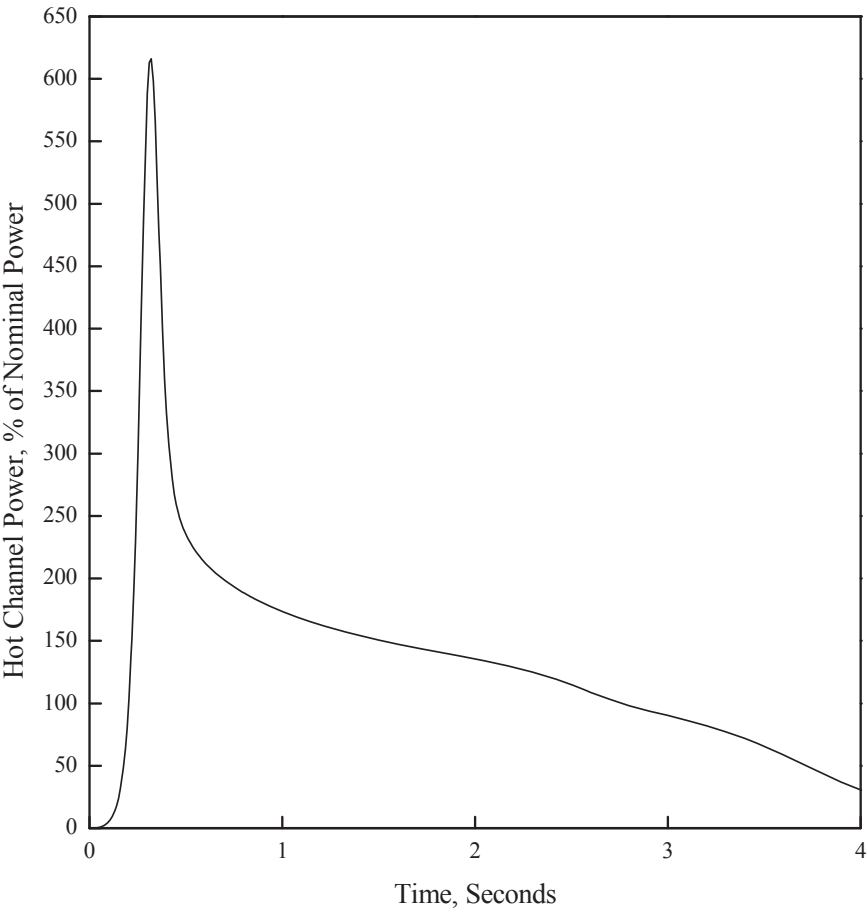
Figure 15.4.8-6 CEA Ejection: Reactivity vs. Time (HFP)

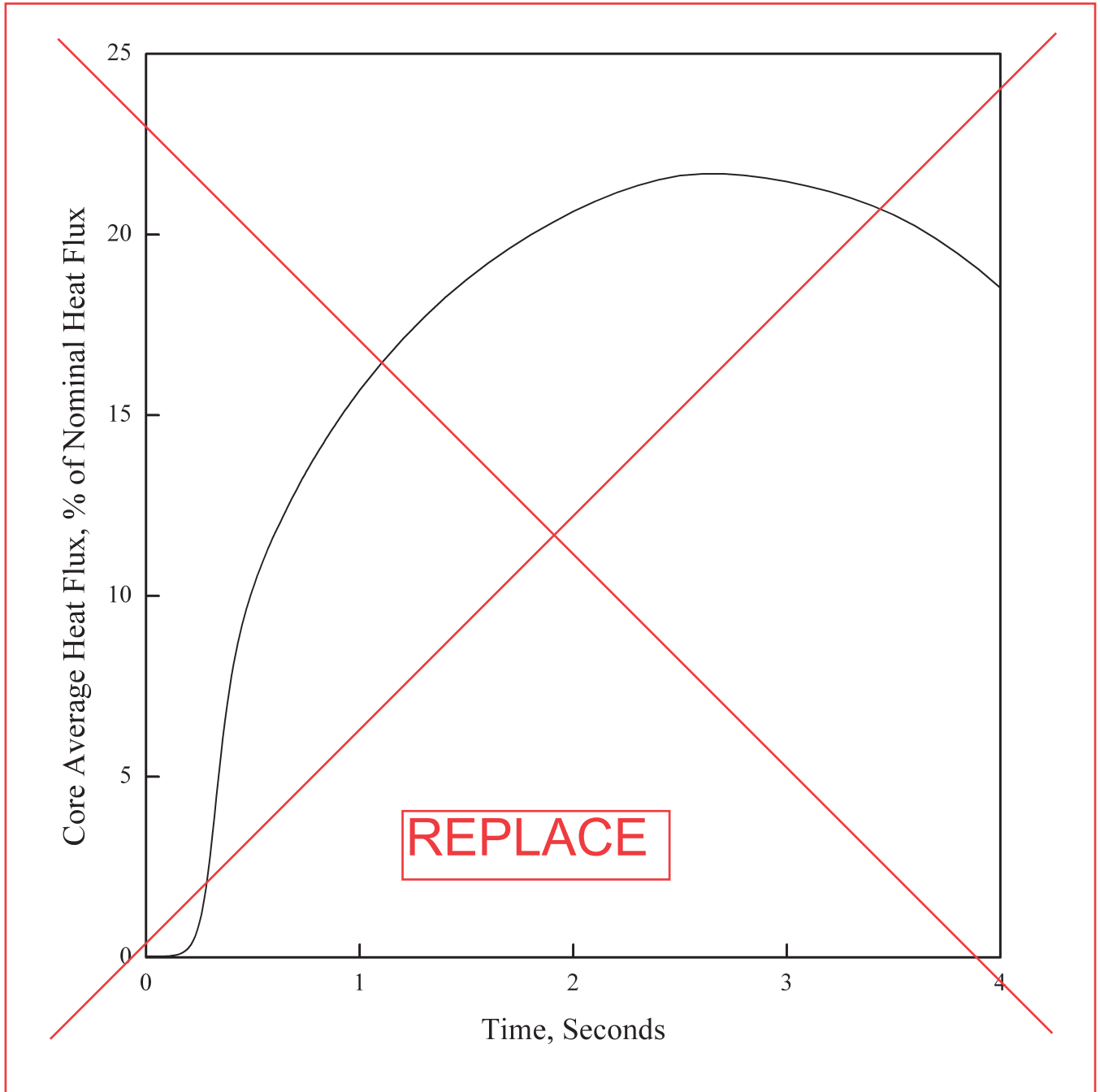


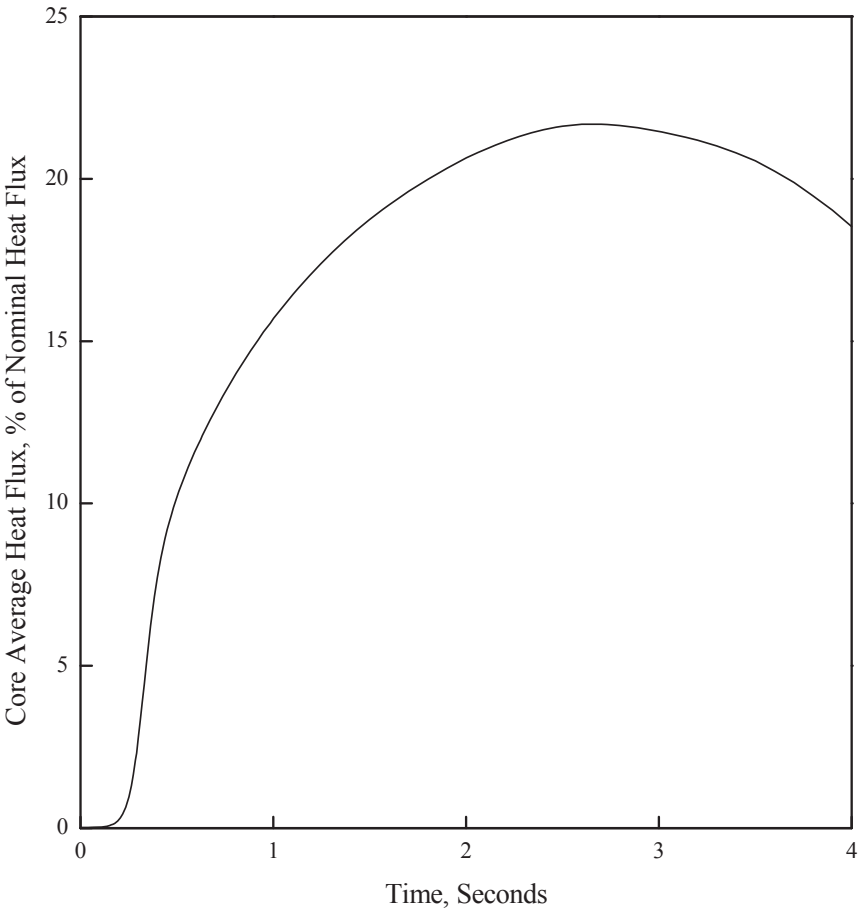
APR1400 DCD TIER 2**Figure 15.4.8-7 CEA Ejection: Core Power vs. Time (HYP)**

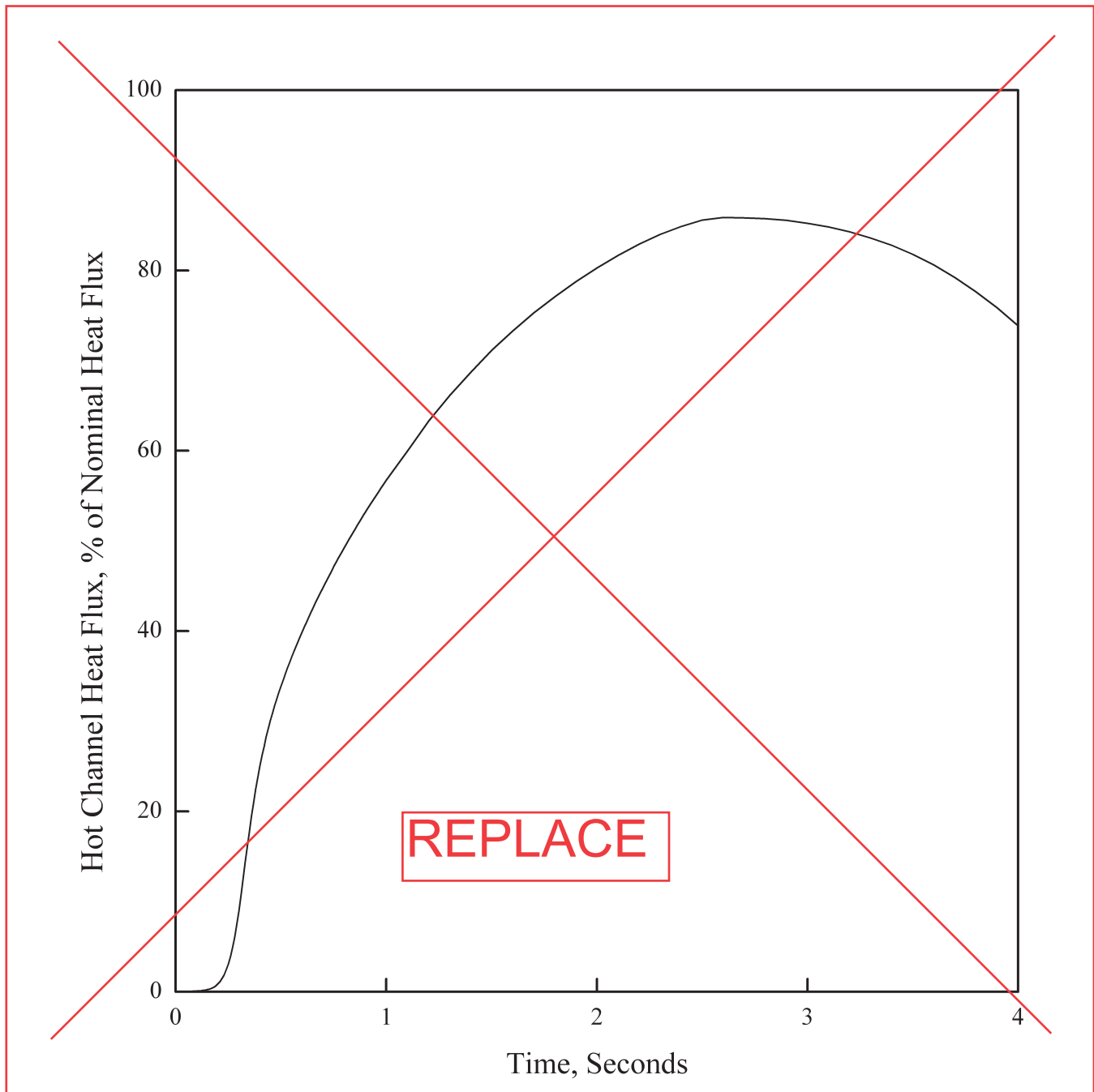


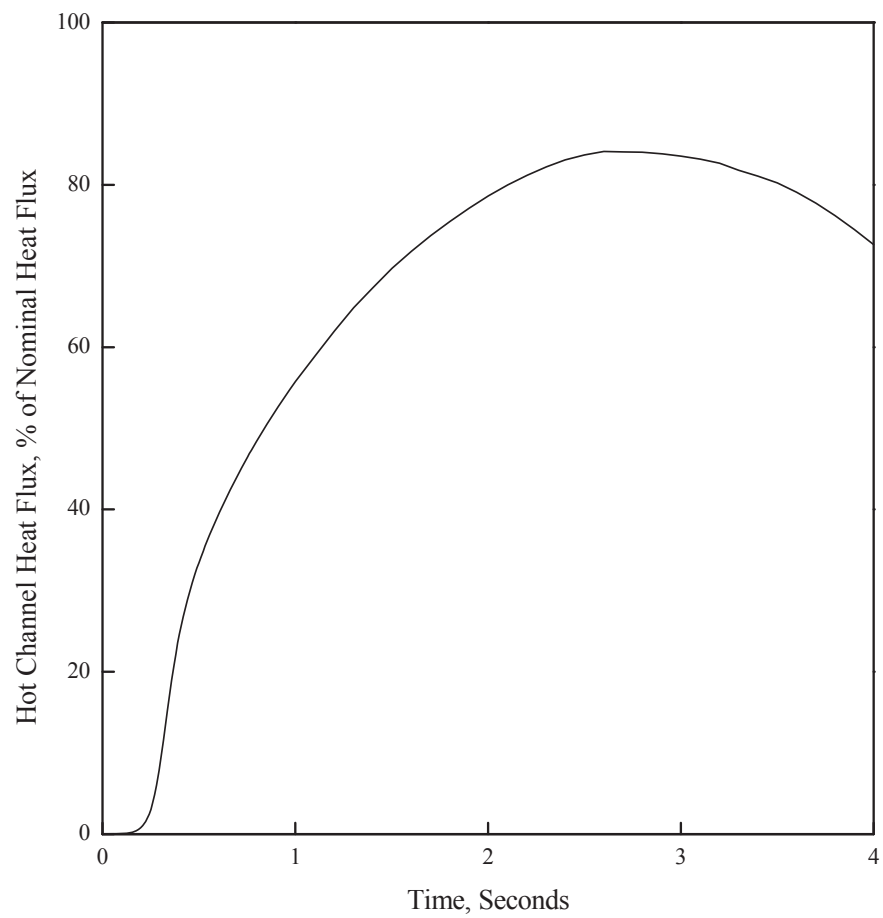
APR1400 DCD TIER 2**Figure 15.4.8-8 CEA Ejection: Hot Channel Power vs. Time (HZP)**



APR1400 DCD TIER 2**Figure 15.4.8-9 CEA Ejection: Core Average Heat Flux vs. Time (HZP)**



APR1400 DCD TIER 2**Figure 15.4.8-10 CEA Ejection: Hot Channel Heat Flux vs. Time (HWP)**



APR1400 DCD TIER 2

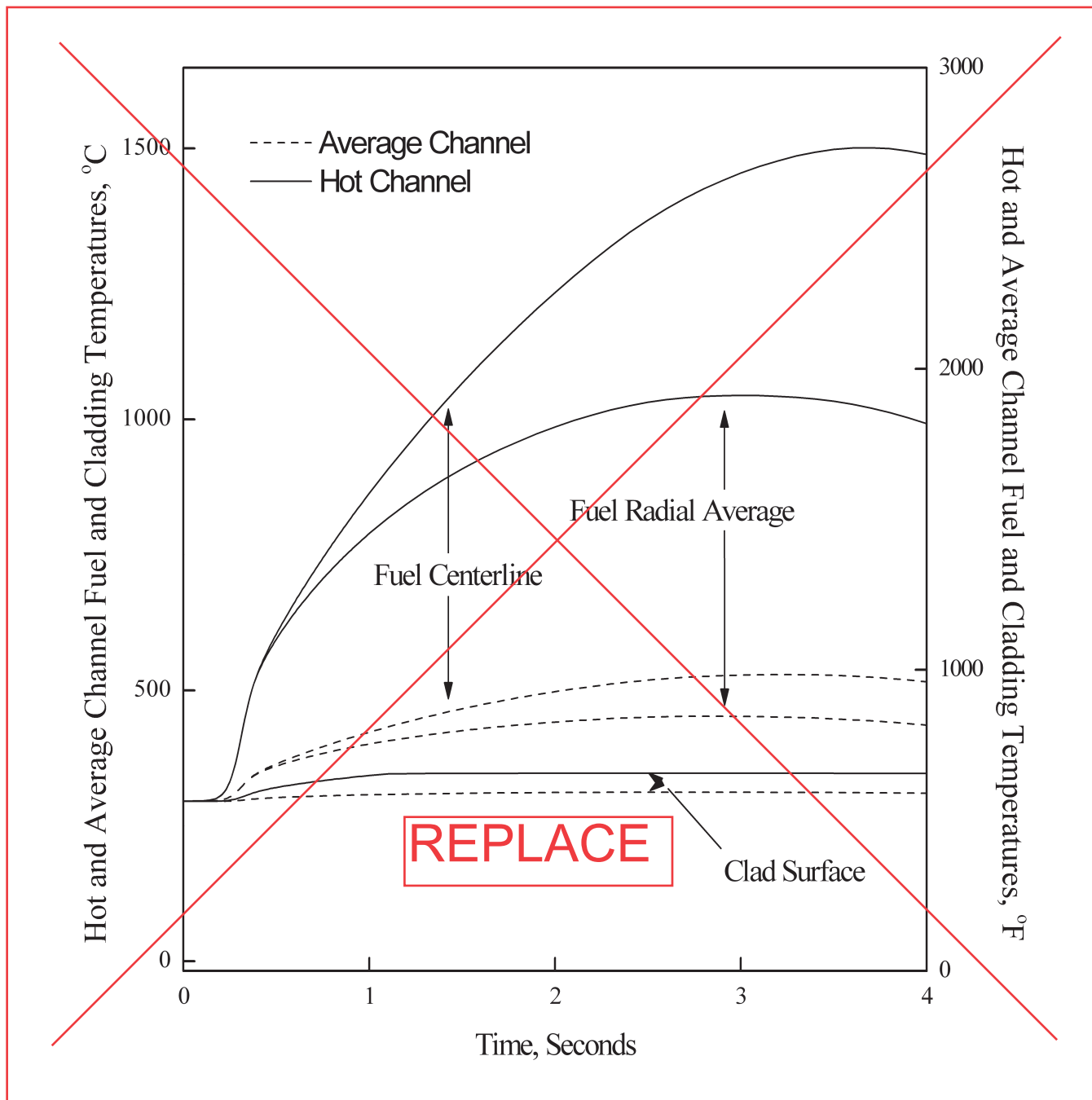
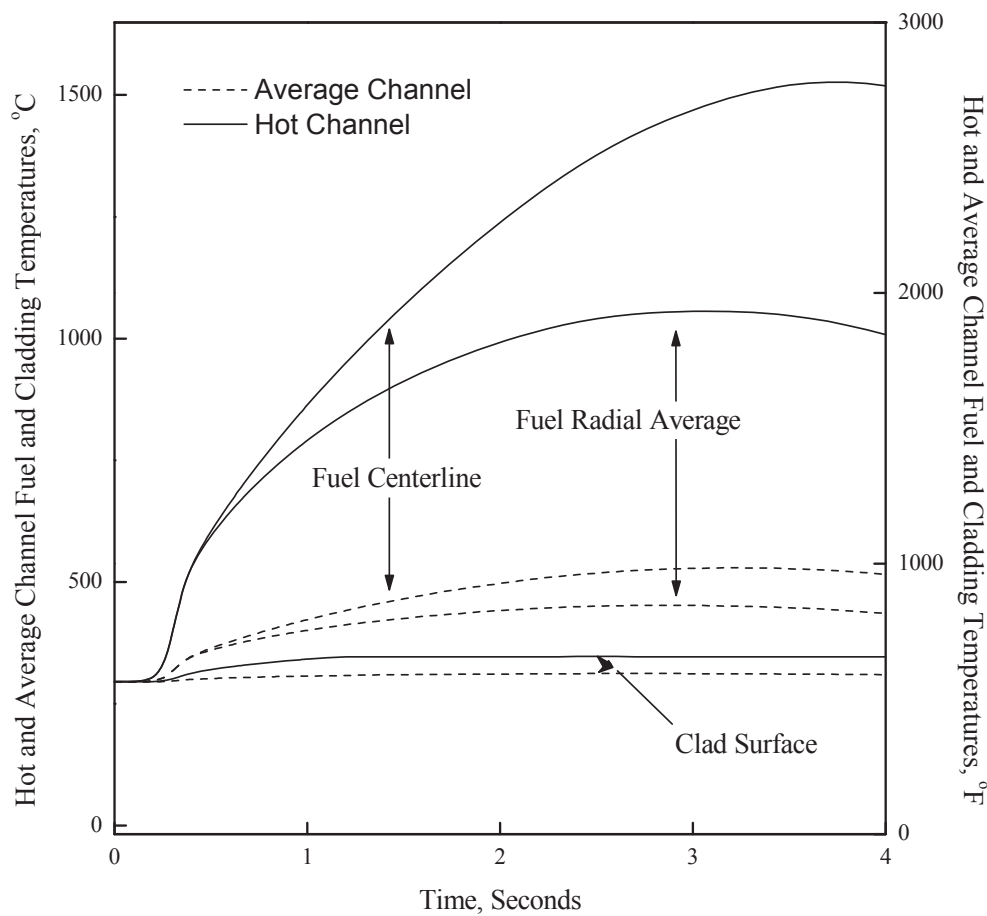


Figure 15.4.8-11 CEA Ejection: Hot and Average Channel Fuel and Cladding Temperatures vs. Time (HZP)



APR1400 DCD TIER 2

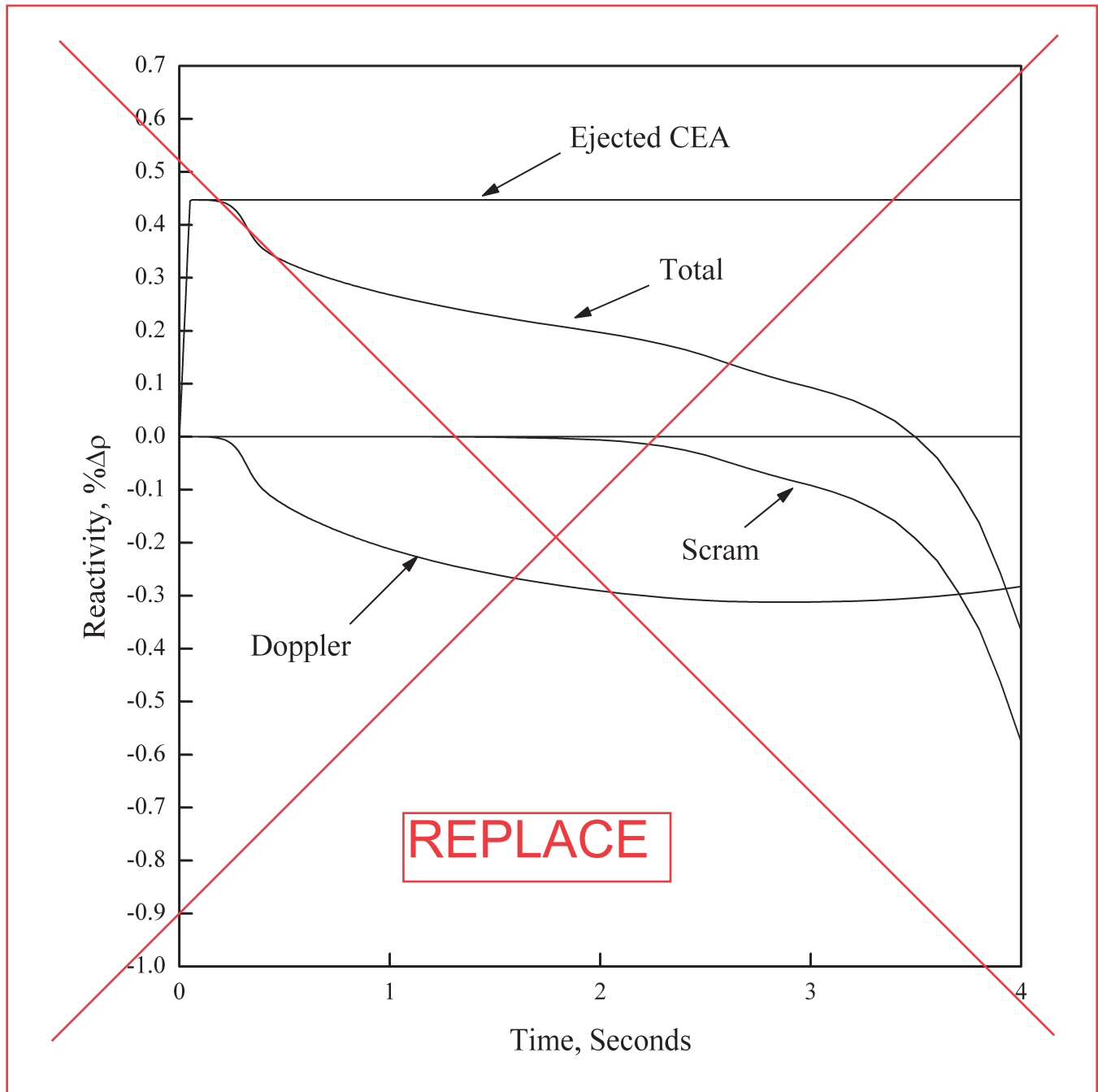
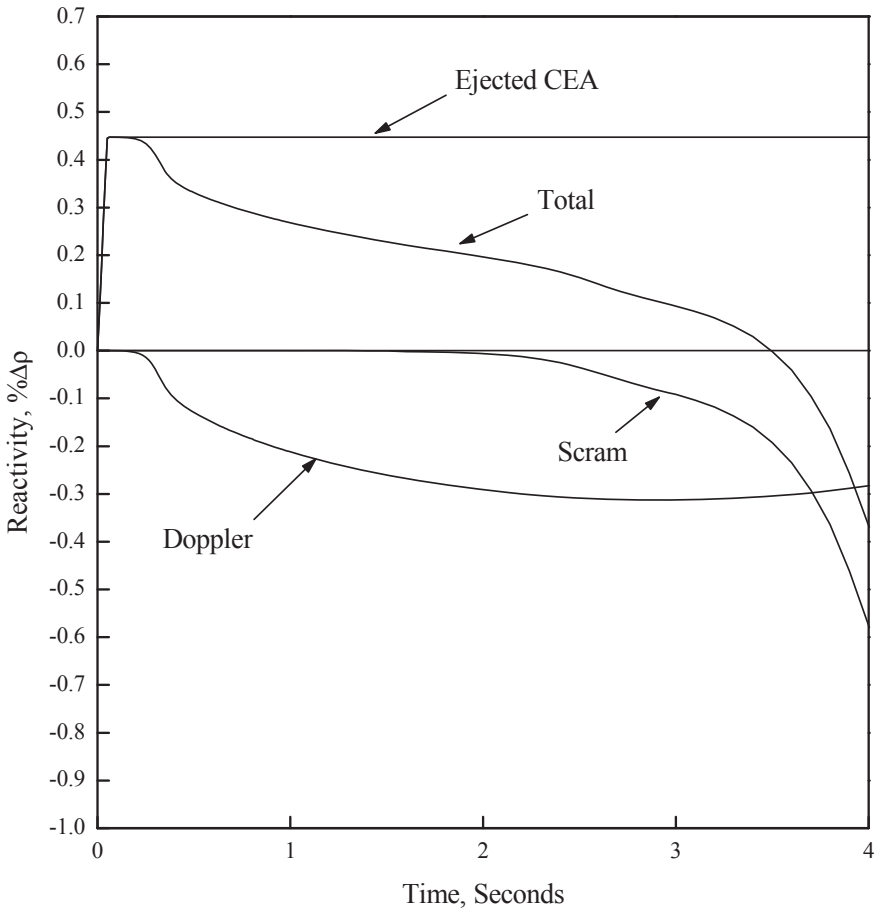
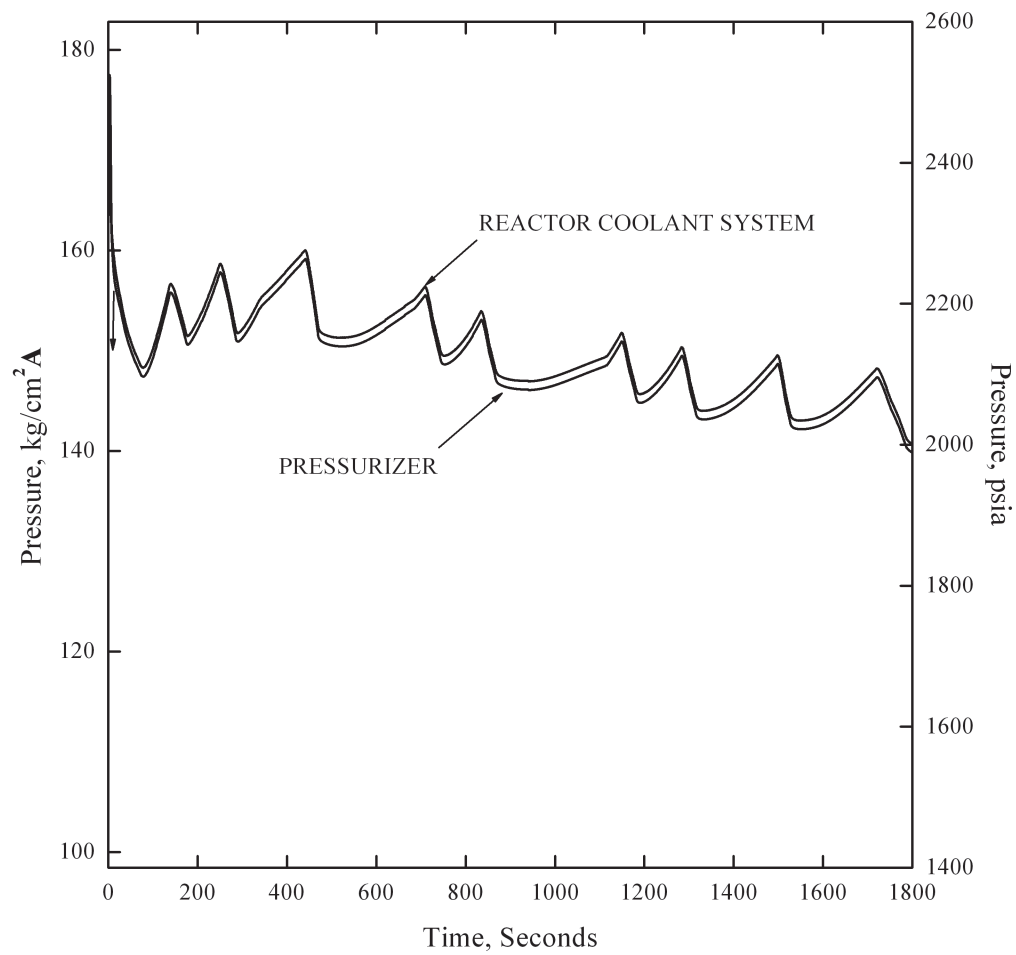


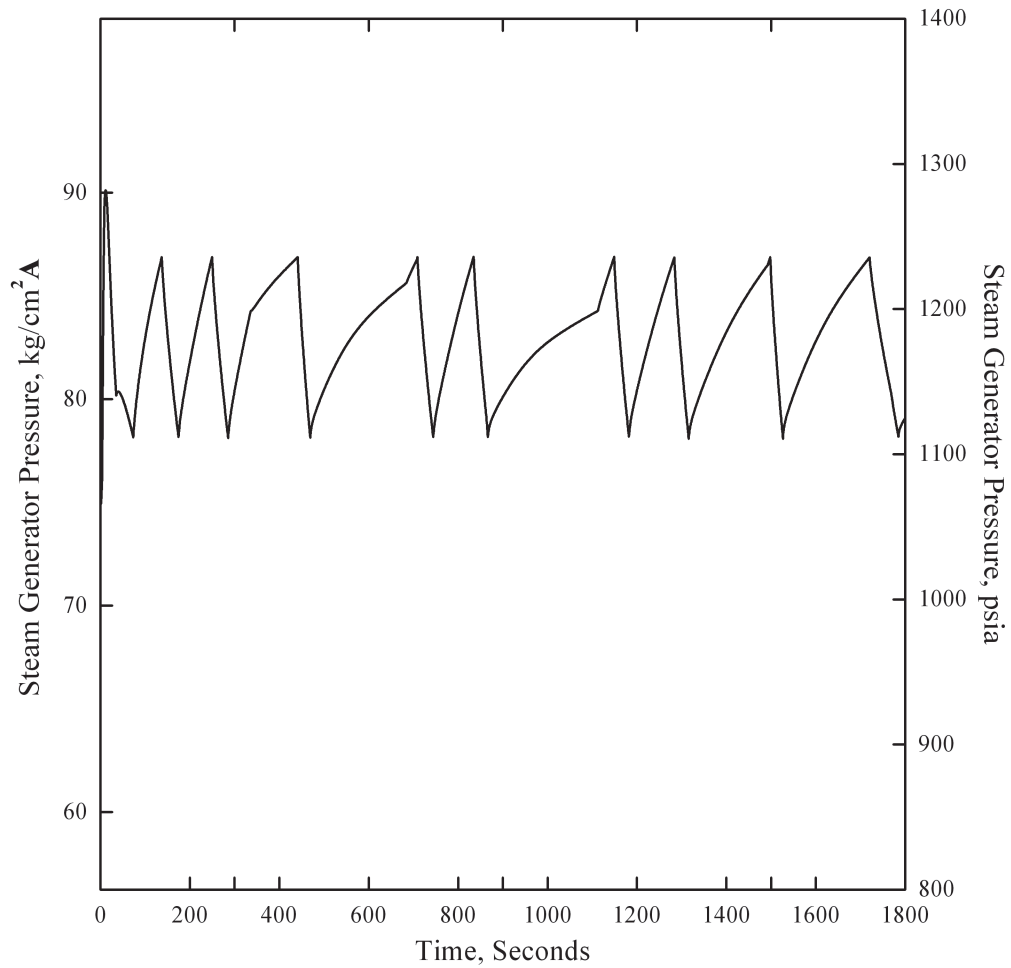
Figure 15.4.8-12 CEA Ejection: Reactivity vs. Time (HZP)

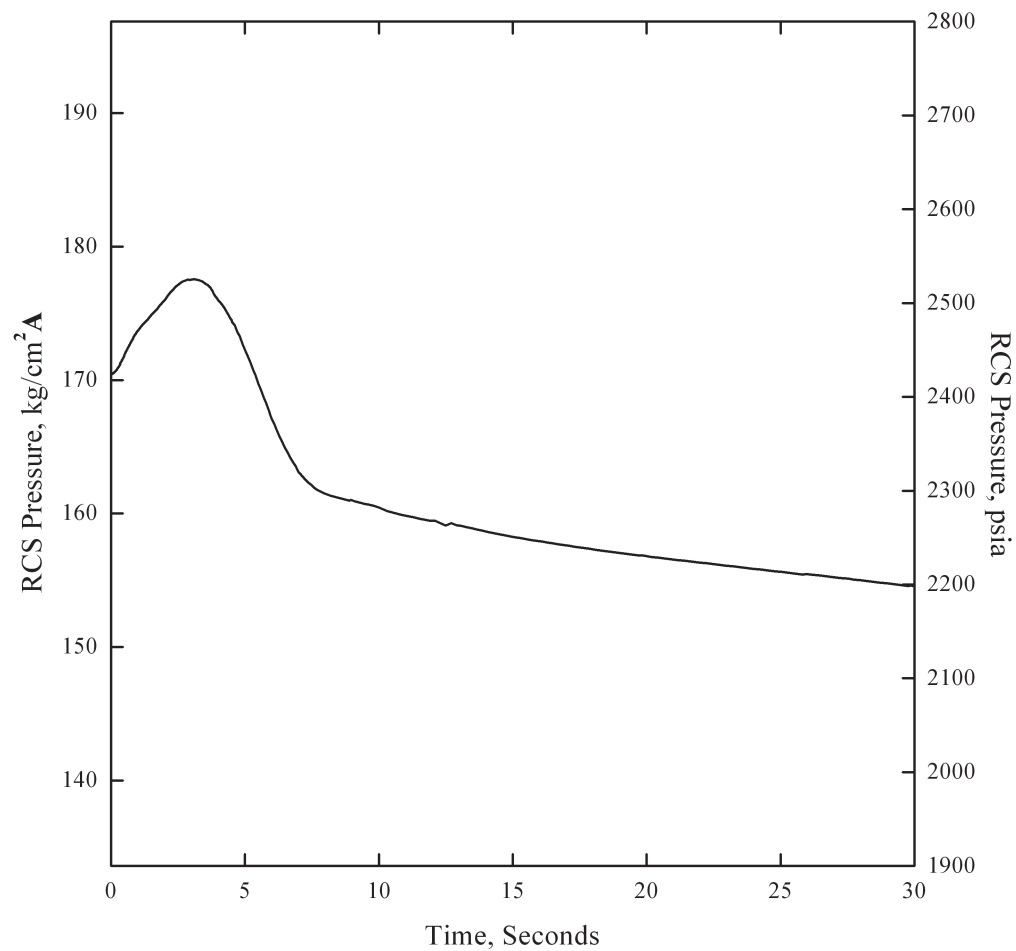


APR1400 DCD TIER 2

* The pressure difference between cold leg at the RCP discharge and the surge line is not included.

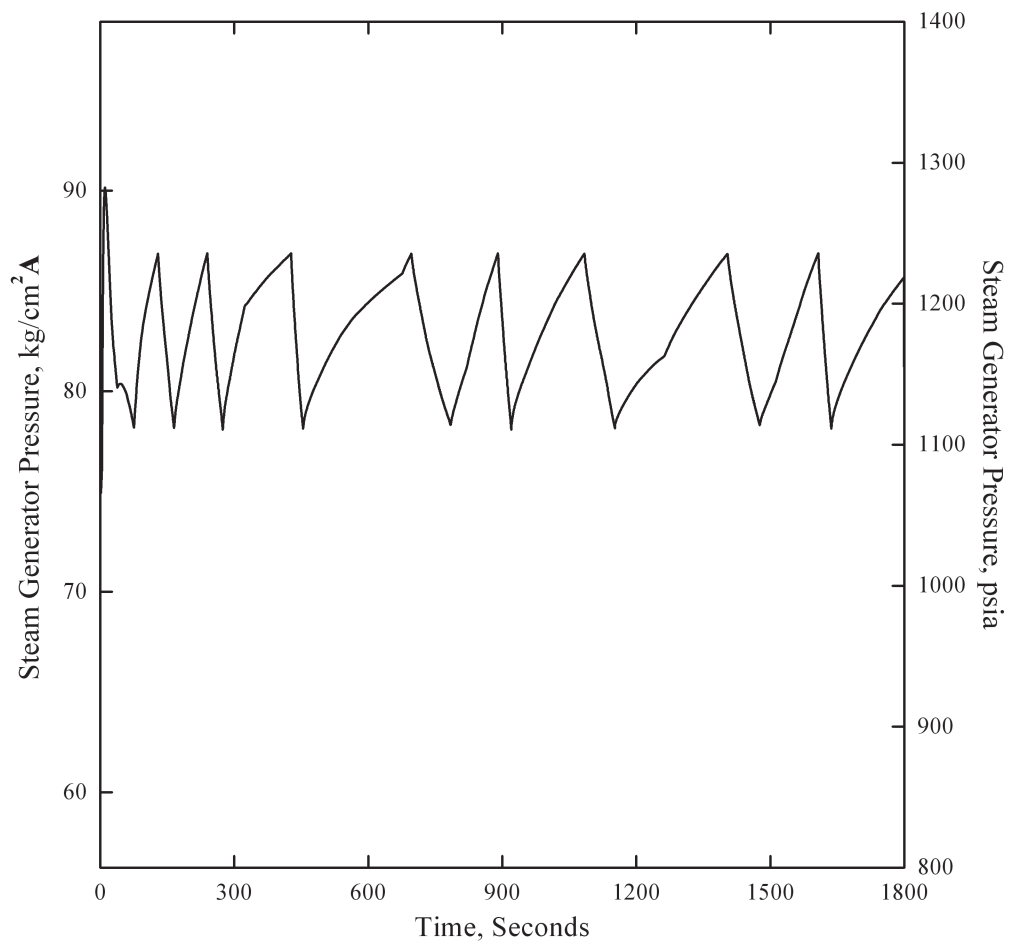
Figure 15.4.8-13 CEA Ejection: RCS and Pressurizer Pressures vs. Time

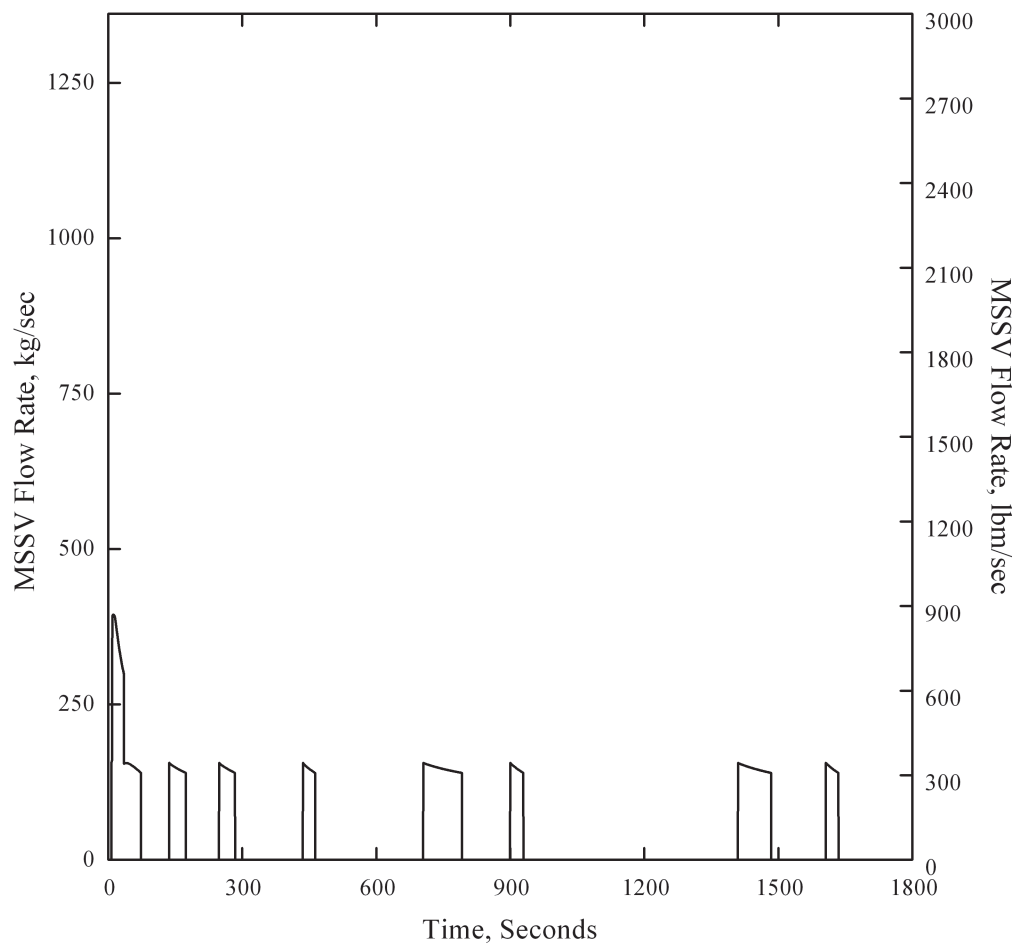
APR1400 DCD TIER 2**Figure 15.4.8-14 CEA Ejection: Steam Generator Pressure vs. Time**

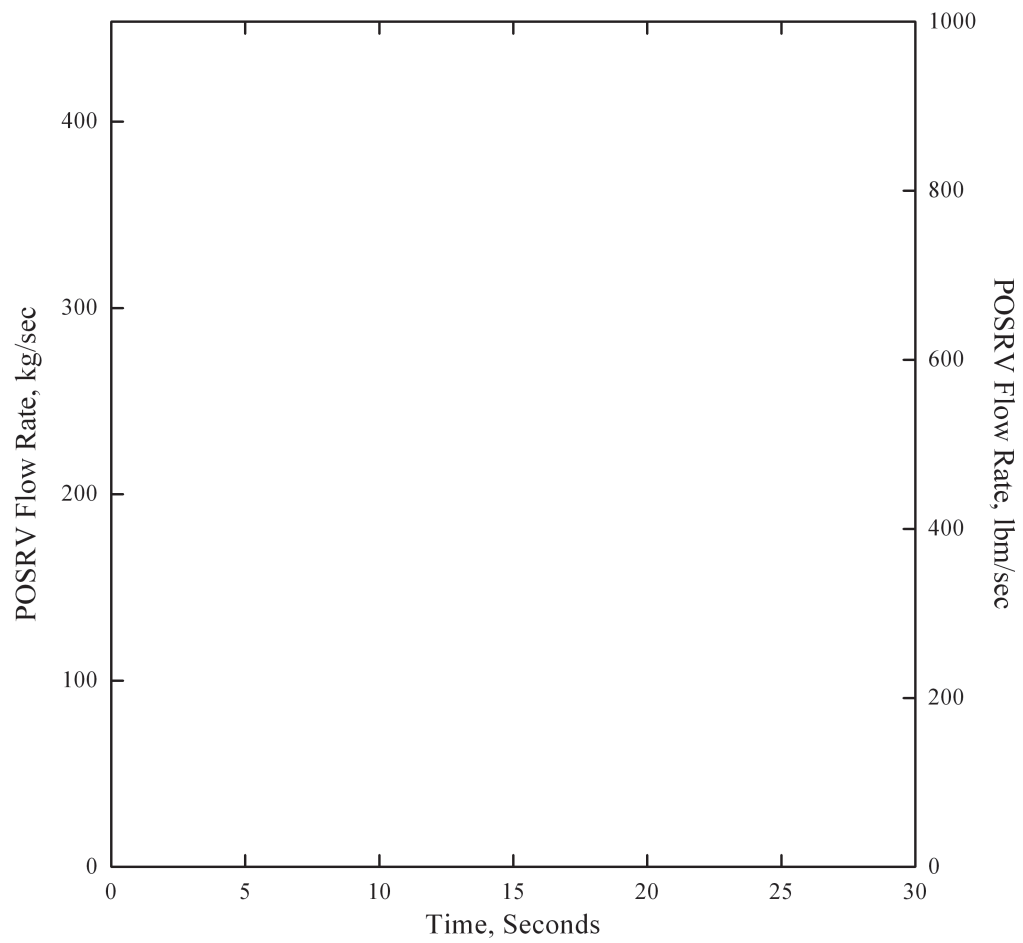
APR1400 DCD TIER 2

*The pressure difference between cold leg at the RCP discharge and the surge line is included.

Figure 15.4.8-15 CEA Ejection: RCS Pressure vs. Time (Peak Pressure Case)

APR1400 DCD TIER 2**Figure 15.4.8-16 CEA Ejection: Steam Generator Pressure vs. Time (Peak Pressure Case)**


APR1400 DCD TIER 2**Figure 15.4.8-17 CEA Ejection: MSSV Flow Rate vs. Time (Peak Pressure Case)**

APR1400 DCD TIER 2**Figure 15.4.8-18 CEA Ejection: POSRV Flow Rate vs. Time (Peak Pressure Case)**

| | | |
|---------------------------|---|--------------------|
| Table 15.6.3-3 | Sequence of Events for a Steam Generator Tube Rupture with a Loss of Offsite Power | 15.6-58 |
| Table 15.6.3-4 | Assumptions and Initial Conditions for the Steam Generator Tube Rupture with a Loss of Offsite Power | 15.6-59 |
| Table 15.6.3-5 | Parameters Used in Evaluating the Radiological Consequences of the Steam Generator Tube Rupture with a Loss of Offsite Power..... | 15.6-60 |
| Table 15.6.3-6 | Radiological Consequences of the Steam Generator Tube Rupture with a Loss of Offsite Power..... | 15.6-63 |
| Table 15.6.5-1 | Uncertainty Parameter Ranges and Distributions | 15.6-64 |
| Table 15.6.5-2 | General System Parameters and Initial Conditions for Large Break ECCS Performance | 15.6-65 |
| Table 15.6.5-3 | Summary of Fuel Rod Performance for Break Spectrum of Large Break LOCA..... | 15.6-67 |
| Table 15.6.5-4 | Sequence of Events for Representative Large Break LOCA..... | 15.6-68 |
| Table 15.6.5-5 | Summary of SRS and Bias Evaluation Results..... | 15.6-69 |
| Table 15.6.5-6 | Safety Injection Pumps Minimum Delivered Flow to RCS (Assuming Two SI Pump Trains Failed) | 15.6-70 |
| Table 15.6.5-7 | General System Parameters and Initial Conditions; Small Break ECCS Performance Analysis..... | 15.6-71 |
| Table 15.6.5-8 | Small Break Spectrum | 15.6-72 |
| Table 15.6.5-9 | Variables Plotted as a Function of Time for Each Small Break in the Spectrum..... | 15.6-73 |
| Table 15.6.5-10 | Peak Cladding Temperature and Oxidation Percentage for the Small Break Spectrum | 15.6-74 |
| Table 15.6.5-11 | Times of Interest for the Small Break Spectrum (Seconds after Break) | 15.6-75 |
| Table 15.6.5-12 | General System Parameters and Initial Conditions Long-Term Cooling SIS Performance..... | 15.6-76 |
| Table 15.6.5-13 | Major Input Parameters Used in Radiological Consequences Analysis for Large Break LOCA | 15.6-77 |
| Table 15.6.5-14 | Radiological Consequences of a Large Break LOCA | 15.6-81 |

delete

insert T D thermal conductivity degradation



| | |
|-------|--------------------------------------|
| TBV | turbine bypass valve |
| TEDE | total effective dose equivalent |
| TSC | technical support center |
| TS | technical specification |
| UGS | upper guide structure |
| USEPA | U.S. Environmental Protection Agency |
| USI | Unresolved Safety Issue |
| VOPT | variable overpower trip |

APR1400 DCD TIER 2

53. NUREG-1465, "Accident Source Terms for Light Water Nuclear Power Plants," U.S. Nuclear Regulatory Commission, February 1995.
54. Regulatory Guide 1.183, "Alternative Radiological Source Terms for Evaluating Design Basis Accidents at Nuclear Power Reactors," U.S. Nuclear Regulatory Commission, July 2000.
55. USEPA, Federal Guidance Report No. 11, EPA 520/1-88-020, "Limiting Values of Radionuclide Intake and Air Concentration and Dose Conversion Factors for Inhalation, Submersion, and Ingestion," September 1993.
56. USEPA, Federal Guidance Report No. 12, EPA 402-R-93-081, "External Exposure to Radionuclides in Air, Water, and Soil," September 1993.
57. 10 CFR 50.34, "Contents of Applications; Technical Information," U.S. Nuclear Regulatory Commission, January 10, 1997.
58. 10 CFR Part 50, Appendix A, "General Design Criteria for Nuclear Power Plants," U.S. Nuclear Regulatory Commission, January 24, 2000.
59. NUREG/CR-6604, "RADTRAD: A Simplified Model for RADionuclide Transport and Removal and Dose Estimation," SNL, December 1997.
60. NUREG-0800, Standard Review Plan, BTP 11-5, "Postulated Radioactive Release Due to Waste Gas System Leak or Failure," Rev.3, U.S. Nuclear Regulatory Commission, March 2007.
61. NUREG-0800, Standard Review Plan, BTP 11-6, "Postulated Radioactive Release Due to Liquid-Containing Tank Failure," Rev.3, U.S. Nuclear Regulatory Commission, March 2007.
62. 10CFR50.46, "Acceptance Criteria for Emergency Core Cooling Systems for Light Water-Cooled Nuclear Power Reactors," U.S. Nuclear Regulatory Commission.
63. APR1400-F-A-TR-12004-P (Proprietary), "Realistic Evaluation Methodology for Large-Break LOCA," KHNP, insert ~ Rev. 1 December 2012 ~ ul ~ 2017
64. Regulatory Guide 1.157, "Best-estimate Calculations of Emergency Core Cooling System Performance," U.S. Nuclear Regulatory Commission, May 1989.

APR1400 DCD TIER 2

65. NUREG/CR-5535, "RELAP5/MOD3 Code Manual Vol. 6, Validation of Numerical Techniques in RELAP5/MOD3.0," Rev.P3, U.S. Nuclear Regulatory Commission, March 2006.
66. NUREG/CR-3716, BNL-NUREG-51754, "CONTEMPT4/MOD4, A Multicompartment Containment System Analysis Program," U.S. Nuclear Regulatory Commission, March 1984.
- NUREG/CR-4001, BNL-NUREG-51894, "CONTEMPT4/MOD5: An improvement to CONTEMPT4/MOD4 multi-compartment containment system analysis program for ice containment analysis," Brookhaven National Laboratory, 1984.
67. APR1400-F-A-NR-14001-P, "Small Break LOCA Evaluation Model," KHNP, September 2014.
68. Letter, O. D. Parr (NRC) to F. M. Stern (C-E), June 13, 1975.
69. CENPD-133P (Proprietary), "CEFLASH-4AS, A Computer Program for Reactor Blowdown Analysis of the Small Break Loss-of-Coolant Accident," Supplement 1, Combustion Engineering, Inc., August 1974.
- CENPD-133 (Proprietary), "CEFLASH-4AS, A Computer Program for the Reactor Blowdown Analysis of the Small Break Loss-of-Coolant Accident," Supplement 3-P, Combustion Engineering, Inc., January 1977.
70. CENPD-134P (Proprietary), "COMPERC-II, A Program for Emergency Refill-Reflood of the Core," Combustion Engineering, Inc., August 1974
- CENPD-134P (Proprietary), "COMPERC-II, A Program for Emergency Refill-Reflood of the Core (Modifications)," Supplement 1, Combustion Engineering, Inc., February 1975.
- CENPD-134 "COMPERC-II, A Program for Emergency Refill-Reflood of the Core," Supplement 2, Combustion Engineering, Inc., June 1985.
71. CENPD-135P (Proprietary), "STRIKIN-II, A Cylindrical Geometry Fuel Rod Heat Transfer Program," Combustion Engineering, Inc., August 1974.

APR1400 DCD TIER 2

CENPD-135P (Proprietary), "STRIKIN-II, A Cylindrical Geometry Fuel Rod Heat Transfer Program (Modifications)," Supplement 2, Combustion Engineering, Inc., February 1975.

CENPD-135 (Proprietary), "STRIKIN-II, A Cylindrical Geometry Fuel Rod Heat Transfer Program," Supplement 4-P, Combustion Engineering, Inc., August 1976.

CENPD-135 (Proprietary), "STRIKIN-II, A Cylindrical Geometry Fuel Rod Heat Transfer Program," Supplement 5-P, Combustion Engineering, Inc., April 1977.

72. CENPD-138P (Proprietary), "PARCH, A FORTRAN-IV Digital Program to Evaluate Pool Boiling, Axial Rod and Coolant Heatup," Combustion Engineering, Inc., August 1974.

CENPD-138P (Proprietary), "PARCH, A FORTRAN-IV Digital Program to Evaluate Pool Boiling, Axial Rod and Coolant Heatup (Modifications)," Supplement 1, Combustion Engineering, Inc., February 1975.

73. APR1400-F-A-NR-14003-P, "Post-LOCA Long Term Cooling Evaluation Model," KHNP, September 2014.

74. CENPD-139-P-A (Proprietary), "C-E Fuel Evaluation Model," Combustion Engineering, Inc., July 1974.

CEN-161 (B)-P-A (Proprietary), "Improvements to Fuel Evaluation Model," Combustion Engineering, Inc., August 1989.

CEN-161 (B)-P (Proprietary) "Improvements to Fuel Evaluation Model," Supplement 1-P-A, Combustion Engineering, Inc., January 1992.

75. CEN-268, "Justification of Trip Two/Leave Two Reactor Coolant Pump Trip Strategy," Rev. 1, Combustion Engineering, Inc., May 1987.
76. APR1400-Z-A-NR-14006-P, "Non-LOCA Safety Analysis Methodology," Rev. 1, KHNP, February 2017.
77. APR1400-Z-J-NR-14005-P, "Setpoint Methodology for Plant Protection System," Rev. 1, KHNP, February 2017.

APR1400 DCD TIER 2

delete

~~78. APR1400-F-A-NR-14002-P, "The Effect of Thermal Conductivity Degradation on APR1400 Design and Safety Analyses," Rev. 0, KHNP, September 2014.~~

78

79. NUREG-1462, "Final Safety Evaluation Report Related to the Certification of the System 80+ Design Docket No. 52-002," Rev. 0, U.S. Nuclear Regulatory Commission, 1994.

79

80. APR1400-Z-A-NR-14014-P, "ATWS Evaluation," Rev. 0, KHNP, November 2014.

80

81. APR1400-F-M-TR-13001-P (Proprietary), "PLUS7 Fuel Design for the APR1400," Rev. 0, KHNP, August 2013.

APR1400 DCD TIER 2

allowable dose criteria limits, which are 100 percent and 10 percent of the 10 CFR 50.34(a)(1) value, respectively. The MCR and TSC doses are also within the dose limit in GDC 19.

15.6.3.2.6 Conclusions

The radiological consequences for the SGTR accident with a LOOP are within the allowable criteria. The RCS and secondary system pressures are below the 110 percent of the design pressure limits, thus providing reasonable assurance of the integrity of these systems. The minimum DNBR is above the DNBR SAFDL value of 1.29. The acceptance criterion regarding fuel performance is met.

For the limiting SGTR event with respect to SG overfill considerations (SGTR with a LOOP), the maximum liquid inventories do not result in an overfill and consequent introduction of liquid water into the steam lines, providing reasonable assurance of the integrity of these steam lines.

After 30 minutes, the operator uses the plant emergency procedure for the SGTR to cool down the plant to shutdown cooling entry conditions.

15.6.4 Radiological Consequences of Main Steam Line Failure Outside Containment (Boiling Water Reactor)

Not applicable to the APR1400.

15.6.5 Loss-of-Coolant Accidents Resulting from the Spectrum of Postulated Piping Breaks within the Reactor Coolant Pressure Boundary

15.6.5.1 Identification of Causes and Frequency Classification

Loss-of-coolant accidents (LOCAs) are hypothetical accidents that result from the loss of reactor coolant at a rate that exceeds the capability of the reactor coolant makeup system. The cause is breaks in the pipes in the reactor coolant pressure boundary up to and including a break equivalent in size to the double-ended rupture of the largest pipe in the RCS.

In the accident analyses for the APR1400, large break and small break LOCAs are both classified as postulated accidents (PAs). They are not expected to occur during the life of the plant but are postulated as a conservative design basis.

APR1400 DCD TIER 215.6.5.2 Sequence of Events and Systems Operation

insert: and burnup to consider thermal conductivity degradation (TCD) effects

15.6.5.2.1 Description of Large Break Loss-of-Coolant Accident

insert: with various burnup cases

A cold leg break between the outlet of the reactor coolant pump (RCP) and the corresponding reactor vessel (RV) inlet nozzle is found to be the most limiting with respect to the peak cladding temperature (PCT) in a large break LOCA. The large break LOCA analysis assumes a Loss Of Offsite Power (LOOP). The RCPs lose power and coast down after the LOOP. In order to determine the limiting break size, a guillotine break spectrum of a 100, 80, and 60 percent break area is studied. The blowdown PCT is a maximum when the break area is 100 percent of the cold leg cross-sectional area. The reflood PCT is a maximum when the break area is 80 percent. However, because the reflood PCT is not as high as the blowdown PCT, the 100 percent break size is chosen as the limiting guillotine break case.

insert: with the burnup of 27,000 MWd/MTU

delete

In the 100 percent guillotine break, the total break area is two times the cold leg cross-sectional area. A 200 percent slot break shows lower PCT in the blowdown phase and the transient is found to be faster by about 4 seconds than that of the 100 percent guillotine break. The PCT of the reflood phase is lower than that of the guillotine break, and the fuel quenching is somewhat earlier. The 100 percent double-ended guillotine break in a cold leg is determined to be the limiting case.

delete

insert: with the burnup of 27,000 MWd/MTU

The scenario is divided into four phases that characterize the events during the transient. The phases are blowdown, refill, early reflood, and late reflood and are defined by the inventory of the reactor pressure vessel and the flow condition of safety injection tank with fluidic device (SIT-FD).

A blowdown is defined as the phase from the opening time of the break to the start time of the SIT-FD injection. The refill phase is defined as the phase from the start time of the SIT-FD injection to the time when the mixture level in the reactor vessel lower plenum reaches the bottom of the active core. The definitions of these two phases are the same as those of the conventional large break LOCA scenario in PWRs.

Unlike the conventional scenario, the reflood phase is divided into early reflood and late reflood phases based on the time in which the SIT-FD becomes empty. The division is intended to address any possibility of core heatup during the late reflood phase in detail because the APR1400 does not have a low-pressure safety injection pump.

APR1400 DCD TIER 2Blowdown Phase

The blowdown phase starts when the break opens and ends when an SIT-FD injection is initiated; blowdown lasts for approximately 15 seconds. During blowdown, the primary coolant is rapidly expelled into the containment through the break. The reactor coolant changes from a subcooled liquid to a two-phase mixture or pure steam due to fluid flashing. By roughly 6 seconds, the core region begins to dry out.

The initial break flow is very high, reflecting the subcooled critical flow at the break. Mass flow from the reactor vessel side of the break is larger than that from the pump side due to the higher hydraulic resistances of the pump and the Steam Generator(SG). As the break flow develops in the reverse direction from the core to the break as well as in the positive direction, the core flow rapidly stagnates and then reverses shortly after the break occurs.

As the primary system depressurizes, flashing occurs first in the hot regions of the system, such as the upper plenum, hot leg, pressurizer, and core, and then proceeds to the relatively cold regions, such as the lower plenum, downcomer, and cold legs. Extensive voiding occurs in all areas of the reactor pressure vessel. Nucleate boiling develops in the core. Fission power that is calculated by a kinetics model drops to the level of decay heat due to the voiding in the core. The flashing also reduces the primary system depressurization rate.

When the critical heat flux (CHF) condition is reached in the core, heat transfer changes from nucleate boiling to post-CHF heat transfer regimes (i.e., transition boiling, film boiling, and forced convection to vapor), and much of the core dries out. Fuel rod cladding temperatures increase rapidly due to the degrading rod-to-fluid heat transfer. The cladding temperature increase during the early blowdown phase is terminated by several processes:

- a. First, as the core rapidly voids, the core power immediately decreases via void reactivity insertion.
- b. Second, the flow at the core reverses after stagnation.
- c. Third, the large coolant inventory of the upper guide structures (UGSs) and upper head moves toward the top of the core by two paths, through the UGS drainage

APR1400 DCD TIER 2

holes in the UGS bottom plate between the UGS and upper plenum and through the guide tube pipes that terminate in the upper inactive core.

As the low pressurizer pressure setpoint is reached, the reactor is tripped. Reactor coolant pumps (RCPs) are modeled to trip and coast down from the beginning of the accident assuming a LOOP. As the primary system pressure continues to decrease, flashing develops in the cold regions of the system. The resultant voiding occurring in the RCP degrades its pumping performance. The break flow rate decreases rapidly as the flow regime changes from subcooled to saturated critical flow at the break.

delete

~~Four SIT FDs begin to deliver flow into the four direct vessel injection (DVI) lines when the primary system pressure falls below its actuation setpoint. The coolant flows through the DVI nozzles into the upper annulus and then begins to refill the reactor pressure vessel. Because the reactor coolant system is still depressurizing, some of the coolant entering the upper annulus is swept out to the break along with entrained liquid from the lower plenum and the downcomer. Although the break flow remains high, the coolant is delivered downward into the downcomer and increases the downcomer water level. Then the coolant injected by the SIT FD eventually reaches the lower plenum.~~

Refill Phase

The refill phase begins when the SIT-FD injection flow is initiated and ends when the water level in the lower plenum reaches the core inlet.

mi~ture

Emergency core cooling (ECC) water in the reactor vessel downcomer can flow down by insert A from ne~t~age swept out to the break by the pressure differential and upward-escaping steam flow that levitates the liquid. Reactor vessel walls and internals are considered as the large metal structures at temperatures above saturation. When subcooled ECC water comes into contact with the metal structures in the downcomer, steam is generated by nucleate boiling, reducing the gravitational head of the fluid in the downcomer. The process of liquid penetration and sweep-out repeats in the downcomer and direct-contact condensation of steam on the subcooled ECC water continues in the upper annulus.

~ottom of the active core

The depressurization of the system wanes as the differential pressure between the RCS and the containment reduces. Owing to the gradual reduction of flashing and break flow, the rate of liquid penetration into the lower plenum increases. With a decreasing steam flow rate, a small amount of the ECC injection is bypassed, and most of it flows downward to

A

Four SIT-FDs begin to deliver flow into the four DFI lines when the primary system pressure falls below their actuation set-point. The coolant flows through the DFI nozzles into the upper annulus and then begins to refill the reactor pressure vessel. The reactor coolant system sees depressurizing because some of the coolant entering the upper annulus is sent out to the steam along with entrained liquid from the lower plenum and the downcomer. Although the steam flow remains high, sufficient flow in the excess of the mass is delivered downward into the downcomer and increases the downcomer water level. Eventually the coolant injected by the SIT-FDs reaches the lower plenum.

APR1400 DCD TIER 2

fill the downcomer and the lower plenum. At this stage, ^{mixture} ~~water~~ levels in the downcomer and the lower plenum increase rapidly.

Heatup, which is almost adiabatic, continues in the core during this phase because there is no inventory to cool the core.

The refill phase ends when the ^{mixture} ~~liquid~~ level in the lower plenum reaches the bottom of the active core.

^{insert and remains full thereafter and conditions are established for continuous core reflooding.}

Early Reflood Phase

The early reflood phase begins when the lower plenum ^{mixture level in the} ~~is completely filled with water~~ and ends when the SIT-FD water is depleted. Near the beginning of the early reflood phase, the safety injection pumps (SIPs) begin to inject water. Initially, the core reflood is quite rapid because of the following:

^{reaches the bottom of the active core}

- The downcomer remains filled with water by the ECC injection.
- The high flow injection of SIT-FD continues.
- There is little loop steam flow and hydraulic resistance in the loop is therefore low.
- There is no severe steam binding.

^{insert control of}

The maximum SIT-FD injection flow is reached during this phase. High flow injection through the standpipe becomes unavailable, and only the flow through the fluidic-device becomes injected. During the high-flow injection, the downcomer and core liquid levels increase rapidly. As the downcomer liquid level approaches the level of the cold legs, much of the coolant spills out of the break, and the vessel side break flow tends to increase. When the water level in the SIT-FD decreases to below the top of the standpipe, the low-flow injection begins. Water levels in the downcomer and core decrease slightly, but the levels increase again within approximately ^{around} ~~10~~ seconds, maintaining downcomer water level ^{above} the level of the cold legs. The combined SIP and SIT-FD flows are injected to maintain the water level in the downcomer and to retard core heatup.

⁵

In the core, heat transfer regimes encompass the entire spectrum. The regimes include single-phase liquid convection, nucleate boiling, transition boiling, film boiling, and single-phase vapor convection.

APR1400 DCD TIER 2

Local quenching could occur due to droplet de-entrainment at the fuel alignment plate and spacer grids. Vapor velocities and liquid entrainment in the central region of the core are higher due to the higher power of this region. The entrained liquid could have a cooling effect on the upper region of the core. Some of the entrained liquid is de-entrained at the fuel alignment plate, and the remainder is carried into the upper plenum, forming a two-phase pool. Liquid from the pool can re-enter the low-powered regions of the core through the fuel alignment plate due to the lower vapor velocities in those regions. A three-dimensional flow pattern can therefore occur: water flows from low-powered to high-powered regions in the core, while the flow is in the opposite direction in the upper plenum. Liquid from the upper plenum pool may be further entrained and carried over into the hot legs and SGs.

As reflooding progresses upward from the lower core region, more liquid is entrained to the upper plenum, and the level of the two-phase mixture in the pool can reach the hot leg. When the entrained liquid reaches the U-tubes of the SGs, it is vaporized by reverse heat transfer from the secondary side to the primary side. Due to the vaporization in the U-tubes, hot side pressure increases and causes steam binding, which deteriorates the reflooding of the core. Because the steam generation rate in the core decreases due to the lower reflood rate, liquid entrainment and the steam binding effect decrease, causing the reflood rate to increase again. Through this cyclical process, the entire core eventually becomes reflooded. The increase of core pressure due to the steam binding causes manometric oscillations between levels in the downcomer and the core.

The early reflood phase ends when SIT-FDs are emptied.

Late Reflood Phase

The late reflood phase begins when the SIT-FDs are emptied. ECC water is supplied only by the Safety Injection Pumps(SIPs) during this phase.

during this ~ hase

Water level in the downcomer decreases somewhat as the SIT flow stops at the beginning of the late reflood phase and falls below the level of the cold legs. Then the core water level becomes stabilized. Liquid levels in the downcomer and core become balanced ~~within approximately 20 seconds.~~ Due to the decreased flow of coolant into the downcomer, liquid temperature in the downcomer can increase to a near saturation temperature under the influence of the residual heat of the metal structures (i.e., vessel walls in the downcomer). Boiling can occur on the surface of the walls depending on the

APR1400 DCD TIER 2

conditions. ECC water is provided by the four SIPs, the possibility of downcomer boiling is suppressed, and the core is found to remain amenable to cooling.

Because the entire core remains in a quenched state during this phase, steam generation in the core is not significant enough to cause any severe ECC water bypass during this phase.

Only safety-related systems or components are credited to mitigate the accident, as follows:

- a. Normally operating plant instrumentation and controls

Steady-state conditions of a large break LOCA analysis are calculated at the normal operating plant conditions (e.g., power, flow rate, pressure, temperature).

- b. Reactor protection system (RPS)

The reactor trip signal is generated from the low pressurizer pressure during the large break LOCA. The trip signal also generates the turbine trip and RCP trip automatically. Coastdown of the RCP progresses after the RCP trip. However, because the CEA insertion is not used for large break LOCA analysis, the negative reactivity of CEA is not credited. For the small break LOCA analysis, the CEA insertion is credited including the signal delay.

- c. Engineered safety feature actuation system (ESFAS)

An ESFAS is generated from the low pressurizer pressure or high-containment pressure during the large break LOCA. Low pressurizer pressure is credited only in the LOCA analysis and actuates the containment isolation actuation signal (CIAS) and safety injection actuation signal (SIAS).

- d. Safety injection system (SIS)

During the LOCA, the SIS provides the direct vessel injection. The discharge of each SIP and SIT is piped directly to a reactor vessel nozzle where the flow is directed into the reactor vessel downcomer region. Storage of fluid for the SIS is accomplished by the IRWST, which contains borated fluid.

- e. Containment spray system (CSS)

APR1400 DCD TIER 2

The CSS is designed to reduce containment pressure and temperature from a main steam line break or LOCA and to remove fission products from the containment atmosphere following a LOCA. The CSS uses the IRWST and has two independent trains. During the large break LOCA, CSS is automatically actuated on a high-high containment pressure signal. Maximum containment spray capacity is assumed to calculate the minimum containment pressure, which is described in Subsection 6.2.1.5.

15.6.5.2.2 Description of Small Break Loss-of-Coolant Accident

Small Break LOCA shows the significantly different behaviors depending on the break size and location. For a smaller break size, a SIP can maintain the RCS coolant inventory, since the reactor operator utilizes the Steam Generator (SG) to depressurize and cool down the system. For a larger break size, the blowdown break flow cannot be compensated by the SIP.

Small Break LOCA behavior can be changed with break location. The scenario of DVI line break, which is known to be the most limiting case of Small Break LOCA, can be generally subdivided into five phases: blowdown, natural circulation, loop seal clearing, core boil-off, and core recovery. The duration and occurrence of each phase are varied with break size and system characteristics.

Blowdown Phase

The break drastically depressurizes the RCS. When the RCS pressure reaches a reactor trip set-point on low pressurizer pressure, the reactor is tripped by the insertion of control rods. Once the RCS is depressurized to the low-low pressurizer pressure, safety injection signal is actuated. And safety injection water is delivered into the RCS after a delay until the injection pump is started. During the blowdown phase, the RCS is mostly filled with fluid in liquid phase and subcooled or saturated coolant is discharged into the containment building through the break. When the RCS is further depressurized to reach a quasi-equilibrium state with the secondary side of SG, the blow-down phase is finished.

Natural Circulation phase

The thermal quasi-equilibrium state can last for hundreds of seconds depending on the break size. Since the Reactor Coolant Pump (RCP) is shut down due to the assumption of Loss-Of-Offsite Power (LOOP), there is no forced circulation flow during this phase. The heat transfer from the primary to the secondary side is carried out by either single or two-

APR1400 DCD TIER 2

phase natural circulation. The coolant is gradually drained from the upper side of reactor coolant system. The phase separation proceeds from the upper side of U tube in SG to the reactor core upper head and then to the reactor upper plenum. The reactor core decay heat is removed via the break and SGs. The loop seal is filled with the coolant not to form the effective flow path for steam so that the steam generated in the reactor core cannot be effectively discharged.

Loop Seal Clearing phase

This phase covers from the termination of natural circulation flow until the loop seal clearing. When the coolant level in the SG side of loop seal becomes lower than the top of horizontal portion of pump suction leg, the loop seal is cleared and the steam isolated in the system is discharged through the break. Before the loop seal is cleared, the two-phase mixture level in the core can be significantly decreased to cause the reactor core uncover within short period of time. After the loop seal clearing, the pressure imbalance in the RCS disappears. The core level recovers up to the cold leg elevation.

Core Boil-Off phase

After the loop seal is cleared, the coolant in the reactor core starts to boil due to the decay heat so that the core mixture level decreases gradually. Consequently, the core uncover could happen again. At this time the cladding temperature can reach its peak value. When the safety injection flow becomes larger than the break flow as RCS pressure decreases, the core mixture level starts to recover.

Core Recovery phase

Core recovery continues from the moment when the core is at its lowest level until it is filled with SI flow. The core can be sufficiently cooled for the prolonged time in this phase by the recovered water level.

15.6.5.2.3 Description of Post Loss-of-Coolant Accident Long-Term Cooling

Immediately following a LOCA, safety injection is initiated to mitigate the short-term consequences of the event by replenishing the lost coolant. Safety injection is characterized by the automatic actuation of SIPs and the passive operation of SITs. Responses by operators are not required in the short term after a LOCA.

APR1400 DCD TIER 2

The post-LOCA long-term phase is defined as beginning when the core is reflooded and ending when the plant is secured. During the long term, operator action is needed to provide reasonable assurance that the core cooling is maintained until the plant is brought to a cold shutdown condition.

The basic function of long-term cooling (LTC) is to maintain the core at safe temperature levels while avoiding the precipitation of boric acid in the RCS. The capability of performing this basic function is reasonably assured until such time that the fuel assemblies are removed from the reactor vessel.

The analysis procedures account for single-failures to provide reasonable assurance that the performance objectives are met even with this assumption. There is a behavioral difference between large and small break LOCAs in the long term. This difference is that the RCS will remain at high pressure for small breaks and the safety injection flow rate will be too low for effective cooling; thus, small breaks require cooling of the RCS by the SGs until shutdown cooling (SDC) can be initiated. Large breaks, on the other hand, are adequately cooled by the safety injection flow because this flow is large due to the low RCS pressure; however, large breaks use simultaneous hot leg and direct vessel injection to flush boric acid from the vessel. As a consequence, the LTC large break and small break analyses are different.

15.6.5.3 Core and System Performance

15.6.5.3.1 Evaluation Model

The acceptance criteria for the emergency core cooling system (ECCS) for light water-cooled reactors are provided in 10 CFR 50.46 (Reference 62). The analyses presented in this section demonstrate that the APR1400 design satisfies these criteria.

Analyses are performed for a complete spectrum of break sizes. The most limiting break, which limits the peak linear heat generation rate (PLHGR), is identified as the 1.0 (break area) × double-ended guillotine at the pump discharge (DEG/PD) break. The results of the analyses demonstrate that for a PLHGR of 446.2 W/cm (13.6 kW/ft), the APR1400 SIS design meets the acceptance criteria of Reference 62. Requirements are as follows:

- a. Criterion 1 – Peak Cladding Temperature

APR1400 DCD TIER 2

The calculated maximum fuel element cladding temperature shall not exceed 1,204 °C (2,200 °F).

b. Criterion 2 – Maximum Cladding Oxidation

The calculated total oxidation of the cladding anywhere shall not exceed 0.17 times (17 percent) of the total cladding thickness before oxidation.

c. Criterion 3 – Maximum Hydrogen Generation

The calculated total amount of hydrogen generated from the chemical reaction of the cladding with water or steam shall not exceed 0.01 times (1 percent) the hypothetical amount that would be generated if all of the metal in the cladding cylinders surrounding the fuel, excluding the cladding surrounding the plenum volume, were to react.

d. Criterion 4 – Coolable Geometry

Calculated changes in core geometry shall be such that the core remains amenable to cooling.

e. Criterion 5 – Long-Term Cooling

After any calculated successful initial operation of the ECCS, the calculated core temperature shall be maintained at an acceptably low value, and decay heat shall be removed for the extended period of time required by the long-lived radioactivity remaining in the core.

Large Break Loss-of-Coolant Accident Evaluation Model

The large break LOCA analysis is performed using the CAREM (Reference 63) realistic evaluation methodology for the criteria of 10 CFR 50.46 (Reference 62). This methodology is based on the models and assumptions described in NRC RG 1.157 (Reference 64).

insert R~ LAP5/ ~ D3.3/ ~ ode~ a modified version of R~ LAP5/ ~ D3.3

In CAREM, the RELAP5/MOD3.3 Code (Reference 65) is used for the calculation of ECCS thermal-hydraulics behavior and cladding temperature. Containment back pressure and temperature calculations are performed by the CONTEMPT4/MOD5 Code (Reference 66). Containment back pressure is affected by the mass and energy release

APR1400 DCD TIER 2

rate, and thermal-hydraulics phenomena is dependent on the containment back pressure. RELAP5/MOD3.3 and CONTEMPT4/MOD5 are merged to exchange their results in every time step.

insert ~ / ~

CAREM quantifies the overall calculation uncertainty by propagating the uncertainty of each parameter. The ranges of uncertainty parameters are determined by auxiliary calculations and literature survey and confirmed by checking experimental data. To quantify the PCT at a 95 percent probability with a 95 percent confidence level, 124 times random sampling calculations are performed adopting non-parametric statistics. This methodology extrapolates the code accuracy to quantify the uncertainty that is applied to plant calculations.

181

A total of 124 input vectors are generated by random sampling, and simple random sampling (SRS) analyses are performed with the application of each input vector. The code uncertainty parameters and their ranges are determined by the evaluation of the code accuracy and confirmation of data covering processes. PCT is determined by applying Wilks' Formula to the SRS results in a 95 percent tolerance limit at a 95 percent confidence level.

181

Cases in which the reflood peak clad temperature differences within 100K compared with the highest reflood peak are selected for scale bias calculations, extracting the highest two cases from 124 cases of SRS. Code biases in the prediction of ECC water bypass and steam binding are evaluated separately. Steam binding bias is evaluated by combining the results of two bias evaluations of droplet de-entrainment in the upper plenum of the reactor vessel and droplet evaporation in the steam generator U-tube. The final values of the third PCT considering the uncertainties of the automatic time step control function and data reading frequency of RELAP5/MOD3.3/K are suggested for the comparison of LOCA criteria.

181

Small Break Loss-of-Coolant Accident Evaluation Model

The calculations presented in this section are performed using the small break evaluation model, which is described in Reference 67 and approved by the Nuclear Regulatory Commission (NRC) in Reference 68. The CEFLASH-4AS (Reference 69) computer program is used to determine the primary system hydraulic parameters during the blowdown phase, and the COMPERC-II (Reference 70) computer program is used to determine the system behavior during the reflood phase. Fuel rod temperatures and clad

APR1400 DCD TIER 2

oxidation percentages are calculated using the STRIKIN-II (Reference 71) and PARCH (Reference 72) computer programs. The interface between these programs is described in detail in Reference 67.

The small break evaluation model already met the requirements of TMI action item II.K.3.30 and II.K.3.31. Details are respectively described in Reference 23 and Section 15.6.5.3.

Post Loss-of-Coolant Accident Long-Term Cooling Evaluation Model

Long-term cooling (LTC) initiates when the core is quenched after a LOCA and terminates when the plant is secured. The objectives of LTC are to maintain the core at safe temperature levels and to avoid the precipitation of boric acid in the core region. To accomplish these objectives, an LTC analysis was performed using the codes and methods documented in Reference 73.

The LTC plan uses one of two procedures depending on the break area. The shutdown cooling system (SCS) is used if the break is sufficiently small that reasonable assurance of a successful operation of the SCS is provided. For large break LOCAs, a simultaneous hot leg and direct vessel injection is used to maintain core cooling and boric acid flushing. The plant operator initiates the appropriate procedure based on the indicated RCS pressure.

Figure 15.6.5-34 shows the LTC sequence of events and the schedule for operator actions for the LTC plan. The operator's first action is to initiate cooldown within 1 hour post-LOCA by releasing steam from the SGs. The steam is released through the turbine bypass system if available or through the atmospheric dump valves. Between 1 and 3 hours post-LOCA, the operator isolates or vents the safety injection tanks (SITs) to avoid injecting a large quantity of nitrogen (noncondensable) gas into the RCS. Between 1 and 4 hours post-LOCA, pressurizer depressurization is initiated. Between 2 and 3 hours post-LOCA, the discharge lines of SIP 3 and 4 are realigned to the hot legs to divide the SIP flow between the hot leg and direct vessel injection connections.

If the RCS pressure is above 31.6 kg/cm²A (450 psia) between 8 to 9 hours post-LOCA, the RCS is filled, which provides reasonable assurance that proper suction is available for entering shutdown cooling. Cooling of the RCS continues until the indicated RCS temperature is lower than the maximum SDC entry temperature including instrument uncertainty. The operator then throttles the SIPs until the RCS pressure is reduced to

APR1400 DCD TIER 2

shutdown cooling entry pressure, including instrument uncertainty, and initiates shutdown cooling.

A prerequisite to throttling or terminating SI flow is that the RCS is in a subcooled condition for the indicated RCS pressure. While reducing RCS pressure to initiate SCS operation, the operator maintains subcooling of the RCS consistent with the emergency operating procedures.

If the SCS is inoperable, the alternative for decay heat removal is the continued use of the SGs. This requires the continued availability of auxiliary feedwater and the atmospheric dump valves or the turbine bypass system. If the SCS becomes operable later, it is put into operation. This path is indicated by the dashed lines in Figure 15.6.5-34.

If the indicated RCS pressure falls below 31.6 kg/cm²A (450 psia) at 8 to 9 hours, the break may be too large for absolute assurance that proper suction is available for the shutdown cooling mode. In this event, a simultaneous hot leg and direct vessel injection by itself cools the core and also flushes the reactor vessel indefinitely.

15.6.5.3.2 Input Parameters and Initial Conditions

Large Break Loss-of-Coolant Accident

The SIS consists of four safety injection pumps (SIPs) and four safety injection tanks (SITs). Automatic operation of the SIPs is actuated by a low pressurizer pressure signal or a high containment pressure signal. Flow is initiated from the SITs by the opening of a check valve when the reactor vessel downcomer pressure drops below the SIT pressure. A fixed internal device in the SIT regulates the flow rate with changing level and pressure. SI flow is delivered by DVI connections.

The most limiting single failure for a large break LOCA is the loss of one SIP train. However, two of the four SIPs are conservatively assumed to be available. The available SIP injection located near the broken cold leg with another available injection located on the opposite side of broken cold leg is used for the large break LOCA analysis.

The operating parameters and ranges for the plant uncertainty evaluation determined in large break LOCA analysis are listed in Table 15.6.5-1. Core and system parameters are prepared by using measurement uncertainty ranges or determined to cover the minimum and maximum ranges of the design data or the limit of the Technical Specifications.

described in Reference 63

~ urnu~ sensitivit~ stud~ to determine the limiting ~ urnu~ is introduced ~ considering T~ D effects. In addition~ since determination of the limiting ~ rea~ si~ e could ~ e affected ~ ~ urnu~ ~ r~ ea~ si~ e sensitivit~ ~ ith various ~ urnu~ cases are evaluated.

The large break LOCA analysis accounts for 10 percent tube plugging of the steam generator tubes that may occur during the life of the plant.

~~The accidents are assumed to occur at the initial burnup for the large break LOCA analysis. The stored energy is the maximum value because the fuel elements show the most densification at the initial burnup (BOC), and the burnup yields the highest cladding temperature in the large break LOCA.~~

Subsection 6.2.1.5 presents the minimum containment pressure analysis that is performed in the analysis of ECCS performance. The analysis identifies the containment parameters used in the large break analysis. The values for the containment parameters are chosen to minimize containment pressure to minimize the core reflood rate.

insert~ ~ ith the ~ urnu~ of 27~000 ~ ~ d~ TU

The worst break in the large break LOCA analysis is the double-ended guillotine at the pump discharge leg (Reference 63). To determine the limiting break area, a guillotine break spectrum of 100 percent, 80 percent, and 60 percent break areas is analyzed, and the limiting break area is applied for 124 cases of SRS calculation.

Small Break Loss-of-Coolant Accident

181

insert~ ~ ith various ~ urnu~

The safety injection system (SIS) consists of four direct vessel injection lines, each supplying flow from one SIT and one SIP. Offsite power is conservatively assumed to be lost upon reactor trip, and the SIPs therefore await diesel generator startup and load sequencing before they can start. The total time delay assumed is 40 seconds from when the SIAS setpoint is reached to when the full SI flow is delivered to the RCS. For breaks in the DVI line, all safety injection flow delivered to the broken line is assumed to spill out of the break.

An analysis of the possible single failures that can occur within the SIS shows that the worst single failure for the small break spectrum is the failure of one SIP train. However, two of the four SIPs are conservatively assumed to be available, thereby minimizing the safety injection available to cool the core.

Based on the above assumptions, the following safety injection flows are credited for the small break LOCA analysis:

- a. For a break in the pump discharge leg, the SI flow credited is full flow from two SIPs and four SITs.

APR1400 DCD TIER 2

- b. For a break in a DVI line, the SI flow credited is full flow from one SIP and three SITs. The flow from the remaining active SIP and from one SIT is assumed to spill out of the break.

Table 15.6.5-6 presents the SIP flow rates assumed at each of the four injection points as a function of RCS pressure.

The significant core and system parameters used in the small break LOCA calculations are presented in Table 15.6.5-7. PLHGR of 492.1 W/cm (15.0 kW/ft) is assumed to occur about 15 percent from the top of the active core. A conservative beginning-of-life moderator temperature coefficient of $0.0 \times 10^{-4} \Delta\rho/^{\circ}\text{C}$ ($0.0 \times 10^{-4} \Delta\rho/^{\circ}\text{F}$) was used in all small break LOCA calculations.

The initial steady-state fuel rod conditions are obtained from the FATES3 (Reference 74) computer program. The small break LOCA analysis uses a hot rod average burnup, which maximizes the amount of stored energy in the fuel.

The small break LOCA analysis uses the containment parameters of the initial containment pressure and the maximum containment volume. Containment parameters do not influence the small break LOCA analysis because the break flow stays critical.

Post Loss-of-Coolant Accident Long-Term Cooling

The major assumptions used in performing the LTC analysis are as follows:

- a. No offsite power is available.
- b. The worst single failure is the loss of two SIP trains with additional conservativeness. This results in the following:
 - 1) Two SIPs are operable.
 - 2) One motor-driven auxiliary feedwater pump is operable.
- c. One atmospheric dump valve on each SG is available to cool down the RCS.
- d. RCS cooldown begins at 2 hours post-LOCA.
- e. The SITs are vented or isolated before establishing shutdown cooling conditions for the small break LTC procedure.

APR1400 DCD TIER 2

- f. The pressurizer is depressurized to establish shutdown cooling conditions for the small break LTC procedure.
- g. RCS cooldown is terminated when the hot leg temperature is below the maximum shutdown cooling entry temperature including instrument uncertainty.
- h. Pump flow rates and initial water source inventories used in the large break LOCA boric acid precipitation analysis are selected to maximize the boric acid concentration in the core.
- i. A boric acid precipitation limit of 29.3 weight percent (Reference 73) is used in the large break LOCA boric acid precipitation analysis. This limit is based on a conservative containment pressure of 1.03 kg/cm²A (14.7 psia).

Significant core and system parameters used in the post-LOCA long-term cooling analysis are presented in Table 15.6.5-12.

The IRWST sump strainer related to GSI-191 is designed to provide reasonable assurance that debris quantities are maintained within the bounds of a post-LOCA long-term cooling analysis. See Subsection 6.8.4.5 for further information.

15.6.5.3.3 Results

Large Break Loss-of-Coolant Accident Analysis Results

Major input variables used in the performance evaluation of the SIS in a large break LOCA are summarized in Table 15.6.5-2. The important results such as the PCT, PCT location, and time results for large break LOCA spectrum analyses are listed in Table 15.6.5-3. Major times of interest are listed in Table 15.6.5-4. The transient behaviors of the NSSS parameters are shown in Figures 15.6.5-2 through 15.6.5-23.

The most limiting break area is a 100 percent of double-ended guillotine at the pump discharge break. Hence, a SRS calculation is performed for a 100 percent double-ended guillotine break at the pump discharge leg.

The cladding temperature behavior result obtained from 124 times SRS calculations is shown in Figure 15.6.5-23. In the 124 times calculations, the highest two PCT cases are excluded. The third highest PCT is 991.3 °C (1,816.4 °F) and maximum cladding oxidation is 3 percent with exceeding the 95 percent at 95 percent confidence level.

The third highest PCT is occurred during reflood phase and the PCTs are increased by the biases. The total PCT bias is evaluated as +9.8 °C and the peak local oxidation and hot rod hydrogen generation are confirmed not to increase by the scale bias calculations. Therefore the final PCT (w/ BIAS) is 1,019.7 °C (1,867.5 °F) and the maximum cladding oxidation (w/ BIAS) is 6.30 percent as shown in Table 15.6.5-4.

The cases in which the clad temperature differences in the second peak are within 100 °C (180 °F) compared with the highest second peak are selected for scale bias calculations. Code biases in the prediction of ECC water bypass and steam binding are evaluated separately. Steam binding bias is evaluated by combining the results of two separate bias evaluations of droplet de-entrainment in the upper plenum of the reactor vessel and droplet evaporation in the steam generator U-tube. Even though reflood cladding temperatures are increased by the biases, they do not exceed the blowdown PCT of 991.3 °C (1,816.4 °F). Total PCT bias is evaluated as +0 °C, as shown in Table 15.6.5-5. The maximum cladding oxidation with bias evaluation is 3 percent as shown in Table 15.6.5-5.

Uncertainties from sources other than code models or plant operation conditions, such as automatic time step control function and data reading frequency of RELAP5/MOD3.3/K, are considered of maximum 10 °C (18 °F). The hot rod average oxidation is calculated lower than one percent. The final PCT, maximum cladding oxidation, and core-wide hydrogen generation combining all the biases are as follows:

$$\begin{aligned}\text{Peak cladding temperature} &= 991.3\text{ °C} + 10\text{ °C} \\ &= 1,001.3\text{ °C (1,834.3 °F)} \\ &= 1,274.5\text{ K} < 1,477.15\text{ K (2,200 °F)}\end{aligned}$$

$$\text{Maximum cladding oxidation} = 3.09\% < 17\%$$

$$\text{Maximum hydrogen generation} \ll 1\%$$

The highest cladding temperature in the large break LOCA analysis is 1,001.3 °C (1,834.3 °F), which is 202.7 °C (365.7 °F) lower than the acceptance criterion of 1,204 °C (2,200 °F).

The final PCT considering the effect of thermal conductivity degradation is still satisfied the acceptance criteria. Details are given in Reference 78. The PCT increase is ended when the core is maintaining a coolable geometry. The heat generated from the fuel is able to be removed properly for a long period.

Based on the results of this analysis, it is concluded that the APR1400 ECCS satisfies the all SRP acceptance criteria of References 62 and 64 (Subsection 15.0.5) for a complete spectrum of large break LOCAs and is adequate to perform its intended function of maintaining the integrity of the core, thereby limiting radiation release to the environment.

APR1400 DCD TIER 2Small Break Loss-of-Coolant Accident Analysis Results

The nine breaks analyzed at 4,062.66 MWt, 102 percent of nominal, include reactor coolant pump discharge leg breaks ranging in size from 465 cm² (0.5 ft²) to 46.5 cm² (0.05 ft²) and DVI line breaks from 372 cm² (0.4 ft²) to 18.6 cm² (0.02 ft²). One break, equal in area to a fully open POSRV, 27.9 cm² (0.03 ft²), is postulated to occur in the top of the pressurizer. Table 15.6.5-8 lists the various break sizes and locations examined for this analysis.

The transient behavior of important NSSS parameters is shown in the figures listed in Table 15.6.5-9. Table 15.6.5-10 summarizes the important results of this analysis. Times of interest for the various breaks analyzed are presented in Table 15.6.5-11. A plot of PCT versus break size is presented in Figure 15.6.5-33. The 372 ft² (0.4 ft²) DVI break results in the highest cladding temperature 624 °C (1,156 °F) of the small breaks analyzed, which is 580 °C (1,044 °F) lower than the acceptance criteria of 1,204 °C (2,200 °F). Of the pump discharge leg and DVI line break locations, the DVI line break is limiting due to the assumed loss of all safety injection flow to the broken line.

For the DVI line break location, as the break size becomes progressively smaller than 372 cm² (0.4 ft²), the inner vessel two phase level follows a definite pattern:

- a. The time of initial core uncover is later.
- b. The depth of core uncover is less.
- c. The rate of level decrease and increase becomes slower.

This trend continues until the core does not uncover at all. These trends predictably affect the PCT.

As the break size decreases, both the later time of the initial core uncover and the shallower depth of uncover tend to mitigate the temperature transient. This trend continues until the core does not uncover as typified by the 18.6 cm² (0.02 ft²) break. By analyzing several break sizes over this range, the behavior of PCT versus break size is adequately determined.

The above behavior of core uncover with break size results from the design characteristics of the SIS. For DVI break sizes below 93 cm² (0.1 ft²), the RCS pressure remains above the SIT pressure and coolant flow injection to the reactor vessel is accomplished entirely by

APR1400 DCD TIER 2

one SIP. For break sizes greater than 93 cm^2 (0.1 ft^2), the transient is terminated by the action of both the SITs and SIPs.

For the cold leg breaks, the additional SIS flow resulting from being able to credit two SIPs precludes core uncover to break sizes up to 93 cm^2 (0.1 ft^2). In addition, the core uncover for break sizes greater than 93 cm^2 (0.1 ft^2) is delayed, and the depth and duration of uncover decreased relative to DVI breaks, which credit only one SIP. This more favorable behavior results in lower cladding temperatures relative to breaks in a DVI line.

In addition to the break locations described above, the rupture of an in-core instrument tube is considered. A break equal in size to a completely severed instrument tube (2.8 cm^2 [0.003 ft^2]) is postulated to occur in the reactor vessel bottom head.

Following rupture, the primary system depressurizes until a reactor scram signal and safety injection actuation signal (SIAS) are generated due to low pressurizer pressure at $109.3 \text{ kg/cm}^2\text{A}$ ($1,555 \text{ psia}$). The assumed LOOP causes the primary coolant pumps and the feedwater pumps to coast down. After the 40-second delay, required to actuate the emergency diesel and the SIPs following the SIAS, safety injection flow is initiated to the RCS. Four SITs are available but do not inject due to the high RCS pressure.

The primary side depressurization continues accompanied by a rise in secondary side pressure until the secondary side pressure reaches the lowest setpoint of the steam generator safety valves. The primary system pressure continues to fall until it is just slightly greater than the secondary side pressure. At this point, the flow from the two operating SIPs (63 kg/sec [139 lbm/sec]) exceeds the leak flow (12 kg/sec [26 lbm/sec]). Therefore, the RCS fills. The decay heat generated in the core is removed in the SGs by steam flow through the secondary side safety valves. The core remains covered and cooled in this condition.

Based on the results of this analysis, it is concluded that the APR1400 ECCS satisfies the all SRP acceptance criteria of References 1 and 62 (Subsection 15.0.5) for small break LOCAs.

Post Loss-of-Coolant Accident Long-term Cooling Evaluation Results

An evaluation of the various break locations showed that the double-ended ($9,104.5 \text{ cm}^2$ [9.8 ft^2]) cold leg break was confirmed to be the limiting break geometry for the boric acid precipitation analysis (Reference 73). The long-term loop seal refilling with a slot break at the top of the cold leg does not significantly affect the boric acid precipitation analysis.

APR1400 DCD TIER 2

For a cold leg break, the core flushing flow is the difference between the hot leg injection flow rate and the core boiloff rate. The initiation of a simultaneous hot leg and direct vessel SIP injection flow at 3 hours post-LOCA provides a substantial and time-increasing core flushing flow as shown in Figure 15.6.5-35. Figure 15.6.5-36 shows that with no core flushing flow, boric acid does not begin to precipitate until 3.2 hours post-LOCA. The margin provided for the prevention of boric acid precipitation by the core flushing flow of 113.6 L/min (30 gpm) is also shown in Figure 15.6.5-36. The analyses also show that all hot leg steam entrainment of injection water is terminated in less than 3 hours post-LOCA. When the operator initiates simultaneous hot leg and direct vessel injection by 3 hours, there is no potential for the hot leg entrainment and boric acid precipitation.

The left branch of the LTC plan in Figure 15.6.5-34 applies to the break areas for which the RCS refills. The LTC analysis predicts that the RCS will refill at various times depending on break area, as shown in Figure 15.6.5-37. As shown, for a break area as large as 37.2 cm² (0.04 ft²), the RCS refills within 8 hours. The LTC analysis determines that more than 14 hours is required to exhaust all of the auxiliary feedwater during cooldown of the RCS. To allow a substantial time margin to avoid exhausting the auxiliary feedwater, a period of 8 to 9 hours is selected for the operator to decide whether the small break LTC procedure is appropriate. These results demonstrate that breaks as large as 37.2 cm² (0.04 ft²) are able to use SCS for the long-term cooling and flushing of the core. The LTC analysis determines that the large break procedures can flush the core for break areas down to 3.7 cm² (0.004 ft²). The overlap in break areas for which either the large break or small break procedures can be used is illustrated in Figure 15.6.5-38.

The operator chooses the appropriate procedure on the basis of the indicated RCS pressure between 8 and 9 hours. Figure 15.6.5-38 lists the RCS pressure at 8 hours for a wide range of break areas, and Figure 15.6.5-39 presents this information graphically. The decision pressure is selected as 31.6 kg/cm²A (450 psia) so that, with consideration of the maximum RCS pressure measurement error up to ± 21.1 kg/cm² (± 300 psia), reasonable assurance is provided that the operator selects the proper procedure for any break area.

The natural circulation cooldown analysis that is performed as part of the LTC analysis determines that the SCS entry temperature of 193 °C (380 °F) is reached at approximately 6.7 hours after the start of the LOCA. The analysis simulates a conservatively slow cooldown rate and consequently, a maximum value for the earliest time that the SCS entry temperature is reached. The analysis takes credit only for safety grade systems, namely, the safety injection system, the auxiliary feedwater system, and the atmospheric dump

APR1400 DCD TIER 2

valves. Reaching the SCS entry temperature at 6.7 hours leaves sufficient time for the operator to depressurize the RCS to the SCS entry pressure and initiate shutdown cooling.

Based on the results of this analysis, it is concluded that the APR1400 ECCS satisfies the all SRP acceptance criteria of References 1 and 62 (Subsection 15.0.5) for LTC.

15.6.5.4 Barrier Performance

In Section 6.2, the barrier performance is described in detail, and the containment vessel pressure that affects the performance of the barriers is evaluated.

15.6.5.5 Radiological Consequence

The radiological consequences for large break LOCAs are performed to determine the post-LOCA doses at the EAB, LPZ, MCR, and TSC using the AST guidance in NRC RG 1.183, plant-specific design inputs, and TEDE dose criteria for the following post-LOCA release paths:

- a. Containment leakage
- b. Engineered safety feature (ESF) leakage
- c. Low volume purge release
- d. Back leakage to the IRWST leakage

The following regulatory requirement and guidance are applied as the acceptance criteria for the receptors at EAB, LPZ, MCR, and TSC:

- a. NRC RG 1.183
- b. 10 CFR 50.34
- c. Standard Review Plan, Subsection 15.0.3

15.6.5.5.1 Evaluation Model

For the design basis LOCA, all fuel assemblies in the core are assumed to be affected, and the maximum core fission product inventory is used. The maximum core fission product inventories are listed in Appendix 15A, Table 15A-1. The remaining isotopes are not

APR1400 DCD TIER 2

Table 15.6.5-1

Uncertainty Parameter Ranges and Distributions

| No. | Parameter | Distribution | Parameter Ranges | | Component |
|-----|-----------------------------|--------------|------------------|----------|----------------|
| | | | Min. | Max | |
| 1 | Fq | Uniform | 1.94 | 2.41 | Fuel |
| 2 | Gap conductance | Uniform | 0.75 | 1.50 | |
| 3 | Fuel conductivity | Normal | 0.8455 | 1.1545 | |
| 4 | Core power | Normal | 0.9691 | 1.0309 | |
| 5 | Decay heat | Normal | 0.89803 | 1.10197 | |
| 6 | Burst temperature dial | Uniform | 0.90 | 1.10 | |
| 7 | Burst strain dial | Uniform | 0.30 | 1.70 | |
| 8 | Oxidization dial | Normal | 0.961 | 1.039 | |
| 9 | Groeneveld CHF dial | Normal | -0.17111 | 2.17111 | Core |
| 10 | Chen nucleate boiling dial | Normal | 0.382 | 1.618 | |
| 11 | Zuber CHF dial | Normal | 0.5365 | 1.4635 | |
| 12 | Dittus Boelter, liquid dial | Normal | 0.606025 | 1.393975 | |
| 13 | Dittus Boelter, vapor dial | Normal | 0.606025 | 1.393975 | |
| 14 | Bromley dial | Normal | 0.42835 | 1.57165 | |
| 15 | Weber number dial | Uniform | 1.350 | 7.0 | |
| 16 | F. Rohsenow dial | Uniform | 0.5 | 1.5 | |
| 17 | Weismann dial | Uniform | 0.40 | 1.60 | |
| 18 | 1-Phase Cd | Normal | 0.7821 | 0.9979 | |
| 19 | 2-Phase Cd | Normal | 0.7026 | 1.4374 | |
| 20 | Pump K-factor | Uniform | 0.239 | 0.577 | Loop |
| 21 | Pump head multiplier | Uniform | 0.0 | 1.0 | |
| 22 | Pump torque multiplier | Uniform | 0.0 | 1.0 | |
| 23 | Pressurizer pressure, bar | Normal | 152.47 | 157.80 | Pressurizer |
| 24 | SIT pressure, bar | Uniform | 40.31 | 44.59 | SIT/Cold Leg |
| 25 | SIT water volume, m3 | Uniform | 50.69 | 54.57 | |
| 26 | SIT water temp, K | Uniform | 283.0 | 321.9 | |
| 27 | SIP flow multiplier | Uniform | -0.5 | 0.5 | |
| 28 | IRWST water temp, K | Uniform | 283.0 | 321.9 | |
| 29 | Thermal Conductivity | Uniform | 1.0 | 2.0 | Downcomer Wall |
| 30 | Heat Capacity | Uniform | 1.0 | 1.5 | |

APR1400 DCD TIER 2

Table 15.6.5-2 (1 of 2)

General System Parameters and Initial Conditions for Large Break ECCS Performance

| Plant Parameters | Reference Conditions |
|---|----------------------|
| Core | |
| 1. Core power, MWt | 3,983 |
| 2. Power peaking factor | 2.258 ← 2.184 |
| 3. Fuel type | 16 × 16 |
| 4. Power output pattern | Figure 15.6.5-1 |
| 5. Decay heat | ANS79 model |
| Reactor Coolant System | |
| 1. Initial core flow rate, kg/hr | 73.3×10^6 |
| Pressurizer | |
| 1. Pressure, bar | 155.1 |
| Steam Generator | |
| 1. Feedwater temperature, K | 505.23 |
| 2. Tube plugging rate, % | 10 |
| Safety Injection System | |
| 1. Safety injection tank coolant volume, m ³ | 52.63 ← 52.61 |
| 2. Safety injection tank gas pressure, bar | 42.45 ← 43.07 |
| 3. Safety injection tank coolant temperature, K | 302.5 ← 302.59 |
| 4. FD K-factor for high injection flow (including piping K) | 25 ← 10 |
| 5. FD K-factor for low injection flow (including piping K) | 120 ← 80 |
| 6. IRWST temperature, K | 302.5 ← 302.59 |

APR1400 DCD TIER 2

Table 15.6.5-2 (2 of 2)

| Plant Parameters | Reference Conditions |
|---|----------------------|
| Containment Building | |
| 1. Initial pressure, bar | 0.98 |
| 2. Initial temperature, K | 283.15 |
| 3. Net Free volume, m ³ | 97,239 |
| 4. Number of spray | 2 |
| 5. Delay time for spray actuation, sec | 0 |
| 6. Spray flow rate (2 pumps), L/min (gpm) | 37,853 |

Replace with next page C

APR1400 DCD TIER 2

Table 15.6.5-3

Summary of Fuel Rod Performance for Break Spectrum of Large Break LOCA

| | Variable | 100 % Break | 80 % Break | 60 % Break |
|--------------------------------------|-----------------|-------------|------------|------------|
| Blowdown | PCT, °C | 892.0 | 870.0 | 768.9 |
| | PCT Location, m | 2.57 | 2.57 | 2.76 |
| | PCT Time, sec | 6.5 | 36.5 | 36.5 |
| Reflood | PCT, °C | 798.9 | 869.5 | 762.5 |
| | PCT Location, m | 2.57 | 2.76 | 2.76 |
| | PCT Time, sec | 36.5 | 64.0 | 71.5 |
| Peak Local Oxidation, % | | 1.50 | 1.92 | 1.24 |
| Peak Zr-H ₂ O location, m | | 2.57 | 2.76 | 2.76 |
| Maximum Hydrogen Generation, % | | < 1.0 | < 1.0 | < 1.0 |
| Hot Fuel Rod Rupture | | N/A | N/A | N/A |

C

Table 15.6.5-2

Summary of Fuel Rod Performance for Break Spectrum of Large Break LOCA

| Variable | | 100 % Break | 80 % Break | 60 % Break |
|--------------------------------------|-----------------|-------------|------------|------------|
| Burn-Up | | 27,000 | 27,000 | 0 |
| Blowdown | PCT, °C | 896.8 | 847.7 | 633.4 |
| | PCT Location, m | 2.76 | 2.76 | 2.76 |
| | PCT Time, sec | 7.2 | 9.2 | 2.7 |
| Reflood | PCT, °C | 846.8 | 887.3 | 796.4 |
| | PCT Location, m | 2.57 | 2.76 | 2.76 |
| | PCT Time, sec | 92.5 | 80.5 | 87.5 |
| Peak Local Oxidation, % | | 2.661 | 2.860 | 0.560 |
| Peak Zr-H ₂ O location, m | | 2.19 | 2.57 | 2.76 |
| Maximum Hydrogen Generation, % | | < 1.0 | < 1.0 | < 1.0 |
| Hot Fuel Rod Rupture | | 28.8 | 27.8 | N/A |

Replace with next page D

APR1400 DCD TIER 2

Table 15.6.5-4

Sequence of Events for Representative Large Break LOCA

| EVENT | 100 % Break (sec) | 80 % Break (sec) | 60 % Break (sec) |
|--|----------------------|---------------------|---------------------|
| Break Occurs | 0 | 0 | 0 |
| Reactor Trip signal Occurs | 6.2 | 6.2 | 7.3 |
| SI Injection signal Occurs | 6.2 | 6.2 | 7.3 |
| SIT Discharge Begins | | | |
| SIT 1 (Broken Cold Leg Side) | 14.4 | 16.2 | 22.2 |
| SIT 2 (Broken Loop Intact Cold Leg Side) | 14.4 | 16.2 | 22.2 |
| SIT 3 (Intact Loop Intact Cold Leg Side 1) | 14.4 | 16.2 | 22.2 |
| SIT 4 (Intact Loop Intact Cold Leg Side 2) | 14.4 | 16.2 | 22.2 |
| Pumped SI Injection | 46.2 | 46.2 | 46.4 |
| Core Water Level Recovery | 44.2 | 40.6 | 45.5 |
| SIT Empty Time | | | |
| SIT 1 (Broken Cold Leg Side) | 201.5 | 207.5 | 206.7 |
| SIT 2 (Broken Loop Intact Cold Leg Side) | 201.5 | 207.5 | 206.8 |
| SIT 3 (Intact Loop Intact Cold Leg Side 1) | 201.5 | 207.5 | 206.7 |
| SIT 4 (Intact Loop Intact Cold Leg Side 2) | 201.5 | 207.5 | 206.6 |

D

Table 15.6.5-3

Sequence of Event for Representative Large Break LOCA

| EVENT | 100 % Break(sec) | 80 % Break(sec) | 60 % Break(sec) |
|--|---------------------|--------------------|--------------------|
| Break Occurs | 0 | 0 | 0 |
| Reactor Trip signal Occurs | 9.51 | 9.57 | 9.77 |
| SI Injection signal Occurs | 9.51 | 9.57 | 9.77 |
| SIT Discharge Begins | | | |
| SIT 1 (Broken Cold Leg Side) | 14.8 | 16.6 | 20.1 |
| SIT 2 (Broken Loop Intact Cold Leg Side) | 14.8 | 16.6 | 20.1 |
| SIT 3 (Intact Loop Intact Cold Leg Side 1) | 14.8 | 16.6 | 20.1 |
| SIT 4 (Intact Loop Intact Cold Leg Side 2) | 14.8 | 16.6 | 20.1 |
| Pumped SI Injection | 48.36 | 48.42 | 48.62 |
| Core Water Level Recovery | 32.5 | 35.5 | 43.0 |
| SIT Empty Time | | | |
| SIT 1 (Broken Cold Leg Side) | 171.4 | 178.7 | 177.9 |
| SIT 2 (Broken Loop Intact Cold Leg Side) | 171.5 | 178.8 | 177.9 |
| SIT 3 (Intact Loop Intact Cold Leg Side 1) | 171.4 | 178.7 | 177.9 |
| SIT 4 (Intact Loop Intact Cold Leg Side 2) | 171.5 | 178.7 | 177.9 |

Replace with next page E

APR1400 DCD TIER 2

Table 15.6.5-5

Summary of SRS and Bias Evaluation Results

| Peak Cladding Temperature (PCT) | | Value, °C |
|---|----------------------------|----------------------|
| SRS Results | Highest PCT | 991.3 |
| | Highest Reflood PCT | 982.9 |
| Scale BIAS Evaluation Results | Final BIAS Reflood PCT | 982.9 |
| | Max. BIAS Case Reflood PCT | 982.9 |
| | – ECC Bypass BIAS | +0.0 |
| | – Steam Binding BIAS | +0.0 |
| Final PCT (w/ BIAS) | | 991.3 ⁽¹⁾ |
| Max. Cladding Oxidation | | Value, % |
| SRS Results | Max. Cladding Oxidation | 3.00 |
| Scale BIAS Evaluation Results | Final BIAS Oxidation | 3.09 |
| | Max. BIAS Case Oxidation | 2.56 |
| | – ECC Bypass BIAS | +0.14 |
| | – Steam Binding BIAS | +0.39 |
| Final Max. Cladding Oxidation (w/ BIAS) | | 3.09 |

- (1) The final PCT with considering thermal conductivity degradation effect is still satisfied the acceptance criteria.

E

Table 15.6.5-4

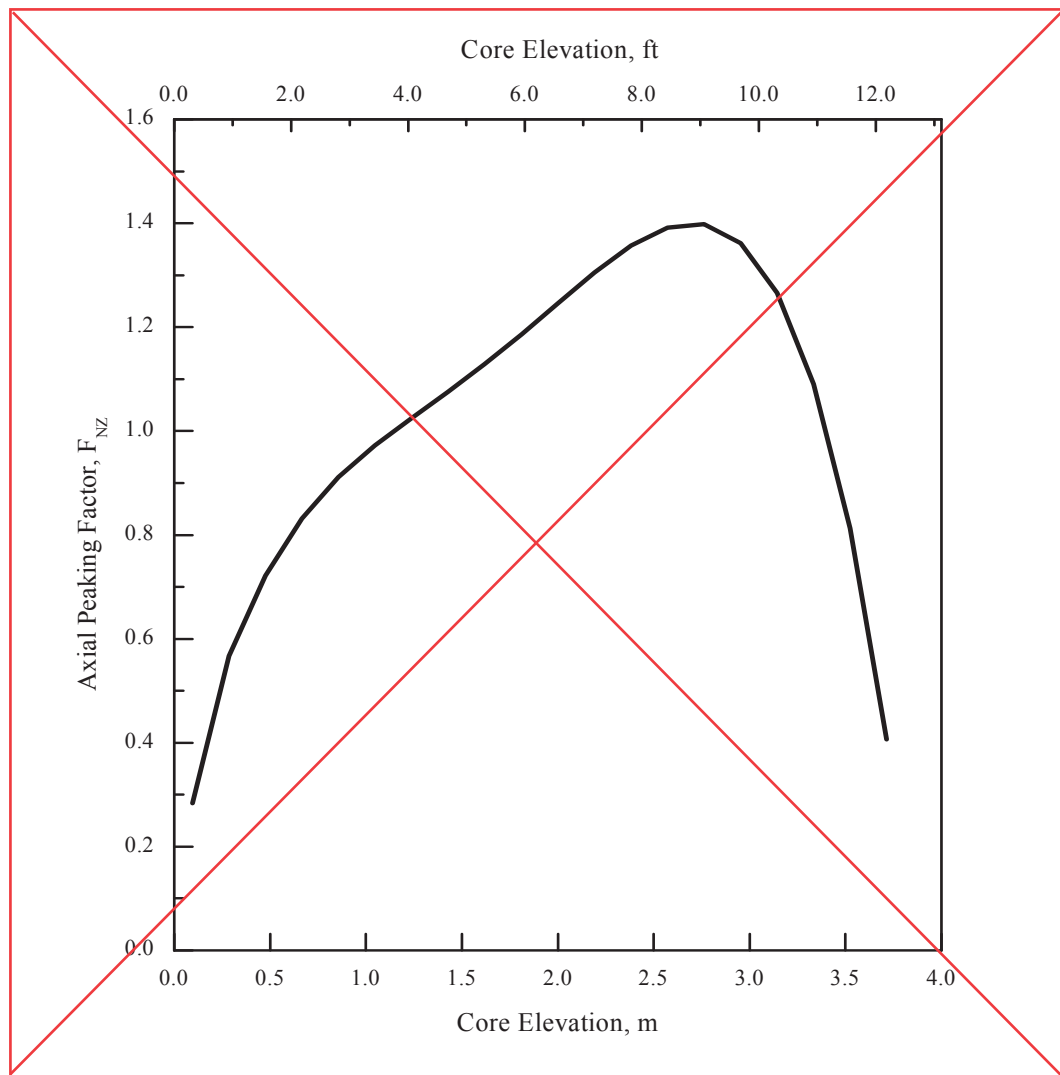
Summary of SRS and Bias Evaluation Results

| Peak Cladding Temperature (PCT) | | Value, °C |
|---|------------------------------------|-----------------------|
| SRS Results | Highest PCT | 1,009.9 |
| | Highest Reflood PCT | 1,009.9 |
| Scale BIAS Evaluation Results | Final BIAS Reflood PCT | 1,019.7 |
| | Max. BIAS Case Reflood PCT | 1,009.9 |
| | - ECC Bypass BIAS | +9.8 |
| | - Steam Binding BIAS | +0.0 |
| Final PCT (w/ BIAS) | | 1,019.7 ¹⁾ |
| Max. Cladding Oxidation | | Value, % |
| SRS Results | Max. Cladding Oxidation | 6.30 |
| Scale BIAS Evaluation Results | Final BIAS Max. Cladding Oxidation | 6.30 |
| | Max. BIAS Case Cladding Oxidation | 6.30 |
| | - ECC Bypass BIAS | +0.0 |
| | - Steam Binding BIAS | +0.0 |
| Final Max. Cladding Oxidation (w/ BIAS) | | 6.30 |

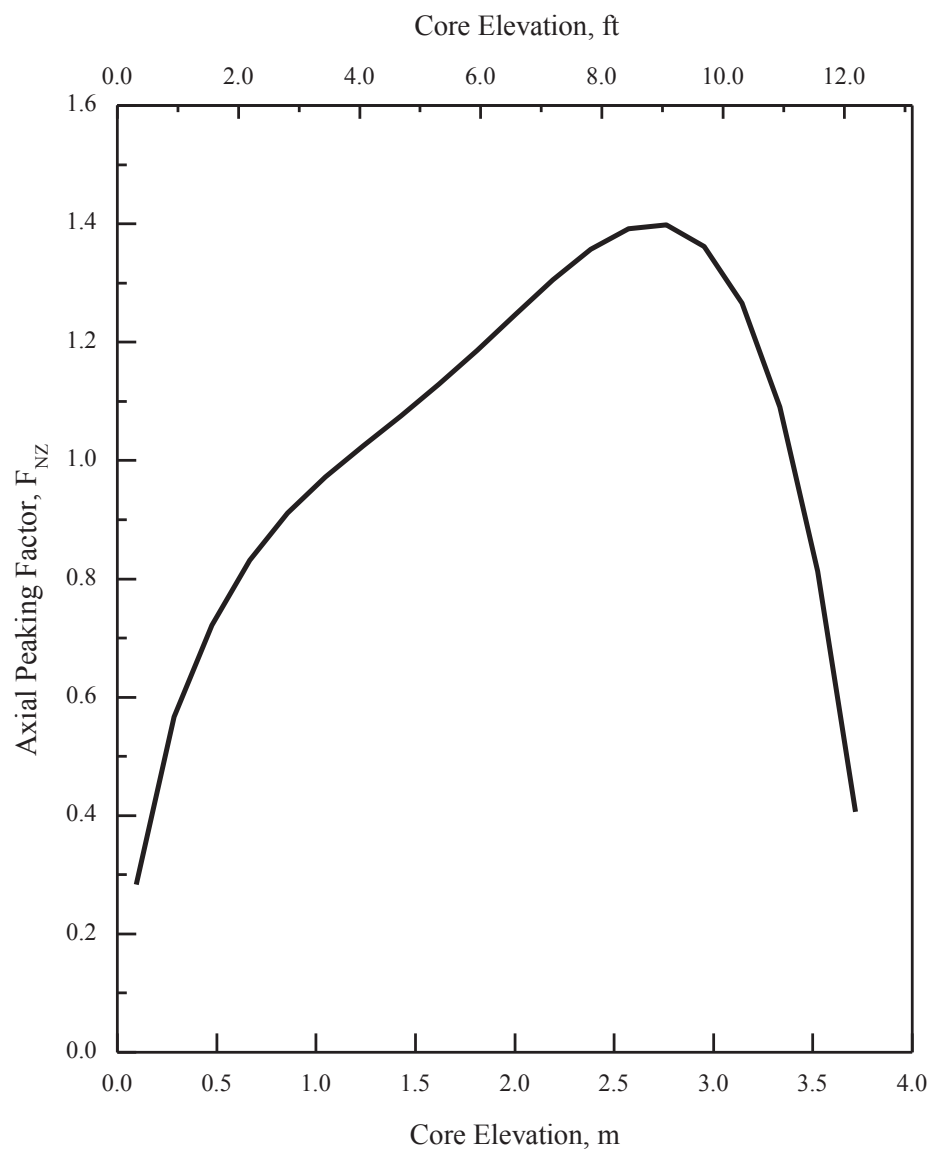
(1) The final PCT with considering thermal conductivity degradation effect is still satisfied the acceptance criteria.

APR1400 DCD TIER 2

Replace with next page F

**Figure 15.6.5-1 Axial Power Distribution at Large Break**

F



APR1400 DCD TIER 2

Replace with next page G

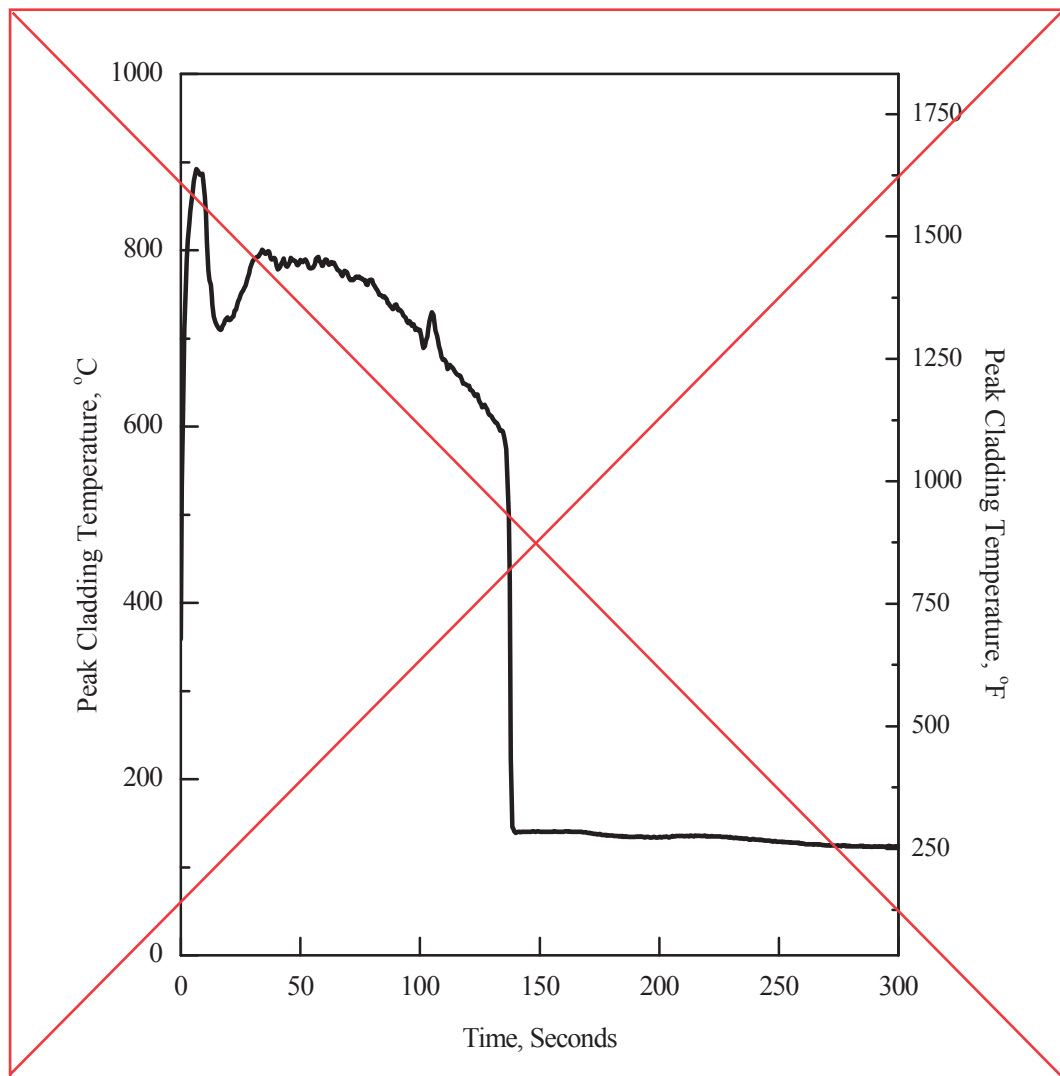
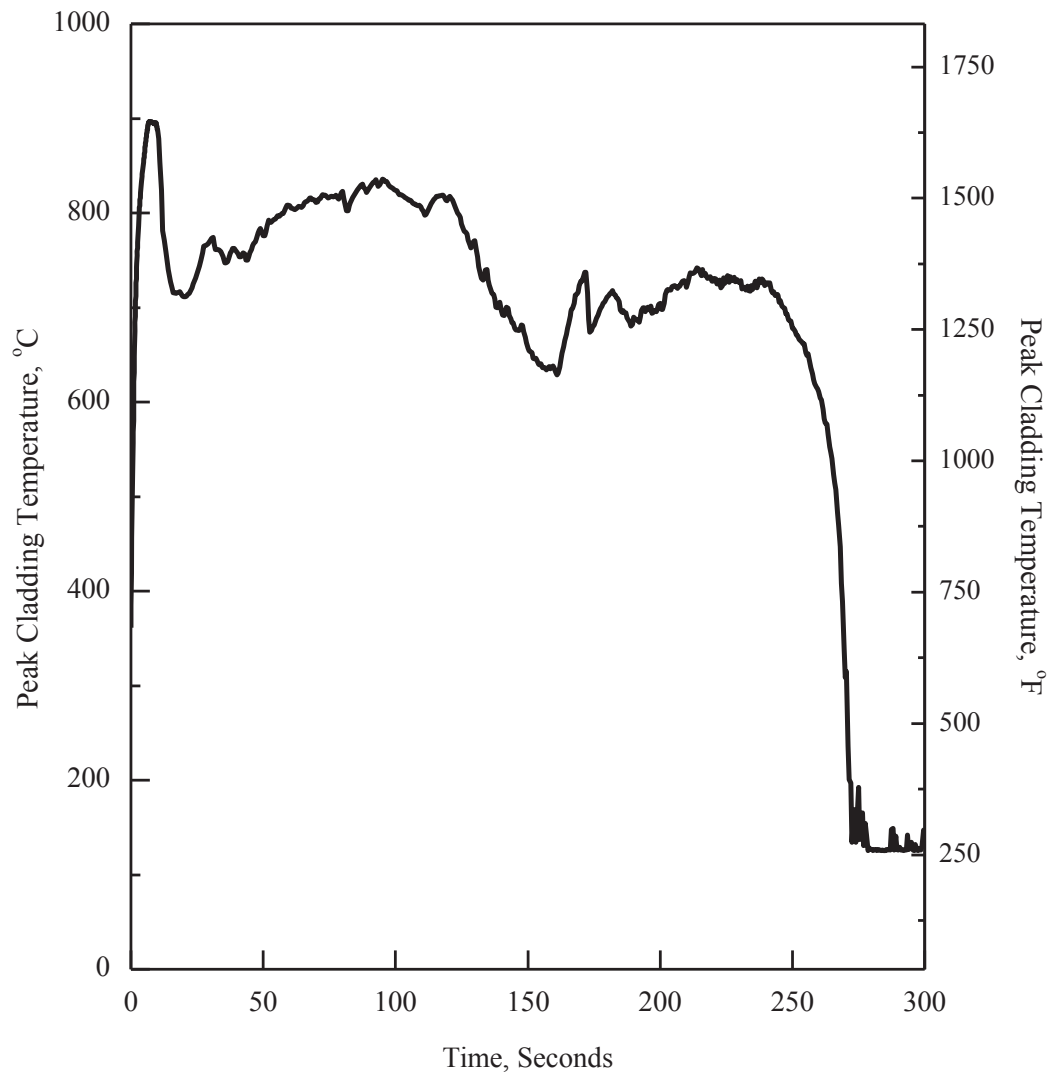


Figure 15.6.5-2 1.0 × Double-ended Guillotine Break in Pump Discharge Leg (Peak Cladding Temperature)

G



APR1400 DCD TIER 2

Replace with next page H

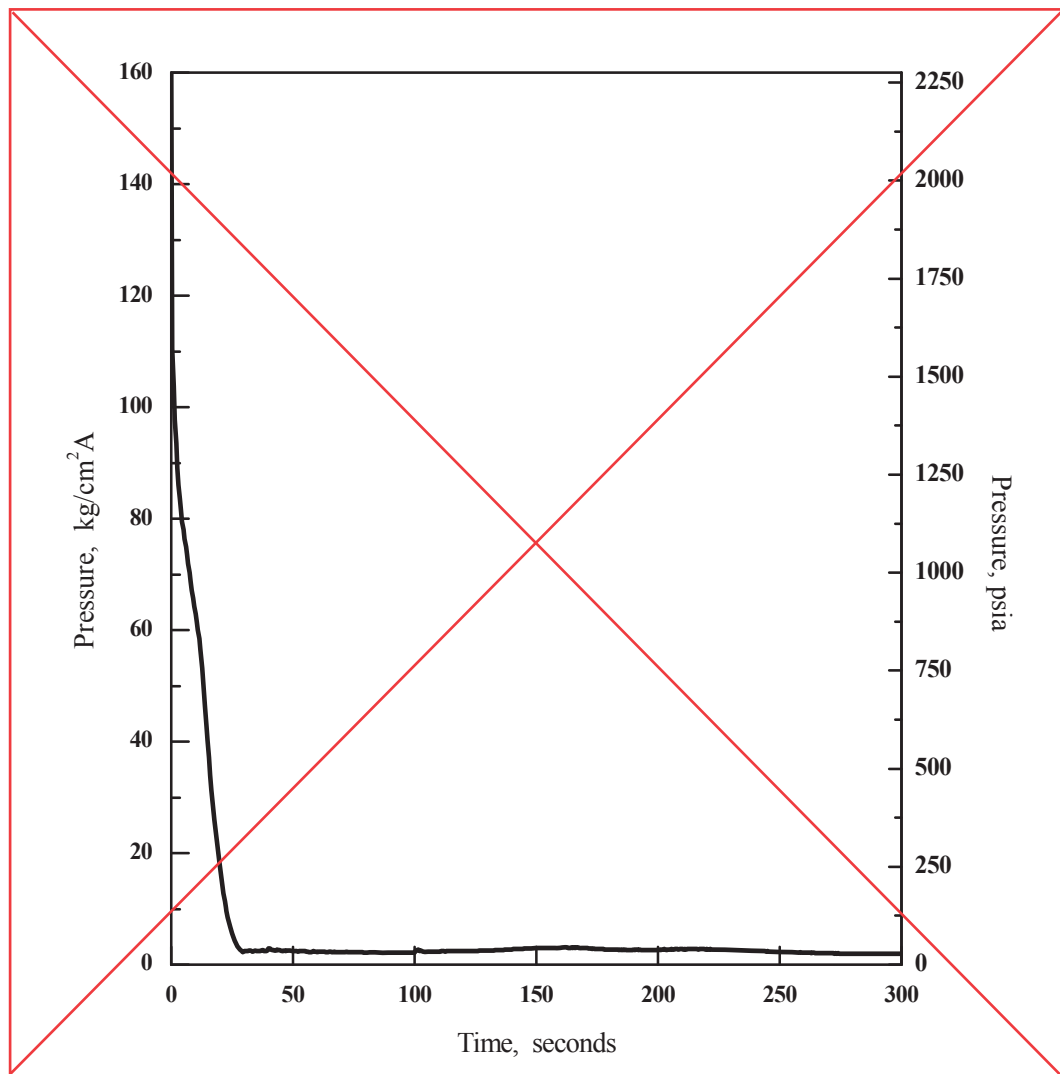
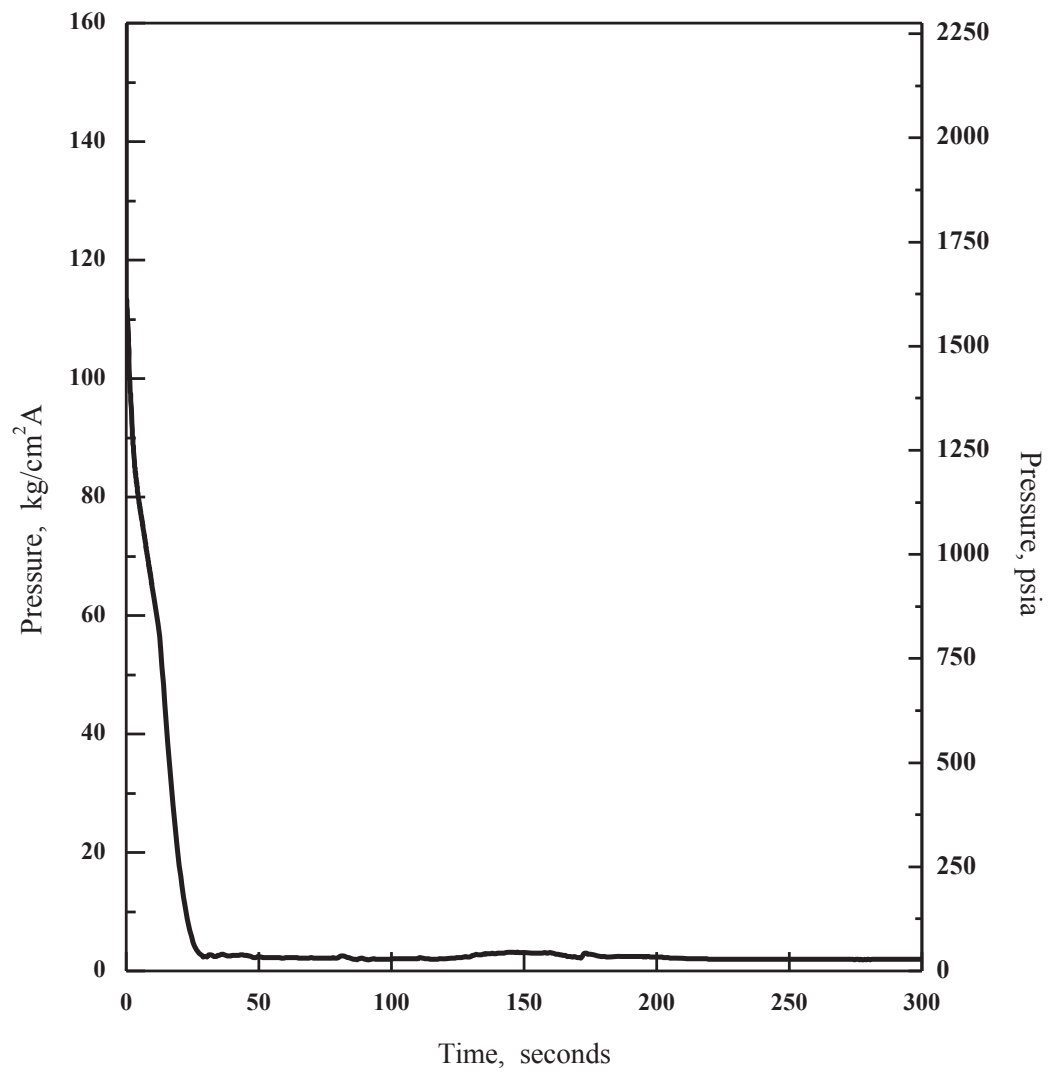


Figure 15.6.5-3 1.0 x Double-ended Guillotine Break in Pump Discharge Leg (Core Pressure)

H



APR1400 DCD TIER 2

Replace with next page I

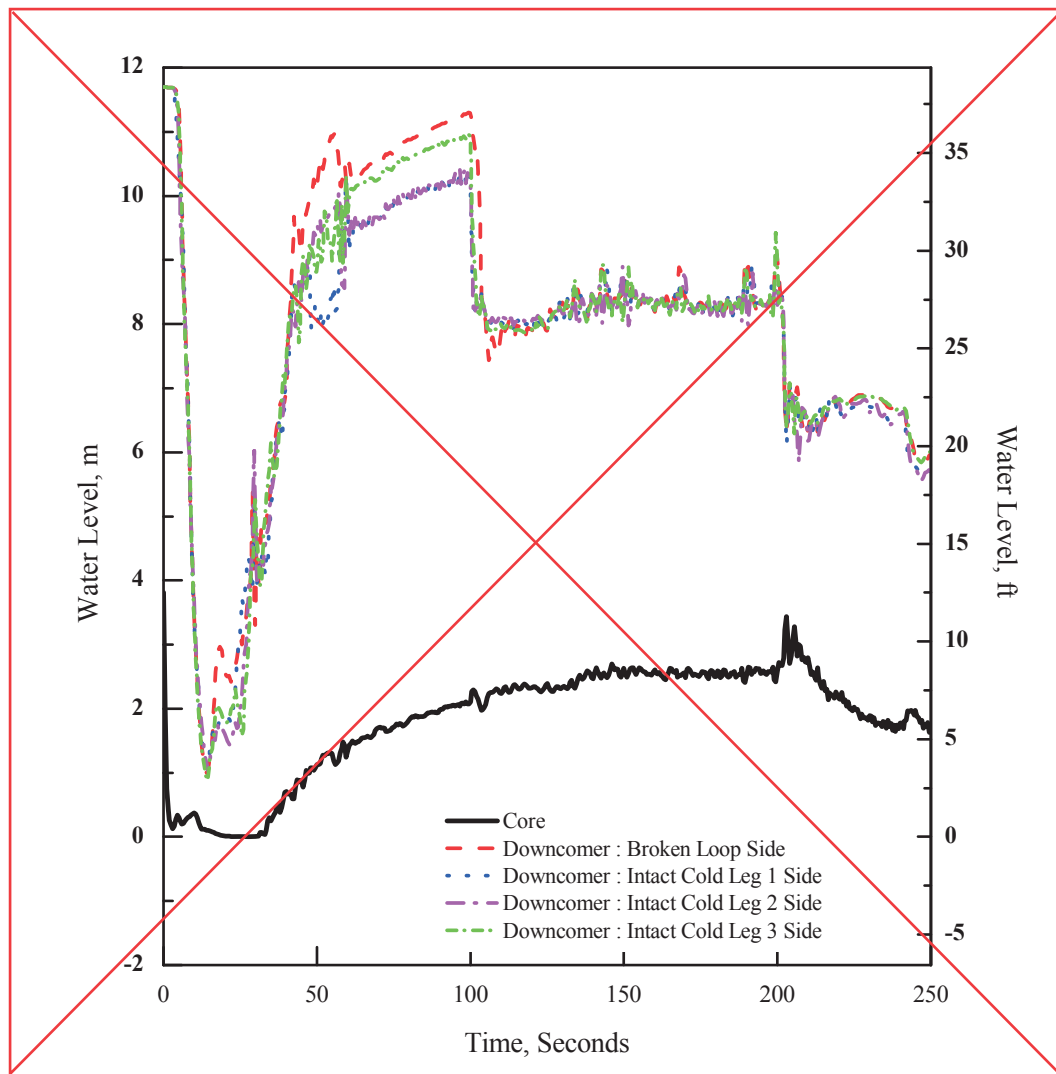
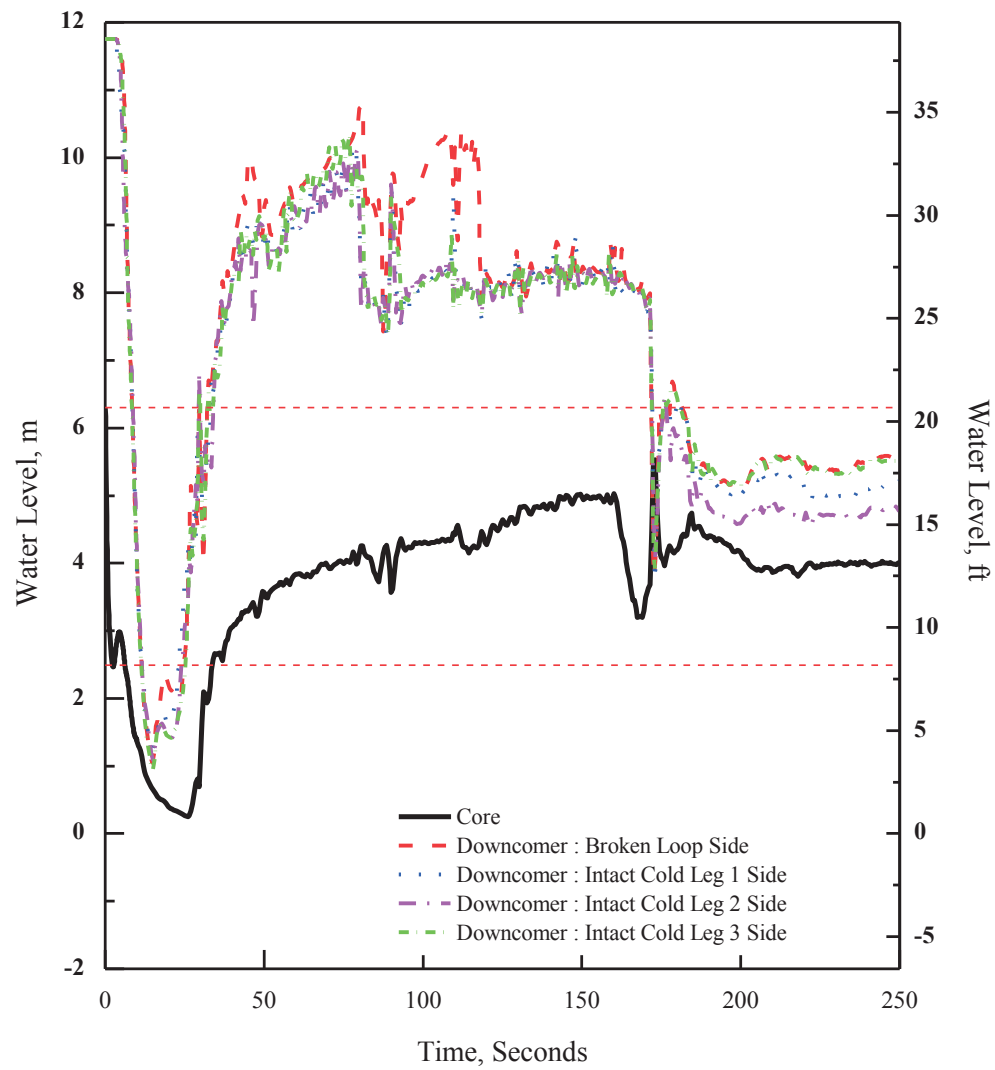


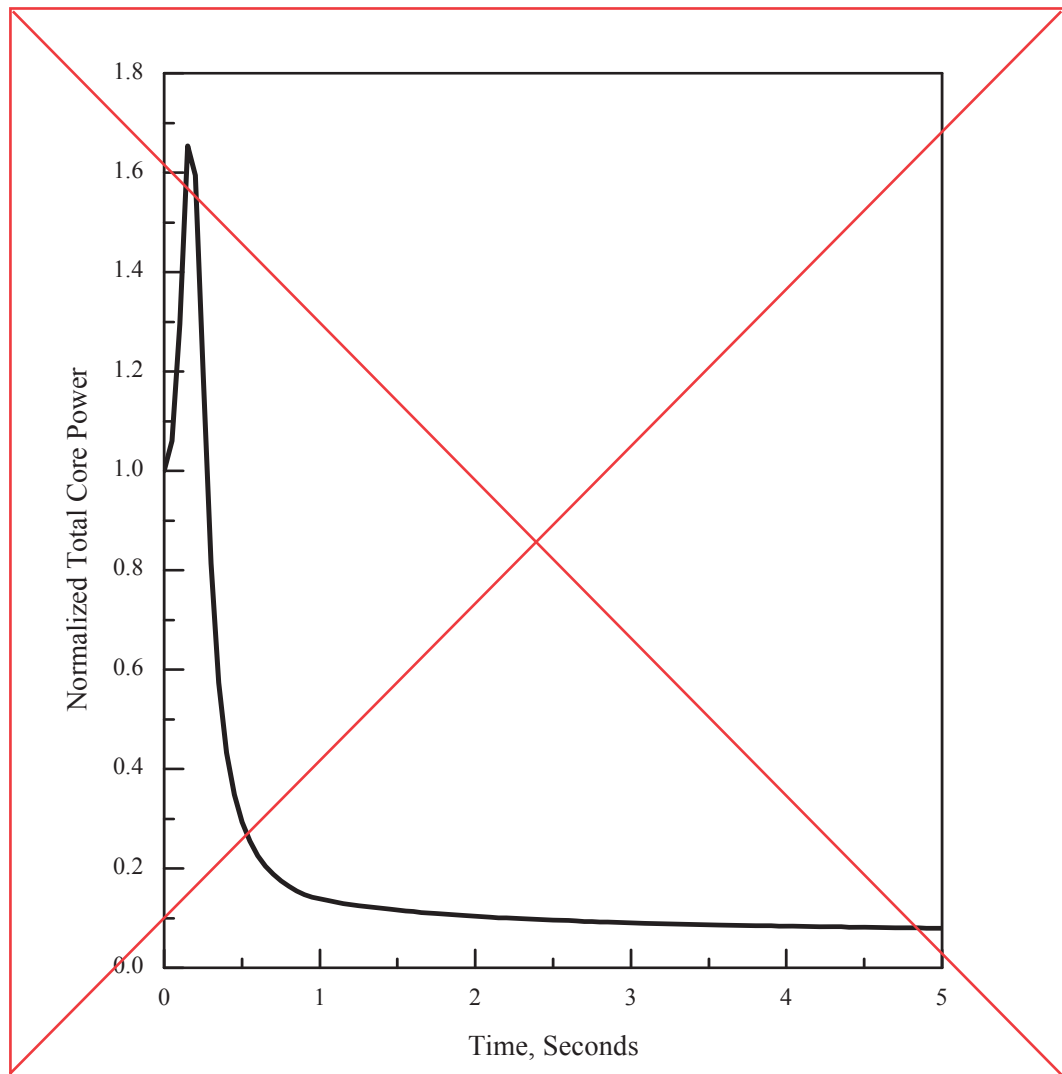
Figure 15.6.5-4 1.0 × Double-ended Guillotine Break in Pump Discharge Leg
(Water Level in Core and Downcommer)

I



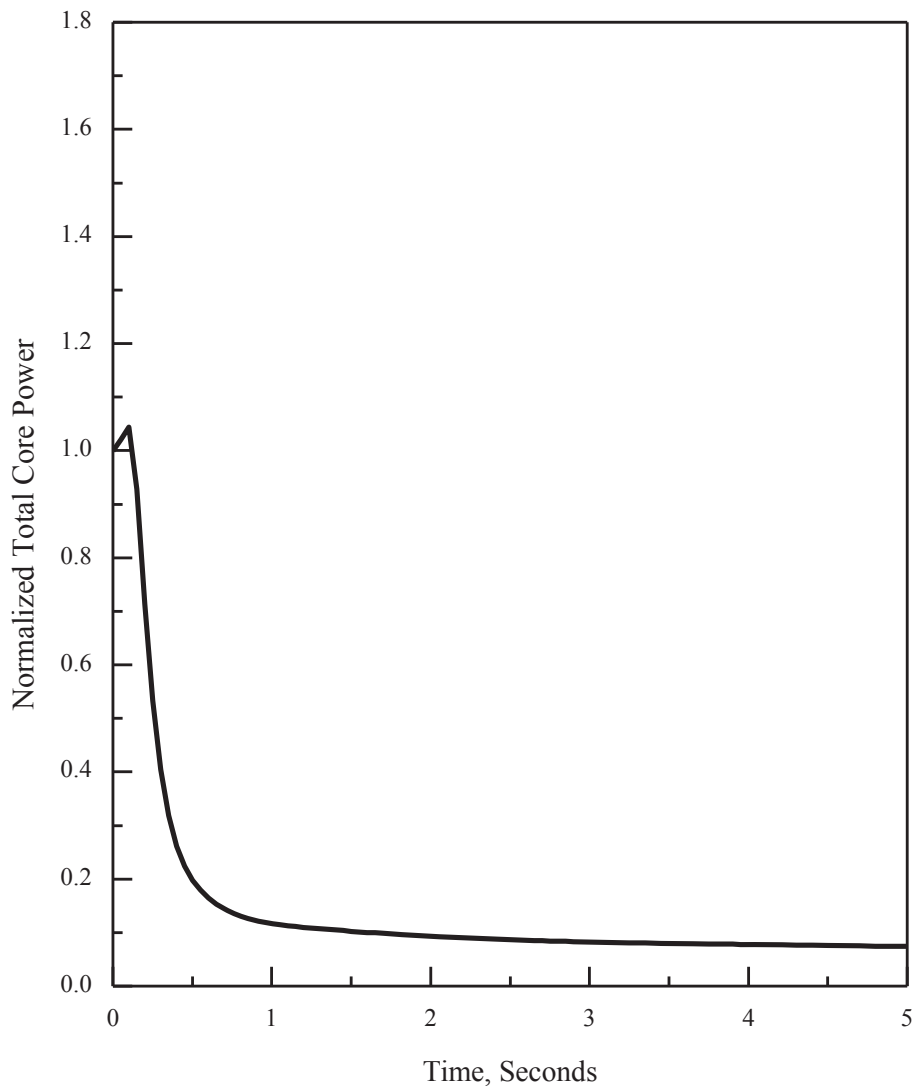
APR1400 DCD TIER 2

Replace with next page J



**Figure 15.6.5-5 1.0 × Double-ended Guillotine Break in Pump Discharge Leg
(Normalized Core Power)**

J



APR1400 DCD TIER 2

Replace with next page K

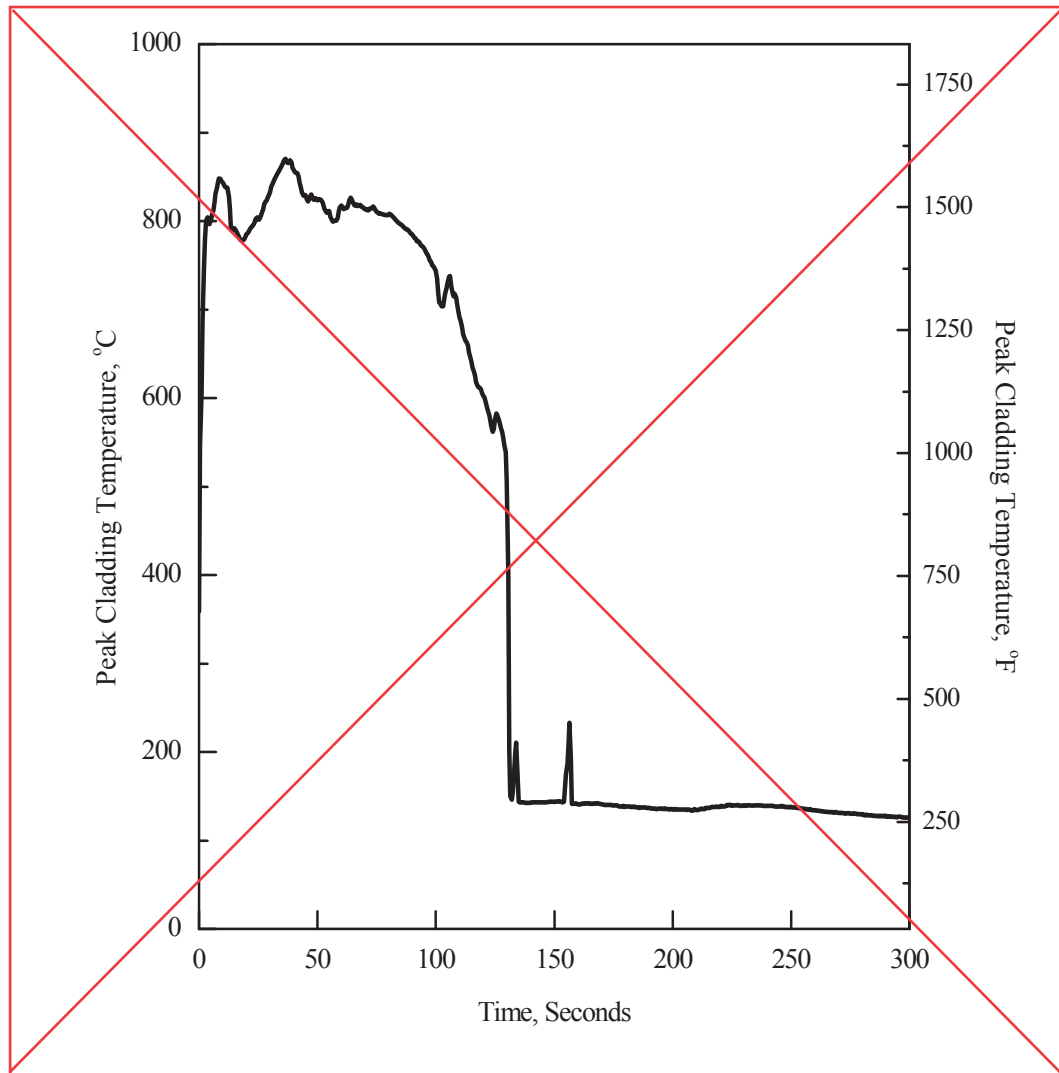
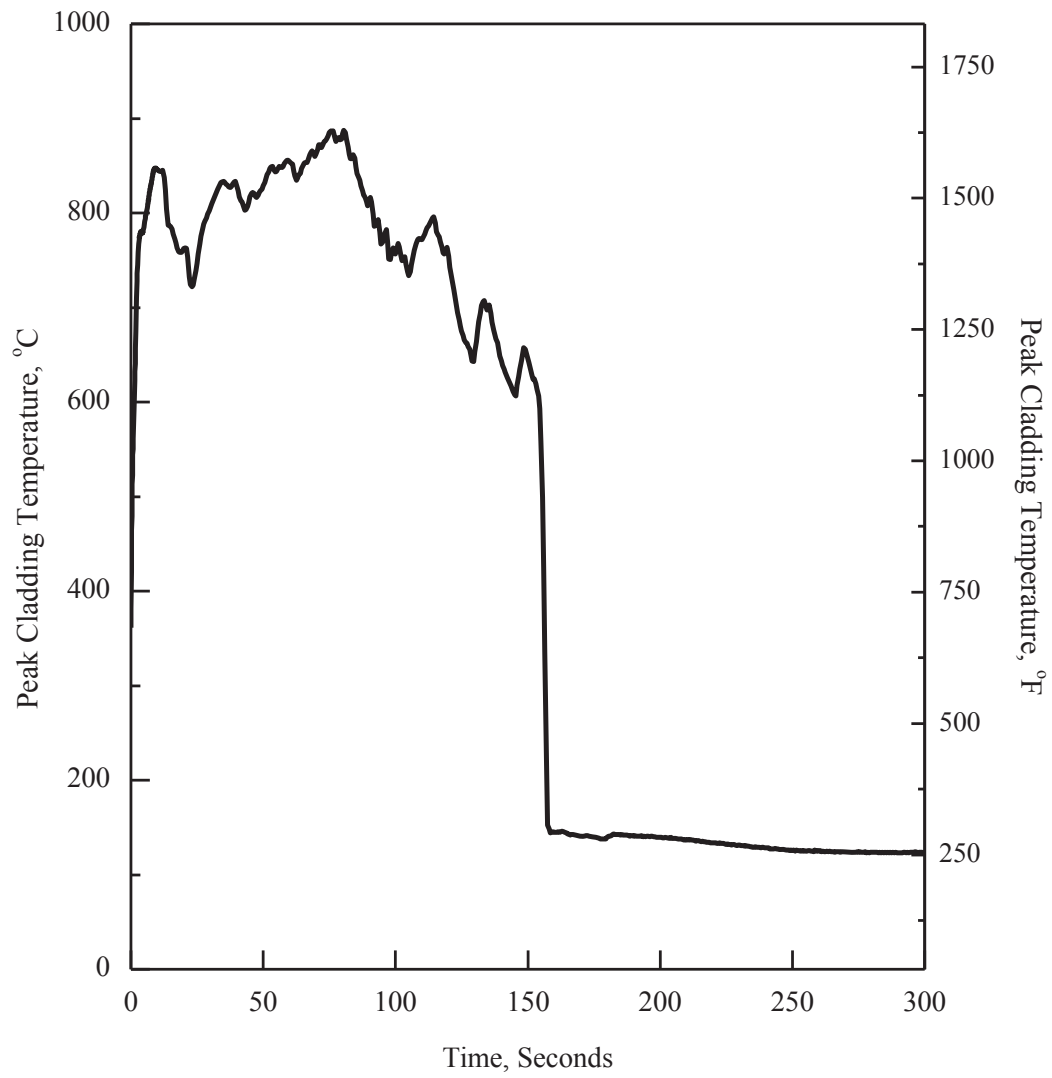


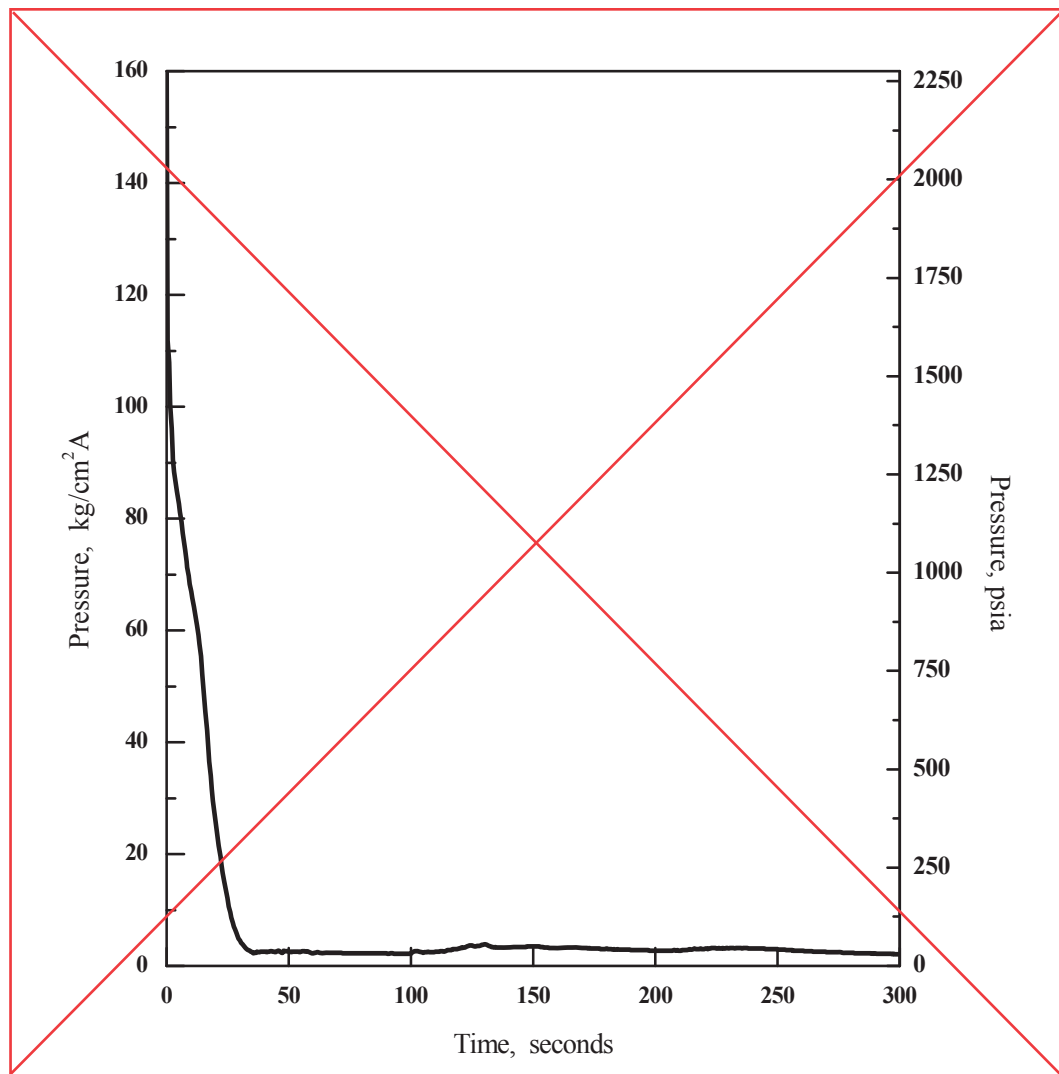
Figure 15.6.5-6 0.8 × Double-ended Guillotine Break in Pump Discharge Leg (Peak Cladding Temperature)

| |
|---|
| K |
|---|



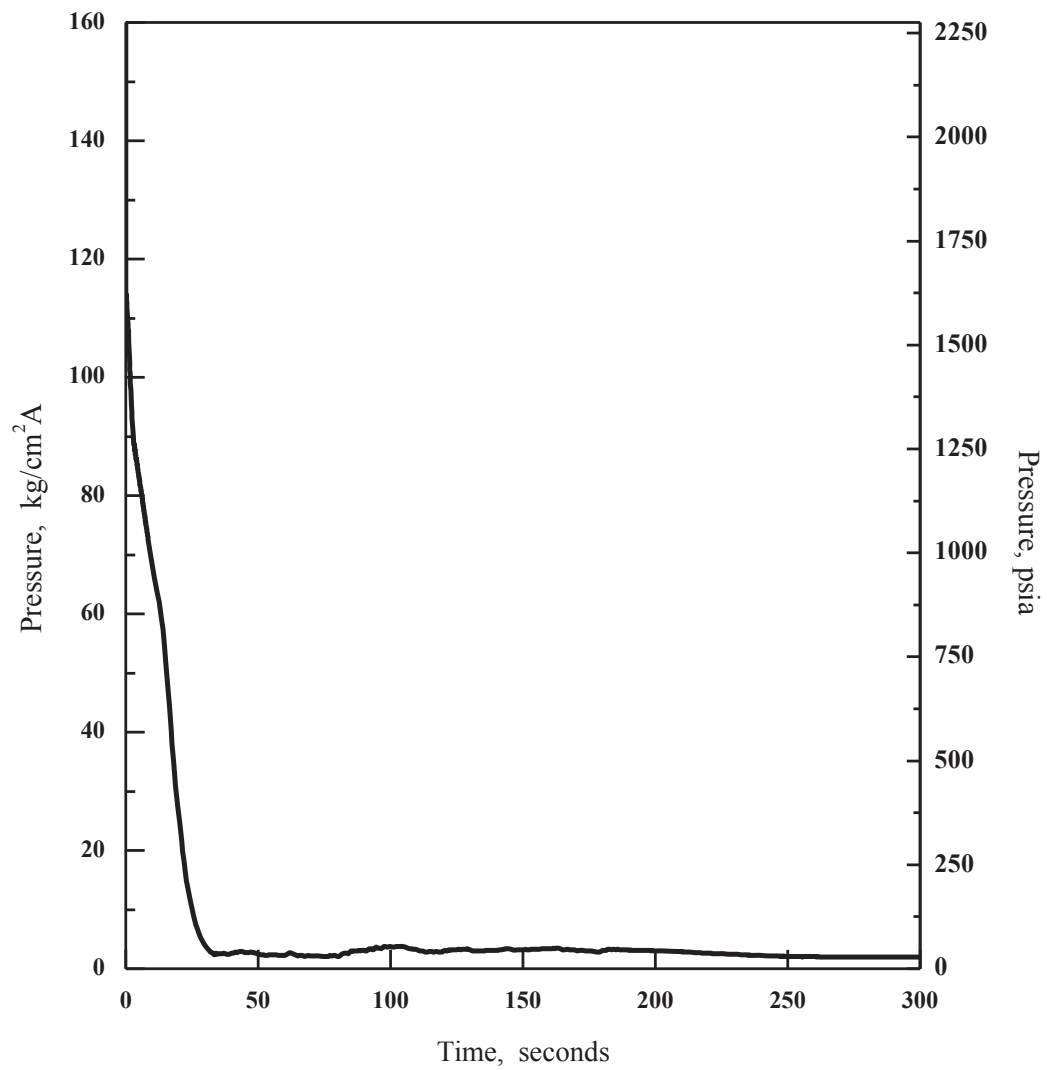
APR1400 DCD TIER 2

Replace with next page L



**Figure 15.6.5-7 0.8 × Double-ended Guillotine Break in Pump Discharge Leg
(Core Pressure)**

L



APR1400 DCD TIER 2

Replace with next page M

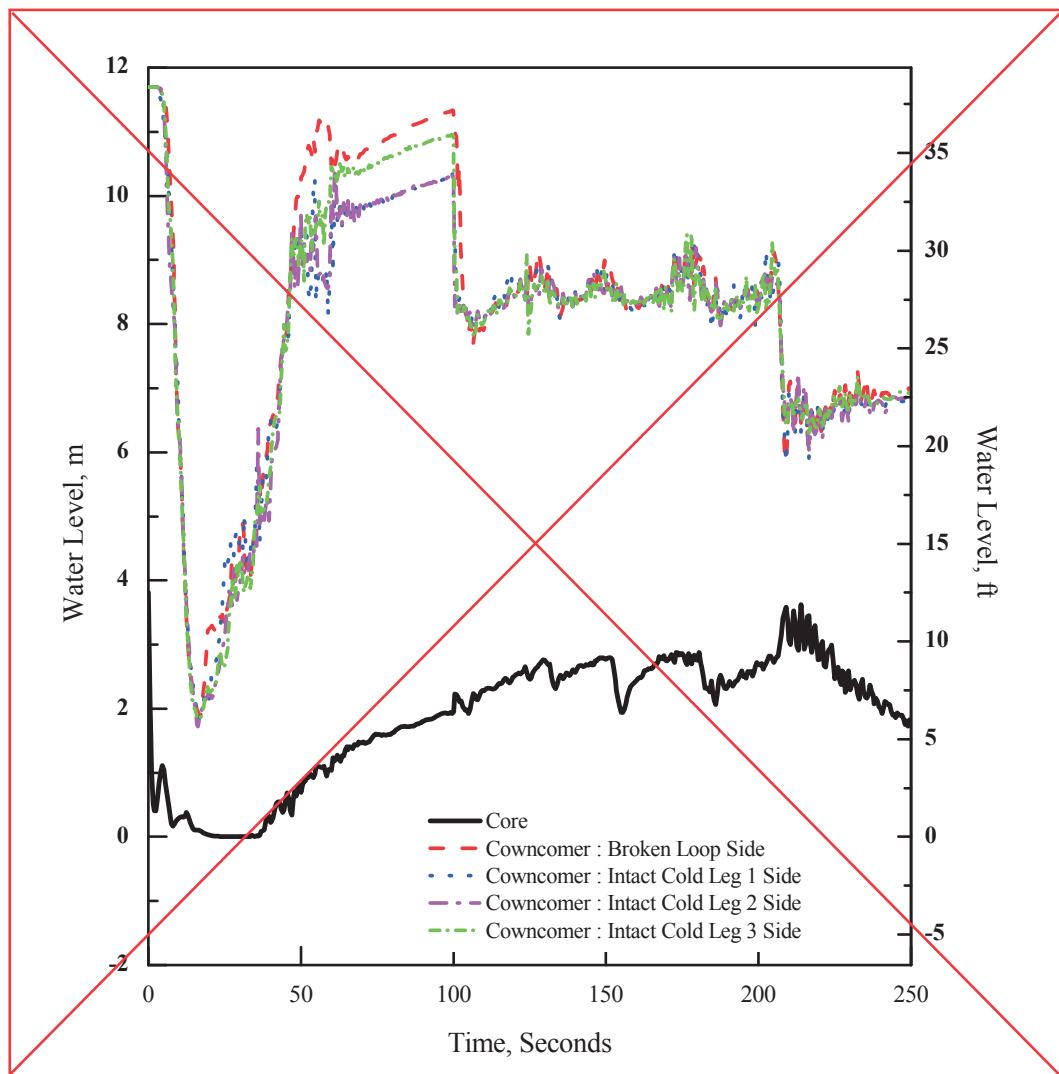
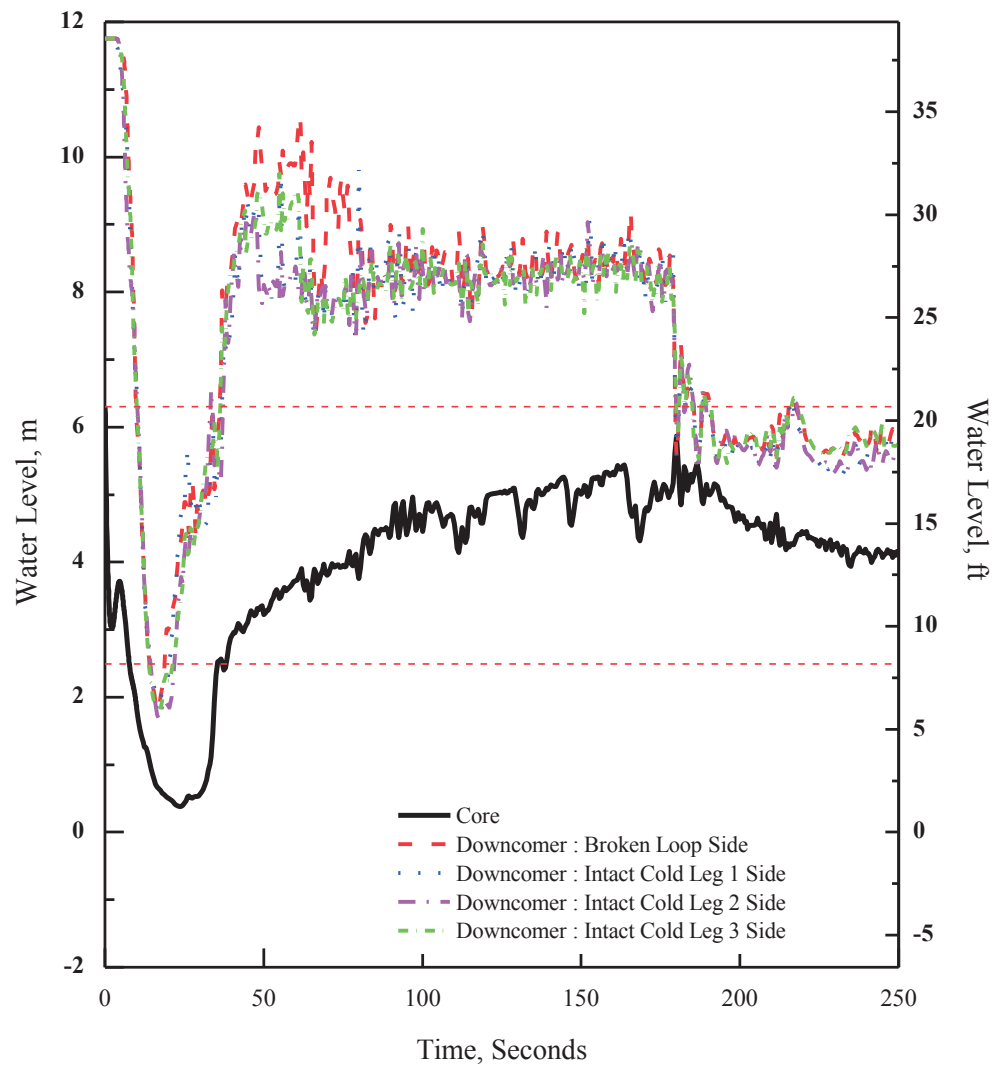


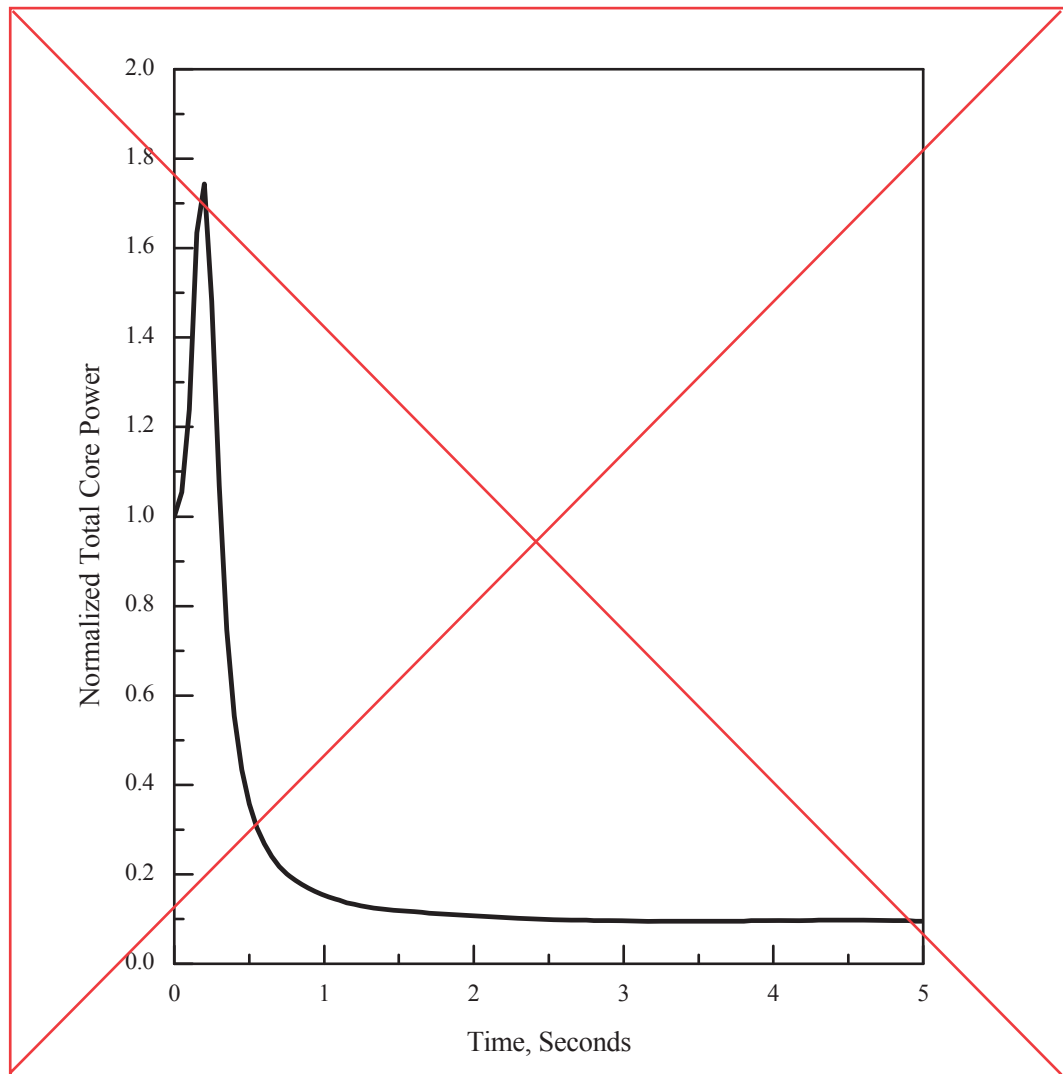
Figure 15.6.5-8 0.8 × Double-ended Guillotine Break in Pump Discharge Leg (Water Level in Core and Downcommer)

M



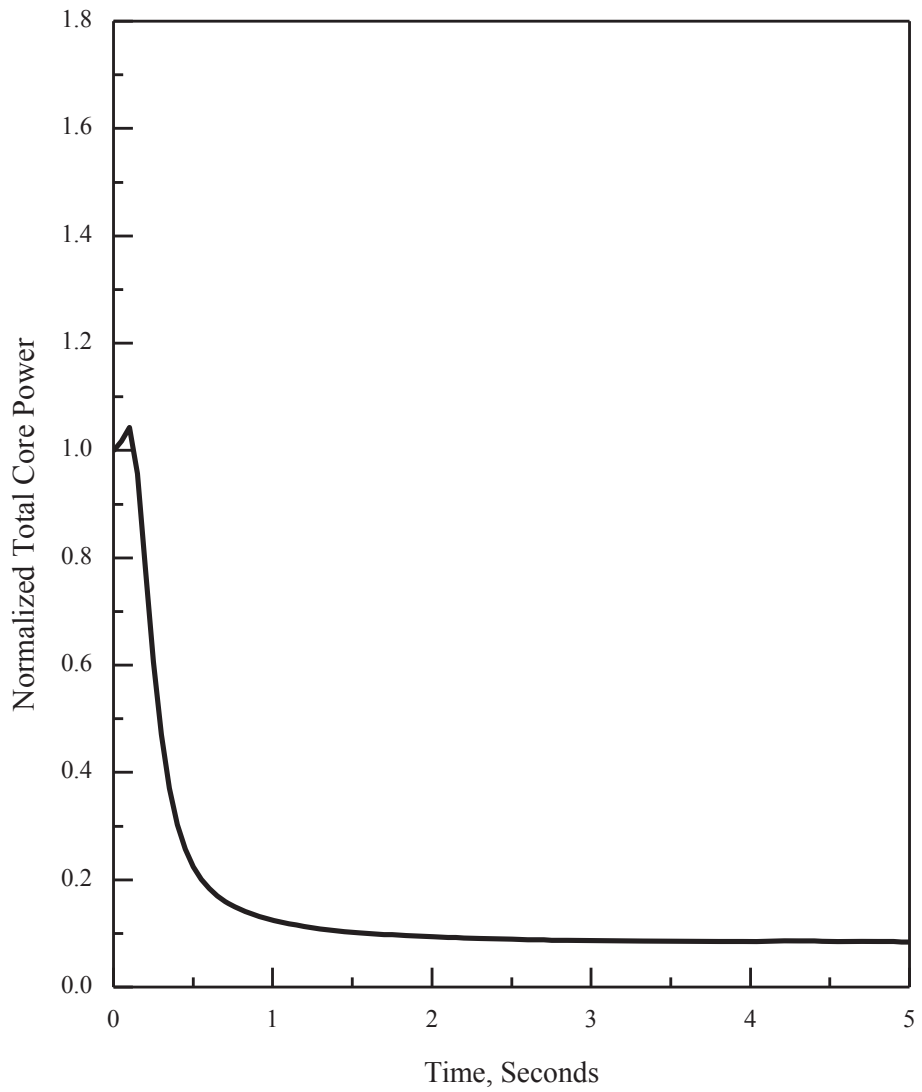
APR1400 DCD TIER 2

Replace with next page N



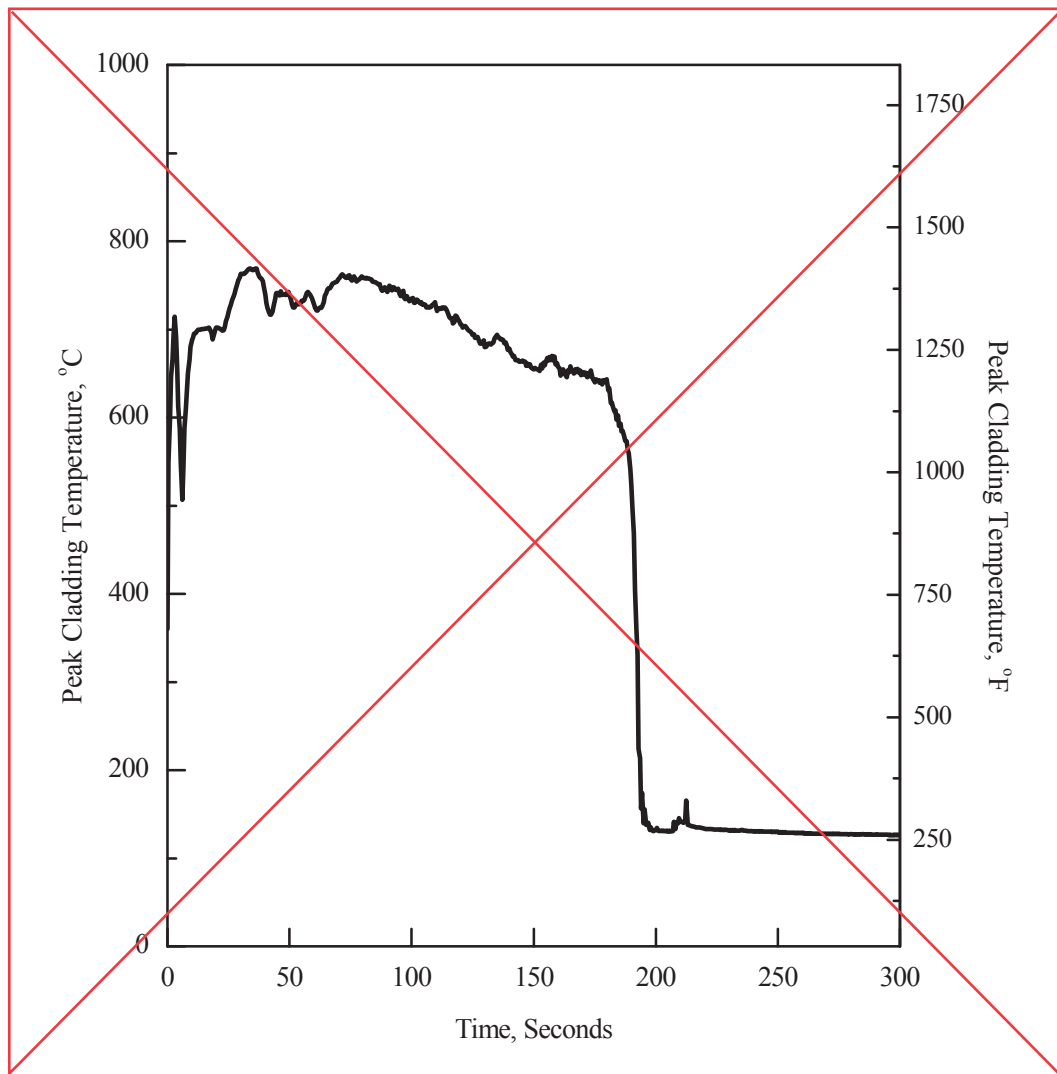
**Figure 15.6.5-9 0.8 × Double-ended Guillotine Break in Pump Discharge Leg
(Normalized Core Power)**

N



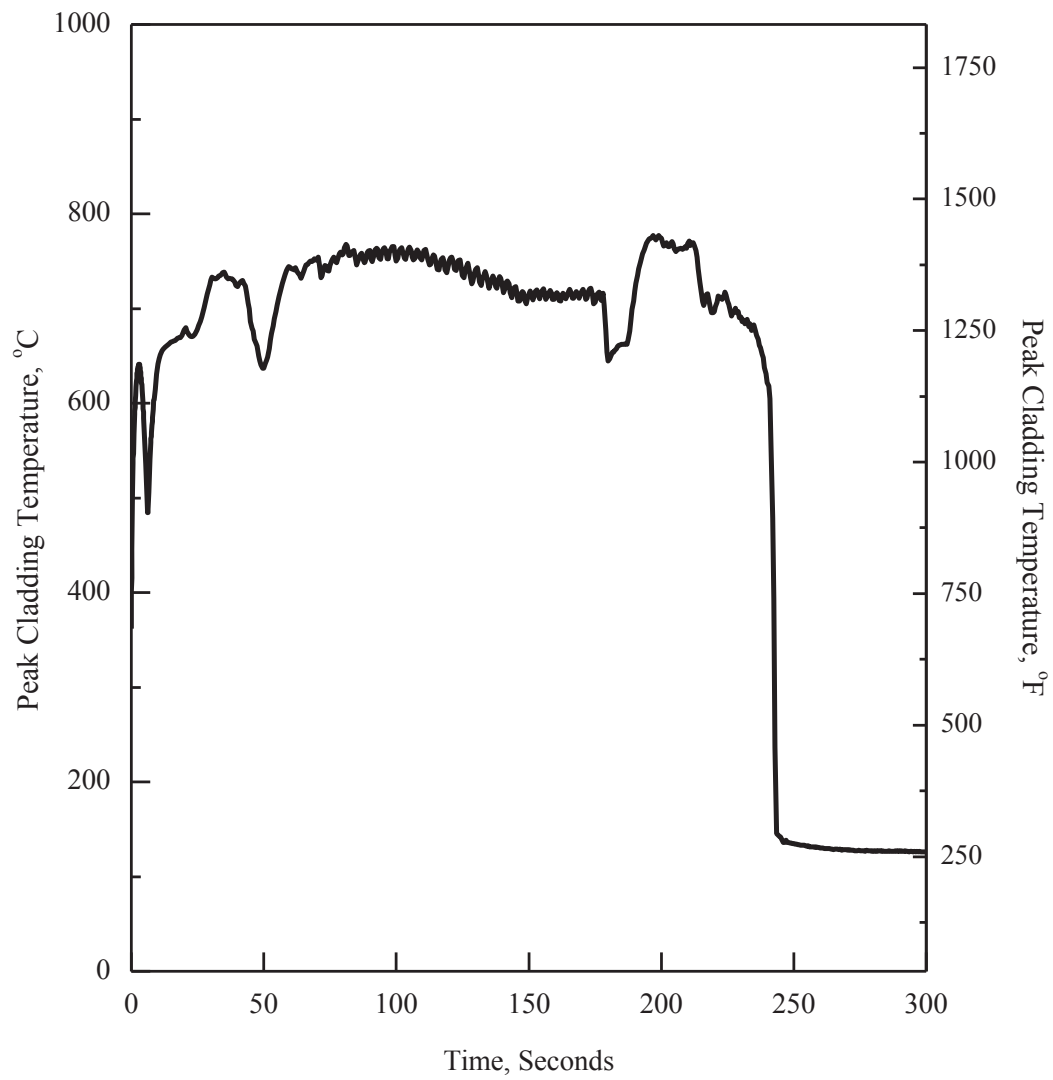
APR1400 DCD TIER 2

Replace with next page O



**Figure 15.6.5-10 0.6 × Double-ended Guillotine Break in Pump Discharge Leg
(Peak Cladding Temperature)**

O



APR1400 DCD TIER 2

Replace with next page P

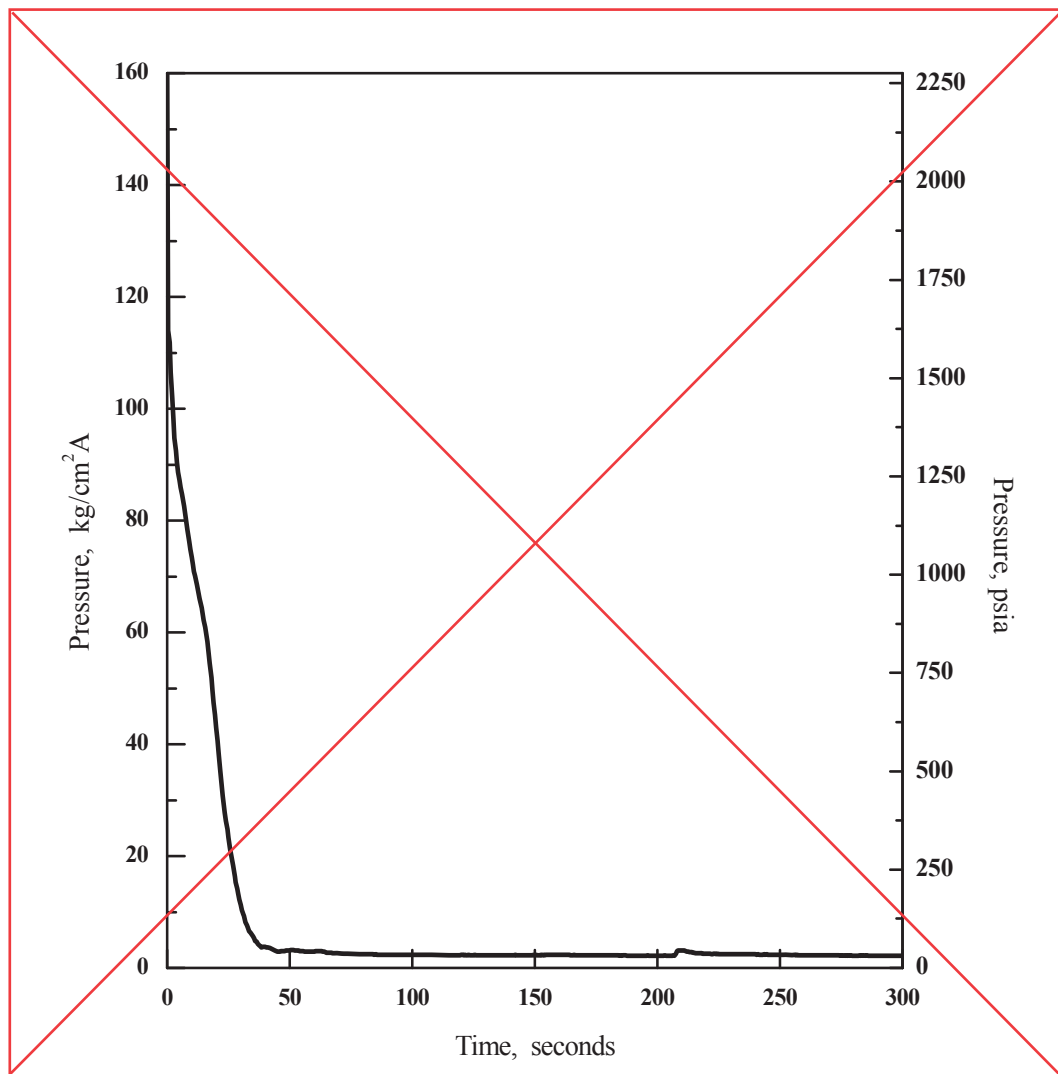
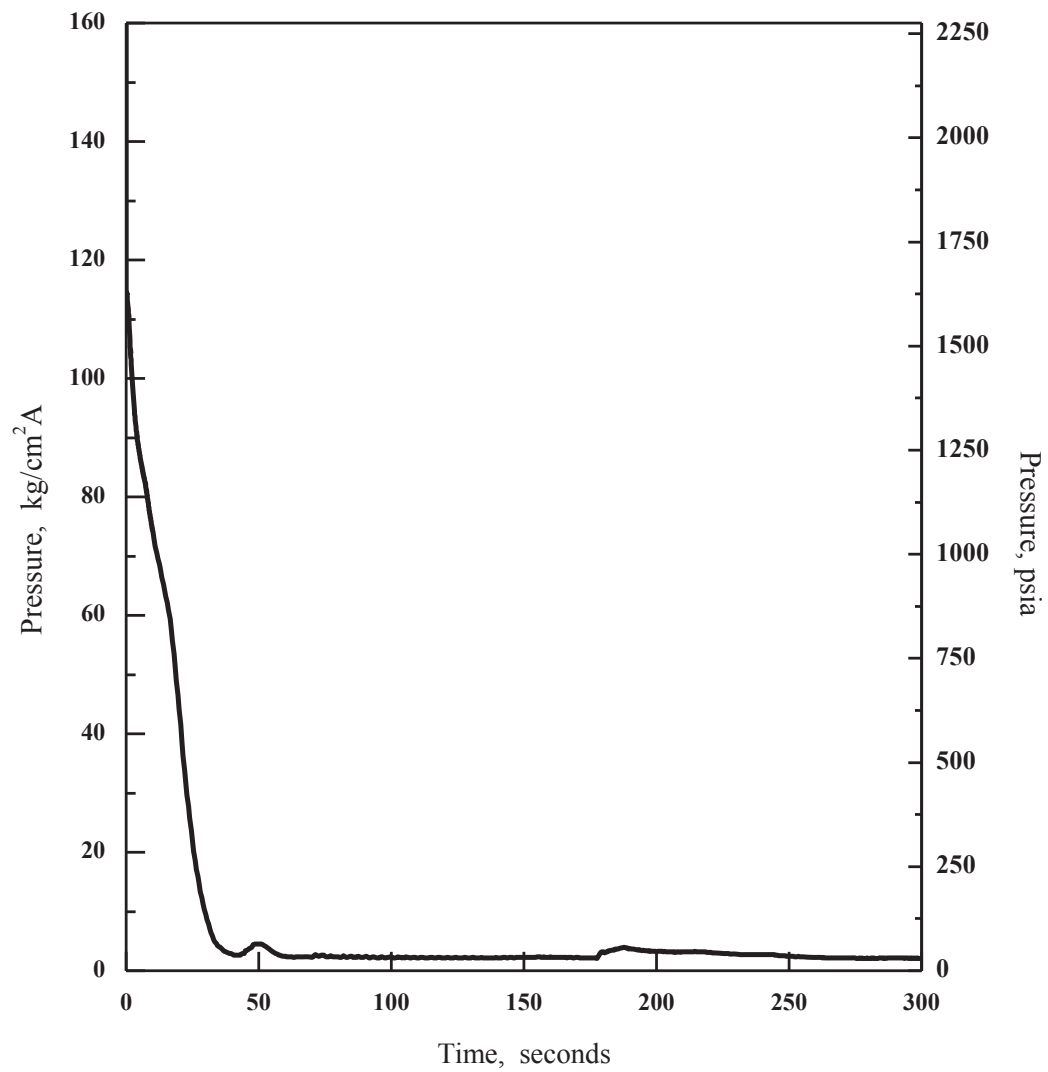


Figure 15.6.5-11 0.6 × Double-ended Guillotine Break in Pump Discharge Leg
(Core Pressure)

P



APR1400 DCD TIER 2

Replace with next page Q

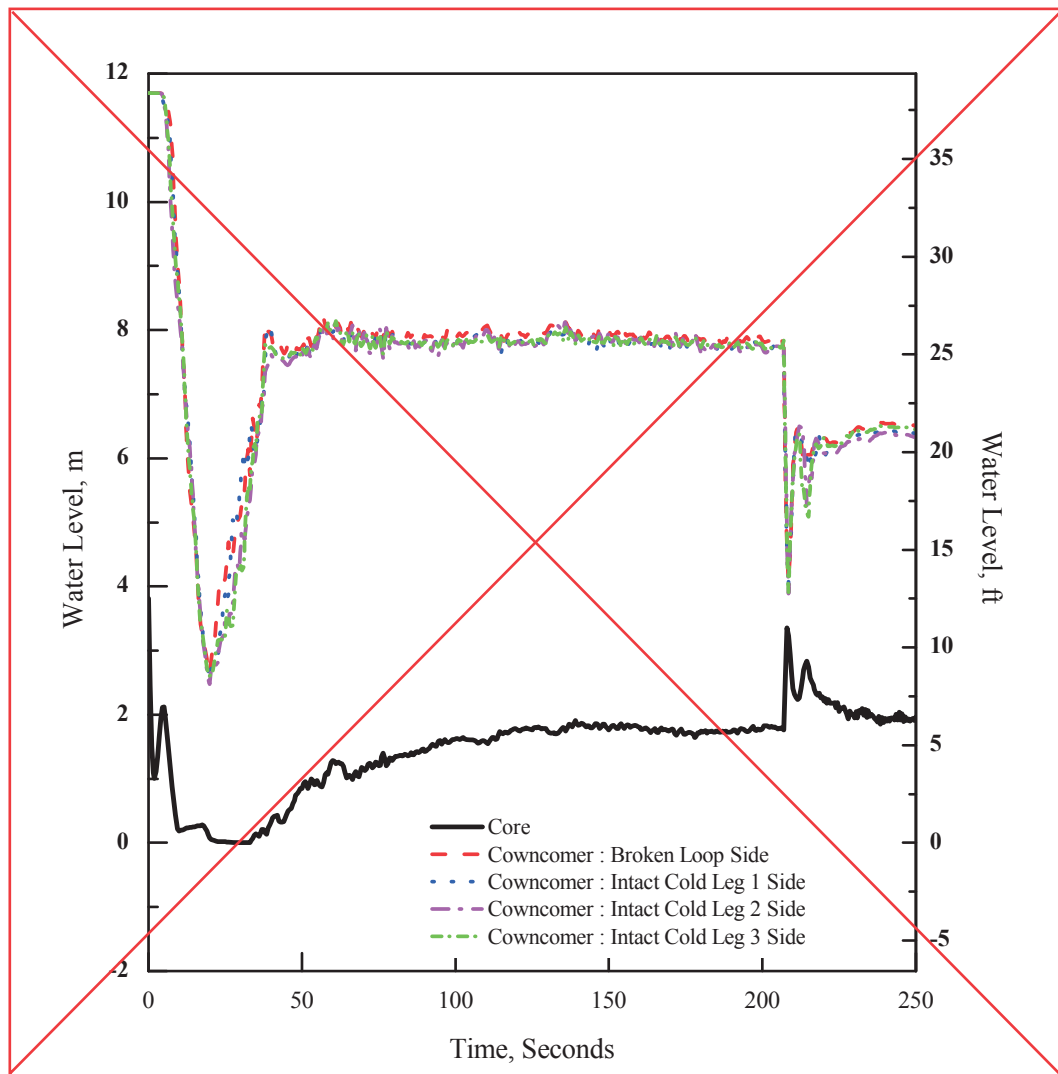
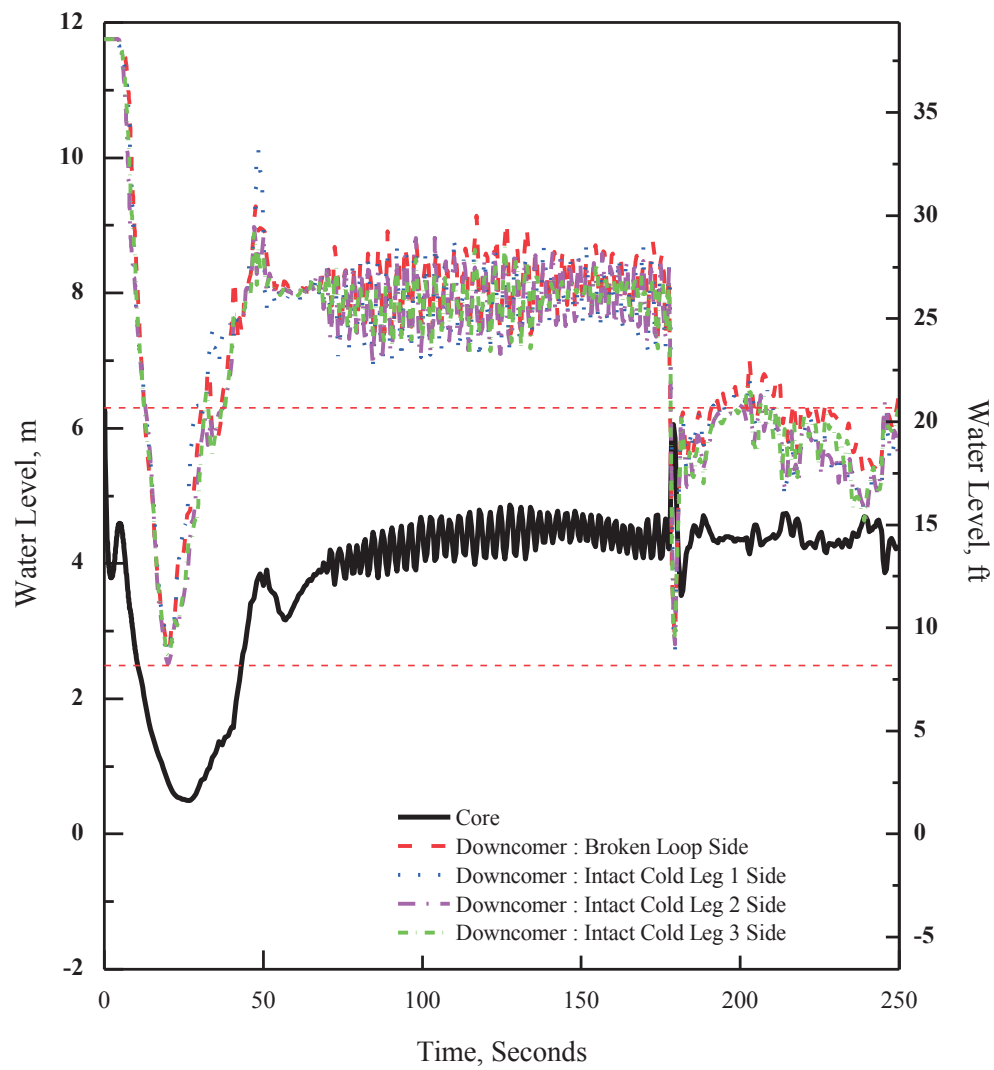


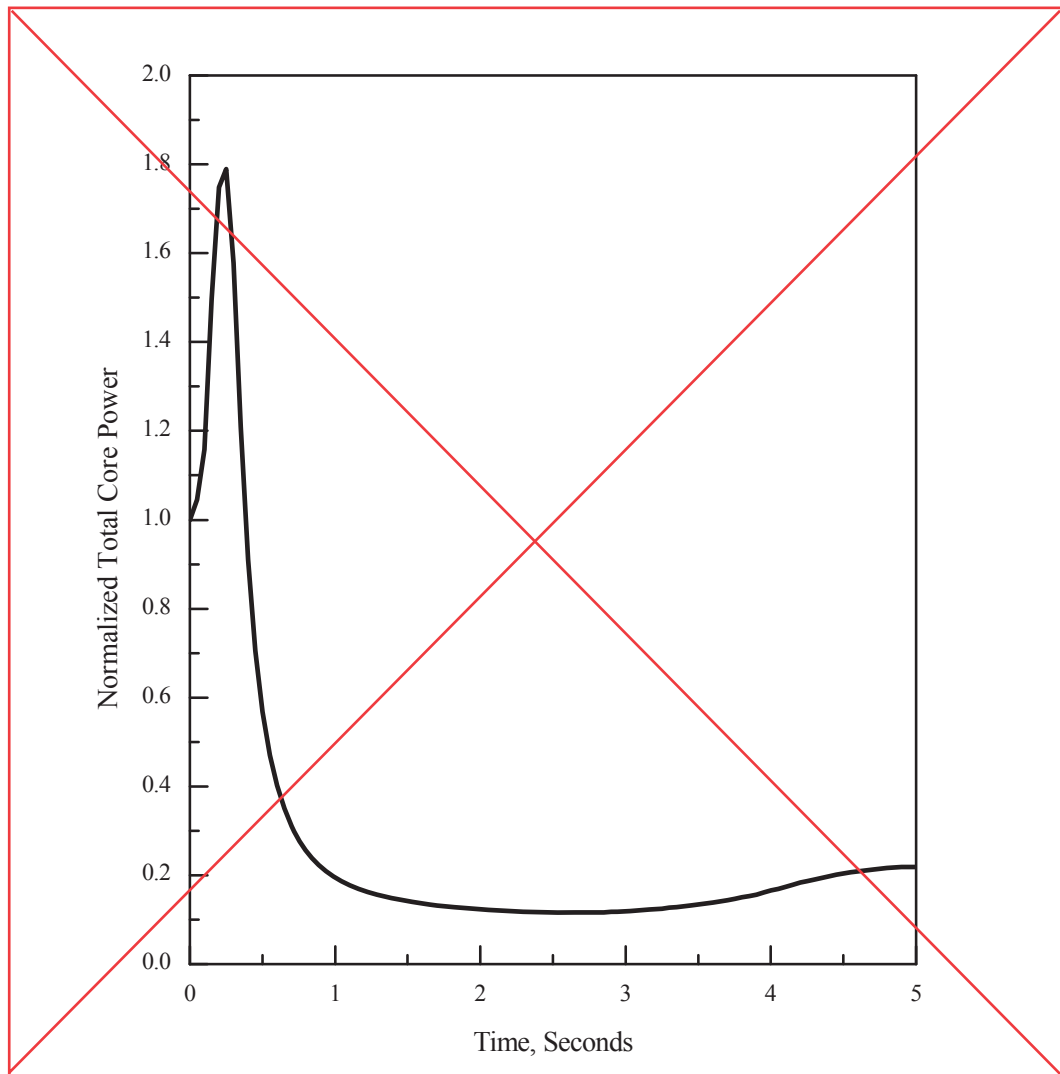
Figure 15.6.5-12 0.6 × Double-ended Guillotine Break in Pump Discharge Leg (Water Level in Core and Downcommer)

Q



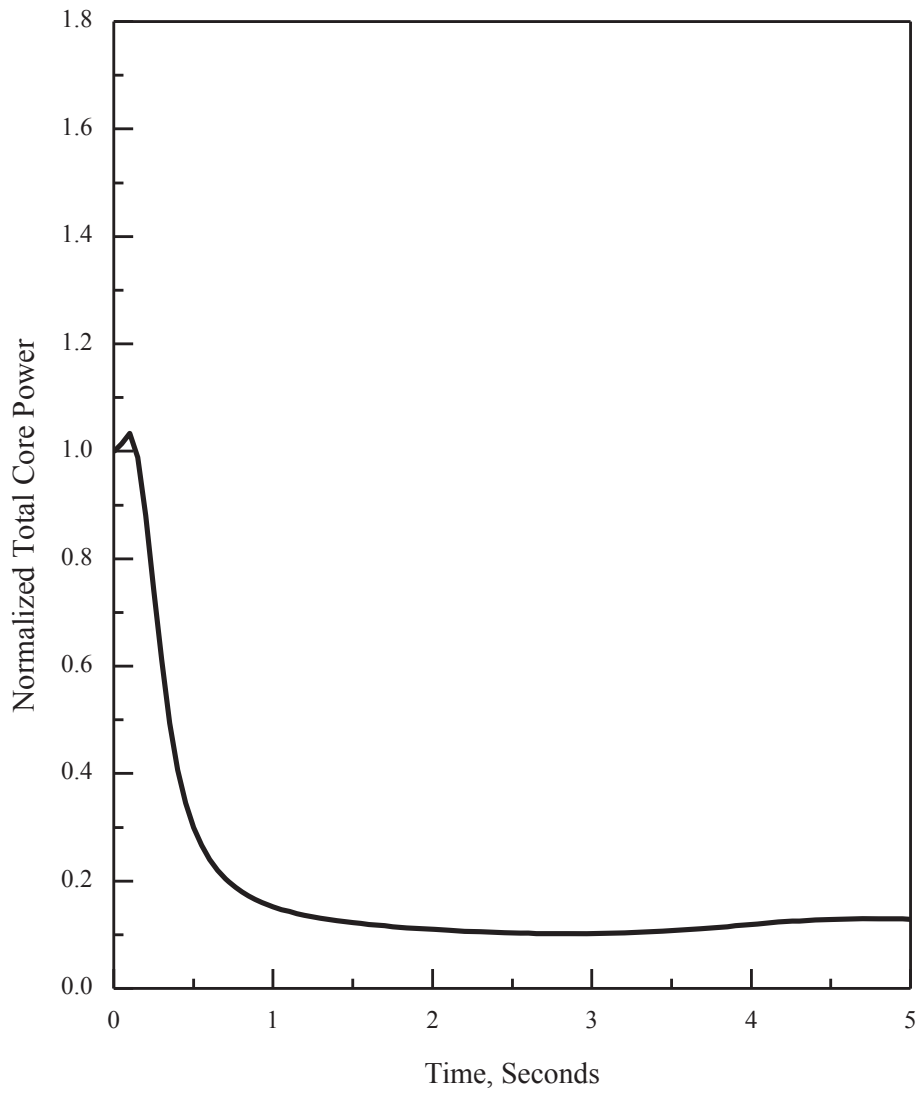
APR1400 DCD TIER 2

Replace with next page R



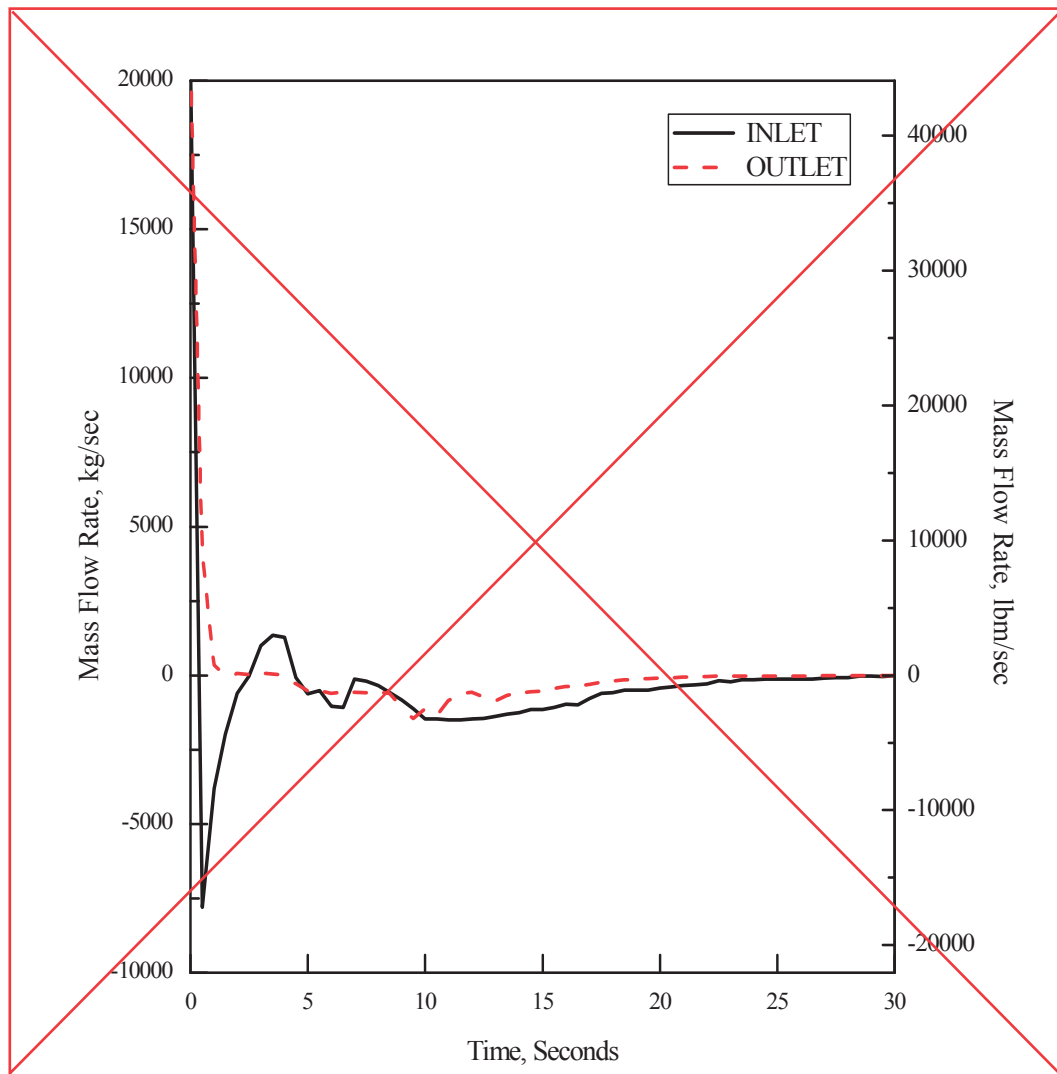
**Figure 15.6.5-13 0.6 × Double-ended Guillotine Break in Pump Discharge Leg
(Normalized Core Power)**

| |
|---|
| R |
|---|



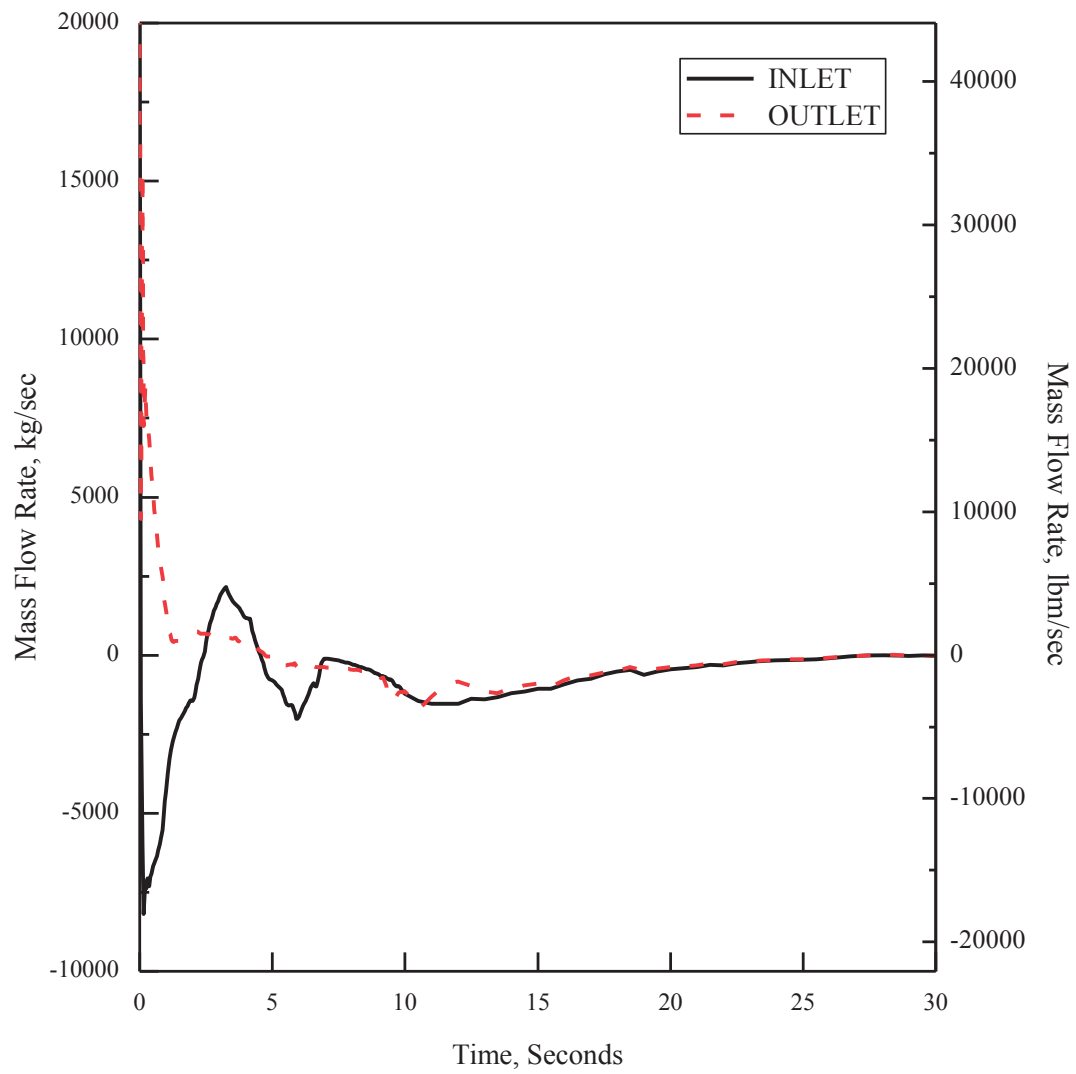
APR1400 DCD TIER 2

Replace with next page S



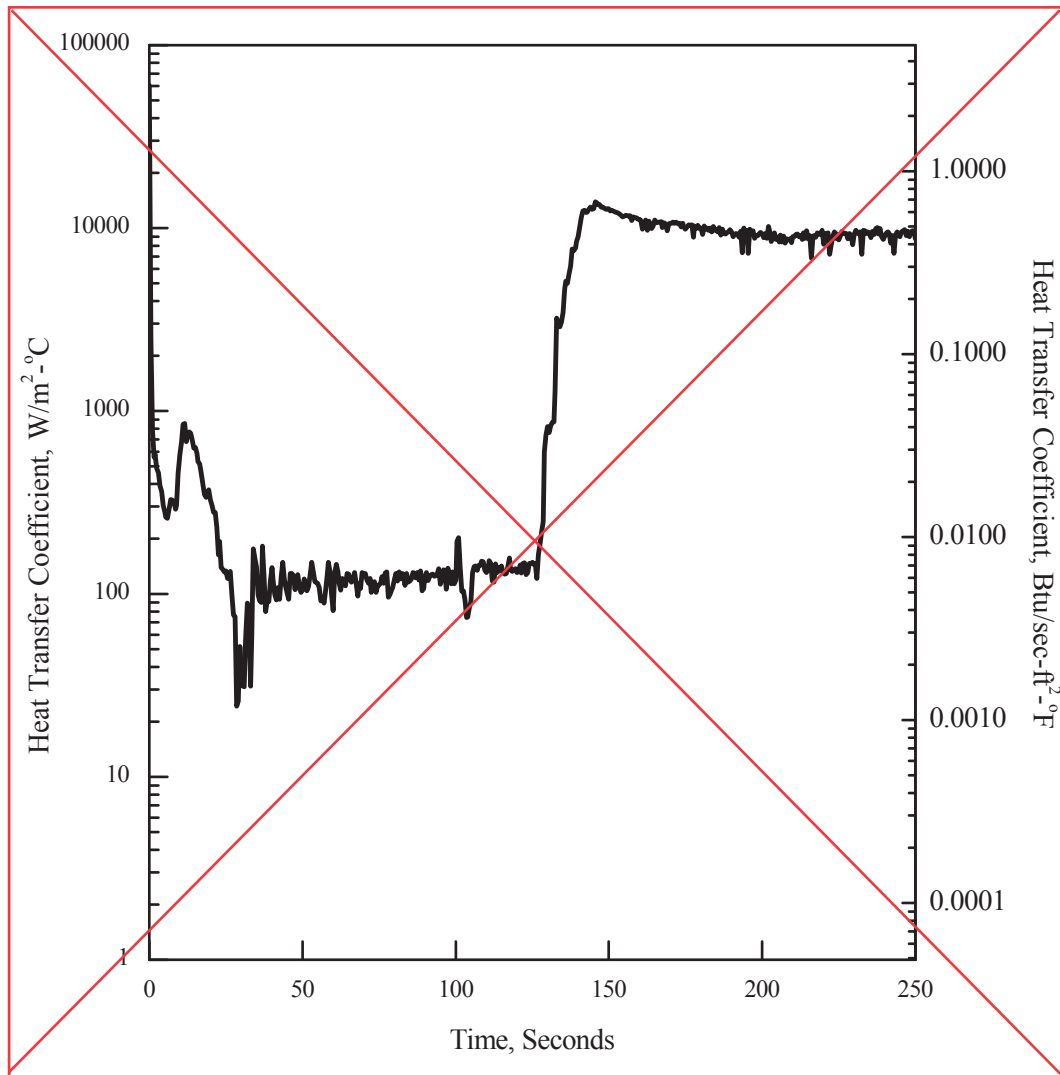
**Figure 15.6.5-14 1.0 × Double-ended Guillotine Break in Pump Discharge Leg
(Core Inlet and Outlet Mass Flow)**

S



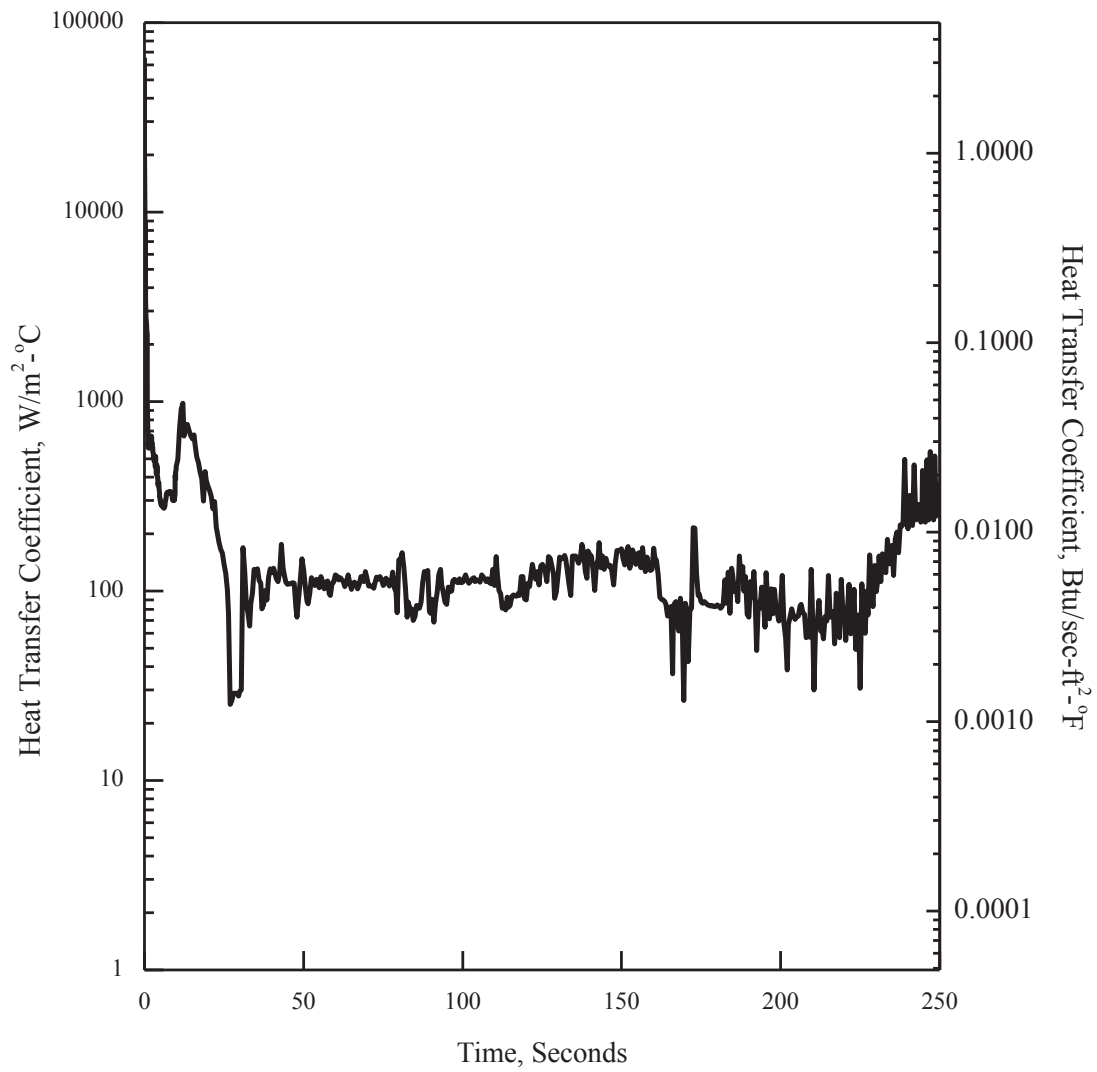
APR1400 DCD TIER 2

Replace with next page T



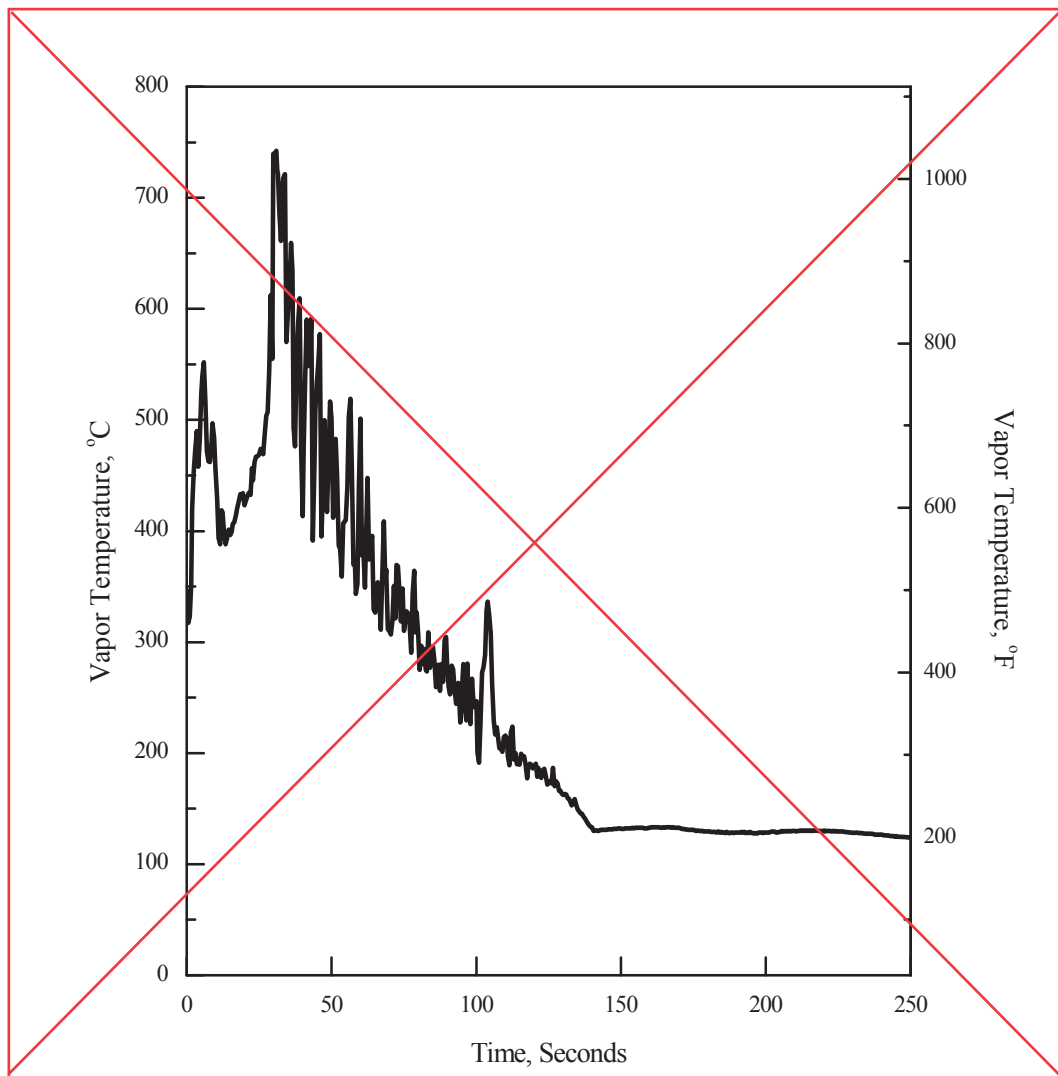
**Figure 15.6.5-15 1.0 × Double-ended Guillotine Break in Pump Discharge Leg
(Hot Spot Heat Transfer Coefficient)**

T



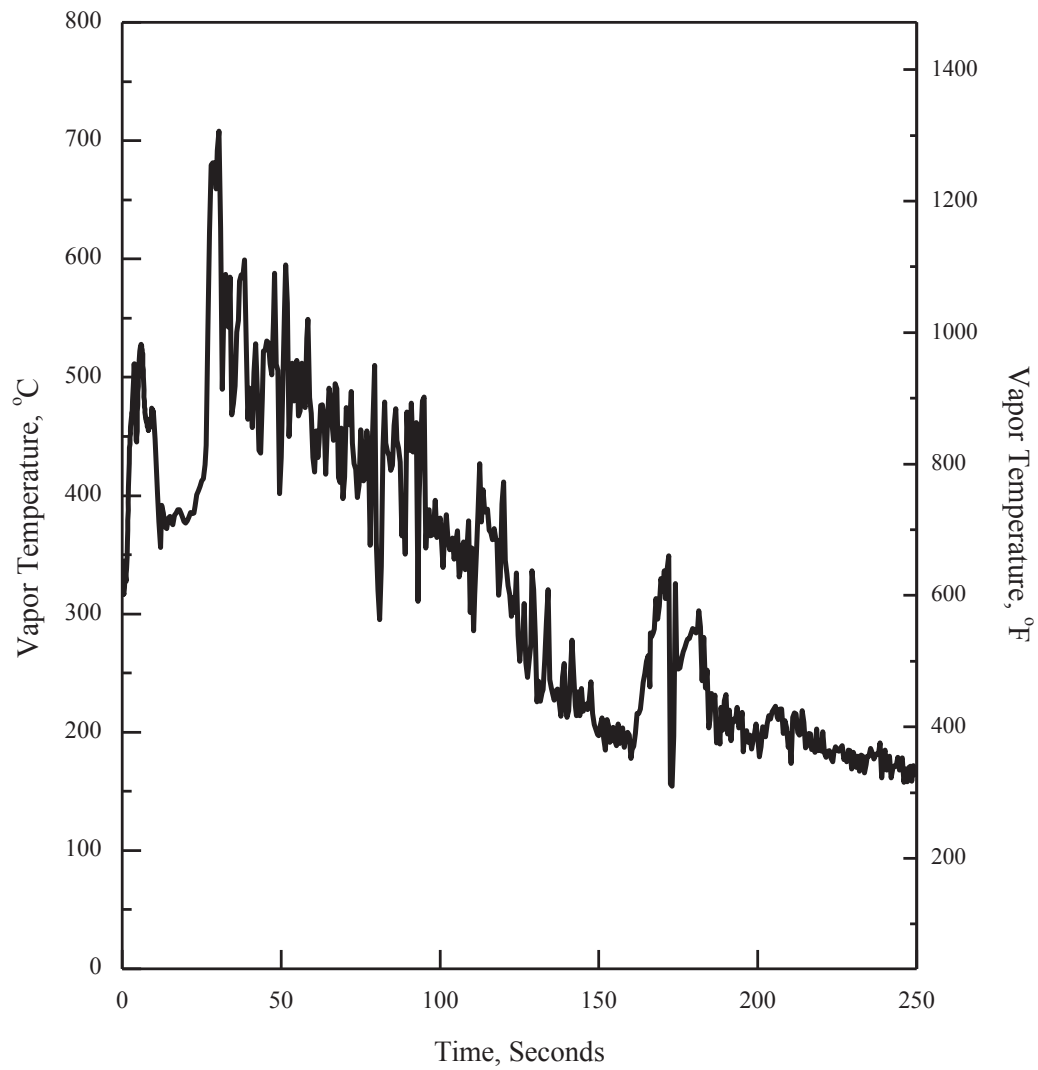
APR1400 DCD TIER 2

Replace with next page U



**Figure 15.6.5-16 1.0 × Double-ended Guillotine Break in Pump Discharge Leg
(Hot Spot Vapor Temperature)**

U



APR1400 DCD TIER 2

Replace with next page V

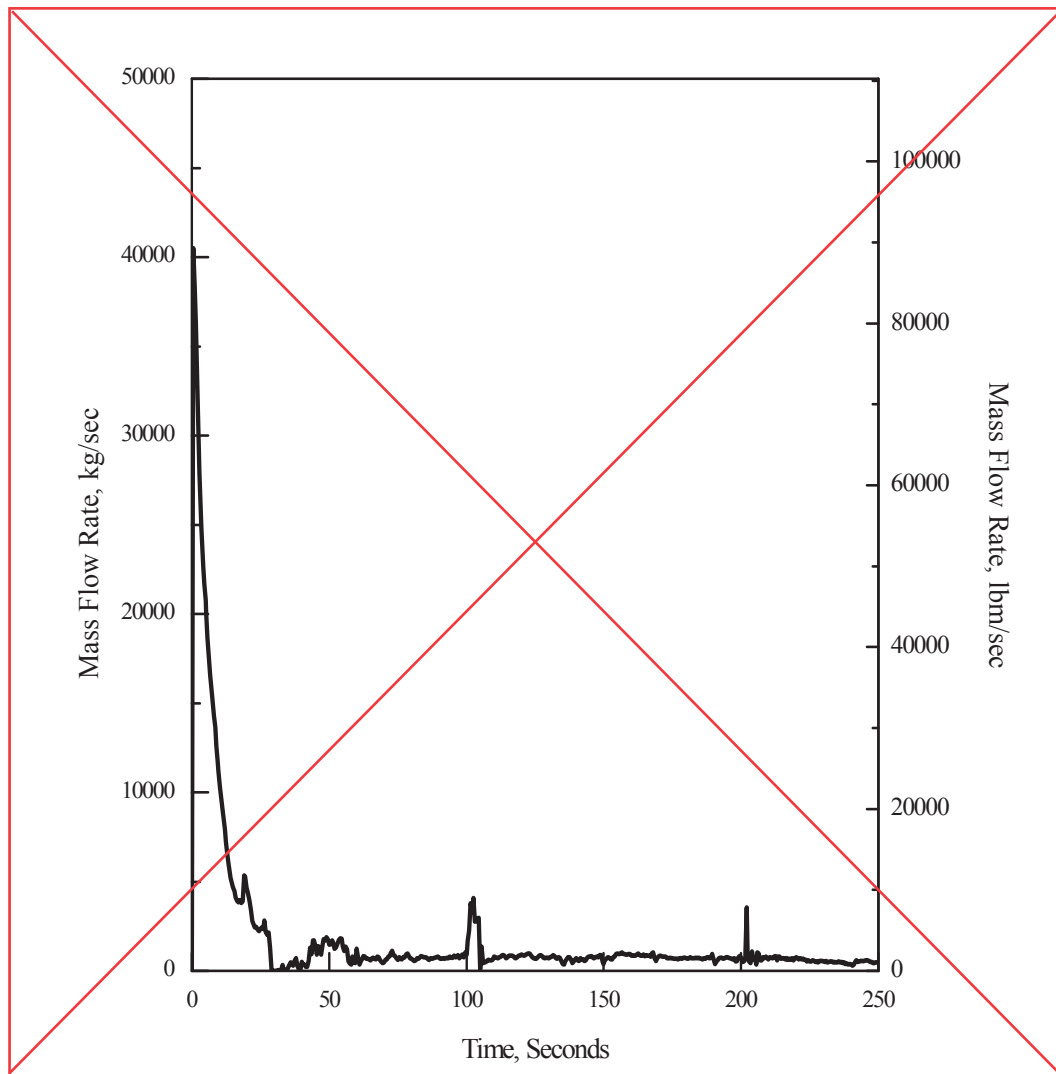
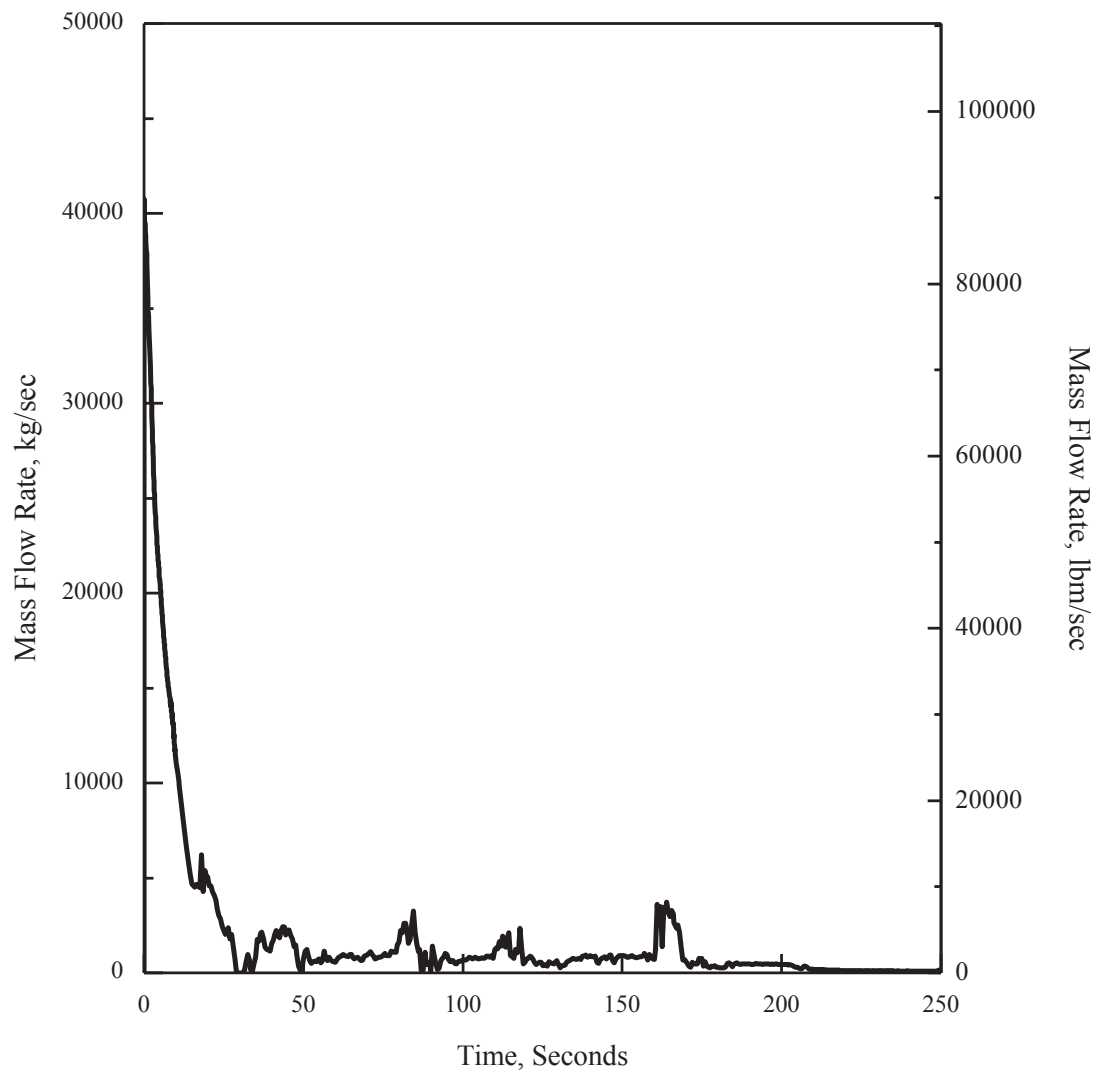


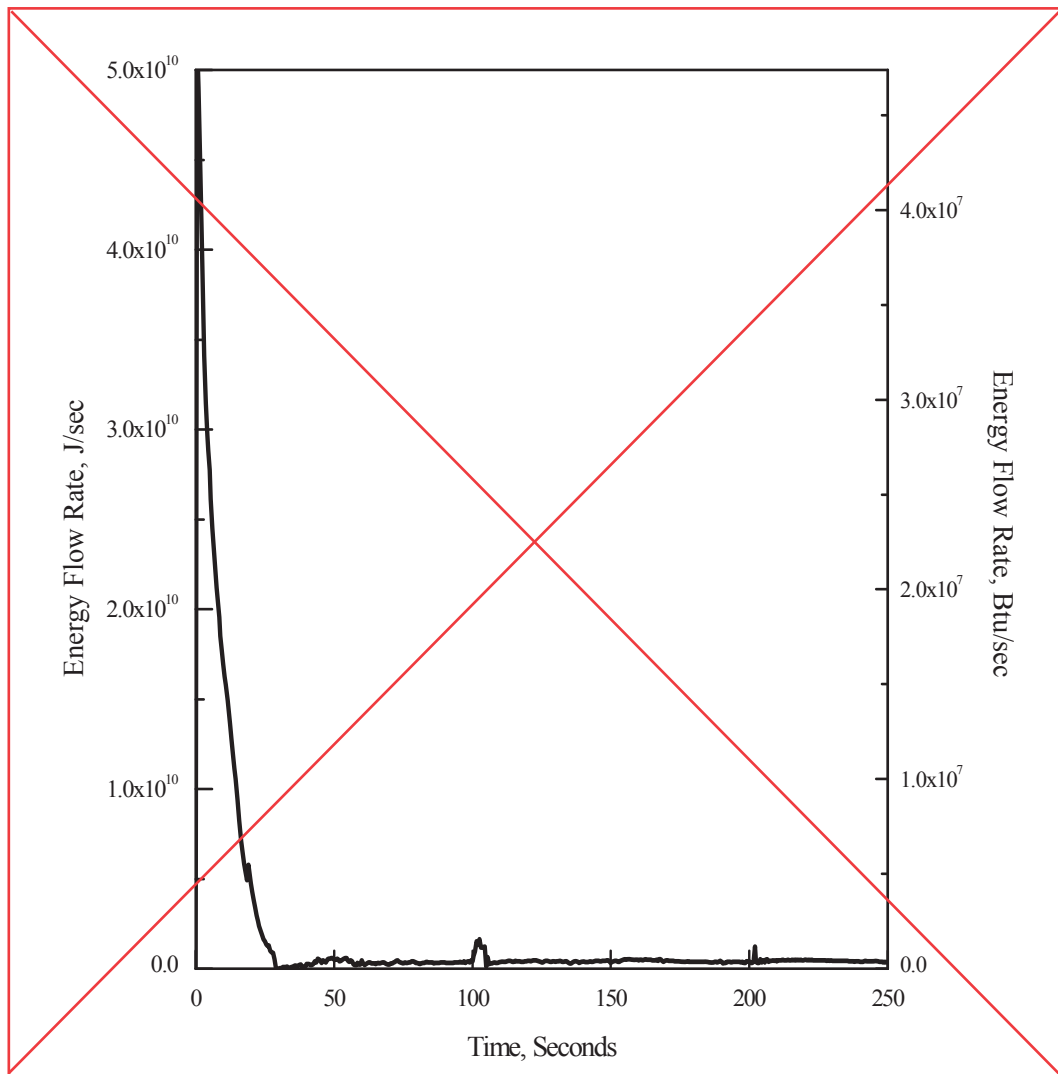
Figure 15.6.5-17 1.0 x Double-ended Guillotine Break in Pump Discharge Leg (Break Flow)

V



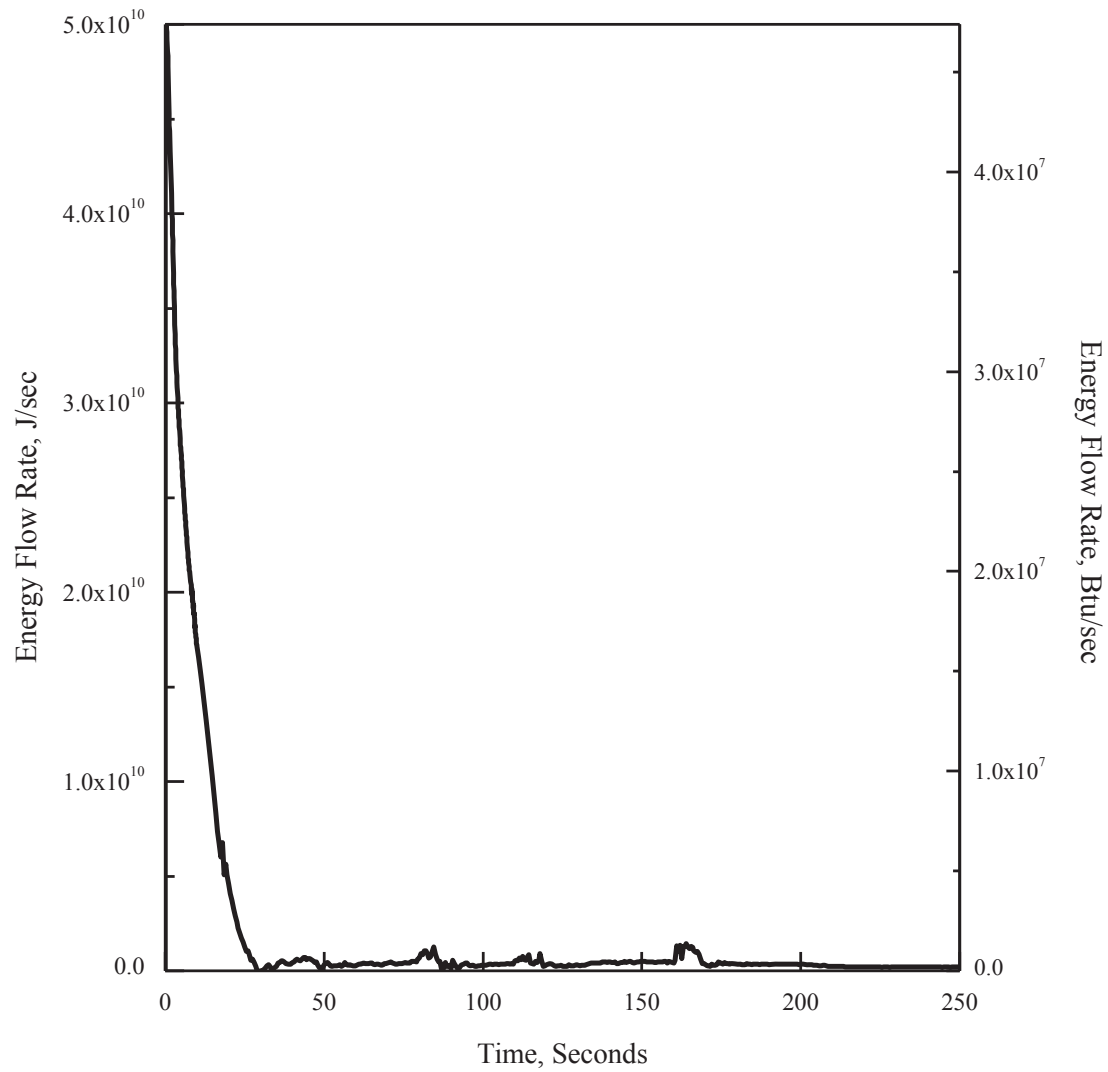
APR1400 DCD TIER 2

Replace with next page W



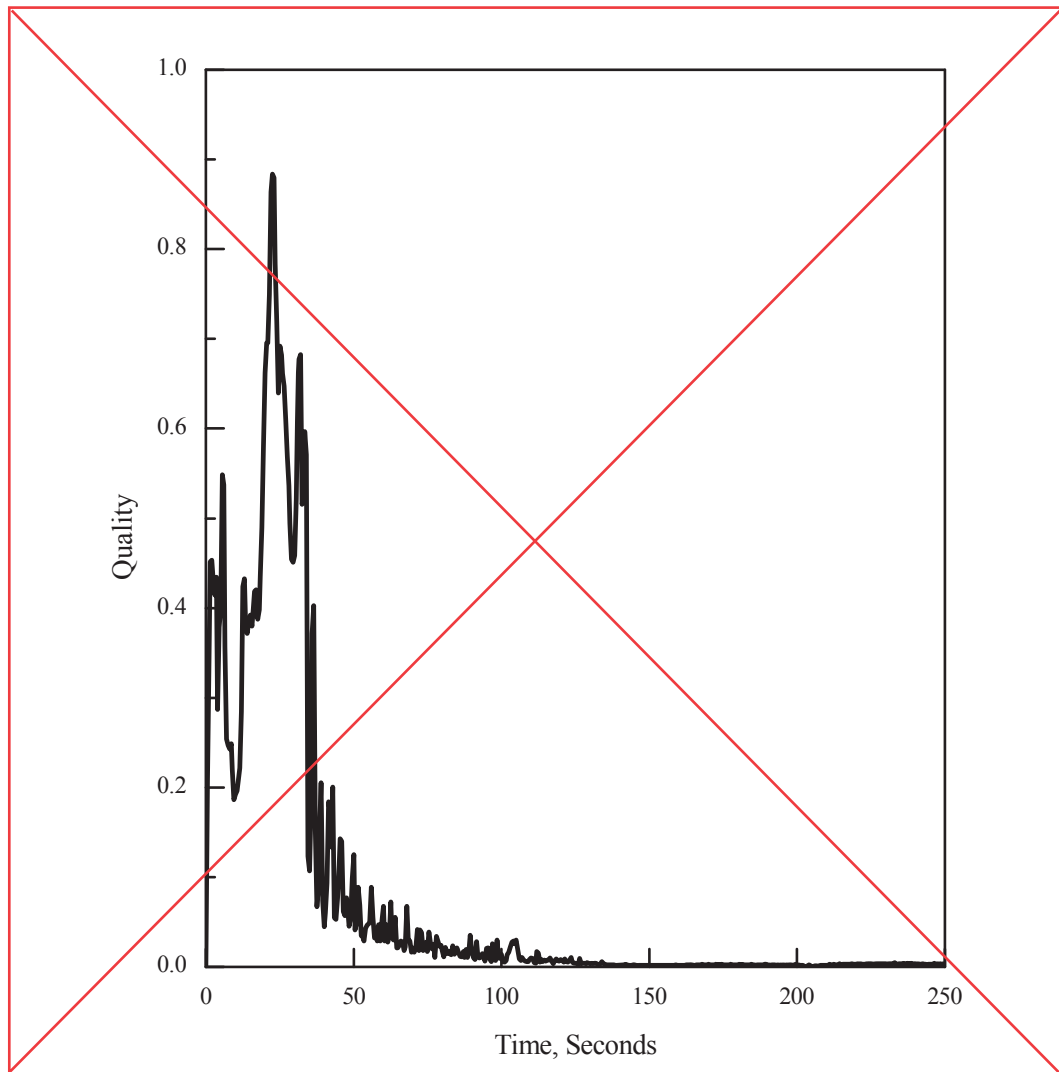
**Figure 15.6.5-18 1.0 × Double-ended Guillotine Break in Pump Discharge Leg
(Break Energy Flow)**

W



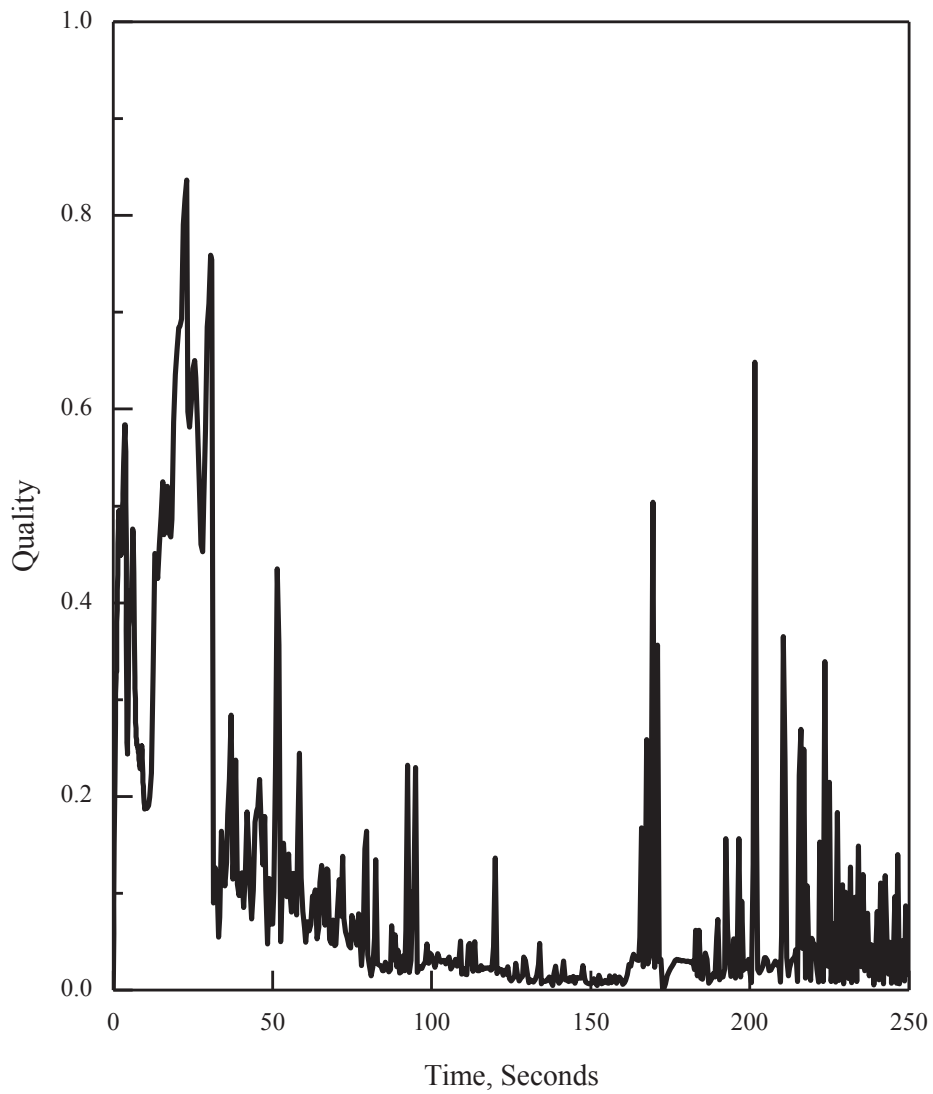
APR1400 DCD TIER 2

Replace with next page X



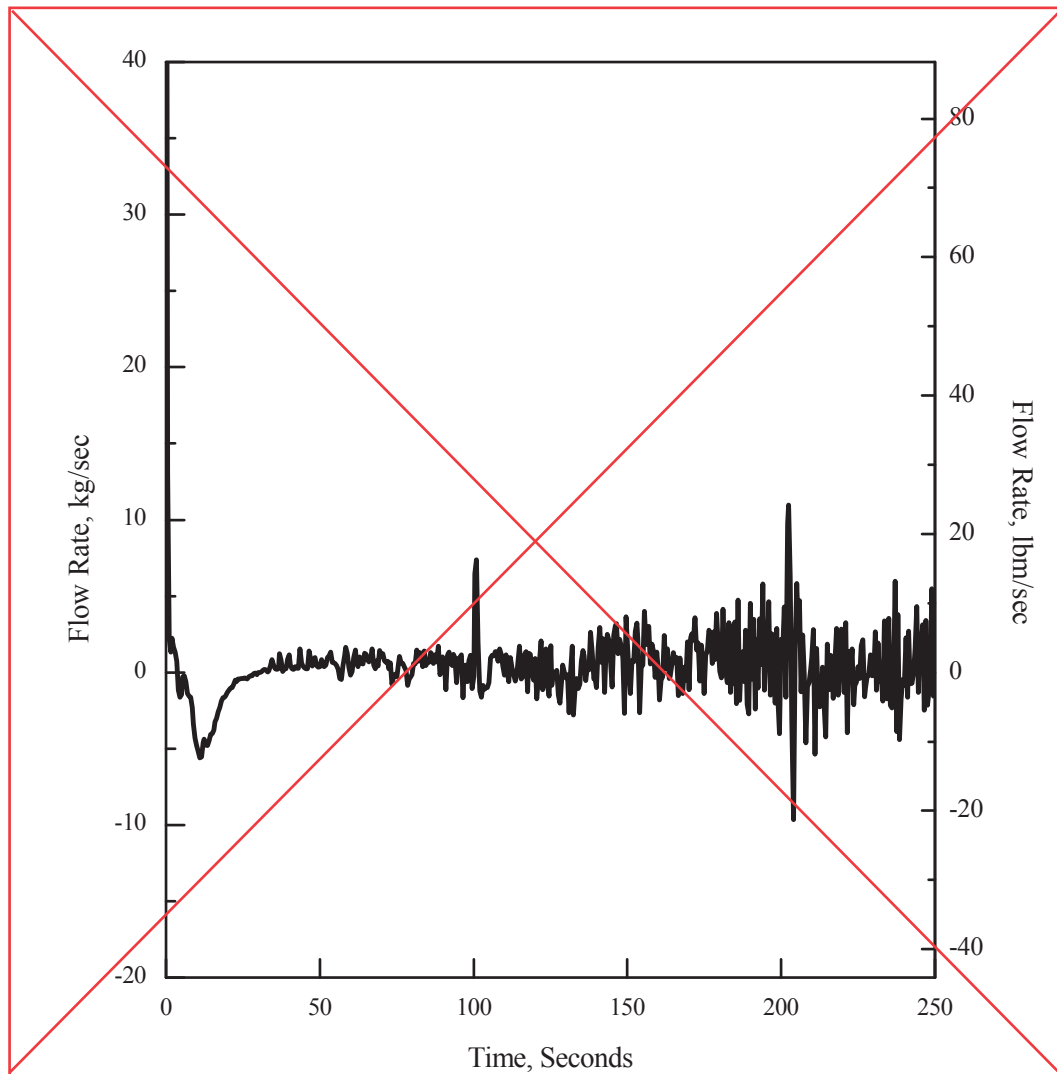
**Figure 15.6.5-19 1.0 x Double-ended Guillotine Break in Pump Discharge Leg
(Hot Assembly Quality)**

X



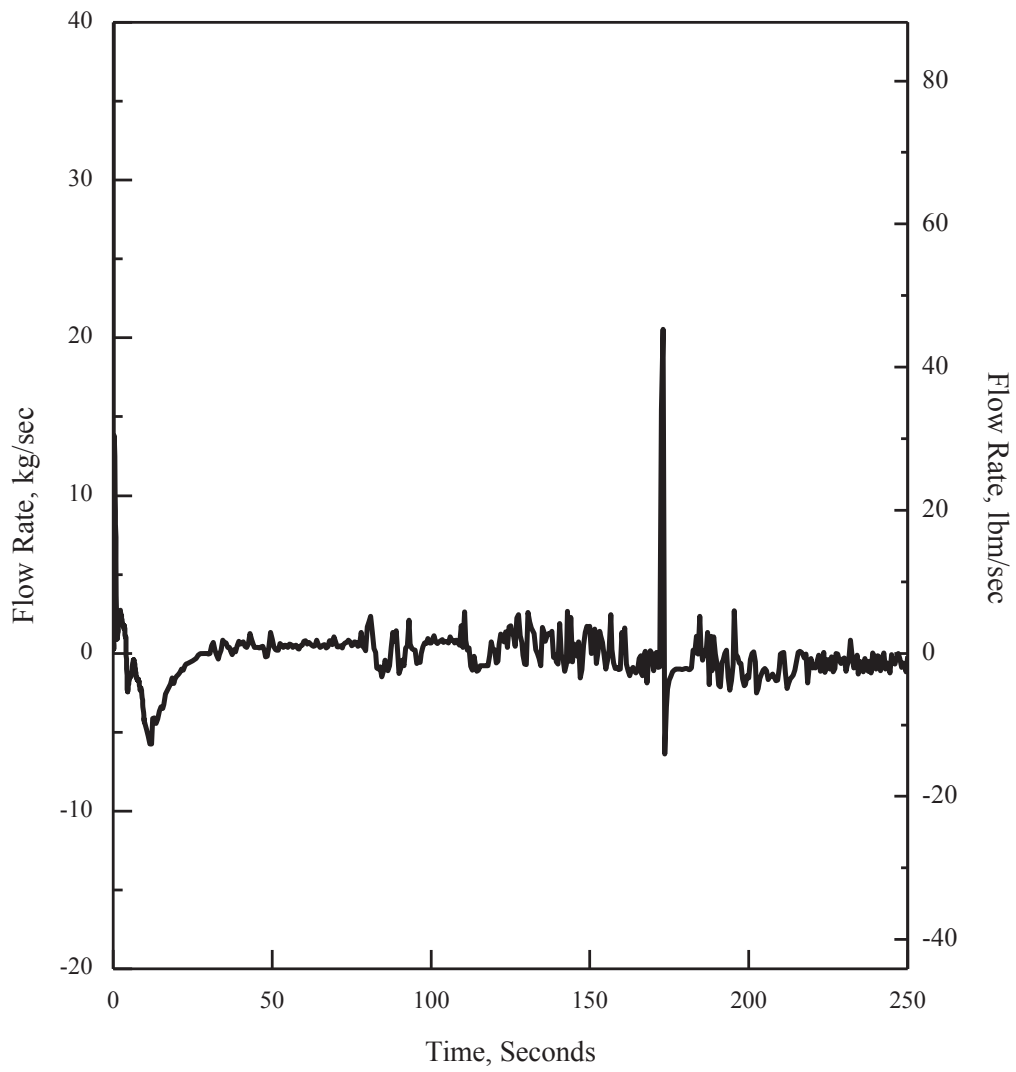
APR1400 DCD TIER 2

Replace with next page Y



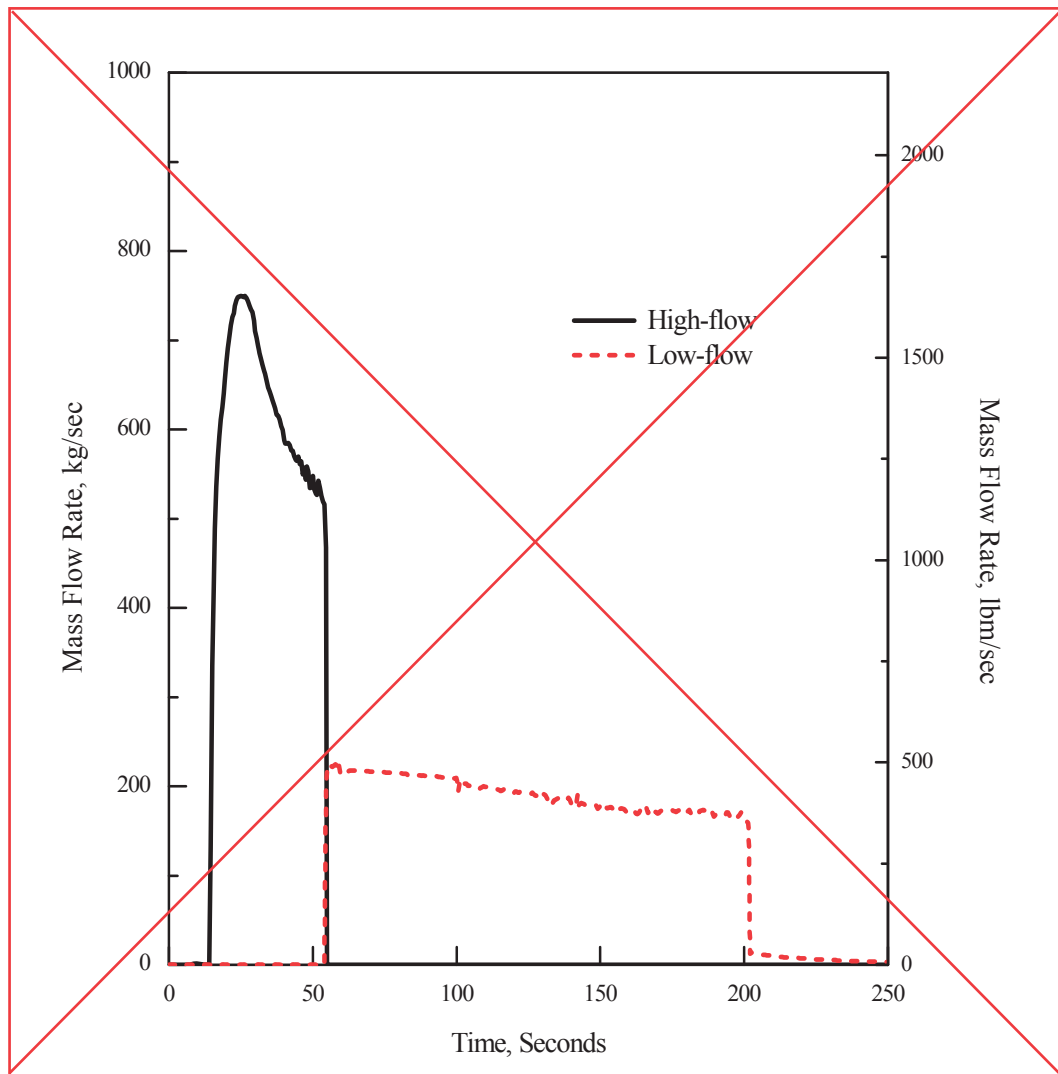
**Figure 15.6.5-20 1.0 x Double-ended Guillotine Break in Pump Discharge Leg
(Hot Assembly Mass Flow Rate)**

Y



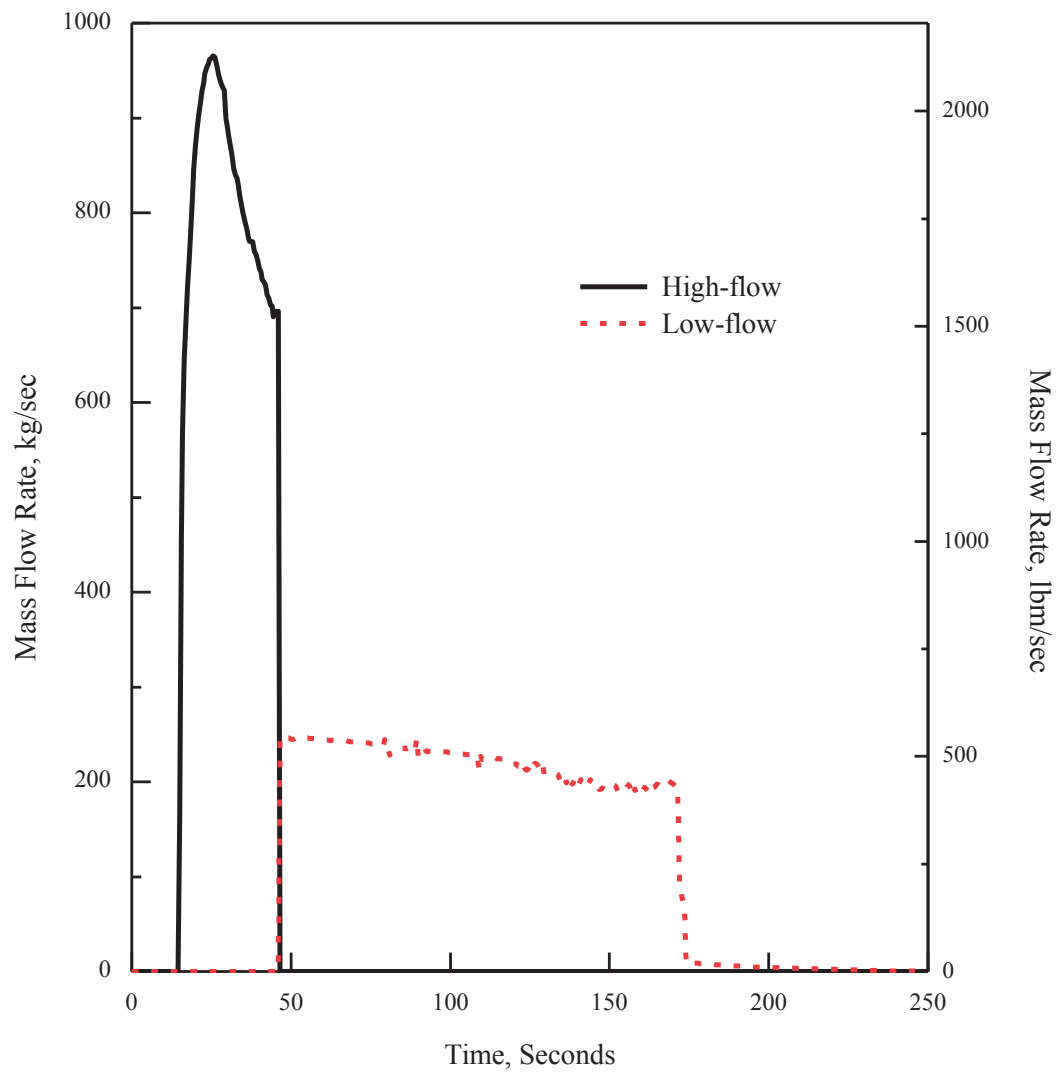
APR1400 DCD TIER 2

Replace with next page Z



**Figure 15.6.5-21 1.0 × Double-ended Guillotine Break in Pump Discharge Leg
(Safety Injection Tank Flow)**

Z



APR1400 DCD TIER 2

Replace with next page AA

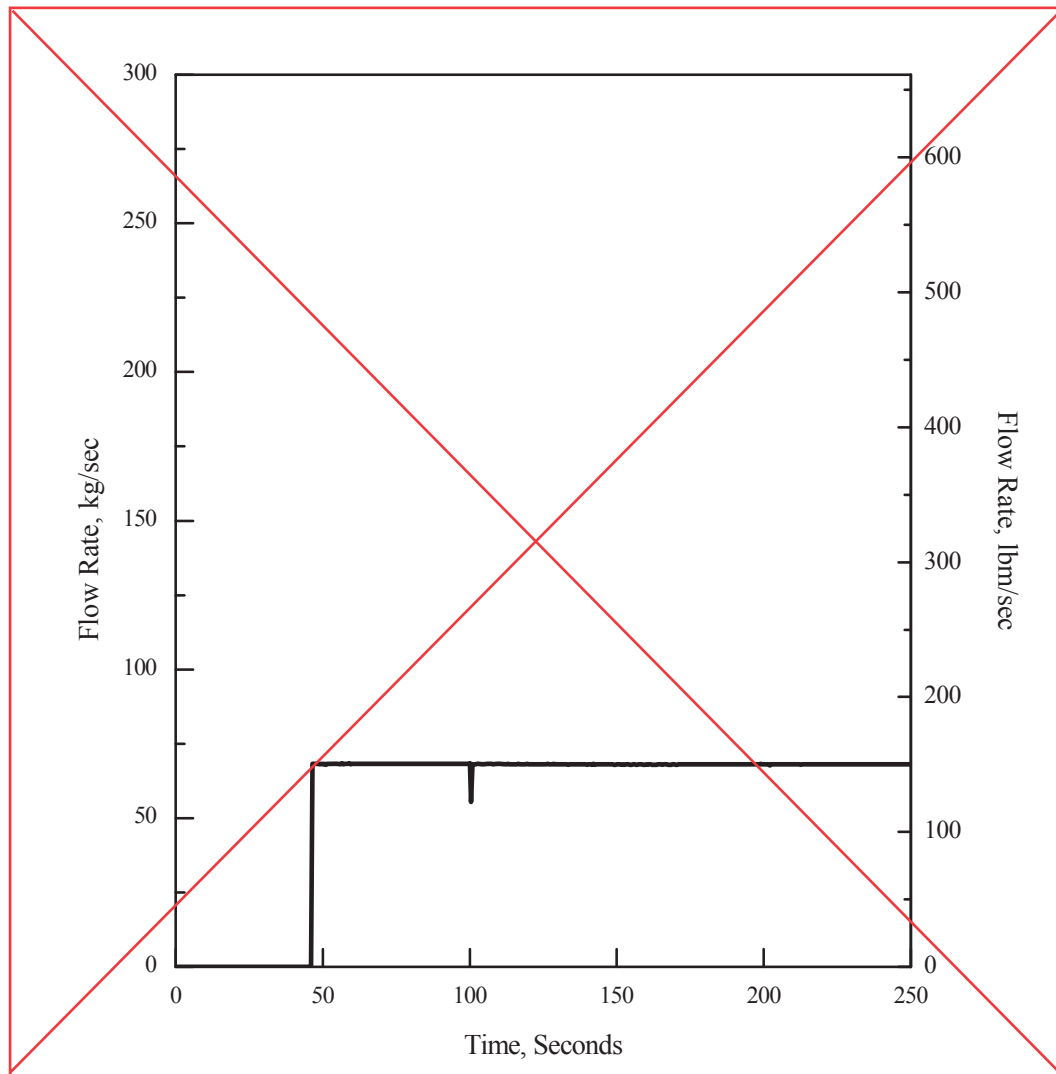
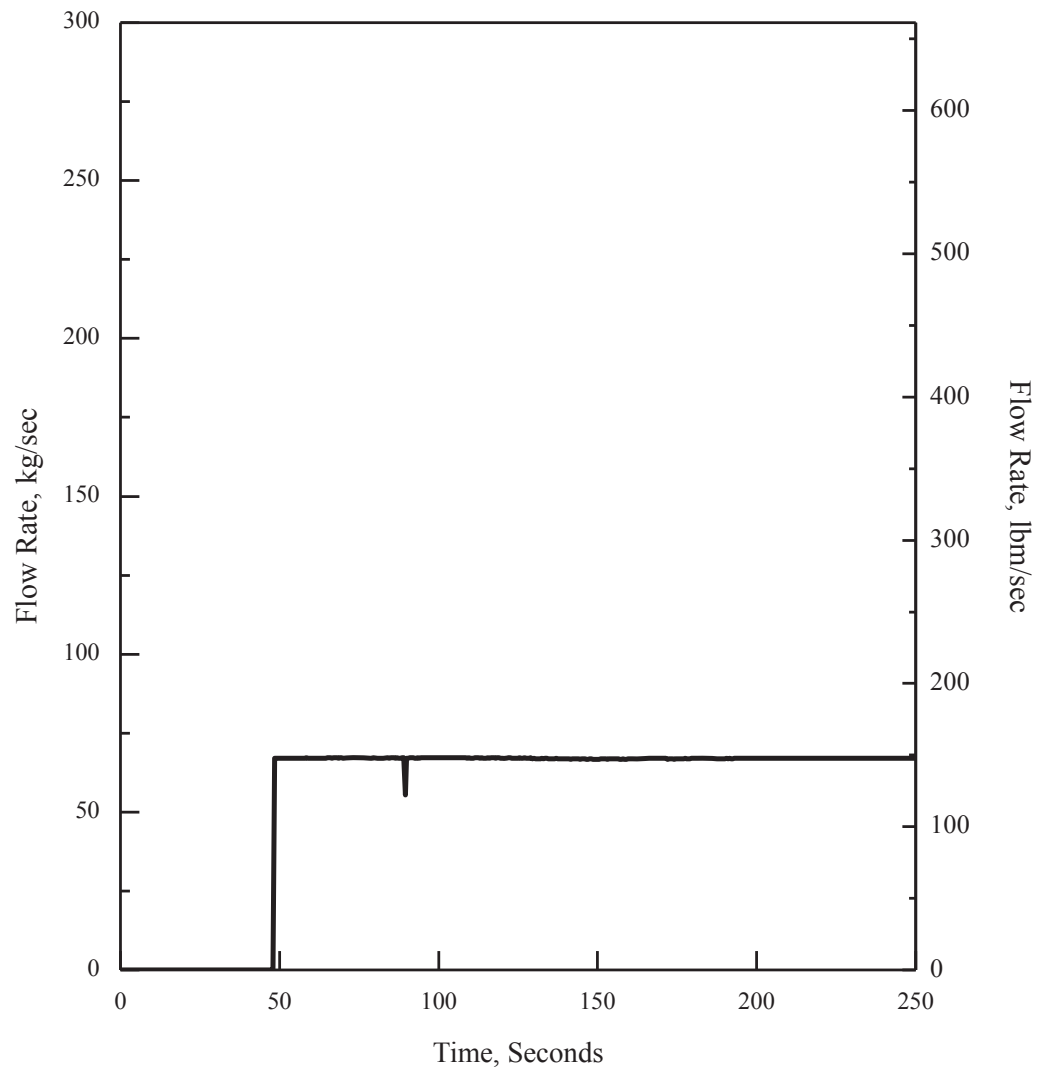


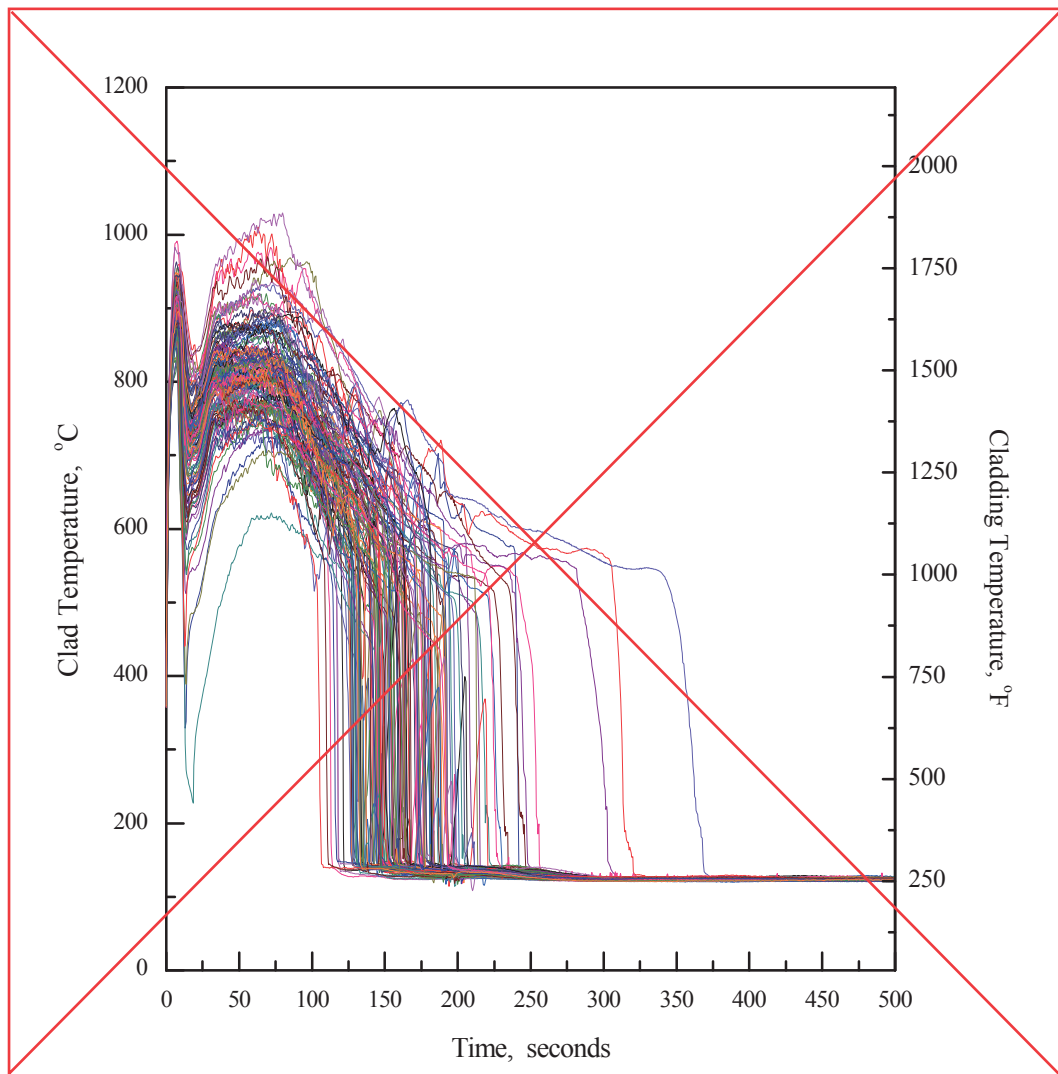
Figure 15.6.5-22 1.0 × Double-ended Guillotine Break in Pump Discharge Leg (SI Pump Flow Rate)

AA

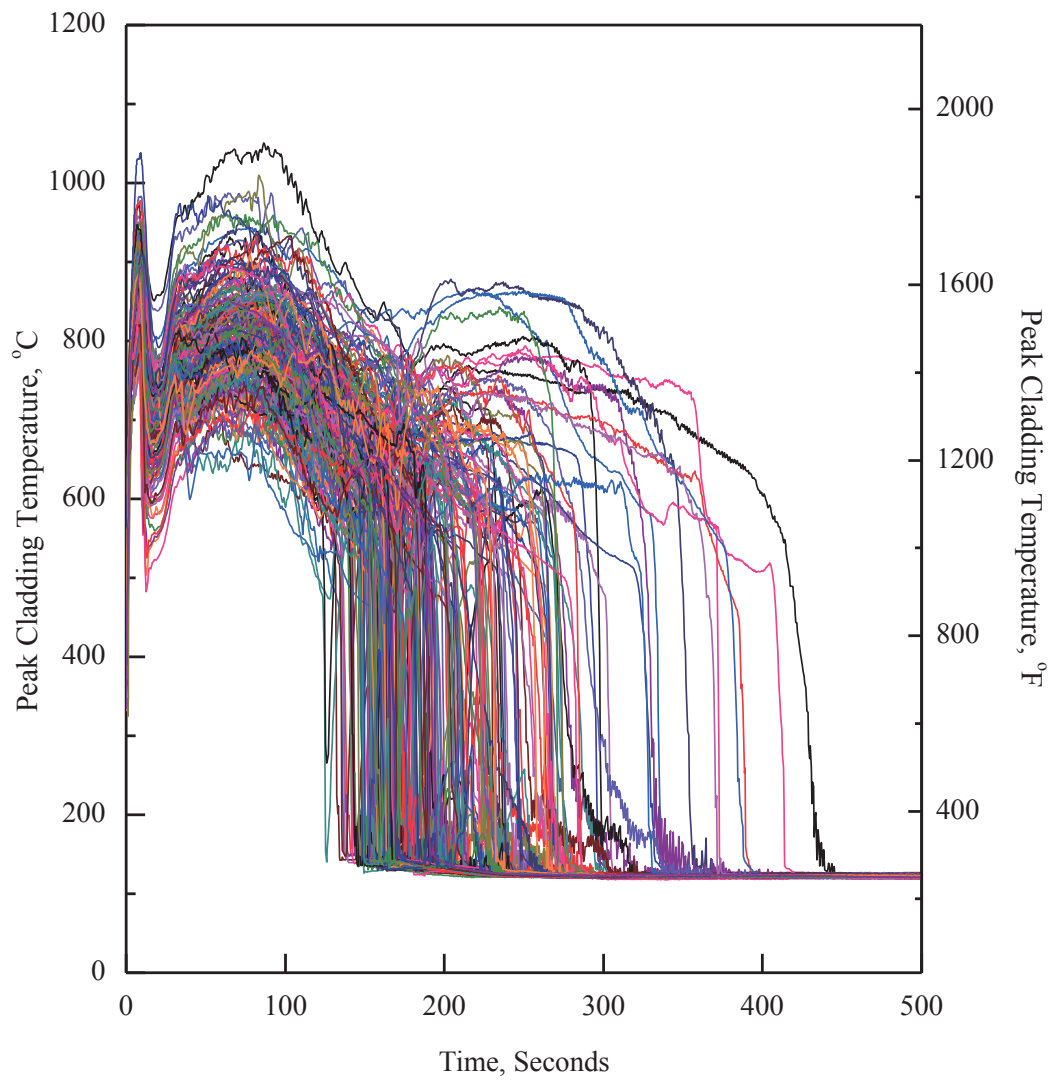


APR1400 DCD TIER 2

Replace with next page AB

**Figure 15.6.5-23 SRS Peak Cladding Temperature**

AB



Non-Proprietary

Criticality Analysis of FR and SFR

APR1400-A-R-14011-P Rev.1

3.5 Criticality Analysis for Spent Fuel Pool Region II

The spent fuel pool region II is designed to accommodate the fuel assemblies with the minimum enrichment which satisfies the criticality acceptance criteria. The criticality analysis is performed using the SAS5/sequence and the RI-ARP with cross section libraries generated using the TRIT-sequence and the DFR-II 238 energy group library.

In order to determine the loading curve the criticality analyses are performed to find the minimum enrichment which results in k_{eff} less than 1.0 at the each initial enrichment of fuel assemblies.

Figures 3.5-8 and 3.5-9 provide the analysis views of SFP region II. As can be seen from the Figure 3.5-8 spent fuel storage racks in SFP region II are based on a high density rack design and at least one neutron absorber plate is placed between adjacent fuel assemblies to maintain sub-criticality.

Design data for fuel storage cells of SFP region II are provided in Figures 3.5-8 3.5-9 and Table 3.1-2 and information for rack interfaces within and between the SFP regions are provided in Subsection 3.5.1.

3.5.1 Depletion Calculations

As discussed in Subsection 3.3.2 the depletion calculations are performed using the RI-ARP with cross section libraries generated using the TRIT-sequence. For the generation of the cross section libraries using the TRIT-sequence, the following reactor parameters described in the Subsection 3.5.1.1 are used. The isotopic concentrations are generated using the RI-ARP at each 2.25 % TU intervals from 0 to 72 % TU for the initial enrichments from 2.0 to 5.0 % ^{235}U with 0.5 % increments of ^{235}U enrichment.

Zero cooling time is taken for conservatism so that the fuel assembly is not allowed to decay after depletion to a desired assembly-average enrichment.

3.5.1.1 Bounding Reactor Parameters for the Depletion Calculation

The bounding reactor parameters are a fuel temperature of T_{fuel} and a ^{235}U concentration of C_{235} . The applied fuel temperature is higher than the maximum fuel temperature of T_{fuel}^{TS} including Thermal Conductivity Degradation (TCD) effect.

- Fuel temperature: Higher fuel temperature causes Doppler broadening and it results in increased plutonium production. Therefore the maximum fuel temperature of T_{fuel}^{TS} is applied to the depletion calculations.

- Fuel enrichment: To maximize fissile material to the depletion calculation.
- Moderator temperature: Higher moderator temperature broadens the energy spectrum hardening. Therefore the maximum moderator temperature of T_{mod}^{TS} is applied to the depletion calculation.
- Soluble boron concentration: Higher soluble boron concentration hardens the spectrum. Therefore the maximum soluble boron concentration of C_{B}^{TS} is applied to the depletion calculation.
- Power level: The sensitivity and level of power level is found that there is no trend in respect to power level as shown in Table 3.5-2. So the maximum power level corresponding to the maximum fuel temperature is used as a bounding reactor parameter.

**KHNP****KOREA HYDRO & NUCLEAR POWER CO., LTD**

70-1312-gil, Yuseong-daero, Yuseong-gu, Daejeon, 305-343, KOREA

Tel: +82-42-870-5400 / Fax: +82-42-870-5449

<http://www.khnp.co.kr>

December 1, 2017
Document Control Desk
U.S. Nuclear Regulatory Commission
Washington, DC 20555-0001

Attention: Mr. William Ward
Division of New Reactor Licensing

Docket No. 52-046
MKD/NW-17-0371L

Subject: Revised Response to RAI 5-7954 on Topical Report “PLUS7 Fuel Design for the APR1400” (Rev.3)

- References:** 1) NRC Request for Additional Information 5-7954, dated June 18, 2015
2) KHNP Letter MKD/NW-15-0055L, Response to RAI 5-7954 on Topical Report “PLUS7 Fuel Design for the APR1400, APR1400-F-M-TR-13001, Rev. 0, dated July 21, 2015
3) KHNP Letter MKD/NW-16-0826L, Response to RAI 5-7954 for Question TR PLUS7 Fuel Design for the APR1400-16, dated July 29, 2016
4) KHNP Letter MKD/NW-17-0201L, Revised Response to RAI 5-7954 on Topical Report “PLUS7 Fuel Design for the APR1400”, dated August 11, 2017
5) KHNP Letter MKD/NW-17-0323L, Revised Response to RAI 5-7954 on Topical Report “PLUS7 Fuel Design for the APR1400” (Rev.2), dated October 16, 2017

KHNP is hereby submitting the response to RAI 5-7954, dated June 18, 2015. The revised response addresses Questions TR PLUS7 Fuel Design for the APR1400-11.

Enclosure 1 contains a copy of the associated affidavit. Enclosure 2 provides the revised response to RAI 5-7954 on topical report “PLUS7 Fuel Design for the APR1400” (Rev.3) (Proprietary). Enclosure 3 provides the revised response to RAI 5-7954 on topical report PLUS7 Fuel Design for the APR1400” (Rev.3) (Non-Proprietary).

If additional information or clarification is required, please contact Daegeun Ahn, Director of KHNP Washington DC Center at ahn.daegeun@khnp.co.kr or 703-388-0592.

Sincerely,

Han-gon Kim
Project Manager
Advanced Reactors Development Laboratory
Korea Hydro & Nuclear Power Co., Ltd.



Enclosures:

1. Affidavit KAW-17-0371
2. Revised Response to RAI 5-7954 on Topical Report “PLUS7 Fuel Design for the APR1400”
(Rev.3) (Proprietary)
3. Revised Response to RAI 5-7954 on Topical Report “PLUS7 Fuel Design for the APR1400”
(Rev.3) (Non-Proprietary)

Enclosure 1

Affidavit KAW-17-0371

I, Yun-ho Kim, state the following:

1. I am the General Manager of Korea Hydro & Nuclear Power Co., Ltd. (KHNP), and as such I am authorized to request withholding the information transmitted with this letter from public disclosure and to execute this affidavit.
2. I am familiar with the criteria applied by KHNP to determine whether certain information is proprietary, and with the policies established by KHNP to ensure the proper application of these criteria.
3. The information, Revised Response to RAI 5-7954 on Topical Report “PLUS7 Fuel Design for the APR1400” (Rev.3) (Proprietary), transmitted with this letter has been classified by KHNP as proprietary in accordance with the policies for the control and protection of proprietary and confidential information. The information regarded as proprietary is identified and marked consistent with the requirements of 10 CFR 2.390, § (b)(1)(i). Accordingly, the proprietary information is enclosed within brackets and the right-hand bracket carries a notation of “TS” to indicate that the trade secret nature of the information claimed to be proprietary is the basis for proposing that the information so identified be withheld from public disclosure.
4. Pursuant to the considerations set forth in 10 CFR Section 2.390(a), KHNP considers the information classified as proprietary to be “trade secret” information since it is design, analysis, or test information that would be difficult for a competitor to reproduce and hence provides an economic and competitive advantage to KHNP.
5. The need for designating the information as proprietary has been raised within KHNP. The information is being treated proprietary and confidential and has not been disclosed by KHNP to the public.
6. Nondisclosure of the proprietary information transmitted with this letter is vital to the competitiveness held by KHNP and, hence, disclosure of the proprietary information transmitted in with this letter would have negative commercial impacts on the competitive position of KHNP in the U.S. nuclear market.
7. In accordance with KHNP policy, proprietary information contained in this document may be, or may have been, made available on a limited basis to regulatory bodies, customers, potential customers, and their agents, suppliers, and licensees, and others under suitable agreements providing for nondisclosure and limited use of the information.



KHNP
KOREA HYDRO & NUCLEAR POWER CO., LTD

I declare that the foregoing statements are true and correct to the best of my knowledge,
information and belief.

Executed on December 1, 2017.

Yun-ho Kim
General Manager
APR1400 Licensing Team
Korea Hydro and Nuclear Power Co., Ltd

Enclosure 3

Revised Response to RAI 5-7954 on Topical Report “PLUS7 Fuel
Design for the APR1400” (Rev.3)

(Non-Proprietary)

December 1, 2017

REVISED RESPONSE TO REQUEST FOR ADDITIONAL INFORMATION

APR1400 Topical Reports

Korea Electric Power Corporation / Korea Hydro & Nuclear Power Co., LTD

Docket No. PROJ 0782

RAI No.: 5-7954

SRP Section: TR PLUS7 Fuel Design for the APR1400

Application Section: PLUS7 Fuel Design for the APR1400
(APR1400-F-M-TR-13001-P)

Date of RAI Issue: 06/18/2015

Question No. TR PLUS7 Fuel Design for the APR1400-11

GDC 10 requires that the reactor core and associated coolant, control, and protection systems shall be designed with appropriate margin to assure that specified acceptable fuel design limits (SAFDLs) are not exceeded during any condition of normal operation, including the effects of anticipated operational occurrences (AOOs). SRP Section 4.2 (II)(1)(B)(v) provides guidance stating that the fuel failure criteria should address excessive fuel enthalpy.

This fuel failure criterion is addressed on Page 3-9 of APR1400-F-M-TR-13001-P for the PLUS7 fuel design. Section 3.4.4 of the topical report states that the code used to analyze this fuel failure mechanism (FATES3B) over predicts fuel thermal conductivity at high burnup. Therefore, it will also under predict fuel enthalpy. The staff notes that Section 3.4.4 provides a qualitative argument to state that the effects of burnup dependence of TCD are bounded by the reduced power capabilities at higher burnups. This raises concerns from the staff on the ability of the excessive fuel enthalpy analysis to demonstrate compliance with the excessive fuel enthalpy SAFDL given all core loading options available.

Please include a discussion, supported by analysis, within Section 3.2.10 and/or 3.4.4 of APR1400-F-M-TR-13001-P regarding the impacts of the fuel enthalpy under prediction and how excessive fuel enthalpy is precluded.

Response - (Rev.3)

A impact of fuel enthalpy will be updated and added in Section 3.6 of topical report (APR1400-F-M-TR-13001-P), which is currently described in Section 3.4.5.

“The impacts of TCD result in increasing the fuel enthalpy and the fuel centerline temperature. The impact on the fuel enthalpy due to TCD would be negligible for fresh fuel even though the maximum power peaking factors exist in the low burnup fuel in the APR1400 reload core designs. For the high burnup fuel which is affected by TCD, the fuel enthalpy and the fuel centerline temperature increase due to TCD are not significant because of the peaking factor burndown effect at higher burnups. The event specific evaluation considering the TCD penalty described in the Section 3.5 was performed and described in DCD Tier 2 Chapter 15.4.8.”

Impact on DCD

Effect on the Design Control Document (DCD) Tier 2 Chapter 15.4.8 for safety analyses will be updated because interface data results based on the thermal conductivity degradation (TCD) penalty methodology are applied.

In addition, for an extent of condition review, TCD-affected chapters will be revised as indicated on the attached markups. The attached markups are classified as follow.

- References (Chapter 4.2.6) : Attachment 2
- Control Requirements (Chapter 4.3.2.4) : Attachment 3
- Containment Functional Design (Chapter 6.2.1) : Attachment 4
- Containment Functional Design (Chapter 6.2.1) : Attachment 5
- Criticality Safety of New Spent Fuel Storage (Chapter 9.1.1) : Attachment 6
- General Information for Safety Analysis (Chapter 15.0.0) and Spectrum of Control Element Assembly Ejection Accidents (15.4.8) : Attachment 7
- Loss-of-Coolant Accidents (Chapter 15.6.5) : Attachment 8

Impact on PRA

There is no impact on the PRA.

Impact on Technical Specifications

There is no impact on the Technical Specifications.

Impact on Technical/Topical/Environmental Reports

PLUS7 fuel design topical report (APR1400-F-M-TR-13001-P) will be revised as indicated on the attached markups (Attachment 1).

Criticality Analysis technical report (APR1400-Z-A-NR-14011-P) will be revised as indicated on the attached markups (Attachment 9).

Non Proprietary

PLUS7 FUEL DESIGN for the APR1400

APR1400-F-M-TR-13001-P Rev.0

Considering the amount of potential increase in rod internal pressure by TCD impact and design margin to the limit, it is judged that the cladding stress criteria are still met with consideration of TCD.

3.4.2 Cladding Strain and Fatigue

The cladding strain is affected by TCD due to the increased fuel thermal expansion. However, the increased thermal expansion can be offset with available design margin to the cladding strain and fatigue limits and conservatism in the input variables such as power history and assumed rod internal pressure. Therefore, cladding strain and fatigue criteria are still satisfied with consideration of TCD.

3.4.3 Fuel Rod Internal Pressure

The effect of increased fuel temperature due to TCD on fission gas release is inherently accounted for in the current performance code, FATES3B (References 3-1 through 3-4) because the model was calibrated to measured data for a full range of fuel rod burnup and operating conditions. Additionally, conservatism is considered in the original FATES3B calibration process and in fuel rod design analysis. However, the rod internal pressure may still increase with TCD due to the increased fuel thermal expansion, which reduces the total fuel rod void volume.

Evaluations show that the reduction of void volume due to increased thermal expansion is not significant in PLUS7 fuel rod design. In addition, the rod internal pressure limit calculation is inherently conservative in that actual gap reopening is predicted to occur at higher pressures.

In conclusion, the increased rod internal pressure can be offset with available design margin to the rod internal pressure limits. Therefore, rod internal pressure criteria are still satisfied considering the effects of TCD.

3.4.4 Overheating of Fuel Pellets

The power to melt limit depends on fuel burnup but the reduced power capability with burnup, which is caused by the depletion of the fissile material in the fuel and the buildup of fission products, offsets the TCD impact. Therefore, it is judged that there will be no safety concerns due to TCD. However, the power to melt values with burnup considering the impact of TCD are calculated and will be provided in the TCD Technical Report which will be submitted to NRC.

In summary, KNF fuel rod design criteria have been reviewed with respect to the potential impacts of TCD, and it is concluded that TCD can be accommodated such that approved fuel rod design criteria will remain satisfied for current fuel rod designs.

3.5 Conclusion

The PLUS7 fuel rod design is verified to maintain the rod integrity up to rod average burnup of 60,000 MWD/MTU based on the thermal performance and mechanical integrity evaluation results

3.4.5 Impacts of Fuel Thermal Expansion

The impacts of TCD result in increasing the fuel enthalpy and the fuel centerline temperature. The impact on the fuel enthalpy due to TCD is negligible for fresh fuel even though the maximum operating factors exist in the low burnup fuel in the APR1400 reload core designs. For the high burnup fuel which is affected by TCD the fuel enthalpy and the fuel centerline temperature increase due to TCD are not significant because of the operating factor burnup effect at higher burnups. The detailed evaluation was performed for the impacts of TCD and summarized in TCD Technical Report in Reference 3-14.

KHNP

3-17

This chapter 3.4.5 will be modified and moved to in the next new draft page.

3.5.2 Fuel Rod Interface Data for Safety Analyses

To generate the fuel rod interface data with TCD effect for safety analyses, the TCD penalty determined as a function of burnup is added to the temperatures calculated by FATES3B code and those TCD penalty-added centerline temperatures of hot and average rods should be provided to safety analyses team.

3.6 Impact of Fuel Enthalpy

The impacts of TCD result in increasing the fuel enthalpy and the fuel centerline temperature. The impact on the fuel enthalpy due to TCD would be negligible for fresh fuel even though the maximum power peaking factors exist in the low burnup fuel in the APR1400 reload core designs. For the high burnup fuel which is affected by TCD, the fuel enthalpy and the fuel centerline temperature increase due to TCD are not significant because of the peaking factor burndown effect at higher burnups. The event specific evaluation considering the TCD penalty described in the Section 3.5 was performed and described in DCD Tier 2 Chapter 15.4.8.

3.7 Conclusion

The PLUS7 fuel rod design criteria considering TCD effect is evaluated using NRC approved FATES3B code and verified acceptable up to rod average burnup of 60,000 MWd/MTU. In addition, the potential impact of TCD on the fuel rod design criteria was evaluated, and it is concluded that TCD can be accommodated. Fuel rod interface data accounting for TCD penalty are generated and transmitted to safety analyses team.

Header 3.4.5 for enthalpy is moved to new header 3.

Note: This change is needed to reflect the TCD effect. This change is same with the Attachment 1 (7/11) in response to RAI 5-7954 Question 12.

APR1400 DCD TIER 2

4.2.6 References

1. 10 CFR Part 50, Appendix A, General Design Criterion for Nuclear Power Plants 10, "Reactor Design," U.S. Nuclear Regulatory Commission.
2. 10 CFR Part 50, Appendix A, General Design Criterion for Nuclear Power Plants 27, "Combined Reactivity Control Systems Capability," U.S. Nuclear Regulatory Commission.
3. 10 CFR Part 50, Appendix A, General Design Criterion for Nuclear Power Plants 35, "Emergency Core Cooling," U.S. Nuclear Regulatory Commission.
4. 10 CFR 50.46, "Acceptance criteria for emergency core cooling systems for light-water nuclear power reactors," U.S. Nuclear Regulatory Commission.
5. APR1400-F-M-TR-13001-P (Proprietary) & NP (Non-Proprietary), "PLUS7 Fuel Design for the APR1400, Rev. 0, KHNP, August 2013." Rev. 1 ~~to be issued.~~ August 2017.
6. NUREG-0800, Standard Review Plan, Section 4.2, "Fuel System Design," Rev. 3, U.S. Nuclear Regulatory Commission, March 2007.
7. CENPD-404-P-A, "Implementation of ZIRLO™ Cladding Material in CE Nuclear Power Fuel Assembly Designs," Rev. 0, Combustion Engineering, Inc., November 2001.
8. WCAP-12610-P-A, "VANTAGE+ Fuel Assembly Reference Core Report," Westinghouse Electric Corporation, April 1995.
9. W. J. O'Donnell and B. F. Langer, "Fatigue Design Basis for Zircaloy Components," Nuc. Sci. Eng., Vol. 20, pp. 1-12, April 1964.
10. Conway, J. B., "The Thermal Expansion and Heat Capacity of UO₂ to 2200 °C," E-NMPD-TM-63-6-6.
11. Christensen, J. A., "Thermal Expansion and Change in Volume on Melting for Uranium Dioxide," HW-75148, October 1962.
12. Jones, J. M. and Murchison D. G., "Optical Properties of Uranium Oxides," Nature, Vol. 205, pp. 663-65, February 1965.

APR1400 DCD TIER 2

coefficient, is described in Subsection 4.3.2.3.2 and shown in Figures 4.3-31 and 4.3-32. The second factor ($\delta T_m / \delta p$) of the second term is a constant because the moderator temperature is controlled to be a linear function of power.

Because the fuel temperature coefficient ($\delta \rho / \delta T_f$) and moderator temperature coefficient ($\delta \rho / \delta T_m$) are functions of one or more independent variables (e.g., burnup, temperature, soluble boron content, xenon worth, CEA insertion), the total power coefficient, dp/dp , also depends on these variables.

The power coefficient tends to become more negative with burnup because the fuel and moderator temperature coefficients become more negative as shown in Figures 4.3-30 through 4.3-32. Insertion of the CEAs, while maintaining constant power, results in a more negative power coefficient because the soluble boron level is reduced and because of the spectral effects of the CEAs themselves. The full-power values of the overall power coefficient for the unrodded core at the beginning and end of the first cycle are shown in Table 4.3-4.

4.3.2.4 Control Requirements

The three basic types of control requirements that influence the design of this reactor are:

4.3.2.3.8 Impact of Thermal Conductivity Degradation on Reactivity Coefficients

The fuel temperature increase due to thermal conductivity degradation (TCD) could have impacts on the prediction results of the fuel temperature coefficients and the core average reactivity due to the change in reactivity feedback of fuel temperature. The least negative or the most negative fuel temperature coefficients are used for safety analysis on an event specific basis, which is limiting for the transient. The fuel temperature coefficients are calculated using the effective fuel temperature changes which are caused by power changes and the corresponding reactivity changes. The nodal average effective fuel temperature correlation as a function of the burnup and linear power density is determined based on the fuel temperatures generated by FATES (References 2 and 3) as described in Subsection 4.3.2.3.7. The prediction results of the reactivity parameters using the effective fuel temperature correlation combined with current nuclear cross section models of DIT (Subsection 4.3.3.1.1.3) have been validated through the operation of OPR1000 plants with designs similar to those of APR1400 in terms of fuel design, operating temperatures and linear power density.

The limiting reactivity parameters based on the fuel temperature correlation and the cross section data are used as input for the safety analysis with the biases and uncertainties which have been determined through the comparison of prediction data to the plant measurement data. Therefore, the reactivity parameters implicitly include the impact of TCD in APR1400 nuclear design since the effective fuel temperature correlations and the biases and uncertainties have been validated against plant measurements.

APR1400 DCD TIER 2

A containment response analysis following a DBA LOCA is also performed to consider the impact from thermal conductivity degradation (TCD) of the fuel pellets. The containment peak pressure of the TCD analysis is 0.3 psi higher than the case without TCD consideration. The TCD case peak pressure remains below the containment design limit, thus ensuring containment integrity at these conditions. A detailed description of the TCD effects on the containment integrity analysis is provided in Reference 5.

3

Consistent with the requirements of GDC 15 and 50, it has been demonstrated that the APR1400 containment design pressure provides more than a 10 percent margin (14.8 percent) above the maximum calculated peak pressure. The calculated containment pressure at 24 hours, 1.521 kg/cm²G (21.64 psig), is 42.35 percent of the peak calculated pressure for the limiting LOCA and thus meets the requirements of GDC 38.

Throughout the LOCA, the containment temperature remains at saturated conditions. Per Reference 3, the DBA LOCA peak saturation temperature of 134.59 °C (274.25 °F), which is higher than the maximum calculated surface temperature of all the containment internal structures including liner plate, is less than the containment design temperature of 143.3 °C (290.0 °F).

6.2.1.1.3.3 Analysis of Containment Response to Secondary System Piping Ruptures

This subsection describes the containment response analysis following a postulated main steam line break (MSLB) event. Containment response analyses to various combinations of power level, break size, and break location were performed to determine the limiting MSLB from a containment peak temperature and pressure standpoint. The bases for the selection of break size, power level, and single failure are discussed in Subsection 6.2.1.4 and listed in Table 6.2.1-1.

The MSLB M&E release data used in the containment response calculation are given in Tables 6.2.1-9 through 6.2.1-18. The methodology, computer codes, and assumptions used for the M&E release analysis are presented in Subsection 6.2.1.4. Additional description of the computer code and methodology for MSLB containment response analyses are provided in Reference 3.

6.2.1.3.2 Energy Sources

The following sources of generated and stored energy in the RCS and secondary coolant system are considered:

- a. Primary coolant
- b. Secondary coolant
- c. Primary walls (including reactor internals)
- d. Secondary walls
- e. Safety injection water
- f. Core power
- g. Decay heat

The core stored energy may be increased slightly by the thermal conductivity degradation (TCD). The containment pressure with the TCD effect is slightly higher (0.3% or less) than the case without TCD. The TCD effect on the LWA is negligible. The detailed methodology descriptions and the P/T results of the TCD effect analysis are provided in Section 3 of Reference 3.

For the conservative analysis, the assumptions about the energy sources are biased to maximize the stored energy.

For considering the stored energy in the coolant, the initial RCS water volumes are conservatively calculated based on the maximum manufacturing tolerances of the reactor vessel and steam generator tubes. Volume expansion of the loop components from cold to hot operating conditions is also considered for the primary and secondary coolant stored energy. The initial water volume in the pressurizer includes an allowance for level instrumentation error. This makes the maximized pressurizer water volume, which includes the maximized stored energy.

For considering the stored energy in the primary and secondary walls, the large specific heat and heat conductivity of carbon steel are conservatively assumed for all of the walls in the RCS.

The core stored energy may be increased slightly by thermal conductivity degradation (TCD). However, the effect of TCD on the M&E release is negligible. The results are described in Reference 5.

For considering the energy in the safety injection water, the liquid break flow is assumed to be mixed with the water in IRWST. The mixed water is taken and discharged into the

The total volume of fluid for two steam lines between the MSIVs and a steam generator is assumed to be the maximum in the analysis. The total volume of fluid between the MSIVs and the turbine stop valves is also assumed to be the maximum in the analysis. The analysis credits the energy stored in the steam and liquid in the affected steam generator.

There are two MFIVs in each feedwater line. The total volume of fluid between the upstream MFIV and each steam generator is assumed to be the maximum. The flashing of this fluid into the affected steam generator and then into the containment is considered in the analysis. These assumed volumes conservatively exceed the actual design values of the APR1400 volumes.

The sources of energy considered in the MSLB analysis include the stored energy in the (1) affected steam generator's metal, including the steam generator tube, (2) water in the affected steam generator, (3) feedwater transferred to the affected steam generator before the closure of the MFIV, and (4) steam from the unaffected steam generator before the closure of the MSIV. The energy sources that are considered also include the energy transferred from the primary coolant to the water in the affected steam generator during blowdown.

6.2.1.4.1 Mass and Energy Release Data

Mass and energy release data for the MSLB cases listed in Table 6.2.1-1 are given in Tables 6.2.1-9 through 6.2.1-18.

6.2.1.4.2 Single Failure Analysis

Non-class 1E electric power is conservatively assumed to be available because it allows the continuation of reactor coolant pump operation, which maximizes the rate of heat transfer to the affected steam generator, which maximizes the rate of an M&E release. With the availability of Non-class 1E electric power, a postulated diesel generator failure is unnecessary.

There is an MSIV in each main steam line. The MSIVs are designed to close based on a conservative calculation that maximizes the dynamic pressure loading on the valve for all possible flow rates and qualities. Each valve has dual control circuits to provide reasonable assurance of closure even with a single failure in the control system. Each valve is tested periodically. A single failure in the actuation signal does not prevent valve

The core stored energy may be increased by the thermal conductivity degradation (TCD). The containment peak pressure with the TCD effect is slightly higher by 0.33 psi than the case without TCD. The TCD effect on the MSLB is negligible. The detailed methodology descriptions and M/E and P/T results of the TCD effect analysis are provided in Section 3 of Reference 3.

APR1400 DCD TIER 2

containment vessel. The ferritic materials meet the fracture toughness criteria and requirements for testing identified in Article NE 2300 of ASME Section III, Division 1 (Reference 39) or Article CC 2520 of ASME Section III, Division 2 (Reference 38) as appropriate for the individual components.


The weld filler materials meet the applicable requirements of ASME Code Section III and conform to the applicable ASME Code Section II material specifications or ASME Code Cases permitted or approved by the NRC.

The COL Applicant is to provide the weld filler material in the supplier specification (COL 6.2(1)).

6.2.8 Combined License Information

COL 6.2(1) The COL Applicant is to provide the weld filler material in the supplier specification.

6.2.9 References

1. APR1400-E-N-NR-14001-P (Proprietary) & NP (Non-Proprietary), "Design Features to Address GSI-191," Rev. 1, KHNP, March 2017.
2. GOTHIC Thermal Hydraulic Analysis Package User Manual, Version 8.0(QA), NAI 8907-02, Rev. 20, Numerical Applications, Inc., January 2012.
3. APR1400-Z-A-NR-14007-P (Proprietary) & (Non-Proprietary), "LOCA Mass and Energy Release Methodology," Rev. 0, KHNP, November 2014.
4. Final Safety Evaluation For FRAMATOME ANP Topical Report BAW-10252(P), "Analysis of Containment Response to Postulated Pipe Ruptures Using GOTHIC" (TAC NO. MC3783), Rev. 0, August 31, 2005.
5. ~~APR1400-F-A-NR-14002-P (Proprietary) & NP (Non-Proprietary), "The Effect of Thermal Conductivity Degradation on APR 1400 Design and Safety Analyses," Rev. 0, KHNP, September 2014.~~ 
6. COMPARE-MOD1A Code Addendum, NUREG/CR-1185, Scientific Los Alamos Laboratory, June 1980.

APR1400 DCD TIER 2

insert Tem erature

| | | |
|-----------------|--|---------|
| Figure 6.2.1-52 | 1.0 x Double-Ended Guillotine Break In Pump Discharge Leg (In-containment Refueling Water Storage Tank) | 6.2-554 |
| Figure 6.2.2-1 | Containment Spray System Flow Diagram | 6.2-555 |
| Figure 6.2.2-2 | Containment Spray Nozzle Orientation | 6.2-556 |
| Figure 6.2.2-3 | Main Spray Nozzle Spray Profiles | 6.2-557 |
| Figure 6.2.2-4 | Spray Nozzle Header Elevations | 6.2-561 |
| Figure 6.2.2-5 | Sprayed Regions | 6.2-562 |
| Figure 6.2.4-1 | Containment Isolation Valve Arrangement | 6.2-564 |
| Figure 6.2.4-2 | Containment Monitoring System Diagram | 6.2-577 |
| Figure 6.2.5-1 | Containment Hydrogen Control System | 6.2-578 |
| Figure 6.3.1-1 | Safety Injection System Schematic Flow Diagram | 6.3-57 |
| Figure 6.3.2-1 | Safety Injection / Shutdown Cooling System Flow Diagram | 6.3-58 |
| Figure 6.3.2-2 | Schematic Diagram of Fluidic Device | 6.3-62 |
| Figure 6.3.2-3 | Safety Injection Pump Head and NPSH Curves (Typical) | 6.3-63 |
| Figure 6.3.2-4 | SIS Elevation Diagram | 6.3-64 |
| Figure 6.3.2-5 | SIT-FD Flow Schematic Characteristics | 6.3-65 |
| Figure 6.4-1 | Control Room Envelope | 6.4-19 |
| Figure 6.4-2 | Control Room HVAC System Flow Diagram (Normal Mode) | 6.4-21 |
| Figure 6.4-3 | Control Room HVAC System Flow Diagram (Emergency Mode) | 6.4-22 |
| Figure 6.4-4 | Control Room HVAC System Flow Diagram (Recirculation Mode) | 6.4-23 |
| Figure 6.4-5 | Onsite Toxic Chemical Location in Site Plot Plan Drawing | 6.4-24 |
| Figure 6.4-6 | Schematic View of MCR Shielding Design | 6.4-25 |
| Figure 6.8-1 | IRWST and HVT Plan View | 6.8-37 |
| Figure 6.8-2 | IRWST and Cavity Flooding System | 6.8-38 |
| Figure 6.8-3 | In-containment Water Storage System Flow Diagram | 6.8-39 |
| Figure 6.8-4 | IRWST Vent Location | 6.8-40 |
| Figure 6.8-5 | Effect of Discharge from Sparger vs. Time on IRWST Loads | 6.8-41 |

APR1400 DCD TIER 2

Pressure values in the affected and unaffected steam generators for each MSLB case listed in Table 6.2.1-1 are given in Tables 6.2.1-9 through 6.2.1-18.

The chronologies of events for the MSLB cases listed in Table 6.2.1-1 are given in Tables 6.2.1-9 through 6.2.1-18.

Feedwater flow to the affected steam generator for each MSLB case listed in Table 6.2.1-1 is shown in Figures 6.2.1-38 through 6.2.1-47.

6.2.1.5 Minimum Containment Pressure Analysis for Performance Capability Studies of the Emergency Core Cooling System

This subsection presents the analysis on the minimum containment pressure that is used in the ECCS performance analysis, which is presented in Subsection 15.6.5.

6.2.1.5.1 Analytical Models

loss-of-coolant acci~ ent (L~ L~ ~ A)

The calculations reported in this subsection are performed using the realistic evaluation methodology for large break LOCA of the APR1400 described in Reference 16 and are in accordance with NRC RG 1.157 (Reference 17). In the code-accuracy-based realistic evaluation method (CAREM), the RELAP5/MOD3.3/K computer program, a modified version of RELAP5/MOD3.3 (Reference 18), is used for the analysis of the ECCS thermal-hydraulic transient calculation and the cladding temperature calculation. A part of the RELAP5/MOD3.3 code's reflood model has been modified to improve the prediction of rods quenching time and to correct coding errors. The minimum containment back pressure and temperature calculations are performed using the CONTEMPT4/MOD5 code (Reference 19).

~ elete

insert~ of the R~ LAP/~ ~ D3.3 co~ e

insert~ the fuel

RELAP5/MOD3.3 is one of the best-estimate safety analysis codes to date. The code has been widely applied in the analysis of system transients of pressurized water reactors, including a postulated large break loss of coolant accident (LBLOCA). The film boiling heat transfer model of the reflood package of RELAP5/MOD3.3 has been modified based on independent assessment calculations against the FLECHT-SEASET data.

L~ L~ ~ A

Containment back pressure depends on mass and energy release rates, and thermal-hydraulic phenomena depend on the containment back pressure. CONTEMPT4/MOD5 is a containment analysis code that is used especially for calculating containment back pressures in case of a LOCA. It includes fan and spray cooling system

insert~ L~

APR1400 DCD TIER 2

models and passive heat sink models that are essential for the calculation of the containment back pressures following a LOCA. It is equipped with the conservation equations of mass, momentum, and energy and can calculate the mass and energy transfer due to the pressure difference between compartments. It also includes state equation of non-condensable gas and can calculate humidity. Heat conduction can be modeled with diverse boundary heat transfer conditions.

RELAP5/MOD3.3 and CONTEMPT4/MOD5 are merged to exchange the containment back pressure calculated by the CONTEMPT4 and the mass and energy release rate calculated by the RELAP5/MOD3.3/K in every time step.

6.2.1.5.2 Mass and Energy Release Data

insert with the urnu of 27000 ~ ~ ~ / TU

The mass and energy released to the containment for a limiting LBLOCA, 100 percent double-ended guillotine break at the pump discharge leg ($1.0 \times \text{DEG/PD}$) are listed as a function of time in Table 6.2.1-39. The quantity of safety injection fluid that spills from the break is described in Subsection 6.2.1.5.6. The analytical models applied in Subsection 15.6.5 best estimate analysis calculate the mass and energy released to the containment. This results are used to the calculation of minimum containment pressure.

6.2.1.5.3 Initial Containment Internal Conditions

The minimum containment temperature, minimum containment pressure, and maximum humidity encountered under limiting normal operating conditions are used for the analysis. The initial containment internal conditions that are used in the analysis are as follows:

| | |
|-------------------------|---|
| Containment temperature | 10 °C (50 °F) (minimum value) |
| IRWST water temperature | 10 °C (50 °F) (minimum value) |
| Containment pressure | 1.024 kg/cm ² A (14.56 psia) (minimum value) |
| Relative humidity | 90 percent (maximum value) |

Each condition is a specified conservative value to minimize the containment pressure, consistent with Branch Technical Position 6-2 (Reference 20).

6.2.1.5.4 Containment Volume

The maximum net free containment volume that is used for the analysis is 97,155 m³ (3,431,000 ft³). The maximum net free volume is determined from the gross containment

APR1400 DCD TIER 2

volume minus the volumes of internal structures such as walls and floors, structural steel, major equipment, and piping with a consideration of uncertainty.

6.2.1.5.5 Active Heat Sinks

In order to conservatively consider the heat removal capacity of the containment active heat sinks, the containment sprays and cooling fans are modeled to actuate immediately with the maximum capacity at the time of the postulated LOCA.

The containment atmosphere cooling systems designed as the non-safety-related system are also modeled to actuate immediately at the time of the postulated LOCA. In addition, the minimum temperature of the stored water for the spray cooling system and the cooling water supplied to the fan coolers, based on technical specification limits, are assumed.

The operating parameters for the containment sprays that are used in the analysis are as follows:

| | | | |
|--------------------------|---|--------------|------------|
| Flow rate (total, pumps) | 2 | 37853 | 10000 |
| | 4 | 75,706 L/min | 20,000 gpm |
| Temperature | | 10.0 °C | (50 °F) |

The heat removal capacity of reactor containment fan cooler (RCFC) is shown in Figure 6.2.1-48.

6.2.1.5.6 Steam-Water Mixing

The spillage of subcooled ECCS water into the containment provides an additional heat sink as the subcooled ECCS water mixes with the steam in the containment by the steam-water mixing. The spilled water from the broken cold leg is determined by the thermal-hydraulic behavior of the core cooling system. It is considered in the analysis model of CONTEMPT4/MOD5.

6.2.1.5.7 Passive Heat Sinks

The passive heat sinks included in the containment evaluation model are established by identifying structures and components within the containment that are influenced the pressure response. The surface areas and thicknesses of all exposed containment passive heat sink, as well as the thermal properties used for the passive heat sinks, are listed in Table 6.2.1-23. The passive heat sink data are conservatively assumed with minimum

insert s

insert the maximum surface area

APR1400 DCD TIER 2

paint thickness and maximum structure thickness. Containment air wall is not considered, conservatively.

6.2.1.5.8 Heat Transfer to Passive Heat Sinks

The conservative condensing heat transfer coefficients for heat transfer to the exposed passive heat sinks during the blowdown and post-blowdown phases of the LOCA are applied. The variations in the condensing heat transfer coefficients between the containment atmosphere and the passive heat sinks are calculated as a function of time and are shown quantitatively in Figure 6.2.1-49. The condensation heat transfer coefficient at the surface of thermal structure is calculated by using Tagami and Uchida correlations shown as below:

$$h_{TAGAMI} = 0.607 \times \left(\frac{U}{V \times tp} \right)^{0.62} \text{ in SI unit}$$

Where:

U = Total released energy from the primary system during the blowdown period

V = Free volume in the containment

tp = Time at the end of blowdown

The heat transfer coefficient during the blowdown period increases linearly from the initial values to a peak value h_{max} and decreases exponentially as shown below. The Uchida heat transfer coefficient is given as the mass ratio function of air and steam:

$$h = h_{stag} + (h_{max} - h_{stag})e^{-0.025(t-t_p)}$$

$$h_{stag} = 1.2 h_{UCHIDA}$$

Where:

h_{max} = Four times of calculated condensing heat transfer coefficient at the end of blowdown

APR1400 DCD TIER 2

6.2.1.5.9 Other Parameters

The minimum containment pressure analysis assumes that the 20.3 cm (8 in) diameter purge system is operating from the time of the LOCA initiation until the isolation valves close, which is after a containment isolation actuation signal. It is conservatively assumed that only dry air is purged from the containment and the maximum mass of air purged is 272.2 kg (600 lbs) for the minimum containment pressure analysis.

6.2.1.5.10 Results

For the limiting ~~large break LOCA~~, 100 percent double-ended guillotine break at the pump discharge leg, the minimum containment pressure response to be used in the ECCS performance analysis is shown in Figure 6.2.1-50. The responses of the containment atmosphere and IRWST temperatures are shown in Figures 6.2.1-51 and 6.2.1-52, respectively.

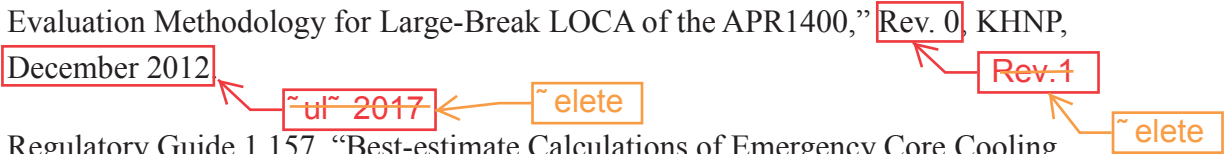
The transient containment response is used in the ECCS performance analysis presented in Subsection 15.6.5.

6.2.1.6 Test and Inspections

This section describes the preoperational testing, in-service testing, and inspection of the containment. The primary objective of testing and inspection is to verify the structural integrity and leak-tight integrity of the containment. The testing and inspection requirements for the containment are described in Subsections 3.8.1.7, 3.8.2.7, 6.2.4, and 6.2.6. Section 14.2, the initial test program, also includes preoperational testing requirements.

Requirements for the structural integrity test are described in Subsection 14.2.12.1.119. The structural integrity test is performed in accordance with ASME Section III, Division 2, CC-6000, to verify the structural integrity of the containment including the liner, concrete structures, all electrical and piping penetrations, equipment hatch, personnel airlocks, and post-tensioning. The pressure will be brought up to 115 percent of the containment design pressure in approximately five or more equal increments. In addition, all ASME Class MC components are tested for their structural acceptance and leak rate at the same time of the structural integrity test. The in-service testing and inspection requirements and methods used for the ASME Class MC components and structural integrity test is described in Subsections 3.8.1.7 and 3.8.2.7.

APR1400 DCD TIER 2

16. APR1400-F-A-TR-12004-P (Proprietary) & NP (Non-Proprietary), "Realistic Evaluation Methodology for Large-Break LOCA of the APR1400," Rev. 0, KHNP, December 2012 
17. Regulatory Guide 1.157, "Best-estimate Calculations of Emergency Core Cooling System Performance," U.S. Nuclear Regulatory Commission, May 1989.
18. NUREG/CR-5535, "RELAP5/MOD3.3 Code Manual," Rev. 3, U.S. Nuclear Regulatory Commission, March 2006.
19. NUREG/CR-3716, "A Multi-compartment Containment System Analysis Program," U.S. Nuclear Regulatory Commission, March 1984.

NUREG/CR-4001, "An Improvement to CONTEMPT4/MOD5 Multi-compartment System Analysis Program for Ice Containment Analysis," U.S. Nuclear Regulatory Commission, September 1984.
20. NUREG-0800, Standard Review Plan, BTP 6-2, "Minimum Containment Pressure Model for PWR ECCS Performance Evaluation," U.S. Nuclear Regulatory Commission, March 2007.
21. Regulatory Guide 1.163, "Performance-Based Containment Leak Test Program," U.S. Nuclear Regulatory Commission, September 1995.
22. ASTM E799-2003(R2009), "Standard Practice for Determining Data Criteria and Processing for Liquid Drop Size Analysis," American Society for Testing and Materia, 2003.
23. ASME Boiler and Pressure Vessel Code, Section XI, "Rules for Inservice Inspection of Nuclear Power Plant Components," The American Society of Mechanical Engineers.
24. ASME OM Code, "Code for Operation and Maintenance of Nuclear Power Plants," The American Society of Mechanical Engineers.
25. 10 CFR Part 50, Appendix A, General Design Criterion 56, "Primary Containment Isolation," U.S. Nuclear Regulatory Commission.
26. Regulatory Guide 1.11, "Instrument Lines Penetrating the Primary Reactor Containment," Rev. 1, U.S. Nuclear Regulatory Commission, March 2010.

APR1400 DCD TIER 2

Table 6.2.1-23 (5 of 7)

Part C. Heat Sink Physical Data for ECCS Performance Analysis

| Heat Sinks | Layer | Material | Thickness | | Surface Area | |
|----------------------|-------|--------------|-----------|----------|----------------|-----------------|
| | | | m | ft | m ² | ft ² |
| Containment cylinder | 1 | E Paint | 0.0000762 | 0.00025 | 7,804.3 | 84,005 |
| | 2 | Z Paint | 0.0000762 | 0.00025 | | |
| | 3 | Carbon Steel | 0.008778 | 0.0288 | | |
| | 4 | Concrete | 1.355994 | 4.4488 | | |
| Dome | 1 | E Paint | 0.0000762 | 0.00025 | 3,316.3 | 35,696.4 |
| | 2 | Z Paint | 0.0000762 | 0.00025 | | |
| | 3 | Carbon Steel | 0.007894 | 0.0259 | | |
| | 4 | Concrete | 1.0668 | 3.5 | | |
| Basemat | 1 | E Paint | 0.000668 | 0.002192 | 1,410.9 | 15,186.3 |
| | 2 | Concrete | 0.9144 | 3 | | |
| | 3 | Carbon Steel | 0.00635 | 0.020833 | | |
| | 4 | Concrete | 3.6576 | 12 | | |
| Embedment Concrete | 1 | E Paint | 0.0000762 | 0.00025 | 726.1 | 7,815.6 |
| | 2 | Z Paint | 0.0000762 | 0.00025 | | |
| | 3 | Carbon Steel | 0.026335 | 0.0864 | | |
| | 4 | Concrete | 0.780776 | 2.5616 | | |

APR1400 DCD TIER 2

Table 6.2.1-23 (6 of 7)

Part C. Heat Sink Physical Data for ECCS Performance Analysis (Continued)

| Heat Sinks | Layer | Material | Thickness | | Surface Area | |
|------------------------|-------|-----------------|------------|----------|----------------|-----------------|
| | | | m | ft | m ² | ft ² |
| Unembedment Concrete | 1 | E Paint | 0.000389 | 0.001275 | 11,120.7 | 119,702 |
| | 2 | Concrete | 0.77254 | 2.534579 | | |
| Refueling Pool | 1 | Stainless Steel | 0.005243 | 0.0172 | 1,153.6 | 12,417.7 |
| IRWST Outside | 1 | E Paint | 0.000668 | 0.002192 | 2,017.4 | 21,714.6 |
| | 2 | Concrete | 0.4572 | 1.5 | | |
| IRWST Inside | 1 | Stainless Steel | 0.00633984 | 0.0208 | 1,038.8 | 11,181.7 |
| | 2 | Concrete | 0.4572 | 1.5 | | |
| Polar Crane and Bridge | 1 | E Paint | 0.0000762 | 0.00025 | 8,291.6 | 89,250 |
| | 2 | Z Paint | 0.0000762 | 0.00025 | | |
| | 3 | Carbon Steel | 0.012192 | 0.04 | | |
| SIT | 1 | E Paint | 0.000152 | 0.0005 | 526.8 | 5,670 |
| | 2 | Carbon Steel | 0.048798 | 0.1601 | | |
| Misc. steel G-A | 1 | E Paint | 0.0000762 | 0.00025 | 10,212.1 | 109,922 |
| | 2 | Z Paint | 0.0000762 | 0.00025 | | |
| | 3 | Carbon Steel | 0.016712 | 0.054831 | | |
| Misc. steel G-B | 1 | Z Paint | 0.0000762 | 0.00025 | 7,062.1 | 76,015.5 |
| | 3 | Carbon Steel | 0.004175 | 0.013698 | | |
| Misc. steel G-C | 1 | E Paint | 0.0000762 | 0.00025 | 3,361.5 | 36,182.7 |
| | 2 | Z Paint | 0.0000762 | 0.00025 | | |
| | 3 | Carbon Steel | 0.00518099 | 0.016998 | | |
| Misc. steel G-D | 1 | Z Paint | 0.0000762 | 0.00025 | 3,664.1 | 39,439.6 |
| | 2 | Carbon Steel | 0.004 | 0.013124 | | |
| Misc. steel G-E | 1 | Z Paint | 0.0000762 | 0.00025 | 21,557.5 | 232,042 |
| | 2 | Carbon Steel | 0.001644 | 0.005393 | | |

APR1400 DCD TIER 2

Table 6.2.1-23 (7 of 7)

Part C. Heat Sink Physical Data for ECCS Performance Analysis (Continued)

| Heat Sinks | Layer | Material | Thickness | | Surface Area | |
|-----------------|-------|-----------------|------------|----------|----------------|-----------------|
| | | | m | ft | m ² | ft ² |
| Misc. steel G-F | 1 | E Paint | 0.0000762 | 0.00025 | 1,589.3 | 17,106.9 |
| | 2 | Z Paint | 0.0000762 | 0.00025 | | |
| | 3 | Carbon Steel | 0.00672846 | 0.022075 | | |
| Misc. steel G-G | 1 | Stainless Steel | 0.00627888 | 0.020600 | 1,872.0 | 20,149.6 |
| Misc. steel G-J | 1 | Z Paint | 0.0000762 | 0.00025 | 1,738.6 | 18,713.6 |
| | 2 | Carbon Steel | 0.009216 | 0.030235 | | |
| Misc. steel G-K | 1 | Stainless Steel | 0.072558 | 0.23805 | 1,269.3 | 13,662.7 |

| | |
|------------------------------|--|
| Thermal Conductivity of: | |
| Steel | 40.6 kcal/m-hr-°C (27.3 Btu/ft-hr-°F) |
| Concrete | 1.94 kcal/m-hr-°C (1.3 Btu/ft-hr-°F) |
| Paint (epoxy) | 0.31 kcal/m-hr-°C (0.21 Btu/ft-hr-°F) |
| Paint (inorganic zinc) | 1.49 kcal/m-hr-°C (1.0 Btu/ft-hr-°F) |
| Volumetric Heat Capacity of: | |
| Steel | 942 kcal/m ³ -°C (58.8 Btu/ft ³ -°F) |
| Concrete | 517 kcal/m ³ -°C (32.3 Btu/ft ³ -°F) |
| Paint (epoxy) | 585 kcal/m ³ -°C (36.5 Btu/ft ³ -°F) |
| Paint (inorganic zinc) | 1,250 kcal/m ³ -°C (78.0 Btu/ft ³ -°F) |

Insert

- (1) The surface area uses its maximum value within the ranges of margin estimated from the geometry uncertainty of each structure.
- (2) The thickness of each structure are determined based on the surface area exposed to the containment atmosphere and the net volume occupied by the structure.
- (3) The thickness of the painting material on the structure is considered as its averaging nominal value.

A detailed description of how to calculate the thickness and surface area is provided in Reference 3.

APR1400 DCD TIER 2

Replace with next page A-1

Table 6.2.1-39 (1 of 4)

Blowdown and Reflood Mass and Energy Release for the Minimum Containment Pressure Analysis

| Time (sec) | Mass Flow | | Enthalpy | | Integral of Mass Flow | | Integral of Energy | |
|---------------|------------|------------|------------|------------|-----------------------|------------|--------------------|------------|
| | (kg/sec) | (lbm/sec) | (kcal/kg) | (Btu/lbm) | (kg) | (lbm) | (kcal) | (Btu) |
| 0.0 | 0.0000E+00 | 0.0000E+00 | 0.0000E+00 | 0.0000E+00 | 0.0000E+00 | 0.0000E+00 | 0.0000E+00 | 0.0000E+00 |
| 0.5 | 3.9083E+04 | 8.6164E+04 | 3.0484E+02 | 5.4870E+02 | 1.9481E+04 | 4.2948E+04 | 5.9366E+06 | 2.3558E+07 |
| 1.0 | 3.7229E+04 | 8.2876E+04 | 3.0525E+02 | 5.4944E+02 | 3.8697E+04 | 8.5313E+04 | 1.1798E+07 | 4.6818E+07 |
| 1.5 | 3.4198E+04 | 7.5395E+04 | 3.0599E+02 | 5.5078E+02 | 5.6465E+04 | 1.2448E+05 | 1.7227E+07 | 6.8364E+07 |
| 2.0 | 3.2051E+04 | 7.0661E+04 | 3.0712E+02 | 5.5282E+02 | 7.3059E+04 | 1.6107E+05 | 2.2314E+07 | 8.8548E+07 |
| 2.5 | 2.9526E+04 | 6.5093E+04 | 3.0870E+02 | 5.5566E+02 | 8.8435E+04 | 1.9497E+05 | 2.7047E+07 | 1.0733E+08 |
| 3.0 | 2.6495E+04 | 5.8411E+04 | 3.1044E+02 | 5.5879E+02 | 1.0245E+05 | 2.2587E+05 | 3.1385E+07 | 1.2455E+08 |
| 3.5 | 2.4309E+04 | 5.3593E+04 | 3.1248E+02 | 5.6246E+02 | 1.1511E+05 | 2.5378E+05 | 3.5328E+07 | 1.4019E+08 |
| 4.0 | 2.2818E+04 | 5.0305E+04 | 3.1483E+02 | 5.6670E+02 | 1.2688E+05 | 2.7972E+05 | 3.9020E+07 | 1.5484E+08 |
| 4.5 | 2.1564E+04 | 4.7541E+04 | 3.1670E+02 | 5.7006E+02 | 1.3793E+05 | 3.0408E+05 | 4.2509E+07 | 1.6869E+08 |
| 5.0 | 2.0493E+04 | 4.5180E+04 | 3.1844E+02 | 5.7320E+02 | 1.4841E+05 | 3.2719E+05 | 4.5840E+07 | 1.8191E+08 |
| 5.5 | 1.9184E+04 | 4.2294E+04 | 3.2188E+02 | 5.7939E+02 | 1.5834E+05 | 3.4908E+05 | 4.9016E+07 | 1.9451E+08 |
| 6.0 | 1.8037E+04 | 3.9764E+04 | 3.2567E+02 | 5.8620E+02 | 1.6764E+05 | 3.6959E+05 | 5.2028E+07 | 2.0646E+08 |
| 6.5 | 1.7038E+04 | 3.7562E+04 | 3.2853E+02 | 5.9136E+02 | 1.7640E+05 | 3.8891E+05 | 5.4895E+07 | 2.1784E+08 |
| 7.0 | 1.6036E+04 | 3.5353E+04 | 3.3182E+02 | 5.9727E+02 | 1.8467E+05 | 4.0713E+05 | 5.7624E+07 | 2.2867E+08 |
| 7.5 | 1.5212E+04 | 3.3536E+04 | 3.3461E+02 | 6.0229E+02 | 1.9247E+05 | 4.2433E+05 | 6.0225E+07 | 2.3899E+08 |
| 8.0 | 1.4582E+04 | 3.2149E+04 | 3.3657E+02 | 6.0582E+02 | 1.9991E+05 | 4.4073E+05 | 6.2721E+07 | 2.4890E+08 |
| 8.5 | 1.4003E+04 | 3.0871E+04 | 3.3755E+02 | 6.0760E+02 | 2.0705E+05 | 4.5647E+05 | 6.5131E+07 | 2.5846E+08 |

APR1400 DCD TIER 2

A-1

Table 6.2.1-39 (1 of 4)

Blowdown and Reflood Mass and Energy Release for the Minimum Containment Pressure Analysis

| Time (sec) | Mass Flow | | Enthalpy | | Integral of Mass Flow | | Integral of Energy | |
|---------------|------------|------------|------------|------------|-----------------------|------------|--------------------|------------|
| | (kg/sec) | (lbm/sec) | (kcal/kg) | (Btu/lbm) | (kg) | (lbm) | (kcal) | (Btu) |
| 0.0 | 0.0000E+00 | 0.0000E+00 | 0.0000E+00 | 0.0000E+00 | 0.0000E+00 | 0.0000E+00 | 0.0000E+00 | 0.0000E+00 |
| 0.5 | 3.8724E+04 | 8.5372E+04 | 3.0481E+02 | 5.4866E+02 | 1.9481E+04 | 4.2948E+04 | 5.9366E+06 | 2.3558E+07 |
| 1.0 | 3.6719E+04 | 8.0951E+04 | 3.0522E+02 | 5.4940E+02 | 3.8697E+04 | 8.5313E+04 | 1.1798E+07 | 4.6818E+07 |
| 1.5 | 3.4041E+04 | 7.5047E+04 | 3.0599E+02 | 5.5078E+02 | 5.6465E+04 | 1.2448E+05 | 1.7227E+07 | 6.8364E+07 |
| 2.0 | 3.1857E+04 | 7.0232E+04 | 3.0710E+02 | 5.5278E+02 | 7.3059E+04 | 1.6107E+05 | 2.2314E+07 | 8.8548E+07 |
| 2.5 | 2.9010E+04 | 6.3957E+04 | 3.0871E+02 | 5.5567E+02 | 8.8435E+04 | 1.9497E+05 | 2.7047E+07 | 1.0733E+08 |
| 3.0 | 2.6322E+04 | 5.8031E+04 | 3.1038E+02 | 5.5868E+02 | 1.0245E+05 | 2.2587E+05 | 3.1385E+07 | 1.2455E+08 |
| 3.5 | 2.4281E+04 | 5.3531E+04 | 3.1241E+02 | 5.6235E+02 | 1.1511E+05 | 2.5378E+05 | 3.5328E+07 | 1.4019E+08 |
| 4.0 | 2.2928E+04 | 5.0548E+04 | 3.1473E+02 | 5.6652E+02 | 1.2688E+05 | 2.7972E+05 | 3.9020E+07 | 1.5484E+08 |
| 4.5 | 2.1645E+04 | 4.7720E+04 | 3.1615E+02 | 5.6907E+02 | 1.3793E+05 | 3.0408E+05 | 4.2509E+07 | 1.6869E+08 |
| 5.0 | 2.0561E+04 | 4.5329E+04 | 3.1811E+02 | 5.7260E+02 | 1.4841E+05 | 3.2719E+05 | 4.5840E+07 | 1.8191E+08 |
| 5.5 | 1.9289E+04 | 4.2526E+04 | 3.2143E+02 | 5.7857E+02 | 1.5834E+05 | 3.4908E+05 | 4.9016E+07 | 1.9451E+08 |
| 6.0 | 1.8132E+04 | 3.9975E+04 | 3.2525E+02 | 5.8545E+02 | 1.6764E+05 | 3.6959E+05 | 5.2028E+07 | 2.0646E+08 |
| 6.5 | 1.7101E+04 | 3.7700E+04 | 3.2825E+02 | 5.9084E+02 | 1.7640E+05 | 3.8891E+05 | 5.4895E+07 | 2.1784E+08 |
| 7.0 | 1.6093E+04 | 3.5480E+04 | 3.3151E+02 | 5.9672E+02 | 1.8467E+05 | 4.0713E+05 | 5.7624E+07 | 2.2867E+08 |
| 7.5 | 1.5240E+04 | 3.3598E+04 | 3.3453E+02 | 6.0215E+02 | 1.9247E+05 | 4.2433E+05 | 6.0225E+07 | 2.3899E+08 |
| 8.0 | 1.4614E+04 | 3.2218E+04 | 3.3647E+02 | 6.0565E+02 | 1.9991E+05 | 4.4073E+05 | 6.2721E+07 | 2.4890E+08 |
| 8.5 | 1.4153E+04 | 3.1202E+04 | 3.3747E+02 | 6.0745E+02 | 2.0705E+05 | 4.5647E+05 | 6.5131E+07 | 2.5846E+08 |

APR1400 DCD TIER 2

Replace with next page A-2

Table 6.2.1-39 (2 of 4)

| Time (sec) | Mass Flow | | Enthalpy | | Integral of Mass Flow | | Integral of Energy | |
|---------------|------------|------------|------------|------------|-----------------------|------------|--------------------|------------|
| | (kg/sec) | (lbm/sec) | (kcal/kg) | (Btu/lbm) | (kg) | (lbm) | (kcal) | (Btu) |
| 9.0 | 1.3295E+04 | 2.9310E+04 | 3.4122E+02 | 6.1420E+02 | 2.1383E+05 | 4.7141E+05 | 6.7437E+07 | 2.6761E+08 |
| 9.5 | 1.2034E+04 | 2.6531E+04 | 3.5498E+02 | 6.3897E+02 | 2.2013E+05 | 4.8530E+05 | 6.9627E+07 | 2.7630E+08 |
| 10.0 | 1.1140E+04 | 2.4560E+04 | 3.6620E+02 | 6.5916E+02 | 2.2592E+05 | 4.9807E+05 | 7.1714E+07 | 2.8458E+08 |
| 11.0 | 9.7376E+03 | 2.1468E+04 | 3.8751E+02 | 6.9752E+02 | 2.3643E+05 | 5.2124E+05 | 7.5655E+07 | 3.0022E+08 |
| 12.0 | 8.3059E+03 | 1.8311E+04 | 4.1727E+02 | 7.5109E+02 | 2.4544E+05 | 5.4110E+05 | 7.9270E+07 | 3.1457E+08 |
| 13.0 | 7.0495E+03 | 1.5541E+04 | 4.4490E+02 | 8.0082E+02 | 2.5319E+05 | 5.5818E+05 | 8.2584E+07 | 3.2772E+08 |
| 14.0 | 5.6965E+03 | 1.2559E+04 | 4.8057E+02 | 8.6502E+02 | 2.5955E+05 | 5.7221E+05 | 8.5525E+07 | 3.3939E+08 |
| 15.0 | 4.6371E+03 | 1.0223E+04 | 5.0858E+02 | 9.1544E+02 | 2.6470E+05 | 5.8357E+05 | 8.8068E+07 | 3.4948E+08 |
| 16.0 | 4.2699E+03 | 9.4135E+03 | 4.6259E+02 | 8.3266E+02 | 2.6917E+05 | 5.9341E+05 | 9.0244E+07 | 3.5812E+08 |
| 17.0 | 4.2033E+03 | 9.2667E+03 | 3.8856E+02 | 6.9941E+02 | 2.7347E+05 | 6.0289E+05 | 9.2034E+07 | 3.6522E+08 |
| 18.0 | 3.9604E+03 | 8.7312E+03 | 3.4041E+02 | 6.1274E+02 | 2.7755E+05 | 6.1190E+05 | 9.3514E+07 | 3.7109E+08 |
| 19.0 | 3.6815E+03 | 8.1162E+03 | 3.1006E+02 | 5.5811E+02 | 2.8146E+05 | 6.2052E+05 | 9.4767E+07 | 3.7607E+08 |
| 20.0 | 3.3936E+03 | 7.4816E+03 | 2.8308E+02 | 5.0955E+02 | 2.8507E+05 | 6.2848E+05 | 9.5825E+07 | 3.8026E+08 |
| 21.0 | 3.1712E+03 | 6.9912E+03 | 2.5108E+02 | 4.5195E+02 | 2.8836E+05 | 6.3572E+05 | 9.6706E+07 | 3.8376E+08 |
| 22.0 | 3.5105E+03 | 7.7394E+03 | 2.1884E+02 | 3.9391E+02 | 2.9193E+05 | 6.4359E+05 | 9.7537E+07 | 3.8706E+08 |
| 23.0 | 3.1260E+03 | 6.8917E+03 | 1.9468E+02 | 3.5043E+02 | 2.9524E+05 | 6.5089E+05 | 9.8226E+07 | 3.8979E+08 |
| 24.0 | 2.3483E+03 | 5.1770E+03 | 1.9237E+02 | 3.4627E+02 | 2.9799E+05 | 6.5696E+05 | 9.8754E+07 | 3.9189E+08 |
| 25.0 | 1.9377E+03 | 4.2719E+03 | 1.7847E+02 | 3.2125E+02 | 3.0006E+05 | 6.6152E+05 | 9.9149E+07 | 3.9346E+08 |
| 26.0 | 1.9829E+03 | 4.3715E+03 | 1.3967E+02 | 2.5141E+02 | 3.0202E+05 | 6.6584E+05 | 9.9457E+07 | 3.9468E+08 |
| 27.0 | 1.7744E+03 | 3.9119E+03 | 1.1880E+02 | 2.1384E+02 | 3.0376E+05 | 6.6968E+05 | 9.9691E+07 | 3.9561E+08 |

APR1400 DCD TIER 2

A-2

Table 6.2.1-39 (2 of 4)

| Time (sec) | Mass Flow | | Enthalpy | | Integral of Mass Flow | | Integral of Energy | |
|---------------|------------|------------|------------|------------|-----------------------|------------|--------------------|------------|
| | (kg/sec) | (lbm/sec) | (kcal/kg) | (Btu/lbm) | (kg) | (lbm) | (kcal) | (Btu) |
| 9.0 | 1.3205E+04 | 2.9113E+04 | 3.4232E+02 | 6.1617E+02 | 2.1383E+05 | 4.7141E+05 | 6.7437E+07 | 2.6761E+08 |
| 9.5 | 1.2105E+04 | 2.6688E+04 | 3.5269E+02 | 6.3484E+02 | 2.2013E+05 | 4.8530E+05 | 6.9627E+07 | 2.7630E+08 |
| 10.0 | 1.1219E+04 | 2.4734E+04 | 3.6500E+02 | 6.5699E+02 | 2.2592E+05 | 4.9807E+05 | 7.1714E+07 | 2.8458E+08 |
| 11.0 | 9.8545E+03 | 2.1725E+04 | 3.8504E+02 | 6.9308E+02 | 2.3643E+05 | 5.2124E+05 | 7.5655E+07 | 3.0022E+08 |
| 12.0 | 8.3606E+03 | 1.8432E+04 | 4.1553E+02 | 7.4795E+02 | 2.4544E+05 | 5.4110E+05 | 7.9270E+07 | 3.1457E+08 |
| 13.0 | 7.0900E+03 | 1.5631E+04 | 4.4297E+02 | 7.9734E+02 | 2.5319E+05 | 5.5818E+05 | 8.2584E+07 | 3.2772E+08 |
| 14.0 | 5.7429E+03 | 1.2661E+04 | 4.7810E+02 | 8.6058E+02 | 2.5955E+05 | 5.7221E+05 | 8.5525E+07 | 3.3939E+08 |
| 15.0 | 4.6607E+03 | 1.0275E+04 | 5.0738E+02 | 9.1328E+02 | 2.6470E+05 | 5.8357E+05 | 8.8068E+07 | 3.4948E+08 |
| 16.0 | 4.5045E+03 | 9.9308E+03 | 4.3551E+02 | 7.8392E+02 | 2.6917E+05 | 5.9341E+05 | 9.0244E+07 | 3.5812E+08 |
| 17.0 | 4.5892E+03 | 1.0117E+04 | 3.4965E+02 | 6.2937E+02 | 2.7347E+05 | 6.0289E+05 | 9.2034E+07 | 3.6522E+08 |
| 18.0 | 6.2080E+03 | 1.3686E+04 | 2.6115E+02 | 4.7008E+02 | 2.7755E+05 | 6.1190E+05 | 9.3514E+07 | 3.7109E+08 |
| 19.0 | 5.3897E+03 | 1.1882E+04 | 2.4960E+02 | 4.4928E+02 | 2.8146E+05 | 6.2052E+05 | 9.4767E+07 | 3.7607E+08 |
| 20.0 | 5.0298E+03 | 1.1089E+04 | 2.1821E+02 | 3.9278E+02 | 2.8507E+05 | 6.2848E+05 | 9.5825E+07 | 3.8026E+08 |
| 21.0 | 4.5887E+03 | 1.0072E+04 | 1.9425E+02 | 3.4965E+02 | 2.8836E+05 | 6.3572E+05 | 9.6706E+07 | 3.8376E+08 |
| 22.0 | 4.0662E+03 | 8.9645E+03 | 1.7118E+02 | 3.0812E+02 | 2.9193E+05 | 6.4359E+05 | 9.7537E+07 | 3.8706E+08 |
| 23.0 | 3.3917E+03 | 7.4775E+03 | 1.5942E+02 | 2.8695E+02 | 2.9524E+05 | 6.5089E+05 | 9.8226E+07 | 3.8979E+08 |
| 24.0 | 2.8318E+03 | 6.2430E+03 | 1.4577E+02 | 2.6238E+02 | 2.9799E+05 | 6.5696E+05 | 9.8754E+07 | 3.9189E+08 |
| 25.0 | 2.2366E+03 | 4.9309E+03 | 1.3316E+02 | 2.3969E+02 | 3.0006E+05 | 6.6152E+05 | 9.9149E+07 | 3.9346E+08 |
| 26.0 | 2.2567E+03 | 4.9752E+03 | 1.1145E+02 | 2.0062E+02 | 3.0202E+05 | 6.6584E+05 | 9.9457E+07 | 3.9468E+08 |
| 27.0 | 1.7760E+03 | 3.9153E+03 | 7.5469E+01 | 1.3584E+02 | 3.0376E+05 | 6.6968E+05 | 9.9691E+07 | 3.9561E+08 |

APR1400 DCD TIER 2

Replace with next page A-3

Table 6.2.1-39 (3 of 4)

| Time (sec) | Mass Flow | | Enthalpy | | Integral of Mass Flow | | Integral of Energy | |
|---------------|-------------|-------------|------------|------------|-----------------------|------------|--------------------|------------|
| | (kg/sec) | (lbm/sec) | (kcal/kg) | (Btu/lbm) | (kg) | (lbm) | (kcal) | (Btu) |
| 28.0 | 5.6570E+02 | 1.2472E+03 | 1.0175E+02 | 1.8315E+02 | 3.0503E+05 | 6.7249E+05 | 9.9830E+07 | 3.9616E+08 |
| 29.0 | -9.8747E+01 | -2.1770E+02 | 3.4733E+02 | 6.2520E+02 | 3.0511E+05 | 6.7265E+05 | 9.9824E+07 | 3.9613E+08 |
| 30.0 | -2.8582E+01 | -6.3013E+01 | 1.3609E+02 | 2.4497E+02 | 3.0507E+05 | 6.7256E+05 | 9.9811E+07 | 3.9608E+08 |
| 35.0 | 2.2727E+02 | 5.0104E+02 | 9.4225E+01 | 1.6961E+02 | 3.0599E+05 | 6.7460E+05 | 9.9938E+07 | 3.9659E+08 |
| 40.0 | 4.0079E+02 | 8.8360E+02 | 1.4478E+02 | 2.6060E+02 | 3.0759E+05 | 6.7813E+05 | 1.0014E+08 | 3.9737E+08 |
| 45.0 | 4.1072E+02 | 9.0548E+02 | 1.4478E+02 | 2.6061E+02 | 3.0931E+05 | 6.8191E+05 | 1.0040E+08 | 3.9840E+08 |
| 50.0 | 2.3177E+03 | 5.1096E+03 | 8.2609E+01 | 1.4870E+02 | 3.1563E+05 | 6.9585E+05 | 1.0100E+08 | 4.0081E+08 |
| 55.0 | 1.6683E+03 | 3.6780E+03 | 8.2492E+01 | 1.4848E+02 | 3.2501E+05 | 7.1652E+05 | 1.0177E+08 | 4.0384E+08 |
| 60.0 | 2.0347E+03 | 4.4857E+03 | 8.2038E+01 | 1.4767E+02 | 3.3385E+05 | 7.3602E+05 | 1.0249E+08 | 4.0673E+08 |
| 65.0 | 1.5550E+03 | 3.4282E+03 | 9.3659E+01 | 1.6859E+02 | 3.4338E+05 | 7.5703E+05 | 1.0330E+08 | 4.0994E+08 |
| 70.0 | 1.1052E+03 | 2.4365E+03 | 9.7418E+01 | 1.7535E+02 | 3.4758E+05 | 7.6628E+05 | 1.0374E+08 | 4.1166E+08 |
| 75.0 | 1.0596E+03 | 2.3359E+03 | 9.9657E+01 | 1.7938E+02 | 3.5262E+05 | 7.7739E+05 | 1.0424E+08 | 4.1364E+08 |
| 80.0 | 7.8015E+02 | 1.7199E+03 | 1.0732E+02 | 1.9318E+02 | 3.5648E+05 | 7.8590E+05 | 1.0465E+08 | 4.1529E+08 |
| 85.0 | 2.3990E+02 | 5.2888E+02 | 1.9546E+02 | 3.5183E+02 | 3.6095E+05 | 7.9577E+05 | 1.0512E+08 | 4.1717E+08 |
| 90.0 | 8.0717E+02 | 1.7795E+03 | 1.0951E+02 | 1.9713E+02 | 3.6243E+05 | 7.9903E+05 | 1.0539E+08 | 4.1822E+08 |
| 95.0 | 6.5211E+02 | 1.4377E+03 | 1.1473E+02 | 2.0651E+02 | 3.6588E+05 | 8.0663E+05 | 1.0579E+08 | 4.1982E+08 |
| 100.0 | 1.7141E+03 | 3.7789E+03 | 9.6159E+01 | 1.7309E+02 | 3.7052E+05 | 8.1686E+05 | 1.0629E+08 | 4.2178E+08 |
| 110.0 | 1.3707E+03 | 3.0219E+03 | 9.3458E+01 | 1.6822E+02 | 3.8066E+05 | 8.3921E+05 | 1.0730E+08 | 4.2582E+08 |
| 120.0 | 1.1553E+03 | 2.5469E+03 | 1.0026E+02 | 1.8046E+02 | 3.9104E+05 | 8.6210E+05 | 1.0835E+08 | 4.2998E+08 |

A-3

APR1400 DCD TIER 2

Table 6.2.1-39 (3 of 4)

| Time (sec) | Mass Flow | | Enthalpy | | Integral of Mass Flow | | Integral of Energy | |
|---------------|-------------|-------------|-------------|-------------|-----------------------|------------|--------------------|------------|
| | (kg/sec) | (lbm/sec) | (kcal/kg) | (Btu/lbm) | (kg) | (lbm) | (kcal) | (Btu) |
| 28.0 | 1.3825E+03 | 3.0478E+03 | 7.4008E+01 | 1.3321E+02 | 3.0503E+05 | 6.7249E+05 | 9.9830E+07 | 3.9616E+08 |
| 29.0 | -4.6888E+01 | -1.0337E+02 | 2.9049E+02 | 5.2288E+02 | 3.0511E+05 | 6.7265E+05 | 9.9824E+07 | 3.9613E+08 |
| 30.0 | -9.2798E+00 | -2.0459E+01 | -3.7440E+02 | -6.7393E+02 | 3.0507E+05 | 6.7256E+05 | 9.9811E+07 | 3.9608E+08 |
| 35.0 | 8.2544E+02 | 1.8198E+03 | 7.0693E+01 | 1.2725E+02 | 3.0599E+05 | 6.7460E+05 | 9.9938E+07 | 3.9659E+08 |
| 40.0 | 1.5654E+03 | 3.4512E+03 | 6.5703E+01 | 1.1826E+02 | 3.0759E+05 | 6.7813E+05 | 1.0014E+08 | 3.9737E+08 |
| 45.0 | 2.2241E+03 | 4.9033E+03 | 6.8862E+01 | 1.2395E+02 | 3.0912E+05 | 6.8149E+05 | 1.0037E+08 | 3.9829E+08 |
| 50.0 | 7.7318E+02 | 1.7046E+03 | 9.6668E+01 | 1.7400E+02 | 3.1457E+05 | 6.9352E+05 | 1.0091E+08 | 4.0045E+08 |
| 55.0 | 7.2726E+02 | 1.6033E+03 | 1.0195E+02 | 1.8351E+02 | 3.2410E+05 | 7.1452E+05 | 1.0169E+08 | 4.0355E+08 |
| 60.0 | 5.4934E+02 | 1.2111E+03 | 1.1092E+02 | 1.9966E+02 | 3.3289E+05 | 7.3389E+05 | 1.0241E+08 | 4.0641E+08 |
| 65.0 | 9.7930E+02 | 2.1590E+03 | 1.0144E+02 | 1.8259E+02 | 3.4263E+05 | 7.5537E+05 | 1.0323E+08 | 4.0966E+08 |
| 70.0 | 9.4834E+02 | 2.0907E+03 | 1.0456E+02 | 1.8820E+02 | 3.4706E+05 | 7.6514E+05 | 1.0369E+08 | 4.1146E+08 |
| 75.0 | 9.2547E+02 | 2.0403E+03 | 1.0588E+02 | 1.9058E+02 | 3.5208E+05 | 7.7621E+05 | 1.0418E+08 | 4.1343E+08 |
| 80.0 | 1.6133E+03 | 3.5567E+03 | 9.9377E+01 | 1.7888E+02 | 3.5606E+05 | 7.8498E+05 | 1.0461E+08 | 4.1511E+08 |
| 85.0 | 2.1460E+03 | 4.7310E+03 | 9.6351E+01 | 1.7343E+02 | 3.6080E+05 | 7.9543E+05 | 1.0510E+08 | 4.1706E+08 |
| 90.0 | 1.0122E+02 | 2.2316E+02 | 2.5144E+02 | 4.5258E+02 | 3.6243E+05 | 7.9903E+05 | 1.0539E+08 | 4.1822E+08 |
| 95.0 | 9.6142E+02 | 2.1196E+03 | 9.9371E+01 | 1.7887E+02 | 3.6588E+05 | 8.0663E+05 | 1.0579E+08 | 4.1982E+08 |
| 100.0 | 6.8324E+02 | 1.5063E+03 | 1.0617E+02 | 1.9111E+02 | 3.7052E+05 | 8.1686E+05 | 1.0629E+08 | 4.2178E+08 |
| 110.0 | 1.2417E+03 | 2.7374E+03 | 1.0184E+02 | 1.8332E+02 | 3.8016E+05 | 8.3811E+05 | 1.0726E+08 | 4.2562E+08 |
| 120.0 | 7.2970E+02 | 1.6087E+03 | 1.0815E+02 | 1.9466E+02 | 3.9050E+05 | 8.6091E+05 | 1.0830E+08 | 4.2976E+08 |

APR1400 DCD TIER 2

Replace with next page A-4

Table 6.2.1-39 (4 of 4)

| Time (sec) | Mass Flow | | Enthalpy | | Integral of Mass Flow | | Integral of Energy | |
|---------------|------------|------------|------------|------------|-----------------------|------------|--------------------|------------|
| | (kg/sec) | (lbm/sec) | (kcal/kg) | (Btu/lbm) | (kg) | (lbm) | (kcal) | (Btu) |
| 130.0 | 8.9815E+02 | 1.9801E+03 | 1.0577E+02 | 1.9039E+02 | 4.0040E+05 | 8.8274E+05 | 1.0933E+08 | 4.3384E+08 |
| 140.0 | 1.1298E+03 | 2.4908E+03 | 1.0262E+02 | 1.8471E+02 | 4.1093E+05 | 9.0594E+05 | 1.1043E+08 | 4.3821E+08 |
| 150.0 | 9.5167E+02 | 2.0981E+03 | 1.0889E+02 | 1.9600E+02 | 4.1912E+05 | 9.2399E+05 | 1.1132E+08 | 4.4175E+08 |
| 160.0 | 1.1363E+03 | 2.5051E+03 | 1.0489E+02 | 1.8881E+02 | 4.3166E+05 | 9.5164E+05 | 1.1261E+08 | 4.4686E+08 |
| 170.0 | 9.1526E+02 | 2.0178E+03 | 1.0773E+02 | 1.9391E+02 | 4.4223E+05 | 9.7495E+05 | 1.1373E+08 | 4.5131E+08 |
| 180.0 | 4.4847E+02 | 9.8870E+02 | 1.2333E+02 | 2.2199E+02 | 4.4953E+05 | 9.9104E+05 | 1.1454E+08 | 4.5453E+08 |
| 190.0 | 4.9428E+02 | 1.0897E+03 | 1.7914E+02 | 3.2245E+02 | 4.5528E+05 | 1.0037E+06 | 1.1524E+08 | 4.5732E+08 |
| 200.0 | 5.4523E+02 | 1.2020E+03 | 1.8537E+02 | 3.3366E+02 | 4.6069E+05 | 1.0157E+06 | 1.1622E+08 | 4.6121E+08 |
| 210.0 | 5.2823E+02 | 1.1645E+03 | 1.8529E+02 | 3.3352E+02 | 4.6557E+05 | 1.0264E+06 | 1.1717E+08 | 4.6496E+08 |
| 220.0 | 5.1639E+02 | 1.1384E+03 | 1.7528E+02 | 3.1550E+02 | 4.7111E+05 | 1.0386E+06 | 1.1813E+08 | 4.6879E+08 |
| 230.0 | 3.4466E+02 | 7.5985E+02 | 2.1803E+02 | 3.9246E+02 | 4.7535E+05 | 1.0480E+06 | 1.1894E+08 | 4.7201E+08 |
| 240.0 | 1.3835E+02 | 3.0501E+02 | 3.4640E+02 | 6.2352E+02 | 4.7706E+05 | 1.0517E+06 | 1.1950E+08 | 4.7422E+08 |
| 250.0 | 1.1657E+02 | 2.5700E+02 | 3.5294E+02 | 6.3529E+02 | 4.7832E+05 | 1.0545E+06 | 1.1994E+08 | 4.7596E+08 |
| 260.0 | 1.1309E+02 | 2.4933E+02 | 3.2035E+02 | 5.7663E+02 | 4.7943E+05 | 1.0576E+06 | 1.2031E+08 | 4.7745E+08 |
| 270.0 | 1.0166E+02 | 2.2411E+02 | 3.5015E+02 | 6.3027E+02 | 4.8051E+05 | 1.0593E+06 | 1.2068E+08 | 4.7889E+08 |
| 280.0 | 1.0073E+02 | 2.2206E+02 | 3.5595E+02 | 6.4071E+02 | 4.8152E+05 | 1.0616E+06 | 1.2104E+08 | 4.8031E+08 |
| 290.0 | 1.0174E+02 | 2.2430E+02 | 3.5329E+02 | 6.3591E+02 | 4.8252E+05 | 1.0638E+06 | 1.2139E+08 | 4.8172E+08 |
| 300.0 | 9.5467E+01 | 2.1047E+02 | 3.4684E+02 | 6.2431E+02 | 4.8351E+05 | 1.0660E+06 | 1.2174E+08 | 4.8310E+08 |

A-4

APR1400 DCD TIER 2

Table 6.2.1-39 (4 of 4)

| Time (sec) | Mass Flow | | Enthalpy | | Integral of Mass Flow | | Integral of Energy | |
|---------------|------------|------------|------------|------------|-----------------------|------------|--------------------|------------|
| | (kg/sec) | (lbm/sec) | (kcal/kg) | (Btu/lbm) | (kg) | (lbm) | (kcal) | (Btu) |
| 130.0 | 4.4106E+02 | 9.7237E+02 | 1.5443E+02 | 2.7797E+02 | 3.9996E+05 | 8.8177E+05 | 1.0928E+08 | 4.3366E+08 |
| 140.0 | 8.9698E+02 | 1.9775E+03 | 1.2583E+02 | 2.2650E+02 | 4.1034E+05 | 9.0465E+05 | 1.1037E+08 | 4.3797E+08 |
| 150.0 | 9.1549E+02 | 2.0183E+03 | 1.2770E+02 | 2.2987E+02 | 4.1868E+05 | 9.2304E+05 | 1.1127E+08 | 4.4156E+08 |
| 160.0 | 7.0149E+02 | 1.5465E+03 | 1.4420E+02 | 2.5956E+02 | 4.3109E+05 | 9.5039E+05 | 1.1255E+08 | 4.4663E+08 |
| 170.0 | 5.7435E+02 | 1.2662E+03 | 1.3331E+02 | 2.3997E+02 | 4.4180E+05 | 9.7401E+05 | 1.1368E+08 | 4.5113E+08 |
| 180.0 | 2.9484E+02 | 6.5000E+02 | 2.9684E+02 | 5.3431E+02 | 4.4929E+05 | 9.9051E+05 | 1.1451E+08 | 4.5442E+08 |
| 190.0 | 4.5837E+02 | 1.0105E+03 | 1.7477E+02 | 3.1459E+02 | 4.5507E+05 | 1.0033E+06 | 1.1520E+08 | 4.5717E+08 |
| 200.0 | 4.3574E+02 | 9.6065E+02 | 1.8588E+02 | 3.3459E+02 | 4.6043E+05 | 1.0151E+06 | 1.1617E+08 | 4.6101E+08 |
| 210.0 | 1.8636E+02 | 4.1085E+02 | 3.1251E+02 | 5.6252E+02 | 4.6531E+05 | 1.0258E+06 | 1.1712E+08 | 4.6478E+08 |
| 220.0 | 1.2309E+02 | 2.7136E+02 | 3.9496E+02 | 7.1094E+02 | 4.7086E+05 | 1.0381E+06 | 1.1809E+08 | 4.6862E+08 |
| 230.0 | 1.0636E+02 | 2.3449E+02 | 4.5244E+02 | 8.1440E+02 | 4.7498E+05 | 1.0471E+06 | 1.1887E+08 | 4.7171E+08 |
| 240.0 | 1.0104E+02 | 2.2275E+02 | 4.7516E+02 | 8.5528E+02 | 4.7692E+05 | 1.0514E+06 | 1.1945E+08 | 4.7403E+08 |
| 250.0 | 1.3263E+02 | 2.9240E+02 | 3.6438E+02 | 6.5588E+02 | 4.7826E+05 | 1.0544E+06 | 1.1992E+08 | 4.7588E+08 |
| 260.0 | 1.3883E+02 | 3.0606E+02 | 3.7319E+02 | 6.7175E+02 | 4.7937E+05 | 1.0568E+06 | 1.2030E+08 | 4.7737E+08 |
| 270.0 | 1.3114E+02 | 2.8912E+02 | 3.6650E+02 | 6.5970E+02 | 4.8046E+05 | 1.0592E+06 | 1.2066E+08 | 4.7882E+08 |
| 280.0 | 1.2790E+02 | 2.8198E+02 | 3.6663E+02 | 6.5994E+02 | 4.8146E+05 | 1.0614E+06 | 1.2102E+08 | 4.8024E+08 |
| 290.0 | 1.3176E+02 | 2.9047E+02 | 3.7484E+02 | 6.7471E+02 | 4.8247E+05 | 1.0637E+06 | 1.2137E+08 | 4.8165E+08 |
| 300.0 | 1.3813E+02 | 3.0452E+02 | 3.6063E+02 | 6.4913E+02 | 4.8341E+05 | 1.0657E+06 | 1.2170E+08 | 4.8296E+08 |

APR1400 DCD TIER 2

Replace with next page B

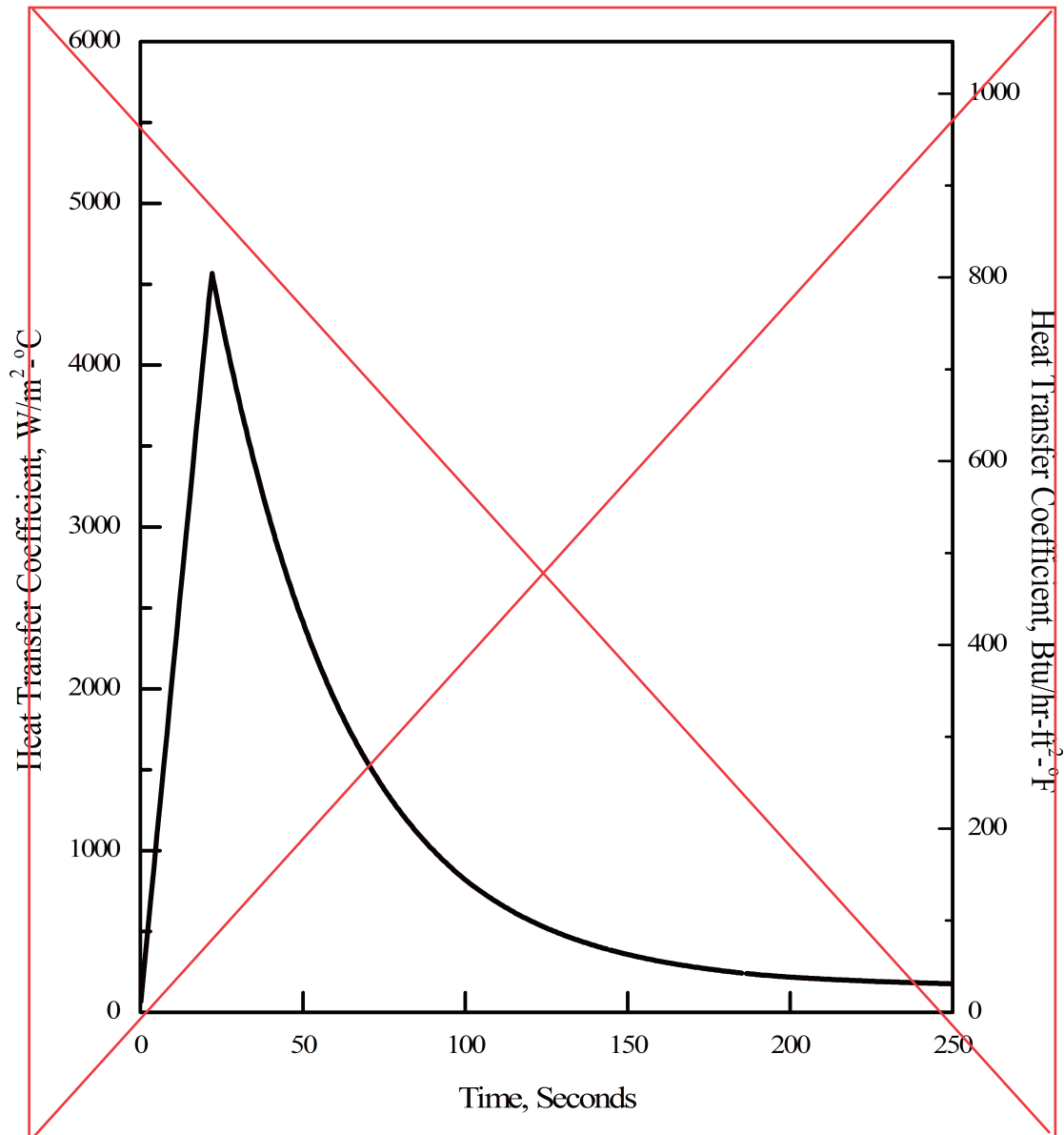
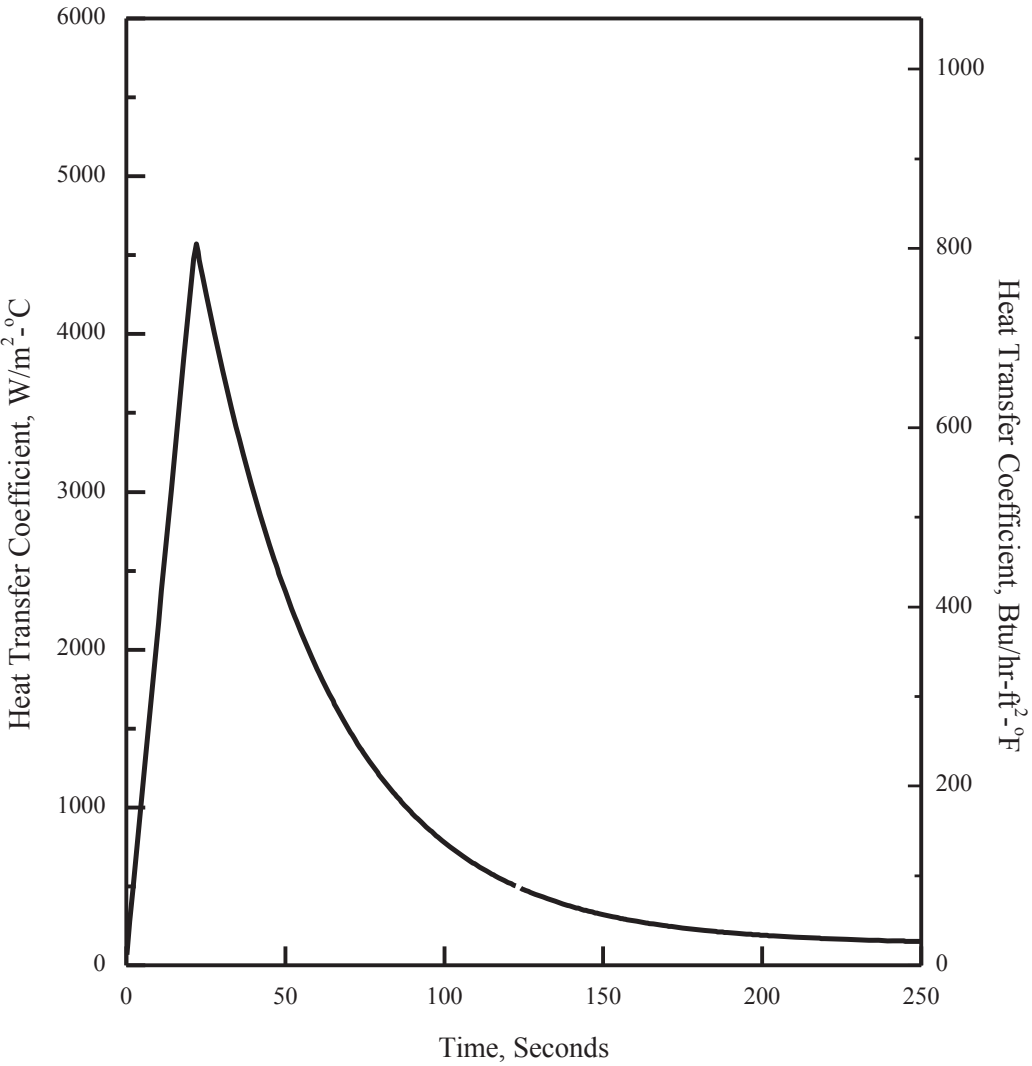


Figure 6.2.1-49 ECCS Performance Analysis
(Condensation Heat Transfer Coefficient for Passive Heat Removal Source)

B



APR1400 DCD TIER 2

Replace with next page C

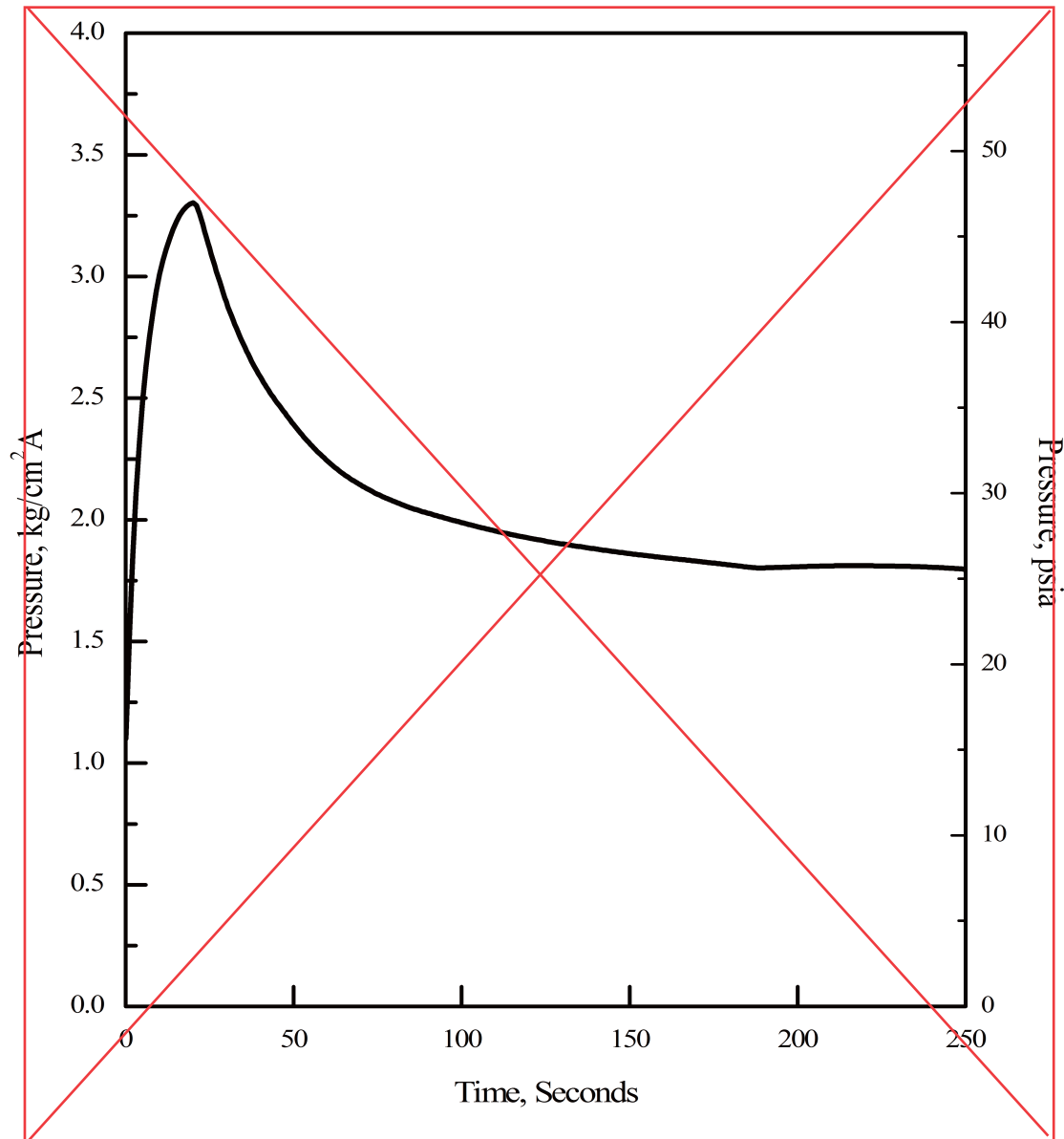
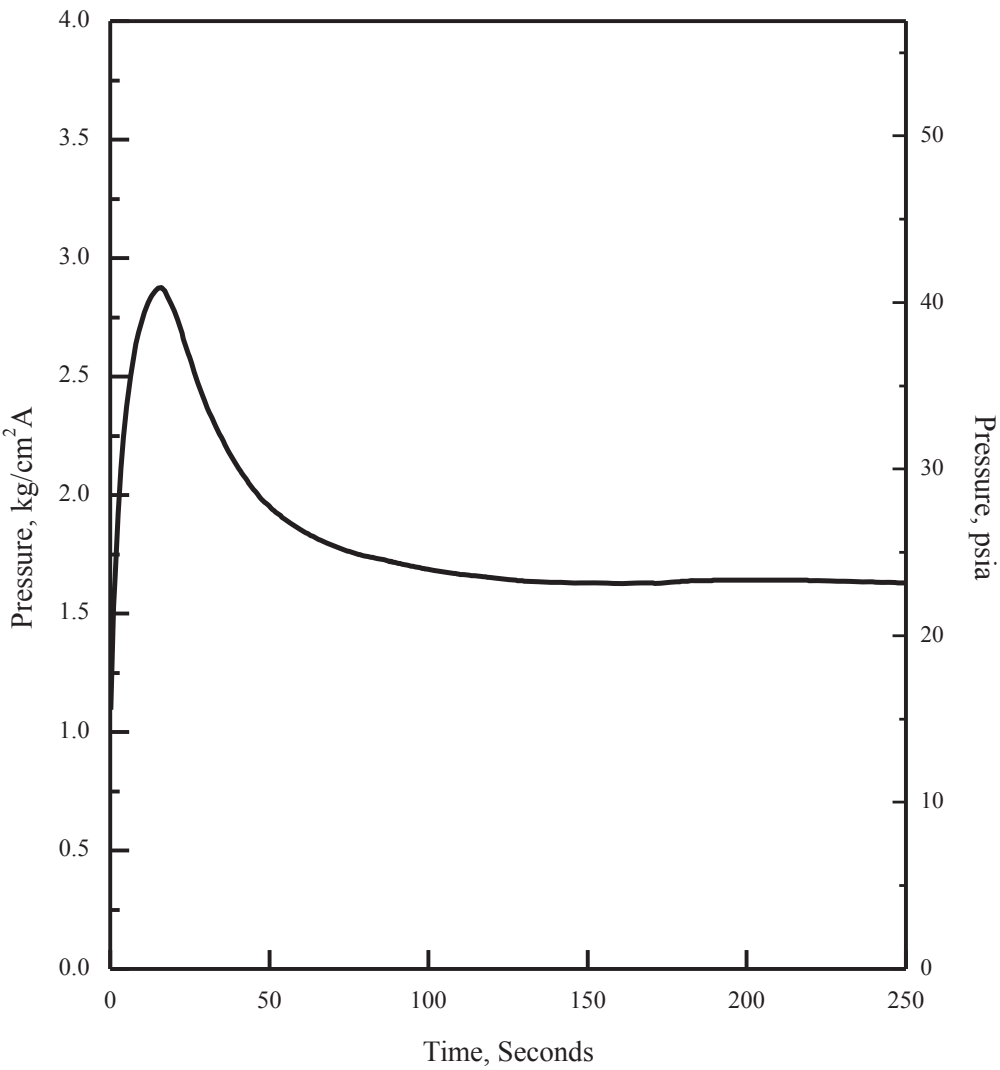


Figure 6.2.1-50 1.0 x Double-Ended Guillotine Break in Pump Discharge Leg
(Min. Containment Pressure for ECCS Performance Analysis)

C



APR1400 DCD TIER 2

Replace with next page D

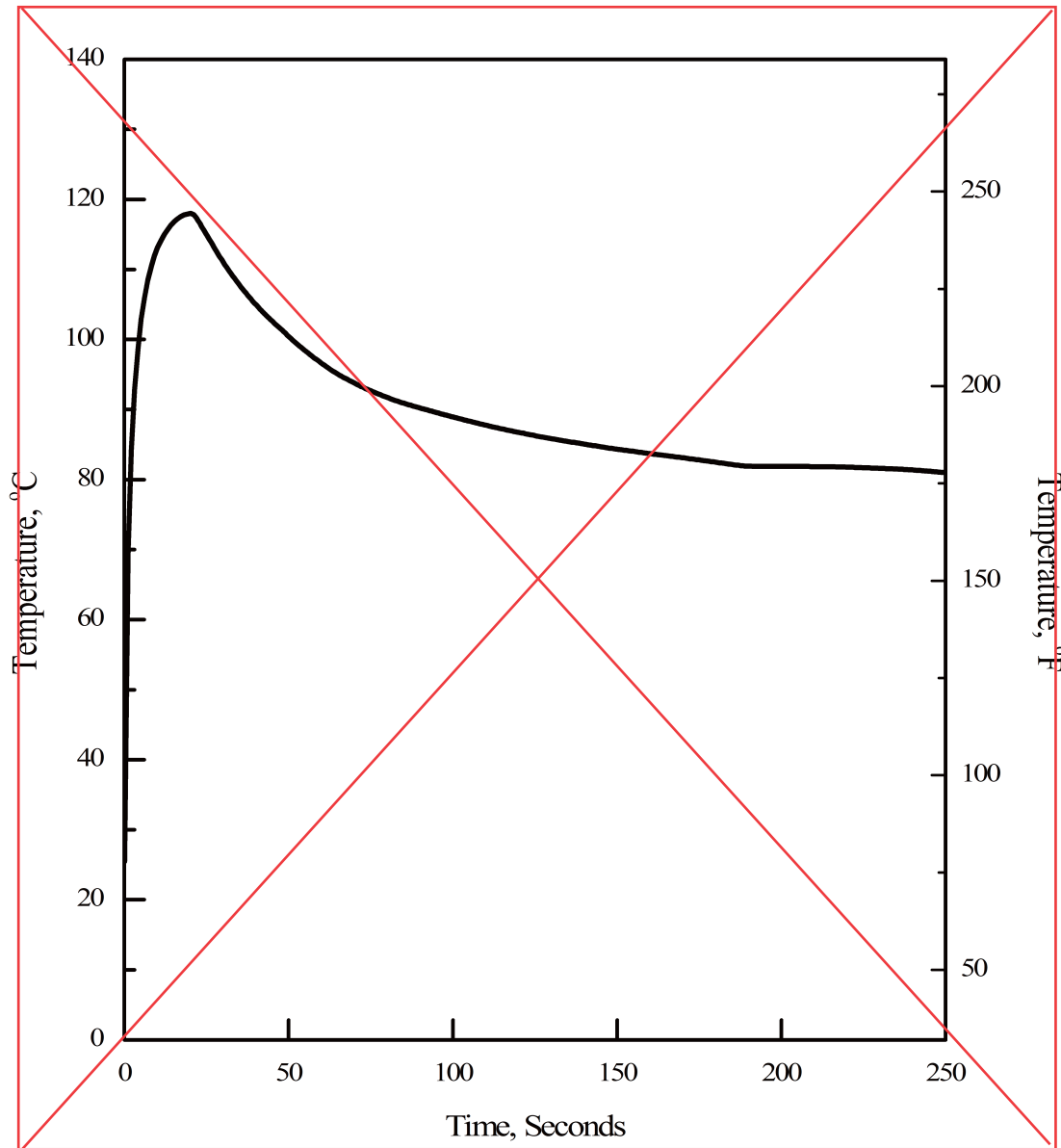
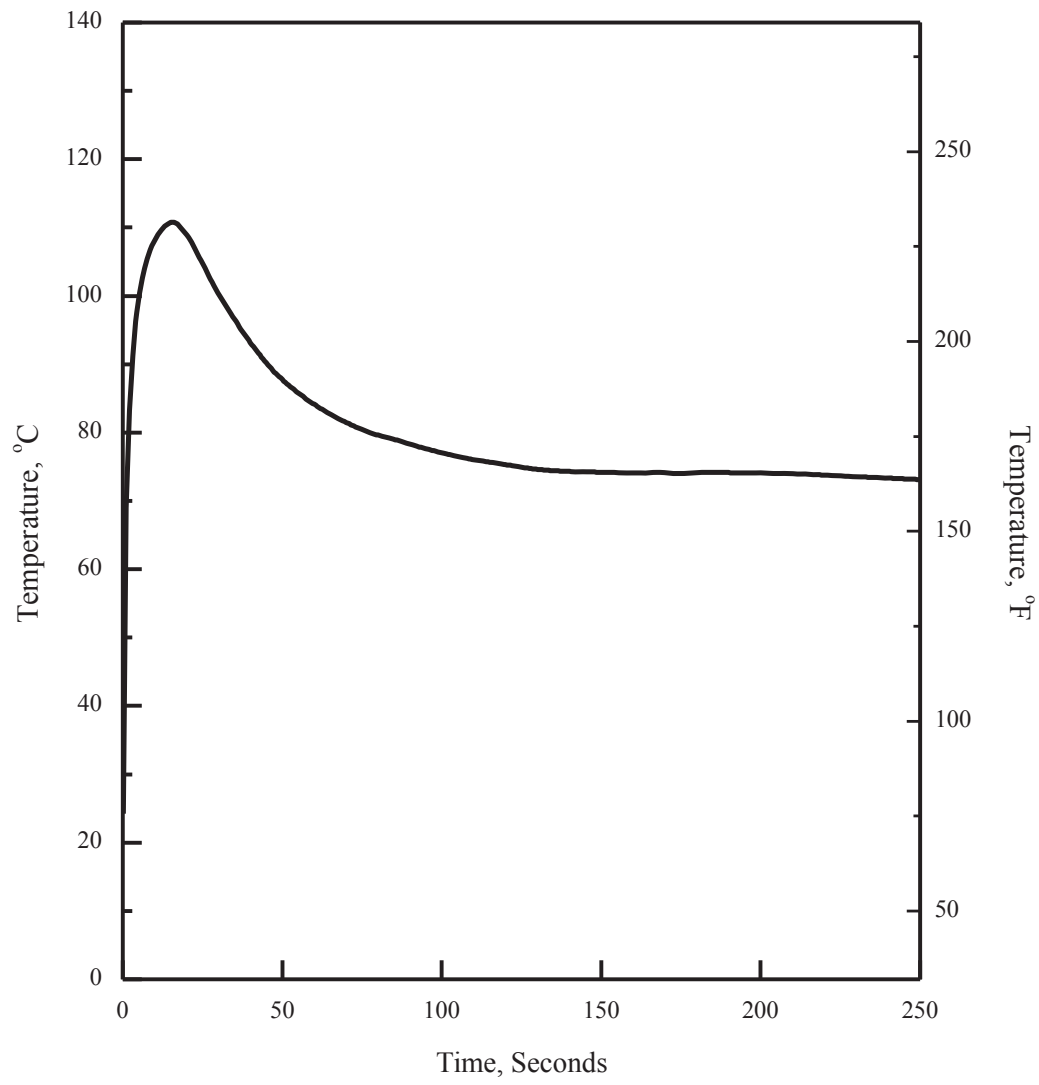


Figure 6.2.1-51 1.0 x Double-Ended Guillotine Break in Pump Discharge Leg (Containment Atmosphere Temperature)

D



APR1400 DCD TIER 2

Replace with next page E

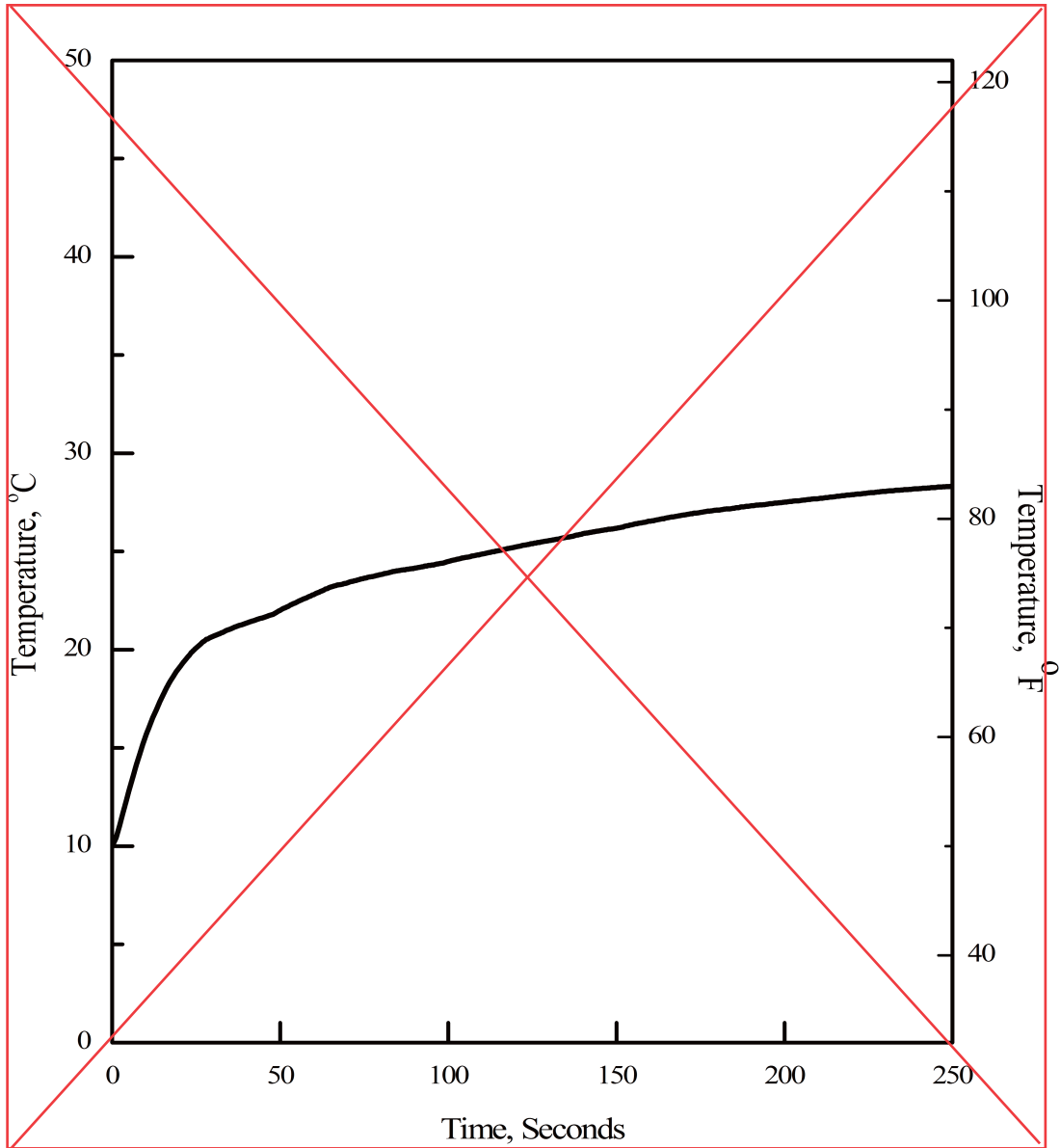
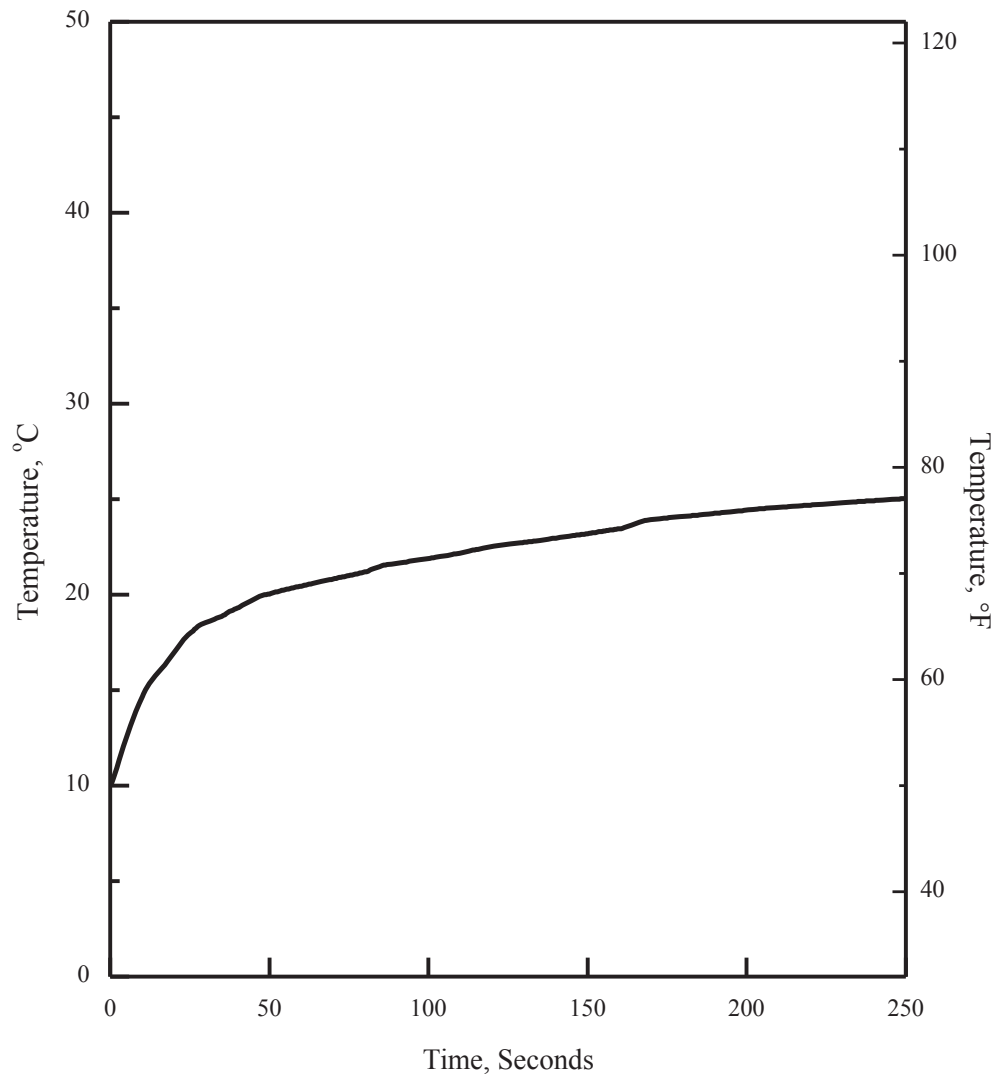


Figure 6.2.1-52 1.0 x Double-Ended Guillotine Break In Pump Discharge Leg
(In-containment Refueling Water Storage Tank)

insert~ Tem~ erature

E



fuel maximum reactivity assumption, worst-case moderator density, and tolerances and uncertainties of the fuel and racks are considered to maximize the calculated K_{eff} for normal conditions and postulated accidents.

The design of the new fuel storage racks is such that K_{eff} (with all biases and uncertainties) must not exceed 0.95 with full density unborated water and 0.98 with optimum moderation in the new fuel rack, at a 95 percent probability and 95 percent confidence level. For the spent fuel storage racks, credit is taken for the presence of soluble boron in the SFP. Therefore, the maximum K_{eff} including all biases and uncertainties must ~~not~~ exceed 0.95 with borated water, and must remain below 1.0 with full density unborated water, at a 95 percent probability and 95 percent confidence level.

The criticality safety evaluation for the new and spent fuel storage racks is performed in accordance with the following acceptance criteria and relevant guidance: 10 CFR Part 50 Appendix A, General Design Criterion (GDC) 62 (Reference 1), 10 CFR Part 50.68 (Reference 2), NRC guidance (Reference 3), and NUREG/CR-6698 (Reference 4). The 10 CFR Part 50.68 (b) items (2) and (3) for new fuel storage racks and item (4) for spent fuel storage racks are applied as the criticality safety design criteria. Criticality analysis codes are validated in accordance with NUREG/CR-6698.

9.1.1.2 Facilities Description

The description of new and spent fuel storage facilities is presented in Subsection 9.1.2.2.

9.1.1.3 Safety Evaluation

Prevention of an inadvertent criticality is provided by the adequate design of fuel handling and storage facilities and by administrative control procedures, considering the double contingency principle. The main methods for criticality control are (1) limiting the size of the array of fuel assemblies and (2) limiting the assembly neutron interaction by fixing the minimum separation and/or providing neutron poisons. In addition, rack cells are maintained in a safe geometry with no deformation in any design basis event. Flooding in the new fuel storage racks and boron dilution in the SFP water are minimized. Fuel mishandling is prevented by the fuel handling procedures.

For criticality safety design, the following analyses are performed to evaluate the degree of subcriticality and to verify conformance with the following design criteria (Reference 10):

condition, an infinite array of fresh fuel assemblies is modeled in the criticality calculation. Criticality for damaged fuel assemblies is separately evaluated and the effects of gap between racks are also evaluated.

- b. For the region II analyses, an infinite array of 2×2 fuel assemblies with various U-235 enrichments, from 2.0 to 5.0 wt%, is used for the criticality calculation. The moderator of pure water is at the temperature (density) within the design limits that yields the largest reactivity. The full density of unborated water is assumed to be 1.0 g/cm^3 (62.4 lbm/ft^3).
- c. Credit is taken for the neutron absorption in the neutron absorbing materials, and only 75 percent of B-10 areal density in the neutron absorbing materials is credited in the analysis. These assumptions provide additional margin in the event that deformation, degradation, or damage to the neutron absorber occur.
- d. Credit is taken for the soluble boron in the SFP. The SFP soluble boron concentration is assumed to be the same or less than the minimum concentration provided in the LCO 3.7.15.
- e. No cooling time is assumed to avoid fission product accumulation and Xe-135 is not included in the criticality calculation to conservatively evaluate the K_{eff} .
- f. The nuclear characteristics of the spent fuel are affected by the core operation parameters, such as fuel temperature, coolant temperature, soluble boron concentration in the coolant, and axial burnup profile. Thus, the most severe operating conditions are conservatively assumed in the fuel burnup calculation.
- g. No CEAs or burnable poison rods in the fuel assembly, and no neutron absorption
- h. The maximum fuel temperature including Thermal Conductivity Degradation (TCD) effect is less than the conservative fuel temperature applied to the criticality analysis.
the SFP filled with water.
- i. The bias and bias uncertainty obtained from benchmark calculation are reflected in the calculated K_{eff} . Uncertainties from mechanical tolerances and variations in the design parameters are added to the total uncertainty. For region II analyses, the effects of axial burnup profile and burnable poison rods, and uncertainty from the depletion calculation methodology are considered in the calculation K_{eff} .

R~ PLA~ ~

APR1400 DCD TIER 2

In ~ on-L~ ~ A anal~ sis~ ma~ imum ga~ con~ uctance use~ in ~ ~ S~ ~ -III co~ e is not affecte~ ~ ~ T~ D ~ ecause the highest ga~ con~ uctance value is o~ taine~ ~ ithout gas generation. An~ minimum ga~ con~ uctance use~ in ~ ~ S~ ~ -III co~ e is not affecte~ ~ ecause the lo~ est ga~ con~ uctance value is o~ taine~ at lo~ ~ urnu~ ~ here fission gas release is negligi~ le. The fuel tem~ erature coefficient reflecting a large uncertaint~ can cover the T~ D. Also~ Do~ ~ ler fee~ ~ ac~ effect in ~ ~ S~ ~ -III co~ e is still conservative ~ ecause of the conservative ga~ con~ uctance assum~ tion.

In D~ ~ anal~ ses~ ~ ~ T~ P/T~ R~ co~ e is not affecte~ ~ ~ T~ D ~ ue to the use of ~ ~ umm~ ~ ro~ s to ~ efine the heat flu~ ~ oun~ ar~ . A ~ umm~ ~ ro~ ~ o~ es not consi~ er the con~ uction heat transfer ~ ithin the fuel ro~ s.

~ ost of store~ energ~ is eliminate~ ~ efore the core uncover~ ~ uring a ~ lo~ ~ o~ n~ hase in small ~ rea~ L~ ~ A (S~ L~ ~ A). ~ ence~ the initial store~ energ~ effects cause~ ~ ~ T~ D are negligi~ le in S~ L~ ~ A.

The im~ acts of T~ D for a ~ ~ A e~ ection acci~ ent an~ L~ ~ L~ ~ A are consi~ ere~ ~ ~ reflecting T~ D ~ enalt~ in initiali~ ng the fuel centerline an~ average tem~ erature. The T~ D ~ enalt~ is ~ rovi~ e~ in Reference 78.

each design basis event.

The setpoints presented in Table 15.0-2 are determined based on the methodology presented above. The main methodology for determining uncertainties and the detailed uncertainty values are provided in Reference 51, which is based on NRC RG 1.105, Rev. 3, "Setpoints for Safety-Related Instrumentation." The setpoint methodology for plant protection system is provided in Reference 77.

15.0.0.10 Thermal Conductivity Degradation

The effects of thermal conductivity degradation (TCD) on non-LOCA and LOCA evaluations, except for a CEA ejection accident and LBLOCA, are negligible. ~~The effects are provided in Reference 78.~~

The results of the evaluation of a CEA ejection accident and LBLOCA are provided in Subsections 15.4.8.3 and 15.6.5.3, respectively.

15.0.1 Radiological Consequence Analysis Using Alternative Source Terms

This subsection is not applicable to the APR1400 because it is prepared to review the application for the initial implementation of an alternative source terms (AST)

they exhibit a
ere is a known
effects of an
n the signal
at calculation
Safety-Related

is random and
are combined
as errors are
algebraically

vironment for
al equipment
at setpoint for

APR1400 DCD TIER 2

In on-L A analysis maximum gas conformance use in S -III code is not affected. T D because the highest gas conformance value is obtained without fission gas release. An minimum gas conformance use in S -III code is not affected because the lowest gas conformance value is obtained at low burnup where fission gas release effect is negligible. The least negative or the most negative fuel temperature coefficients use in on-L A analysis cover the impact of T D since the effective fuel temperature correlation and the biases and uncertainties are determined using measured data. Also Doeller feedback effect in S -III code is still conservative because of the conservative gas conformance assumption.

In D analysis T P/T R code is not affected. T D due to the use of summation rods to refine the heat flux boundary. A summation rods does not consider the conduction heat transfer within the fuel rods.

Most of stored energy is eliminated before the core uncover using a low power phase in small area L A (S L A). Hence the initial stored energy effects caused T D are negligible in S L A.

The impacts of T D for a A ejection accident and L L A are considered reflecting T D enalt in initializing the fuel centerline and average temperature. The T D enalt is provided in Reference 81.

they exhibit a
there is a known
effects of an
in the signal
at calculation
Safety-Related

is random and
are combined
as errors are
algebraically

environment for
al equipment
at setpoint for

ogy presented

above. The main methodology for determining uncertainties and the detailed uncertainty values are provided in Reference 51, which is based on NRC RG 1.105, Rev. 3, "Setpoints for Safety-Related Instrumentation." The setpoint methodology for plant protection system is provided in Reference 77.

15.0.0.10 Thermal Conductivity Degradation

The effects of thermal conductivity degradation (TCD) on non-LOCA and LOCA evaluations, except for a CEA ejection accident and LBLOCA, are negligible. ~~The effects are provided in Reference 78.~~

The results of the evaluation of a CEA ejection accident and LBLOCA are provided in Subsections 15.4.8.3 and 15.6.5.3, respectively.

15.0.1 Radiological Consequence Analysis Using Alternative Source Terms

This subsection is not applicable to the APR1400 because it is prepared to review the application for the initial implementation of an alternative source terms (AST)

delete

APR1400-F-M-TR-13001-P PLUS7 Fuel Design for the APR1400
Rev. 1 P To be issue

Intentional plan

78. ~~APR1400-F-A-NR-14002-P, "The Effect of Thermal Conductivity Degradation on APR1400 Design and Safety Analyses," Rev. 0, KHNP, September 2014.~~
79. NUREG-1462, "Final Safety Evaluation Report Related to the Certification of the System 80+ Design Docket No. 52-002," Rev. 0, U.S. Nuclear Regulatory Commission, 1994.
80. APR1400-Z-A-NR-14014-P, "ATWS Evaluation," Rev. 0, KHNP, November 2014.
81. APR1400-F-M-TR-13001-P (Proprietary), "PLUS7 Fuel Design for the APR1400,"
~~Rev. 0, KHNP, August 2013.~~

Rev. 1 P August 2017.

APR1400 DCD TIER 2

- i. A top-peaked axial power distribution is set to maximize the energy content in the hottest fuel pellet.
- j. The maximum delay time is 0.55 second (including time to open the reactor trip switchgear) for the VOPT and 0.5 second for CEA holding coil decay time.

15.4.8.3.3 Results

For peak fuel rod temperature and fuel rod enthalpy analysis, the results are summarized in Table 15.4.8-3. For the HZP case, the fuel radial average enthalpy of hot spot is well below the high cladding temperature failure criterion. The prompt fuel enthalpy rise is less than 251.2 kJ/kg (60 cal/g), which is the lowest criterion of the PCMI failure depicted in Figure B-1 of SRP 4.2 and the oxide to wall thickness ratio is less than 0.2 (the maximum cladding oxide thickness is less than 100 μ m, Reference 81). The PCMI

. For T~ D effects~ the T~ D ~enalt~ ~escri~ e~ in Reference 81 ~ as reflecte~ in initial~ ing the fuel centerline an~ average tem~ erature.

and the HZP case. The non-prompt scenarios that do not exhibit a prompt critical or narrow pulse power excursion, such as the HFP case and the 50 percent power case, would be not concerned with PCMI cladding failure.

In the results, there are no fuel failures due to the high fuel enthalpy and PCMI. From a core coolability perspective, the peak fuel radial average enthalpy and the fuel centerline temperature meet the criterion. The maximum fuel cladding temperature is not high enough to cause fuel rupture or significant rod ballooning. Therefore, there is no loss of core coolable geometry. The interim criteria for reactivity-initiated accident (RIA) described in NUREG-0800 (SRP 4.2 Appendix B) are met.

~~The centerline temperature is increased by 157.2 °C (315 °F) in case of considering the thermal conductivity degradation (TCD) effect (Reference 78). However, the maximum centerline temperature is below the melting temperature and met the criterion.~~

Following a postulated CEA ejection event, 10.0 percent of the fuel is calculated to undergo DNB. As all fuel pins that undergo DNB are conservatively assumed to suffer clad failure, 10.0 percent of fuel failure is used in the offsite dose evaluation in Subsection 15.4.8.5. The case initiated from HFP initial conditions is expected to result in the greatest potential for offsite dose consequences.

APR1400 DCD TIER 2

Table 15.4.8-1 (1 of 3)

Sequence of Events for the CEA Ejection

| Power | Time (sec) | Event | Setpoint or Value |
|-------|------------|---|-------------------|
| HFP | 0.00 | Mechanical failure | |
| | 0.03 | Core power reaches variable overpower reactor trip analysis setpoint, % of design power | |
| | 0.05 | CEA fully ejected | - |
| | 0.07 | Maximum core power, % of design power | 156.3 |
| | 1.08 | CEAs begin to drop into core | - |
| | 3.30 | Maximum radial average fuel enthalpy in the hot spot, kJ/kg (cal/gm) | 522.1 (124.7) |
| | 3.43 | Maximum clad surface temperature in the hot spot, °C (°F) | 567.2 (1,053.0) |
| 50% | 3.67 | Maximum fuel centerline temperature in the hot spot, °C (°F) | 2,490.2 (4,514.3) |
| | 0.00 | Mechanical failure | |
| | 0.03 | Core power reaches variable overpower reactor trip analysis setpoint, % of design power | 75.0 |
| | 0.05 | CEA fully ejected | |
| | 0.08 | Maximum core power, % of design power | 127.1 |
| | 1.08 | CEAs begin to drop into core | |
| | 3.20 | Maximum clad surface temperature in the hot spot, °C (°F) | 569.2 (1,056.5) |
| | 3.31 | Maximum radial average fuel enthalpy in the hot spot, kJ/kg (cal/gm) | 504.1 (120.4) |
| | 3.72 | Maximum fuel centerline temperature in the hot spot, °C (°F) | 2,370.9 (4,299.6) |

APR1400 DCD TIER 2

Maximum clad surface temperature in the hot spot
(°F)

Table 15.4.8-1 (2 of 3)

Maximum radial average fuel enthalpy in the hot spot
(cal/gm)

| Power | Time (sec) | Event | |
|-------|------------|---|-------------------|
| 20% | 0.00 | Mechanical failure of CEDM causes CEA to eject | - |
| | 0.04 | Core power reaches variable overpower reactor trip analysis setpoint, % of design power | 45.0 |
| | 0.05 | CEA fully ejected | - |
| | 0.10 | Maximum core power, % of design power | 140.3 |
| | 1.09 | CEAs begin to drop into core | - |
| | 3.30 | Maximum radial average fuel enthalpy in the hot spot, kJ/kg (cal/gm) | 473.5 (113.1) |
| | 3.62 | Maximum clad surface temperature in the hot spot, °C (°F) | 586.7 (1,088.1) |
| | 3.67 | Maximum fuel centerline temperature in the hot spot, °C (°F) | 2,331.3 (4,228.4) |
| HZP | 0.00 | Mechanical failure of CEDM causes CEA to eject | - |
| | 0.21 | Core power reaches variable overpower reactor trip analysis setpoint, % of design power | 25.0 |
| | 0.05 | CEA fully ejected | - |
| | 0.32 | Maximum core power, % of design power | 141.3 |
| | 1.26 | CEAs begin to drop into core | - |
| | 2.48 | Maximum clad surface temperature in the hot spot, °C (°F) | 346.9 (656.5) |
| | 3.04 | Maximum radial average fuel enthalpy in the hot spot, kJ/kg (cal/gm) | 314.8 (75.2) |
| | 3.67 | Maximum fuel centerline temperature in the hot spot, °C (°F) | 1,501.5 (2,734.7) |

2.32

3.2

3.87

348.2 (~ 58.7)

500.4 (119.~)

2,388.8 (4,331.8)

2.~ 1

3.09

3.74

(~ 5~ .4)

319.1 (7~ .2)

1,52~ .5 (2,779.7)

APR1400 I R 2

Table

Results of the CEA Ejection Analysis

| Parameter | Power | | | |
|--|----------------------|----------------------|----------------------|----------------------|
| | HZP | 20% | 50% | HFP |
| Maximum radial average fuel enthalpy at hot spot, kJ/kg (cal/gm) | 314.8 (75.2) | 473.5 (113.1) | 504.1 (120.4) | 522.1 (124.7) |
| Maximum fuel centerline temperature, °C (°F) | 1,501.5 (2,734.7) | 2,331.3 (4,228.4) | 2,370.9 (4,299.6) | 2,490.2 (4,514.3) |
| Maximum prompt enthalpy rise, ⁽¹⁾ kJ/kg (cal/gm) | 90.9 (21.7) | 138.6 (33.1) | 160.8 (38.4) | 118.9 (28.4) |
| Maximum cladding surface temperature, °C (°F) | 347.0 (656.6) | 586.7 (1,088.1) | 569.2 (1,056.5) | 567.2 (1,053.0) |

(1) Maximum energy deposition during the prompt power pulse width. For HFP and 50 percent power case, the prompt enthalpy rise is the value at 1.0 second.

347.9
(~ 57.4)

348.2
(~ 58.7)

524.1
(975.3)

527.8
(980.3)

139.0
(33.2)

172.0
(38.7)

122.3
(29.2)

APR1400 DCD TIER 2

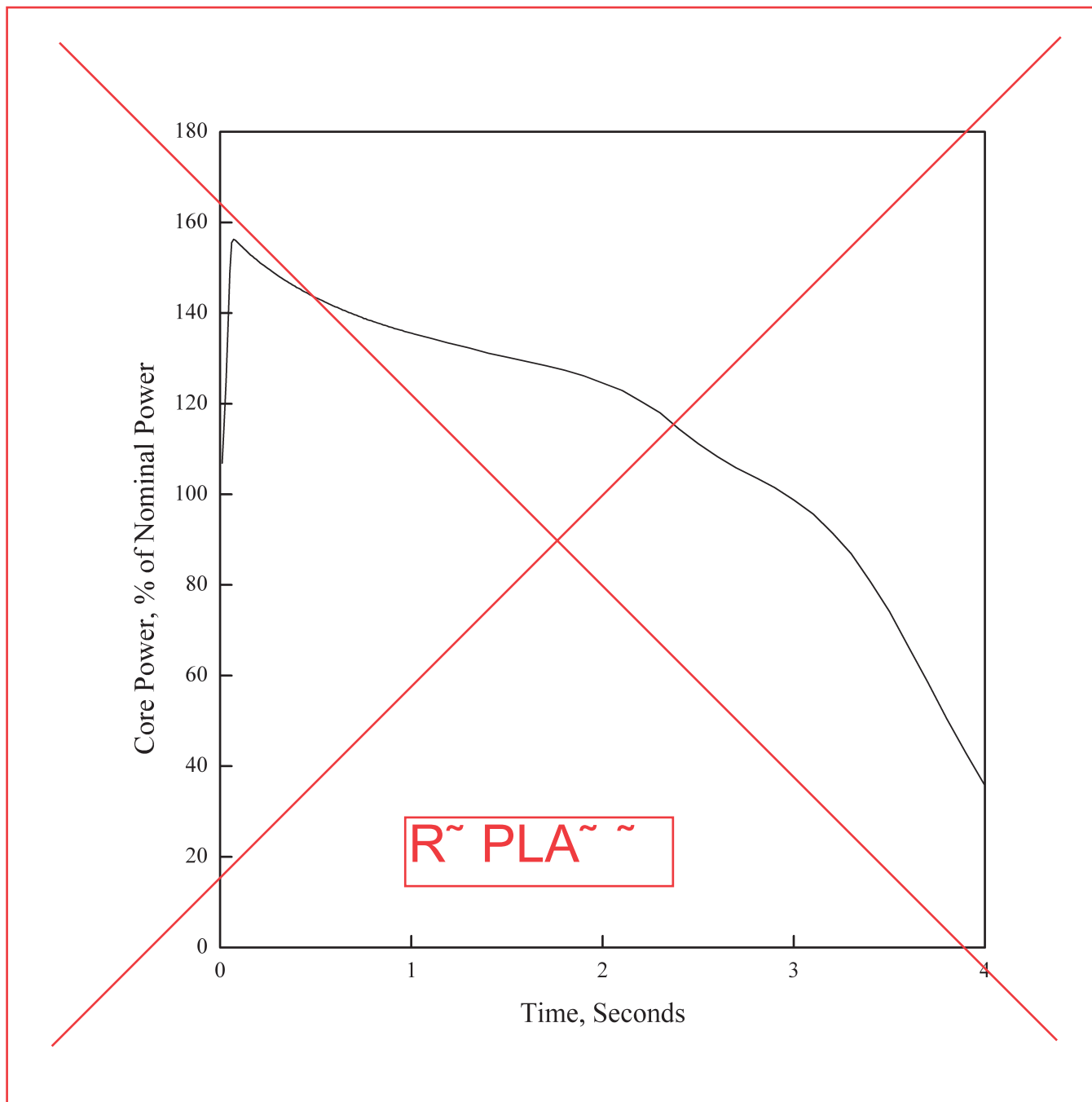
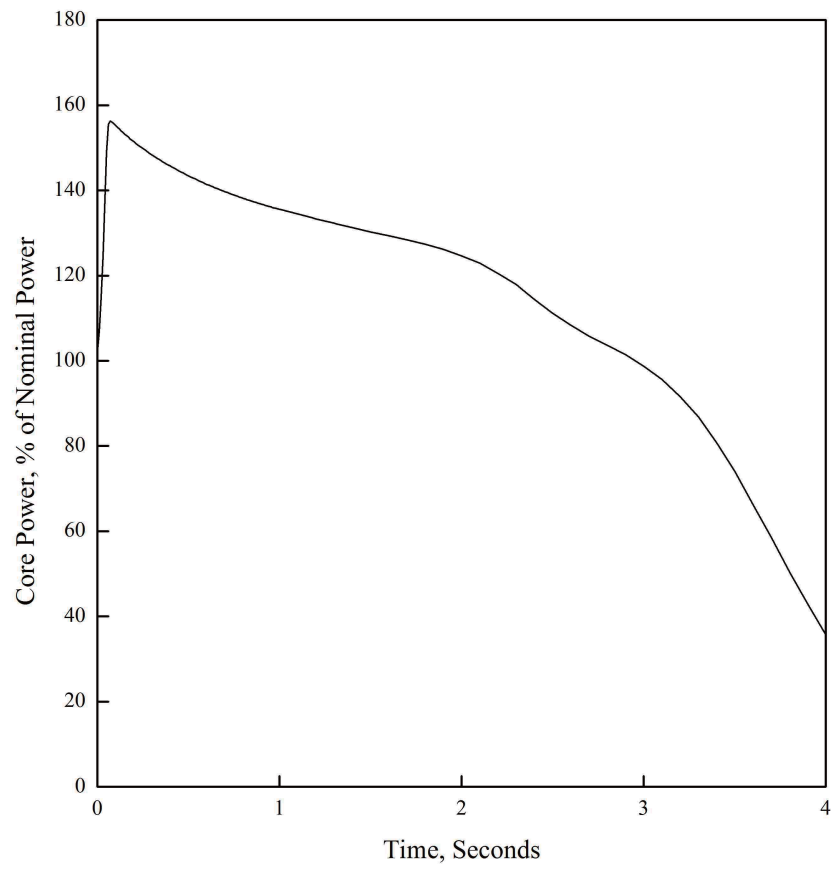


Figure 15.4.8-1 CEA Ejection: Core Power vs. Time (HFP)



APR1400 DCD TIER 2

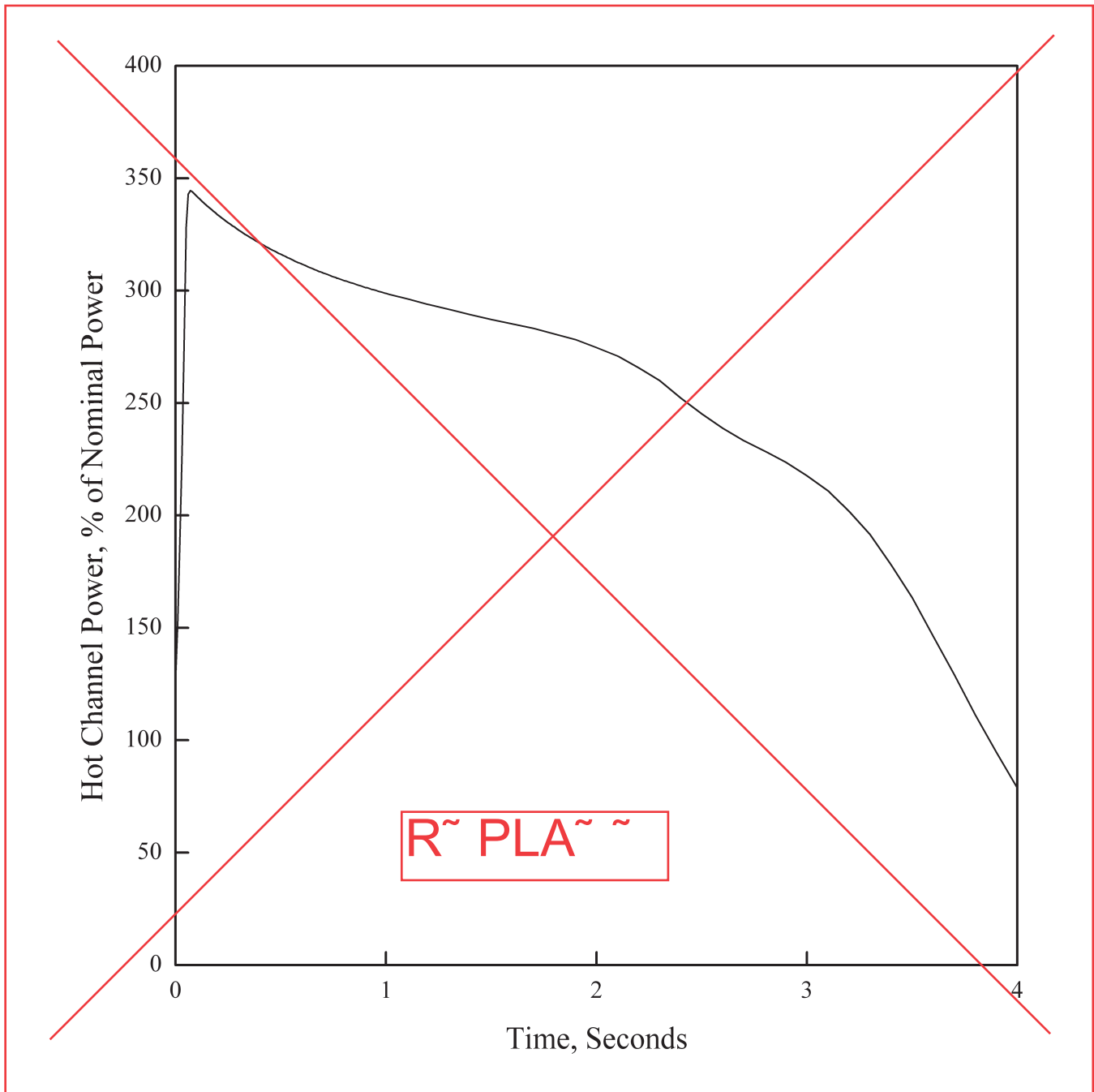
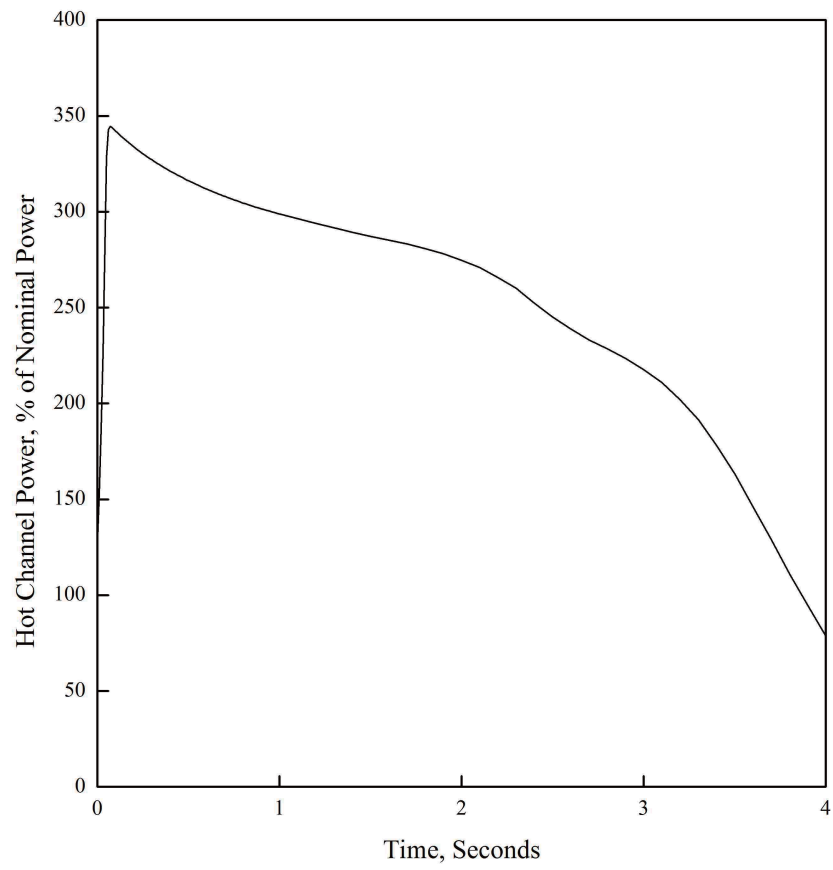


Figure 15.4.8-2 CEA Ejection: Hot Channel Power vs. Time (HFP)



APR1400 DCD TIER 2

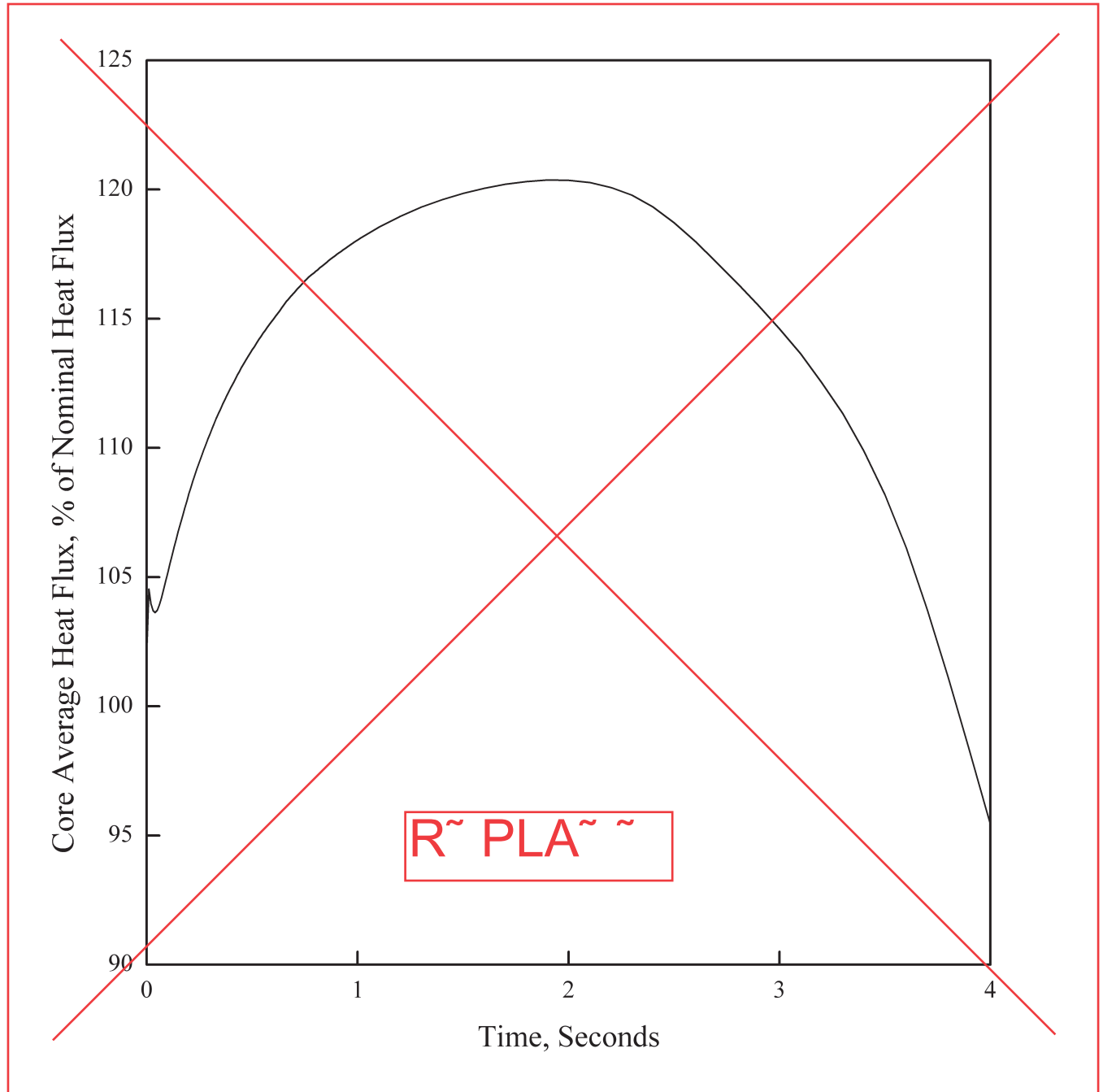
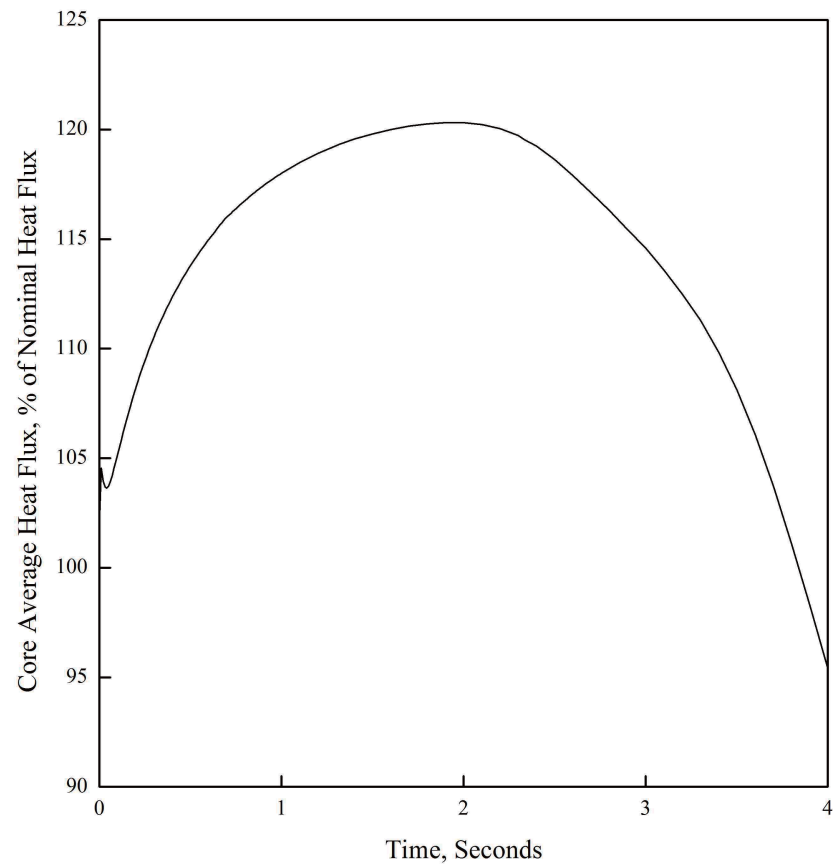


Figure 15.4.8-3 CEA Ejection: Core Average Heat Flux vs. Time (HFP)



APR1400 DCD TIER 2

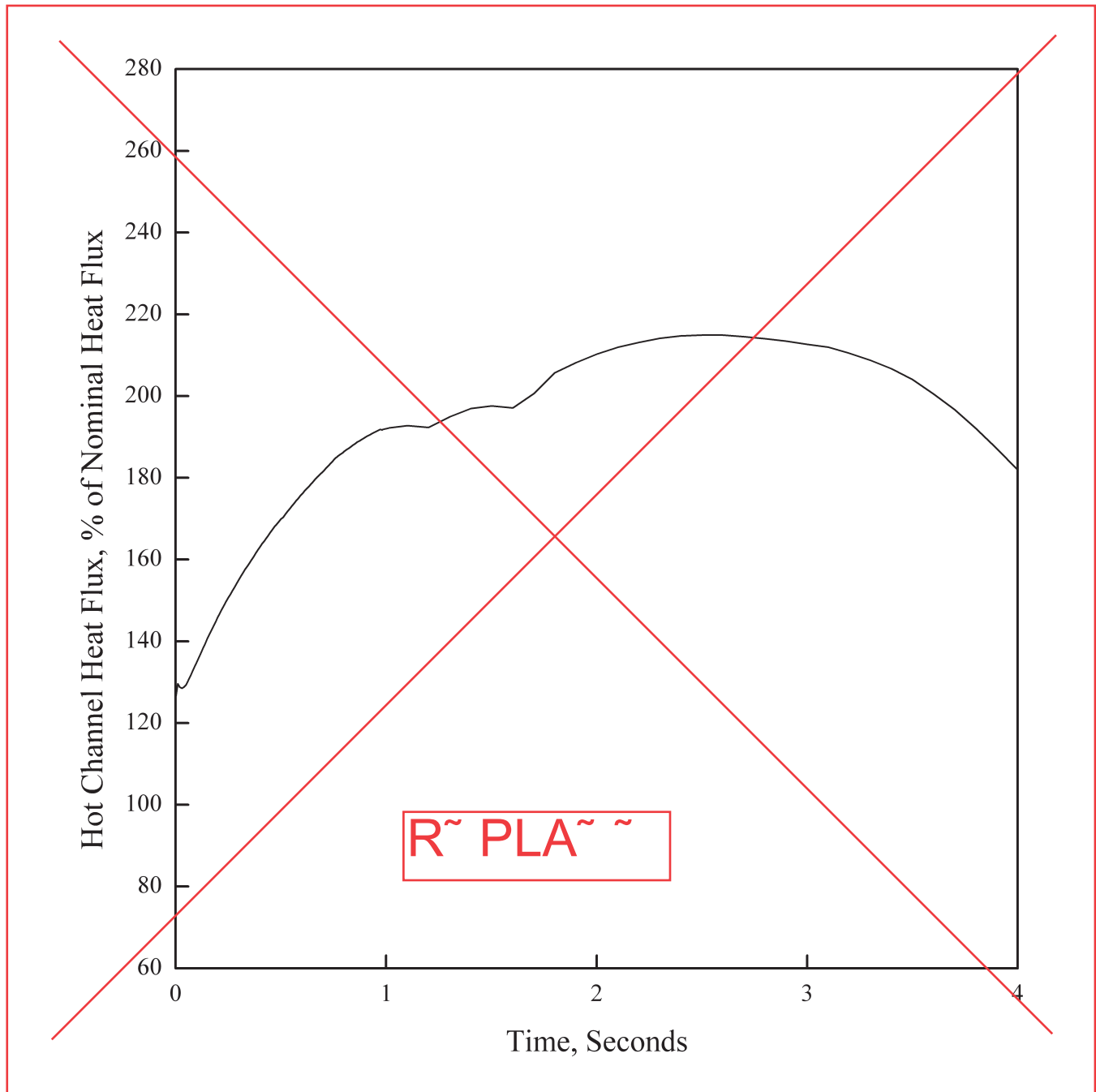
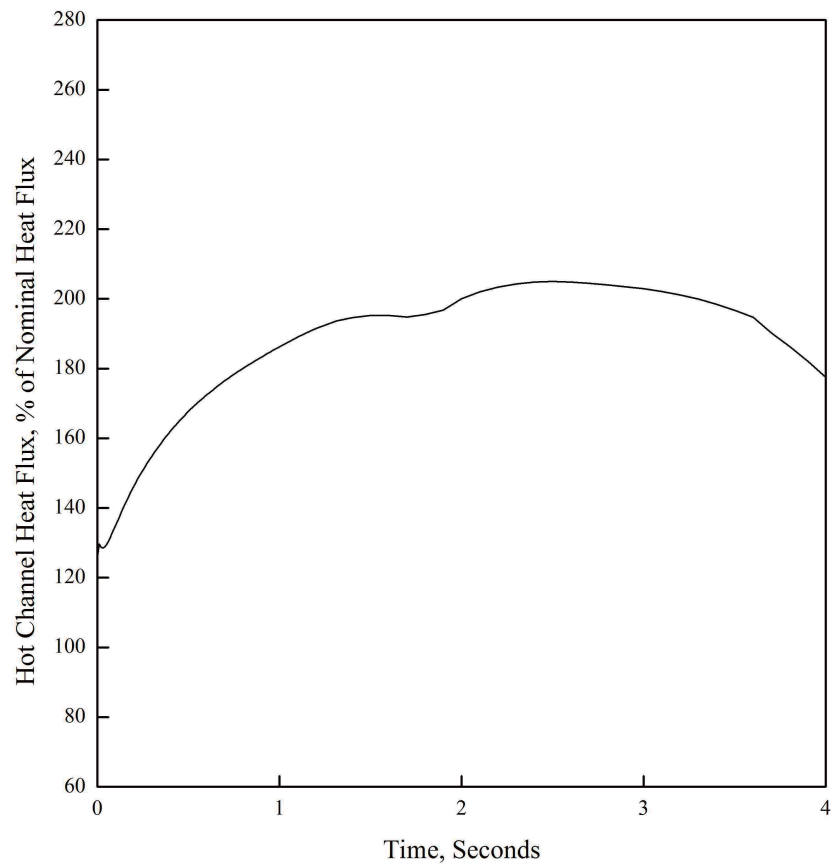


Figure 15.4.8-4 CEA Ejection: Hot Channel Heat Flux vs. Time (HFP)



APR1400 DCD TIER 2

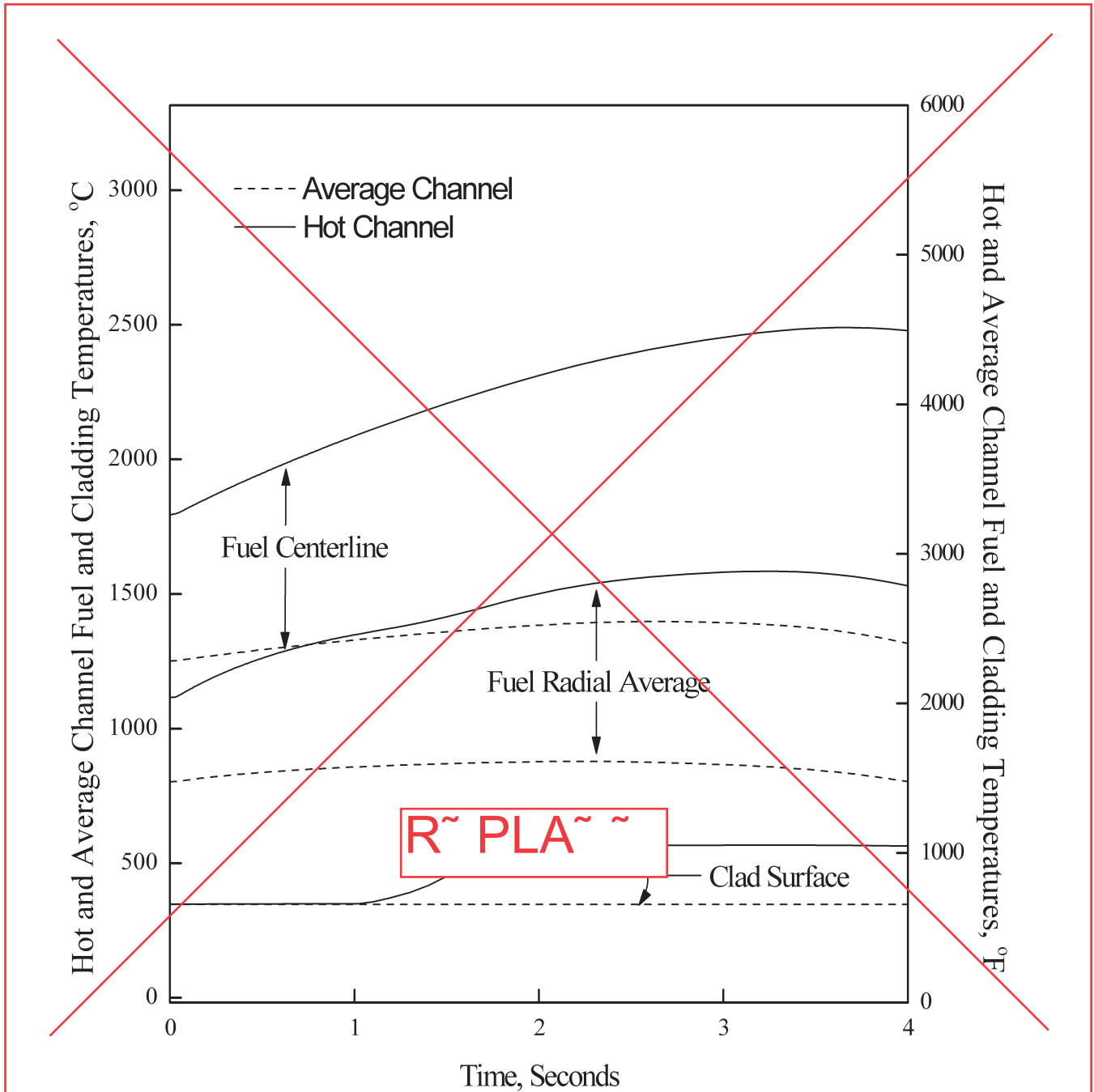
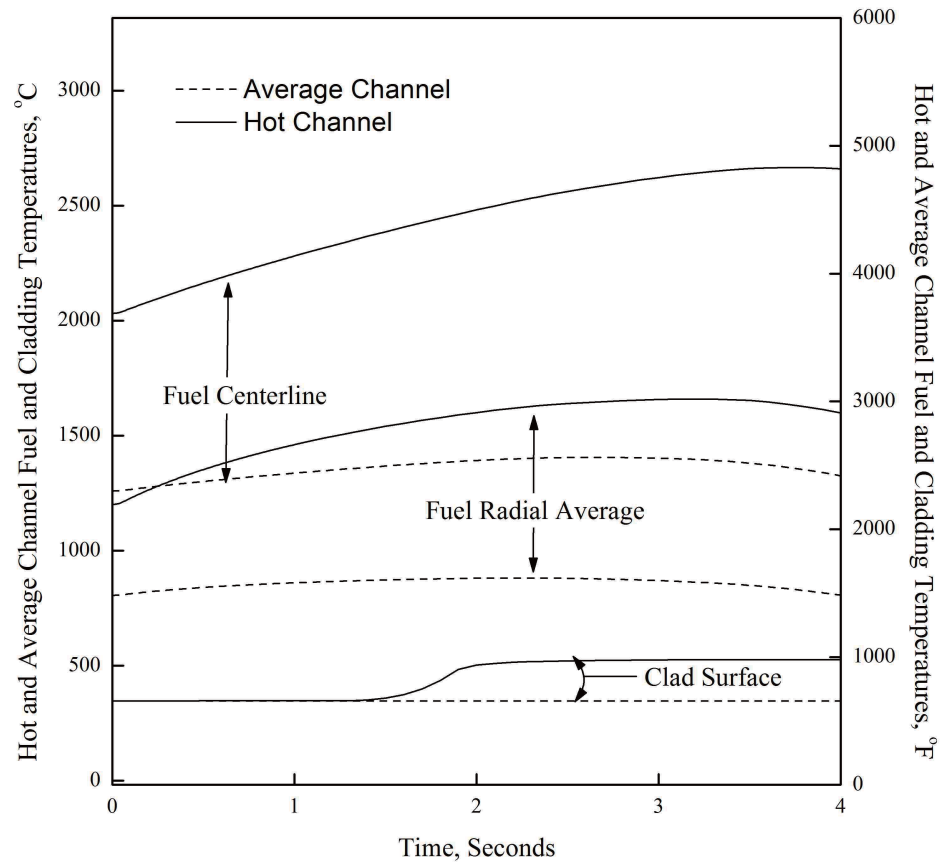


Figure 15.4.8-5 CEA Ejection: Hot and Average Channel Fuel and Cladding Temperatures vs. Time (HFP)

insert



APR1400 DCD TIER 2

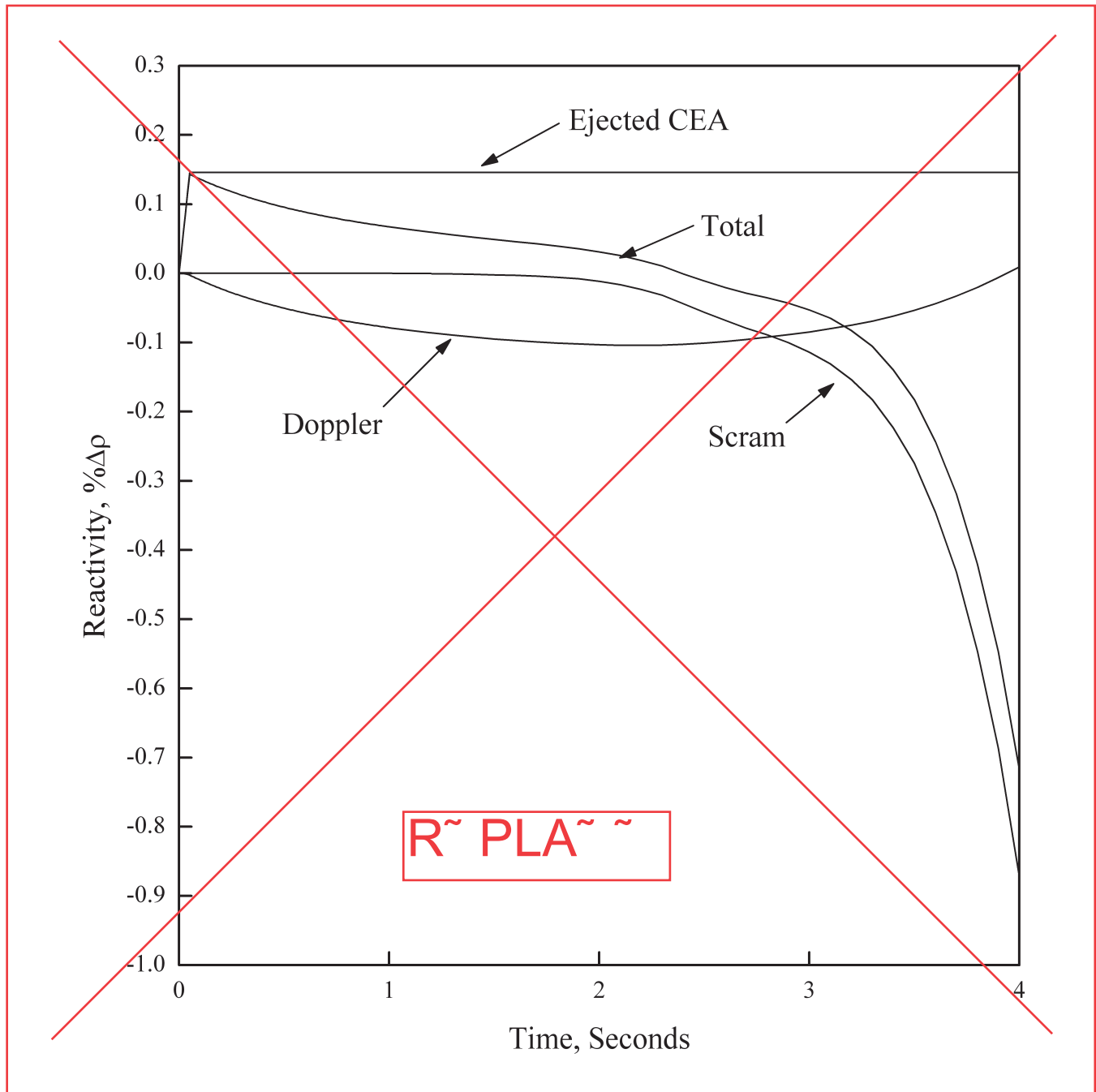
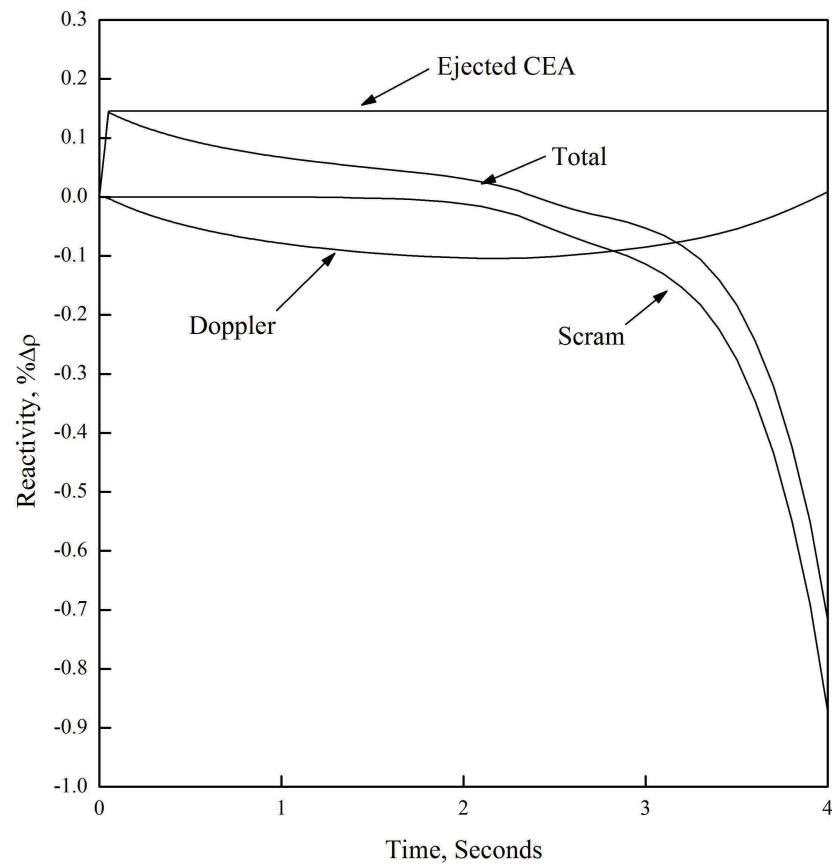


Figure 15.4.8-6 CEA Ejection: Reactivity vs. Time (HFP)



APR1400 DCD TIER 2

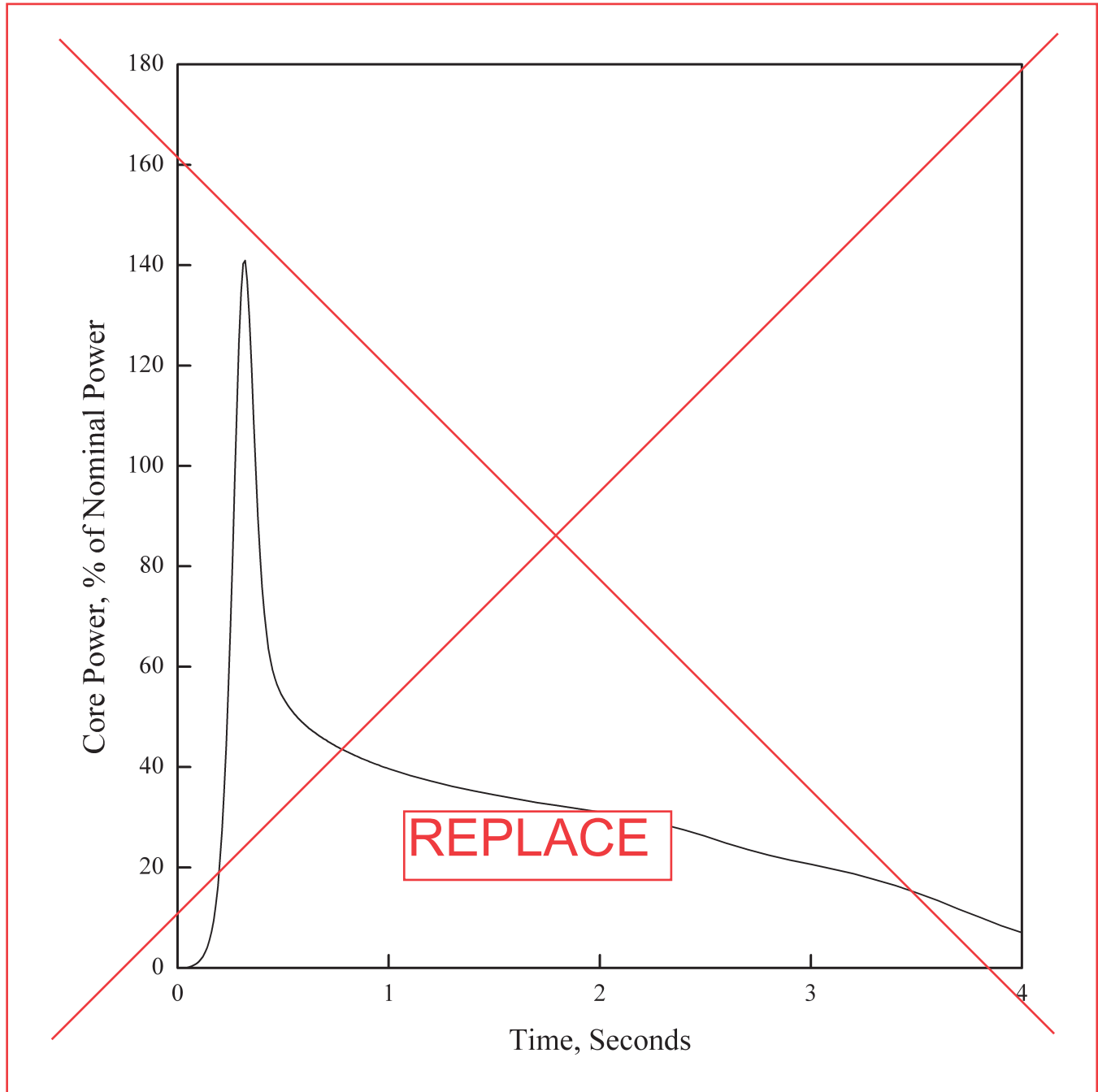
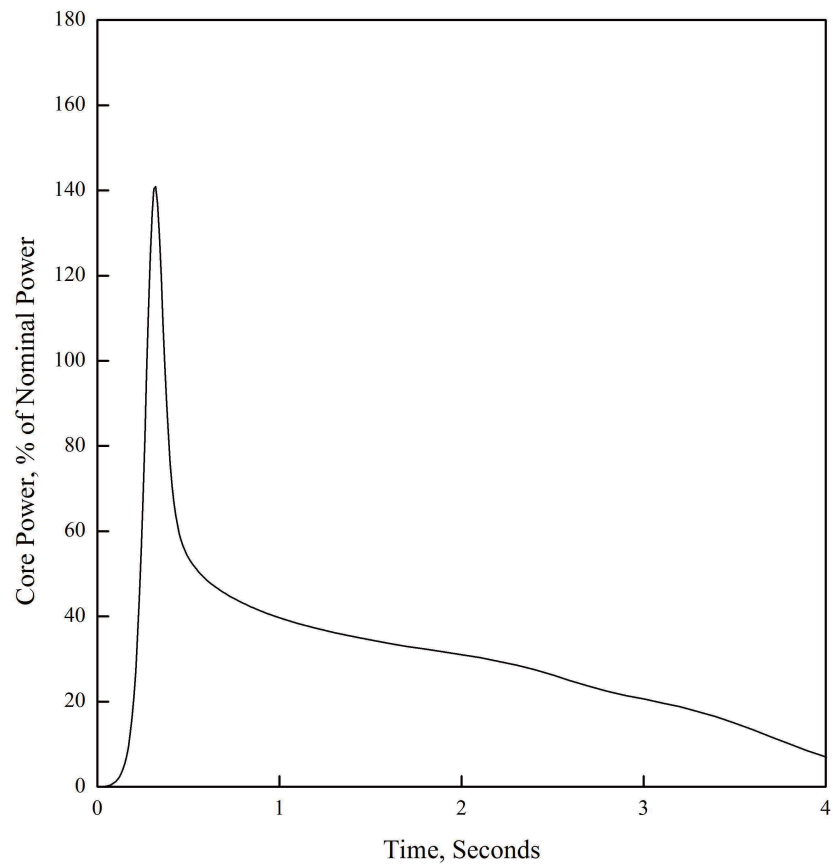


Figure 15.4.8-7 CEA Ejection: Core Power vs. Time (HZP)



APR1400 DCD TIER 2

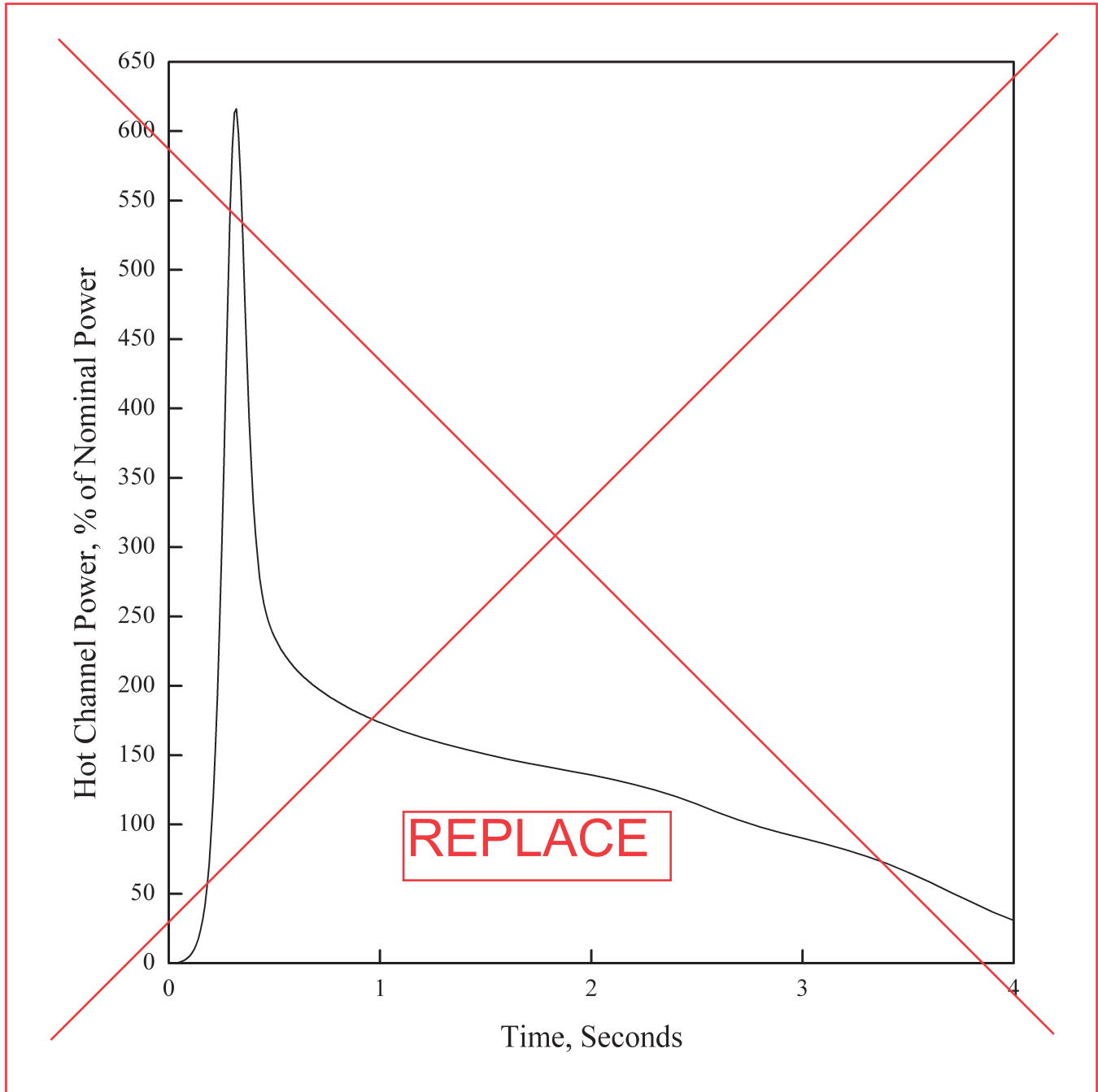
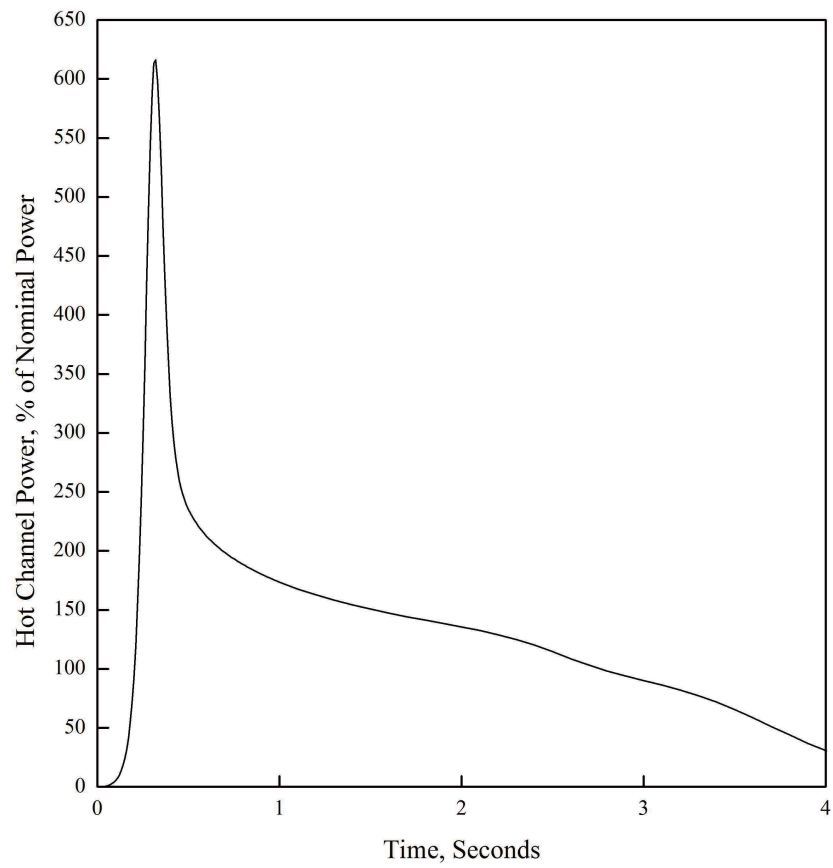
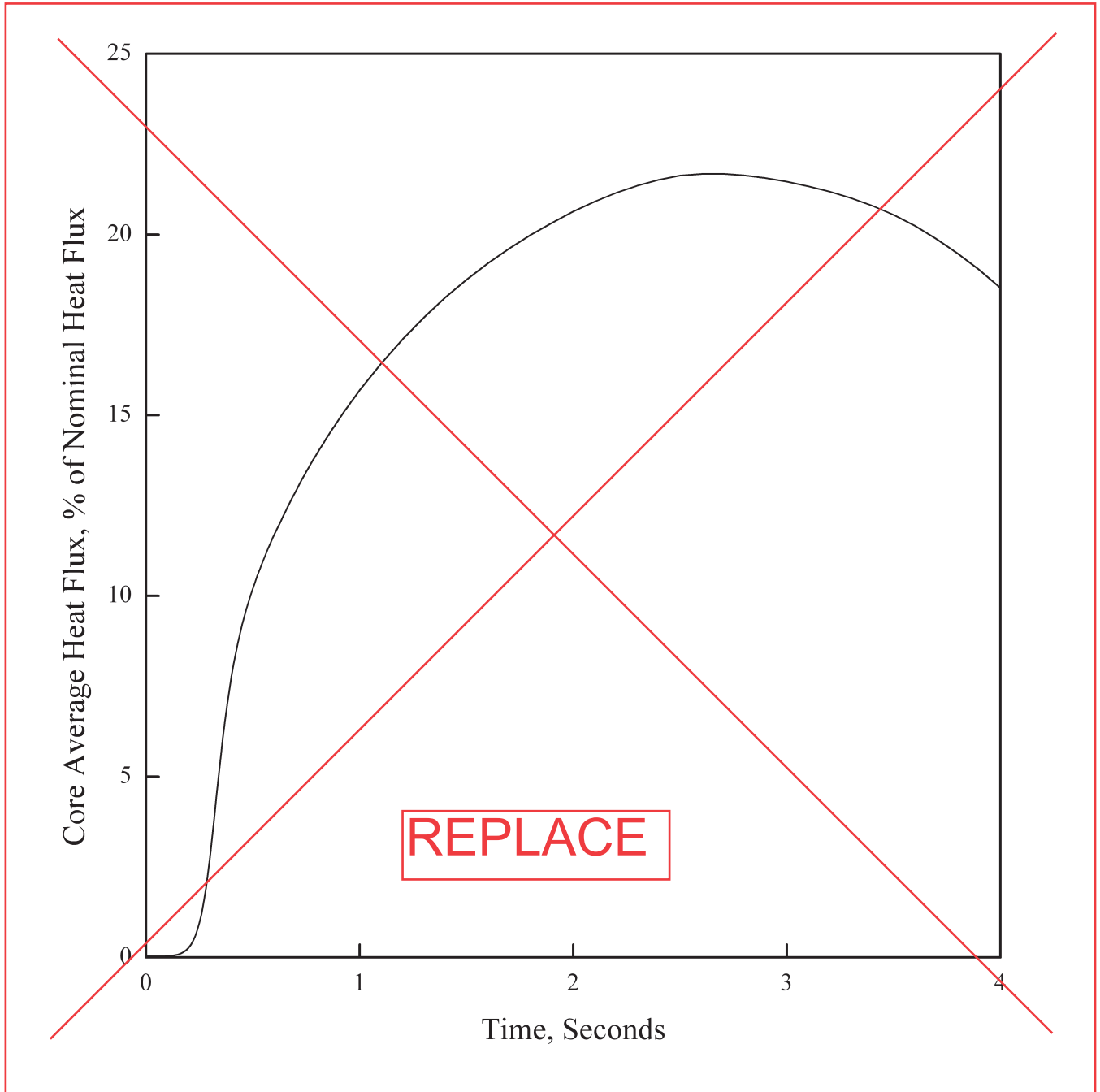
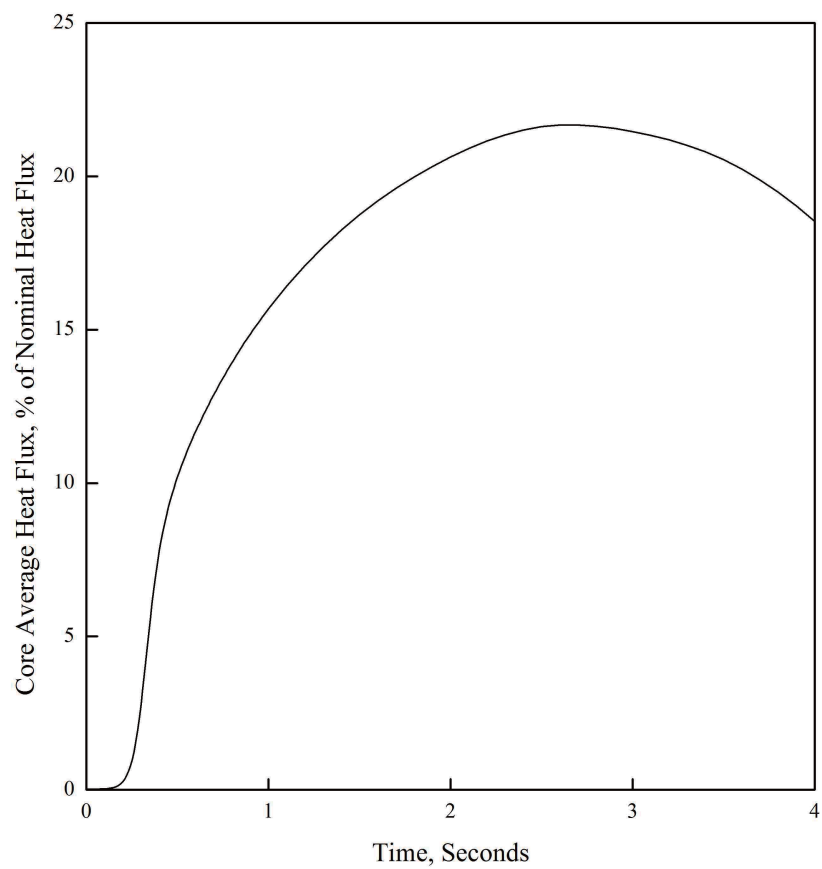


Figure 15.4.8-8 CEA Ejection: Hot Channel Power vs. Time (HCP)

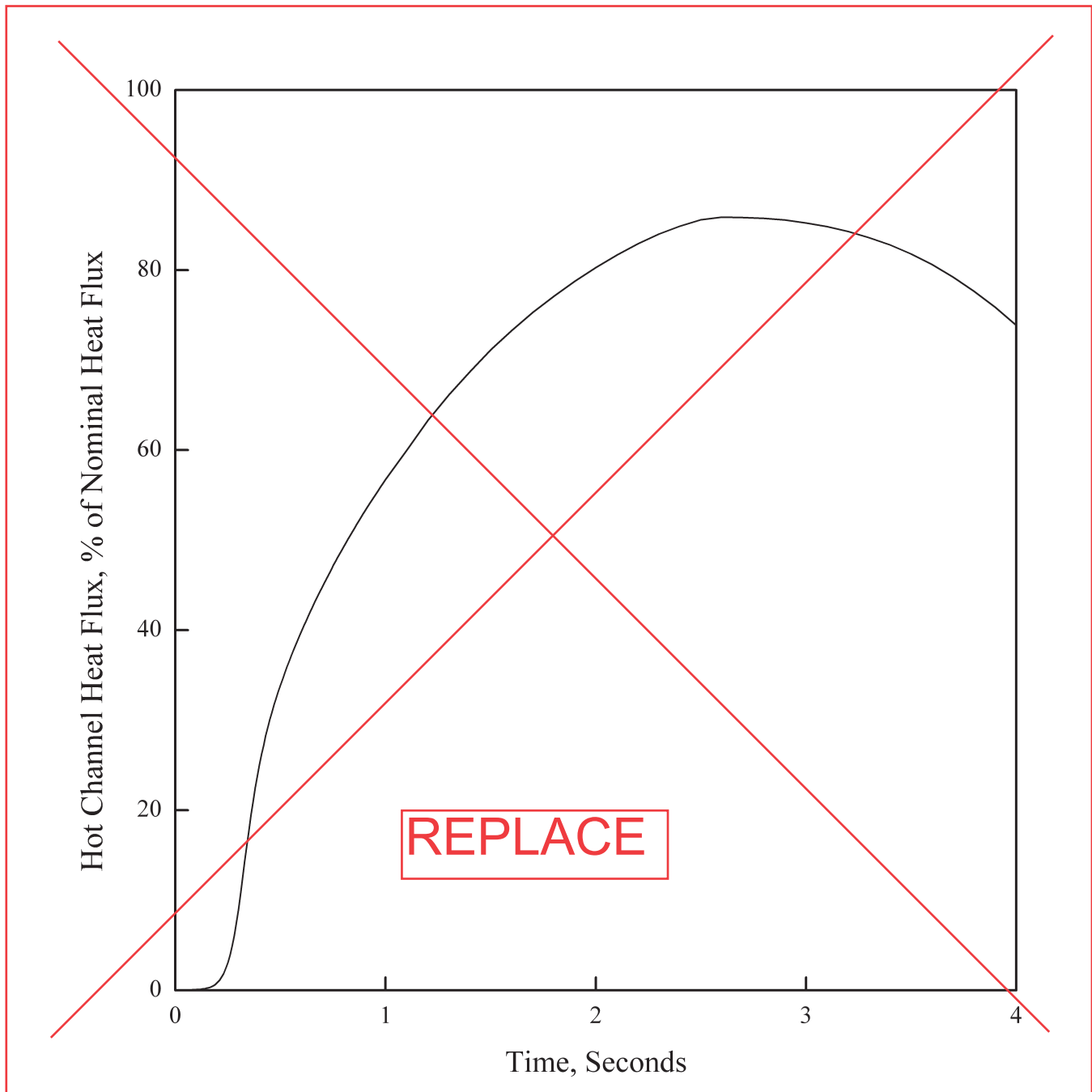


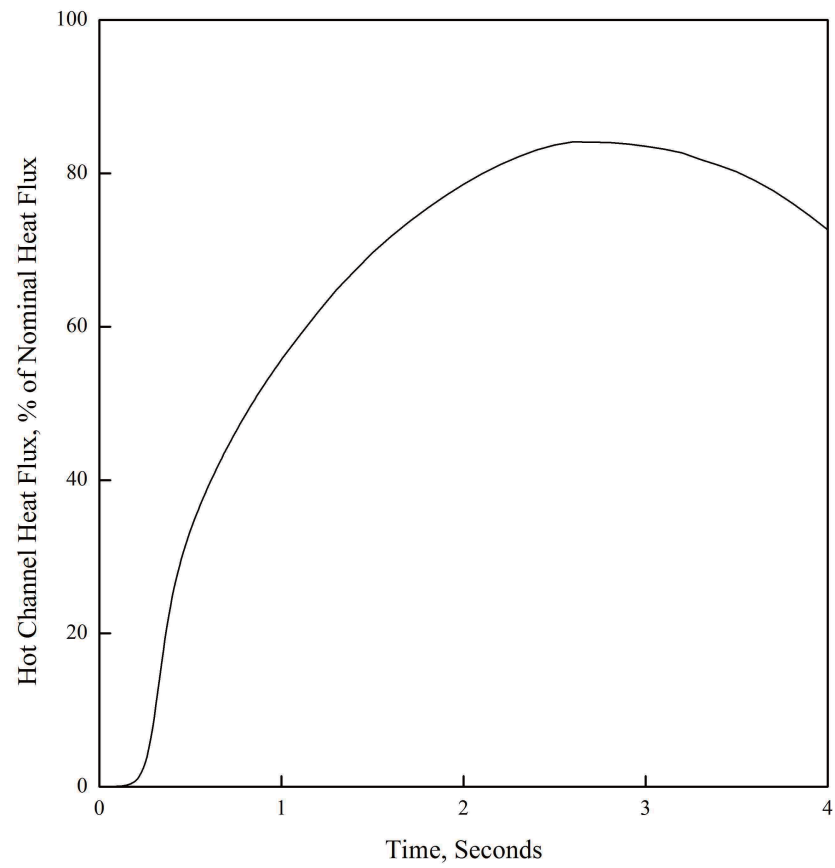
APR1400 DCD TIER 2

**Figure 15.4.8-9 CEA Ejection: Core Average Heat Flux vs. Time (HZP)**



APR1400 DCD TIER 2

**Figure 15.4.8-10 CEA Ejection: Hot Channel Heat Flux vs. Time (HWP)**



APR1400 DCD TIER 2

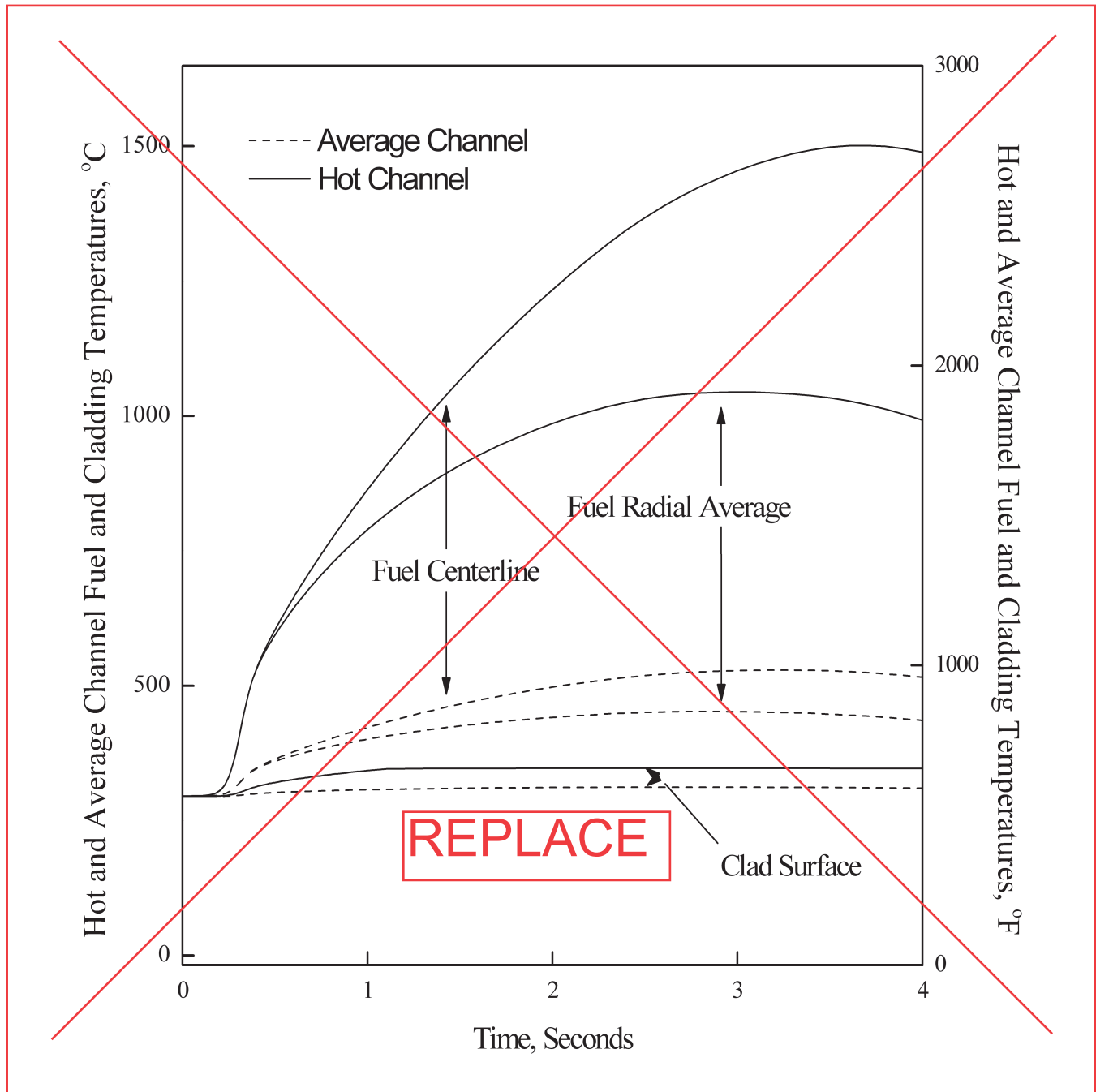
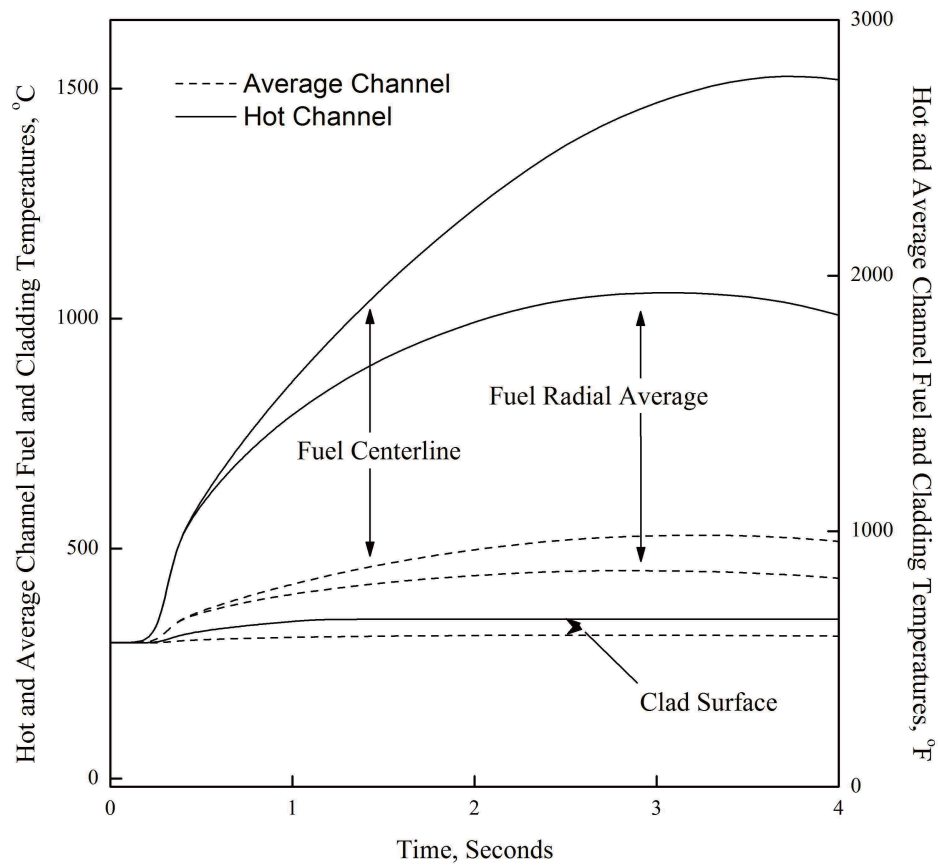


Figure 15.4.8-11 CEA Ejection: Hot and Average Channel Fuel and Cladding Temperatures vs. Time (HZIP)



APR1400 DCD TIER 2

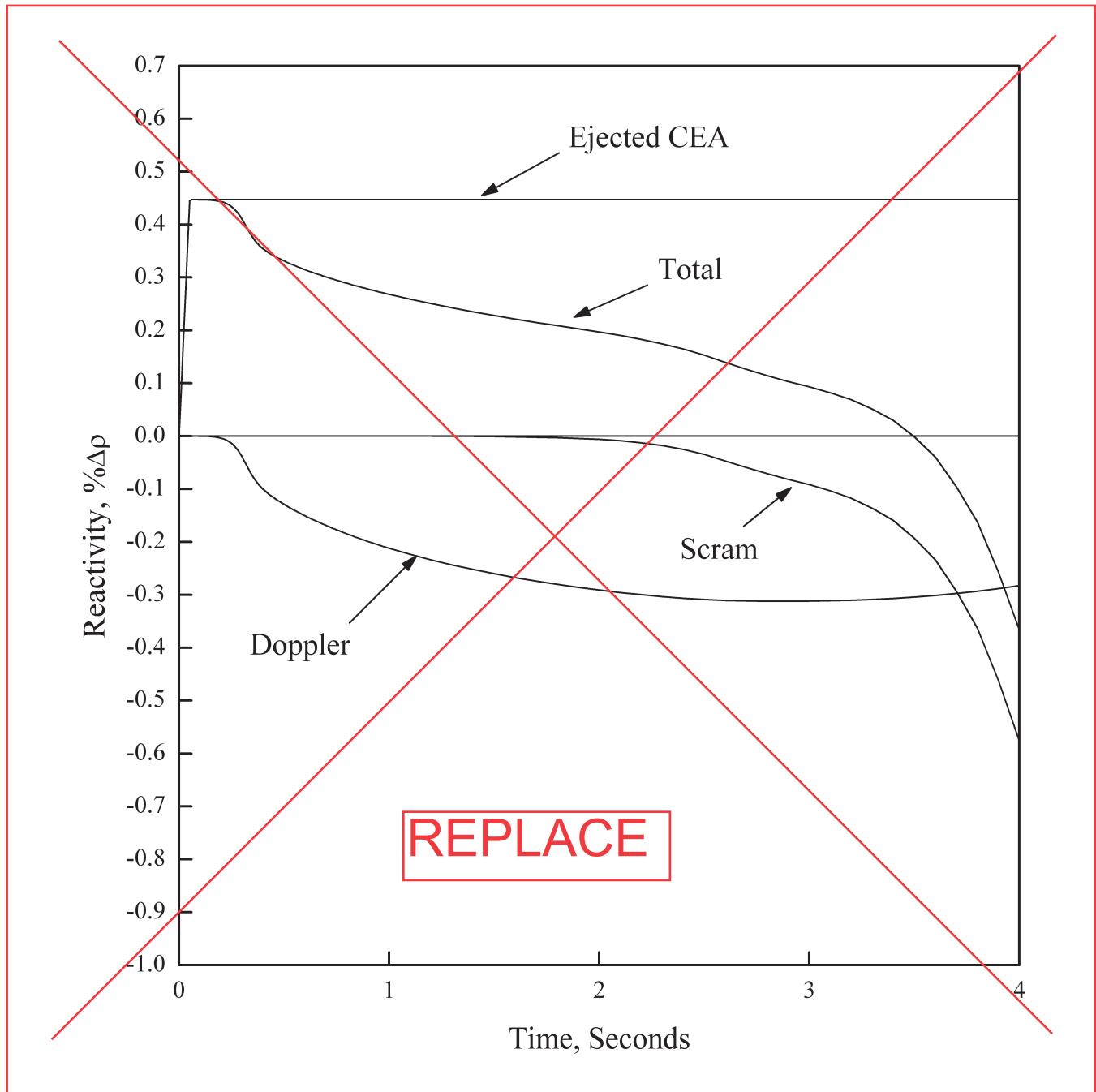
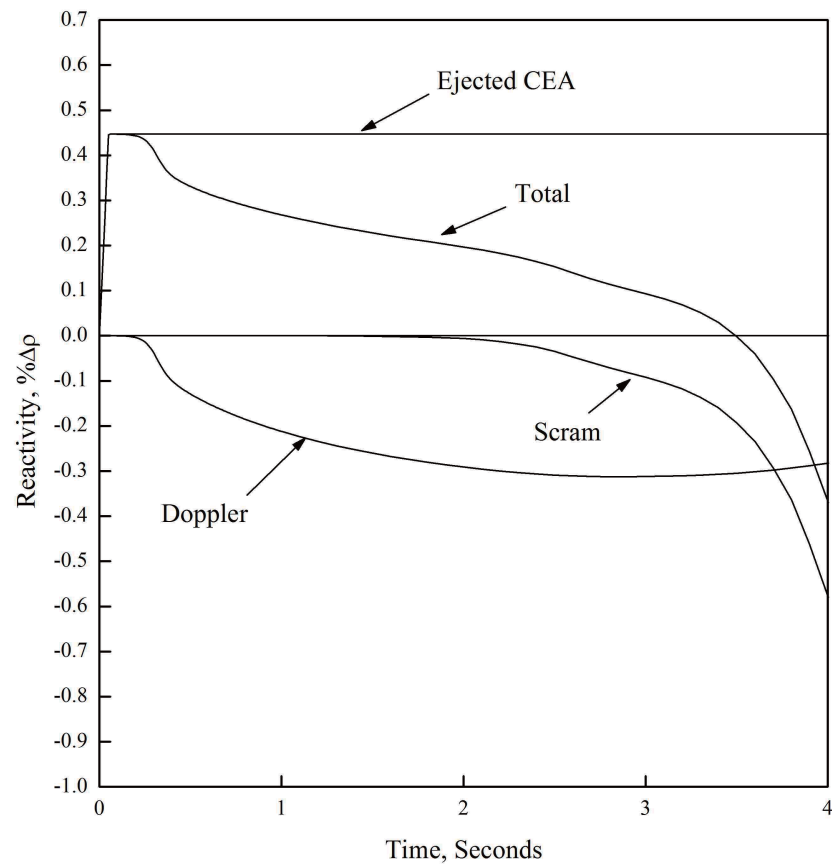


Figure 15.4.8-12 CEA Ejection: Reactivity vs. Time (HZP)



| | | |
|---------------------------|---|--------------------|
| Table 15.6.3-3 | Sequence of Events for a Steam Generator Tube Rupture with a Loss of Offsite Power | 15.6-58 |
| Table 15.6.3-4 | Assumptions and Initial Conditions for the Steam Generator Tube Rupture with a Loss of Offsite Power | 15.6-59 |
| Table 15.6.3-5 | Parameters Used in Evaluating the Radiological Consequences of the Steam Generator Tube Rupture with a Loss of Offsite Power..... | 15.6-60 |
| Table 15.6.3-6 | Radiological Consequences of the Steam Generator Tube Rupture with a Loss of Offsite Power..... | 15.6-63 |
| Table 15.6.5-1 | Uncertainty Parameter Ranges and Distributions | 15.6-64 |
| Table 15.6.5-2 | General System Parameters and Initial Conditions for Large Break ECCS Performance | 15.6-65 |
| Table 15.6.5-3 | Summary of Fuel Rod Performance for Break Spectrum of Large Break LOCA..... | 15.6-67 |
| Table 15.6.5-4 | Sequence of Events for Representative Large Break LOCA..... | 15.6-68 |
| Table 15.6.5-5 | Summary of SRS and Bias Evaluation Results..... | 15.6-69 |
| Table 15.6.5-6 | Safety Injection Pumps Minimum Delivered Flow to RCS (Assuming Two SI Pump Trains Failed) | 15.6-70 |
| Table 15.6.5-7 | General System Parameters and Initial Conditions; Small Break ECCS Performance Analysis..... | 15.6-71 |
| Table 15.6.5-8 | Small Break Spectrum | 15.6-72 |
| Table 15.6.5-9 | Variables Plotted as a Function of Time for Each Small Break in the Spectrum..... | 15.6-73 |
| Table 15.6.5-10 | Peak Cladding Temperature and Oxidation Percentage for the Small Break Spectrum | 15.6-74 |
| Table 15.6.5-11 | Times of Interest for the Small Break Spectrum (Seconds after Break) | 15.6-75 |
| Table 15.6.5-12 | General System Parameters and Initial Conditions Long-Term Cooling SIS Performance..... | 15.6-76 |
| Table 15.6.5-13 | Major Input Parameters Used in Radiological Consequences Analysis for Large Break LOCA | 15.6-77 |
| Table 15.6.5-14 | Radiological Consequences of a Large Break LOCA | 15.6-81 |

~ delete



insert~ TCD thermal con~ uctivity ~ egra~ ation

| | |
|-------|--------------------------------------|
| TBV | turbine bypass valve |
| TEDE | total effective dose equivalent |
| TSC | technical support center |
| TS | technical specification |
| UGS | upper guide structure |
| USEPA | U.S. Environmental Protection Agency |
| USI | Unresolved Safety Issue |
| VOPT | variable overpower trip |

APR1400 DCD TIER 2

53. NUREG-1465, "Accident Source Terms for Light Water Nuclear Power Plants," U.S. Nuclear Regulatory Commission, February 1995.
54. Regulatory Guide 1.183, "Alternative Radiological Source Terms for Evaluating Design Basis Accidents at Nuclear Power Reactors," U.S. Nuclear Regulatory Commission, July 2000.
55. USEPA, Federal Guidance Report No. 11, EPA 520/1-88-020, "Limiting Values of Radionuclide Intake and Air Concentration and Dose Conversion Factors for Inhalation, Submersion, and Ingestion," September 1993.
56. USEPA, Federal Guidance Report No. 12, EPA 402-R-93-081, "External Exposure to Radionuclides in Air, Water, and Soil," September 1993.
57. 10 CFR 50.34, "Contents of Applications; Technical Information," U.S. Nuclear Regulatory Commission, January 10, 1997.
58. 10 CFR Part 50, Appendix A, "General Design Criteria for Nuclear Power Plants," U.S. Nuclear Regulatory Commission, January 24, 2000.
59. NUREG/CR-6604, "RADTRAD: A Simplified Model for RADionuclide Transport and Removal and Dose Estimation," SNL, December 1997.
60. NUREG-0800, Standard Review Plan, BTP 11-5, "Postulated Radioactive Release Due to Waste Gas System Leak or Failure," Rev.3, U.S. Nuclear Regulatory Commission, March 2007.
61. NUREG-0800, Standard Review Plan, BTP 11-6, "Postulated Radioactive Release Due to Liquid-Containing Tank Failure," Rev.3, U.S. Nuclear Regulatory Commission, March 2007.
62. 10CFR50.46, "Acceptance Criteria for Emergency Core Cooling Systems for Light Water-Cooled Nuclear Power Reactors," U.S. Nuclear Regulatory Commission.
63. APR1400-F-A-TR-12004-P (Proprietary), "Realistic Evaluation Methodology for Large-Break LOCA," KHNP, December 2012 ~uly 2017 Decem~er 2012
64. Regulatory Guide 1.157, "Best-estimate Calculations of Emergency Core Cooling System Performance," U.S. Nuclear Regulatory Commission, May 1989.

APR1400 DCD TIER 2

~ elete

~~78. APR1400-F-A-NR-14002-P, "The Effect of Thermal Conductivity Degradation on APR1400 Design and Safety Analyses," Rev. 0, KHNP, September 2014.~~

7~

~~79.~~ NUREG-1462, "Final Safety Evaluation Report Related to the Certification of the System 80+ Design Docket No. 52-002," Rev. 0, U.S. Nuclear Regulatory Commission, 1994.

79

~~80.~~ APR1400-Z-A-NR-14014-P, "ATWS Evaluation," Rev. 0, KHNP, November 2014.

0

~~81.~~ APR1400-F-M-TR-13001-P (Proprietary), "PLUS7 Fuel Design for the APR1400," Rev. 0, KHNP, August 2013.

REPLACE ~ ith Ne~t Page

APR1400 DCD TIER 2

~Intentionally ~lan~~

78. ~~APR1400 F A NR-14002 P, “The Effect of Thermal Conductivity Degradation on APR1400 Design and Safety Analyses,” Rev. 0, KHNP, September 2014.~~
79. NUREG-1462, “Final Safety Evaluation Report Related to the Certification of the System 80+ Design Docket No. 52-002,” Rev. 0, U.S. Nuclear Regulatory Commission, 1994.
80. APR1400-Z-A-NR-14014-P, “ATWS Evaluation,” Rev. 0, KHNP, November 2014.
81. APR1400-F-M-TR-13001-P (Proprietary), “PLUS7 Fuel Design for the APR1400,”
~~Rev. 0, KHNP, August 2013.~~


Rev. 1~~~ NP~ August 2017.

APR1400 DCD TIER 2

allowable dose criteria limits, which are 100 percent and 10 percent of the 10 CFR 50.34(a)(1) value, respectively. The MCR and TSC doses are also within the dose limit in GDC 19.

15.6.3.2.6 Conclusions

The radiological consequences for the SGTR accident with a LOOP are within the allowable criteria. The RCS and secondary system pressures are below the 110 percent of the design pressure limits, thus providing reasonable assurance of the integrity of these systems. The minimum DNBR is above the DNBR SAFDL value of 1.29. The acceptance criterion regarding fuel performance is met.

For the limiting SGTR event with respect to SG overfill considerations (SGTR with a LOOP), the maximum liquid inventories do not result in an overfill and consequent introduction of liquid water into the steam lines, providing reasonable assurance of the integrity of these steam lines.

After 30 minutes, the operator uses the plant emergency procedure for the SGTR to cool down the plant to shutdown cooling entry conditions.

15.6.4 Radiological Consequences of Main Steam Line Failure Outside Containment (Boiling Water Reactor)

Not applicable to the APR1400.

15.6.5 Loss-of-Coolant Accidents Resulting from the Spectrum of Postulated Piping Breaks within the Reactor Coolant Pressure Boundary

15.6.5.1 Identification of Causes and Frequency Classification

Loss-of-coolant accidents (LOCAs) are hypothetical accidents that result from the loss of reactor coolant at a rate that exceeds the capability of the reactor coolant makeup system. The cause is breaks in the pipes in the reactor coolant pressure boundary up to and including a break equivalent in size to the double-ended rupture of the largest pipe in the RCS.

In the accident analyses for the APR1400, large break and small break LOCAs are both classified as postulated accidents (PAs). They are not expected to occur during the life of the plant but are postulated as a conservative design basis.

APR1400 DCD TIER 2

15.6.5.2 Sequence of Events and Systems Operation

~~delete~~ → ~~insert: and burnup to consider thermal conductivity degradation (TCD) effects~~ → ~~insert: (LBLOCA)~~

15.6.5.2.1 Description of Large Break Loss-of-Coolant Accident

~~delete~~ → ~~insert: with various burnup cases~~ → ~~insert: s~~ → ~~insert: and burnup~~

A cold leg break between the outlet of the reactor coolant pump (RCP) and the corresponding reactor vessel (RV) inlet nozzle is found to be the most limiting with respect to the peak cladding temperature (PCT) in a large break LOCA. The ~~large break LOCA~~ analysis assumes a Loss Of Offsite Power (LOOP). The RCPs lose power and coast down after the LOOP. In order to determine the limiting break size, a guillotine break spectrum of ~~a~~ 100, 80, and 60 percent break area is studied. The blowdown PCT is a maximum when the break area is 100 percent of the cold leg cross-sectional area. The reflood PCT is a maximum when the break area is 80 percent. However, because the reflood PCT is not as high as the blowdown PCT, the 100 percent break size is chosen as the limiting guillotine break case.

In the 100 percent guillotine break, the total break area is two times the cold leg cross-sectional area. A 200 percent slot break shows lower PCT in the blowdown phase and the transient is found to be faster ~~by about 4 seconds~~ than that of the 100 percent guillotine break. The PCT of the reflood phase is lower than that of the guillotine break, and the fuel quenching is ~~somewhat~~ earlier. ~~The~~ 100 percent double-ended guillotine break in a cold leg is determined to be the limiting case. ~~Therefore, the~~

~~delete~~ → ~~insert: with the burnup of 27,000 MWd/MTU~~ → ~~insert: behaviors~~

The scenario is divided into four phases that characterize the events during the transient. The phases are blowdown, refill, early reflood, and late reflood and are defined by the inventory of the reactor pressure vessel and the flow condition of safety injection tank with fluidic device (SIT-FD).

A blowdown is defined as the phase from the opening time of the break to the start time of the SIT-FD injection. The refill phase is defined as the phase from the start time of the SIT-FD injection to the time when the mixture level in the reactor vessel lower plenum reaches the bottom of the active core. The definitions of these two phases are the same as those of the conventional ~~large break LOCA~~ scenario in PWRs.

Unlike the conventional scenario, the reflood phase is divided into early reflood and late reflood phases based on the time in which the SIT-FD becomes empty. The division is intended to address any possibility of core heatup during the late reflood phase in detail because the APR1400 does not have a low-pressure safety injection pump.

APR1400 DCD TIER 2

delete one space

Blowdown Phase

The blowdown phase starts when the break opens and ends when an SIT-FD injection is initiated; blowdown lasts for approximately 15 seconds. During blowdown, the primary coolant is rapidly expelled into the containment through the break. The reactor coolant changes from a subcooled liquid to a two-phase mixture or pure steam due to fluid flashing. By roughly 6 seconds, the core region begins to dry out.

The initial break flow is very high, reflecting the subcooled critical flow at the break. Mass flow from the reactor vessel side of the break is larger than that from the pump side due to the higher hydraulic resistances of the pump and the Steam Generator(SG). As the break flow develops in the reverse direction from the core to the break as well as in the positive direction, the core flow rapidly stagnates and then reverses shortly after the break occurs.

As the primary system depressurizes, flashing occurs first in the hot regions of the system, such as the upper plenum, hot leg, pressurizer, and core, and then proceeds to the relatively cold regions, such as the lower plenum, downcomer, and cold legs. Extensive voiding occurs in all areas of the reactor pressure vessel. Nucleate boiling develops in the core. Fission power that is calculated by a kinetics model drops to the level of decay heat due to the voiding in the core. The flashing also reduces the primary system depressurization rate.

When the critical heat flux (CHF) condition is reached in the core, heat transfer changes from nucleate boiling to post-CHF heat transfer regimes (i.e., transition boiling, film boiling, and forced convection to vapor), and much of the core dries out. Fuel rod cladding temperatures increase rapidly due to the degrading rod-to-fluid heat transfer. The cladding temperature increase during the early blowdown phase is terminated by several processes:

- a. First, as the core rapidly voids, the core power immediately decreases via void reactivity insertion.
- b. Second, the flow at the core reverses after stagnation.
- c. Third, the large coolant inventory of the upper guide structures (UGSs) and upper head moves toward the top of the core by two paths, through the UGS drainage

APR1400 DCD TIER 2

~ elete

holes in the UGS bottom plate between the UGS and upper plenum and through the guide tube pipes that terminate in the upper inactive core.

~ elete

~~As the low pressurizer pressure setpoint is reached, the reactor is tripped.~~ Reactor coolant pumps (RCPs) are modeled to trip and coast down from the beginning of the accident assuming a LOOP. As the primary system pressure continues to decrease, flashing develops in the cold regions of the system. The resultant voiding occurring in the RCP degrades its pumping performance. The break flow rate decreases rapidly as the flow regime changes from subcooled to saturated critical flow at the break.

~~Four SIT-FDs begin to deliver flow into the four direct vessel injection (DVI) lines when the primary system pressure falls below its actuation setpoint. The coolant flows through the DVI nozzles into the upper annulus and then begins to refill the reactor pressure vessel. Because the reactor coolant system is still depressurizing, some of the coolant entering the upper annulus is swept out to the break along with entrained liquid from the lower plenum and the downcomer. Although the break flow remains high, the coolant is delivered downward into the downcomer and increases the downcomer water level. Then the coolant injected by the SIT-FD eventually reaches the lower plenum.~~

Refill Phase

The refill phase begins when the SIT-FD injection flow is initiated and ends when the ~~water~~ level in the lower plenum reaches ~~the core inlet~~

mi~ ture

~ ottom of the active core

~~Emergency core cooling (ECC) water in the reactor vessel downcomer can flow down by~~ swept out to the break by the pressure differential and upward-escaping steam flow that levitates the liquid. Reactor vessel walls and internals are considered as the large metal structures at temperatures above saturation. When subcooled ECC water comes into contact with the metal structures in the downcomer, steam is generated by nucleate boiling, reducing the gravitational head of the fluid in the downcomer. The process of liquid penetration and sweep-out repeats in the downcomer and direct-contact condensation of steam on the subcooled ECC water continues in the upper annulus.

The depressurization of the system wanes as the differential pressure between the RCS and the containment reduces. Owing to the gradual reduction of flashing and break flow, the rate of liquid penetration into the lower plenum increases. With a decreasing steam flow rate, a small amount of the ECC injection is bypassed, and most of it flows downward to

insert A from ne~ t page

A

Direct vessel injection (DVI)



Four SIT-FDs begin to deliver flow into the four **DVI** lines when the primary system pressure falls below their actuation set-point. The coolant flows through the DVI nozzles into the upper annulus and then begins to refill the reactor pressure vessel. The reactor coolant system keeps depressurizing because some of the coolant entering the upper annulus is swept out to the steam generator along with entrained air from the lower plenum and the steam generator. Although the steam flow remains high, sufficient flow in the excess of the bypass is delivered to the steam generator and increases the steam generator water level. Eventually the coolant injected by the SIT-FDs reaches the lower plenum.

APR1400 DCD TIER 2

fill the downcomer and the lower plenum. At this stage, ~~water~~ levels in the downcomer and the lower plenum increase rapidly.

Heatup, which is almost adiabatic, continues in the core during this phase because there is no inventory to cool the core.

The refill phase ends when the ~~liquid~~ level in the lower plenum reaches the bottom of the active core.

insert~ It remains full thereafter an~ con~ itions are esta~ lishe~ for continuous core refloo~ ing.

Early Reflood Phase

The early reflood phase begins when the lower plenum ~~is completely filled with water~~ and ends when the SIT-FD water is depleted. Near the beginning of the early reflood phase, the safety injection pumps (SIPs) begin to inject water. Initially, the core reflood is quite rapid because of the following:

- a. The downcomer remains filled with water by the ECC injection.

The hy~ raulic resistance in the loop is lo~ ~ since there is small loop steam flo~ .

- b. The high flow injection of SIT-FD continues.

- c. There is little loop steam flow and hydraulic resistance in the loop is therefore low.

- d. There is no severe steam binding.

insert~ control port of

The maximum SIT-FD injection flow is reached during this phase. High flow injection through the standpipe becomes unavailable, and only the flow through the fluidic-device becomes injected. During the high-flow injection, the downcomer and core liquid levels increase rapidly. As the downcomer liquid level approaches the level of the cold legs, much of the coolant spills out of the break, and the vessel side break flow tends to increase. When the water level in the SIT-FD decreases to below the top of the standpipe, the low-flow injection begins. Water levels in the downcomer and core decrease slightly, but the levels increase again within approximately 10 seconds, maintaining downcomer water level ~~above~~ the level of the cold legs. The combined SIP and SIT-FD flows are injected to maintain the water level in the downcomer and to retard core heatup.

In the core, heat transfer regimes encompass the entire spectrum. The regimes include single-phase liquid convection, nucleate boiling, transition boiling, film boiling, and single-phase vapor convection.

APR1400 DCD TIER 2

Local quenching could occur due to droplet de-entrainment at the fuel alignment plate and spacer grids. Vapor velocities and liquid entrainment in the central region of the core are higher due to the higher power of this region. The entrained liquid could have a cooling effect on the upper region of the core. Some of the entrained liquid is de-entrained at the fuel alignment plate, and the remainder is carried into the upper plenum, forming a two-phase pool. Liquid from the pool can re-enter the low-powered regions of the core through the fuel alignment plate due to the lower vapor velocities in those regions. A three-dimensional flow pattern can therefore occur: water flows from low-powered to high-powered regions in the core, while the flow is in the opposite direction in the upper plenum. Liquid from the upper plenum pool may be further entrained and carried over into the hot legs and SGs.

~ elete

As reflooding progresses upward from the lower core region, more liquid is entrained to the upper plenum, and the level of the two-phase mixture in the pool can reach the hot leg. When the entrained liquid reaches the U-tubes of the SGs, it is vaporized by reverse heat transfer from the secondary side to the primary side. Due to the vaporization in the U-tubes, hot side pressure increases and causes steam binding, which deteriorates the reflooding of the core. Because the steam generation rate in the core decreases due to the lower reflood rate, liquid entrainment and the steam binding effect decrease, causing the reflood rate to increase again. Through this cyclical process, the entire core eventually becomes reflooded. The increase of core pressure due to the steam binding causes manometric oscillations between levels in the downcomer and the core.

The early reflood phase ends when SIT-FDs are emptied.

Late Reflood Phase

The late reflood phase begins when the SIT-FDs are emptied. ECC water is supplied only by the Safety Injection Pumps(SIPs) during this phase.

~ uring this phase

Water level in the downcomer decreases somewhat as the SIT flow stops at the beginning of the late reflood phase and falls below the level of the cold legs. Then the core water level becomes stabilized. Liquid levels in the downcomer and core become balanced ~~within approximately 20 seconds.~~ Due to the decreased flow of coolant into the downcomer, liquid temperature in the downcomer can increase to a near saturation temperature under the influence of the residual heat of the metal structures (i.e., vessel walls in the downcomer). Boiling can occur on the surface of the walls depending on the

APR1400 DCD TIER 2

conditions. ECC water is provided by the four SIPs, the possibility of downcomer boiling is suppressed, and the core is found to remain amenable to cooling.

Because the entire core remains in a quenched state during this phase, steam generation in the core is not significant enough to cause any severe ECC water bypass during this phase.

Only safety-related systems or components are credited to mitigate the accident, as follows:

- a. Normally operating plant instrumentation and controls

Steady-state conditions of a large break LOCA analysis are calculated at the normal operating plant conditions (e.g., power, flow rate, pressure, temperature).

- b. Reactor protection system (RPS)

The reactor trip signal is generated from the low pressurizer pressure during the large break LOCA. The trip signal also generates the turbine trip and RCP trip automatically. Coastdown of the RCP progresses after the RCP trip. However, because the CEA insertion is not used for large break LOCA analysis, the negative reactivity of CEA is not credited. For the small break LOCA analysis, the CEA insertion is credited including the signal delay.

- c. Engineered safety feature actuation system (ESFAS)

An ESFAS is generated from the low pressurizer pressure or high-containment pressure during the large break LOCA. Low pressurizer pressure is credited only in the LOCA analysis and actuates the containment isolation actuation signal (CIAS) and safety injection actuation signal (SIAS).

- d. Safety injection system (SIS)

During the LOCA, the SIS provides the direct vessel injection. The discharge of each SIP and SIT is piped directly to a reactor vessel nozzle where the flow is directed into the reactor vessel downcomer region. Storage of fluid for the SIS is accomplished by the IRWST, which contains borated fluid.

- e. Containment spray system (CSS)

Reactor coolant pumps (RCPs) are monitored to trip and coast down from the beginning of the accident assuming L~ ~ P.

APR1400 DCD TIER 2

LBLOCA

The CSS is designed to reduce containment pressure and temperature from a main steam line break or LOCA and to remove fission products from the containment atmosphere following a LOCA. The CSS uses the IRWST and has two independent trains. During the large break LOCA, CSS is automatically actuated on a high-high containment pressure signal. Maximum containment spray capacity is assumed to calculate the minimum containment pressure, which is described in Subsection 6.2.1.5.

15.6.5.2.2 Description of Small Break Loss-of-Coolant Accident

Small Break LOCA shows the significantly different behaviors depending on the break size and location. For a smaller break size, a SIP can maintain the RCS coolant inventory, since the reactor operator utilizes the Steam Generator (SG) to depressurize and cool down the system. For a larger break size, the blowdown break flow cannot be compensated by the SIP.

Small Break LOCA behavior can be changed with break location. The scenario of DVI line break, which is known to be the most limiting case of Small Break LOCA, can be generally subdivided into five phases: blowdown, natural circulation, loop seal clearing, core boil-off, and core recovery. The duration and occurrence of each phase are varied with break size and system characteristics.

Blowdown Phase

The break drastically depressurizes the RCS. When the RCS pressure reaches a reactor trip set-point on low pressurizer pressure, the reactor is tripped by the insertion of control rods. Once the RCS is depressurized to the low-low pressurizer pressure, safety injection signal is actuated. And safety injection water is delivered into the RCS after a delay until the injection pump is started. During the blowdown phase, the RCS is mostly filled with fluid in liquid phase and subcooled or saturated coolant is discharged into the containment building through the break. When the RCS is further depressurized to reach a quasi-equilibrium state with the secondary side of SG, the blow-down phase is finished.

~ lo ~ o ~ n

Natural Circulation phase

L ~ P The thermal quasi-equilibrium state can last for hundreds of seconds depending on the break size. Since the Reactor Coolant Pump (RCP) is shut down due to the assumption of Loss-Of-Offsite Power (LOOP), there is no forced circulation flow during this phase. The heat transfer from the primary to the secondary side is carried out by either single or two-

APR1400 DCD TIER 2

phase natural circulation. The coolant is gradually drained from the upper side of reactor coolant system. The phase separation proceeds from the upper side of U-tube in SG to the reactor core upper head and then to the reactor upper plenum. The reactor core decay heat is removed via the break and SGs. The loop seal is filled with the coolant not to form the effective flow path for steam so that the steam generated in the reactor core cannot be effectively discharged.

U-tu~es

~elete

Loop Seal Clearing phase

This phase covers from the termination of natural circulation flow until the loop seal clearing. When the coolant level in the SG side of loop seal becomes lower than the top of horizontal portion of pump suction leg, the loop seal is cleared and the steam isolated in the system is discharged through the break. Before the loop seal is cleared, the two-phase mixture level in the core can be significantly decreased to cause the reactor core uncover within short period of time. After the loops seal clearing, the pressure imbalance in the RCS disappears. The core level recovers up to the cold leg elevation.

Core Boil-Off phase

After the loop seal is cleared, the coolant in the reactor core starts to boil due to the decay heat so that the core mixture level decreases gradually. Consequently, the core uncover could happen again. At this time the cladding temperature can reach its peak value. When the safety injection flow becomes larger than the break flow as RCS pressure decreases, the core mixture level starts to recover.

Core Recovery phase

Core recovery continues from the moment when the core is at its lowest level until it is filled with SI flow. The core can be sufficiently cooled for the prolonged time in this phase by the recovered water level.

15.6.5.2.3 Description of Post Loss-of-Coolant Accident Long-Term Cooling

Immediately following a LOCA, safety injection is initiated to mitigate the short-term consequences of the event by replenishing the lost coolant. Safety injection is characterized by the automatic actuation of SIPs and the passive operation of SITs. Responses by operators are not required in the short term after a LOCA.

APR1400 DCD TIER 2

The post-LOCA long-term phase is defined as beginning when the core is reflooded and ending when the plant is secured. During the long term, operator action is needed to provide reasonable assurance that the core cooling is maintained until the plant is brought to a cold shutdown condition.

The basic function of long-term cooling (LTC) is to maintain the core at safe temperature levels while avoiding the precipitation of boric acid in the RCS. The capability of performing this basic function is reasonably assured until such time that the fuel assemblies are removed from the reactor vessel.

The analysis procedures account for single-failures to provide reasonable assurance that the performance objectives are met even with this assumption. There is a behavioral difference between large and small break LOCAs in the long term. This difference is that the RCS will remain at high pressure for small breaks and the safety injection flow rate will be too low for effective cooling; thus, small breaks require cooling of the RCS by the SGs until shutdown cooling (SDC) can be initiated. Large breaks, on the other hand, are adequately cooled by the safety injection flow because this flow is large due to the low RCS pressure; however, large breaks use simultaneous hot leg and direct vessel injection to flush boric acid from the vessel. As a consequence, the LTC large break and small break analyses are different.

15.6.5.3 Core and System Performance

15.6.5.3.1 Evaluation Model

The acceptance criteria for the emergency core cooling system (ECCS) for light water-cooled reactors are provided in 10 CFR 50.46 (Reference 62). The analyses presented in this section demonstrate that the APR1400 design satisfies these criteria.

Analyses are performed for a complete spectrum of break sizes. The most limiting break, which limits the peak linear heat generation rate (PLHGR), is identified as the 1.0 (break area) × double-ended guillotine at the pump discharge (DEG/PD) break. The results of the analyses demonstrate that for a PLHGR of 446.2 W/cm (13.6 kW/ft), the APR1400 SIS design meets the acceptance criteria of Reference 62. Requirements are as follows:

- a. Criterion 1 – Peak Cladding Temperature

APR1400 DCD TIER 2

The calculated maximum fuel element cladding temperature shall not exceed 1,204 °C (2,200 °F).

b. Criterion 2 – Maximum Cladding Oxidation

The calculated total oxidation of the cladding anywhere shall not exceed 0.17 times (17 percent) of the total cladding thickness before oxidation.

c. Criterion 3 – Maximum Hydrogen Generation

The calculated total amount of hydrogen generated from the chemical reaction of the cladding with water or steam shall not exceed 0.01 times (1 percent) the hypothetical amount that would be generated if all of the metal in the cladding cylinders surrounding the fuel, excluding the cladding surrounding the plenum volume, were to react.

d. Criterion 4 – Coolable Geometry

Calculated changes in core geometry shall be such that the core remains amenable to cooling.

e. Criterion 5 – Long-Term Cooling

After any calculated successful initial operation of the ECCS, the calculated core temperature shall be maintained at an acceptably low value, and decay heat shall be removed for the extended period of time required by the long-lived radioactivity remaining in the core.

L~ L~ CA

Large Break Loss-of-Coolant Accident Evaluation Model

The ~~large break LOCA~~ analysis is performed using the CAREM (Reference 63) realistic evaluation methodology for the criteria of 10 CFR 50.46 (Reference 62). This methodology is based on the models and assumptions described in NRC RG 1.157 (Reference 64).

~~insert~ RELAP5/~ ~ D3.3/~ Co~ e~ a mo~ ifie~ version of RELAP5/~ ~ D3.3~~

In CAREM, the ~~RELAP5/MOD3.3 Code~~ (Reference 65) is used for the calculation of ECCS thermal-hydraulics behavior and cladding temperature. Containment back pressure and temperature calculations are performed by the CONTEMPT4/MOD5 Code (Reference 66). Containment back pressure is affected by the mass and energy release

~~insert~ RELAP5/~ ~ D3.3/~ Co~ e~ a mo~ ifie~ version of RELAP5/~ ~ D3.3
Co~ e (References ~ 3 an~ ~ 5)~~

Delete

APR1400 DCD TIER 2

rate, and thermal-hydraulics phenomena is dependent on the containment back pressure. RELAP5/MOD3.3 and CONTEMPT4/MOD5 are merged to exchange their results in every time step.

insert ~ / ~

CAREM quantifies the overall calculation uncertainty by propagating the uncertainty of each parameter. The ranges of uncertainty parameters are determined by auxiliary calculations and literature survey and confirmed by checking experimental data. To quantify the PCT at a 95 percent probability with a 95 percent confidence level, 124 times random sampling calculations are performed adopting non-parametric statistics. This methodology extrapolates the code accuracy to quantify the uncertainty that is applied to plant calculations.

1 ~ 1

A total of 124 input vectors are generated by random sampling, and simple random sampling (SRS) analyses are performed with the application of each input vector. The code uncertainty parameters and their ranges are determined by the evaluation of the code accuracy and confirmation of data covering processes. PCT is determined by applying Wilks' Formula to the SRS results in a 95 percent tolerance limit at a 95 percent confidence level.

1 ~ 1

Cases in which the reflood peak clad temperature differences within 100K compared with the highest reflood peak are selected for scale bias calculations, extracting the highest two cases from 124 cases of SRS. Code biases in the prediction of ECC water bypass and steam binding are evaluated separately. Steam binding bias is evaluated by combining the results of two bias evaluations of droplet de-entrainment in the upper plenum of the reactor vessel and droplet evaporation in the steam generator U-tube. The final values of the third PCT considering the uncertainties of the automatic time step control function and data reading frequency of RELAP5/MOD3.3/K are suggested for the comparison of LOCA criteria.

1 ~ 1

Small Break Loss-of-Coolant Accident Evaluation Model

The calculations presented in this section are performed using the small break evaluation model, which is described in Reference 67 and approved by the Nuclear Regulatory Commission (NRC) in Reference 68. The CEFLASH-4AS (Reference 69) computer program is used to determine the primary system hydraulic parameters during the blowdown phase, and the COMPERC-II (Reference 70) computer program is used to determine the system behavior during the reflood phase. Fuel rod temperatures and clad

APR1400 DCD TIER 2

oxidation percentages are calculated using the STRIKIN-II (Reference 71) and PARCH (Reference 72) computer programs. The interface between these programs is described in detail in Reference 67.

The small break evaluation model already met the requirements of TMI action item II.K.3.30 and II.K.3.31. Details are respectively described in Reference 23 and Section 15.6.5.3.

Post Loss-of-Coolant Accident Long-Term Cooling Evaluation Model

Long-term cooling (LTC) initiates when the core is quenched after a LOCA and terminates when the plant is secured. The objectives of LTC are to maintain the core at safe temperature levels and to avoid the precipitation of boric acid in the core region. To accomplish these objectives, an LTC analysis was performed using the codes and methods documented in Reference 73.

The LTC plan uses one of two procedures depending on the break area. The shutdown cooling system (SCS) is used if the break is sufficiently small that reasonable assurance of a successful operation of the SCS is provided. For large break LOCAs, a simultaneous hot leg and direct vessel injection is used to maintain core cooling and boric acid flushing. The plant operator initiates the appropriate procedure based on the indicated RCS pressure.

LBLOCAs

Figure 15.6.5-34 shows the LTC sequence of events and the schedule for operator actions for the LTC plan. The operator's first action is to initiate cooldown within 1 hour post-LOCA by releasing steam from the SGs. The steam is released through the turbine bypass system if available or through the atmospheric dump valves. Between 1 and 3 hours post-LOCA, the operator isolates or vents the safety injection tanks (SITs) to avoid injecting a large quantity of nitrogen (noncondensable) gas into the RCS. Between 1 and 4 hours post-LOCA, pressurizer depressurization is initiated. Between 2 and 3 hours post-LOCA, the discharge lines of SIP 3 and 4 are realigned to the hot legs to divide the SIP flow between the hot leg and direct vessel injection connections.

If the RCS pressure is above 31.6 kg/cm²A (450 psia) between 8 to 9 hours post-LOCA, the RCS is filled, which provides reasonable assurance that proper suction is available for entering shutdown cooling. Cooling of the RCS continues until the indicated RCS temperature is lower than the maximum SDC entry temperature including instrument uncertainty. The operator then throttles the SIPs until the RCS pressure is reduced to

APR1400 DCD TIER 2

shutdown cooling entry pressure, including instrument uncertainty, and initiates shutdown cooling.

A prerequisite to throttling or terminating SI flow is that the RCS is in a subcooled condition for the indicated RCS pressure. While reducing RCS pressure to initiate SCS operation, the operator maintains subcooling of the RCS consistent with the emergency operating procedures.

If the SCS is inoperable, the alternative for decay heat removal is the continued use of the SGs. This requires the continued availability of auxiliary feedwater and the atmospheric dump valves or the turbine bypass system. If the SCS becomes operable later, it is put into operation. This path is indicated by the dashed lines in Figure 15.6.5-34.

If the indicated RCS pressure falls below 31.6 kg/cm²A (450 psia) at 8 to 9 hours, the break may be too large for absolute assurance that proper suction is available for the shutdown cooling mode. In this event, a simultaneous hot leg and direct vessel injection by itself cools the core and also flushes the reactor vessel indefinitely.

15.6.5.3.2 Input Parameters and Initial Conditions

Large Break Loss-of-Coolant Accident

The SIS consists of four safety injection pumps (SIPs) and four safety injection tanks (SITs). Automatic operation of the SIPs is actuated by a low pressurizer pressure signal or a high containment pressure signal. Flow is initiated from the SITs by the opening of a check valve when the reactor vessel downcomer pressure drops below the SIT pressure. A fixed internal device in the SIT regulates the flow rate with changing level and pressure. SI flow is delivered by DVI connections.

The most limiting single failure for a ~~large break LOCA~~ is the loss of one SIP train. However, two of the four SIPs are conservatively assumed to be available. The available SIP injection located near the broken cold leg with another available injection located on the opposite side of broken cold leg is used for the ~~large break LOCA~~ analysis.

The operating parameters and ranges for the plant uncertainty evaluation determined in ~~large break LOCA~~ analysis are listed in Table 15.6.5-1. Core and system parameters are prepared by using measurement uncertainty ranges or determined to cover the minimum and maximum ranges of the design data or the limit of the Technical Specifications.

~ escri~ e~ in Reference ~ 3

burnup sensitivity study to determine the limiting burnup is introduced by considering TCD effects. In addition since determination of the limiting reactivity could be affected by burnup reactivity sensitivity with various burnup cases are evaluated.

The ~~large break LOCA~~ analysis accounts for 10 percent tube plugging of the steam generator tubes that may occur during the life of the plant. **LBLOCA**

~~The accidents are assumed to occur at the initial burnup for the large break LOCA analysis. The stored energy is the maximum value because the fuel elements show the most densification at the initial burnup (BOC), and the burnup yields the highest cladding temperature in the large break LOCA.~~

Delete → **insert ~ ith the ~ burnup of 27~000 ~ ~ ~ /~ TU**

LBLOCA

Subsection 6.2.1.5 presents the minimum containment pressure analysis that is performed in the analysis of ECCS performance. The analysis identifies the containment parameters used in the ~~large break~~ analysis. The values for the containment parameters are chosen to minimize containment pressure to minimize the core reflood rate.

insert ~ ith the ~ burnup of 27~000 ~ ~ ~ /~ TU **LBLOCA**

The worst break in the ~~large break LOCA~~ analysis is the double-ended guillotine at the pump discharge leg (Reference 63). To determine the limiting break area, a guillotine break spectrum of 100 percent, 80 percent, and 60 percent break areas is analyzed, and the limiting break area is applied for 124 cases of SRS calculation.

insert: and burnup

conditions are

Small Break Loss-of-Coolant Accident

1~1

insert ~ ith various ~ burnup

~~ith various ~ burnups are~~
The safety injection system (SIS) consists of four direct vessel injection lines, each supplying flow from one SIT and one SIP. Offsite power is conservatively assumed to be lost upon reactor trip, and the SIPs therefore await diesel generator startup and load sequencing before they can start. The total time delay assumed is 40 seconds from when the SIAS setpoint is reached to when the full SI flow is delivered to the RCS. For breaks in the DVI line, all safety injection flow delivered to the broken line is assumed to spill out of the break.

An analysis of the possible single failures that can occur within the SIS shows that the worst single failure for the small break spectrum is the failure of one SIP train. However, two of the four SIPs are conservatively assumed to be available, thereby minimizing the safety injection available to cool the core.

Based on the above assumptions, the following safety injection flows are credited for the small break LOCA analysis:

- For a break in the pump discharge leg, the SI flow credited is full flow from two SIPs and four SITs.

APR1400 DCD TIER 2

- b. For a break in a DVI line, the SI flow credited is full flow from one SIP and three SITs. The flow from the remaining active SIP and from one SIT is assumed to spill out of the break.

Table 15.6.5-6 presents the SIP flow rates assumed at each of the four injection points as a function of RCS pressure.

The significant core and system parameters used in the small break LOCA calculations are presented in Table 15.6.5-7. PLHGR of 492.1 W/cm (15.0 kW/ft) is assumed to occur about 15 percent from the top of the active core. A conservative beginning-of-life moderator temperature coefficient of $0.0 \times 10^{-4} \Delta\rho/^{\circ}\text{C}$ ($0.0 \times 10^{-4} \Delta\rho/^{\circ}\text{F}$) was used in all small break LOCA calculations.

The initial steady-state fuel rod conditions are obtained from the FATES3 (Reference 74) computer program. The small break LOCA analysis uses a hot rod average burnup, which maximizes the amount of stored energy in the fuel.

The small break LOCA analysis uses the containment parameters of the initial containment pressure and the maximum containment volume. Containment parameters do not influence the small break LOCA analysis because the break flow stays critical.

Post Loss-of-Coolant Accident Long-Term Cooling

The major assumptions used in performing the LTC analysis are as follows:

- a. No offsite power is available.
- b. The worst single failure is the loss of two SIP trains with additional conservativeness. This results in the following:
 - 1) Two SIPs are operable.
 - 2) One motor-driven auxiliary feedwater pump is operable.
- c. One atmospheric dump valve on each SG is available to cool down the RCS.
- d. RCS cooldown begins at 2 hours post-LOCA.
- e. The SITs are vented or isolated before establishing shutdown cooling conditions for the small break LTC procedure.

APR1400 DCD TIER 2

- f. The pressurizer is depressurized to establish shutdown cooling conditions for the small break LTC procedure.
- g. RCS cooldown is terminated when the hot leg temperature is below the maximum shutdown cooling entry temperature including instrument uncertainty.
- h. Pump flow rates and initial water source inventories used in the ~~large break LOCA~~ boric acid precipitation analysis are selected to maximize the boric acid concentration in the core.
- i. A boric acid precipitation limit of 29.3 weight percent (Reference 73) is used in the ~~large break LOCA~~ boric acid precipitation analysis. This limit is based on a conservative containment pressure of 1.03 kg/cm²A (14.7 psia).

Significant core and system parameters used in the post-LOCA long-term cooling analysis are presented in Table 15.6.5-12.

The IRWST sump strainer related to GSI-191 is designed to provide reasonable assurance that debris quantities are maintained within the bounds of a post-LOCA long-term cooling analysis. See Subsection 6.8.4.5 for further information.

15.6.5.3.3 Results

Large Break Loss-of-Coolant Accident Analysis Results

Major input variables used in the performance evaluation of the SIS in a ~~large break LOCA~~ are summarized in Table 15.6.5-2. The important results such as the PCT, PCT location, and time results for ~~large break LOCA~~ spectrum analyses are listed in Table 15.6.5-3. Major times of interest are listed in Table 15.6.5-4. The transient behaviors of the NSSS parameters are shown in Figures 15.6.5-2 through 15.6.5-23.

The most limiting break area is a 100 percent of double-ended guillotine at the pump discharge break. Hence, a SRS calculation is performed for a 100 percent double-ended guillotine break at the pump discharge leg.

The cladding temperature behavior result obtained from 124 times SRS calculations is shown in Figure 15.6.5-23. In the 124 times calculations, the highest two PCT cases are excluded. The third highest PCT is 991.3 °C (1,816.4 °F) and maximum cladding oxidation is 3 percent with exceeding the 95 percent at 95 percent confidence level.

The third highest PCT is occurred during reflood phase and the PCTs are increased by the biases. The total PCT bias is evaluated as +9.8 °C and the peak local oxidation and hot rod hydrogen generation are confirmed not to increase by the scale bias calculations. Therefore the final PCT (w/ BIAS) is 1,019.7 °C (1,867.5 °F) and the maximum cladding oxidation (w/ BIAS) is 6.30 percent as shown in Table 15.6.5-4.

The cases in which the clad temperature differences in the second peak are within 100 °C (180 °F) compared with the highest second peak are selected for scale bias calculations. Code biases in the prediction of ECC water bypass and steam binding are evaluated separately. Steam binding bias is evaluated by combining the results of two separate bias evaluations of droplet de-entrainment in the upper plenum of the reactor vessel and droplet evaporation in the steam generator U-tube. ~~Even though reflood cladding temperatures are increased by the biases, they do not exceed the blowdown PCT of 991.3 °C (1,816.4 °F). Total PCT bias is evaluated as +0 °C, as shown in Table 15.6.5-5. The maximum cladding oxidation with bias evaluation is 3 percent as shown in Table 15.6.5-5.~~

Uncertainties from sources other than code ~~models~~ or plant operation conditions, such as automatic time step control function and data reading frequency of RELAP5/MOD3.3/K, are considered of maximum 10 °C (18 °F). The hot rod average oxidation is calculated lower than one percent. The final PCT, maximum cladding oxidation, and core-wide hydrogen generation combining all the biases are as follows:

$$\begin{aligned} \text{Peak cladding temperature} &= \cancel{991.3\text{ °C} + 10\text{ °C}} && 1,019.7\text{ °C} + 10\text{ °C} \\ &= \cancel{1,001.3\text{ °C} (1,834.3\text{ °F})} && 1,029.7\text{ °C} (1,885.5\text{ °F}) < 1,204.4\text{ °C} (2,200\text{ °F}) \\ &= \cancel{1,274.5\text{ K} < 1,477.15\text{ K} (2,200\text{ °F})} \end{aligned}$$

$$\text{Maximum cladding oxidation} = \cancel{3.09\%} < 17\%$$

$$\text{Maximum hydrogen generation} \ll 1\%$$

The highest cladding temperature in the large break LOCA analysis is ~~1,001.3 °C (1,834.3 °F)~~, which is ~~202.7 °C (365.7 °F)~~ lower than the acceptance criterion of ~~1,204 °C (2,200 °F)~~.

~~The final PCT considering the effect of thermal conductivity degradation is still satisfied the acceptance criteria. Details are given in Reference 78. The PCT increase is ended when the core is maintaining a coolable geometry. The heat generated from the fuel is able to be removed properly for a long period.~~

Based on the results of this analysis, it is concluded that the APR1400 ECCS satisfies the all SRP acceptance criteria of References 62 and 64 (Subsection 15.0.5) for a complete spectrum of large break LOCAs and is adequate to perform its intended function of maintaining the integrity of the core, thereby limiting radiation release to the environment.

REPLACE ~ ith ne~t page

The third highest PCT is occurred during reflood phase and the PCTs are increased by the biases. The total PCT bias is evaluated as +9.8 °C and the peak local oxidation and hot rod hydrogen generation are confirmed not to increase by the scale bias calculations. Therefore the final PCT (w/ BIAS) is 1,020 °C (1,868 °F) and the maximum cladding oxidation (w/ BIAS) is 6.3 percent as shown in Table 15.6.5-4.

The cases in which the clad temperature differences in the second peak are within 100 °C (180 °F) compared with the highest second peak are selected for scale bias calculations. Code biases in the prediction of ECC water bypass and steam binding are evaluated separately. Steam binding bias is evaluated by combining the results of two separate bias evaluations of droplet de-entrainment in the upper plenum of the reactor vessel and droplet evaporation in the steam generator U-tube. Even though reflood cladding temperatures are increased by the biases, they do not exceed the blowdown PCT of 991.3 °C (1,816.4 °F). Total PCT bias is evaluated as +0 °C, as shown in Table 15.6.5-5. The maximum cladding oxidation with bias evaluation is 3 percent as shown in Table 15.6.5-5.

Uncertainties from sources other than code models or plant operation conditions, such as automatic time step control function and data reading frequency of RELAP5/MOD3.3/K, are considered of maximum 10 °C (18 °F). The hot rod average oxidation is calculated lower than one percent. The final PCT, maximum cladding oxidation, and core-wide hydrogen generation combining all the biases are as follows:

$$\begin{aligned} \text{Peak cladding temperature} &= 991.3\text{ °C} + 10\text{ °C} \\ &= 1,001.3\text{ °C (1,834.3 °F)} \\ &= 1,274.5\text{ K} < 1,477.15\text{ K (2,200 °F)} \end{aligned}$$

$$\text{Maximum cladding oxidation} = 3.09\% < 17\%$$

$$\text{Maximum hydrogen generation} \ll 1\%$$

The highest cladding temperature in the large break LOCA analysis is 1,001.3 °C (1,834.3 °F), which is 202.7 °C (365.7 °F) lower than the acceptance criterion of 1,204 °C (2,200 °F).

The final PCT considering the effect of thermal conductivity degradation is still satisfied the acceptance criteria. Details are given in Reference 78. The PCT increase is ended when the core is maintaining a coolable geometry. The heat generated from the fuel is able to be removed properly for a long period.

Based on the results of this analysis, it is concluded that the APR1400 ECCS satisfies the all SRP acceptance criteria of References 62 and 64 (Subsection 15.0.5) for a complete spectrum of large break LOCAs and is adequate to perform its intended function of maintaining the integrity of the core, thereby limiting radiation release to the environment.

APR1400 DCD TIER 2Small Break Loss-of-Coolant Accident Analysis Results

The nine breaks analyzed at 4,062.66 MWt, 102 percent of nominal, include reactor coolant pump discharge leg breaks ranging in size from 465 cm² (0.5 ft²) to 46.5 cm² (0.05 ft²) and DVI line breaks from 372 cm² (0.4 ft²) to 18.6 cm² (0.02 ft²). One break, equal in area to a fully open POSRV, 27.9 cm² (0.03 ft²), is postulated to occur in the top of the pressurizer. Table 15.6.5-8 lists the various break sizes and locations examined for this analysis.

The transient behavior of important NSSS parameters is shown in the figures listed in Table 15.6.5-9. Table 15.6.5-10 summarizes the important results of this analysis. Times of interest for the various breaks analyzed are presented in Table 15.6.5-11. A plot of PCT versus break size is presented in Figure 15.6.5-33. The 372 ft² (0.4 ft²) DVI break results in the highest cladding temperature 624 °C (1,156 °F) of the small breaks analyzed, which is 580 °C (1,044 °F) lower than the acceptance criteria of 1,204 °C (2,200 °F). Of the pump discharge leg and DVI line break locations, the DVI line break is limiting due to the assumed loss of all safety injection flow to the broken line.

For the DVI line break location, as the break size becomes progressively smaller than 372 cm² (0.4 ft²), the inner vessel two phase level follows a definite pattern:

- a. The time of initial core uncover is later.
- b. The depth of core uncover is less.
- c. The rate of level decrease and increase becomes slower.

This trend continues until the core does not uncover at all. These trends predictably affect the PCT.

As the break size decreases, both the later time of the initial core uncover and the shallower depth of uncover tend to mitigate the temperature transient. This trend continues until the core does not uncover as typified by the 18.6 cm² (0.02 ft²) break. By analyzing several break sizes over this range, the behavior of PCT versus break size is adequately determined.

The above behavior of core uncover with break size results from the design characteristics of the SIS. For DVI break sizes below 93 cm² (0.1 ft²), the RCS pressure remains above the SIT pressure and coolant flow injection to the reactor vessel is accomplished entirely by

APR1400 DCD TIER 2

15.6.5.5.1.4 Post-LOCA Back-Leakage to In-Containment Refueling Water Storage Tank

The IRWST is located inside the containment, and a minimum flow line is provided on each CSS pump discharge line, which is connected to the CSS suction line. Any post-LOCA leakage that occurs from the minimum flow line components is confined within the containment pressure boundary and not directly released to the environment.

15.6.5.5.2 Input Parameters and Initial Conditions

The radiological consequences of the LOCA are analyzed using a conservative set of assumptions and the APR1400 design inputs. Input parameter values used in the analysis are presented in Table 15.6.5-13.

12

Credit is taken only for the accident mitigation features that are classified as safety-related, are required to be operable by the Technical Specifications, are powered by emergency power sources, and are either automatically actuated or, in limited cases, have actuation requirements addressed in emergency operating procedures. The operations of the containment spray system, containment purge valve isolation, AB emergency exhaust system, and main control room HVAC system, including filtration efficiencies credited in the analysis to mitigate the dose consequences, are operable by the Technical Specifications. The control room HVAC system intake radiation monitor capability to align with the less contaminated air intake is also credited in the analysis.

The numeric values used in this analysis are chosen as inputs with the objective of maximizing the postulated dose. The use of the filter efficiencies lower than or equal to the actual tested efficiencies, use of a ground release that leads to the most conservative MCR and AB air intake χ/Q values regardless of actual source-receptor configuration, and the use of the most limiting U.S. meteorological hourly data demonstrate the inherent conservatism in the analysis. Many of the design input parameter values used in the analysis are those specified in the Technical Specifications.

The χ/Q values used in the analysis for EAB, LPZ, MCR, and TSC are described in Subsection 2.3.4 and are listed in Tables 2.3-1 through 2.3-12; breathing rates are given in Table 15A-12.

APR1400 DCD TIER 215.6.5.5.3 Results

13

The radiological consequences due to large break LOCA are presented in Table 15.6.5-14. The results of large break LOCA analyses indicate that the EAB and LPZ doses are within their allowable dose limits in 10 CFR 50.34(a)(1). The MCR and TSC doses are also within the limit in GDC 19.

15.6.6 Combined License Information

No COL information is required with regard to Section 15.6.

APR1400 DCD TIER 2

Table 15.6-1

Uncertainty Parameter Ranges and Distributions

| No. | Parameter | Distribution | Parameter Ranges | | Component |
|-----|-----------------------------|--------------|------------------|----------|----------------|
| | | | Min. | Max | |
| 1 | Fq | Uniform | 1.94 | 2.41 | Fuel |
| 2 | Gap conductance | Uniform | 0.75 | 1.50 | |
| 3 | Fuel conductivity | Normal | 0.8455 | 1.1545 | |
| 4 | Core power | Normal | 0.9691 | 1.0309 | |
| 5 | Decay heat | Normal | 0.89803 | 1.10197 | |
| 6 | Burst temperature dial | Uniform | 0.90 | 1.10 | |
| 7 | Burst strain dial | Uniform | 0.30 | 1.70 | |
| 8 | Oxidization dial | Normal | 0.961 | 1.039 | |
| 9 | Groeneveld CHF dial | Normal | -0.17111 | 2.17111 | Core |
| 10 | Chen nucleate boiling dial | Normal | 0.382 | 1.618 | |
| 11 | Zuber CHF dial | Normal | 0.5365 | 1.4635 | |
| 12 | Dittus Boelter, liquid dial | Normal | 0.606025 | 1.393975 | |
| 13 | Dittus Boelter, vapor dial | Normal | 0.606025 | 1.393975 | |
| 14 | Bromley dial | Normal | 0.42835 | 1.57165 | |
| 15 | Weber number dial | Uniform | 1.350 | 7.0 | |
| 16 | F. Rohsenow dial | Uniform | 0.5 | 1.5 | |
| 17 | Weismann dial | Uniform | 0.40 | 1.60 | |
| 18 | 1-Phase Cd | Normal | 0.7821 | 0.9979 | |
| 19 | 2-Phase Cd | Normal | 0.7026 | 1.4374 | |
| 20 | Pump K-factor | Uniform | 0.239 | 0.577 | Loop |
| 21 | Pump head multiplier | Uniform | 0.0 | 1.0 | |
| 22 | Pump torque multiplier | Uniform | 0.0 | 1.0 | |
| 23 | Pressurizer pressure, bar | Normal | 152.47 | 157.80 | Pressurizer |
| 24 | SIT pressure, bar | Uniform | 40.31 | 44.59 | SIT/Cold Leg |
| 25 | SIT water volume, m3 | Uniform | 50.69 | 54.57 | |
| 26 | SIT water temp, K | Uniform | 283.0 | 321.9 | |
| 27 | SIP flow multiplier | Uniform | -0.5 | 0.5 | |
| 28 | IRWST water temp, K | Uniform | 283.0 | 321.9 | |
| 29 | Thermal Conductivity | Uniform | 1.0 | 2.0 | Downcomer Wall |
| 30 | Heat Capacity | Uniform | 1.0 | 1.5 | |

APR1400 DCD TIER 2

Table 15.6.5-2 (1 of 2)

General System Parameters and Initial Conditions for Large Break ECCS Performance

| Plant Parameters | Reference Conditions |
|---|------------------------|
| Core | |
| 1. Core power, MWt | 3,983 |
| 2. Power peaking factor | 2.258 ← 2.184 |
| 3. Fuel type | 16 × 16 |
| 4. Power output pattern | Figure 15.6.5-1 |
| 5. Decay heat | ANS79 model |
| Reactor Coolant System | |
| 1. Initial core flow rate, kg/hr | 73.3×10^6 |
| Pressurizer | |
| 1. Pressure, bar | 155.1 |
| Steam Generator | |
| 1. Feedwater temperature, K | 505.23 |
| 2. Tube plugging rate, % | 10 |
| Safety Injection System | |
| 1. Safety injection tank coolant volume, m ³ | 52.63 ← 52.61 |
| 2. Safety injection tank gas pressure, bar | 42.45 ← 43.07 |
| 3. Safety injection tank coolant temperature, K | 302.5 ← 302.59 ← 302.6 |
| 4. FD K-factor for high injection flow (including piping K) | 25 ← 10 |
| 5. FD K-factor for low injection flow (including piping K) | 120 ← 80 |
| 6. IRWST temperature, K | 302.5 ← 302.59 ← 302.6 |

APR1400 DCD TIER 2

Table 15.6.5-2 (2 of 2)

| Plant Parameters | Reference Conditions |
|---|----------------------|
| Containment Building | |
| 1. Initial pressure, bar | 0.98 |
| 2. Initial temperature, K | 283.15 |
| 3. Net Free volume, m ³ | 97,239 |
| 4. Number of spray | 2 |
| 5. Delay time for spray actuation, sec | 0 |
| 6. Spray flow rate (2 pumps), L/min (gpm) | 37,853 |

Replace with next page C

APR1400 DCD TIER 2

Table 15.6.5-3

Summary of Fuel Rod Performance for Break Spectrum of Large Break LOCA

| | Variable | 100 % Break | 80 % Break | 60 % Break |
|--------------------------------------|-----------------|-------------|------------|------------|
| Blowdown | PCT, °C | 892.0 | 870.0 | 768.9 |
| | PCT Location, m | 2.57 | 2.57 | 2.76 |
| | PCT Time, sec | 6.5 | 36.5 | 36.5 |
| Reflood | PCT, °C | 798.9 | 869.5 | 762.5 |
| | PCT Location, m | 2.57 | 2.76 | 2.76 |
| | PCT Time, sec | 36.5 | 64.0 | 71.5 |
| Peak Local Oxidation, % | | 1.50 | 1.92 | 1.24 |
| Peak Zr-H ₂ O location, m | | 2.57 | 2.76 | 2.76 |
| Maximum Hydrogen Generation, % | | < 1.0 | < 1.0 | < 1.0 |
| Hot Fuel Rod Rupture | | N/A | N/A | N/A |

C

Table 15.6.5-2

Summary of Fuel Rod Performance for Break Spectrum of Large Break LOCA

| Variable | | 100 % Break | 80 % Break | 60 % Break |
|--------------------------------------|-----------------|-------------|------------|------------|
| Burnup (MWd/MTU) | | 27,000 | 27,000 | 0 |
| Blowdown | PCT, °C | 896.8 | 847.7 | 633.4 |
| | PCT Location, m | 2.76 | 2.76 | 2.76 |
| | PCT Time, sec | 7.2 | 9.2 | 2.7 |
| Reflood | PCT, °C | 846.8 | 887.3 | 796.4 |
| | PCT Location, m | 2.57 | 2.76 | 2.76 |
| | PCT Time, sec | 92.5 | 80.5 | 87.5 |
| Peak Local Oxidation, % | | 2.66 | 2.86 | 0.56 |
| Peak Zr-H ₂ O location, m | | 2.19 | 2.57 | 2.76 |
| Maximum Hydrogen Generation, % | | < 1.0 | < 1.0 | < 1.0 |
| Hot Fuel Rod Rupture Time, sec | | 28.8 | 27.8 | N/A |

Replace with next page D

APR1400 DCD TIER 2

Table 15.6.5-4

Sequence of Events for Representative Large Break LOCA

| EVENT | 100 % Break (sec) | 80 % Break (sec) | 60 % Break (sec) |
|--|----------------------|---------------------|---------------------|
| Break Occurs | 0 | 0 | 0 |
| Reactor Trip signal Occurs | 6.2 | 6.2 | 7.3 |
| SI Injection signal Occurs | 6.2 | 6.2 | 7.3 |
| SIT Discharge Begins | | | |
| SIT 1 (Broken Cold Leg Side) | 14.4 | 16.2 | 22.2 |
| SIT 2 (Broken Loop Intact Cold Leg Side) | 14.4 | 16.2 | 22.2 |
| SIT 3 (Intact Loop Intact Cold Leg Side 1) | 14.4 | 16.2 | 22.2 |
| SIT 4 (Intact Loop Intact Cold Leg Side 2) | 14.4 | 16.2 | 22.2 |
| Pumped SI Injection | 46.2 | 46.2 | 46.4 |
| Core Water Level Recovery | 44.2 | 40.6 | 45.5 |
| SIT Empty Time | | | |
| SIT 1 (Broken Cold Leg Side) | 201.5 | 207.5 | 206.7 |
| SIT 2 (Broken Loop Intact Cold Leg Side) | 201.5 | 207.5 | 206.8 |
| SIT 3 (Intact Loop Intact Cold Leg Side 1) | 201.5 | 207.5 | 206.7 |
| SIT 4 (Intact Loop Intact Cold Leg Side 2) | 201.5 | 207.5 | 206.6 |

D

Table 15.6.5-3

Sequence of Event for Representative Large Break LOCA

| EVENT | 100 % Break(sec) | 80 % Break(sec) | 60 % Break(sec) |
|--|---------------------|--------------------|--------------------|
| Break Occurs | 0 | 0 | 0 |
| Reactor Trip signal Occurs | 9.51 | 9.57 | 9.77 |
| SI Injection signal Occurs | 9.51 | 9.57 | 9.77 |
| SIT Discharge Begins | | | |
| SIT 1 (Broken Cold Leg Side) | 14.8 | 16.6 | 20.1 |
| SIT 2 (Broken Loop Intact Cold Leg Side) | 14.8 | 16.6 | 20.1 |
| SIT 3 (Intact Loop Intact Cold Leg Side 1) | 14.8 | 16.6 | 20.1 |
| SIT 4 (Intact Loop Intact Cold Leg Side 2) | 14.8 | 16.6 | 20.1 |
| Pumped SI Injection | 48.36 | 48.42 | 48.62 |
| Core Water Level Recovery | 32.5 | 35.5 | 43.0 |
| SIT Empty Time | | | |
| SIT 1 (Broken Cold Leg Side) | 171.4 | 178.7 | 177.9 |
| SIT 2 (Broken Loop Intact Cold Leg Side) | 171.5 | 178.8 | 177.9 |
| SIT 3 (Intact Loop Intact Cold Leg Side 1) | 171.4 | 178.7 | 177.9 |
| SIT 4 (Intact Loop Intact Cold Leg Side 2) | 171.5 | 178.7 | 177.9 |

Replace with next page E

APR1400 DCD TIER 2

Table 15.6.5-5

Summary of SRS and Bias Evaluation Results

| Peak Cladding Temperature (PCT) | | Value, °C |
|---|----------------------------|----------------------|
| SRS Results | Highest PCT | 991.3 |
| | Highest Reflood PCT | 982.9 |
| Scale BIAS Evaluation Results | Final BIAS Reflood PCT | 982.9 |
| | Max. BIAS Case Reflood PCT | 982.9 |
| | – ECC Bypass BIAS | +0.0 |
| | – Steam Binding BIAS | +0.0 |
| Final PCT (w/ BIAS) | | 991.3 ⁽¹⁾ |
| Max. Cladding Oxidation | | Value, % |
| SRS Results | Max. Cladding Oxidation | 3.00 |
| Scale BIAS Evaluation Results | Final BIAS Oxidation | 3.09 |
| | Max. BIAS Case Oxidation | 2.56 |
| | – ECC Bypass BIAS | +0.14 |
| | – Steam Binding BIAS | +0.39 |
| Final Max. Cladding Oxidation (w/ BIAS) | | 3.09 |

- (1) The final PCT with considering thermal conductivity degradation effect is still satisfied the acceptance criteria.

E

Table 15.6.5-4

Summary of SRS and Bias Evaluation Results

| Peak Cladding Temperature (PCT) | | Value, °C |
|---|------------------------------------|-----------------------|
| SRS Results | Highest PCT | 1,009.9 |
| | Highest Reflood PCT | 1,009.9 |
| Scale BIAS Evaluation Results | Final BIAS Reflood PCT | 1,019.7 |
| | Max. BIAS Case Reflood PCT | 1,009.9 |
| | - ECC Bypass BIAS | +9.8 |
| | - Steam Binding BIAS | +0.0 |
| Final PCT (w/ BIAS) | | 1,019.7 ¹⁾ |
| Max. Cladding Oxidation | | Value, % |
| SRS Results | Max. Cladding Oxidation | 6.3 |
| Scale BIAS Evaluation Results | Final BIAS Max. Cladding Oxidation | 6.3 |
| | Max. BIAS Case Cladding Oxidation | 6.3 |
| | - ECC Bypass BIAS | +0.0 |
| | - Steam Binding BIAS | +0.0 |
| Final Max. Cladding Oxidation (w/ BIAS) | | 6.3 |

(1) The final PCT with considering thermal conductivity degradation effect is still satisfied the acceptance criteria.

APR1400 DCD TIER 2

Table 15.6.5-6

5

Safety Injection Pumps Minimum Delivered Flow to RCS
(Assuming Two SI Pump Trains Failed)

| RCS Pressure, kg/cm ² (psig) | Flow Rate Per Injection Point, ⁽¹⁾ L/min (gpm) | |
|--|--|---------------|
| | A | B |
| 112 (1,600) | 0 (0) | 0 (0) |
| 105 (1,500) | 1,096 (290) | 1,096 (290) |
| 98 (1,400) | 1,524 (403) | 1,524 (403) |
| 91 (1,300) | 1,843 (487) | 1,843 (487) |
| 84 (1,200) | 2,107 (557) | 2,107 (557) |
| 77 (1,100) | 2,337 (617) | 2,337 (617) |
| 70 (1,000) | 2,542 (672) | 2,542 (672) |
| 63 (900) | 2,730 (721) | 2,730 (721) |
| 56 (800) | 2,903 (767) | 2,903 (767) |
| 49 (700) | 3,064 (810) | 3,064 (810) |
| 42 (600) | 3,216 (850) | 3,216 (850) |
| 35 (500) | 3,360 (888) | 3,360 (888) |
| 32 (450) | 3,429 (906) | 3,429 (906) |
| 28 (400) | 3,496 (924) | 3,496 (924) |
| 25 (350) | 3,562 (941) | 3,562 (941) |
| 21 (300) | 3,627 (958) | 3,627 (958) |
| 18 (250) | 3,690 (975) | 3,690 (975) |
| 14 (200) | 3,752 (991) | 3,752 (991) |
| 11 (150) | 3,812 (1,007) | 3,812 (1,007) |
| 7 (100) | 3,872 (1,023) | 3,872 (1,023) |
| 4 (50) | 3,929 (1,038) | 3,929 (1,038) |
| 0 (0) | 3,986 (1,053) | 3,986 (1,053) |

- (1) For breaks assumed at the DVI location, Injection Point A is assumed to be the broken line. Injection Point B is the intact injection line. There is no flow delivered to the two injection points in the other loop due to the assumed failure of one emergency generator.

APR1400 DCD TIER 2

Table 15.6.5-7

General System Parameters and Initial Conditions:
Small Break ECCS Performance Analysis

| Quantity | Value |
|---|---|
| Core Power Level (102 % of Nominal), MWt | 4,062.66 |
| Average Linear Heat Generation Rate, W/cm (kW/ft) | 187.5 (5.715) |
| Peak Linear Heat Generation Rate (PLHGR), W/cm (kW/ft) | 492.1 (15.0) |
| Gap Conductance at PLHGR, kcal/hr-m ² -°C (Btu/hr-ft ² -°F) | 10,289 (2,107) |
| Fuel Centerline Temperature at PLGHR, °C (°F) | 1,965 (3,568) |
| Fuel Average Temperature at PLHGR, °C (°F) | 1,200 (2,192) |
| Hot Rod Gas Pressure, kg/cm ² A (psia) | 52.0 (740) |
| Moderator Temperature Coefficient, Δρ/°C (Δρ/°F) | 0.0 × 10 ⁻⁴ (0.0 × 10 ⁻⁴) |
| Initial RCS Flow Rate, kg/hr (lbm/hr) | 75.6 × 10 ⁶ (166.6 × 10 ⁶) |
| Initial Core Flow Rate, kg/hr (lbm/hr) | 73.3 × 10 ⁶ (161.6 × 10 ⁶) |
| Initial RCS Pressure, kg/cm ² A (psia) | 158.2 (2,250) |
| Initial Reactor Vessel Inlet Temperature, °C (°F) | 290.6 (555.0) |
| Initial Reactor Vessel Outlet Temperature, °C (°F) | 324.4 (615.9) |
| Low Pressurizer Pressure Reactor Trip Setpoint, kg/cm ² A (psia) | 109.3 (1,555) |
| SIAS Setpoint on Low Pressurizer Pressure, kg/cm ² A (psia) | 109.3 (1,555) |
| SIT Gas Pressure, kg/cm ² A (psia) | 41.1 (584.7) |

APR1400 DCD TIER 2

Table 15.6.5-8

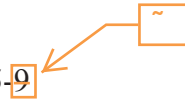
7

Small Break Spectrum

| Break Size and Location | Abbreviation | Figure No. |
|--|---------------------------|------------|
| 465 cm ² (0.5 ft ²) break in pump discharge leg | 465 cm ² /PD | 15.6.5-24 |
| 325 cm ² (0.35 ft ²) break in pump discharge leg | 325 cm ² /PD | 15.6.5-25 |
| 93 cm ² (0.1 ft ²) break in pump discharge leg | 93 cm ² /PD | 15.6.5-26 |
| 46.5 cm ² (0.05 ft ²) break in pump discharge leg | 46.5 cm ² /PD | 15.6.5-27 |
| 372 cm ² (0.4 ft ²) break in DVI line | 372 cm ² /DVI | 15.6.5-28 |
| 93 cm ² (0.1 ft ²) break in DVI line | 93 cm ² /DVI | 15.6.5-29 |
| 46.5 cm ² (0.05 ft ²) break in DVI line | 46.5 cm ² /DVI | 15.6.5-30 |
| 18.6 cm ² (0.02 ft ²) break in DVI line | 18.6 cm ² /DVI | 15.6.5-31 |
| 27.9 cm ² (0.03 ft ²) break in top of pressurizer | 27.9 cm ² /HL | 15.6.5-32 |

APR1400 DCD TIER 2

Table 15.6.5-9

Variables Plotted as a Function of Time for Each Small Break in the Spectrum

| Variable | Figure Symbol |
|---------------------------------------|---------------|
| Normalized total core power | A |
| Inner vessel pressure | B |
| Break flow rate | C |
| Inner vessel inlet flow rate | D |
| Inner vessel two-phase mixture level | E |
| Heat transfer coefficient at hot spot | F |
| Coolant temperature at hot spot | G |
| Hot spot clad surface temperature | H |

APR1400 DCD TIER 2

Table 15.6.5-10

9

Peak Cladding Temperature and Oxidation Percentage
for the Small Break Spectrum

| Break | Peak Cladding Temperature, °C (°F) | Maximum Cladding Oxidation, % | Maximum Core-Wide Oxidation, % |
|---------------------------|------------------------------------|-------------------------------|--------------------------------|
| 465 cm ² /PD | 498 (929) | 0.0017 | < 0.0003 |
| 325 cm ² /PD | 492 (917) | 0.0015 | < 0.0002 |
| 93 cm ² /PD | 565 (1,049) | 0.0010 | < 0.0001 |
| 46.5 cm ² /PD | 568 (1,054) | 0.0008 | < 0.0002 |
| 372 cm ² /DVI | 624 (1,156) | 0.0195 | < 0.0029 |
| 93 cm ² /DVI | 569 (1,056) | 0.0069 | < 0.0009 |
| 46.5 cm ² /DVI | 571 (1,059) | 0.0018 | < 0.0003 |
| 18.6 cm ² /DVI | 616 (1,140) | 0.0029 | < 0.0006 |
| 27.9 cm ² /HL | 568 (1,055) | 0.0006 | < 0.0002 |

APR1400 DCD TIER 2

Table 15.6.5-11

10

Times of Interest for the Small Break Spectrum
(Seconds after Break)

| Break | SIP Flow Delivered to RCS | SIT Flow Delivered to RCS | Hot Spot Peak Cladding Temperature Occurs |
|---------------------------|------------------------------|------------------------------|--|
| 465 cm ² /PD | 57 | 150 | 167 |
| 325 cm ² /PD | 62 | 218 | 105 |
| 93 cm ² /PD | 138 | 1,128 | 100 |
| 46.5 cm ² /PD | 248 | 2,984 | 208 |
| 372 cm ² /DVI | 60 | 192 | 239 |
| 93 cm ² /DVI | 138 | 1,092 | 100 |
| 46.5 cm ² /DVI | 250 | N/A ⁽¹⁾ | 210 |
| 18.6 cm ² /DVI | 624 | N/A ⁽¹⁾ | 1,184 |
| 27.9 cm ² /HL | 795 | N/A ⁽¹⁾ | 750 |

(1) Calculation terminated before initiation of SIT discharge

APR1400 DCD TIER 2

Table 15.6.5-12

11

General System Parameters and Initial Conditions
Long-Term Cooling SIS Performance

| Quantity | | Value |
|--|-------|---------------------------|
| Reactor Power Level (102 % of Nominal), MWt | | 4,062.66 |
| SCS Entry Temperature, °C (°F) | | 193 (380) |
| SCS Entry Pressure, kg/cm ² A (psia) | | 28.1 (400) |
| Atmospheric Dump Valve Capacity, per Valve at 70.3 kg/cm ² A (1,000 psia), kg/hr (lbm/hr) | | 430,900 (950,000) (min) |
| Auxiliary Feedwater Storage Tank Capacity, per tank, L (gal) | | 1,870,000 (494,000) (min) |
| Boric Acid Concentration, wt% (ppm) | RCS | 0.94 (1,650) (max) |
| | IRWST | 2.52 (4,400) (max) |
| | SIT | 2.52 (4,400) (max) |

APR1400 DCD TIER 2

Table 15.6.5-13 (1 of 4)

Major Input Parameters Used in Radiological
Consequences Analysis for Large Break LOCA

| Parameter | Value | |
|--|---|-------------------------------|
| Containment Leakage Parameters | | |
| Reactor Core Power Level | 4,062.66 MWt | |
| Core Inventory | See Table 15A-1 | |
| Radionuclide Composition | | |
| Group | Elements | |
| Noble Gases | Xe, Kr | |
| Halogens | I, Br | |
| Alkali Metals | Cs, Rb | |
| Tellurium | Te, Sb, Se, Ba, Sr | |
| Noble Metals | Ru, Rh, Pd, Mo, Tc, Co | |
| Lanthandies | La, Zr, Nd, Eu, Nb, Pm, Pr, Sm, Y, Cm, Am | |
| Cerium | Ce, Pu, Np | |
| Timing of Release Phases | | |
| Phase | Onset | Duration |
| Gap Release | 0.0083 hr | 0.5 hr |
| Early In-Vessel Release | 0.5083 hr | 1.3 hr |
| Fraction of Core Inventory Released into Containment | | |
| Group | Gap Release Phase | Early In-Vessel Release Phase |
| Noble Gases | 0.05 | 0.95 |
| Halogens | 0.05 | 0.35 |
| Alkali Metals | 0.05 | 0.25 |
| Tellurium Metals | 0.00 | 0.05 |
| Ba, Sr | 0.00 | 0.02 |
| Noble Metals | 0.00 | 0.0025 |
| Cerium | 0.00 | 0.0005 |
| Lanthanides | 0.00 | 0.0002 |

APR1400 DCD TIER 2

Table 15.6.5-13 (2 of 4)

| Parameter | Value |
|--|--|
| Activity Transport Parameters in Primary Containment | |
| Containment Net Free Volume | $8.86 \times 10^4 \text{ m}^3$ ($3.13 \times 10^6 \text{ ft}^3$) |
| Sprayed Volume | $6.64 \times 10^4 \text{ m}^3$ ($2.35 \times 10^6 \text{ ft}^3$) |
| Unsprayed Volume | $2.21 \times 10^4 \text{ m}^3$ ($7.82 \times 10^5 \text{ ft}^3$) |
| Primary Containment Leak Rate | 0.1 v/o/day (0 ~ 24 hr) 0.05 v/o/day (24 ~ 270 hr) |
| Flow Rate Between Sprayed and Unsprayed Regions | 736 m ³ /min (26,000 cfm) (Mixing Flow) 2 turnovers of unsprayed volume/hr |
| Spray Initiation Time | 110 sec (Delay time) |
| Spray Recirculation Phase Initiation Time | Spray water is circulated from IRWST for entire duration of accident (IRWST→CS→HVT→IRWST) |
| Containment Spray Removal Coefficients | 20 hr ⁻¹ (0 ~ 2.25 hr until DF is 200) |
| Elemental (λ_E) | 6.25 hr ⁻¹ (0 ~ 2.40 hr until DF is 50) |
| Particulate (λ_P) | 0.625 hr ⁻¹ (2.40 ~ 4 hr) |
| ESF Leakage Parameters | |
| Minimum IRWST Water Volume | $2.44 \times 10^3 \text{ m}^3$ ($8.61 \times 10^4 \text{ ft}^3$) |
| ESF Leakage Rate | 37.8 L/hr (10 gal/hr) |
| ESF Leakage Initiation Time | 0.0 min |
| Long-term Minimum IRWST Water pH | > 7 |
| ESF Leakage Flashing Factor | 10 % (0 ~ 3 hr) 2 % (3 ~ 16.67 hr) 10 % (> 16.67 hr) |
| Post-LOCA Sump Water Temperature | |
| 3.0 hr | 107 °C (225 °F) |
| 7.64 hr | 113 °C (235.5 °F) |
| 16.67 hr | 107 °C (225 °F) |

APR1400 DCD TIER 2

Table 15.6.5-13 (3 of 4)

| Parameter | Value |
|--|--|
| Chemical Form of Iodine in ESF | |
| Elemental | 97 % |
| Organic | 3 % |
| Fraction of Core Iodine in Sump Water | 40 % |
| Auxiliary Building Emergency Ventilation Charcoal Filter Efficiency (elemental and organic iodines removal) | 95% |
| Filter Loading Model Parameters | |
| MCR Wall Thickness | |
| East | 0.91 m (3.0 ft) |
| West | 0.91 m (3.0 ft) |
| North | 0.91 m (3.0 ft) |
| South | 0.91 m (3.0 ft) |
| Ceiling | 0.46 m (1.5 ft) |
| Minimum MCR Envelope Concrete Shielding | 0.46 m (1.5 ft) |
| Emergency Ventilation HVAC Filter Charcoal Density | 0.45 g/cc (28.1 lb/ft ³) |
| Emergency Ventilation HVAC Filter Charcoal Tray Dimension | 1.65 m (L) × 1.65 m (W) × 2.34 m (H) 1.65 m (L) × 1.65 m (W) × 1.65 m (H) |
| MCR and TSC Model Parameter | |
| Envelope Volume | 5,663 m ³ (200,000 ft ³) |
| Normal Ventilation Flow Rate (unfiltered) | 105 m ³ /min (3,700 cfm) |
| Emergency Ventilation Makeup Rate (filtered) | 105 m ³ /min (3,700 cfm) |
| Emergency Ventilation Recirculation Flow Rate (filtered) | 122 m ³ /min (4,300 cfm) |
| Emergency HVAC Delay Time | 5 min |
| Emergency Ventilation Charcoal Filter Efficiency (elemental and organic iodine removal) | 99 % |
| Emergency Ventilation HEPA Filter Efficiency (particulate removal) | 99 % |
| Unfiltered Inleakage | 2.83 m ³ /min (100 cfm) |

APR1400 DCD TIER 2

Table 15.6.5-13 (4 of 4)

| Parameter | Value |
|--|---|
| Occupancy Factors | |
| 0 ~ 24 hr | 100 % |
| 24 ~ 96 hr | 60 % |
| 96 ~ 720 hr | 40 % |
| Onsite χ/Q_s | See Tables 2.3.2 ~ 2.3.12 |
| Containment Low Volume Purge System (CLVPS) Release Parameters | |
| CLVPS Valve Closure Time | 5.0 sec |
| Volume Flow Rate of CLVPS Release | 11 m ³ /sec (2.34×10^4 cfm) |
| Reactor Coolant Mass | 300,000 kg (661,000 lbm) |
| Reactor Coolant Specific Activity | 3.7×10^4 Bq/g (1.0 μ Ci/g) DE I-131 2.15×10^7 Bq/g (580 μ Ci/g) DE Xe-133 RCS concentrations with 1% fuel defect for Alkali Metal |
| Onsite χ/Q_s | See Tables 2.3.2 ~ 2.3-12 |
| Offsite Model Parameters | |
| χ/Q_s | See Table 2.3-1 |
| Breathing Rate | See Table 15A-12 |
| Minimum Concrete Density | 2,240 kg/m ³ (140 lb/ft ³) |

APR1400 DCD TIER 2

Table 15.6.5-14

13

Radiological Consequences of a Large Break LOCA

| Post-LOCA Activity Release Path | TEDE Dose (mSv) | | |
|------------------------------------|-----------------|----------|----------|
| | MCR and TSC | EAB | LPZ |
| Containment Leakage | 2.73E+01 | 1.99E+02 | 9.94E+01 |
| ESF Leakage | 3.16E-01 | 1.18E+00 | 6.70E+00 |
| CLVPS Release | 1.54E-01 | 2.30E-02 | 5.05E-03 |
| Containment Shine | 0.00E+00 | 0.00E+00 | 0.00E+00 |
| External Cloud | 6.22E+00 | 0.00E+00 | 0.00E+00 |
| Emergency Ventilation Filter Shine | 1.29E+01 | 0.00E+00 | 0.00E+00 |
| Total | 4.69E+01 | 2.00E+02 | 1.06E+02 |
| Allowable TEDE Limit | 5.00E+01 | 2.50E+02 | 2.50E+02 |

APR1400 DCD TIER 2

Replace with next page F

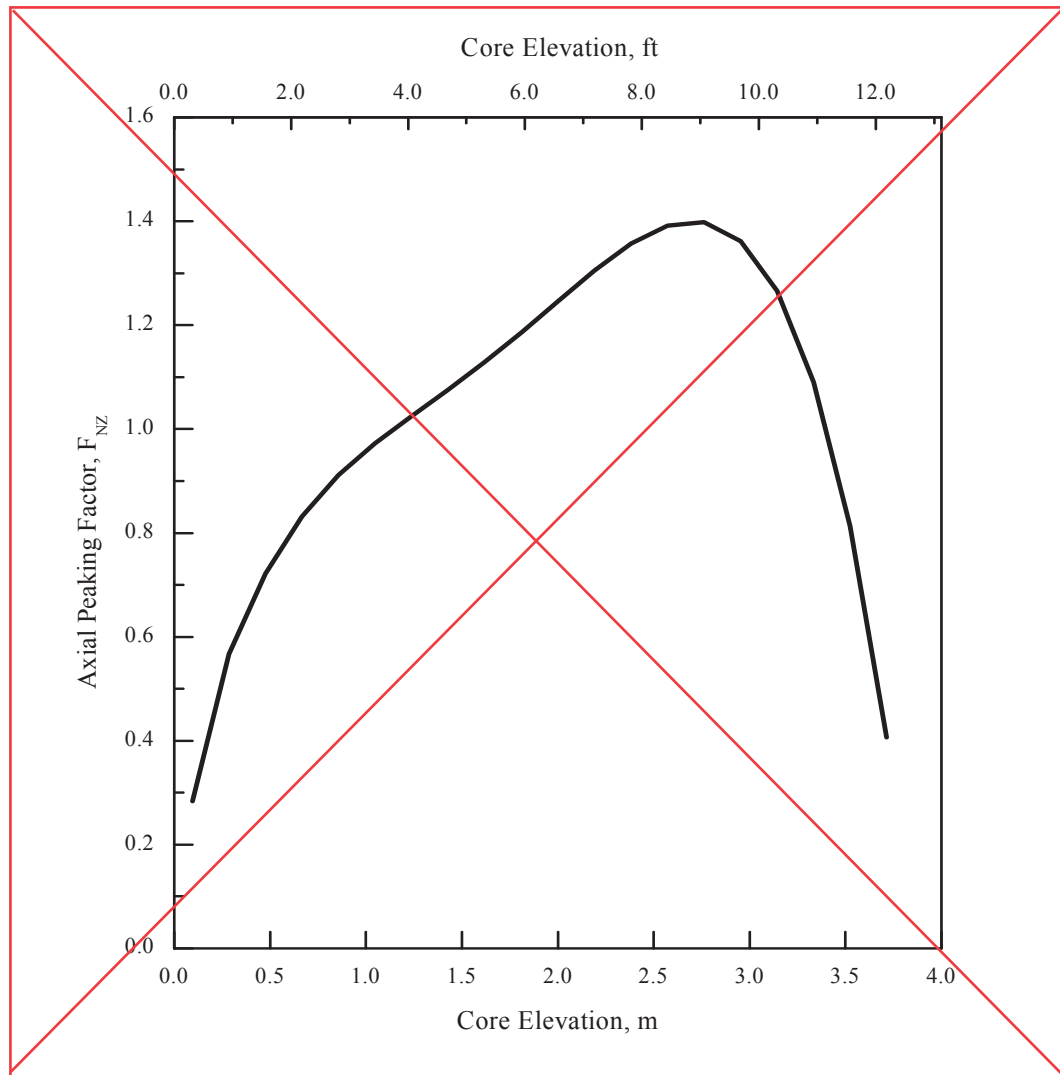
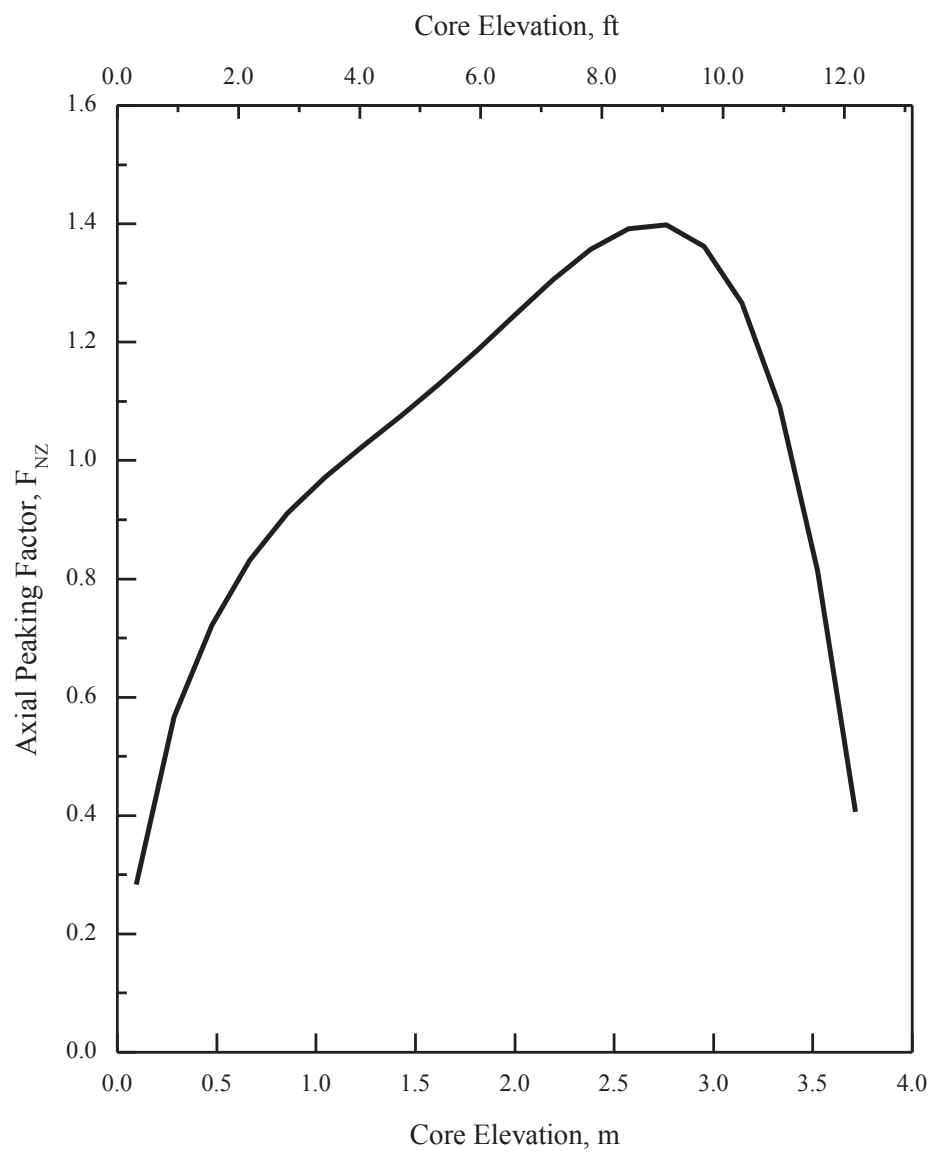


Figure 15.6.5-1 Axial Power Distribution at Large Break

F



APR1400 DCD TIER 2

Replace with next page G

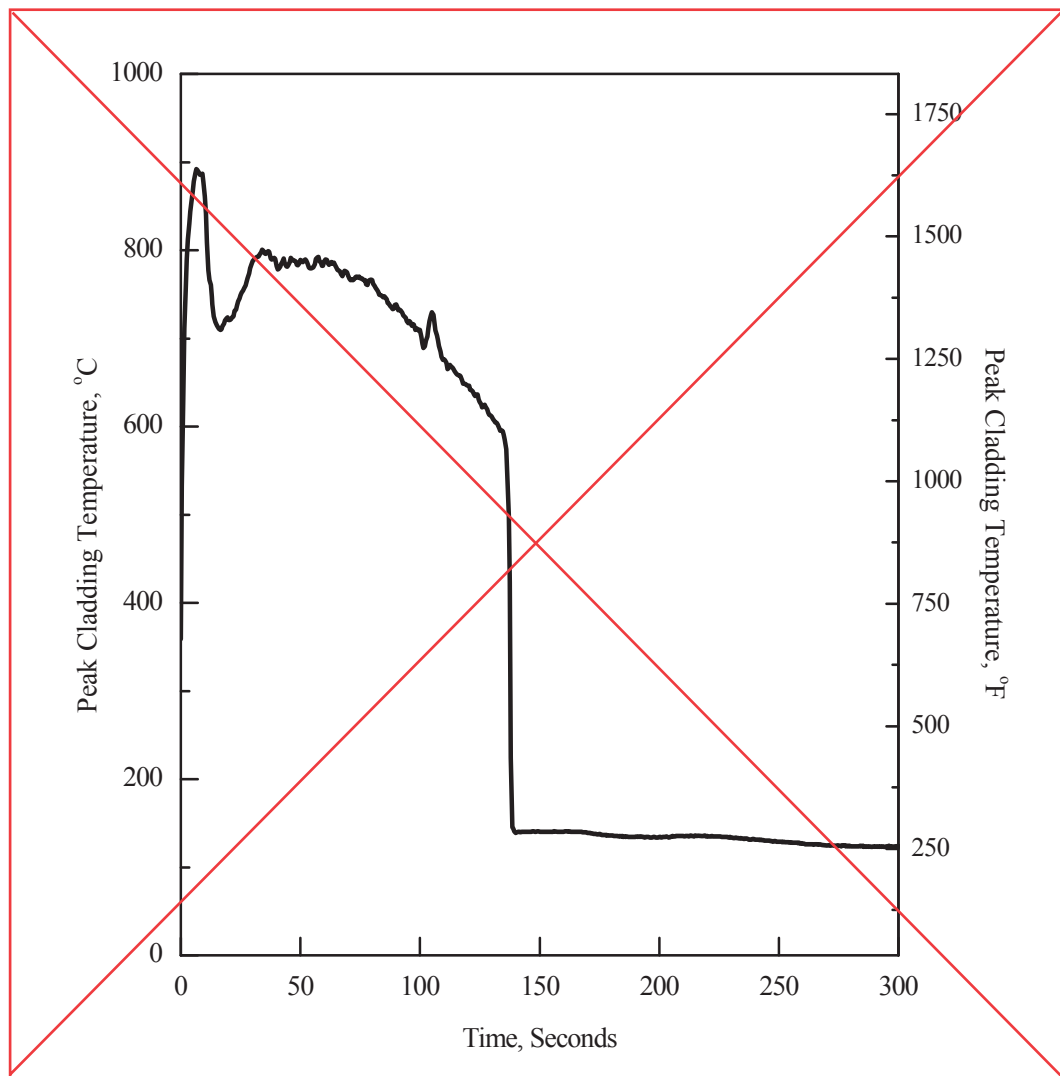
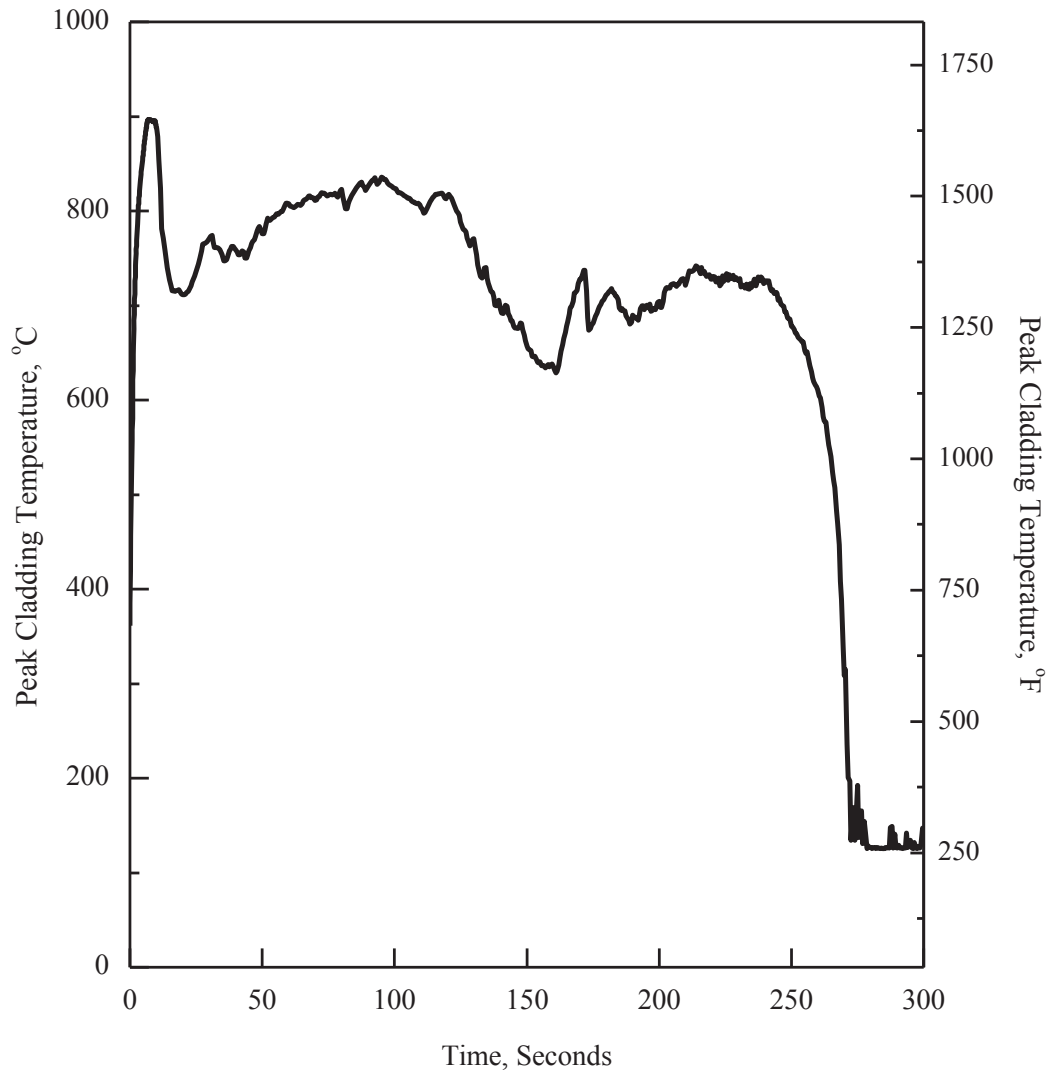


Figure 15.6.5-2 1.0x Double-ended Guillotine Break in Pump Discharge Leg (Peak Cladding Temperature)

G



APR1400 DCD TIER 2

Replace with next page H

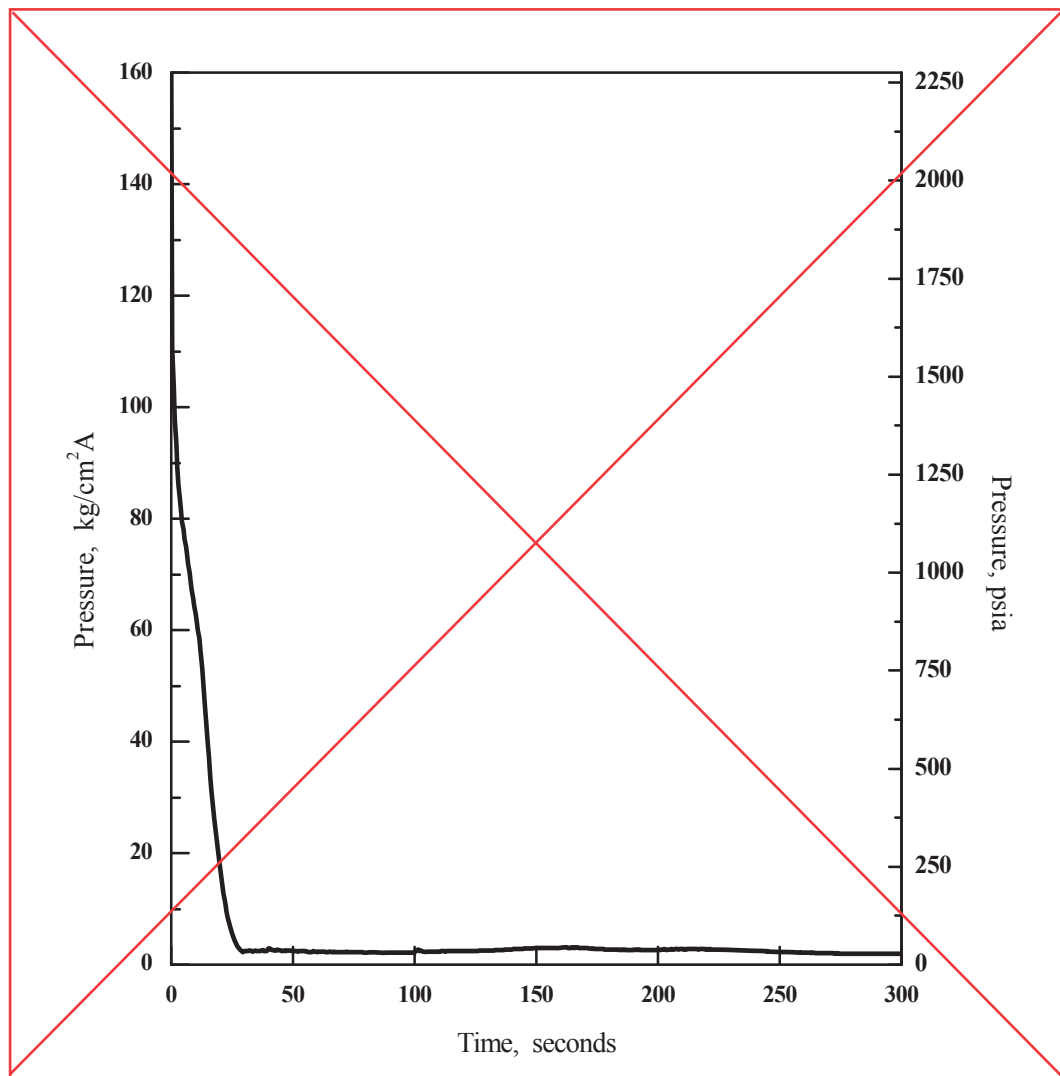
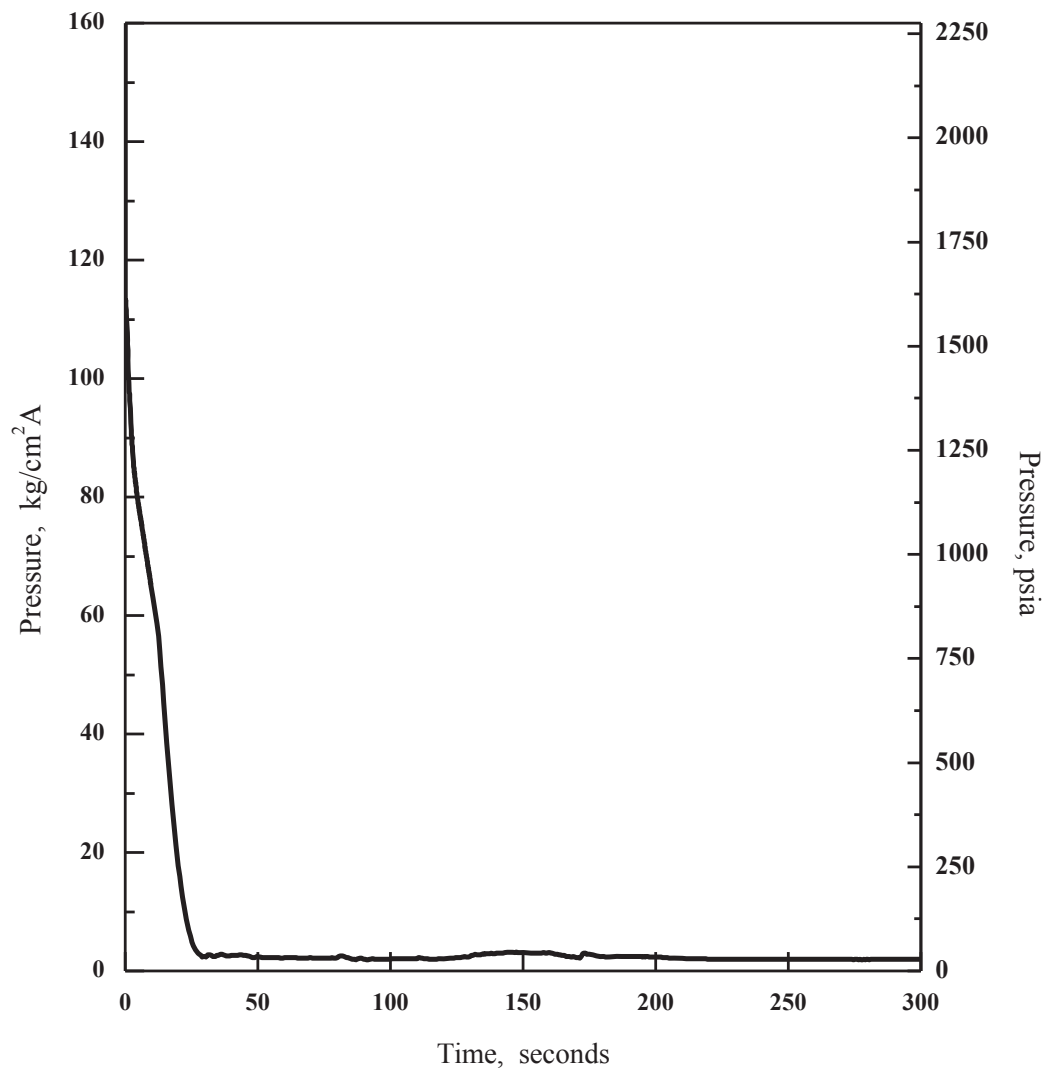


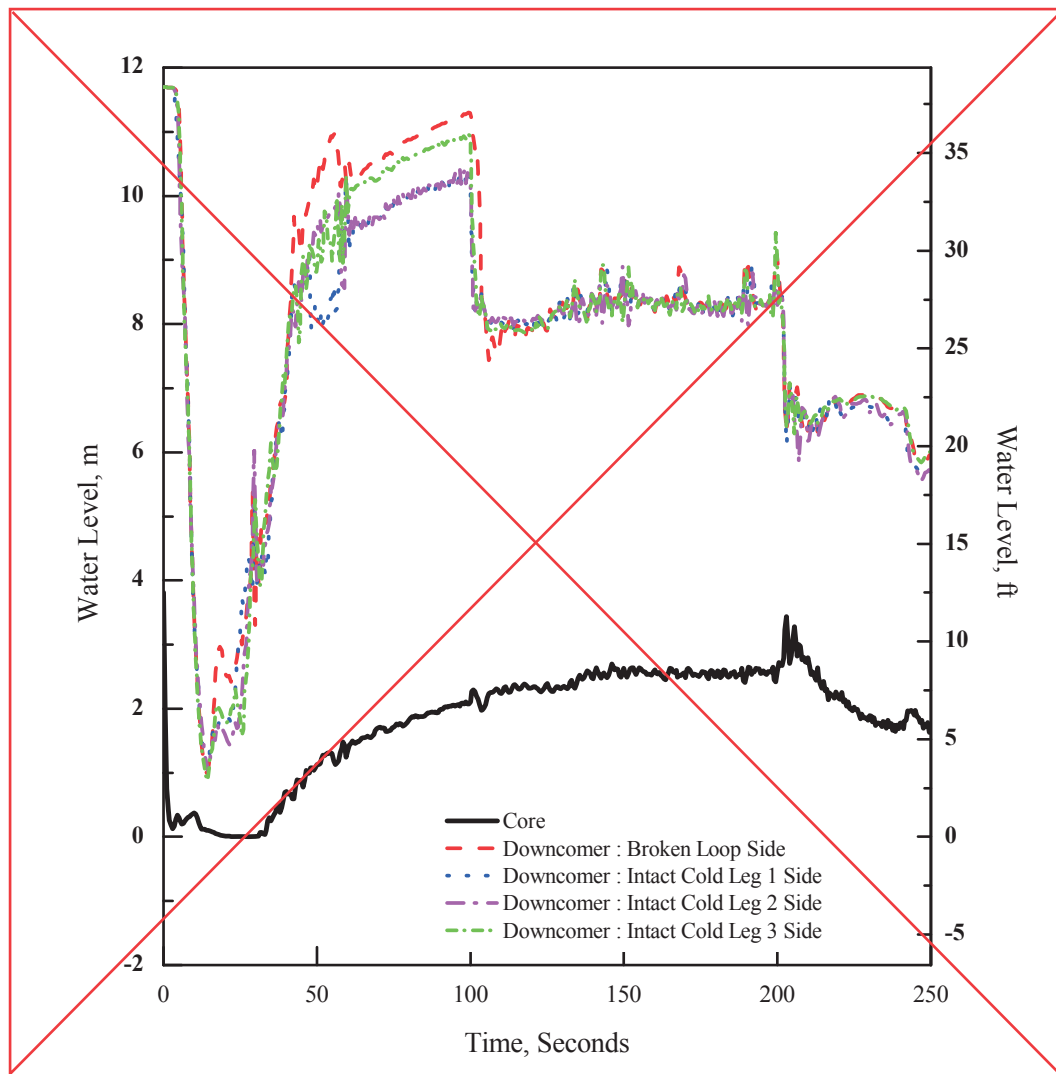
Figure 15.6.5-3 1.0 x Double-ended Guillotine Break in Pump Discharge Leg (Core Pressure)

H



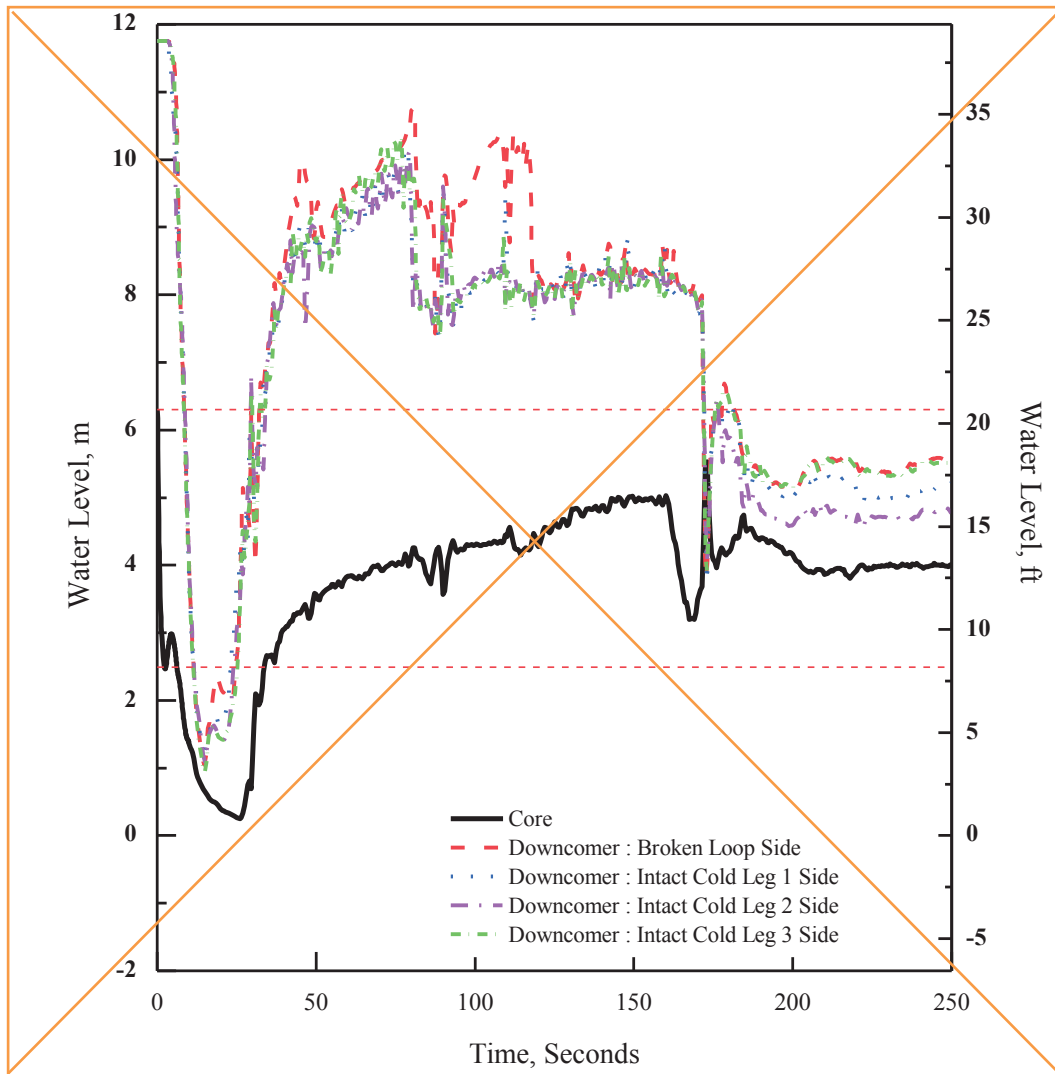
APR1400 DCD TIER 2

Replace with next page I

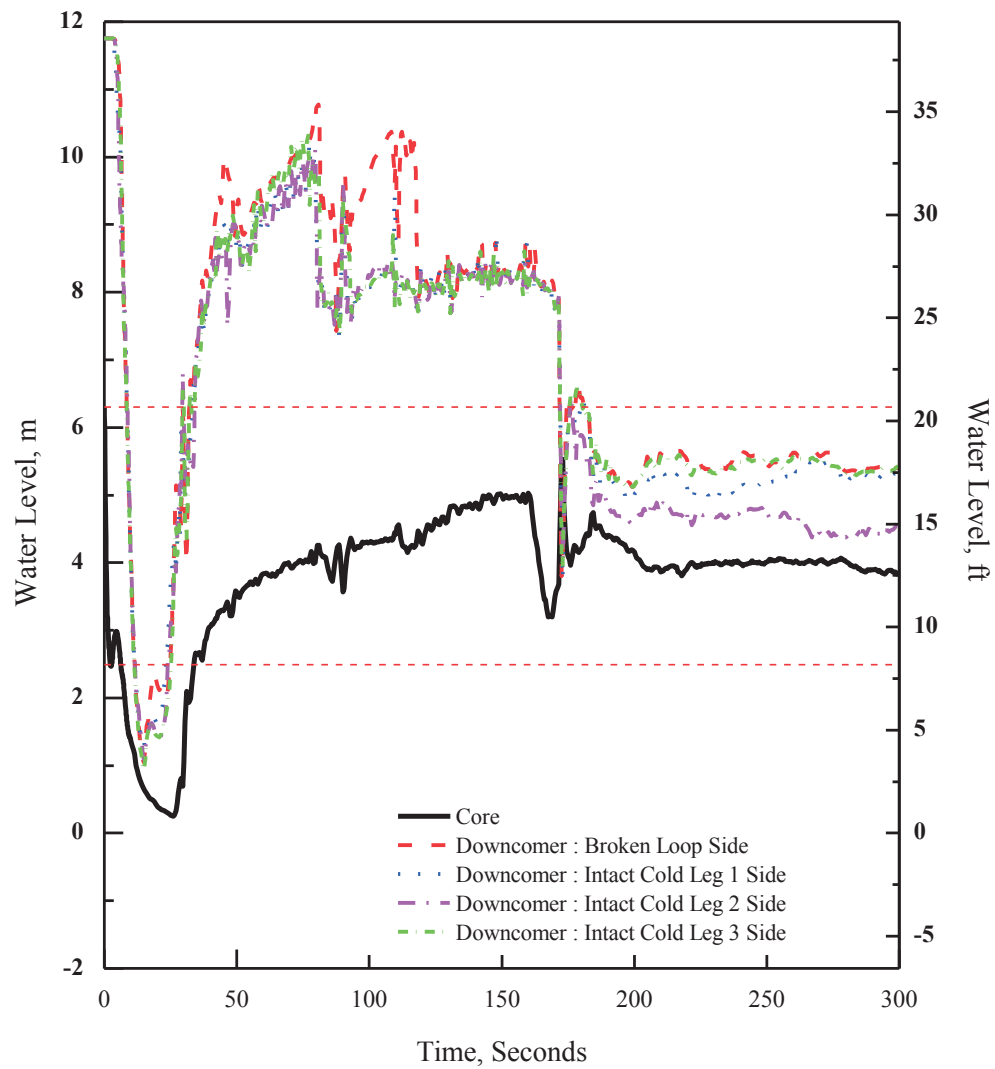


**Figure 15.6.5-4 1.0 × Double-ended Guillotine Break in Pump Discharge Leg
(Water Level in Core and Downcommer)**

I

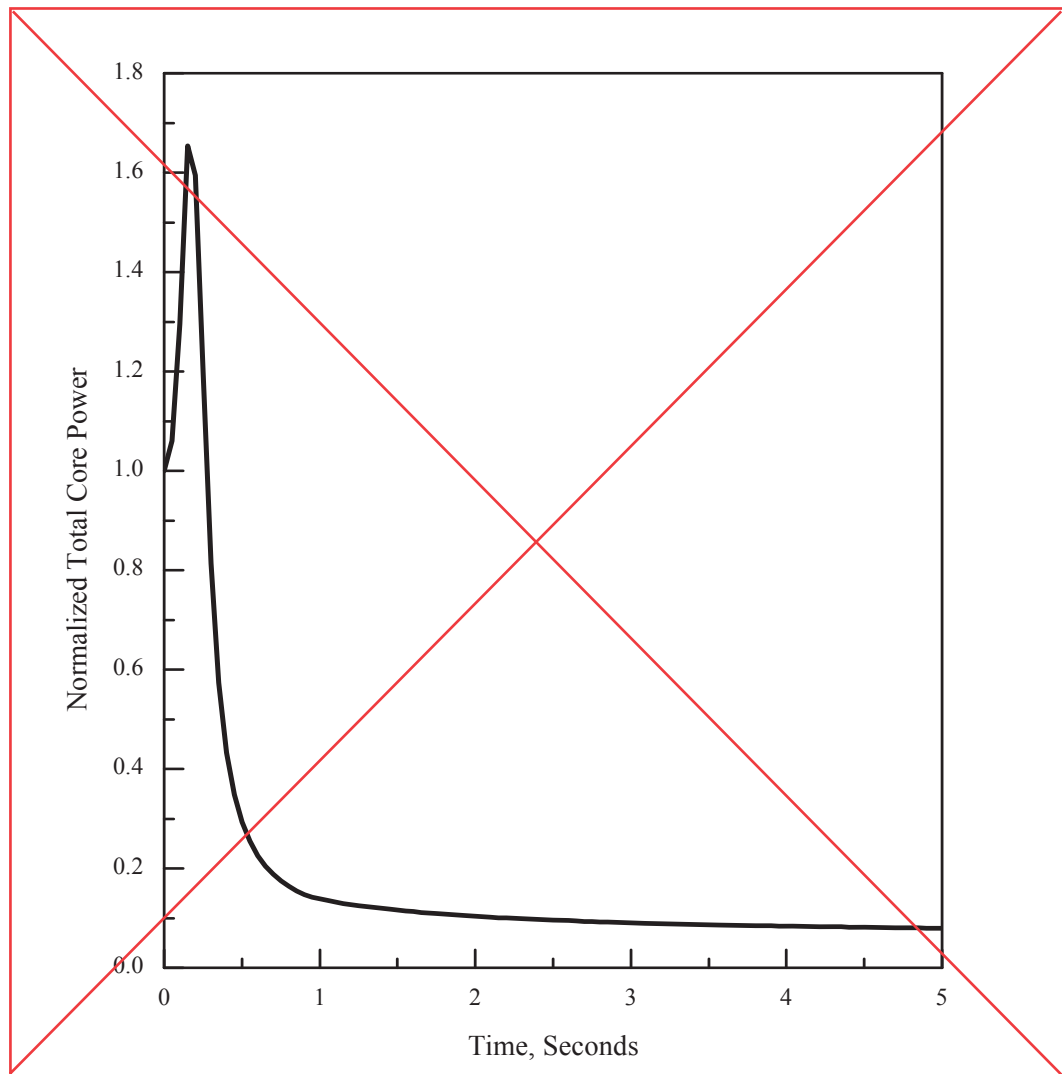


I



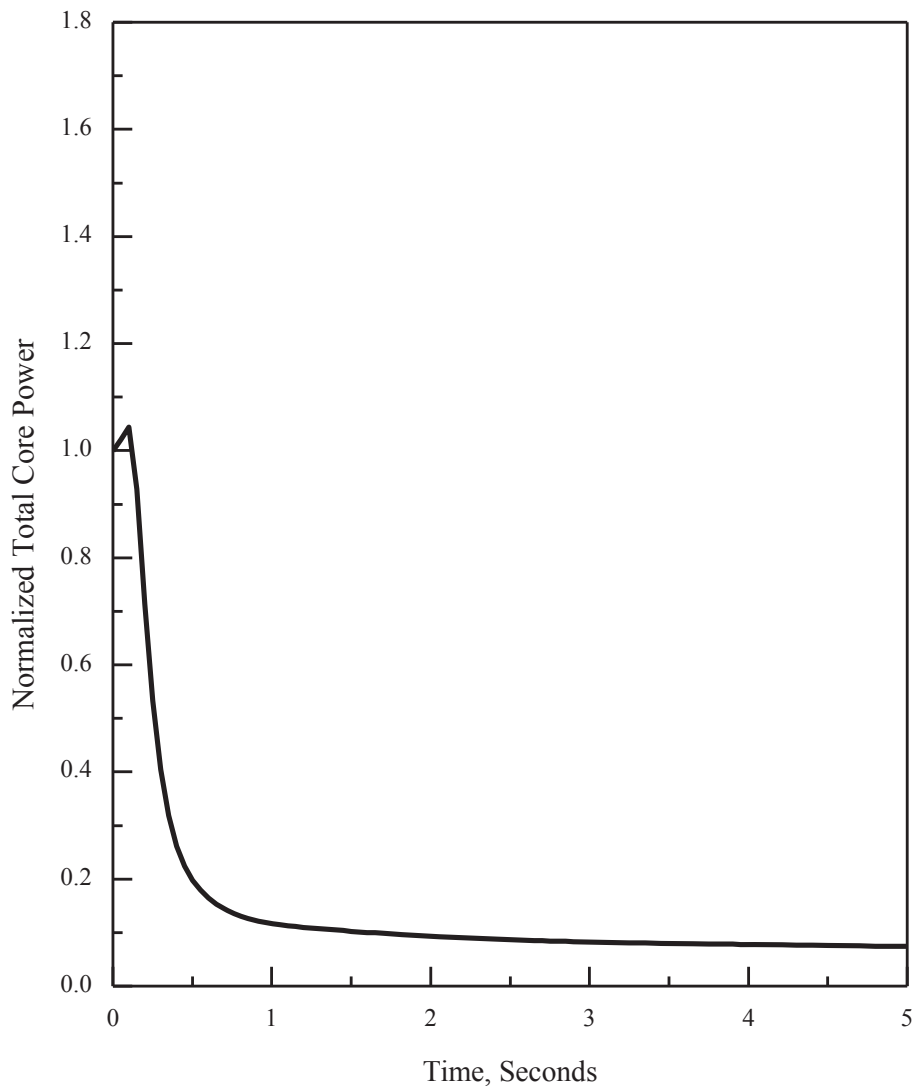
APR1400 DCD TIER 2

Replace with next page J



**Figure 15.6.5-5 1.0 x Double-ended Guillotine Break in Pump Discharge Leg
(Normalized Core Power)**

J



APR1400 DCD TIER 2

Replace with next page K

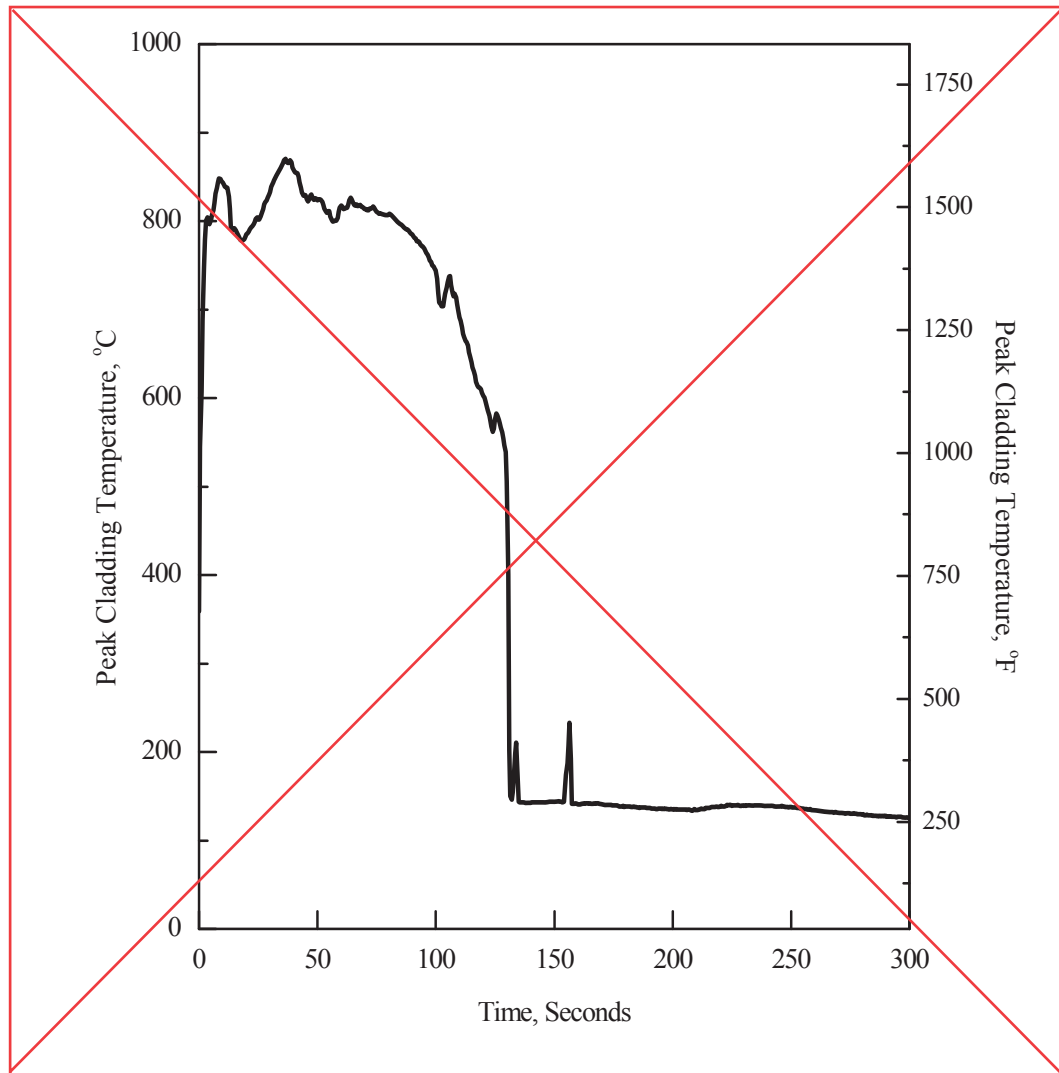
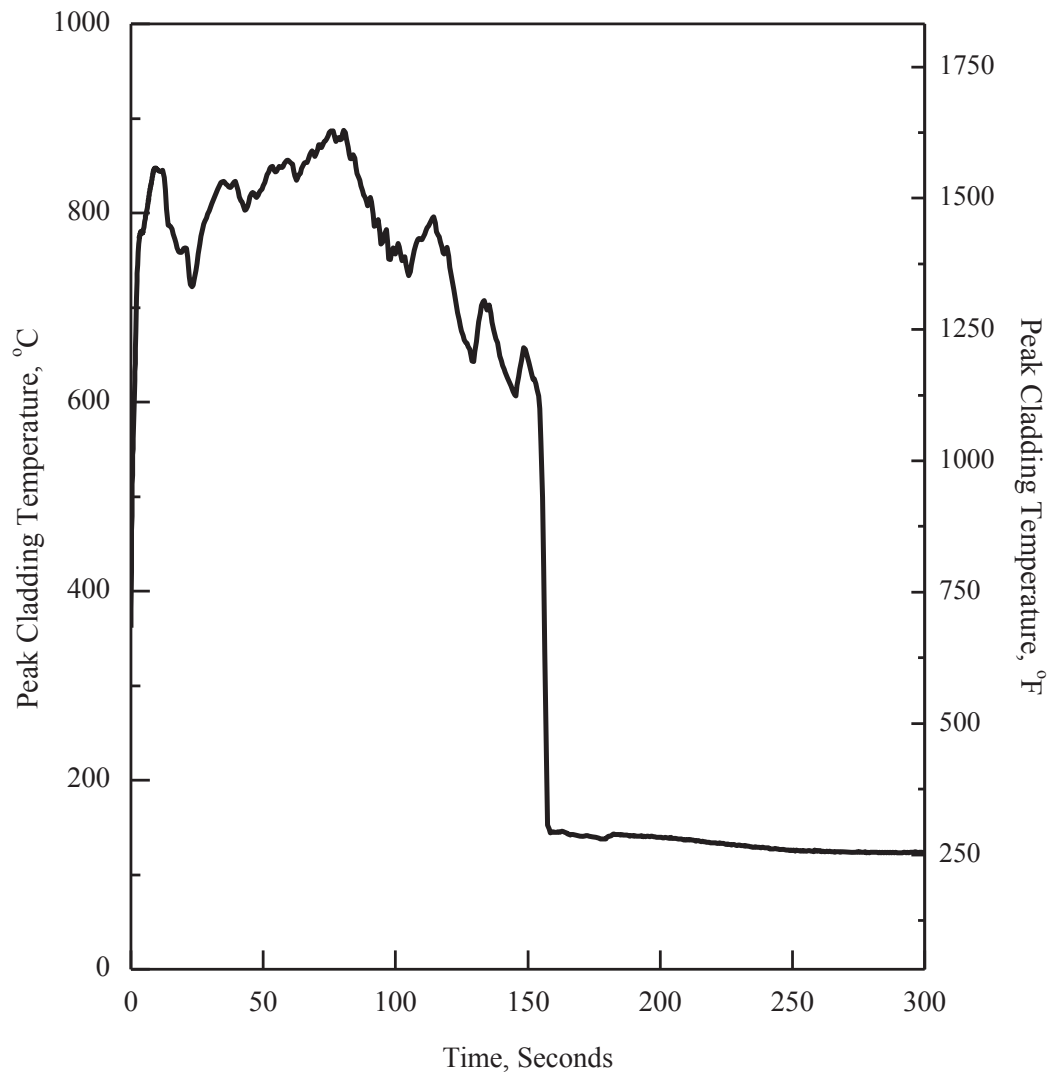


Figure 15.6.5-6 0.8 × Double-ended Guillotine Break in Pump Discharge Leg (Peak Cladding Temperature)

K



APR1400 DCD TIER 2

Replace with next page L

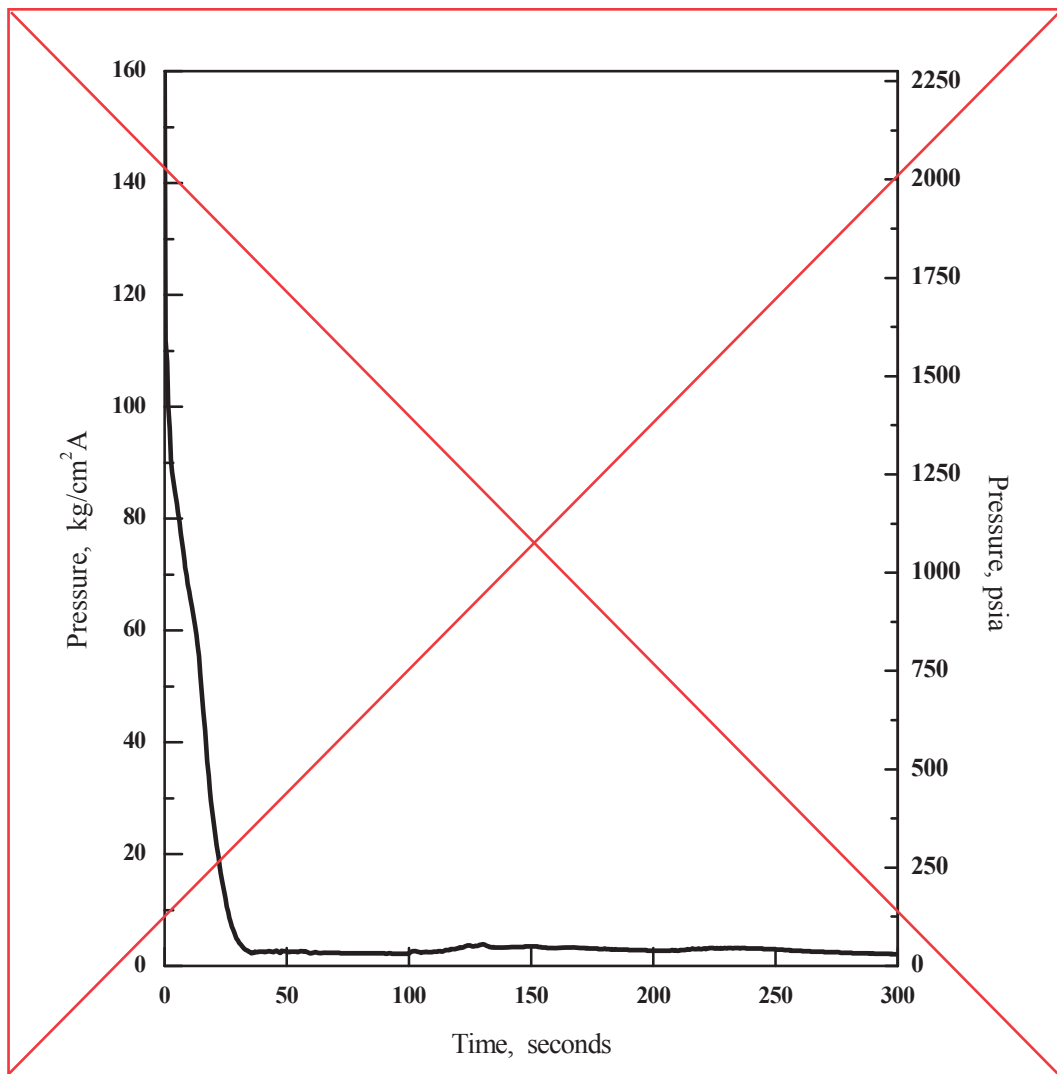
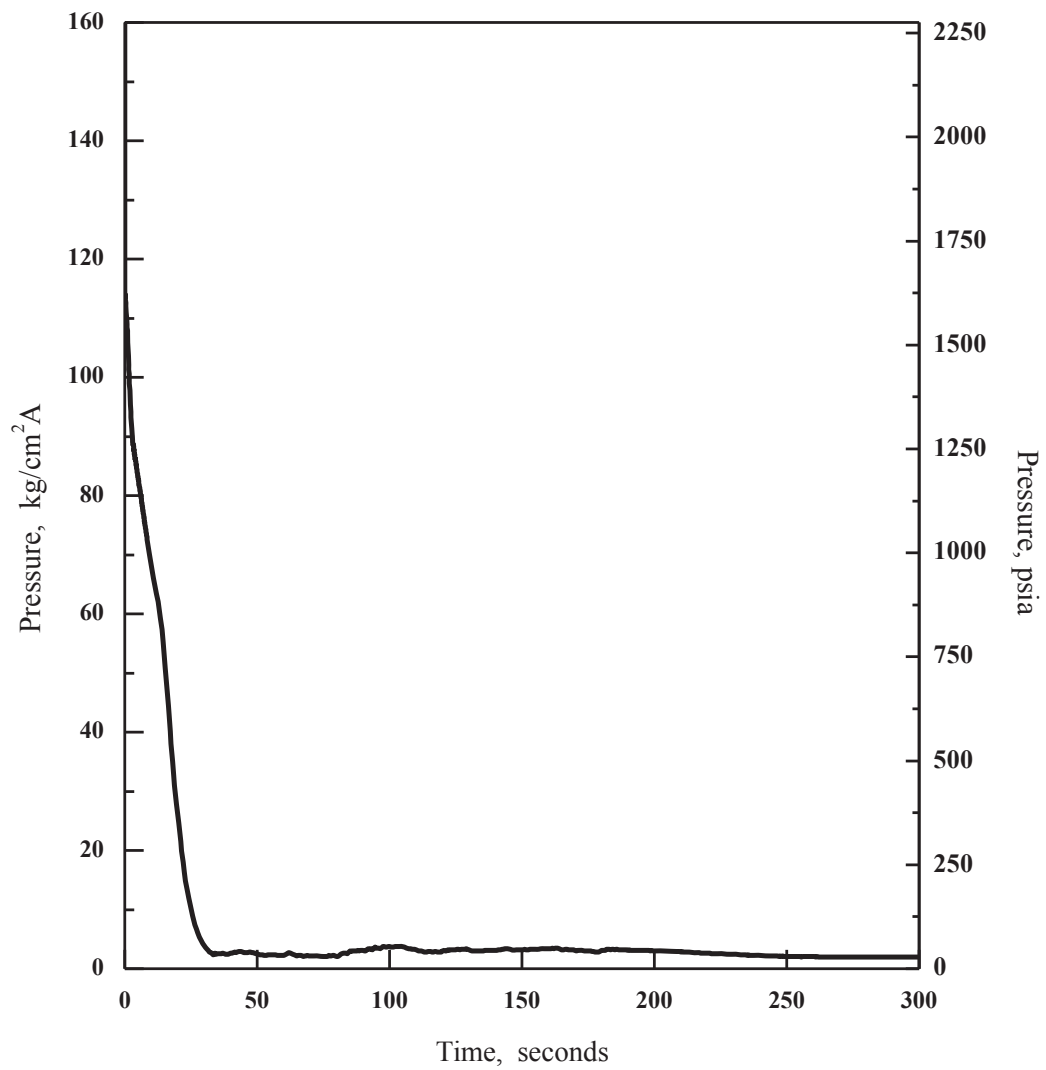


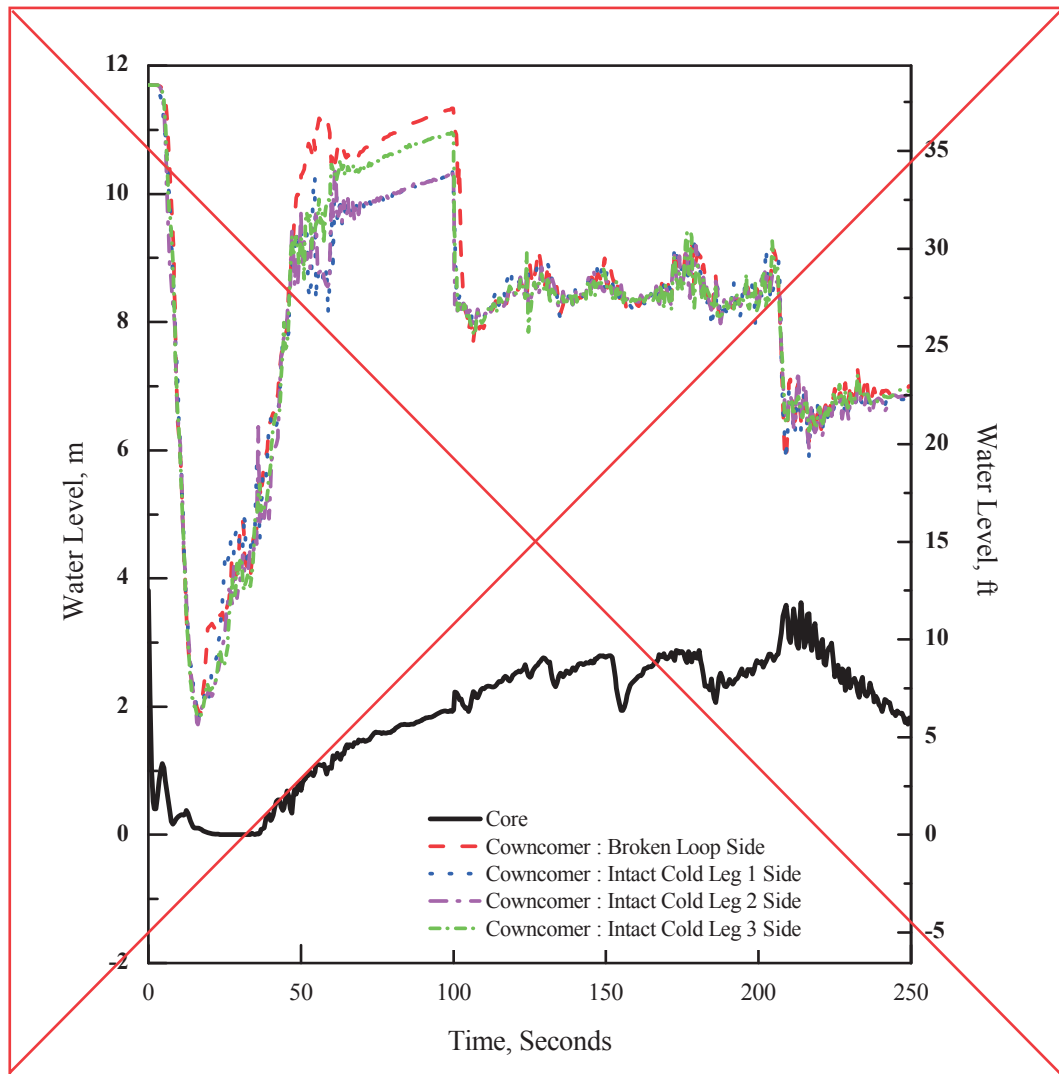
Figure 15.6.5-7 0.8 × Double-ended Guillotine Break in Pump Discharge Leg
(Core Pressure)

L



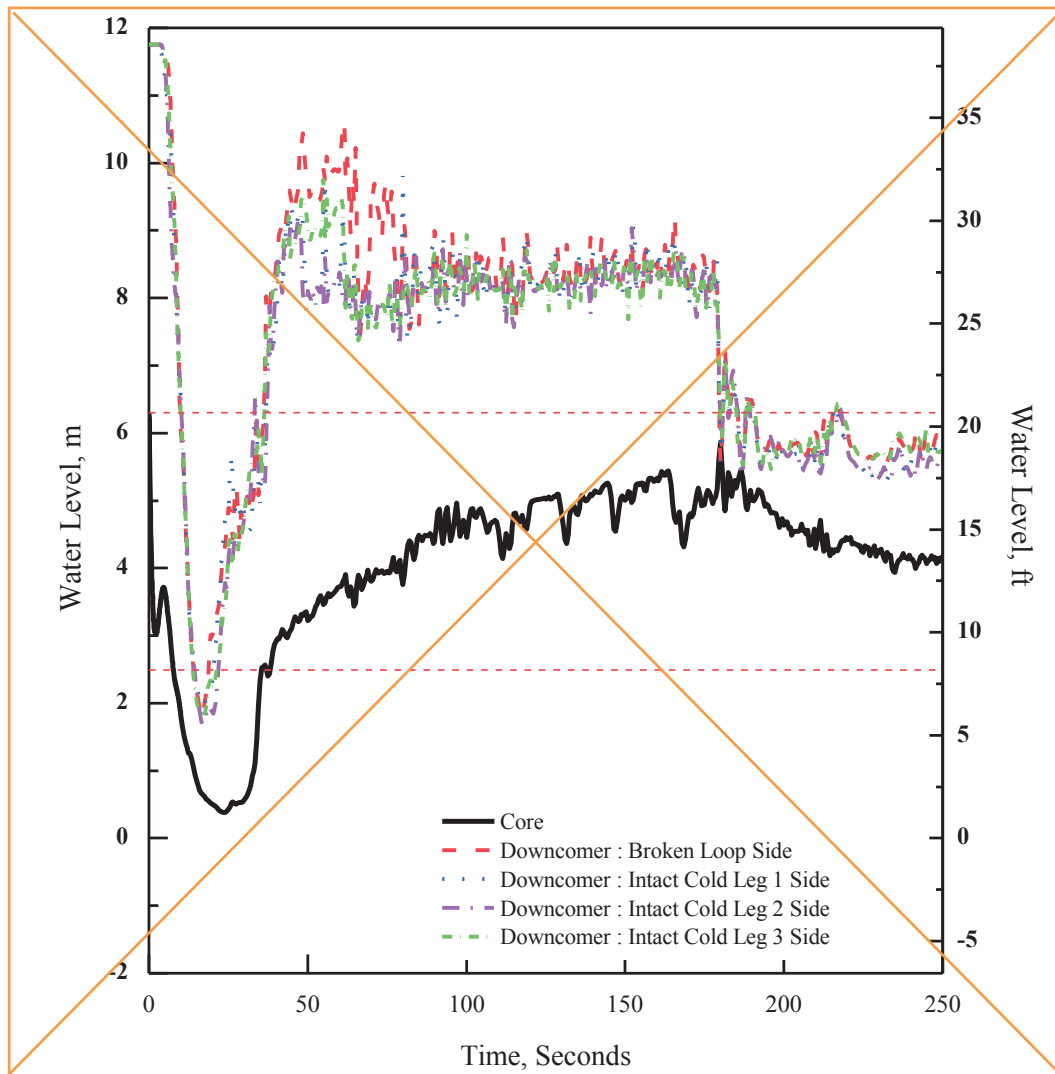
APR1400 DCD TIER 2

Replace with next page M

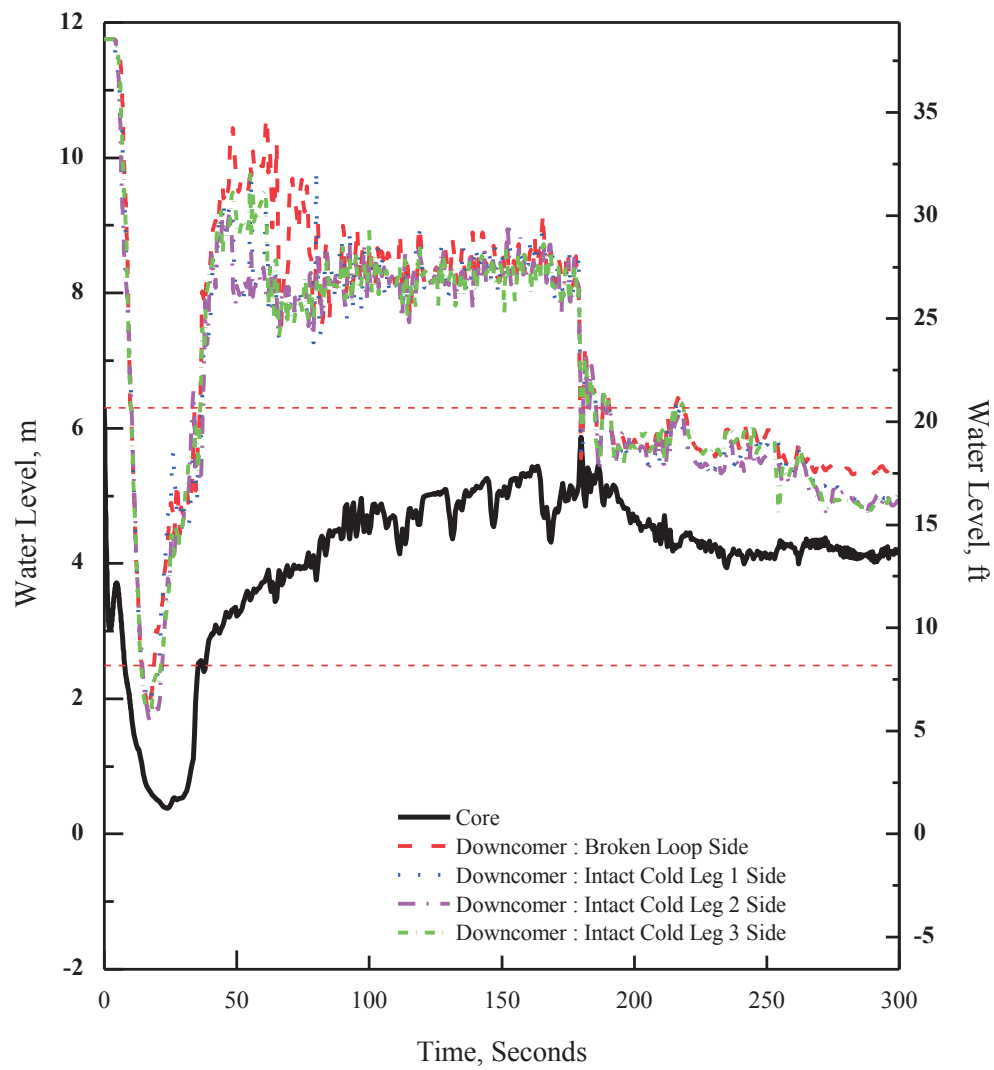


**Figure 15.6.5-8 0.8 × Double-ended Guillotine Break in Pump Discharge Leg
(Water Level in Core and Downcommer)**

M

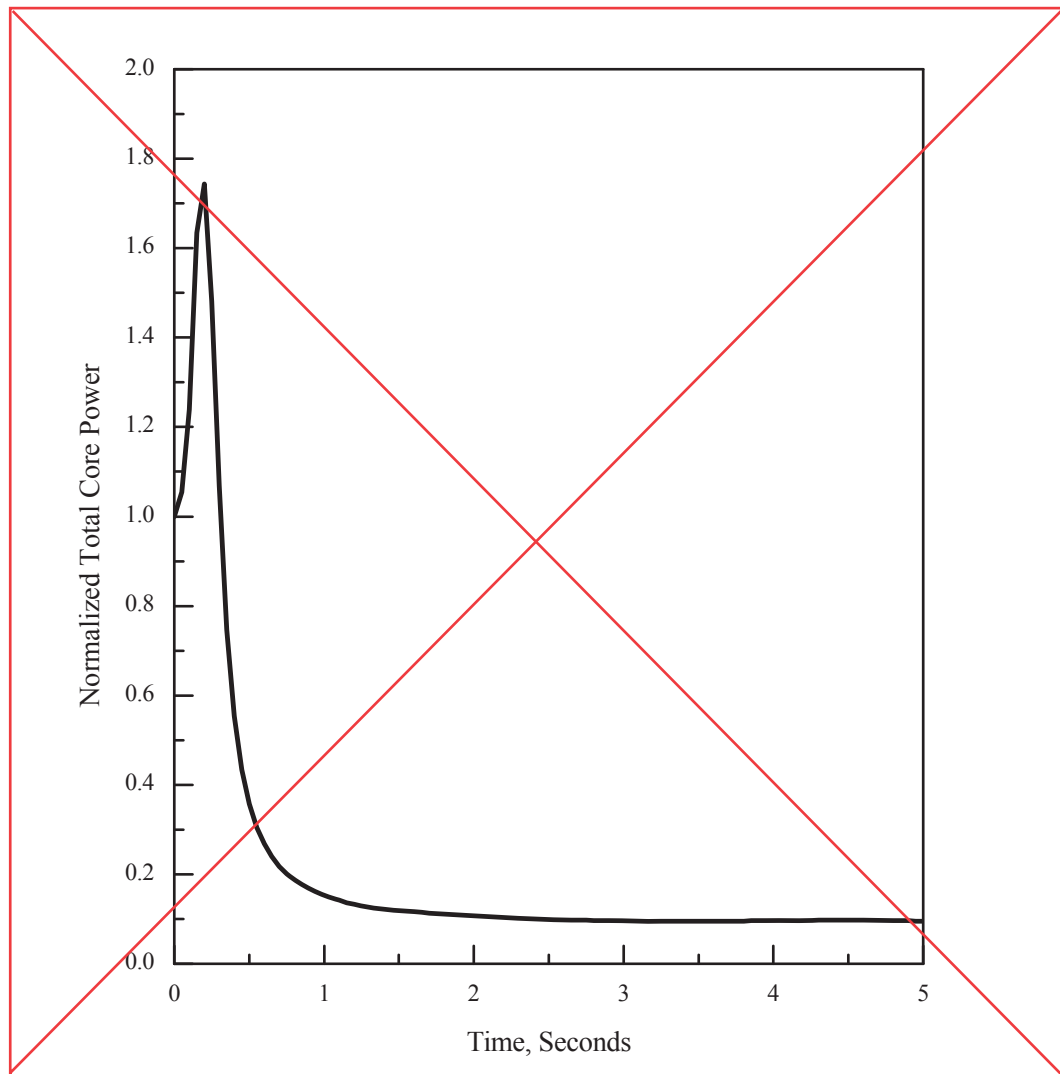


M



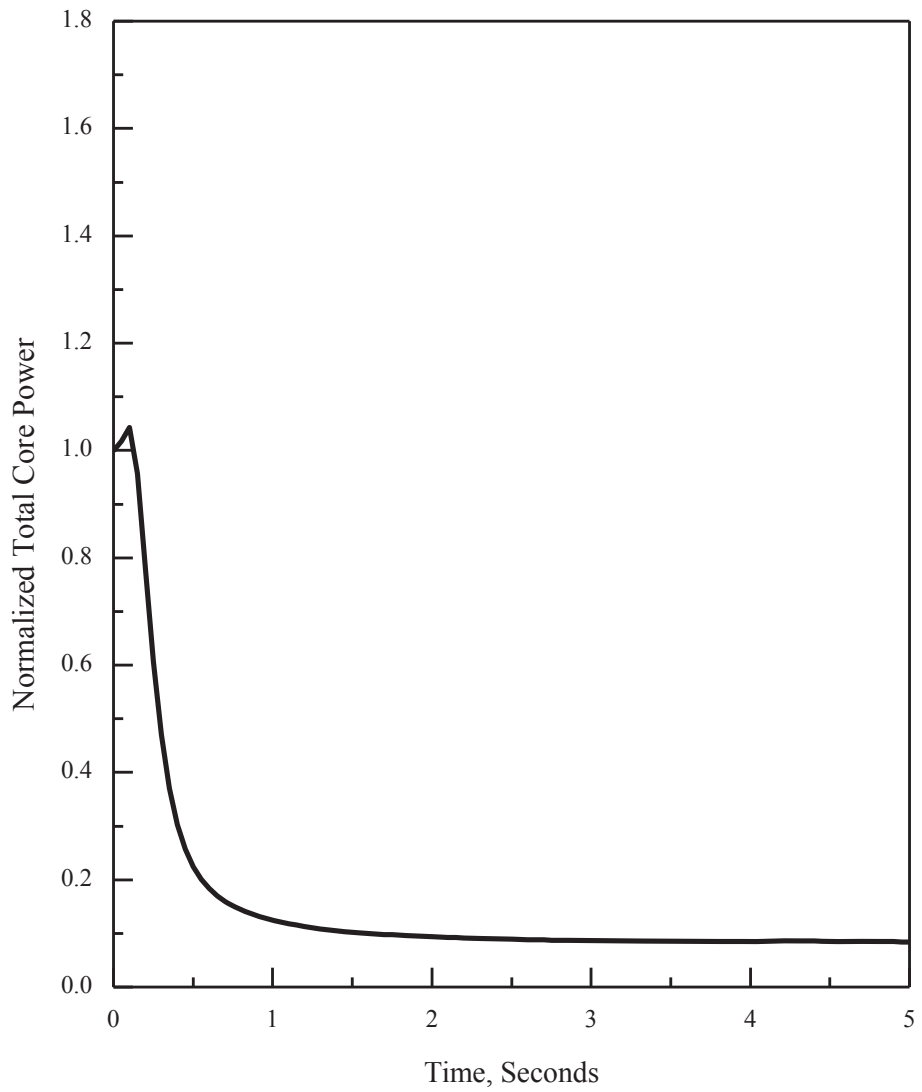
APR1400 DCD TIER 2

Replace with next page N



**Figure 15.6.5-9 0.8 × Double-ended Guillotine Break in Pump Discharge Leg
(Normalized Core Power)**

N



APR1400 DCD TIER 2

Replace with next page O

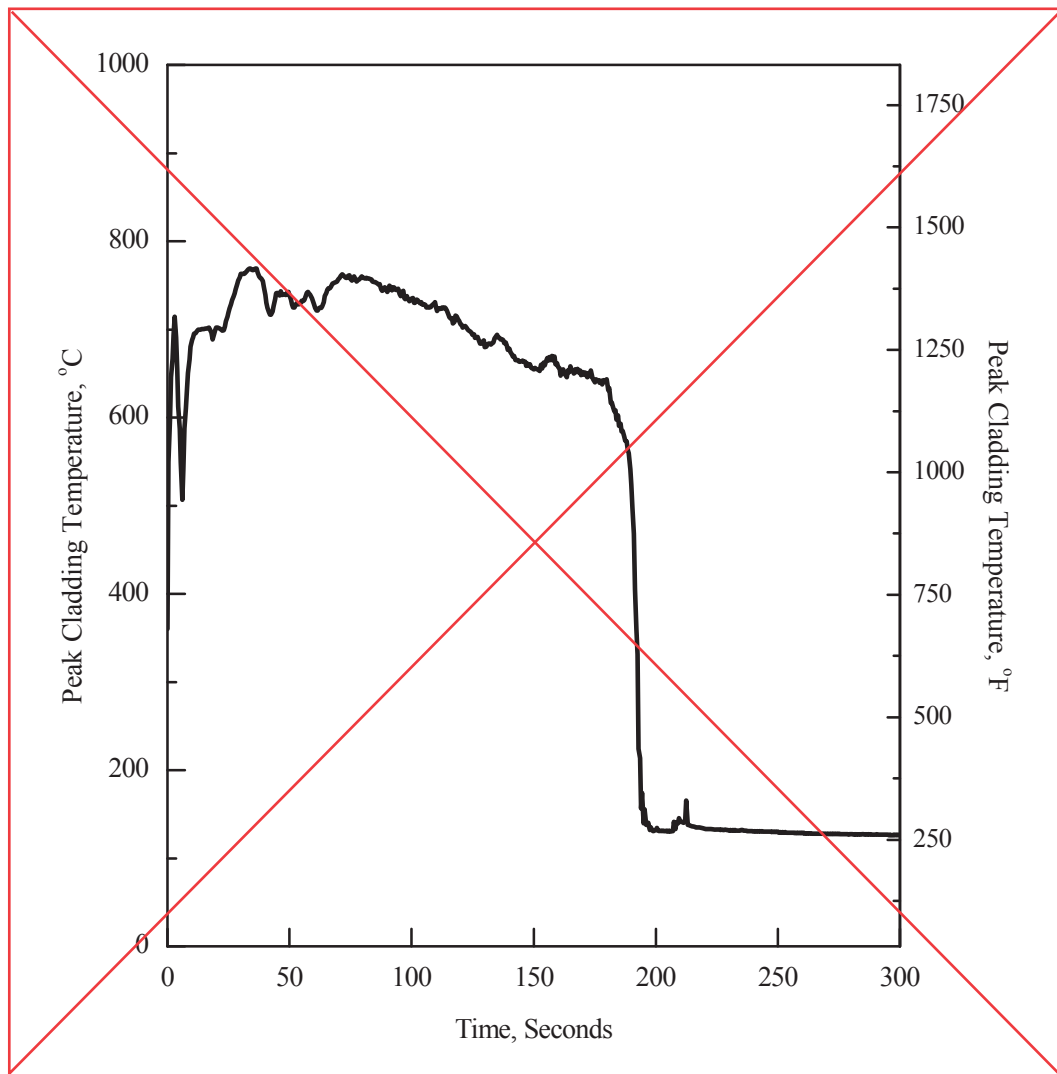
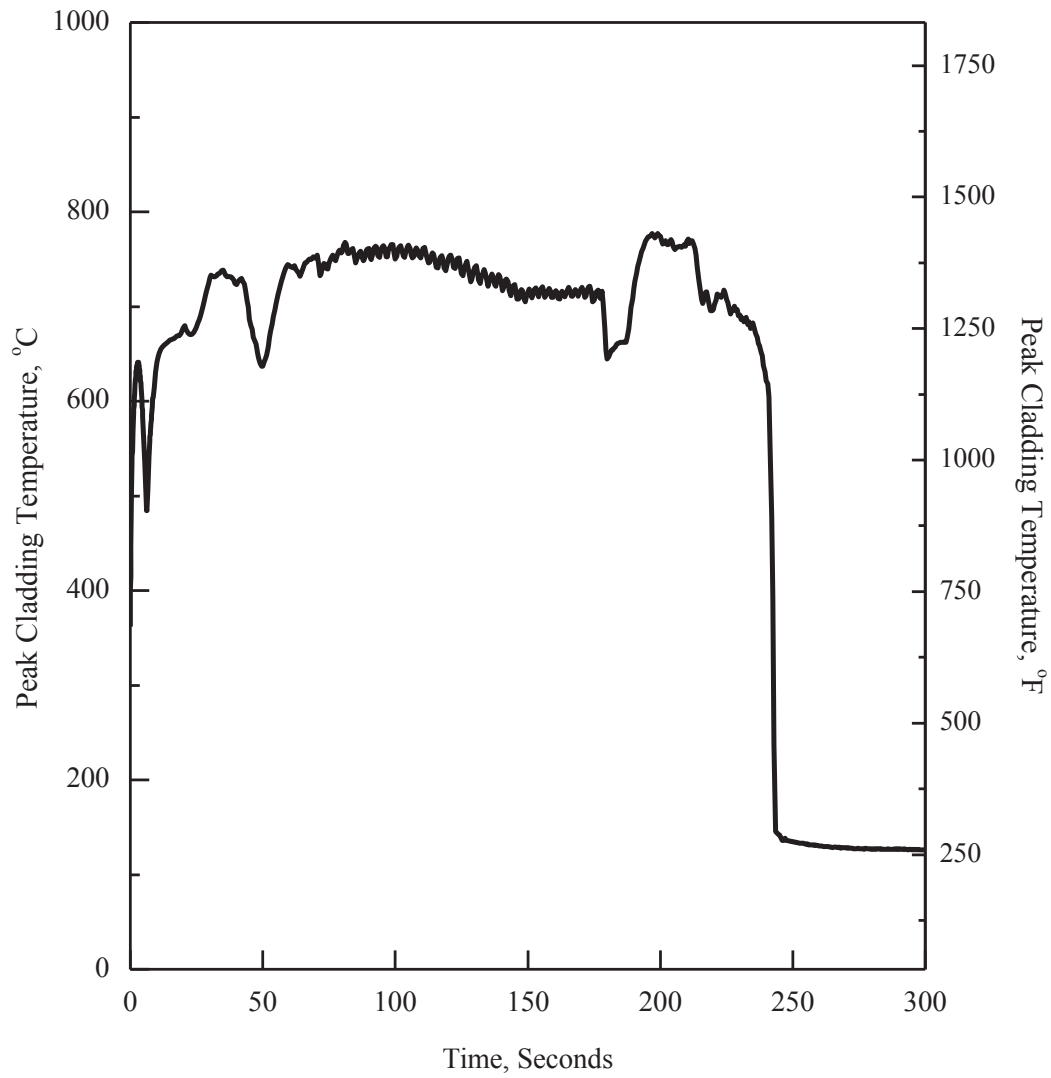


Figure 15.6.5-10 0.6 × Double-ended Guillotine Break in Pump Discharge Leg (Peak Cladding Temperature)

O



APR1400 DCD TIER 2

Replace with next page P

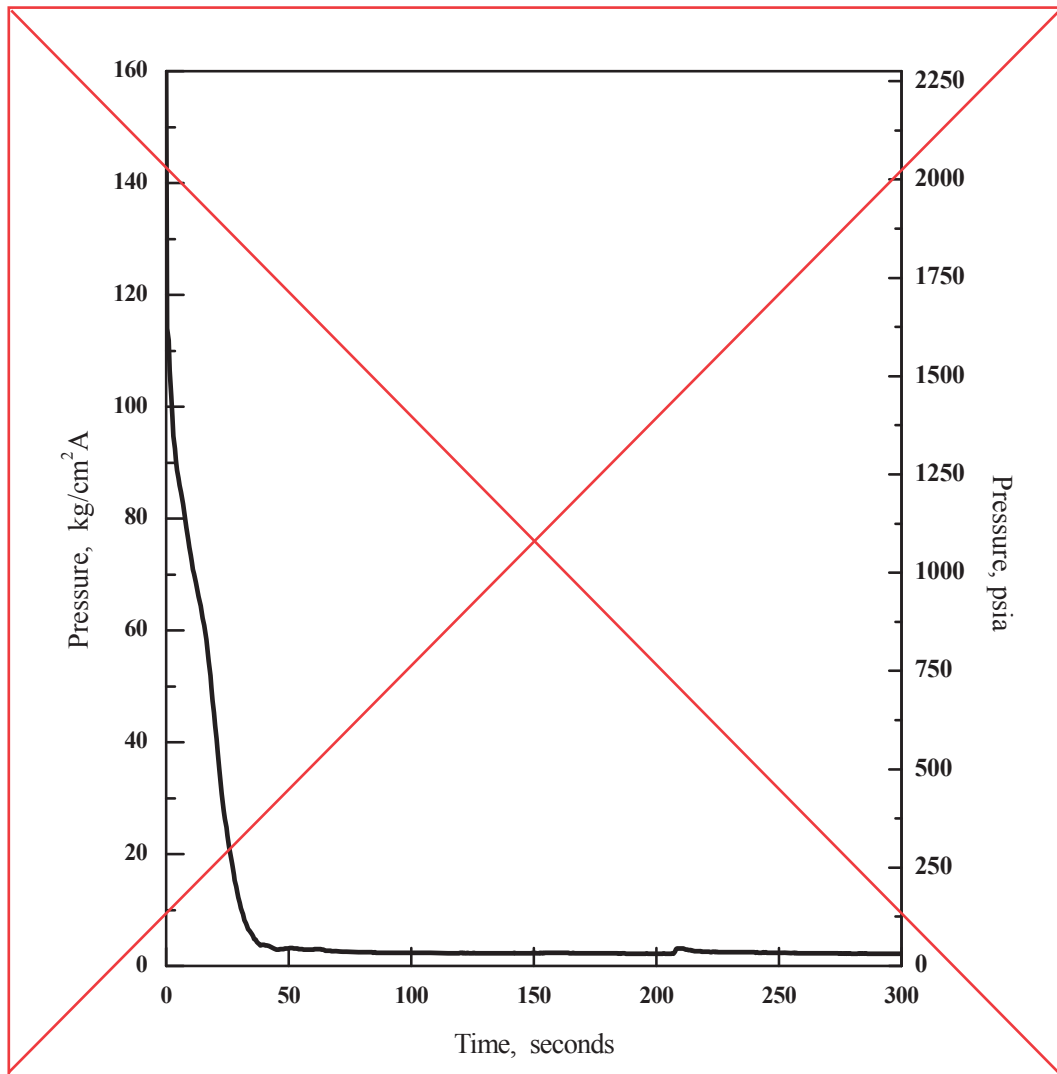
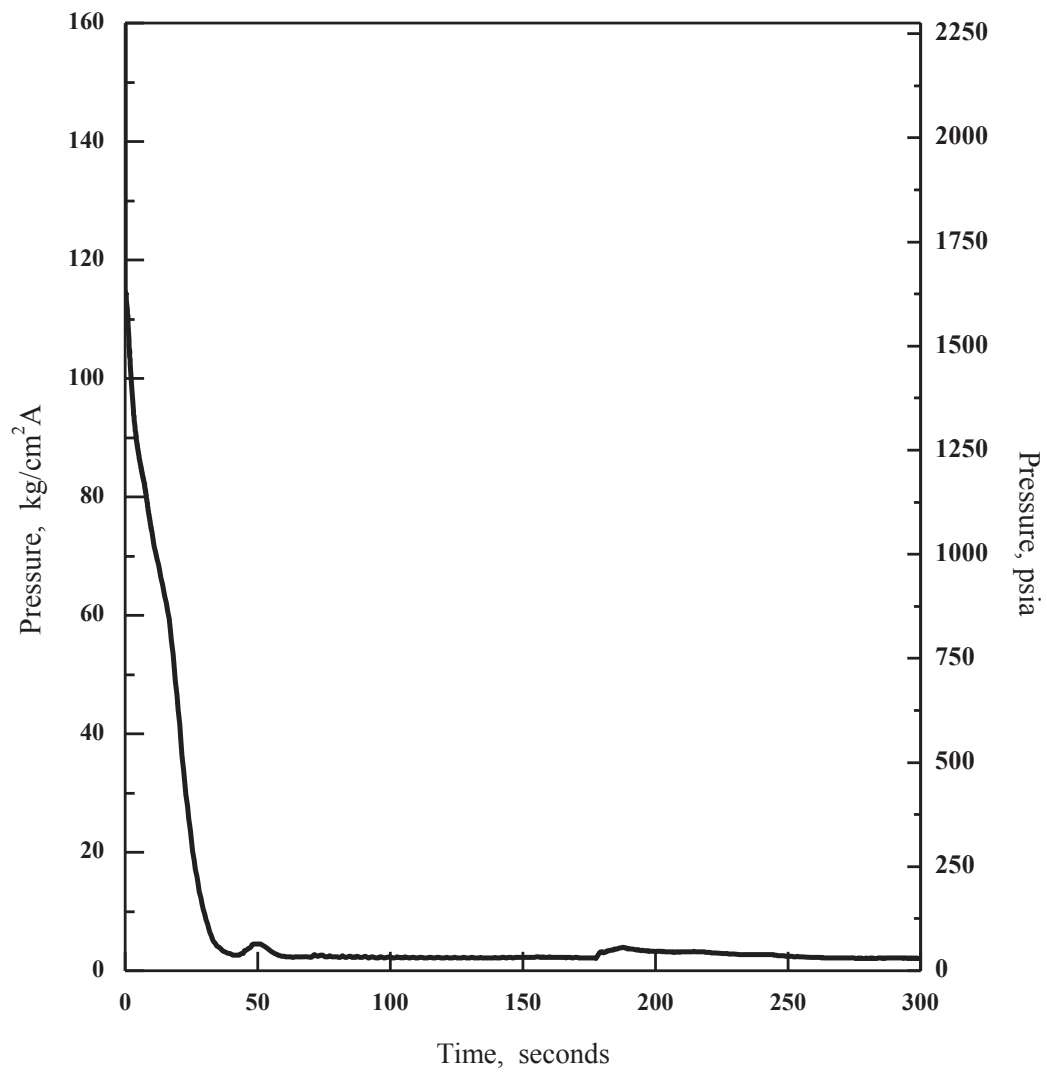


Figure 15.6.5-11 0.6 × Double-ended Guillotine Break in Pump Discharge Leg
(Core Pressure)

P



APR1400 DCD TIER 2

Replace with next page Q

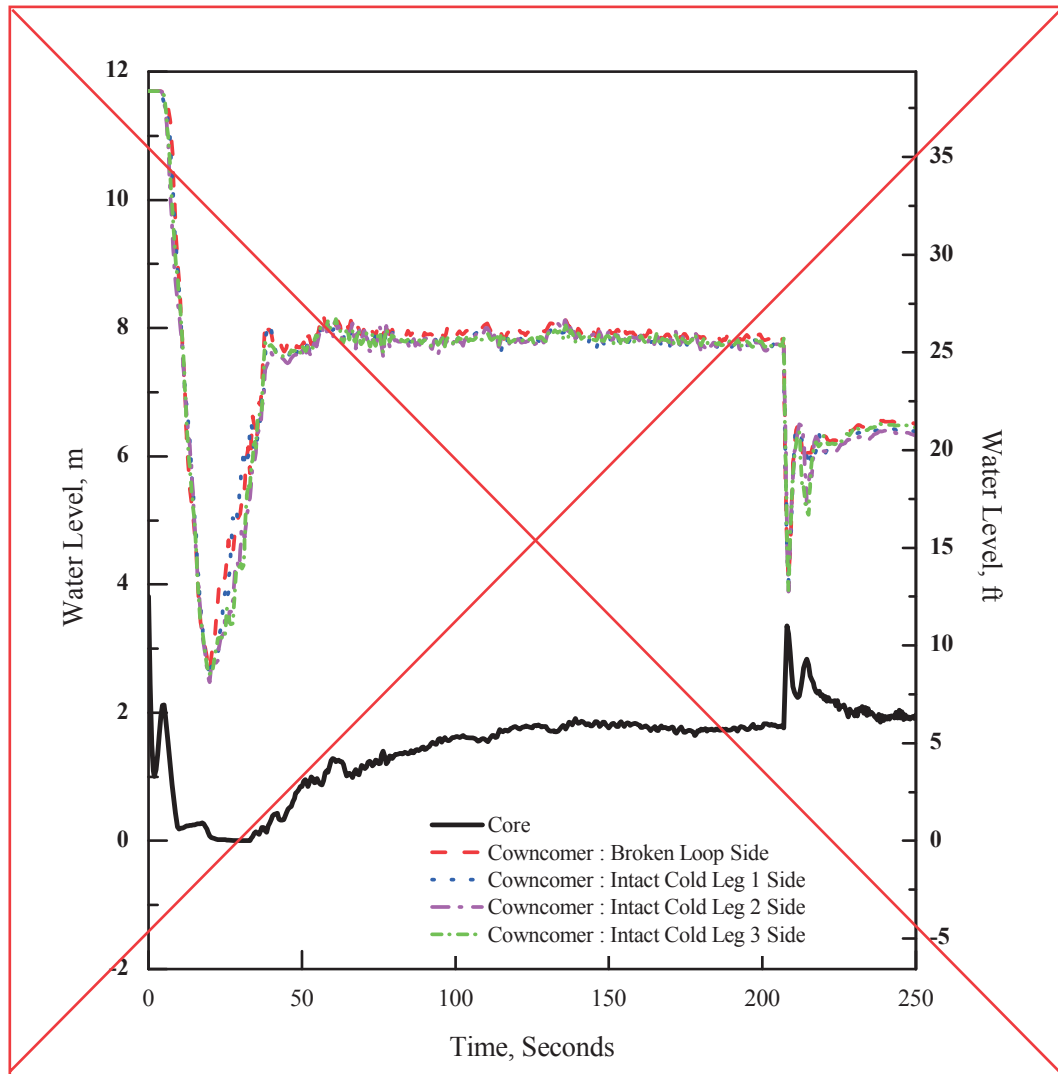
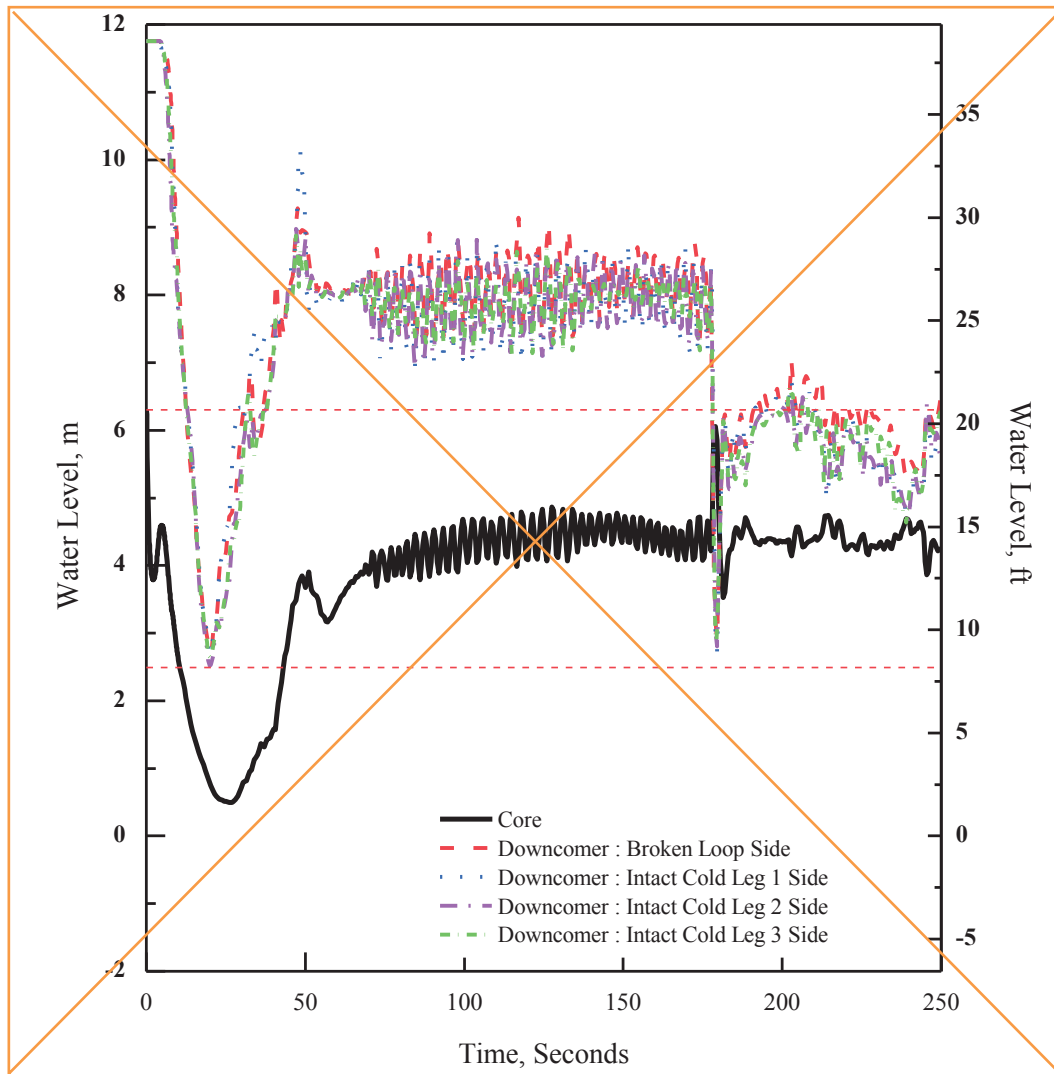
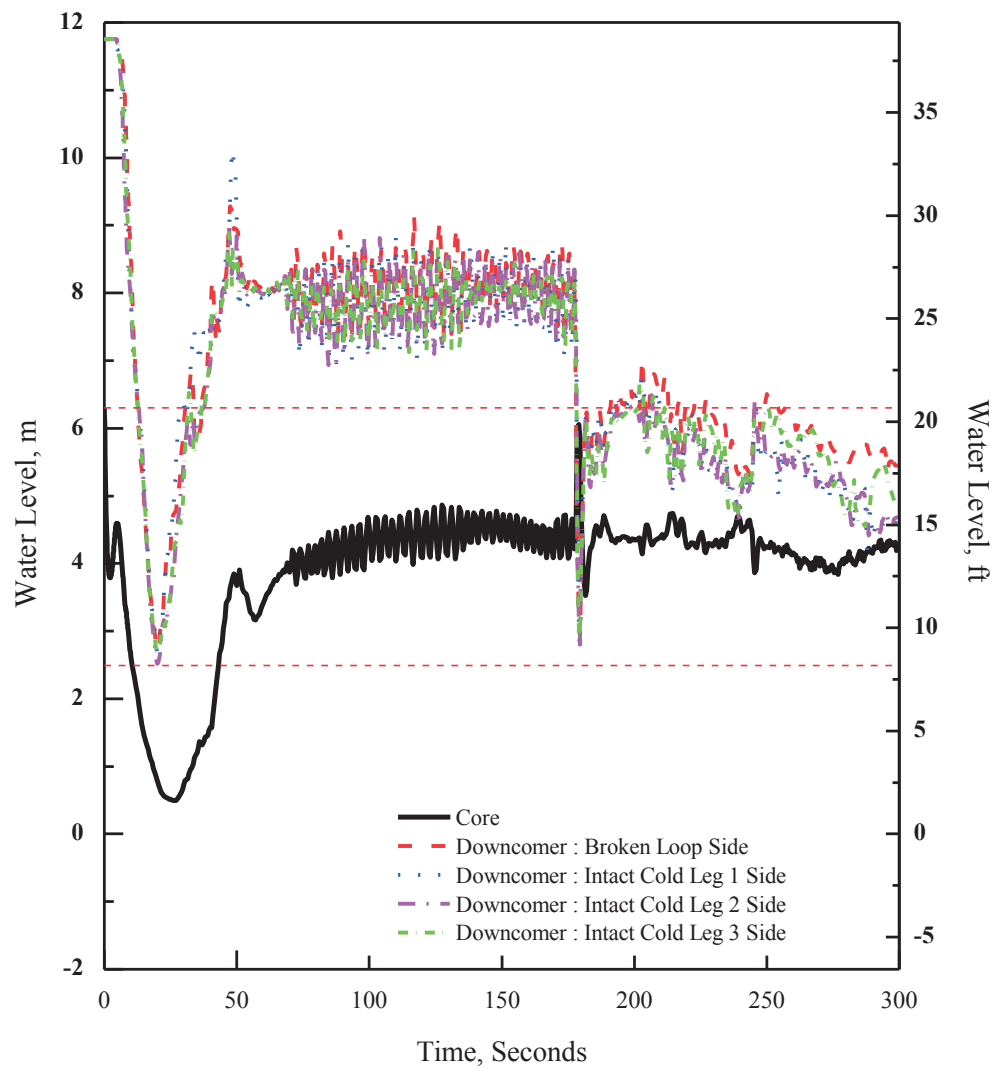


Figure 15.6.5-12 0.6 × Double-ended Guillotine Break in Pump Discharge Leg (Water Level in Core and Downcommer)

Q

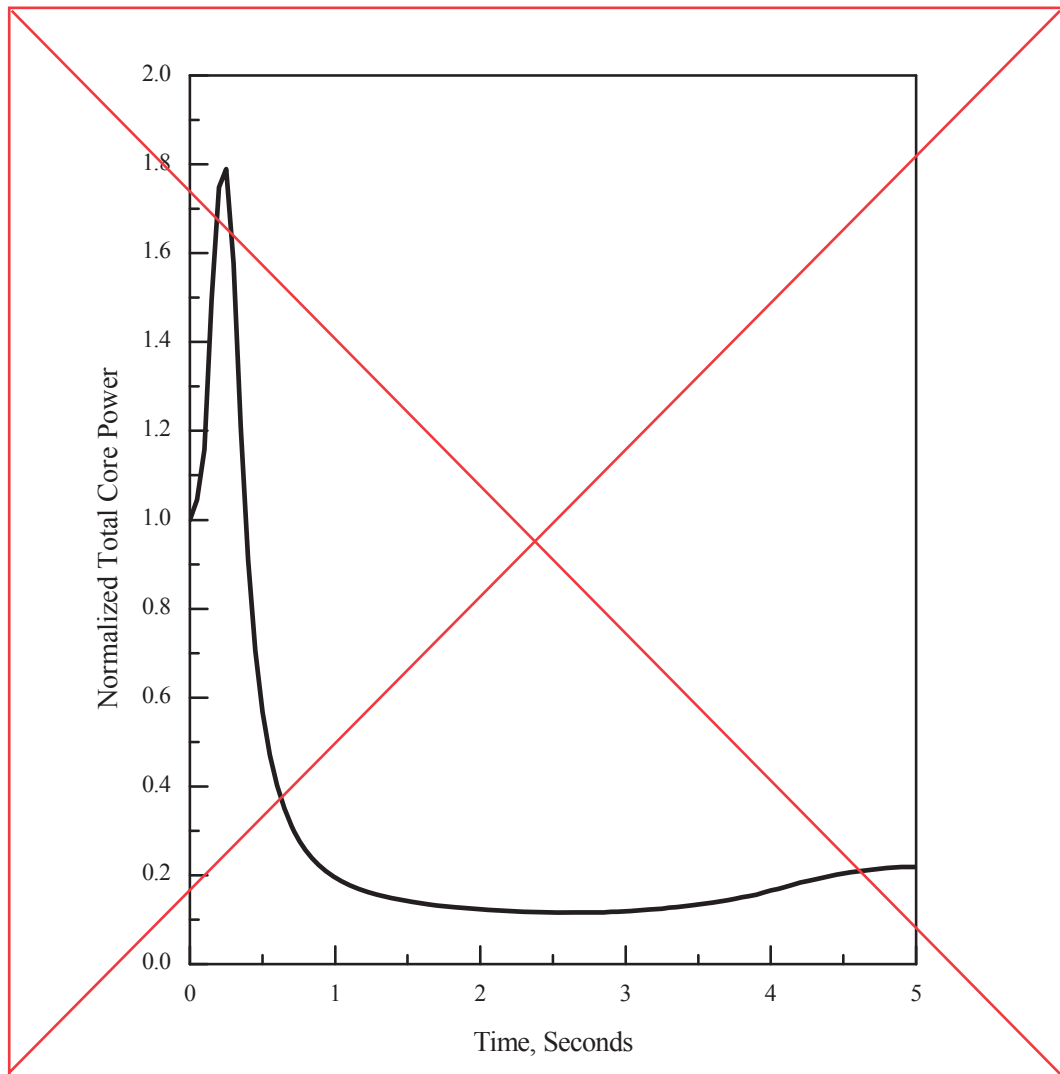


Q



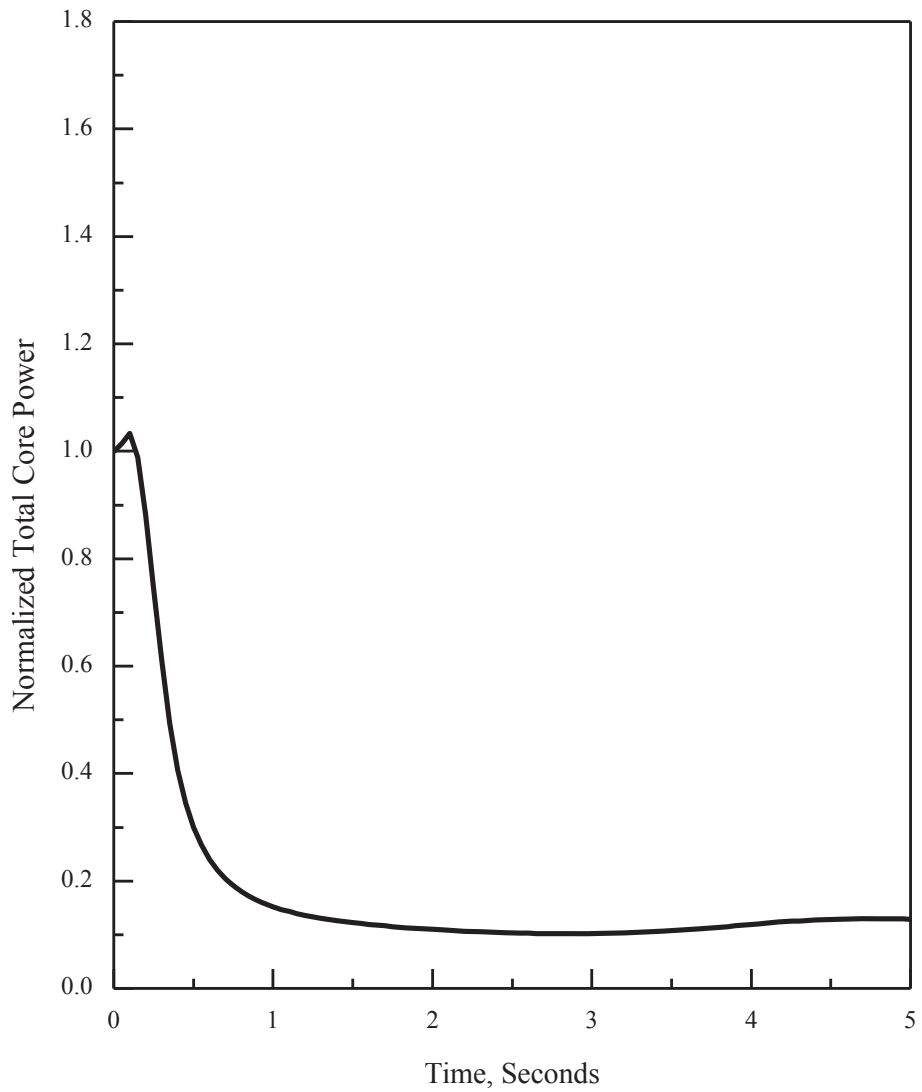
APR1400 DCD TIER 2

Replace with next page R



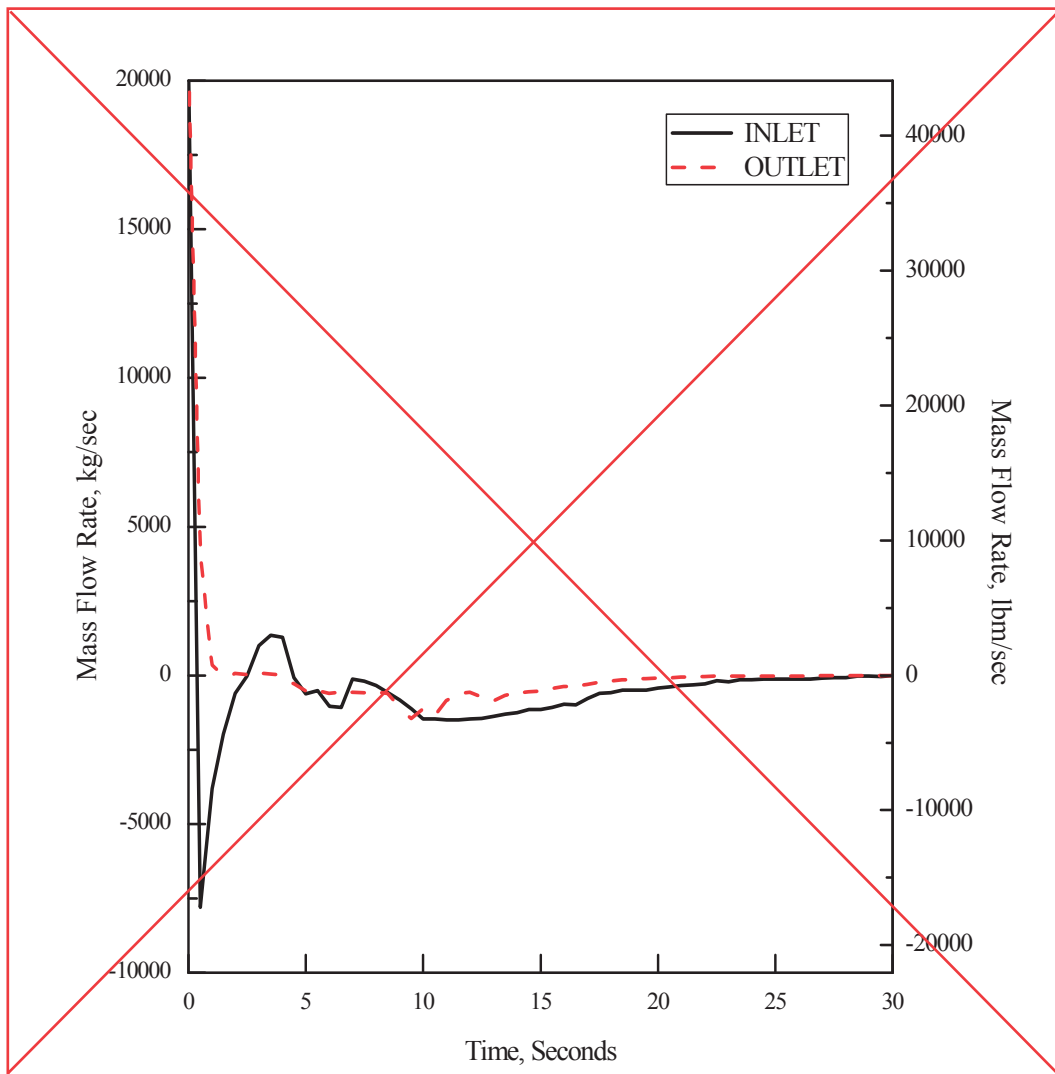
**Figure 15.6.5-13 0.6 × Double-ended Guillotine Break in Pump Discharge Leg
(Normalized Core Power)**

R



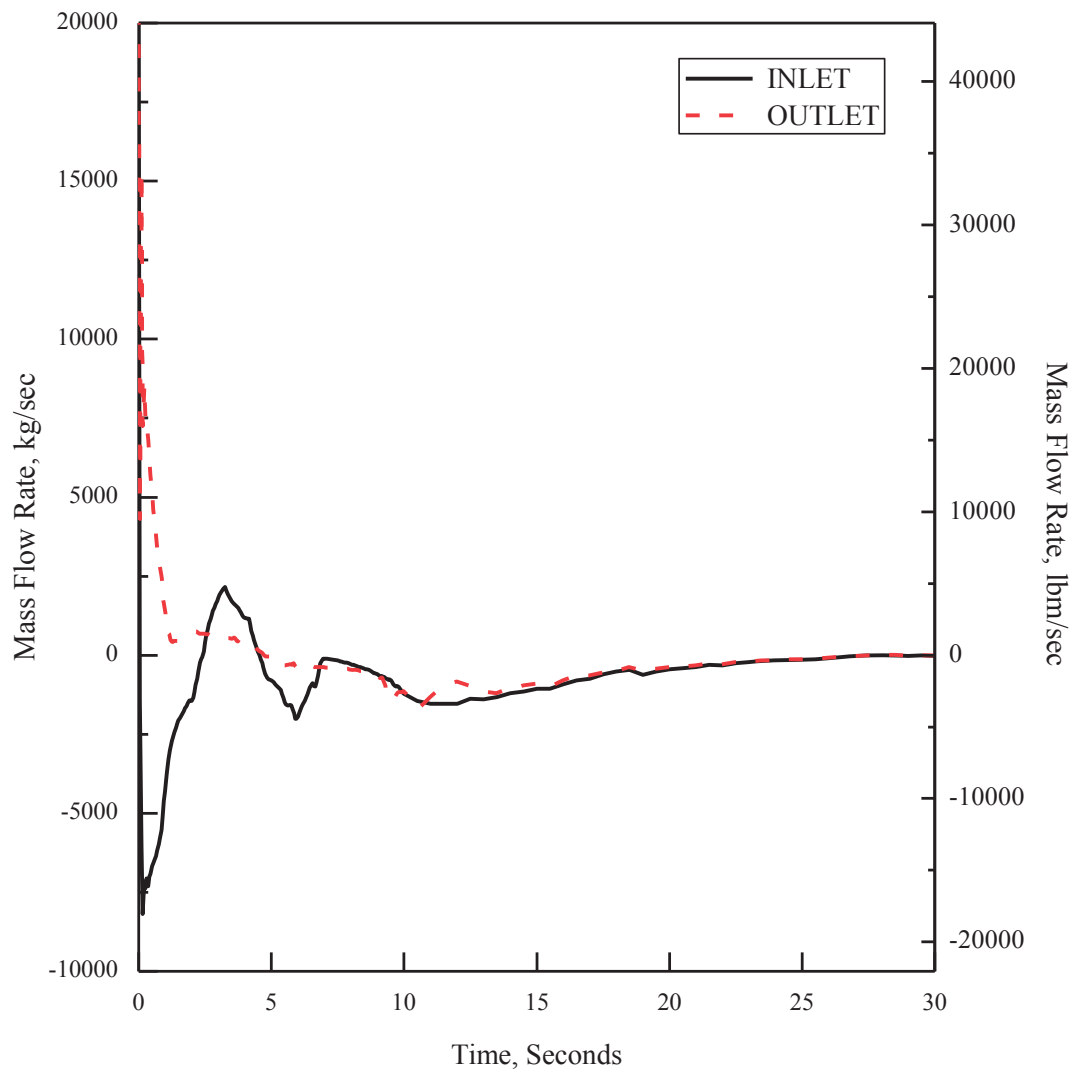
APR1400 DCD TIER 2

Replace with next page S



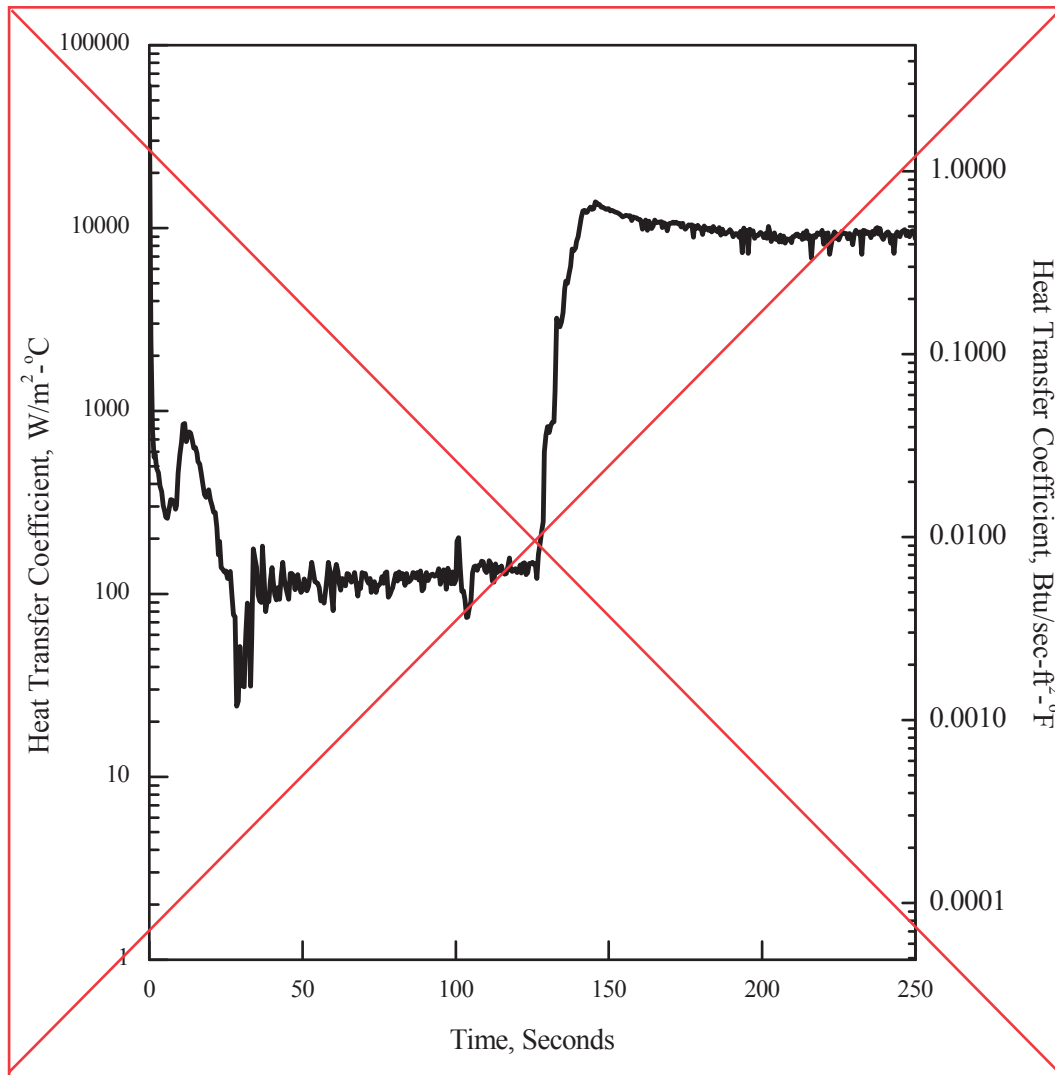
**Figure 15.6.5-14 1.0 × Double-ended Guillotine Break in Pump Discharge Leg
(Core Inlet and Outlet Mass Flow)**

S



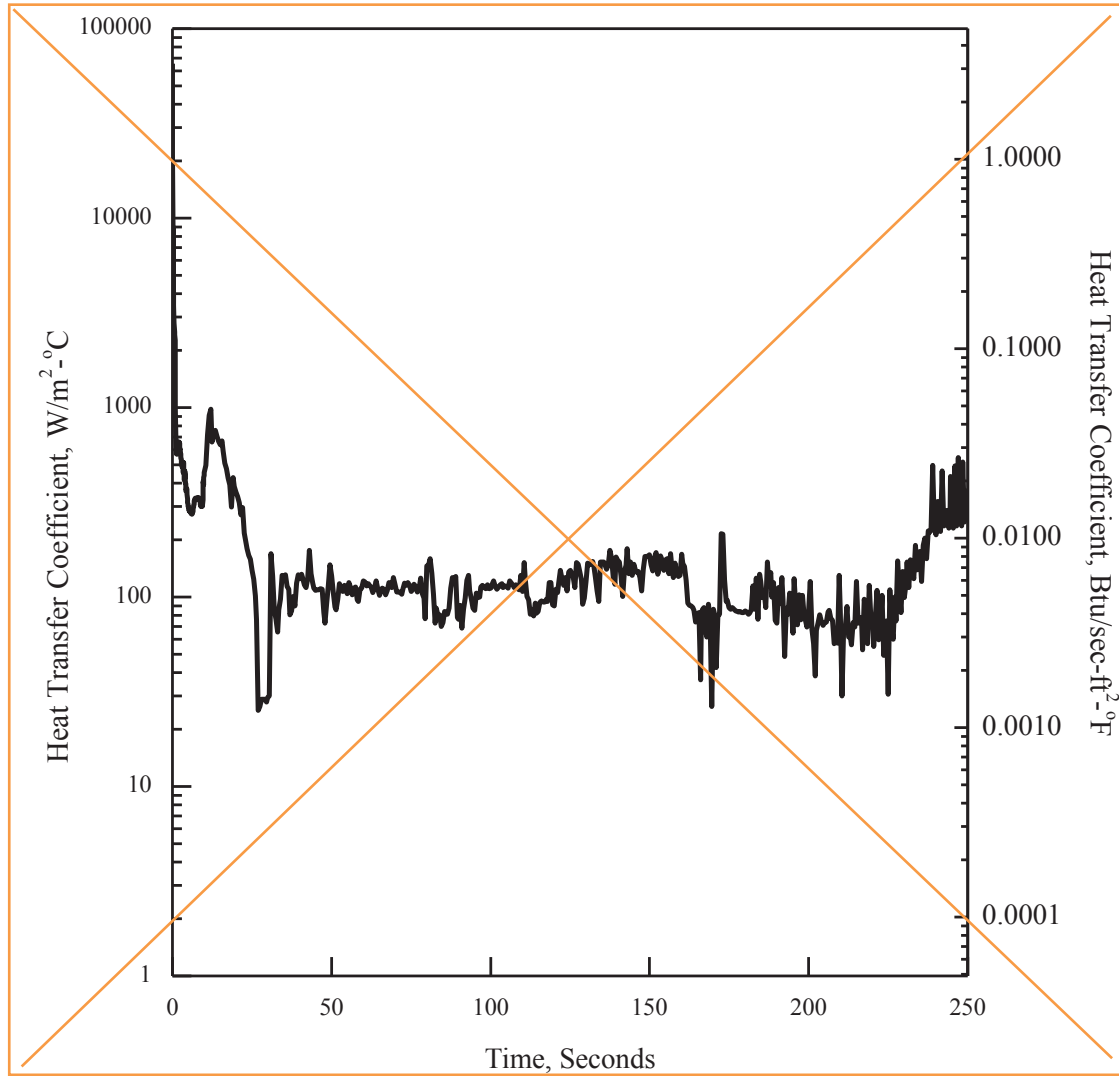
APR1400 DCD TIER 2

Replace with next page T

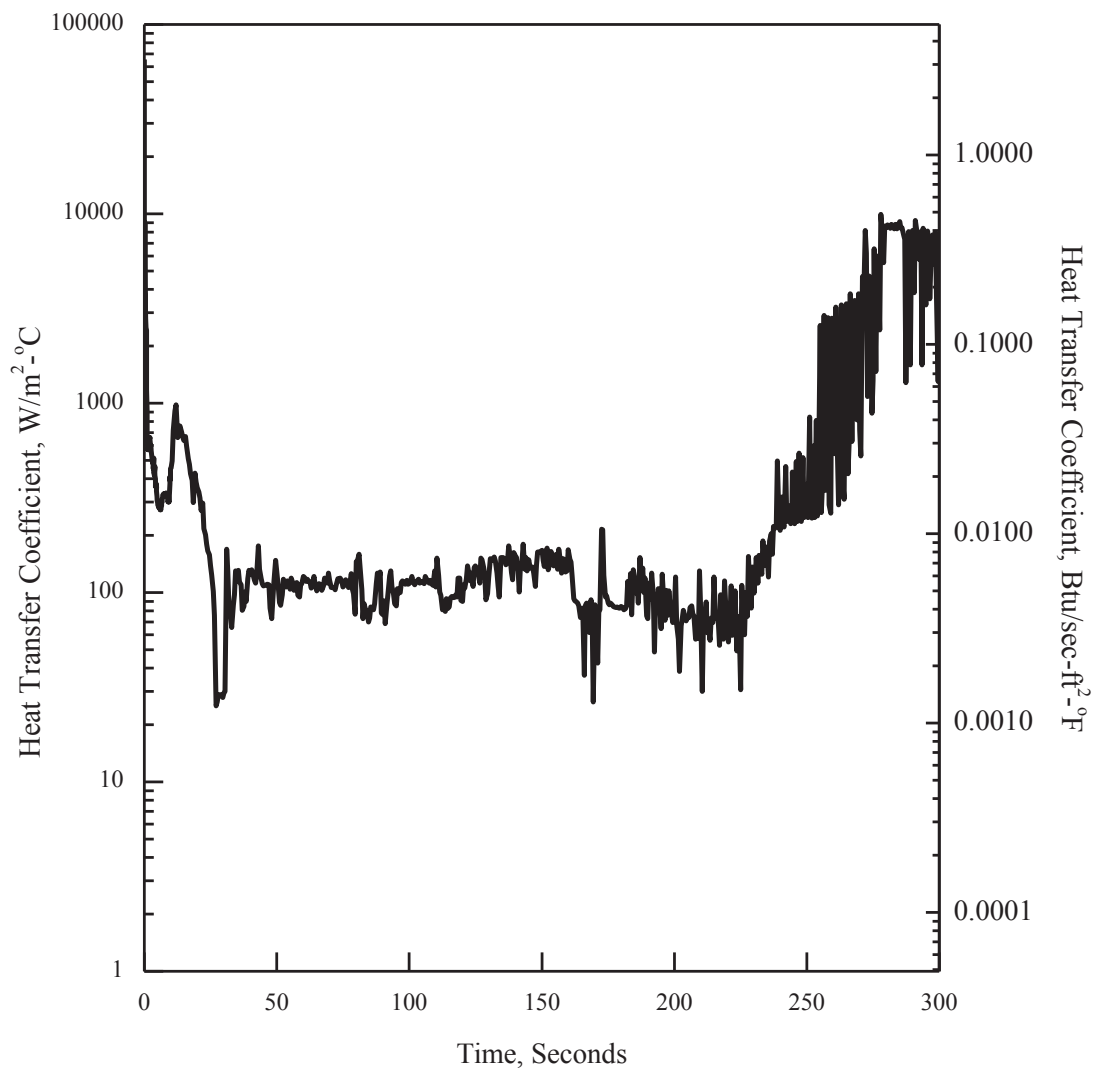


**Figure 15.6.5-15 1.0 × Double-ended Guillotine Break in Pump Discharge Leg
(Hot Spot Heat Transfer Coefficient)**

T



T



APR1400 DCD TIER 2

Replace with next page U

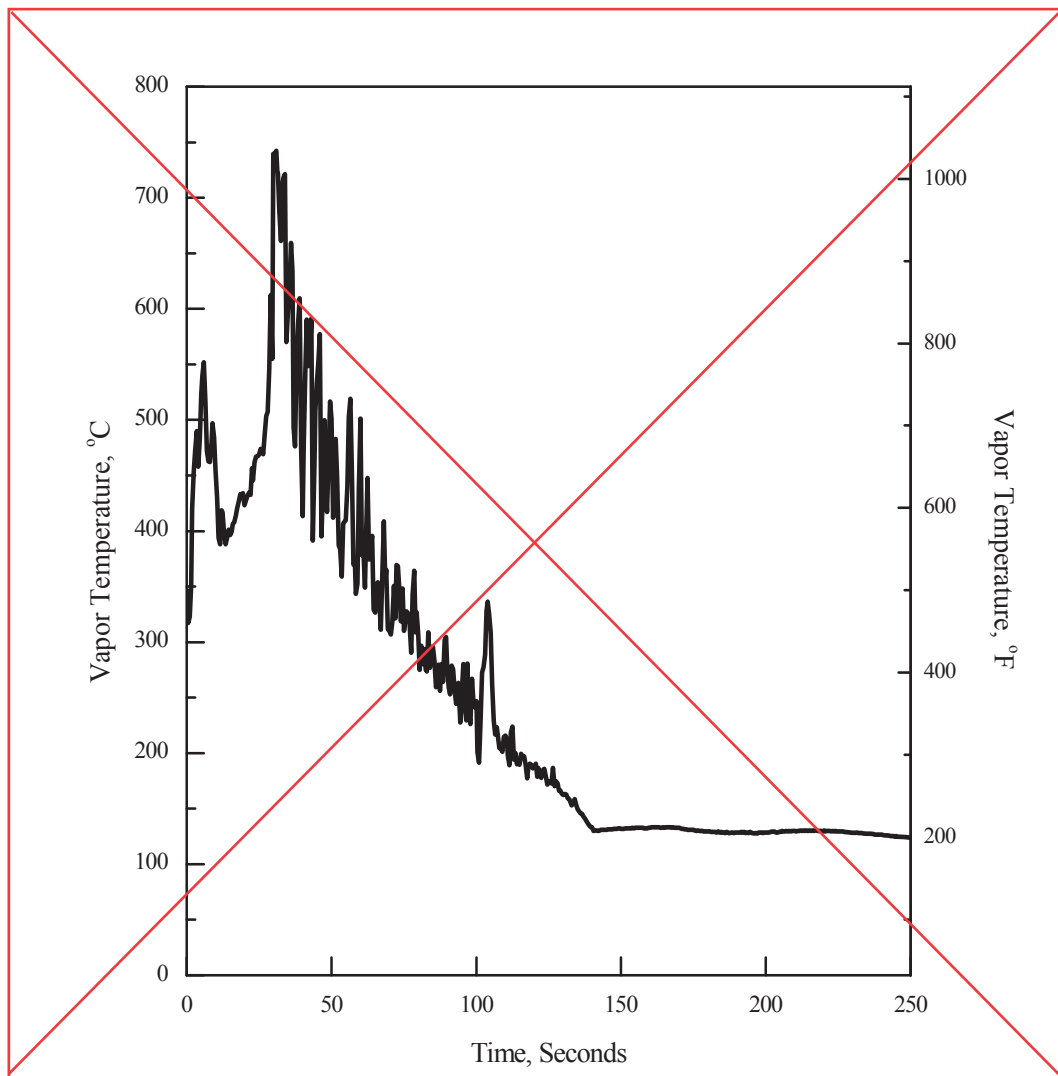
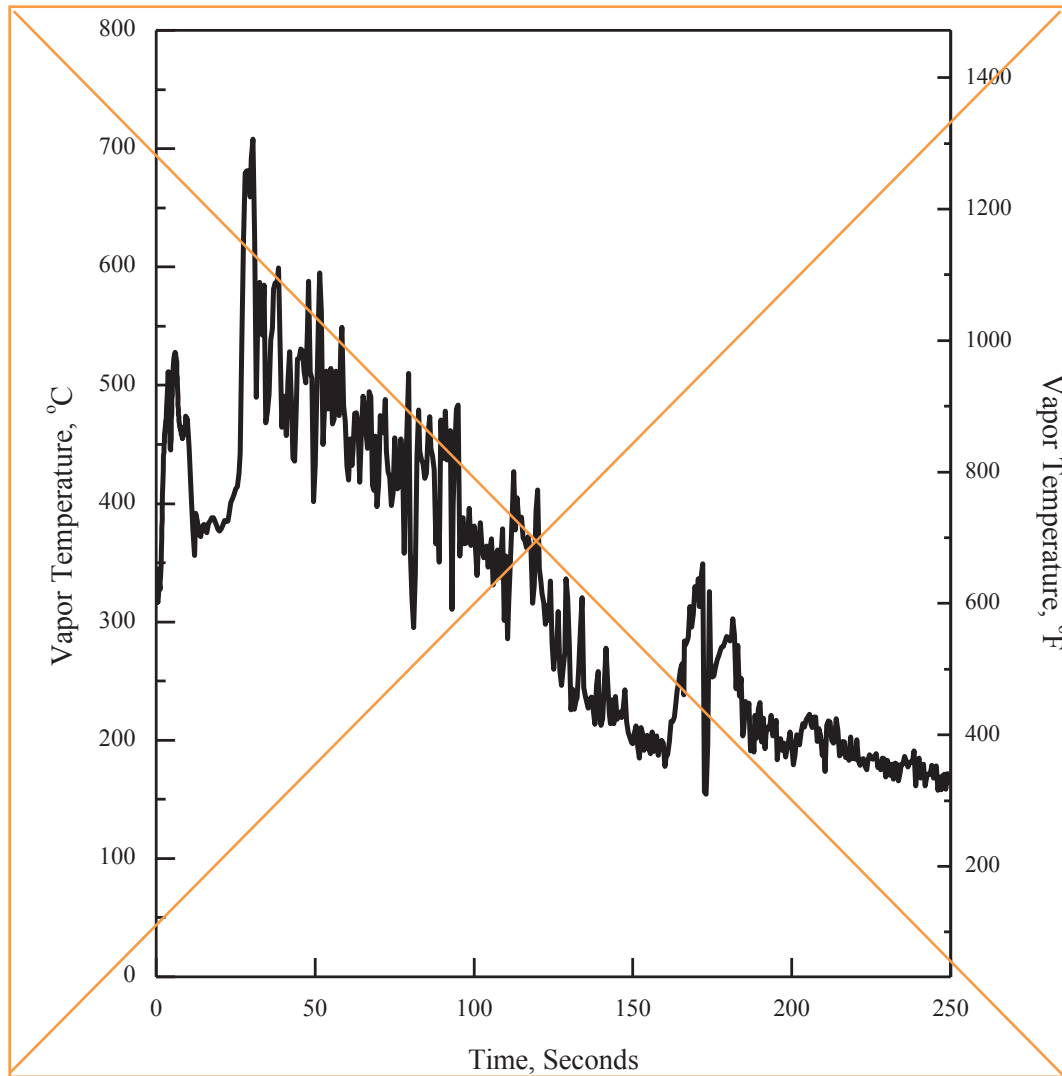
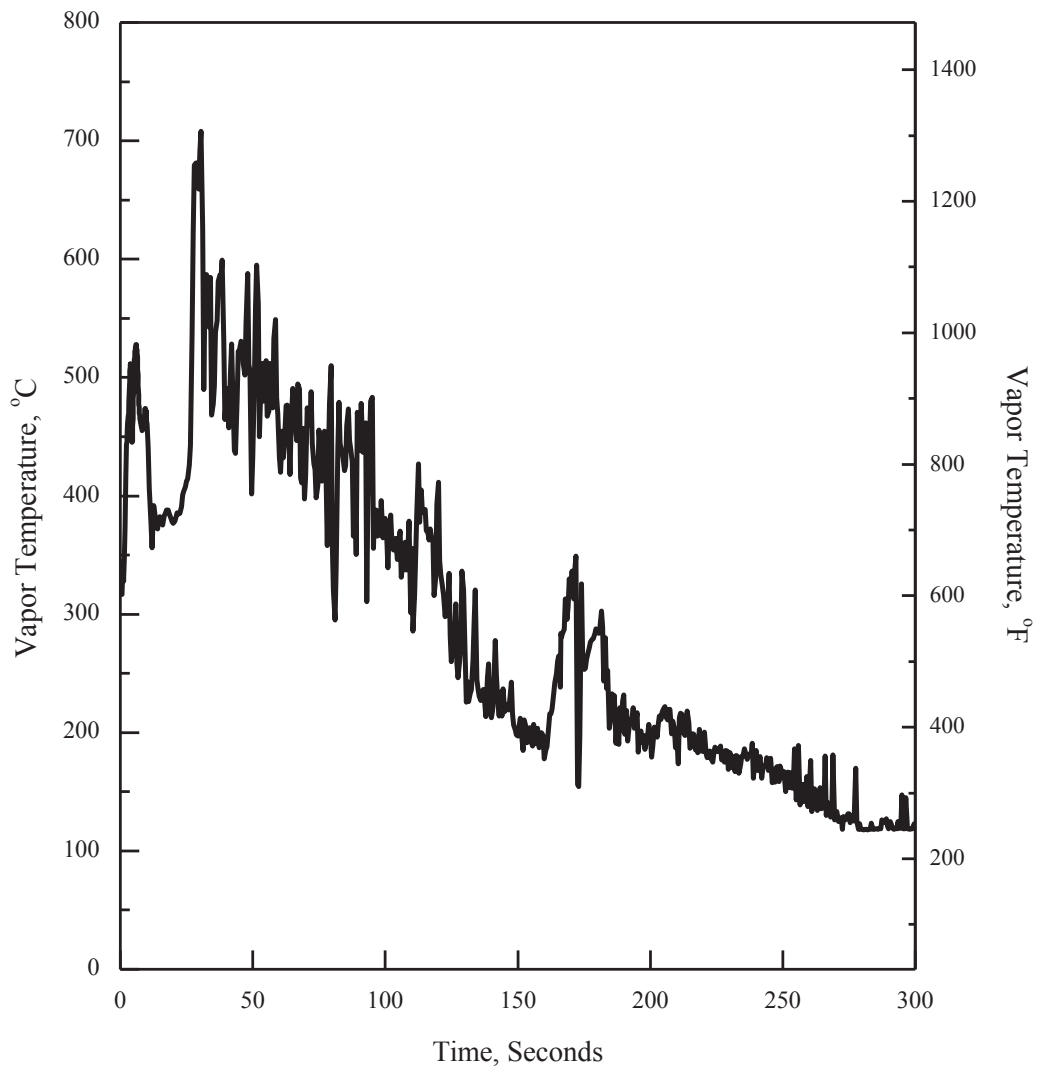


Figure 15.6.5-16 1.0 × Double-ended Guillotine Break in Pump Discharge Leg (Hot Spot Vapor Temperature)

U



U



APR1400 DCD TIER 2

Replace with next page V

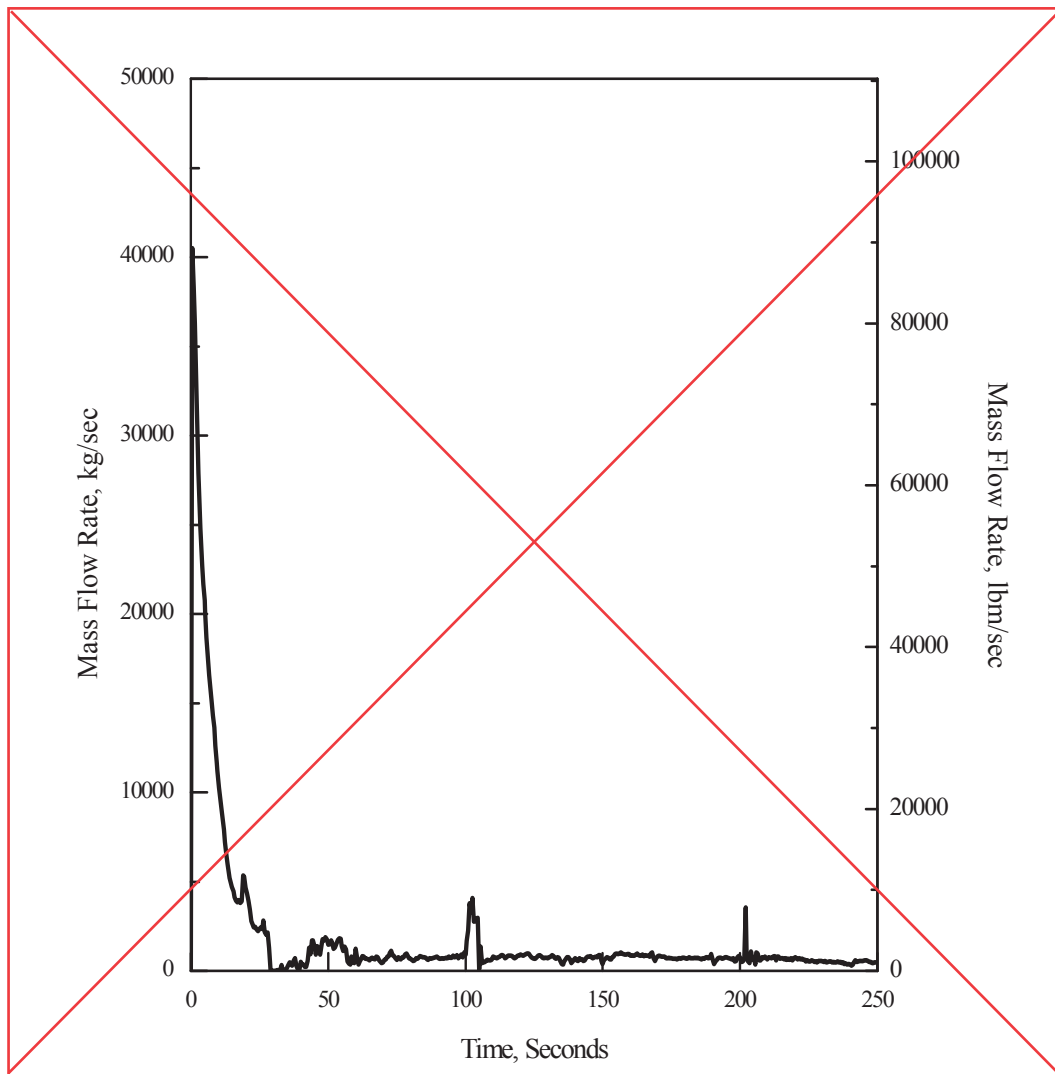
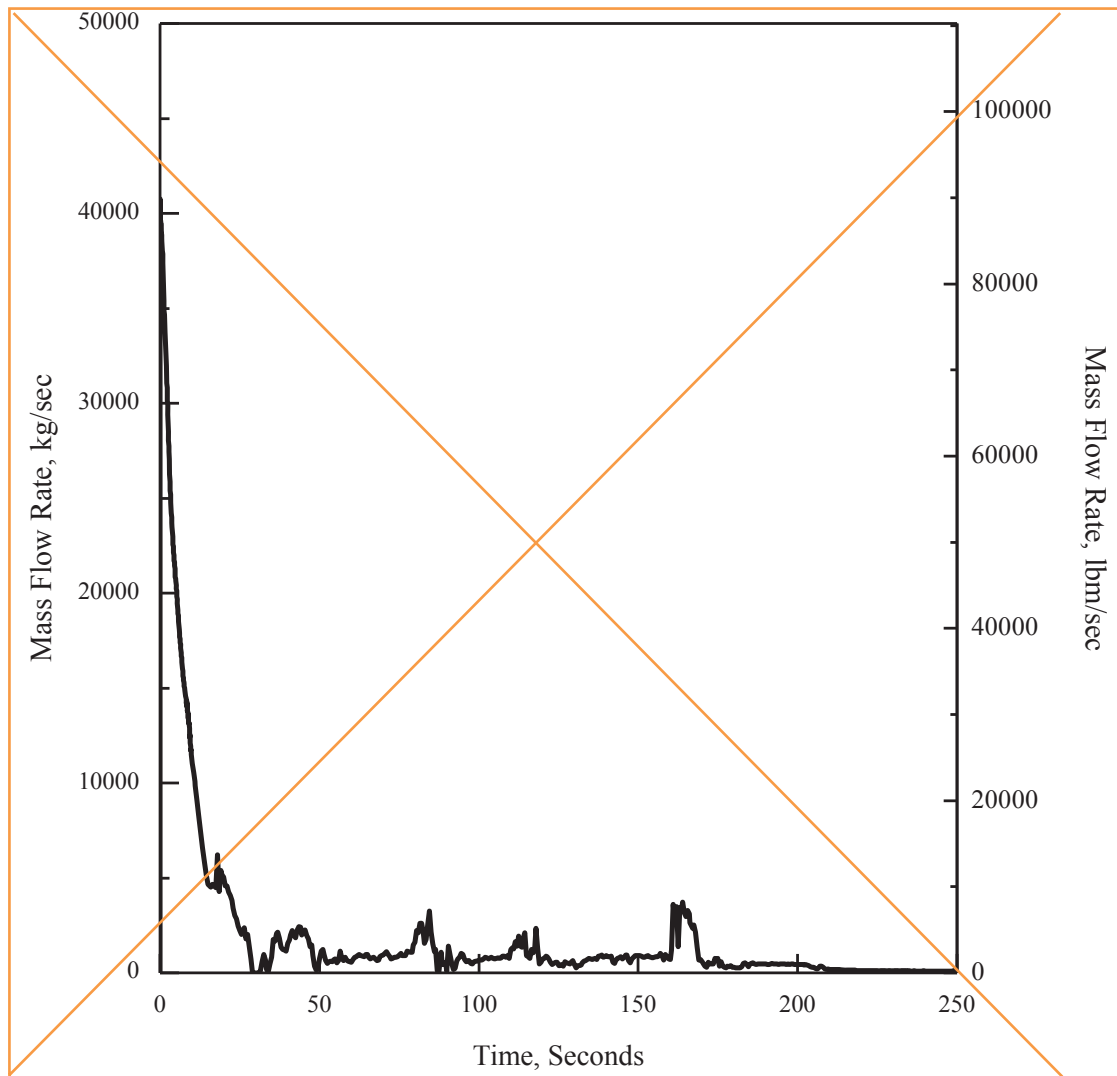
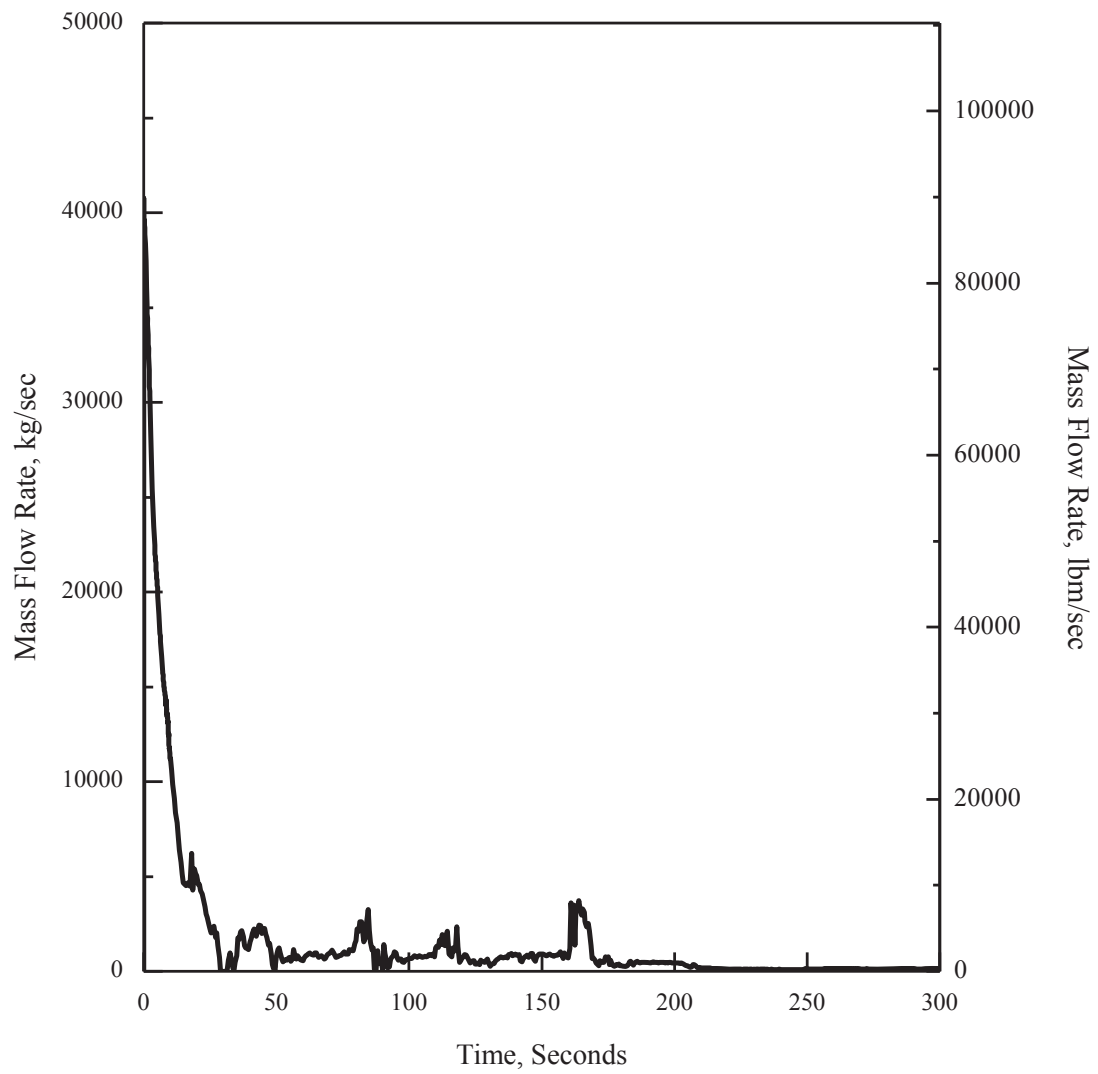


Figure 15.6.5-17 1.0 x Double-ended Guillotine Break in Pump Discharge Leg (Break Flow)

V

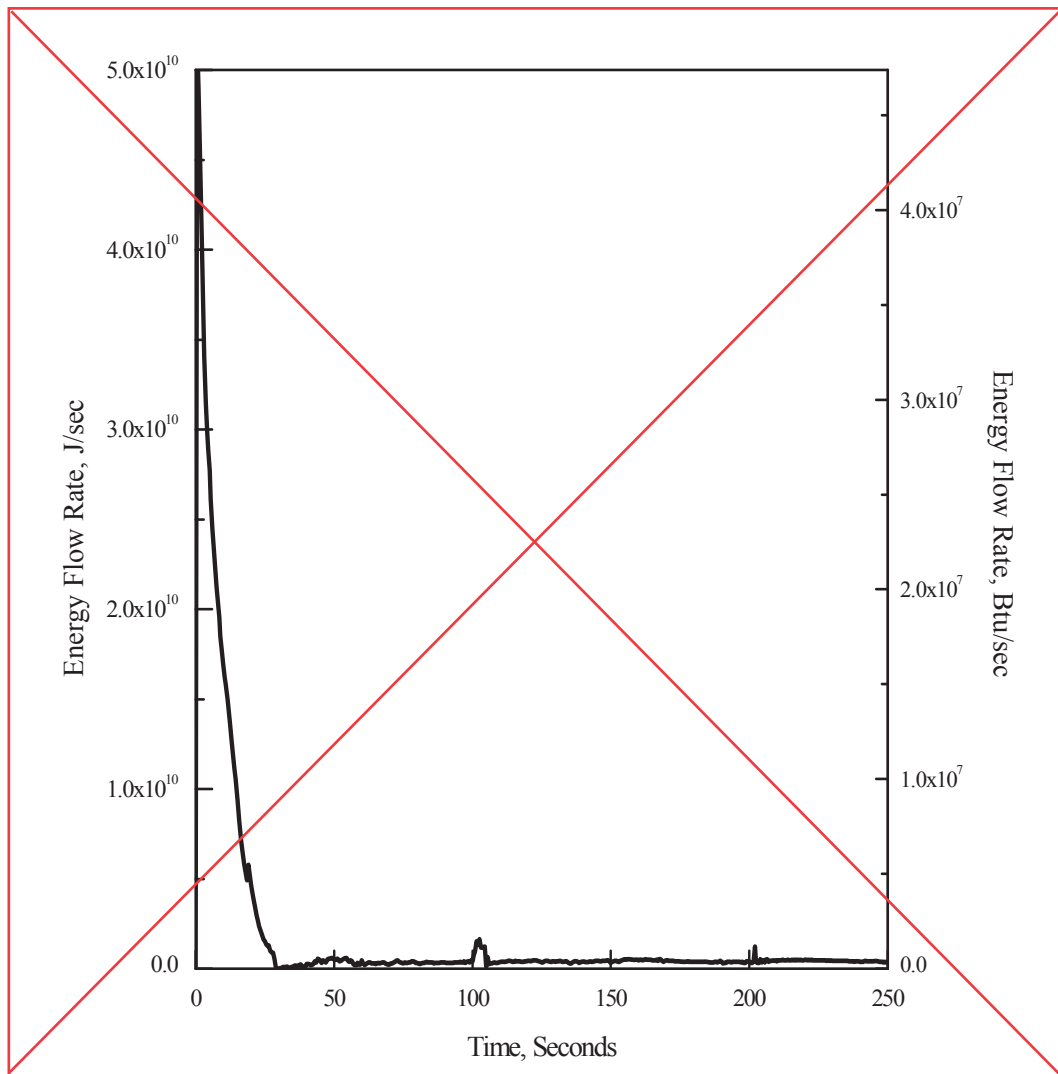


V



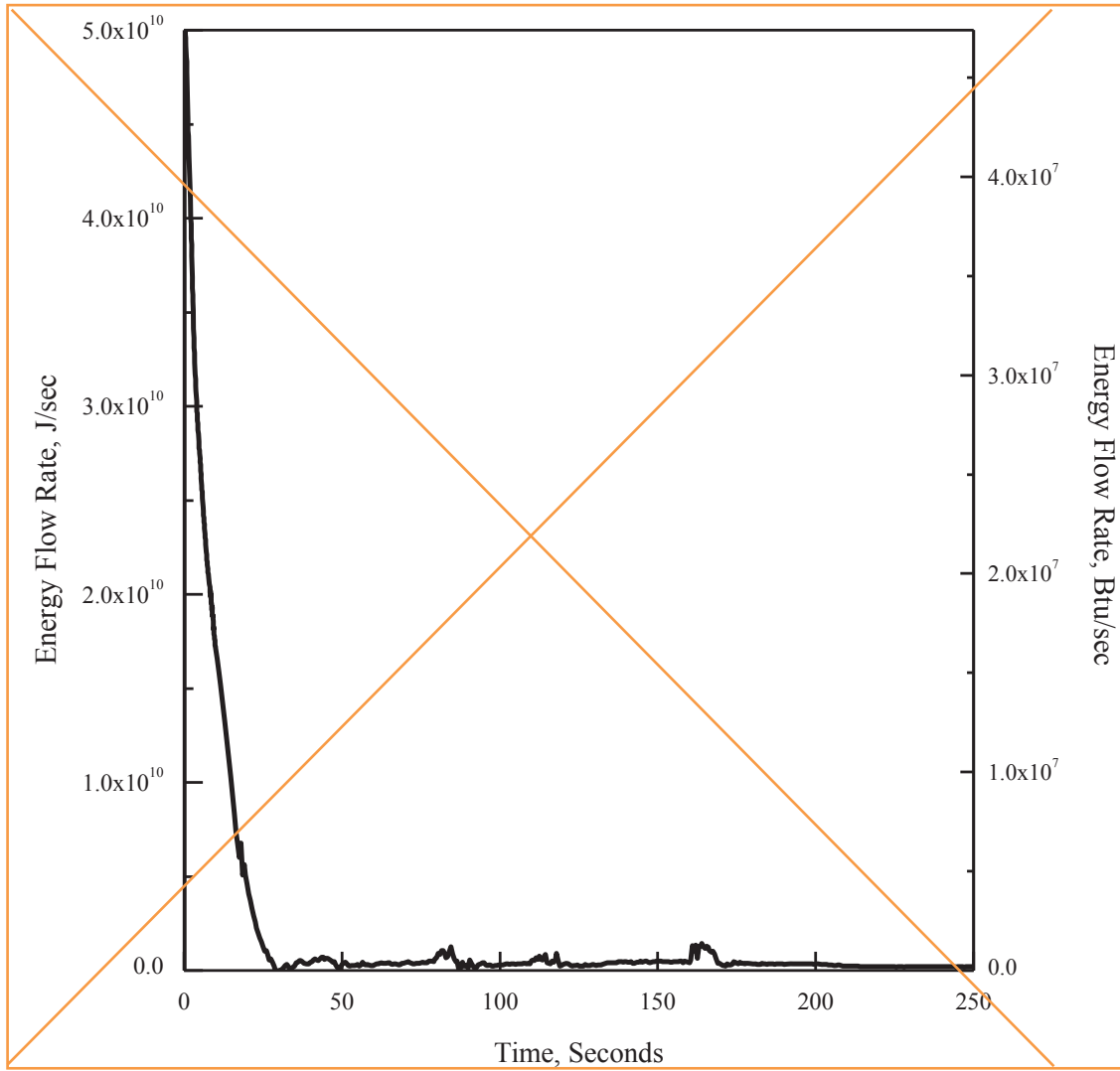
APR1400 DCD TIER 2

Replace with next page W

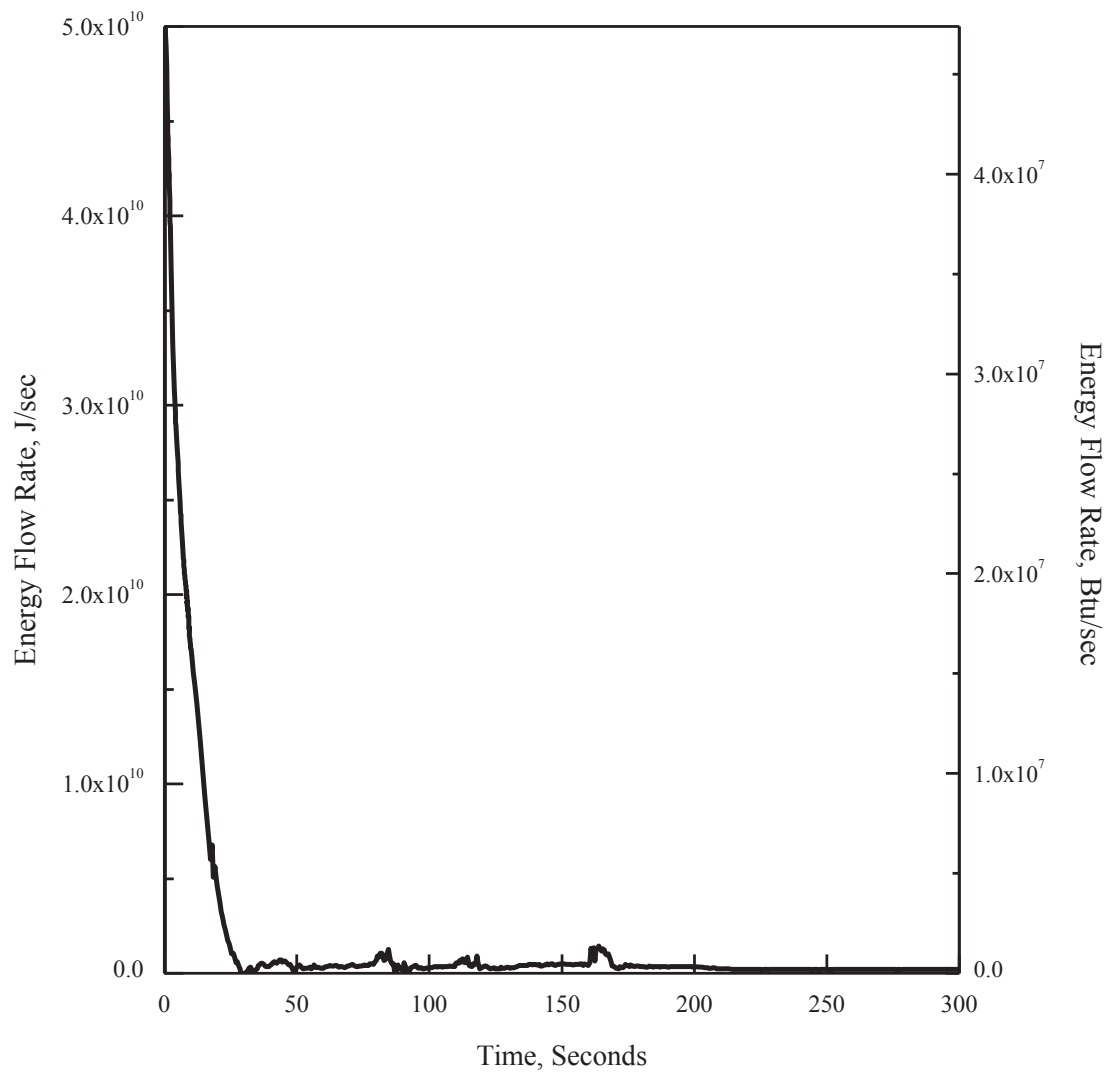


**Figure 15.6.5-18 1.0 × Double-ended Guillotine Break in Pump Discharge Leg
(Break Energy Flow)**

W



W



APR1400 DCD TIER 2

Replace with next page X

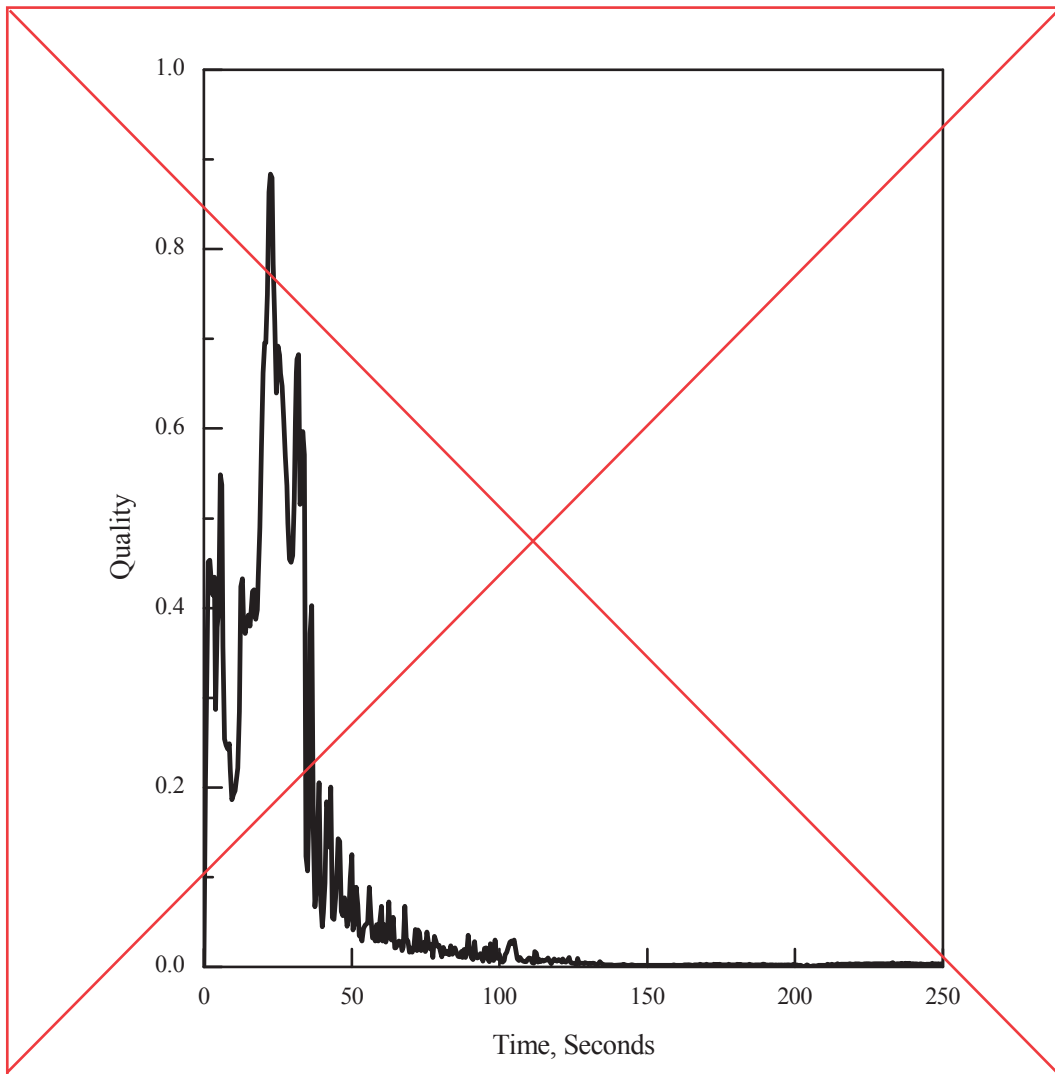
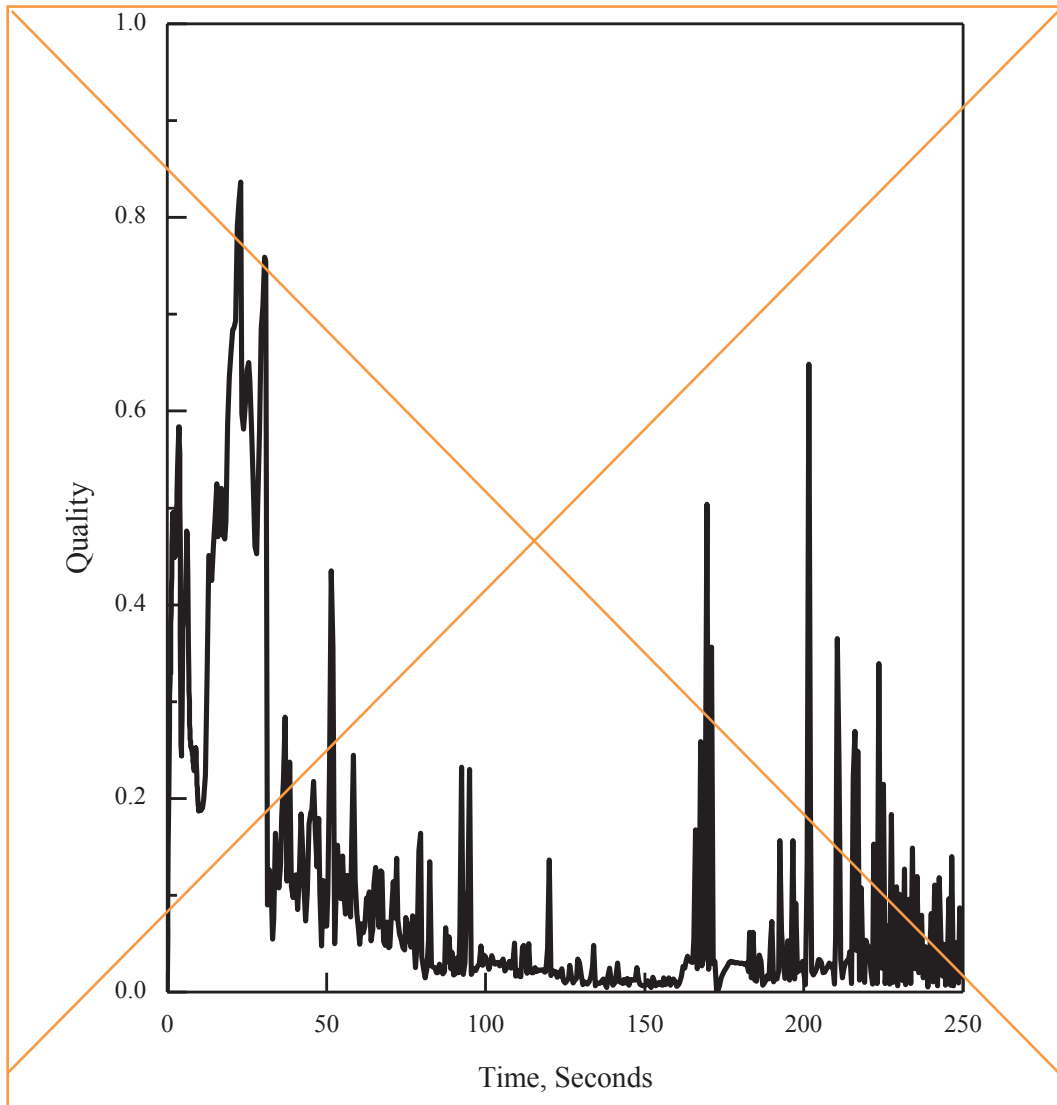
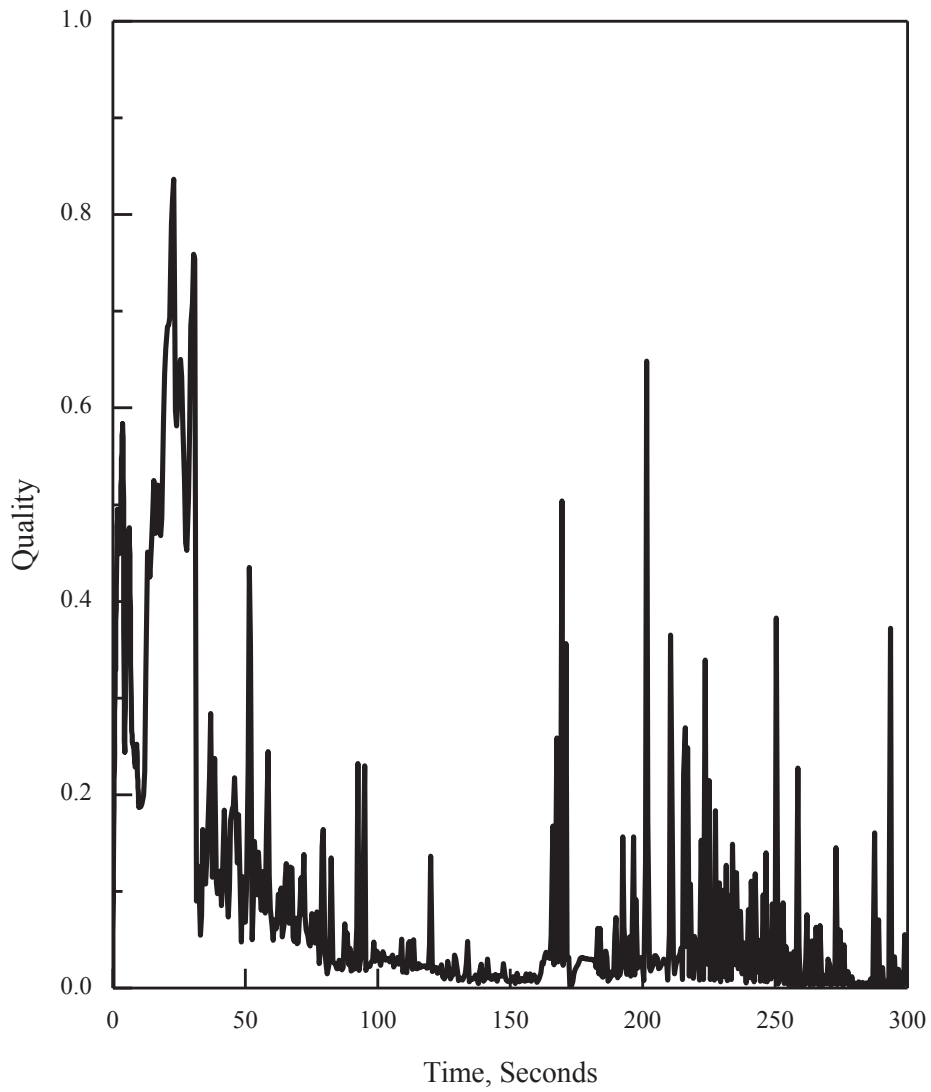


Figure 15.6.5-19 1.0 x Double-ended Guillotine Break in Pump Discharge Leg (Hot Assembly Quality)

X

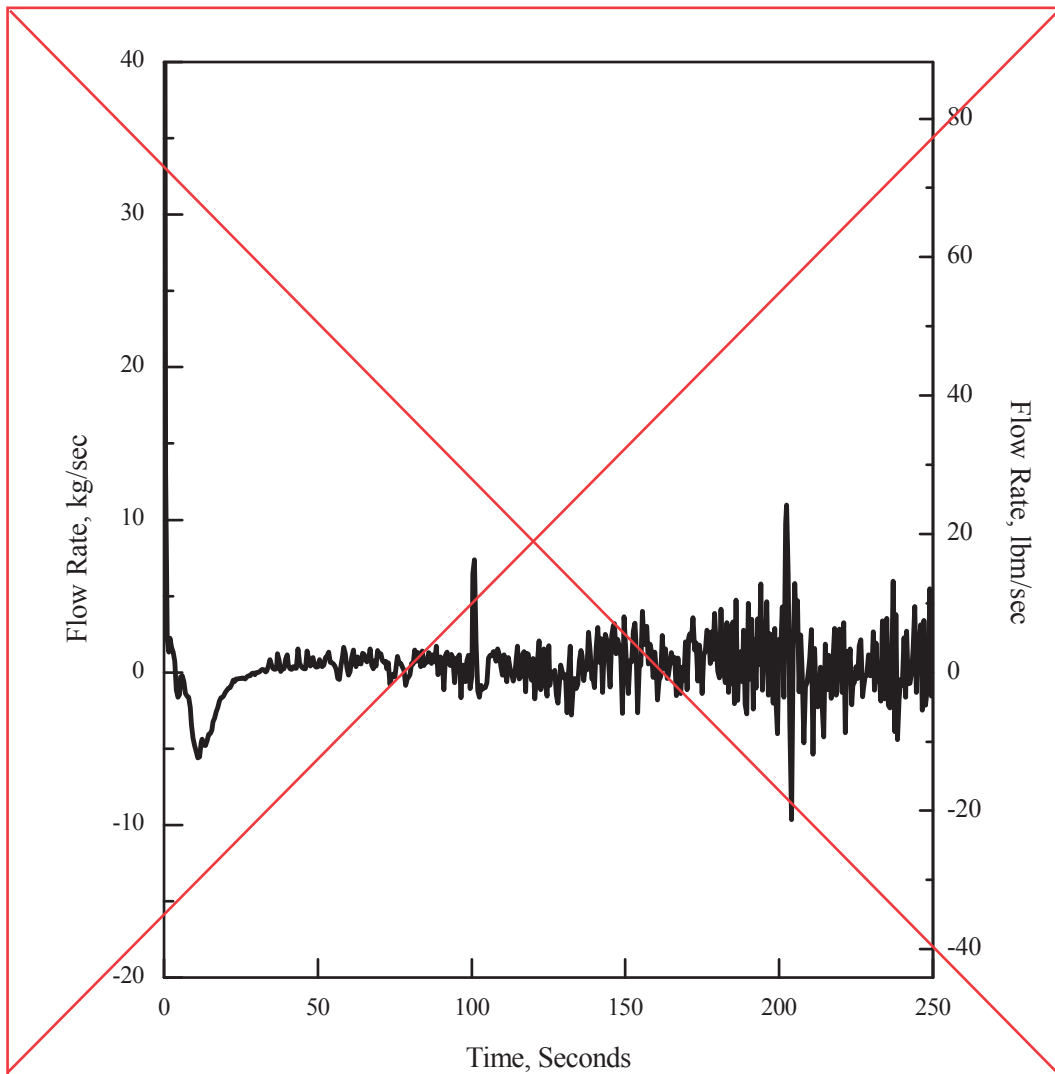


X



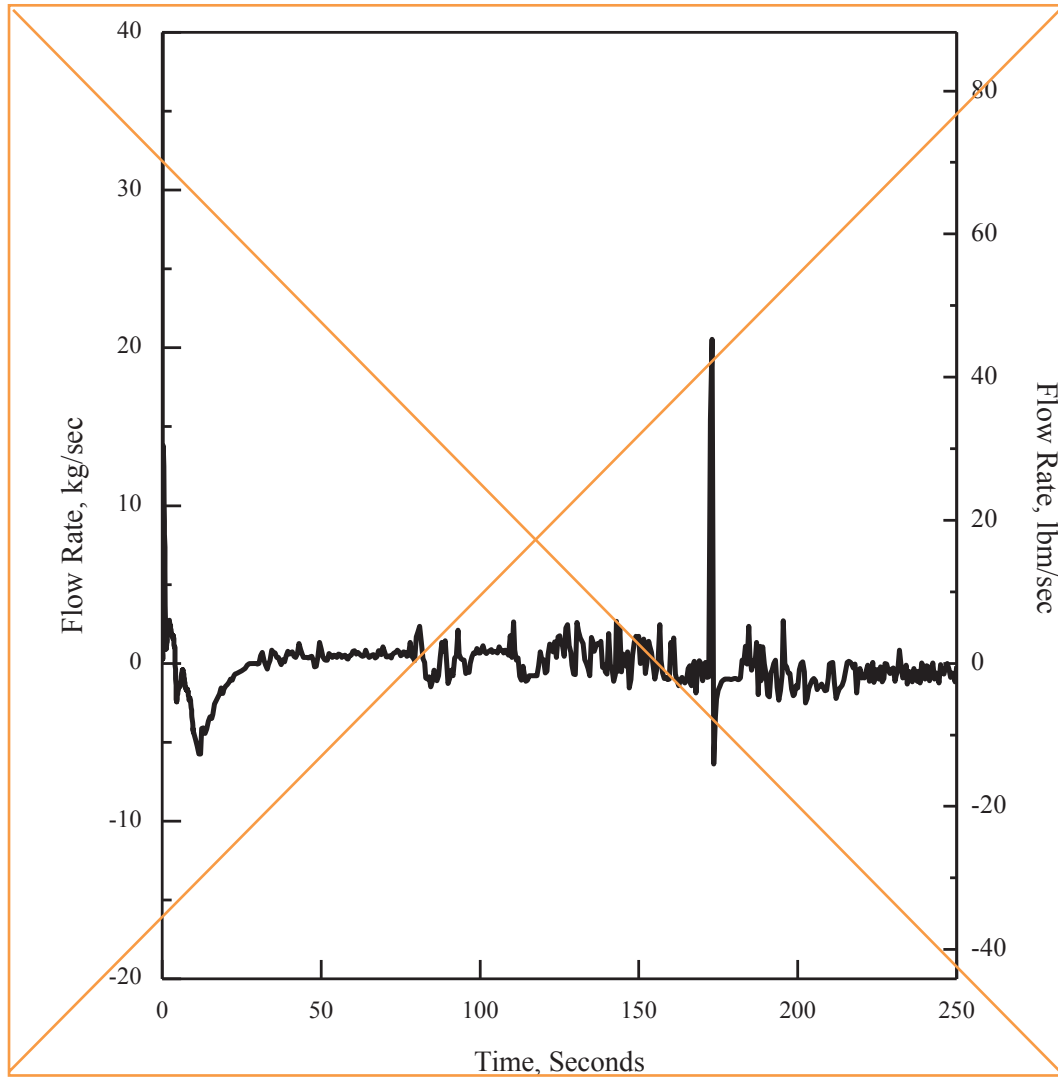
APR1400 DCD TIER 2

Replace with next page Y

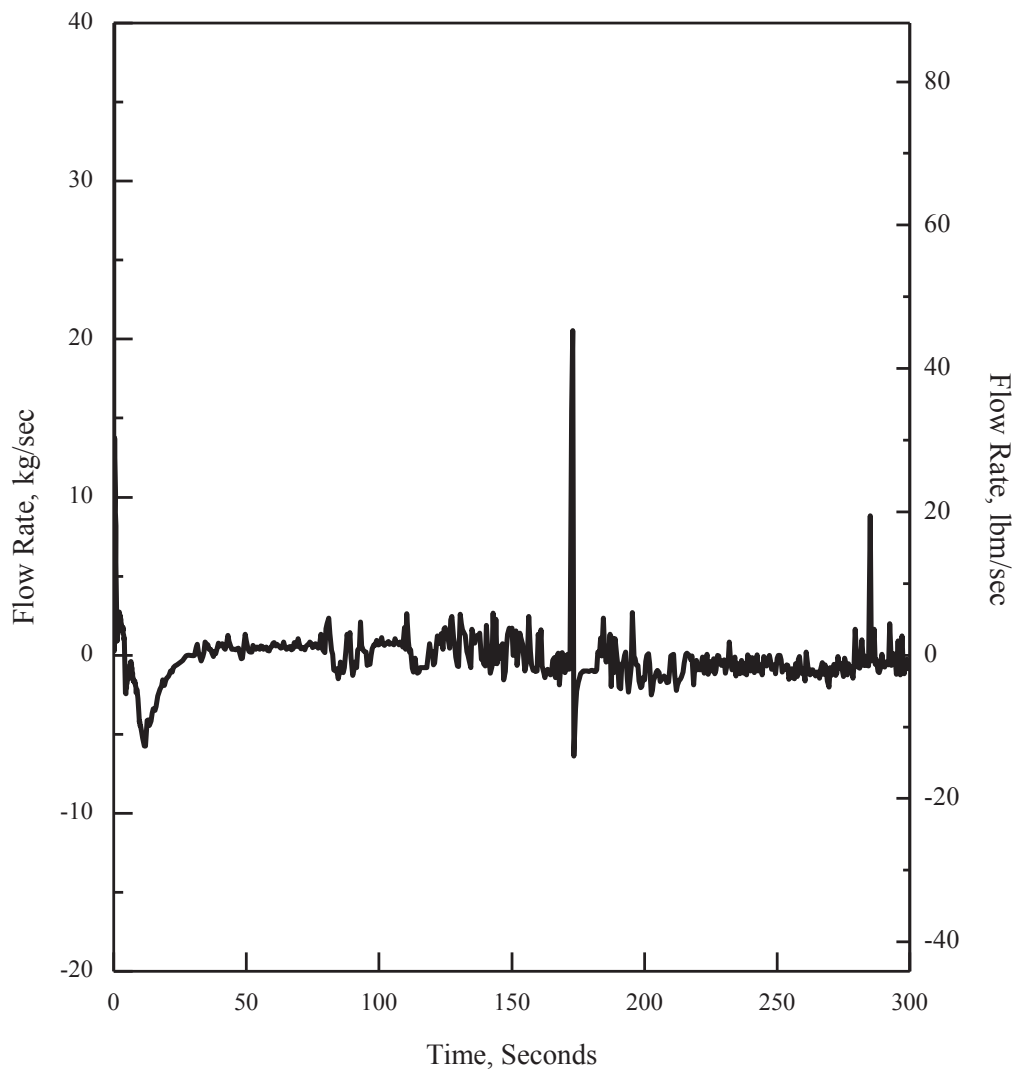


**Figure 15.6.5-20 1.0 x Double-ended Guillotine Break in Pump Discharge Leg
(Hot Assembly Mass Flow Rate)**

Y



Y



APR1400 DCD TIER 2

Replace with next page Z

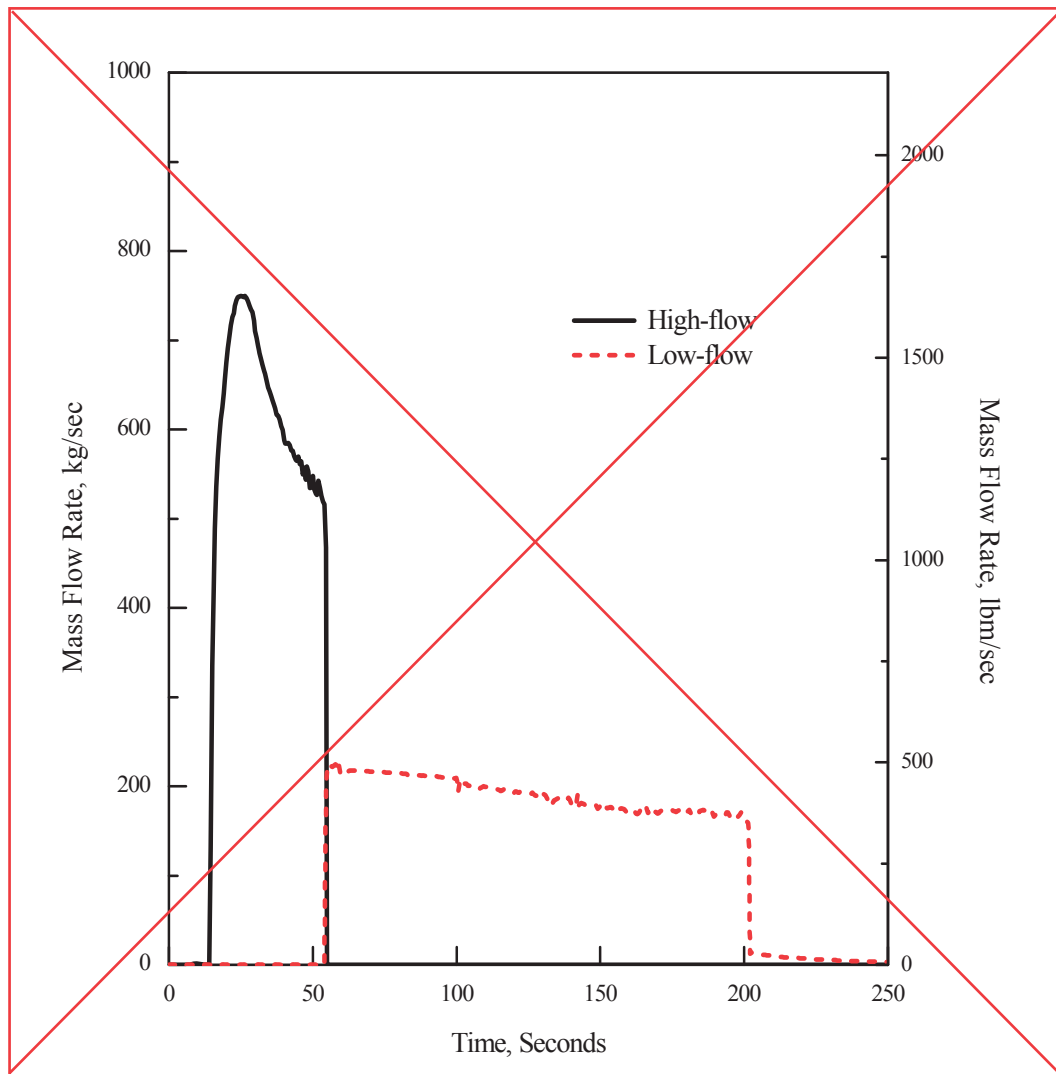
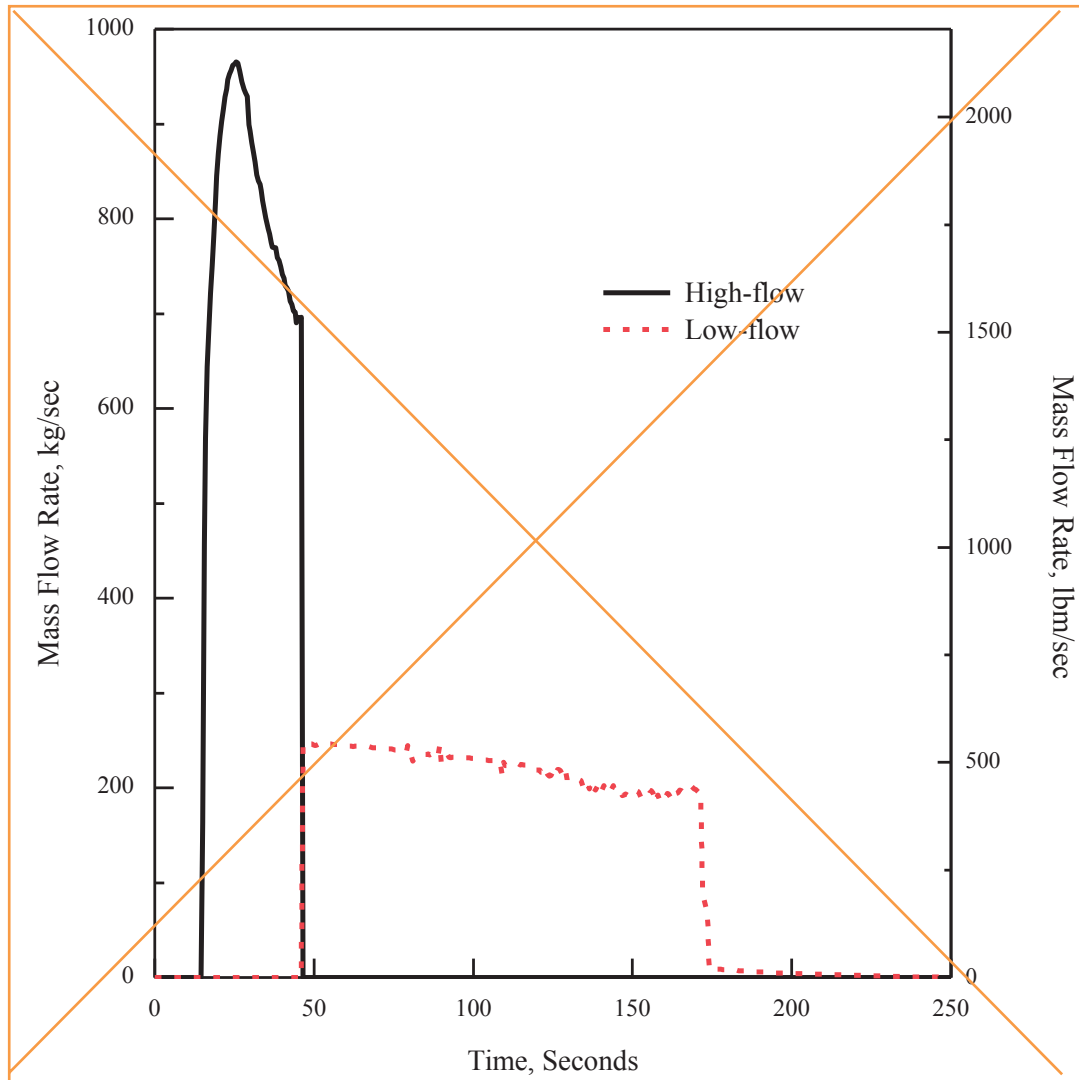
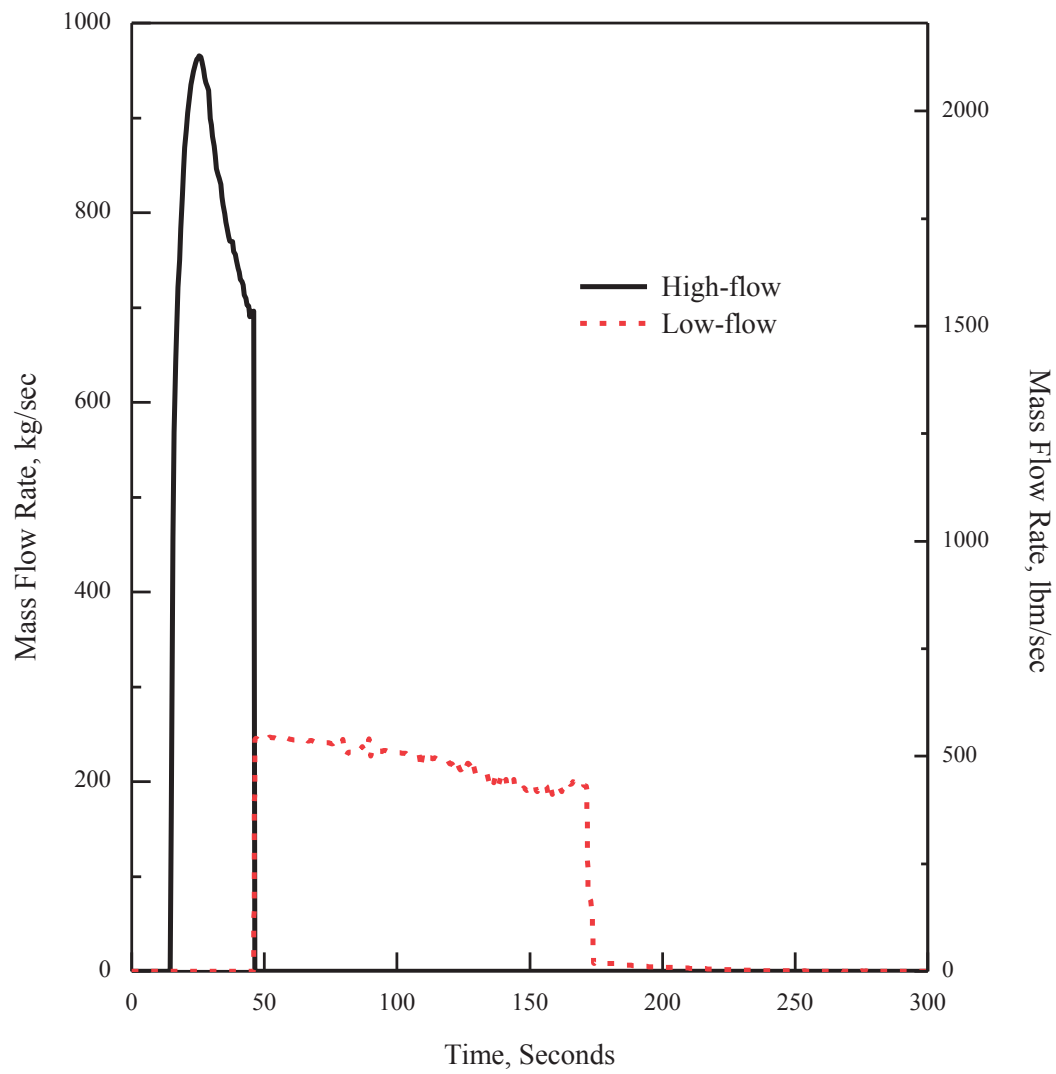


Figure 15.6.5-21 1.0 × Double-ended Guillotine Break in Pump Discharge Leg (Safety Injection Tank Flow)

Z



Z



APR1400 DCD TIER 2

Replace with next page AA

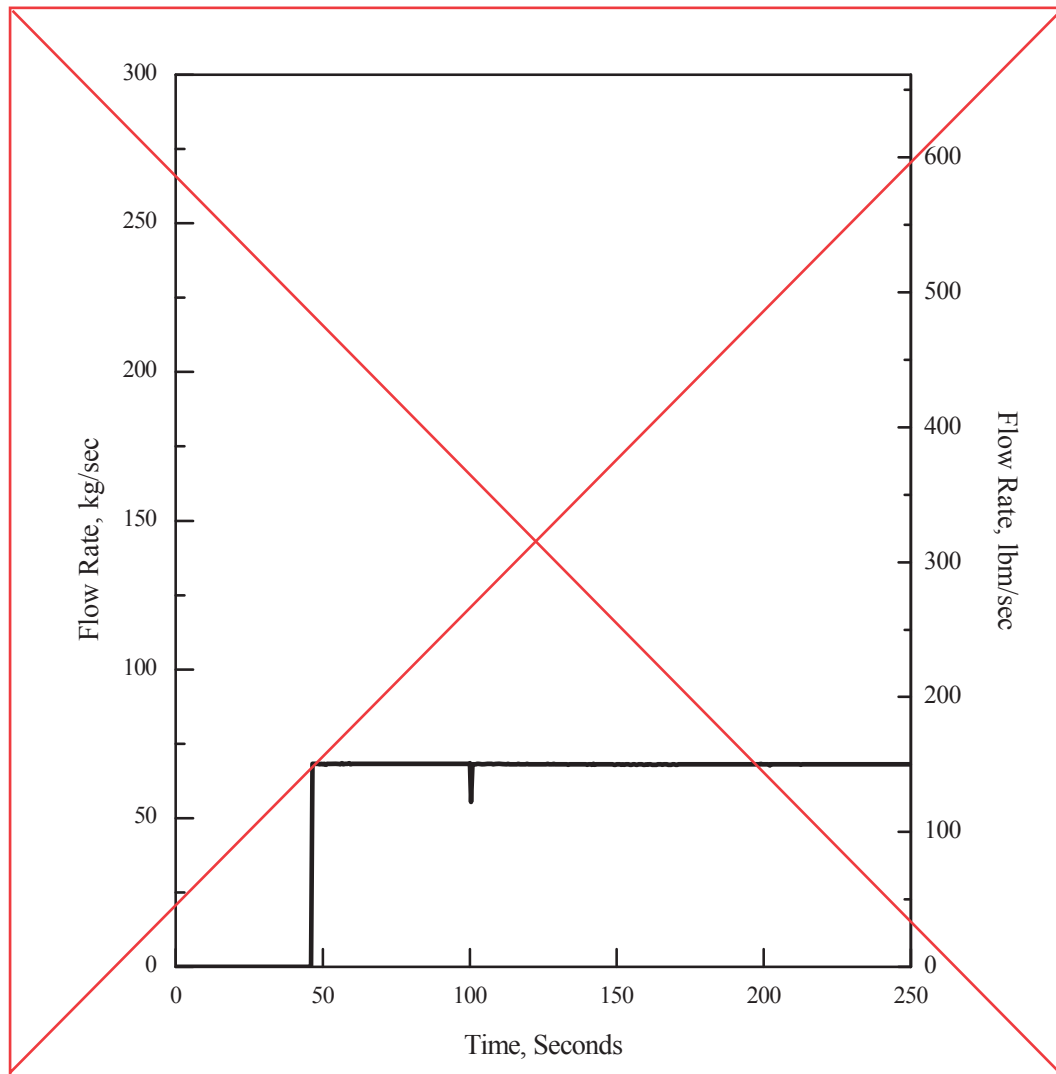
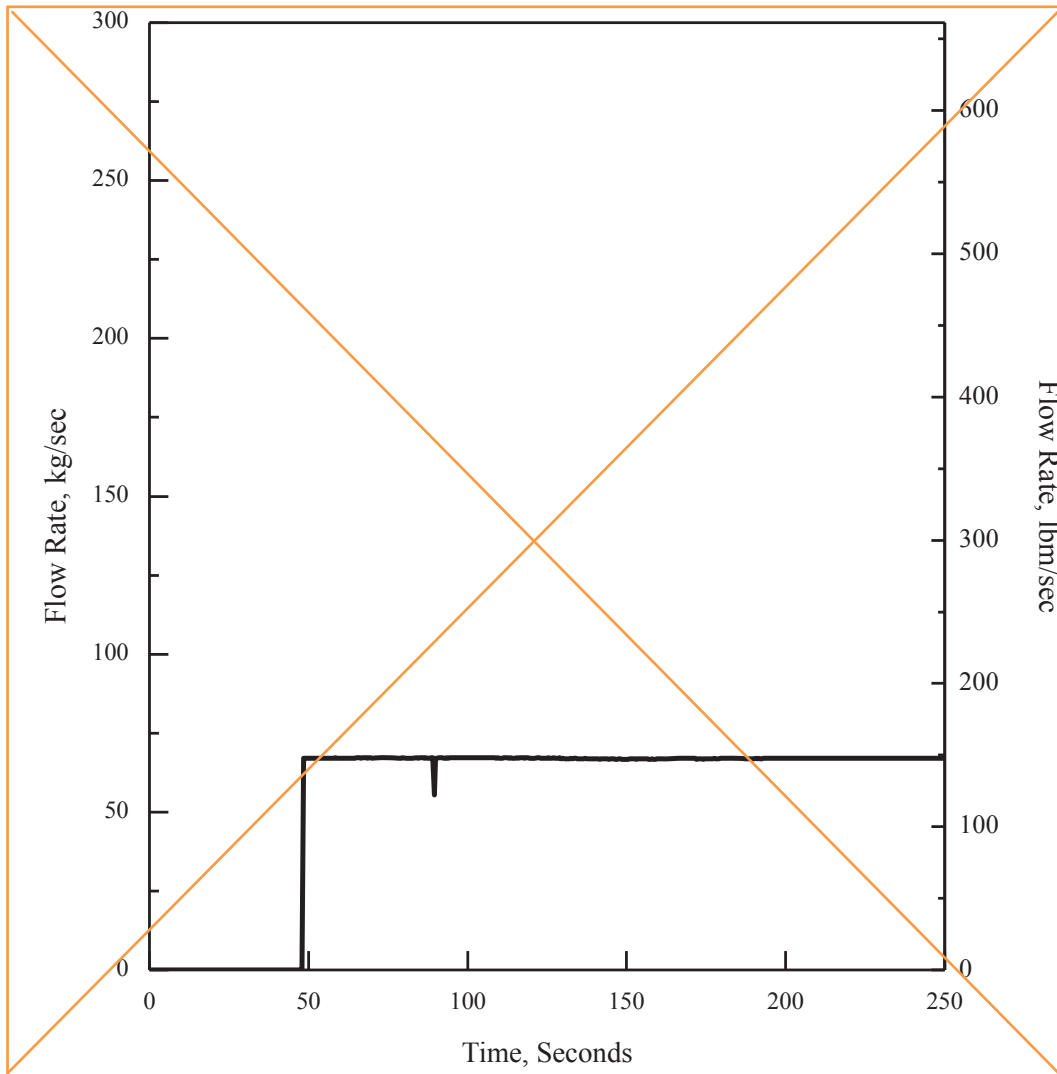
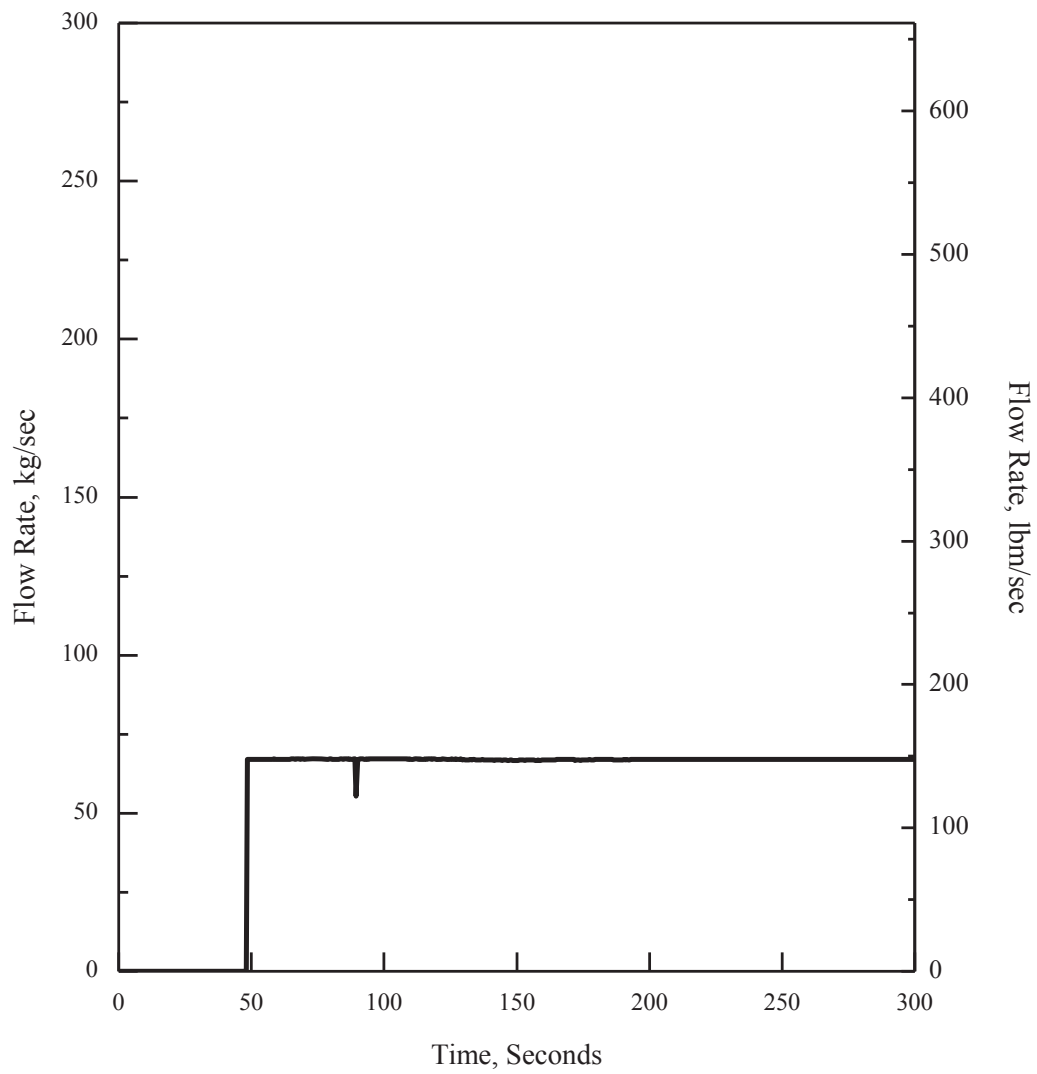


Figure 15.6.5-22 1.0 x Double-ended Guillotine Break in Pump Discharge Leg (SI Pump Flow Rate)

AA



AA



APR1400 DCD TIER 2

Replace with next page AB

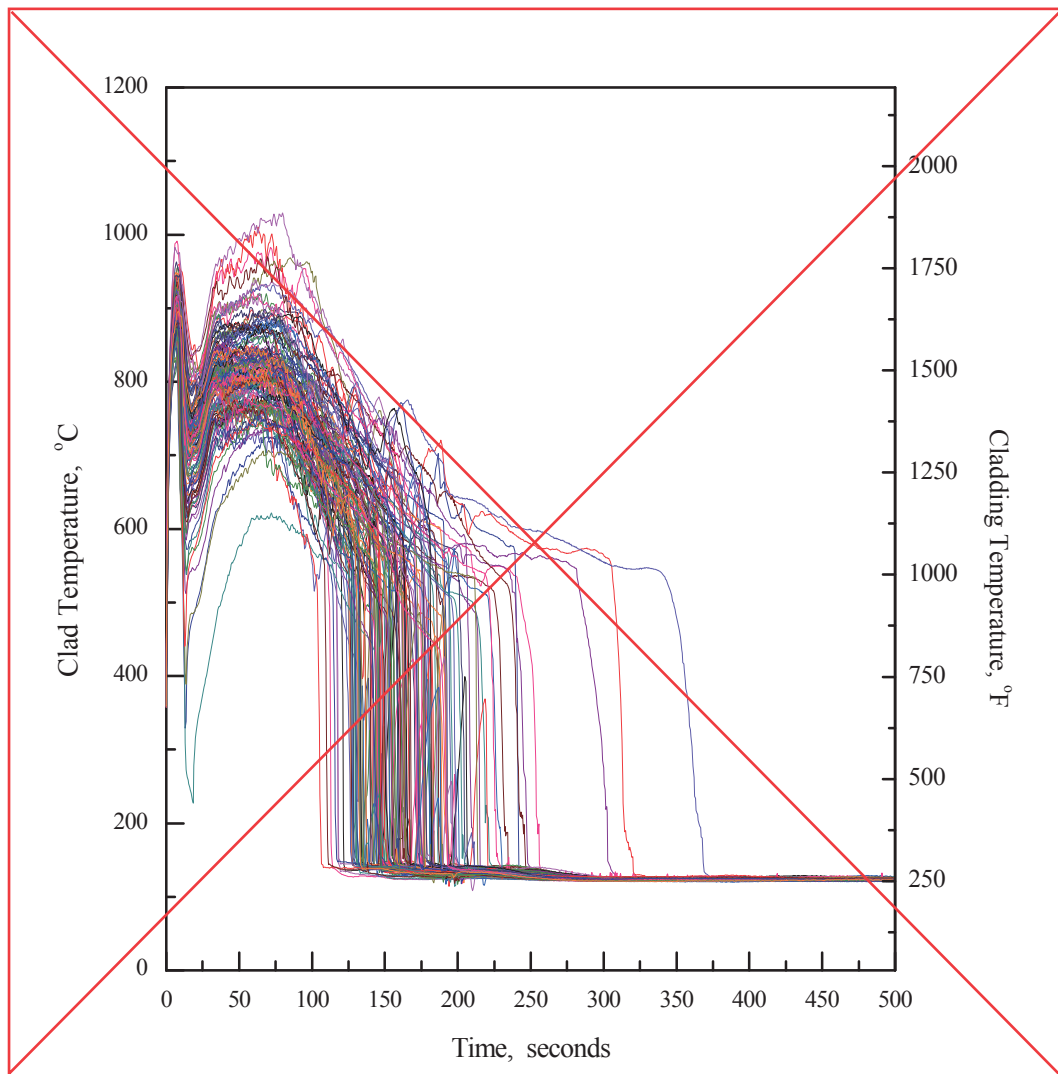
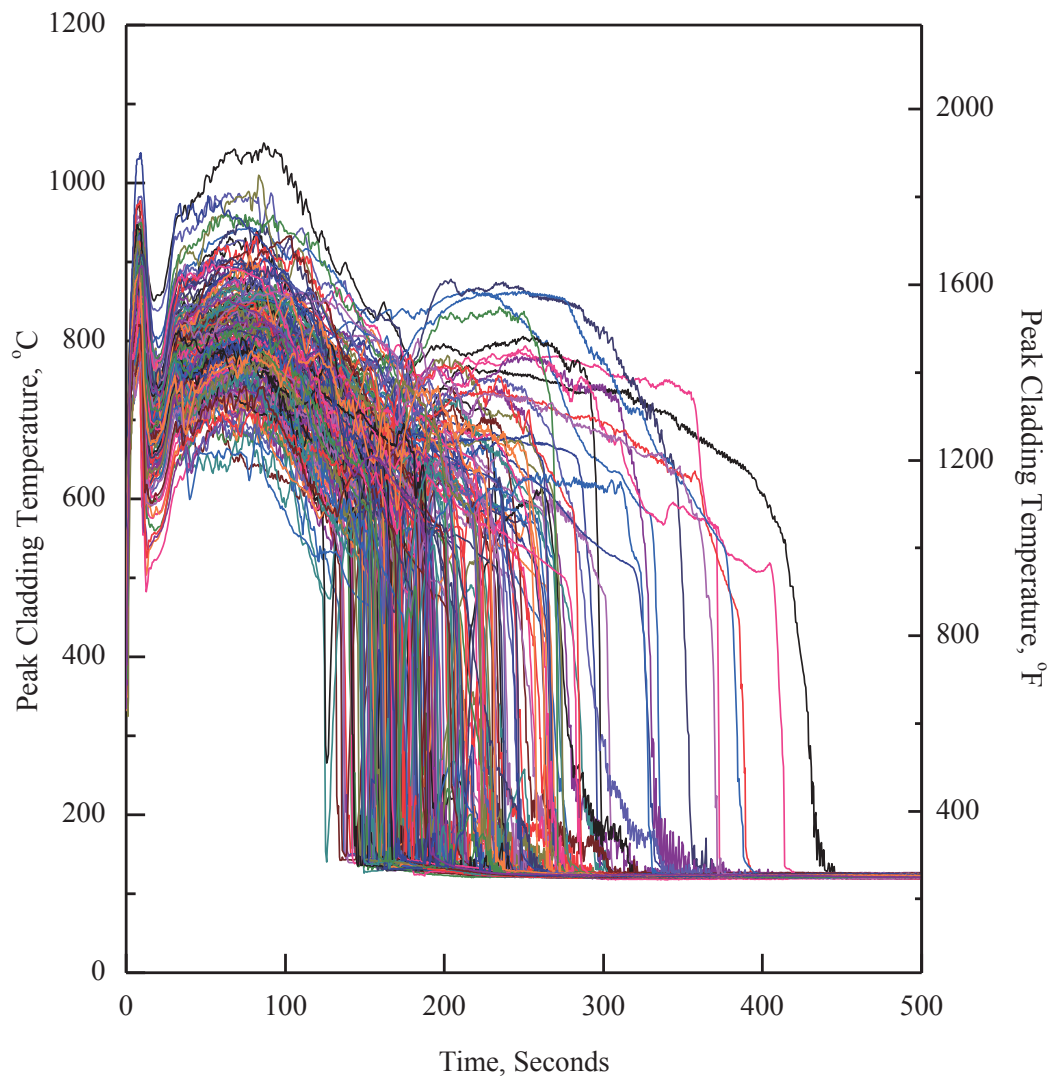


Figure 15.6.5-23 SRS Peak Cladding Temperature

AB



Non-Proprietary

Criticality Analysis of NFR and SFR

APR1400-A-NR-14011-NP Rev.1

3.5 Criticality Analysis for Spent Fuel Pool Region II

The spent fuel pool region II is designed to accommodate the fuel assemblies with the minimum burnup which satisfies the criticality acceptance criteria. The criticality analysis is performed using the CSAS5/ ENDF-7.1a sequence and the RI EN-ARP with cross section libraries generated using the TRITON and the ENDF-7.123 energy group library.

In order to determine the loading curve the criticality analyses are performed to find the minimum burnup which provides a k_{eff} less than 1.0 at the each initial enrichment of fuel assemblies.

Figures 3.5-1 and 3.5-9 provide the top and side views of SFP region II. As can be seen from the Figure 3.5-1 spent fuel storage racks in SFP region II are based on a high density rack design and at least one neutron absorber plate is placed between adjacent fuel assemblies to maintain sub-criticality.

Design data for fuel storage cells of SFP region II are provided in Figures 3.5-2 to 3.5-9 and Table 3.1-2 and information for rack interfaces within and between the SFP regions are provided in Subsection 3.5.1.

3.5.1 Depletion Calculations

As discussed in Subsection 3.3.2 the depletion calculations are performed using the RI EN-ARP with cross section libraries generated using the TRITON sequence. For the generation of the cross section libraries using the TRITON sequence, the following reactor parameters described in the Subsection 3.5.1.1 are used. The isotopic concentrations are generated by the RI EN-ARP at each 2.25 % F TU intervals from 0 to 72 % F TU for the initial enrichments from 2.0 to 5.0 % ^{235}U with 0.5 % increments of U-235 enrichment.

Zero cooling time is taken for conservatism so that the fuel assembly is not allowed to decay after depletion to a desired assembly-average burnup.

3.5.1.1 Bounding Reactor Parameters for the Depletion Calculation

The bounding reactor parameters are a fuel temperature, fuel concentration and a power level.

The applied fuel temperature is higher than the maximum fuel temperature of []^{TS} including Thermal Conductivity Degradation (TCD) effect.

- Fuel temperature: Higher fuel temperature causes Doppler broadening and it results in increased plutonium production. Therefore the maximum fuel temperature of []^{TS} is applied to the depletion calculations.

- Fuel density: To maximize fissile fuel density, the maximum fuel density is applied to the depletion calculation.

- Moderator temperature: Higher moderator temperature hardens the energy spectrum hardening. Therefore the maximum moderator temperature is applied to the depletion calculation.

- Soluble boron concentration: Higher soluble boron concentration hardens the energy spectrum. Therefore the maximum soluble boron concentration is applied to the depletion calculation.

- Power level: The sensitivity and uncertainty analysis shows that there is no trend in respect to power level as shown in Table 3.5-2. So the maximum power level corresponding to the maximum fuel temperature is used as a bounding reactor parameter.

Non-Proprietary

SECTION E

Non-Proprietary

Page intentionally left blank

**KHNP****KOREA HYDRO & NUCLEAR POWER CO., LTD**

70-1312-gil, Yuseong-daero, Yuseong-gu, Daejeon, 305-343, KOREA

Tel: +82-42-870-5740 / Fax: +82-42-870-5779

<http://www.khnp.co.kr>

January 27, 2016
Document Control Desk
U.S. Nuclear Regulatory Commission
Washington, DC 20555-0001

Attention: Mr. Jeff Ciocco
Division of New Reactor Licensing

Docket No. 52-046
MKD/NW-16-0069L

Subject: Response to RAI TOP 6-8322

Reference: NRC Request for Additional Information TOP 6-8322, dated October 27, 2015

KHNP is hereby submitting the response to RAI TOP 6-8322, dated October 27, 2015. The response addresses Question TR PLUS7 Fuel Design for the ARP1400-24.

Enclosure 1 contains a copy of the associated affidavit. Enclosure 2 provides the response to RAI TOP 6-8322 (Proprietary). Enclosure 3 provides the response to RAI TOP 6-8322 (Non-Proprietary).

If additional information or clarification is required, please contact Daegeun Ahn, Director of KHNP Washington DC Center at ahn.daegeun@khnp.co.kr or 703-388-0592.

Sincerely,

Jae-yong Lee
Project Manager
Advanced Reactors Development Laboratory
Korea Hydro and Nuclear Power Co., Ltd

Enclosures:

1. Affidavit KAW-16-0069
2. Response to RAI TOP 6-8322 (Proprietary)
3. Response to RAI TOP 6-8322 (Non-Proprietary)

Enclosure 1

Affidavit KAW-16-0069

I, Yun-ho Kim, state the following:

1. I am the General Manager of Korea Hydro & Nuclear Power Co., Ltd. (KHNP), and as such I am authorized to request withholding the information transmitted with this letter from public disclosure and to execute this affidavit.
2. I am familiar with the criteria applied by KHNP to determine whether certain information is proprietary, and with the policies established by KHNP to ensure the proper application of these criteria.
3. The information, Response to RAI TOP 6-8322 (Proprietary), transmitted with this letter has been classified by KHNP as proprietary in accordance with the policies for the control and protection of proprietary and confidential information. The information regarded as proprietary is identified and marked consistent with the requirements of 10 CFR 2.390, § (b)(1)(i). Accordingly, the proprietary information is enclosed within brackets and the right-hand bracket carries a notation of “TS” to indicate that the trade secret nature of the information claimed to be proprietary is the basis for proposing that the information so identified be withheld from public disclosure.
4. Pursuant to the considerations set forth in 10 CFR Section 2.390(a), KHNP considers the information classified as proprietary to be “trade secret” information since it is design, analysis, or test information that would be difficult for a competitor to reproduce and hence provides an economic and competitive advantage to KHNP.
5. The need for designating the information as proprietary has been raised within KHNP. The information is being treated proprietary and confidential and has not been disclosed by KHNP to the public.
6. Nondisclosure of the proprietary information transmitted with this letter is vital to the competitiveness held by KHNP and, hence, disclosure of the proprietary information transmitted in with this letter would have negative commercial impacts on the competitive position of KHNP in the U.S. nuclear market.
7. In accordance with KHNP policy, proprietary information contained in this document may be, or may have been, made available on a limited basis to regulatory bodies, customers, potential customers, and their agents, suppliers, and licensees, and others under suitable agreements providing for nondisclosure and limited use of the information.

I declare that the foregoing statements are true and correct to the best of my knowledge, information and belief.

Executed on January 27, 2016.



Yun-ho Kim
General Manager
APR1400 Licensing Team
Central Research Institute
Korea Hydro and Nuclear Power Co., Ltd

Enclosure 3

Response to RAI TOP 6-8322

(Non-Proprietary)

January 27, 2016

RESPONSE TO REQUEST FOR ADDITIONAL INFORMATION

APR1400 Topical Reports

Korea Electric Power Corporation / Korea Hydro & Nuclear Power Co., LTD

Docket No. PROJ 0782

RAI No.: TOP 6-8322

SRP Section: TR PLUS7 Fuel Design for the APR1400

Application Section: PLUS7 Fuel Design for the APR1400
(APR1400-F-M-TR-13001-P)

Date of RAI Issue: 10/27/2015

Question No. TR PLUS7 Fuel Design for the APR1400-24

GDC 10 requires that the reactor core and associated coolant, control, and protection systems shall be designed with appropriate margin to assure that specified acceptable fuel design limits (SAFDLs) are not exceeded during any condition of normal operation, including the effects of anticipated operational occurrences (AOOs). GDC 27 requires that the reactivity control system is designed with appropriate margin and, in conjunction with the ECCS, is capable of controlling reactivity and cooling the core under post-accident conditions. SRP Section 4.2 (II)(1)(B)(viii) and Appendix A provides review guidance related to mechanical fracturing based on seismic and LOCA applied loads. It is also stated specifically that control rod insertability must be maintained.

This topic is addressed in Section 2.2.2 of APR1400-F-M-TR-13001-P, in the response to Question 2 of RAI 4-7542 (ML14177A220), and in the response to Question 23 of RAI 5-7954. In Question 23 of RAI 5-7954 (ML15169A118), the staff requested supporting technical justification that the proposed guide tube stress limits would meet GDC 27. The response provides an analysis which compares the calculated stresses for the PLUS7 fuel assemblies under seismic and LOCA loads with the material's yield stress and concludes that the yield stress is never exceeded. This response does not address the staff's concerns because the original RAI requested justification for the proposed limits, not an analysis of the applied loads.

Provide a discussion that covers the proposed stress-strain limits and what level of damage could occur to the components based on those limits. If damage could occur to the guide tubes, include a description of the tests and results that demonstrate control rod insertability. Update the topical report, as necessary, to capture these points.

Response

For the evaluation of guide tube stresses induced by the lateral displacements and the axial loads on fuel assembly during seismic and LOCA events, Appendix F of ASME Section III is

used as the general stress criteria: 1) the general primary membrane stress intensity P_m shall not exceed the lesser of $2.4S_m$ and $0.7S_u$, 2) the primary membrane plus primary bending stress intensity P_m+P_b shall not exceed 150% of the limit for P_m . The proposed stress limit (i.e., $1.05 S_u$) and the associated strain ($\epsilon_{1.05}$) for the SRA ZIRLO guide tube are depicted in Figure 24-1.

Since the ASME stress criteria are based on an elastic analysis, the triangular strain energy density over yield stress can be converted to equivalent strain energy on the actual stress-strain curve as shown in the figure. Therefore, the actual strain ($\epsilon'_{1.05}$) is slightly increased by the equivalent strain energy density and the resulting damage will be slightly greater than proportional permanent strain. The following considerations explain that the damage will not create an excessive deformation of the guide tube that would prevent control rod insertability.

- The loadings during the seismic and LOCA events are not a static load, but an oscillating dynamic load that will be diminished after several seconds, so the actual stress on the guide tube is lower than the one given by the static elastic analysis that is based on an instantaneous deflection,
- Only a portion of the guide tube's cross section has stresses that exceed yield at a particular elevation,
- Only a limited portion of the axial length of the guide tube has stresses that exceed yield, and
- Strain hardening of the guide tube when loaded beyond yield increases the elastic strain range of the material, thereby decreasing the permanent deformation of the guide tube associated with a loading beyond yield.

TS

Figure 24-1 PLUS7 Guide Thimble Stress-Strain Relation

Impact on DCD

There is no impact on the DCD.

Impact on PRA

There is no impact on the PRA.

Impact on Technical Specifications

There is no impact on the Technical Specifications.

Impact on Technical/Topical/Environmental Report

There is no impact on any Technical, Topical, or Environmental Report.

**KHNP****KOREA HYDRO & NUCLEAR POWER CO., LTD**

70-1312-gil, Yuseong-daero, Yuseong-gu, Daejeon, 305-343, KOREA

Tel: +82-42-870-5400 / Fax: +82-42-870-5449

<http://www.khnp.co.kr>

July 31, 2017

Document Control Desk

U.S. Nuclear Regulatory Commission

Washington, DC 20555-0001

Attention: Mr. William Ward

Division of New Reactor Licensing

Docket No. 52-046

MKD/NW-17-0130L

Subject: Revised Response to RAI TOP 6-8322**References: 1) NRC Request for Additional Information TOP 6-8322, dated October 27, 2015****2) KHNP Letter MKD/NW-16-0069L, Response to RAI TOP 6-8322, dated January 27, 2016**

KHNP is hereby submitting the response to RAI TOP 6-8322, dated October 27, 2015. The RAI revised response addresses Question TR PLUS7 Fuel Design for the ARP1400-24.

Enclosure 1 contains a copy of the associated affidavit. Enclosure 2 provides the revised response to RAI TOP 6-8322 (Proprietary). Enclosure 3 provides the revised response to RAI TOP 6-8322 (Non-Proprietary).

If additional information or clarification is required, please contact Daegeun Ahn, General Manager of KHNP Washington DC Center at ahn.daegeun@khnp.co.kr or 703-388-0592.

Sincerely,



Han-gon Kim

Project Manager

Advanced Reactors Development Laboratory

Korea Hydro & Nuclear Power Co., Ltd.

Enclosures:

1. Affidavit KAW-17-0130

2. Revised Response to RAI TOP 6-8322 (Proprietary)

3. Revised Response to RAI TOP 6-8322 (Non-Proprietary)

Enclosure 1

Affidavit KAW-17-0130

I, Yun-ho Kim, state the following:

1. I am the General Manager of Korea Hydro & Nuclear Power Co., Ltd. (KHNP), and as such I am authorized to request withholding the information transmitted with this letter from public disclosure and to execute this affidavit.
2. I am familiar with the criteria applied by KHNP to determine whether certain information is proprietary, and with the policies established by KHNP to ensure the proper application of these criteria.
3. The information, KHNP Revised Response to RAI TOP 6-8322 (Proprietary), transmitted with this letter has been classified by KHNP as proprietary in accordance with the policies for the control and protection of proprietary and confidential information. The information regarded as proprietary is identified and marked consistent with the requirements of 10 CFR 2.390, § (b)(1)(i). Accordingly, the proprietary information is enclosed within brackets and the right-hand bracket carries a notation of “TS” to indicate that the trade secret nature of the information claimed to be proprietary is the basis for proposing that the information so identified be withheld from public disclosure.
4. Pursuant to the considerations set forth in 10 CFR Section 2.390(a), KHNP considers the information classified as proprietary to be “trade secret” information since it is design, analysis, or test information that would be difficult for a competitor to reproduce and hence provides an economic and competitive advantage to KHNP.
5. The need for designating the information as proprietary has been raised within KHNP. The information is being treated proprietary and confidential and has not been disclosed by KHNP to the public.
6. Nondisclosure of the proprietary information transmitted with this letter is vital to the competitiveness held by KHNP and, hence, disclosure of the proprietary information transmitted in with this letter would have negative commercial impacts on the competitive position of KHNP in the U.S. nuclear market.
7. In accordance with KHNP policy, proprietary information contained in this document may be, or may have been, made available on a limited basis to regulatory bodies, customers, potential customers, and their agents, suppliers, and licensees, and others under suitable agreements providing for nondisclosure and limited use of the information.



KHNP
KOREA HYDRO & NUCLEAR POWER CO., LTD

I declare that the foregoing statements are true and correct to the best of my knowledge,
information and belief.

Executed on July 31, 2017.

Yun-ho Kim
General Manager
APR1400 Licensing Team
Korea Hydro and Nuclear Power Co., Ltd

Enclosure 3

Revised Response to RAI TOP 6-8322

(Non-Proprietary)

July 31, 2017

REVISED RESPONSE TO REQUEST FOR ADDITIONAL INFORMATION

APR1400 Topical Reports

Korea Electric Power Corporation / Korea Hydro & Nuclear Power Co., LTD

Docket No. PROJ 0782

RAI No.: TOP 6-8322

SRP Section: TR PLUS7 Fuel Design for the APR1400

Application Section: PLUS7 Fuel Design for the APR1400
(APR1400-F-M-TR-13001-P)

Date of RAI Issue: 10/27/2015

Question No. TR PLUS7 Fuel Design for the APR1400-24

GDC 10 requires that the reactor core and associated coolant, control, and protection systems shall be designed with appropriate margin to assure that specified acceptable fuel design limits (SAFDLs) are not exceeded during any condition of normal operation, including the effects of anticipated operational occurrences (AOOs). GDC 27 requires that the reactivity control system is designed with appropriate margin and, in conjunction with the ECCS, is capable of controlling reactivity and cooling the core under post-accident conditions. SRP Section 4.2 (II)(1)(B)(viii) and Appendix A provides review guidance related to mechanical fracturing based on seismic and LOCA applied loads. It is also stated specifically that control rod insertability must be maintained.

This topic is addressed in Section 2.2.2 of APR1400-F-M-TR-13001-P, in the response to Question 2 of RAI 4-7542 (ML14177A220), and in the response to Question 23 of RAI 5-7954. In Question 23 of RAI 5-7954 (ML15169A118), the staff requested supporting technical justification that the proposed guide tube stress limits would meet GDC 27. The response provides an analysis which compares the calculated stresses for the PLUS7 fuel assemblies under seismic and LOCA loads with the material's yield stress and concludes that the yield stress is never exceeded. This response does not address the staff's concerns because the original RAI requested justification for the proposed limits, not an analysis of the applied loads.

Provide a discussion that covers the proposed stress-strain limits and what level of damage could occur to the components based on those limits. If damage could occur to the guide tubes, include a description of the tests and results that demonstrate control rod insertability. Update the topical report, as necessary, to capture these points.

Response - (Rev.1)

The stress limits of the normal operation and anticipated operational occurrence (AOO) condition will be used to assure that the components do not deformed severely enough to interfere with control rod insertion at the faulted conditions. The fuel assembly components for CEA insertion are guide thimble, outer guide post, adapter plate and holddown plate. The stress limits of fuel assembly components for CEA insertion are:

$$(a) P_m \leq S_m$$

$$(b) P_m + P_b \leq 1.5 \cdot S_m$$

Where:

P_m = primary membrane stress intensity,

P_b = primary bending stress intensity

S_m = allowable design stress intensity defined in the ASME Section III

DCD APR1400-K-X-FS-14002-P Rev.1, technical report APR1400-Z-M-NR-14010-P Rev.1 and topical report APR1400-F-M-TR-13001-P Rev.0 will be revised to add the limits of the fuel assembly components as indicated in the attachment 1, 2 and 3.

Based on analyses of Seismic and LOCA events, the stress intensities results of the fuel assembly components for CEA insertion are less than the normal operation and AOO limits. Satisfying the normal operation and AOO limits ensures that no permanent deformation of the guide tubes within manufacturing tolerances will occur, so there is no impact on CEA insertability. Evaluation results of the fuel assembly components for the CEA insertion will be included in technical report APR1400-Z-M-NR-14010-P Rev.0 as indicated in the attachment 3.

Impact on DCD

DCD Rev.1 4.2.1.5.3 will be revised as indicated on the Attachment 1.

Impact on PRA

There is no impact on PRA.

Impact on Technical Specifications

There is no impact on the Technical Specifications.

Impact on Technical/Topical/Environmental Reports

Technical Report APR1400-Z-M-NR-14010-P Rev.1 will be revised as indicated on the Attachment 2.

Topical Report APR1400-F-M-TR-13001-P Rev.0 will be revised as indicated on the Attachment 3.

APR1400 DCD TIER 2

- c. Two-thirds of the specified minimum yield strength (S_y) at room temperature
- d. Ninety percent of the yield strength at temperature

For the zirconium alloy, the design stress intensity on the unirradiated yield strength is conservative.

The design stress intensity of zirconium alloy is defined as follows:

- a. Two-thirds of the minimum yield strength at temperature

4.2.1.5.3 Postulated Accident Loads

Worst-case abnormal loads during postulated accidents are represented by seismic and LOCA loads. For these conditions, the reactor is able to be brought to a safe shutdown condition, and the core is kept subcritical with the acceptable heat transfer geometry. This requirement is met by demonstrating that, under the most severe anticipated loading of fuel assemblies for postulated accidents, no damage to the fuel assembly structure is severe enough to prevent a coolable geometry from being maintained or to preclude CEA insertion.

The fuel assembly structural component stresses under faulted conditions are evaluated using primarily the methods in Appendix F of ASME Section III (Reference 23). The faulted condition stress limits for fuel assembly structural components are:

- a. General primary membrane stress intensity limit: S_m'
- b. Primary membrane plus bending stress intensity: $1.5 S_m'$

Where:

S_m' = the lesser value of $2.4 S_m$ and $0.7 S_u$

4.2.1.6 In-Core Control Components

Additionally the stresses of the fuel assembly components for the CEA insertion are evaluated using the normal operation and AOO stress limits to assure that the components do not deformed severely enough to interfere with CEA insertion even under the faulted conditions. The fuel assembly components for CEA insertion are guide thimble, outer guide post, adapter plate and holddown plate. The stress limits of fuel assembly components for CEA insertion are same as the normal operation and AOO stress limits in subsection 4.2.1.5.2.

$$P_m \leq S_m'$$
$$P_m + P_b \leq 1.5 \cdot S_m'$$

Where,

P_m = calculated primary membrane stress

P_b = calculated primary bending stress

S_m = allowable design stress intensity defined in the ASME Section III

S_u = minimum ultimate tensile strength at unirradiated condition

S_m' = allowable design strength for the accident conditions (a smaller value of $2.4 S_m$ and $0.7 S_u$)

(3) Evaluation

The structural integrity of the PLUS7 components is verified in Section 2.3 for all conditions.

The fuel assembly evaluation for seismic and LOCA loads is performed in accordance with the NRC licensed CE methodology (Reference 2-1). The fuel assembly model and characteristics were determined as analysis of fuel assembly mechanical test and used to the core analysis predicted fuel assembly deflected shapes and grid impact forces. Grid buckling strength was determined from dynamic impact testing for PLUS7 grids, and compared with predicted grid impact forces. The stresses for remaining components during seismic and LOCA are calculated through deflection shapes and axial loads, and then evaluated against each stress criteria. The evaluation of fuel assembly for seismic and LOCA loads will be addressed in DCD tier 2, Section 4.2.

2.2.2.2 Rod-to-Top Nozzle Axial Clearance

(1) Basis

Additionally the stresses of the fuel assembly components for the CEA insertion are evaluated using the normal operation and AOO stress limits to assure that the components do not deformed severely enough to interfere with control rod insertion even under the postulated accident conditions. The fuel assembly components for CEA insertion are guide thimble, outer guide post, adapter plate and holddown plate. The stress limits of fuel assembly components for CEA insertion are same as the normal operation and AOO stress limits.


(3) Evaluation

Based on the calculation of the axial gap between the fuel rod and top nozzle considering their irradiation growths, the axial clearance is maintained during the fuel lifetime. The PLUS7 PSE results confirmed the sufficient gap after three cycles of irradiation as shown in the Section 4.2.3.

2.2.2.3 Hydraulic Stability

(1) Basis

Since the fuel assembly lift-off may cause the fuel assembly and in-core structure failure, the fuel assembly shall not be lifted off during the normal operation. The fuel assembly and fuel rod vibration causing the fuel failure shall not occur over the full range of flow rates of the plant.



Results of the fuel assembly stress analysis in this section did not exceed each stress limit during postulated accidents. In addition, as a result of core analysis in Section 3 and 4, grid impact loads did not exceed the grid crush strength in Section 5.

Consequently, the fuel assembly satisfied the requirements to maintain control rod insertability and core coolability.

Additionally the stresses of fuel assembly components for the CEA insertion are compared with the normal operation and anticipated operational occurrence (AOO) stress limits to ensure the CEA insertability. The stresses of guide thimble, outer guide post, adapter plate and holddown plate did not exceed the stress limits of normal operation and anticipated operational occurrence (AOO) condition. It is evaluated that these components will not interfere with control rod insertion under the postulated accident conditions.

7. FAULTED CONDITION CRITERIA FOR FUEL ASSEMBLY PERFORMANCE EVALUATION

7.1 Introduction

This section presents the criteria that must be met for fuel assembly components, such as nozzles and guide thimbles, during seismic and pipe rupture events. According to Reference 7-1, to meet the requirement related to control rod insertability and core coolability for postulated accidents (seismic and

Additionally the stresses of the fuel assembly components for the CEA insertion are evaluated using the normal operation and anticipated operational occurrence (AOO) stress limits to assure that the components do not deformed severely enough to interfere with control rod insertion even under the postulated accident conditions. The fuel assembly components for CEA insertion are guide thimble, outer guide post, adapter plate and holddown plate. The stress limits of fuel assembly components for CEA insertion are:

- (a) $P_m \leq S_m$
- (b) $P_m + P_b \leq 1.5 \cdot S_m$

would be based on ASME Boiler and Pressure Vessel Code values.

7.2 Grid

The grids have an important role for coolable geometry of the fuel assembly in maintaining the appropriate spacing between adjacent fuel rods. The evaluation of grids for this function is performed by comparing the peak impact load for the grid in the core analysis with the lateral impact strength of the grid. This grid crush strength is determined by the grid impact test described in Appendix A and by analyzing the test results described in Section 5.

7.3 Components Except Grid

As described in Section 2, the fuel assembly is made from Type 304 stainless steel including Grade CF-3, Inconel 718, and zirconium alloy. The structural integrity of these components to withstand the loads during seismic and pipe rupture accidents are evaluated by comparing the calculated stress intensities for each component with stress limits defined by:

- (a) $P_m \leq S_m'$
- (b) $P_m + P_b \leq 1.5 \cdot S_m'$

Where:

P_m = primary membrane stress intensity,
 P_b = primary bending stress intensity
 S_m' = design intensity value for faulted conditions.

S_m = allowable design stress intensity defined in the ASME Section III

~~For holddown springs that are fabricated from Inconel 718 wire, their performance is evaluated by calculating the shear stress resulting from the spring being compressed to its solid height. This calculated shear stress must not exceed the yield strength in shear for this material.~~

7.4 References for Section 7

- 7-1 NUREG-0800, Standard Review Plan Section 4.2 Rev. 03, "Fuel System Design," March 2007.